Fall 2010

Measuring blast induced rock damage from pre-splitting sandstone by applying the multichannel analysis of surface waves geophysical method

Charles Bradford Zdazinsky

MEASURING BLAST INDUCED ROCK DAMAGE FROM PRE-SPLITTING SANDSTONE BY APPLYING THE MULTICHANNEL ANALYSIS OF SURFACE WAVES GEOPHYSICAL METHOD

by

CHARLES BRADFORD ZDAZINSKY

A THESIS

Presented to the Faculty of the Graduate School of the

MISSOURI UNIVERSITY OF SCIENCE AND TECHNOLOGY

In Partial Fulfillment of the Requirements for the Degree

MASTER OF SCIENCE IN EXPLOSIVES ENGINEERING

2010

Approved by

Jason Baird, Advisor

Paul Worsey

Kwame Awuah-Offei

ABSTRACT

Many blasting applications in the mining industry demand that the hard rock being blasted remains structurally competent. For example, pre-splitting is a common technique to reduce fracturing, and operators of dimension stone quarries use this blasting method to eliminate overbreak. When pre-split design parameters are not applied correctly, there will be a redistribution of stresses within the rock, resulting in Blast Induced Rock Damage (BID). Advances in geophysical technology are enabling blast technicians to monitor BID and then use the results to correctly design their blasts.

The Multichannel Analysis of Surface Waves (MASW) geophysical method is new technology that is applied in many industries to determine the structural integrity of the subsurface. However, it has never been applied to monitor and quantify BID. Nonetheless, the author of this research intended to determine whether the MASW geophysical method can be applied on a large scale in surface mining by quantifying the amount of BID that is produced from pre-splitting and comparing this BID to rock mass competency, and high-wall stability. The author did so by performing a series of pre-split shots at a sandstone dimension stone quarry. Pre and post blast MASW surveys were gathered and compared to determine the extent that unwanted damage was occurring from the pre-split at specific depth intervals from the split line.

The MASW method will produce high resolution data when it is used in optimal conditions. However, geological anomalies that are typical at mine sites prevent accurate MASW data to be processed with high resolution. Therefore, MASW is not applicable to monitor BID produced from pre-splitting with precision. However, MASW is capable of collecting detailed information at mine sites when it is performed on a large scale and this research shows that it will identify zones where the stone has been disturbed from the blast at depths several meters from the split line which compromises the structural integrity of the remaining rock mass and negatively influences the outcome of later shots performed in that area. This research generated recommendations for work that could be done to further utilize the MASW method as it was intended for.

ACKNOWLEDGEMENTS

I would like to thank my advisor, Dr. Jason Baird, as well as Dr. Paul Worsey and Dr. Kwame Awuah-Offei for their advice, expert knowledge, and serving on my graduate committee. Their friendship has had a priceless impact on this project's success as well as on my education.

I would like to thank the Missouri University of Science and Technology for funding this project as well as supplying many of the tools, equipment and facilities that were used to complete the work. I would also like to thank representatives of the Mining Engineering Program, especially: Jimmy Taylor, DeWayne Phelps, Barbara Robertson, Shirley Hall, Dr. David Summers, Alex Hopkins, Matt Ortel, Mathew Turner, and Phillip Mulligan.

I would like to thank University faculty outside of the Mining Engineering Program including: Dr. Neil Anderson, Oleg Kovin, Evgeniy Torgashov, Dr. Leslie Gertsch, John Tyler, Dr. John P. Hogan, Dr. Beth Cudney, Dr. Dan Reardon, Vicki Hudgins, Dr. Mary Bixby, and Phoebe Shyla Wiles.

Many companies and representatives of the Mining, Geotechnical, and Explosives industries have advised and supported the success of this project as well, including: Dyno Nobel, Orica, Brunner and Lay, Crazy Horse, Davey Bickford, Cold Springs Granite, Tom Barkley, Steve Iverson, Justin Davis, Vernon Smith, Bret Smith, Dr. Patrick Walter, Jim Lally, and Howard Bell.

I must also thank Jim DiPardo for allowing me to use his quarry as the location to perform my research as well as donating his time and machinery to extract the stone after it had been blasted.

Finally, I would like to thank my family and friends for their patience, love, and support while I have been finishing my academic career.

TABLE OF CONTENTS

Page

LIST OF ILLUSTRATIONS

Figure Page

LIST OF TABLES

1. INTRODUCTION

When applicable, the use of explosives allows the mining industry to swiftly, and effectively complete a job. When blasting techniques are properly used, the job becomes more safe and economic than any other excavation method. In turn, engineers are able to make a large net value of the product that is blasted.

Occasionally in conventional blasting, the explosive has been misused in such a way as to destroy the quality of the remaining rock. The explosive energy penetrates far into the rock, and the resulting systems of cracks result in overbreak [Kihlstrom, 1978]. Though the competence of the stone depends on the geology of the region -- free from joints and intrusions -- the blaster does have some control over fractures induced by explosives. Many applications demand that the hard rock being blasted remain competent and keep its structural integrity. For example, pre-splitting and smooth-wall blasting are common techniques to reduce fracturing, and operators of dimension stone quarries use these blasting methods to eliminate overbreak. The stone that is separated from the rock mass in a dimension stone quarry is defined as a loaf. In order to gain saleable product, the blast must not compromise the strength of the rock. The loaves that are being extracted and the rock mass left behind (to be blasted at a later time) must have minimal damage. Careful control of the loaf shot is vital; overshooting can fracture the entire loaf and ruin several thousand tons of product [Lownds, 2000].

To prevent unwanted damage in blasted stone, every shot must be designed correctly. To understand how the blasted rock is affected by the explosives, engineers and blast technicians have performed research studies to obtain tomographic images of the blasted material at specific depth intervals from the borehole location where the explosives were placed. Tomography is imaging by sectioning, by using waves of energy [Tomography, 2010]. Tomographic images are commonly obtained by performing seismic wave field studies using geotechnical equipment. The tomographic images are then processed and analyzed to obtain information about the structural integrity of the subsurface at specified depth intervals into the material.

The author of this research project used the Multichannel Analysis of Surface Waves (MASW) geophysical method to obtain tomographic images of the subsurface before and after a pre-split shot in a sandstone dimension stone quarry. This geophysical method is commonly applied in the mining exploration industry, but it has never been used to monitor and quantify unwanted damage in blasted stone. The MASW data were examined and compared to interpret the extent to which the explosives had damaged the stone from the split line at specific depth intervals. The main objective of this research experiment was to determine whether or not the MASW method could be applied to monitor the damage that explosives used in pre-splitting induce on the remaining stone once the loaves have been extracted from the shot area. The tomographic data generated from the MASW software would also quantify the damage at specific depth intervals into the rock mass from the borehole locations where the explosives were placed.

The MASW geophysical method is a relatively new technology, and applying it to monitor and quantify Blast Induced Rock Damage (BID) from pre-splitting in a dimension stone quarry is "ground-breaking" work. In addition, the set-up parameters that are presented in this project have not been attempted before this work. As such, no published baseline data were available, so all of the information had to be obtained by performing tests. Fortunately, the author was able to do these tests on a large scale in an operating sandstone dimension stone quarry. The information was gathered in a real situation and saleable production stone was acquired after each blast. This made the field work more interesting and applicable to the surface mining industry. However, because geology is a major factor in blasting, the author had to make some adjustments in the blast design and set-up parameters to both accommodate and take advantage of the geological variability present in the sandstone quarry. The author approached this work with no preconceptions of outcomes, considering the unique nature of the experimental location's geology as well as sources of variation and error that were present in the MASW process. From this study, the author developed conclusions regarding the work performed and generated recommendations for work that could be done to further utilize the MASW method as it was intended for.

2. REVIEW OF THE LITERATURE

To better understand the direction of this thesis project, the author conducted a literature search for material related to pre-split blast design including shock wave theory and velocity of detonation. The conventional blasting techniques that have been used in pre-splitting applications and in the mining industry for many years were also reviewed. Several recent experiments performed by Explosive Engineers to improve dimension stone mining were also researched. This search made it evident to the author that Explosive Engineers have dramatically improved blast designs within the past several decades, and that blasting has evolved from an art into a scientific discipline. In addition, advancements in geophysical technology were investigated that enable Explosives Engineers to mitigate Blast Induced Rock Damage (BID) that occurs during the shot using seismic wave travel time. The MASW method was studied to learn how it works, its common applications, its field requirements and equipment, and its limitations. The following review of relevant literature explains the science behind the work:

2.1. DIMENSION STONE BLASTING DESIGN

A typical quarry shot design has multiple rows of holes. Explosives are packed into the holes and detonated in order to fracture the rock throughout and displace the fragmented stone in a muck pile, away from its original resting place. The detonation of explosives produces shock pressures that radiate outward and break the rock mass to a more desirable size. In the case of dimension stone, the goal is not to fracture the rock throughout, nor to throw it away from the deposit into a muck pile. Dimension stone quarries aim to split the rock into manageable sized blocks without compromising the integrity of the stone itself. Dimension stone companies typically work with hard rock, such as marble or granite, and are dedicated to producing aesthetically appealing stone that is to be used in architecture and sculptures. Dimension stone is not limited to granite and marble, however. For example, sandstone can be resistant to weathering, yet it is easy to work with. These qualities makes sandstone a common building material; to acquire large blocks of sandstone by means of dimension stone blasting is not

uncommon. Blast technicians use pre-splitting in these quarries to create a smooth cut where machines will be able to later enter the site, and extract the loaf from the deposit.

Because the blast expands in every direction, blast technicians must apply special techniques to ensure the stone is split only in line with the design while the rock's interior structural integrity is preserved. Certain "rules of thumb" (Table 2.1) apply when engineers design a pre-split or smooth wall blast. Though they cannot be applied in every situation, these "rules" offer a good starting place and are quite reliable.

Table 2.1: Pre-split "rules of thumb" [Worsey, 2006].

Maximum Depth	250 x hole diameter
Spacing	10 x hole diameter
Minimum Burden	30 x hole diameter
Specialist Pre-split Charge Diameter	1/4 x hole diameter
Stemming (Changes when boreholes are drilled at a shallow depth)	25 x hole diameter

Every design aspect is significant when creating a pre-split shot: hole diameter, burden, spacing, timing, charge weight, and confinement. Precision drilling and blasting requires the blast holes to be closely spaced and relatively small in diameter (3.18 cm (1 ¼")). Larger diameters allow wider spacing and deeper holes, but the resultant split will not be as smooth and BID will radiate further into the stone [Worsey, 2006].

A standard explosive used in this type of blasting is detonating cord with nominal charge weights of 1.5, 3.6, and 8 grams/meter (7.5, 18, and 40 grains/foot). This is a significantly smaller amount of explosive than one would see in a typical quarry shot.

Detonating cord fires at a high velocity of detonation which causes high pressures within the borehole during initiation. This pressure causes the pre-split to propagate between holes, and separate the loaf from the deposit. Moreover, because detonating cord has a small charge weight and diameter, it produces little damage to the surrounding stone when it is used correctly.

The charge weight of explosives used should be varied depending on the geology of the blast area. Some stone is more brittle (e.g., granite) than others and will split away from the rock mass very easily. However, some stone is very porous and the shock wave and gas pressures created by the explosive are absorbed by the stone. In porous stone, the desired split may not be achieved as easily.

Another blasting problem influenced by geology is when there are fractures or joint sets in the shot area. The gas pressures produced from the explosives will escape to these void areas, the pressure in the blast hole is decreased considerably, and the split will not be achieved.

The two geologically-influenced problems described above are common in sandstone dimension stone quarries. This sedimentary rock is deposited in layers and often has mud seams present throughout. In addition, it is porous and very absorbent. Joint sets, seams and fractures are characteristic in sandstone as well. Due to these conditions, the blaster must pay close attention to the charge weight, loaf orientation, and the hole diameter in order to achieve a good split.

These problems can be solved by following the “rules of thumb” mentioned above regarding charge weight diameter and/or increasing the confinement in the blast hole. This in turn will cause the pressure in the blast hole to be increased during the shot. Crushed stone, sand, and water are common stemming materials that are used in these instances to increase the confinement. Stemming is also very important to reduce air blasts and surface cratering [Worsey, 2006].

Stone deposits have compressive stresses pushing from every direction. The correct spacing is needed for the split to propagate and break the loaf free. Otherwise, the explosives will not have the strength to split the rock. In turn, all the energy will be

wasted by blowing the stemming into the air rather than splitting the rock. To utilize the energy created from the explosive, it is necessary for the row of holes to have relief in order for the pre-split to be successful and split the loaf away from the rock mass. The blaster must locate the row of holes correctly spaced and in line with an existing split or connect the row of holes perpendicular to a free face.

2.1.1. Sequential Timing Delays. Pre-splitting of rock in closely spaced holes works best when the holes fire nearly simultaneously. Figure 2.1 represents the different results that occur when detonators are fired independently versus instantaneously. When the detonators were fired separately, a rough split was produced and excessive radial fracturing resulted around every hole at lengths approximately equal to the spacing between detonators. When the detonators were fired simultaneously, the resultant split was very straight and radial fracturing was minimized. This experiment was performed in plexi-glass, and though the effects would be different in rock, it is evident that firing instantaneously is superior.

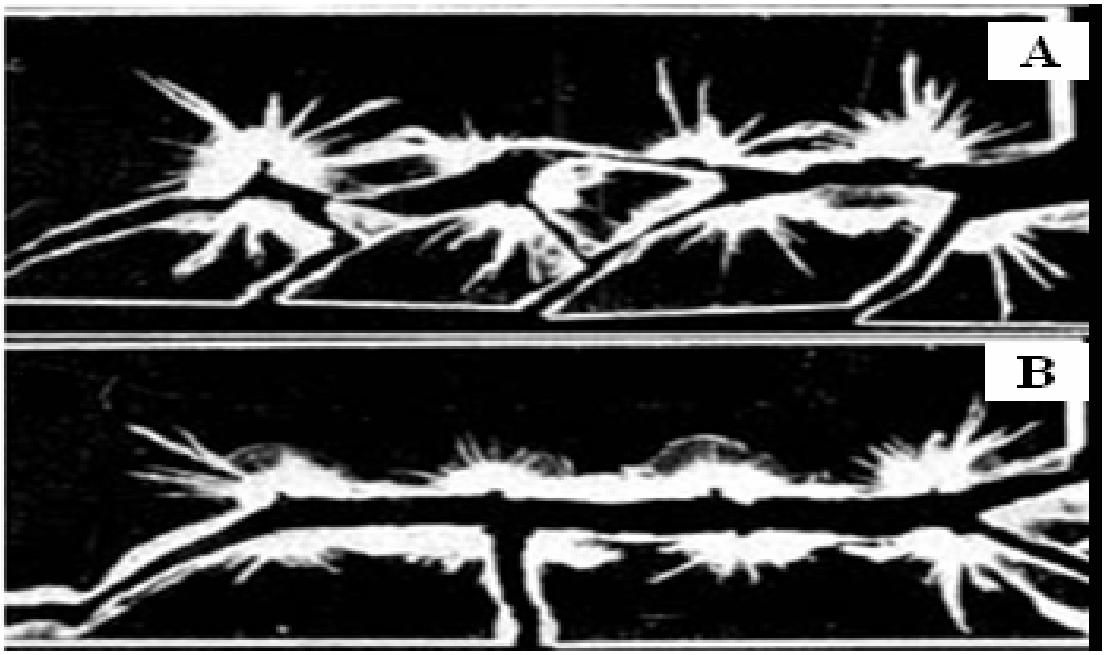

Figure 2.1: Blasting experiment in plexi-glass [Kihlstrom, 1978]: A) Independent shots; B) instantaneous shots.

Quick initiation allows the stress fields from adjacent holes to interact and makes the cracks propagating parallel between the holes the dominant split. Moreover, radial fracturing occurs as unwanted cracks propagate outward -- perpendicular to the desired split line. The goal of pre-splitting is to minimize radial fracturing to preserve the structural integrity of the blasted material. However, the stress fields take a finite time to be established because the stress waves travel at a finite velocity. Cracks from the first hole fired cannot be influenced by the next hole fired until the stress wave traveling backwards from the second fired hole fired meets these cracks. When this happens, the cracks become one and tend to form a smooth split in line with the row of holes [Lownds, 2000].

A study of sequential timing in pre-split design was performed at a granite dimension stone quarry by Lownds [2000]. At this quarry, the normal spacing between holes to achieve good splitting was 14 cm (5.5”). The velocity of crack propagation through hard rock was not measured in Lownds’ test, but it was assumed to travel at 1 mm/µs. With this information, it was determined that the best timing sequence the granite quarry should use in their pre-split designs was 20 µs between holes. Figure 2.2 shows specifically why this timing sequence works.

The cracks from the first hole fired will propagate uniformly in all directions until the stress fields interact, after which the splitting crack is dominant. During this time, the severity of cracks that deviate away from the split depends on the pressure in the holes. Higher pressures will cause more cracks to develop. Ideally the explosive induced stress should be just enough to propagate two cracks from each hole (forward and backward with respect to the direction of the drilled row of holes). When the stress is too great in the rock, there will be extra energy that will drive cracks away from the split line and compromise the integrity of the stone [Lownds, 2000].

When an explosive detonates, the shock waves travel at speeds specific to the media through which they are traveling. Each type of rock has unique physical characteristics. Compressive shock waves will travel at high speeds through competent matter [Lownds, 2000]. Conversely, they will travel slower through fractured material. To achieve smooth splitting, the velocity of the compressive waves through the stone, the

velocity of crack propagation, and the velocity of detonation should be incorporated into the design if possible.

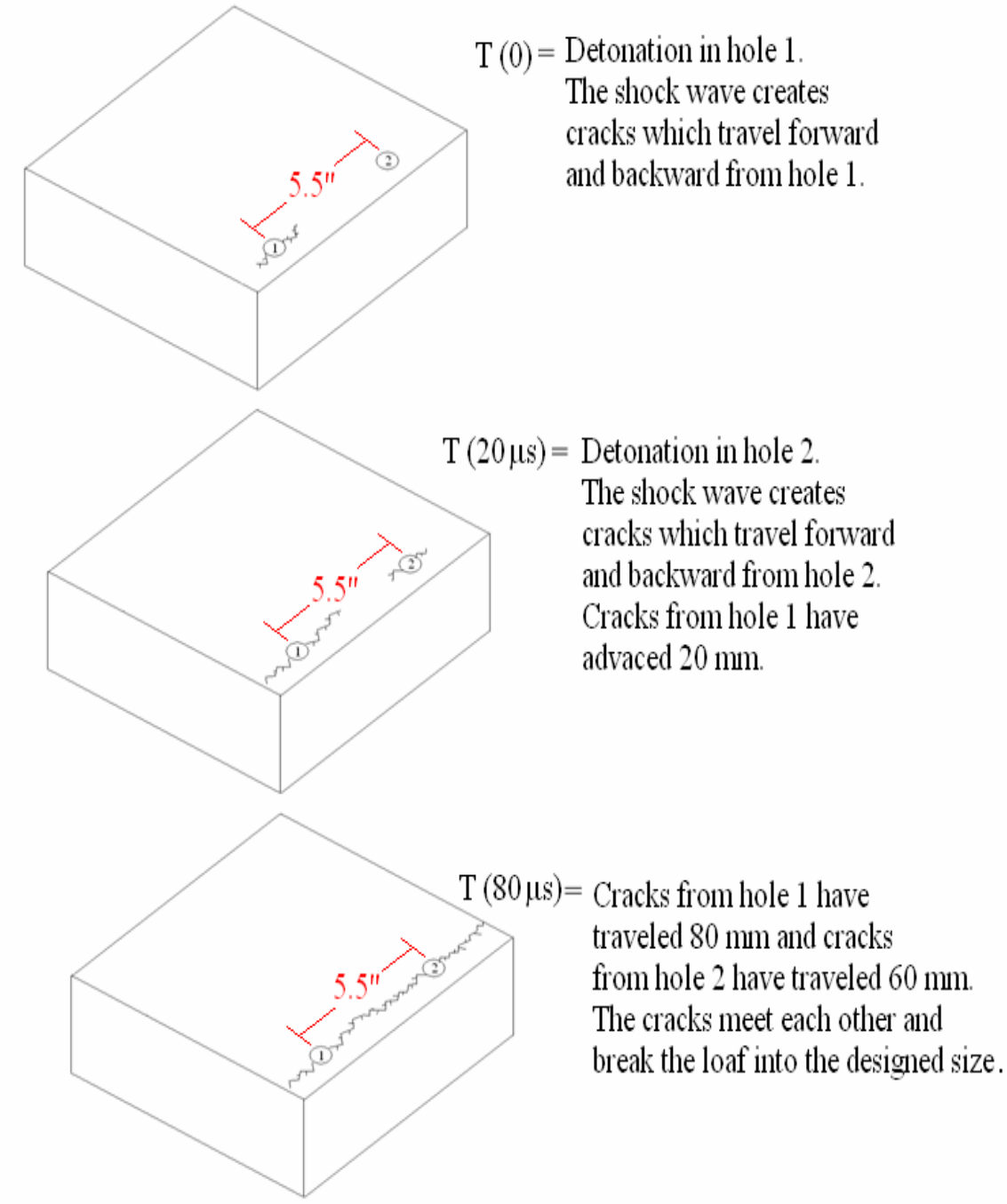

Figure 2.2: Velocity of crack propagation from pre-splitting in granite [Lownds, 2000].

2.2. COMPARISON OF BLAST PRESSURES FROM HIGH VELOCITY DETONATING CORD THROUGH DIFFERENT COUPLING MEDIAS

During a pre-split shot, the severity of radial fracturing that deviate away from the split depends on the pressure in the holes [Lownds, 2000]. Cold Springs Granite is a company in the Northwestern United States that specializes in dimension stone mining. At the turn of the millennium, Explosive Engineers completed several tests that studied different techniques to characterize and quantify the shock pressure created by pre-splitting, using detonating cord as the primary explosive. The quarry's standard blast procedures were applied, but a second parallel row of holes was drilled and commercial tourmaline pressure gauges were suspended in water in each of them (Figure 2.3). Pressure magnitude-duration graphs were then produced from the data acquired by the instrumentation [Lownds, 2000].

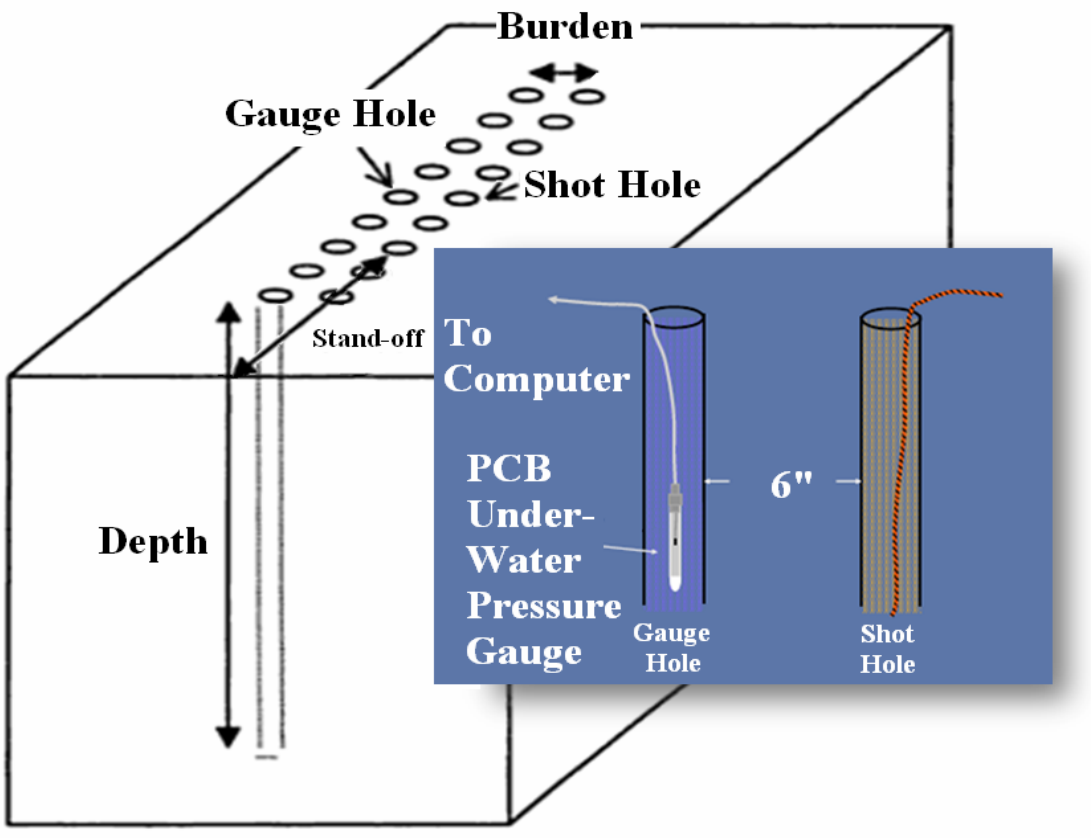

Figure 2.3: Cold Springs test set-up [Barkley, 2001].

The Cold Springs' study also tested five different types of coupling media in the blast holes. The goal was to determine which media would allow the explosive to adequately break the loaf away from the rock mass, but also absorb the pressure wave enough to preserve the stone's integrity. The five media were air, sand, water, and two B-Gel compositions developed by Viking Explosives & Supply, Inc. The pressure traces within each group of replicates displayed significant variation, but they were nevertheless reproducible enough to show important differences between the various explosive charges and fill media in the holes [Lownds, 2000].

This experiment determined that a split will not be achieved in granite unless a pressure of at least 1 MPa is maintained for the first 80 microseconds. Pressures higher than 2 MPa during the first 40 microseconds were not needed, and contribute to blast damage. Any significant pressure after 100 microseconds was unnecessary and probably would cause unwanted damage after the split was achieved [Lownds, 2000].

2.3. COMPARISON OF BLAST PRESSURES FROM LOW VELOCITY DETONATING CORD THROUGH DIFFERENT COUPLING MEDIAS

Unwanted damage is caused by the quick release of energy and pressure that explosives produce. Cold Springs Granite believed that by reducing the detonation velocity of the cord, the pressure within the borehole would be reduced as well. A new concept in detonating cord manufacturing has provided a radically different performing explosive. The explosive powder in the cord is mixed with other low strength and inert materials to reduce the detonation velocity [Product Manual, 2005]. This new Cord (LV cord) has reduced the velocity of detonation by approximately 30% (Table 2.2). The LV cord has a lower and longer sustained pressure pulse. In addition, it develops more gas than conventional cords. At the same time it maintains all of the handling and reliability advantages of conventional detonating cord and may be manufactured at the same nominal charge weights as the high velocity (HV) cord [Barkley, 2001]. Cold Springs decided to perform tests with an identical set up procedure that they used previously with HV cord, except that this second experiment would study LV cord in addition to HV cord [Barkley, 2001].

Table 2.2: Comparison of high velocity cord to low velocity cord [Barkley, 2001].

	HV Cord	**LV Cord**
Velocity of Detonation	6,700 m/s (23,000 fps)	4,700 m/s (15,400 fps)
Detonation Pressure	9.19 x 10^6 kPa (1.33 x 10^6 psi)	4.19 x 10^6 kPa (608,000 psi)

Cold Springs examined the blocks of granite after both of these experiments. By simply searching for surface cracks and measuring their lengths, Cold Springs concluded which explosive and stemming combination worked best (Table 2.3). No interior damage was measured or analyzed.

Table 2.3: The cracks present on the surface of a loaf using LV cord compared to the cracks present on the surface of a loaf using HV cord [Barkley, 2001].

	Maximum Crack Length (cm)	**Minimum Crack Length (cm)**	**Average Crack Length (cm)**	**Number of Stickers [Cracks longer than 15.2 cm (6")] per slab**
LV Cord	22.1 (8.7")	3.6 (1.4")	4.8 (1.9")	2.6
HV Cord	51.1 (20.1")	4.1 (1.6")	12.2 (4.8")	7.5
LV/HV	0.4	0.9	0.4	0.3
% Change	-60%	-10%	-60%	-70%

2.4. VELOCITY OF SEISMIC WAVES THROUGH FRACTURED AND UNFRACTURED STONE

Blast Induced Rock Damage (BID) is a concern in mining because it contributes to a redistribution of stresses within rock, resulting in rock mass strength weakening from resultant blasting fractures. Measurement of BID can thus be a useful tool to help refine blasting techniques for reduced rock fracturing [Iverson, 2009]. Tomography is imaging by sectioning, using waves of energy to generate information of a material at specific depth intervals. The mining industry has been using tomographic imaging and seismic data frequently for the past few decades to study stress distribution and fracturing within rock masses. Specifically, this process has been used to maintain safe working conditions in underground mines [Iverson, 2009]. BID may be determined by measuring the velocity of seismic wave energy and to generate tomographic images of blasted stone.

High resolution seismic methods have the potential to assess the extent of BID by analyzing P-wave velocity variation with depth into a rock mass. P-waves are compression waves observed in elastic media. The P-wave velocity increases with increasing consolidation of material and decreases with fracture density [Iverson, 2009]. By measuring P-wave velocities in a single rock type, one should be able to determine that specific rock's consolidation and/or structural integrity as a function of depth. These waves recorded before a blast, compared to waves recorded after a blast, will determine the extent of the BID.

A group of engineers from the University of Montana studied seismic refraction travel time tomography as an inversion method for estimating P-wave velocities to ultimately quantify BID in a concrete block. Variation of P-wave first arrival times were used to iteratively update a grid of velocities over the surveyed area. Their approach was to use seismic refraction travel time tomography to determine P-wave velocity as a function of depth into the concrete block [Iverson, 2009]. This survey was conducted on the concrete block before and after a blast was initiated. By comparison of the pre and post blast P-wave velocities, the engineers were able to quantify the amount of BID produced from the shot. The explosive used was Dyno AP emulsion.

To collect the P-wave velocity data, a line of holes was drilled horizontally into the concrete block to an equal and specific depth. Engineers attached geophones and strain gauges on the end of stud anchor bolts that were driven into the holes which were then filled with an epoxy. A small hammer with an electronic trigger was the source for the seismic data. This trigger attached to the hammer and the bolt completed a simple circuit when the bolt was struck by the hammer. The impact on the end of the bolt sent a signal to the system, which instructed it to begin recording. The bolts also had an aluminum wedge attached to them to hold an accelerometer in place for accurate data collection. Other recording equipment consisted of a Geode seismograph and compatible software to store the data on a laptop computer [Iverson, 2009]. The drill hole and instrumentation geometry is shown in Figure 2.4.

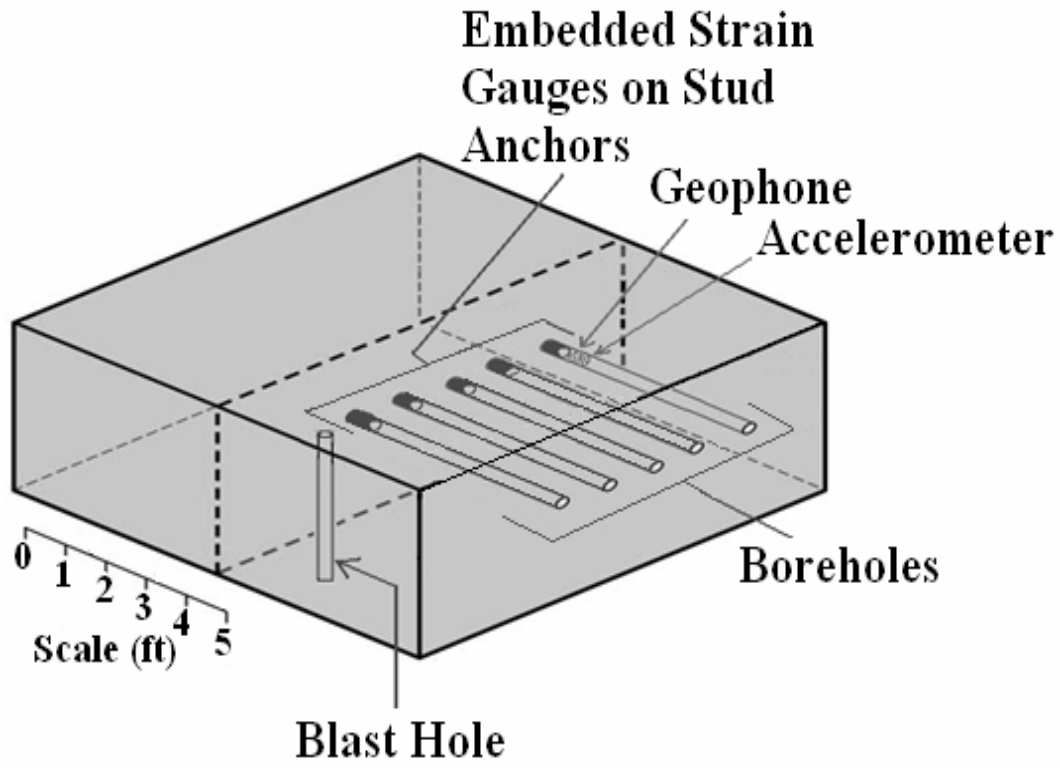

Figure 2.4: P-wave experiment drill hole and instrumentation set-up [Iverson, 2009].

The Rayfract software was applied to produce tomograms which recorded P-wave velocity within the concrete before (Figures 2.5) and after (Figure 2.6) a blast. The blast destroyed a large portion of the concrete block and therefore only half of the stud anchor bolt and geophone detector units were used in the post blast survey. In addition, the back side of the concrete block was destroyed and the post blast survey could only generate data to a depth of 0.2 meters (approximately 8"). The engineers then identified the low velocity zones related to BID by comparing the pre and post blast tomograms and determining the negative change in the P-wave velocity (Figure 2.7). The areas that were most affected by the explosives were highly fractured, thus they had a larger negative change in P-wave velocity at that depth.

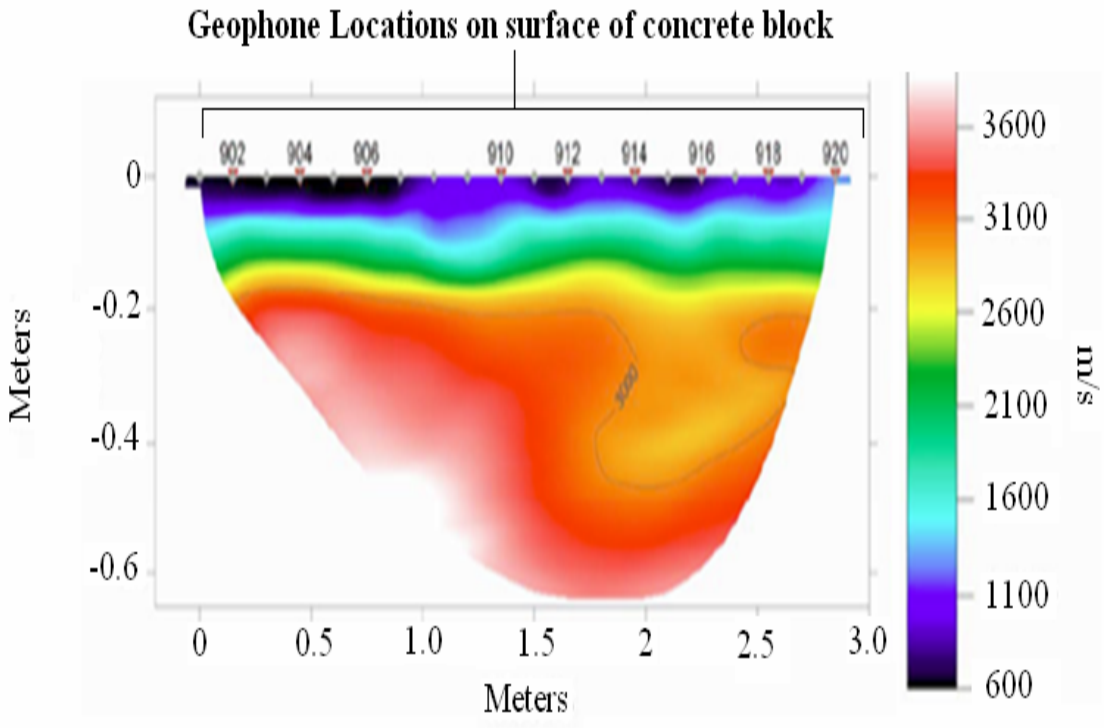

Figure 2.5: Tomographic imaging for a concrete block prior to a blast [Iverson, 2009].

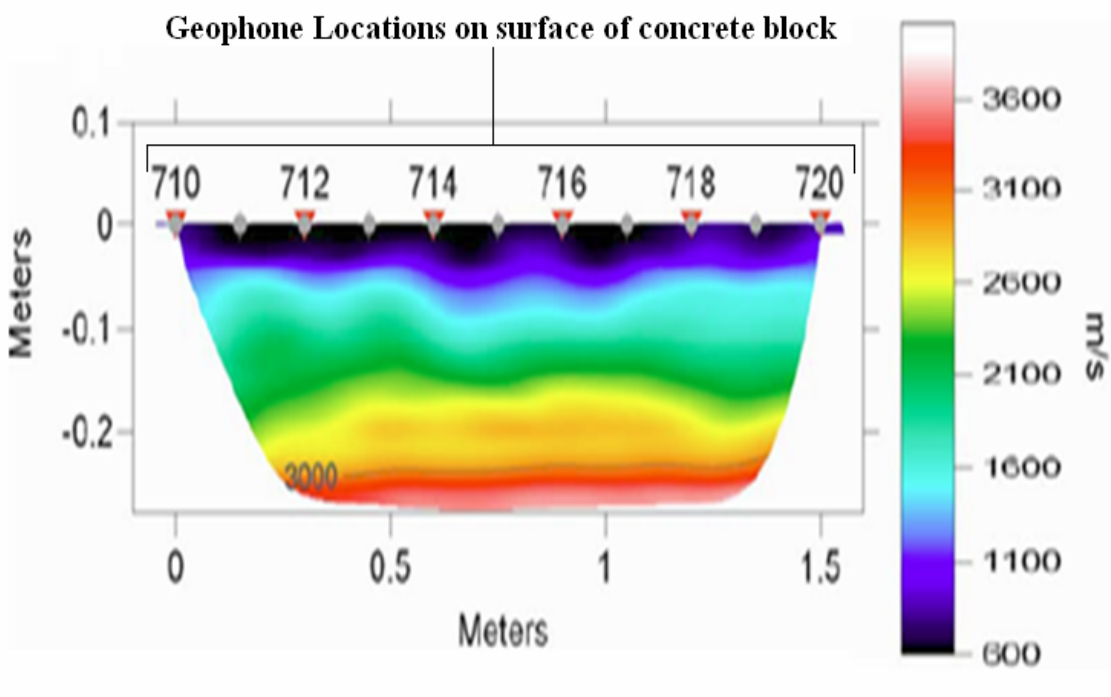

Figure 2.6: Tomographic imaging for a concrete block post blast [Iverson, 2009].

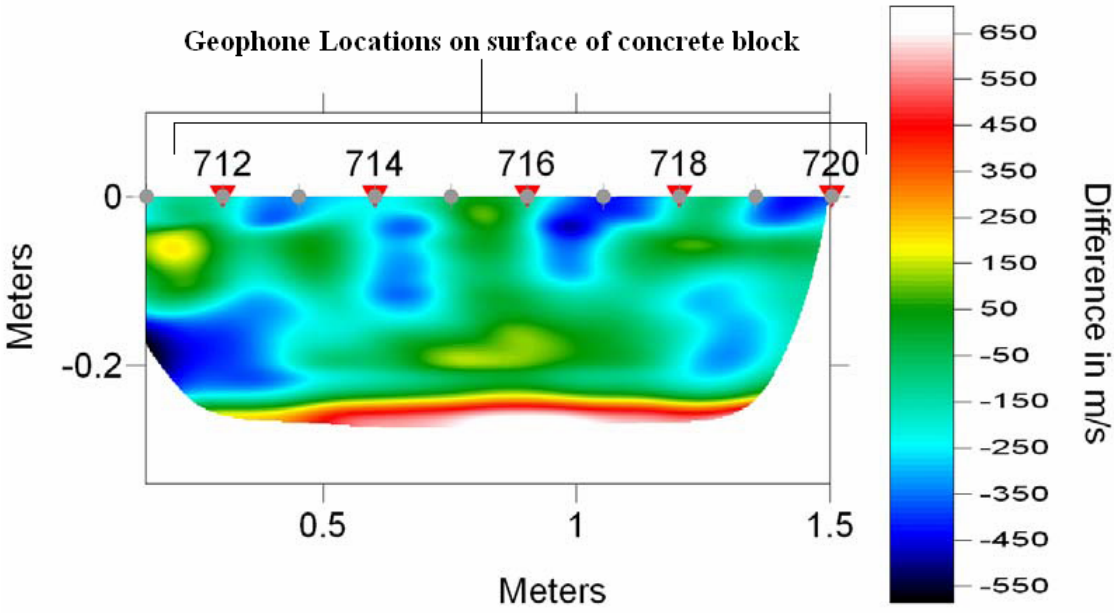

Figure 2.7: Comparison analysis shows the zones of the concrete block that were most affected by the blast due to the change in P-wave velocities [Iverson, 2009].

2.5. GEOPHYSICAL METHODS

Geophysics, a major discipline of the Earth Sciences, is the study of the whole Earth by the quantitative observation of its physical properties. Geophysical techniques have been used by engineers since the mid 19th century, but recent advances in technology have enabled geophysics to be a very versatile science and have allowed it to be applied to many different situations. As previously emphasized, many mining applications demand that the extracted stone remain structurally sound after the blast. The stone that is left behind (often to be blasted at a later time to produce additional saleable loaves, or to serve as a high-wall or portal entry) must remain competent as well. Iverson [2009] and the engineers at the University of Montana used geotechnical methods to quantify the BID that is produced by explosives that are commonly used in the mining industry. The research performed by the author of this report further investigates BID that occurs when performing pre-split shots using a similar approach that was utilized at the University of Montana.

The author of this research did not have access to either the tomographic imaging software or the geophysical instrumentation that was used by the group of engineers at the University of Montana. Therefore, the author researched other geophysical methods that would obtain seismic velocity profiles of the subsurface at specific depths to translate the extent of BID in a pre-split shot.

2.5.1. Seismic Wave Research. Seismic energy is produced by earthquakes or by other sources of near-surface disturbance such as an explosion, an automobile, or a sledgehammer impacting the surface. Geophysical methods can use this seismic energy to generate information regarding the structural integrity of the subsurface [Anderson, 2010]. Two types of seismic waves travel through the subsurface as a result of near-surface impact: body waves and surface waves. When interpreting geophysical data, one must understand the difference between these two types of seismic waves.

P-waves and Shear waves are the two types of body waves. Each of these waves propagates three-dimensionally into the subsurface as it is generated. P-waves travel faster than Shear waves and disturb the medium through which they travel by

compressing and extending the particles in the solid. P-waves occur as vibrations parallel to the travel direction of the wave energy. Conversely, Shear waves are body waves in which the disturbance is an elastic deformation perpendicular to the direction of motion of the wave. The Shear waves that are generated from the source radiate spherically outward forming alternating compressions and rarefactions [Anderson, 2010].

When seismic waves are generated at or near the earth's surface, surface waves are also generated. These waves propagate radially in two dimensions away from the source. Surface wave particle motion is confined essentially to the earth-air interface, so the shallow subsurface can be interpreted by analyzing surface waves. One type of surface wave generated is referred to as a Rayleigh wave. These waves are frequently used in non destructive testing (NDT) for detecting anomalies in the Earth's subsurface because they generally have high frequencies [Rayleigh Wave, 2010].

The frequencies of seismic waves travel through the subsurface at different speeds depending on the density of the material through which they are propagating. The speed of waves in the Earth typically increases with depth from the surface due to consolidation. The low frequency waves typically travel faster than the high frequency waves at the greatest depths. Similarly, intermediate frequencies involve particle motions at intermediate frequencies and depths. The highest frequencies travel slowest at the shallowest depths [Rayleigh Wave, 2010]. Geophysical equipment and software records the frequency and the travel time of seismic waves traveling through the subsurface and can thus relate the frequencies recorded to a depth [Anderson, 2010]. Ultimately, the seismic wave velocities with their associated frequencies can be transformed into a tomographic image of the subsurface, profiling depth vs. seismic wave velocity.

Rayleigh waves have unique properties that allow them to be transformed into near-surface Shear wave velocity profiles [Surf-Seis, 2006]. The speed of Rayleigh waves is mostly a function of the Shear wave velocity of the medium through which they are propagating [Rayleigh Wave, 2010], thus engineers transform Rayleigh wave phase velocities into Shear wave velocity profiles of the subsurface with simple conversion calculations.

2.5.2. Surface Wave Applications. Rayleigh waves in the ultrasonic frequency range are used in NDT applications to help find cracks and other imperfections in materials. There are many applications of surface waves in geophysical engineering. However, to determine the structural integrity of the subsurface material, it is only necessary to discuss how engineers have used surface waves to generate Shear wave velocity profiles. This is done by inverting Rayleigh wave phase velocity to generate corresponding Shear wave data of the desired region.

During the data acquisition phase, a seismic source is applied onto the earth's surface, and energy in the form of Rayleigh waves travels along the surface of the earth. Seismographs connected to geophones coupled to the earth's surface record the magnitude and arrival time of surface wave energy. Associated geophysical software converts the recorded information into images (shot gathers) which can then be converted into a dispersion curve. This curve maps the Rayleigh wave phase velocity as compared to its frequency. Rayleigh wave phase velocities are a function of both the Shear wave and the Compression wave velocities of the subsurface. The inter-relationships between Rayleigh wave velocities (V_R), Shear wave velocities (β), and Compression wave velocities (α) in a uniform medium are expressed in Equation 2.1 [Anderson, 2010]:

$$V_R^6 - 8\beta^2 V_R^4 + (24 - 16\beta^2/\alpha^2)\beta^4 V_R^2 + 16(\beta^2/\alpha^2 - 1)\beta^6 = 0 \qquad \text{Equation 2.1.}$$

Equation 2.1 might initially suggest that it would be difficult to extract Shear wave velocity because the equation contains two unknowns (Shear and Compression wave velocities). Fortunately, this is not the case because Rayleigh wave phase velocities are influenced much less by changes in Compression wave velocity than by changes in Shear wave velocity. Rayleigh wave velocity (V_R) and Shear wave velocity (β**)** in a uniform medium are related by Equation 2.2 [Anderson, 2010]:

$$\beta = V_R/C \qquad \text{Equation 2.2.}$$

The variable C is a constant that changes slightly depending on the Poisson's ratio of the material through which the seismic waves travel. Even in extreme variations of Poisson's ratio, C only ranges from 0.874 to 0.955 [Anderson, 2010]. If a value for C is assumed, and the frequencies with their respective surface wave velocities are recorded, then a Shear wave velocity profile can be developed through analysis, and a velocity image of the subsurface can be generated [Anderson, 2010].

2.6. MULTICHANNEL ANALYSIS OF SURFACE WAVES

Multichannel Analysis of Surface Waves (MASW) is a relatively new geophysical method that was introduced to the industry by the Kansas Geological Survey at the turn of this century. It applies the relationship between surface waves and Shear waves as explained above to ultimately generate a Shear wave velocity profile of the subsurface. It has been commonly applied in mining exploration to determine the depths and thicknesses of the geological strata at a potential mine site. It may also be applied on much smaller scales in the transportation industry to identify damaged areas on asphalt or concrete pavements with high resolution [Anderson, 2010]. A very similar method, Spectral Analysis of Surface Waves (SASW), has been employed by geophysicists for some time, but the MASW method has surpassed its counterpart by giving increasingly more accurate, and detailed information. While SASW collects data using two detector units, the MASW method uses an array of 24 geophones to collect data. This array gives geophysicists a more readily interpretable image of the subsurface [Anderson, 2010]. Three types of MASW methods exist: Active, Passive Remote, and Passive Roadside. Each type of method has its advantages and limitations, but the general idea of all three is the same [Surf-Seis, 2006]. The two passive methods utilize surface waves generated from cultural (and natural) activities (e.g., traffic, thunder, tidal motion, atmospheric pressure changes, etc.). The active method (Figure 2.8) is the most common type of MASW method. It is the conventional mode of survey using a sledge hammer, a dropping weight, and in some instances a small explosive detonation on the surface to generate an active seismic source that will gather field data [Surf-Seis, 2006]. This project uses the general layout scheme of the active method and the report discusses only its specifics.

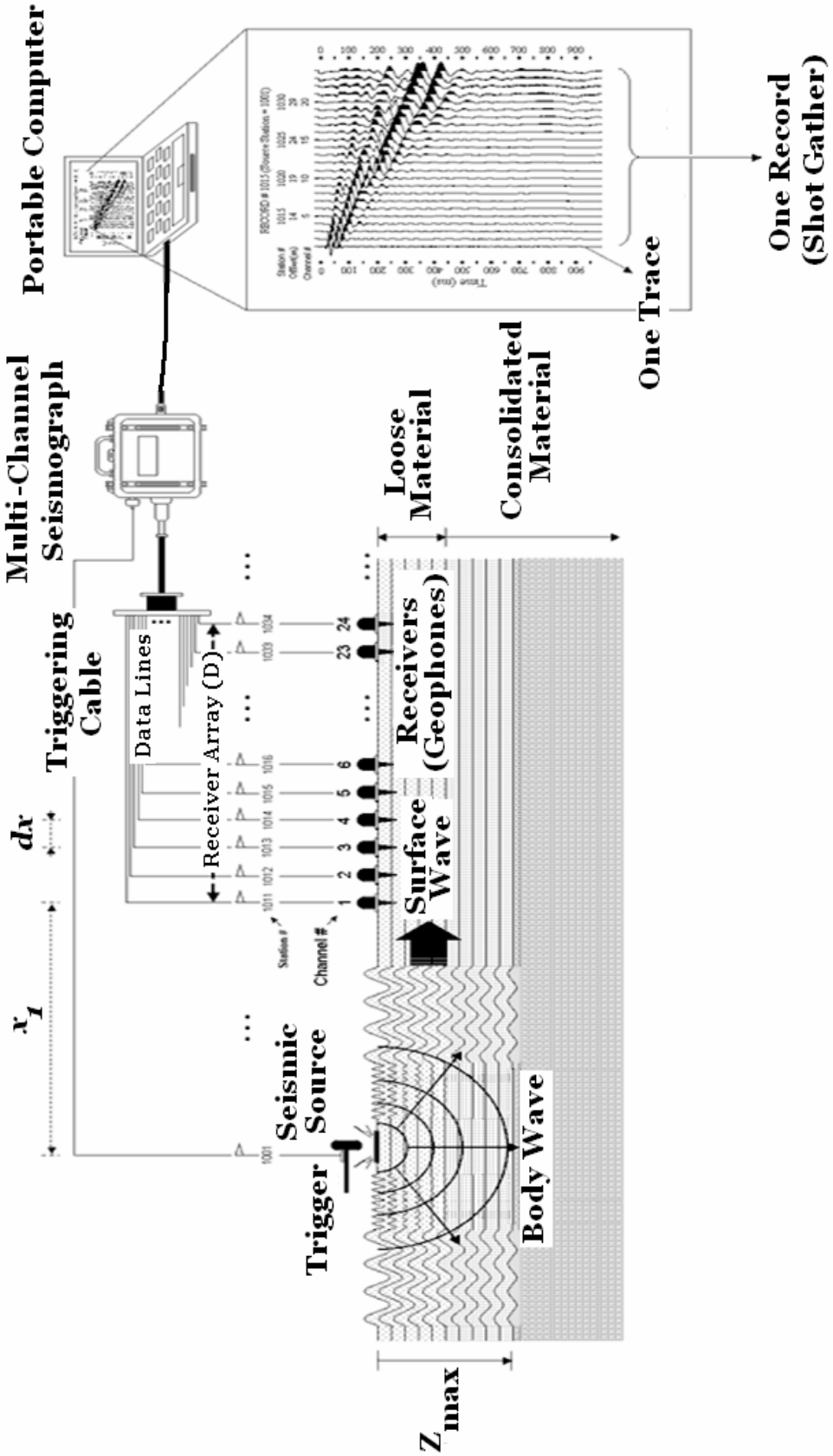

Figure 2.8: Active MASW method [Surf-Seis, 2006].

2.6.1. MASW Equipment. Typical seismic acquisition systems consist of the following components:

- *Seismic Source* -- This is nothing more than an apparatus for delivering seismic energy into the ground. When conducting the survey on soft ground, a metallic or rubber impact plate is recommended to help the source impact point become less intrusive into soil. However if conducting the survey on stone ground, this is not needed. Sources can vary greatly in their size and complexity. All, however, share the following characteristics:
    - They must be repeatable. That is, the nature of the energy delivered into the ground (its amount and the time duration over which it is delivered) should not change as the source is used in different locations. Also, the source should be able to generate a vibration in the ground that will be able to be recorded by the resonant frequency of the chosen geophones.
    - Time of delivery of the source must be controllable. Because first time arrivals of the surface waves are being recorded, the engineer must be able to tell exactly when the source delivered its energy into the ground ("time zero"). In some cases, the time of delivery must be recorded manually by the field technician. In others, an instrument records the time the source delivered its energy. This is typically controlled by a lap top computer equipped with the appropriate software [Surf-Seis, 2006].
- *Geophones* -- These are devices capable of measuring ground motion generated by the seismic source. These typically convert the ground motion into electrical signals (voltages) that are recorded by a separate device. Through research, low-frequency (e.g., 4.5 Hz) geophones have proven to give the most accurate data and are used when mapping to very deep zones (10-30 meters (30'-100')). The effectiveness of somewhat higher-frequency phones (e.g., 100 Hz), however, is often comparable to that of much lower-frequency ones and are recommended especially if one is acquiring information about the shallow subsurface (1-6 meters (3'-20')). Hence, the resonant frequency of the chosen geophones depends on what depth the field study is attempting to map. Vertical (instead of

horizontal) phones must be used to acquire accurate data. This means that the geophone must be placed vertically relative to the surface on which the source is discharged. The Kansas Geological Survey recommends using spike-coupled geophones because they generally obtain the highest sensitivity in typical active MASW field geometries [Surf-Seis, 2006].

- *Recording System* -- This consists of a number of components. In essence, this entire system does nothing more than record the ground motion detected by the array of geophones and stores the resulting data. In addition to recording ground motion, this system must also control the synchronization of the source. It consists of not only the seismograph to store information but also numerous electrical connections to the geophones, and usually a device to select subsets of the installed geophones to record [Surf-Seis, 2006].

2.6.2. MASW Field Geometry. Similar to the type of equipment chosen, how the instrumentation is set up during a field study depends on the application and the data one is attempting to obtain from the study.

The maximum depth of investigation that can be achieved is usually in the 10-30 meters (30'-100') range, but this can vary with sites, equipment set-up parameters, and types of active sources used. Field procedures and data processing steps are briefly explained below [Surf-Seis, 2006].

The length of the receiver spread (D) in Figure 2.8 is commonly referred to as the array. The array (Equation 2.3 [Surf-Seis, 2006]) is directly related to the longest wavelength (λ_{MAX}) that can be confidently analyzed, which in turn determines the maximum depth of investigation (z_{MAX}):

$$D = \lambda_{MAX} = z_{MAX} \qquad \text{Equation 2.3.}$$

In practice, the maximum depth of investigation in an active survey is usually limited by the seismic source as it is the most influential factor. On the other hand, the minimum receiver spacing (dx) is given in Equation 2.4 [Surf-Seis, 2006]. It is related to the shortest wavelength (λ_{MIN}) and therefore the shallowest resolvable depth of investigation (z_{MIN}):

$$dx = \lambda_{MIN} = z_{MIN} \qquad \text{Equation 2.4.}$$

The source offset (x_1) controls the degree of contamination by the near-field effects. Equation 2.5 [Surf-Seis, 2006] suggests it to be a value of about 20% of D:

$$x_1 = 0.2D \qquad \text{Equation 2.5.}$$

It is imperative to record clear and concise field notes when conducting these surveys. When the shot gathers are taken back to the laboratory for analysis, the software requires the interpreter to supply the source offset location and distance away from the array as well as the geophone spacing used in the field geometry. Without precise information, the final velocity profiles will be incorrect and meaningless.

2.6.3. Three Steps of MASW Process. The entire procedure for MASW usually consists of three steps (Figure 2.9) [Surf-Seis, 2006]: First the engineer must acquire multichannel records (shot gathers). These records are then taken back to the lab and the fundamental-mode dispersion curves are extracted. These curves represent the surface wave phase velocity of the shot gather versus the frequency generated from the impact source. Finally, these curves are inverted to obtain two-dimensional profiles of the Shear wave velocity related to depth.

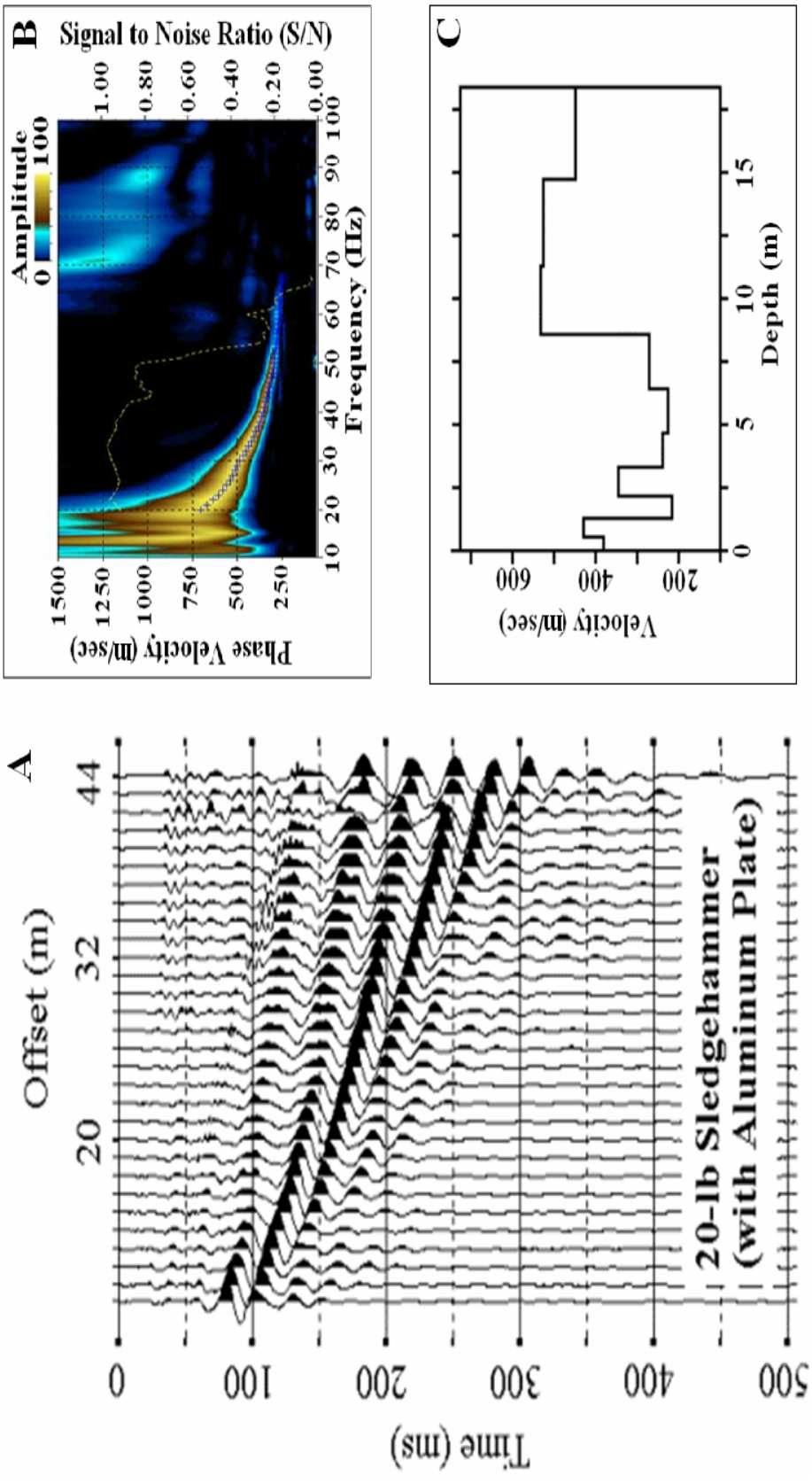

Figure 2.9: Three steps in the MASW process [Surf-Seis, 2006]: A) One shot gather record generates B) one dispersion curve, which in turn generates C) one velocity profile.

2.6.4. Velocity Profile Processing. The MASW geophysical method and its analytical computer software, Surf-Seis (Version 2.05), were developed by the Kansas Geological Survey. Surf-Seis automatically interprets shot gathers collected by the active MASW method to develop a dispersion curve and a velocity profile related to each field log [Surf-Seis, 2006]. It is relatively simple software and displays results that are easily interpreted by the engineer. To project a Shear wave velocity profile from the uploaded shot gathers, the engineer must input the field parameters used into the program. Depending on these parameters and the first arrival times of the Rayleigh waves, a dispersion curve is then generated that maps the surface wave phase velocity versus associated frequencies created from the impact source. The extraction of dispersion data from field-recorded Rayleigh wave data is a standard, established mathematical process that does not require any interactive input from the interpreter [Anderson, 2010]. The analysis of the output dispersion data and the selection of optimum phase velocities, in contrast, requires qualitative input from the interpreter. Hence, there is potential for human error [Anderson, 2010]. To minimize this potential, the interpreter must be experienced with the MASW method and record accurate field notes.

The selection of optimum phase velocities from dispersion data is usually straightforward if good quality Rayleigh wave data are acquired in the field. Dispersion data should be characterized by a narrow, well-defined peak. In this case, the interpreter merely selects phase velocities that fall along the well defined peak [Anderson, 2010]. Figure 2.10 shows three phase velocity placements on a quality dispersion curve. Figure 2.10.B shows phase velocities that were properly chosen along the smooth defined peak while 2.10.A and 2.10.C show points that have been misplaced.

It is imperative for the interpreter to correctly place the chosen points so phase velocities correspond to the correct frequencies and in turn display an accurate velocity profile. Different frequencies travel through the depths of the subsurface at different speeds. When points are chosen on the dispersion curve, the software associates a phase velocity with a specific depth. Each depth interval is then assigned an average velocity as it is plotted on the profile [Anderson, 2010].

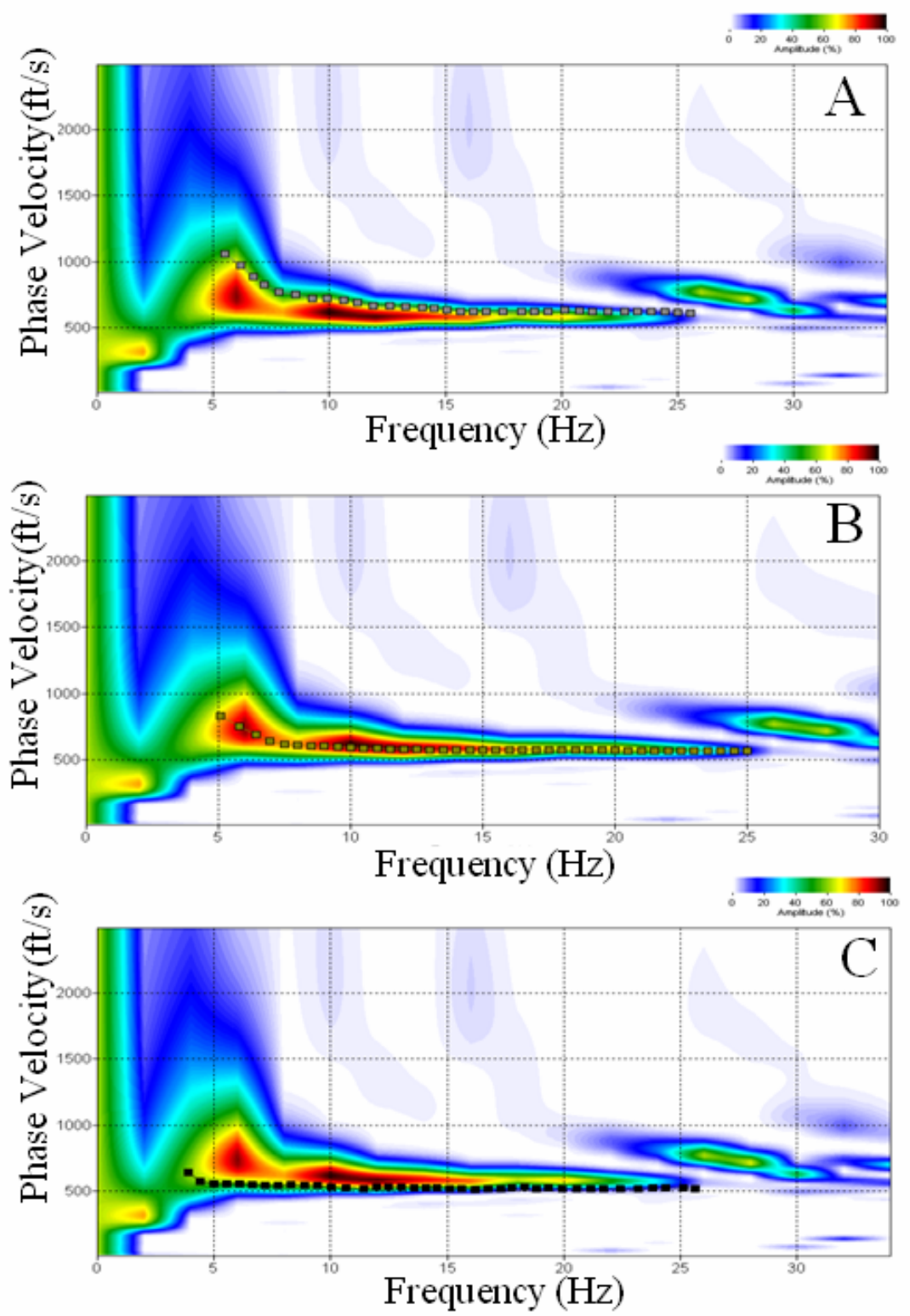

Figure 2.10: Chosen phase velocity placements along the dispersion curve: A) Misplaced points; B) correctly placed points; C) misplaced points [Anderson, 2010].

Shear wave velocity is the dominant parameter influencing changes in Rayleigh wave phase velocity. For the purposes of inversion, Poisson's ratio and therefore the constant C in Equation 2.2 can be assumed. Surf-Seis (Version 2.05) is the software package that the Missouri University of Science and Technology utilizes with their MASW equipment to generate velocity profiles of the subsurface. Surf-Seis presets the value of C to be 0.88. Based on multiple modeling studies using realistic Compression and Shear wave velocities, the Kansas Geological Survey confirmed that this assumption introduces minimal error (generally <3%) into the output Shear wave velocity data [Anderson, 2010].

2.6.5. MASW Limitations. Soft, flat ground is best to set the MASW instrumentation up on because it allows the geophones to have a strong coupling to the soil without unnecessary anomalies present in the topography of the region (Figure 2.11). Uneven surfaces act as potential planes for the Rayleigh waves to reflect off of and cause errors in the data readouts that is referred to as "noise." Any surface relief whose dimension is greater than 10% of the receiver-spread length will cause a significant hindrance to surface wave generation [Surf-Seis, 2006].

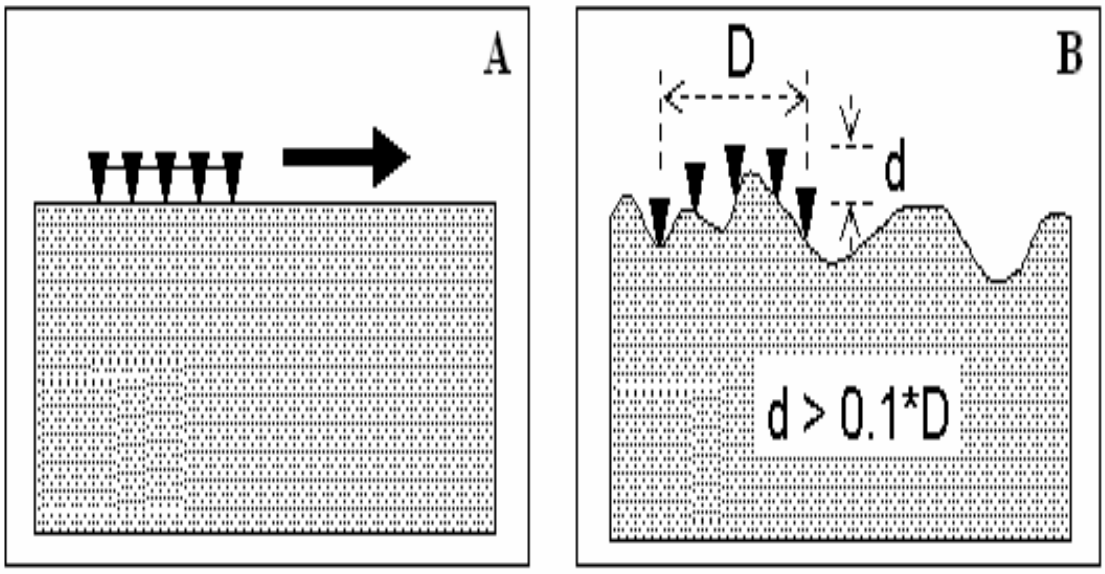

Figure 2.11: Flat or gentle slopes are preferable for active MASW. Topography can interfere with surface wave propagation: A) flat; B) uneven ground [Surf-Seis, 2006].

Surface waves generated by natural or cultural sources outside the intended impact can skew the shot gathers acquired in the field (Figure 2.12). If performing the test in a quarry, it is best to do so in areas where there is no operating machinery that will add "noise" to the acquired data. If possible, one must make the proper accommodations to eliminate all outside sources of "noise" at the test site before acquiring data.

Some of the waves generated by intended or outside sources are reflected and scattered as they encounter shallow and surface objects (e.g., building foundations, culverts, ditches, boulders, and so forth) and become "noise." In the mining industry one must pay close attention to the natural geology in the region where the instrumentation is being set up. Clay seams, voids, or large joint sets and fractures in the subsurface will act as a plane for wave reflection and scattering [Anderson, 2010].

In addition to surface waves, P-waves are generated from impact sources as well. These waves travel faster than surface waves and will be seen at the top of the shot gather above the surface waves. The P-waves are also sources of "noise" when interpreting MASW data and must be removed from the shot gather to generate a velocity profile that will be easy to interpret [Anderson, 2010].

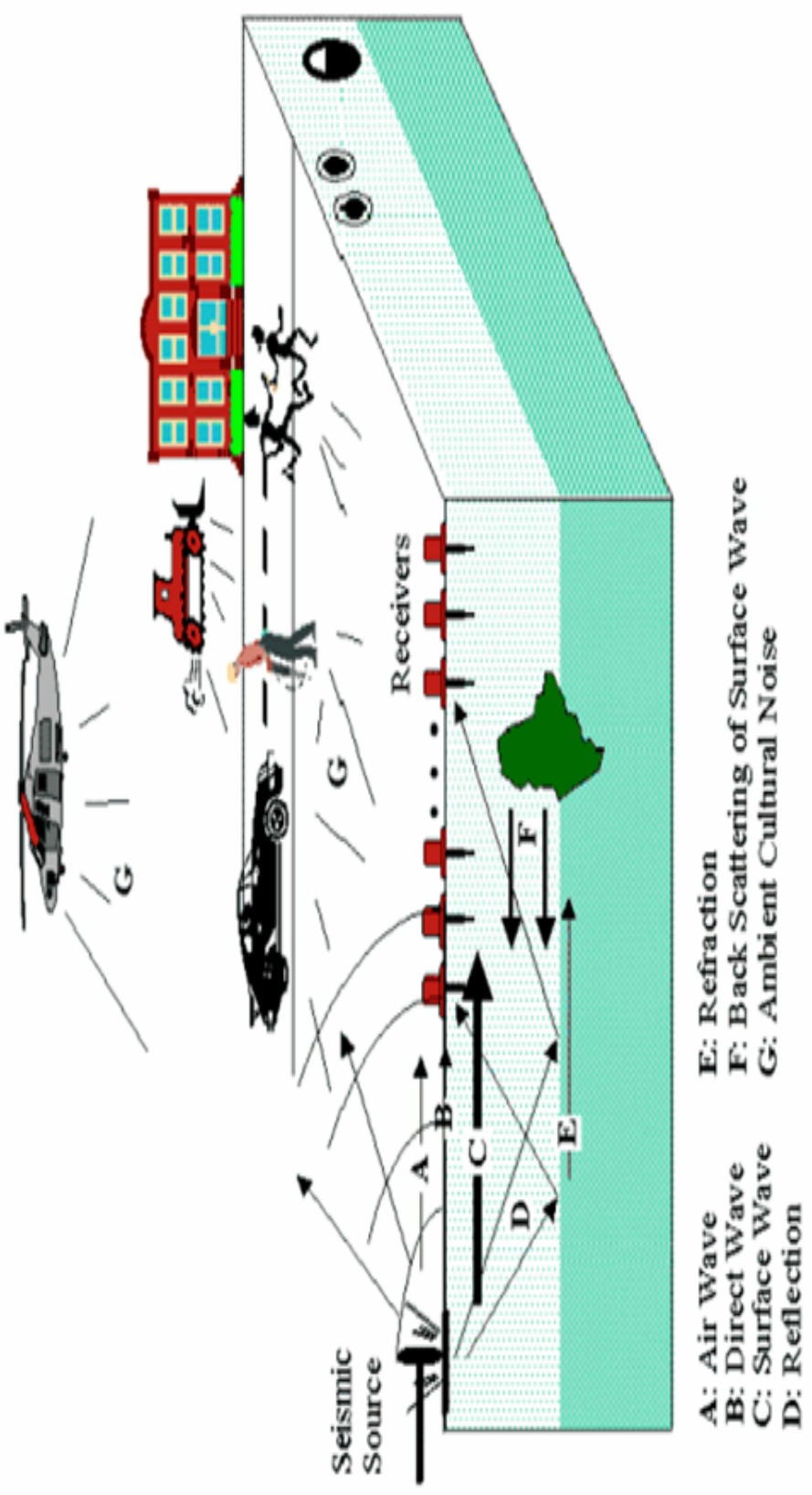

Figure 2.12: Potential outside sources of "noise" during an MASW field test [Surf-Seis, 2006].

3. PROBLEM STATEMENT

Mining Engineers have applied tomographic imaging to identify stress distribution, consolidation, rock integrity and strength, and to monitor damage or disturbance that has resulted from different rock excavation techniques. Blast Induced Rock Damage (BID) contributes to a redistribution of stresses within stone such that the rock mass weakens from resultant blasting fractures. Advances in geophysical sciences provide an opportunity for NDT methods to be researched in an attempt to attain the BID data more efficiently. The MASW geophysical method has many NDT applications in the construction, transportation, and mining exploration industries. It is a simple process that generates tomographic images of the subsurface that are easily interpreted by the engineer. However, MASW has not been applied to monitor and quantify BID produced from pre-split shots that are commonly used to create safe high-wall working conditions in surface mines or to produce saleable loaves at dimension stone quarries.

The goal of pre-splitting at a dimension stone quarry is to split stone and separate it from the rest of the deposit while preserving the structural integrity of the loaf extracted as well as the rock mass left behind. Pre-split design requires explosives that fire nearly simultaneously. Simultaneous initiation requires explosives that possess a high velocity of detonation and create high pressures within the borehole during shot-firing. BID is caused by the impulsive release of energy and pressure that explosives produce. Advances in explosive manufacturing provide the ability to reduce the detonation velocity of the primary explosive (detonating cord) that is commonly used in pre-splitting, so the pressure within the borehole will be reduced as well.

This experiment was divided into two phases. The author performed 19 pre-split shots in an isolated portion of a sandstone dimension stone quarry in phase 1 of the experiment using a detonating cord with a low velocity of detonation fired in sand-filled boreholes. Phase 2 included 20 pre-split shots which gathered information on blasts that used a cord with a high velocity of detonation also fired in sand-filled boreholes. Previous research discussed in the Review of the Literature (see Sections 2.2 and 2.3) indicated that using cord with a lower velocity of detonation in pre-splitting will yield less BID than a cord with a high velocity of detonation. The author used the MASW

method to gather Shear wave velocity data on a sandstone deposit before and after a pre-split shot. The decrease in the Shear wave velocity provided information on the BID caused by the two strengths of 8 grams/meter (40 grains/foot) detonating cord used in this experiment.

The main objective of this research experiment was to determine whether or not the MASW geophysical method could be applied to monitor the damage that explosives used in pre-splitting induce on the remaining stone. The tomographic data generated from the MASW software would also quantify the damage at specific depth intervals into the rock mass from the borehole locations where the explosives were placed. Secondly, the author wanted to confirm the previous research to determine that less BID is produced from low velocity detonating cord as compared to high velocity detonating cord.

3.1. HYPOTHESIS

Cold Springs Granite Dimension Stone Quarry determined an optimal blast design by comparing the blast pressures induced from HV and LV detonating cord through different coupling medias (see Sections 2.2 and 2.3). The studies conducted by Cold Springs indicate that a low velocity of detonation fired in sand-filled boreholes produce the best results with very little BID. The author believed that a similar outcome would result when performing both HV and LV pre-split shots in a sandstone dimension stone quarry.

The MASW method measures the seismic wave velocities that travel through rock to determine consolidation as a function of depth. Likewise, this measurement shows the structural integrity of the stone before any one event compromises its strength. These waves recorded before a blast, compared to waves recorded after a blast, would determine the extent of the BID. The author believed that the MASW geophysical method would show slight decreases in the Shear wave velocity at shallow depths within the sandstone deposit, indicative of BID.

3.2. APPLICATION/IMPORTANCE OF INVESTIGATION

Dimension stone quarrying requires its blast design to have a limited amount of perpendicular damage to the finished cut line. This is critical to the economic recovery of saleable stone. Smooth-wall blasting is performed in surface and underground quarries as well as in construction to create safe high walls, portal entries, tunnels, and pillar supports. Large rock sculptures such as Crazy Horse and Mount Rushmore, require the remaining rock to be unharmed as well. The Explosive Engineers at these mountains are most concerned with preserving the structural integrity of the stone that is left behind after each blast. In order for the sculpture to be successful, preserved, and able to effectively support itself, careful drilling must take place prior to every engineered blast. All of these applications demand that the rock being blasted as well as the rock mass left behind remain competent and that it keeps its structural integrity. Careful control of the blast is vital. Overshooting, bad designs, excessive borehole pressures, and delay scatter could potentially ruin several thousand tons of saleable product and/or create unsafe working conditions.

If the research performed proves that the MASW method may be applied to monitor and quantify BID at pre-splitting operations, the Explosive Engineers will then be able to take this information to correctly design their blasts. The MASW method should not be used on every blast. Rather the engineers may gather BID data in different geological conditions and from different blast designs to then apply the correct blast parameters in similar geologic conditions once the engineers have determined which designs produce a minimum amount of BID. Through this research, the author intended to determine whether the MASW geophysical method can be applied on a large scale in surface mining by quantifying the amount of BID that is produced from typical pre-split applications and comparing this BID to mine requirements for saleable product, loaf production, rock mass competency, and high-wall stability.

4. GEOLOGY OF THE EXPERIMENTAL LOCATION

The experimental location for this project was the DiPardo Sandstone Quarry. It is approximately 227 meters north of the Maramec Spring Geological Quadrant in Rosati, Missouri (Figure 4.1). Approximately 290 meters (950') above sea level, the operating quarry consists primarily of the Roubidoux Formation. This quarry is located South of interstate Highway 44, on County Road 3630. This is a unique dimension stone quarry. It is owned and operated primarily by one man, Jim DiPardo. Though the quarry originally started producing dimension stone in the 1960s it had ceased to be in operation until when DiPardo purchased the land and reopened it for production in 1983. For the most part, he is the sole employee, although when big jobs come along he may have as many as six people working part time.

Once common in the building trades, sandstone fell out of favor over the years. This may reflect a common trait in sandstone; it can be very friable, making it considerably less resistant to weathering and unable to support substantial loads. However, the opposite can also be true. In the right conditions, well-cemented sandstone can be very strong and is ideal material for buildings and paving roads.

The sandstone at the DiPardo quarry varies in strength and nature within very short distances. The overburden stone tends to be very weathered and friable. However, the deeper deposits show an increase in strength, and therefore DiPardo must separate each piece of stone according to his customers' demands. He has tests performed on the stone to make sure it will hold up under a variety of uses. He mainly interacts with architects, builders, and homeowners (Figure 4.2).

4.1. LOCAL GEOLOGY

The author researched three of Missouri's Geological Quadrangles to understand the depositional origin, stratigraphy, lithology, structure, and mineralization of the regional geology and its specifics are discussed in Appendix H. In the 1980s, when DiPardo restarted production at Rosati Sandstone Quarry, he had the Missouri Division

of Geology and Land Survey make a geological assessment of his land. Several formations of the Paleozoic era are deposited in the surrounding areas (including the Ordovician age Gasconade, Roubidoux, and Jefferson City Formations, as well as the Pennsylvanian age Formation), but the assessment's results show that the dimension stone quarry consists completely of Roubidoux sandstone. In light of this information, the author researched the Roubidoux Formation more extensively and its characteristics have been solely considered throughout the project.

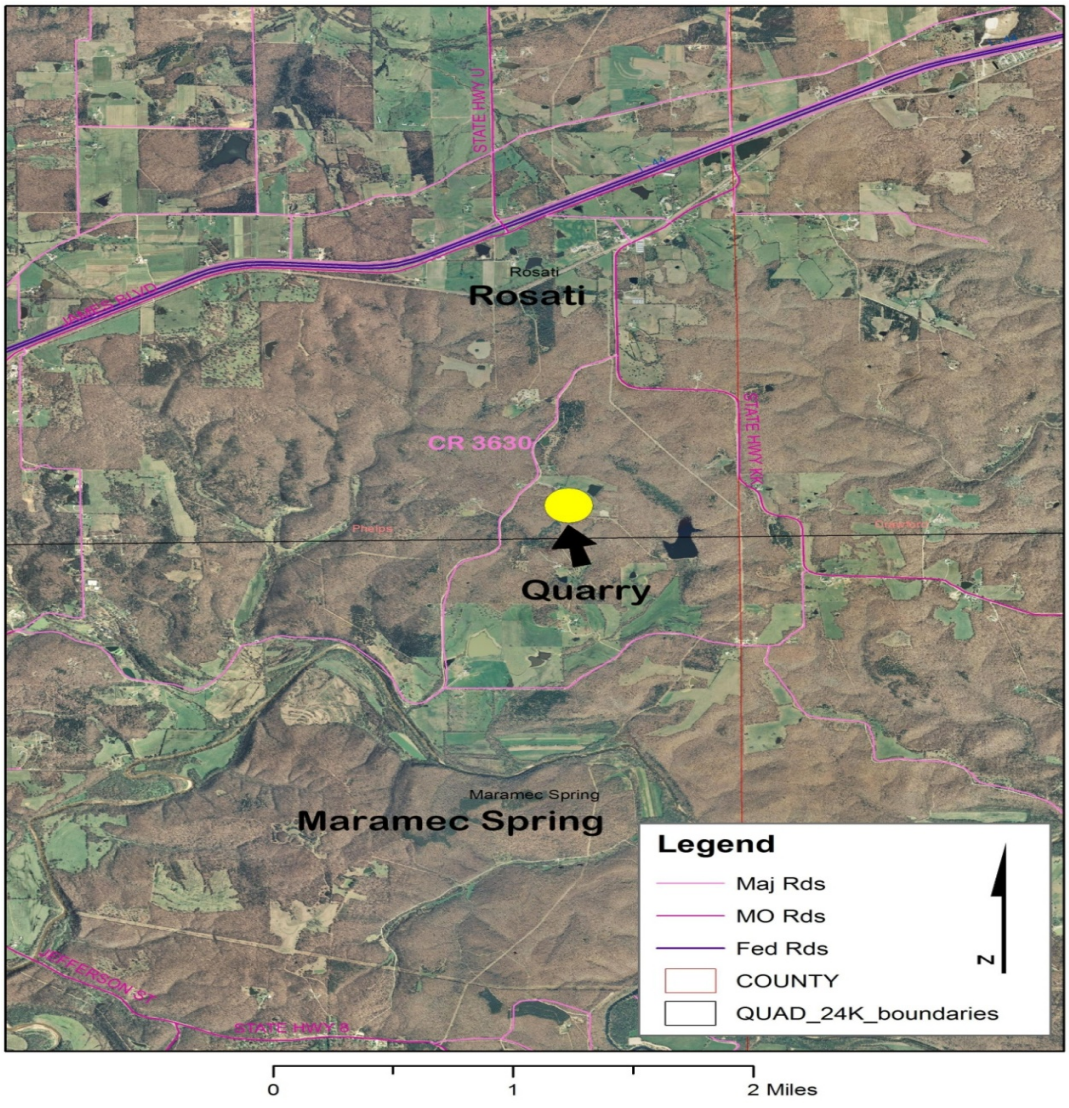

Figure 4.1: Aerial map of the DiPardo Sandstone Quarry location [Proctor, 1993].

Figure 4.2: Typical structures that the stone produced from DiPardo Quarry is used for. A) Ripple marked planar slabs on the exterior of a small house. B) A welcoming gate in Rolla, MO.

The Roubidoux sandstone at the quarry is ideal for producing competent architectural dimension stone. The stone extends approximately 30 meters (100') below the bottom of the quarry pit with almost no evidence of interlaying beds of chert, shale, clay, or dolomite. The mining progress shows this very well. Approximately 10 meters (30') has been excavated to date. The high-walls that resulted from DiPardo's mining sequence show a cross section of the upper geology in the quarry (Figure 4.3). Sandstones of the Roubidoux Formation are prevalent throughout as one massive deposit with many horizontal bedding planes and evidence of weathering.

Figure 4.3: The high-wall produced by DiPardo's excavation methods shows a cross section of the sandstone being mined at the quarry.

4.1.1. Natural Seams, Bedding Planes, and Fractures. Sandstone deposits characteristically possess definite horizontal bedding planes and vertical seams. Unlike massive deposits such as granite, marble or limestone, the extent to which the sand grains in sandstone deposits are cemented together is much less, and this allows sandstone's

bedding planes to cleanly break free from the rest of the rock mass when the stone is being mined. It is because of this that DiPardo has been able to produce stone effectively for more than 20 years without the use of explosives.

Very little blasting has been performed at the Rosati quarry. DiPardo hired contract blasters in the past, but he has harvested most of the stone himself using “feathers and wedges” and a “darter-splitter.” DiPardo carefully examines each rock and then drills holes on natural seams, bedding planes or fractures with an air drill. The “darter-splitter” is a hydraulic splitter that is inserted in the hole and used to "bump" the rock into 3-to-4-ton blocks. Though this method is reliable, the split created with this method can be very unpredictable. The cracks that propagate from the wedging method follow the natural split by going to areas that are least resistant to stress. This commonly creates dimension stone that is awkward in size and shape, unlike the blocks of stone that can be produced from drilling and blasting.

The dimension stone that DiPardo typically markets ranges from 1-3 cubic meters (2-6 tons). Any stone produced larger than this is not manageable for the excavation equipment that he owns and has to be broken into smaller pieces before moving it. Anything smaller has limited use and often it is considered waste.

Because of the desired size of blocks, the natural seams and bedding planes were incorporated into the blast design for this research project, in order to achieve the product and to mine safely. The seams and bedding planes acted as natural pre-splits, and during the shot, the stone would mostly break perfectly along these lines in addition to splitting along the designed row of drill holes (Figure 4.4). The proper application of blasting design greatly increased the efficiency and productivity of this quarry by allowing the area to be safely mined in a series of benches with reduced waste, by harvesting stone of appropriate shape and size for DiPardo to market as product.

Natural seams and fractures could also cause the pre-split to propagate away from its intended path. The gas pressure escaped to the natural joints and fractures during the blast, and as a result, the rock split in the direction of jointed and fractured areas in

addition to the line of drilled holes. This caused some of the stone produced from some shots to be small and in most cases had to be disregarded (Figure 4.5).

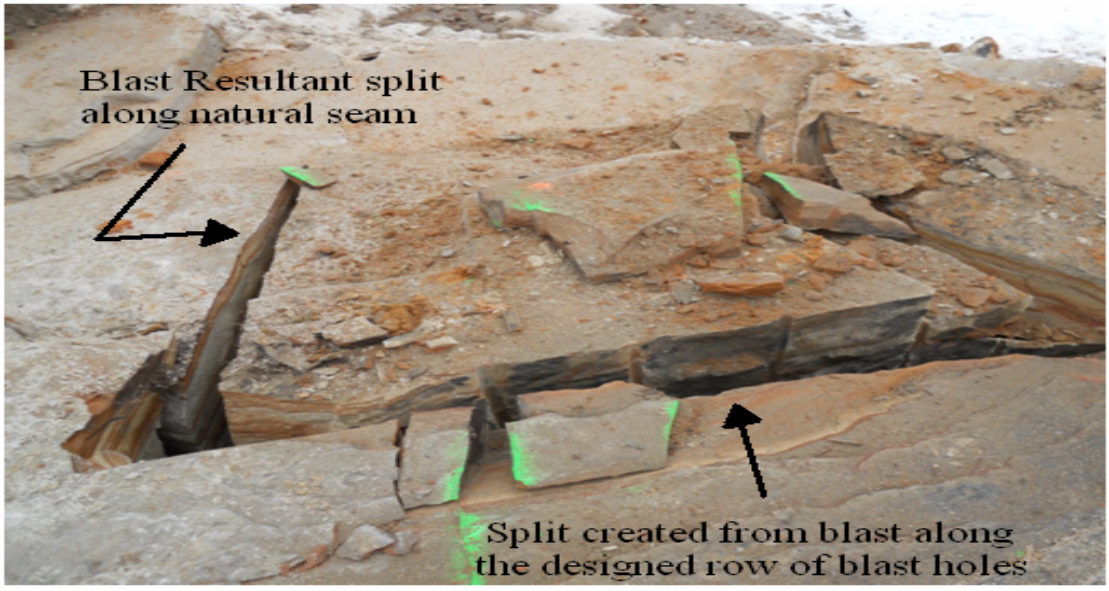

Figure 4.4: Seams and bedding planes acted as natural pre-splits. During the shots, the stone broke along these lines in addition to splitting along the row of drill holes.

Figure 4.5: Fractures present in the shot area caused some of the stone to break into small rocks during the blast and had to be regarded as waste.

In twenty years of operation, DiPardo has never applied blasting applications at his quarry by himself, but on several occasions he had a crew of blasters extract small portions of the pit. The experimental location was directly adjacent to a portion of the pit that DiPardo contracted out to a local drill and blasting company. The blast designs that were used by the contract company are unknown, but evidence remains on the high-walls from drill marks and radial fracturing that was produced from the shots (Figure 4.6). It appears that the boreholes were overloaded due to the excessive amount of radial fracturing surrounding the drill holes. In addition, one drill hole was practically in contact with the experimental section in the north end of the pit. The north end of the experimental location was very fractured at every level during the project's mining sequence (Figure 4.7).

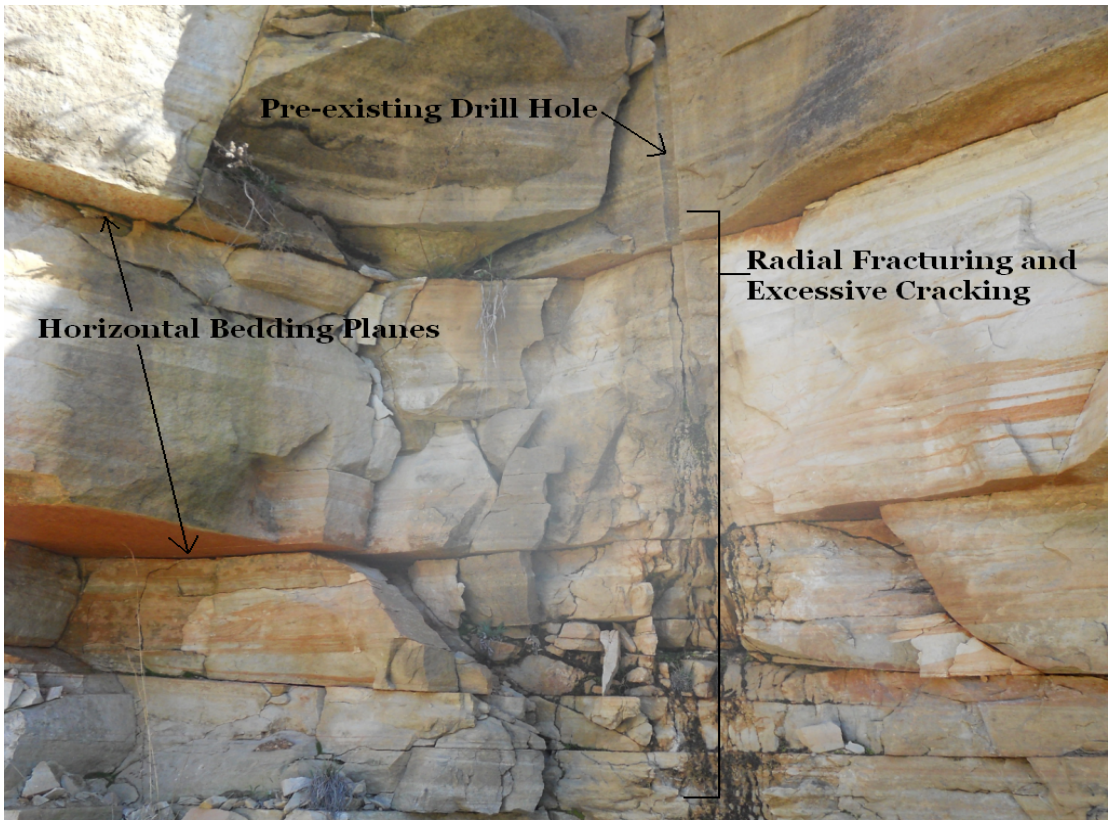

Figure 4.6: The drill hole markings are evidence of former blasting operations. Radial fracturing and excessive cracking surround the drill holes where the charge was placed.

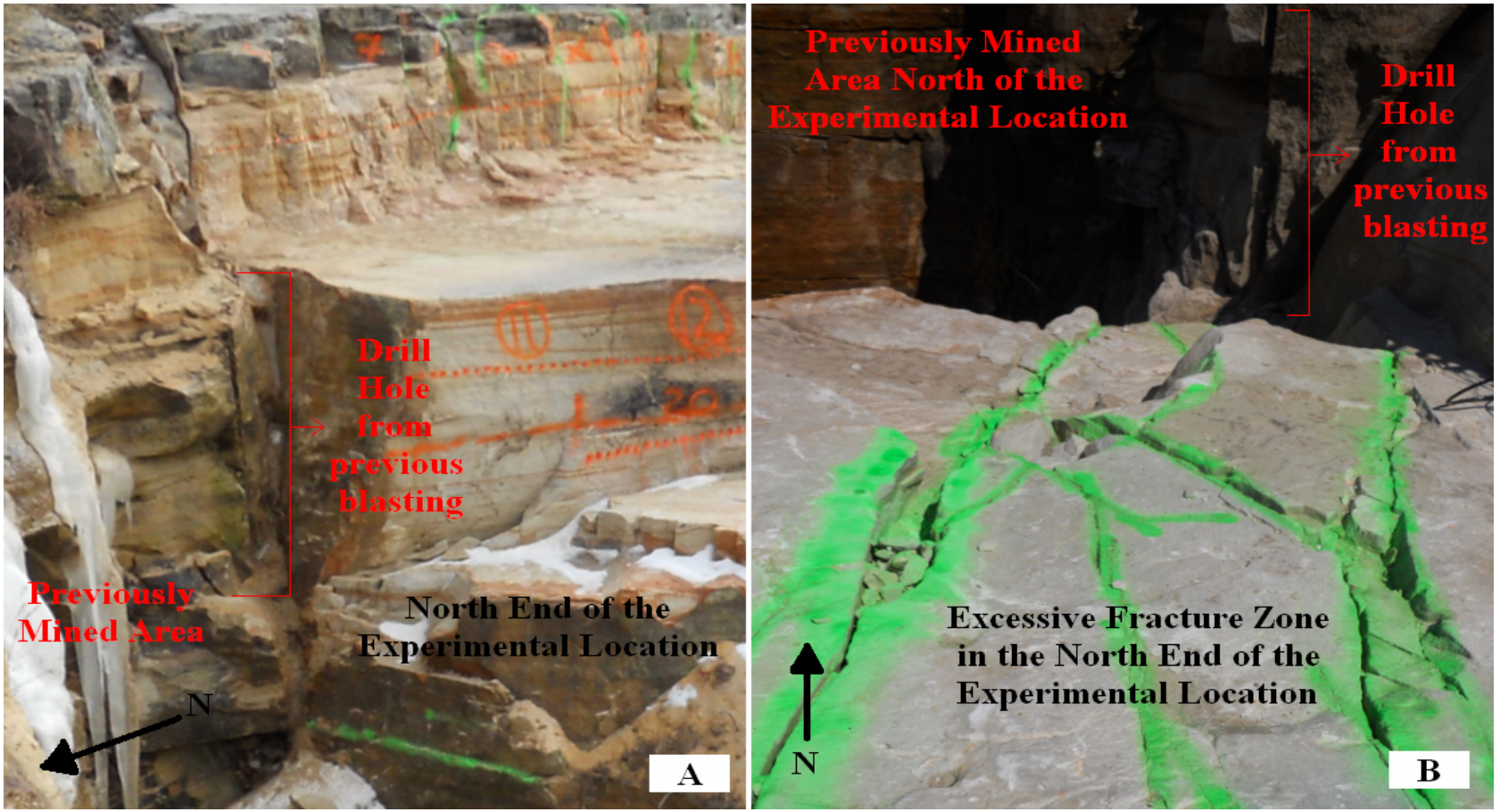

Figure 4.7: Previous blasting operations resulted in excessive fractures in the north end of the experimental location: A) Photo taken from the most northern end of the quarry, above the experimental location; B) photo taken on the third bench created in this project.

4.1.2. Virgin Deposit. To best control the data being gathered, the tests needed to be completed in a virgin deposit – an area of the pit that had not been used as a production zone before. Had explosives been used directly on the site location in the past, there would have been a chance that radial fracturing damaged the deposit (as the example in Figure 4.6 shows) to an unknown depth. In addition, because any previous implemented design and techniques that were used are not exactly the same as those that were being tested, an extra variable would be introduced to the experiment and the produced data would not be as accurate or meaningful. This type of variation could not be controlled, and an attempt to make sense of the data would potentially be difficult.

Fortunately the experimental location was a virgin deposit. The location had never before been directly exposed to blasting or the other extraction methods that DiPardo used on a regular basis. However, severe fracturing was prevalent in the north section of the pit from an adjacent blast as was previously discussed. Nonetheless, the virgin deposit enabled the author to interpret and compare the data confidently because he was aware of the strength of the explosives and the blast design parameters that were implemented while blasting each shot area.

4.1.3. Weathered and Unweathered Sandstone. Because the experimental location was a virgin deposit, the top of the stone was exposed to constant weathering (Figure 4.8). Trees, shrubbery, grass and moss grew on top of the grayish surface of the sandstone mass. This is evidence that the seams and fractures are conduits for fluid flow and the weathered stone was prevalent within the first 2.13 meters (7') of the surface. Several series of blasts had to be completed before truly competent unweathered sandstone was completely uncovered. The unweathered stone is typically white with bands of orange and brown that comes from minerals in the soil such as iron and manganese. Sandstone is not homogeneous, but from samples one can determine how the region has changed slightly through short distances. To determine the elastic properties of the stone, the density was found by performing a submersion test of rock samples from each shot area. Two rock samples were taken from each shot location, and the average density was calculated from the results of submersion tests. The results of the submersion tests may be found in Appendix H. The density of the stone changed

slightly throughout the experimental test location, ranging from 2.05-2.58 grams per cubic centimeter.

Figure 4.8: A view of the experimental blast location prior to any shots or data gathering. The area was a virgin deposit and was exposed to constant weathering.

5. EXPERIMENTAL APPROACHES AND PROCEDURES

The main objective of this experiment was to determine whether or not the MASW geophysical method could be used to monitor and quantify the BID that is produced from pre-splitting applications by measuring the Shear wave velocity at specific shallow depth intervals into the stone from the split line. Secondly, the author wanted to confirm that an explosive with a lower velocity of detonation would yield less BID than an explosive with a higher velocity of detonation. To accomplish both of these goals, it was necessary for the author to follow a scientific method to obtain an adequate statistical sample on shots that were performed when using a low detonation velocity as well as on shots that were performed when using a high detonation velocity.

Due to the unique nature of the test site and the methods that were used in this project, the experimental approach and procedure had to be carefully prepared. Quality planning and maintained equipment ensured that proper blasting techniques were applied to create the desired product while generating a smooth wall that would give meaningful MASW data for all of the shots performed in the experiment. Also, to minimize variation in the process, the same procedure was followed for every blast and MASW set-up.

5.1. PRE-SPLIT APPROACH, BLAST CONSTANTS AND VARIABLES

Though the strength of the stone changed within short distances at the quarry, the rock being blasted was consistent in geologic deposition, lithology, and stratigraphy and this was originally considered to be a constant. The stemming used to confine the explosives within the borehole was also constant for every shot; sand was the chosen stemming material. The blast hole design parameters remained constant for all of the shots. The pre-split “rules of thumb” that were discussed in the Review of the Literature (see Table 2.1) were applied to the procedures.

Detonating cord is a common explosive used in pre-splitting due to its small charge weight and high velocity of detonation. However, a high velocity of detonation will yield high pressures in the borehole during the blast. This condition is the cause of

BID. Decreasing the pressure within in the hole during detonation will in turn decrease the BID. The variable in this project was the explosive used to create the split. Both detonating cords used in this project had nominal charge weights of 8 grams/meter (40 grains/foot) and they were made specifically for pre-splitting. However, Fire-line 8/40 HMX LS Ribbon is a cord that has a high velocity of detonation as it is manufactured to detonate at 7,500 m/s (24,600 fps) [Product Manual, 2005]. Prima-Shear 8 g/m was the second type of detonating cord used in this project. When this cord is manufactured, the normal explosive composition of detonating cord is mixed with other low strength and inert materials. This still allows for a high velocity of detonation when initiated but Prima-Shear detonates at 5,000 m/s (16,400 fps) [Product Manual, 2005].

This project included two phases of pre-split shots performed at DiPardo's sandstone dimension stone quarry. As such, 19 separate shots were conducted in Phase 1 of the experiment using Prima-Shear (LV cord) while 20 shots were conducted in Phase 2 of the experiment when using Fire-line (HV cord) as the explosive.

5.1.1. High Speed Photography of Detonation Velocity. The given velocities of the cords (HV cord – 7,500 m/s, LV cord – 5,000 m/s) were obtained from technical consultants that work for the manufacturer, Dyno Nobel. However, a number of potential variations present during the manufacturing process could have changed the velocity of detonation, none of which the author had control over. To ensure that the detonating cord selected met its specifications, the author checked these given velocities by performing high speed photography tests of each lot of detonating cord that was used in the project.

The Phantom V5.1 high speed video camera was used to determine the actual detonation velocity of both cords used in this project and it has capability of filming at 90,000 frames per second. Each explosive's velocity of detonation was tested separately. To best capture the image and calculate the detonation velocity of each cord, the tested cord was tied horizontally between two points. The Phantom software requires that the image displayed on the lap top screen to include a scaled distance to calculate the speed at which events were occurring. A sheet of ply-wood that was painted with alternating red and white 10.16 cm (4") stripes was placed behind the cord to provide the scale. The tests were conducted on a clear, sunny day when there was enough light to enable camera

operation. Figure 5.1 shows eight frames that were taken by the Phantom system while testing the HV Fire-line.

When observing the LV Prima-Shear the sample rate at which the Phantom was adjusted to was 10,000 frames per second. There was a 256x256 resolution, a 30 µs exposure, and a post trigger of 29,188. To account for human error when picking points on the Phantom software, the author recorded three different velocity readings of each tested cord. The LV Prima-Shear performed within its specifications as the average velocity calculated was 4,911 m/s (16,112 fps).

When observing the HV Fire-line, the sample rate was increased to 13,029 frames per second. The resolution and post trigger were kept constant, but the exposure was increased to 35 µs. The HV Fire-line also proved to be within specifications as the average velocity of detonation was determined to be 7,472 m/s (24,514 fps).

5.1.2. Blast Procedure. As is consistent in the industry, safety was the primary concern before carrying out any scheduled work or blast. To ensure safety, good communication techniques and resources were shared at the experimental test site. Standard operating procedures were followed by properly trained personnel to comply with the Code of Federal Regulations that is governed by the Mine Safety and Health Administration (MSHA) and the Office of Surface Mining (OSM). The author often required assistance when carrying out the experiment at the quarry. Missouri S&T provides undergraduate research assistants for projects such as the one discussed in this report. When working within 1.83 meters (6') to the edge of the bench, the workers were properly harnessed and securely tied off to a large oak tree. The equipment was also tied off to the same tree in these circumstances. All regular personal protective equipment was used when conditions required them at the quarry.

To avoid any tripping hazards, and to prevent the equipments' hoses, ropes, and cables from getting snagged, the benches were kept clean of debris that developed naturally from every blast. This also made it easier to visually inspect the post blast site for natural joints and seams as well as BID.

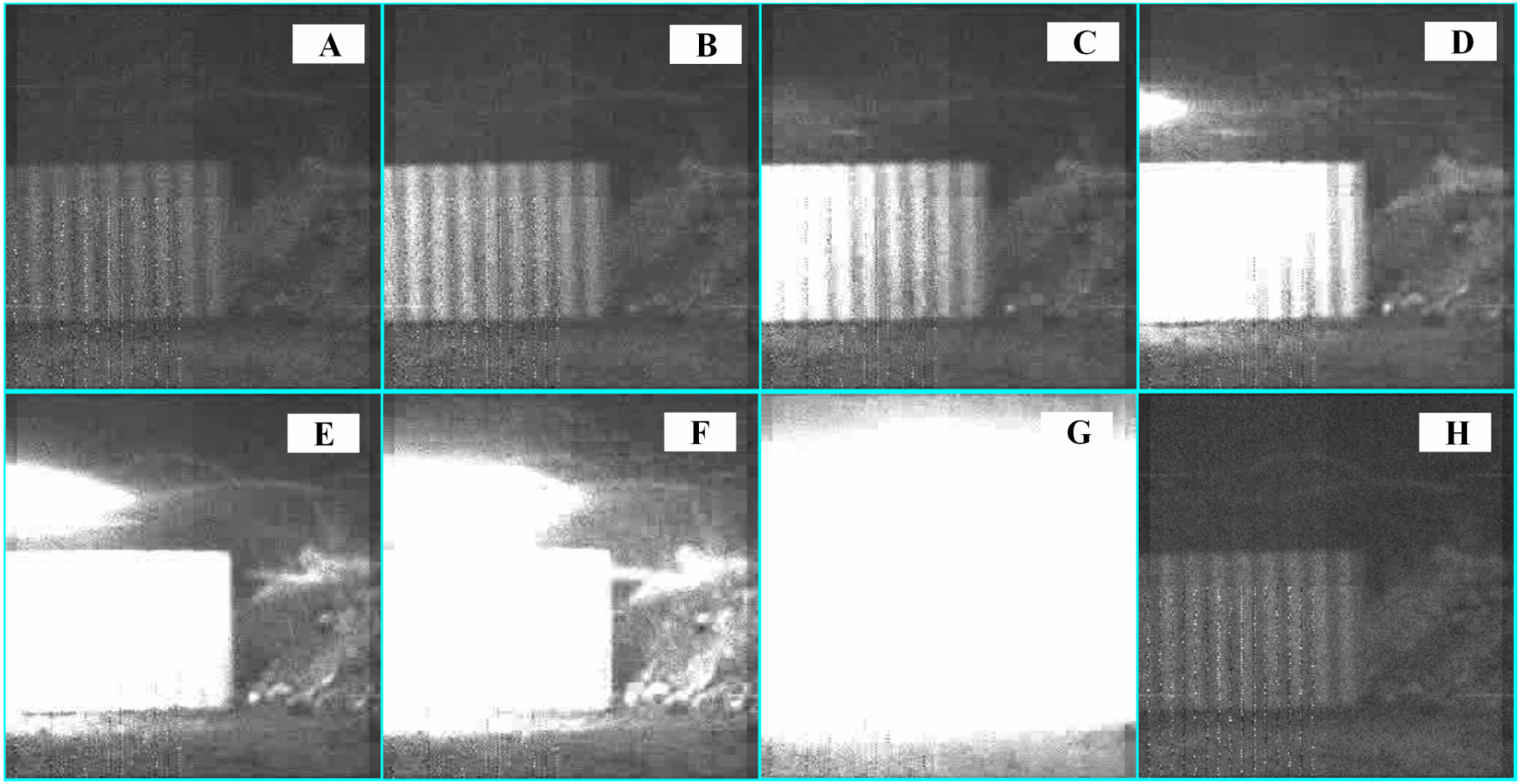

Figure 5.1: High speed photography was used to determine the detonation velocity of a sample of each cord. Eight captured frames of the HV Fire-line test are shown. A) T_0 = 0µs, B) T_1 = 77 µs, C) T_2 = 154 µs, D) T_3 = 230 µs, E) T_4 = 307 µs, F) T_5 = 384µs, G) T_6 = 691 µs, H) T_7 = 13,434 µs.

As mentioned, the spacing relationship and hole diameter was constant for every blast. The holes' diameters were 3.18 cm (1 ¼") and they were drilled 30.48 cm (12") apart. However, before drilling began, measurements were marked to ensure the holes were spaced correctly and that at least a burden 30 times the hole diameter was achieved for the blast. The burden for each hole was then documented after drilling. The blast area was also inspected very closely to search for indications of prevalent seams or joints. When the blast was performed in a heavily fractured or jointed zone, the rock would not only split along the designed row of holes, but also the fractured zones would create a lot of waste rock. Fracture zones were indicated with green marker paint (Figure 5.2). This was documented in the field notes and in digital pictures that were taken.

Most shots contained five blast holes. However, the natural seams and joint sets could be used to the driller's advantage as was discussed in the Geology portion of this report (Section 4.1.1). Likewise, some shots had as little as three holes, while others had as many as six (Figure 5.2).

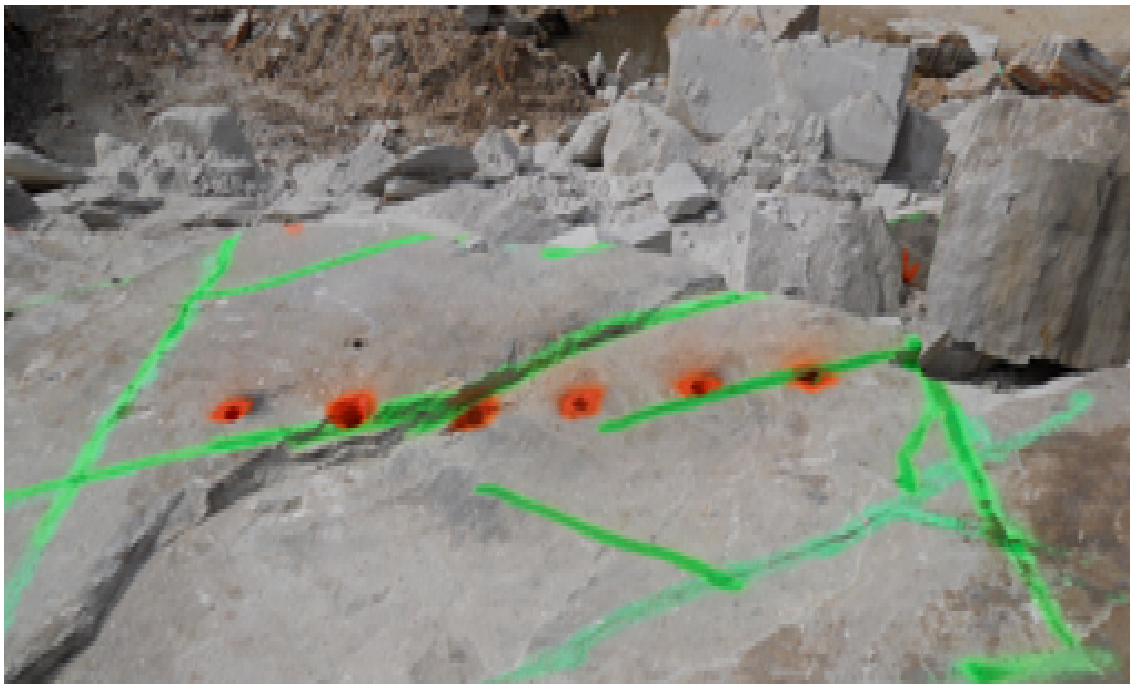

Figure 5.2: After drilling, the final burden for each hole was documented, and the natural seams and joint sets were marked with green paint.

The geology of this region is very horizontally layered. The author used this feature to his advantage when determining the depth of each shot. The extent to which the sand grains in the quarry are cemented together allowed the bedding planes to cleanly break free from the rest of the rock mass when the stone was being blasted (Figure 5.3). This phenomenon helped easily create safe workable benches (Figure 5.4) without requiring "lift" shots. Likewise, the depths of the holes were determined by the distance from the surface to the next horizontal shelf. This depth also had to be measured before every shot to properly lift the stone away from the shelf. Typical depths drilled ranged between 0.91 and 1.22 meters (3' and 4'), but sometimes as deep as 1.83 meters (6'). The blast parameters for each shot may be found in Appendices E and F.

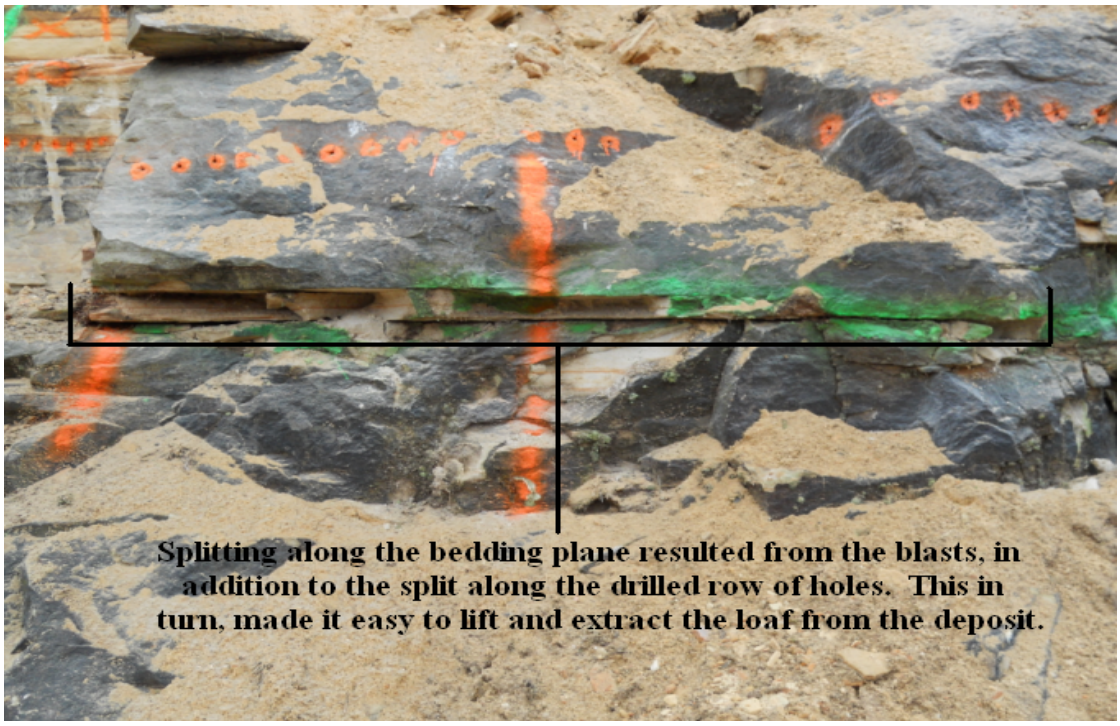

Figure 5.3: The holes were drilled to a depth that would cause the stone to split horizontally along the bedding plane. The bedding plane was marked with green paint.

Figure 5.4: Safe workable benches were easily created without performing “lift” shots.

When drilling the holes in their respective locations, the author was very careful to ensure each hole was drilled vertically and did not drift at an angle. The holes were drilled using a Midwest S-84-F Sinker Drill. The author was mindful to blow out the hole several times while drilling to avoid the drill cuttings clogging up the hole and causing the drill steel to become lodged down in the hole. After the drilling was finished, the holes were cleaned out with an air hose to ensure the holes were free from any drill cuttings and to check for any accumulation of water.

Sandstone is a very absorbent rock, and though it is friable, the pre-split “rules of thumb” regarding minimum charge diameter must be applied. Likewise 3.18 cm (1 ¼”) holes require a charge diameter of at least 0.80 cm (5/16”). To achieve this charge diameter, six lengths of the 8 grams/meter (40 grains/foot) detonating cord were used in

every hole. Electrical tape was used every few centimeters to keep the six lengths bound together (Figure 5.5).

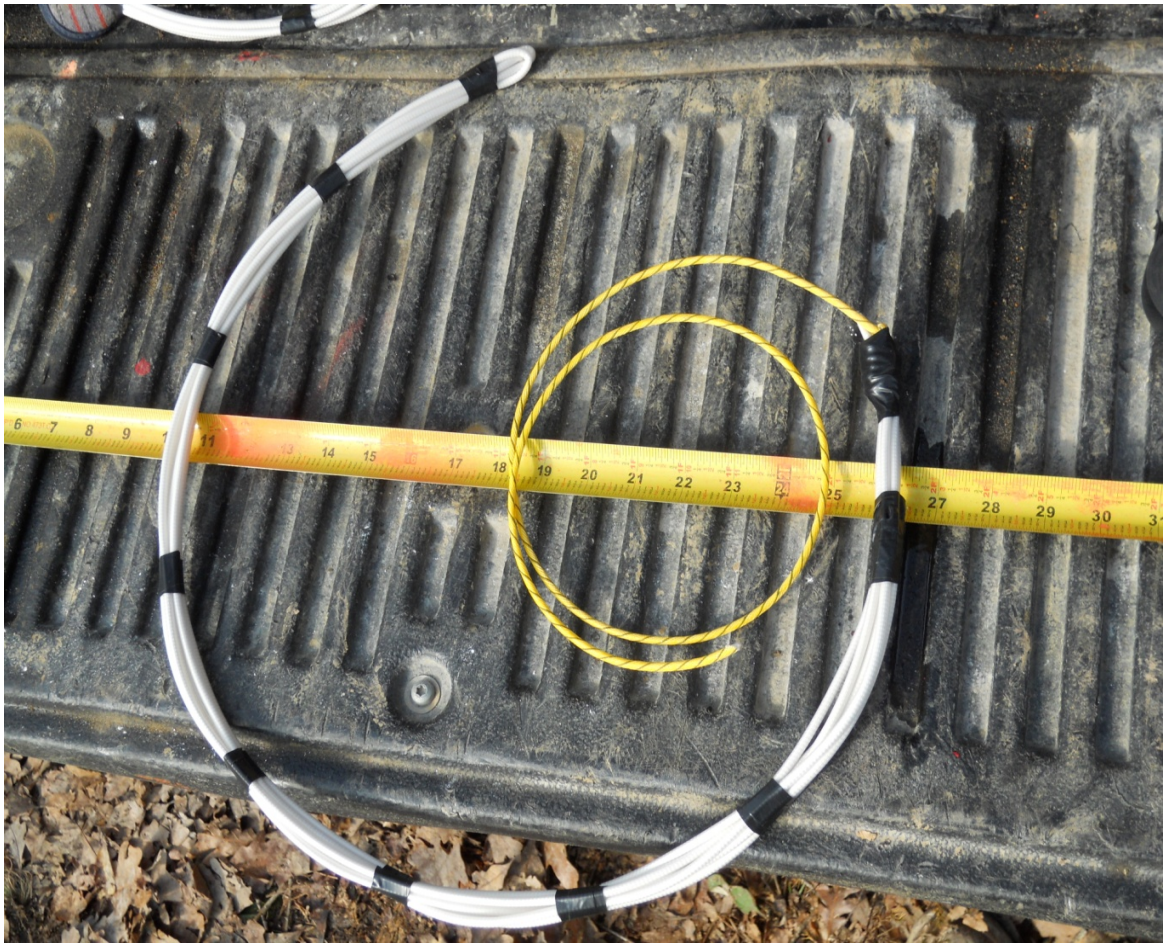

Figure 5.5: Electrical tape kept the six lengths of detonating cord bound together.

When loading the explosive in the boreholes, the detonating cord went from the bottom of the hole to approximately 5 cm from the top of the hole. Each hole was then loaded with the sand stemming medium. To reduce variation in the blasting procedure, the stemming material was kept constant in every test. Often, the drill cuttings and fines produced from the mining process would be wet and poorly sorted material. Had this been used as stemming, air gaps would most likely form in the borehole, and the

explosive would not be properly confined. "All Purpose" bagged sand was brought onto the sight and used to stem the holes (Figure 5.6). This ensured that the sand was completely dry, well sorted, and had uniform granular size.

Figure 5.6: Sand was used as stemming media to confine the explosives in the boreholes.

The blast cable extended out to a distance approximately 4.5 meters (15') away from the shot location. The author then carried out the "1 cap-18 grain donor method" (see Section 5.1.3). At request of the property owner, the detonating cord and blasting detonator on the surface was then covered with a blast mat to reduce the noise and vibration that would come from the shot. A recording seismograph with an air blast monitor was also placed at the closest inhabitable structure which was approximately 100

meters away. All of the shots were well below noise limits, recording less than 100 dB at the structure.

At this point, the shot was ready to be initiated. The property owner was informed that the shot was ready as the blasters went to a safe shooting location after they ensured that there were no personnel or equipment by the blast site that could be injured or damaged from the shot. Before each initiation, the blast team used routine audible and visual warnings.

After each detonation, the blasters waited momentarily before returning to the blast area for inspection. The split was then examined and field notes were taken. The blast cable was reeled up, and the remains of the blasting detonator were discarded. The procedure at this point was either to continue with the next shot by restarting the entire process, or to instruct the excavation equipment operator to enter the site and to remove the stone from the blast area.

A ramp was strategically created along with the production shots in order for excavation equipment to easily tram onto the working benches to remove the blasted stone. A safety berm was constructed on the edge of the cliff to protect the machinery that drove onto the site during each excavation phase. In most circumstances, this equipment included a Bobcat 865 skid steer, a Bobcat 331 mini excavator, and a Caterpillar 920 fork lift (Figure 5.7).

During task planning, the author ensured that the materials listed in Table 5.1 would be on site, maintained and available when performing pre-split shots.

Figure 5.7: Machinery aided in excavating the blasted stone. Some of the equipment used included: A) Caterpillar 920 fork lift; B) Bobcat 331 mini excavator.

Table 5.1: Materials necessary during scheduled blast days.

Shovels, pry bar, tool box	Tape Measure	Marking paint
45 meters (150') of Air Hose with Chicago End fittings	Air Compressor	Air Sinker Drill
7 meters (20') of Air Hose with Chicago End fittings	Rock Drill Oil	Drill Oiler "PIG"
Drill Steel 0.91 meters (3') in length with a 3.18 cm (1 ¼") bit	Field Notebook	Digital Camera
Drill Steel 1.83 meters (6') in length with a 3.18 cm (1 ¼") bit	4 x Whip Checks	Electrical Tape
Air Powered Hole Cleaner with shut-off valve	Knife	Electric Detonators
Fire-line or Prima-Shear detonating cord	Blast Mat	Blast Cable
3.6 grams/meter (18 grains/foot) detonating cord	Seismograph	Blast Box

5.1.3. Initiation Method. As discussed in the Review of the Literature (Section 2.1.1), pre-splitting works best when the shots initiate almost simultaneously. Simultaneous initiation allows the stress fields from adjacent holes to interact and makes the rock split preferentially along the cracks propagating between the holes. Moreover, crack propagation in the unwanted directions are reduced, and the structural integrity of the blasted material is preserved [Lownds, 2000]. Similarly, when an explosive detonates, the shock waves travel at speeds specific to the media through which they travel. The velocity of crack propagation is dependent on the speed at which the shock waves are traveling through the stone. Each type of rock has unique physical

characteristics, but pre-splitting is most effective when the velocity of crack propagation is determined and incorporated into the timing of the design.

Electronic initiation would be preferable in pre-split designs where the "down-the-hole" initiation should fire in millisecond intervals to incorporate the velocity of crack propagation into the design. However, currently electronic initiation is not accurate enough to program the detonators to fire at microsecond intervals. To incorporate the velocity of crack propagation into the timing of this experiment's pre-split design, the detonators would have to fire in microsecond intervals.

Nonetheless, an advantage of using electronic detonators is that they fire very precisely and have eliminated the variation of delay scatter. Delay scatter is typical in detonators that utilize pyrotechnic energy as a means of delay and initiation and this scatter prevents exact initiation timing. As this occurs, the explosive damages the stone's integrity rather than performing the desired task [Cunningham, 2000].

Unfortunately, this experiment was not supplied with electronic detonators. Therefore, pyrotechnic blasting detonators had to be used as the means of initiation. In light of this, the author aimed to eliminate delay scatter and ensure all holes fired simultaneously. Had individual pyrotechnic detonators been used "down-the-hole," logically one would assume that delay scatter would occur, and no procedure could combat this. Delay scatter would introduce significant variation into the project, and likely cause BID. However, if only one electric detonator was used to initiate individual lengths of detonating cord, each of which then initiated an explosive column, no chance of scatter would be present.

The "1 cap-18 grain donor" method securely ties a low strength detonating cord, 1.22 meters (4') in length onto the top of each "down-the-hole" column of explosives (Figure 5.8). This length of low strength cord sits on the surface and acts as a fuse or a donor cord to top initiate the explosives in the holes. Only one electric detonator was used in the initiation process and delay scatter variation was eliminated. Each surface donor cord was connected to the electric detonator (Figure 5.9). All of the donor cords were taken from the same spool and shared an equal velocity of detonation. After

connecting the donor cords individually to each “down-the-hole” cord, the lengths of the low strength cords were measured to ensure that the distance between the detonator to the start of the top of the explosive column was exactly the same for each hole in the shot thus ensuring simultaneous detonation of the holes in each pre-split (Figure 5.10).

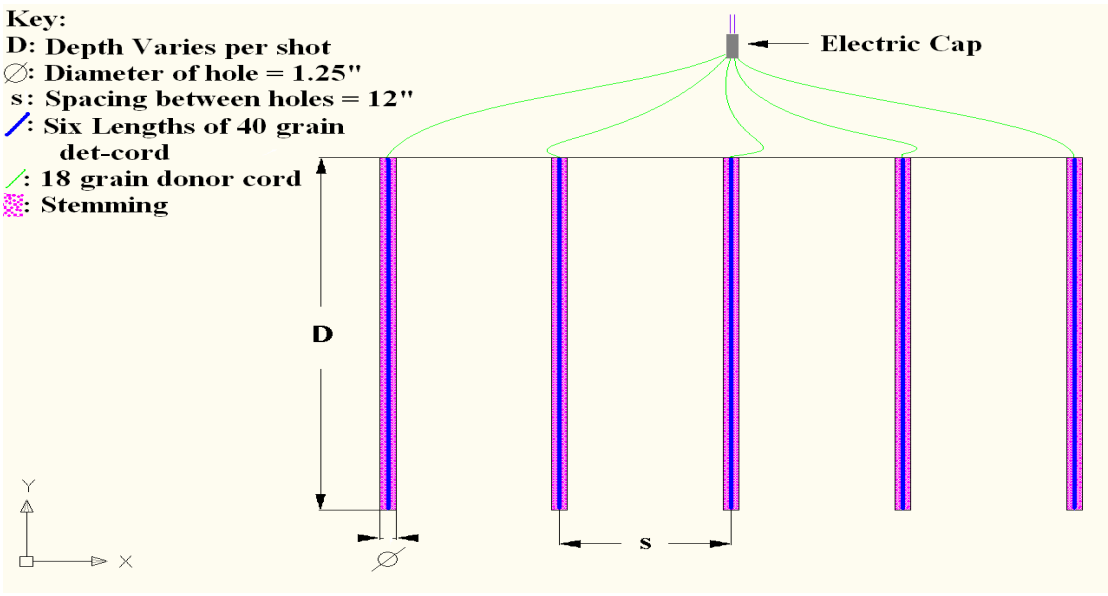

Figure 5.8: “1 cap-18 grain donor” initiation method.

Figure 5.9: Five equal lengths of donor cord connected to one electric detonator.

Figure 5.10: The length of each donor cord was measured to ensure that the distance between the detonator connection to the "down-the-hole" cord connection was exactly the same for each hole in the shot. Tips were cut off of the donor cords to make them uniform in length.

To prevent misfires or cut-offs when tying detonating cords together, they must intersect at right angles or be parallel to each other. Knot connections in detonating cord should be pulled tight to create positive contact between the two lines [Product Manual, 2005]. The author was very conscientious when tying the donor cord to the "down-the-hole" cord in order to create a positive contact. This initiation method required the author to create a connection which wraps the donor cord around the "down-the-hole" cord several times and keeps the two cords parallel to each other. The connection was also wrapped in tape to keep the two cords from losing contact (Figure 5.11).

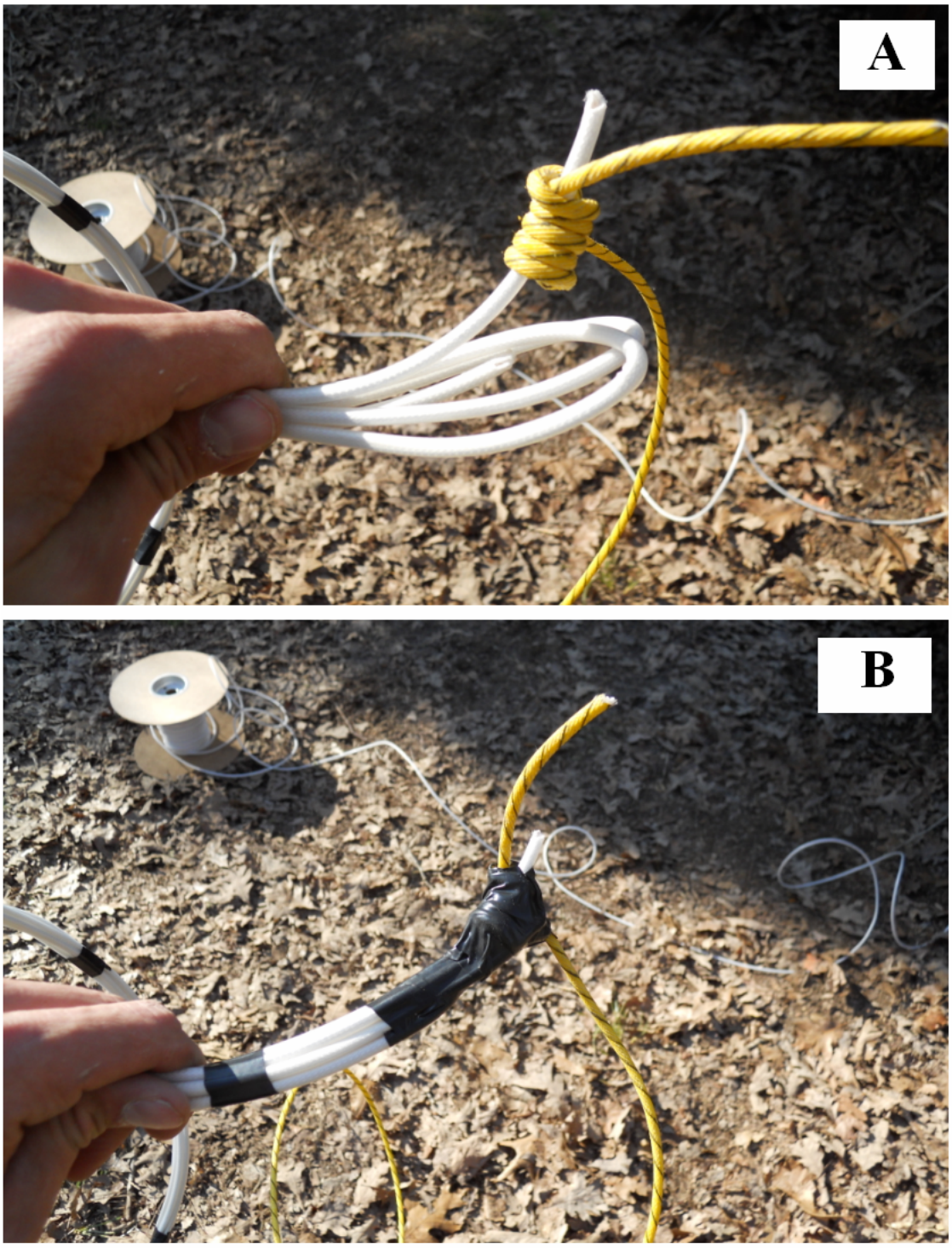

Figure 5.11: The low strength donor cord acted as a fuse for the “down-the hole” cord: A) Positive connection between the donor cord and the “down-the-hole” cord; B) the connection was wrapped in tape to prevent losing a secure contact between the two cords.

The “1 cap-18 grain donor” method is plausible to use in pre-splitting when the number of holes in the design are few and closely spaced. However, this method could be very difficult to accomplish safely on larger shots. Larger shots would require more low strength donor cord to be present on the surface. In turn, this would create more of an air blast during initiation. Also, the longer lengths of low strength donor cord could easily become a tripping hazard or become entangled together and “cut-offs” and/or misfires would result.

5.1.4. 18 Grain Reliability Tests. When detonating cord is designated as a donor, as the detonator detonates, the purpose of the donor is to initiate all detonating cord “down-lines.” Sometimes the industry refers to donors as “trunk lines.” Some detonating cords will not reliably self-to-self initiate. When selecting a detonating cord trunk line, one must consider what the trunk line must initiate and what must initiate the cord using the following guideline:

- Detonating cords between 3.6 and 10.6 grams/meter (18 and 50 grains/foot) initiate each other and themselves when they are securely tied together, unless specified otherwise. Normally cords with a core load less than 3.6 grams/meter (18 grains/foot) do not initiate themselves [Product Manual, 2005].

For this reason, the author chose 3.6 gram/meter (18 grains/foot) cord to serve as the donor in order to prevent misfiring by reliably initiating both of the 8 grams/meter (40 grains/foot) cords that were used in this project. Misfires could ruin the pre-split because the hole-to-hole spacing would be increased, and the shot would step outside the boundaries of the blast design “rules of thumb.”

To ensure the 3.6 grams/meter (18 grains/foot) donor cord would reliably initiate both the HV Fire-line and the LV Prima-Shear, a test was conducted prior to application in the field. A length of the 3.6 grams/meter (18 grains/foot) cord was tied between two points at the Missouri S&T experimental quarry. HV Fire-line was tested first by suspending five lengths of the HV cord to the 3.6 grams/meter (18 grains/foot) donor cord using the recommended clove hitch. When the shot fired, two of the suspended lengths of HV Fire-line did not initiate, and upon inspection, the explosive powder was

still present in the cord. The lack of initiation was because the clove hitches did not provide a secure contact between the donor cord and the Fire-line.

The LV Prima-Shear cord was tested next. The same set up procedure was followed, but when the clove hitches were tied to the 3.6 grams/meter (18 grains/foot) cord, the author wrapped the knot with electrical tape to keep the two cords from losing contact. In this test, all five suspended lengths of Prima-Shear were initiated.

The results of this test encouraged the author to be very mindful to create a positive and secure connection when tying the donor cord to the "down-the-hole" cord. The results also encouraged the author to wrap the knot with tape before using it in the field. As a result, no misfires occurred during experimentation.

5.2. MASW APPROACH

The velocity of the seismic waves that travel through the shallow subsurface of competent stone should show relative uniformity. However, when the seismic waves travel through stone that has been structurally damaged from a blast, the velocity will be decreased compared to a pre blast reading. One of the applications for which the MASW method was developed is to image areas of the subsurface that are structurally incompetent by analyzing the change in velocity of the Shear waves. The experimental set-up involved the active MASW method and a sequence of repetitive steps to indicate areas where the pre-split shot had caused BID, or to indicate that the blast was properly designed and little or no overbreak occurred during the blasting process. This is shown by comparing Shear wave velocity profiles gathered before a blast to profiles gathered after a blast.

The most noticeable difference in the set-up parameters from the instructions provided by the Kansas Geological Survey (discussed in Section 2.6.2) was that the geophone array was horizontally coupled to the face of the rock rather than vertically embedded on the ground surface. The Review of the Literature indicates that vertical geophones must be used with the MASW method in order to attain accurate data [Surf-

Seis, 2006]. This means that the geophones must be placed vertically relative to the surface on which the source is discharged. The seismic source that was used in this procedure was a 4.5 kilogram (10 lb.) sledge hammer. The seismic source was discharged on the deposit's face -- the same surface where the geophones were vertically located (Figure 5.12). An attempt was made to hit the surface of the rock face with the same force to send the same frequency through the stone each time. The frequency created from the impact source determined the depth of investigation that was obtained from the geophones. The author of this project was only interested in imaging the shallow subsurface (to a depth of 3.50 meters (10')). The author assumed that BID caused from pre-splitting should not affect the stone more than approximately 1 meter (3') into the rock mass from the row of blast holes. Therefore, 100 Hz geophones were chosen to effectively acquire information of the shallow subsurface.

Figure 5.12: A 4.5 kilogram (10 lb.) sledge hammer was used as the impact source on the rock face where the geophones were embedded into the stone.

Figure 5.13 shows the three main steps in the experiment's process. Pre blast MASW readings were taken prior to every pre-split shot when it was safe to do so. The instrumentation was removed from the site and the field data were taken back to the computer lab to be analyzed. The next scheduled work day was designated for blasting. Once the blasted stone was excavated from this region, the MASW equipment was brought back to the site and set up onto the freshly blasted rock face. Then a post blast reading was taken. The field data were again taken back to the computer lab to be analyzed. The two sets of data were compared to determine the extent at which the pre-split blast damaged the stone at each 30.48 cm (1') interval.

5.2.1. Applied Field Geometry. The recommended field geometry of the MASW equipment was discussed in the Review of the Literature (Section 2.6.2). The author closely followed these parameters while determining a source offset. However, due to the parameters of the blast design, the geological condition of the area, and because a new unique field application was being tested, some of the geometric parameters had to be significantly altered as discussed below. Nonetheless, an attempt was made to use a field set-up that was similar to the recommended field geometry.

When imaging the subsurface using MASW, the equipment allows the linear array of geophones to be quite large (10-30 meters (30'-100')) to acquire images of the subsurface to depths ranging from 10-30 meters (30'-100') with great accuracy. Small arrays are uncommon and not routinely used in heterogeneous material. However, the author was interested only in imaging the depth into the face within the first 3.50 meters (10'). Typically blasted sections were 1.52 meters (5') wide. The author was interested in obtaining a velocity profile specific to each section blasted. To limit the seismic data to each blasted section, the geophone array and the spacing had to be significantly decreased from a typical field geometry. Two different arrays were utilized during this experiment. The geophones were spaced 7.62 cm (3") apart with an array of 1.83 meters (6') (Figure 5.14) as well as spaced 15.24 cm (6") apart with an array of 3.68 meters (12') (Figure 5.15).

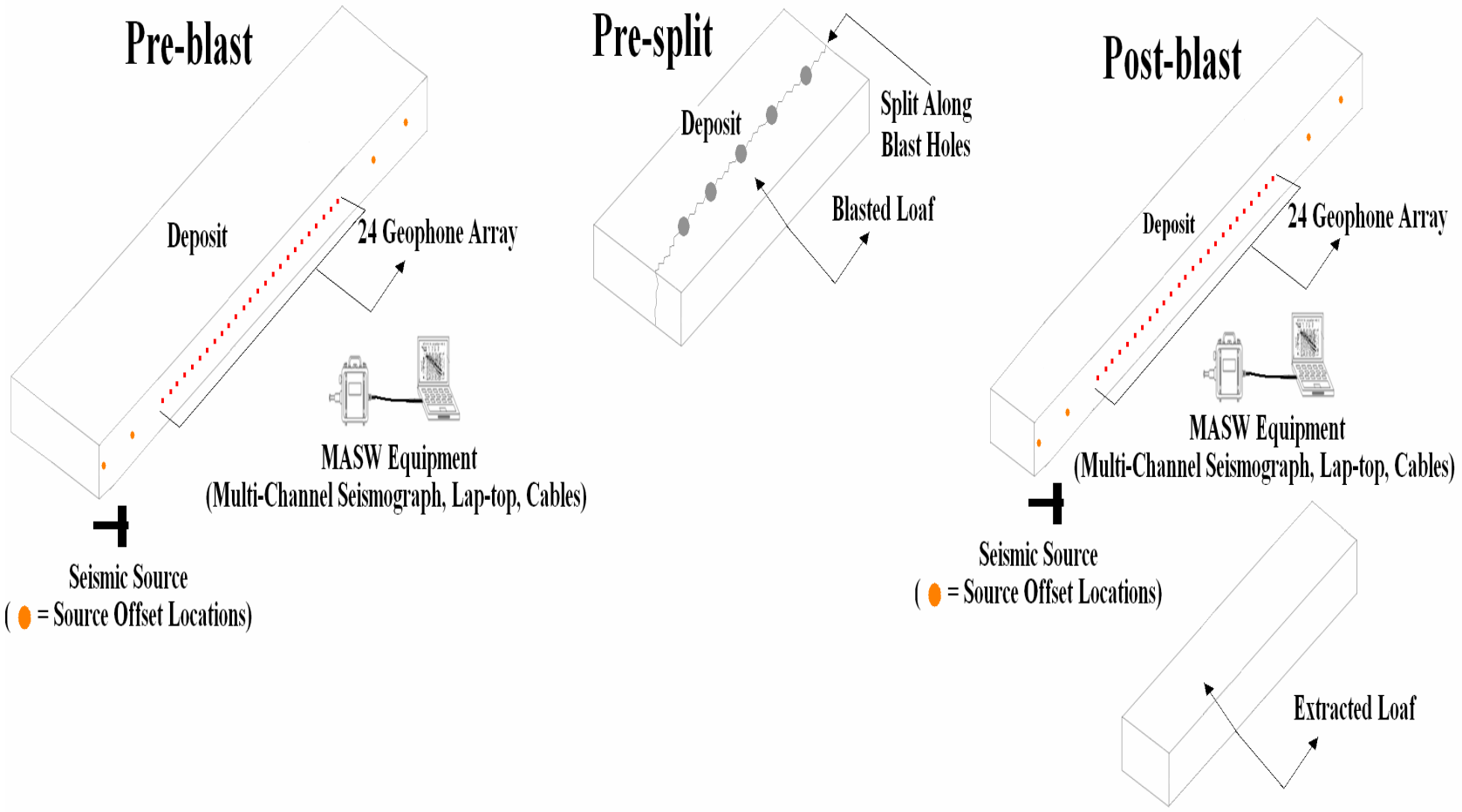

Figure 5.13: The three steps in the experimental process.

Figure 5.14: Shot area 15 was analyzed using an MASW geophone array of 1.83 meters (6’). The gathered data were specific to the 1.52 meters (5’) wide section of stone blasted in shot 15.

Figure 5.15: Shot areas 15 and 25 were adjacent blast sections together spanning over a 3.05 meters (10’) wide area. They were both analyzed together using a 3.66 meters (12’) array.

The data processed using the array of 1.83 meters (6') (Figure 5.14) generated velocity profiles that were very unpredictable and inconsistent. Some of the profiles produced logical data. Conversely, other profiles produced data that were obviously incorrect and/or difficult for the MASW software to analyze. This was most likely a result of the small geophone spacing, the location of the source impact relative to the geophone array, as well as unavoidable reflective surfaces being present within the heterogeneous material at the array location. To combat this issue, many repetitive shot gathers were taken from each array location. Typically, eight shot gathers were acquired per array. This procedure consisted of gathering two sets of data at each impact location. The impact locations were on both the left and the right of the array at source offsets of both 0.76 and 1.52 meters (2.5' and 5.0').

Yet, anomalous data were consistent when using the array of 1.83 meters (6'). The processed velocity profiles were still unpredictable and inconsistent. Therefore, the author repetitively collected data with a larger geophone spacing (15.24 cm (6")), and a 3.66 meters (12') array (Figure 5.15). While the 1.83 meters (6') array was specific to a 1.52 meters (5') wide blasted section, the 3.66 meters (12') array expanded over two adjacent blasted sections. Once the MASW software interpreted the data that were obtained from the 3.66 meters (12') array, the velocity profiles would display Shear wave velocities at each depth interval of both blasted sections averaged together. This undoubtedly introduced error into the gathered data but it was necessary considering that often the 1.83 meters (6') array did not always produce reliable read-outs.

The experimental location was a deposit located in an area of the sandstone dimension stone quarry that had never been mined before. The experimental location had many cliff ledges before the blasting operations created a series of safe benches to walk on. Therefore, some of the first sections blasted did not have corresponding pre blast data because it was unsafe to acquire. However, adjacent areas were used to gather pre blast data, and the velocity profiles show that the stone was relatively similar to each other in these sections. The shot areas where pre blast data could not be gathered were assigned pre blast readings of adjacent areas where the pre blast survey was able to be

safely performed. Though this introduced error and variation into the data collection, it was absolutely necessary to protect the safety of the project's personnel and equipment.

5.2.2. MASW Software. The author used the RAS-24 equipment and software to obtain pre and post blast geophysical data in the field. RAS-24 is a modular 24-channel, high resolution, signal enhancement seismograph designed for shallow geophysical exploration. This versatile software operates through Windows XP/Vista. RAS-24 is self configuring and has a familiar "point and click" interface which is easy to learn and operate. This seismograph was chosen because it provides a unique flexibility not always found in other engineering seismographs. The system connects to a laptop and the 24-channel refraction seismograph becomes ready for field operation [Seistronix, 2010].

The shot gathers attained from the RAS-24 software were interpreted by the Surf-Seis (Version 2.05) software -- developed by the Kansas Geological Survey. Surf-Seis interprets shot gathers collected by the active MASW method to develop a dispersion curve and velocity profile related to each field log. It is relatively simple software and displays results that are easily interpreted by the engineer.

5.2.3. MASW Procedure. In order to minimize variation in the process and acquire consistent and reliable data, a major attempt was made to keep the set-up procedure constant every time. The MASW equipment was borrowed from the Missouri University of Science and Technology – Geological Engineering Program. To avoid variation in the instrumentation, the same geophones, impact source, laptop, and cables were used during every test. Scheduled work days were efficiently coordinated to gather multiple pre and/or post blast readings. Prior to transporting the MASW equipment to the quarry to gather data, the test site was cleaned of blasted stone and debris to avoid any tripping hazard and to keep the geophysical cables from getting snagged or damaged. All of the bench surfaces were also cleaned off with the compressed air hose. The face was examined and any loose stone was scaled down and discarded. All MASW tests were performed when no heavy machinery was in operation that would provide outside sources of "noise." In addition, field work was not scheduled during wet weather due to the effects that accumulated ground water has on the equipment and data readouts.

As the source impacts the stone surface, the seismic waves that travel through the stone reflect off of any surface present, and creates “noisy” data. Geologic features that are common in Gasconade, Jefferson City, and Pennsylvanian Formations such as karsts, sinkholes, air voids, water accumulation, banded layers of chert, and clay create troublesome reflective areas that the MASW method cannot avoid. The information produced in areas that contain such geological features would have made it very difficult to analyze and interpret the data. Fortunately, the Roubidoux Formation that was present in the experimental location did not consist of the geological features that are common in Gasconade, Jefferson City and Pennsylvanian Formations. These conditions allowed for conclusive MASW data to be gathered.

As discussed earlier, reflective surfaces that could potentially produce “noisy” data were prevalent in the experimental location. Fractures, seams, joint sets, bedding planes, ground water, and geological imperfections are common in sandstone. In addition, the top and bottom surfaces of the face, intermediate ledges, and the edge of the deposit provide surfaces off of which seismic waves to bounce (Figure 5.16). These reflective surfaces were very difficult to avoid considering the set-up parameters and geology of the region. However, the author attempted to locate the geophones at a suitable distance from these surfaces so the “noisy” data would be minimized.

Holes were drilled into the rock face in order to insert the spike-coupled geophones. When collecting post blast readings, the objective was to have the geophones set-up at the same orientation (e.g., the same height on the face) as they were during the pre blast readings. However, it was more important to couple the geophones on a smooth vertical surface in order to avoid reflective surfaces and to acquire meaningful data. Likewise, at times the holes were drilled several centimeters up or down from the pre blast geophone orientation. This minor change did not make a significant difference in the data output, since the stone was relatively uniform in each blast region.

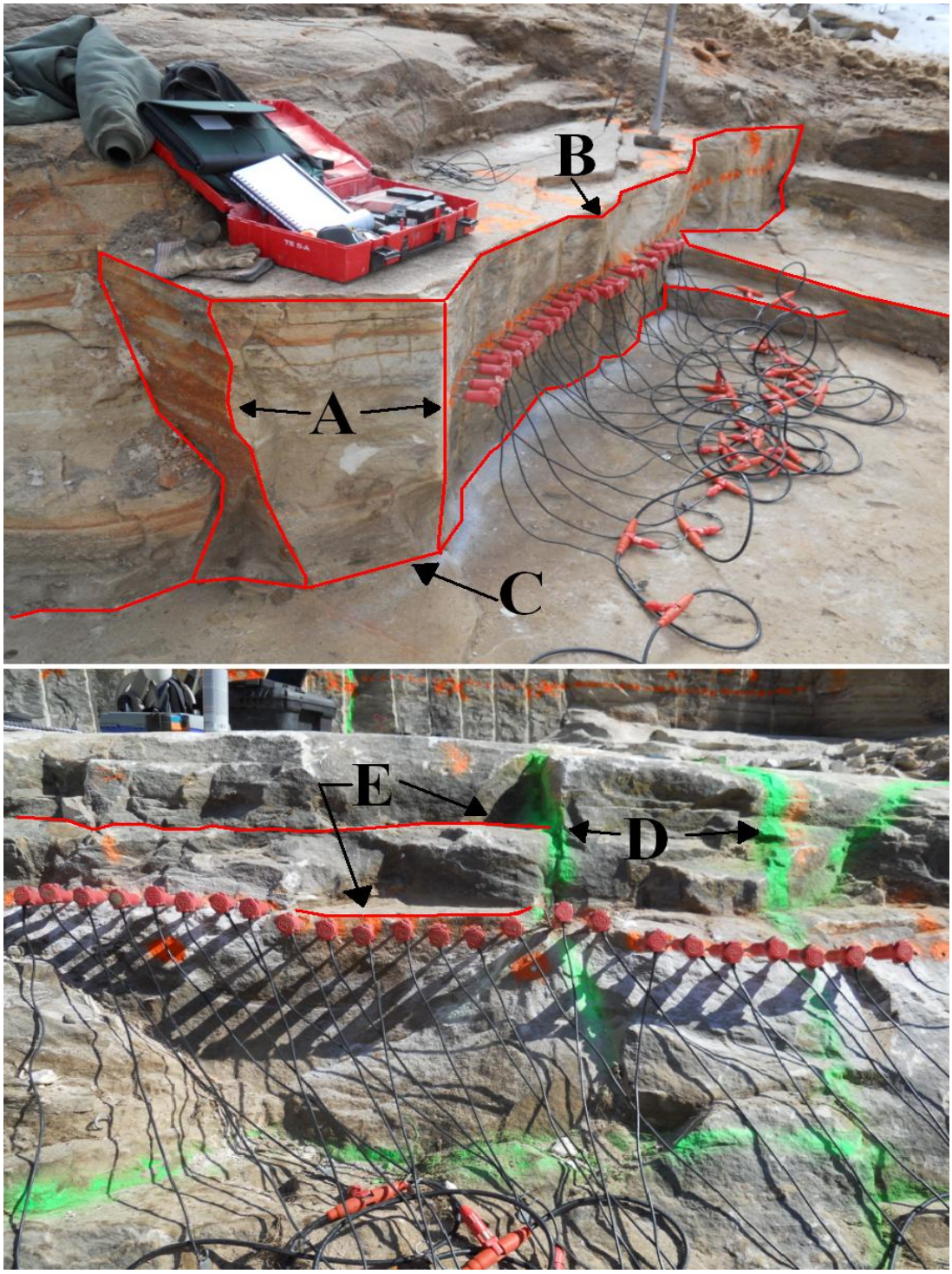

Figure 5.16: The set-up parameters and the geologic conditions of the quarry provided many surfaces off which seismic waves reflected: A) edge of deposit; B) top surface of face; C) bottom surface of face; D) seams and fractures; E) intermediate ledges.

Once the author identified a smooth location on the face where the seismic wave could best avoid any potential reflective surfaces, he made a marking on the face at 7.62 cm (3") intervals. An attempt was made to keep all of the drilled holes level and in line with one another. The hammer drill was then used to drill 0.635 cm (¼") holes approximately 7.62 cm (3") deep at every mark on the tested face. This size hole normally provided very good coupling for the geophones, and quality signals resulted. Once the geophones were coupled to the holes, and the seismograph and the computer were set-up, all of the instrumentation's cable connections were made and the test commenced.

During task planning, the author ensured the materials listed in Table 5.2 were on site, maintained and available when gathering MASW data.

Table 5.2: MASW materials necessary when performing geophysical field work.

Marking paint and large Sharpee marker	Shovels, pry bar, tool box	Measuring Tools
Hilti battery charger and 400 watt car inverter	0.635 cm (¼") hammer drill bits	Field Notebook
Hilti portable Hammer drill equipped with two charged batteries	24 x 100 Hz Geophones	Digital Camera
Fully charged Laptop computer with RAS-24 software	24 channel intermediate cable	Mueller cable
Power cable with alligator clips	12 V battery	Trigger cable
4.5 kilograms (10 lb.) Sledge hammer with trigger	24 channel Seismograph	Computer cable

6. DATA COLLECTION AND ANALYSIS

The data collected from the MASW field work were very extensive and detailed. The author attempted to analyze this data in a number of ways in order to gather meaningful information about the MASW geophysical method and its application to the mining and explosives industry. In addition, the author expected the two explosives used (HV Fire-line and LV Prima-Shear detonating cords) in this project to produce results that differed from one another, confirming that LV cord produces less BID than the HV cord due to less pressure in the boreholes during initiation. The author approached this work with no preconceptions of outcomes, considering the unique nature of the experimental location's geology as well as sources of variation and error that were present in the process. From this study, the author developed conclusions regarding the work performed and generated recommendations for work that could be done to further utilize the MASW method as it was intended for.

6.1. UNCONTROLLABLE SOURCES OF VARIATION

Process variation must be minimized to achieve a quality product. In this project's procedure, the author made a strong attempt to eliminate sources of variation by using well-maintained equipment, quality explosives, dry and well sorted stemming, properly trained personnel, and a consistent, repetitive process. However, events often occurred in the testing environment that introduced sources of variation over which the author had no control. The following sections discuss the events that could have an effect on the amount of BID produced from each blast, as well as the quality and accuracy of the MASW data that were collected from the experimental location:

6.1.1. Variations in Blasting. The blast design pattern did not change for any of the tests. The 3.18 cm (1 ¼") holes were spaced 30.48 cm (12") apart, and the minimum changes in the burden and depth did not have an impact on the collected data. However, the drill bits naturally became dull and decreased in size as a result of every hole drilled. Likewise, the borehole diameter decreased from one hole to the next. It would not have been cost effective or time efficient to change the drill steel bit after each hole drilled.

The author noticed a significant change to the drill bits' diameter after approximately 100 holes were drilled. To minimize variation, the bits were changed out at this time. This change in hole diameter was ignored and each hole was assumed to be 3.18 cm (1 ¼").

The stemming media in every shot was uniform. "All Purpose" bagged sand was loaded in the entire length of the borehole to provide adequate coupling of the explosives, prevent surface cratering, and minimize noise and ground vibration. However, the geology of the region possessed many fractures, seams and bedding planes. Some of the holes that were drilled were interconnected with these geological features and the stemming media did not hold in the holes. It would slowly "leak" into the natural seams and fractures before the shot was detonated. The seams and fractures extended to unknown depths, so it would have been ineffective to continue pouring stemming into the hole until it was plugged. As a result some holes resulted in having no stemming and the explosives therefore were not confined. Unfortunately the project was not supplied with the current mining technology that has been developed specifically to combat this issue (e.g., hole linings). Again this minor variation was ignored for the purpose of this study, and all of the holes were assumed to be loaded completely with sand.

The holes were drilled to a depth of a subsequent underlying horizontal bedding plane. This was an advantage of blasting in sandstone because each shot could be designed to break the dimension stone away from the rock mass without using explosives in "lifter" holes. Because of this, some sets of holes were drilled as deep as 182.88 cm (72"). This produced several problems and sources of variation. The detonating cord is not rigid and it was generally difficult to completely load to the bottom of holes that were deeper than 152.40 cm (60"). The cord was attempted to be kept centered in the hole but logically this was impossible to do. The cord would become bunched together down in the hole, and as a result the bottom 7.62-30.48 cm (3"-12") of deep holes did not contain explosives. Also as the explosives became bunched together in the hole, a "plug" or "decking" was created not allowing the stemming to pass and the entire length of the explosives would not be confined in sand. The depths of these "deckings" were unknown, but it was evident that they existed when the holes became filled with sand considerably quicker as compared to an adjacent hole that was drilled to an equal depth.

These problems were uncommon, as a majority of shots were drilled to a depth of approximately 121.92 cm (48”). Similarly, this minor variation was ignored for the purpose of this study, and all of the holes were assumed to be loaded from top to bottom with the detonating cord coupled by sand.

The faults and fractures present in the experimental location acted as conduits for fluid to flow. When scheduled blast days occurred after periods of high precipitation, it was found that some of the holes contained water after being drilled. Though the holes were cleaned out with compressed air, water quickly found its way back to the holes as it traveled through the natural seams and fractures in the area. The holes were nonetheless loaded with the explosives and stemming and the shots were performed as scheduled. This source of variation was uncommon, and all of the holes were assumed to be loaded only with dry-well graded sand.

6.1.2. Variations in MASW. It is optimal to perform the MASW method in dry conditions. Water has very different properties than the stone. The physical nature of sandstone is changed after periods of high precipitation since it is a very absorbent stone. In addition, water collects in natural faults and fractures. The velocity of the seismic waves that propagate through the rock during the data collection would not be the same in wet stone as in dry stone.

As moisture accumulates in faults and fractures, it causes these voids to enlarge. The voids increase exponentially especially when the accumulated moisture has a chance to freeze and expand. This circumstance could potentially enlarge fractures created from BID, thus the data being analyzed would be skewed.

The water from precipitation flows on the ground surface, picking up sediment such as dirt, clay and sand particles along the way. As this water flows through the natural faults and fractures, these transferred particles accumulate in the stone and change the sandstone’s natural properties.

The author attempted to not gather readings immediately after periods of heavy precipitation. Unfortunately at times this was unavoidable in order to proceed with the project and to stay on schedule.

An attempt was made to gather the MASW data as soon as possible after each blast. However, due to weather, availability, equipment maintenance, and the excavation phase, at times there were long gaps in between the shot and the post blast data collection. The days in between a shot using low velocity cord and the post blast data collection ranged from 9-85 days while the days in between a shot using high velocity cord and the post blast data collection ranged from 2-8 days.

The author consulted with a geophysicist who was well trained in the MASW method. He advised that field data were better recorded on warm days rather than on frigid days [Anderson, 2010]. Freezing temperatures change the physical properties of the stone, and when the impact source strikes the surface, the frequency generated from the source that propagates through the rock is different from when the test is performed in warmer weather. Much of the field work was performed in the winter months. It was often necessary to perform field work on cold days in order to proceed with the project and to stay on schedule.

The force at which the sledge hammer source impacted the stone face was not constant for every gathered record. Though the field technicians attempted to strike the rock face with the same force every time, logically this was impossible to do. This project was not supplied with a "rebound hammer" which would have ensured the source impact generated the same frequency through the stone for every record.

The spike-coupled geophones that were used in this project required 0.635 cm (¼") holes to be drilled horizontally into the face of the rock. The author questioned if drilling these holes into the blasted face could have possibly created new fractures that were not a result of the blasts and/or increase the severity of BID fractures which skewed the post blast data. If this were the case, these additional changes made in the rock could be significant enough to create inaccuracies in the post blast MASW data.

There are geophones that are attached to flat plates rather than spikes that may be coupled to the surface and they are known to generate very good data [Anderson, 2010]. Due to time constraints, spike coupled geophones were the most practical pieces of instrumentation to use, and the variation discussed above could not be avoided.

Geophones attached to flat plates are generally used when performing MASW tests on bridges or roads to locate deteriorated areas or corroded rebar infrastructure. The plates are attached to the ground by applying an adhesive epoxy onto the bottom surfaces of the plates before setting them in their measurement locations. Obviously the rock face was not as smooth as an asphalt road, and if this type of equipment was used, it would have been difficult to adequately couple the geophone plates onto the stone. Also, it would have been very time consuming to allow the epoxy to dry. More than one pre and/or post blast survey was done while the equipment was onsite; the geophones were relocated several times on scheduled MASW days. For all of these reasons it would have been very impractical to use geophones coupled to the stone's face on flat plates with epoxy.

The linear row of 0.635 cm (¼") holes that were drilled into the stone was sunk consistently to the same depth in order for the geophones to have adequate coupling. However, the natural joints and fractures in the rock caused air voids to be present, and sometimes in these regions, the geophones did not have strong coupling to the stone. Weak geophone coupling is very problematic for the MASW method and typically generates "noisy" shot gathers.

Generally, the topography of the blasted face was flat. However, there were times when large fractures, bedding planes or the end of the deposit became an issue and potentially interfered with the surface wave propagation. As discussed in Section 5.2.3 of the Procedures, these geological features presented surfaces off of which the seismic waves to reflect. Also due to the varying height of the benches, the distance from the geophones to the top or bottom ledges of the benches changed for every field set-up. These uncontrollable sources of variation within the geology typically generated moderate or excessive "noise" in the shot gathers.

The rock face topography was rarely flat when pre blast surveys were conducted on a virgin face. In these instances, the geophones were located on a very weathered surface that was sloped (Figure 6.1). This was very problematic for the instrumentation and created velocity profiles that were difficult to interpret.

Figure 6.1: Two examples of pre blast stone surfaces that displayed topographical changes and impacted the accuracy and quality of the collected MASW data. Both A (top view) and B (side view) are the same set-up location. Both C (top view) and D (plane view) are the same set-up location.

Originally the local geology was considered to be an unchanging variable in the experimental procedure because it was consistent in geologic deposition, lithology, and stratigraphy. However, as mentioned, this deposit was virgin rock that had never been mined. Though this was beneficial in some aspects, it also presented variation within the tests. Of the 19 shots performed using low velocity cord, 12 of the shots were performed on virgin stone. Of the 20 shots performed using high velocity cord, only 5 of the shots were performed on virgin stone. Before any shot was performed on a virgin face, the depth to which the weathered surfaces extended to were unknown, as they ranged anywhere from approximately 1-2 meters (3'-7'). The weathered rock generated MASW pre-blast velocity profiles that were approximately one-third of the values of those generated in non-virgin stone. When compiling the statistical analysis, these variations needed consideration.

Finally, as the personnel working on this project became more familiar with the location and more experienced with the equipment, the efficiency of the work improved with the quality of their work. This was certainly the case for both blasting operations as well as with MASW field work. Most noticeably, the author had no experience analyzing or interpreting the geophysical data on the Surf-Seis software before beginning this project. Hundreds of shot gathers were processed. As the author became more familiar with the software and its requirements, the data readouts became more consistent and more accurate.

6.2. DATA PROCESSING AND ANALYSIS ON SURF-SEIS

The shot gathers that were collected from field work were analyzed in the geophysics lab at the Missouri University of Science and Technology. Surf-Seis (Version 2.05) is very efficient software that is effectively able to generate dispersion curves and velocity profiles from MASW shot gathers. A total of 473 shot gathers were taken and analyzed during the experiment. However due to "noisy" data, only 270 of the shot gathers were used during interpretation. Appendix A presents all 270 sets of shot gathers, dispersion curves, and velocity profiles that were used to interpret the data. The

uncontrollable sources of error provided the opportunity for "noise" to be present in the collected data. Shot gathers that were "noisy" often produced inaccurate dispersion curves, and many of the lines had to be disregarded and not included in data analysis.

It is the responsibility of the engineer to specify the field parameters in the Surf-Seis program, which include the geophone spacing, the source offset, and the location of the source impact relative to the geophone array. The engineer must also manually pick the phase velocity locations on the dispersion curve to be measured by the software (the white dots that trace the amplitude curve in Figure 6.2-B). The potential human error that is present when choosing these phase velocity locations was illustrated with Figure 2.10.

P-waves and surface waves are generated when seismic sources impact the earth-air interface. The P-waves act as "noise" when analyzing surface waves; the author muted the P-waves in each shot gather during analysis so the software would generate accurate dispersion curves. The shot gathers displayed in Appendix A are print screens after the P-waves had been muted from the analysis.

Typically the shot gathers should evenly slope downward when each geophone in the array receives the seismic energy at consistent arrival times. Smooth shot gathers are preferred to obtain quality dispersion curves that will create meaningful velocity profiles. The author was only interested in profiling the first 3.05 meters (10') of the subsurface, since he did not expect there to be any damage to the stone from the blast after approximately the first meter (several feet) into the stone. Additionally, he did not expect there to be much variation in the stone within the first 3.05 meters (10'), so the velocity profiles should have generally displayed consistent linear velocities at each depth interval as illustrated in Figure 6.2. The author expected noticeable changes in velocity to only have been found when BID was present in the post blast MASW surveys.

This however was not the case. It was very common in this experiment to record shot gathers that displayed moderate or excessive "noise." This could have been a result of bad coupling, precipitation accumulation, reflective surfaces present in the survey location, the altering strength of the stone, the location of the source impact relative to the geophone array, or human error. The dispersion curves associated with "noisy" shot

gathers were often not completely smooth, and sometimes displayed inconsistent velocity profiles (Figure 6.3). Extremely "noisy" shot gathers (Figure 6.4) characteristically would generate dispersion curves that could not be interpreted (Figure 6.5). The dispersion curves similar to those shown in Figure 6.5 would not generate an accurate velocity profile, and this was one of the reasons why some of the lines were disregarded.

A lot of repetitive field work was necessary in order to gather a sufficient amount of meaningful data for each pre and/or post blast survey. The unique set-up parameters as well as the troublesome features present at the experimental location provided a potential for many uncontrollable sources of variation which interrupted the quality of the gathered data. Of the 270 sets of MASW data that were kept, the shapes of the curves and the displayed graphs were constantly changing. These are shown in Appendix A.

6.3. DATA INTERPRETATION

Once the velocity profiles were obtained from Surf-Seis, the author had to record and interpret the Shear wave velocity at each depth interval. The author narrowed the depth of investigation within the first 3.05 meters (10') from the impact surface. The velocities were then recorded at each 30.48 cm (1') depth interval. The MASW software will provide high resolution on surfaces that are not weathered, that do not possess excessive reflection areas, and are of uniform thickness and strength [Anderson, 2010]. Commonly, the MASW method is used on asphalt or concrete pavements to identify damaged areas within thicknesses of less than 15.24 cm (6") at depth intervals of 7.62 cm (3") [Anderson, 2010]. The troublesome geology at the experimental location made it difficult for the MASW software to interpret depth intervals smaller than 30.48 cm (1') with as high of a resolution that is used to locate damaged zones in asphalt pavements.

Much of the data had velocities that changed abruptly and excessively within the 3.05 meters (10') depth of investigation. Often the velocities were not constant throughout a 30.48 cm (1') interval so the recorded value had to be estimated. Figure 6.6 illustrates how Shear wave velocity estimations were recorded at each 30.48 cm (1') depth interval when the velocity profile produced inconsistent (abruptly changing) data.

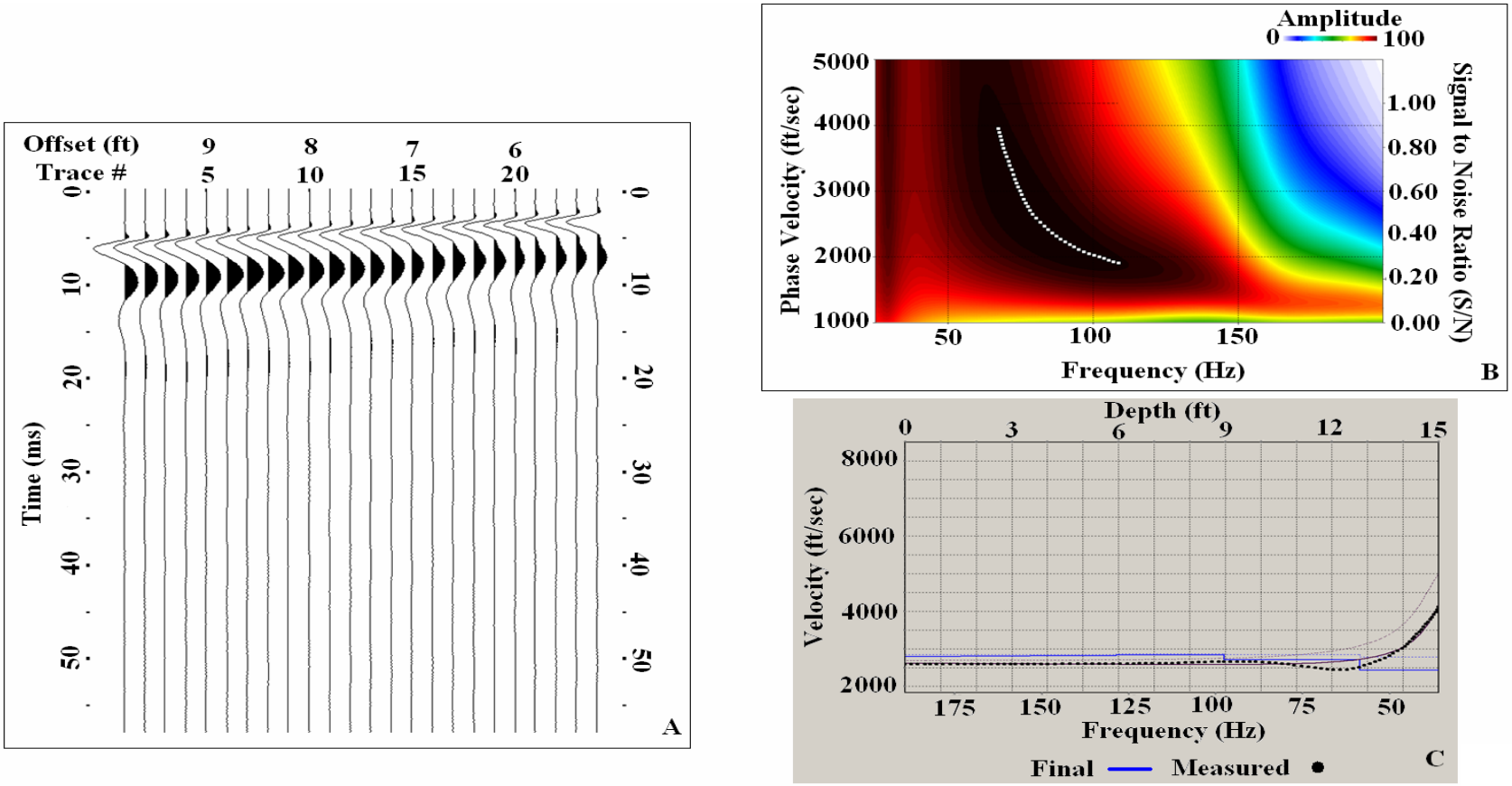

Figure 6.2: A smooth, consistent shot gather curve generated smooth, consistent quality dispersion curves, which in turn would generate a consistent linear velocity profile: A) Shot gather (P-waves muted); B) dispersion curve; C) velocity profile.

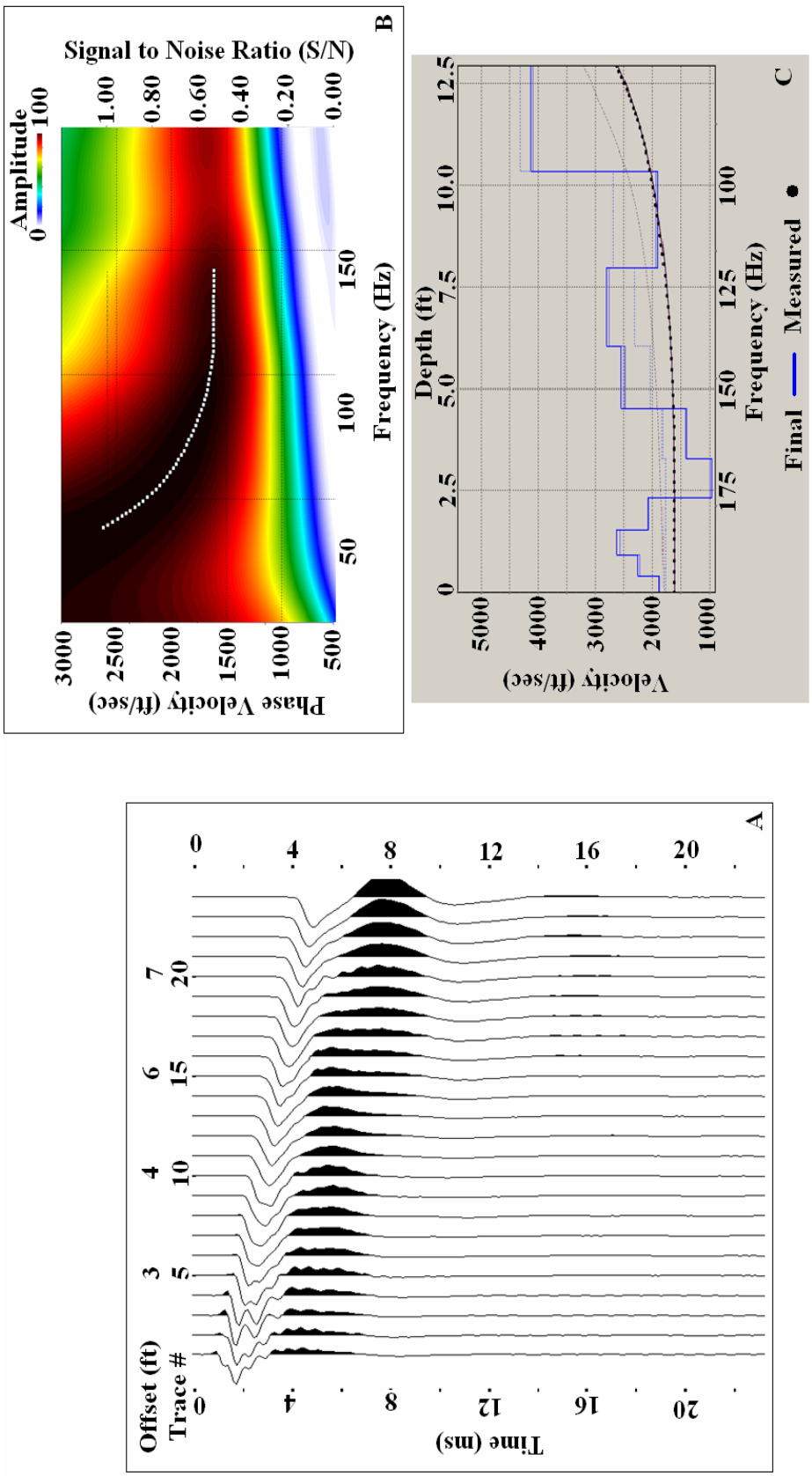

Figure 6.3: "Noisy" shot gathers often displayed smooth dispersion curves, but inconsistent velocity profiles resulted: A) Shot gather (P-waves muted); B) dispersion curve; C) velocity profile.

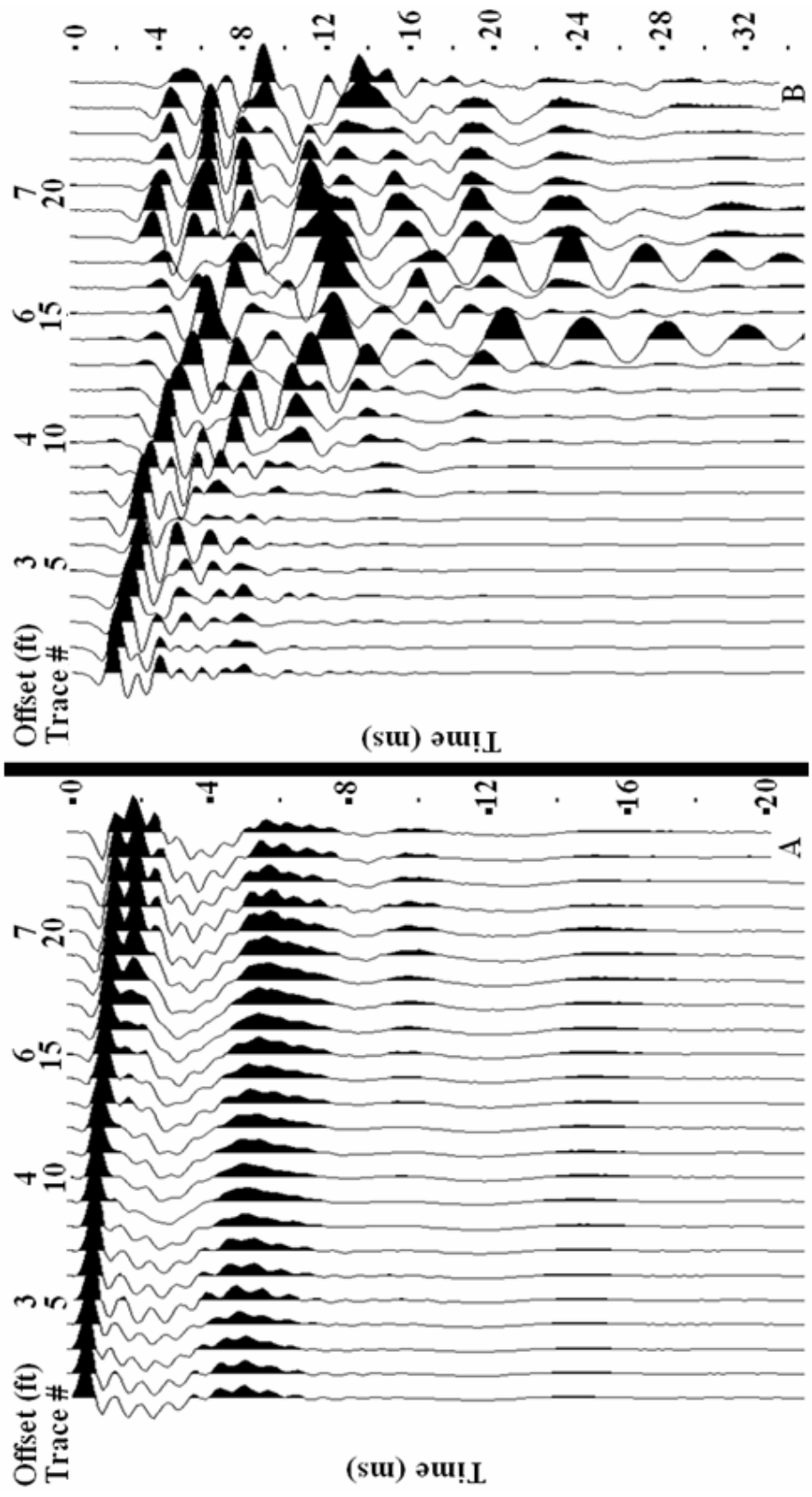

Figure 6.4: "Noisy" shot gathers typically would not be useful to generate dispersion curves: A) Most likely caused by excessive reflection points; B) most likely caused by reflection and/or bad geophone coupling.

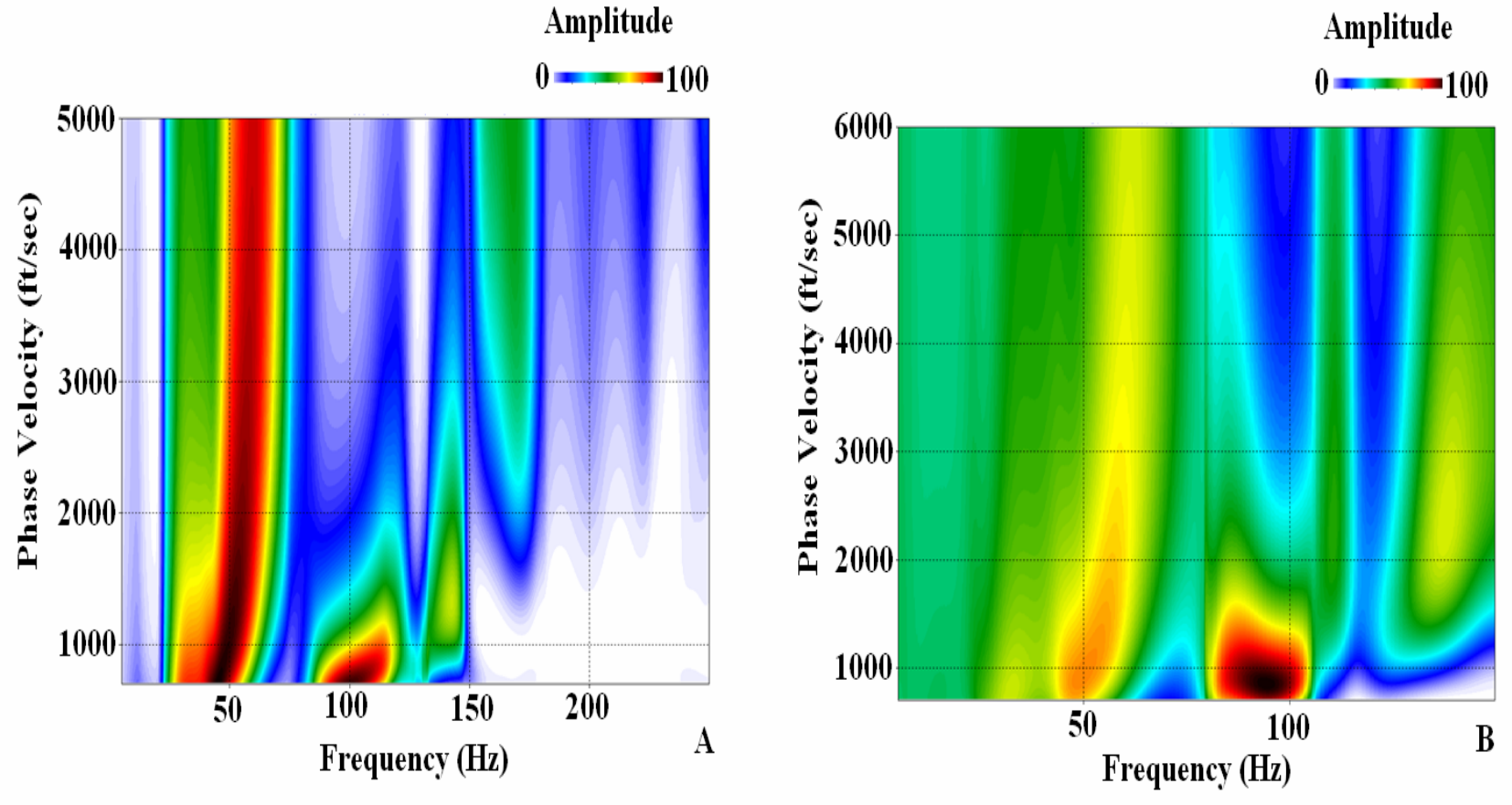

Figure 6.5: Two examples of dispersion curves that were generated from "noisy" shot gathers and were unable to produce a reliable or meaningful velocity profile.

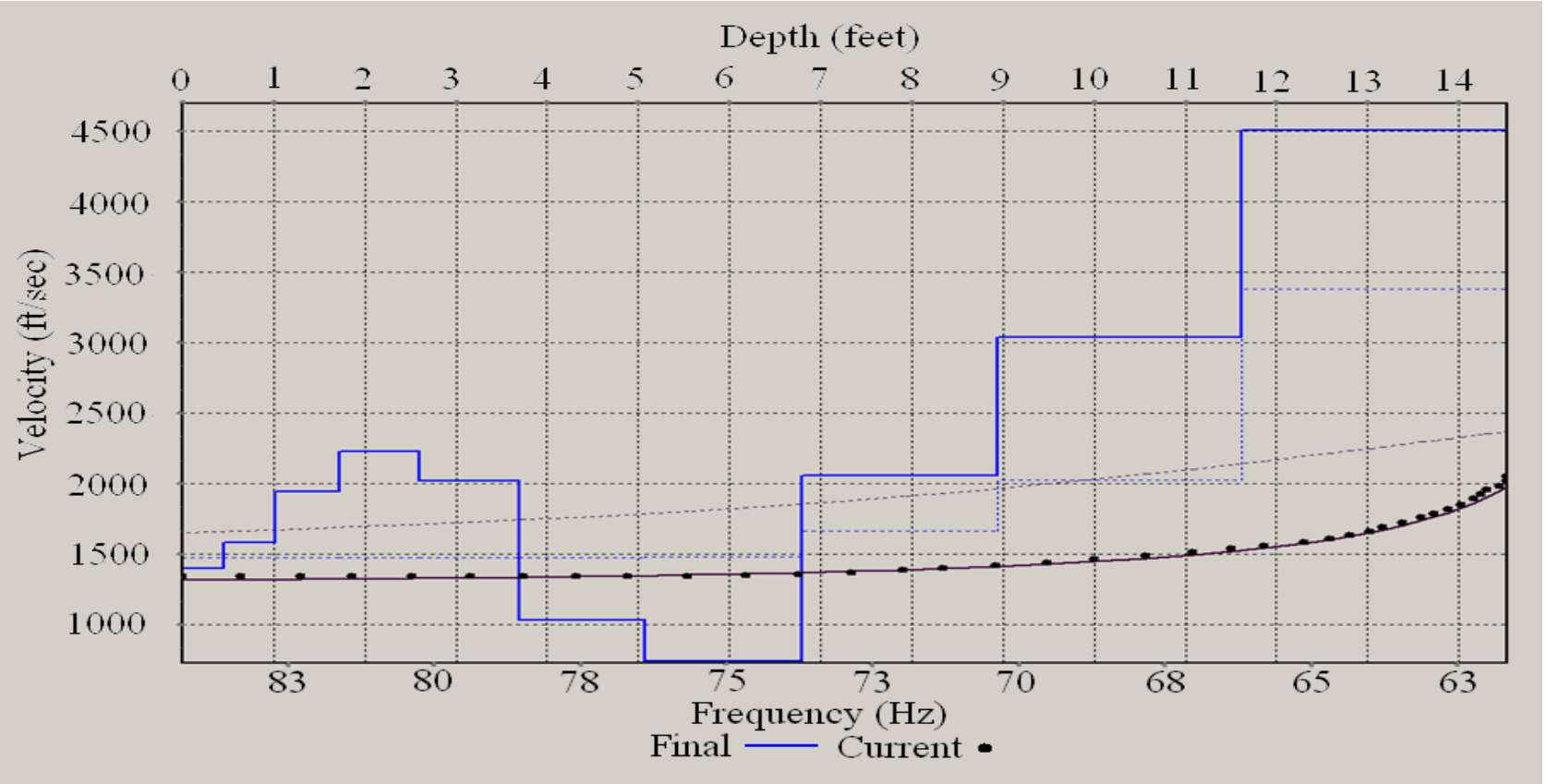

Figure 6.6: Often the velocities abruptly changed in the middle of a depth interval and the recorded velocity had to be estimated. The following are the recorded velocities (fps) at each depth interval: 0'-1' = 1500; 1'-2' = 2100; 2'-3' = 2100; 3'-4' = 1750; 4'-5' = 1000; 5'-6' = 500; 6'-7' = 750; 7'-8' = 2050; 8'-9' = 2050; 9'-10' = 3000.

The author maintained a very detailed field log to ensure that he was relating the correct data to each pre and/or post blast areas. Once all of the pre and post blast velocities were recorded, they were interpreted with Microsoft Excel. Appendix B contains the blast parameters and the recorded velocities associated with each shot area that used the LV detonating cord in the boreholes. The pre and post blast average velocities of each depth interval were then calculated and graphically plotted so one would be able to interpret the structural integrity of the stone before and after a blast.

Similarly, Appendix C contains the blast parameters and the recorded velocities associated with each shot area that used the high velocity detonating cord in the boreholes. The same interpretation process was conducted by averaging the pre and post blast velocities of each depth interval and graphically plotting them so one would be able to easily interpret the structural integrity of the stone before and after a blast.

The recorded pre and post blast average depth interval velocities of each shot area in Appendices B and C were copied to Appendix D. The 19 low velocity shots were compiled together in one chart. Then the average post blast Shear wave velocity was subtracted from the average pre blast Shear wave velocity at each 30.48 cm (1') depth interval. These values were then averaged together at depth intervals of 30.48 cm (1') into the deposit from the borehole location to calculate the "Delta Bar Interval Average" (DBIA). This same procedure was done separately for the 20 shots that used the high velocity cord. These values enabled the author to analyze the LV and HV shots separately by interpreting the average change in the Shear wave velocity at each depth interval away from the split line from 0-0.30 meters (0'-1') to 2.13-2.44 meters (7'-8'). However, because the burden changed on every shot, the sample population decreased as the depth from the split line increased.

The burden ranged from 0.61 to 2.13 meters (2'-7'), but typically the burden blasted away was 0.91 or 1.22 meters (3' or 4'). The burden on each shot was measured from the face where the pre blast survey geophones were located to the row of drilled blast holes. This distance was then rounded to the nearest 30.48 cm (1') because the author was specifically interested in determining the change in the Shear wave velocity within the stone deposit at depth intervals of 30.48 cm (1') from the split line.

A post blast survey that showed a decrease in the Shear wave velocity indicated that the structural integrity of the stone had been compromised from the blast at that specific depth interval from the split line and one could then quantify the BID. In this instance, the DBIA would be positive. However, due to the presence of instrument and human error, a decrease in the Shear wave velocity of approximately 60 m/s (200 fps) was tolerated [Anderson, 2010] and the author only concluded that a significant amount of BID occurred when the DBIA was greater than 60 m/s (200 fps). Conversely, a DBIA that was less than or equal to zero indicated that the post blast Shear wave velocity was higher than the pre blast Shear wave velocity. In theory, this indicates that the blast improved the structural integrity of the stone. The author attributes this to not having ideal MASW field parameters, not being experienced with the MASW software, and the constant change in geology of the region from weathered to non weathered stone.

When pre blast MASW data were analyzed in the lab, very low seismic velocities were characteristic of the weathered areas. A pre blast survey that was conducted on a virgin face would typically generate velocity profiles that were approximately 365-550 m/s (1200-1800 fps). Once the virgin rock was blasted away, a non weathered surface was exposed to conduct a post blast survey on. The exposed non weathered surface was considerably more structurally competent than the virgin face, and the velocity profiles generated typically ranged from 610-1100 m/s (2000-3600 fps), depending on the region. Figure 6.7 illustrates this, not only showing how the integrity of the region changed through short distances, but also that the blasting practices that were implemented were properly splitting the stone and not damaging the strength of the remaining rock mass. For the purpose of this study, when the DBIA was less than or equal to the tolerance level of 60 m/s (200 fps), the author concluded that the shot did not significantly change the Shear wave velocity of the sandstone, and therefore no BID resulted from the shot.

Because the author determined that the velocity profiles generated on virgin faces were much different than those generated on non-virgin faces, a DBIA was calculated for "all shots inclusive," for "only virgin faces," as well as for "virgin faces excluded." These values were then graphically plotted so one could easily compare them (Figures 6.8 and 6.9).

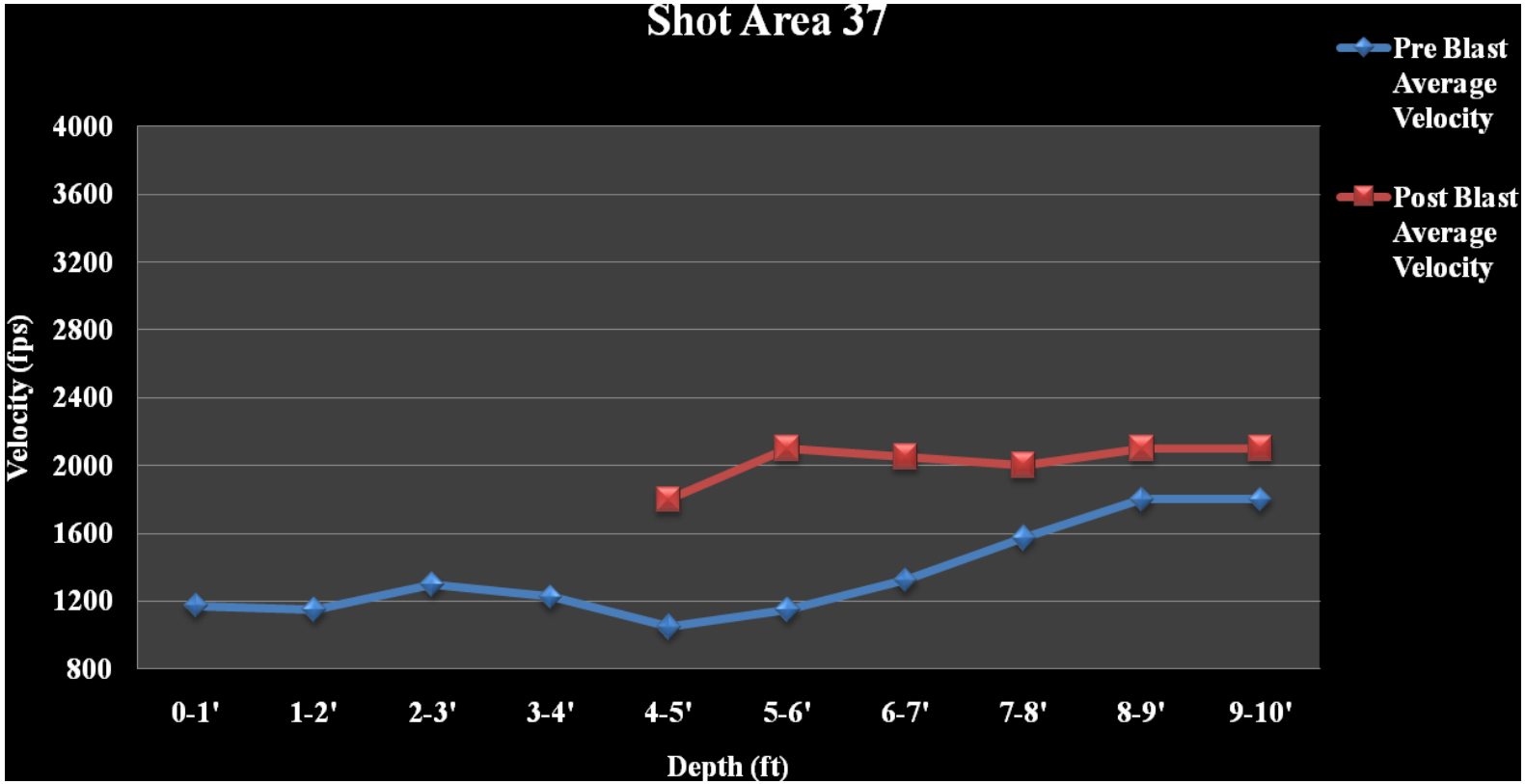

Figure 6.7: When shots were performed on virgin faces, the weathered surfaces were blasted away exposing a non weathered face. The post blast surface was considerably more structurally competent than the weathered surface where the pre blast survey was conducted. The MASW data illustrated this phenomenon.

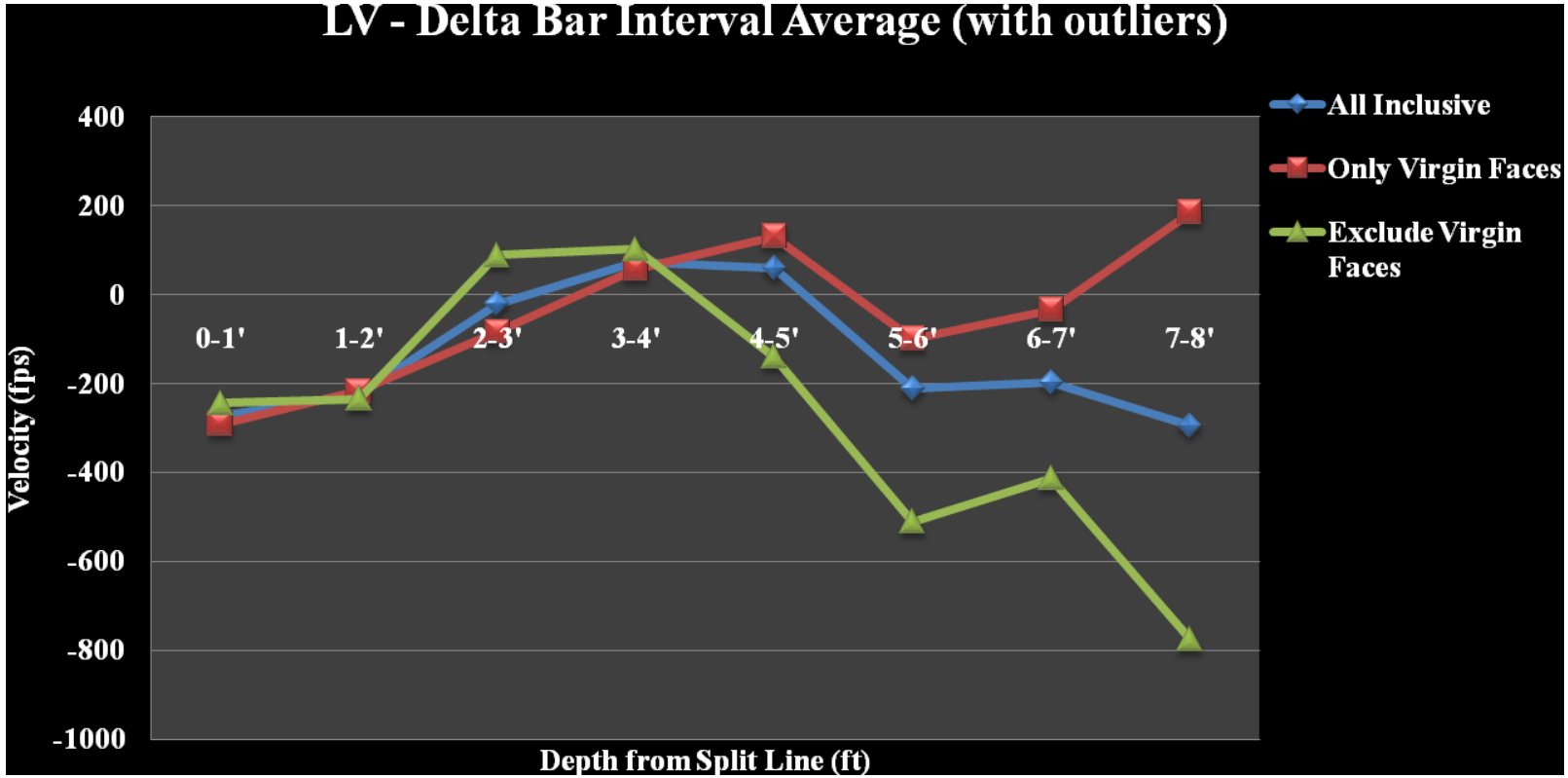

Figure 6.8: Using the low velocity detonating cord, the "Delta Bar Interval Averages" were plotted separately for "all shots inclusive," "only virgin faces," as well as "virgin faces excluded."

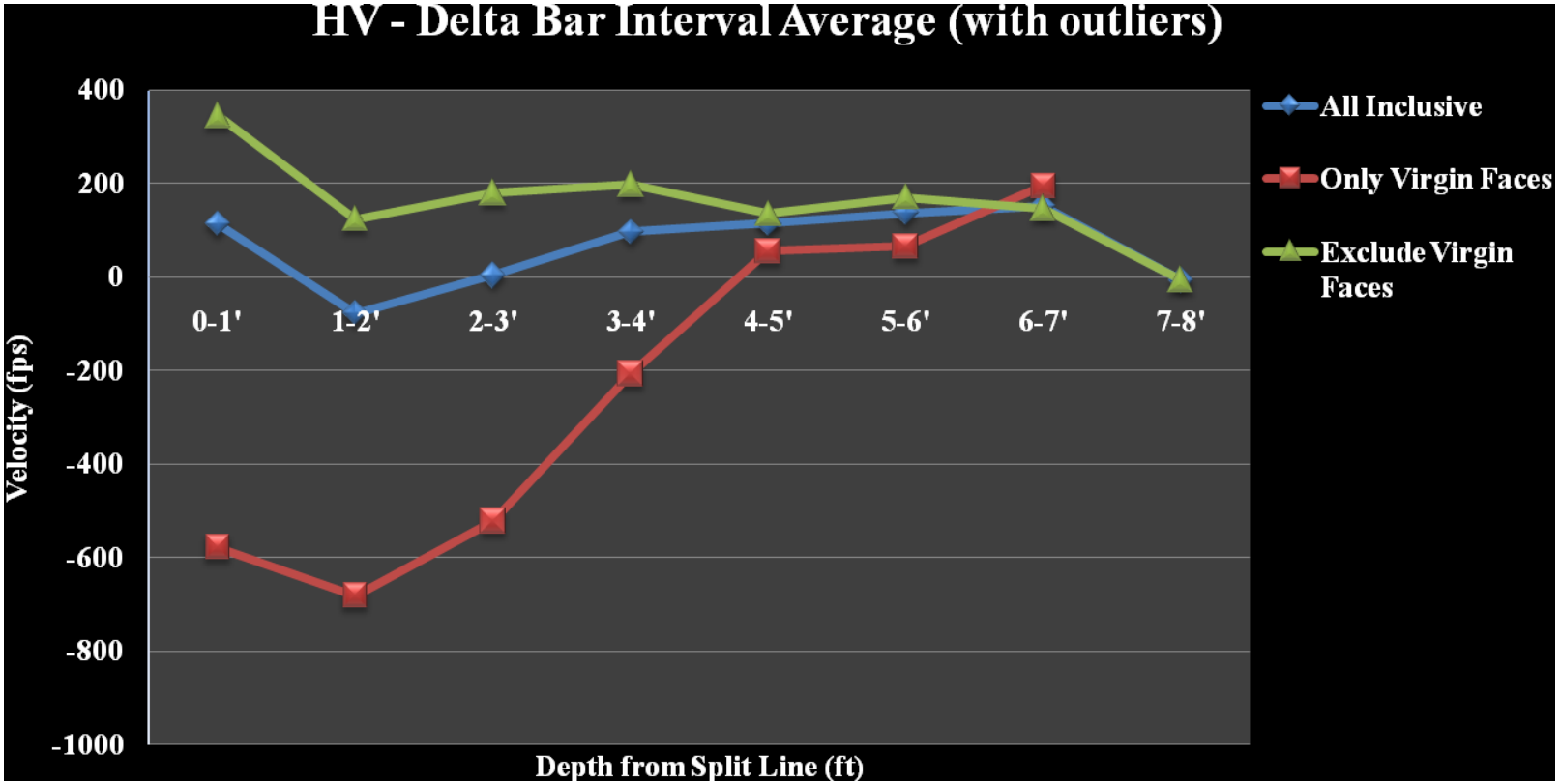

Figure 6.9: Using the high velocity detonating cord, the "Delta Bar Interval Averages" were plotted separately for "all shots inclusive," "only virgin faces," as well as "virgin faces excluded."

Upon investigation, these graphs did not seem accurate to the author and further interpretation was necessary to reach a conclusion about BID and the affect the explosives were having on the stone with some degree of accuracy or precision. There was a wide statistical variance amongst the values that were used to generate the "Delta Bar Interval Averages" for both LV and HV shots. The standard deviation shows how much variation there is from the sample's average. A low standard deviation indicates that the data points tend to be very close to the average, whereas a high standard deviation indicates that the data are spread out over a large range of values [Standard Deviation, 2010]. In theory, the standard deviation of each DBIA should have been very small indicating that the average change in the Shear wave velocity was similar from one shot area to the next at each depth interval away from the split line. However, this was not the case as the shot areas' interval averages used to generate the DBIAs displayed much variance. The standard deviation of each DBIA was calculated in Appendix D. The sets of data produced using the low velocity cord varied as high as 277 m/s (909 fps) away from the DBIA, while the sets of data produced using the high velocity cord varied as high as 308 m/s (1012 fps) away from the DBIA. To reduce the standard deviation of each DBIA, the author reanalyzed the data that are presented in Appendix B and C but eliminated values from the averages that were to be considered outliers. In turn, this would construct new data that was normally distributed and would be much more manageable to formulate meaningful conclusions with.

The uncontrollable sources of error produced "noisy" data. In turn, the velocity profiles were inconsistent at each depth interval as indicated by the high standard deviation of each DBIA. Appendices B and C present the average pre and post blast Shear wave velocities of each depth interval specific to each shot area. These values were calculated by averaging all of the Shear wave velocities that were recorded during the data processing of each shot area individually. The velocities in each of these depth intervals were not normally distributed. That is, though several of the recorded Shear wave velocities repeated themselves in each depth interval, many values varied significantly away from the normal, and skewed the calculated average Shear wave velocity in the depth interval. These gross deviations were outliers [Kiemele, 1994] and prevented the author from generating accurate data. To acquire a normal distribution at

each depth interval, the author used equation 6.1 [Kiemele, 1994] to eliminate the outliers.

$X \pm (1.96)(s/\sqrt{n})$ Equation 6.1

Where:

X = average Shear wave velocity of the depth interval
1.96 = 95% Confidence Interval constant
s = standard deviation
n = sample size

Equation 6.1 eliminates values that deviate significantly away from the average Shear wave velocity with a 95% confidence level. Any recorded value that was not within an allowable range ($\pm$ 1.96*(s/√n)) of the overall depth interval Shear wave average velocity was excluded from the data set and not used to calculate the final average pre or post blast Shear wave velocity in that depth interval. Table 6.1 illustrates a typical amount of recorded values that were ultimately determined outliers after applying Equation 6.1. The values in red are the velocities that fell outside of that depth interval's allowable range.

Appendix E contains the blast parameters and the recorded velocities associated with each shot location that used the low velocity detonating cord in the boreholes once the outliers were defined but not included in the averages. Similarly, Appendix F contains the blast parameters and the recorded velocities associated with each shot location that used the high velocity detonating cord in the boreholes once the outliers were defined but not included in the averages. To graphically display the average pre and post blast Shear wave velocity at each depth interval of the newly constructed data, the same interpretation process that was conducted in Appendices B and C was completed in Appendices E and F so one would be able to easily interpret the structural integrity of the stone before and after a blast.

Table 6.1: The red values are Shear wave velocities that were considered to be outliers. In the event any recorded value did not fall between the upper and lower limit of the 95% confidence level allowable range (gray values in the last two rows of each depth interval) the values were excluded from the depth interval data set and not used to calculate the average pre or post blast Shear wave velocity of that depth interval.

Line	0-1’	1-2’	2-3’	3-4’	4-5’	5-6’	6-7’	7-8’	8-9’	9-10’
1343	3200	3500	3600	3500	3500	2350	2350	2300	2300	2300
1334	2500	2450	2450	2300	2250	2250	2300	2300	2450	2500
1335	2500	2350	2250	2150	2000	2000	2500	2500	2600	2750
1336	2600	2600	2600	2600	2600	2500	2500	2500	2500	2500
1337	2750	2750	2750	2600	2600	2500	2500	2500	2550	2500
95% CI +	2966	3130	3186	3089	3088	2502	2515	2516	2581	2650
95% CI -	2454	2330	2274	2171	2092	2138	2345	2324	2379	2370
1360	Burden Blasted Away				2000	2400	1900	1500	1650	2700
1361					2100	1750	1400	1800	2850	3000
1362					2500	3400	3200	2500	1500	1800
1363					2700	2750	2900	2900	2650	2400
1368					2150	1750	2250	3100	3250	2500
1369					2250	1900	2200	2750	3000	2500
1370					2600	2600	2700	2600	2350	2200
1371					2400	2400	2450	2500	2300	2150
95% CI +					2512	2762	2771	2833	2875	2657
95% CI -					2163	1976	1979	2080	2012	2143

The recorded average pre and post blast average velocities from Appendices E and F were copied to Appendix G, and the same procedure used on the values which included the outliers was conducted to calculate a “Delta Bar Interval Average” and a standard deviation of the new data set that eliminated the outliers. The standard deviation was noticeably decreased, which indicated that the data were more consistent as they varied much less away from the DBIA and the author could then make meaningful conclusions. As before, this procedure was carried out for the 19 shots that used the low velocity cord separately from the 20 shots that used the high velocity cord. The author

was able to collect data on the change in the Shear wave velocity from depth intervals of 0-0.30 meters (0'-1') to 1.52-1.83 meters (5'-6') into the stone from the split line.

An obvious problem with eliminating the outliers from the data was that the data were being manipulated in order to obtain meaningful and useful results. Some of the shot areas that were reanalyzed in Appendices E and F include more values that were considered outliers than values that were used during interpretation. The author questioned the statistical accuracy of eliminating so many values in the pre and post blast Shear wave velocity profiles. However, due to the unique nature of this experiment, and the results formulated without excluding outliers from the data, it would have been very difficult for the author to make any conclusions on the performed work or make any recommendations for future research that could be performed. The fact that so many values were determined to be outliers indicates that it is troublesome for the MASW method to generate consistent, high resolution, accurate data with this project's unique field geometry as it was applied in a sedimentary rock which changed in structural nature within short distances, and possessed many reflective surfaces.

With the outliers eliminated from the data, it was still evident that the velocity profiles generated on virgin faces were much different from those generated on non-virgin faces. Again a DBIA was calculated for "all shots inclusive," for "only virgin faces," as well as for "virgin faces excluded" (Figures 6.10 and 6.11).

The LV cord worked very well overall. Figure 6.10 shows that when low velocity cord was used to pre-split the sandstone, no BID was produced from the shot as the DBIAs are well below the tolerated level of approximately 60 m/s (200 fps) at every depth interval. The average Shear wave velocity never decreased more 30 m/s (100 fps) at every depth interval when LV cord was used in the shots. However, it was very interesting to notice that the change in the Shear wave velocities represented by the DBIAs increased after approximately the first meter (0'-3') from the split line. This is evidence that disturbance in the stone at depth intervals more than one meter from the split line was possibly occurring.

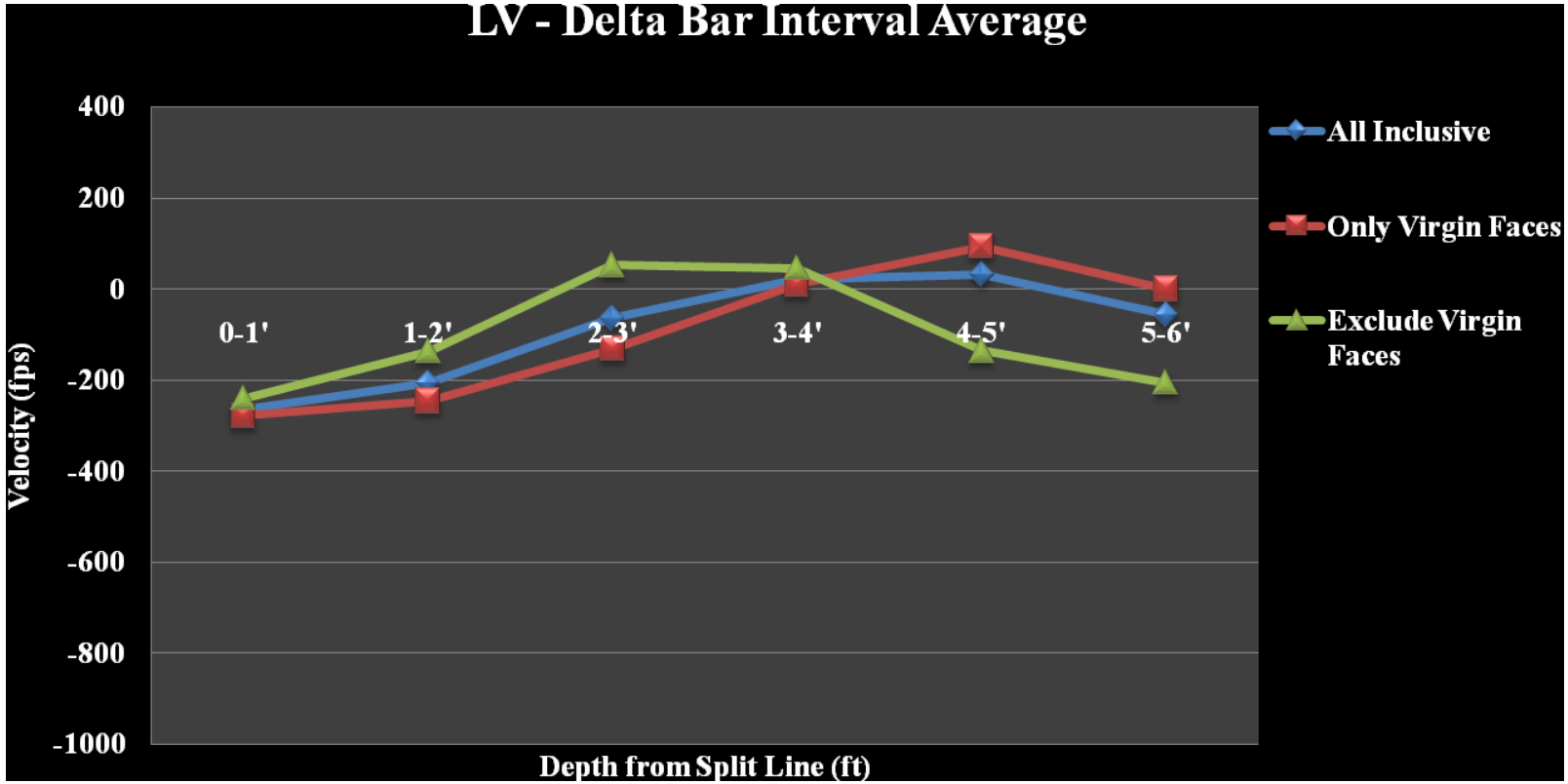

Figure 6.10: Using the low velocity detonating cord, the "Delta Bar Interval Averages" were plotted separately for "all shots inclusive," "only virgin faces," as well as "virgin faces excluded" with outliers excluded from the data.

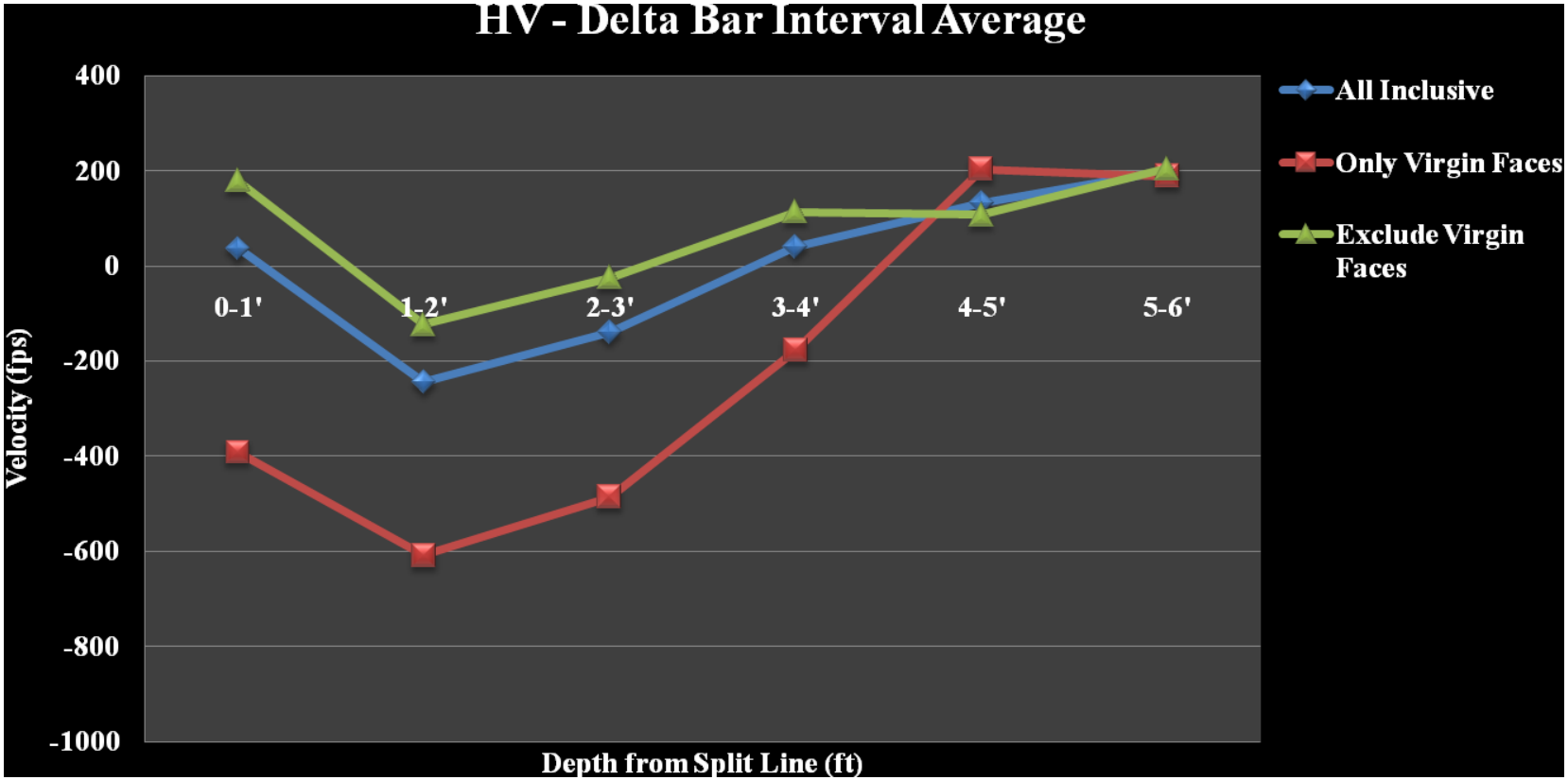

Figure 6.11: Using the high velocity detonating cord, the "Delta Bar Interval Averages" were plotted separately for "all shots inclusive," "only virgin faces," as well as "virgin faces excluded" with outliers excluded from the data.

Figure 6.11 shows that the high velocity cord also performed very well overall in this pre-splitting application as the change in the Shear wave velocity is consistently below the tolerated level of 60 m/s (200 fps) at every depth interval. Again, this change should be tolerated considering the potential for instrument and human error. Therefore, no significant BID can be determined when HV cord was used in this sandstone dimension stone quarry. However, it was again very interesting to notice that the DBIAs peaked at depth intervals several meters into the stone from the split line. This is evidence that the blast was disturbing the stone at depth intervals several meters from the split line, but not damaging the stone within the first meter from the boreholes where the explosives were placed.

To confirm that the low velocity cord produces less BID than the HV cord, the author compared the LV cord to the HV cord individually for "all shots inclusive," "only virgin faces," as well as "virgin faces excluded." Figures 6.12-6.14 show how the explosives performed in this pre-splitting application and which cord created less decrease in the Shear wave velocity at each depth interval from the split line.

The graphical plots indicate that both cords generated little or no damage overall. The cords acted very similarly when all shots were included. Never was the decrease in the Shear wave velocity more than approximately 60 m/s (200 fps) and this change can be tolerated considering the potential for instrument and human error. However, this research showed that the DBIAs for both cords consistently peaked at depth intervals several meters from the split line, away from the borehole location where the detonating cord was in contact with the surface of the sandstone. This potentially indicates a disturbance in the stone at these depths. The author researched explosives applications in the mining industry to formulate theoretical considerations of the results which would answer if a disturbance at a depth within the rock was common, and this will be discussed in Section 7.

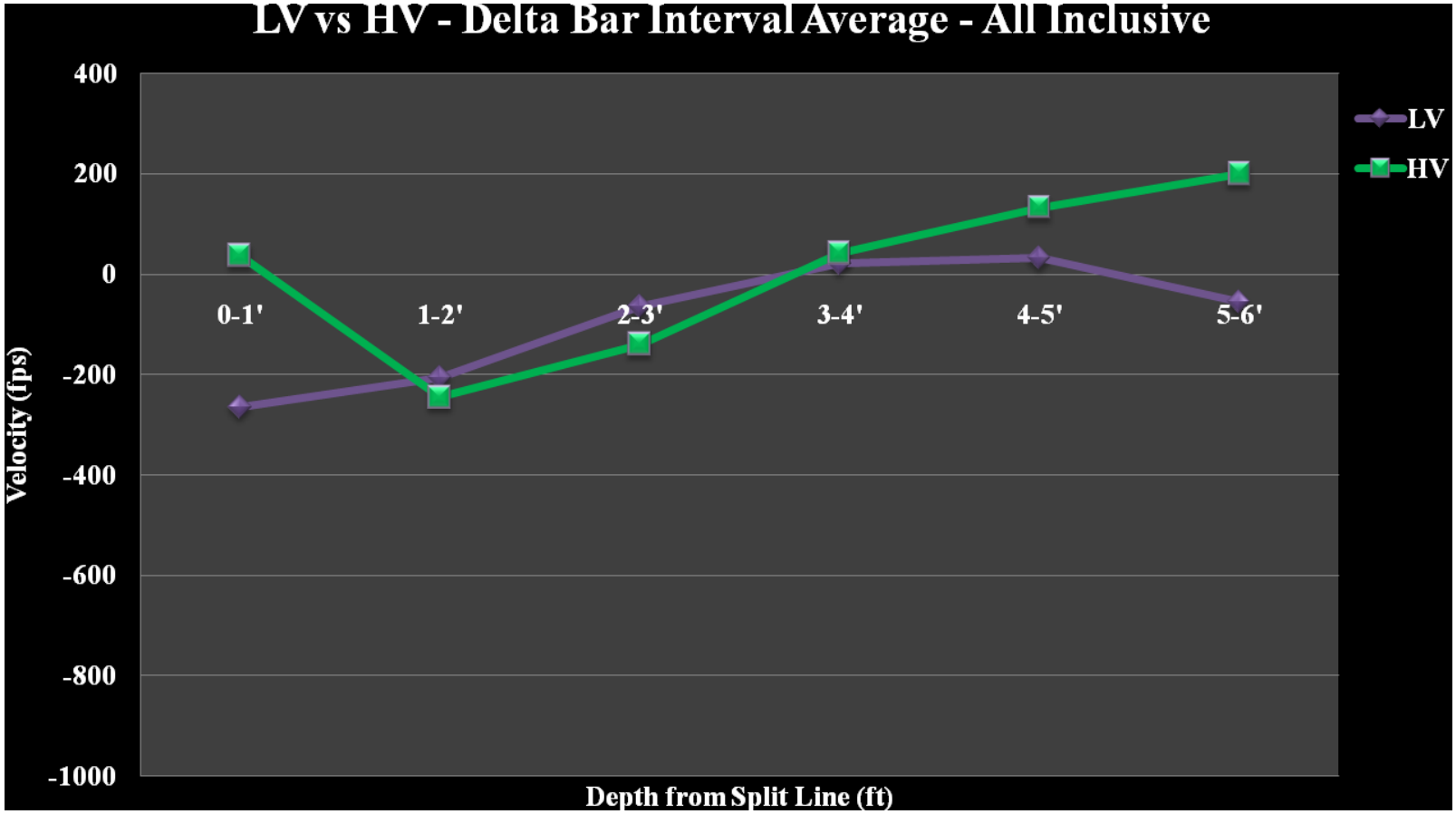

Figure 6.12: "Delta Bar Interval Averages" for shots "all inclusive" compare the low velocity cord to the high velocity cord.

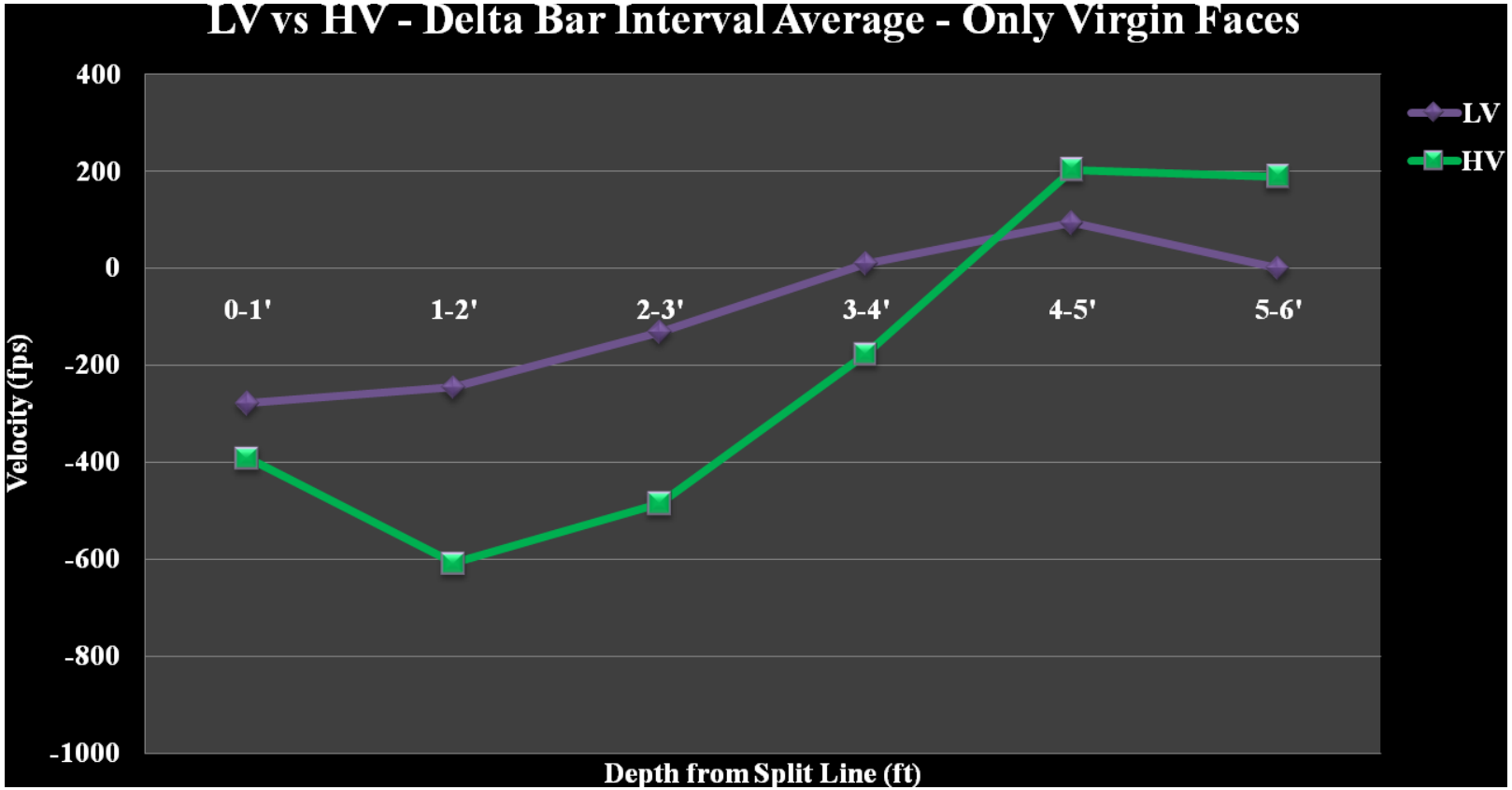

Figure 6.13: "Delta Bar Interval Averages" for shots "only virgin faces" compare the low velocity cord to the high velocity cord.

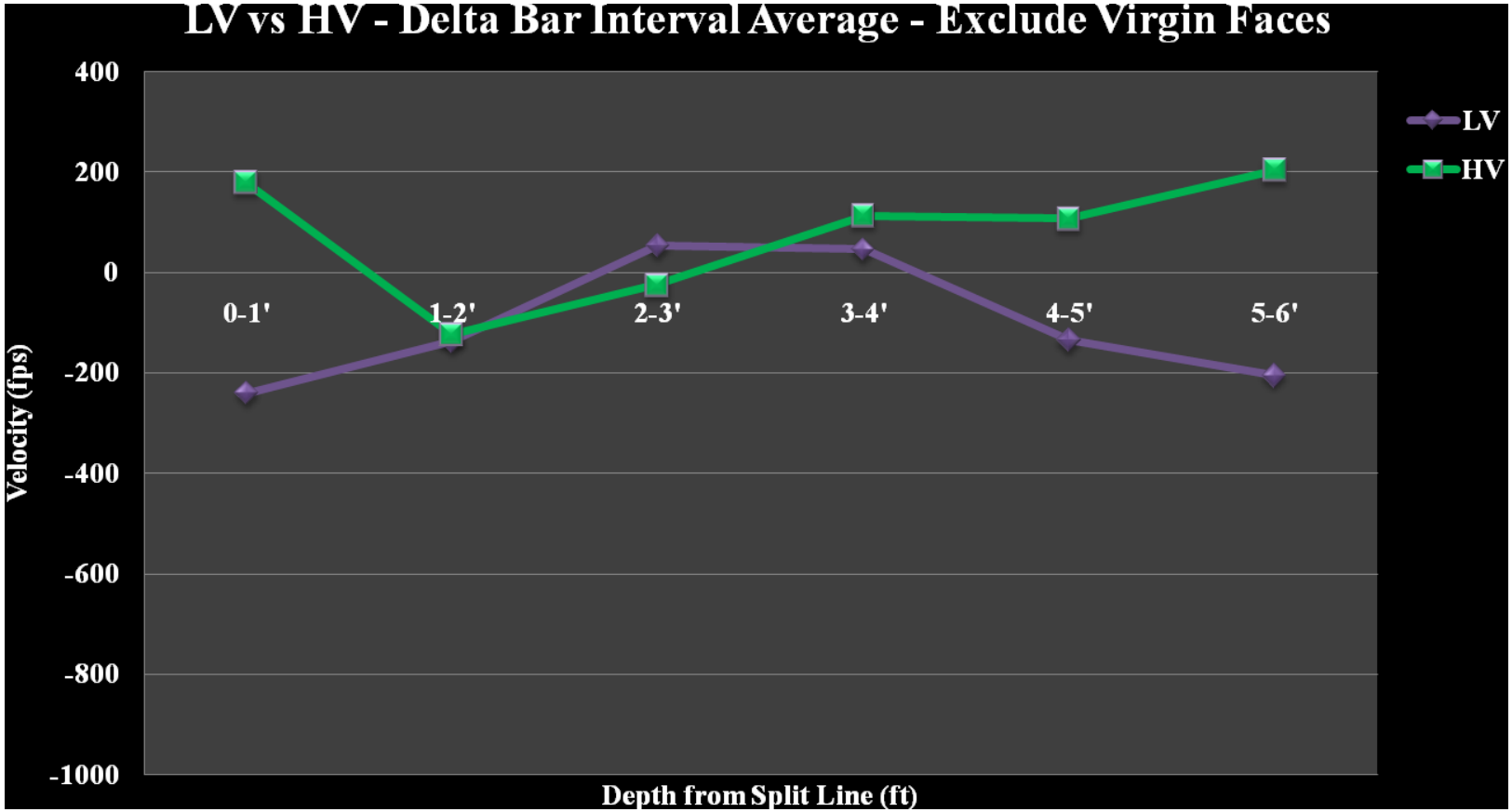

Figure 6.14: "Delta Bar Interval Averages" for shots "exclude virgin faces" compare the low velocity cord to the high velocity cord.

7. THEORETICAL CONSIDERATIONS OF THE RESULTS

After the outliers were eliminated from each shot area's pre and post blast averaged data, it was much easier to interpret results and formulate conclusions. Once the DBIAs excluded the outliers from the recorded velocities, the author reanalyzed the change in the Shear wave velocity at each depth interval from the split line individually to determine exactly where BID was occurring within the stone for LV and HV shots separately. The graphical plots generated during data interpretation (Figures 6.10-6.14) shows that both detonating cords work very well overall. No BID can be determined within the 3.05 meters (10') depth of investigation since the Shear wave velocity was not being decreased from the shots by more than 60 m/s (200 fps); this decrease was tolerated considering the potential for human and instrument error. However, the author noticed that the Shear wave velocity was generally mostly decreased at depth intervals several meters into the stone indicating that the structural integrity of the stone was being disturbed from the shot at these locations within the sandstone but not closest to the borehole location where the explosive charges were placed. To explain this phenomenon, the author speculated elastic rebound was occurring from the shots creating a disturbance in the structural integrity of the stone at depths several meters from the split line.

7.1. SPECULATION OF ELASTIC REBOUND

The main reason for this research was to determine whether or not the MASW method could be applied in mining and explosive engineering to monitor and quantify the BID produced at shallow depths into the stone from pre-split blasts. Moreover, the author expected BID to be evident at depths closest to where the explosives were placed by comparing the pre and post blast MASW surveys and observing a decrease in the Shear wave velocity. The Shear wave velocities of the pre and post blast surveys were expected to be practically identical at depths greater than approximately one meter (3') from the blasted surface. In turn, this would indicate that the structural integrity of the stone at depths greater than approximately one meter (3') from the split line was not compromised from the blast, as illustrated in Figure 7.1.

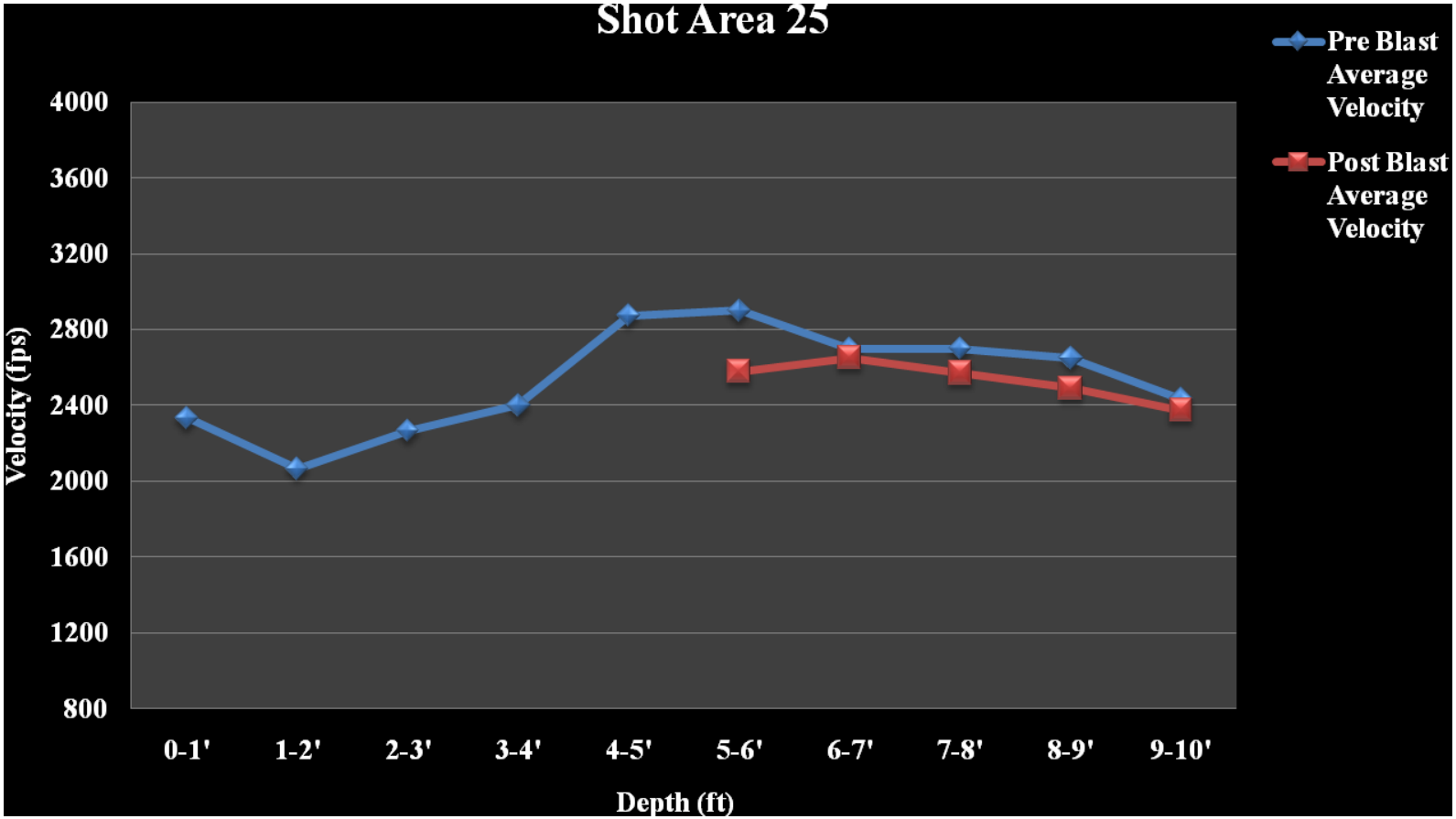

Figure 7.1: Shot area 25 illustrates how the author expected the Shear wave velocity to react from the blast.

Figure 7.1 is a comparison of the pre and post blast average Shear wave velocities at shot area 25 and the author expected most of the comparison graphs to resemble this. Within the first depth interval from the split line, the post blast average velocity decreased by 97.54 m/s (320 fps). The post blast Shear wave velocity then closely resembles the pre blast average velocity curve for the remainder of the graph indicating that the structural integrity of the stone is unchanged at these depths away from the split line.

However, the results from the data interpretation indicate that a pre-split blast may generate a decrease in the Shear wave velocity at depths several meters (3'-7') from the split line, while it is not decreased at depths closest to the boreholes' location, where the explosives were placed. This disturbance at depth intervals several meters into the stone can be a common result when pre-splitting is conducted in sandstone geology [Worsey, 2006].

The sandstone geology at the experimental location included many natural fractures, joint sets and seams. These geological features were essentially small air voids within the rock. The joints and seams developed naturally as the sandstone mass was deposited and the fractures most likely resulted from previous blasting operations performed at the sandstone quarry directly adjacent to the experimental testing location. Many of these air voids were evident by observing the surface of the stone. However, other air voids were certainly present that could not be detected, since they were very small or embedded within the stone and could not be seen on the surface of the rock. These air voids present in the sandstone deposit were potential areas that would allow elastic rebound to result from a pre-split blast [Worsey, 2006].

When the blast was initiated, the explosives provided a force onto the stone on both sides of the intended split line. The energy from the explosives pushed the burden away from the deposit and produced a loaf of dimension stone. The remainder of the stone in the deposit also reacted to the blast. The air voids in the sandstone deposit were potential areas where the stone could be pushed to when the blast supplied energy onto the deposit at the borehole locations. Rock is an elastic material. As the stone in the deposit was pushed into these air voids, it came into contact with the remainder of the

rock mass and then elastically rebounded away from the deposit to create an air void at that depth, several meters away from the split line (Figure 7.2). The rock rebounded a distance more than the original width of the air void, making this void larger than it was before the blast when the pre blast MASW survey was conducted [Worsey, 2006].

The seams, joint sets, and fractures present in the experimental test location that were potential areas where elastic rebound could occur ranged from a few centimeters wide to planes that were fractions of a millimeter. When the air voids were incredibly small, the pre blast MASW survey would not have detected this imperfection, and the Shear wave velocity would have remained generally uniform at every depth interval. However, after the rock elastically rebounded, and the small air voids were enlarged several meters away from the split line, the post blast survey was able to detect this area; therefore the Shear wave velocity profile showed an abrupt decrease at a depth interval several meters into the stone. The Shear wave velocity would then gradually increase and eventually show a velocity profile equal to the recorded pre blast Shear wave velocity, several meters after the rebound location [Worsey, 2006]. Figure 7.3 is a comparison of the pre and post blast average Shear wave velocities at shot area 19. The author found that the post blast Shear wave velocity profiles recorded from the MASW method would react in this manner in shot areas where there was potential for elastic rebound.

Elastic rebound is an important phenomenon for the Explosives Engineer to be aware of because it is disturbance of the structural integrity within the rock mass as a result of the blast. Air voids that are enlarged as a result of elastic rebound create areas within the stone that are not cemented together and are structurally incompetent. The natural features of the stone being blasted must be known to determine how the geology will react from the blast. The blaster must properly design each shot accordingly to preserve the integrity of the product, and to create a pre-split that creates a safe work area at the mine.

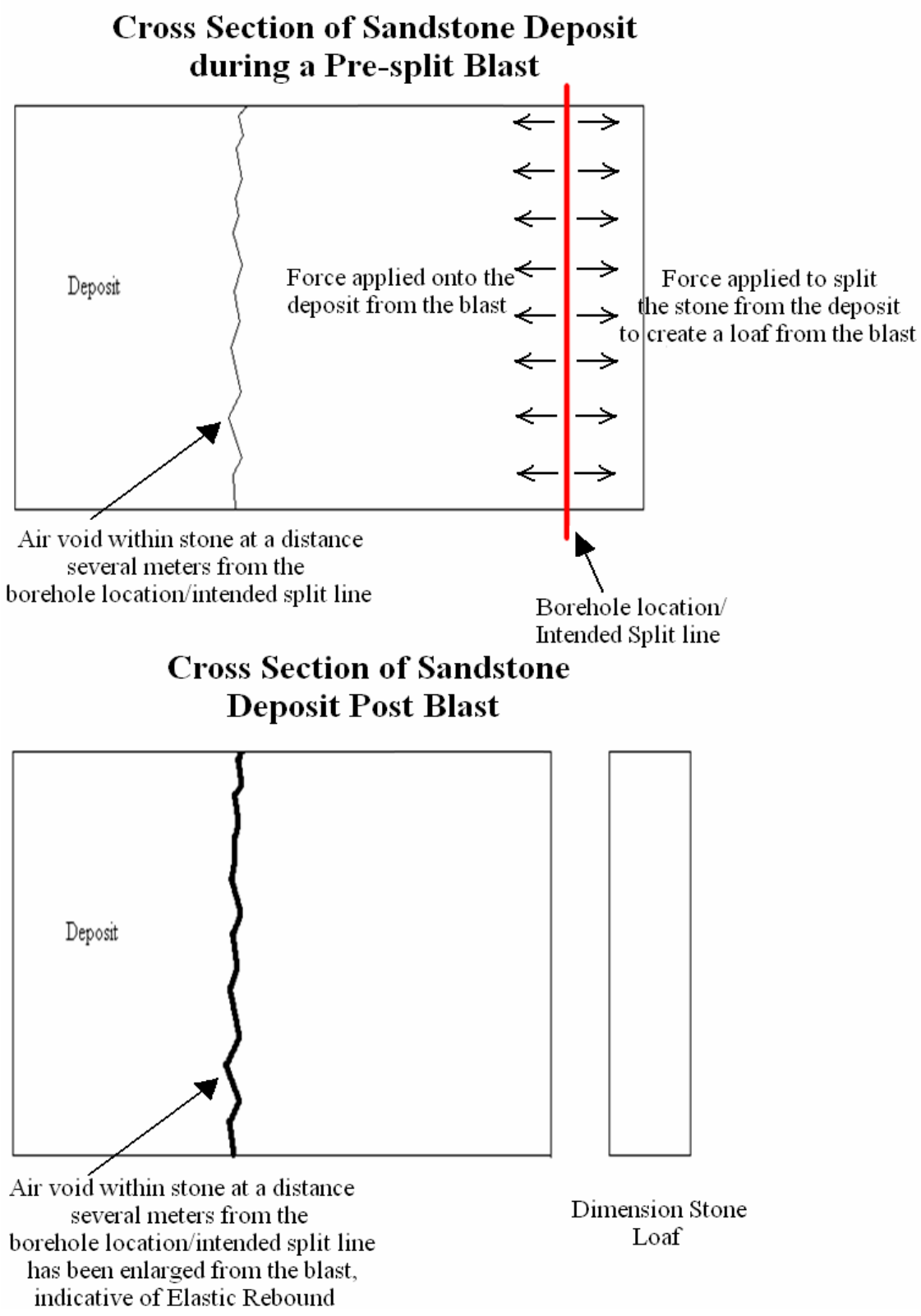

Figure 7.2: Cross Section of Sandstone before and after a Pre-split.

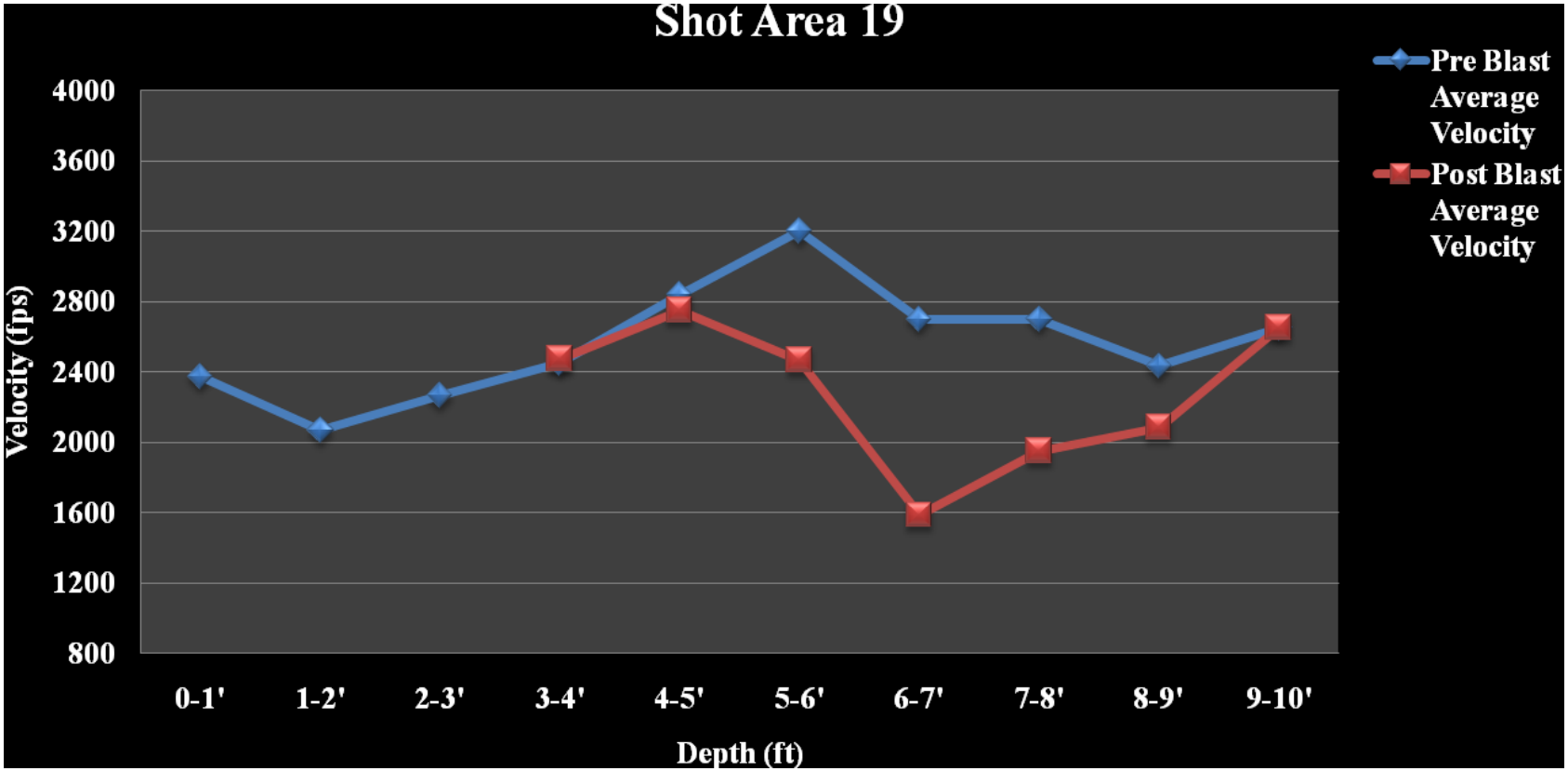

Figure 7.3: Shot area 19 illustrates how elastic rebound potentially was the cause of an abrupt decrease in the Shear wave velocity at depths 3'-7' from the split line. No change is noticed from the pre to the post blast average velocity until the depth interval of 5'-6' which is 3'-4' from the split line. The post blast average velocity was then consistently less than the pre blast average velocity until the last depth interval of 6'-7' from the split line, when it was reunited with the pre blast average velocity.

8. CONCLUSIONS

The main objective of this research experiment was to apply the MASW geophysical method to monitor and quantify Blast Induced Rock Damage that was produced from pre-splitting. The obtained data would answer whether or not the MASW method could be used regularly in the mining and explosives industry to quantify BID which in turn could improve blast design and create safe high-wall working conditions in surface mines, preserve the structural integrity of the rock deposit left behind, or to produce saleable loaves at dimension stone quarries.

The MASW geophysical method is relatively new technology that has a wide variety of applications. It has been used in mining exploration to determine the depths and thicknesses of the geological strata at a potential mine site. In these circumstances, typically the MASW instrumentation is spread linearly over a large area (10-30 meters) to image to depths as deep as 30 meters [Anderson, 2010]. It has been used extensively in the construction industry to develop information regarding the structural integrity of the subsurface or on much smaller scales in the transportation industry to identify damaged areas on asphalt or concrete pavements that are less than 15.24 cm (6”) thick at depth intervals of 7.62 cm (3”) with high resolution [Anderson, 2010].

Considering the blast parameters and the corresponding MASW field geometry utilized in this project, the MASW data should have been analyzed at 7.62 cm (3”) depth intervals within approximately the first meter (3’) from the split line to determine where BID was occurring from the shot because pre-splitting will not produce radial fracturing to depths more than half the spacing between boreholes [Worsey, 2006]. Unfortunately, the troublesome geology at the experimental location made it difficult for the MASW software to interpret depth intervals smaller than 30.48 cm (1’) with as high of a resolution that is used to locate damaged zones on asphalt pavements [Anderson, 2010]. The MASW software will provide high resolution on surfaces that are not weathered, that do not possess excessive reflection areas, and are of uniform thickness and strength [Anderson, 2010]. As these features were characteristic at the sandstone dimension stone quarry where this experiment was performed, this research could not take advantage of the MASW high resolution capabilities. The physical properties of the surface that is

being imaged by the MASW equipment is one of the most influencing factors as one is attempting to gather high resolution data (e.g., to depths of 7.62 cm (3")). Because the geology at mine sites is typically weathered, possesses excessive reflection areas (e.g., joint sets, fractures, and karst features), and is rarely of uniform thickness and strength, the MASW method should not be applied to monitor and quantify BID.

Because the MASW method cannot provide adequate resolution for this project, and considering the presence of instrumental and human error when processing the data, the author tolerated a decrease in the Shear wave velocity of 60 m/s (200 fps) before concluding that significant BID was resultant from the blast. In light of this, the author concludes that both LV Prima-Shear and HV Fire-line detonating cords perform very well in pre-splitting applications and neither of them produces a significant amount of BID when used correctly. However, the secondary objective of this experiment was to confirm that the low velocity cord produces less BID than the high velocity cord in pre-splitting applications. The Review of the Literature (see Section 2.3) indicated that the LV detonating cord will produce less pressure in the borehole during initiation which would yield less damage to the stone perpendicular to preferred split direction. However, the author could not draw a conclusion as to which detonating cord produced less BID by comparing the MASW pre and post blast data specifically because of the uncontrollable sources of error present in the geology of the region which disrupted the resolution and quality of the MASW data.

Though MASW is not applicable to monitor BID produced from pre-splitting, it is capable of performing on a larger scale to identify zones where existing joints or fractures have been enlarged from the blast. Often there would be rapid decreases in the post blast Shear wave velocity several meters from the split line, allowing the author to speculate that elastic rebound had occurred from the blast. Though the author did not intend to discover this phenomenon which is common when pre-splitting sedimentary stone, it is important to consider when blasting rock, for this disturbance at depths several meters from the borehole locations could compromise the structural integrity of the remaining rock mass or negatively influence the outcome of later shots performed in that area.

9. COMMENTS ON OPERATIONAL PROCEDURES AND RECOMMENDATIONS FOR POTENTIAL FUTURE WORK

The author concluded that the MASW geophysical method is not applicable to monitor and quantify Blast Induced Rock Damage from pre-splitting applications due to problems that will result when the subsurface being imaged possesses excessive reflection areas and is of heterogeneous thicknesses and strengths. Nonetheless, the MASW method is a very powerful geophysical tool when it is applied as it was intended for. The following operational procedures must be considered when performing MASW fieldwork:

To obtain meaningful information when applying the MASW geophysical method, a skilled geophysicist should process the data gathered from the field. To better analyze the shot gathers, dispersion curves, and velocity profiles, the interpreter must be experienced with the MASW software and all of its capabilities.

The MASW method is best performed in dry and warm conditions [Anderson, 2010]. Therefore, this method should be performed in the dry summer months when heavy precipitation will not affect the quality of the data recorded.

To obtain quality MASW data, the geophysicist must be mindful of the local geology. Faults, fractures and anomalies present in the deposit significantly influence the quality of the obtained information [Anderson, 2010]. These features create reflective surfaces for the seismic wave energy to bounce off. The MASW method produces the best results when it is performed in geological formations whose grains are very well cemented together, and do not possess any air voids in the stone -- such as karst features, natural bedding planes, joint sets, and/or fractures.

When the MASW method is performed in strata that vary in thickness and strength (e.g., in mining exploration), it should apply the MASW field geometry recommended by the instrumentation's manufacturer described in Section 2.6.2 of this report. The spacing between geophones determines the shallowest depth of investigation, as they are equal to each other [Surf-Seis, 2006]. Therefore, when applying MASW to mining exploration, the equipment will produce the best results when it images a wide

area of land (10-30 meters (30'-100')). Likewise, the geophone spacing must be at least 31.50 cm (12.41") in these circumstances.

The geophone spacing constraint discussed above further gives reason why MASW cannot be used to quantify BID from pre-splitting in heterogeneous material since ideally, to quantify BID, the depth intervals investigated should be approximately 7.62 cm (3") or less. The experiment discussed in this report required the geophone spacing and array to be radically decreased in order to gather information specific to each 1.52 meters (5') section of blasted stone. Though the MASW method did perform with this field geometry, high resolution data could not be acquired due to the troublesome geologic features characteristic in sandstone. To monitor and quantify BID from pre-splitting in heterogeneous material, different methods should be researched that will produce high resolution data when the experiment is performed over a larger scale (e.g., at least 10 meters wide). The following operational procedures must be considered when performing future work with a different geotechnical method:

Future work performed on a larger scale will demand that the drilling and blasting techniques be altered. The pre-split "rules of thumb" given in the Section 2.1 of the Review of the Literature should still be applied. Larger holes spaced farther apart will have to be implemented to effectively perform the experiment on a larger scale. In turn, this potentially allows future work to research precise sequential timing by incorporating the velocity of crack propagation and the velocity of detonation into the blast design. To do this, electronic initiation must be used with individual electronic blasting detonators tied to the "down-the-hole" explosive as they provide precise sequential timing. The holes should be programmed to initiate sequentially at millisecond intervals that are determined by the time it takes the stress fields between adjacent holes to interact (see Section 2.1.1).

Regardless of the geotechnical method that is used to gather BID data in future work, the sample population at each depth interval should be constant for the explosives being tested. In the project discussed in this report, 19-20 values were used to calculate the DBIAs within approximately one meter (0'-3') from the split line, while the depth intervals from 1.22-2.13 meters (4'-7') from the split line were calculated with as little as

two values. Using the blast design parameters that were applied to this project, the author concluded that the data should have been analyzed at 7.62 cm (3") depth intervals to determine where BID was occurring from the shot within approximately the first meter (3') from the split line. A smaller depth of investigation would ensure that the sample population at each depth interval is constant because the burden blasted away should have been no less than approximately one meter (3') with the blast parameters used in this experiment.

The strength of the stone that was blasted in this project changed within very short distances. Regardless of the geotechnical method that is further researched, all of the pre and post blast surveys should both be conducted on surfaces that have similar physical properties, therefore, the data can be interpreted as "all inclusive" rather than having to separate the shots performed on virgin faces from the shots performed on non-weathered stone. The weathered rock capped the competent stone for approximately the first 0.91-2.13 meters (3'-7'). This significantly disrupted the quality of the MASW data and introduced variation into the experimental procedure.

Variation in the experimental process creates data that are difficult to analyze and interpret. As conducted in this experiment's procedure, the researcher must make every attempt to minimize variation by keeping most of the variables constant and using maintained equipment, quality explosives, properly trained personnel, and a consistent, repetitive process. Uncontrollable sources of variation can be minimized by performing the experiment in different conditions, and with specialty personnel.

Different high resolution geotechnical methods need to be researched to obtain information regarding the structural integrity of a stone deposit before and after a blast. The data can then be compared to quantify the extent of BID that is being supplied by the explosives used in the blast design. Future work potentially will determine a method that has the ability to perfect pre-splitting applications in any type of geology, but it is imperative to limit the variation present in the procedure to obtain reliable and meaningful information of the Blast Induced Rock Damage.

APPENDIX A

MASW SHOT GATHERS, DISPERSION CURVES, AND VELOCITY PROFILES GENERATED FROM SURF-SEIS VERSION 2.05

1. INTRODUCTION

Included with this thesis is a CD-ROM, which contains the 270 sets of MASW data that was generated from conducting field work and from processing the data with the MASW software, Surf-Seis (Version 2.05). Each shot gather acquired from the field produced one dispersion curve and one velocity profile. Many sets of data were used for more than one pre and/or post blast survey. Each data set indicates which pre and/or post blast survey it was used for when the Shear wave velocities were recorded. All data sets are displayed in Microsoft Word 2007 document files. To view the file, the reader must have a computer equipped with Adobe 2007.

2. CONTENTS

Appendix A (MASW).pdf

APPENDIX B

PRE AND POST BLAST MASW DATA AND SHOT PARAMETERS FOR ALL LOW VELOCITY SHOTS

APPENDIX C

PRE AND POST BLAST MASW DATA AND SHOT PARAMETERS FOR ALL HIGH VELOCITY SHOTS

APPENDIX D

LV AND HV DELTA BAR INTERVAL AVERAGES AND STANDARD DEVIATIONS OF EACH DEPTH INTERVAL FROM THE SPLIT LINE

APPENDIX E

PRE AND POST BLAST MASW DATA AND SHOT PARAMETERS FOR ALL LOW VELOCITY SHOTS WITH OUTLIERS EXCLUDED

APPENDIX F

PRE AND POST BLAST MASW DATA AND SHOT PARAMETERS FOR ALL HIGH VELOCITY SHOTS WITH OUTLIERS EXCLUDED

APPENDIX G

LV AND HV DELTA BAR INTERVAL AVERAGES AND STANDARD DEVIATIONS OF EACH DEPTH INTERVAL FROM THE SPLIT LINE WITH OUTLIERS EXCLUDED

APPENDIX H

DETAILED INFORMATION OF THE REGIONAL GEOLOGY

BIBLIOGRAPHY

Anderson, Neil. Missouri University of Science and Technology. Geological Engineering Professor. 2010.

Barkley, Thomas L. Lee, Robert. Rodgers, Jay. *A New Detonating Cord for Reducing Unwanted Damage in Controlled Blasting*. ISEE Proceedings. 2001.

Cunningham, C.V.B. *The effect of timing precision on control of blasting effects*. Explosives and Blasting Techniques. Holmberg, Roger. Netherlands. 2000.

Iverson, Stephan R. Link, Curtis A. Singer, Janae A. *High Resolution Seismic Refraction Tomography for Determining Depth of blast Induced Damage in a Mine Wall*. ISEE Proceedings. 2009.

Kiemele, Mark J. Schmidt, Stephen R. Berdine, Ronald J. *Basic Statistics; Tools for Continuous Improvement*. Fourth Edition. Colorado Springs, CO. 1995.

Kihlstrom, B. Langefors, U. *The Modern Technique of Rock Blasting*. Third Edition. Wiley and Sons. 1978.

Lownds, C.M. *Measured shock pressures in the splitting of dimension stone*. Explosives and Blasting Techniques. Holmberg, Roger. Netherlands. 2000.

Proctor, Paul Dean. *Guidebook to the Geology of the Waynesville, Rolla and St. James Areas, Missouri*. Department of Geology and Geophysics. University of Missouri, Rolla. Second Edition. 1993.

Product Manual. *Non-el and Prima-cord*. 2005. Retrieved February 3, 2010 from: http://www.dynonobel.com/ProductAppGuideNONELDetCord.pdf.

Rayleigh Wave. *Wikipedia*. Retrieved February 3, 2010 from: http://en.wikipedia.org/wiki/Rayleigh_wave.

Seistronix. *RAS-24 Exploration Seismograph*. Retrieved February 3, 2010 from: http://seistronix.com/ras_g.htm.

Standard Deviation. *Wikipedia*. Retrieved May 20, 2010 from: http//en.wikipedia.org/wiki/Standard_deviation.

Surf-Seis. *Multi Channel Analysis of Surface Waves*. 2006. Retrieved February 3, 2010 from: http://www.kgs.ku.edu/software/surfseis/masw.html.

Tomography. *Wikipedia*. Retrieved June 1, 2010 from: http://en.wikipedia.org/wiki/Tomography.

Thompson, Thomas L. *The Stratigraphic Succession in Missouri*. Missouri Department of Natural Resources, Division of Geology and Land Survey. 1995.

Worsey, Paul N. *Bulk Blasting vs. Presplit Blasting*. Mining Engineering 307 Lecture. University of Missouri, Rolla. Rolla, MO. 2006.

VITA

Charles B. Zdazinsky (born in St. Louis, Missouri, on July 21, 1985) has always shown great perseverance and hard work ethic in tasks that were presented before him. His goal oriented personality excels mostly in areas that he shows great passion for. Charles found explosive design and theory very fascinating early in his college years and strived to complete the necessary steps in order to turn this passion into his career.

Charles was very fond of his grandfather, Louis Jantzen, and wished to follow in his footsteps by studying to be an engineer. He was accepted into the University of Missouri, Rolla (UMR) and graduated Magna Cum Laude from the Mining Department in December, 2008.

As an undergraduate student, he focused his education in blasting by completing extra technical explosive courses and earned both a minor and a certificate in Explosive Engineering. Though he had the opportunity to enter the mining industry as an engineer, he decided to follow his passion and earn a Master of Science degree in Explosive Engineering by August, 2010. This decision allowed him to not only become more specialized in the explosives field, but to improve his problem solving and project management skills.

Charles Zdazinsky is a “high-caliber, forward thinking, energetic, engineer” and his "can-do" attitude will enable him to thrive in any working environment. Charles is very proud to hold his degrees from Missouri S&T and credits the University for helping him accomplish his goals.

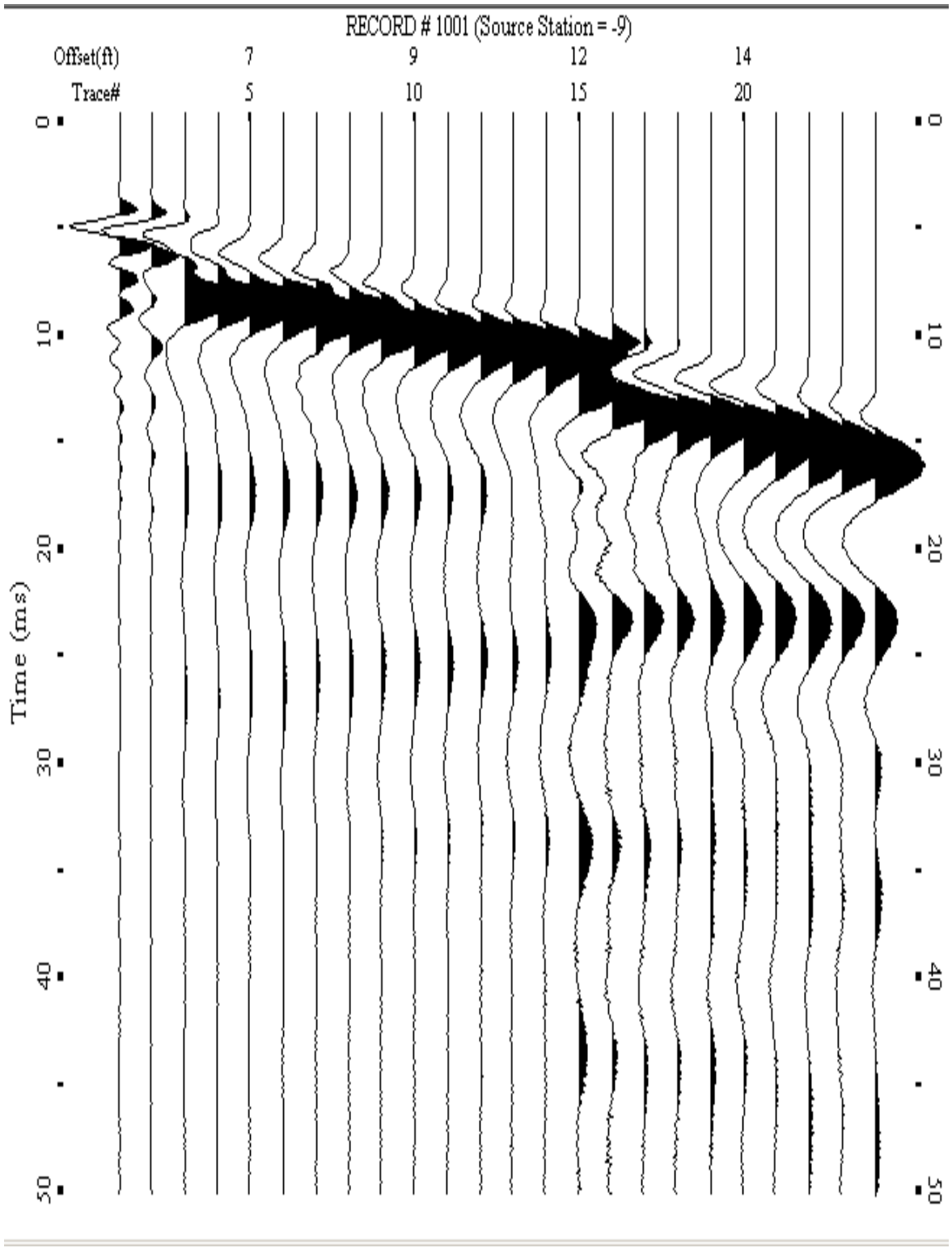

A.001: Shot Gather Line 1000 used in Pre-blast 6

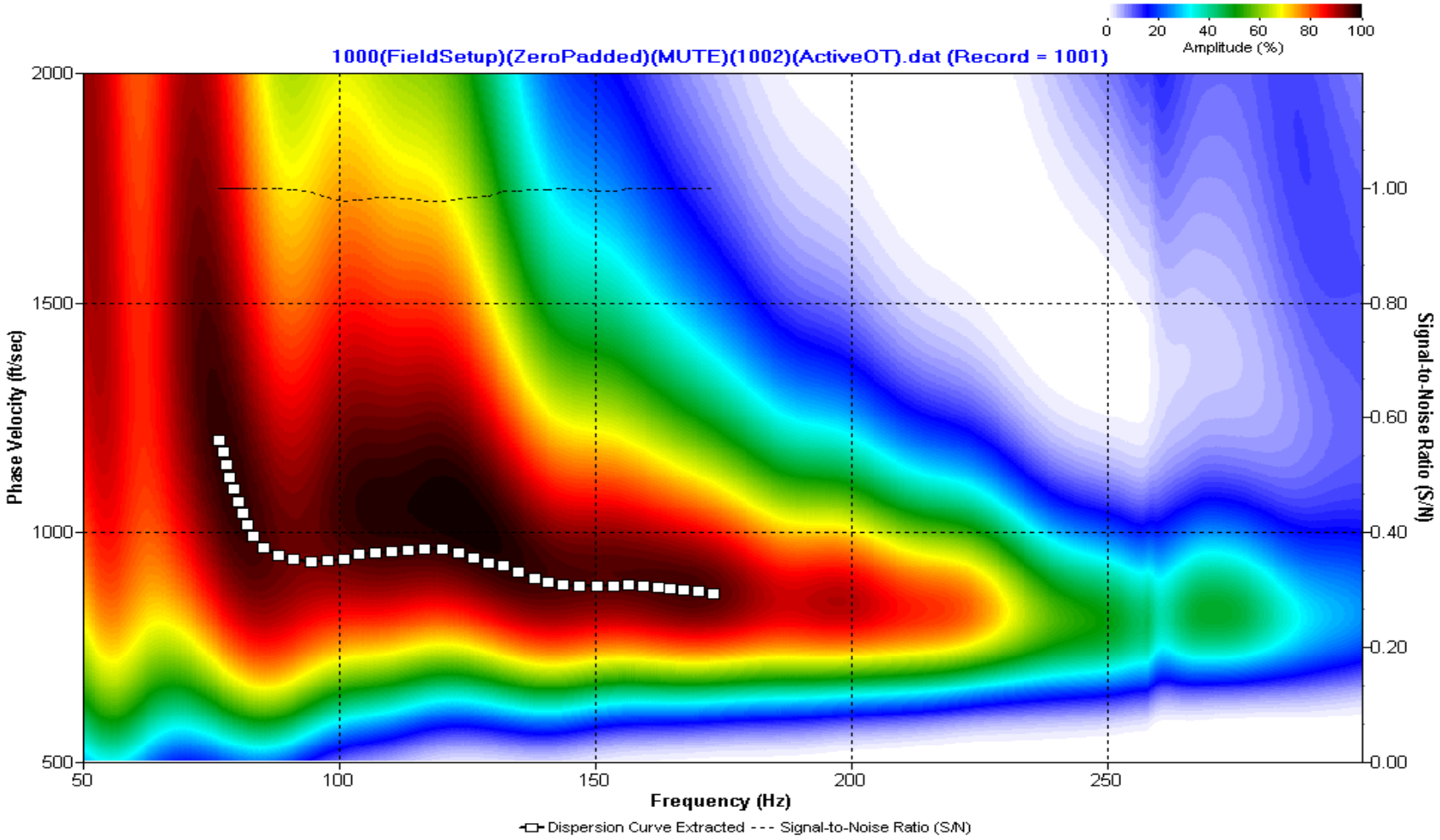

A.002: Dispersion Curve Line 1000 used in Pre-blast 6

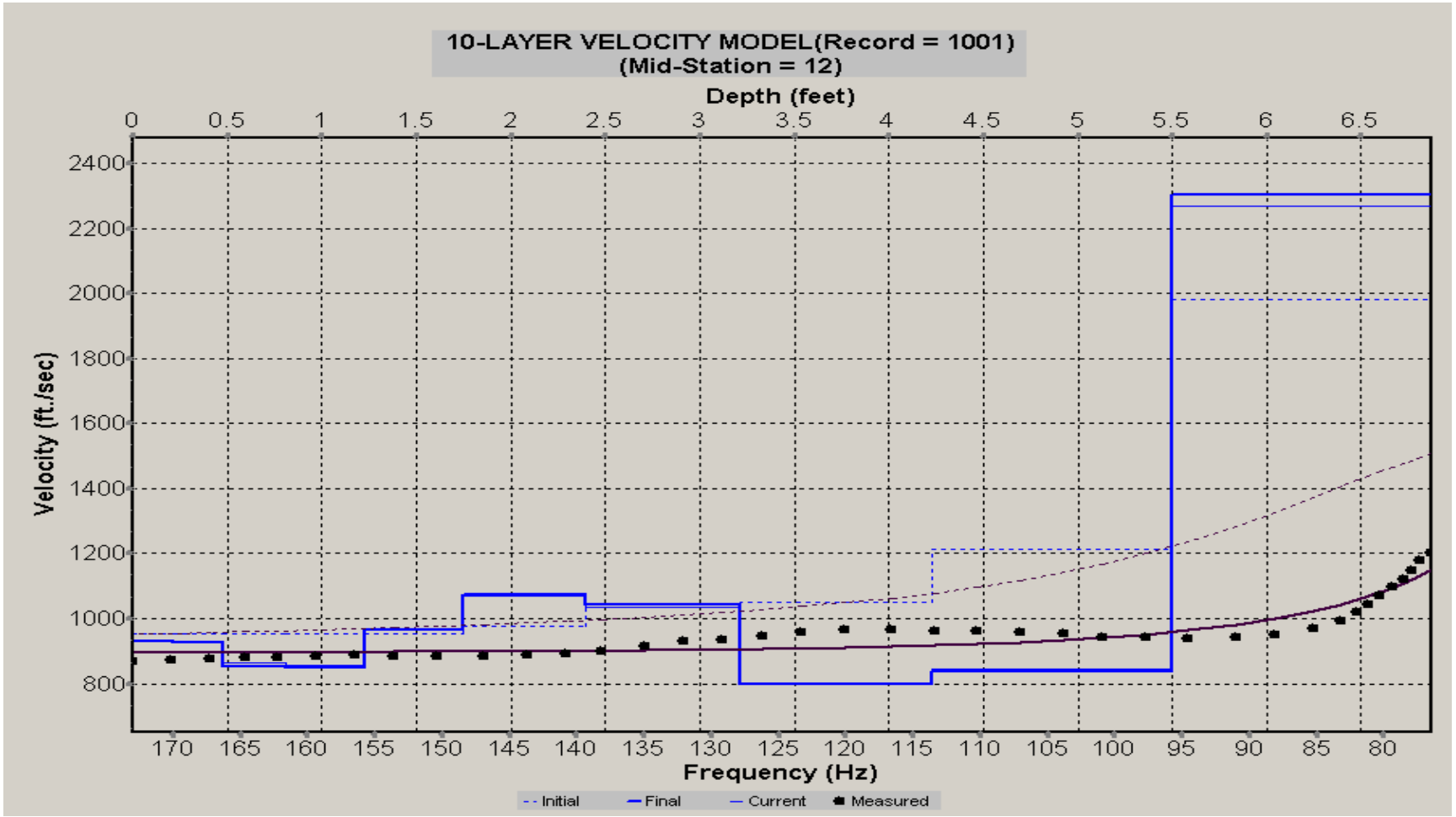

A.003: Velocity Profile Line 1000 used in Pre-blast 6

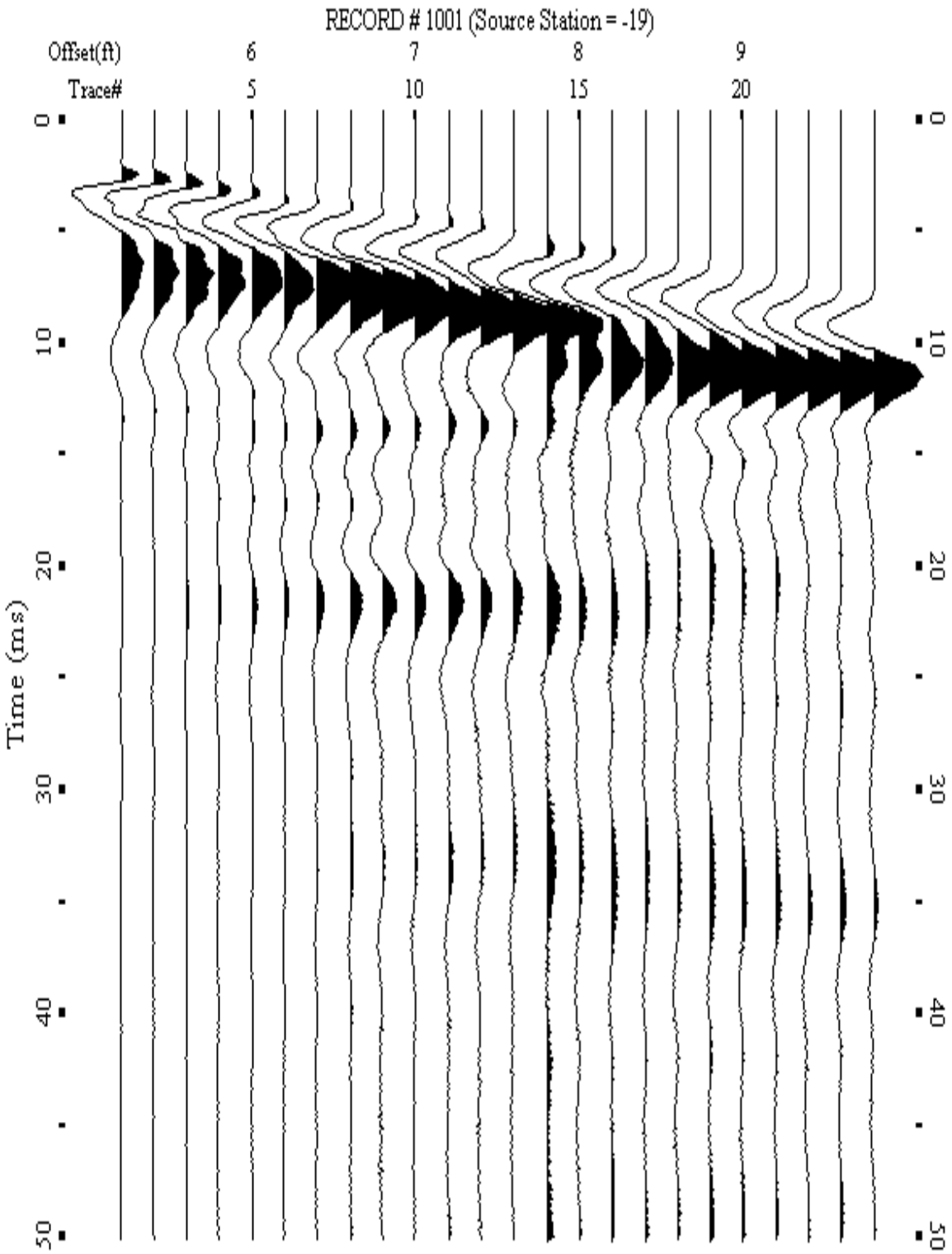

A.004: Shot Gather Line 1001 used in Pre-blast 6

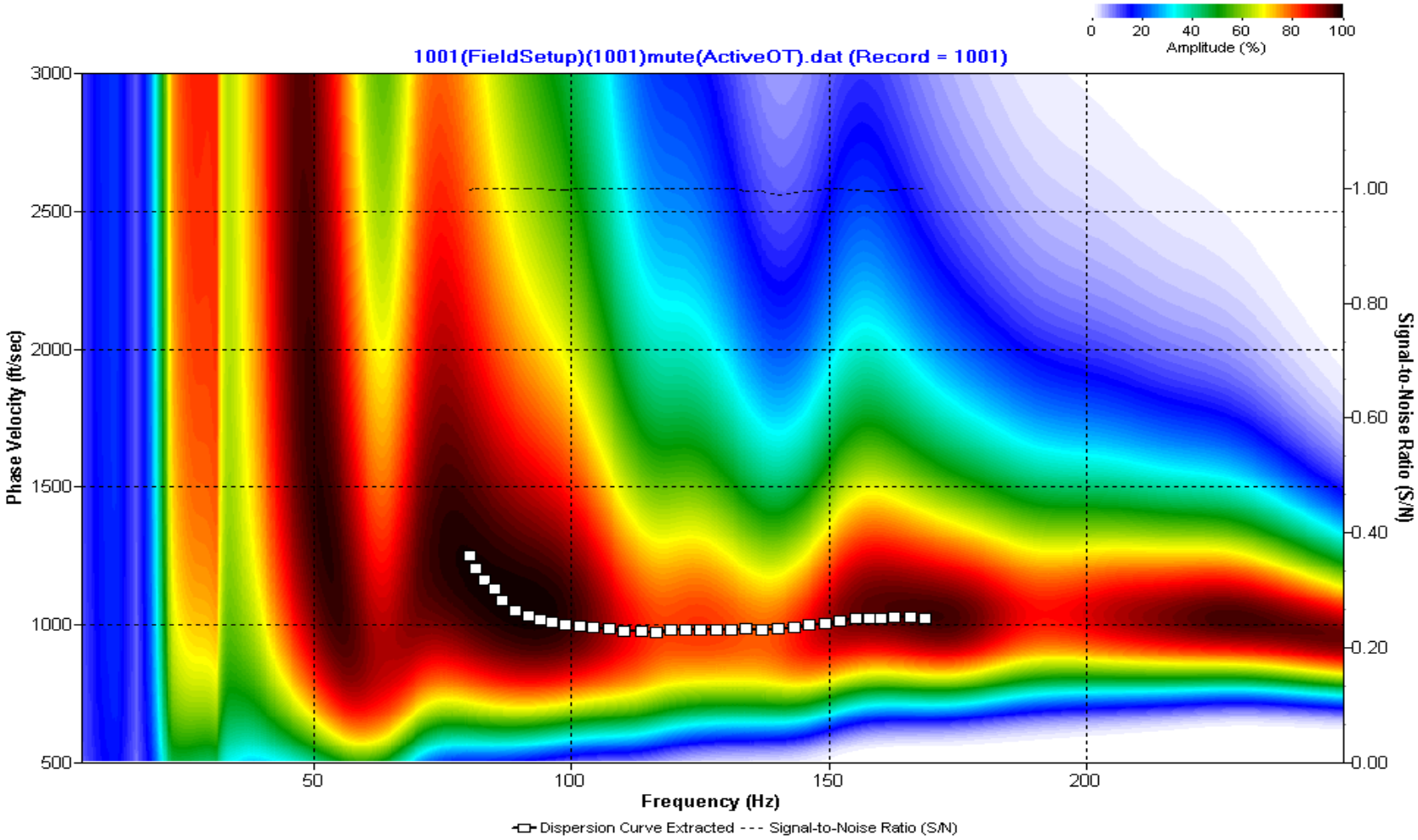

A.005: Dispersion Curve Line 1001 used in Pre-blast 6

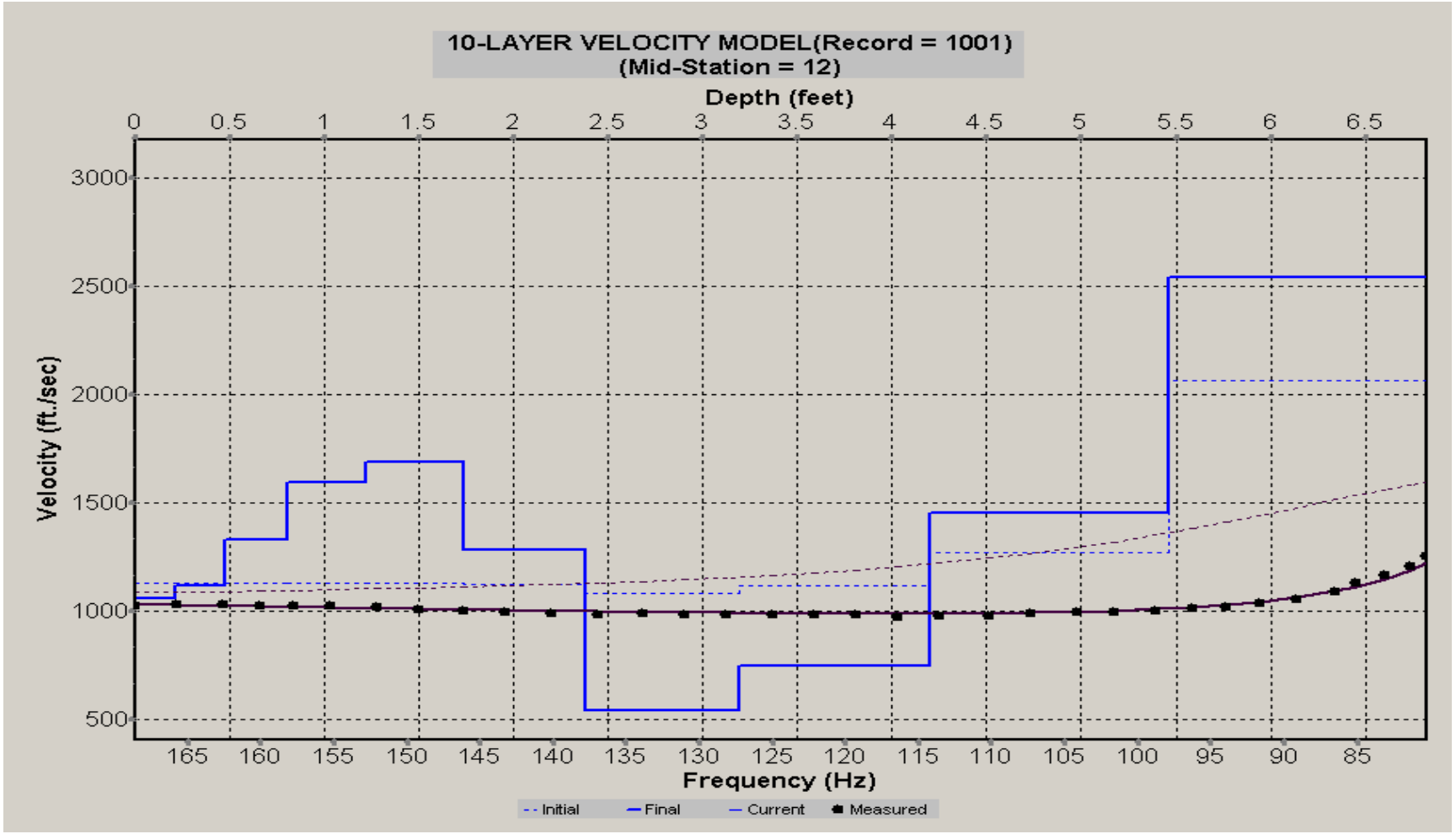

A.006: Velocity Profile Line 1001 used in Pre-blast 6

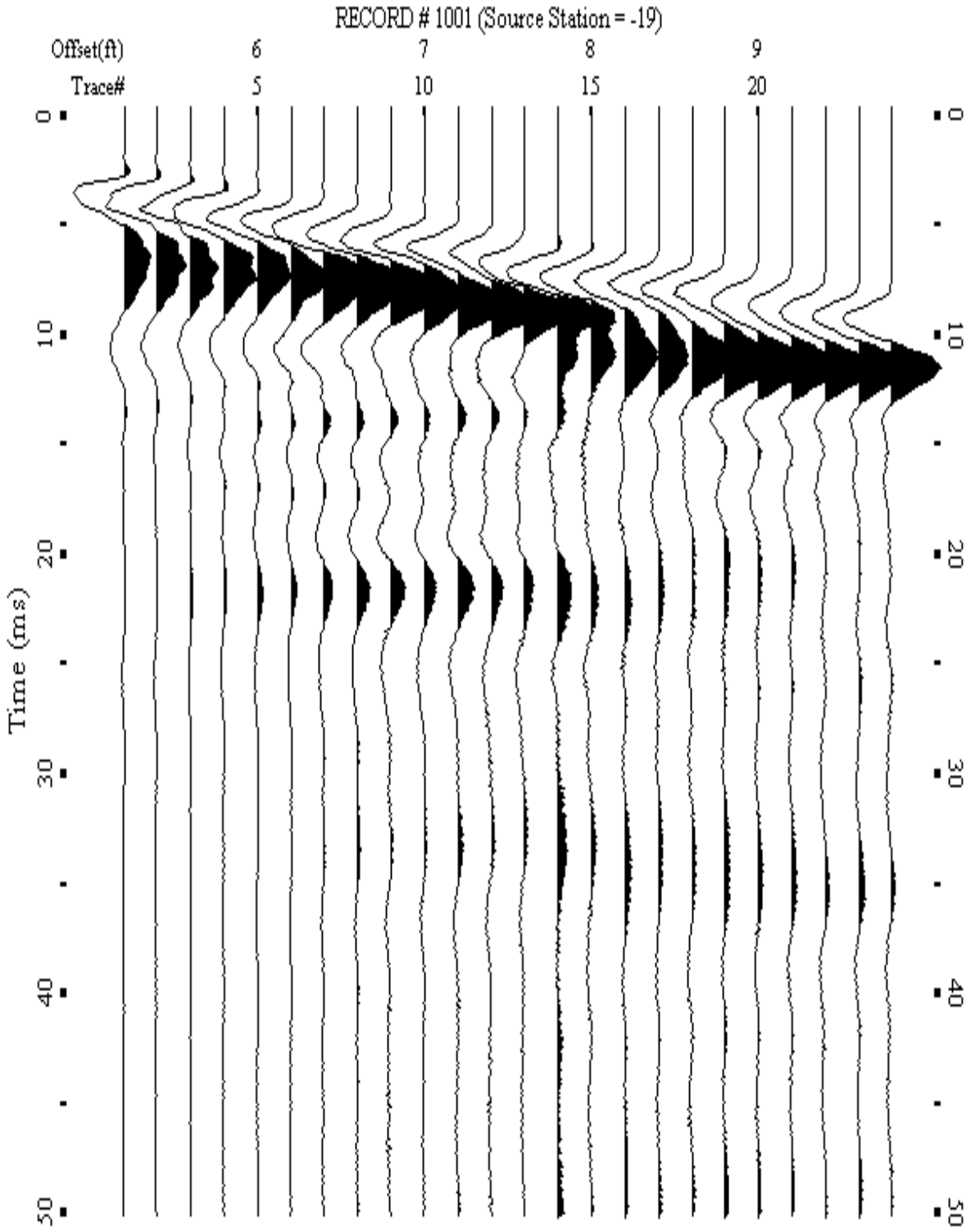

A.007: Shot Gather Line 1002 used in Pre-blast 6

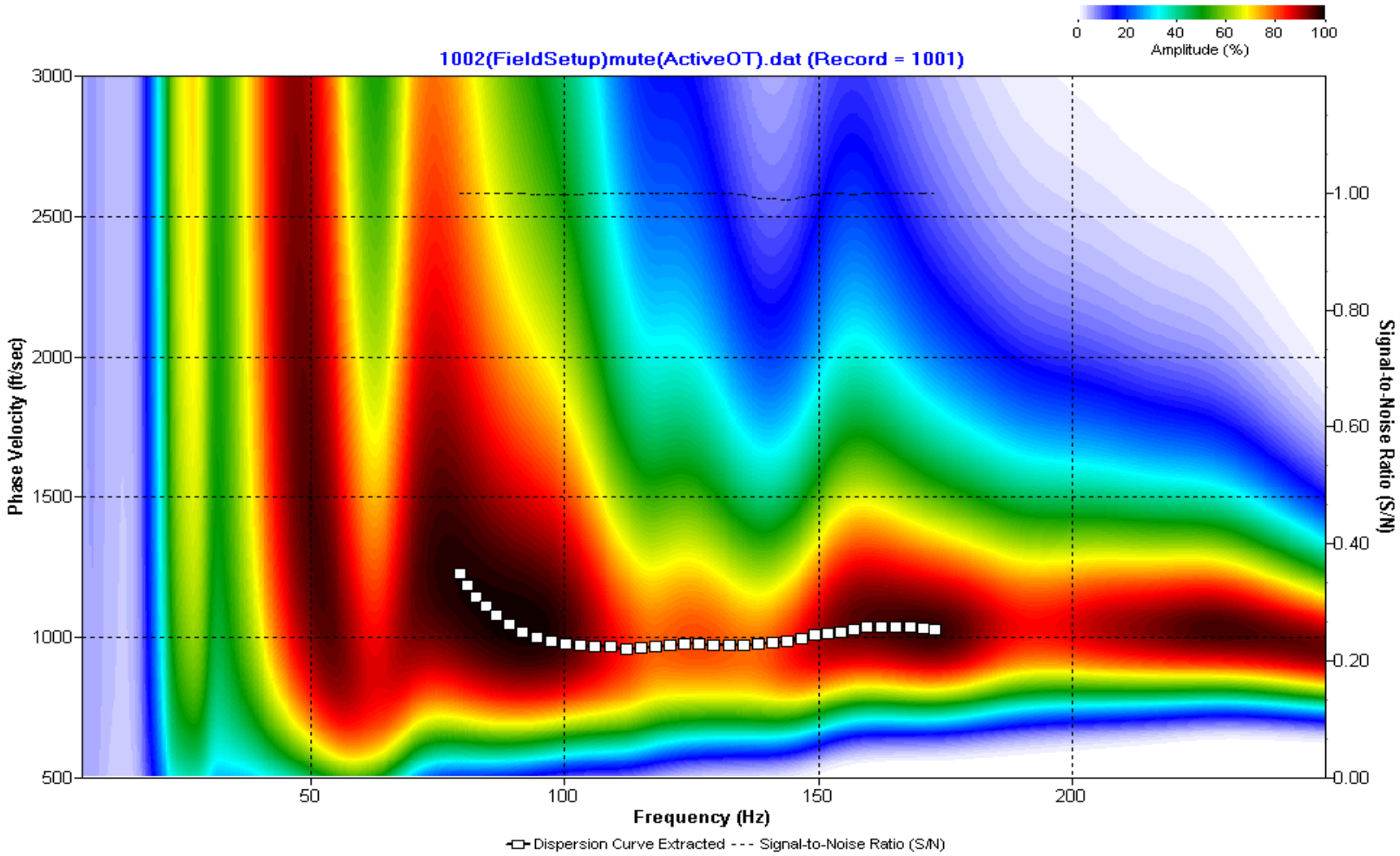

A.008: Dispersion Curve Line 1002 used in Pre-blast 6

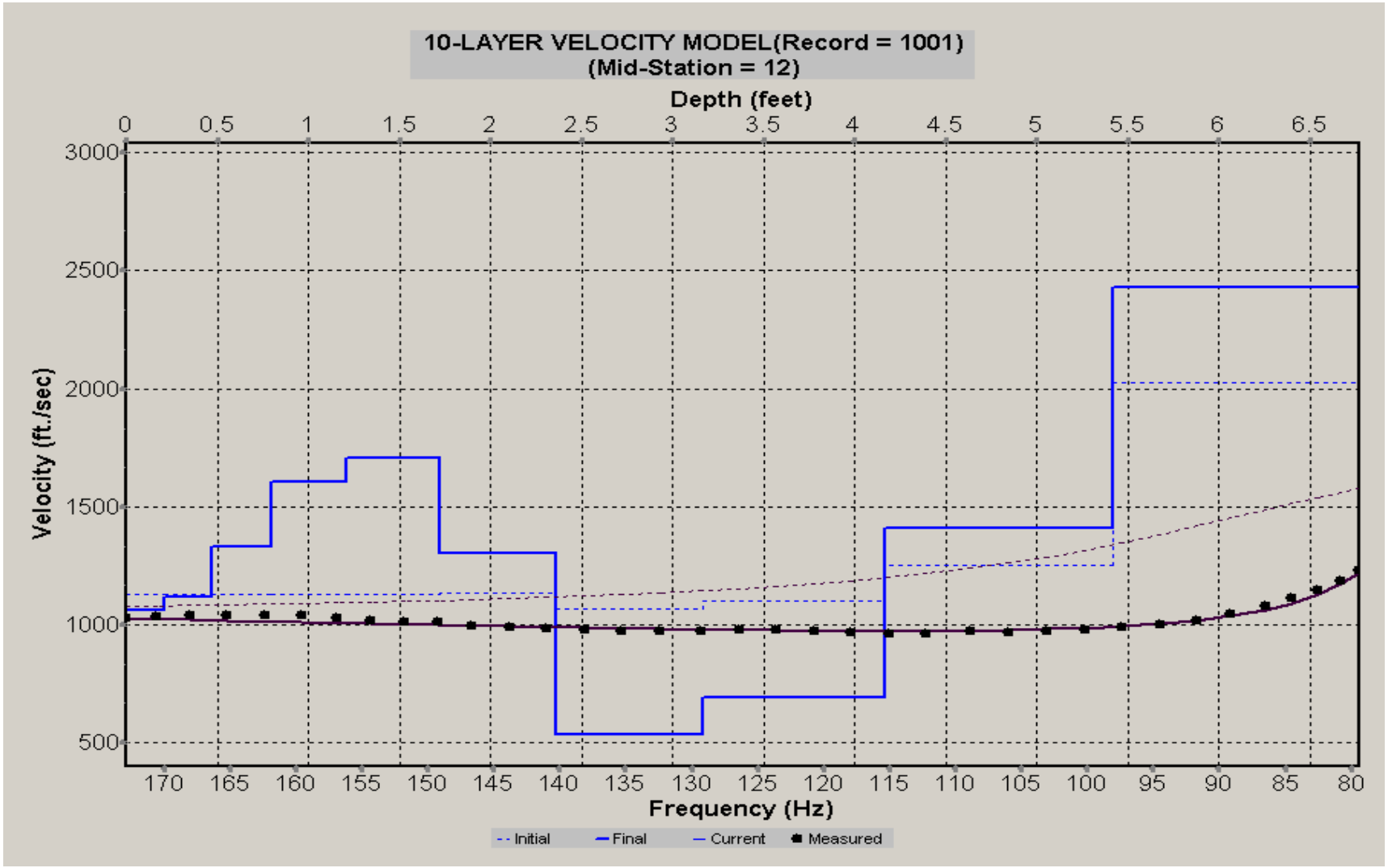

A.009: Velocity Profile Line 1002 used in Pre-blast 6

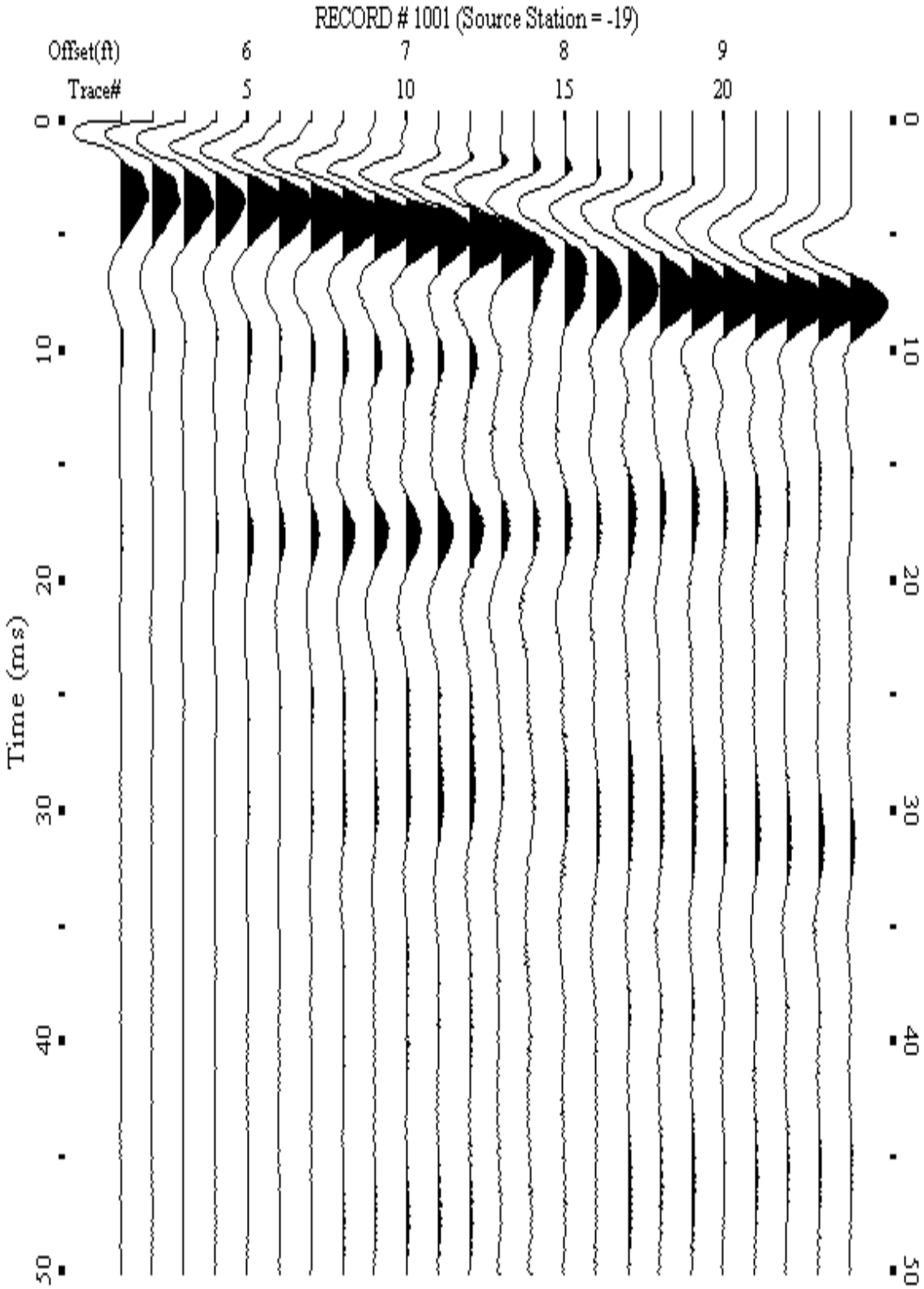

A.010: Shot Gather Line 1003 used in Pre-blast 6

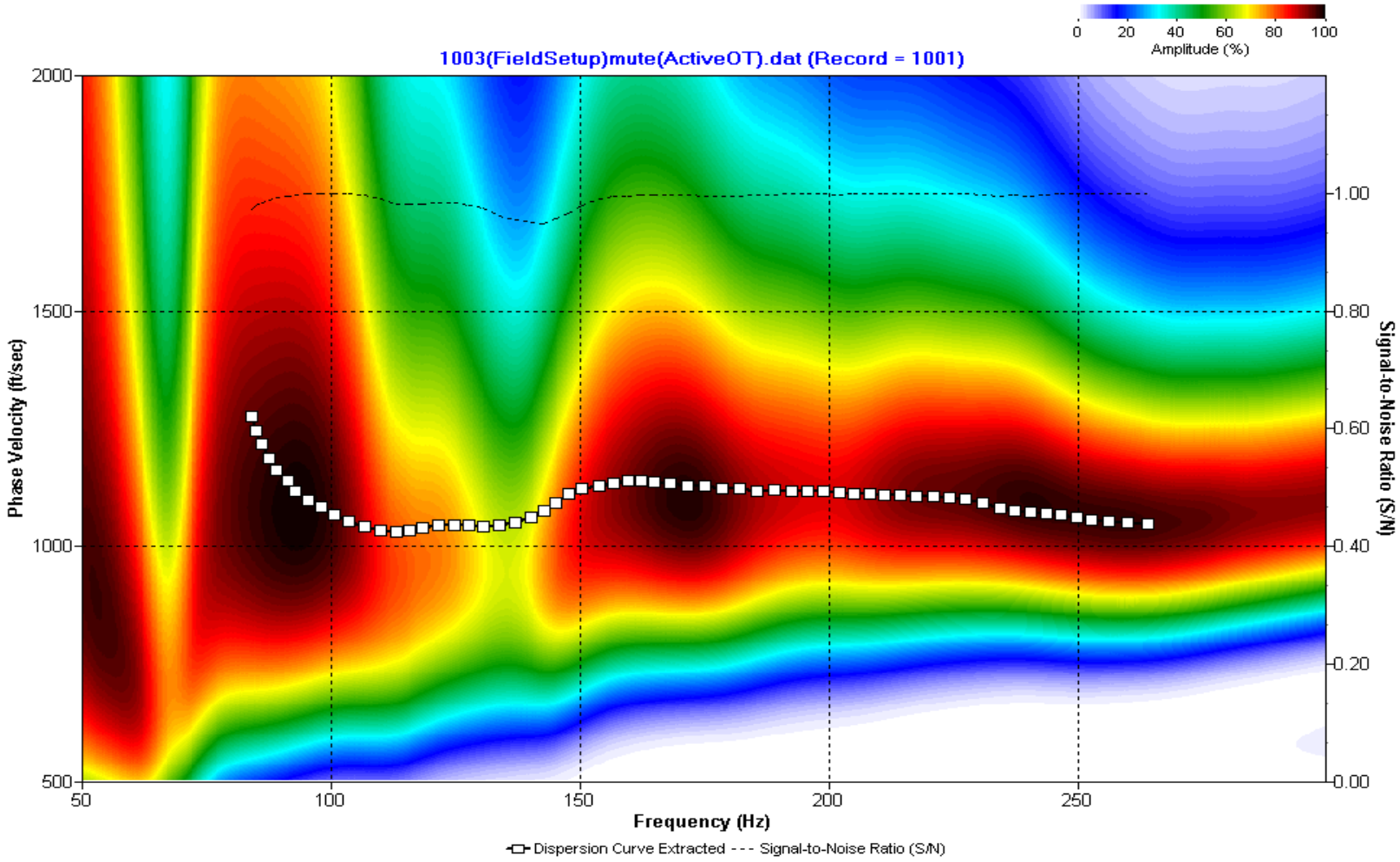

A.011: Dispersion Curve Line 1003 used in Pre-blast 6

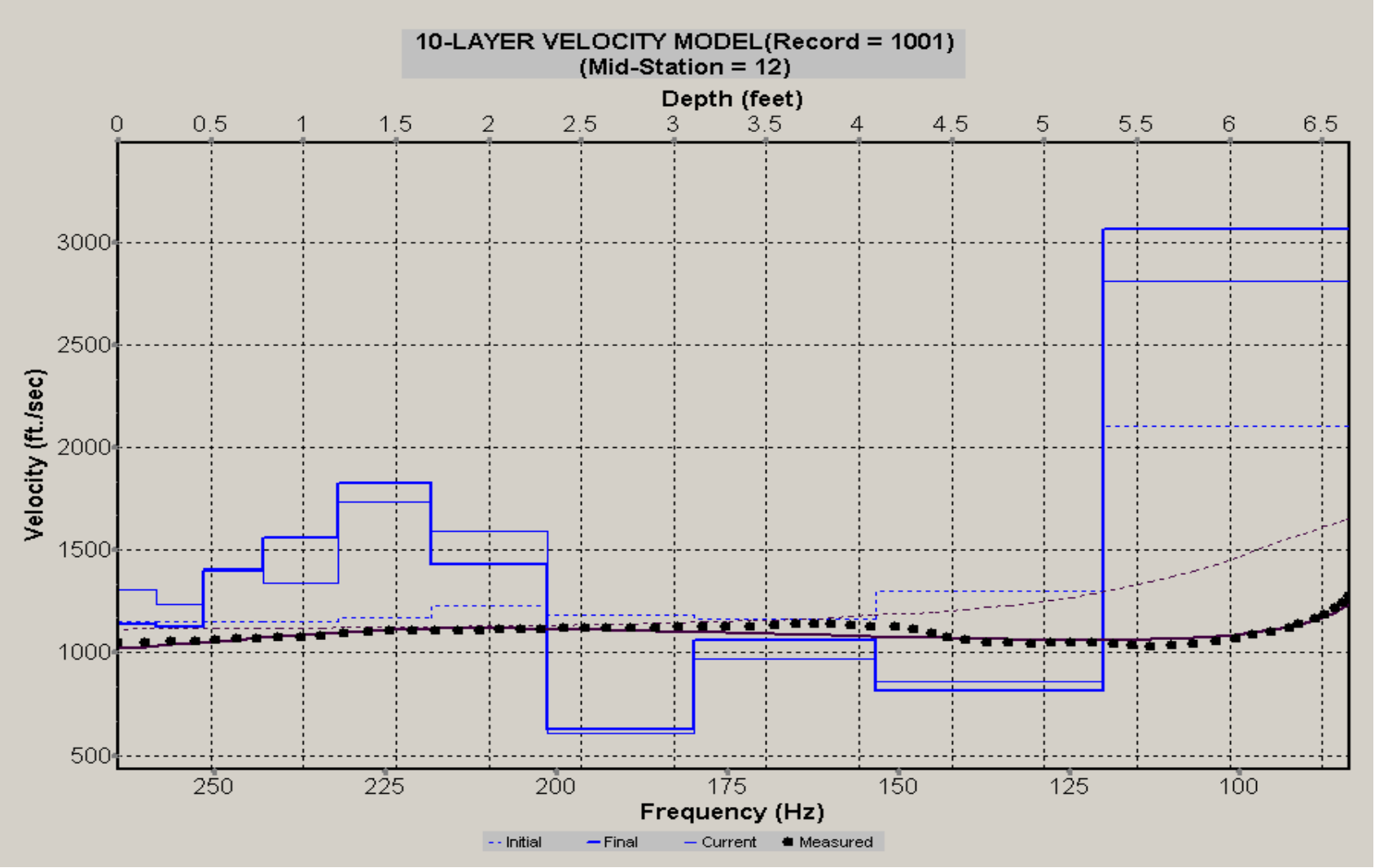

A.012: Velocity Profile Line 1003 used in Pre-blast 6

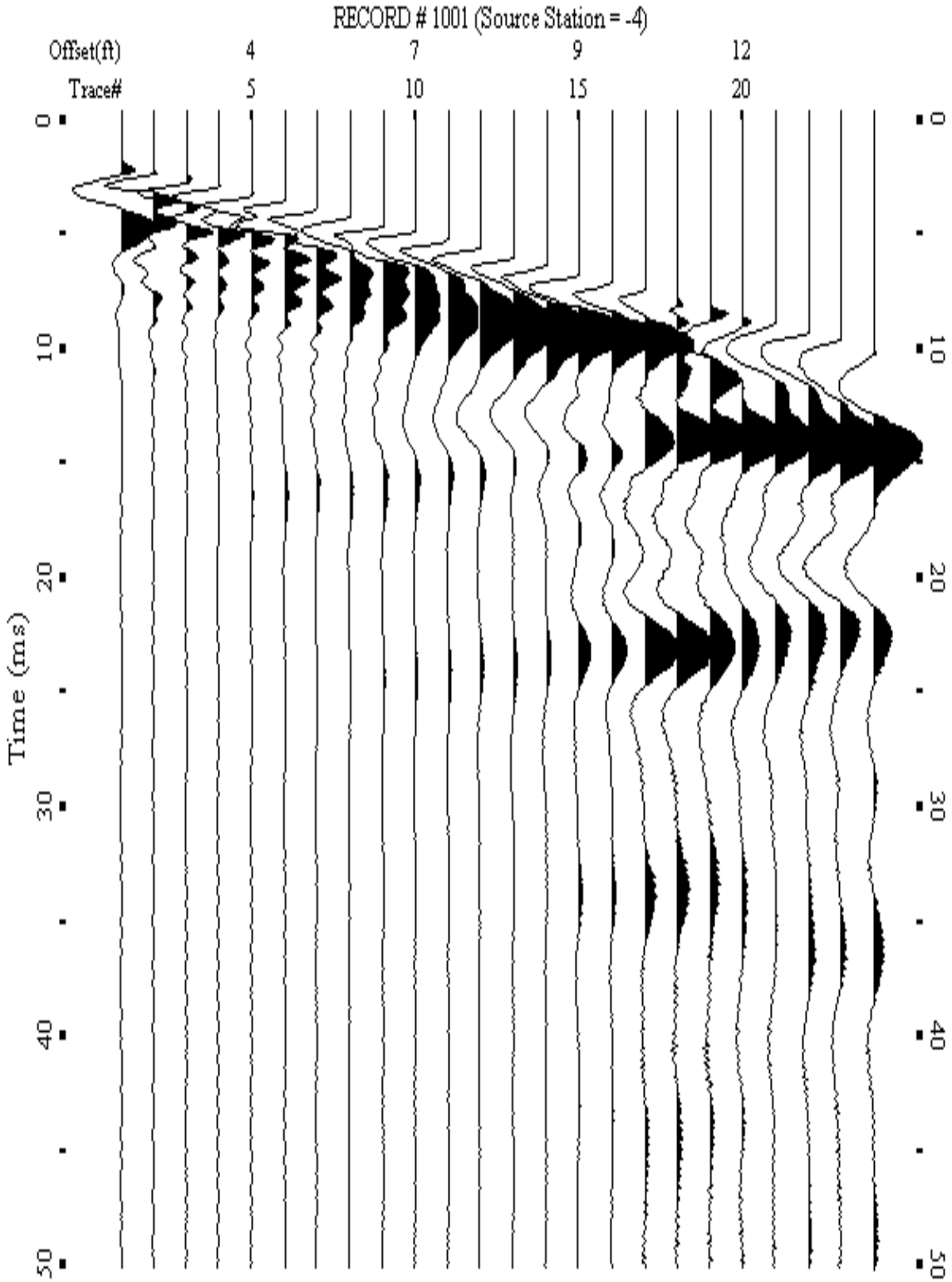

A.013: Shot Gather Line 1023 used in Pre-blast 6 and Pre-blast 7

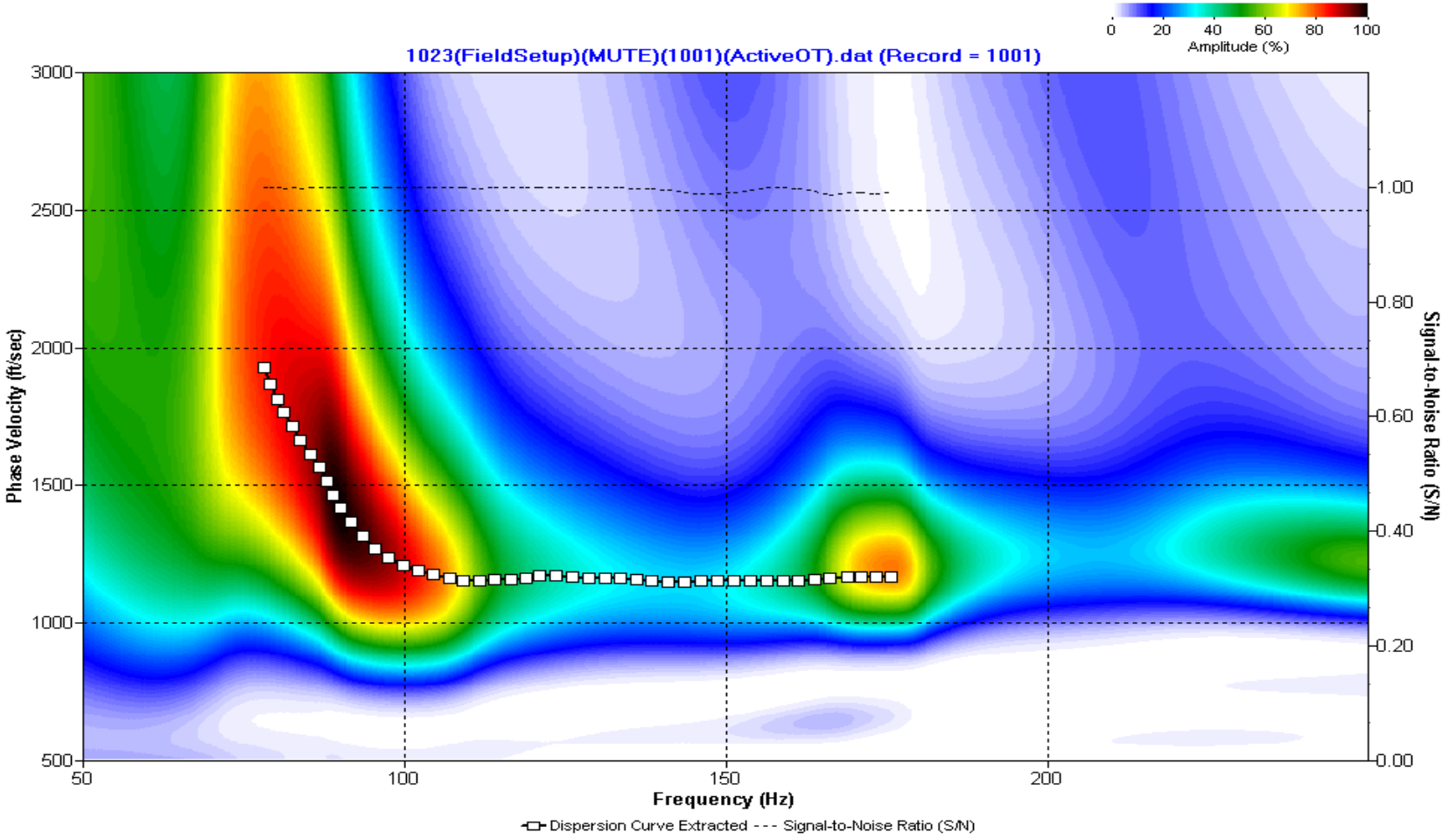

A.014: Dispersion Curve Line 1023 used in Pre-blast 6 and Pre-blast 7

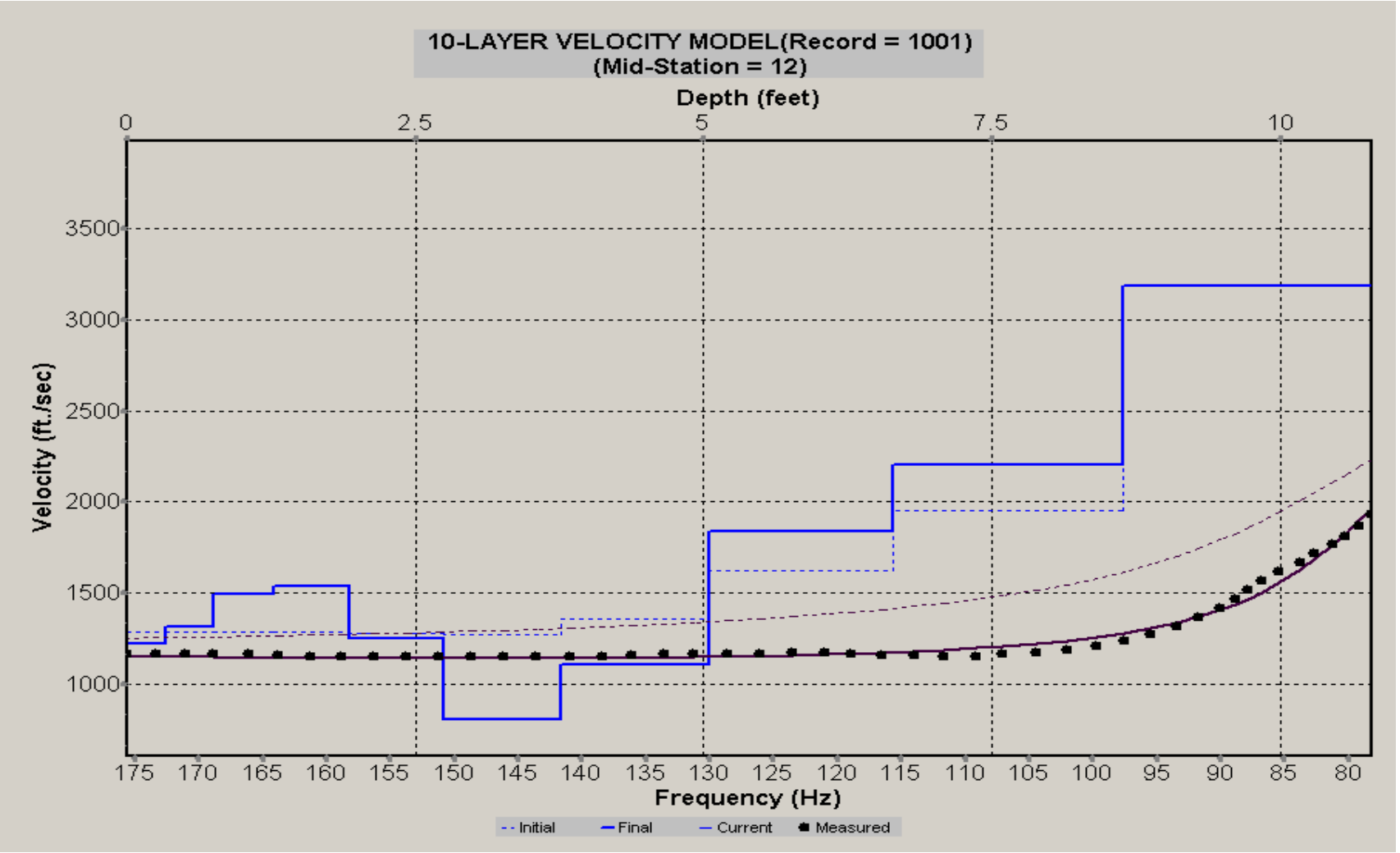

A.015: Velocity Profile Line 1023 used in Pre-blast 6 and Pre-blast 7

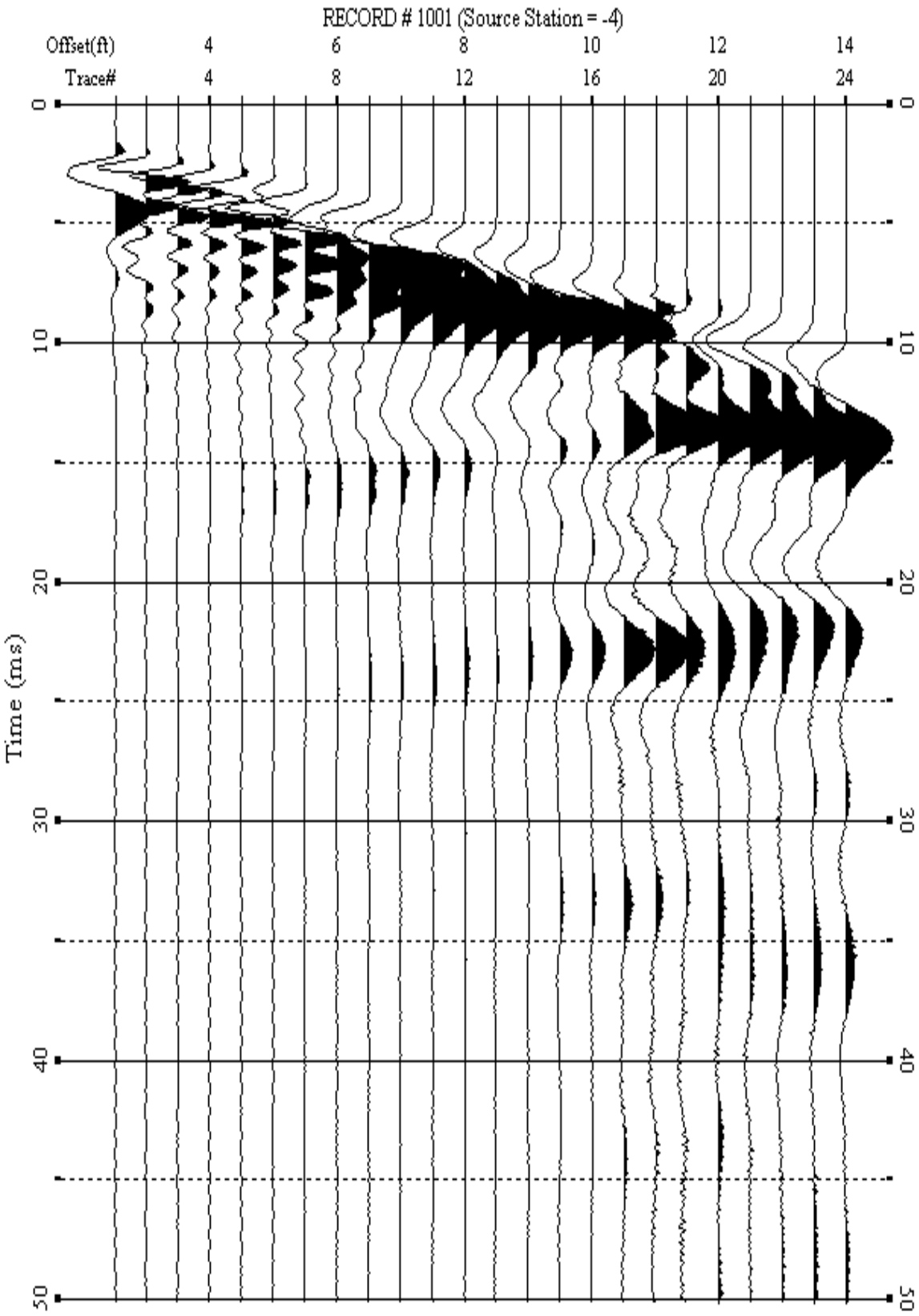

A.016: Shot Gather Line 1024 used in Pre-blast 6 and Pre-blast 7

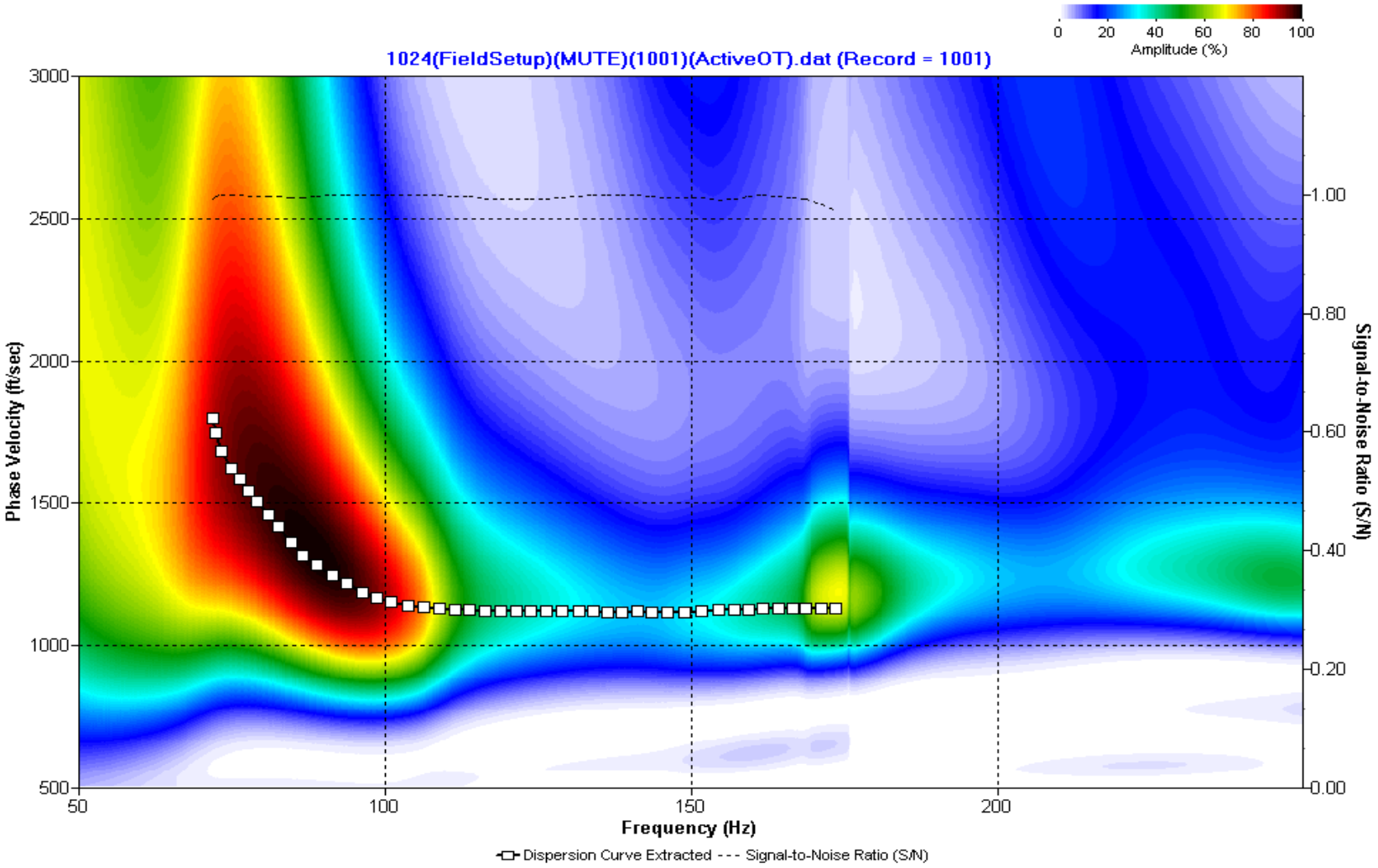

A.017: Dispersion Curve Line 1024 used in Pre-blast 6 and Pre-blast 7

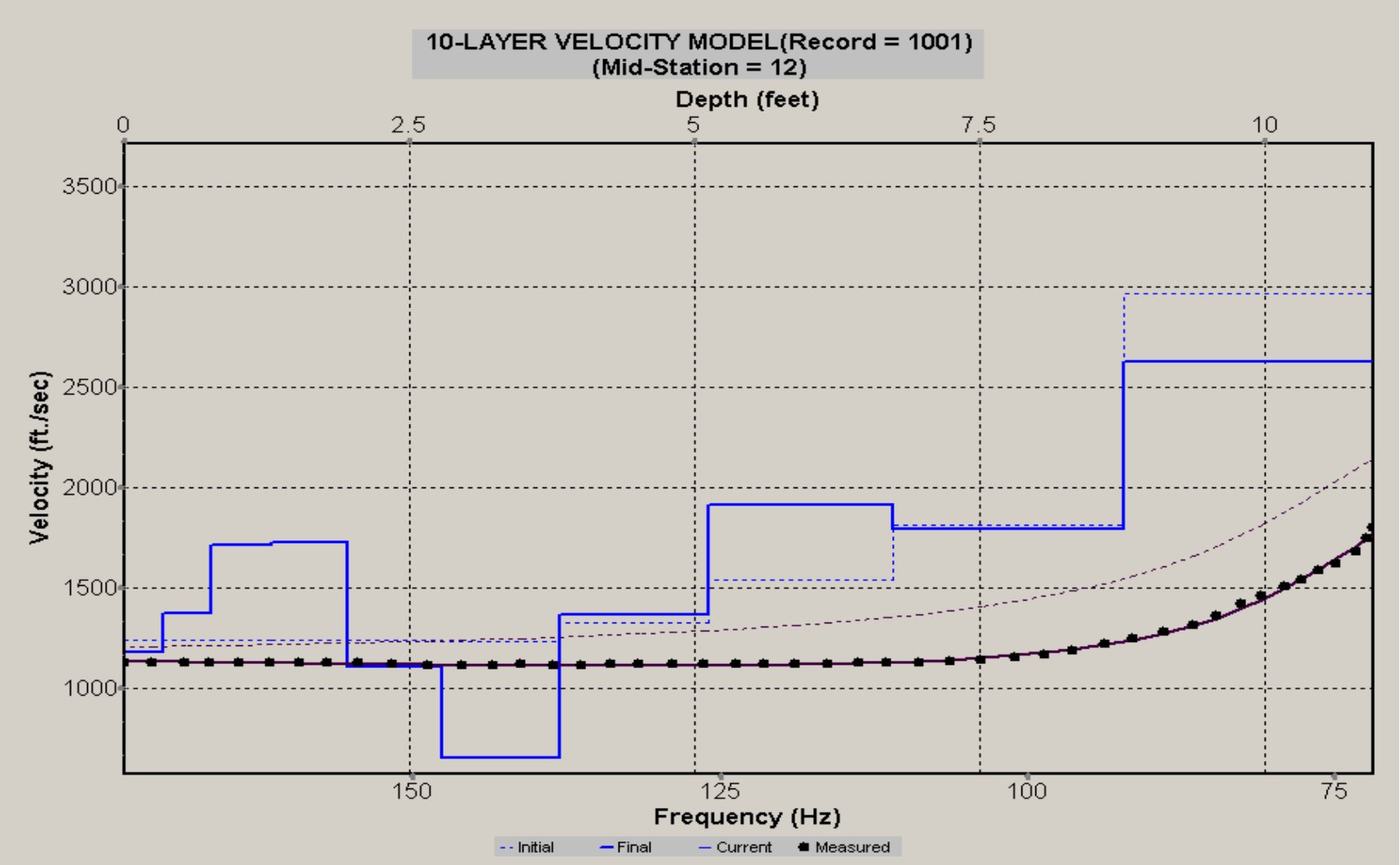

A.018: Velocity Profile Line 1024 used in Pre-blast 6 and Pre-blast 7

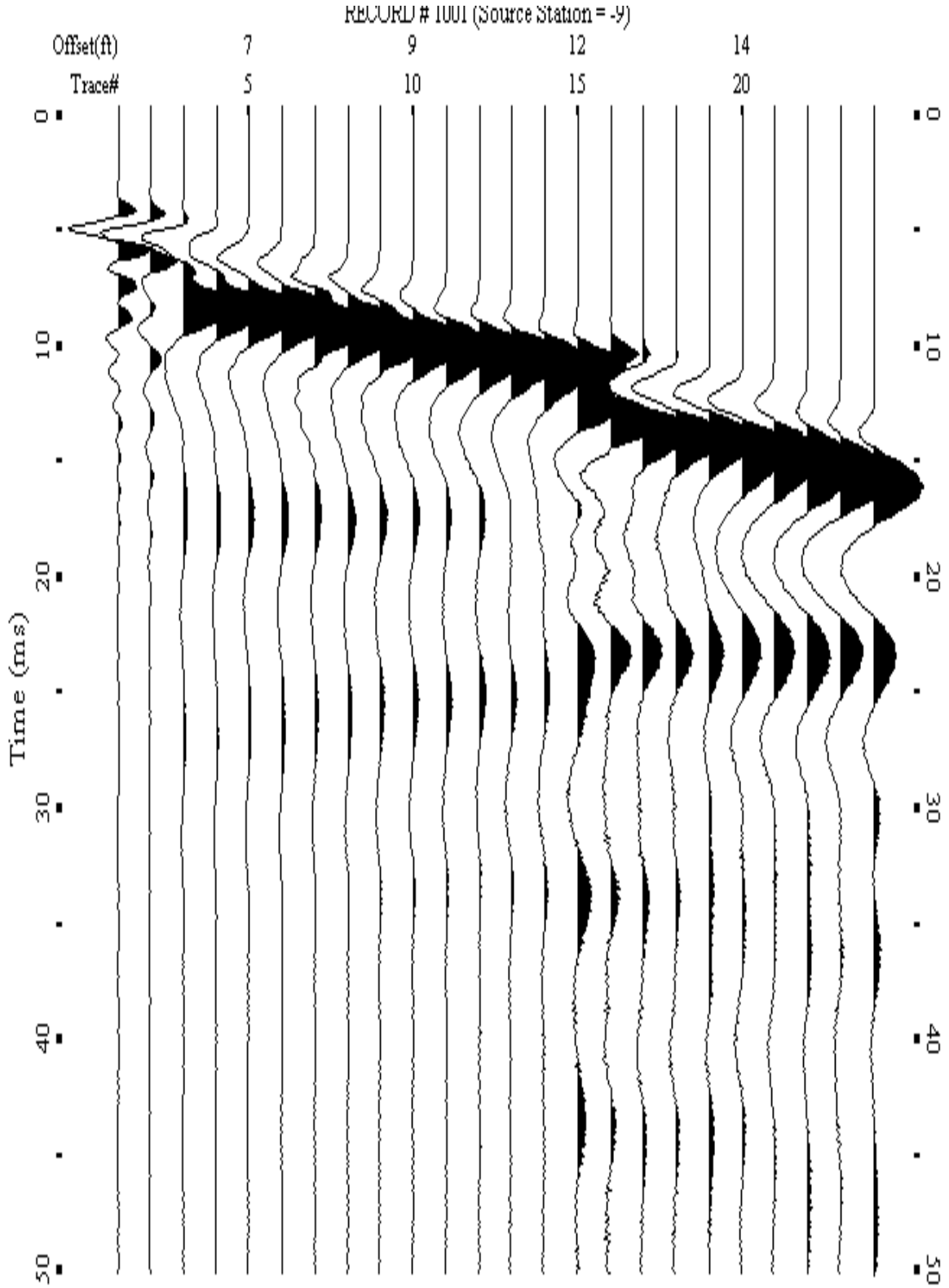

A.019: Shot Gather Line 1025 used in Pre-blast 6

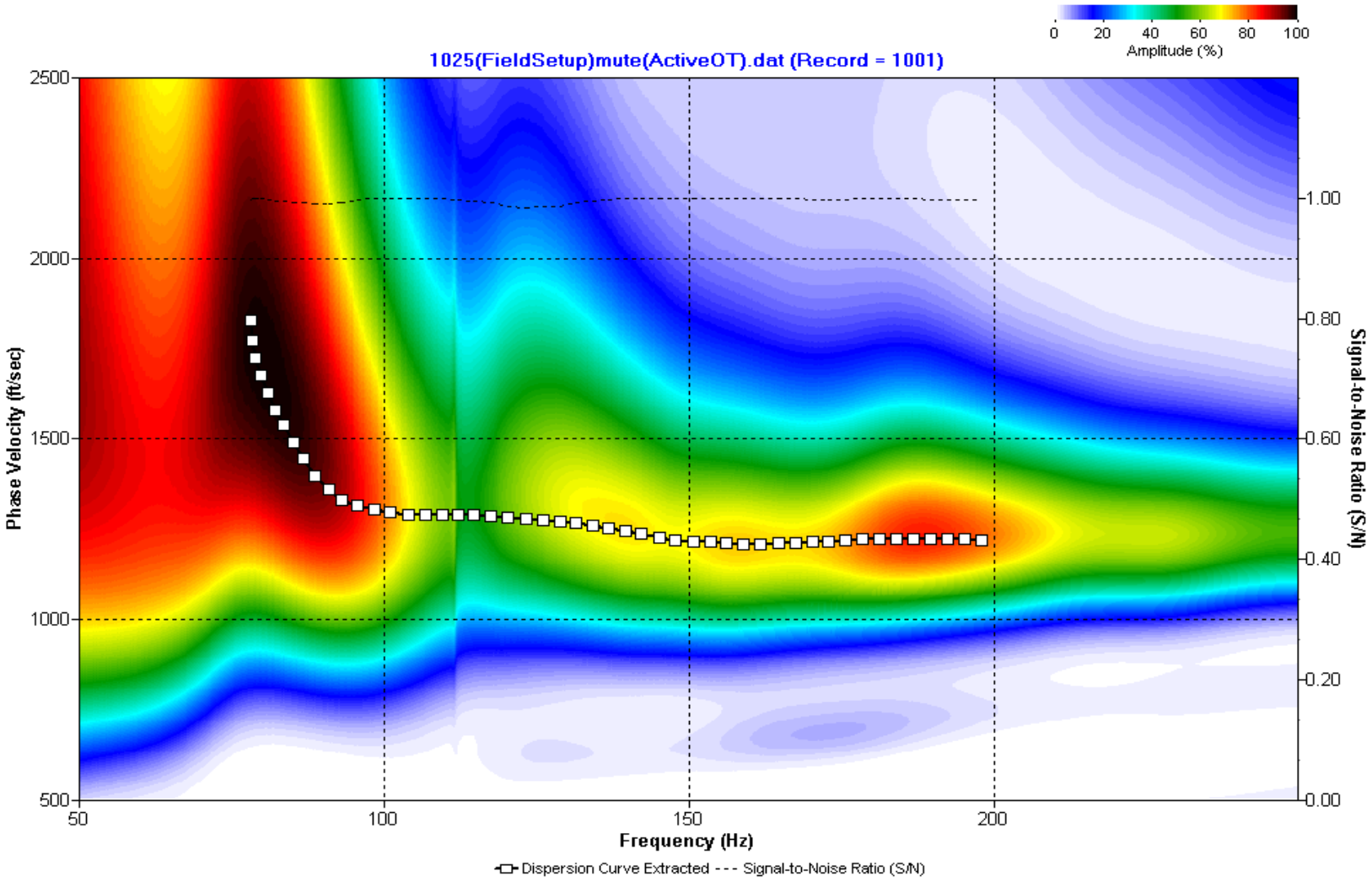

A.020: Dispersion Curve Line 1025 used in Pre-blast 6

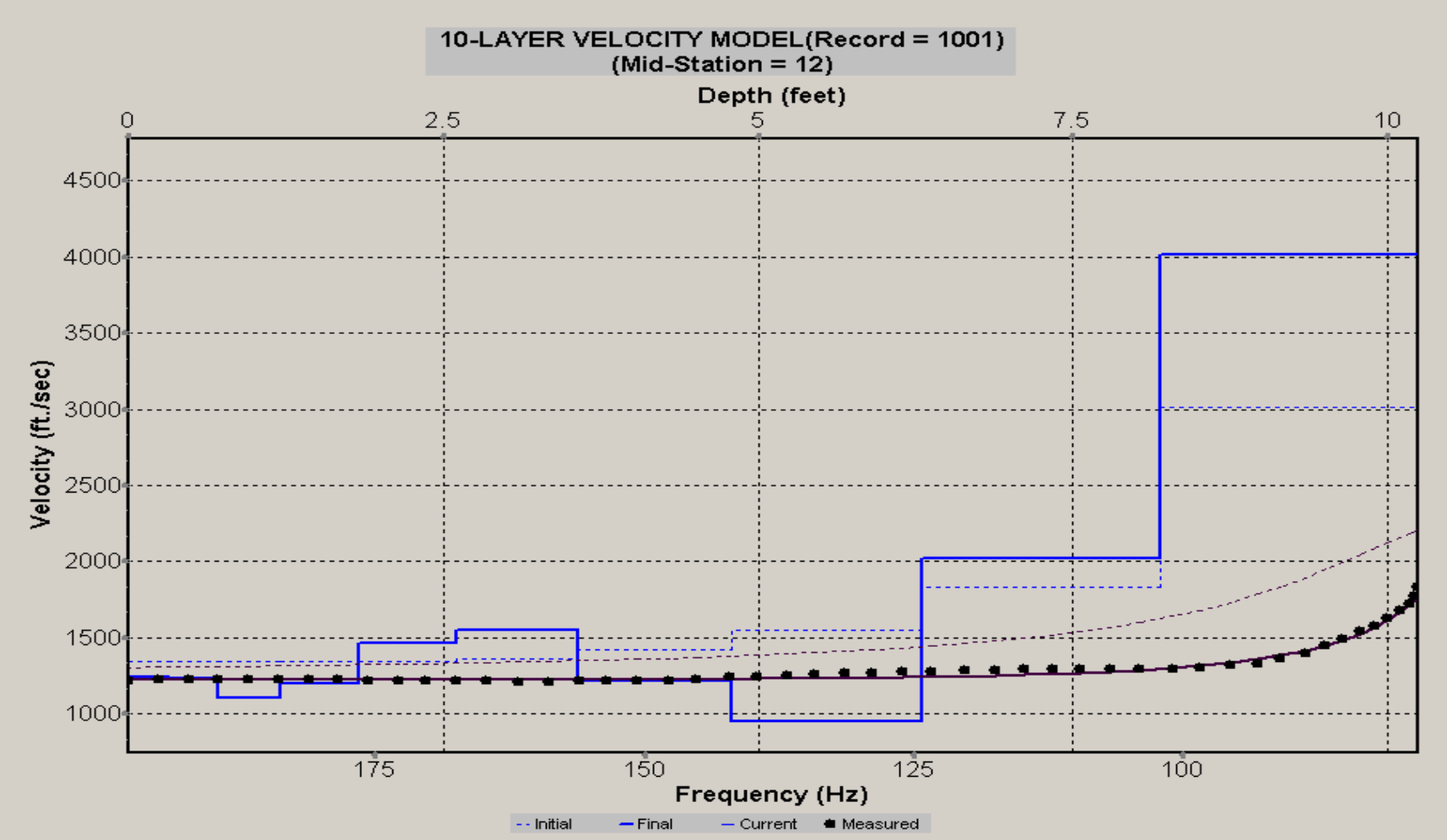

A.021: Velocity Profile Line 1025 used in Pre-blast 6

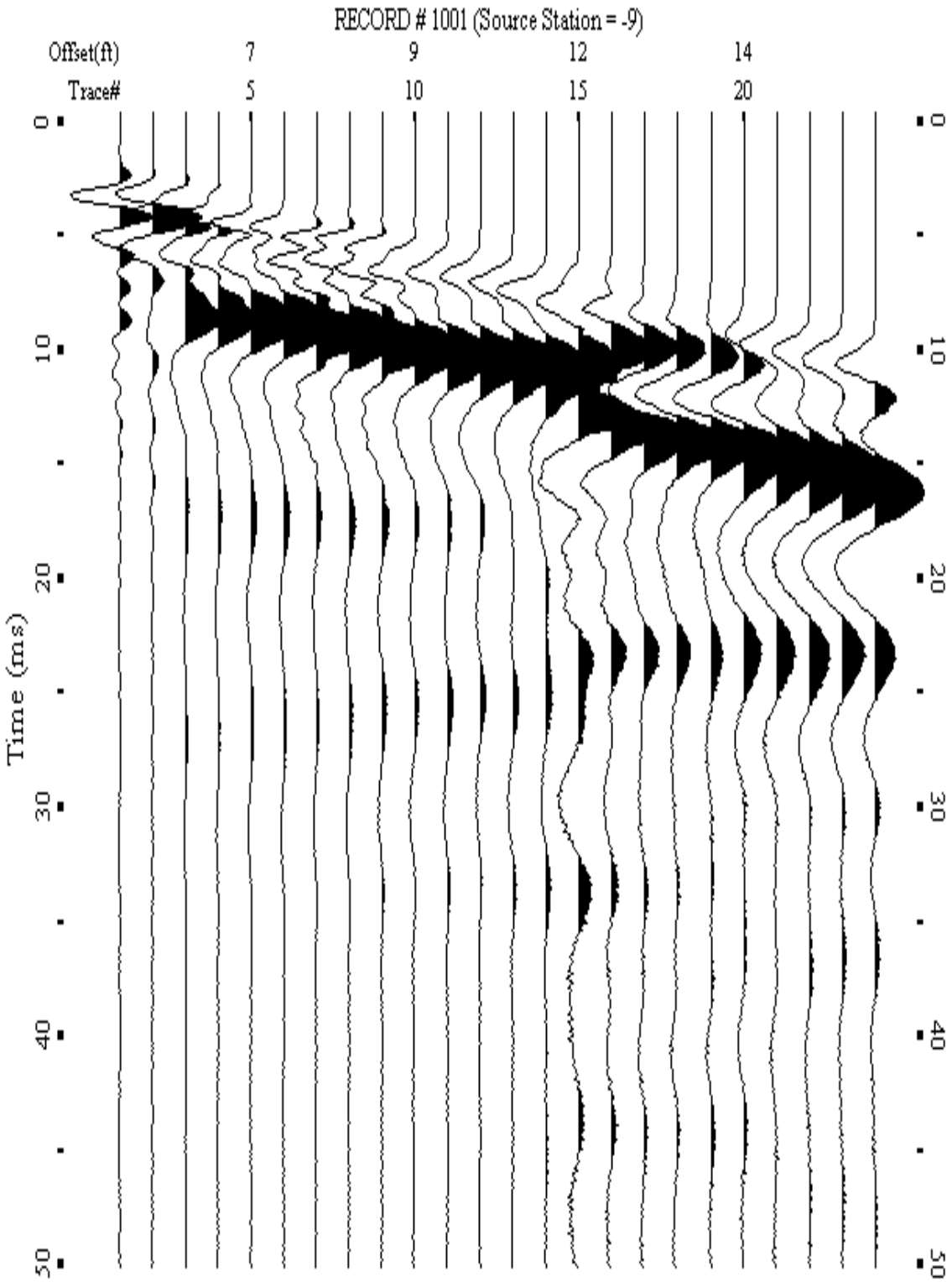

A.022: Shot Gather Line 1026 used in Pre-blast 6

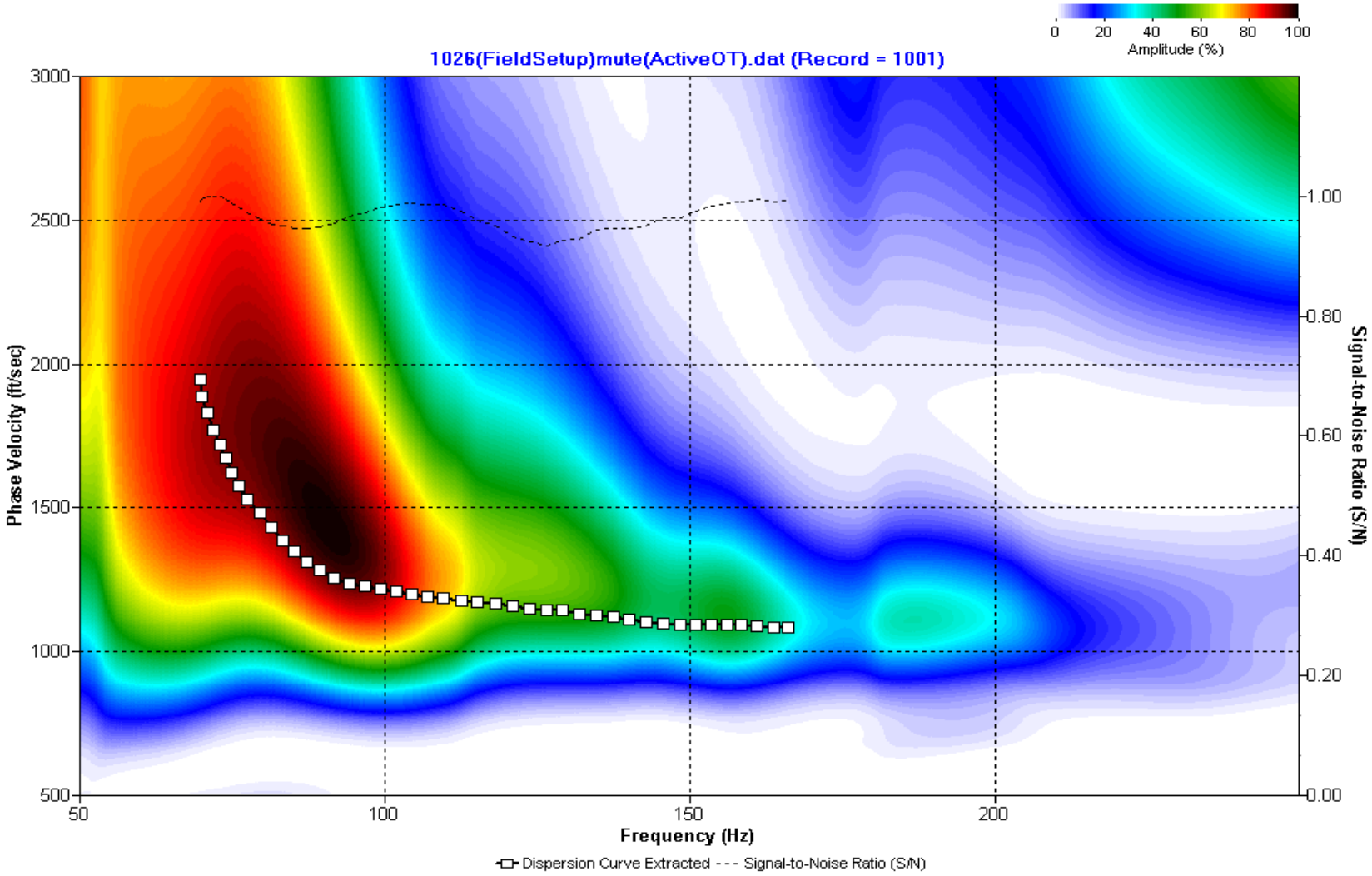

A.023: Dispersion Curve Line 1026 used in Pre-blast 6

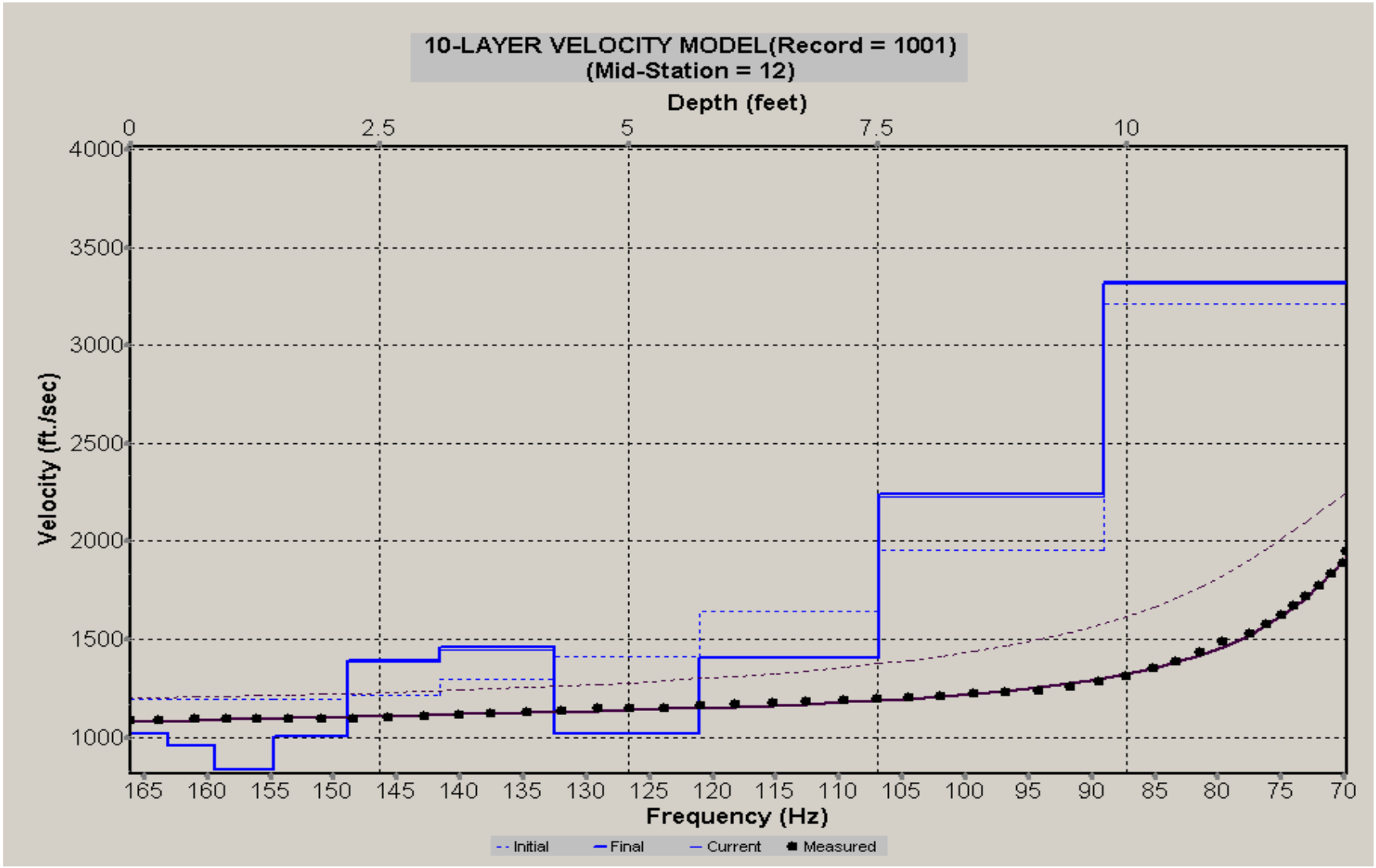

A.024: Velocity Profile Line 1026 used in Pre-blast 6

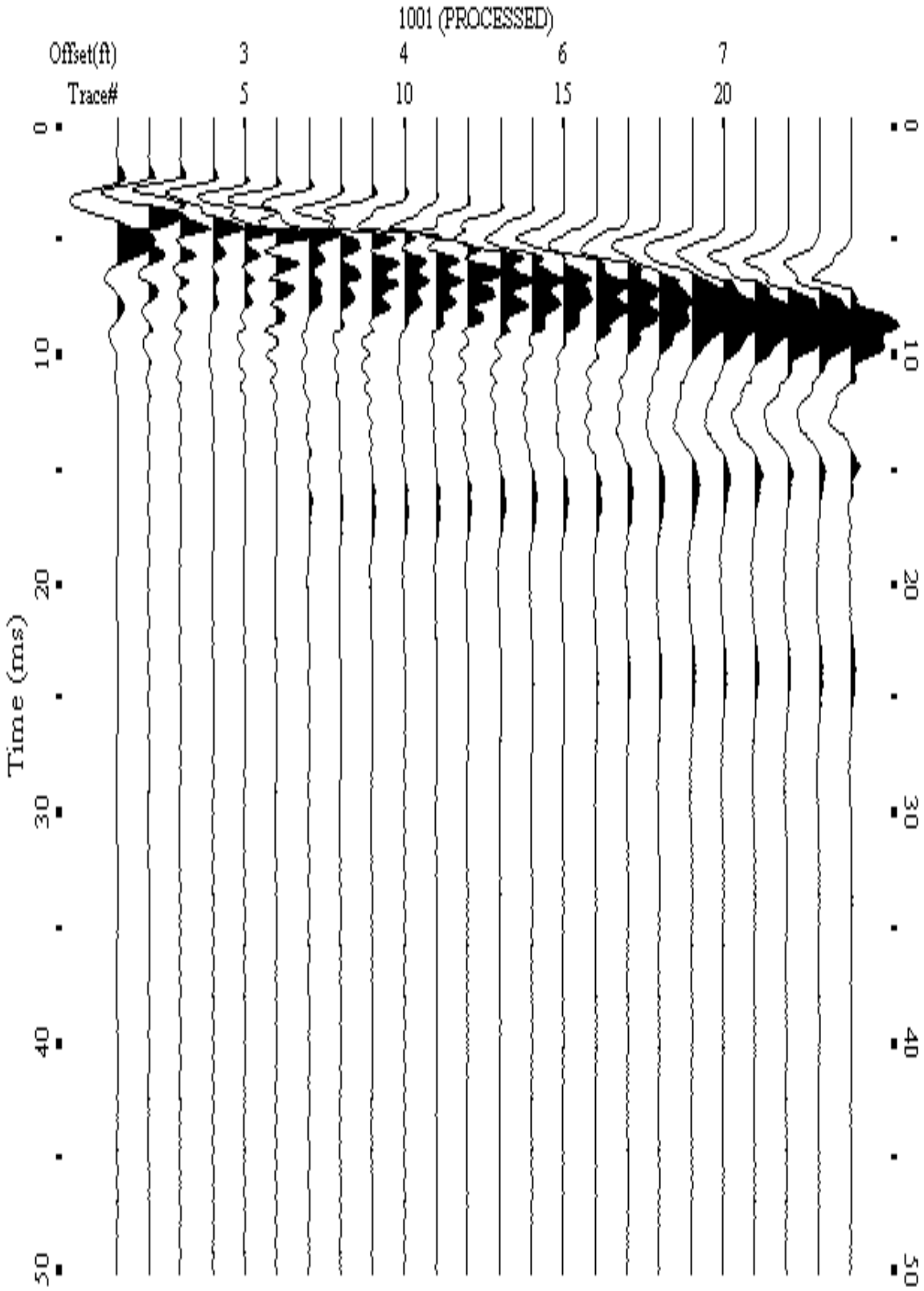

A.025: Shot Gather Line 1027 used in Pre-blast 7

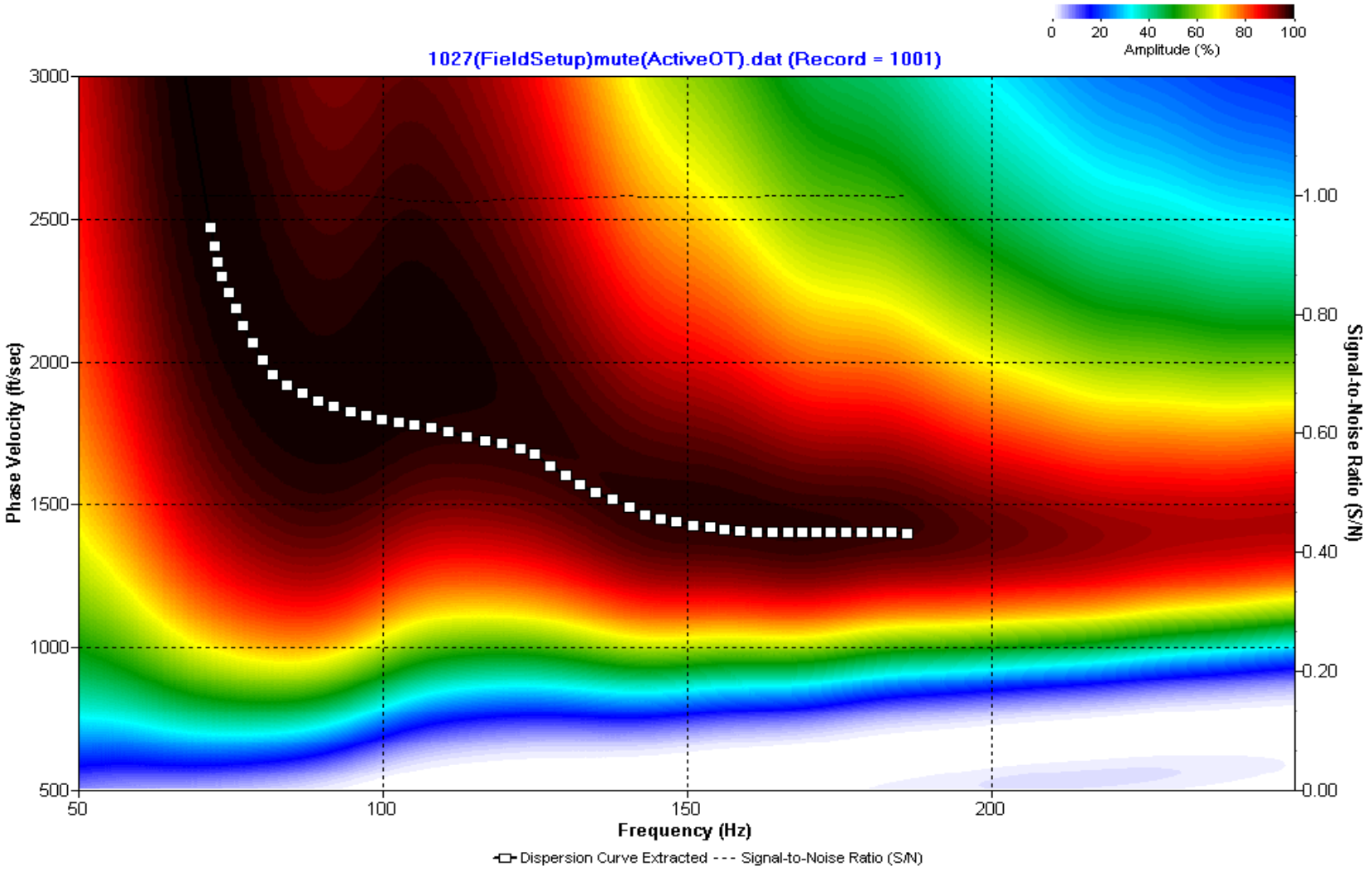

A.026: Dispersion Curve Line 1027 used in Pre-blast 7

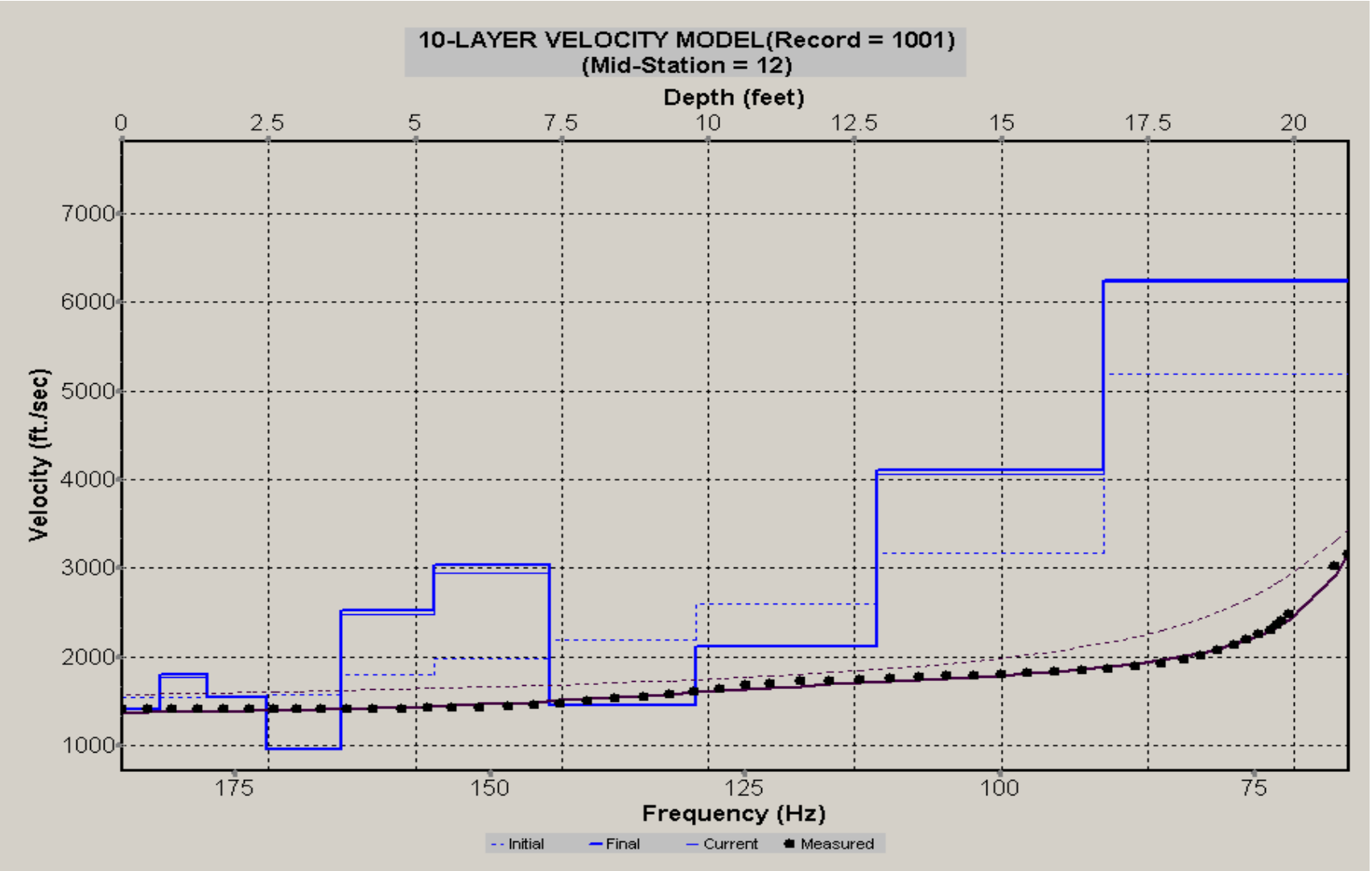

A.027: Velocity Profile Line 1027 used in Pre-blast 7

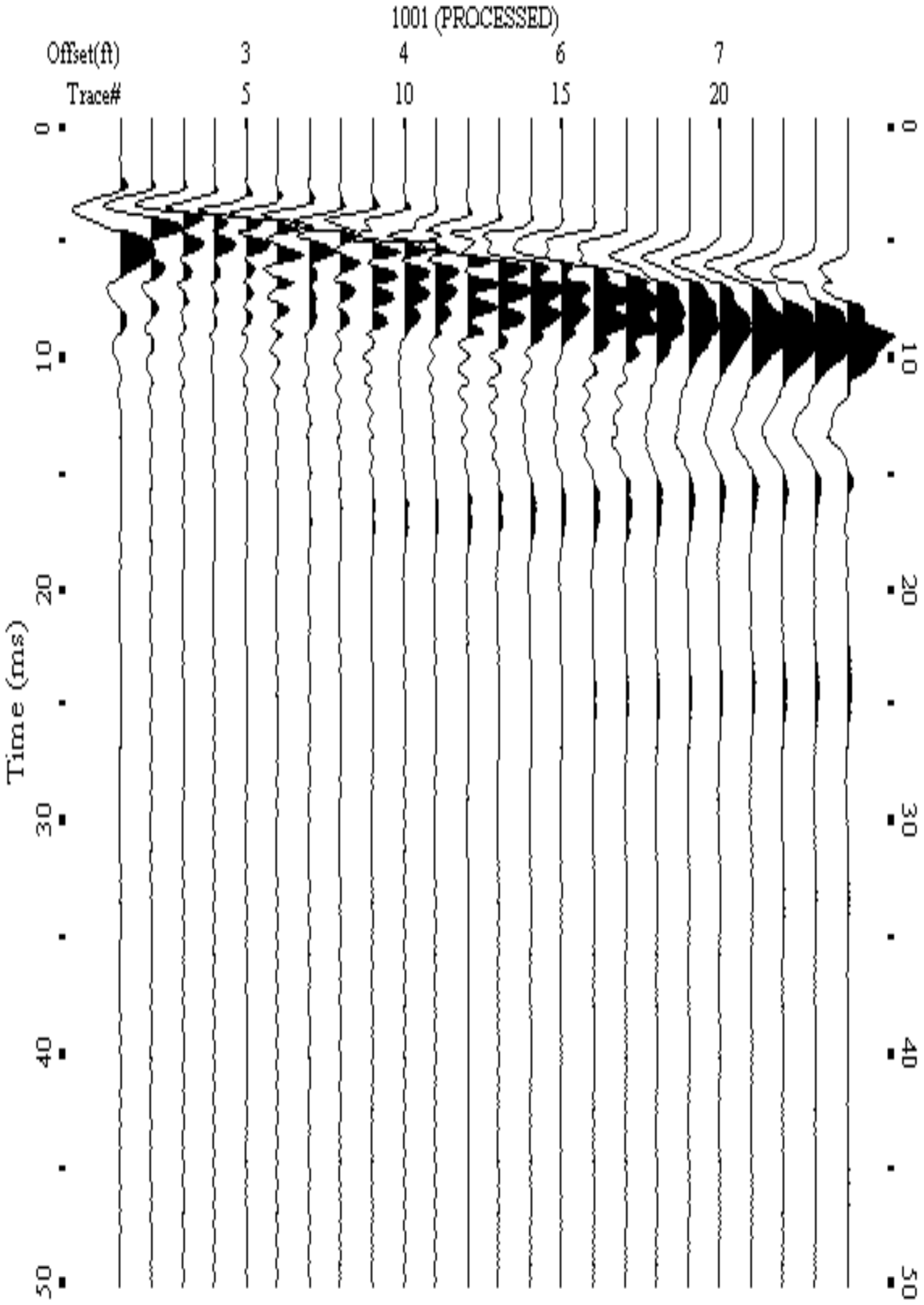

A.028: Shot Gather Line 1028 used in Pre-blast 7

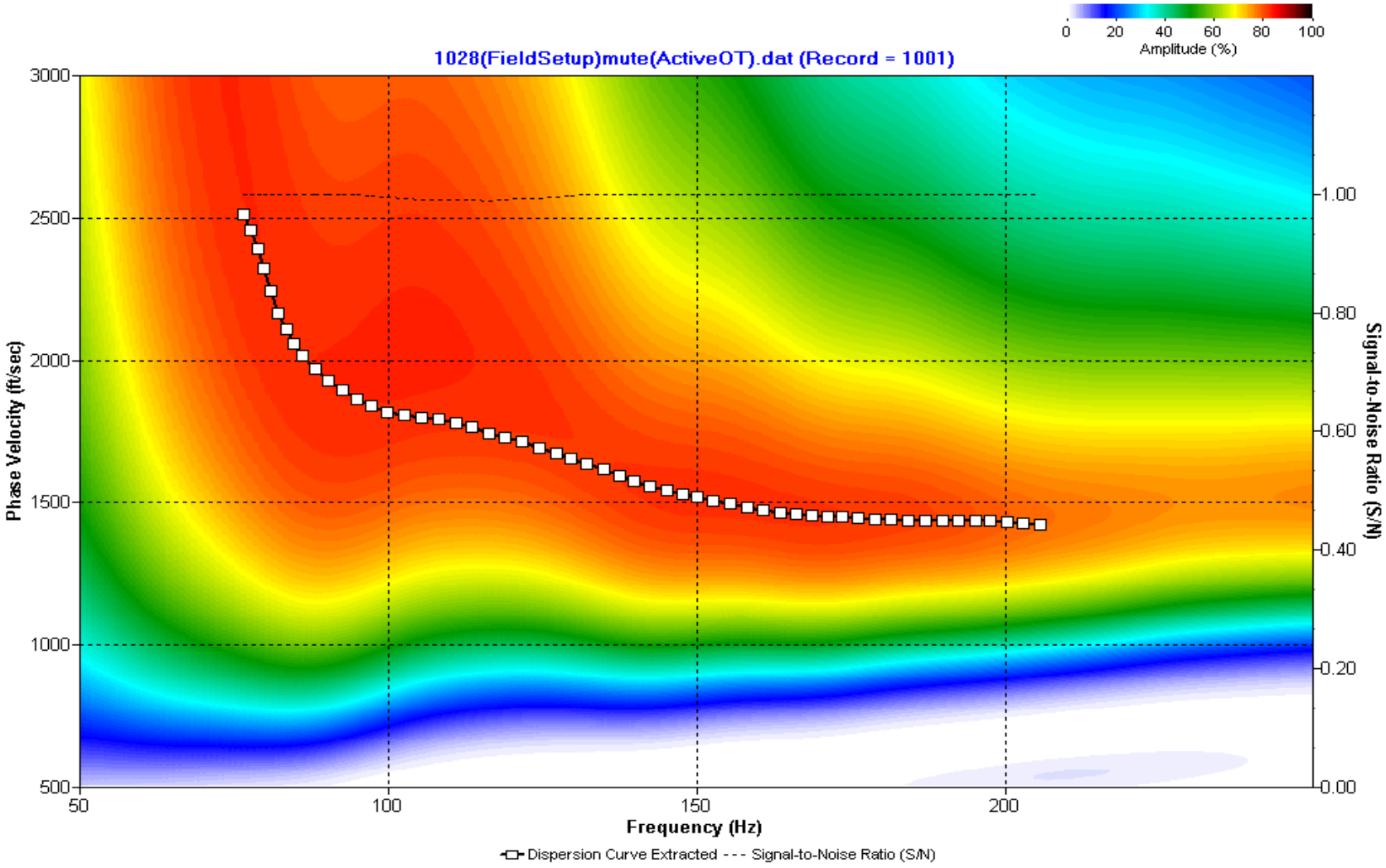

A.029: Dispersion Curve Line 1028 used in Pre-blast 7

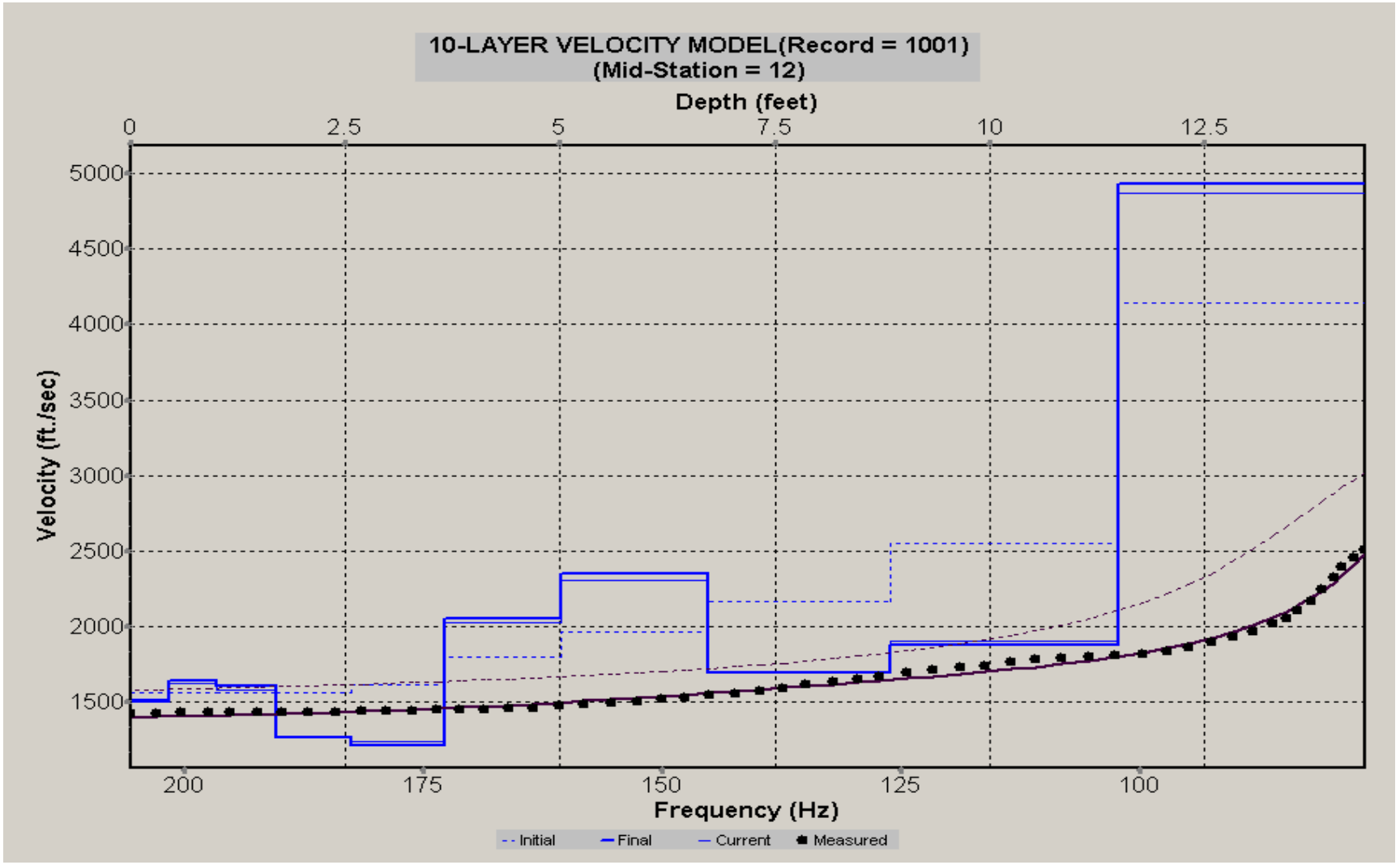

A.030: Velocity Profile Line 1028 used in Pre-blast 7

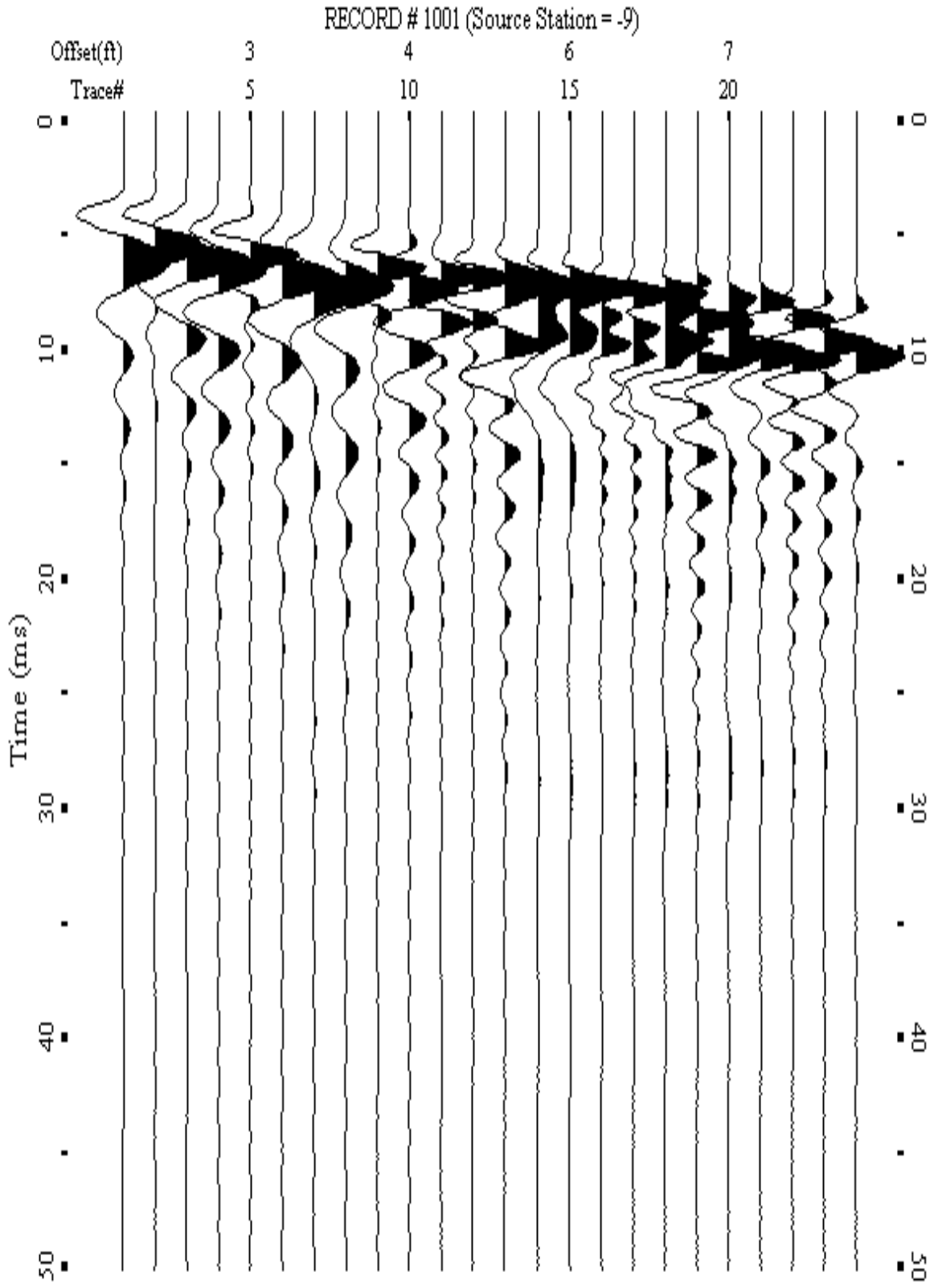

A.031: Shot Gather Line 1031 used in Pre-blast 8

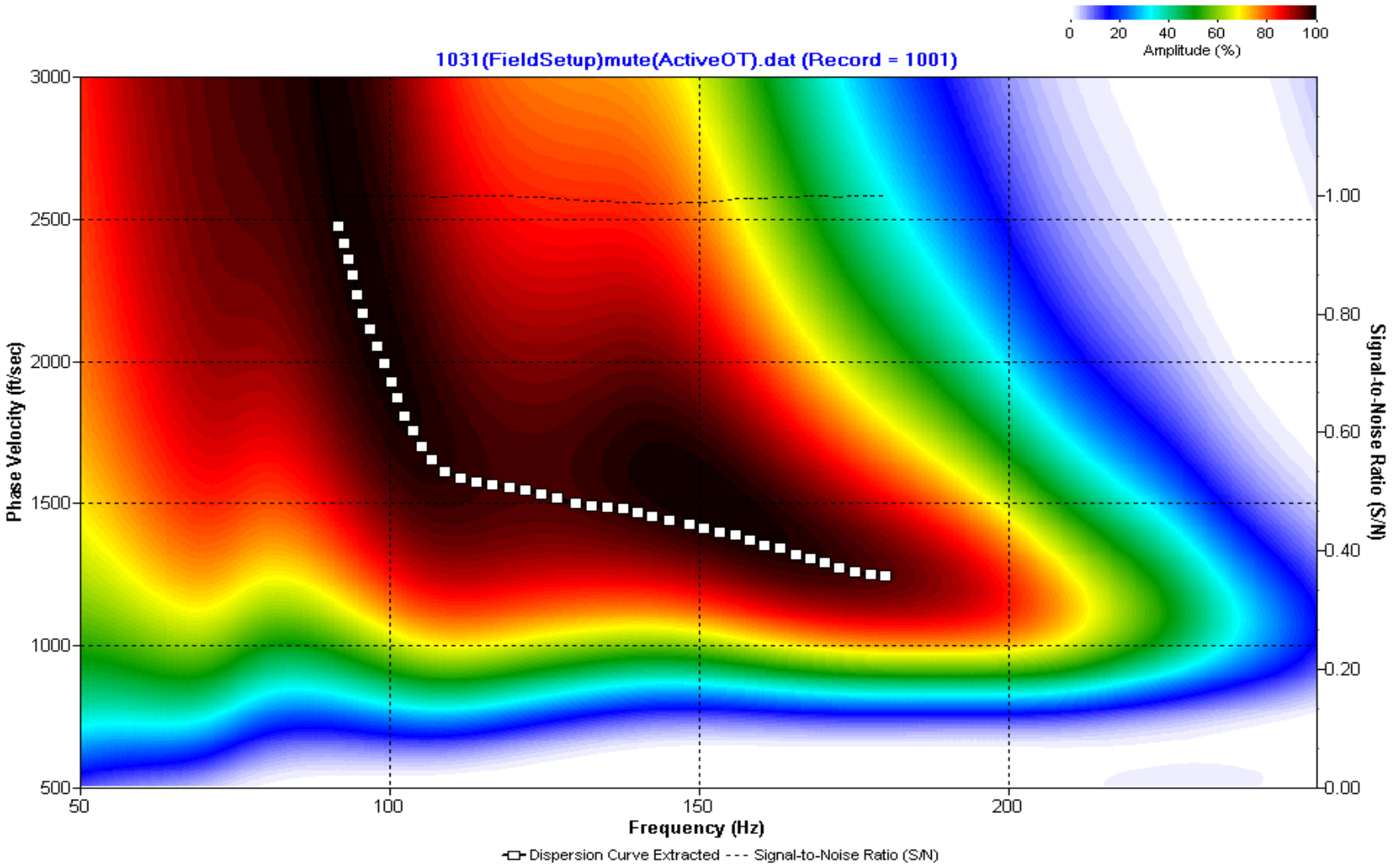

A.032: Dispersion Curve Line 1031 used in Pre-blast 8

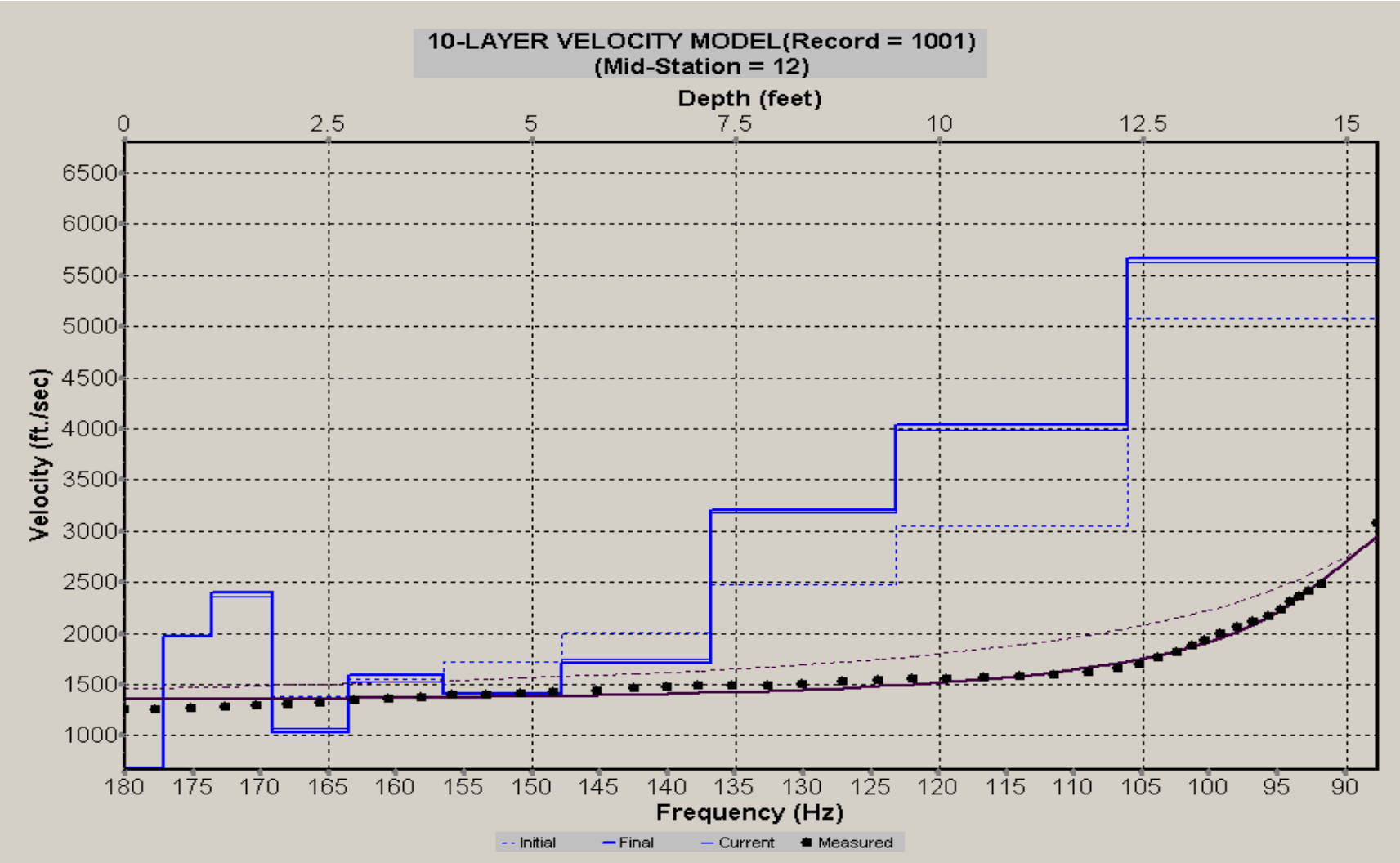

A.033: Velocity Profile Line 1031 used in Pre-blast 8

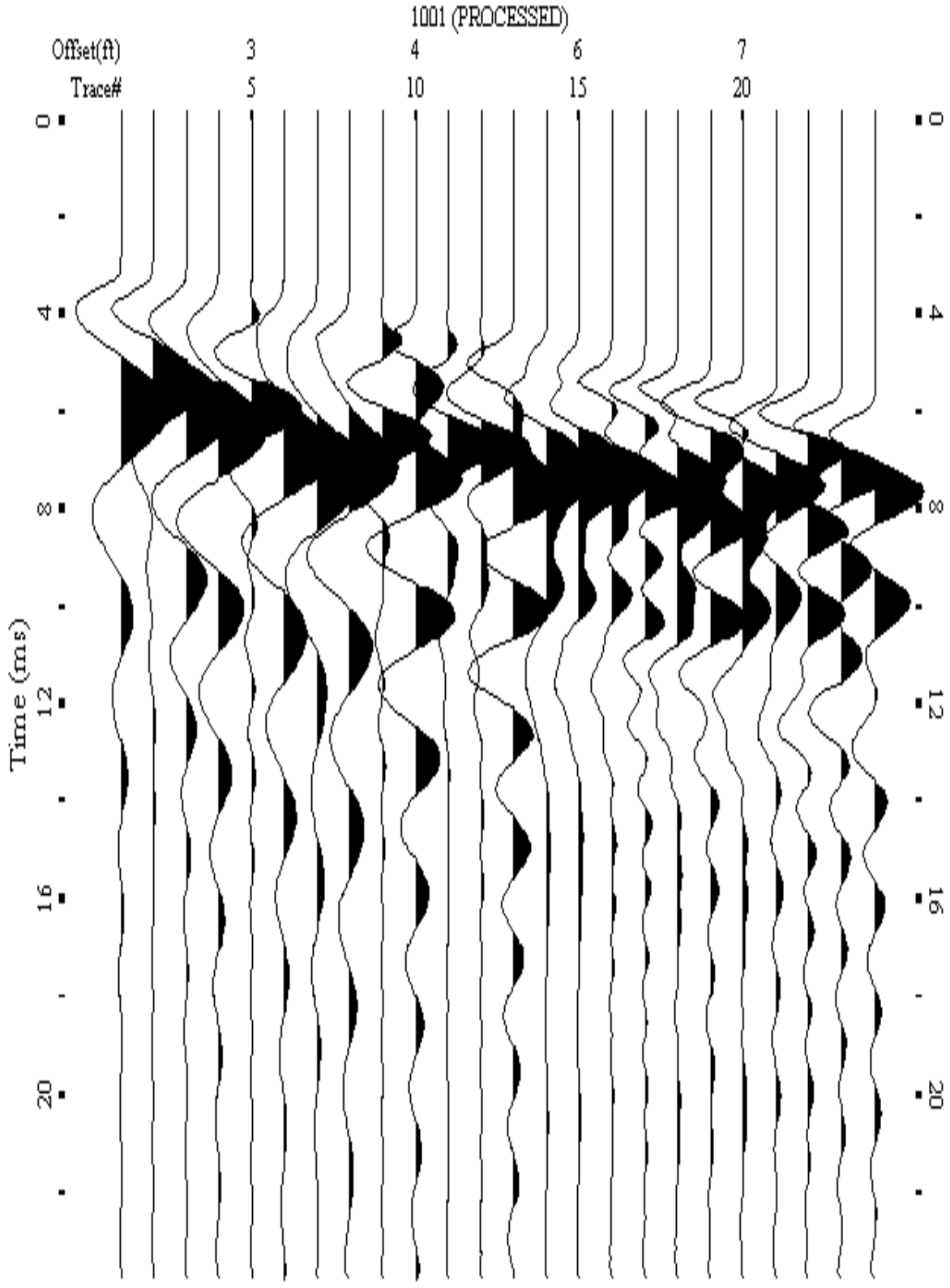

A.034: Shot Gather Line 1032 used in Pre-blast 8

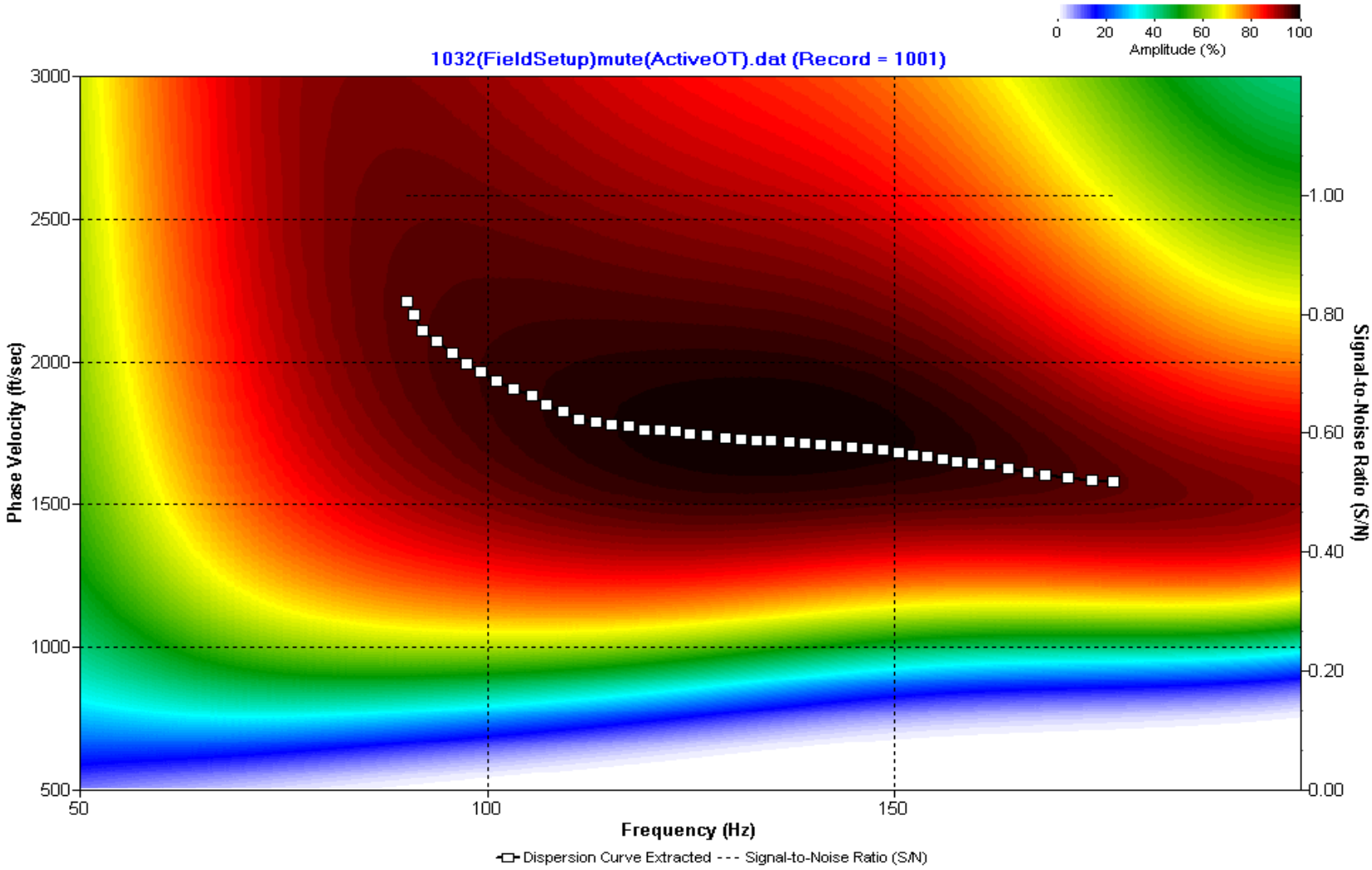

A.035: Dispersion Curve Line 1032 used in Pre-blast 8

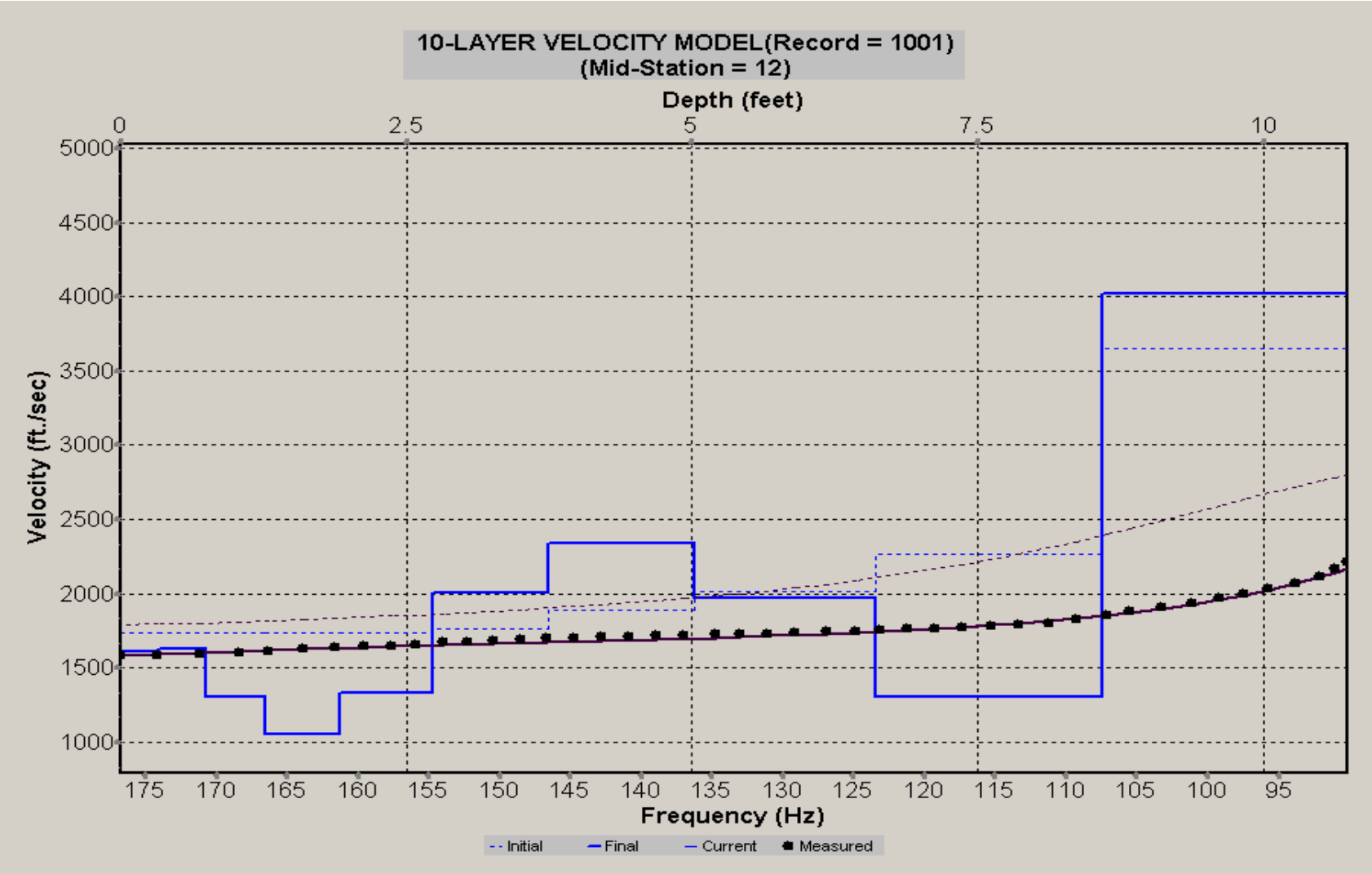

A.036: Velocity Profile Line 1032 used in Pre-blast 8

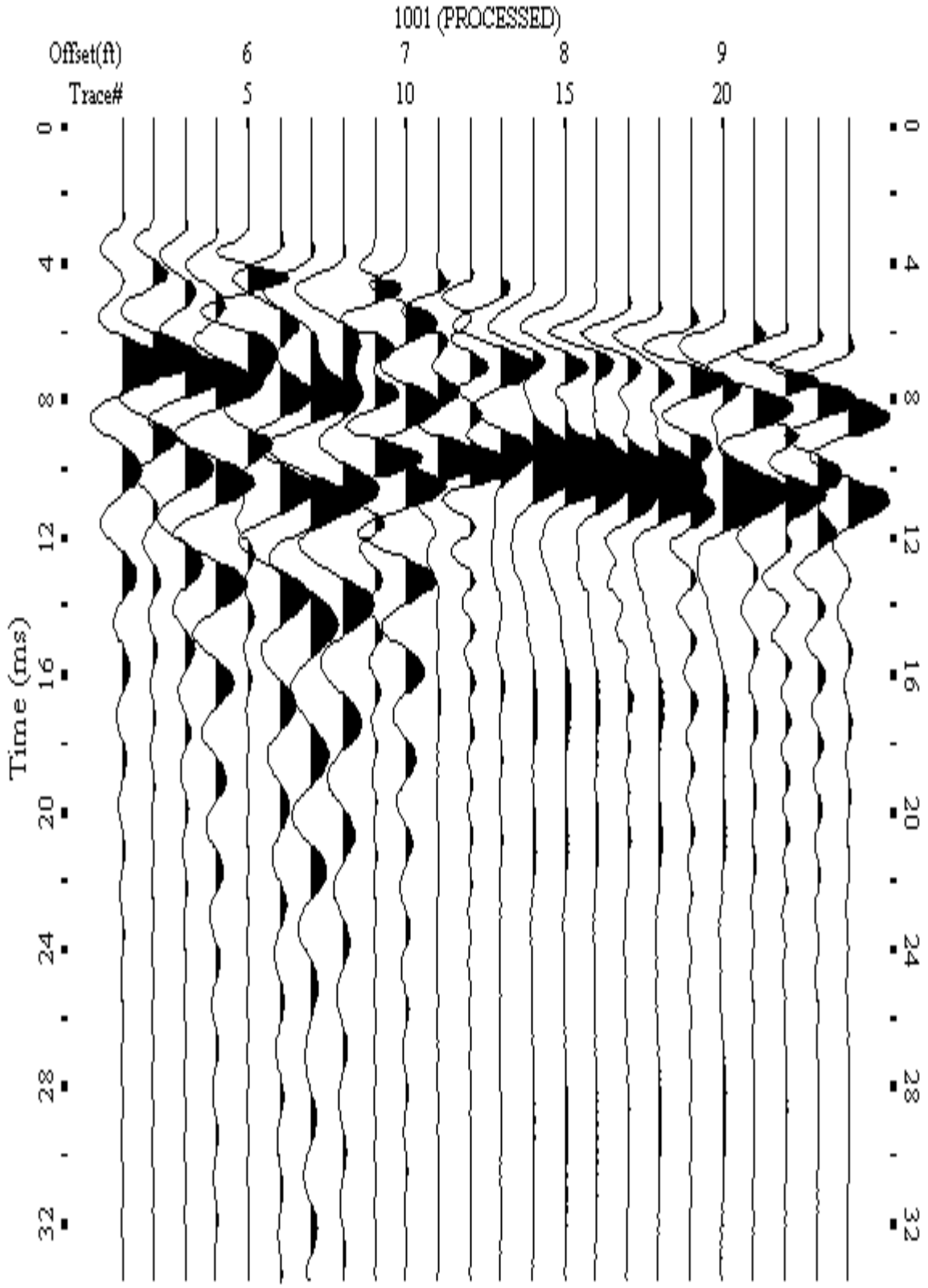

A.037: Shot Gather Line 1033 used in Pre-blast 8

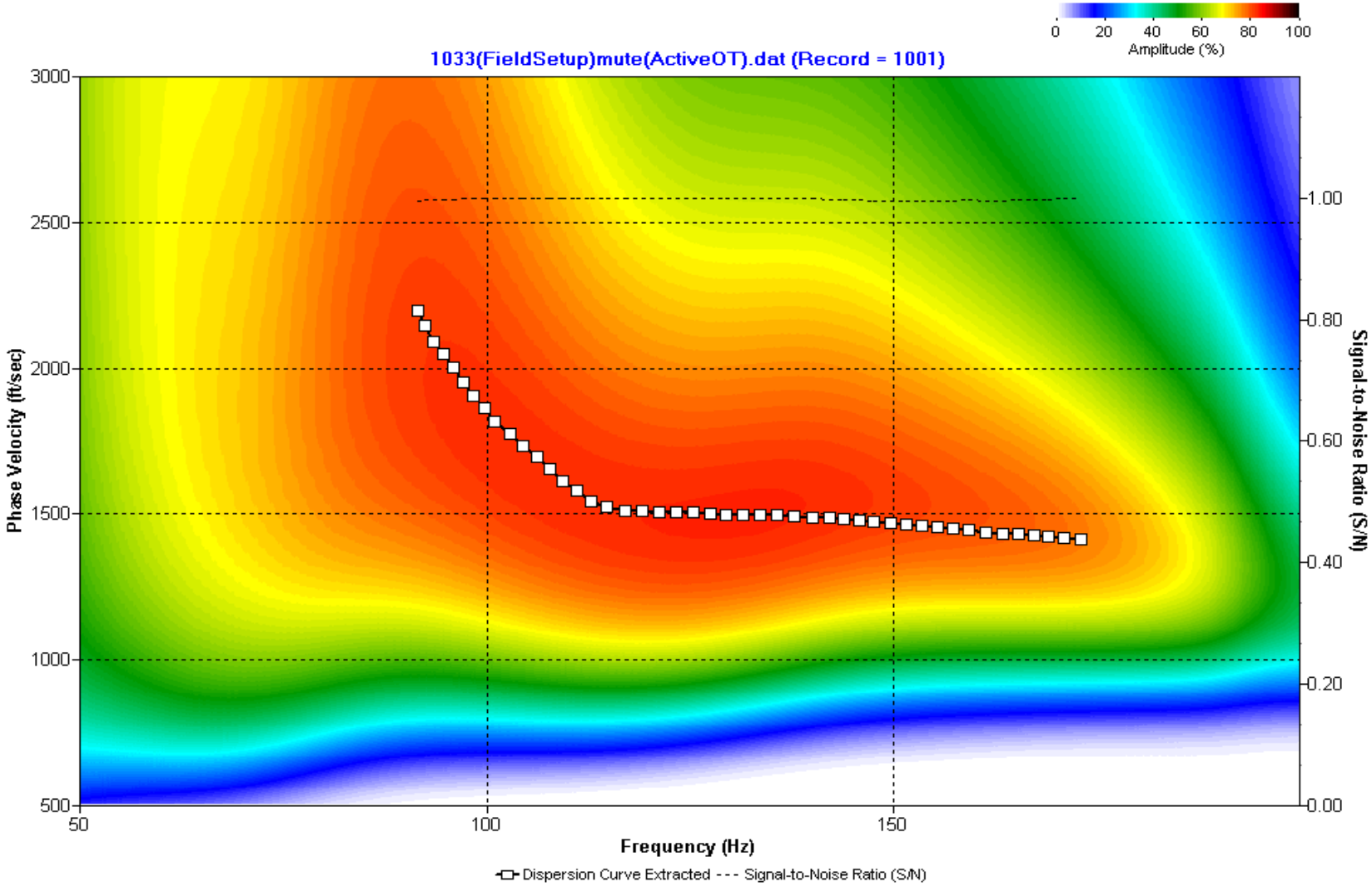

A.038: Dispersion Curve Line 1033 used in Pre-blast 8

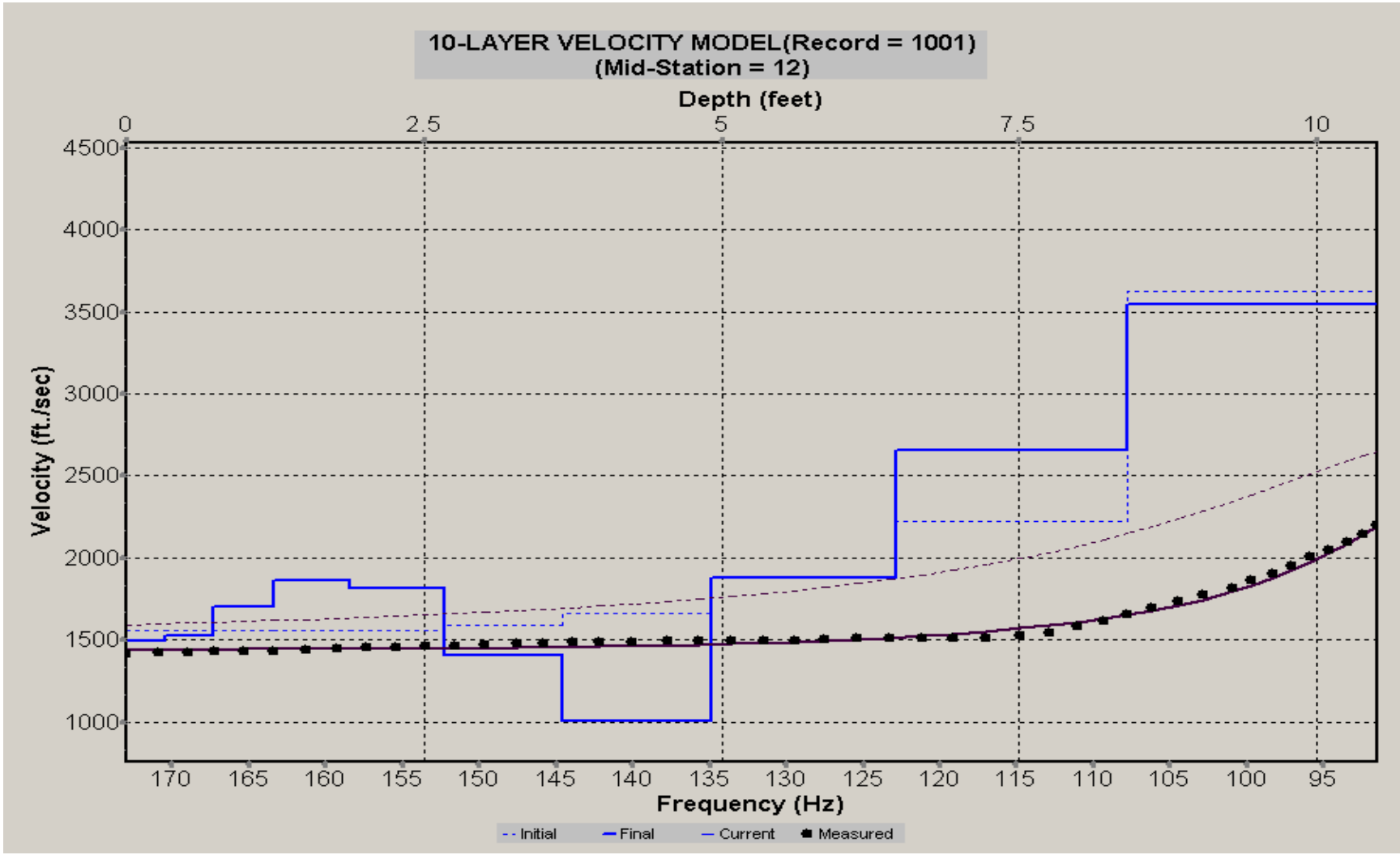

A.039: Velocity Profile Line 1033 used in Pre-blast 8

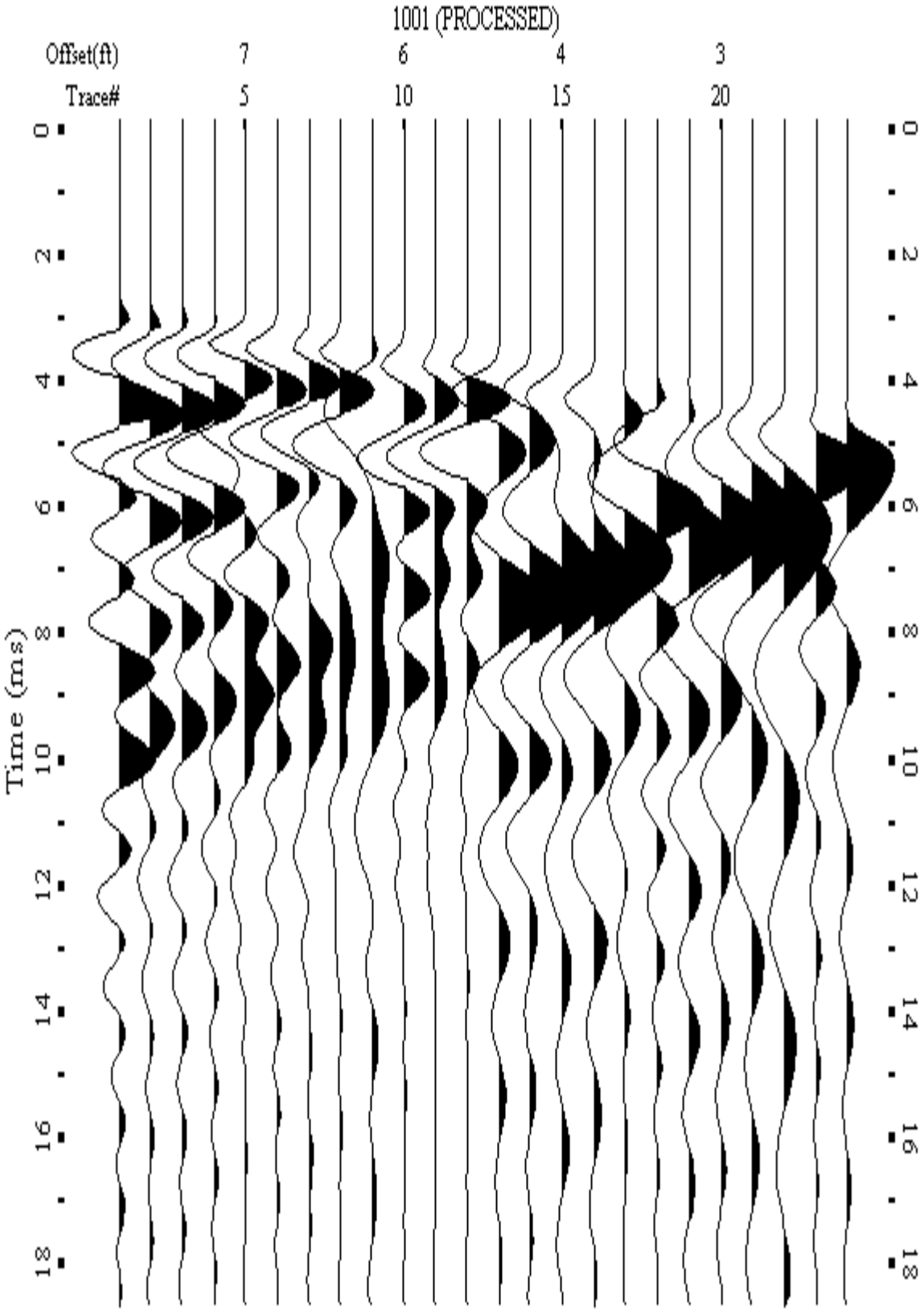

A.040: Shot Gather Line 1035 used in Pre-blast 9 and Pre-blast 10

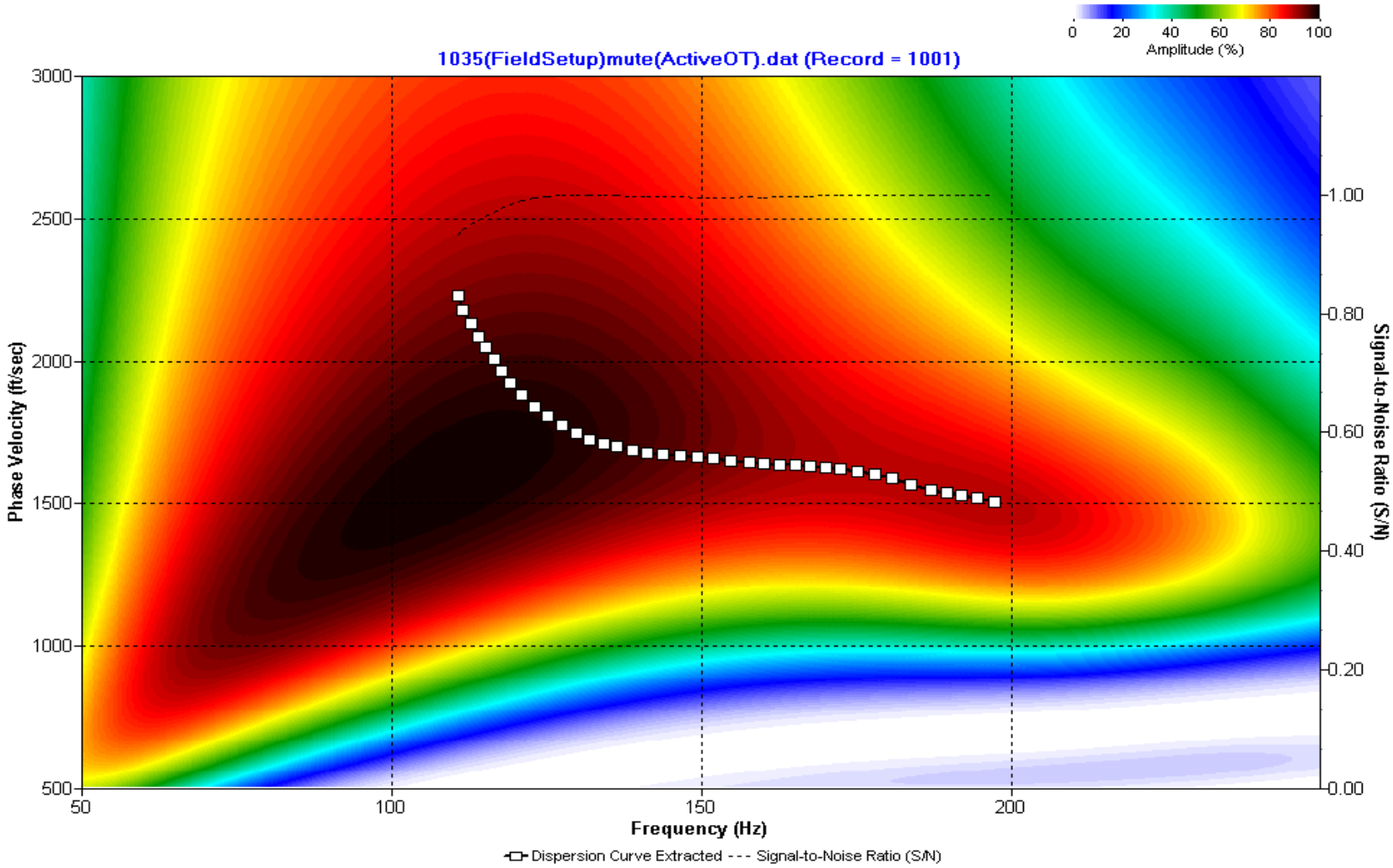

A.041: Dispersion Curve Line 1035 used in Pre-blast 9 and Pre-blast 10

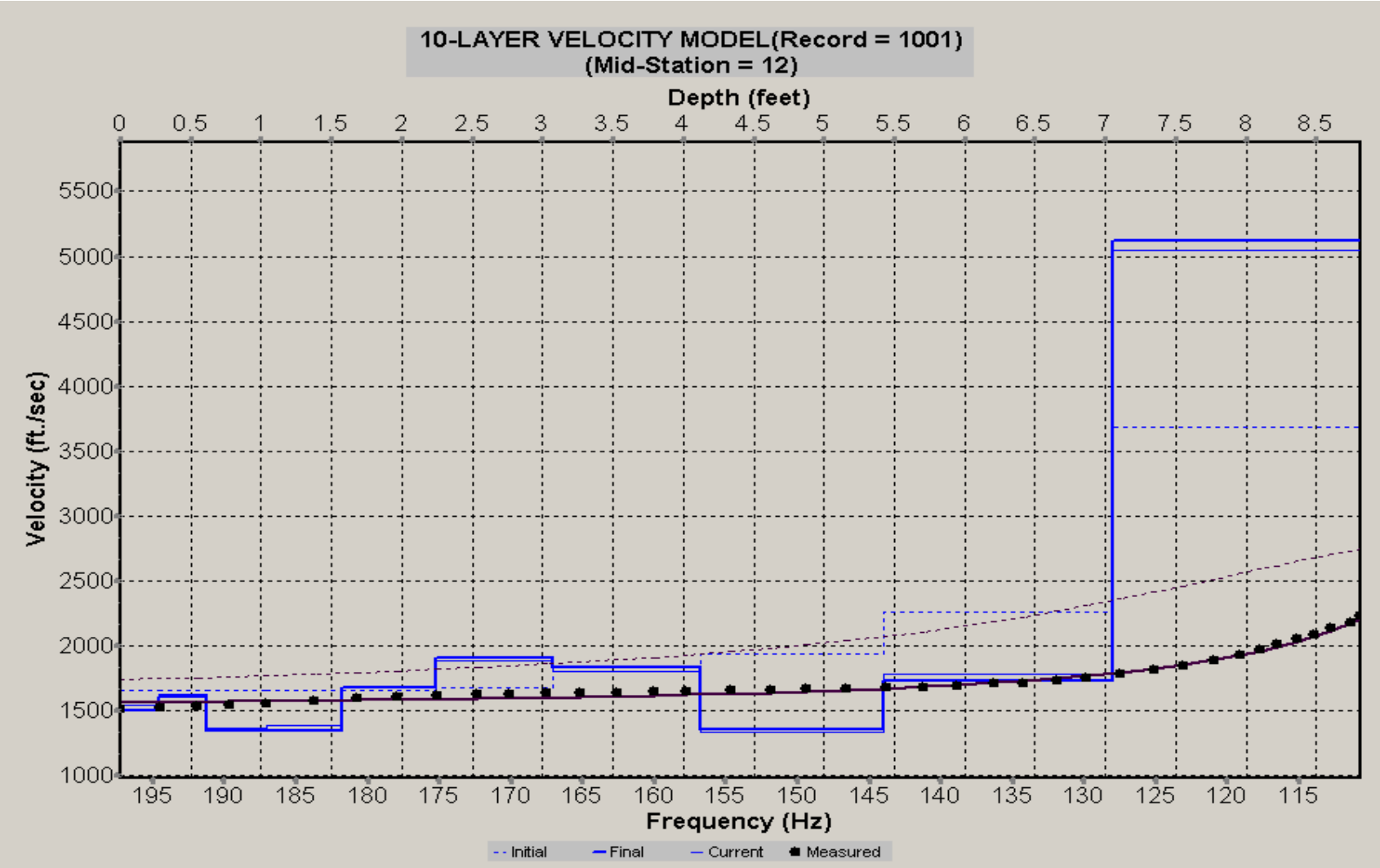

A.042: Velocity Profile Line 1035 used in Pre-blast 9 and Pre-blast 10

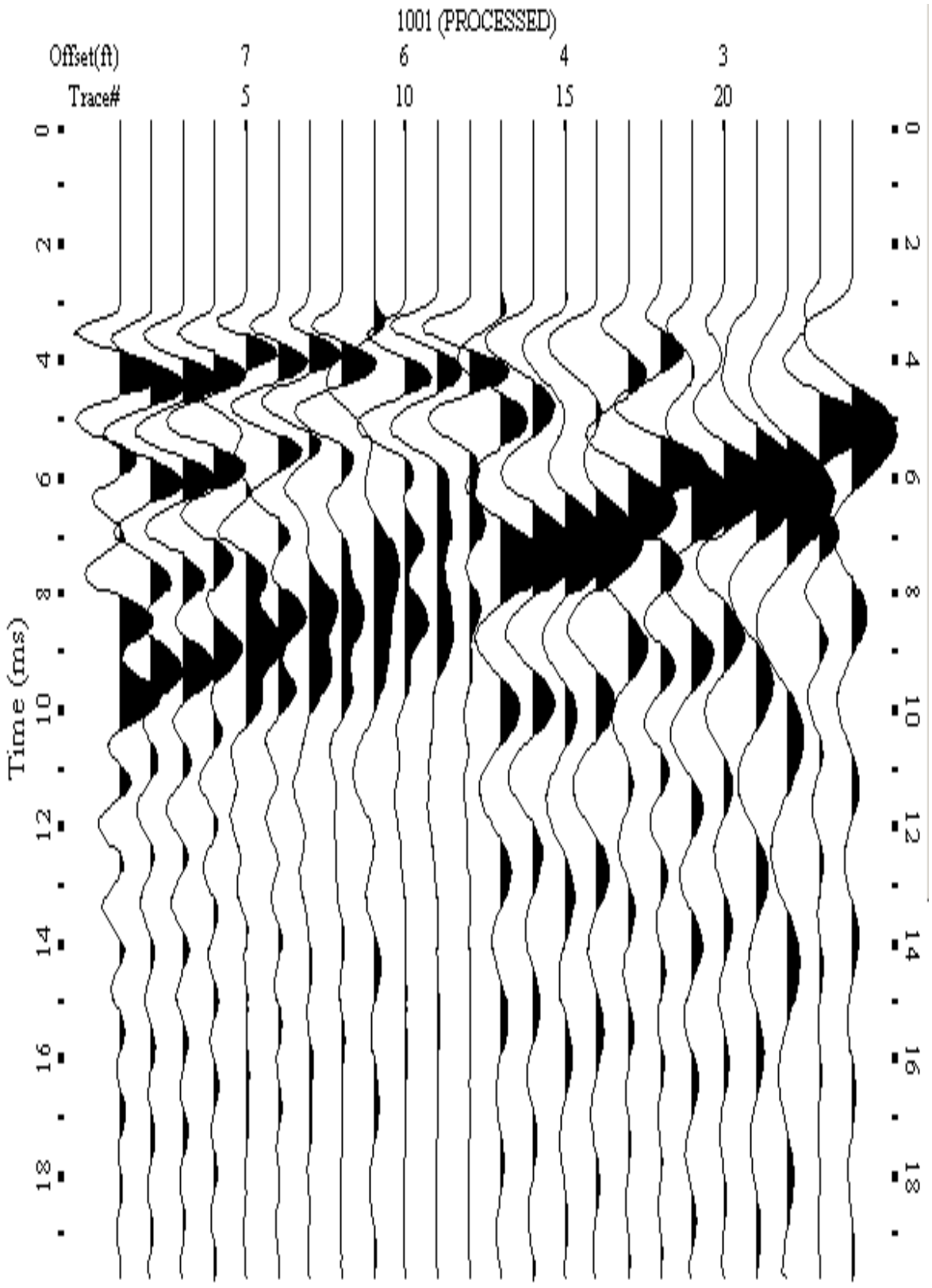

A.043: Shot Gather Line 1036 used in Pre-blast 9 and Pre-blast 10

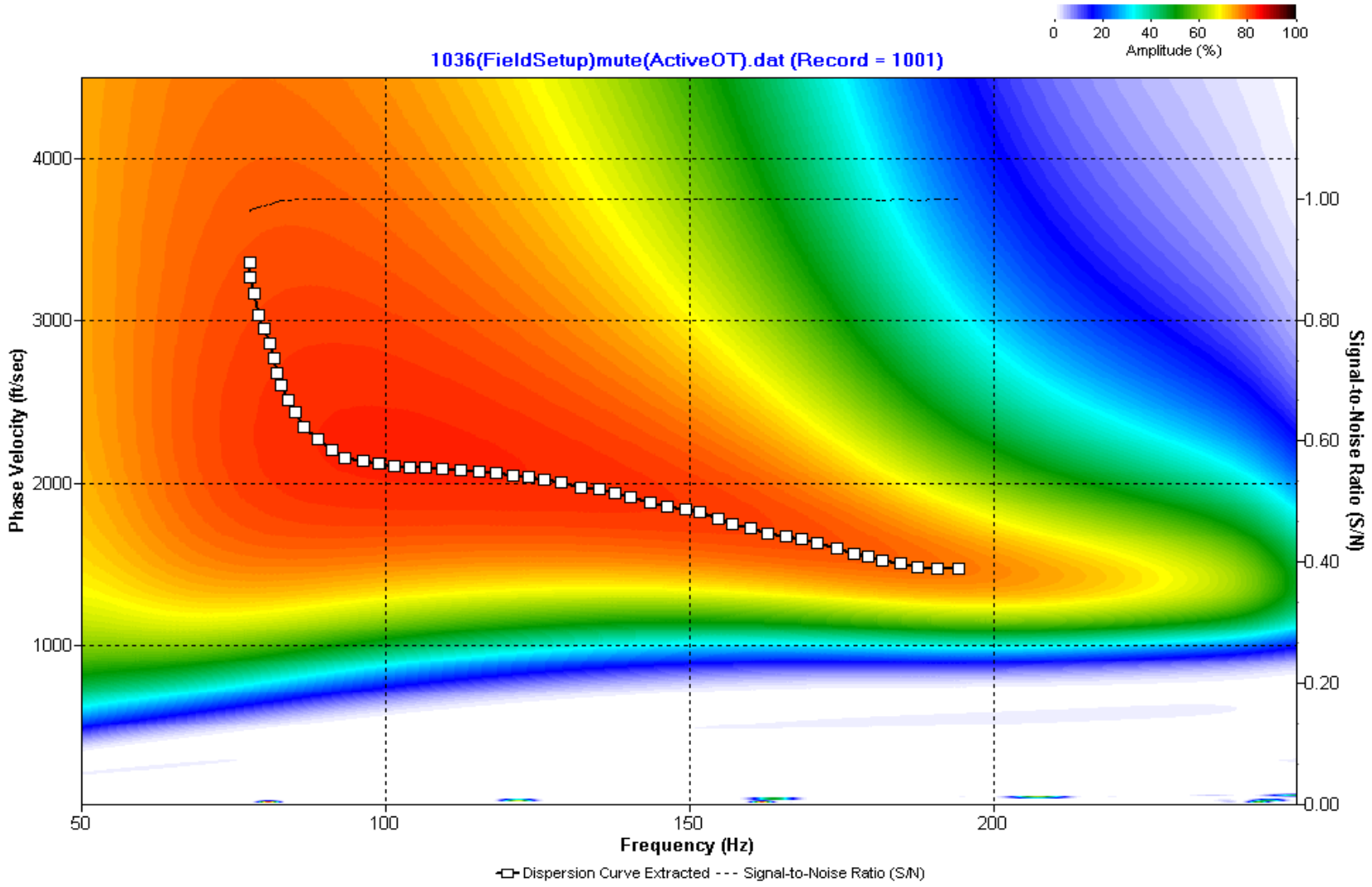

A.044: Dispersion Curve Line 1036 used in Pre-blast 9 and Pre-blast 10

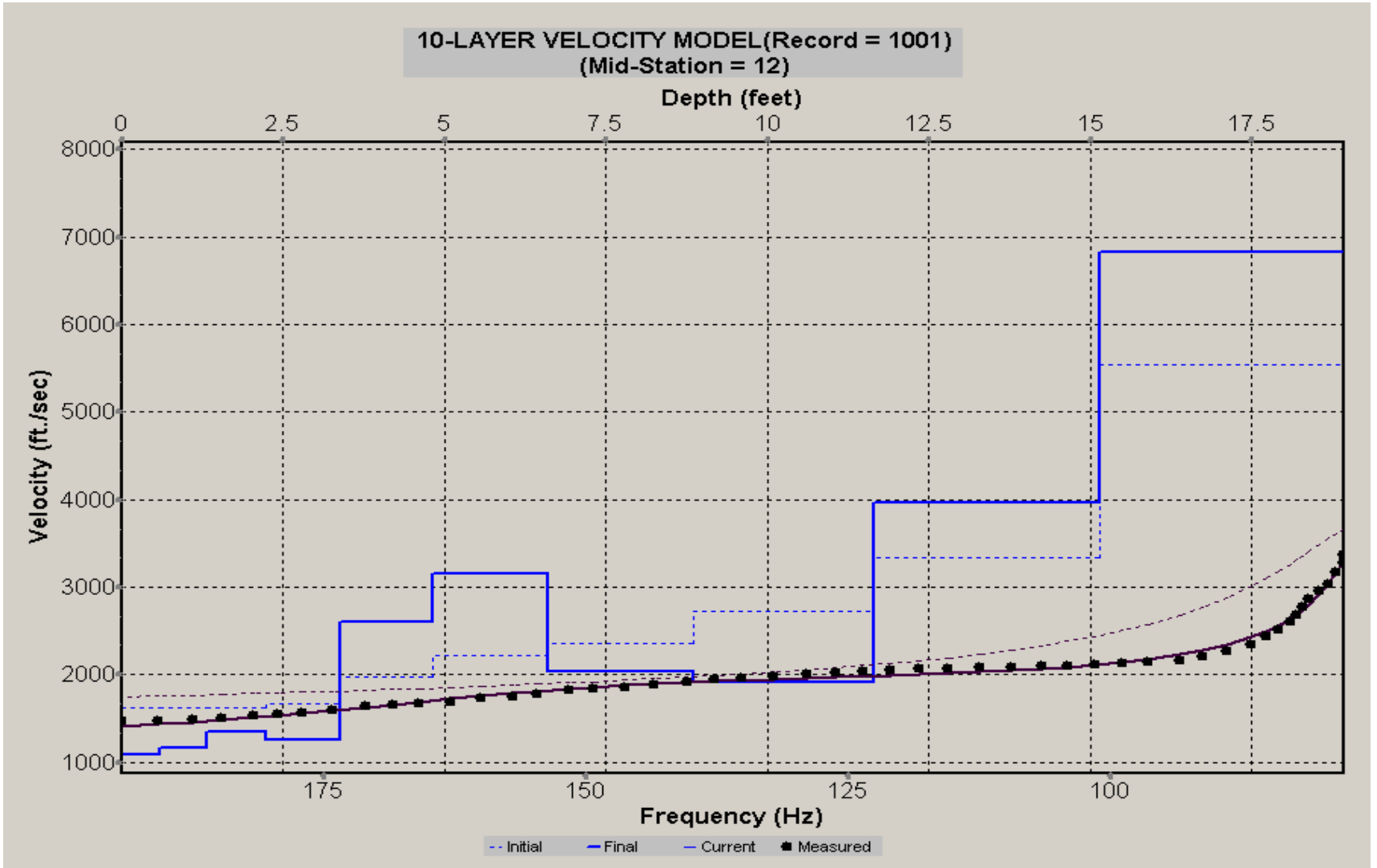

A.045: Velocity Profile Line 1036 used in Pre-blast 9 and Pre-blast 10

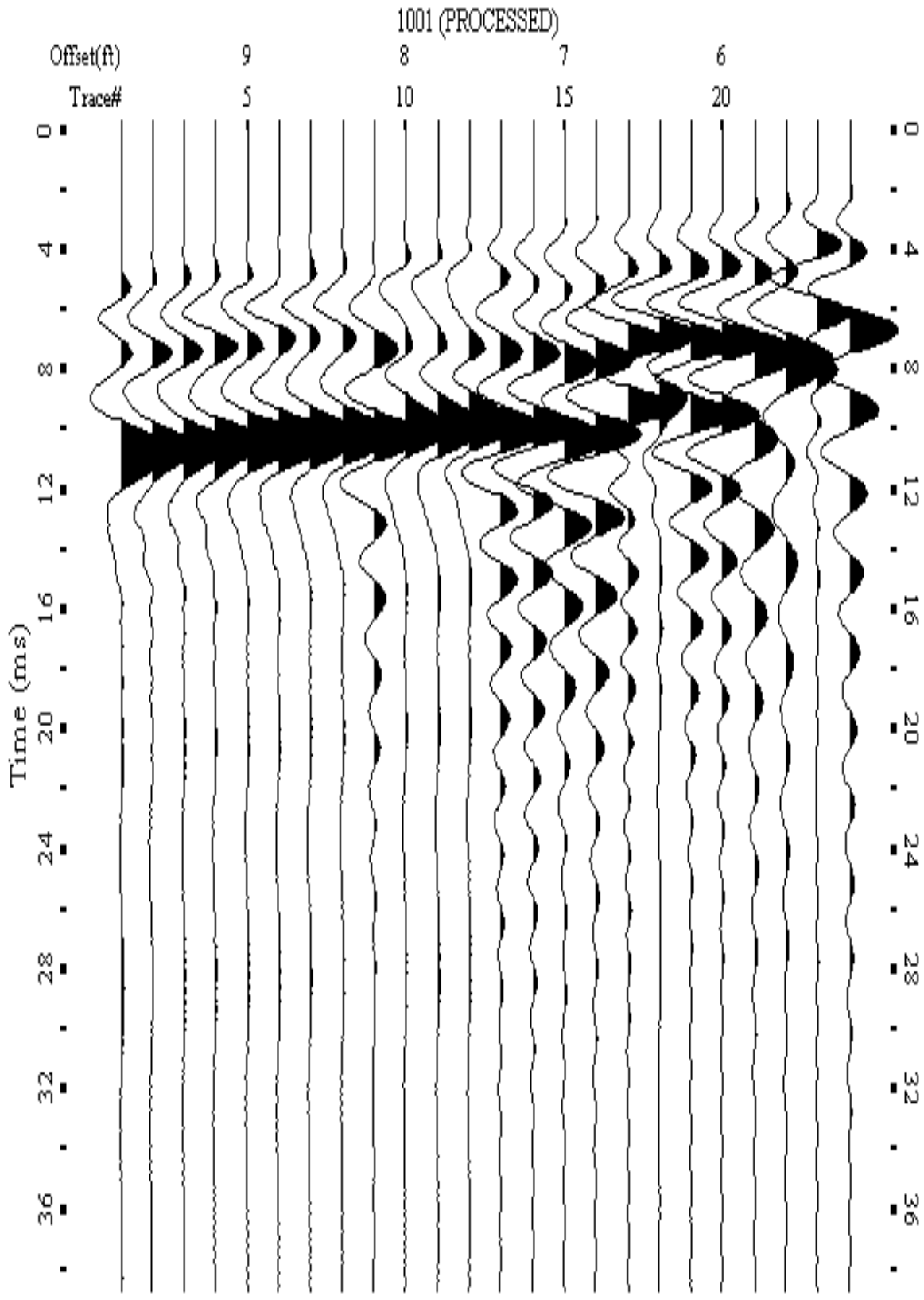

A.046: Shot Gather Line 1037 used in Pre-blast 9 and Pre-blast 10

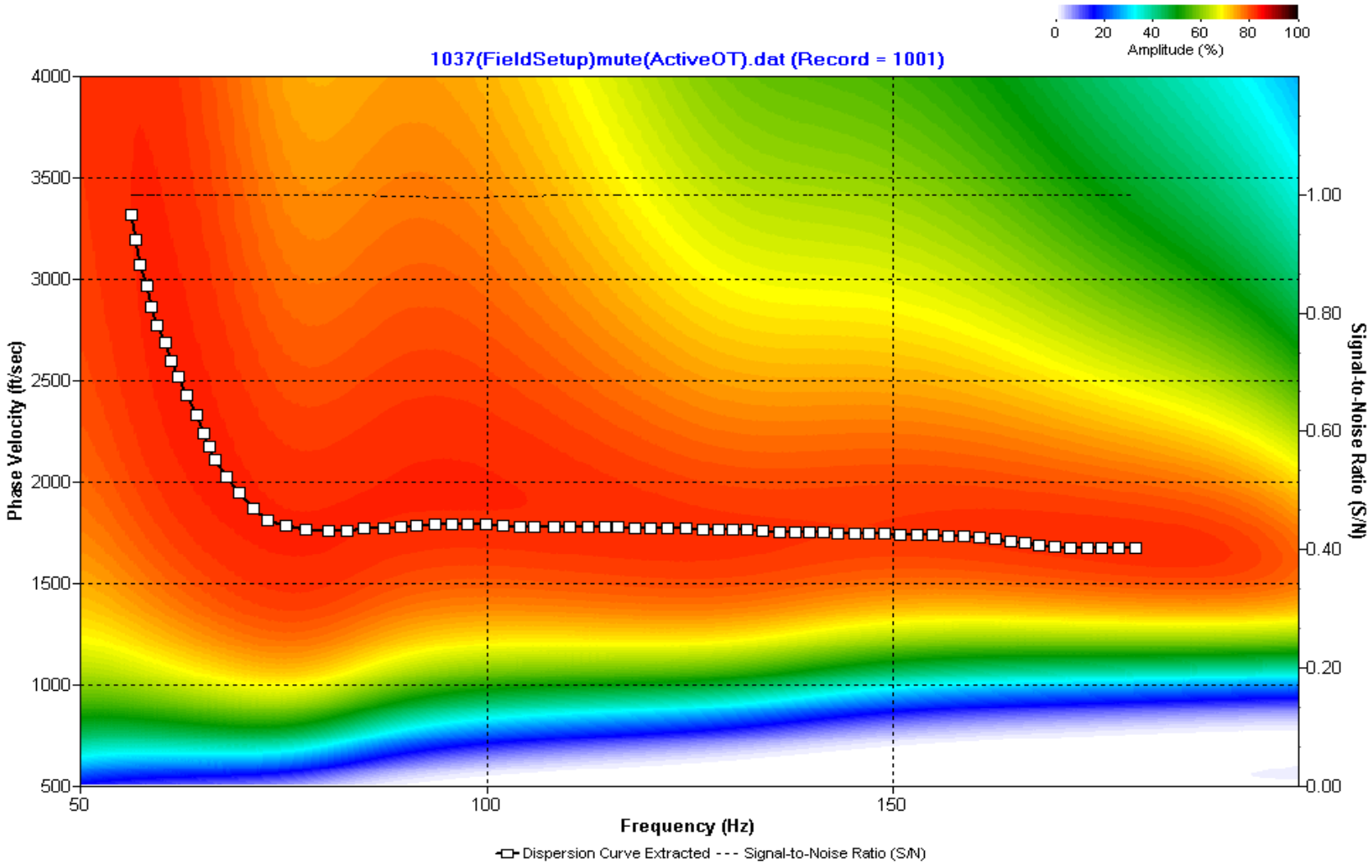

A.047: Dispersion Curve Line 1037 used in Pre-blast 9 and Pre-blast 10

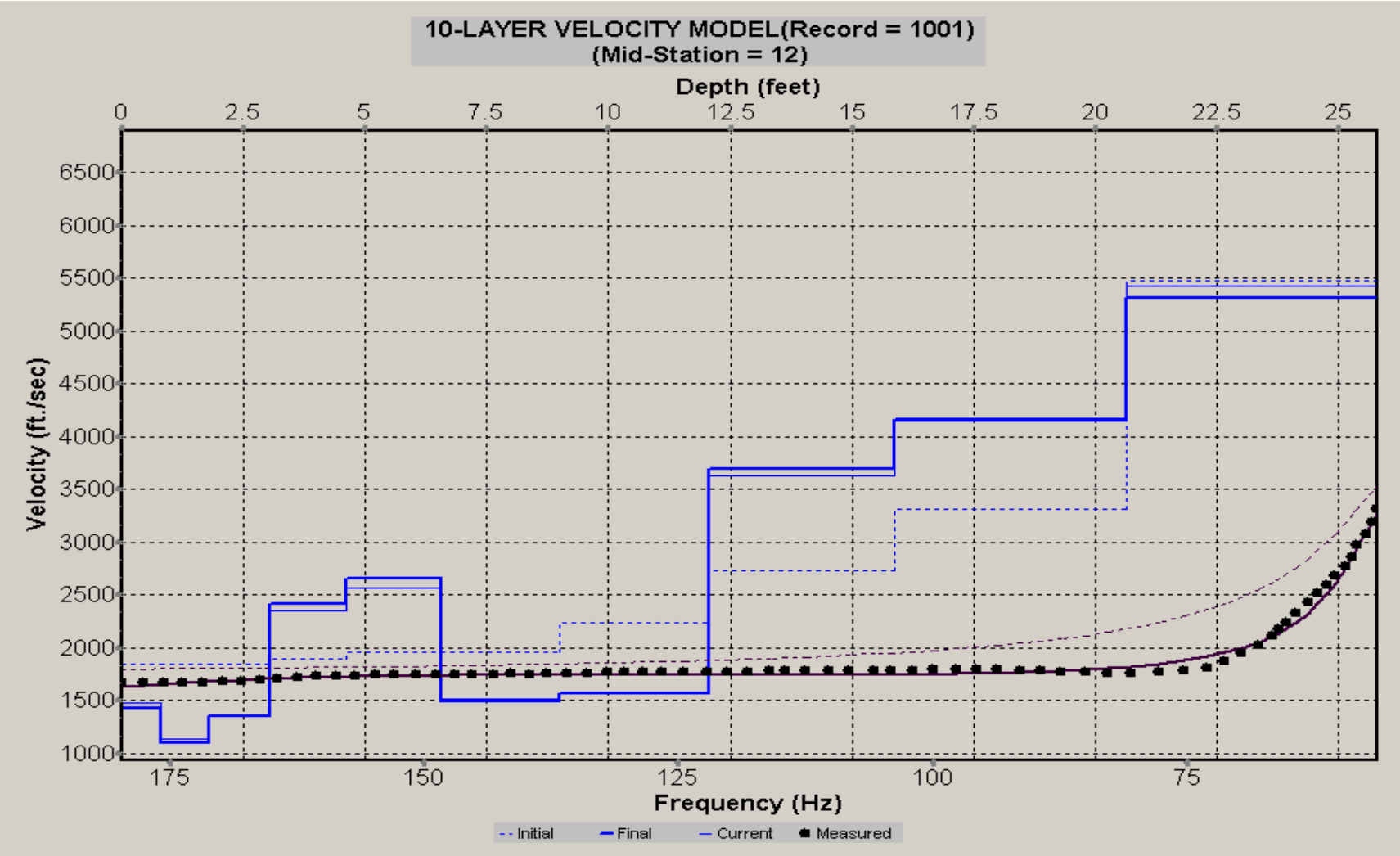

A.048: Velocity Profile Line 1037 used in Pre-blast 9 and Pre-blast 10

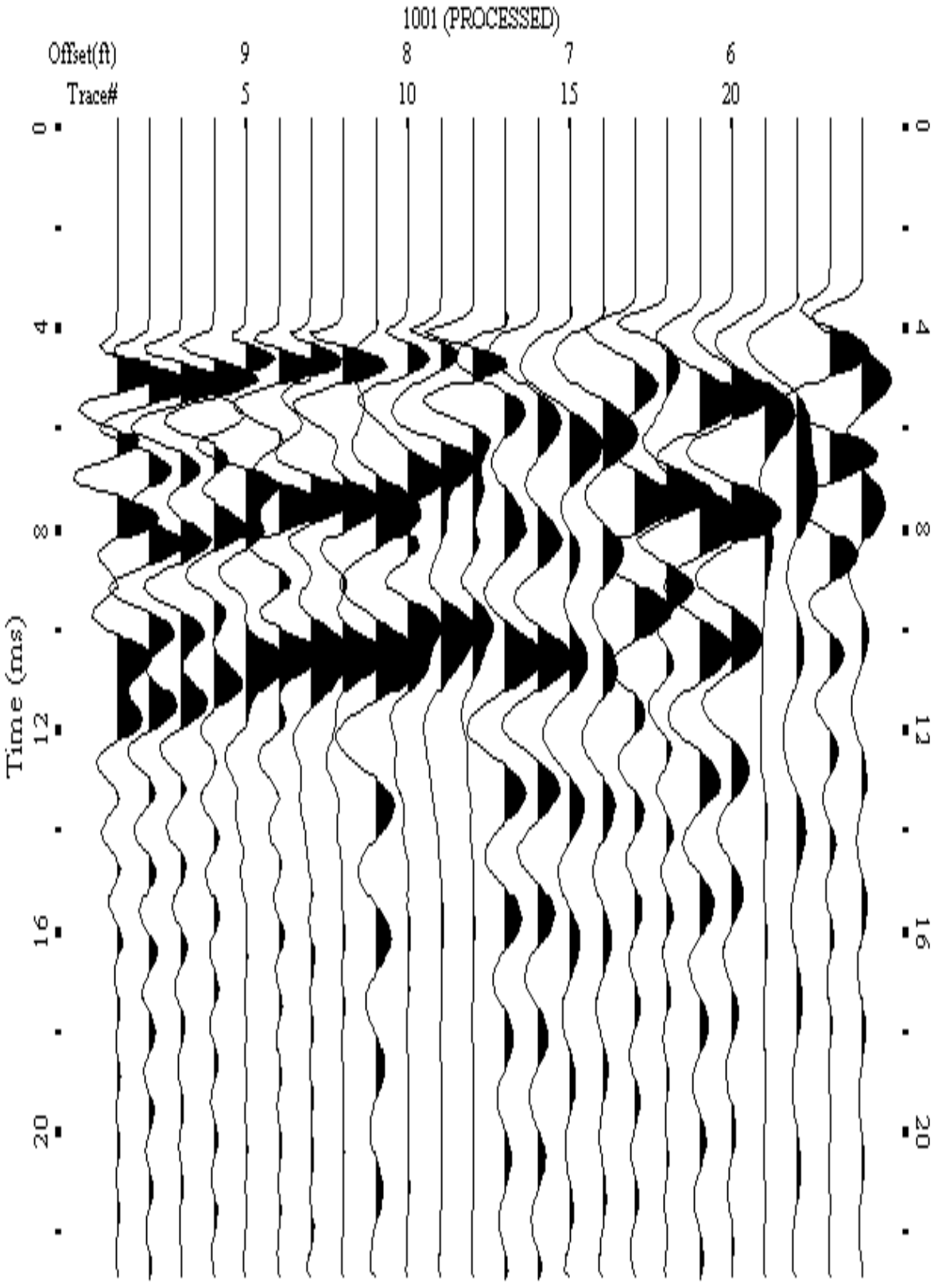

A.049: Shot Gather Line 1038 used in Pre-blast 9 and Pre-blast 10

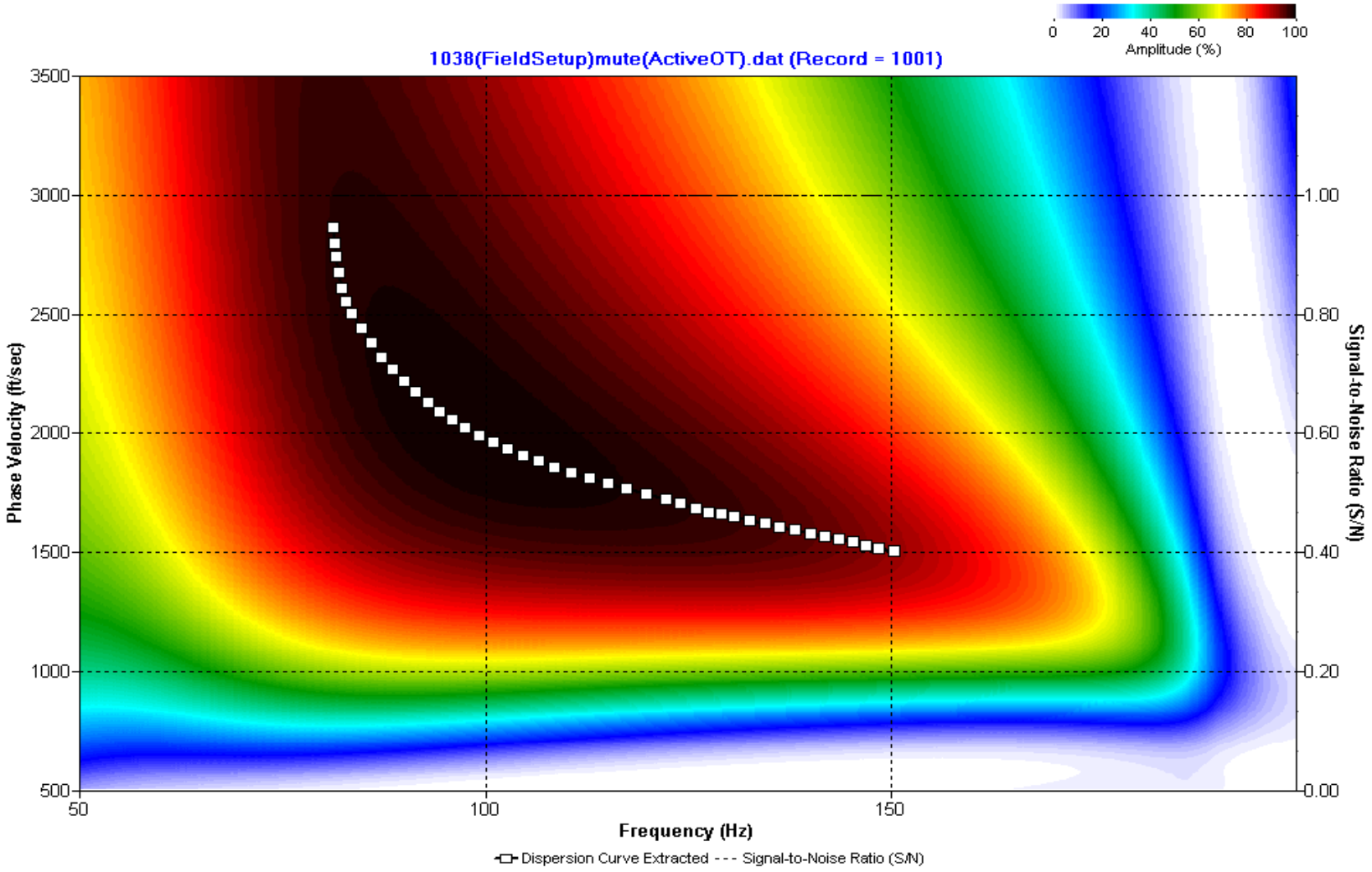

A.050: Dispersion Curve Line 1038 used in Pre-blast 9 and Pre-blast 10

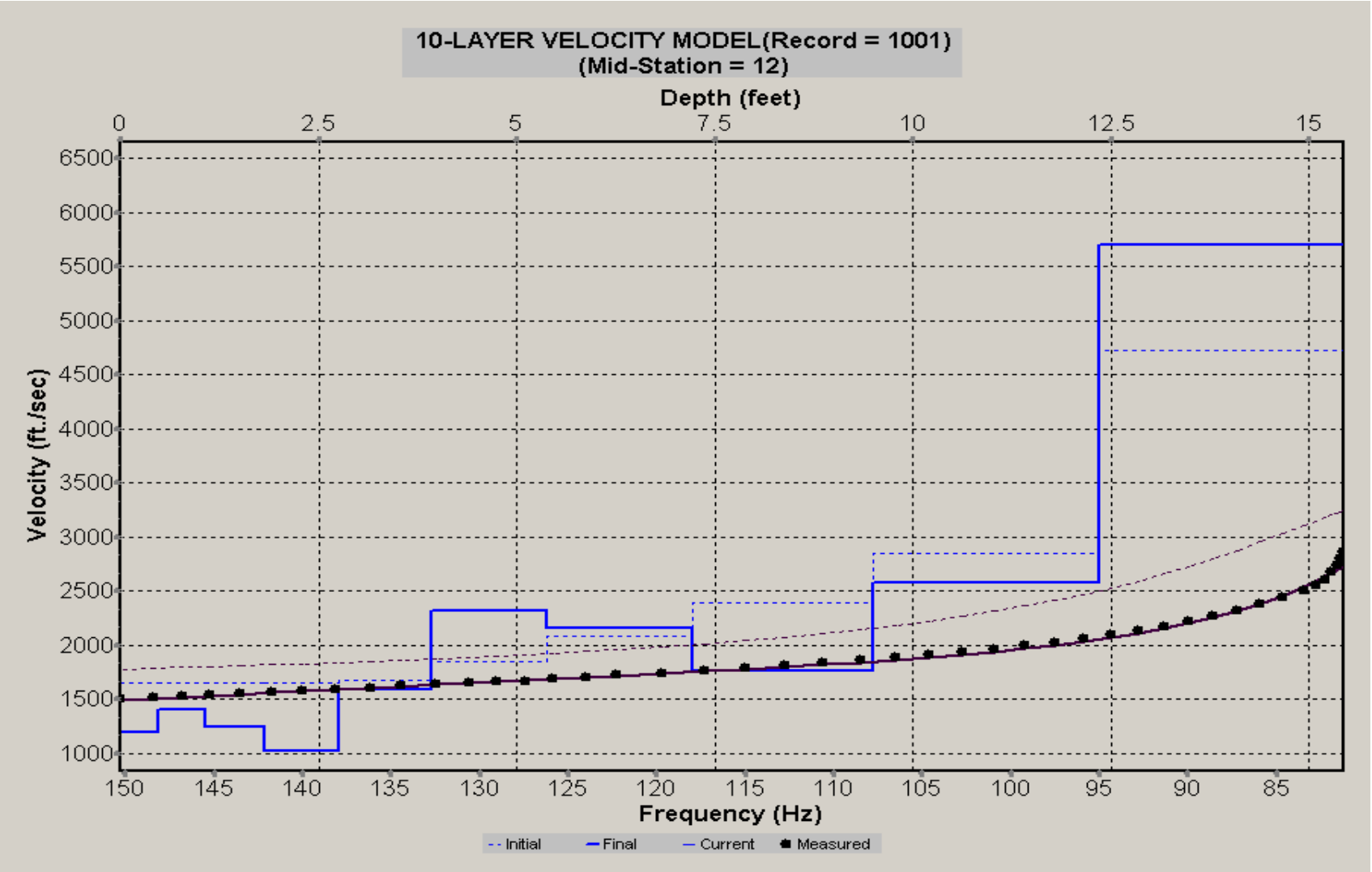

A.051: Velocity Profile Line 1038 used in Pre-blast 9 and Pre-blast 10

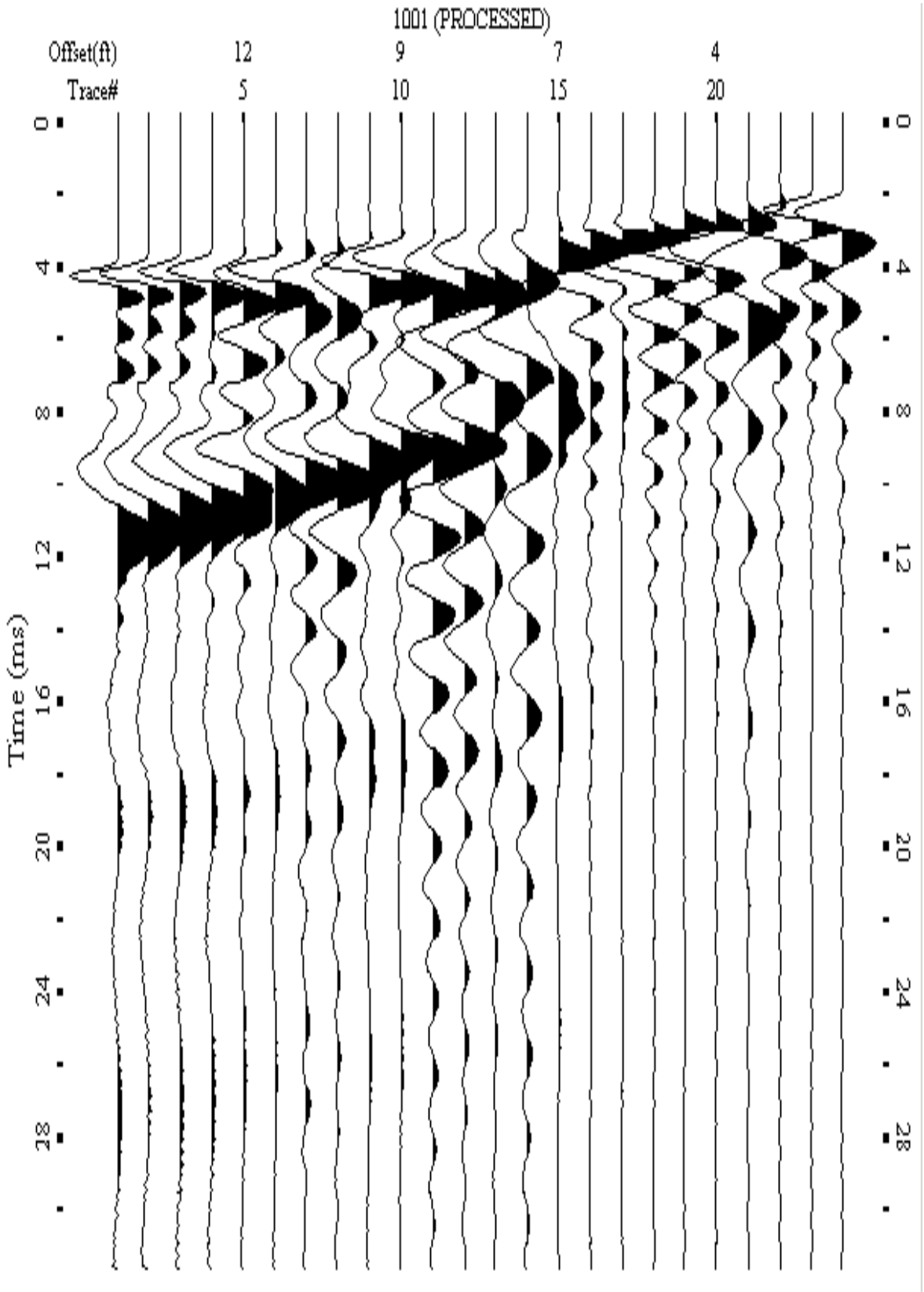

A.052: Shot Gather Line 1039 used in Pre-blast 8, Pre-blast 9 and Pre-blast 10

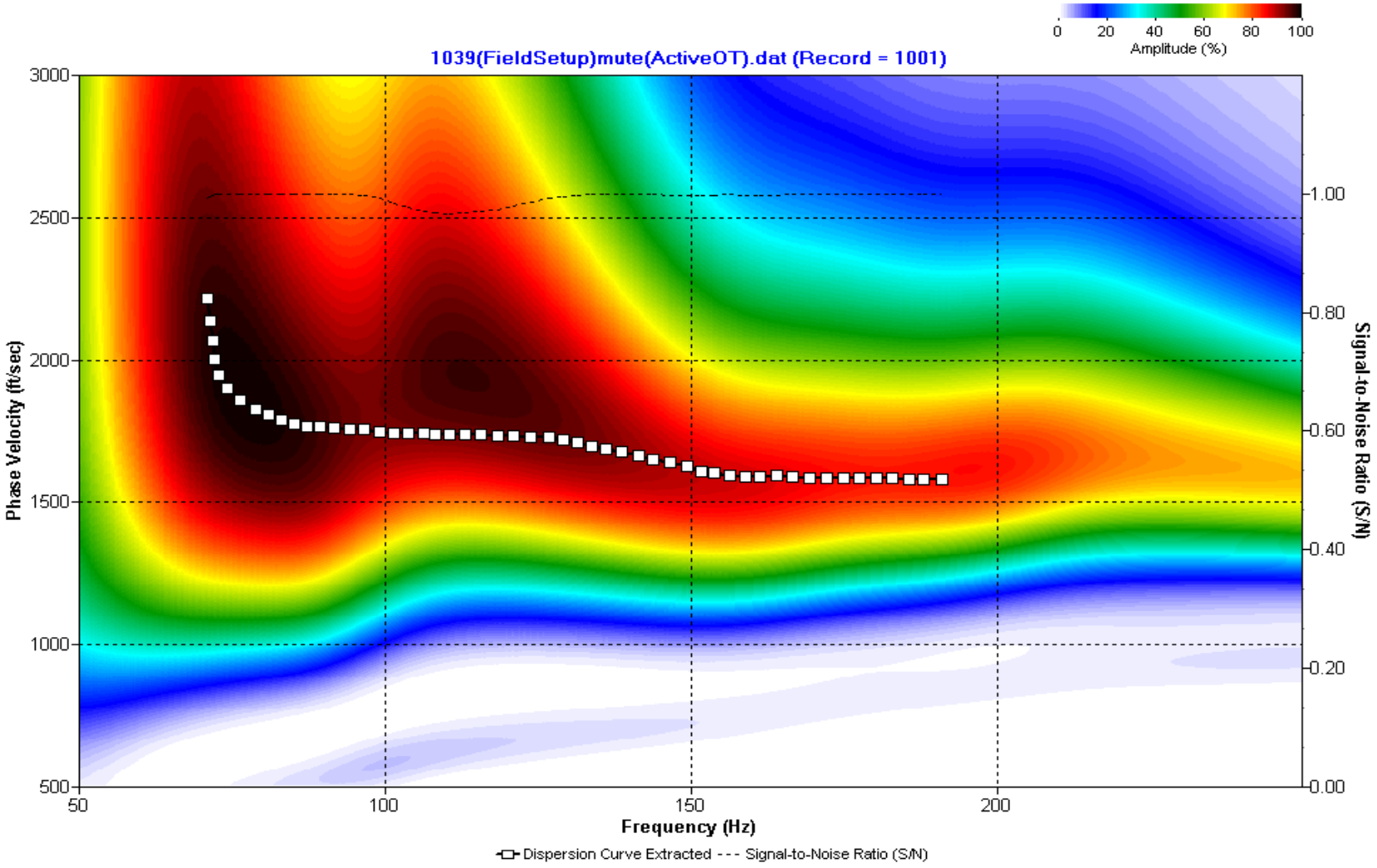

A.053: Dispersion Curve Line 1039 used in Pre-blast 8, Pre-blast 9 and Pre-blast 10

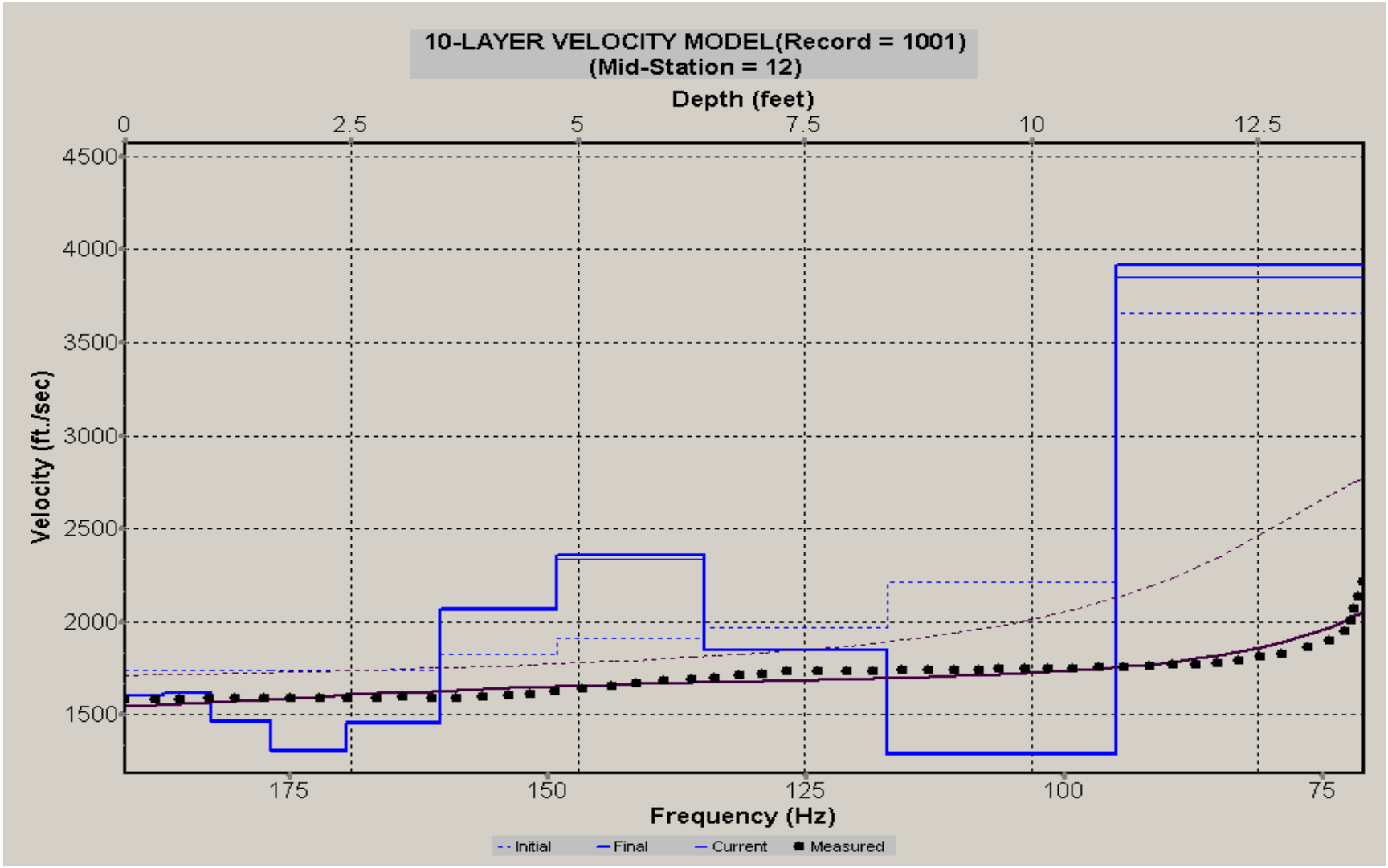

A.054: Velocity Profile Line 1039 used in Pre-blast 8, Pre-blast 9 and Pre-blast 10

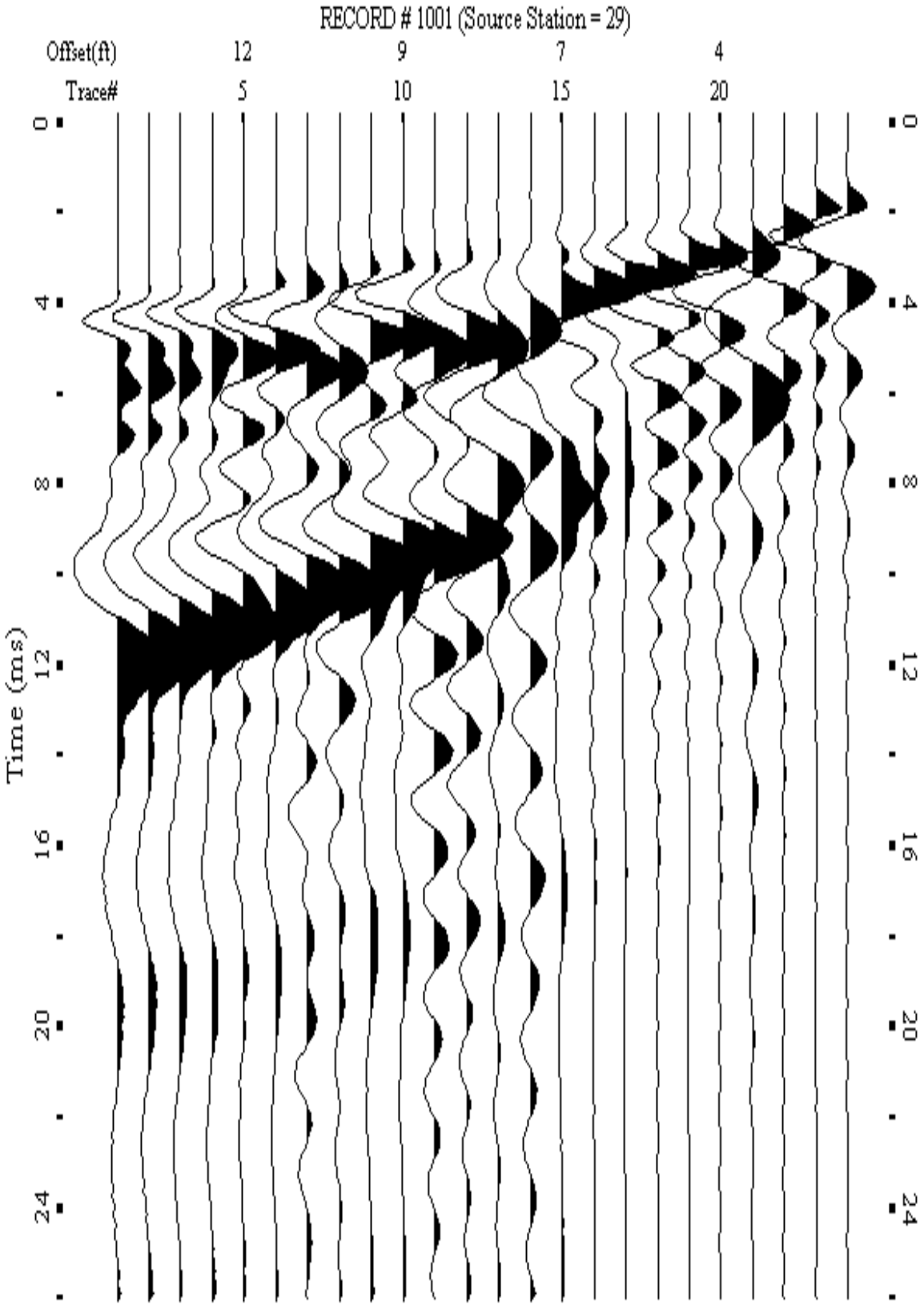

A.055: Shot Gather Line 1040 used in Pre-blast 8, Pre-blast 9 and Pre-blast 10

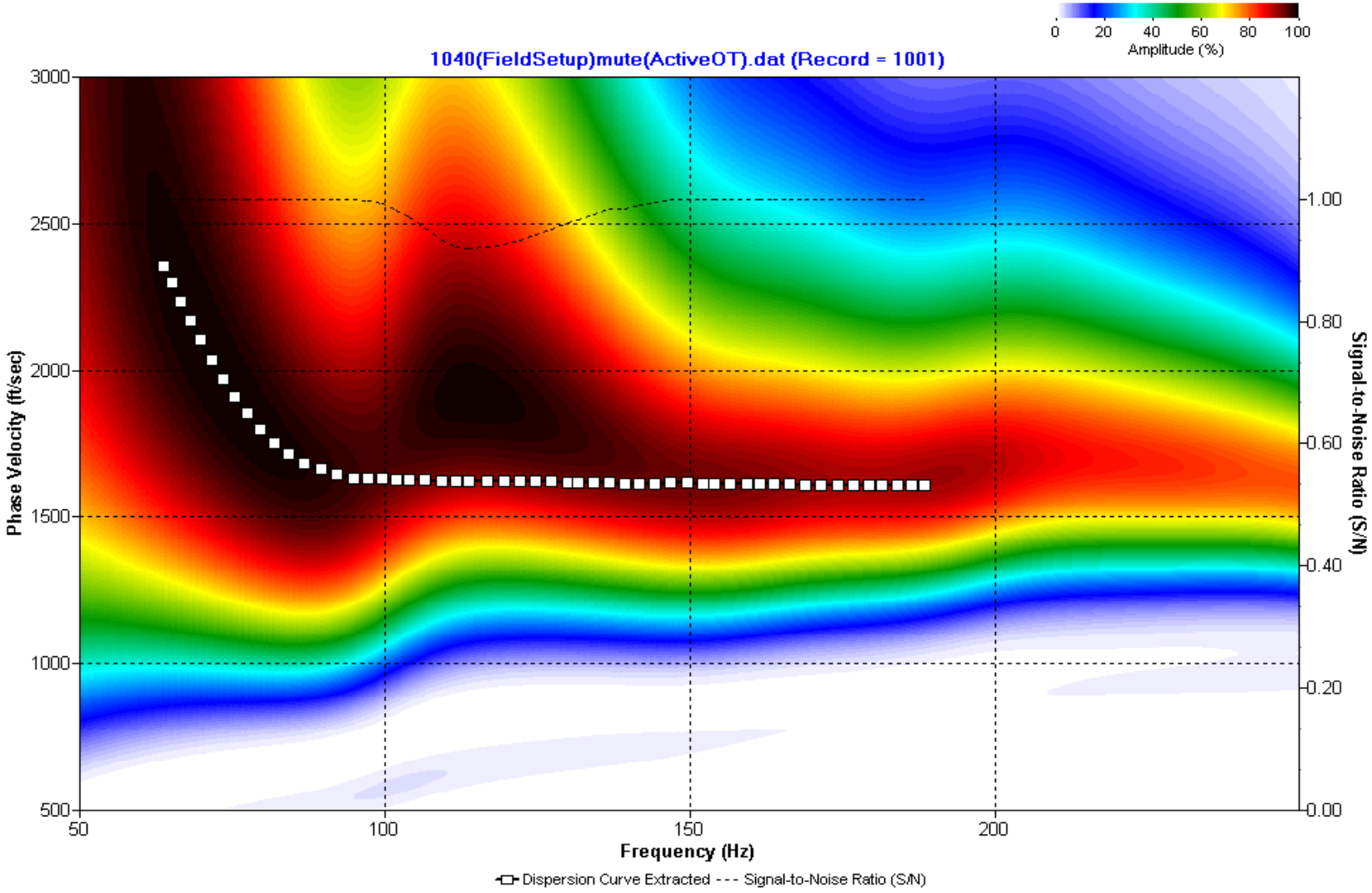

A.056: Dispersion Curve Line 1040 used in Pre-blast 8, Pre-blast 9 and Pre-blast 10

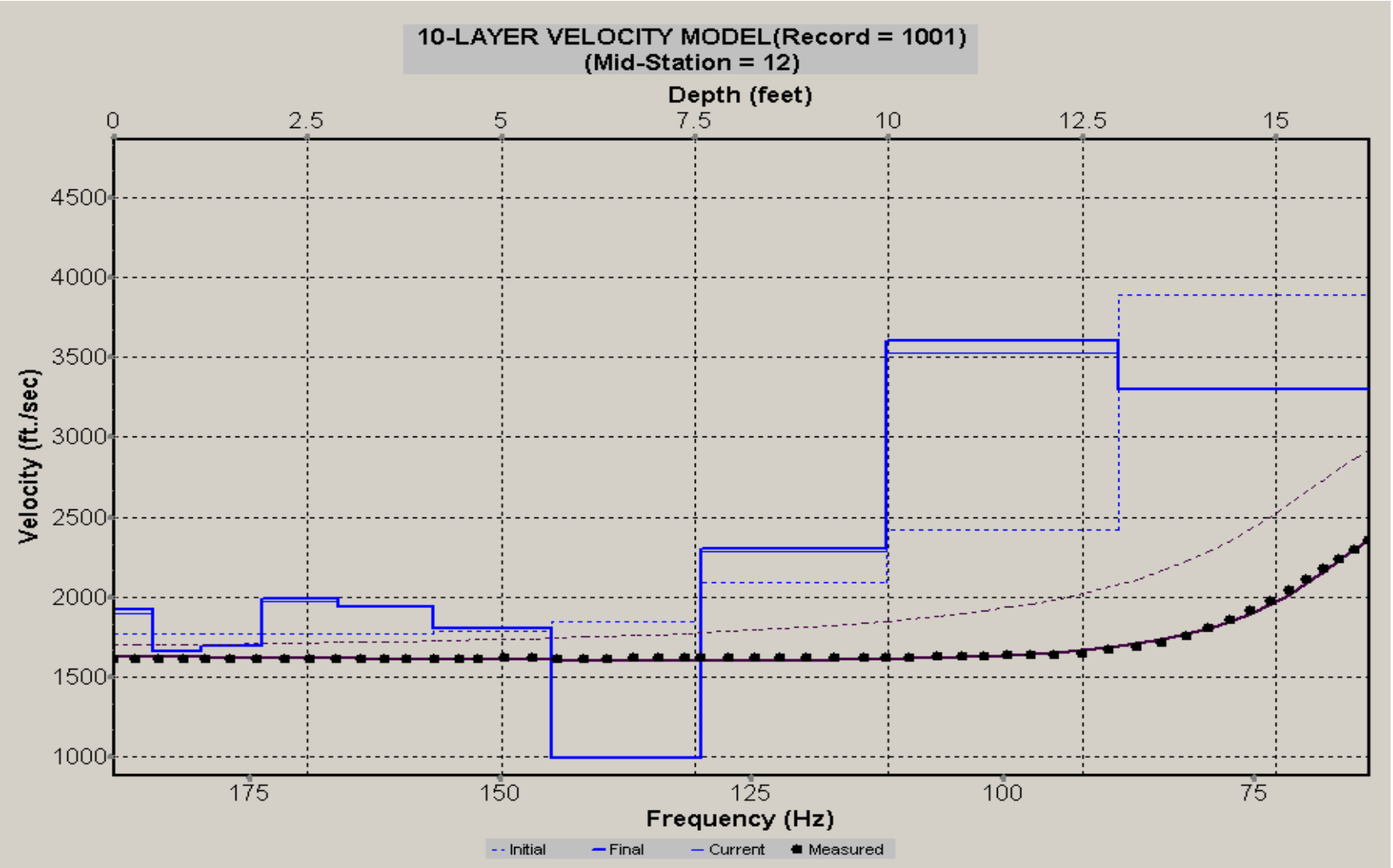

A.057: Velocity Profile Line 1040 used in Pre-blast 8, Pre-blast 9 and Pre-blast 10

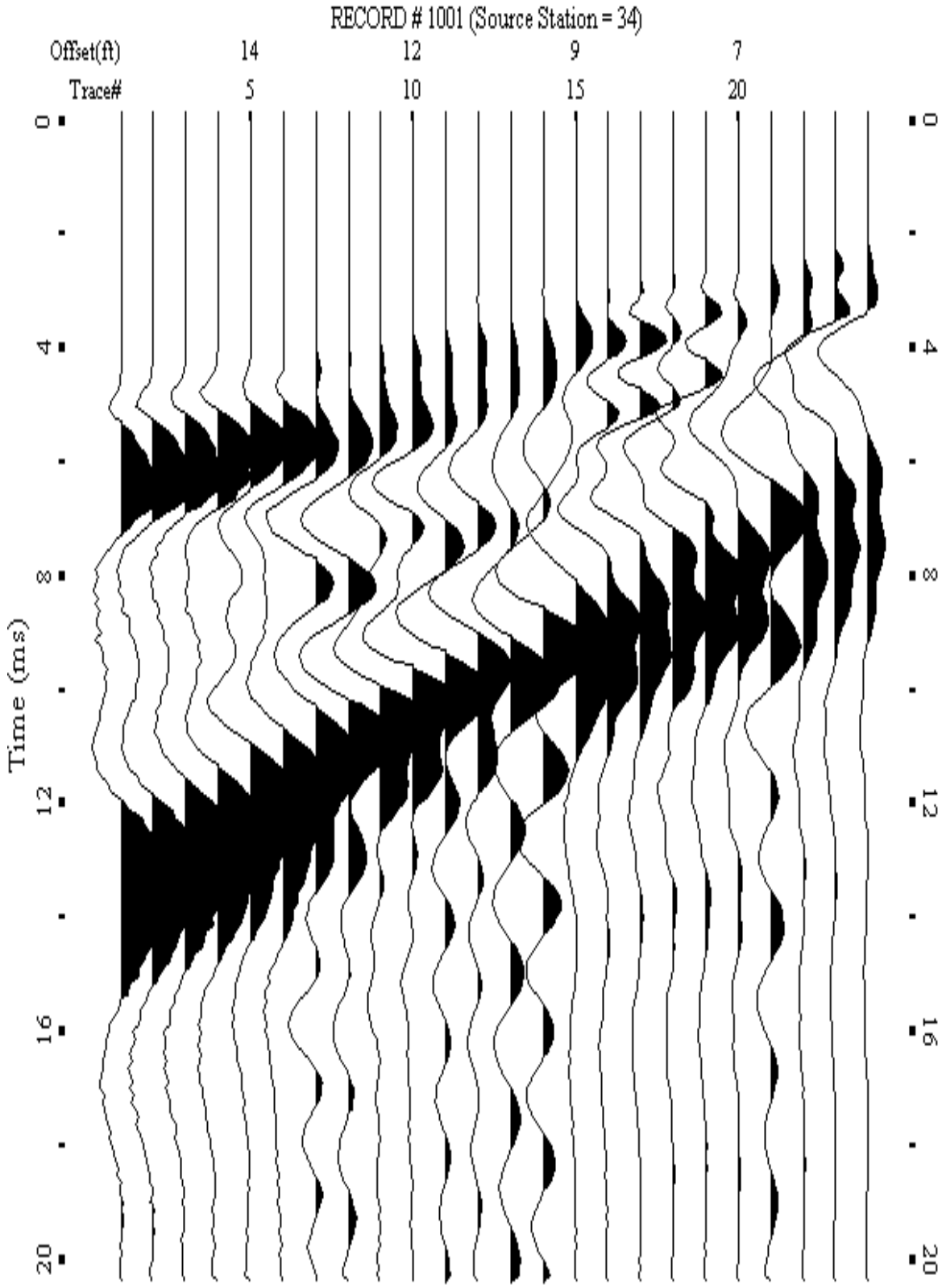

A.058: Shot Gather Line 1041 used in Pre-blast 8, Pre-blast 9 and Pre-blast 10

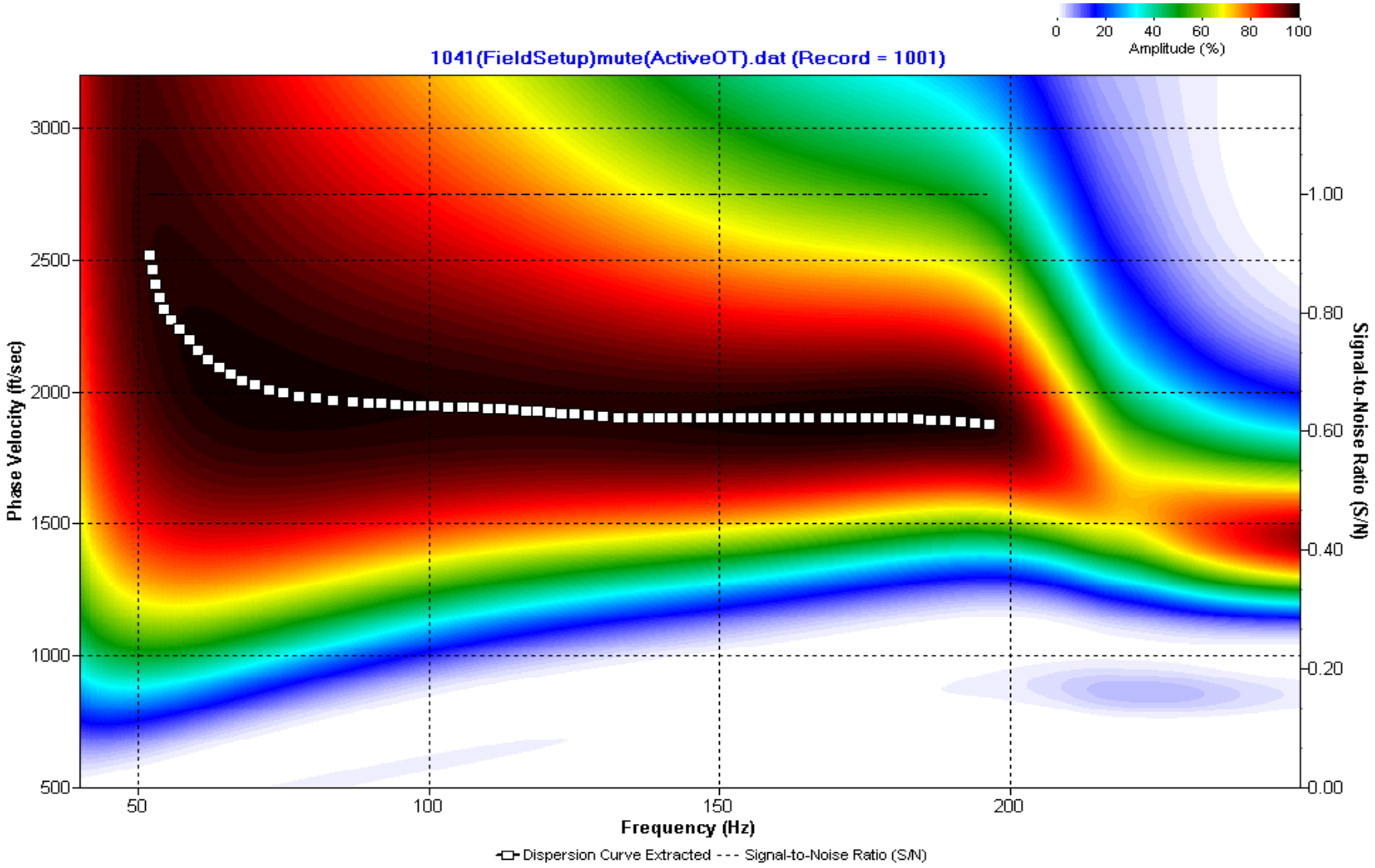

A.059: Dispersion Curve Line 1041 used in Pre-blast 8, Pre-blast 9 and Pre-blast 10

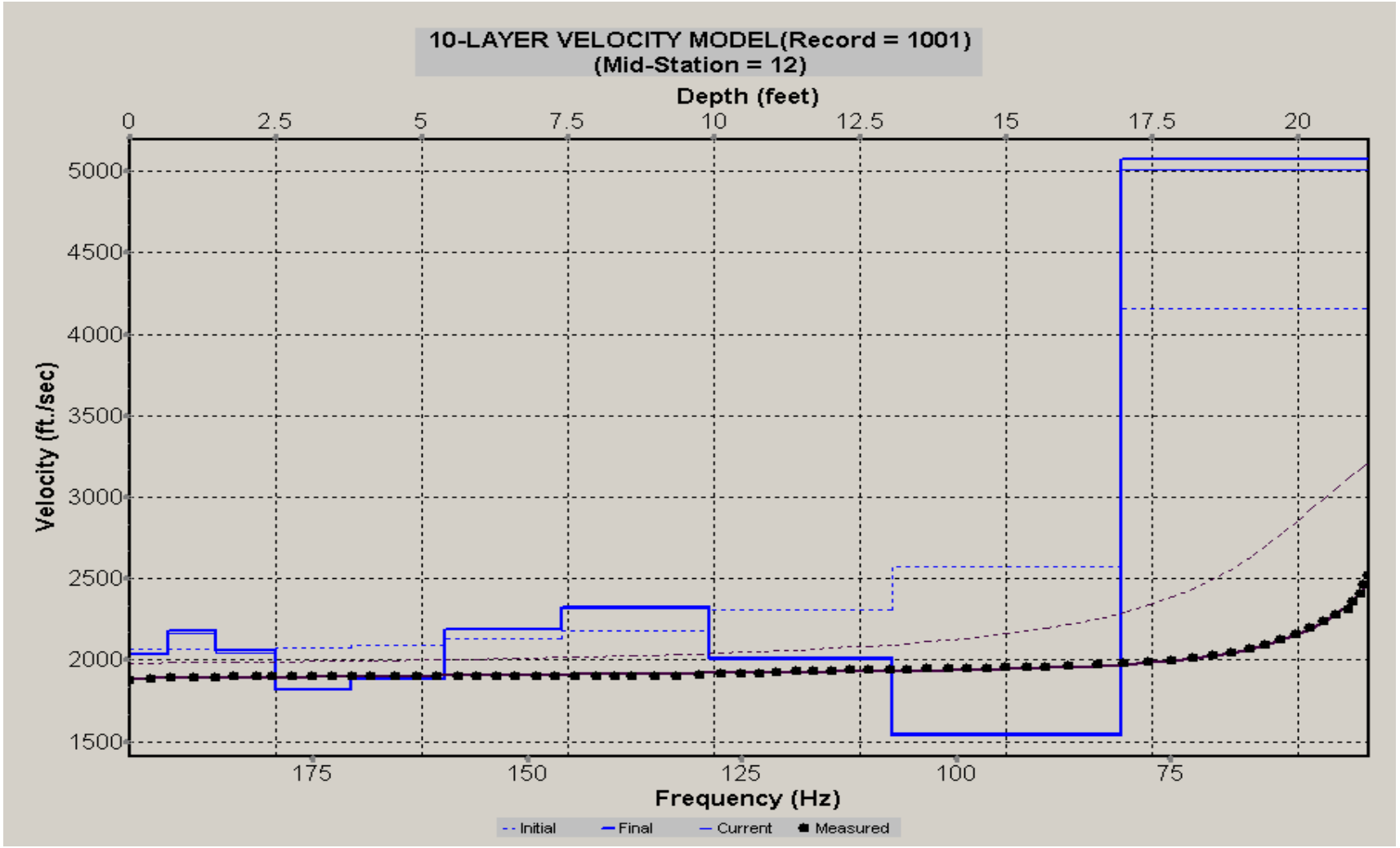

A.060: Velocity Profile Line 1041 used in Pre-blast 8, Pre-blast 9 and Pre-blast 10

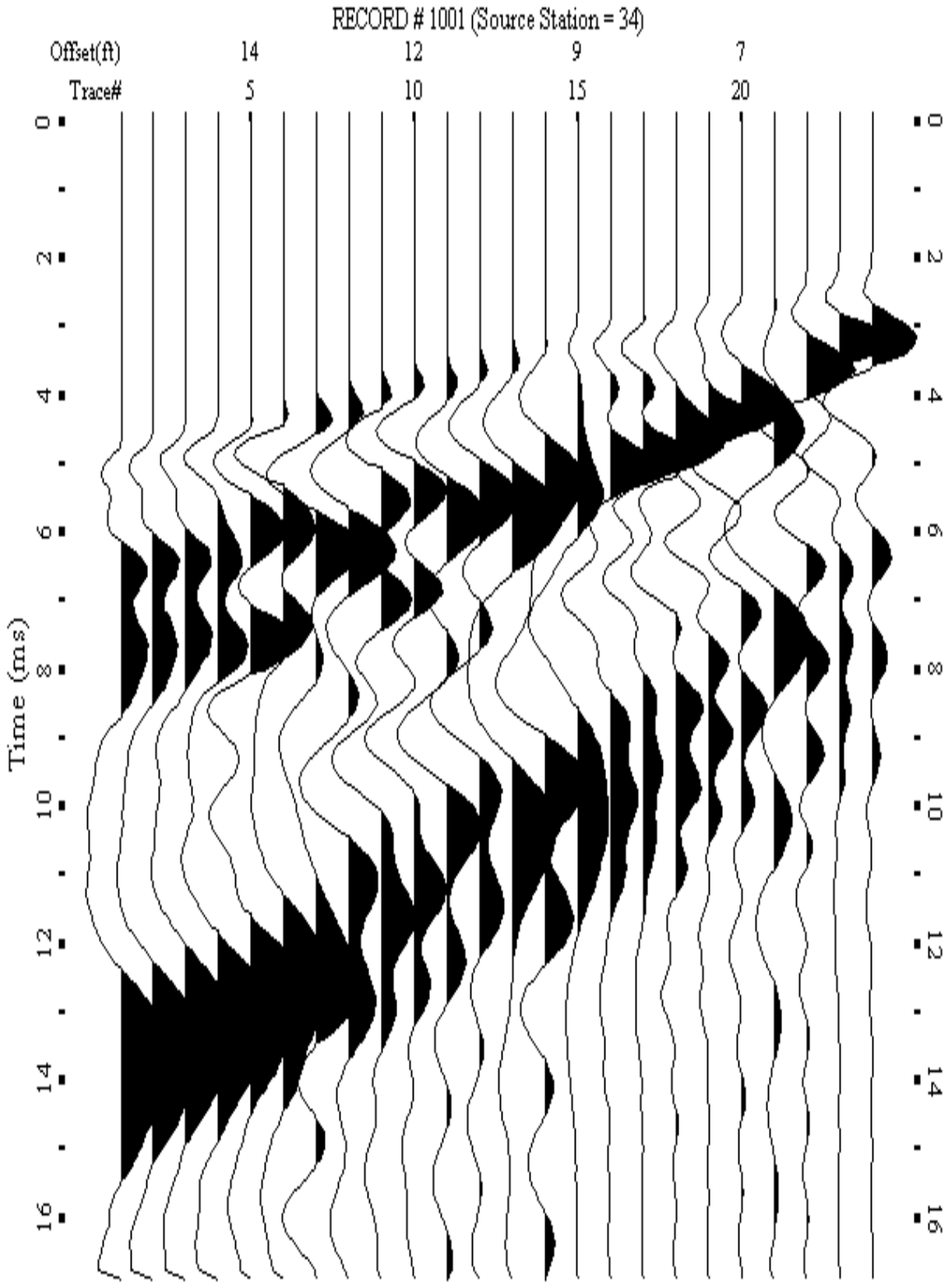

A.061: Shot Gather Line 1042 used in Pre-blast 8, Pre-blast 9 and Pre-blast 10

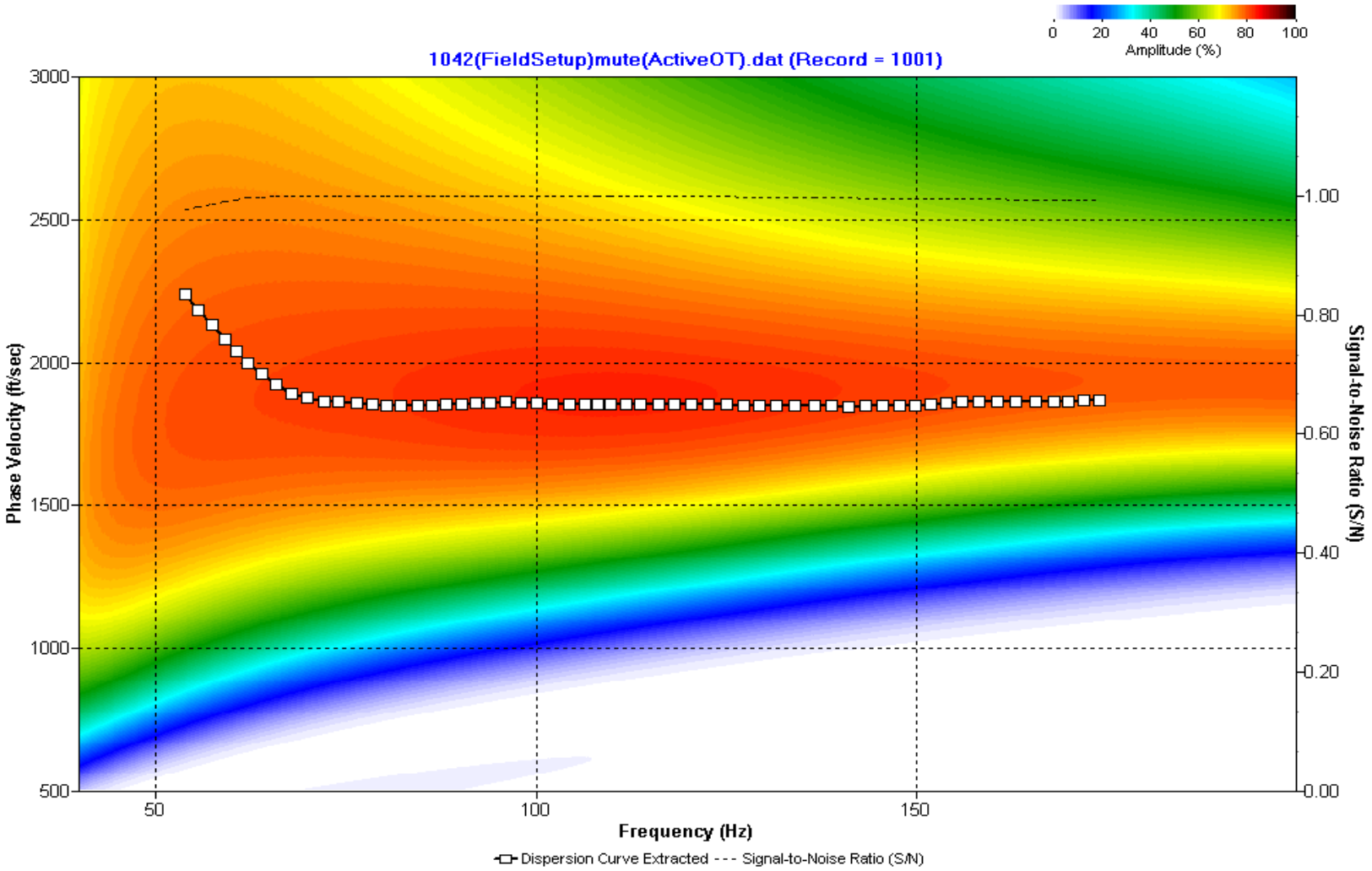

A.062: Dispersion Curve Line 1042 used in Pre-blast 8, Pre-blast 9 and Pre-blast 10

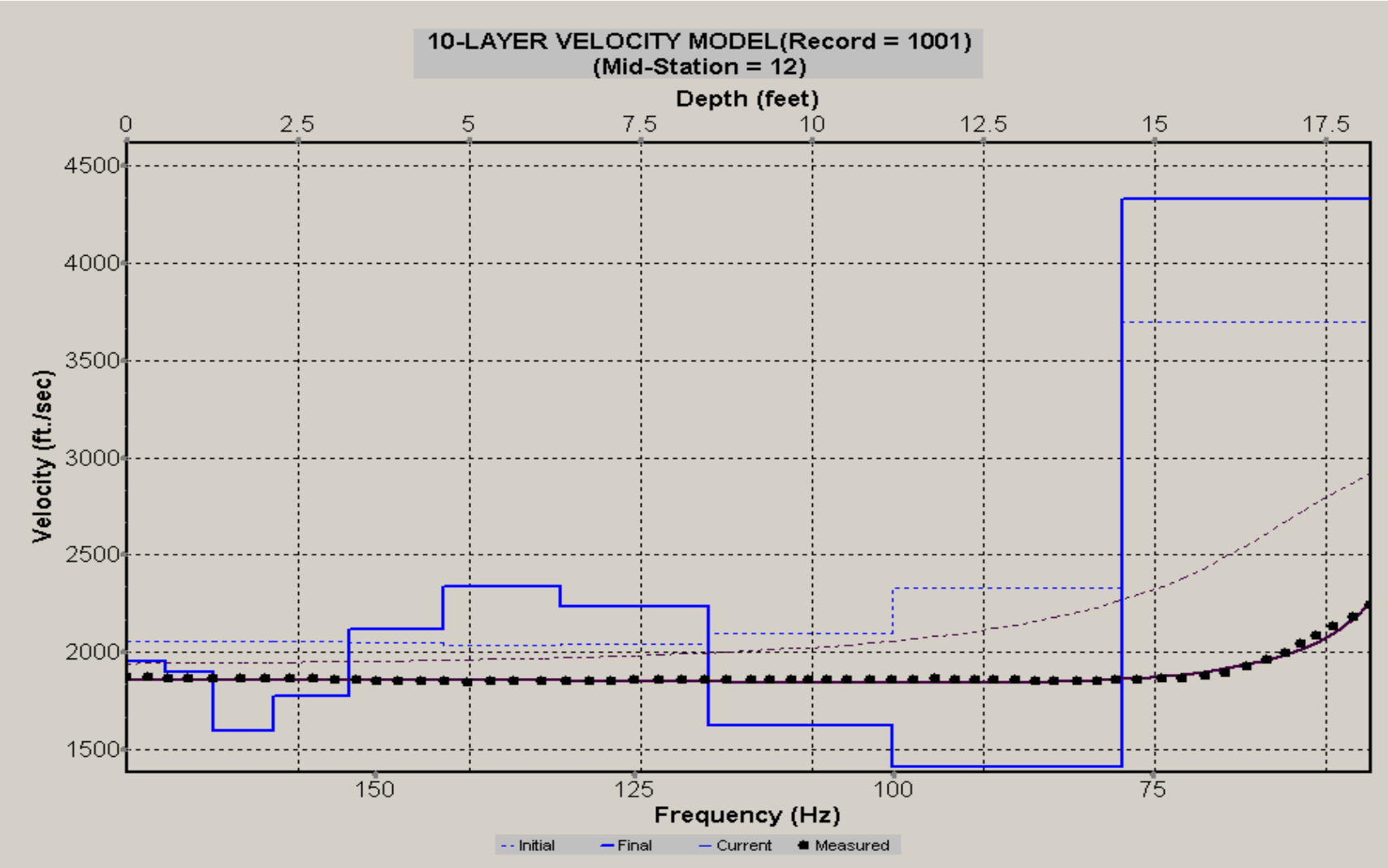

A.063: Velocity Profile Line 1042 used in Pre-blast 8, Pre-blast 9 and Pre-blast 10

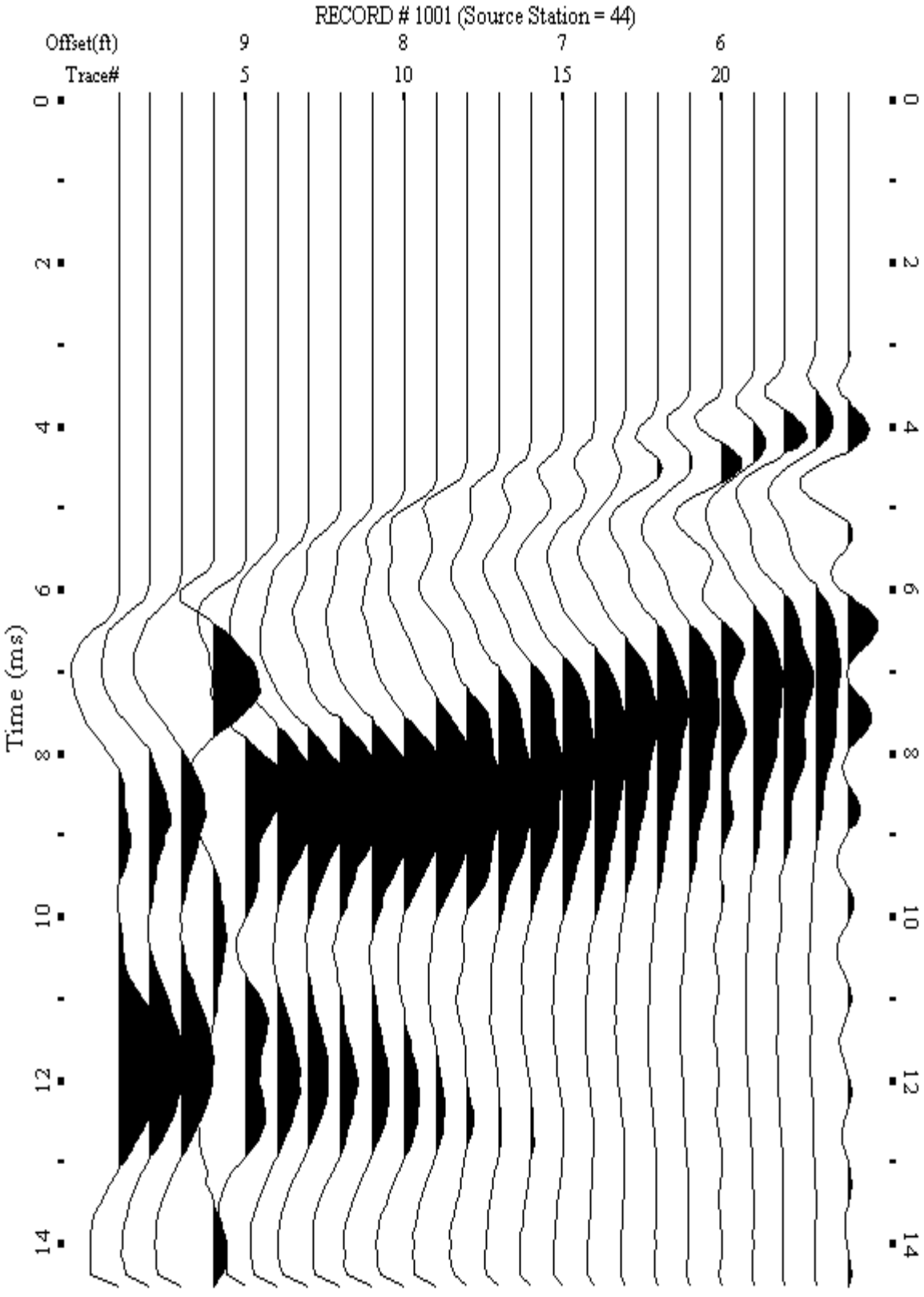

A.064: Shot Gather Line 1069 used in Post-blast 10 and Pre-blast 16

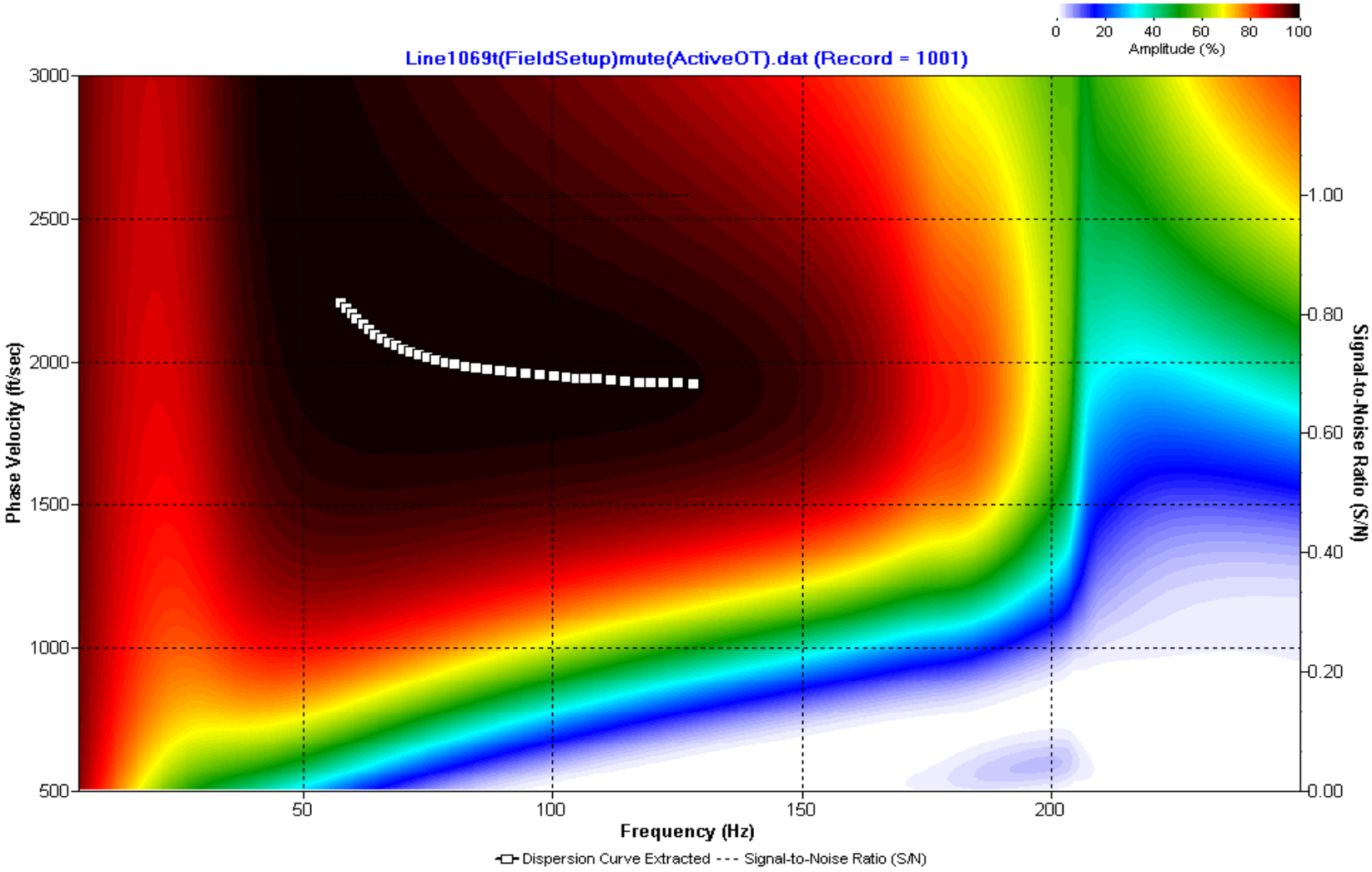

A.065: Dispersion Curve Line 1069 used in Post-blast 10 and Pre-blast 16

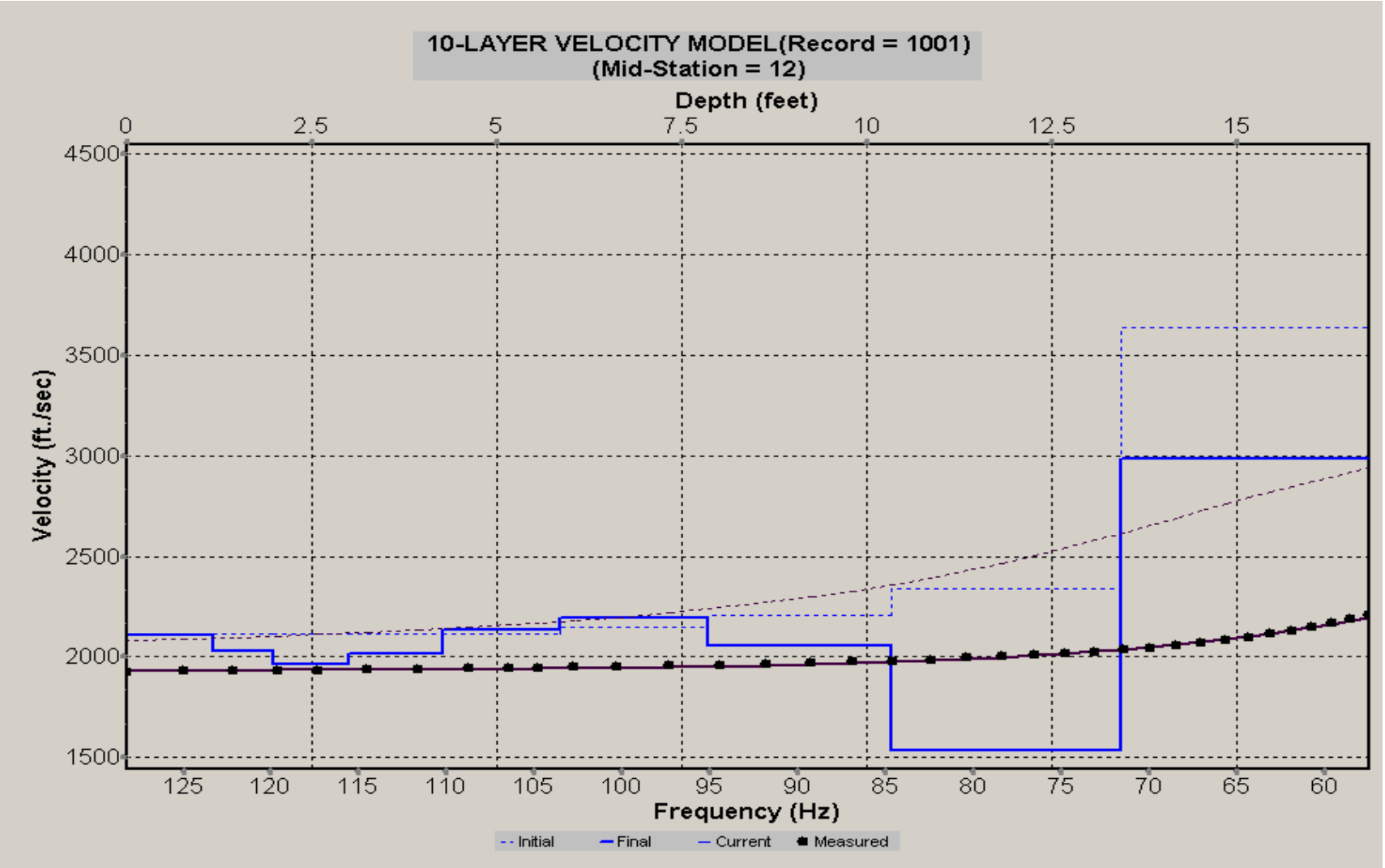

A.066: Velocity Profile Line 1069 used in Post-blast 10 and Pre-blast 16

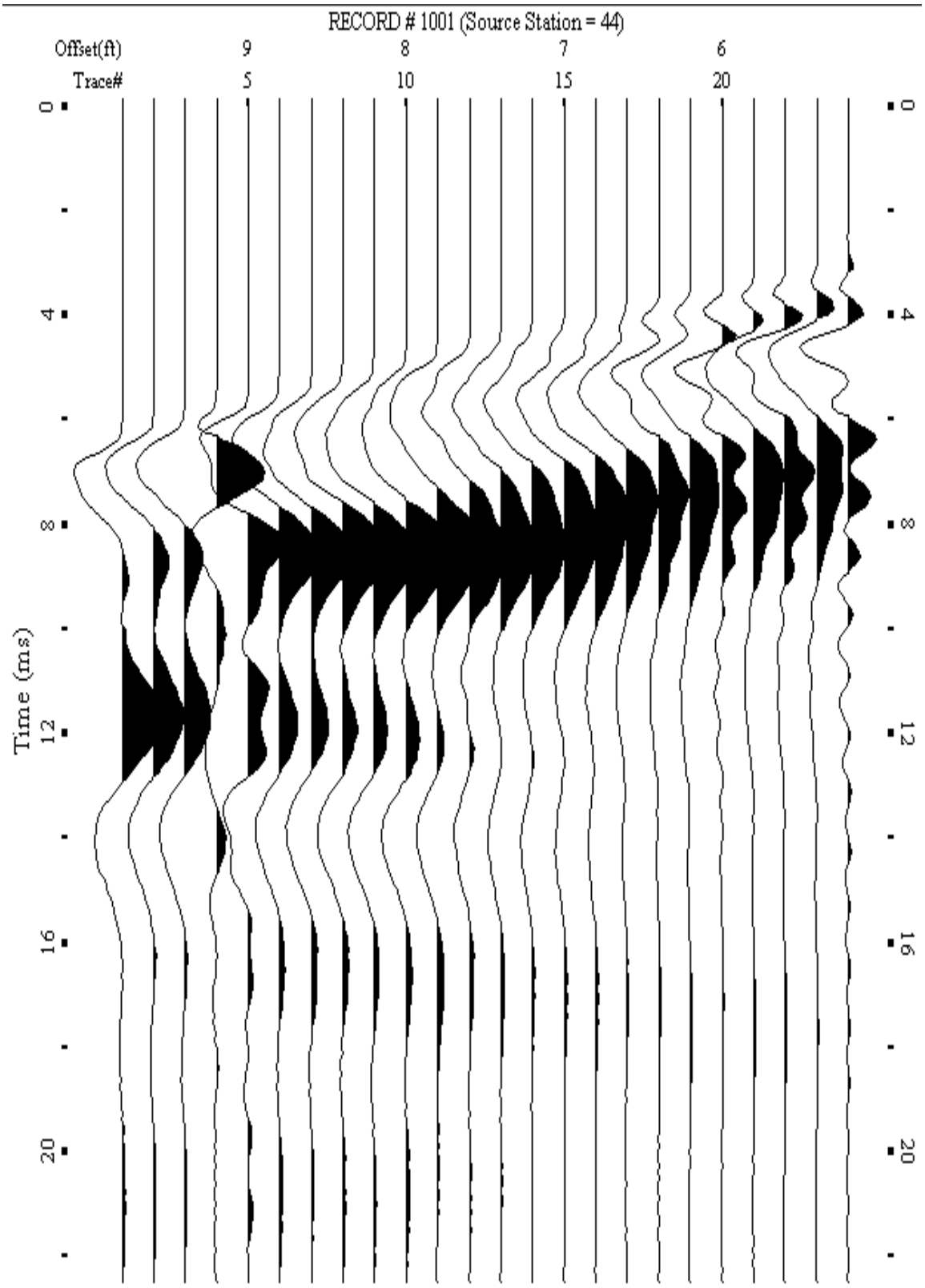

A.067: Shot Gather Line 1070 used in Post-blast 10 and Pre-blast 16

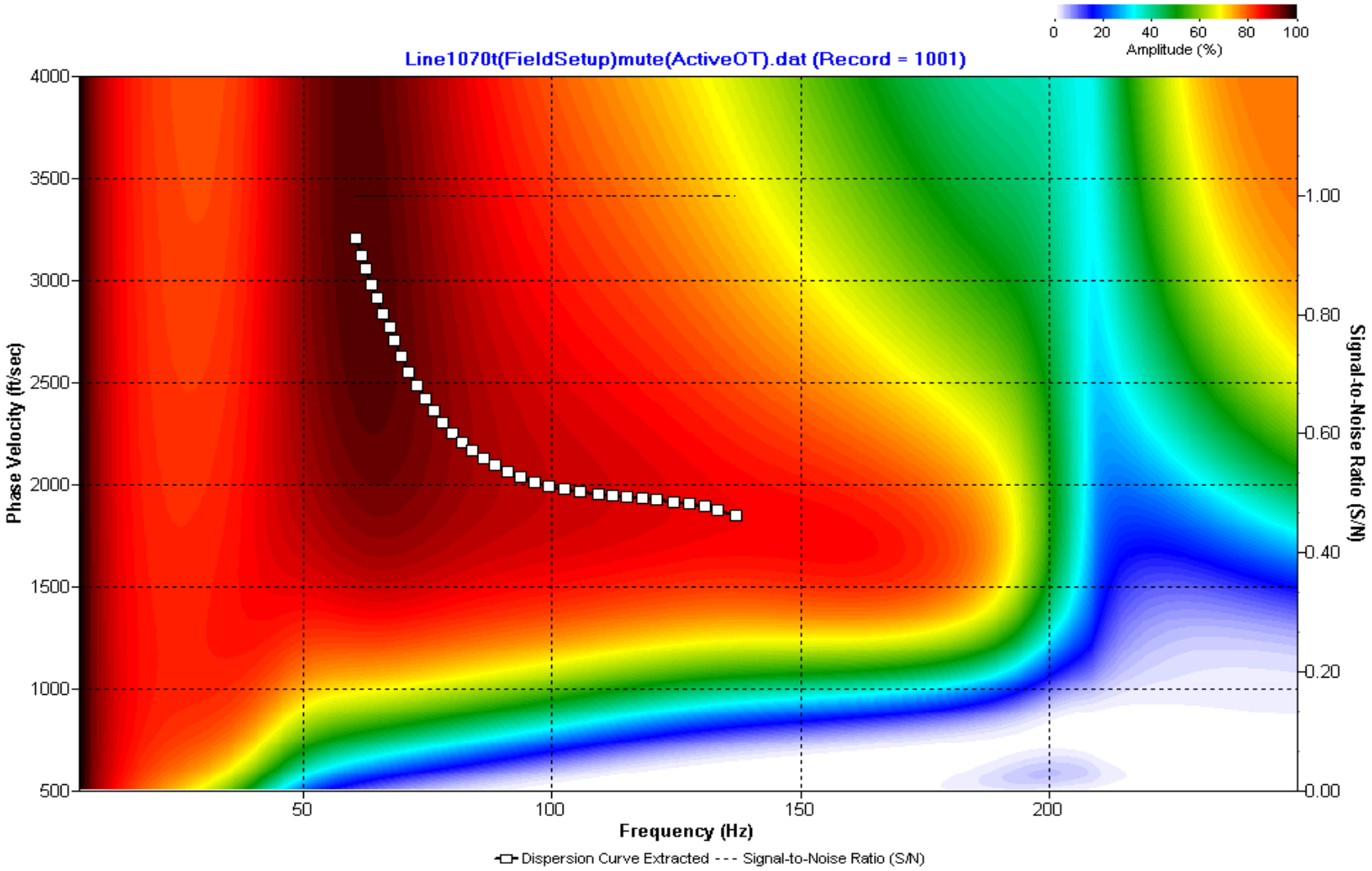

A.068: Dispersion Curve Line 1070 used in Post-blast 10 and Pre-blast 16

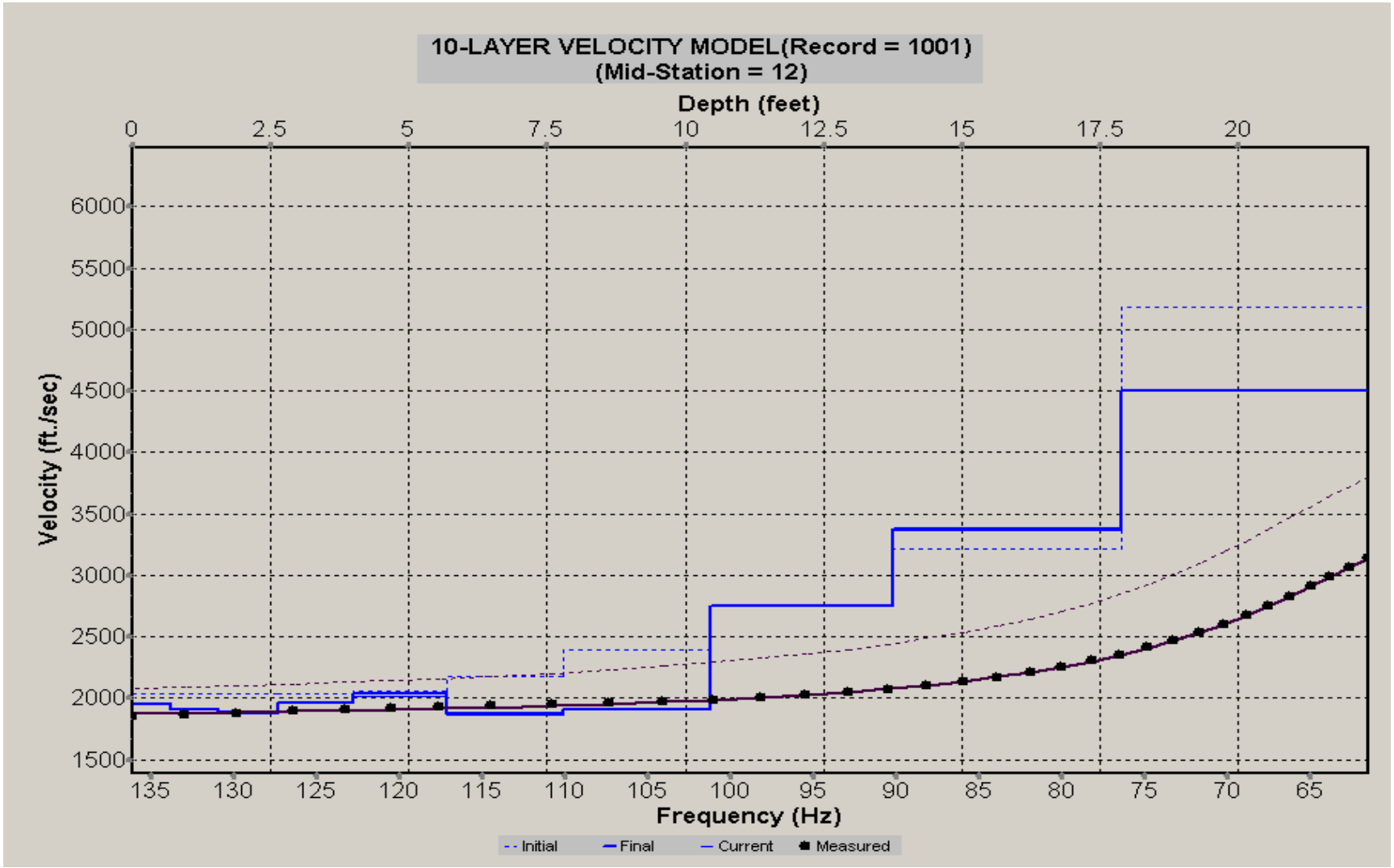

A.069: Velocity Profile Line 1070 used in Post-blast 10 and Pre-blast 16

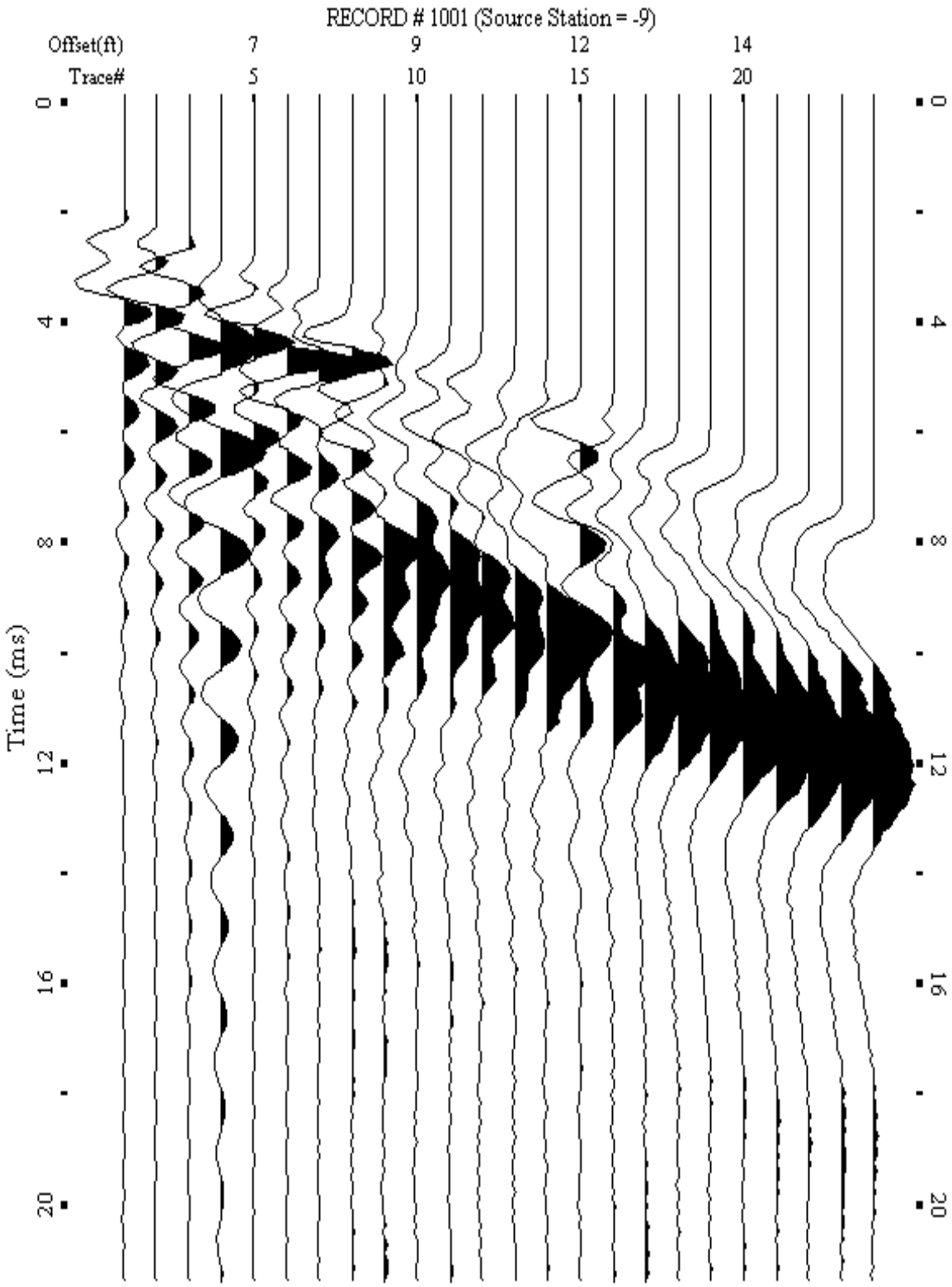

A.070: Shot Gather Line 1071 used in Post-blast 10, Pre-blast 16, Pre-blast 17, and Pre-blast 18

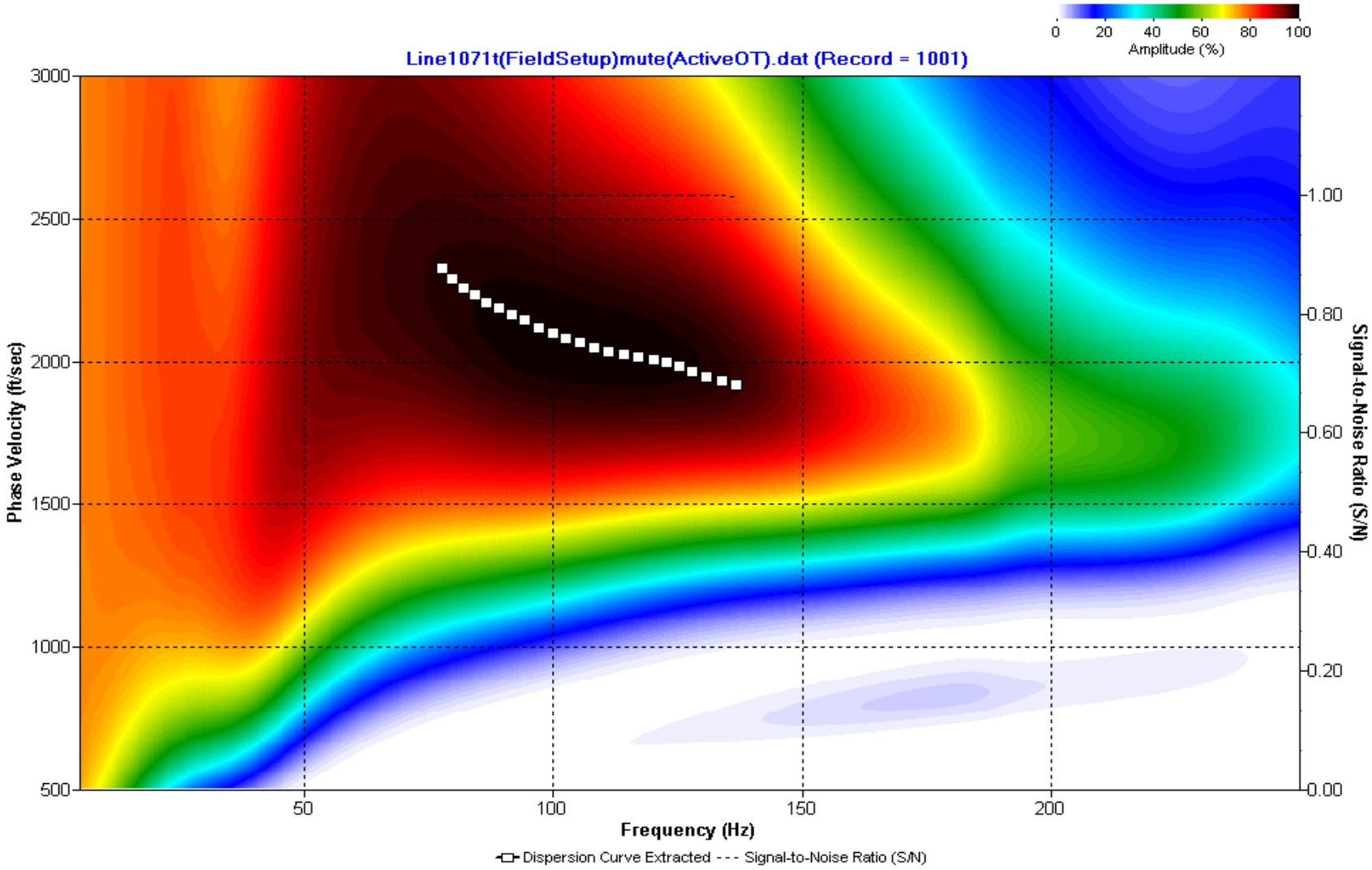

A.071: Dispersion Curve Line 1071 used in Post-blast 10, Pre-blast 16, Pre-blast 17, and Pre-blast 18

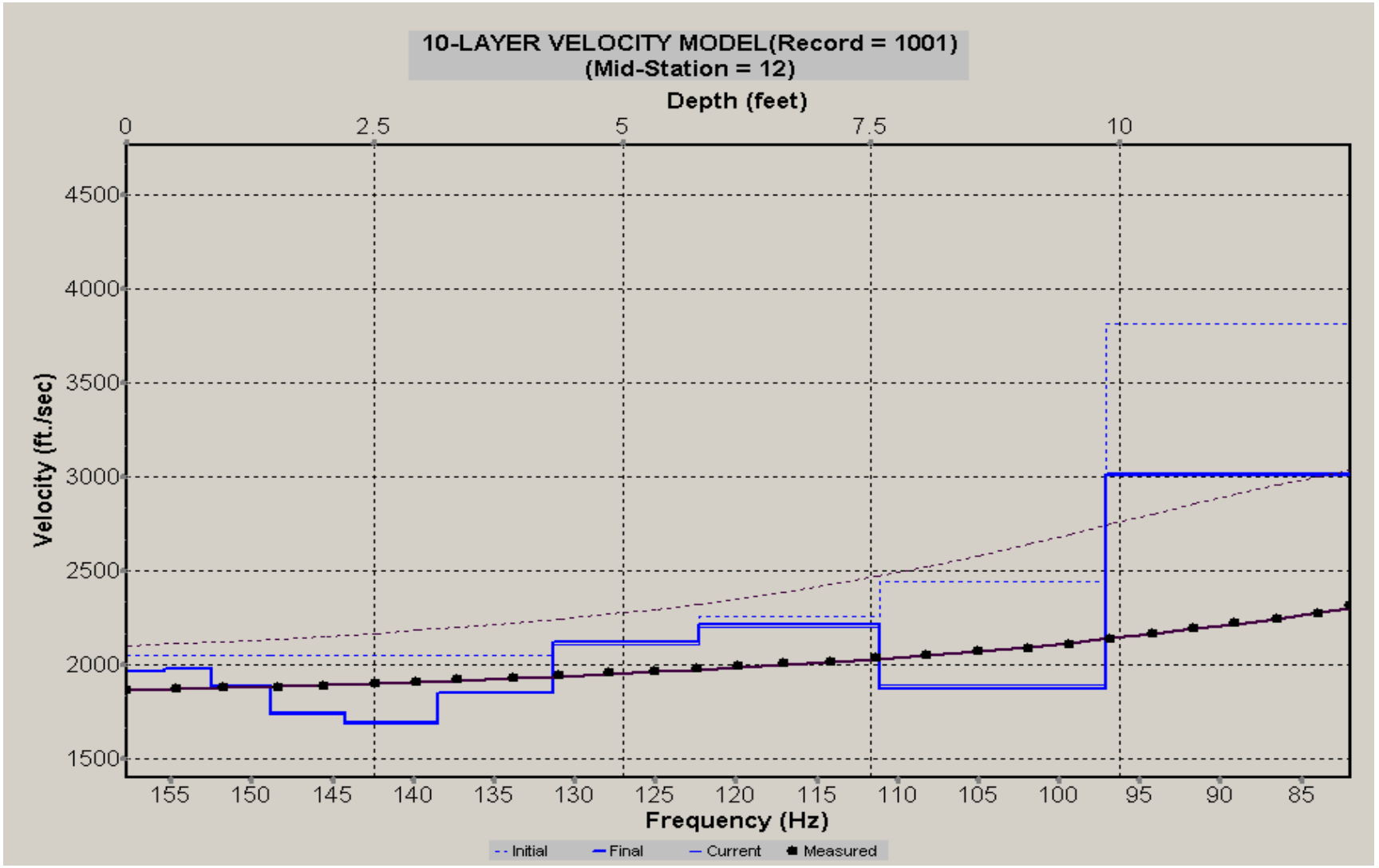

A.072: Velocity Profile Line 1071 used in Post-blast 10, Pre-blast 16, Pre-blast 17, and Pre-blast 18

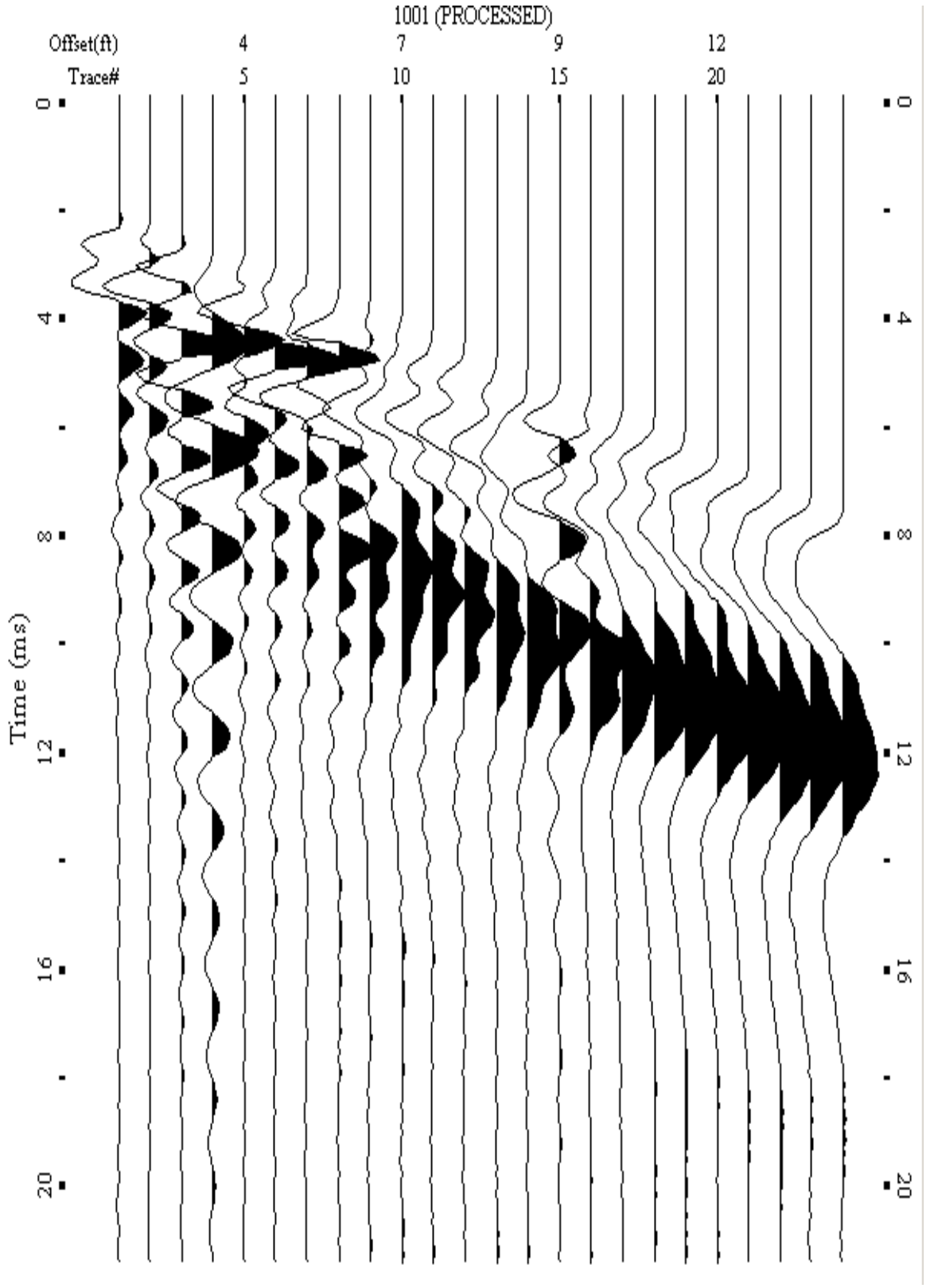

A.073: Shot Gather Line 1072 used in Post-blast 10, Pre-blast 16, Pre-blast 17, and Pre-blast 18

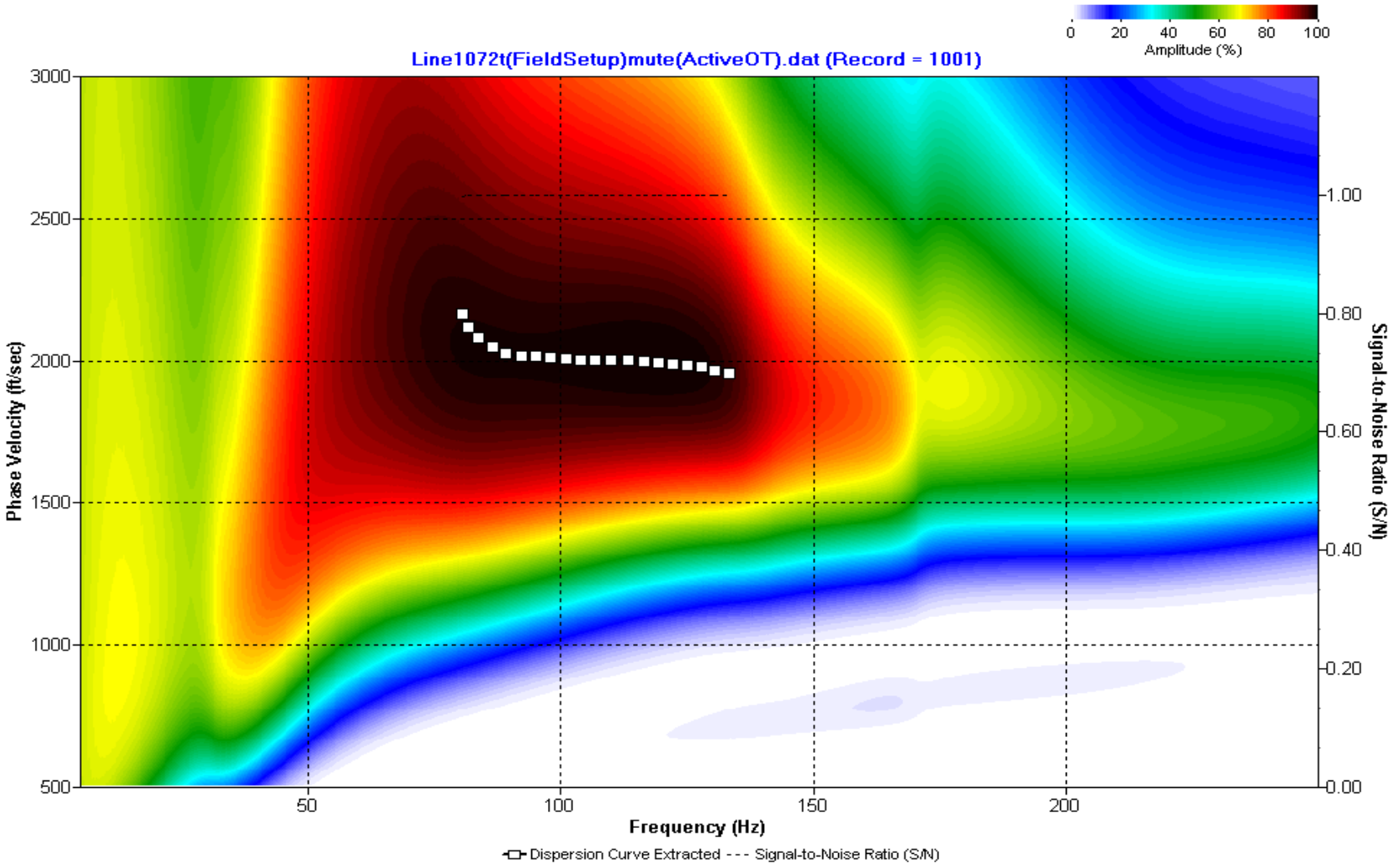

A.074: Dispersion Curve Line 1072 used in Post-blast 10, Pre-blast 16, Pre-blast 17, and Pre-blast 18

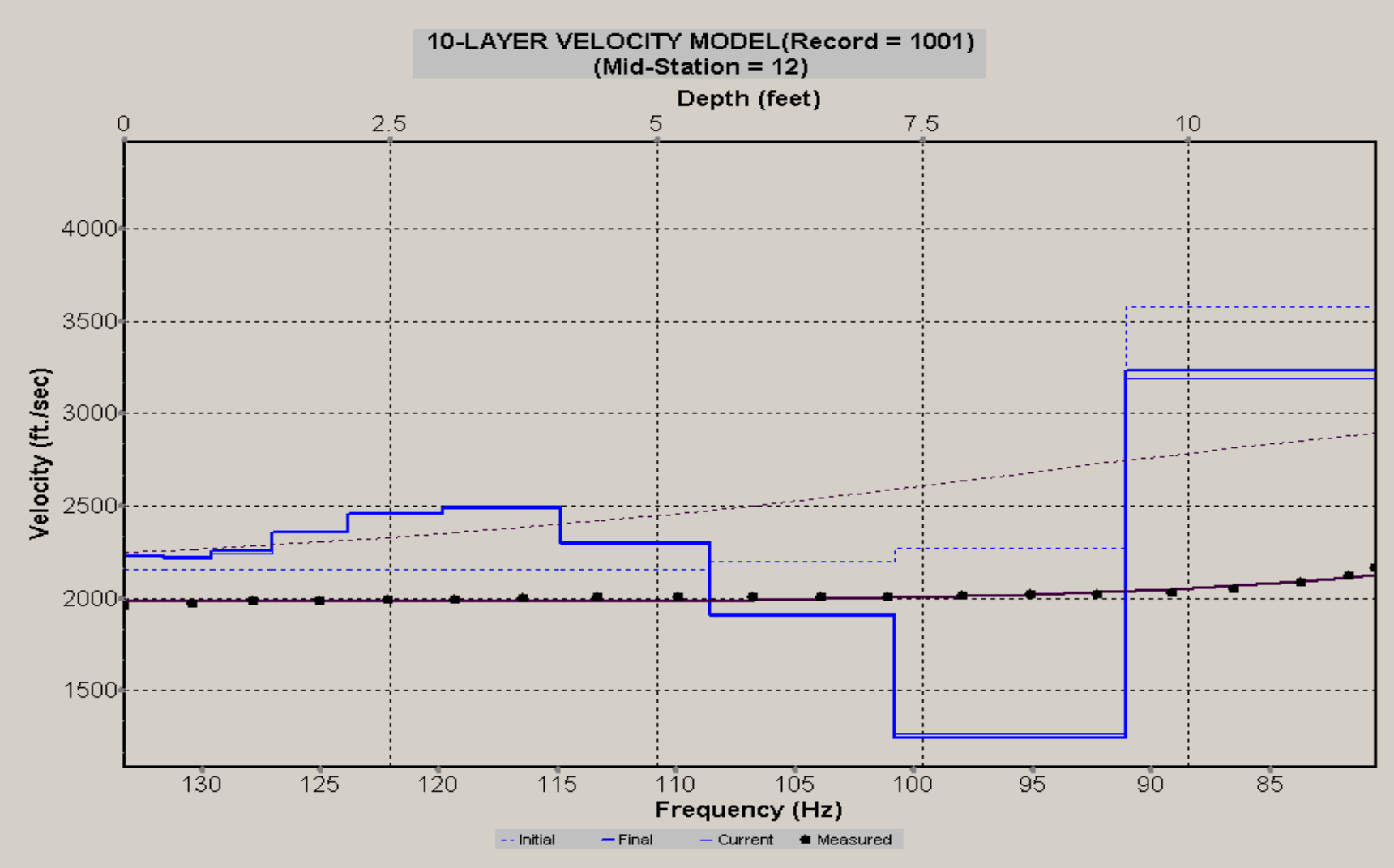

A.075: Velocity Profile Line 1072 used in Post-blast 10, Pre-blast 16, Pre-blast 17, and Pre-blast 18

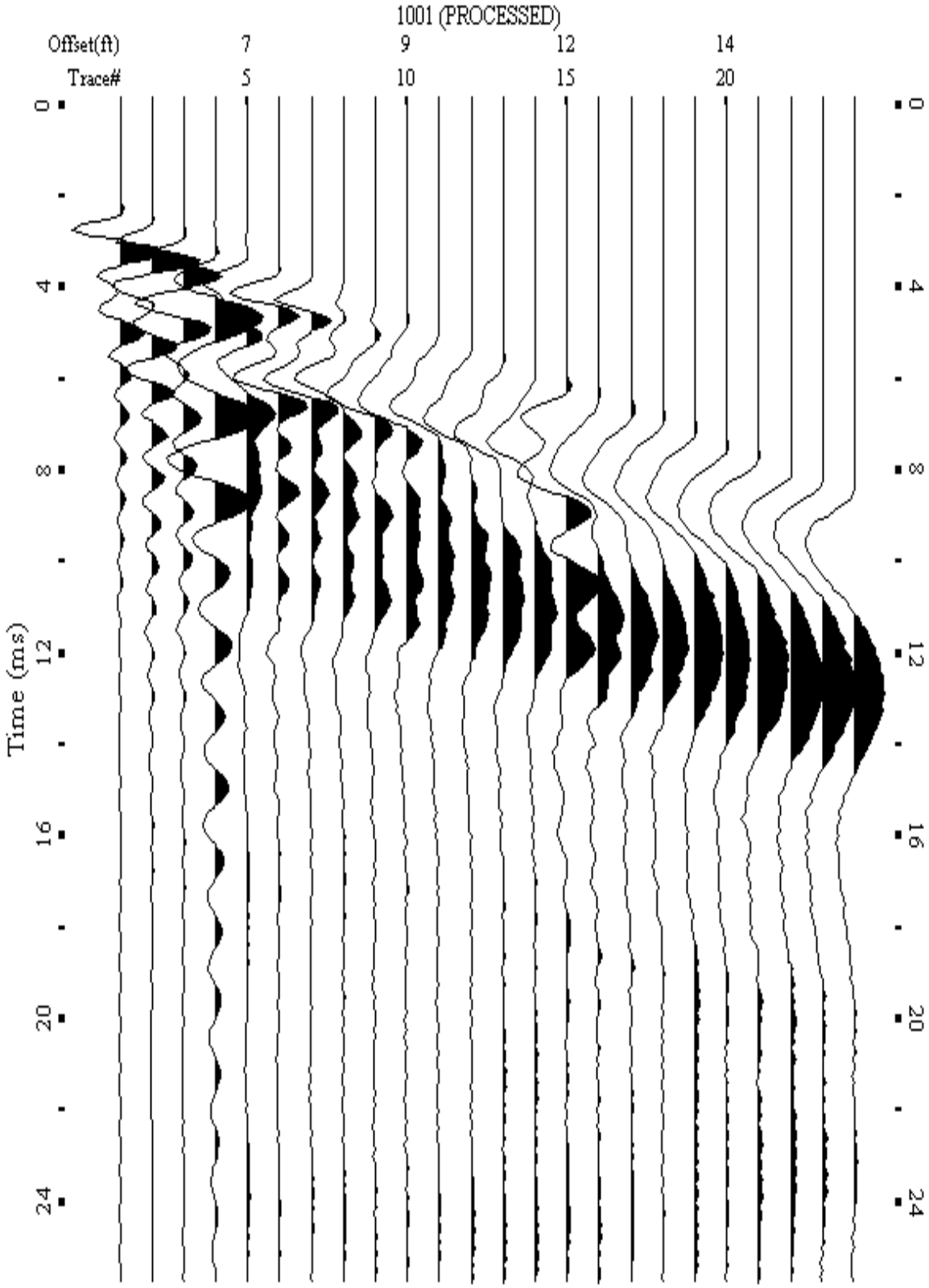

A.076: Shot Gather Line 1073 used in Post-blast 10, Pre-blast 16, Pre-blast 17, and Pre-blast 18

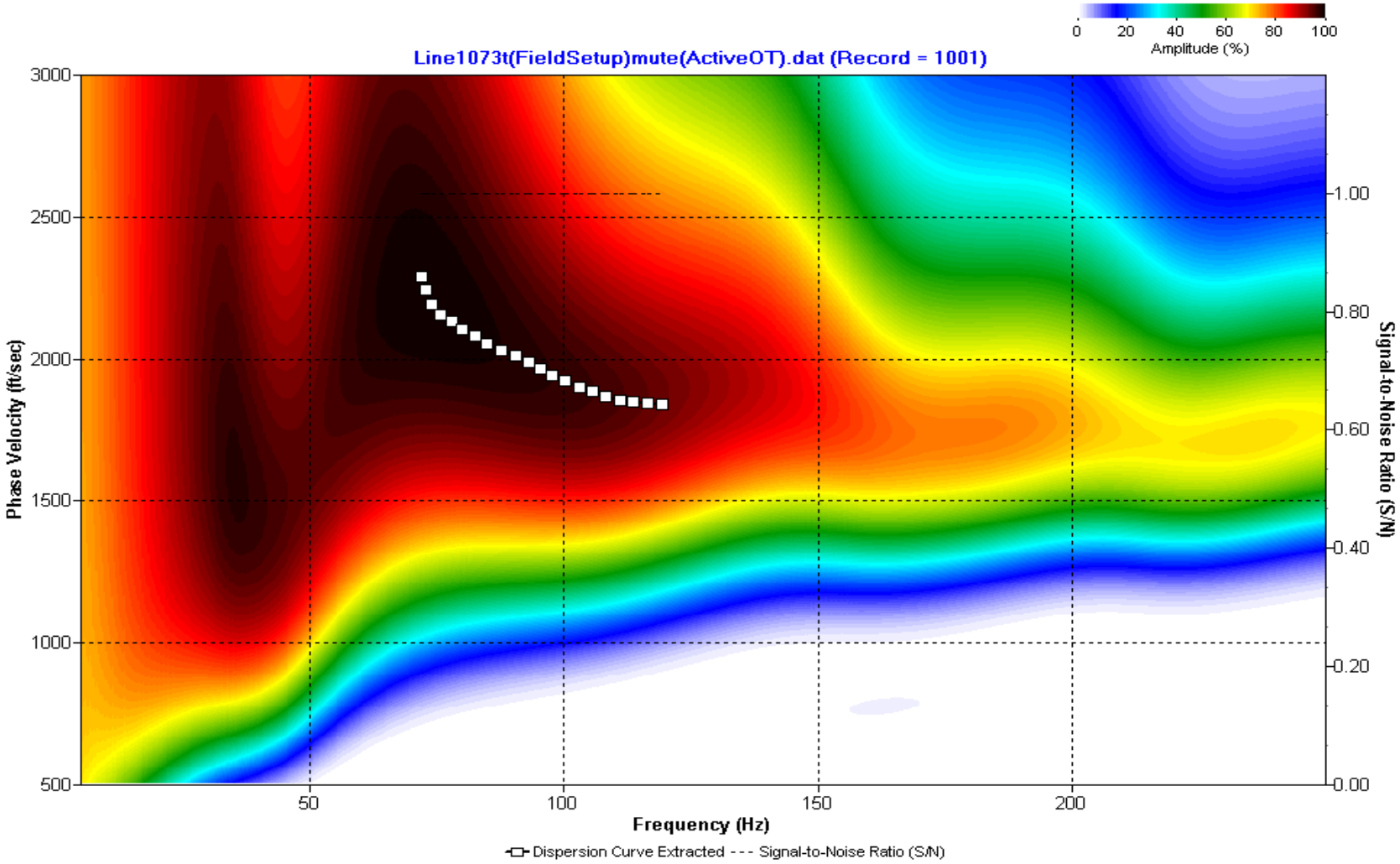

A.077: Dispersion Curve Line 1073 used in Post-blast 10, Pre-blast 16, Pre-blast 17, and Pre-blast 18

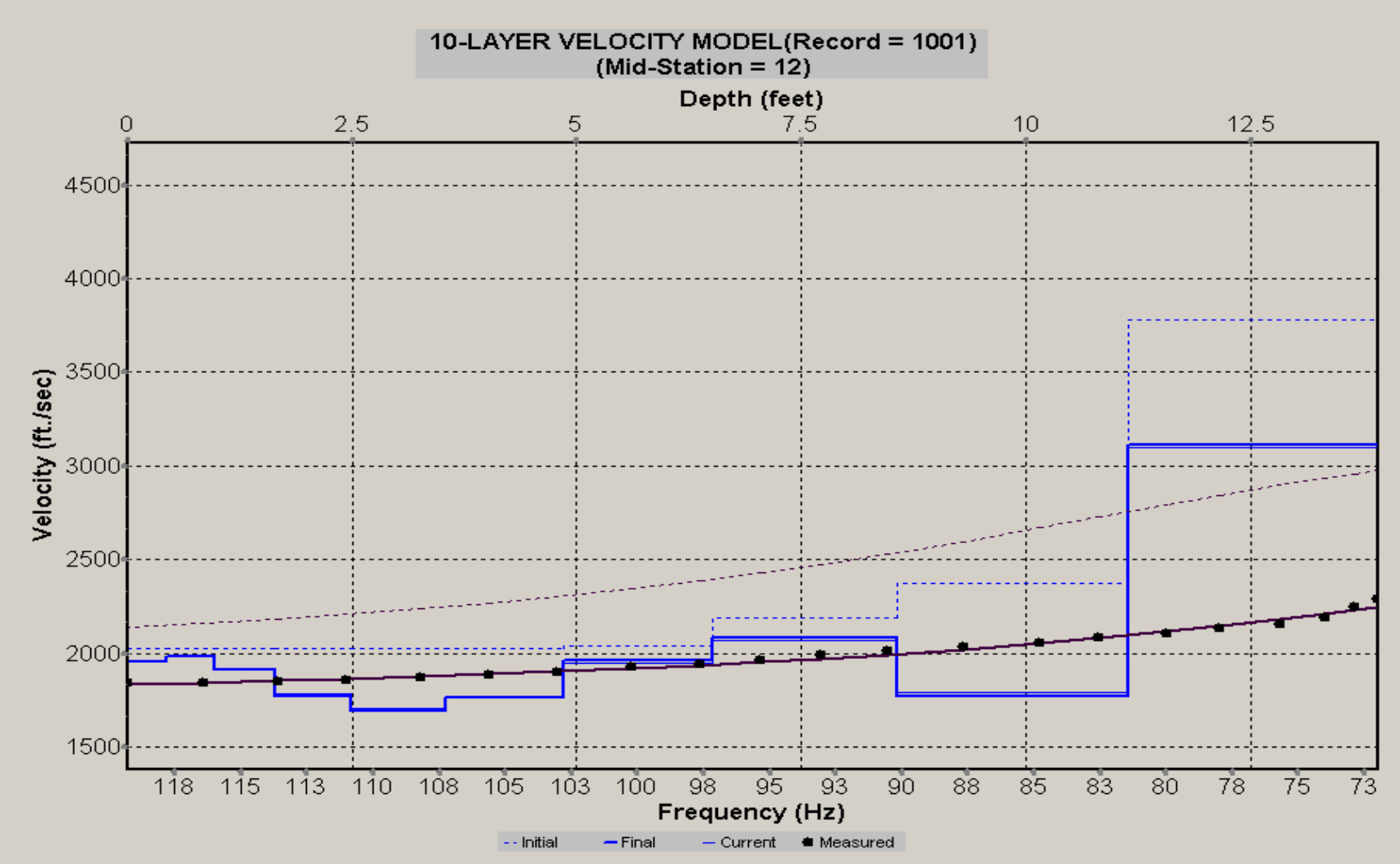

A.078: Velocity Profile Line 1073 used in Post-blast 10, Pre-blast 16, Pre-blast 17, and Pre-blast 18

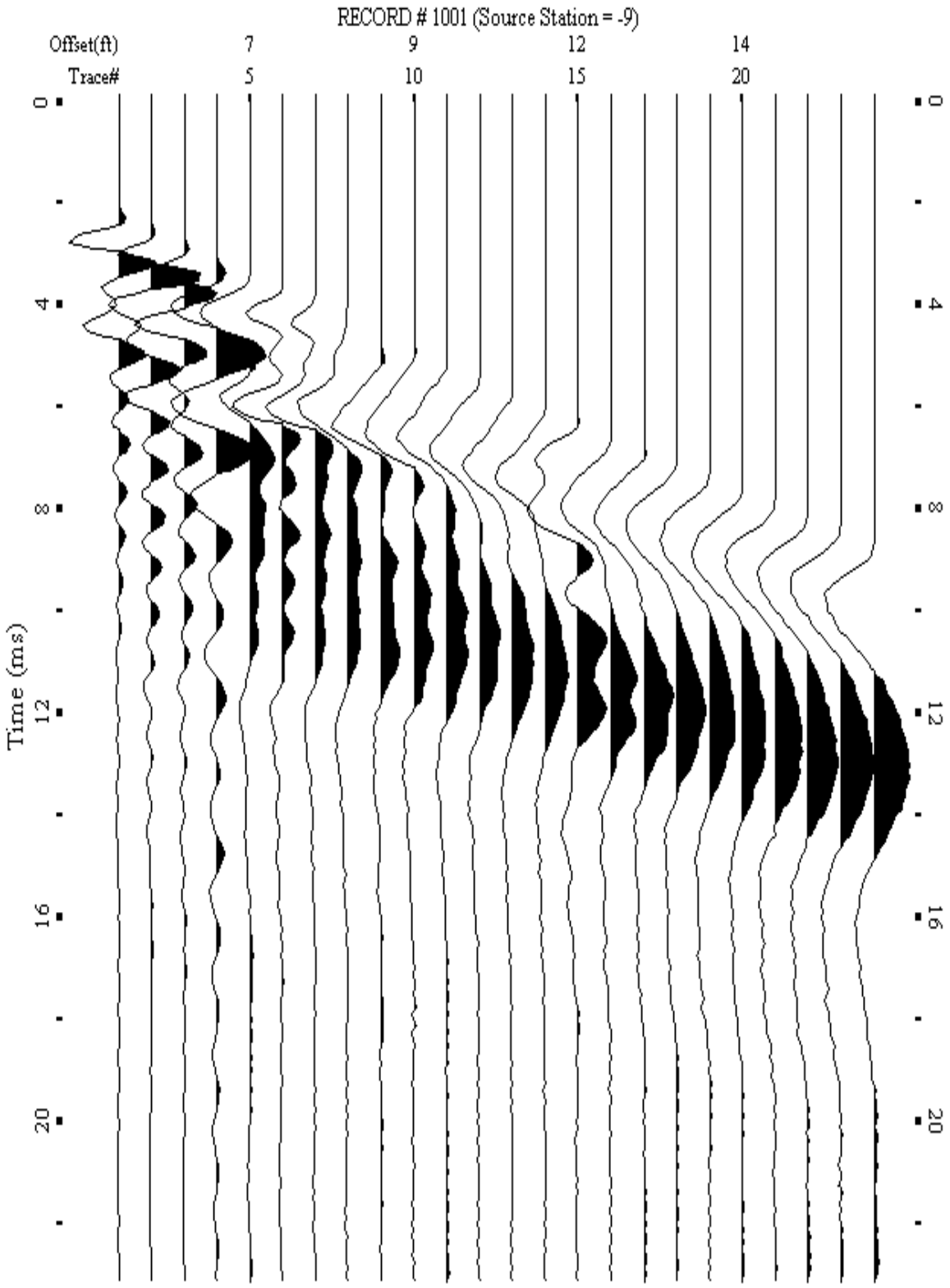

A.079: Shot Gather Line 1074 used in Post-blast 10, Pre-blast 16, Pre-blast 17, and Pre-blast 18

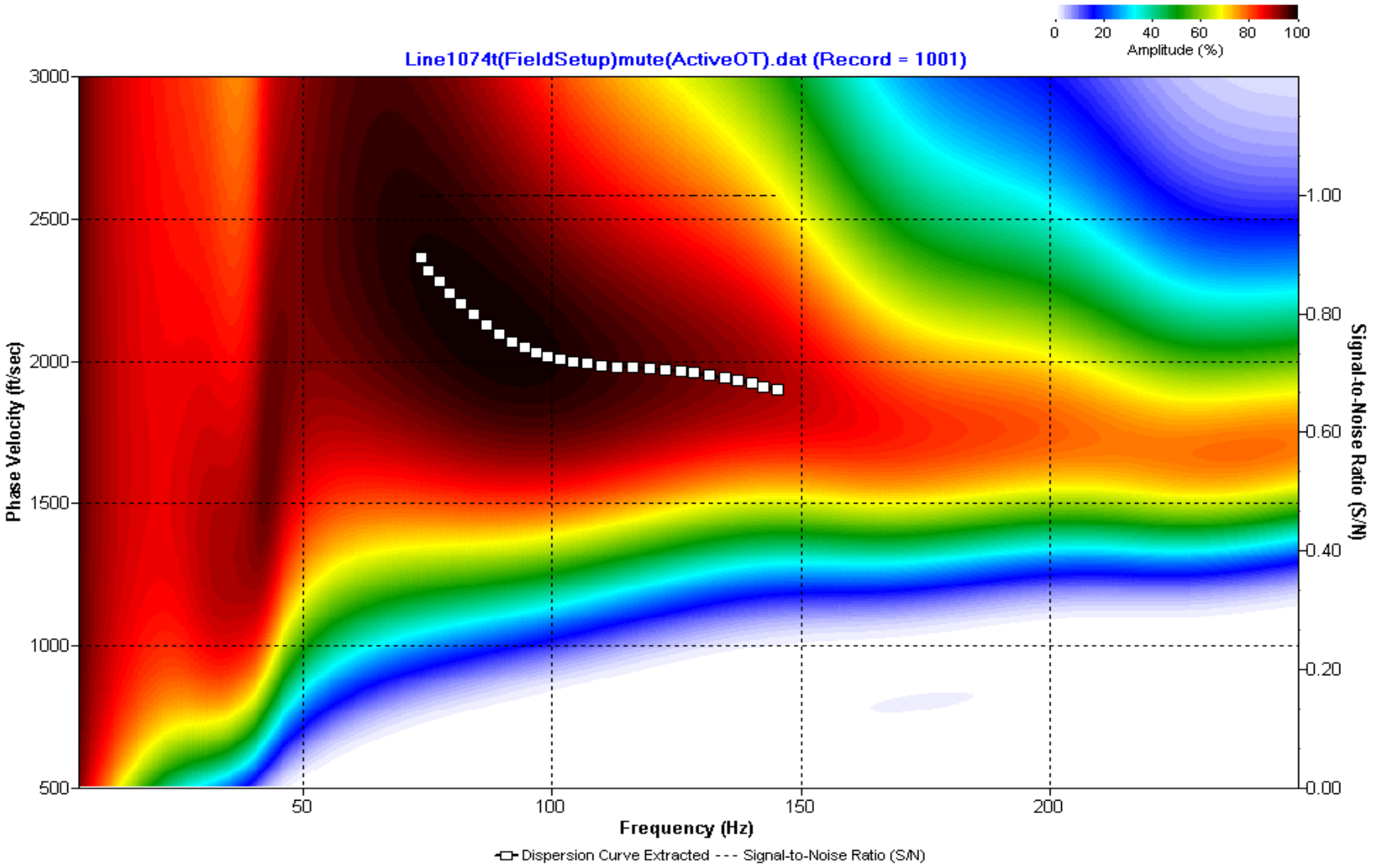

A.080: Dispersion Curve Line 1074 used in Post-blast 10, Pre-blast 16, Pre-blast 17, and Pre-blast 18

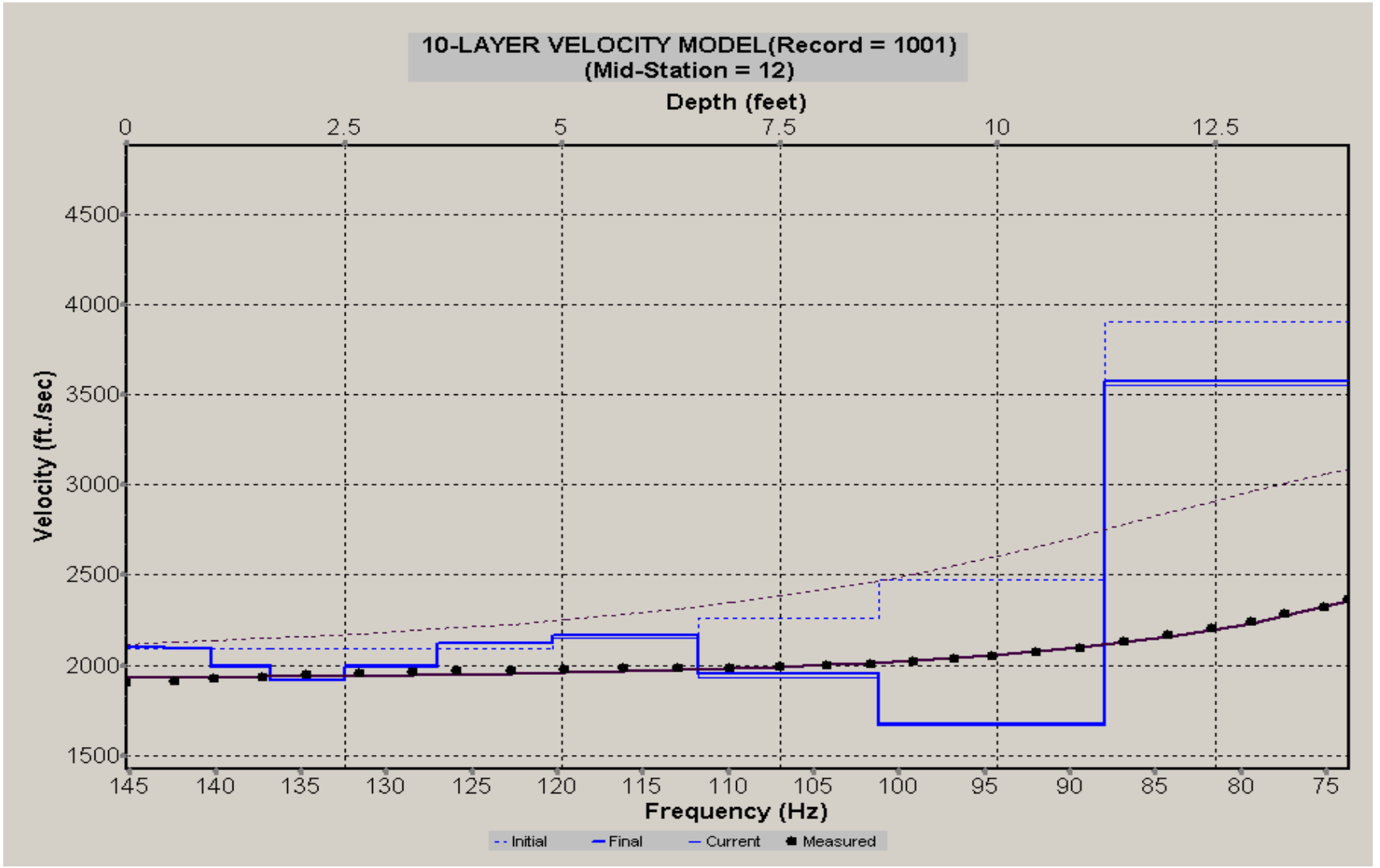

A.081: Velocity Profile Line 1074 used in Post-blast 10, Pre-blast 16, Pre-blast 17, and Pre-blast 18

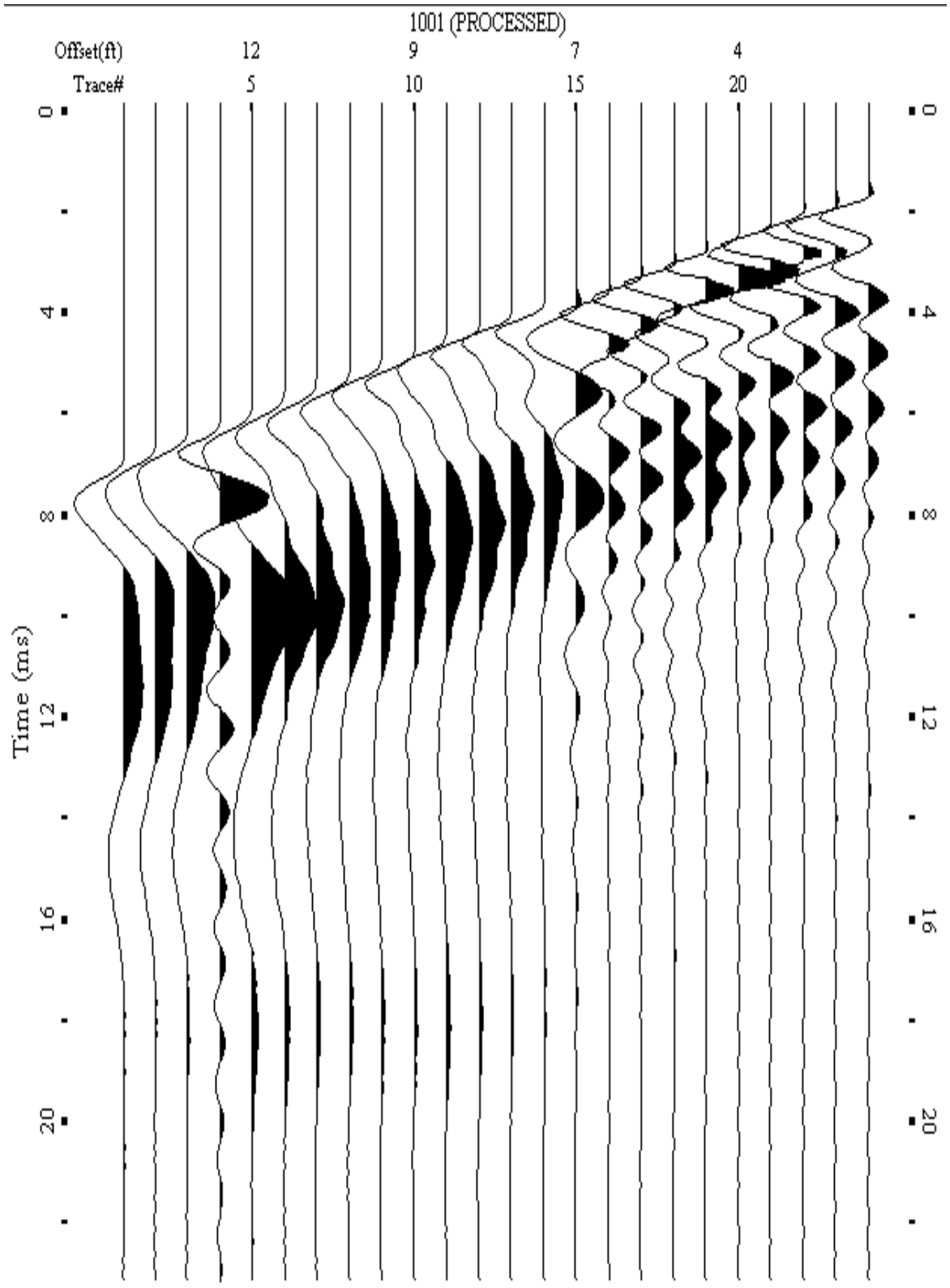

A.082: Shot Gather Line 1075 used in Post-blast 10, Pre-blast 16, Pre-blast 17, and Pre-blast 18

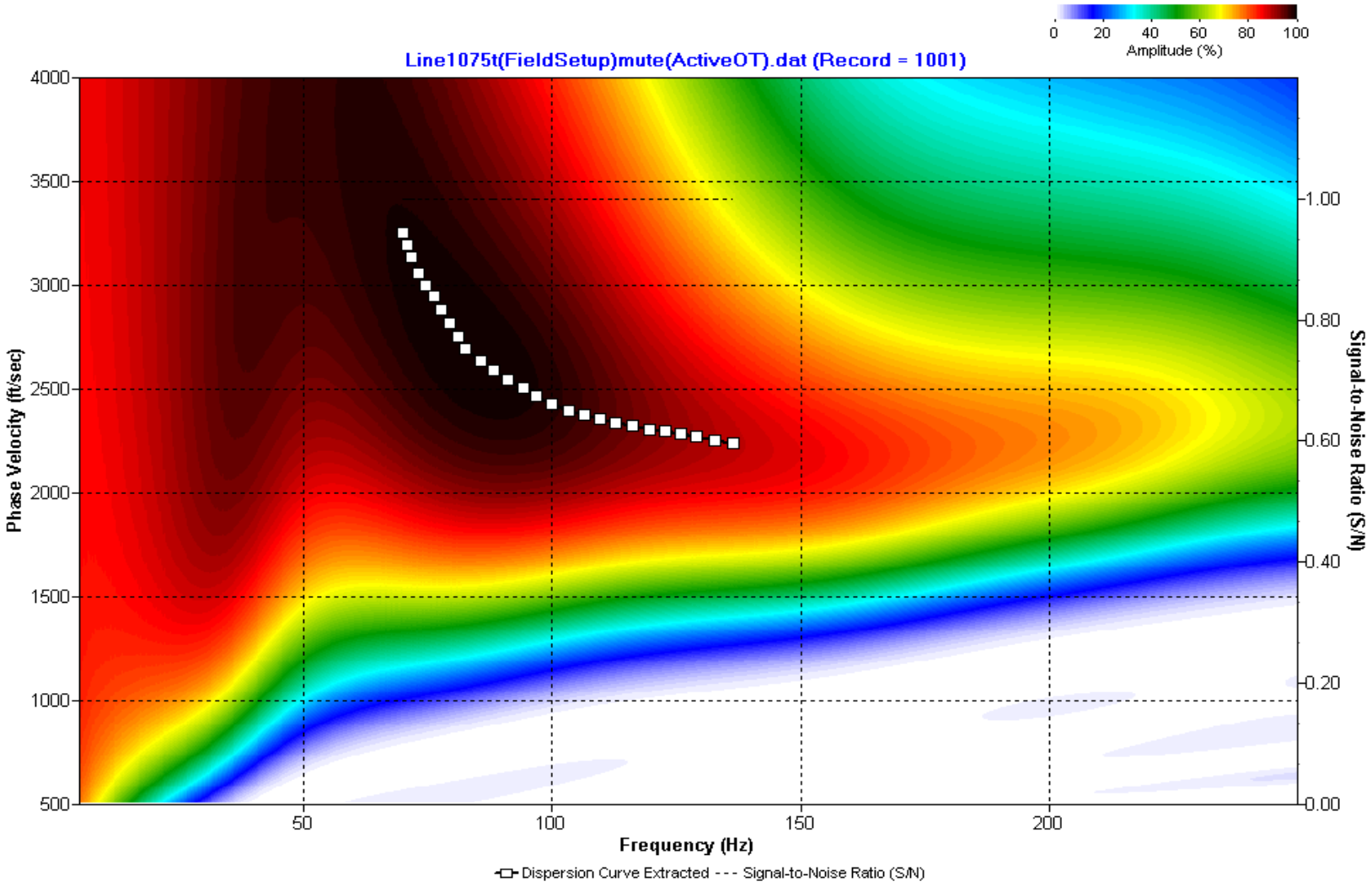

A.083: Dispersion Curve Line 1075 used in Post-blast 10, Pre-blast 16, Pre-blast 17, and Pre-blast 18

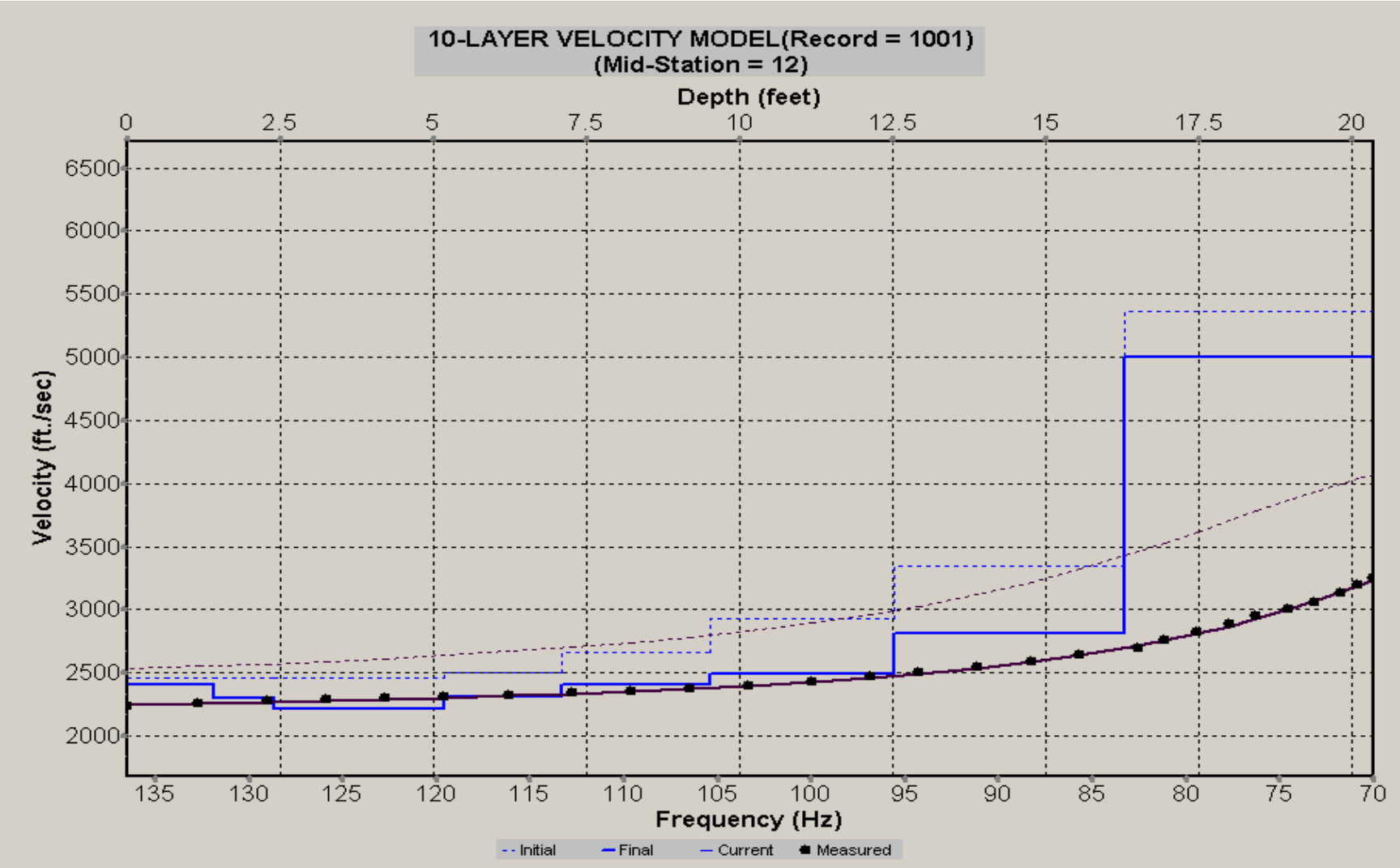

A.084: Velocity Profile Line 1075 used in Post-blast 10, Pre-blast 16, Pre-blast 17, and Pre-blast 18

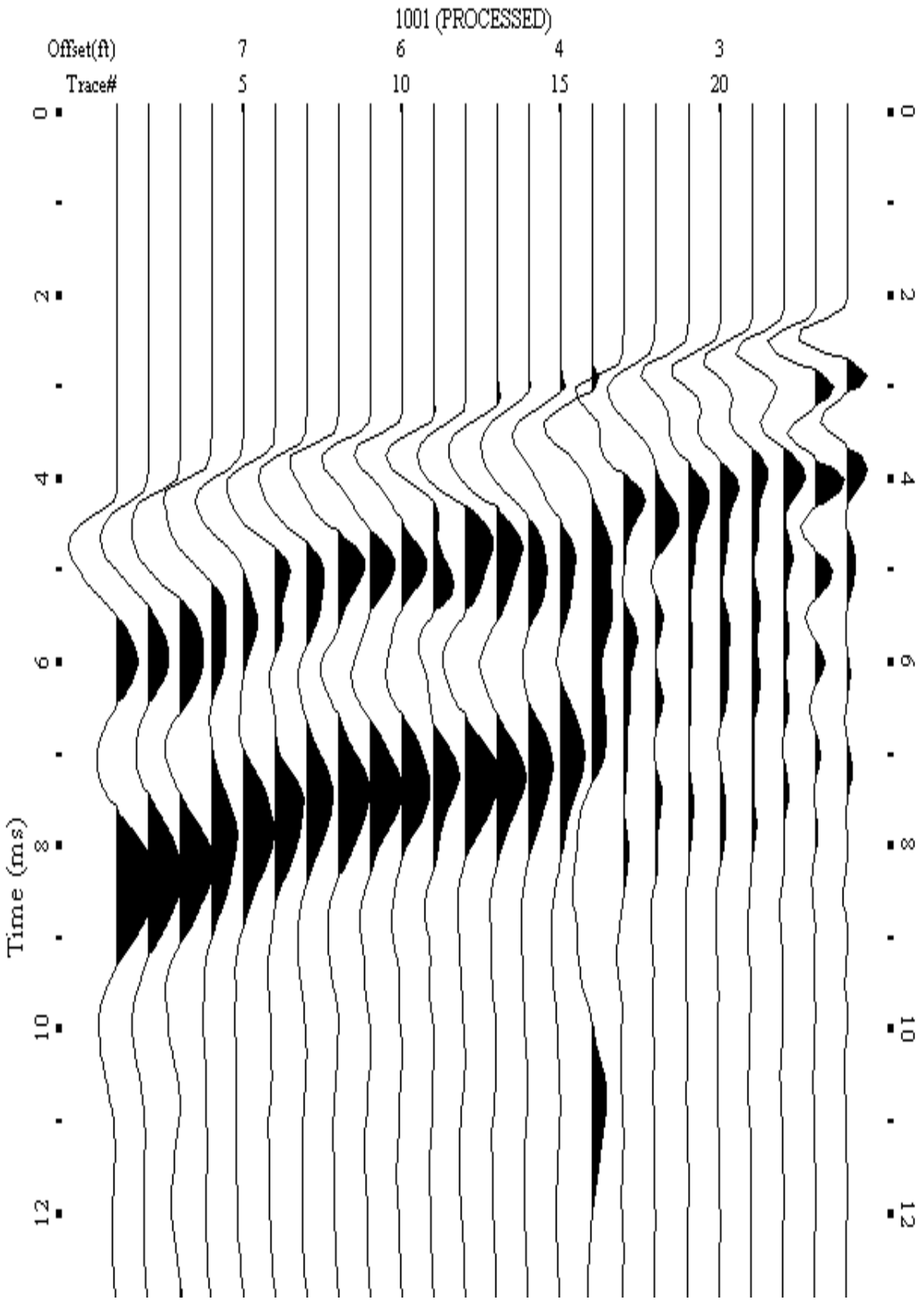

A.085: Shot Gather Line 1090 used in Pre-blast 21

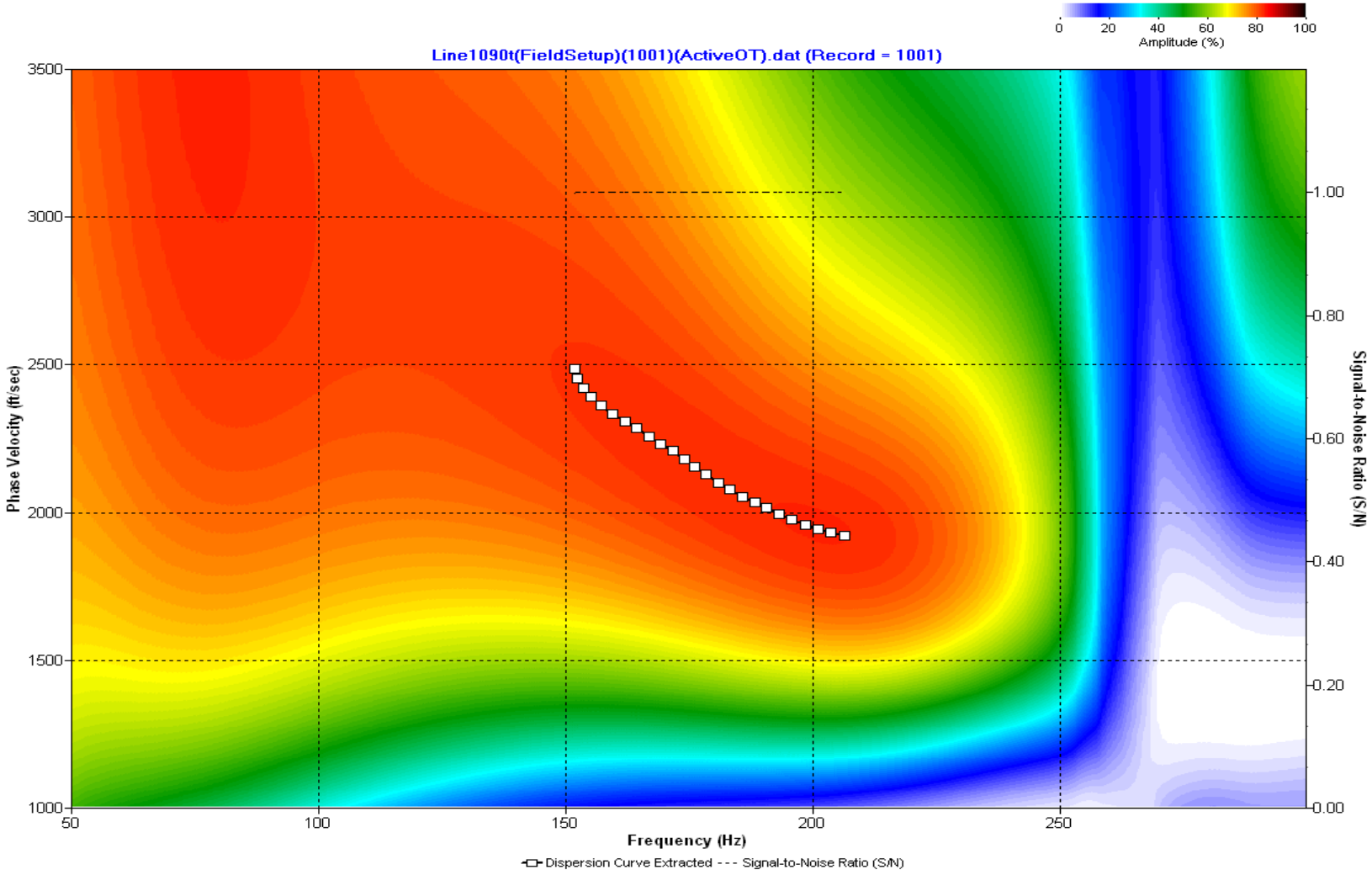

A.086: Dispersion Curve Line 1090 used in Pre-blast 21

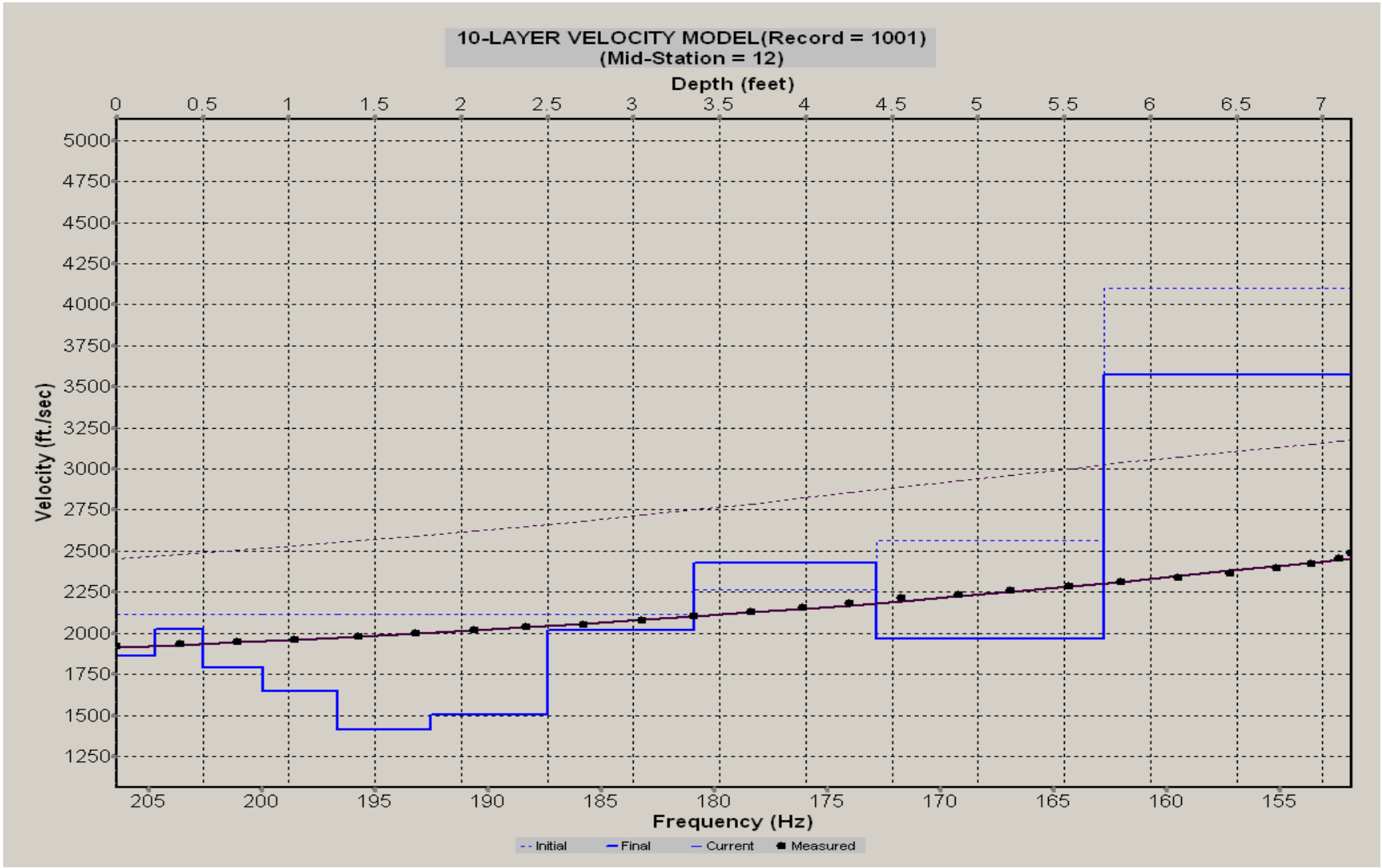

A.087: Velocity Profile Line 1090 used in Pre-blast 21

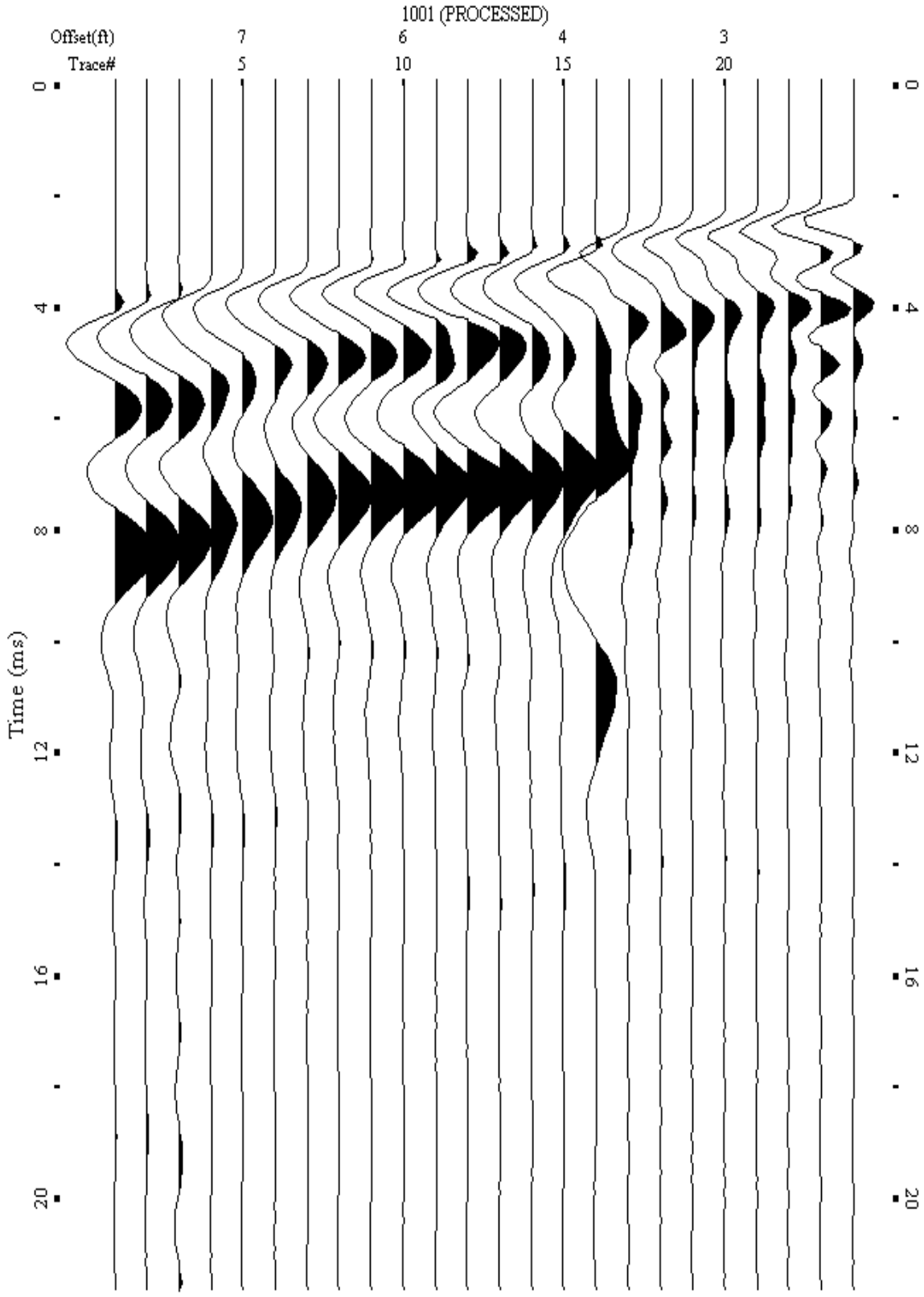

A.088: Shot Gather Line 1091 used in Pre-blast 21

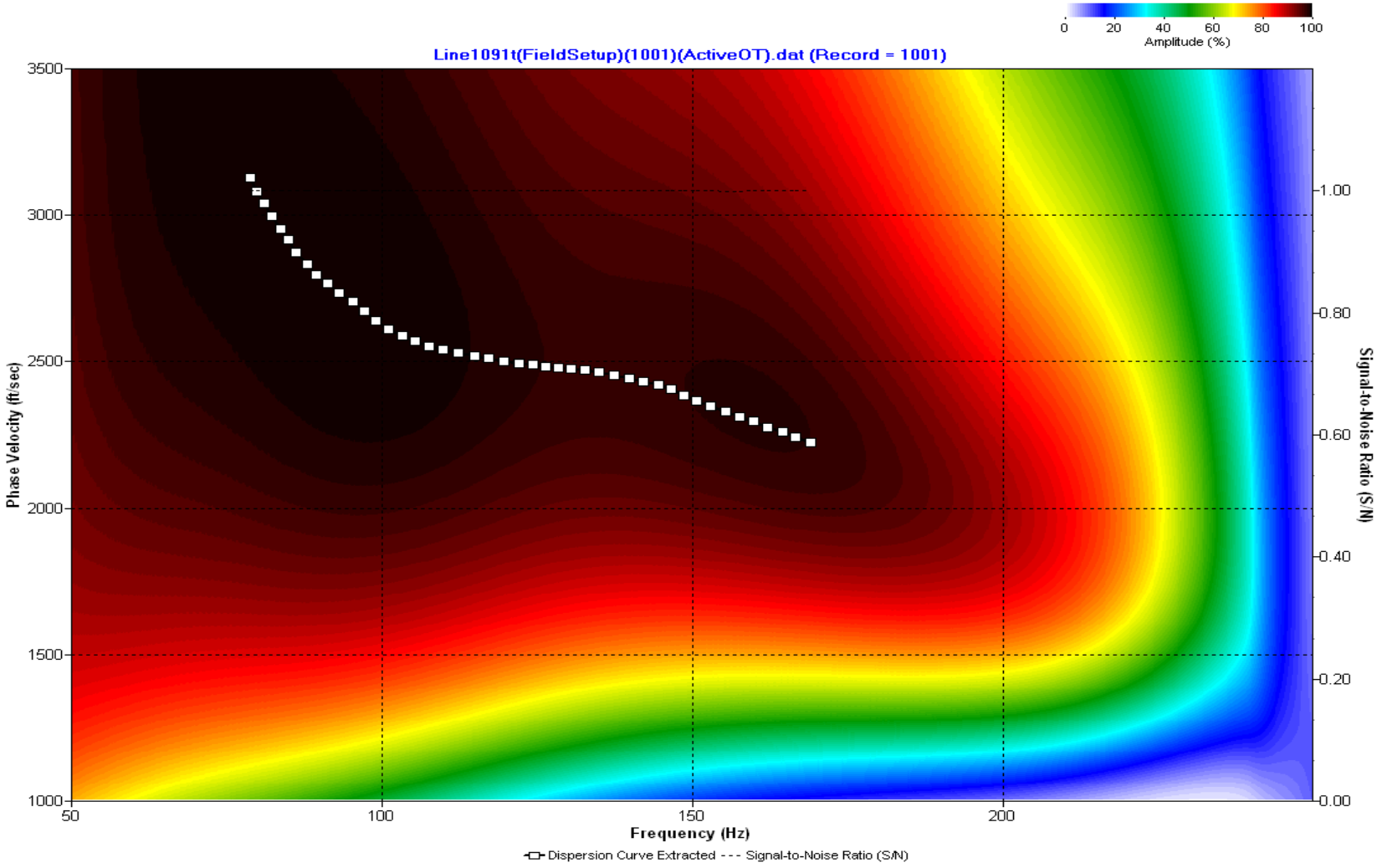

A.089: Dispersion Curve Line 1091 used in Pre-blast 21

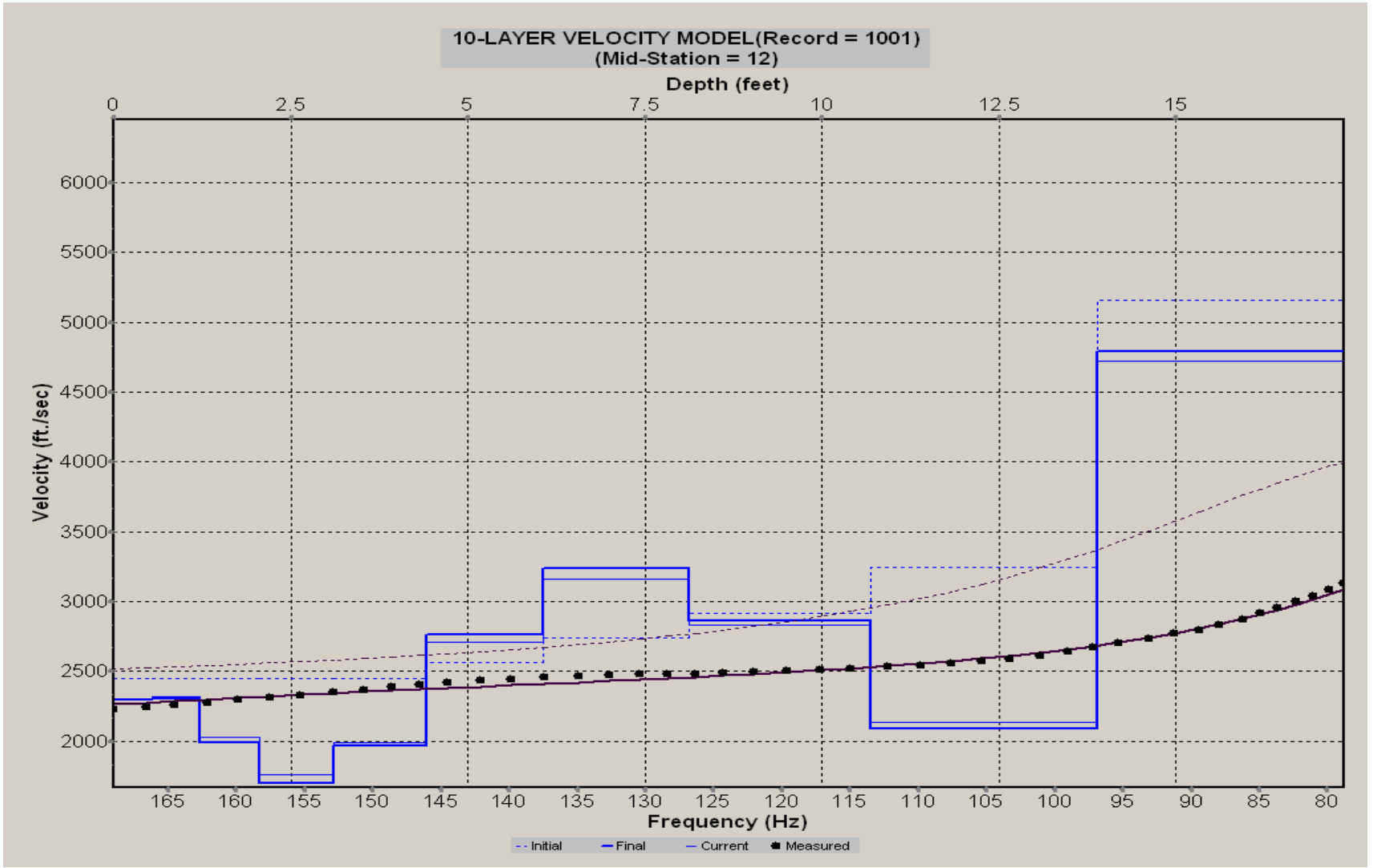

A.090: Velocity Profile Line 1091 used in Pre-blast 21

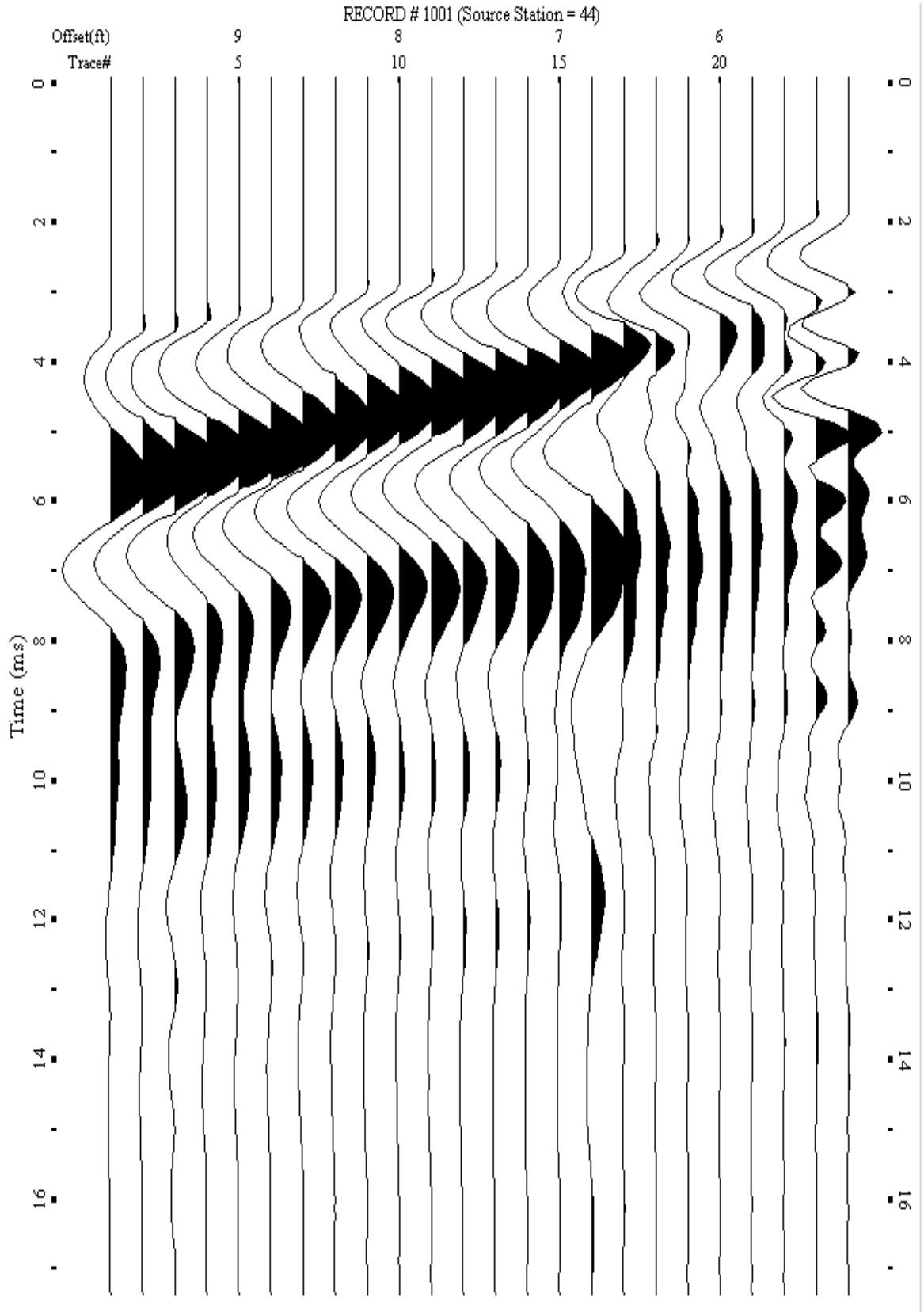

A.091: Shot Gather Line 1092 used in Pre-blast 21

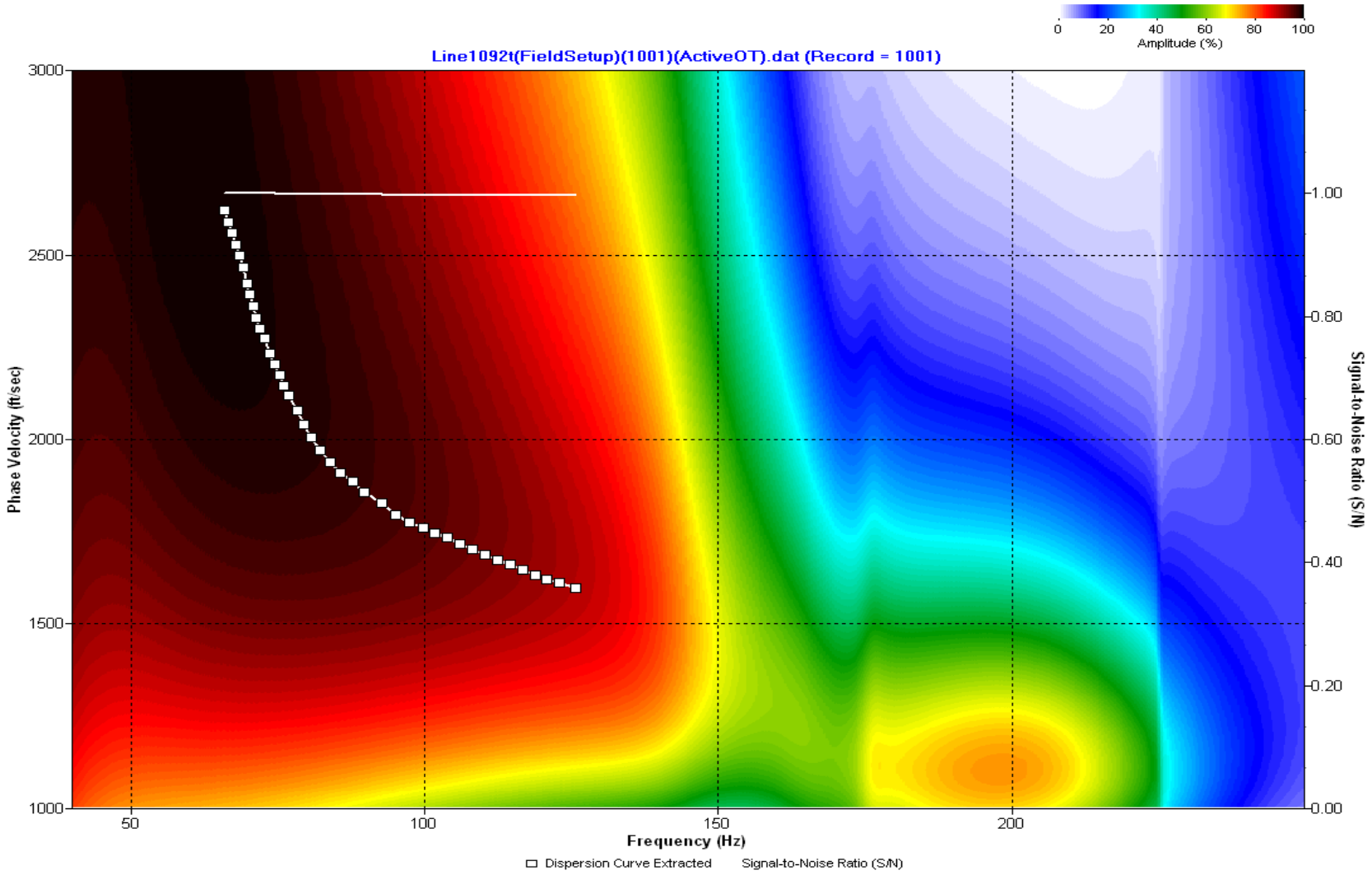

A.092: Dispersion Curve Line 1092 used in Pre-blast 21

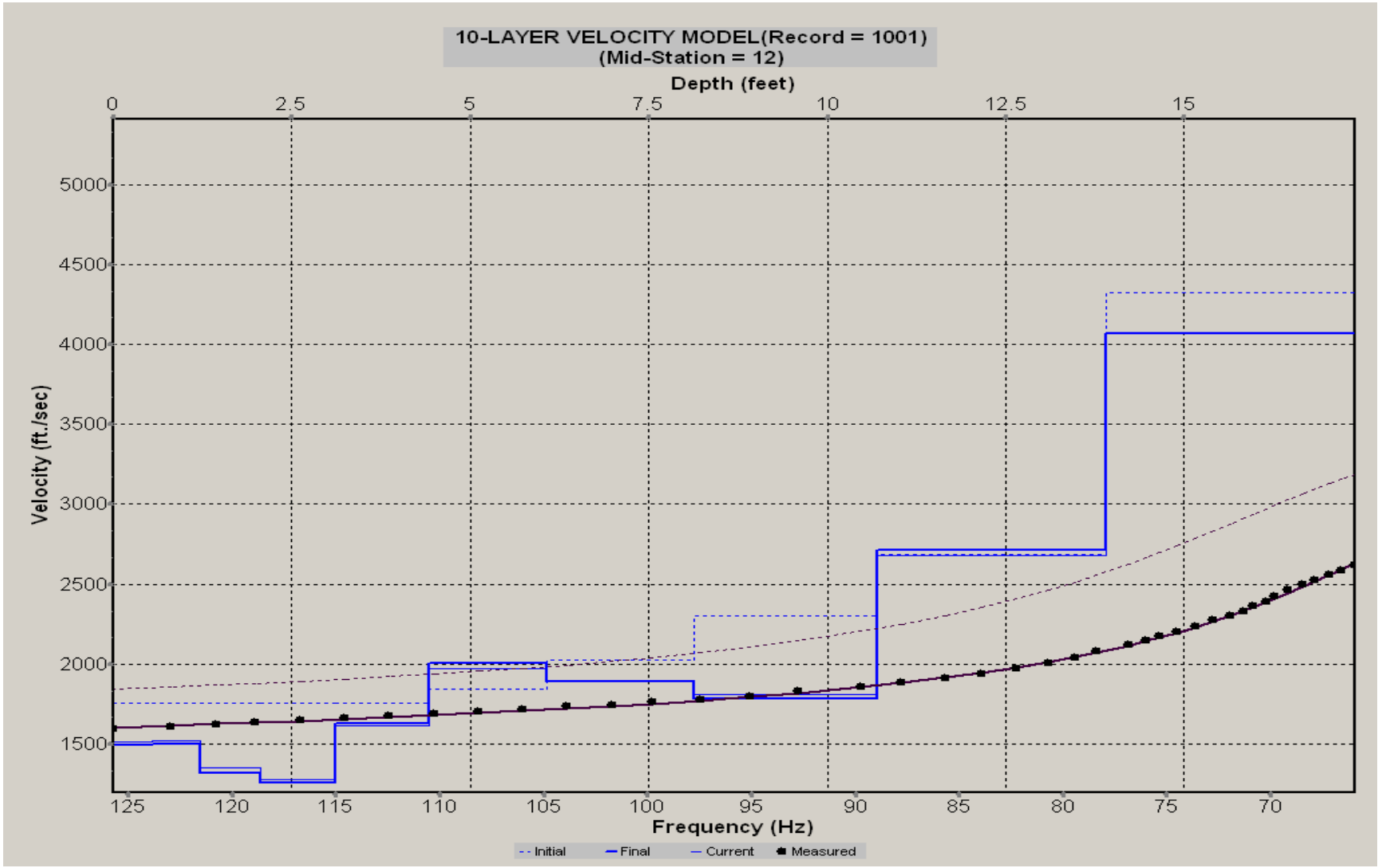

A.093: Velocity Profile Line 1092 used in Pre-blast 21

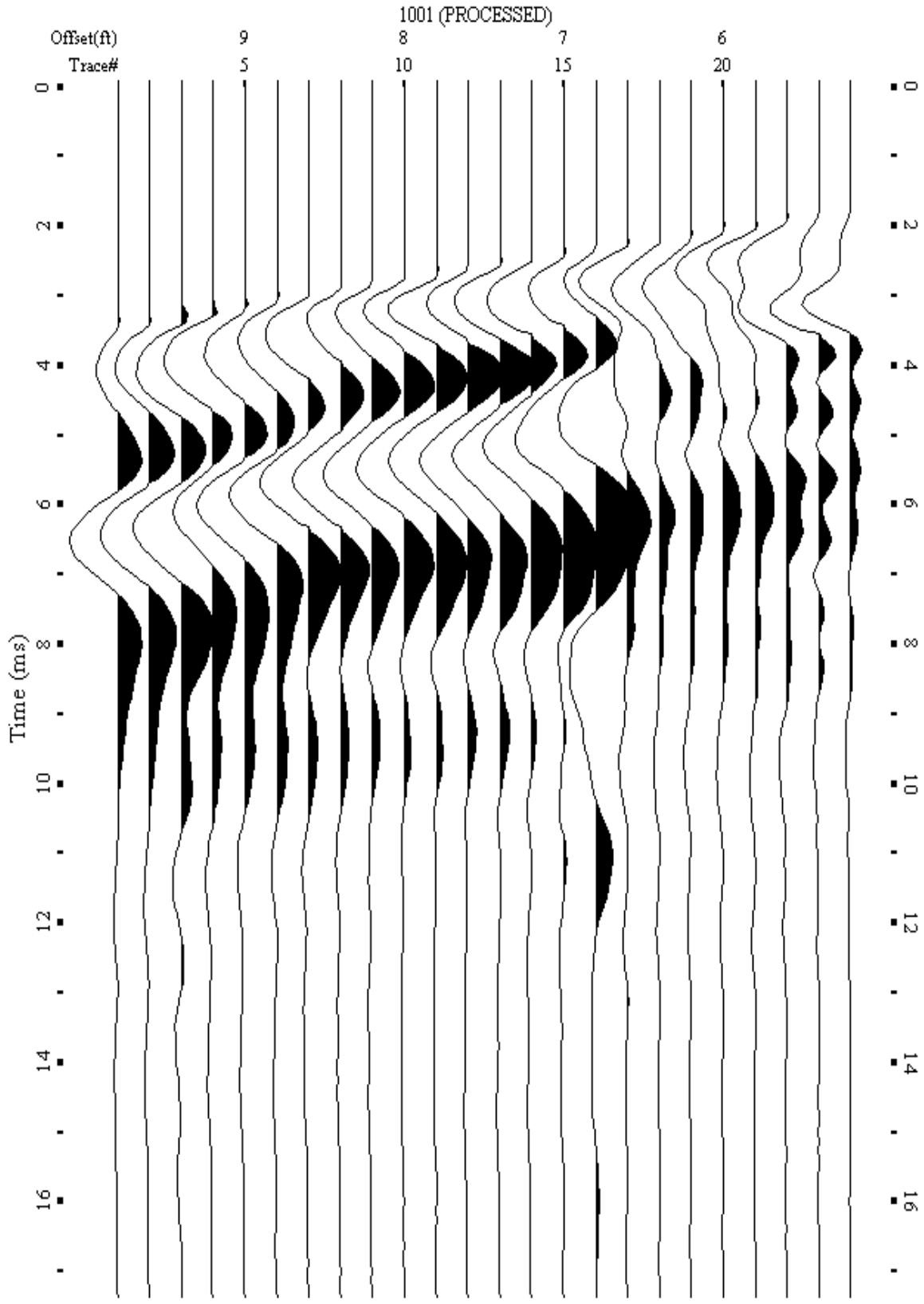

A.094: Shot Gather Line 1093 used in Pre-blast 21

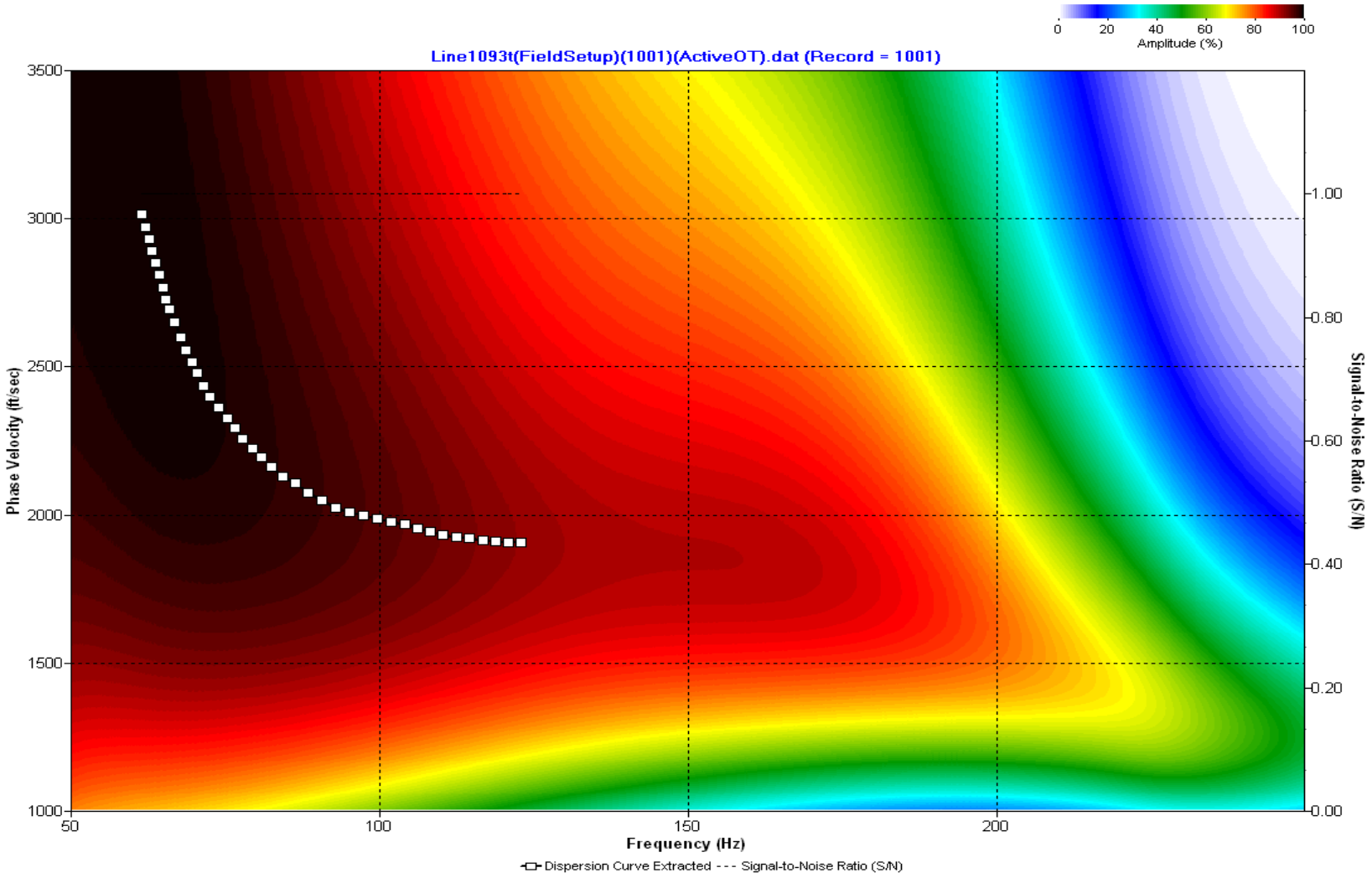

A.095: Dispersion Curve Line 1093 used in Pre-blast 21

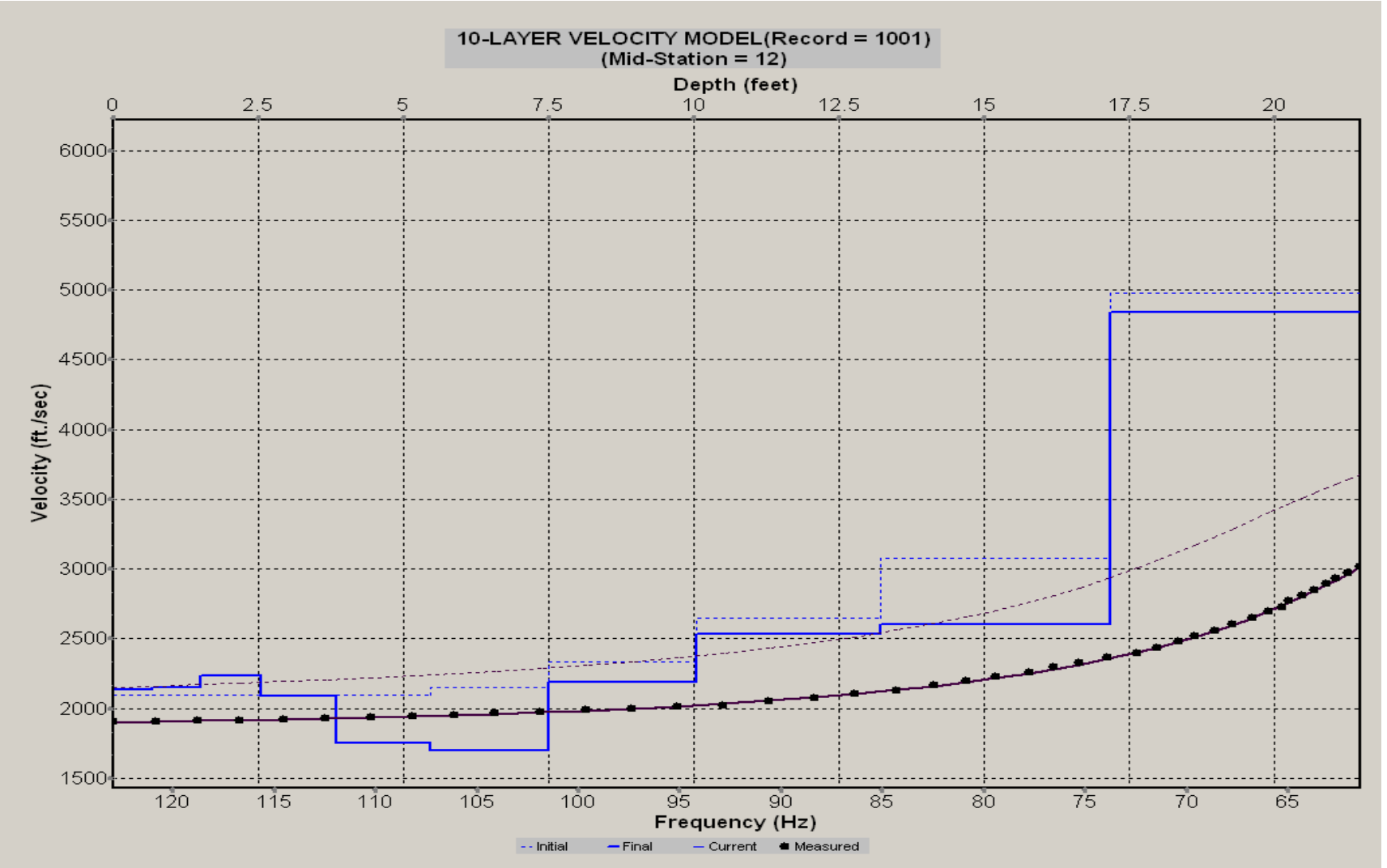

A.096: Velocity Profile Line 1093 used in Pre-blast 21

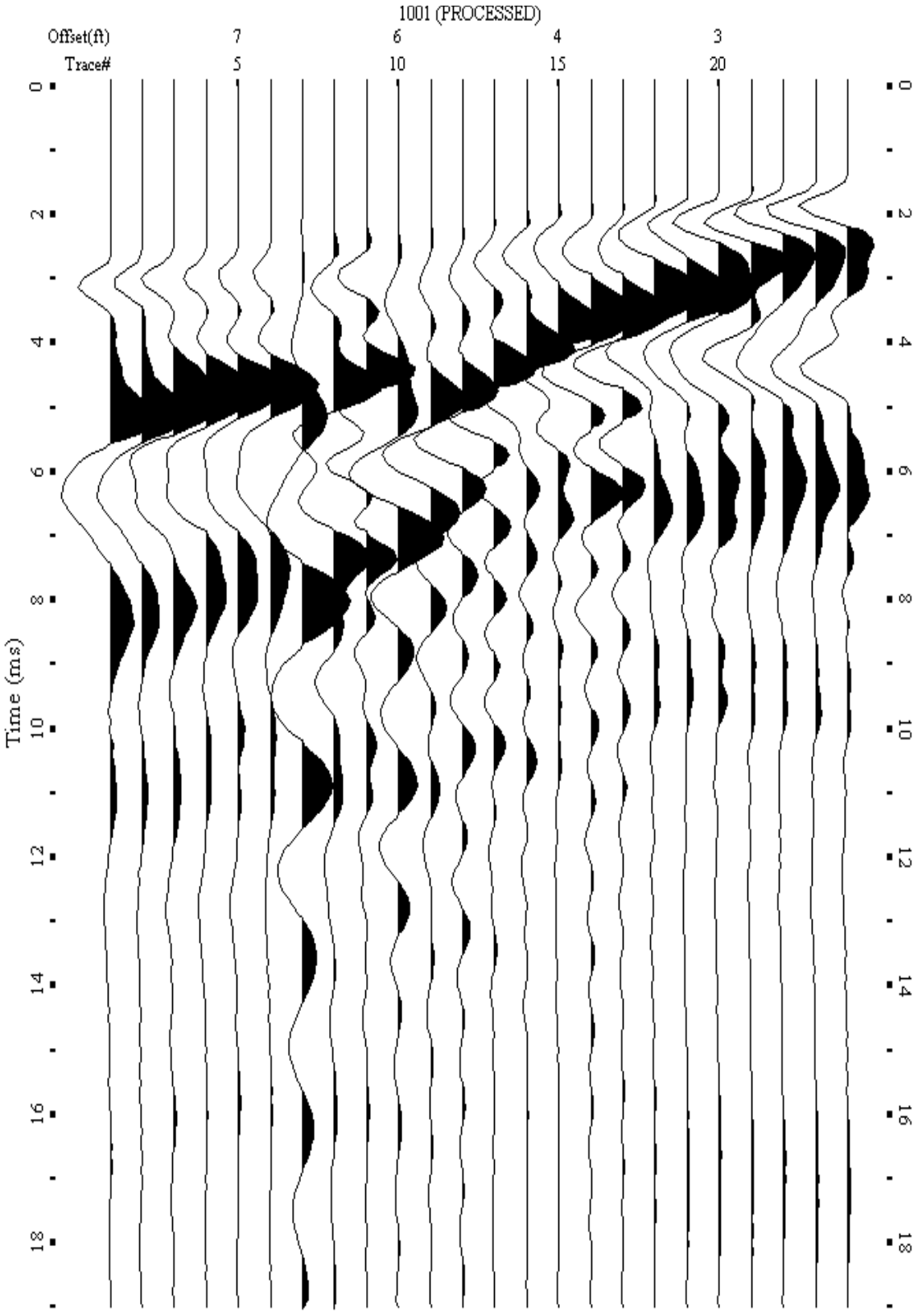

A.097: Shot Gather Line 1102 used in Pre-blast 22

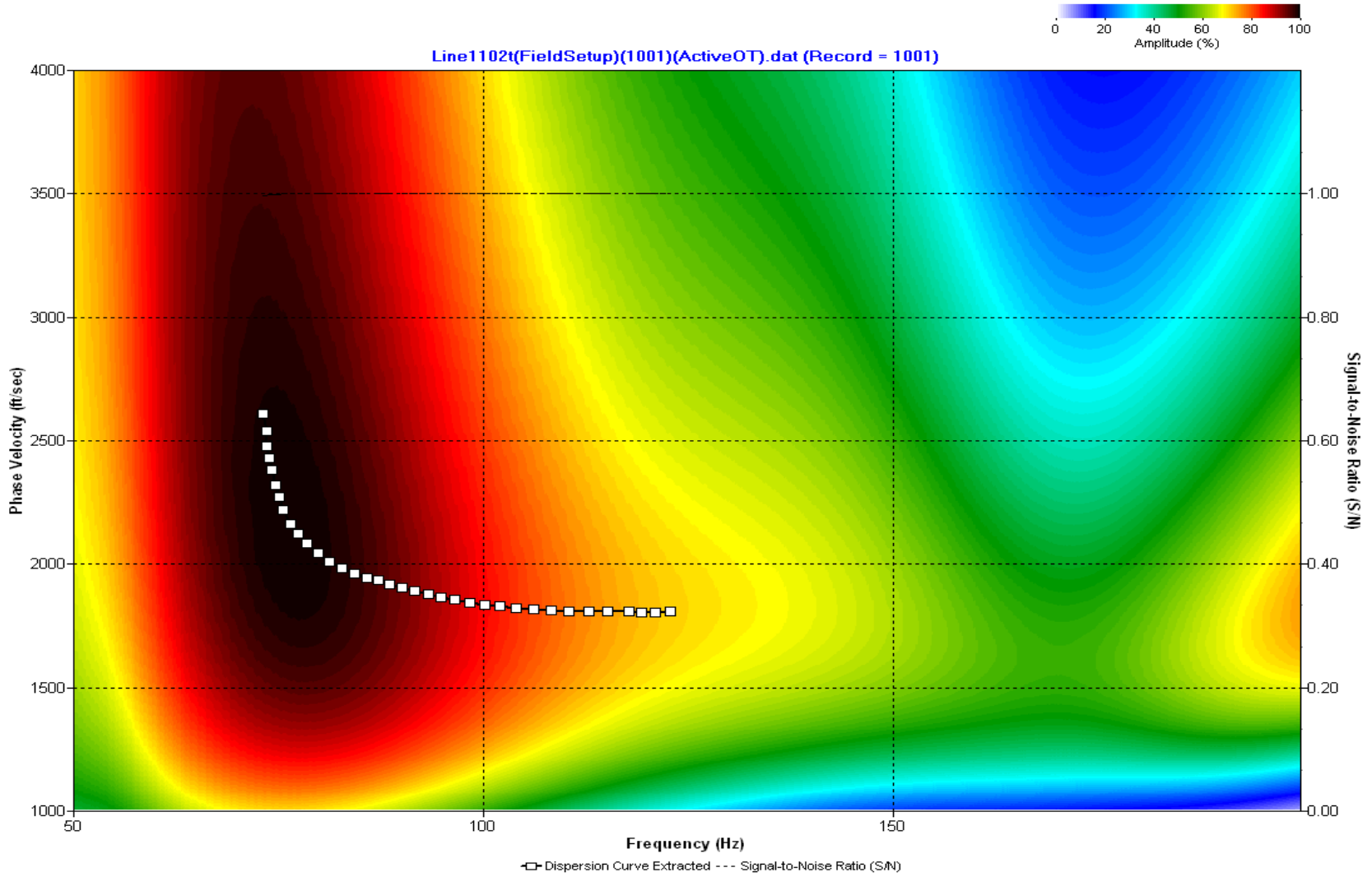

A.098: Dispersion Curve Line 1102 used in Pre-blast 22

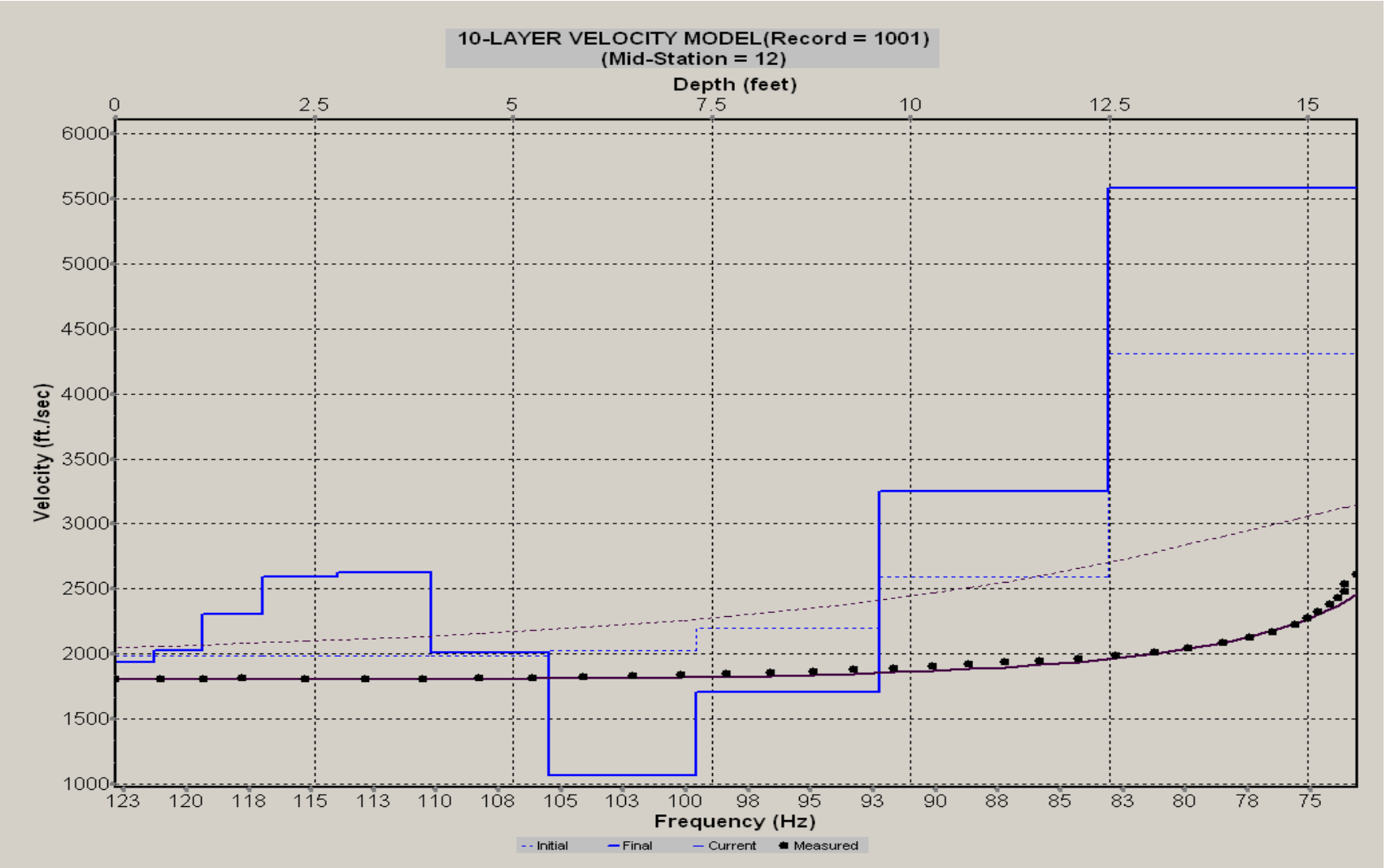

A.099: Velocity Profile Line 1102 used in Pre-blast 22

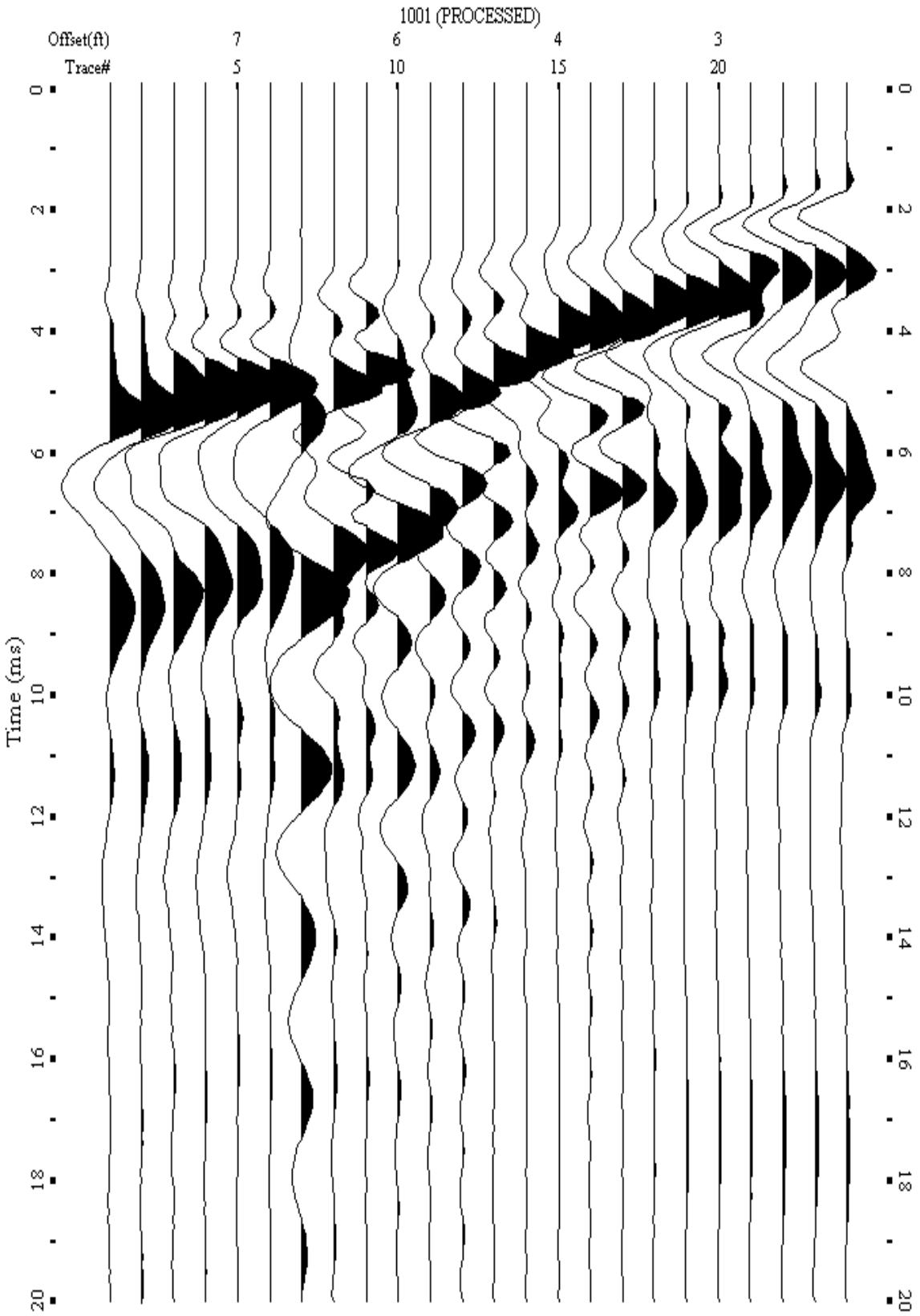

A.100: Shot Gather Line 1103 used in Pre-blast 22

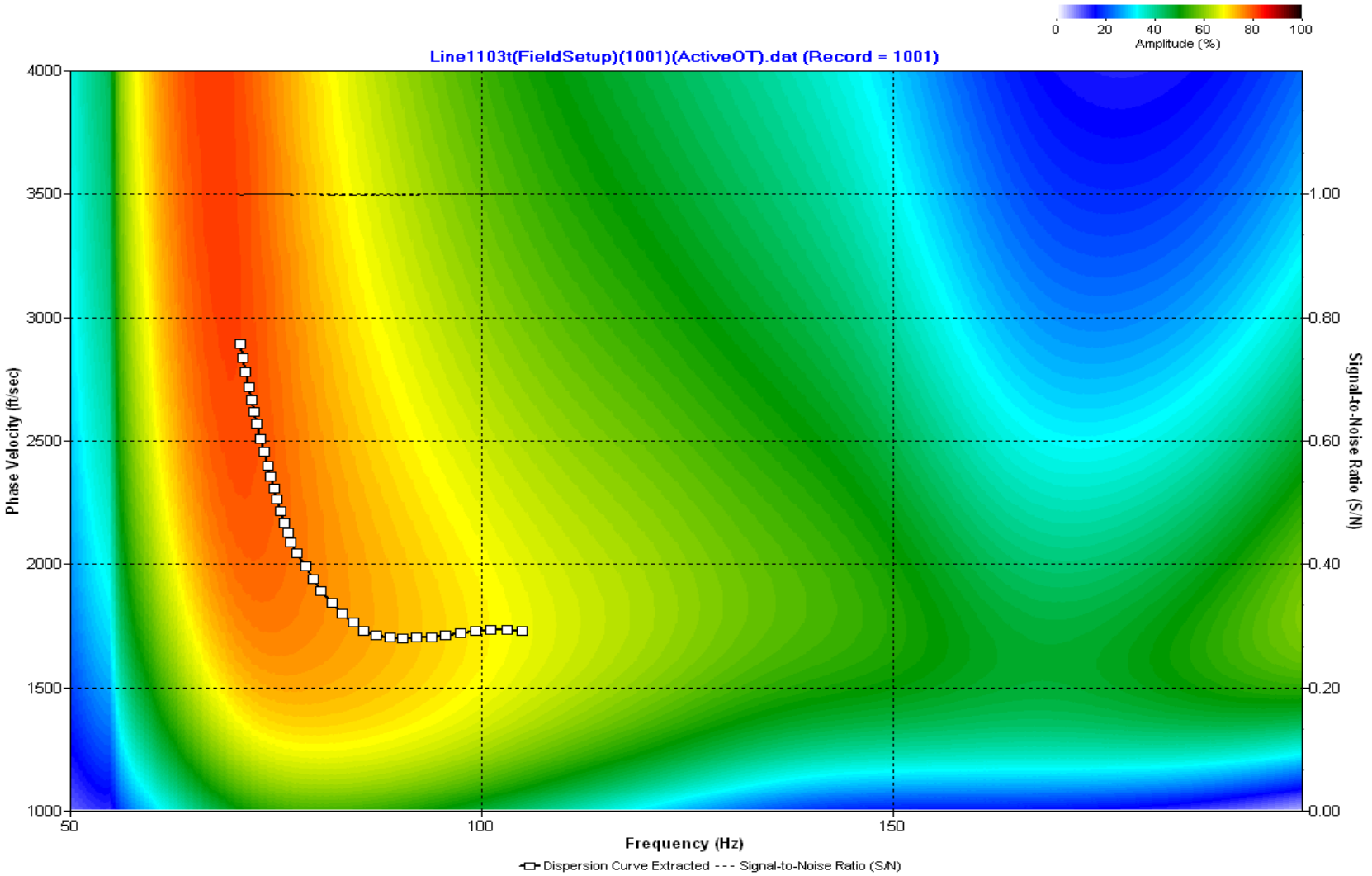

A.101: Dispersion Curve Line 1103 used in Pre-blast 22

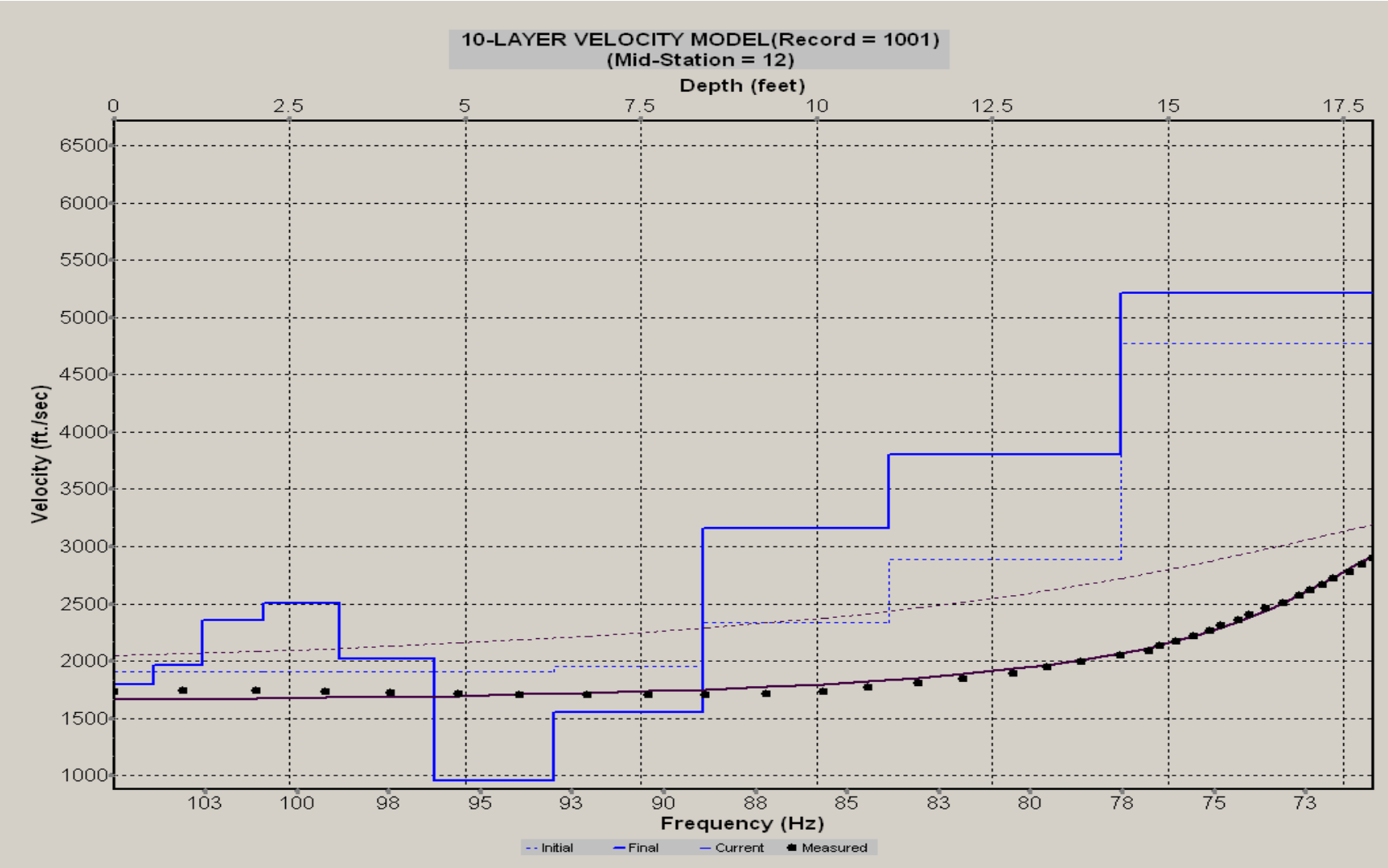

A.102: Velocity Profile Line 1103 used in Pre-blast 22

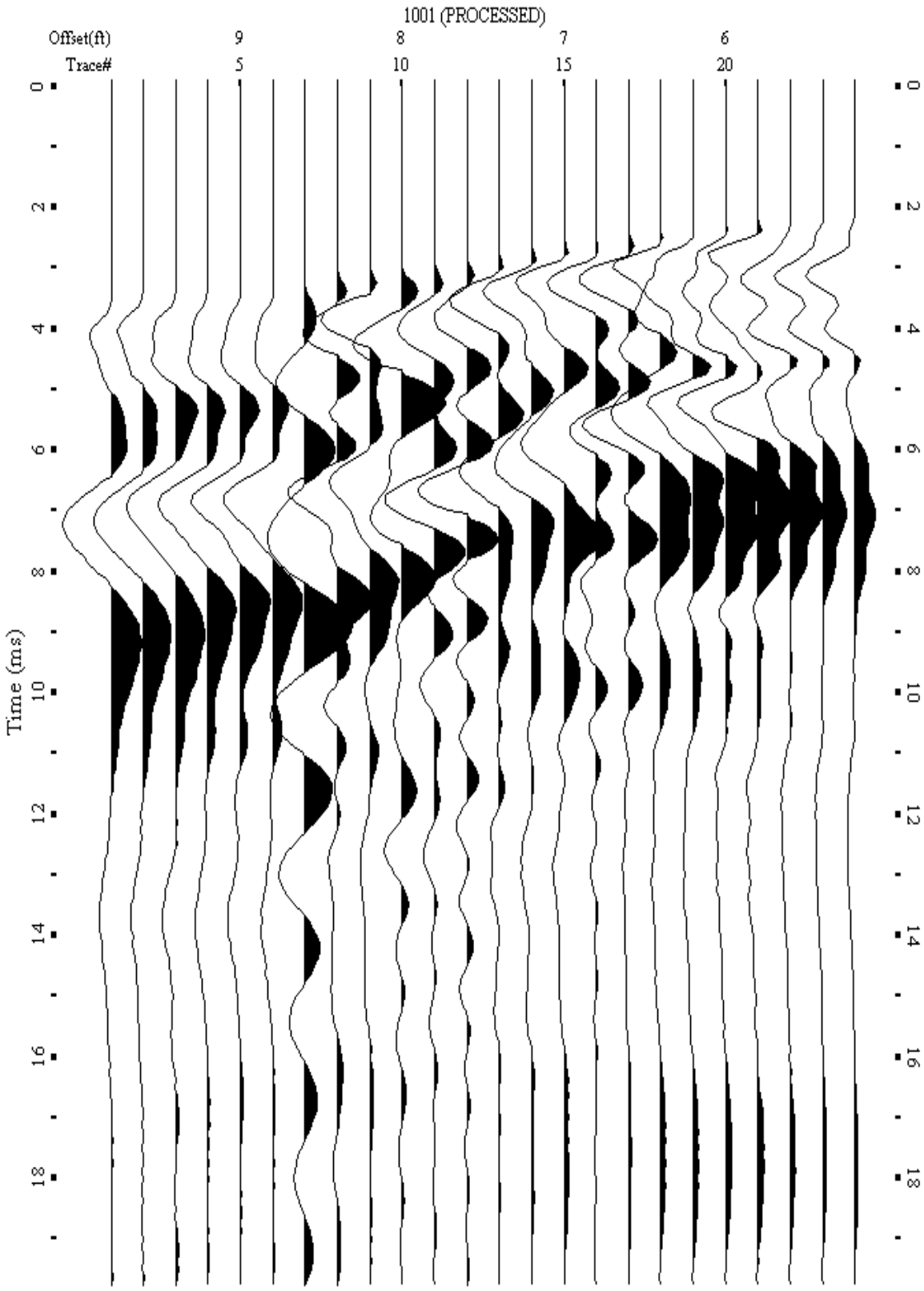

A.103: Shot Gather Line 1105 used in Pre-blast 22

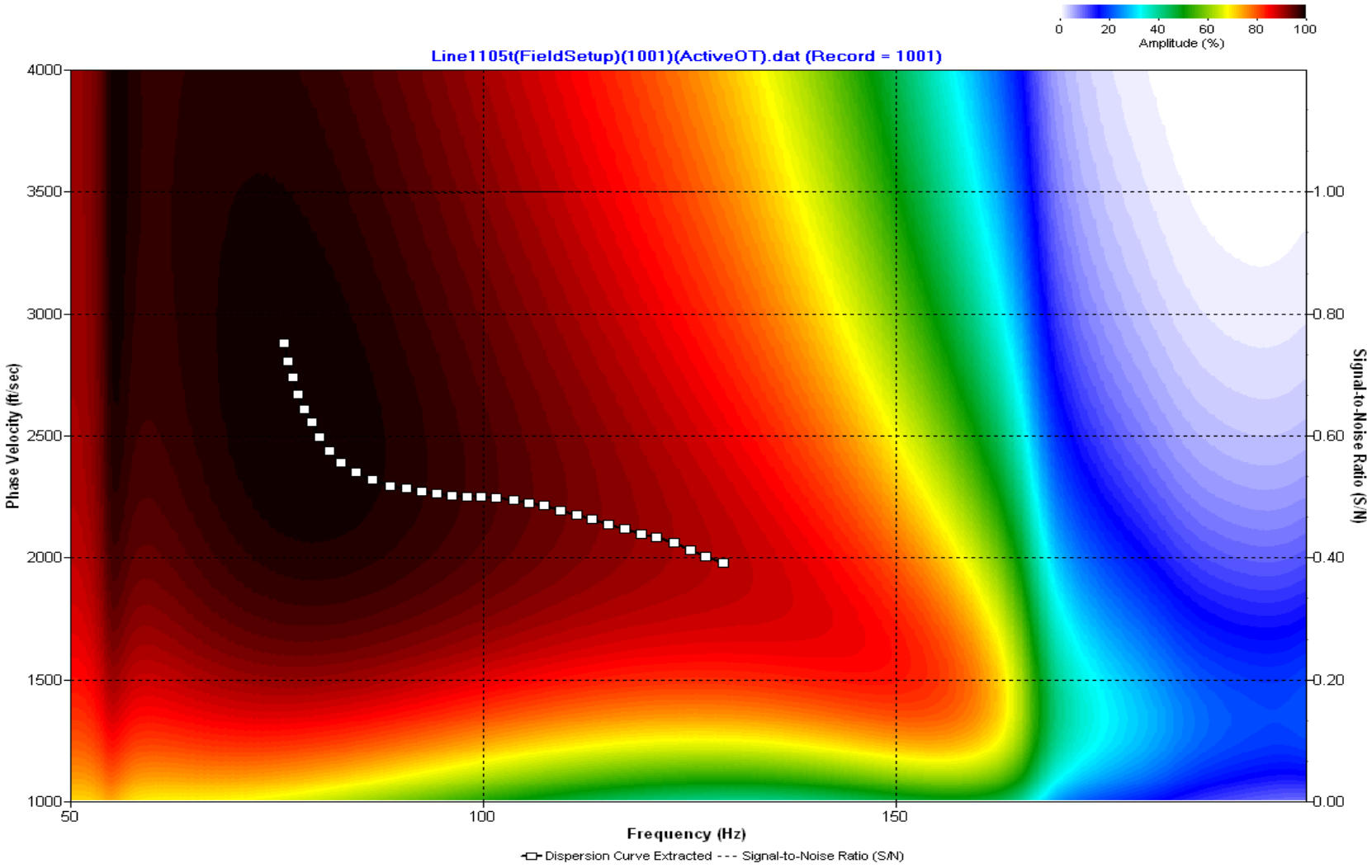

A.104: Dispersion Curve Line 1105 used in Pre-blast 22

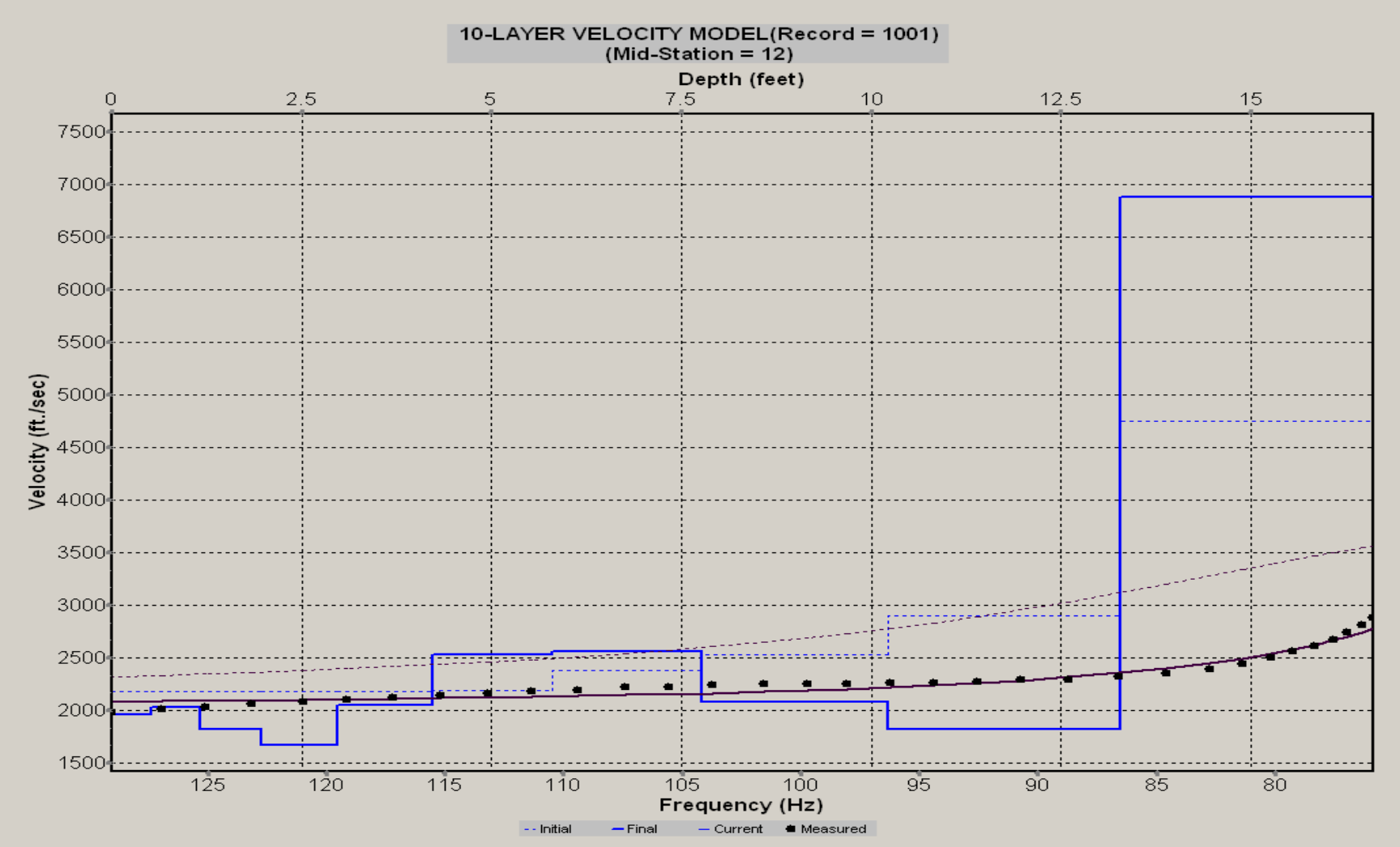

A.105: Velocity Profile Line 1105 used in Pre-blast 22

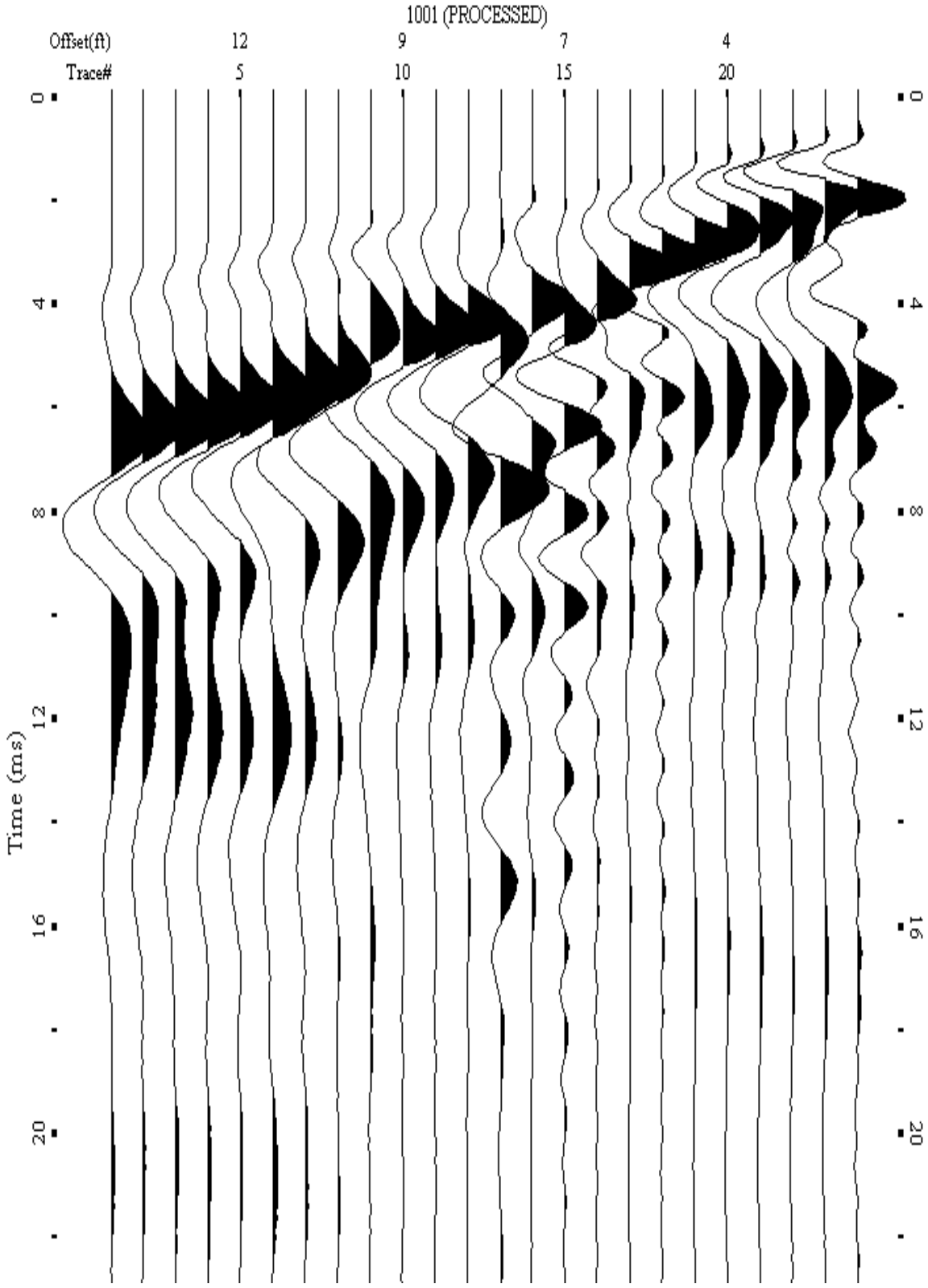

A.106: Shot Gather Line 1110 used in Pre-blast 22

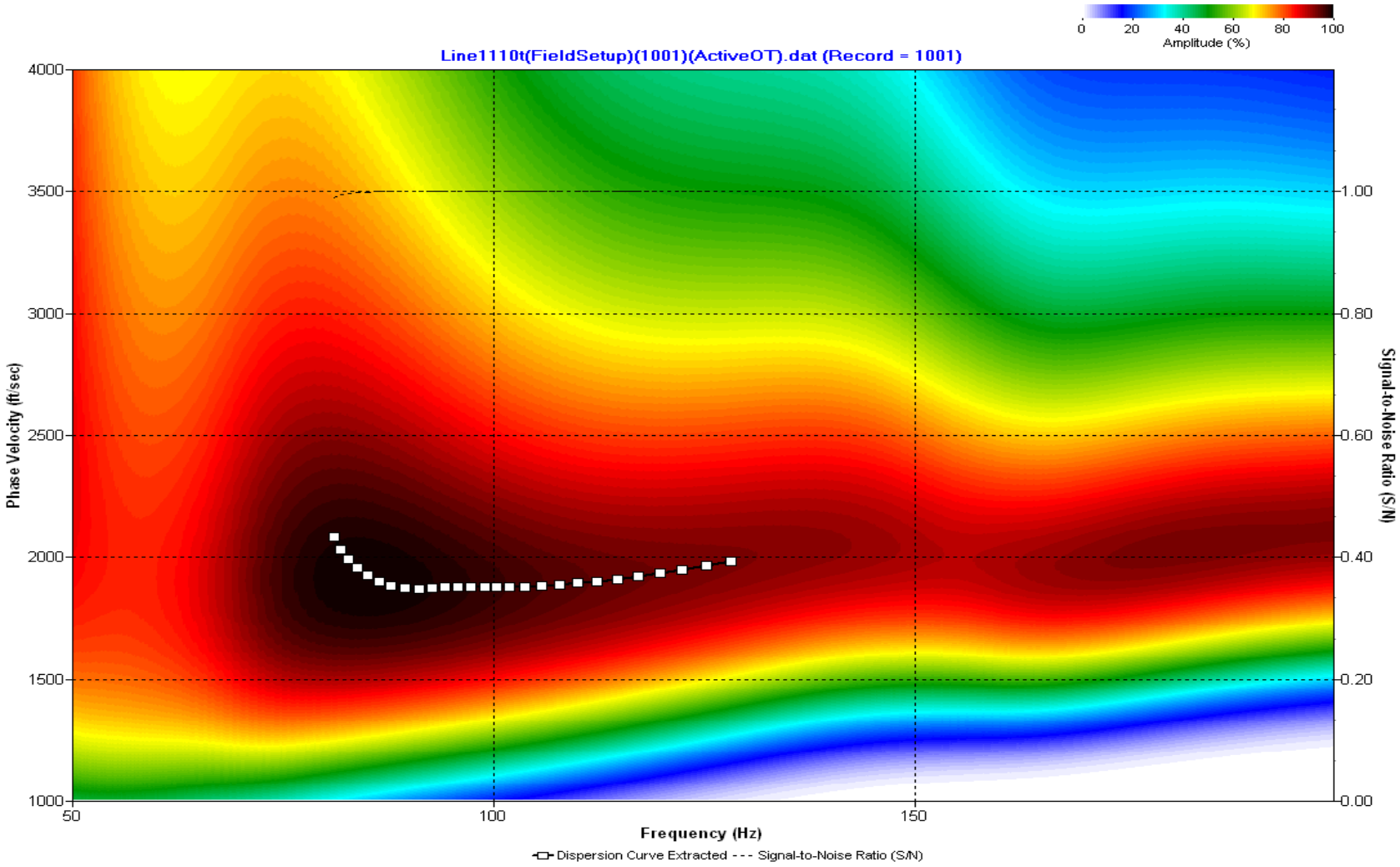

A.107: Dispersion Curve Line 1110 used in Pre-blast 22

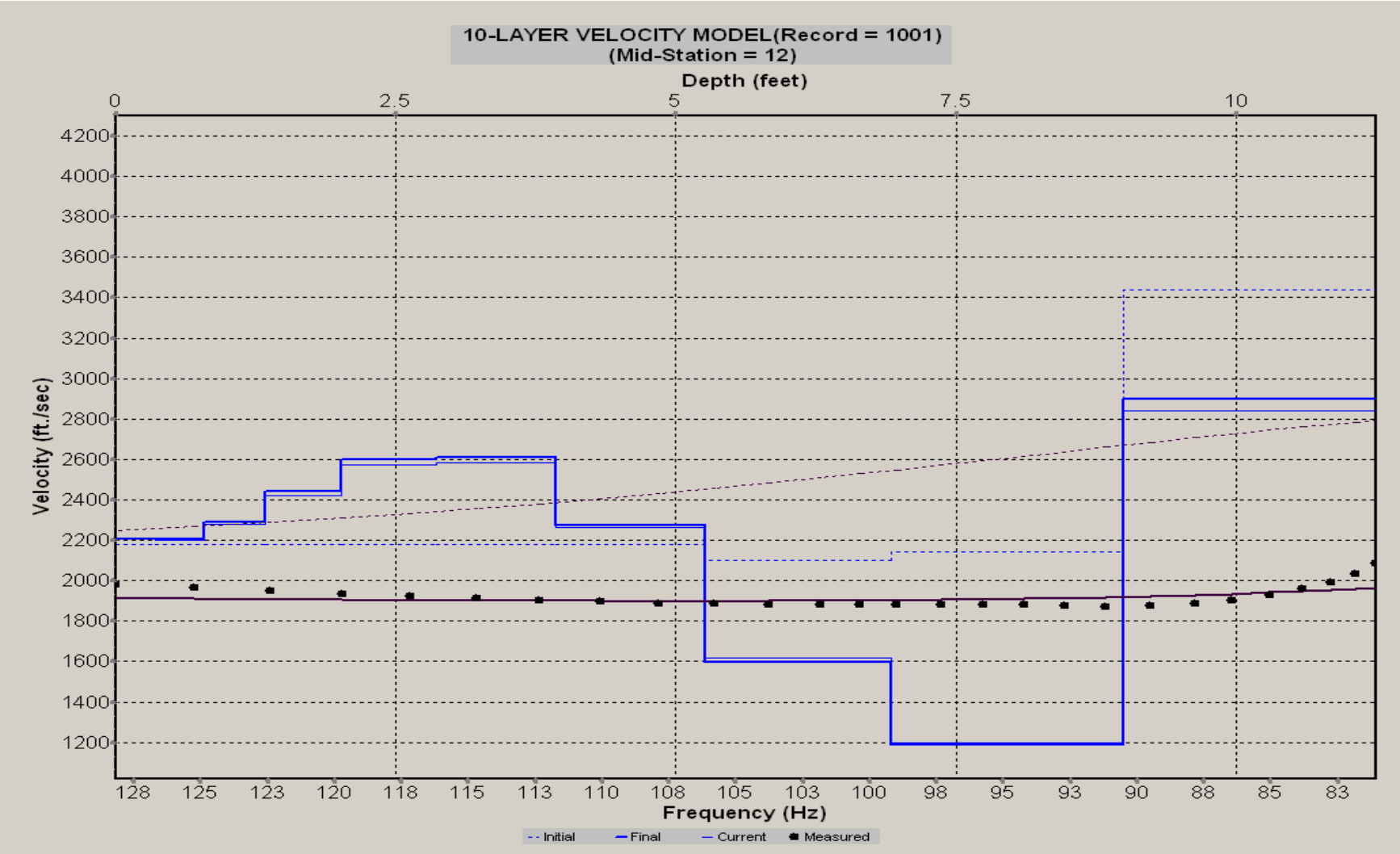

A.108: Velocity Profile Line 1110 used in Pre-blast 22

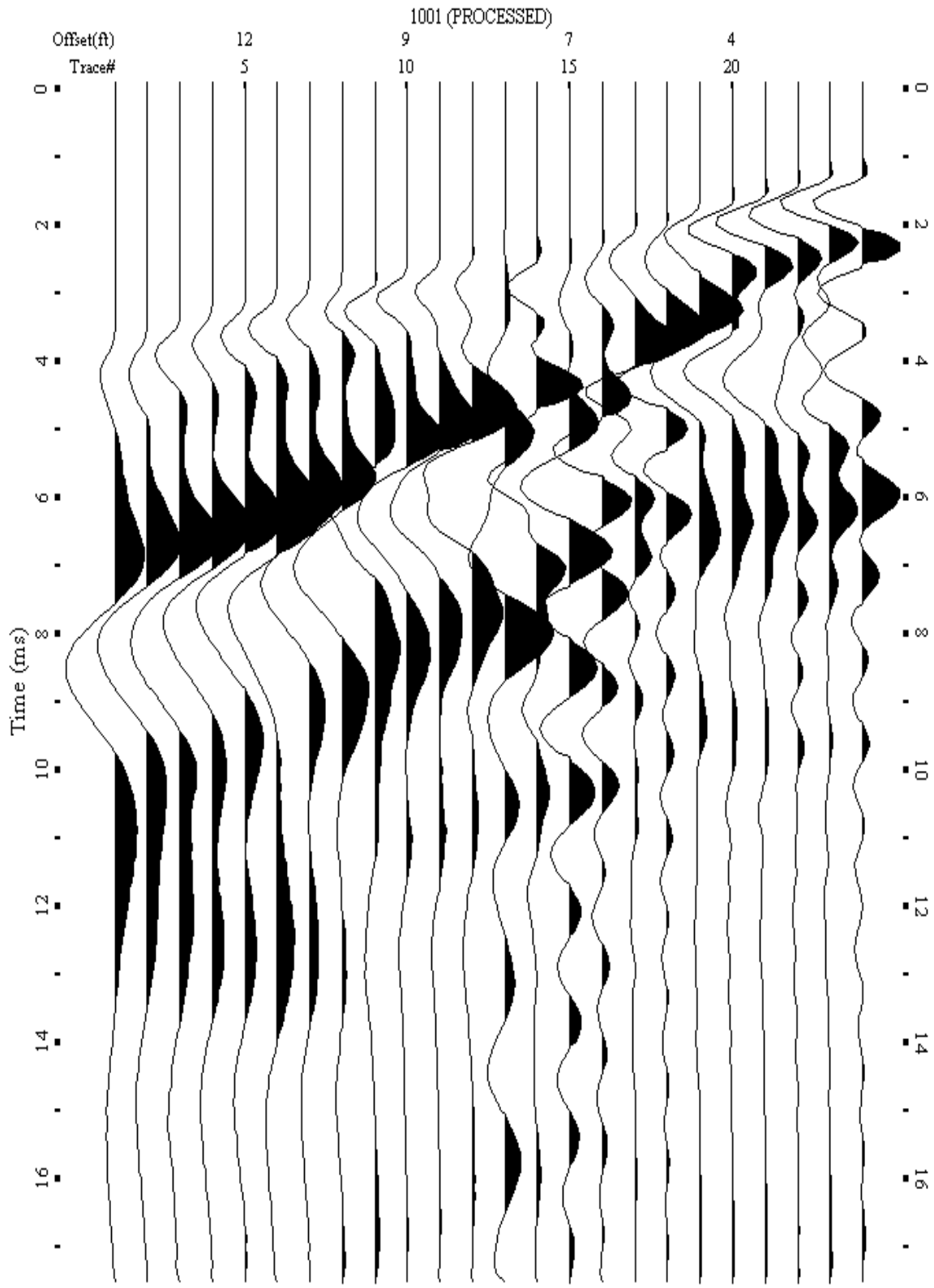

A.109: Shot Gather Line 1111 used in Pre-blast 21 and Pre-blast 22

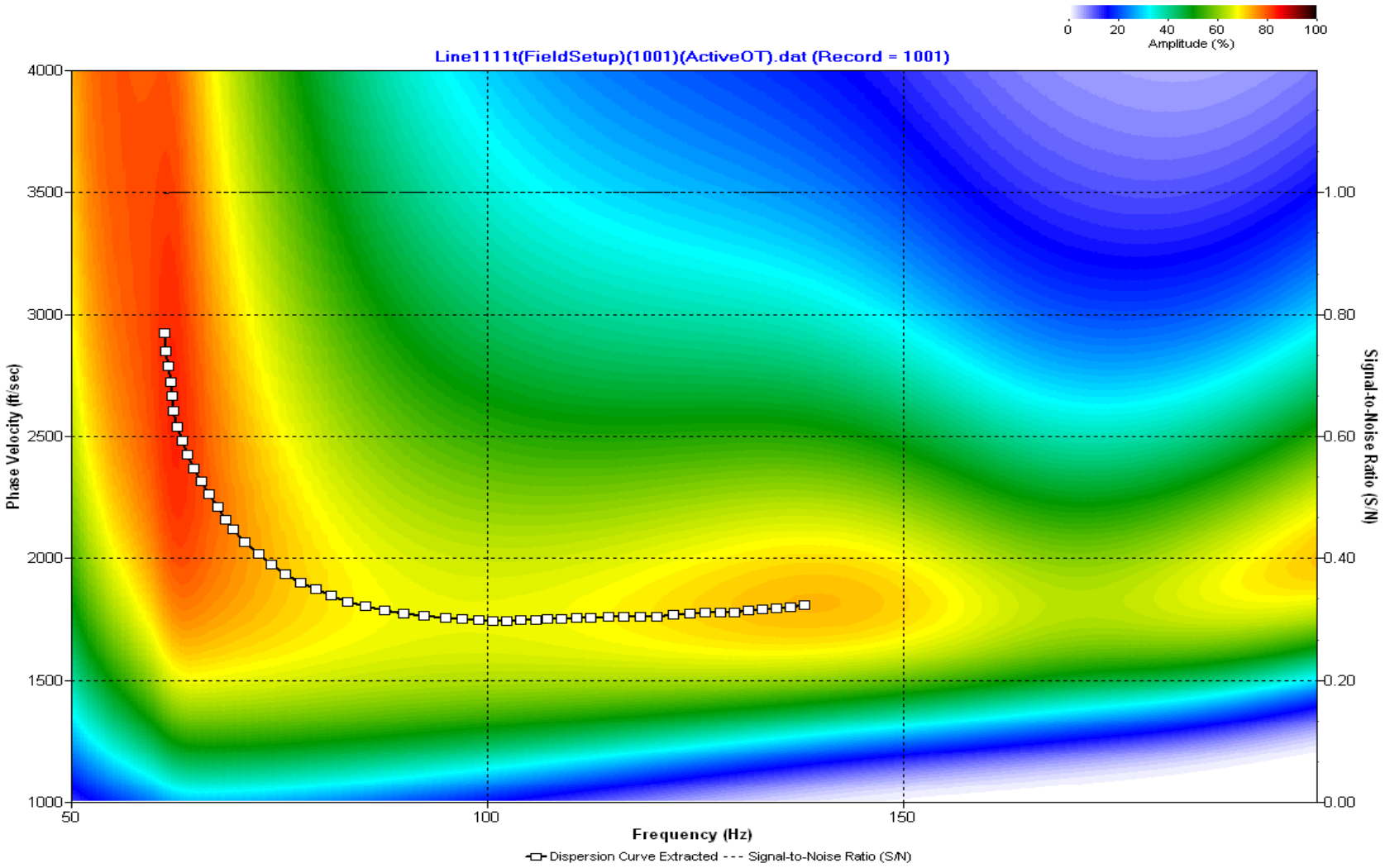

A.110: Dispersion Curve Line 1111 used in Pre-blast 21 and Pre-blast 22

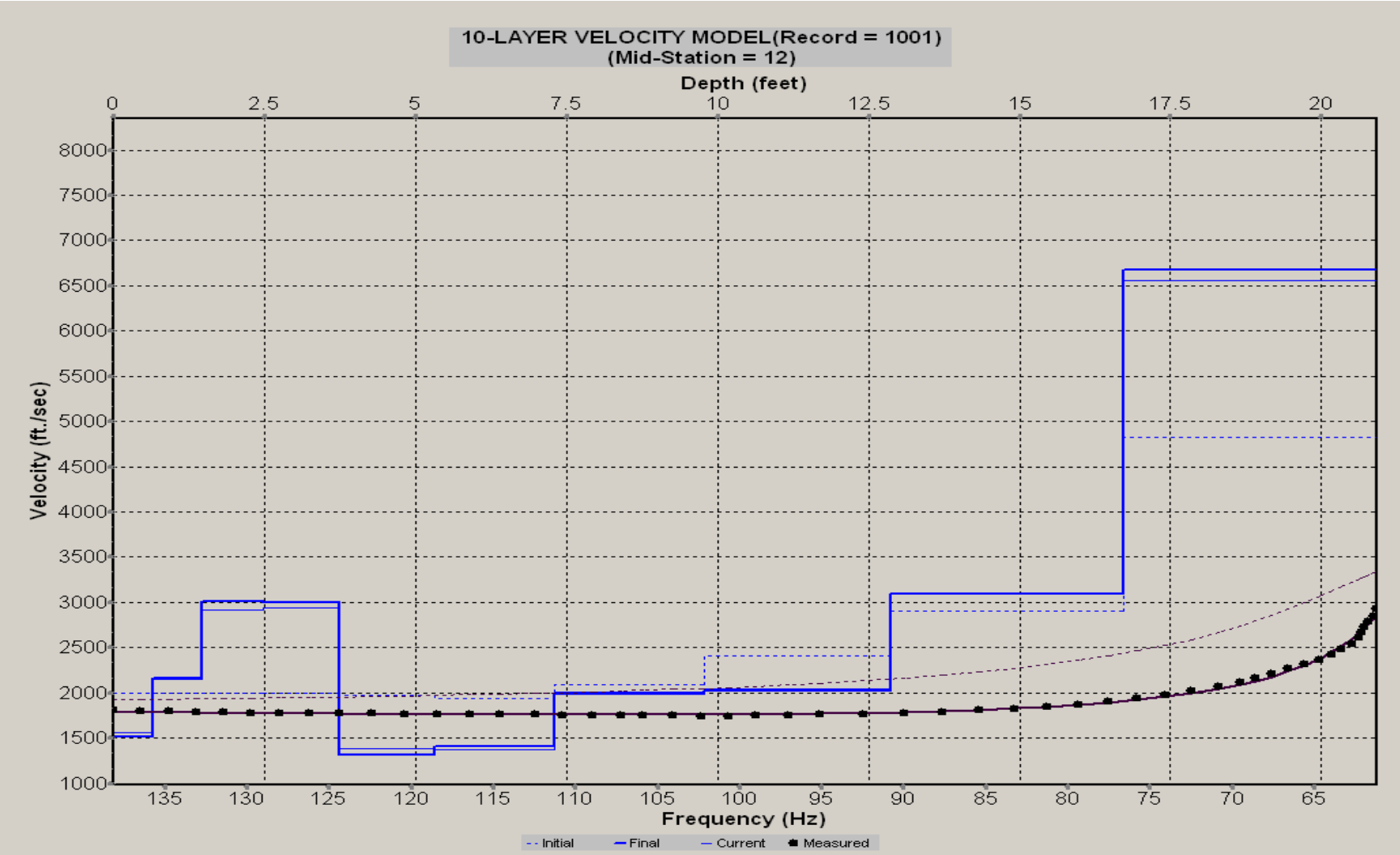

A.111: Velocity Profile Line 1111 used in Pre-blast 21 and Pre-blast 22

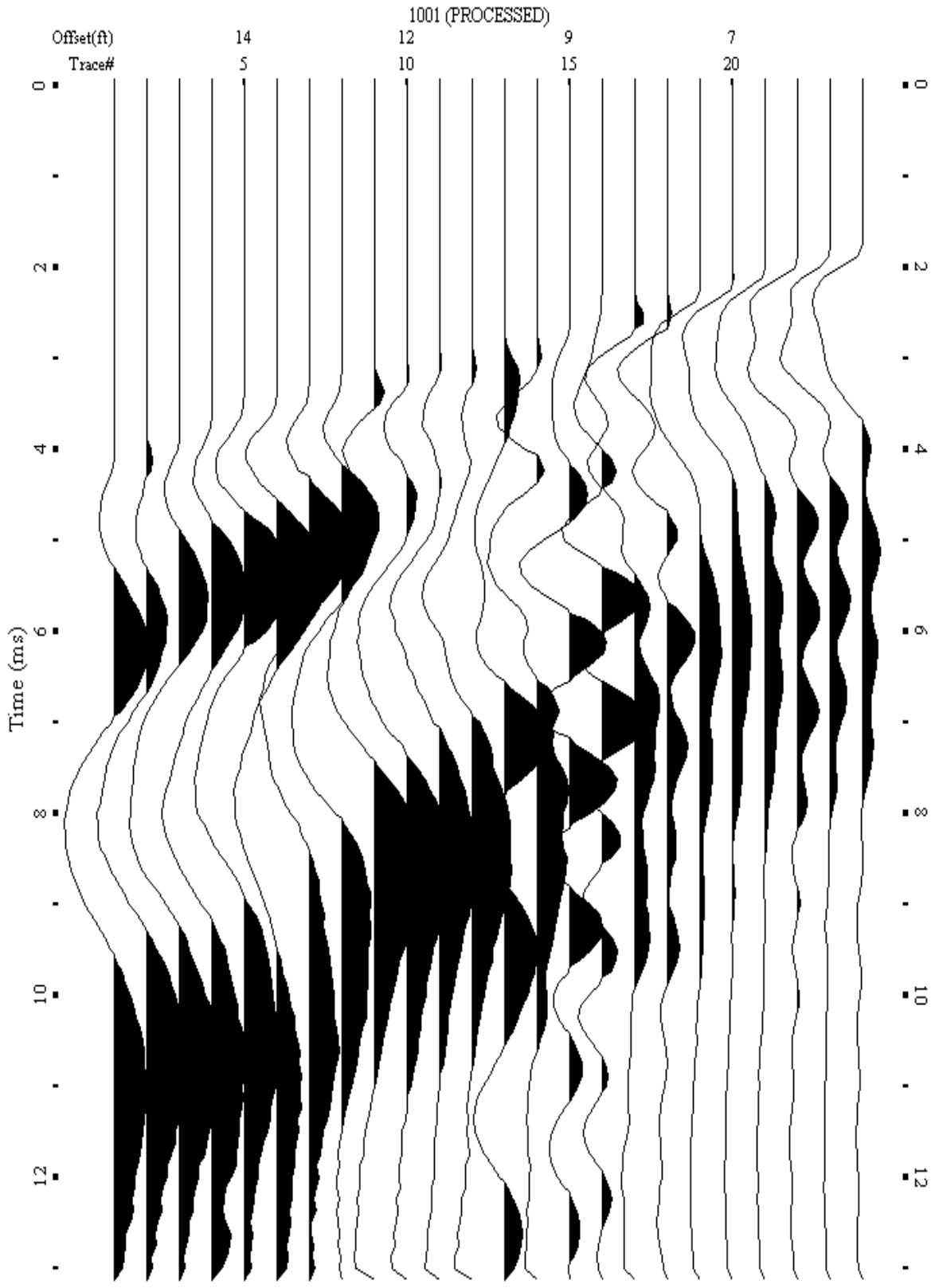

A.112: Shot Gather Line 1112 used in Pre-blast 21 and Pre-blast 22

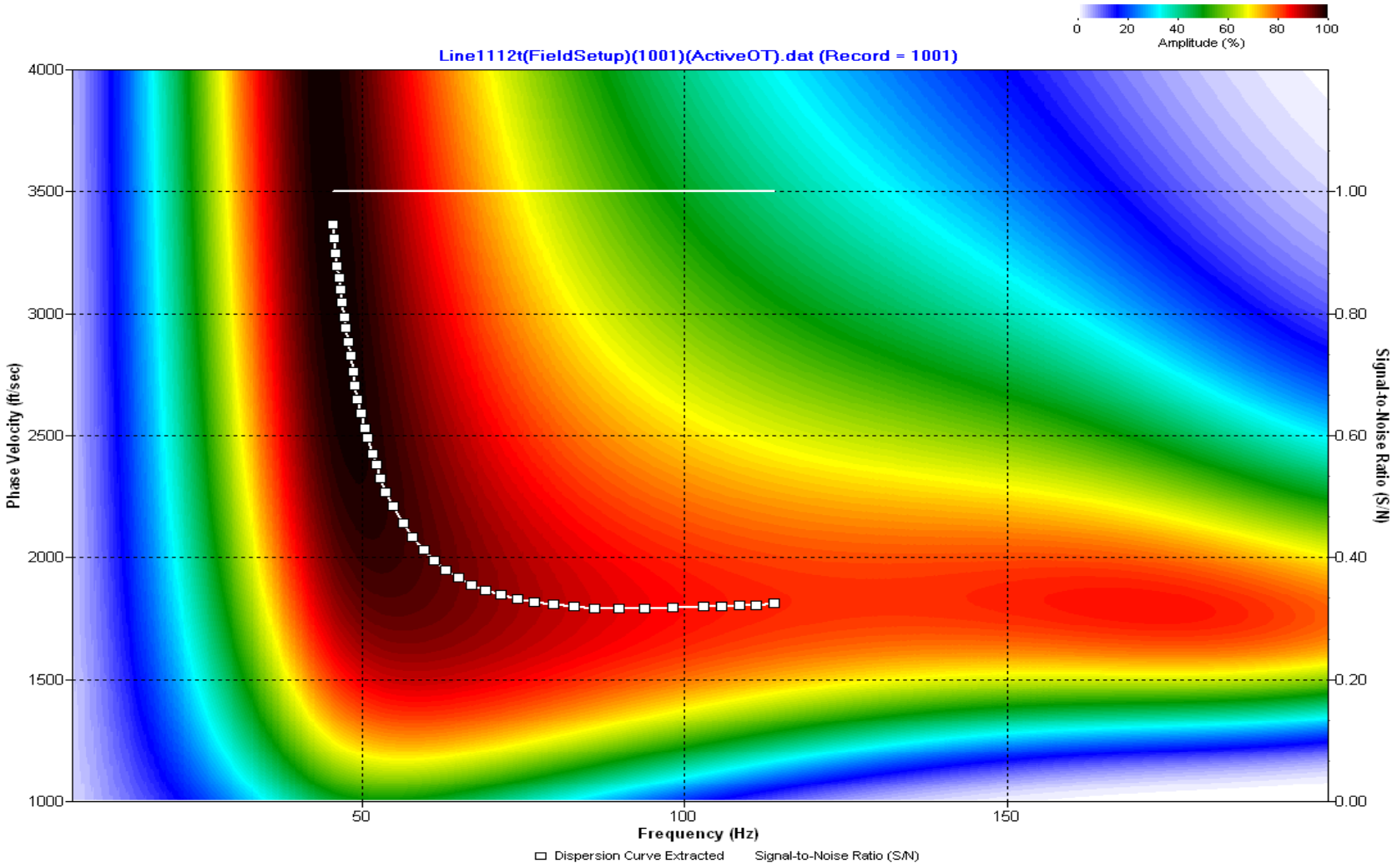

A.113: Dispersion Curve Line 1112 used in Pre-blast 21 and Pre-blast 22

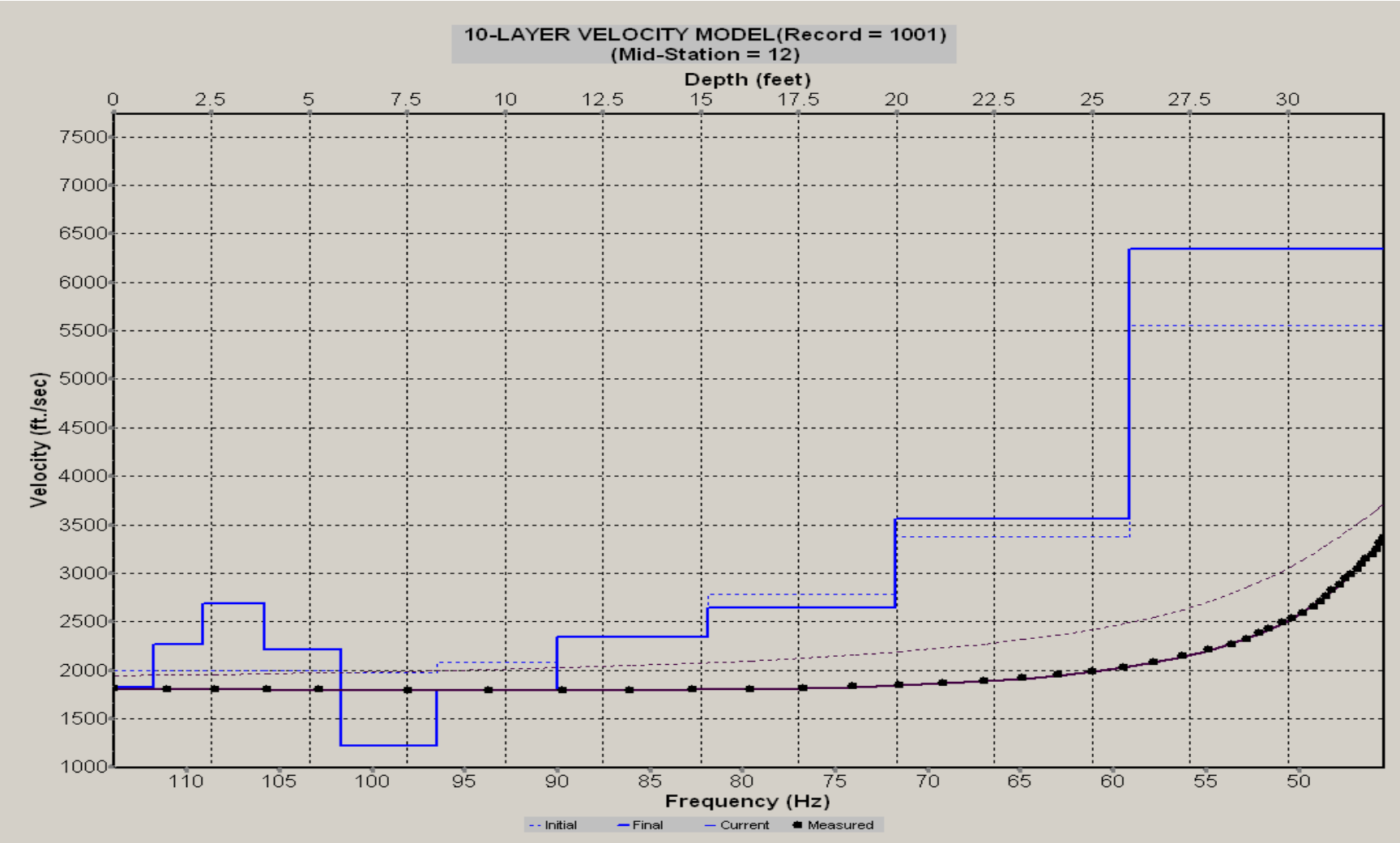

A.114: Velocity Profile Line 1112 used in Pre-blast 21 and Pre-blast 22

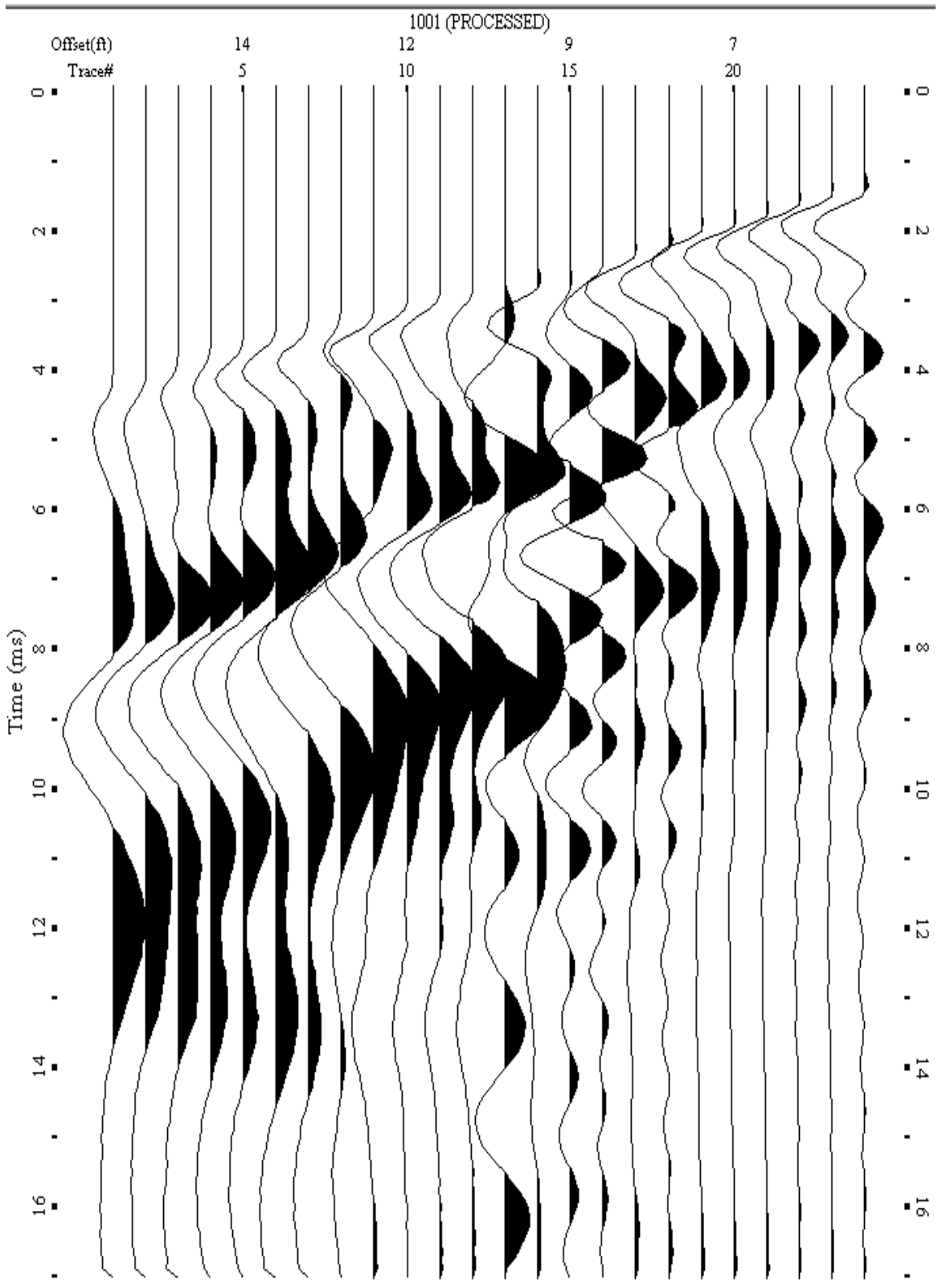

A.115: Shot Gather Line 1113 used in Pre-blast 21 and Pre-blast 22

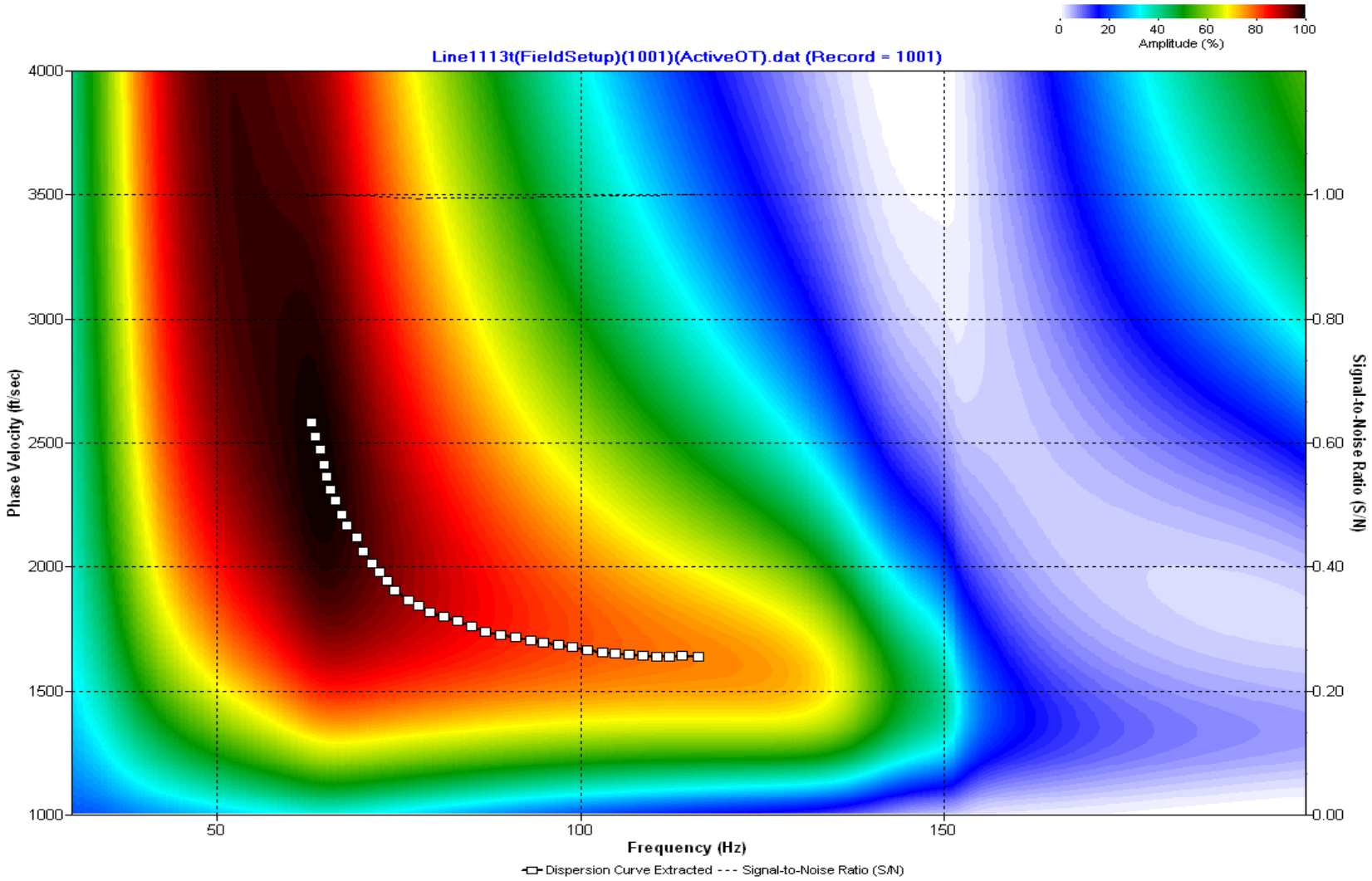

A.116: Dispersion Curve Line 1113 used in Pre-blast 21 and Pre-blast 22

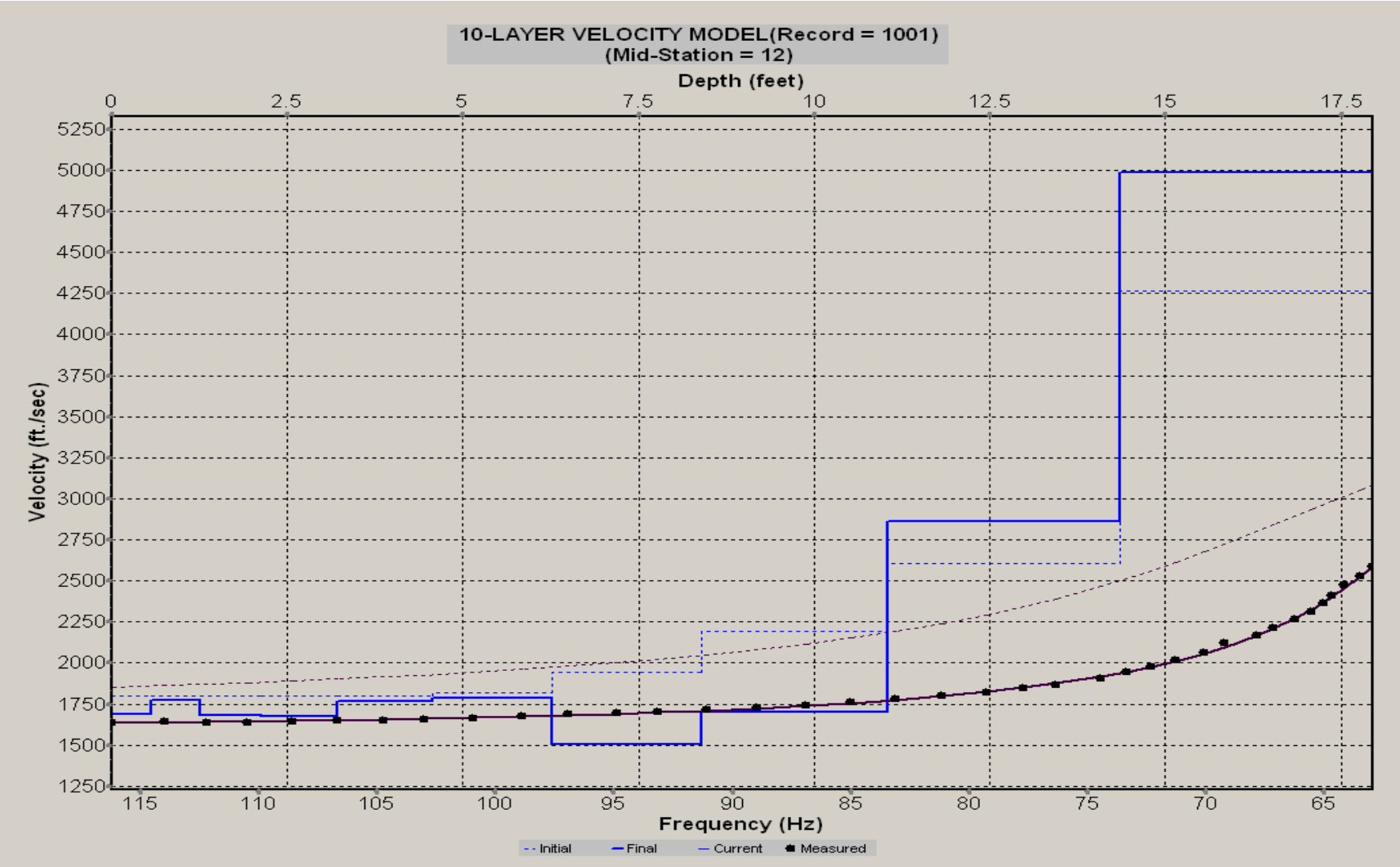

A.117: Velocity Profile Line 1113 used in Pre-blast 21 and Pre-blast 22

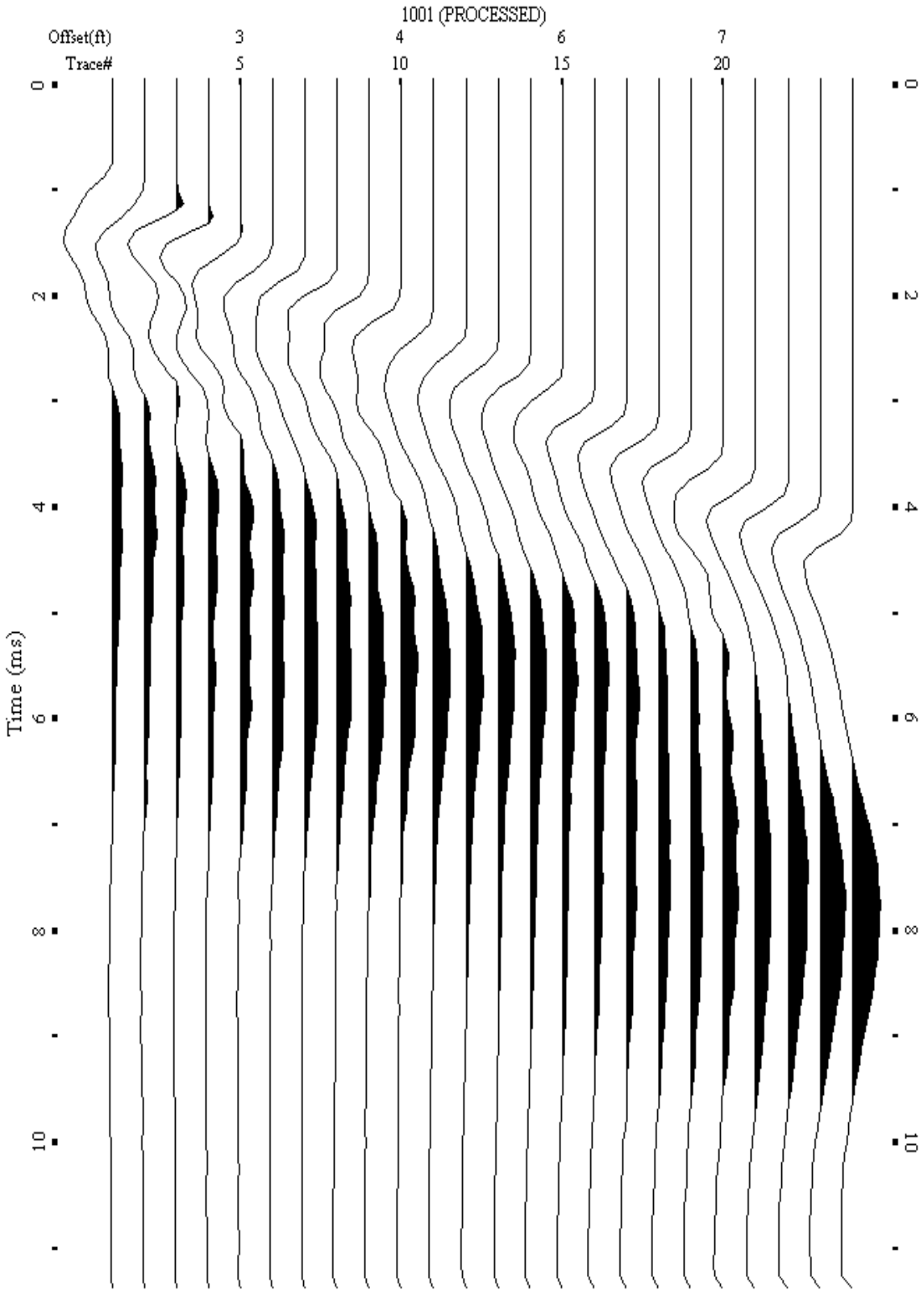

A.118: Shot Gather Line 1114 used in Post-blast 6

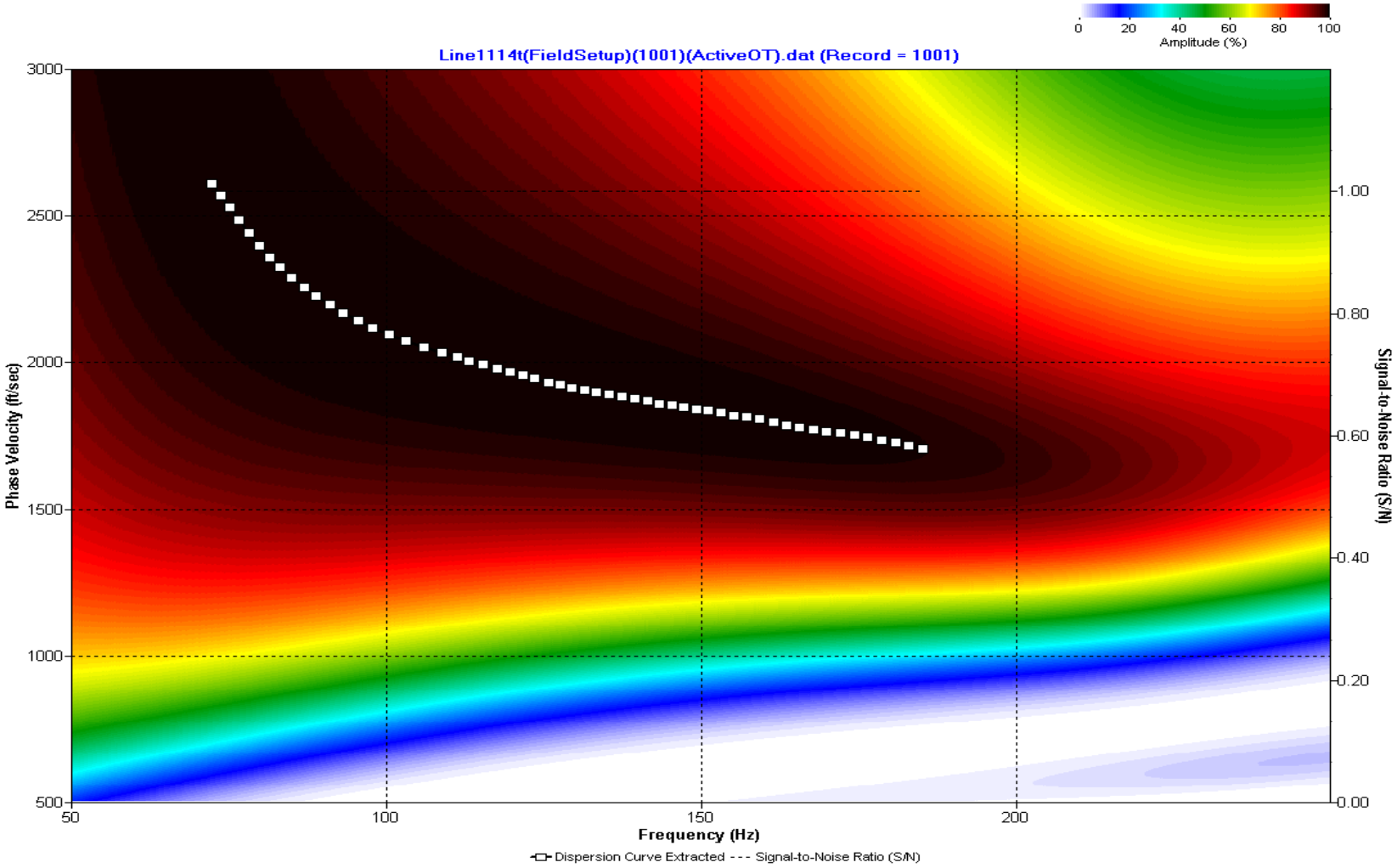

A.119: Dispersion Curve Line 1114 used in Post-blast 6

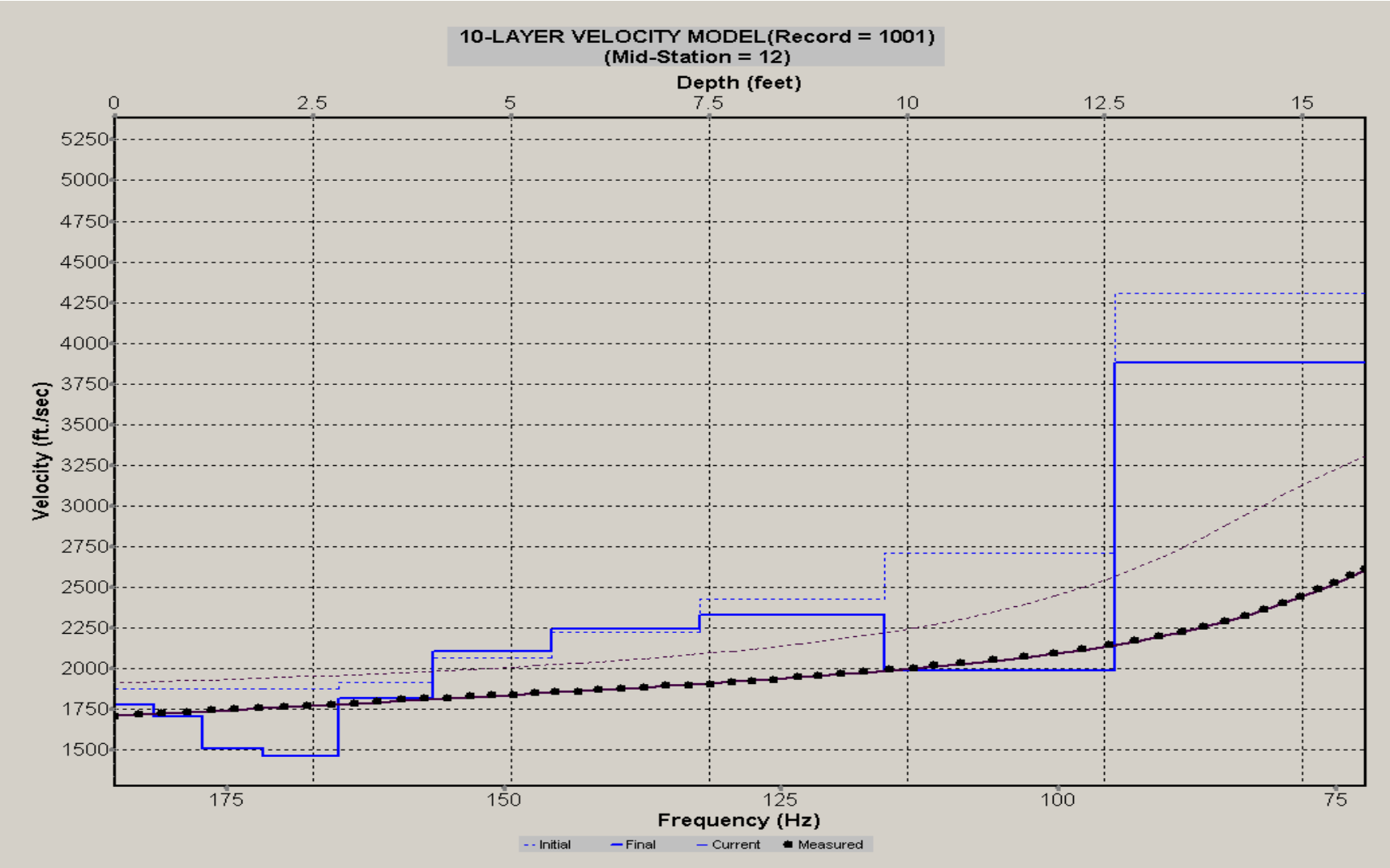

A.120: Velocity Profile Line 1114 used in Post-blast 6

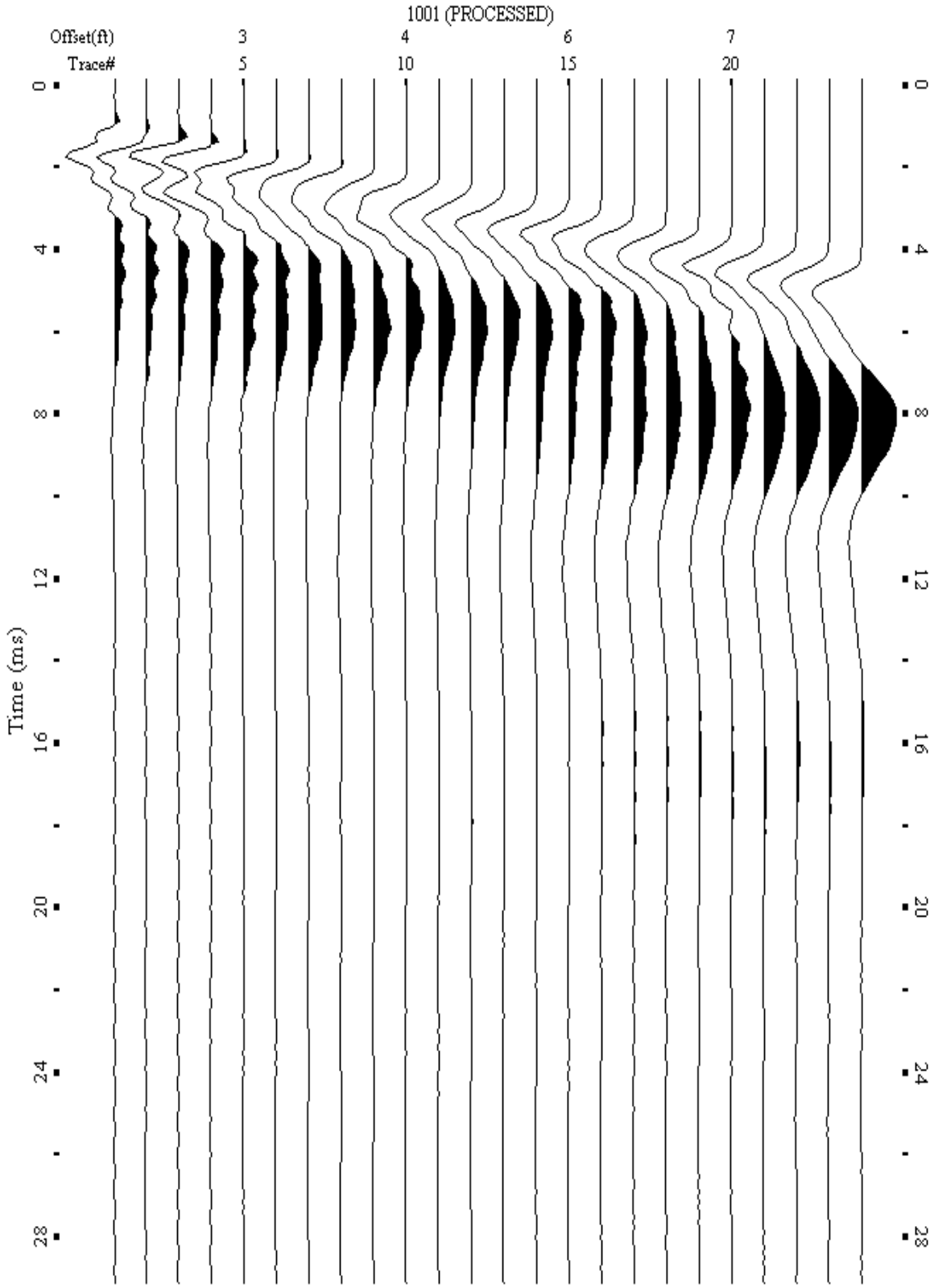

A.121: Shot Gather Line 1115 used in Post-blast 6

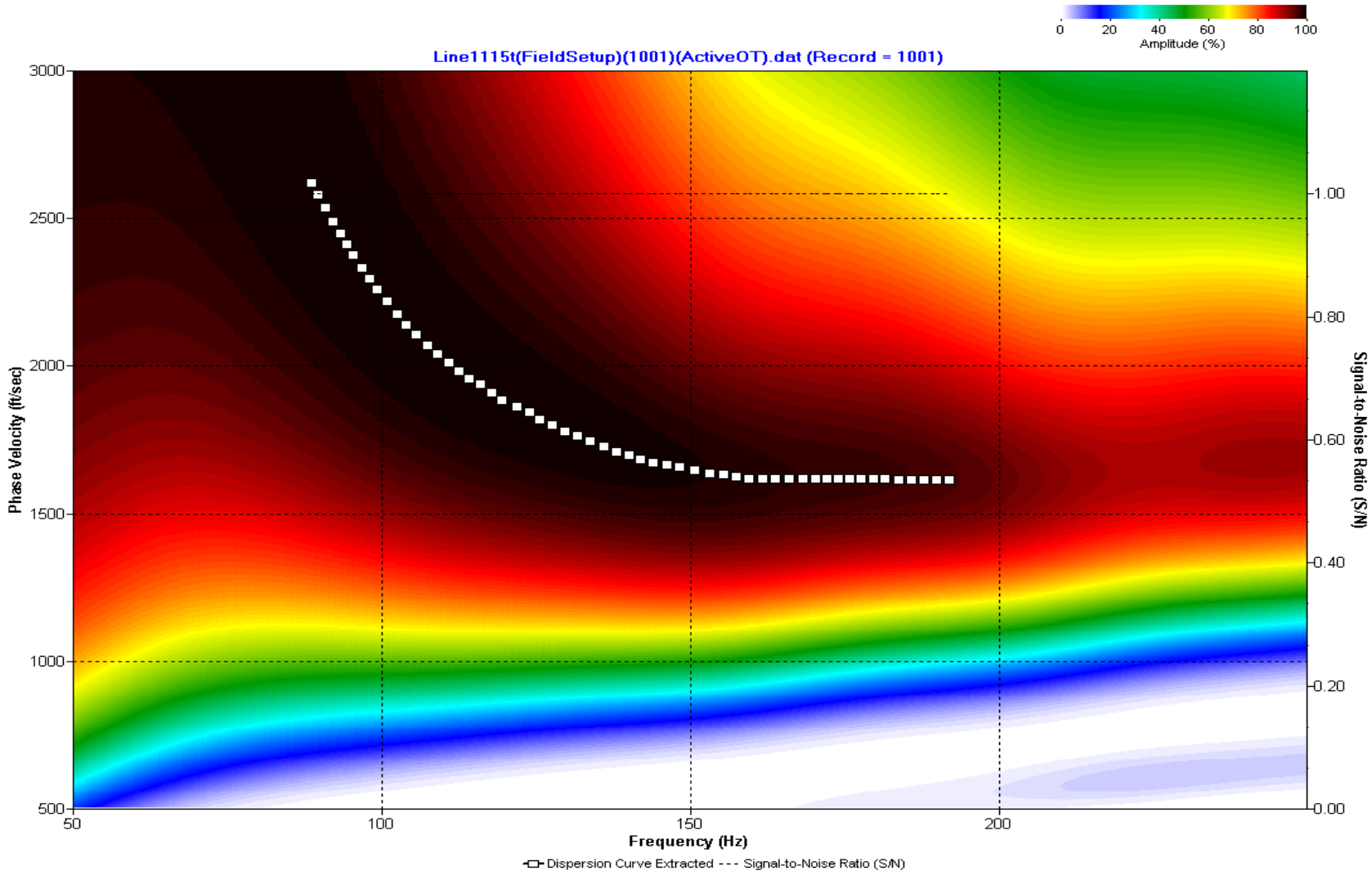

A.122: Dispersion Curve Line 1115 used in Post-blast 6

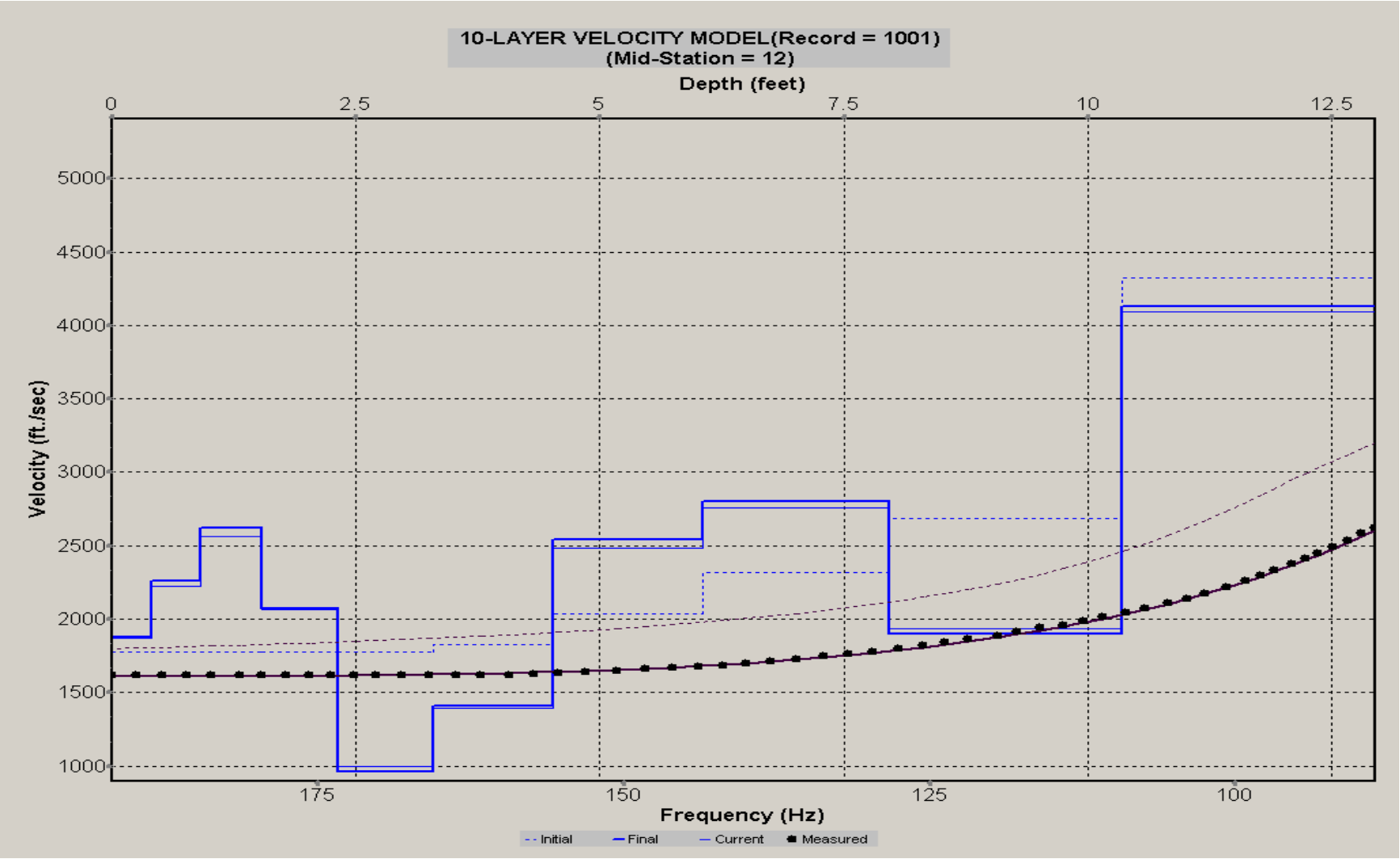

A.123: Velocity Profile Line 1115 used in Post-blast 6

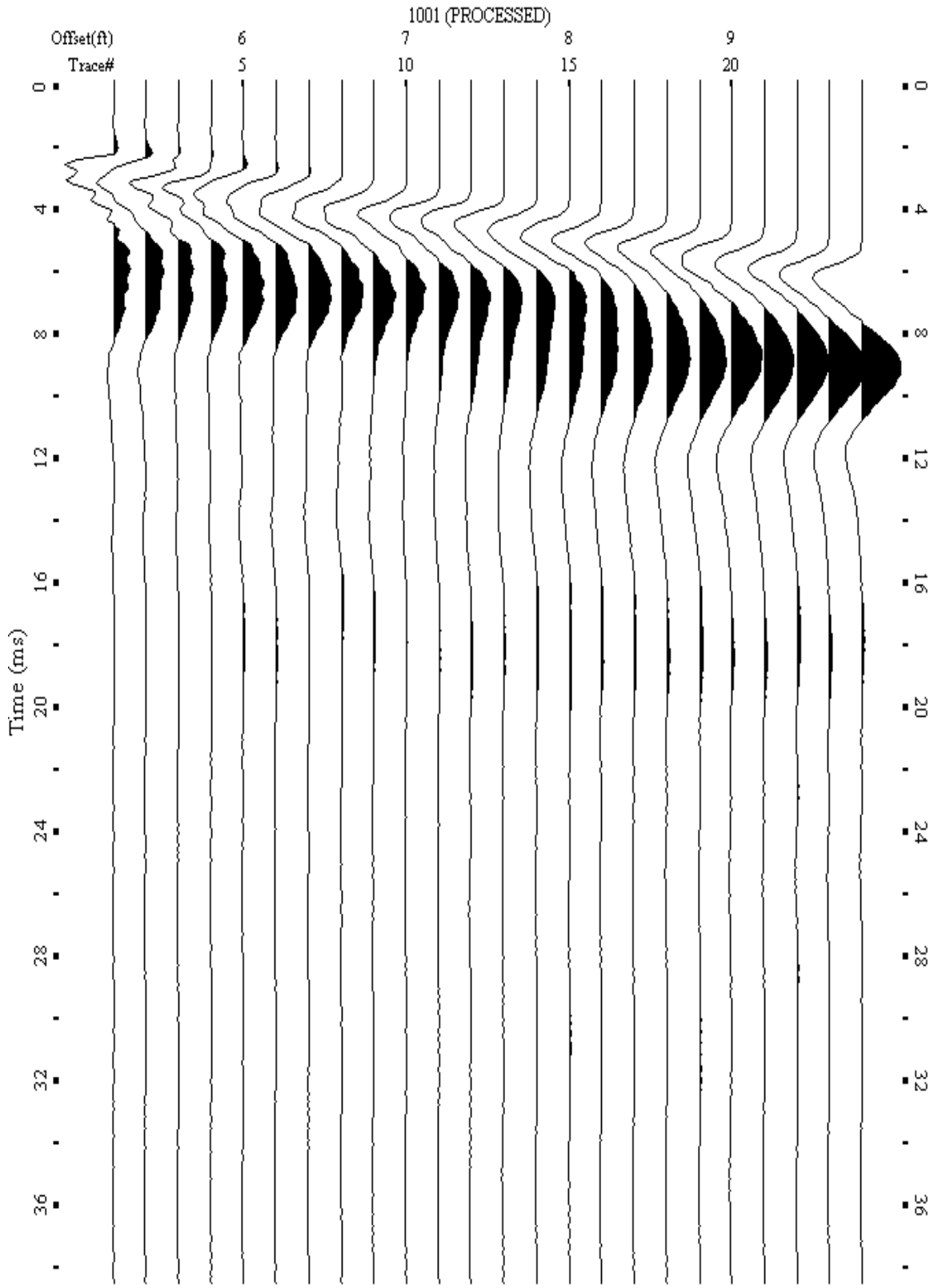

A.124: Shot Gather Line 1116 used in Post-blast 6

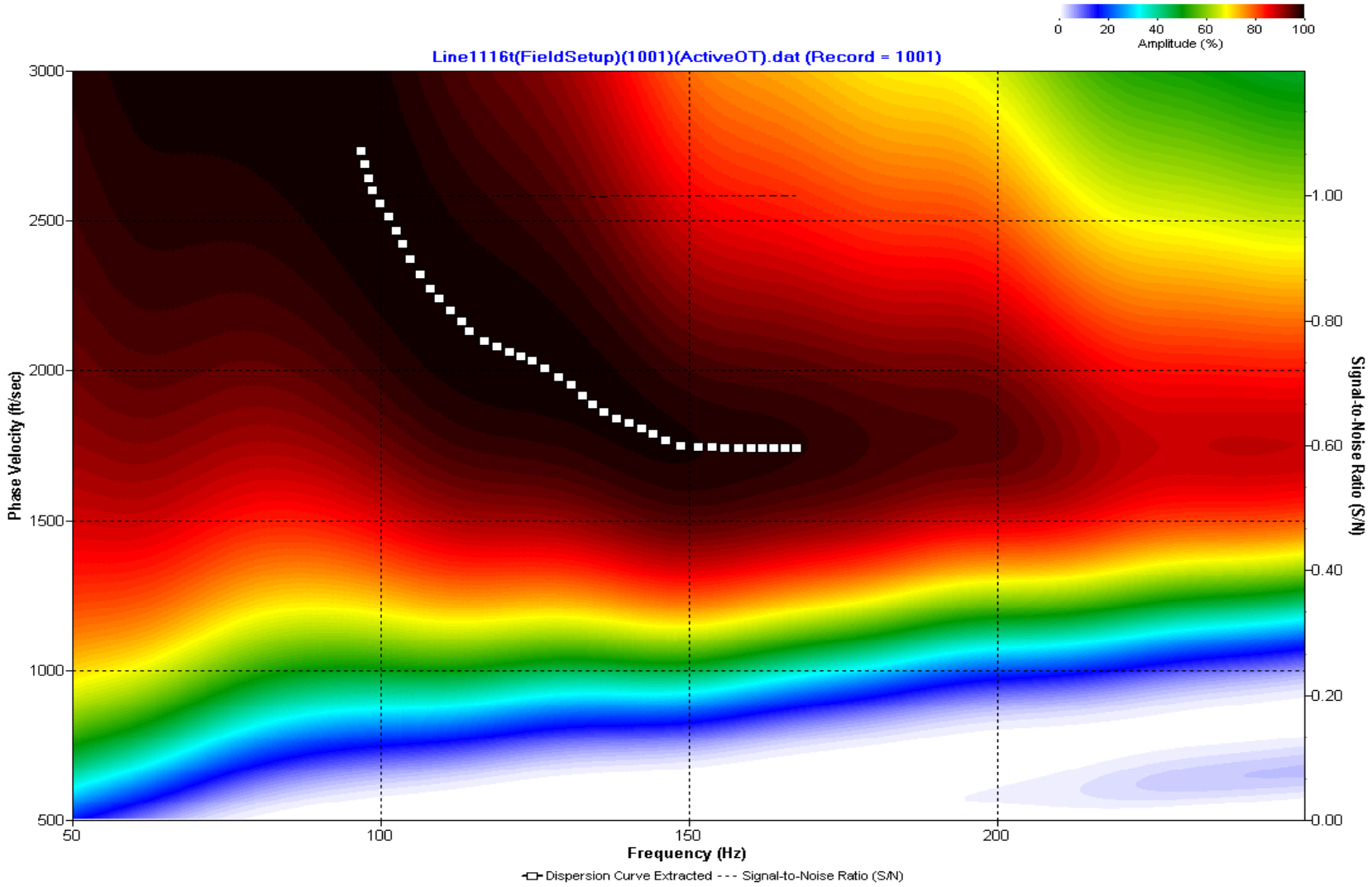

A.125: Dispersion Curve Line 1116 used in Post-blast 6

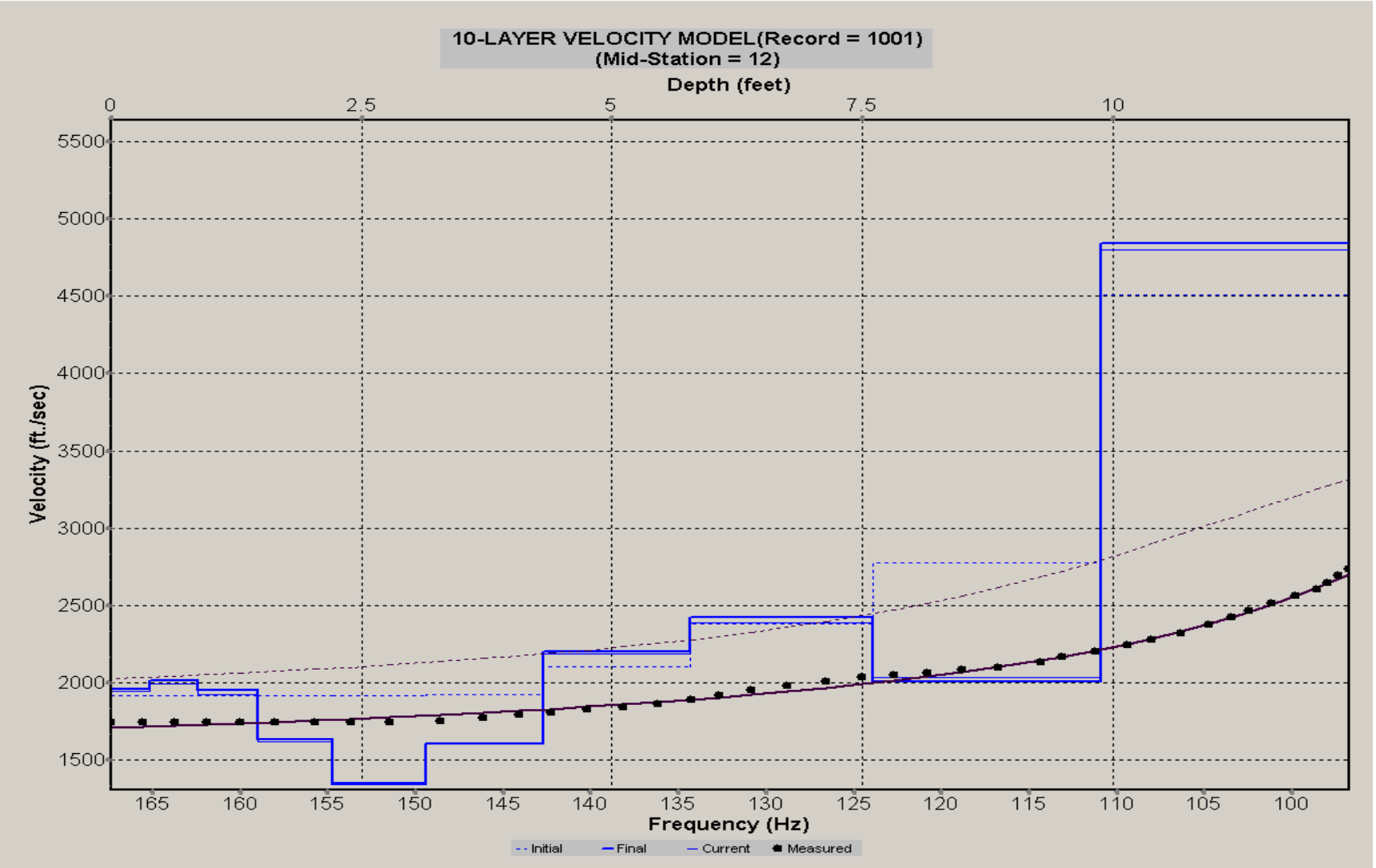

A.126: Velocity Profile Line 1116 used in Post-blast 6

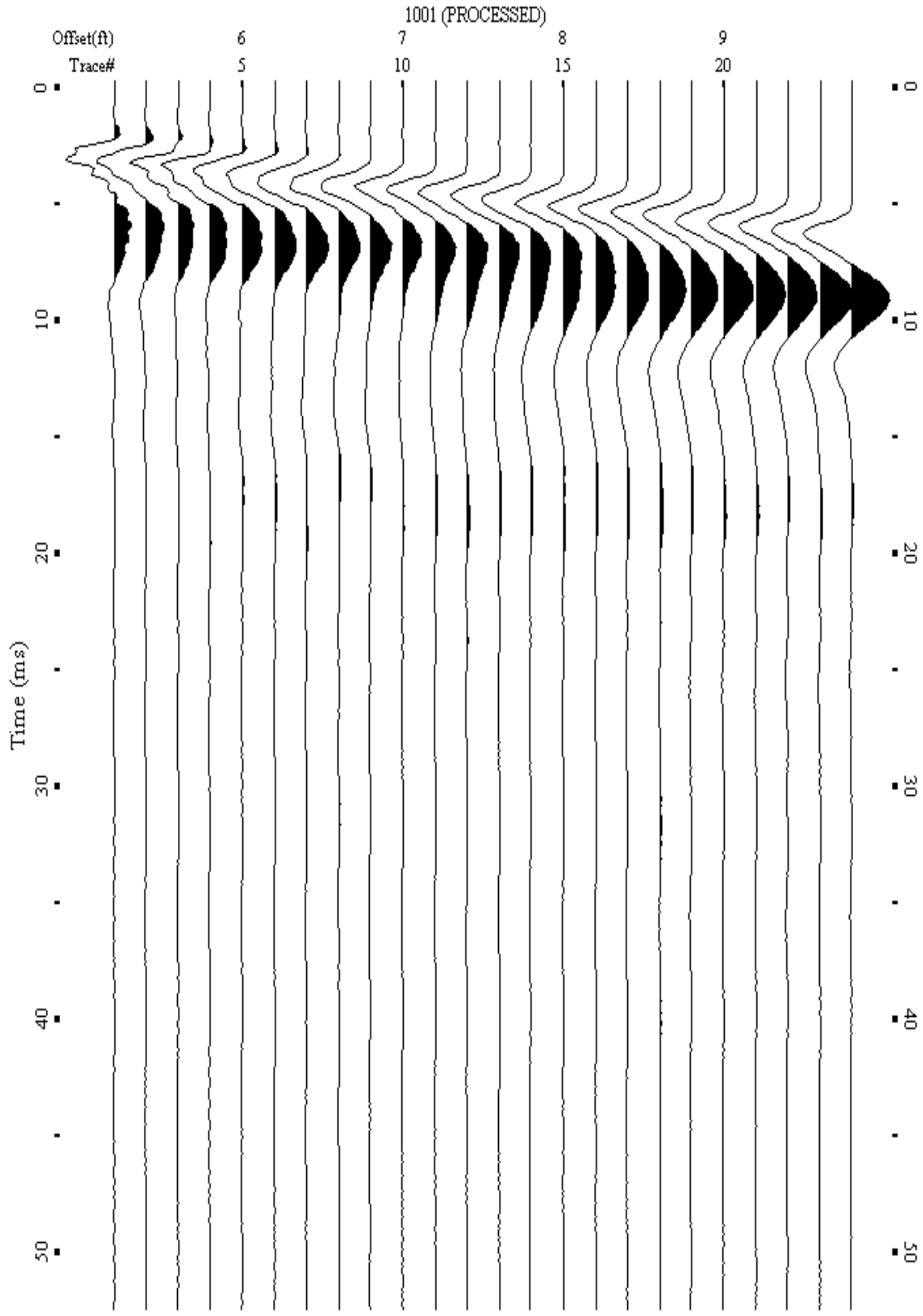

A.127: Shot Gather Line 1117 used in Post-blast 6

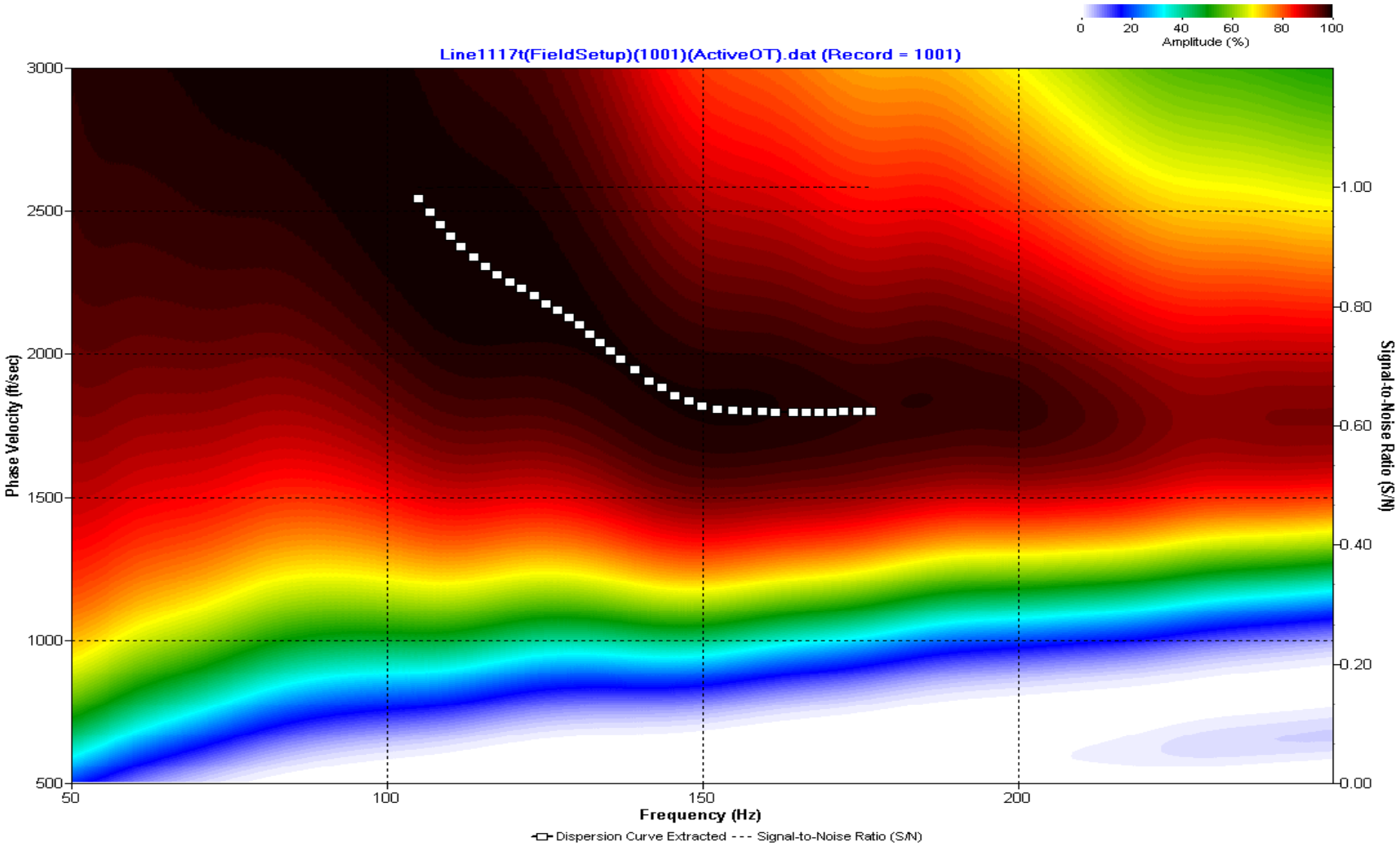

A.128: Dispersion Curve Line 1117 used in Post-blast 6

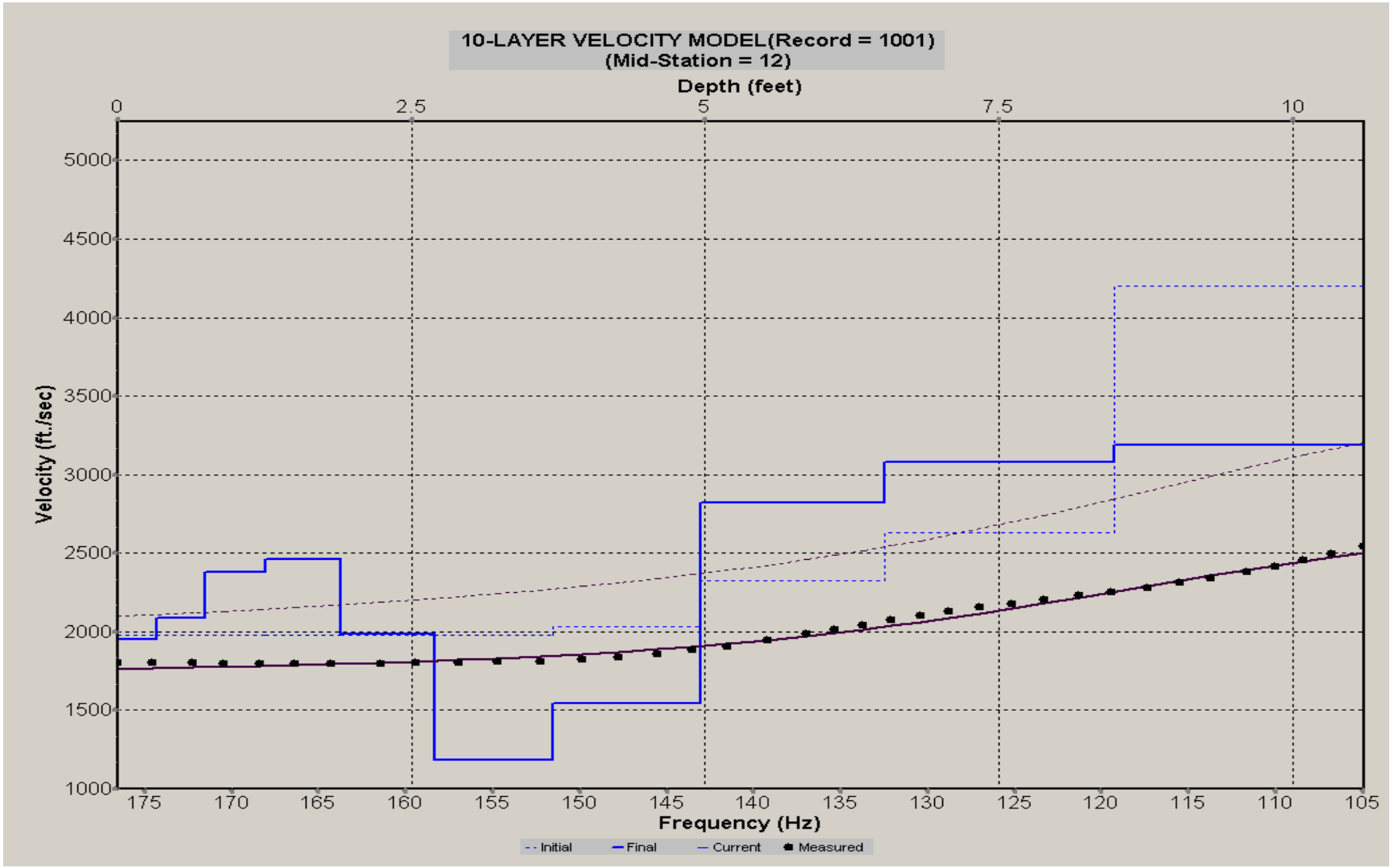

A.129: Velocity Profile Line 1117 used in Post-blast 6

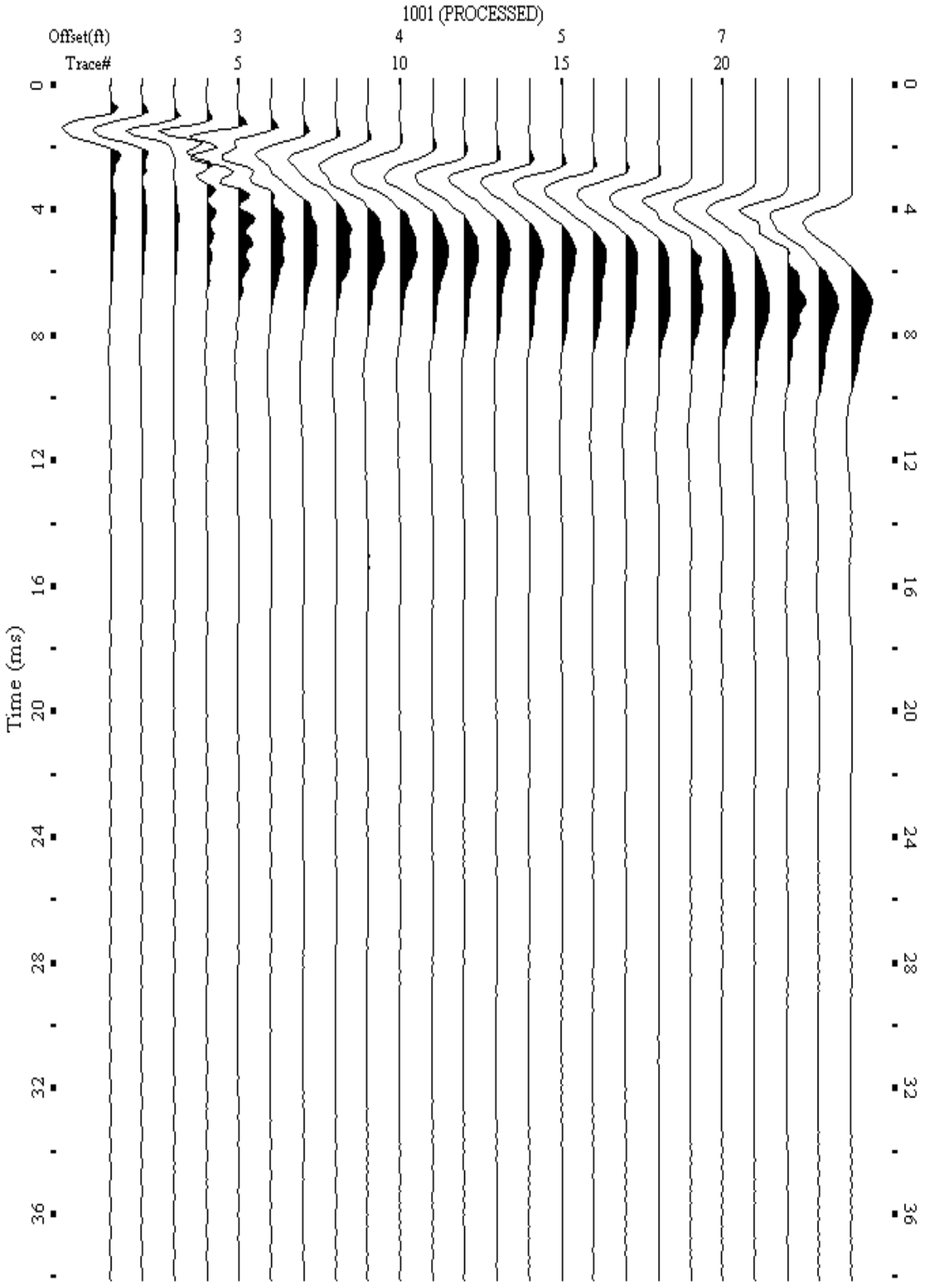

A.130: Shot Gather Line 1118 used in Post-blast 7

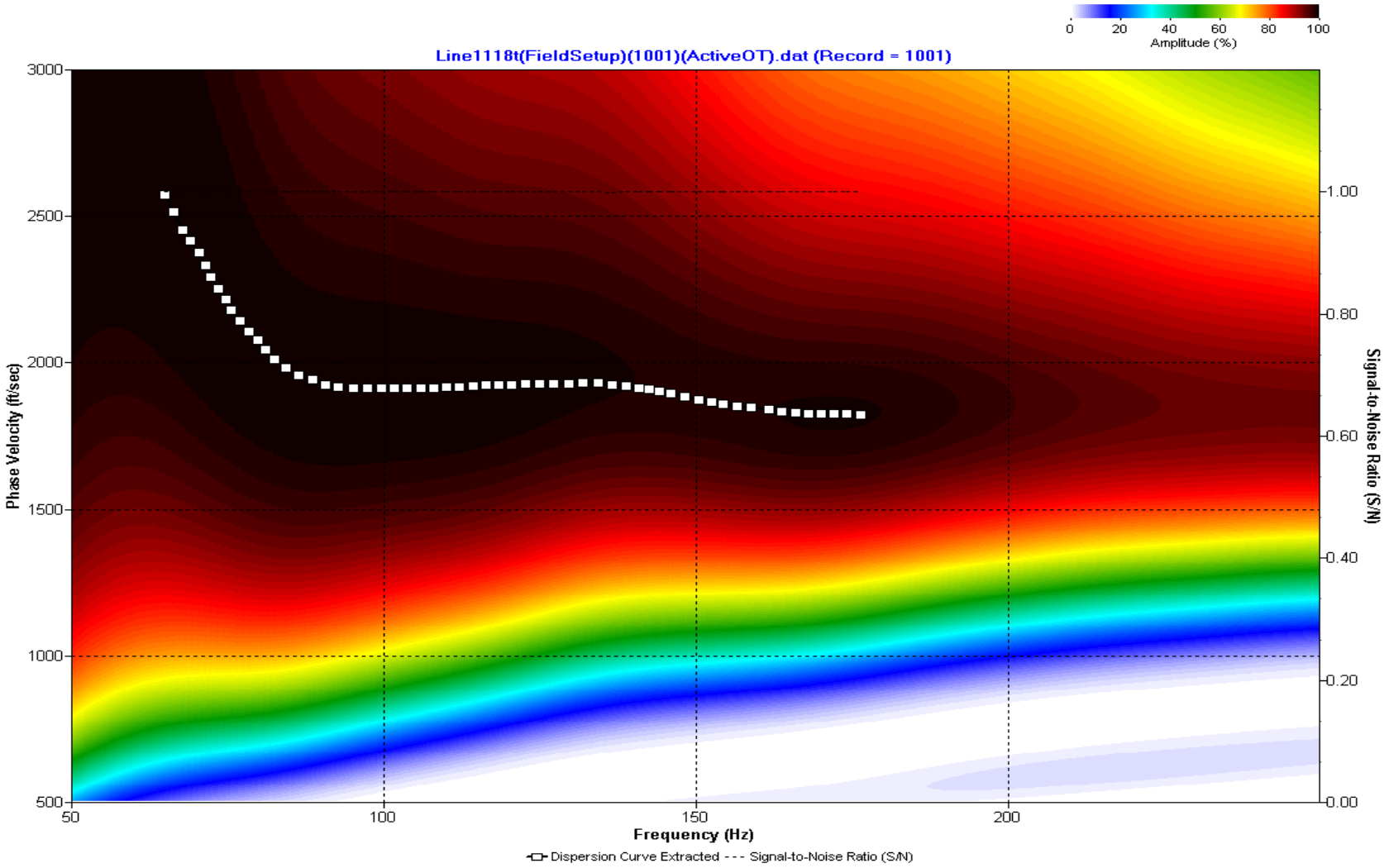

A.131: Dispersion Curve Line 1118 used in Post-blast 7

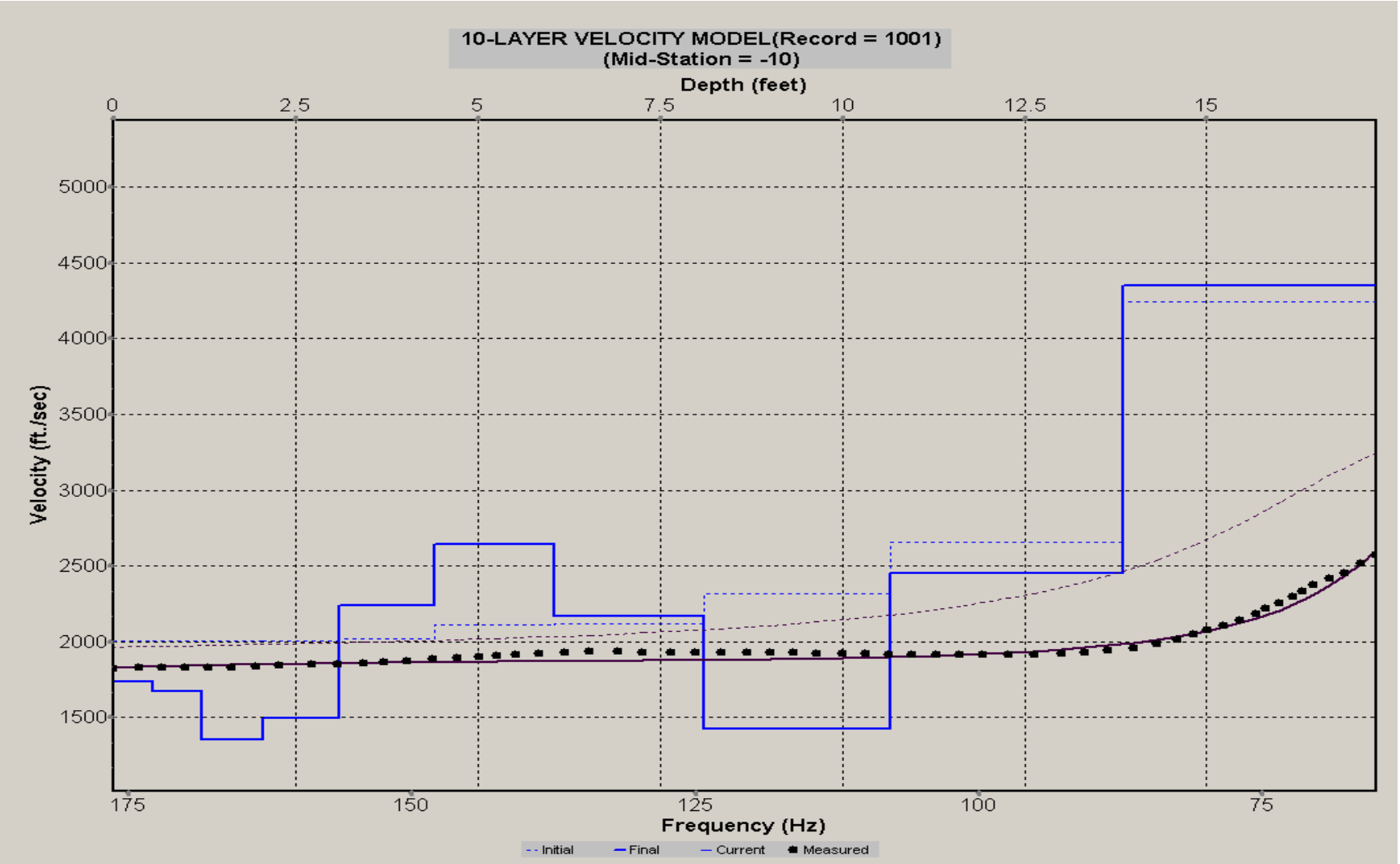

A.132: Velocity Profile Line 1118 used in Post-blast 7

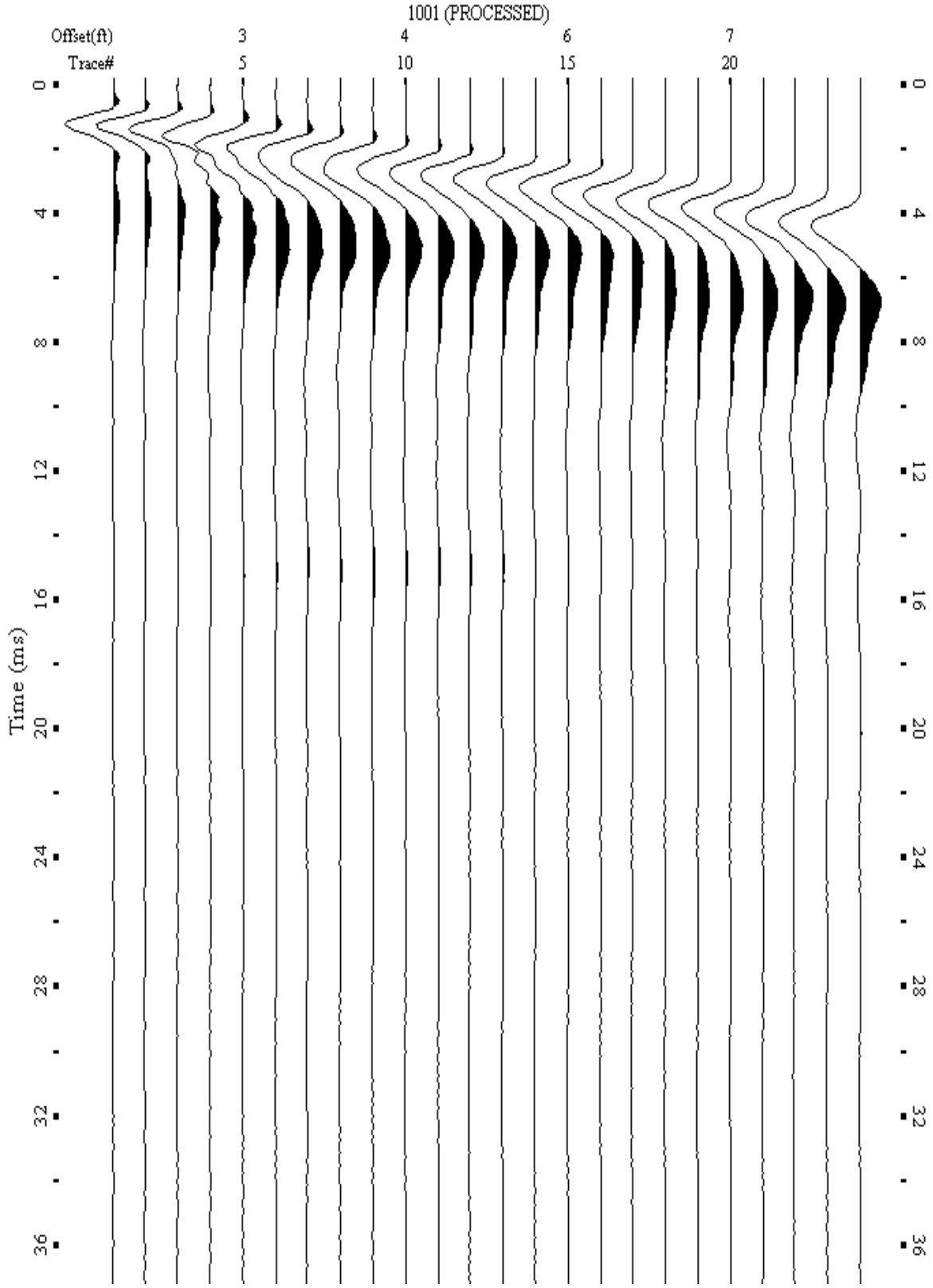

A.133: Shot Gather Line 1119 used in Post-blast 7

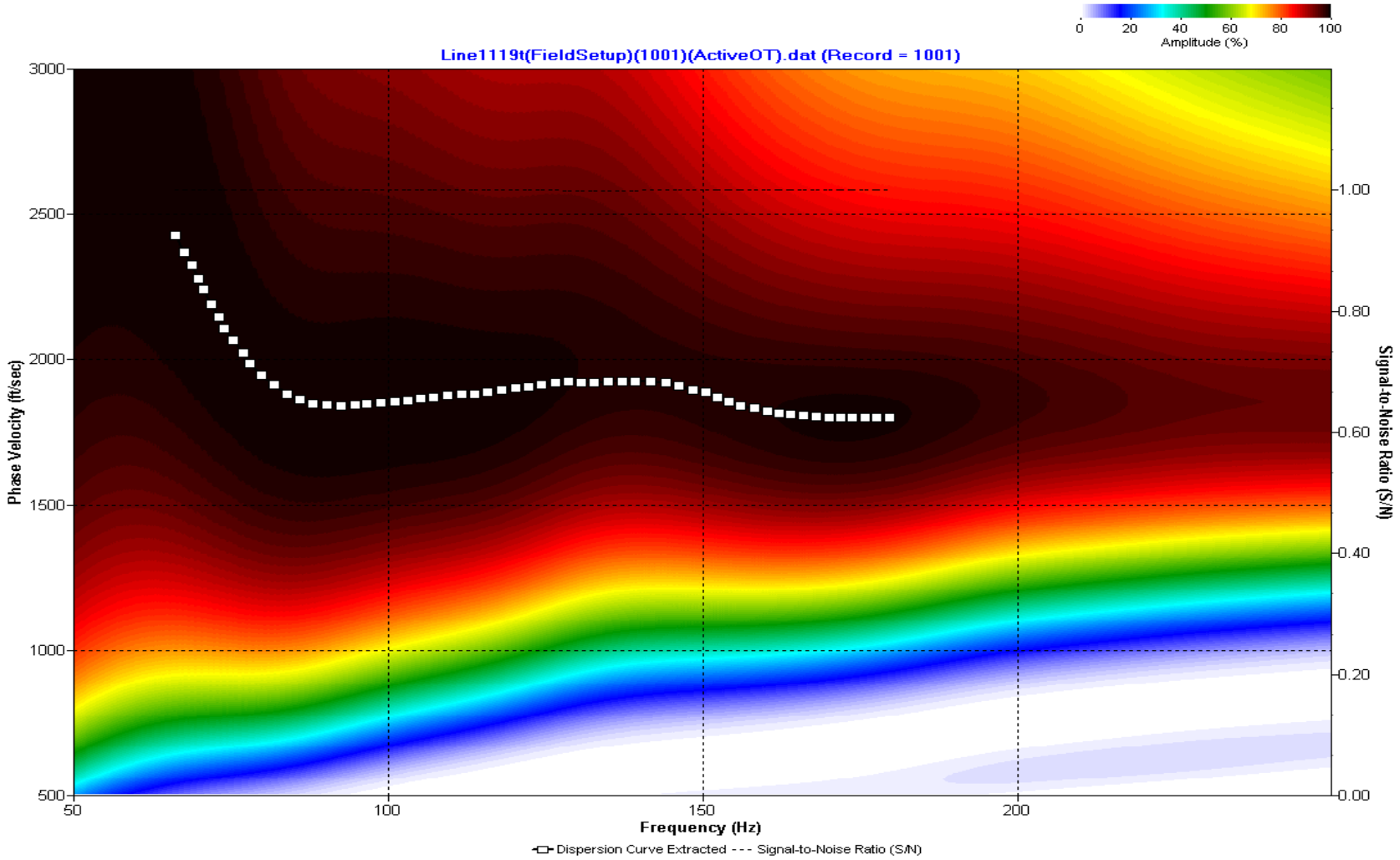

A.134: Dispersion Curve Line 1119 used in Post-blast 7

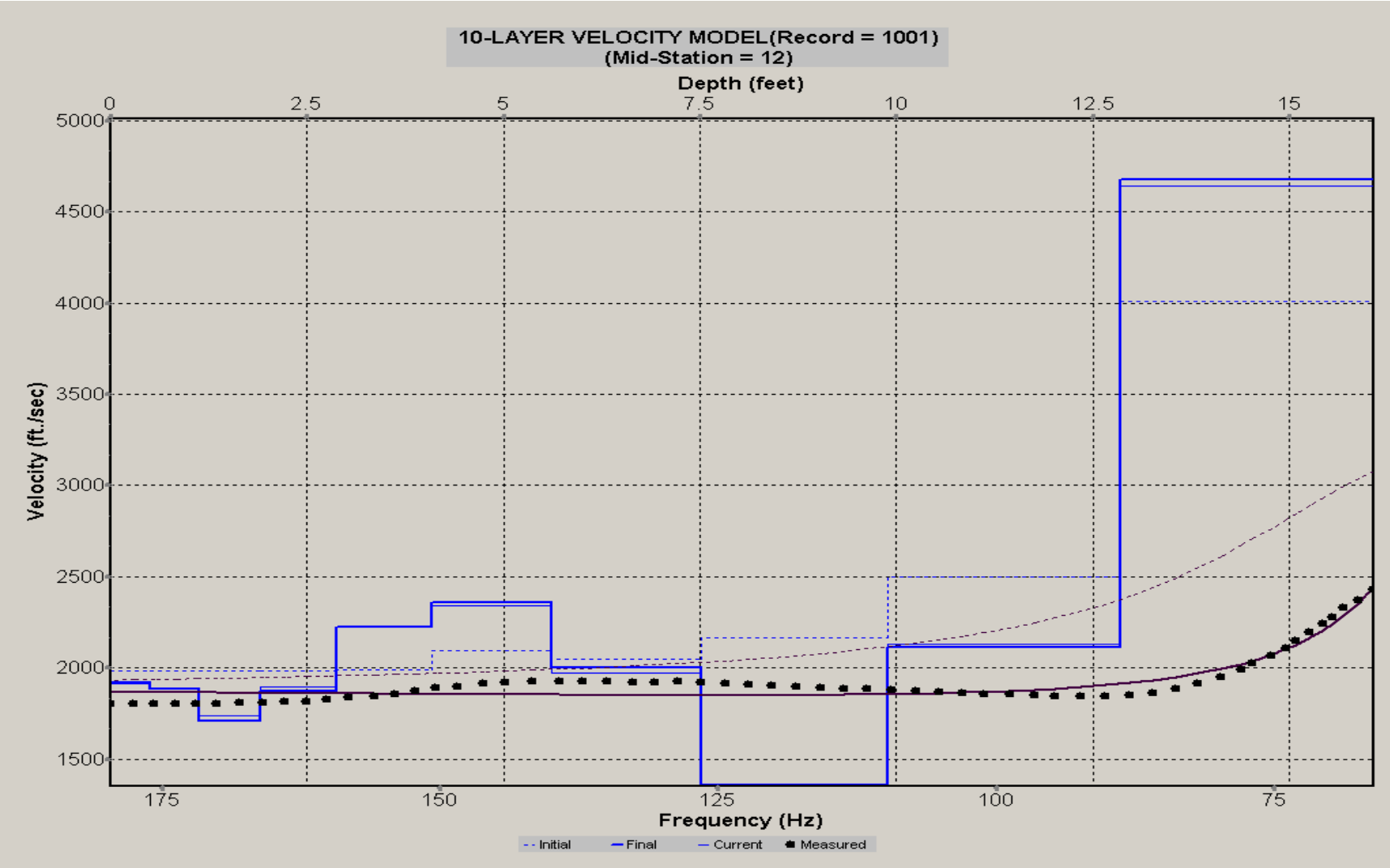

A.135: Velocity Profile Line 1119 used in Post-blast 7

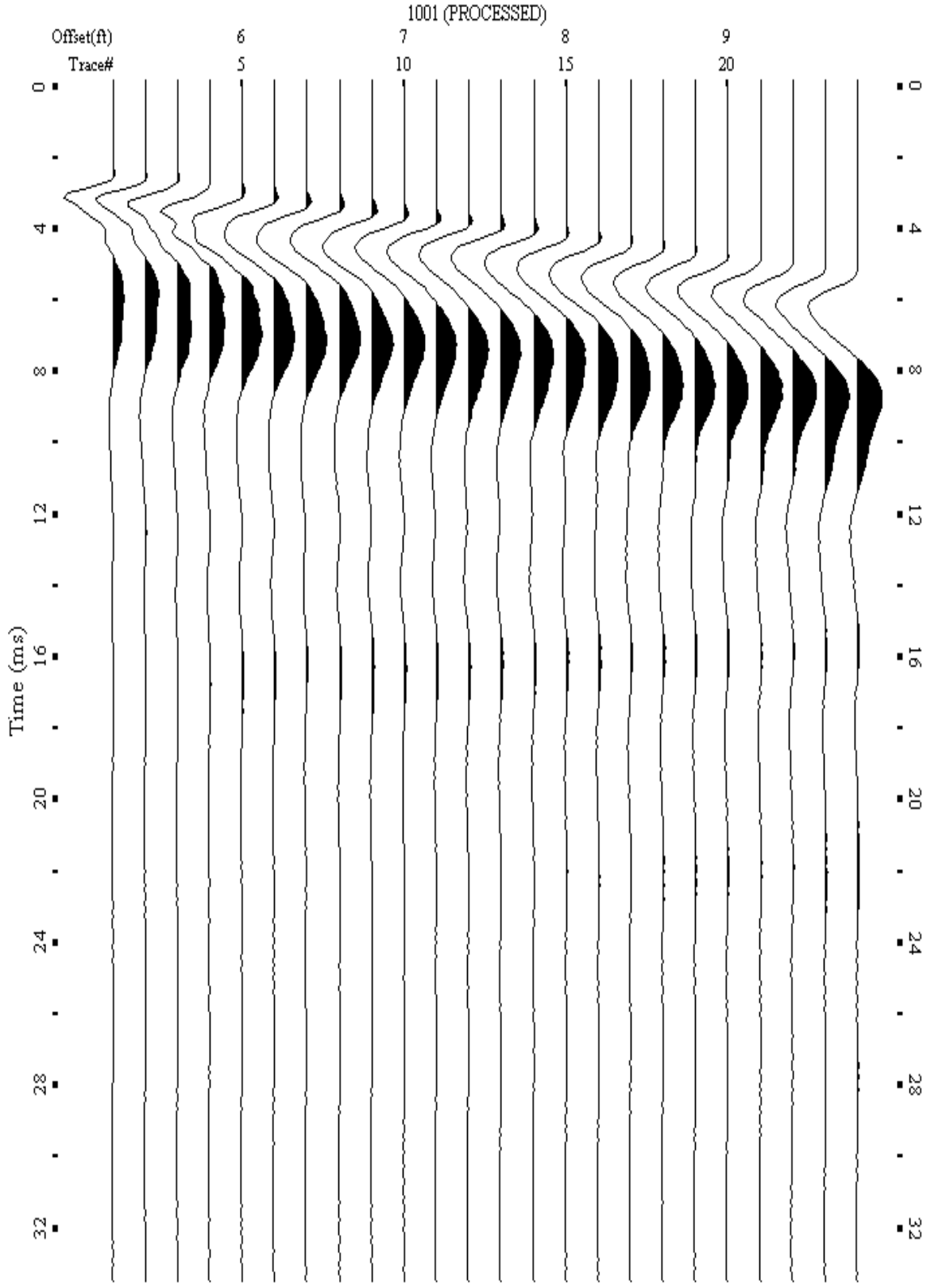

A.136: Shot Gather Line 1121 used in Post-blast 7

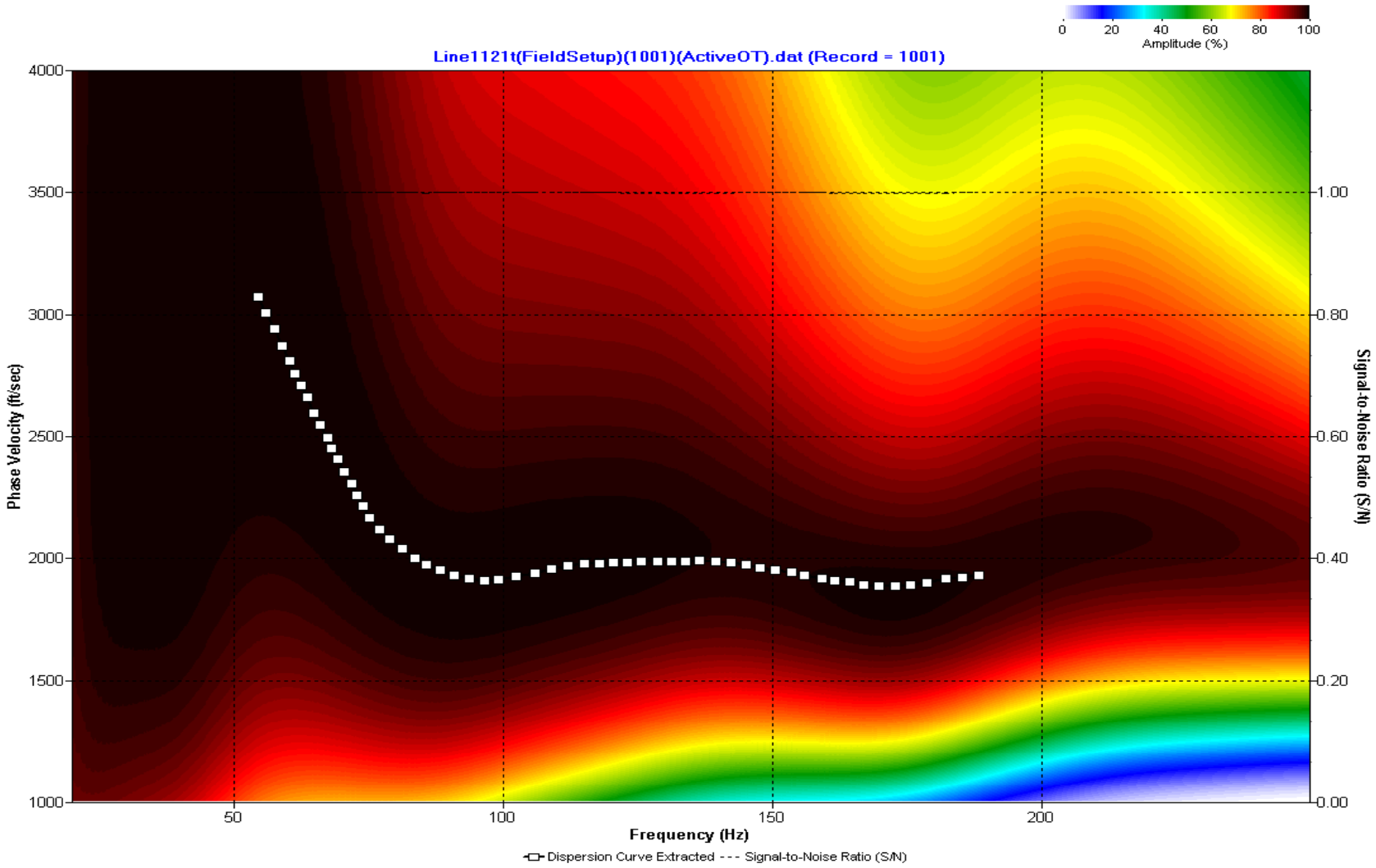

A.137: Dispersion Curve Line 1121 used in Post-blast 7

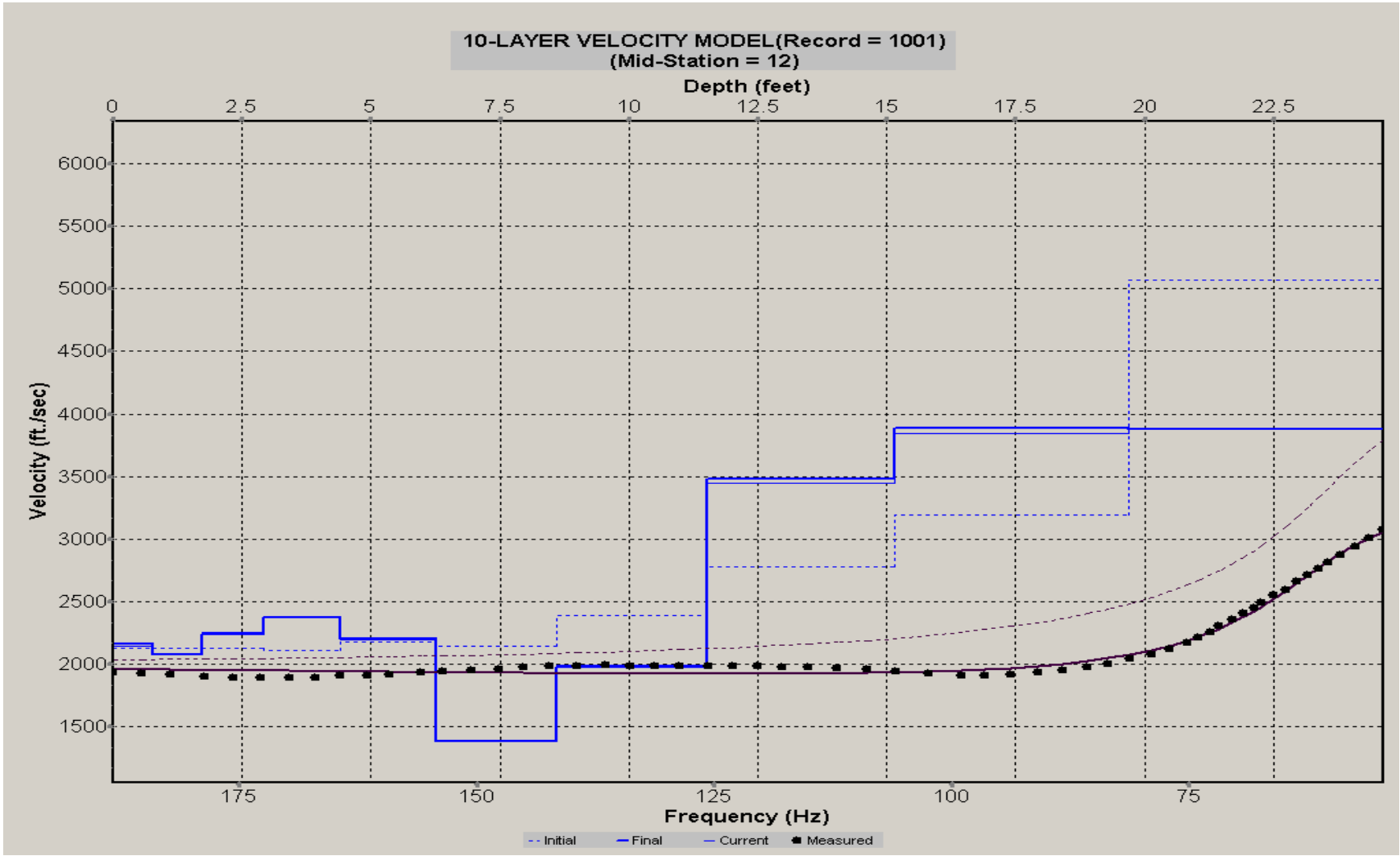

A.138: Velocity Profile Line 1121 used in Post-blast 7

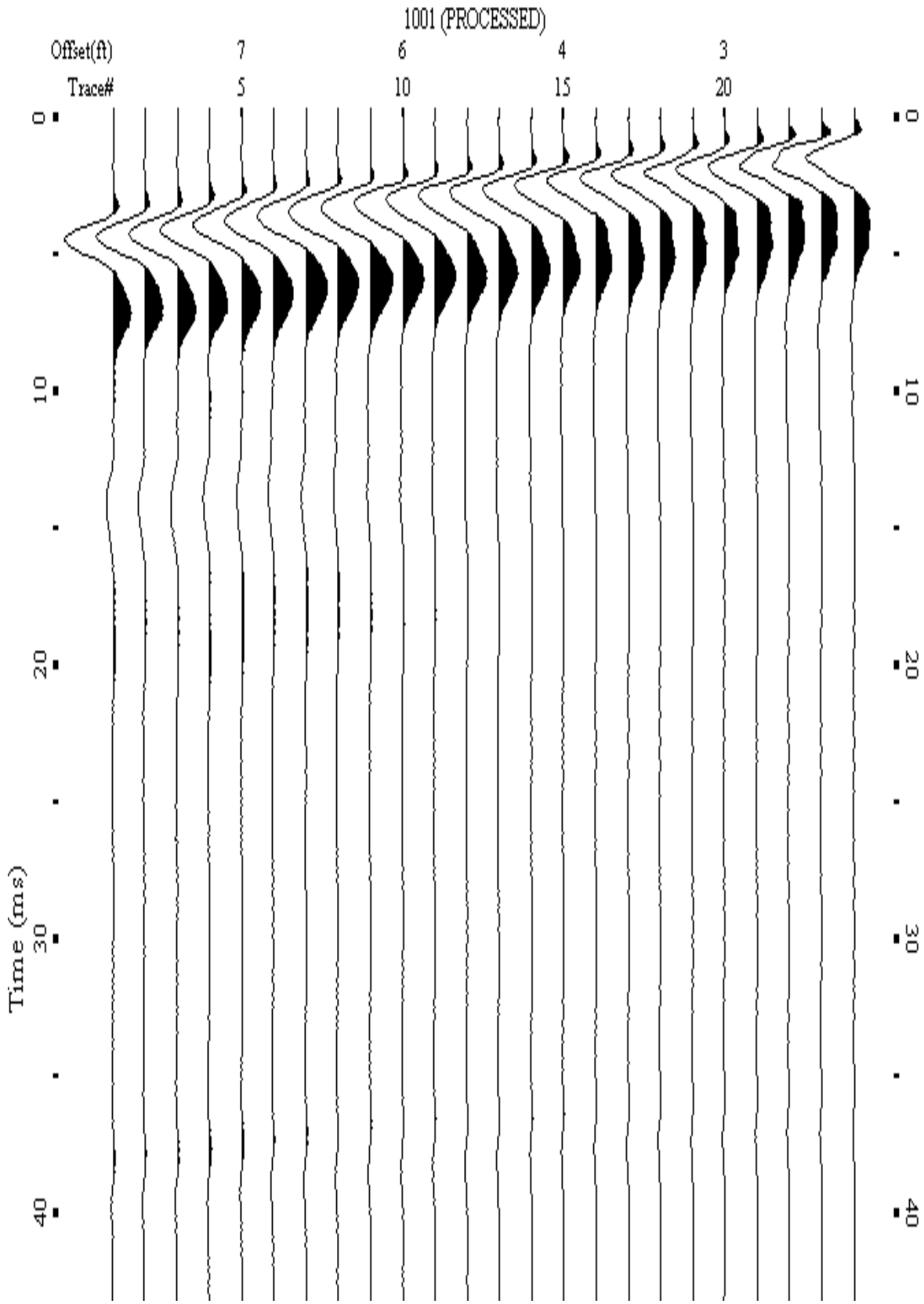

A.139: Shot Gather Line 1122 used in Post-blast 7

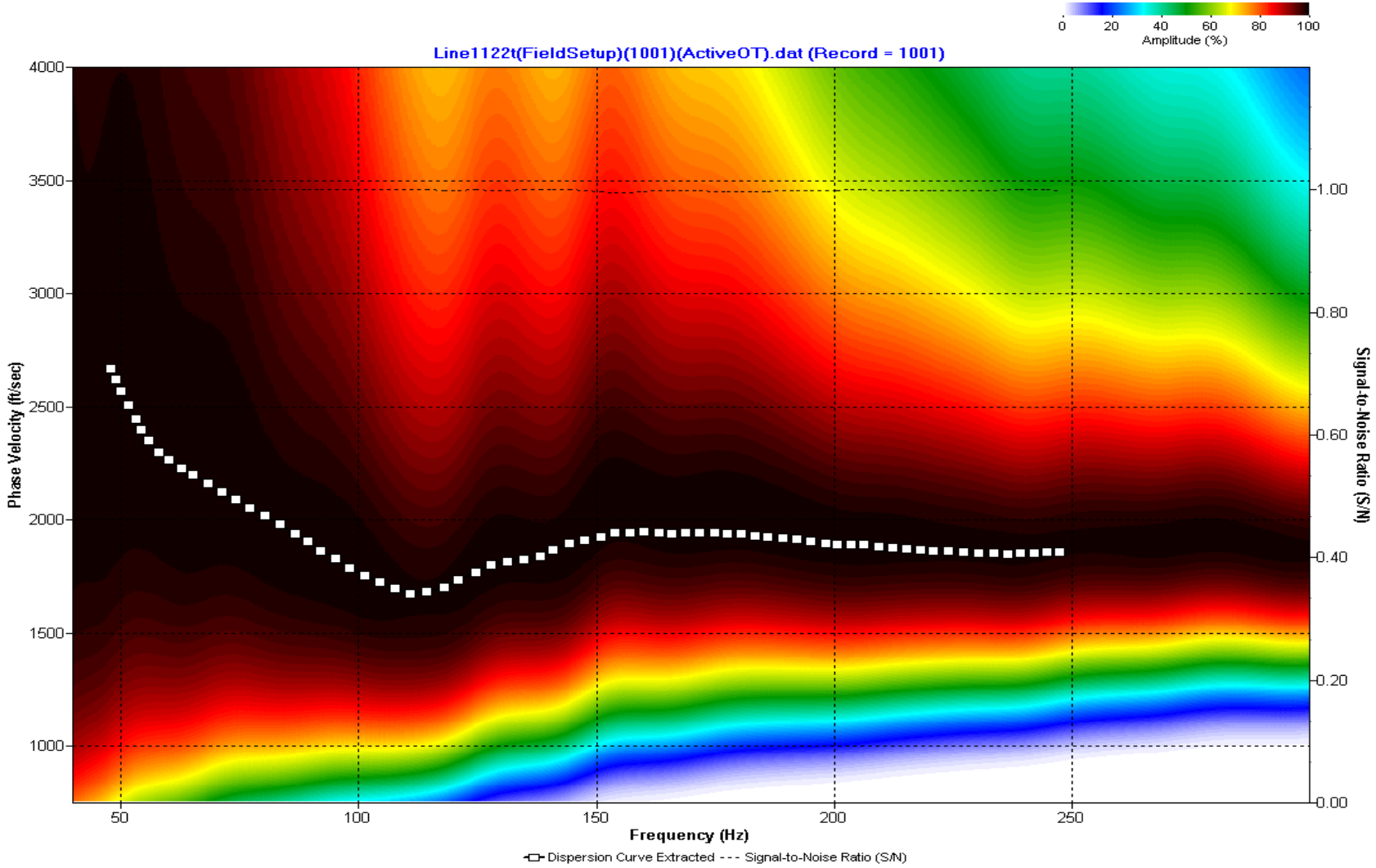

A.140: Dispersion Curve Line 1122 used in Post-blast 7

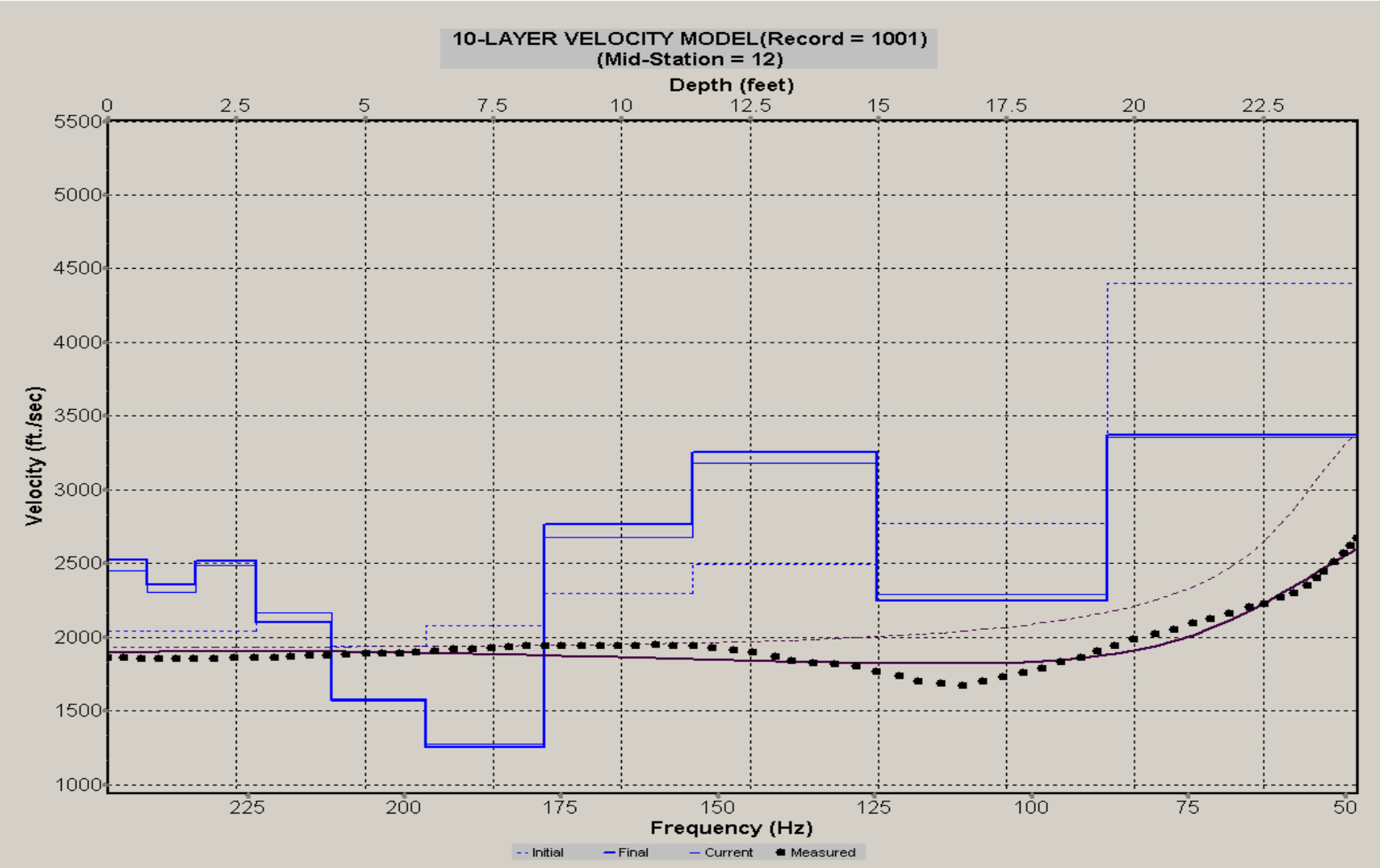

A.141: Velocity Profile Line 1122 used in Post-blast 7

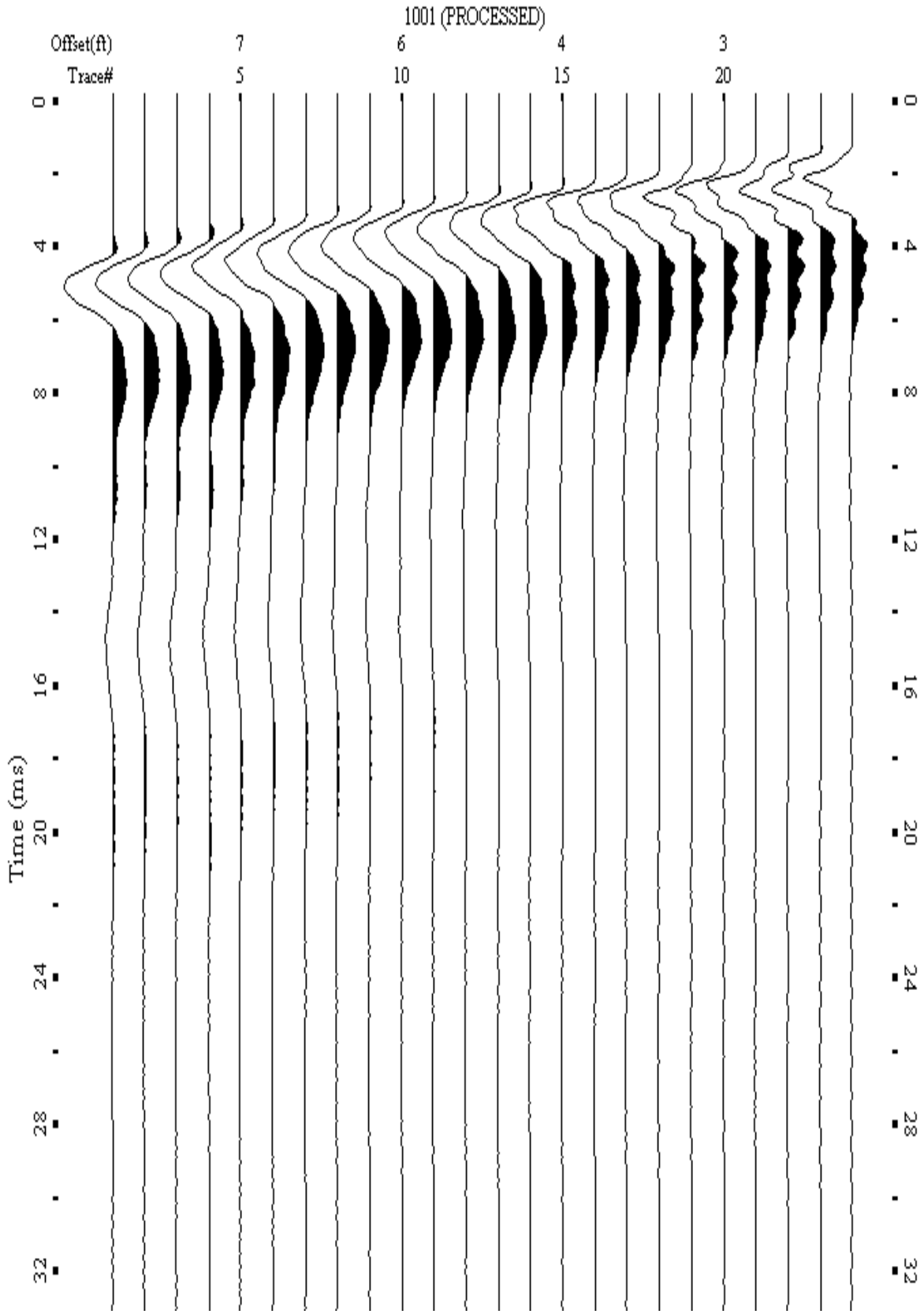

A.142: Shot Gather Line 1123 used in Post-blast 7

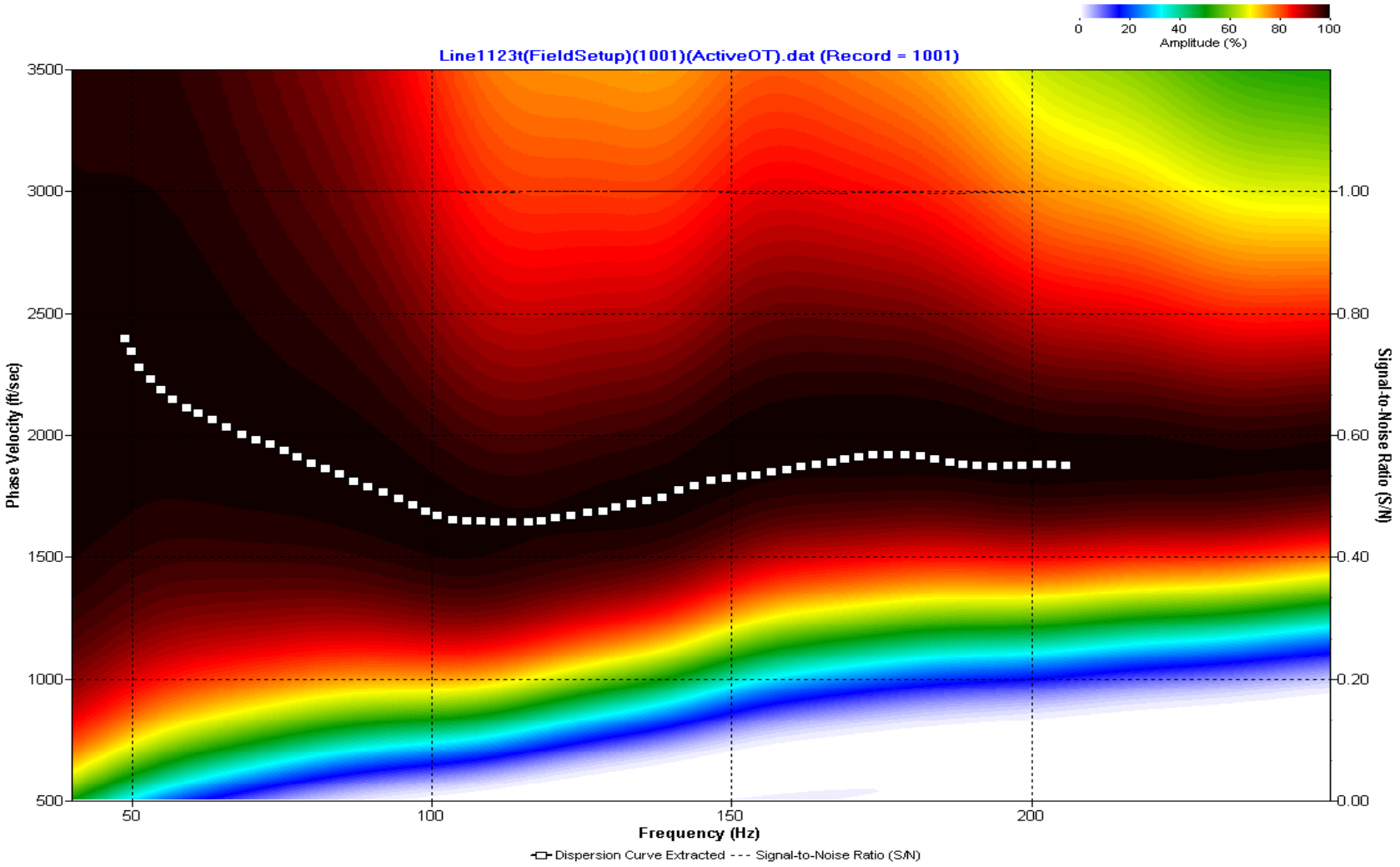

A.143: Dispersion Curve Line 1123 used in Post-blast 7

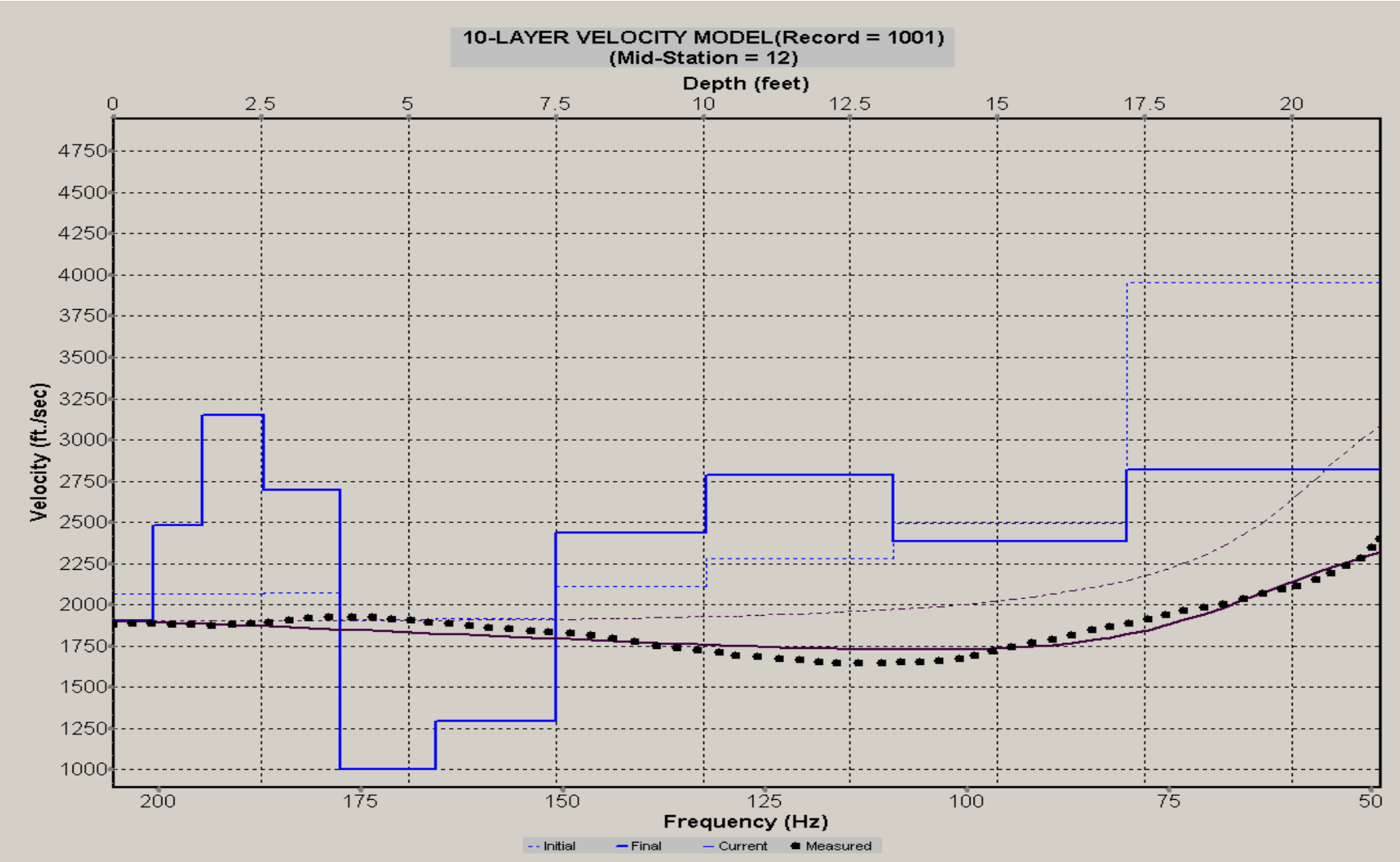

A.144: Velocity Profile Line 1123 used in Post-blast 7

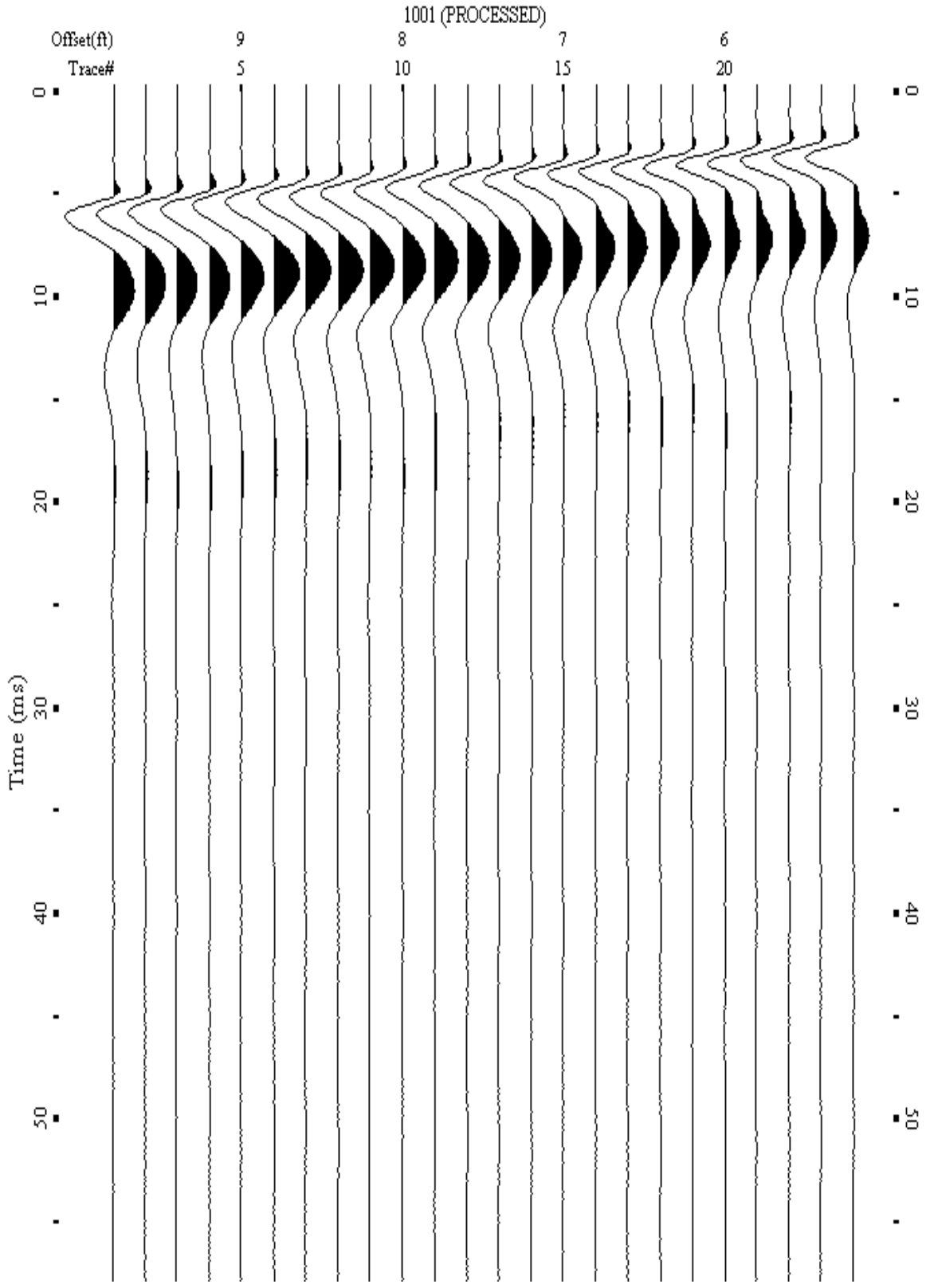

A.145: Shot Gather Line 1124 used in Post-blast 7

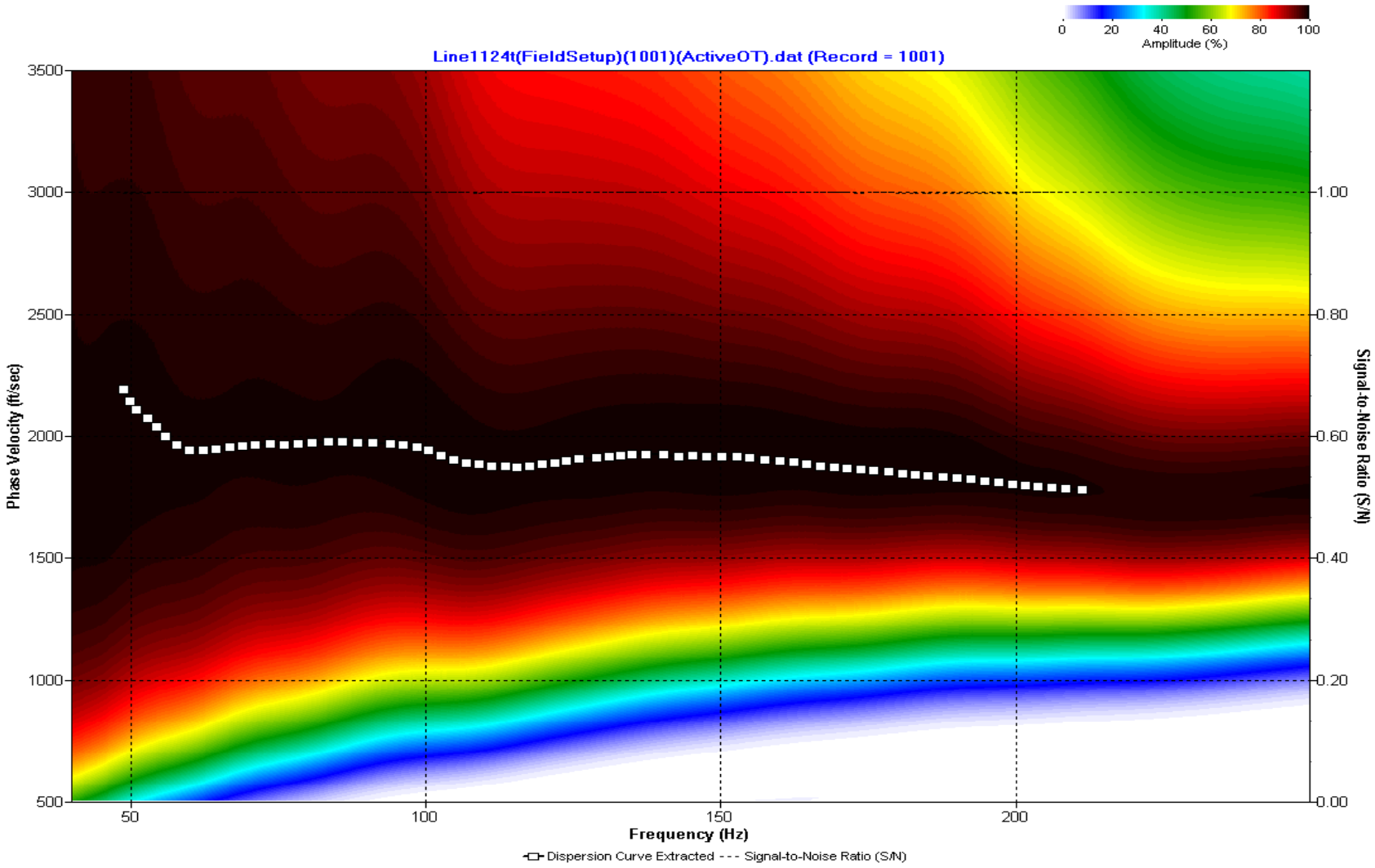

A.146: Dispersion Curve Line 1124 used in Post-blast 7

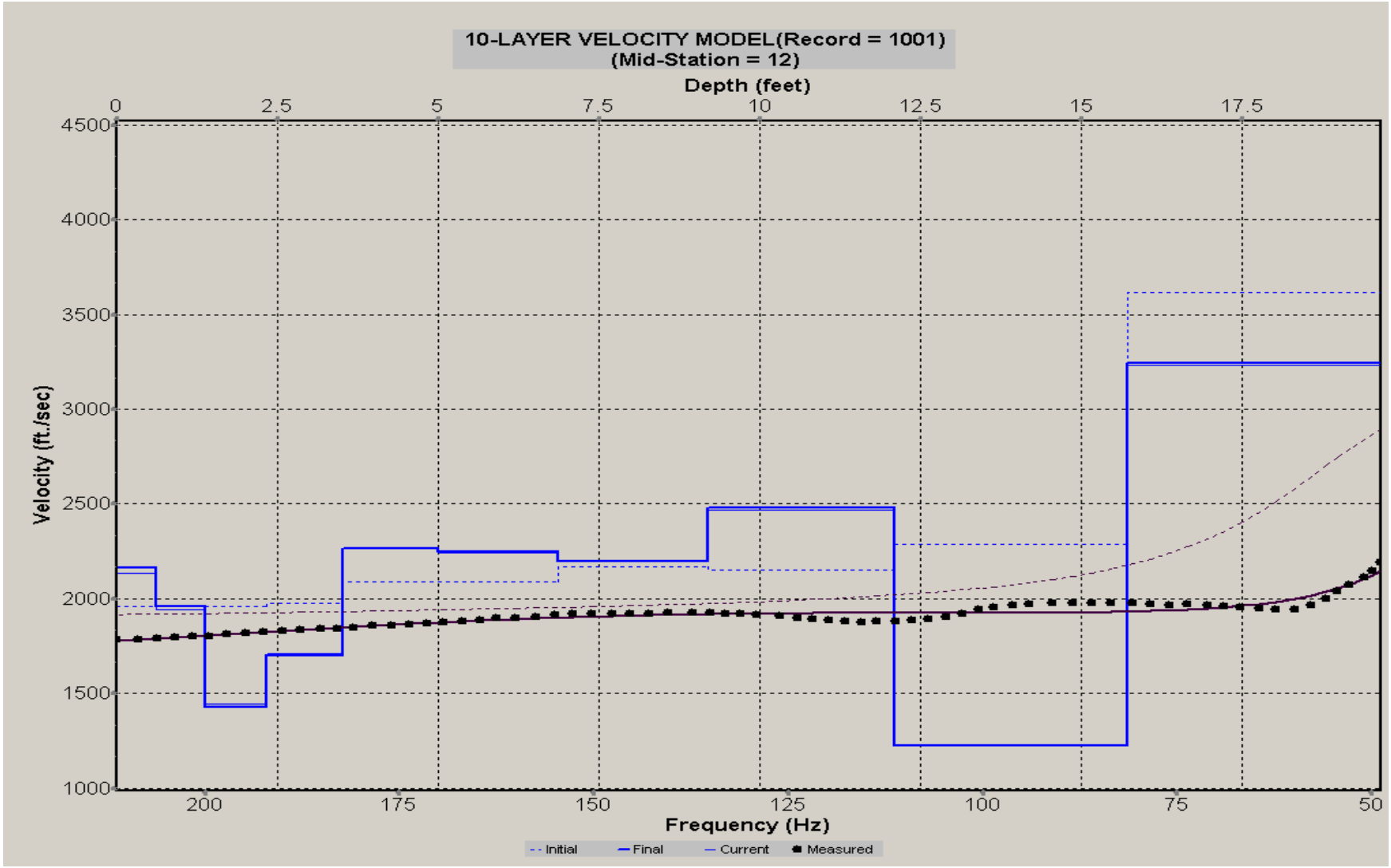

A.147: Velocity Profile Line 1124 used in Post-blast 7

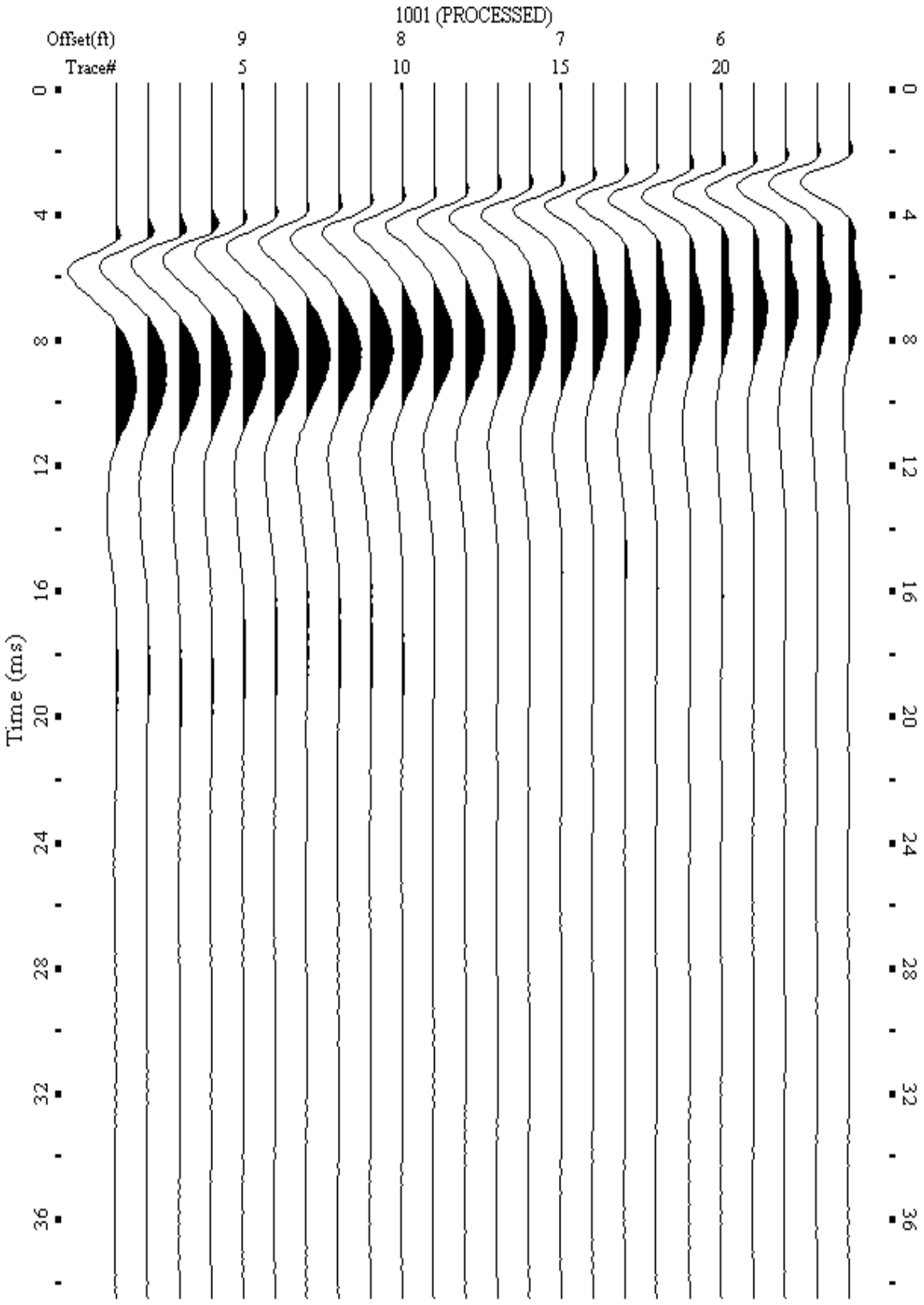

A.148: Shot Gather Line 1125 used in Post-blast 7

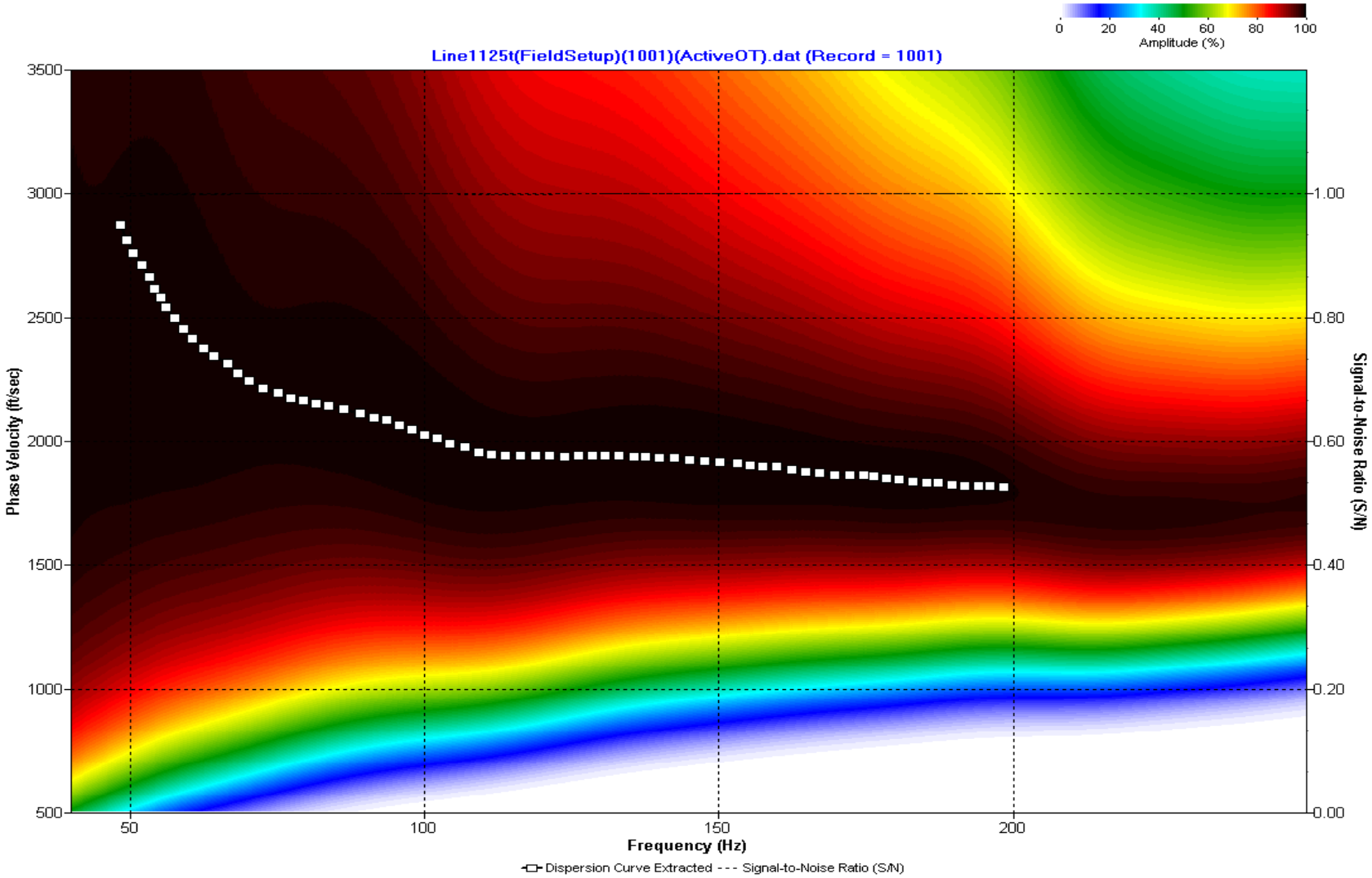

A.149: Dispersion Curve Line 1125 used in Post-blast 7

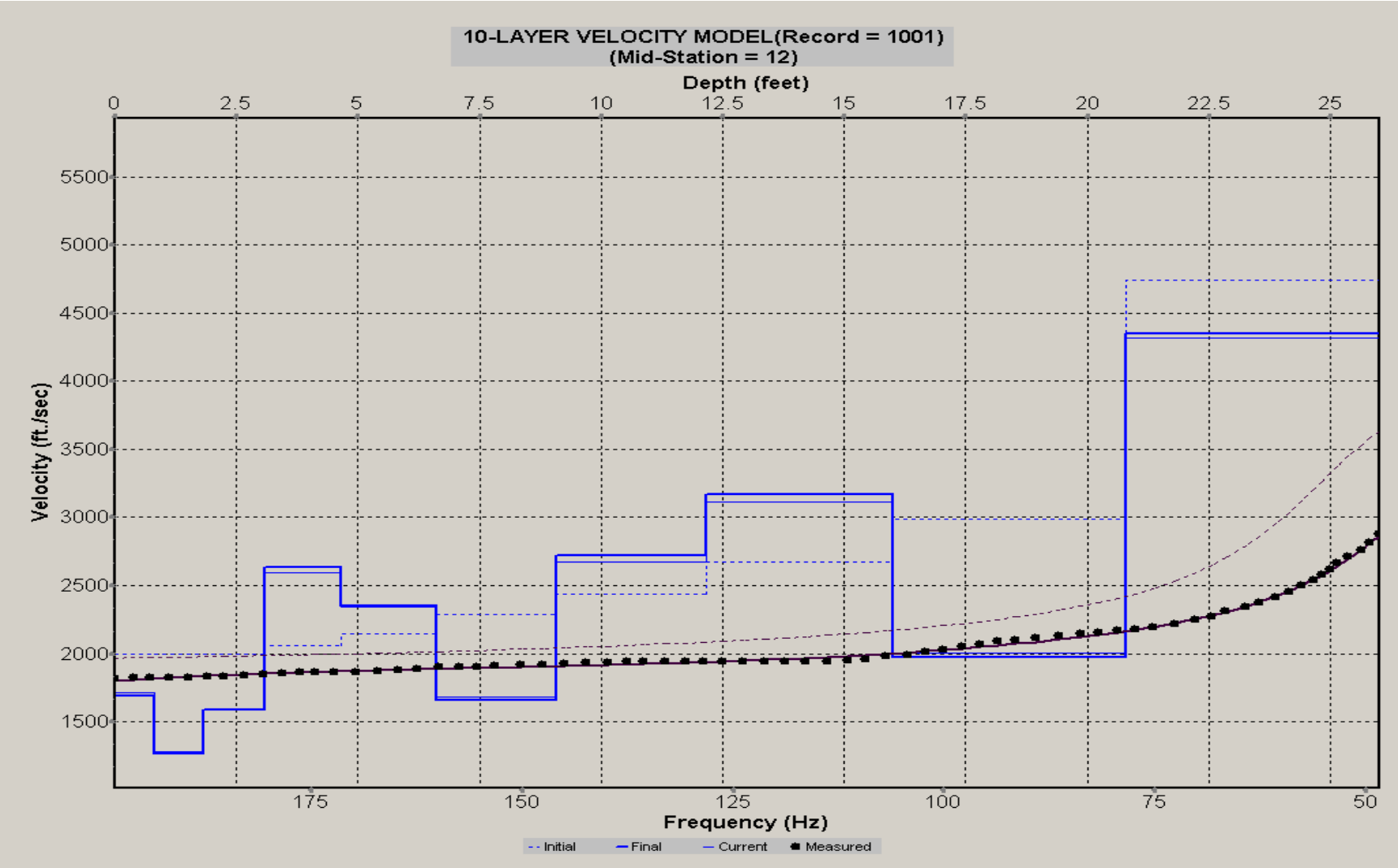

A.150: Velocity Profile Line 1125 used in Post-blast 7

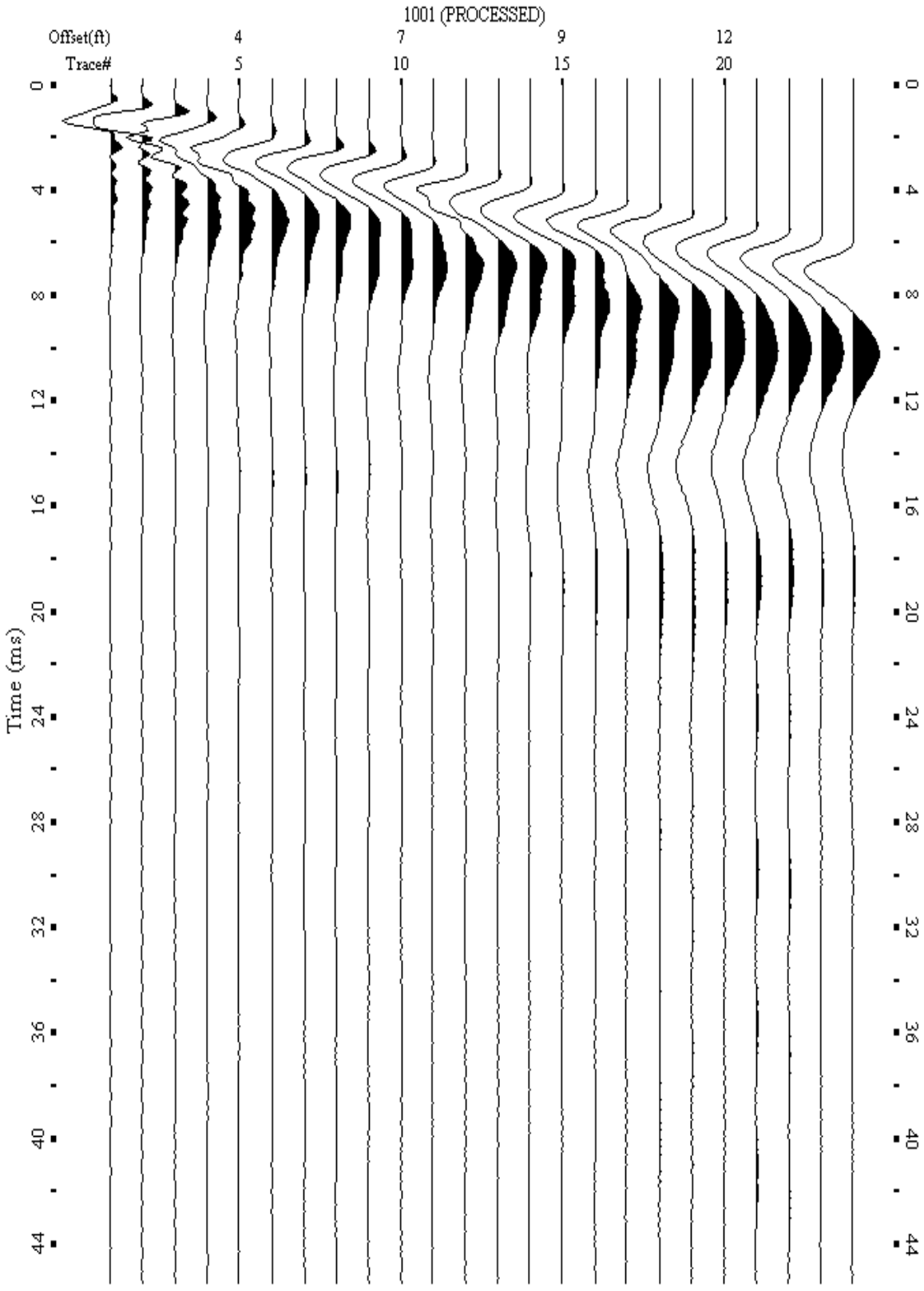

A.151: Shot Gather Line 1126 used in Post-blast 6 and Post-blast 7

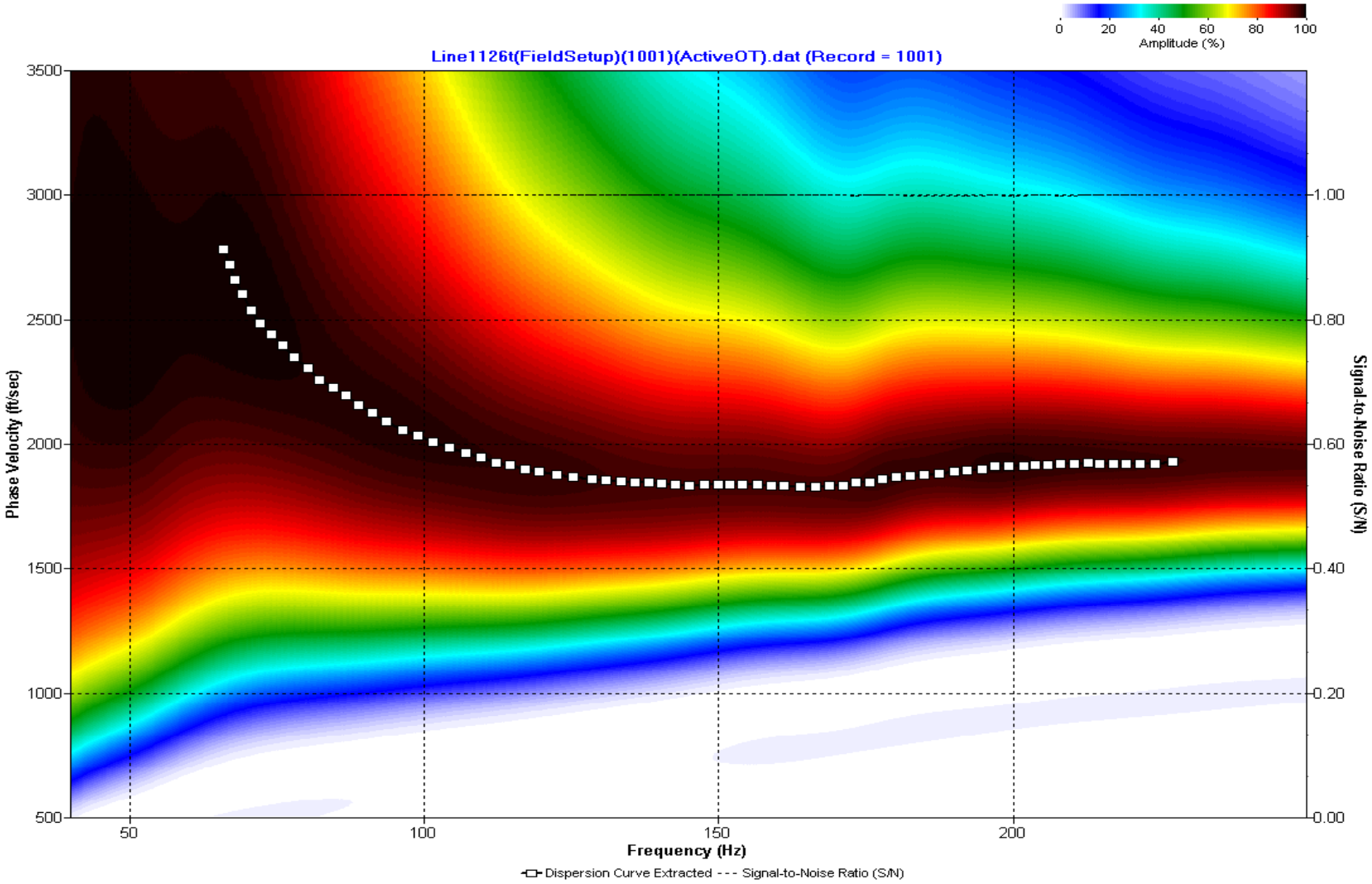

A.152: Dispersion Curve Line 1126 used in Post-blast 6 and Post-blast 7

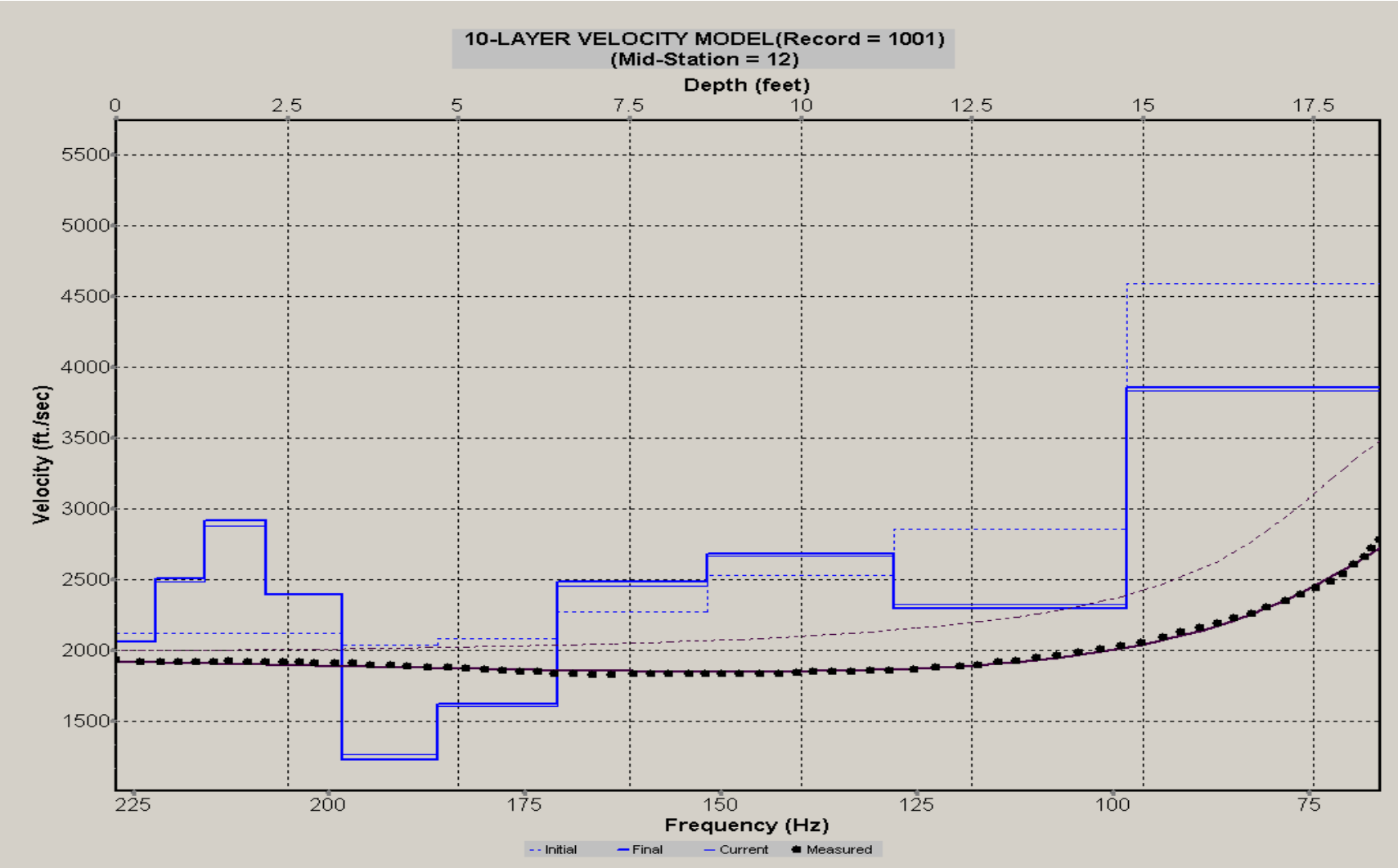

A.153: Velocity Profile Line 1126 used in Post-blast 6 and Post-blast 7

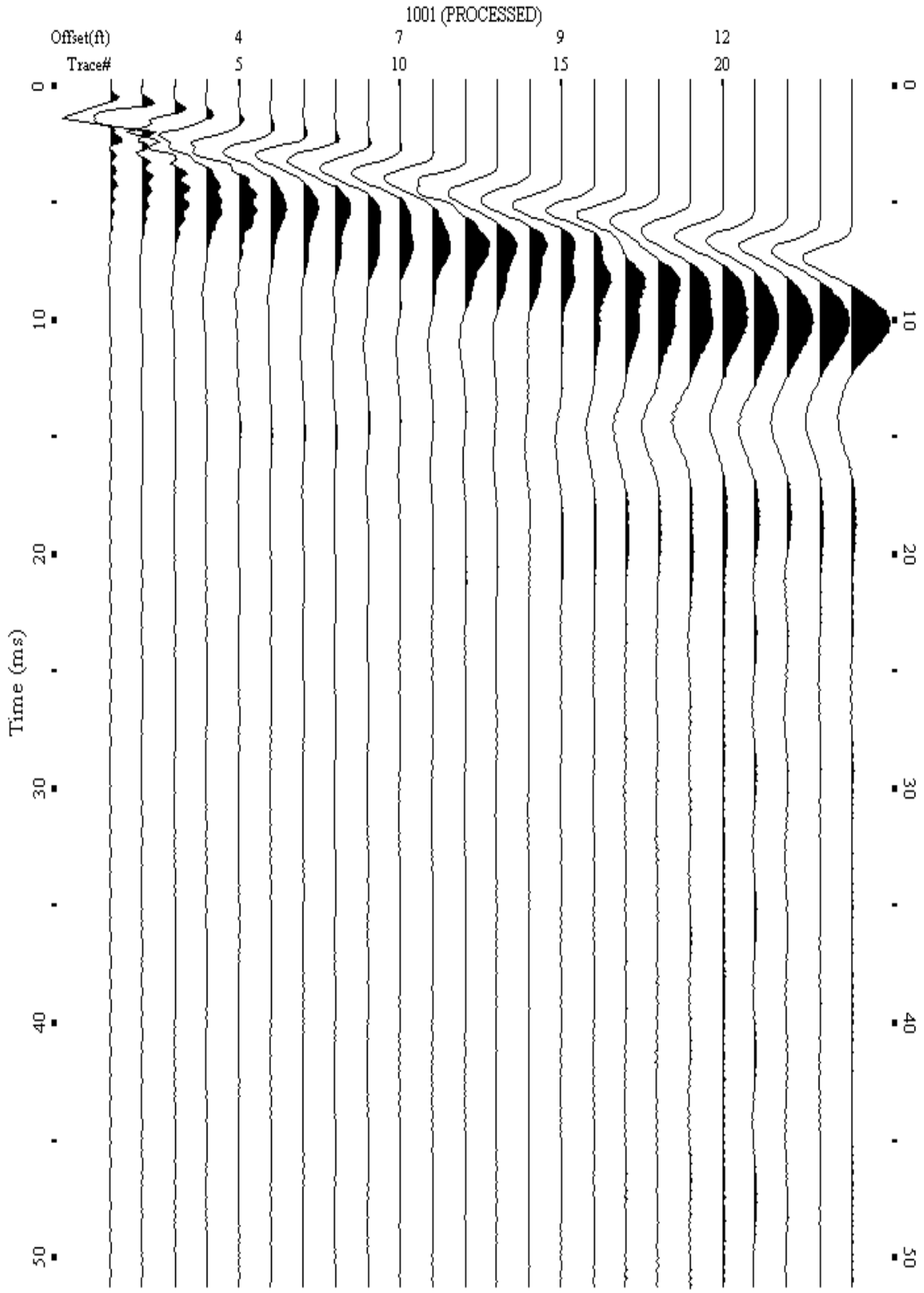

A.154: Shot Gather Line 1127 used in Post-blast 6 and Post-blast 7

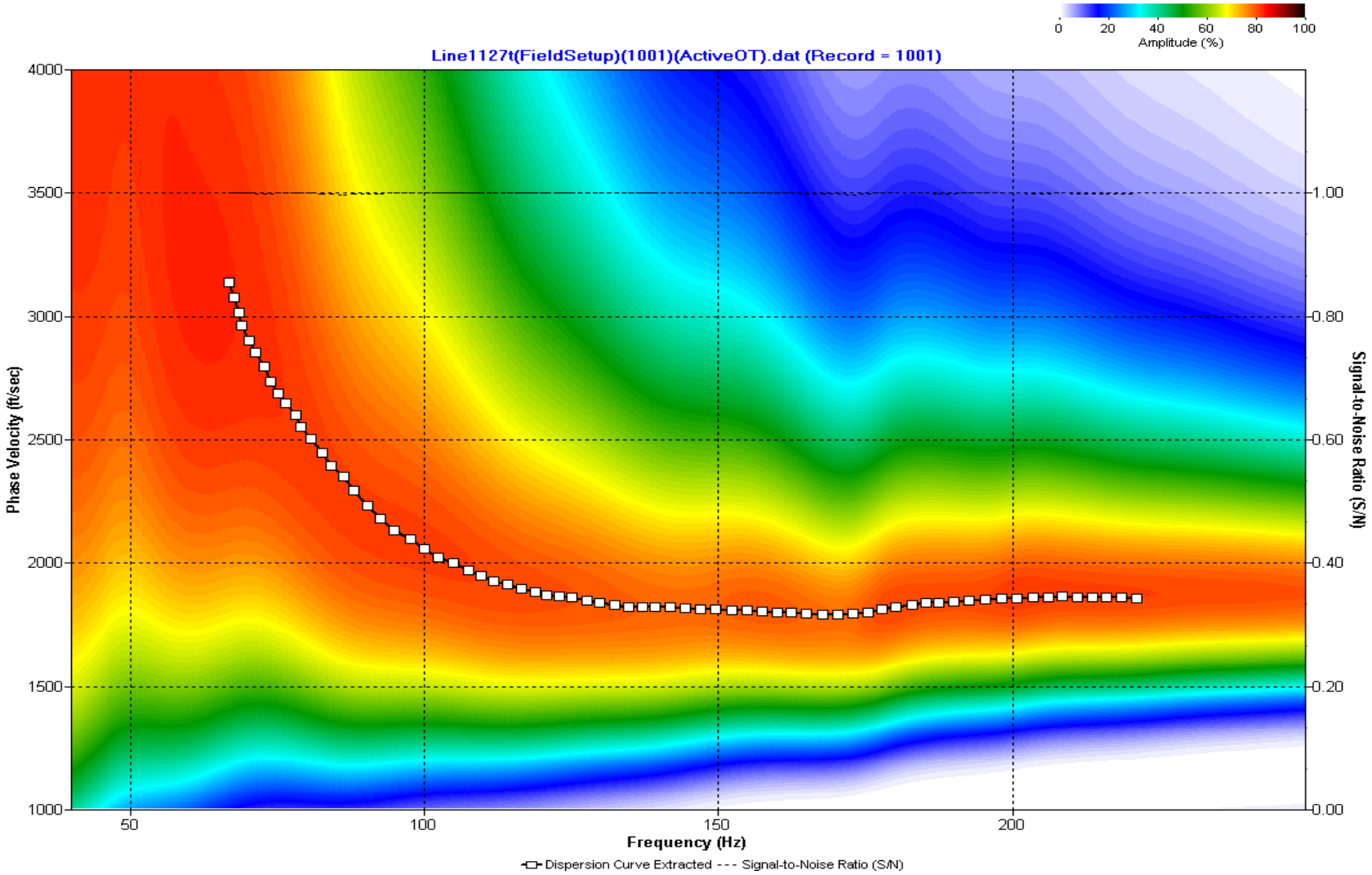

A.155: Dispersion Curve Line 1127 used in Post-blast 6 and Post-blast 7

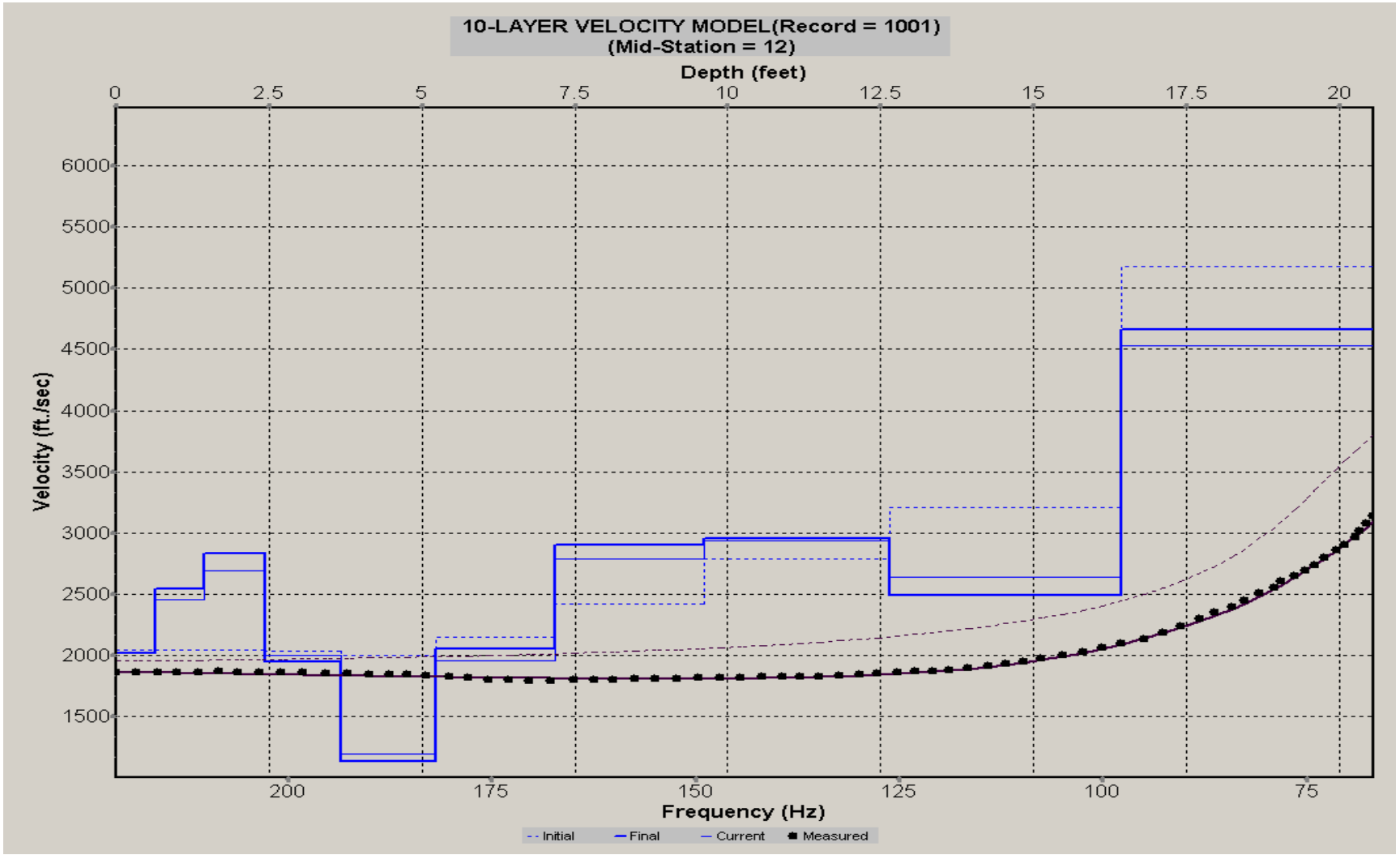

A.156: Velocity Profile Line 1127 used in Post-blast 6 and Post-blast 7

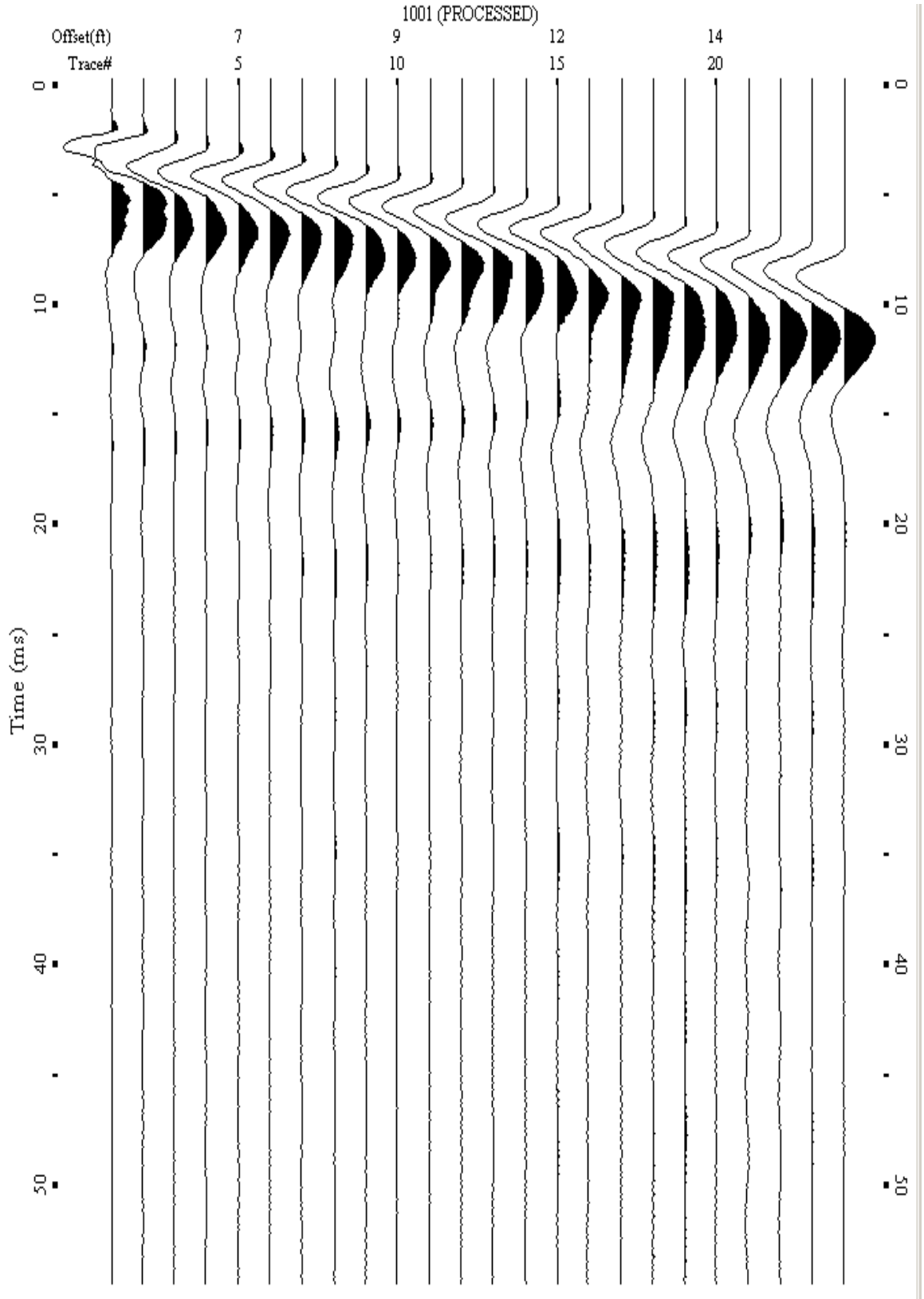

A.157: Shot Gather Line 1128 used in Post-blast 6 and Post-blast 7

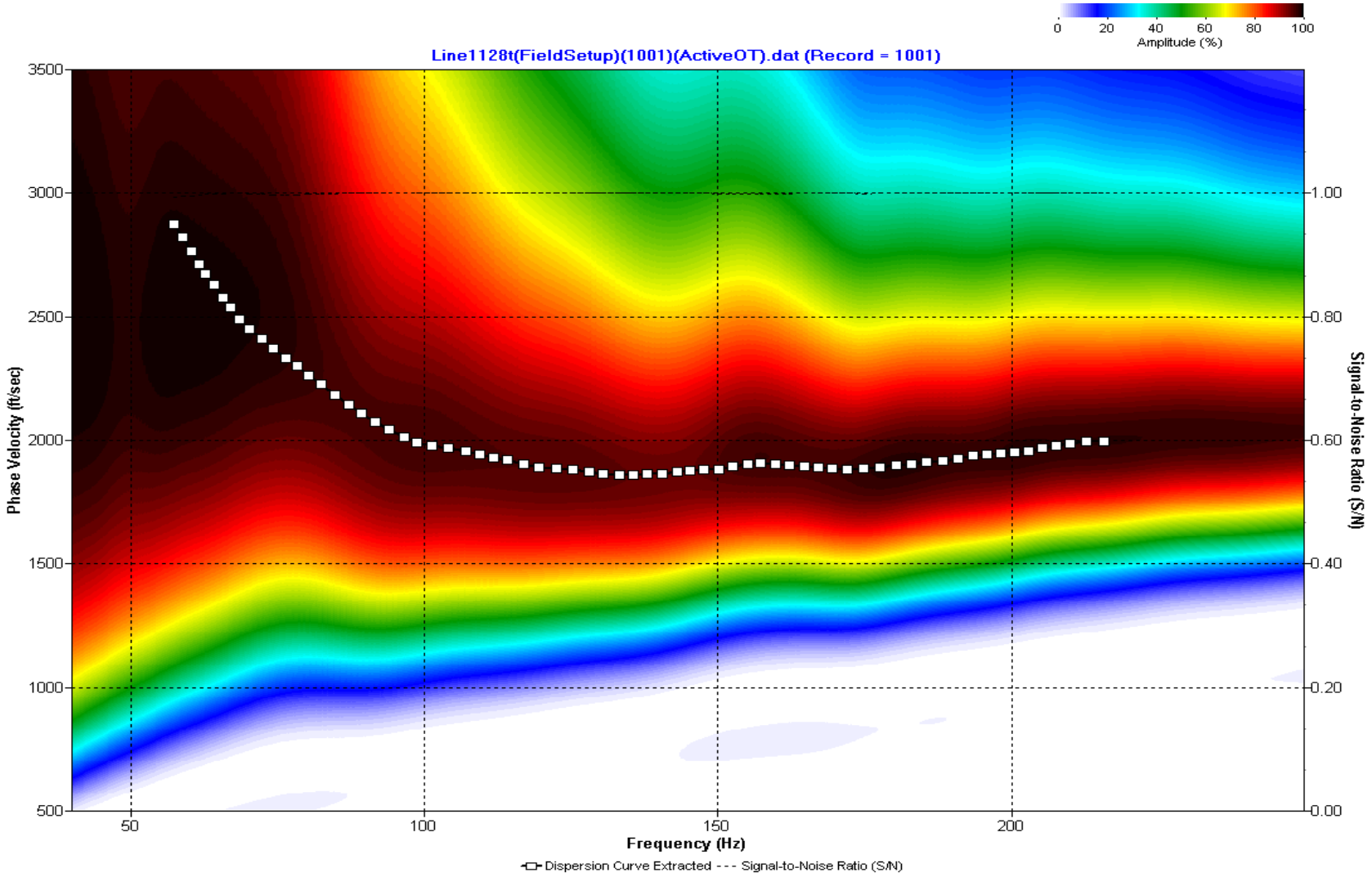

A.158: Dispersion Curve Line 1128 used in Post-blast 6 and Post-blast 7

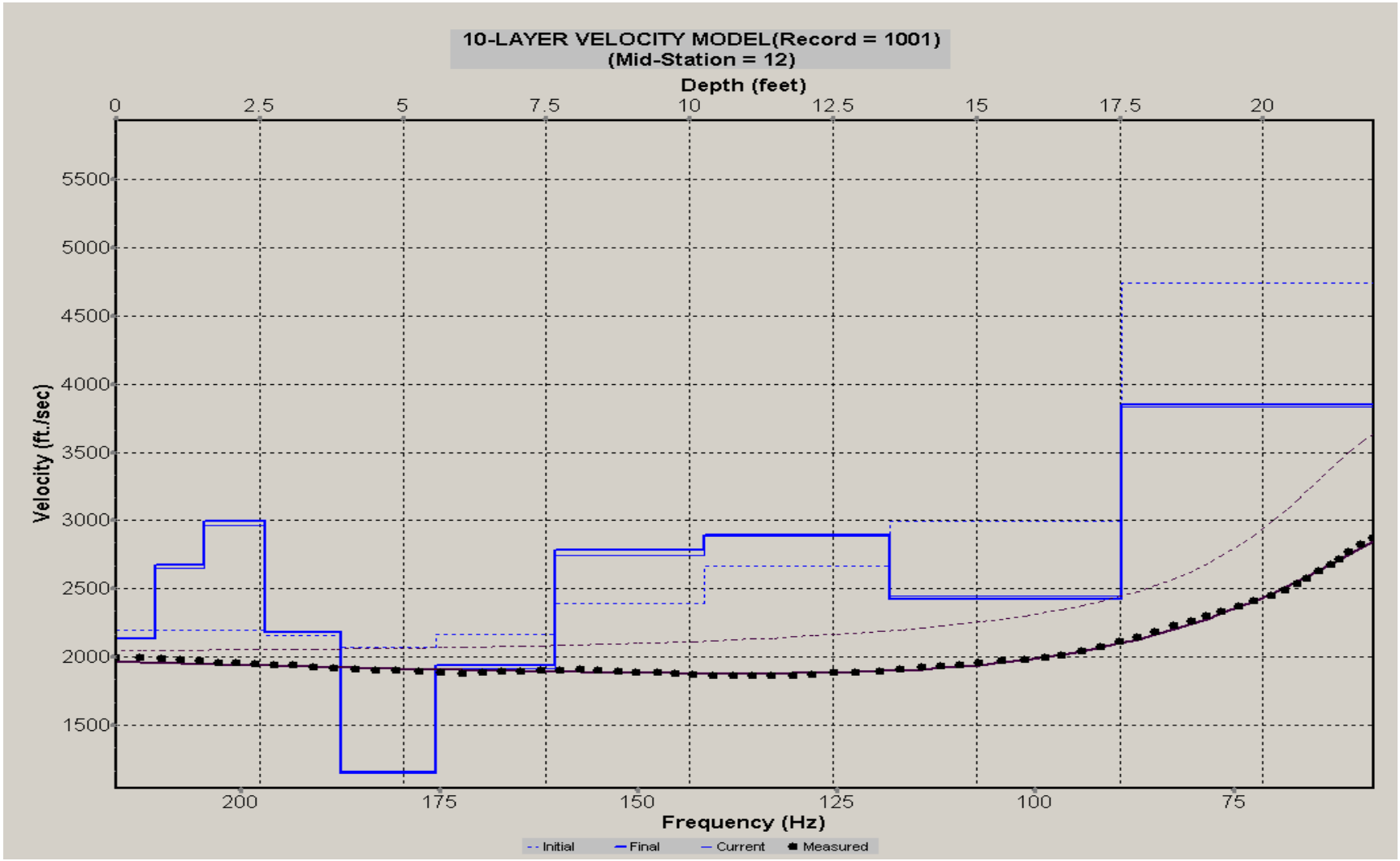

A.159: Velocity Profile Line 1128 used in Post-blast 6 and Post-blast 7

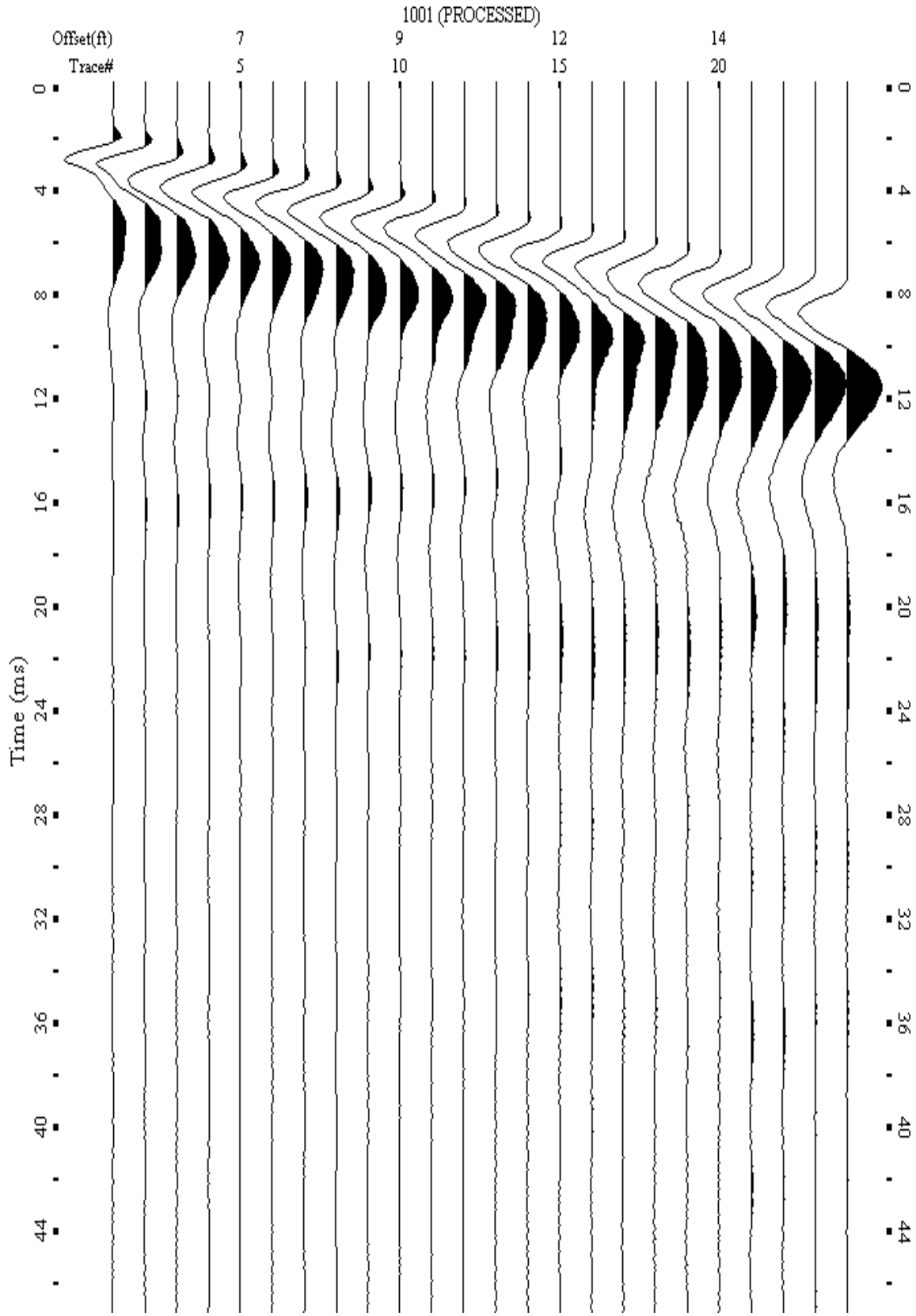

A.160: Shot Gather Line 1129 used in Post-blast 6 and Post-blast 7

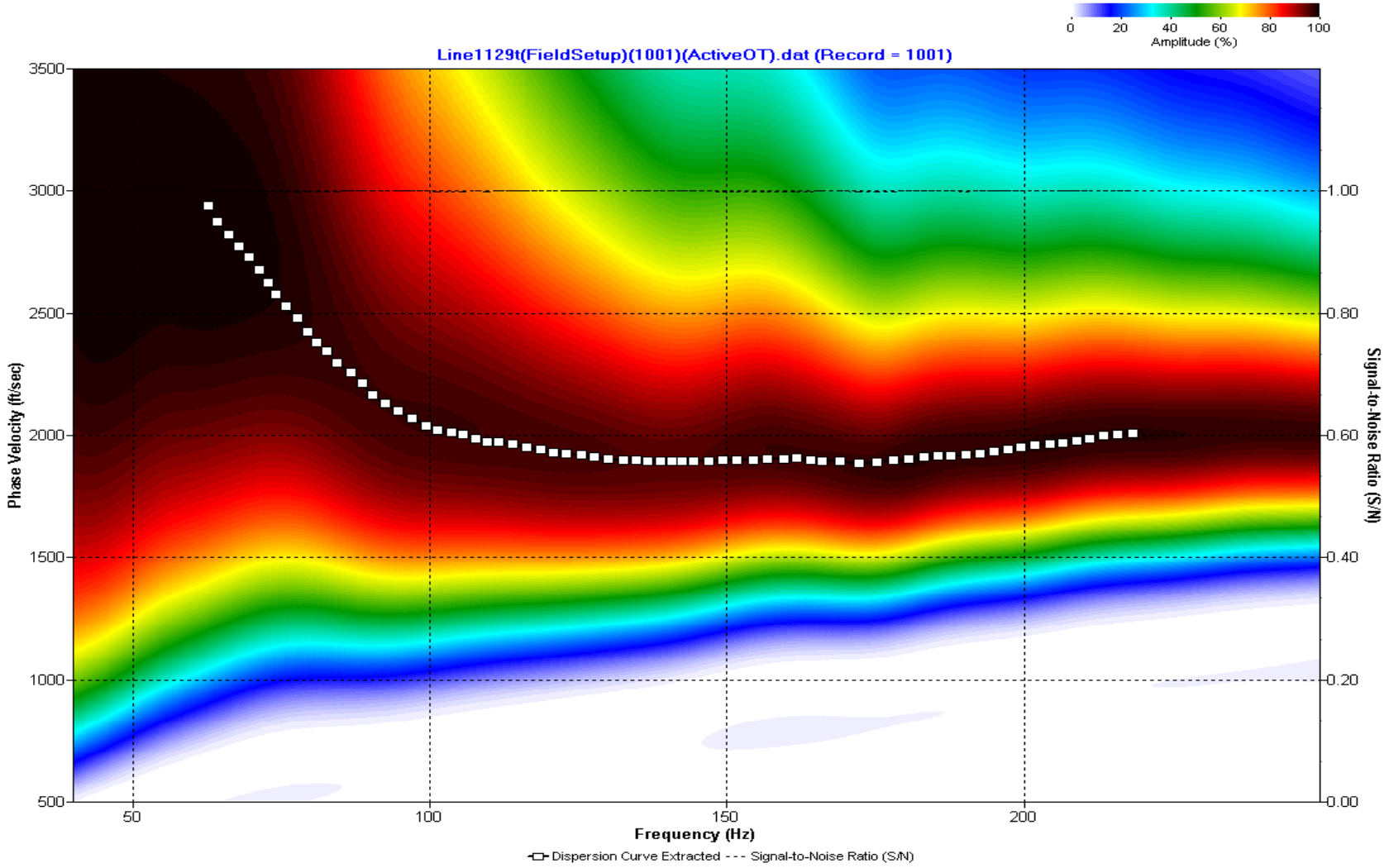

A.161: Dispersion Curve Line 1129 used in Post-blast 6 and Post-blast 7

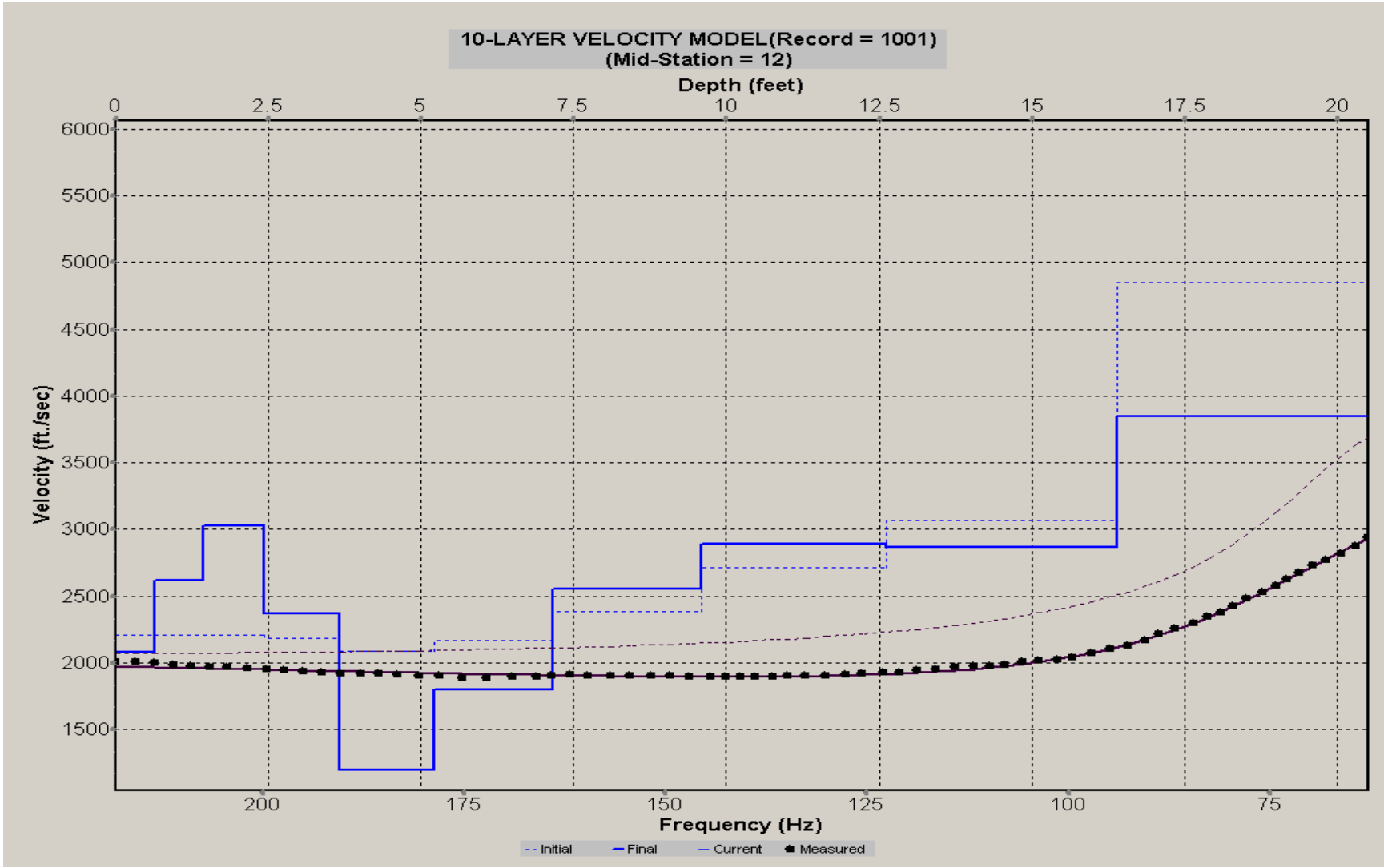

A.162: Velocity Profile Line 1129 used in Post-blast 6 and Post-blast 7

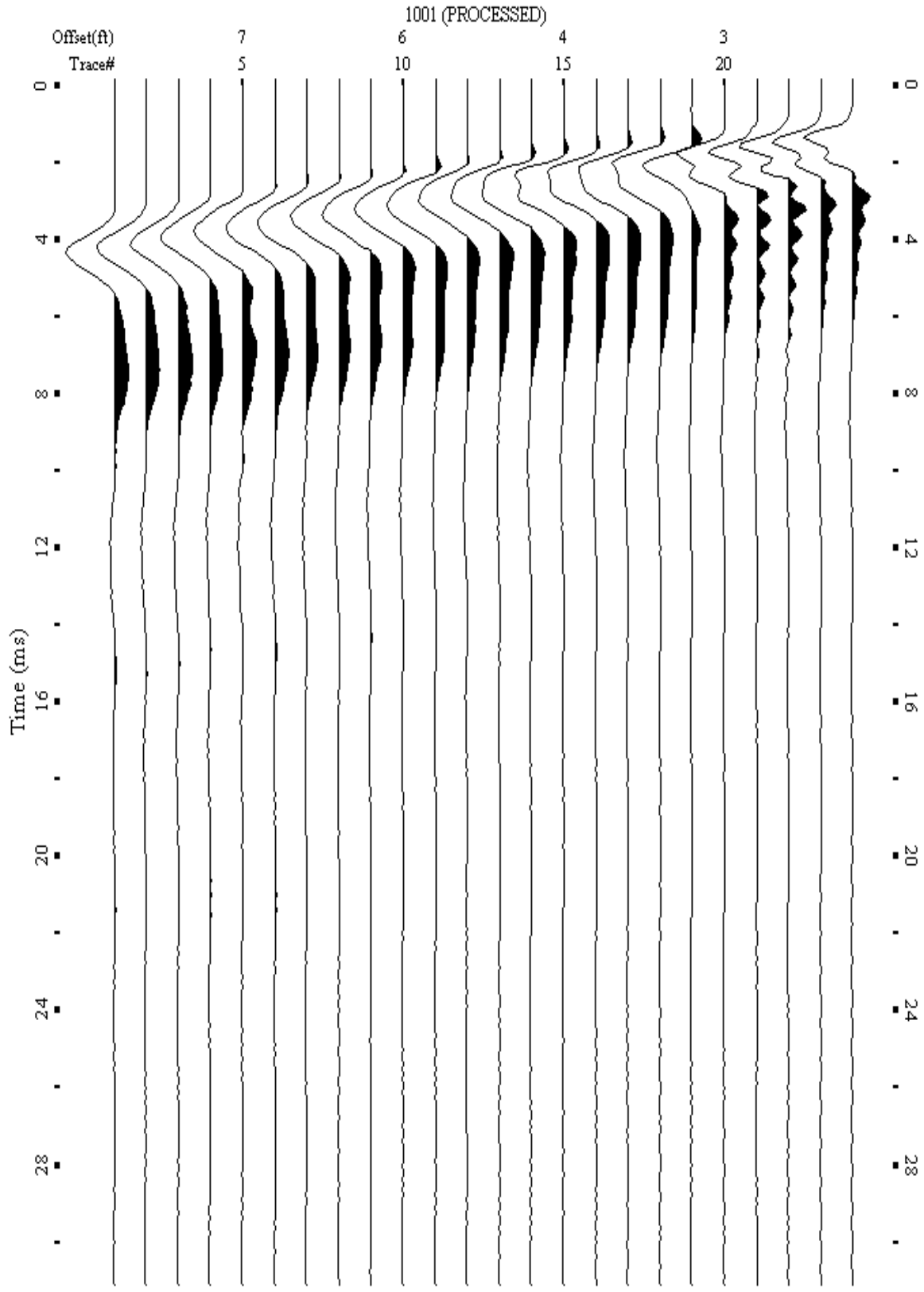

A.163: Shot Gather Line 1130 used in Post-blast 8

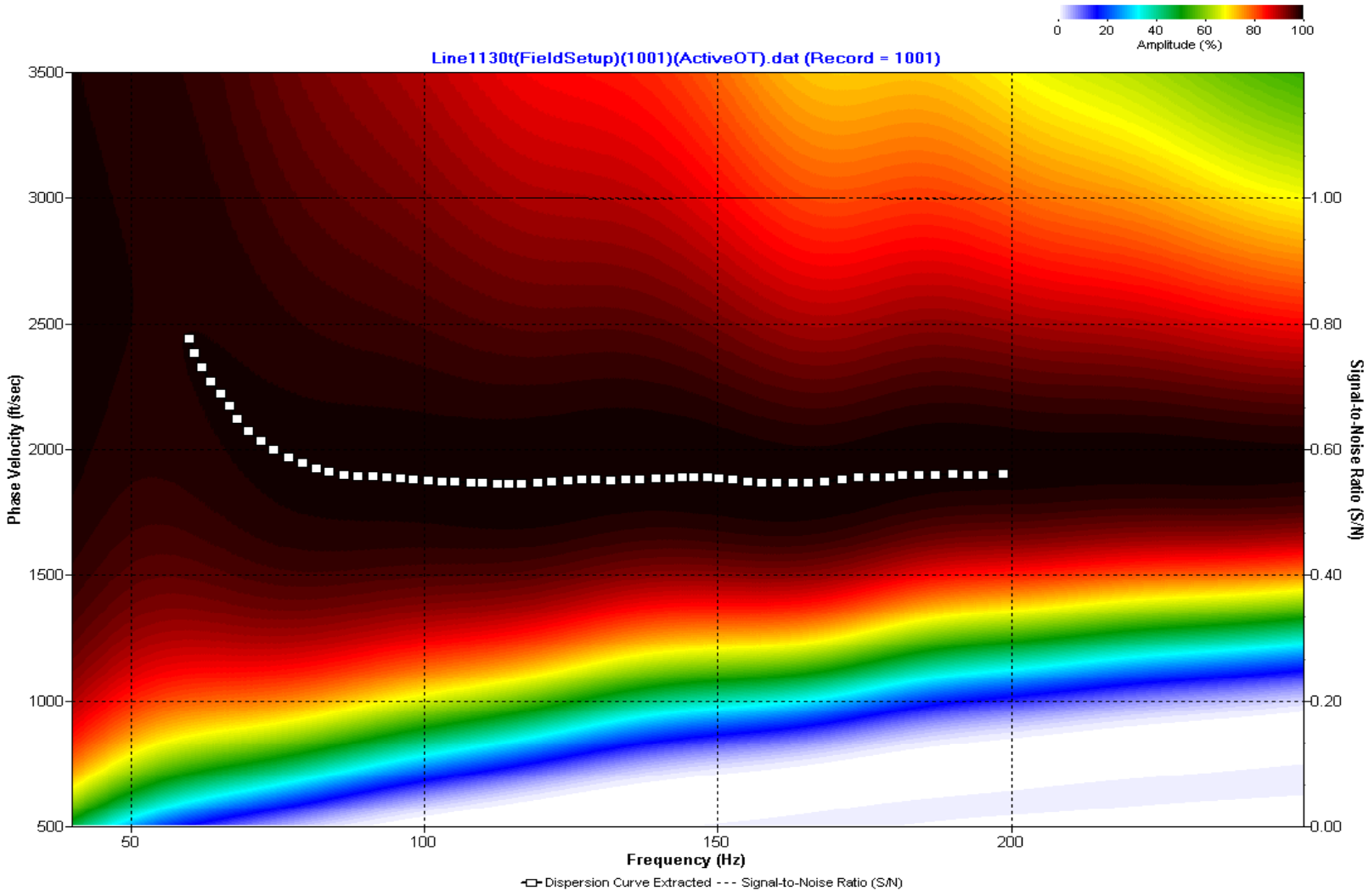

A.164: Dispersion Curve Line 1130 used in Post-blast 8

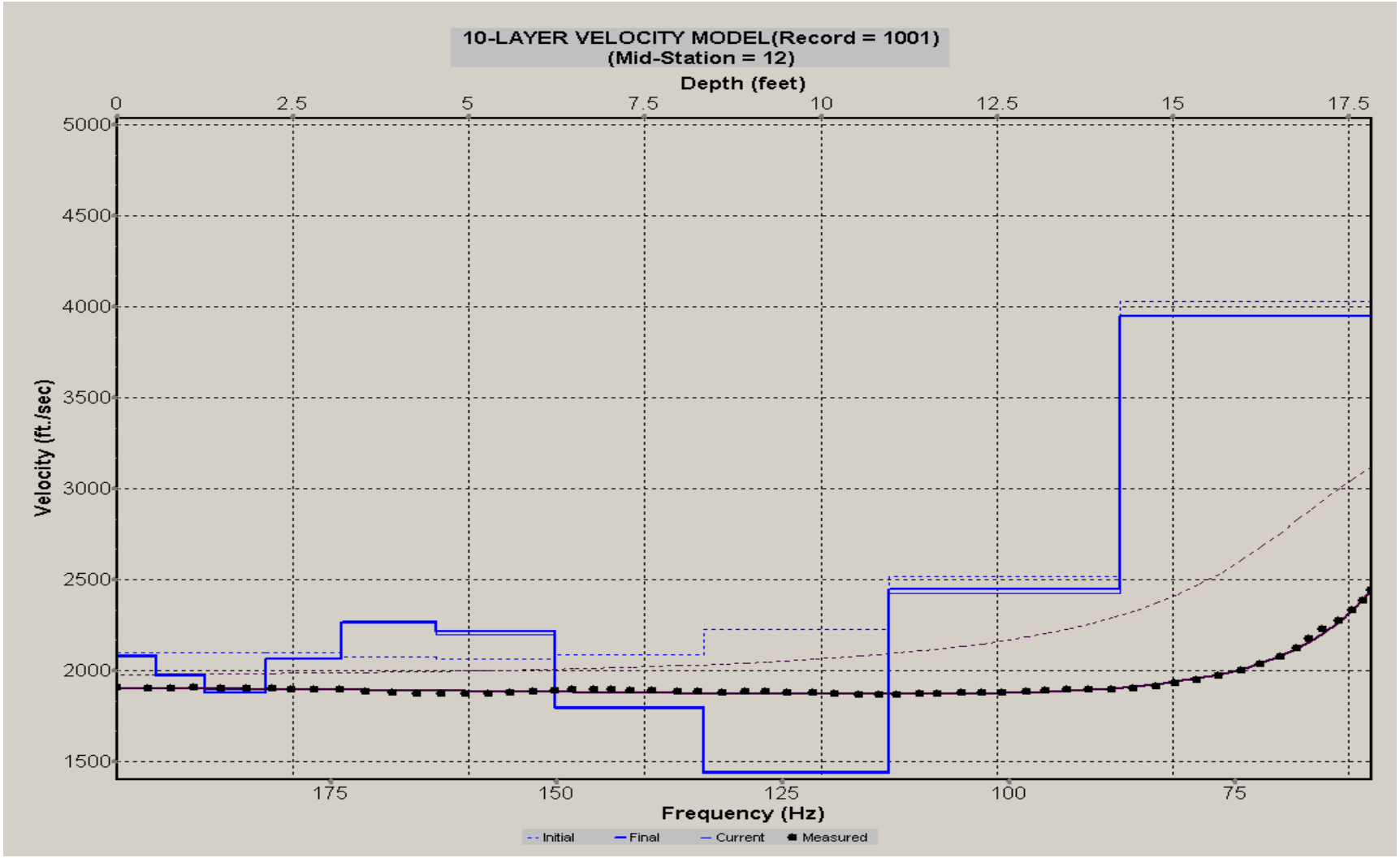

A.165: Velocity Profile Line 1130 used in Post-blast 8

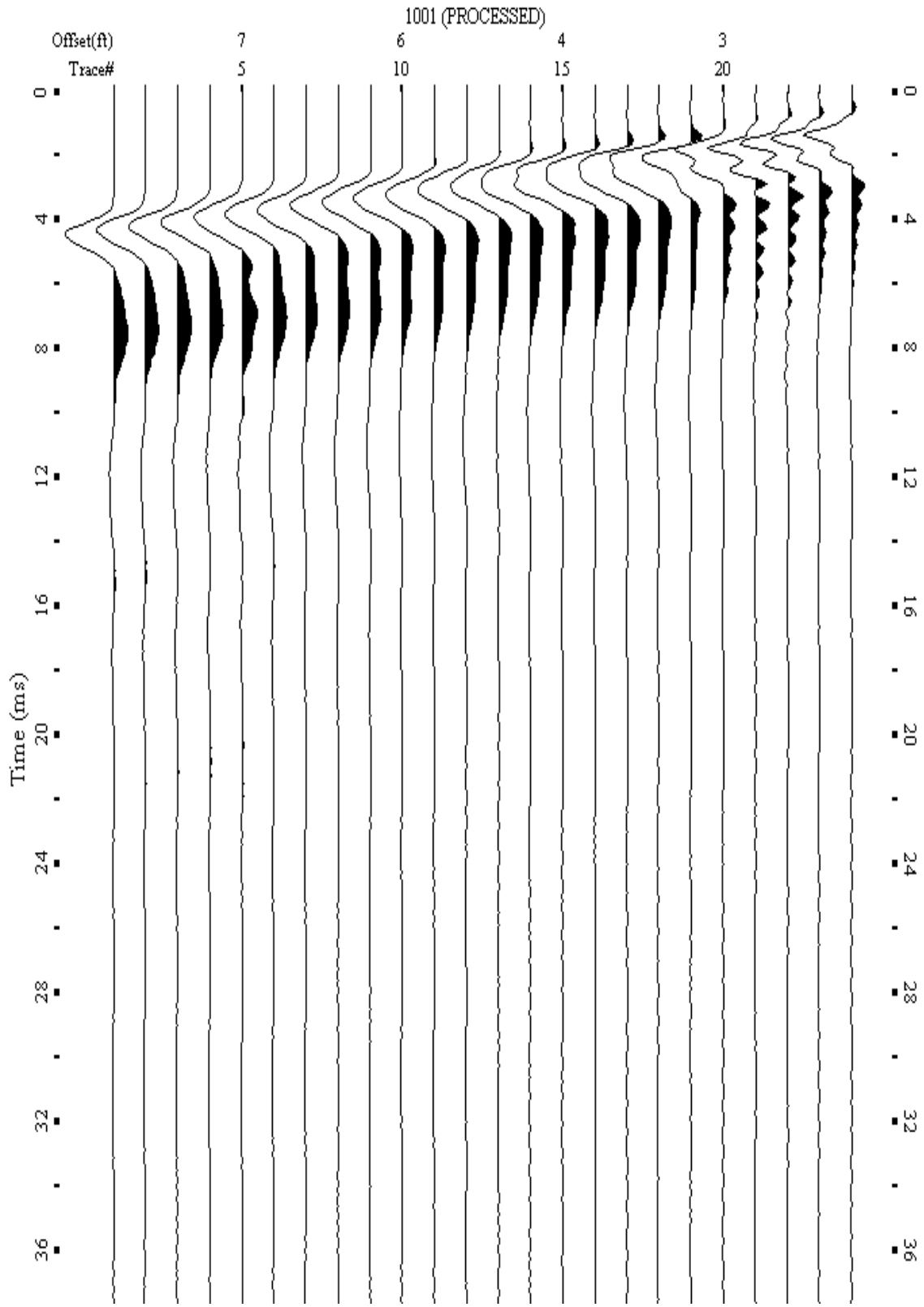

A.166: Shot Gather Line 1131 used in Post-blast 8

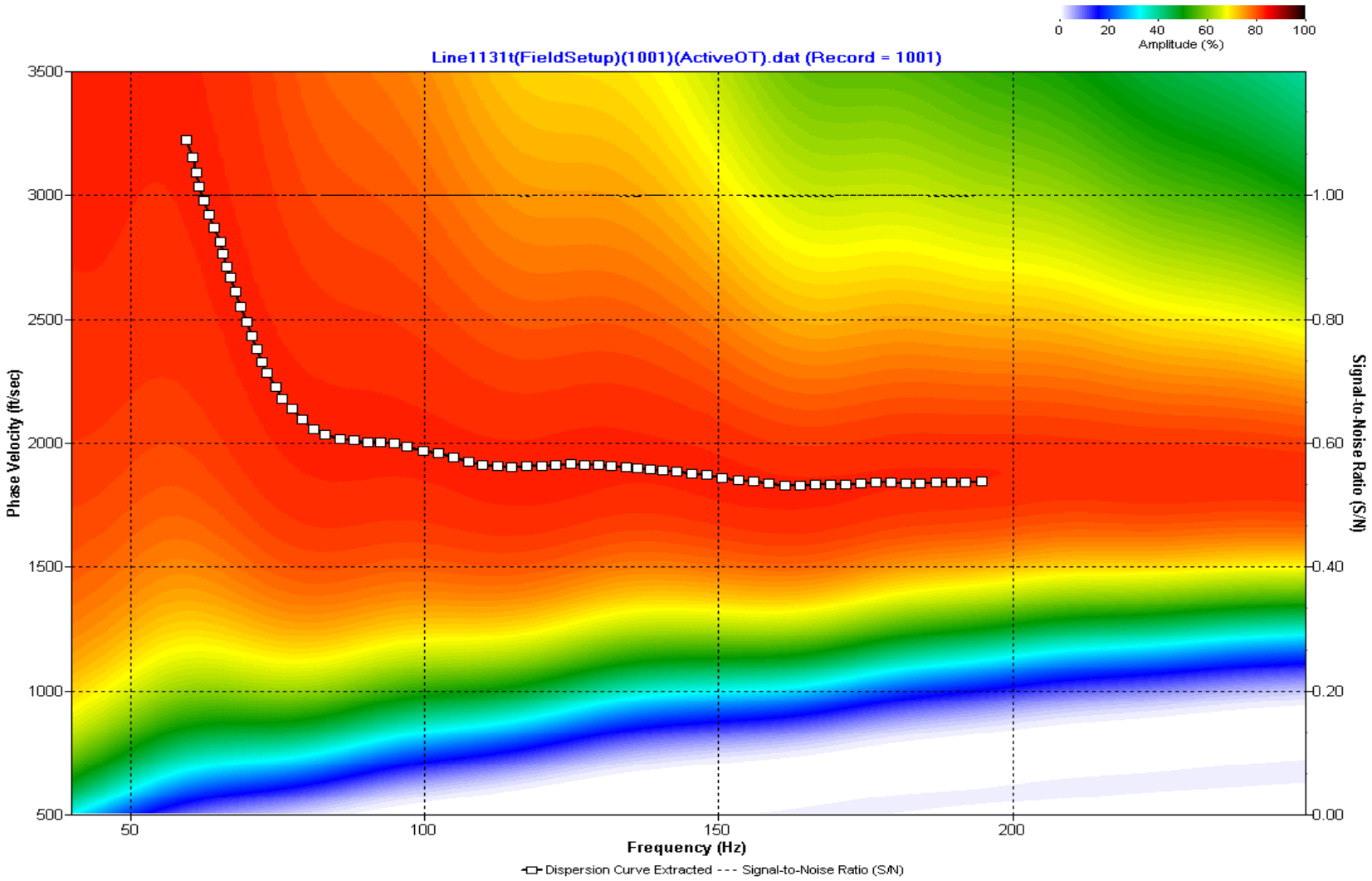

A.167: Dispersion Curve Line 1131 used in Post-blast 8

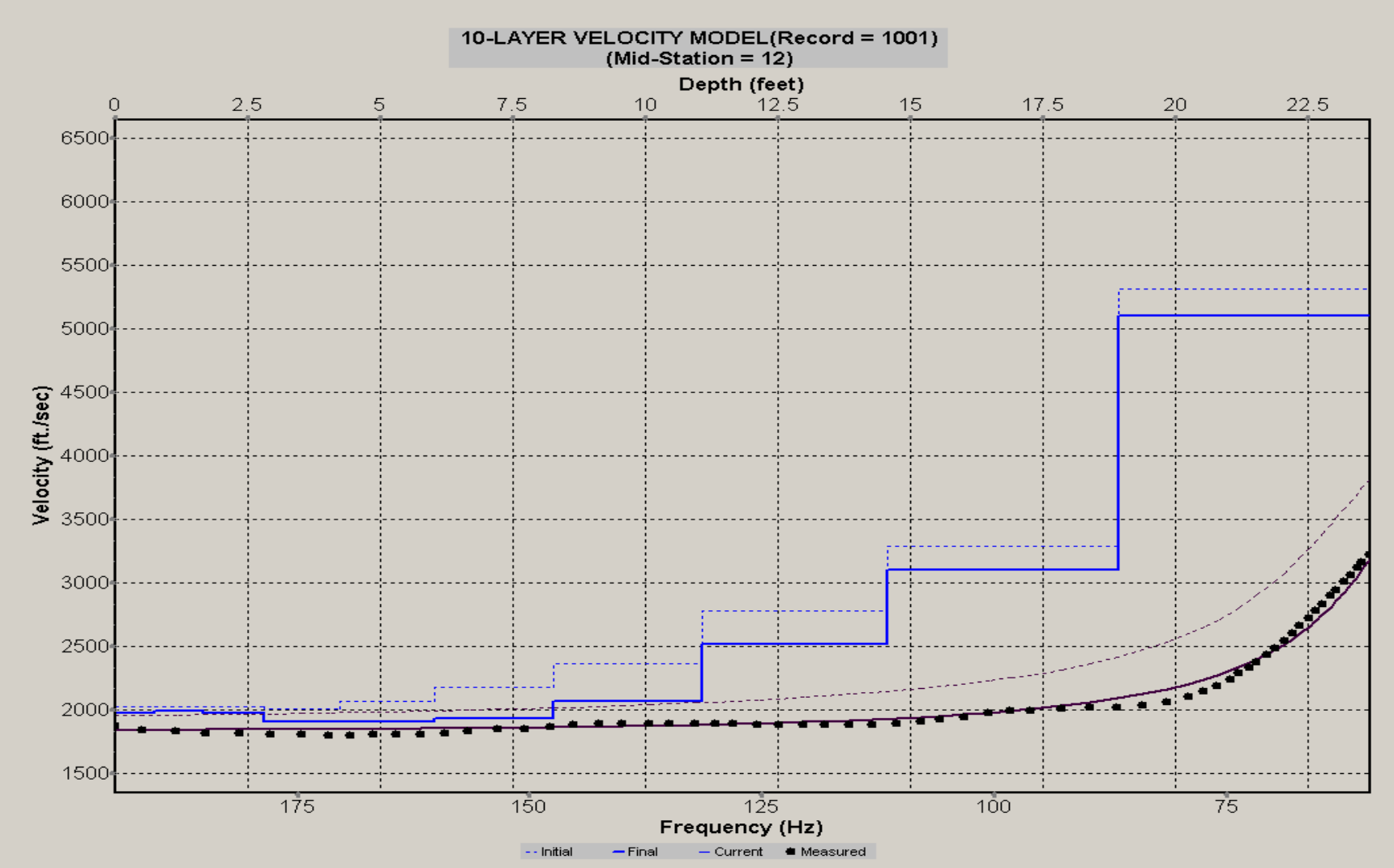

A.168: Velocity Profile Line 1131 used in Post-blast 8

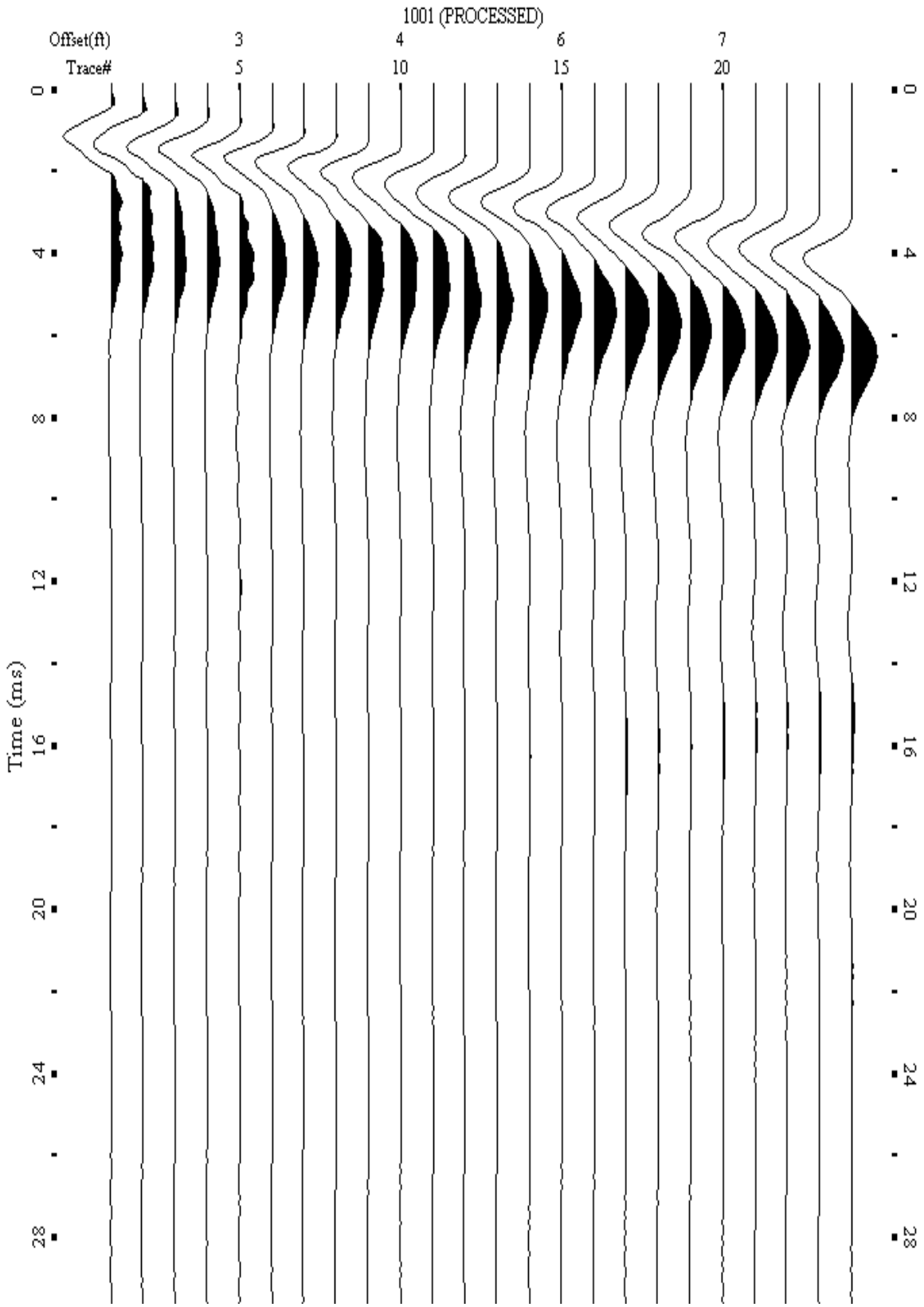

A.169: Shot Gather Line 1134 used in Post-blast 8

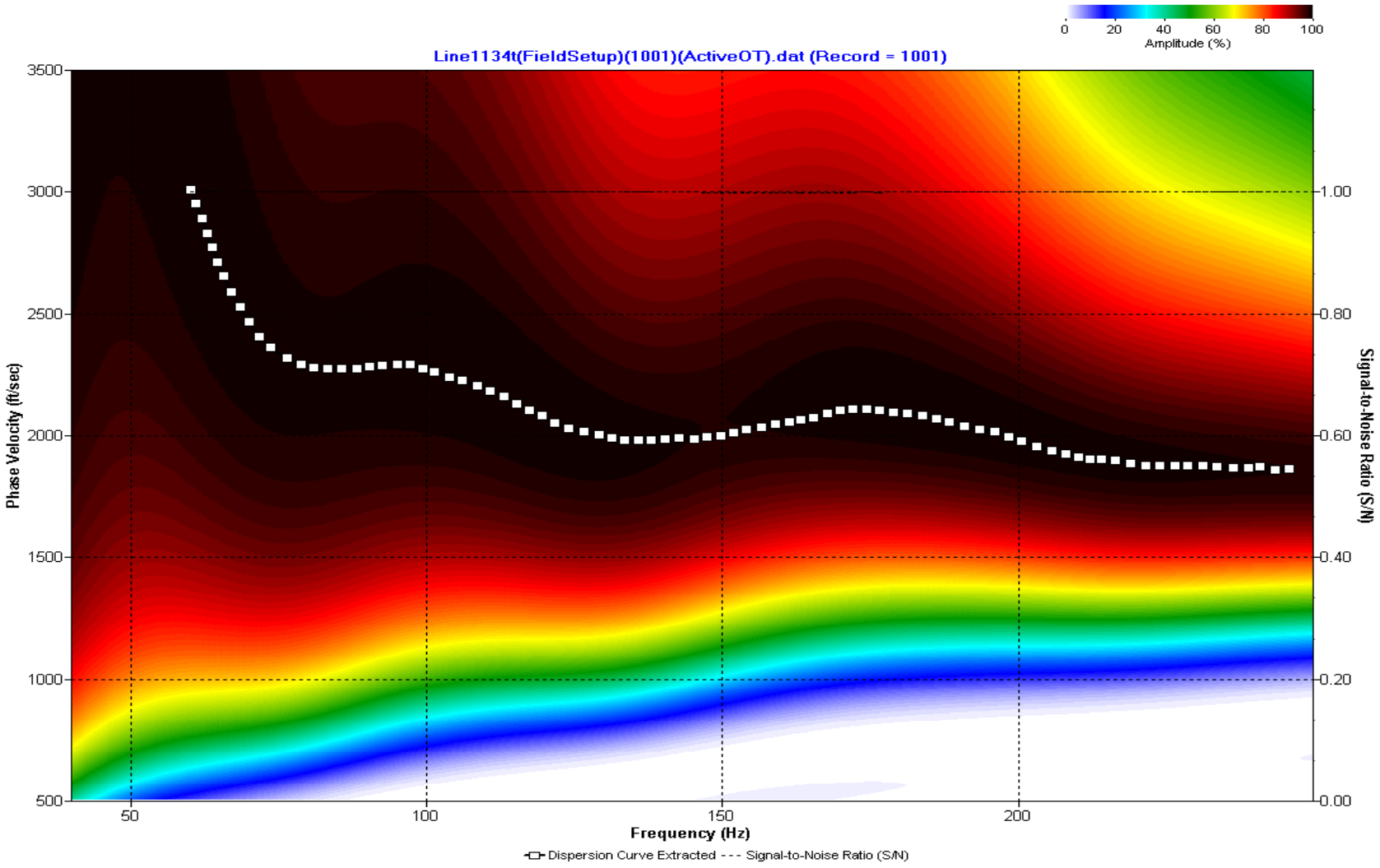

A.170: Dispersion Curve Line 1134 used in Post-blast 8

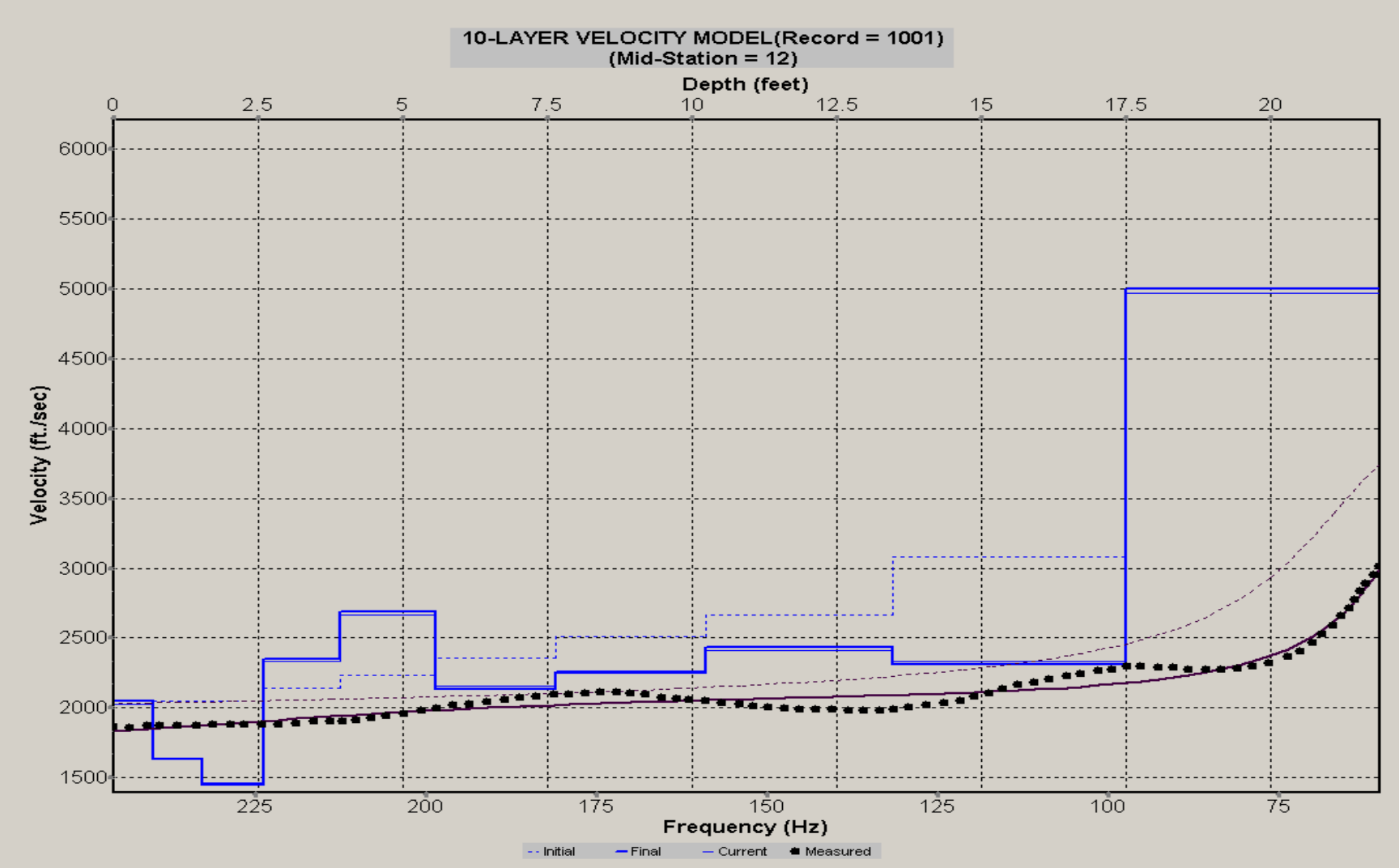

A.171: Velocity Profile Line 1134 used in Post-blast 8

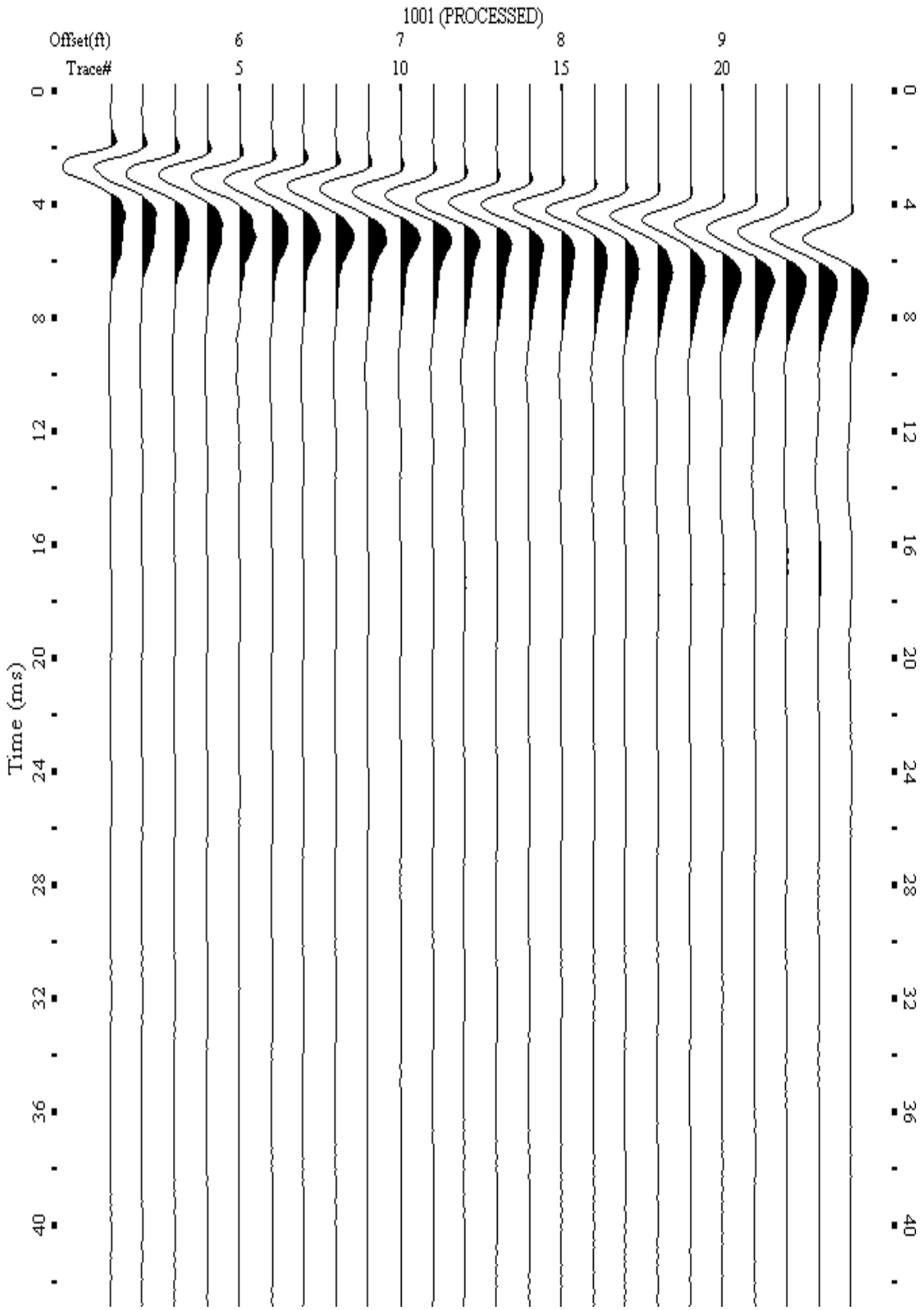

A.172: Shot Gather Line 1136 used in Post-blast 8

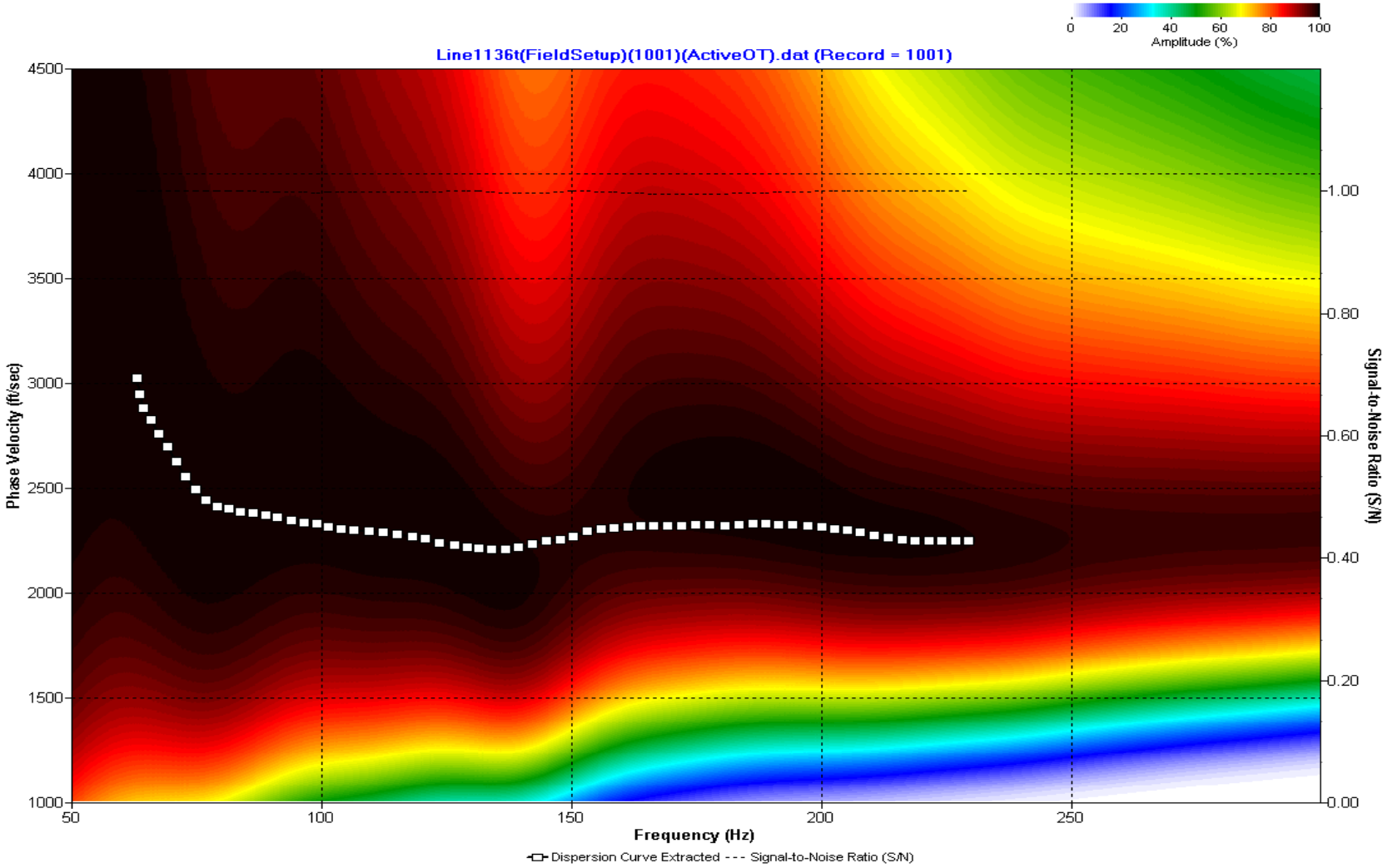

A.173: Dispersion Curve Line 1136 used in Post-blast 8

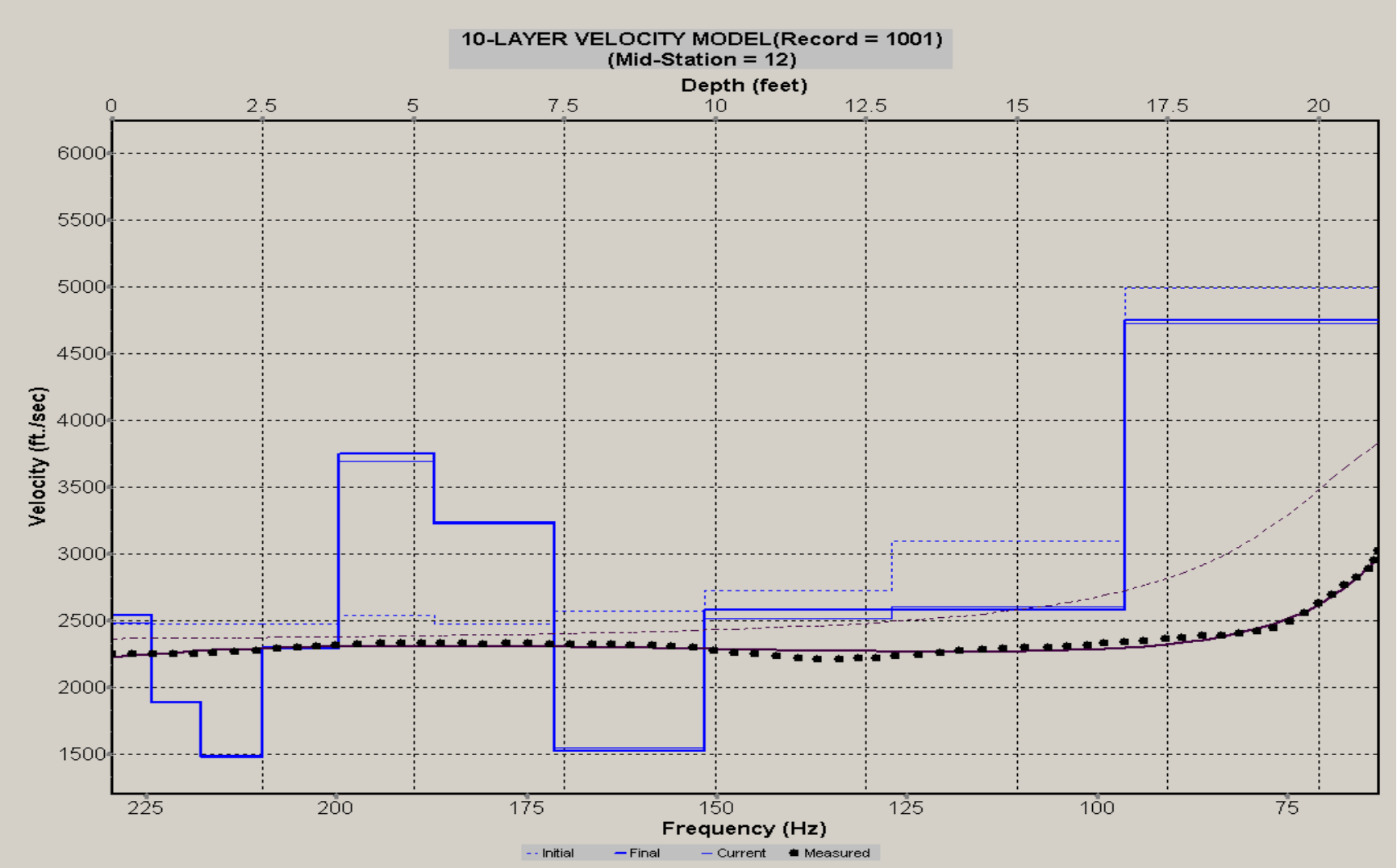

A.174: Velocity Profile Line 1136 used in Post-blast 8

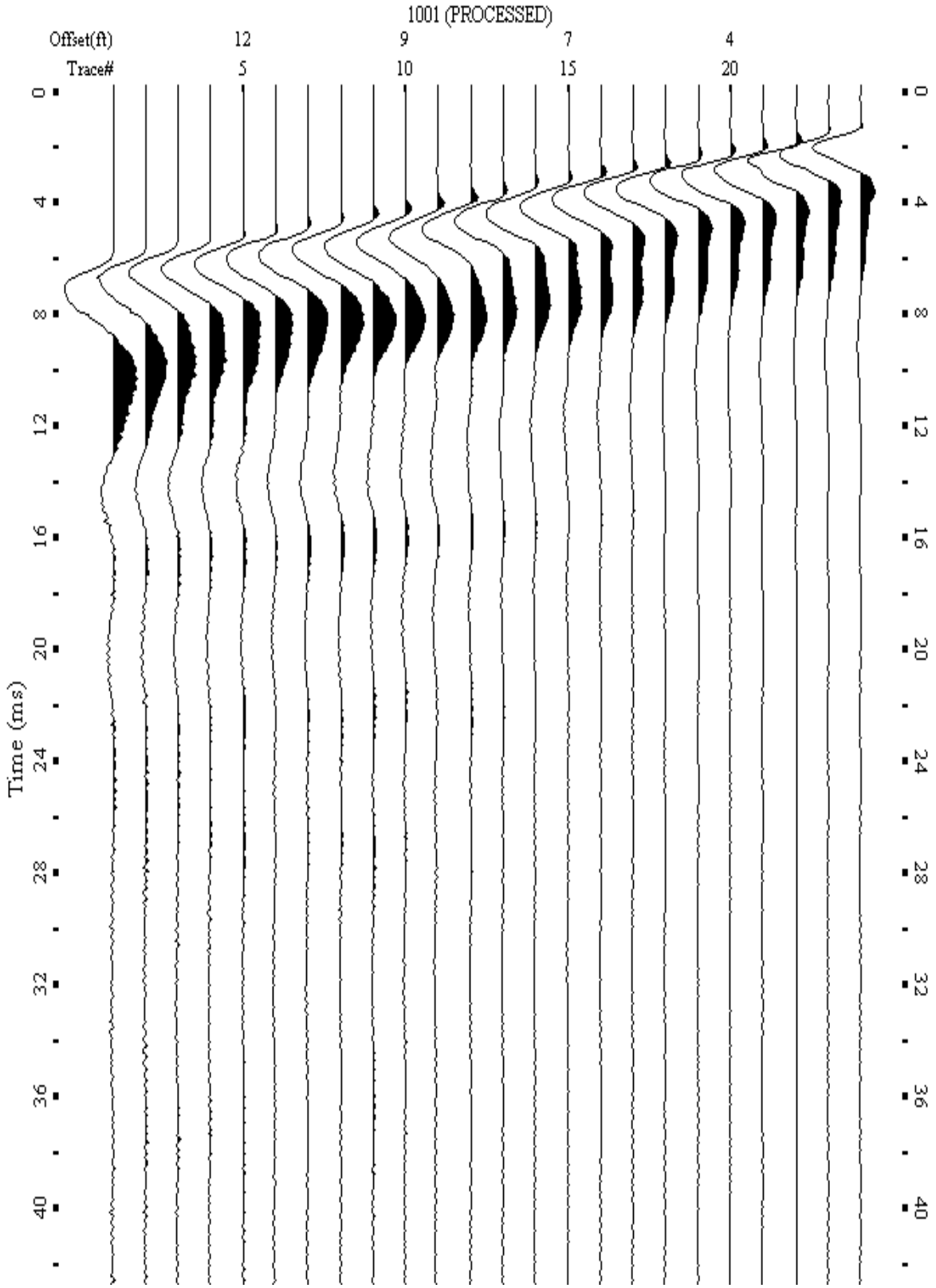

A.175: Shot Gather Line 1138 used in Post-blast 8 and Post-blast 9

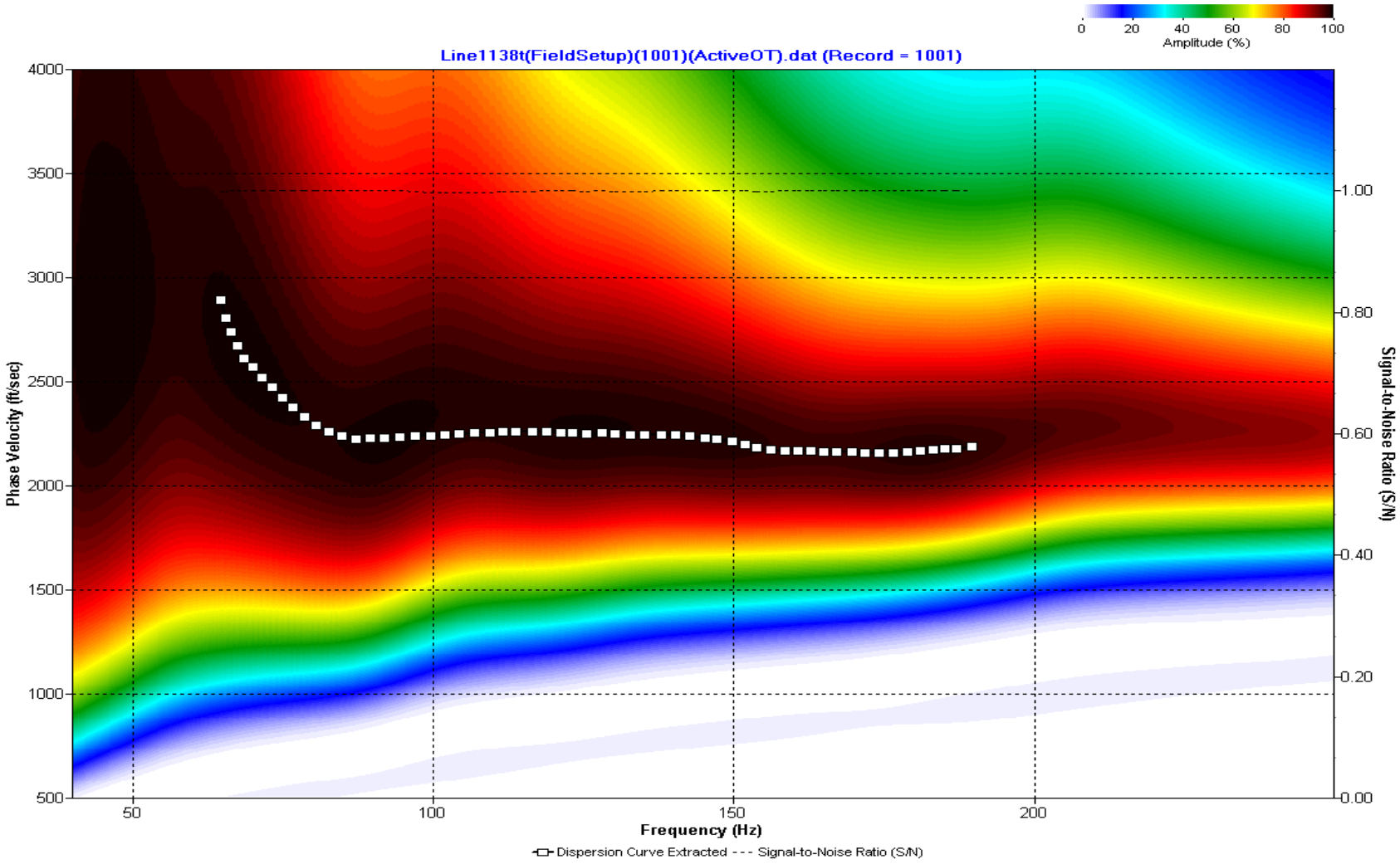

A.176: Dispersion Curve Line 1138 used in Post-blast 8 and Post-blast 9

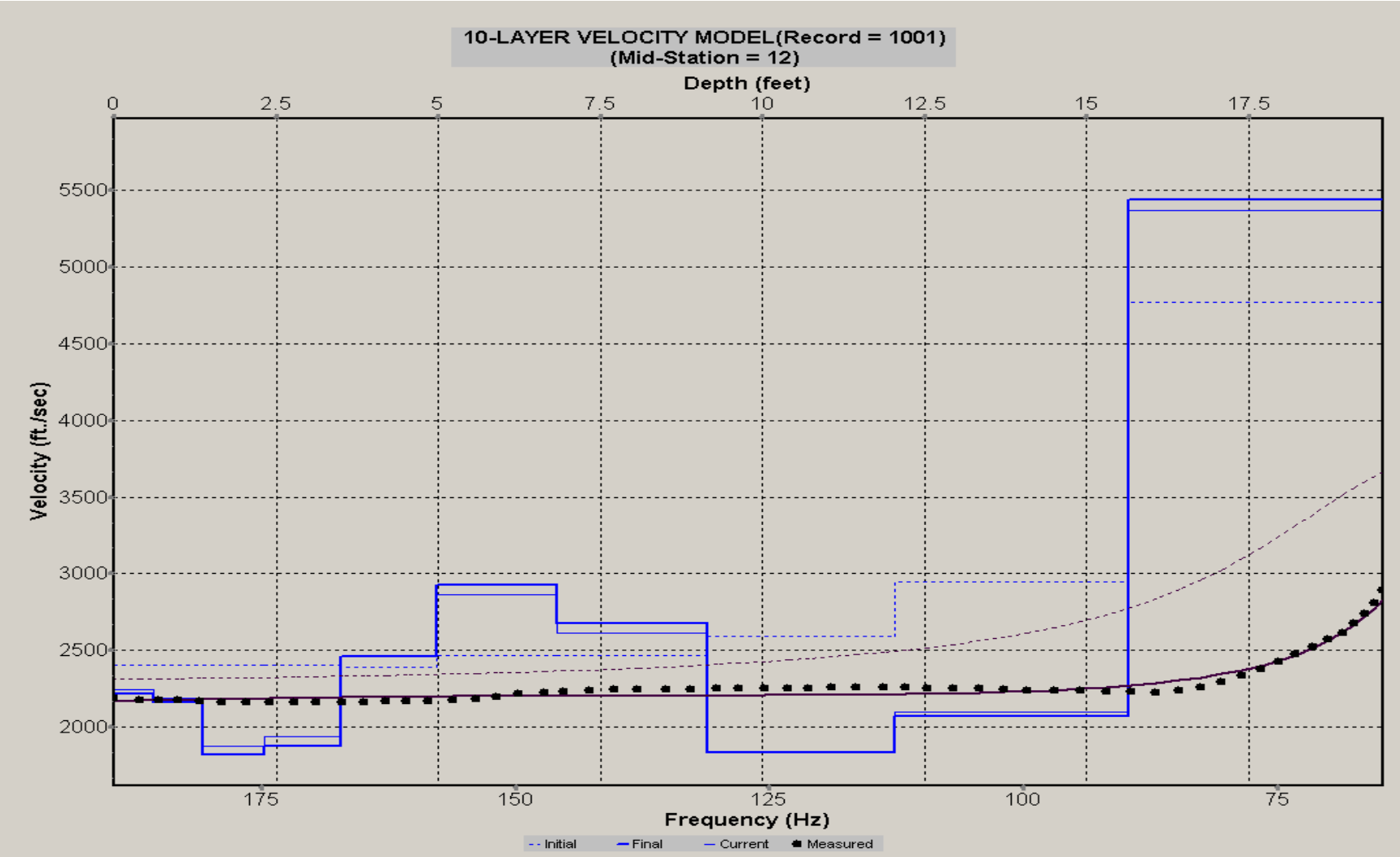

A.177: Velocity Profile Line 1138 used in Post-blast 8 and Post-blast 9

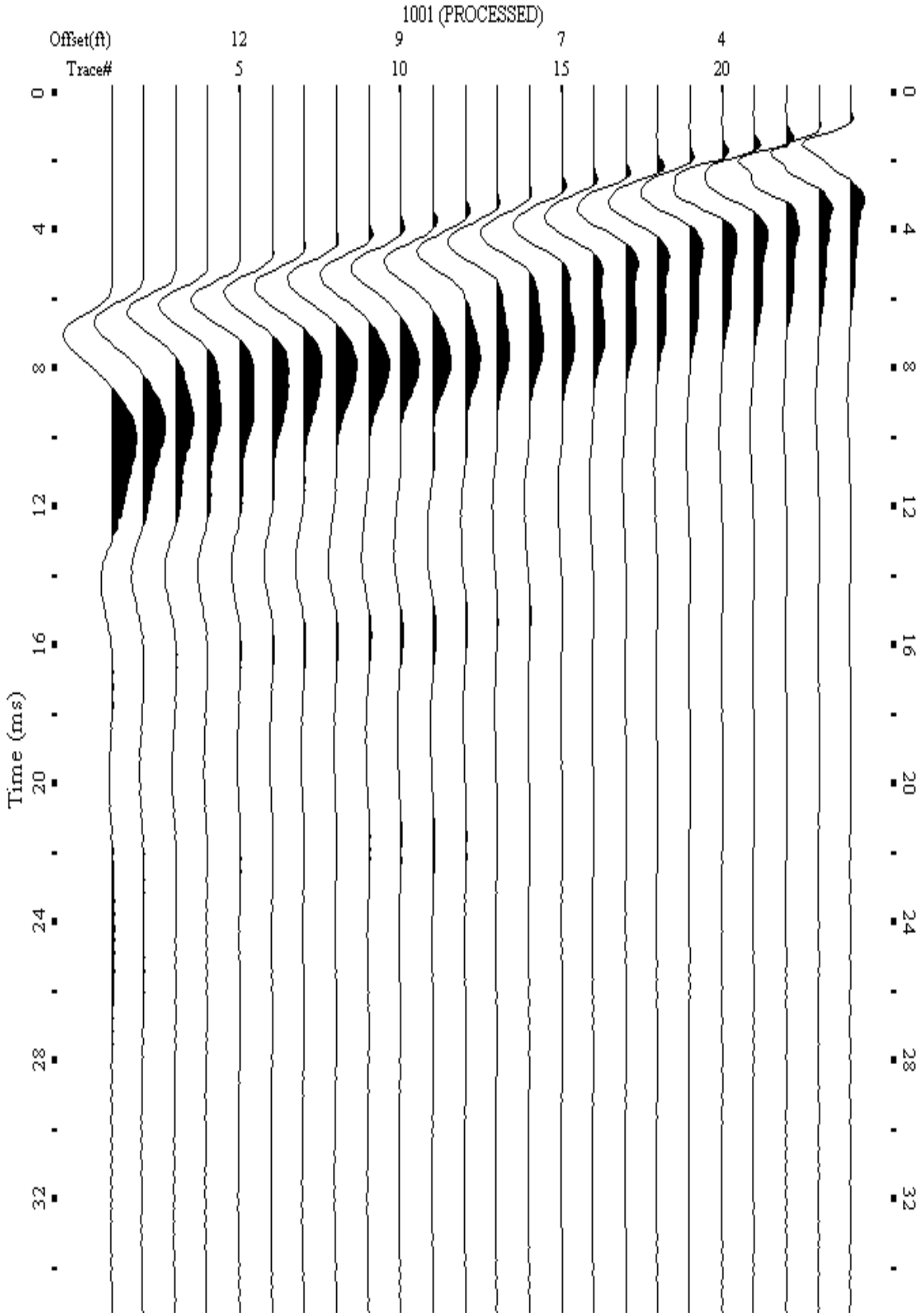

A.178: Shot Gather Line 1139 used in Post-blast 9

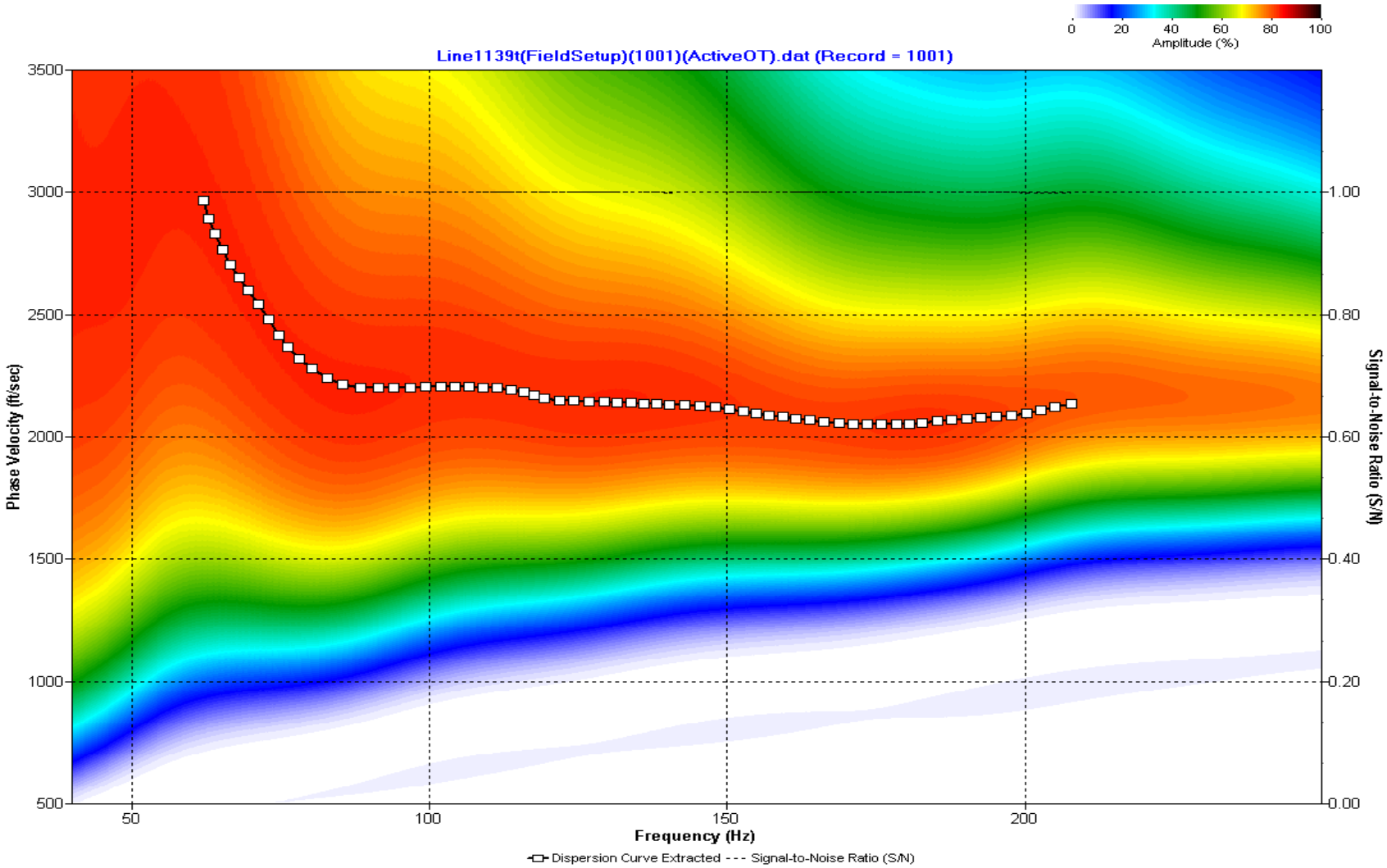

A.179: Dispersion Curve Line 1139 used in Post-blast 9

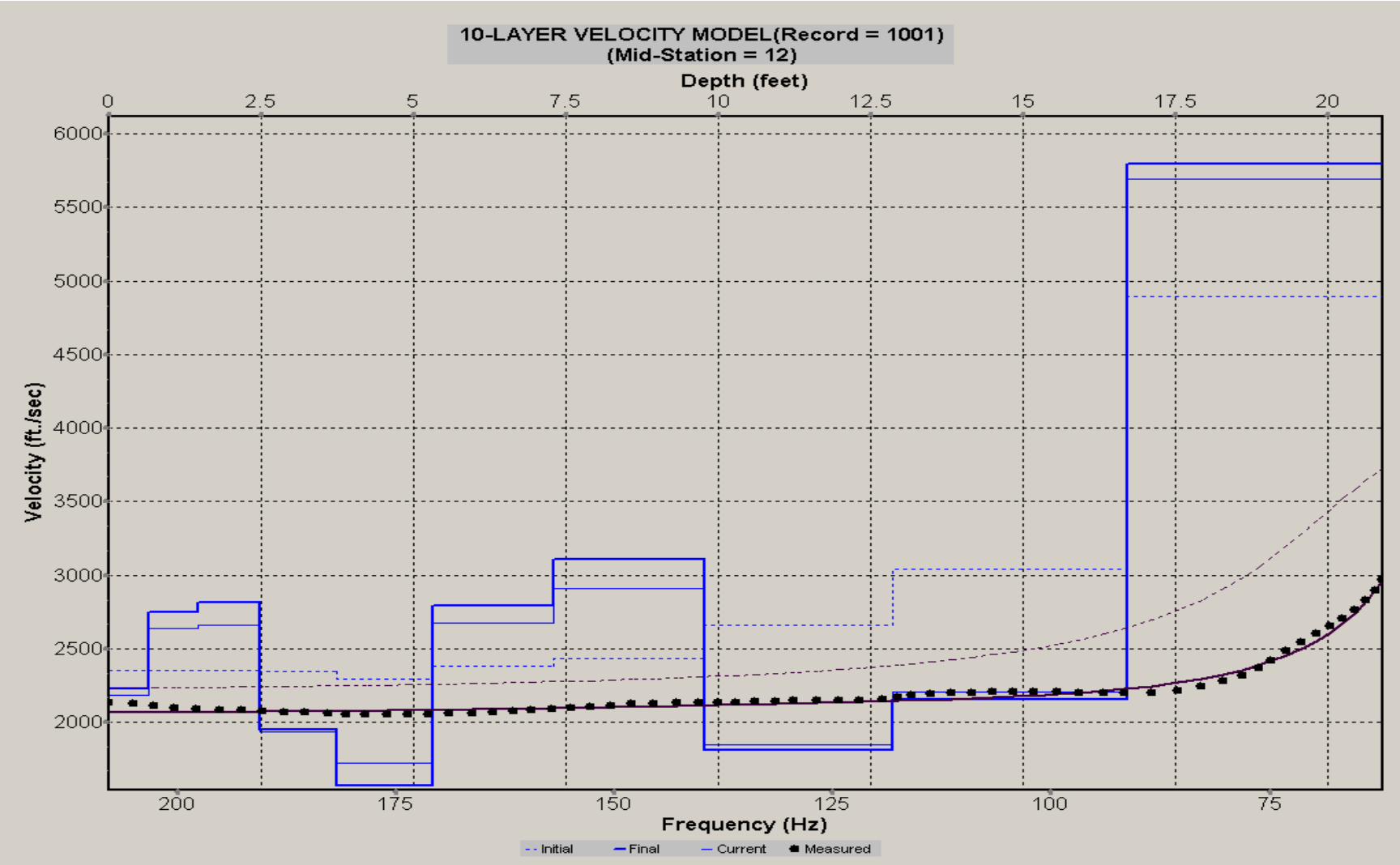

A.180: Velocity Profile Line 1139 used in Post-blast 9

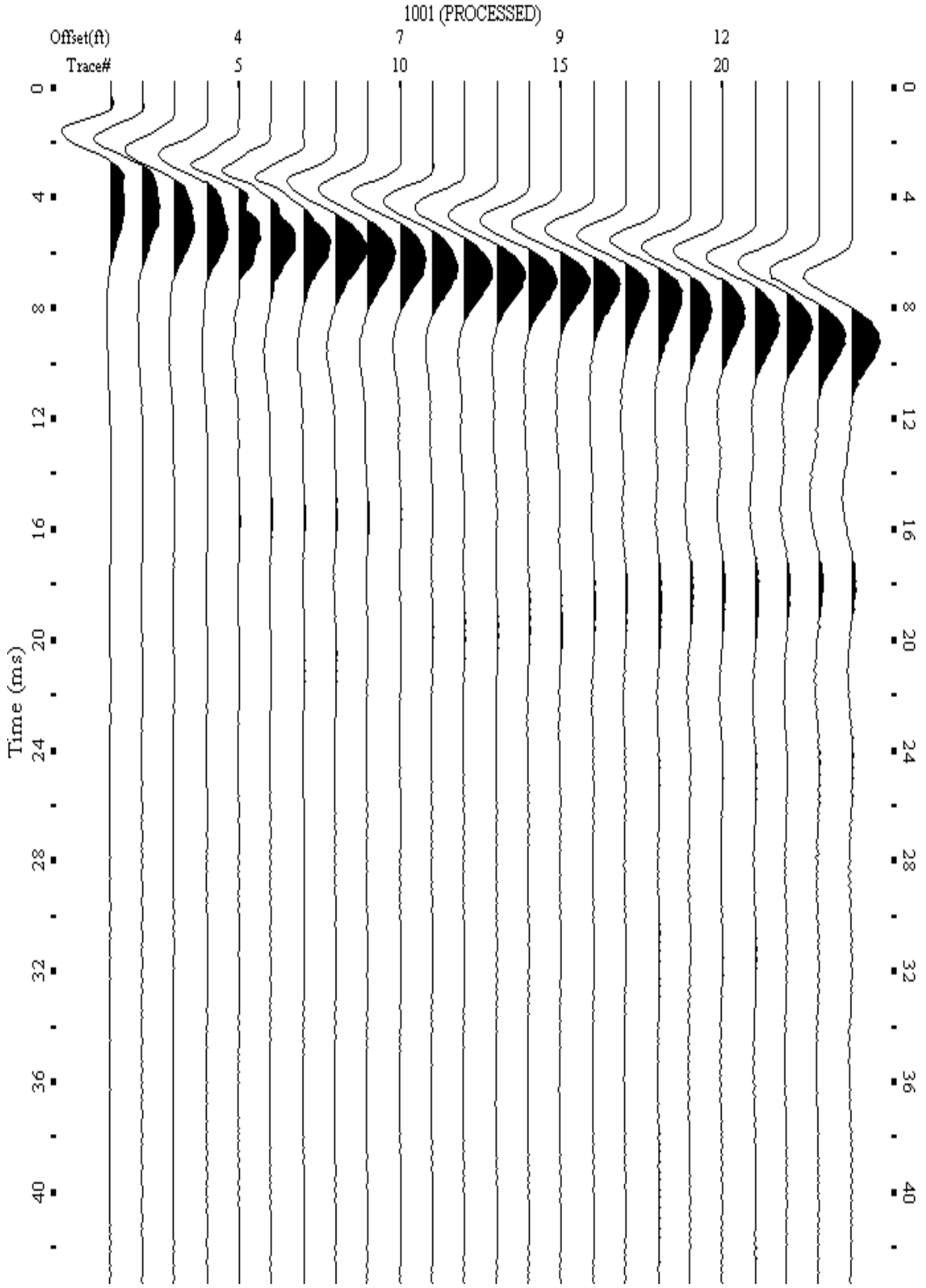

A.181: Shot Gather Line 1143 used in Post-blast 8 and Post-blast 9

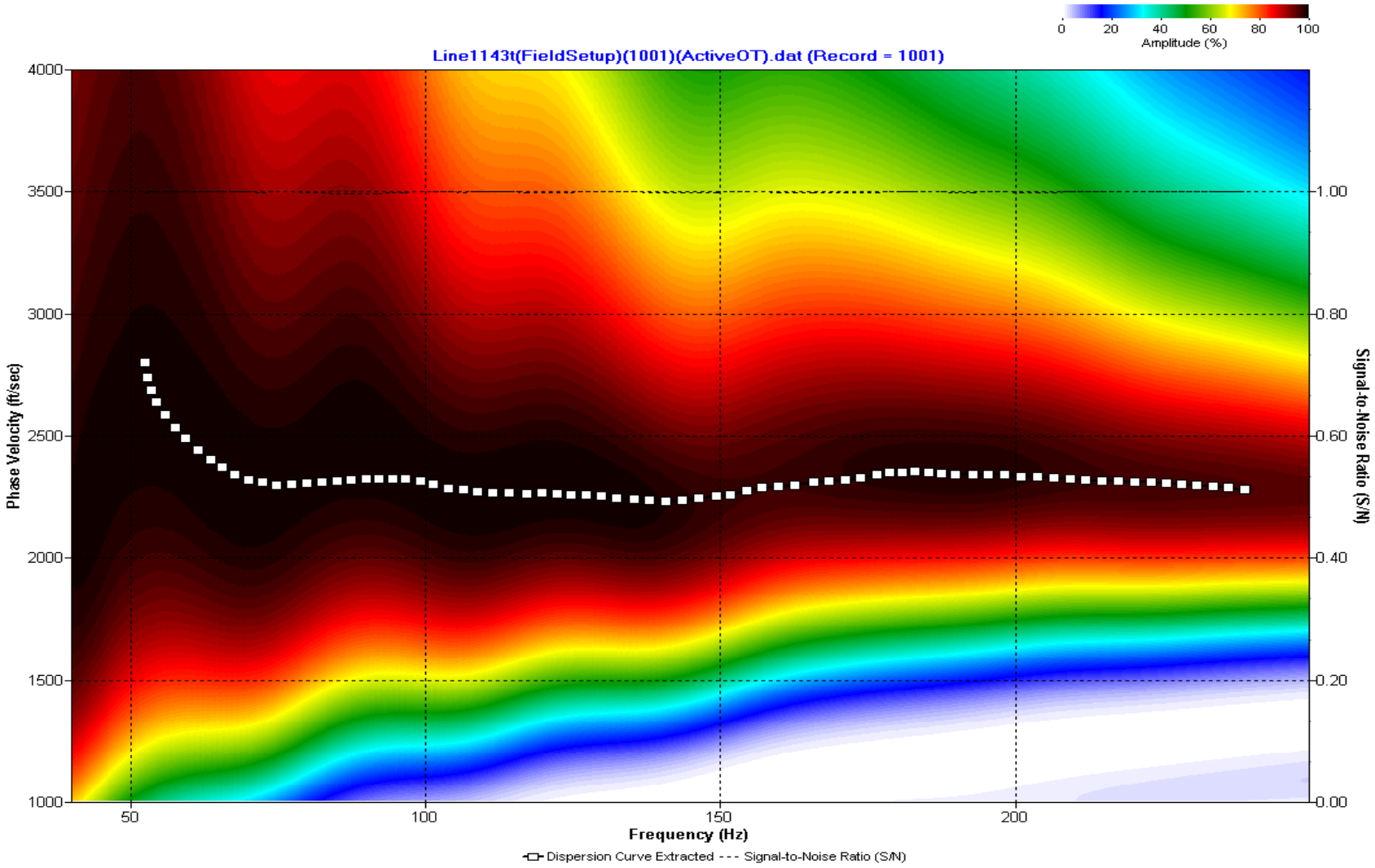

A.182: Dispersion Curve Line 1143 used in Post-blast 8 and Post-blast 9

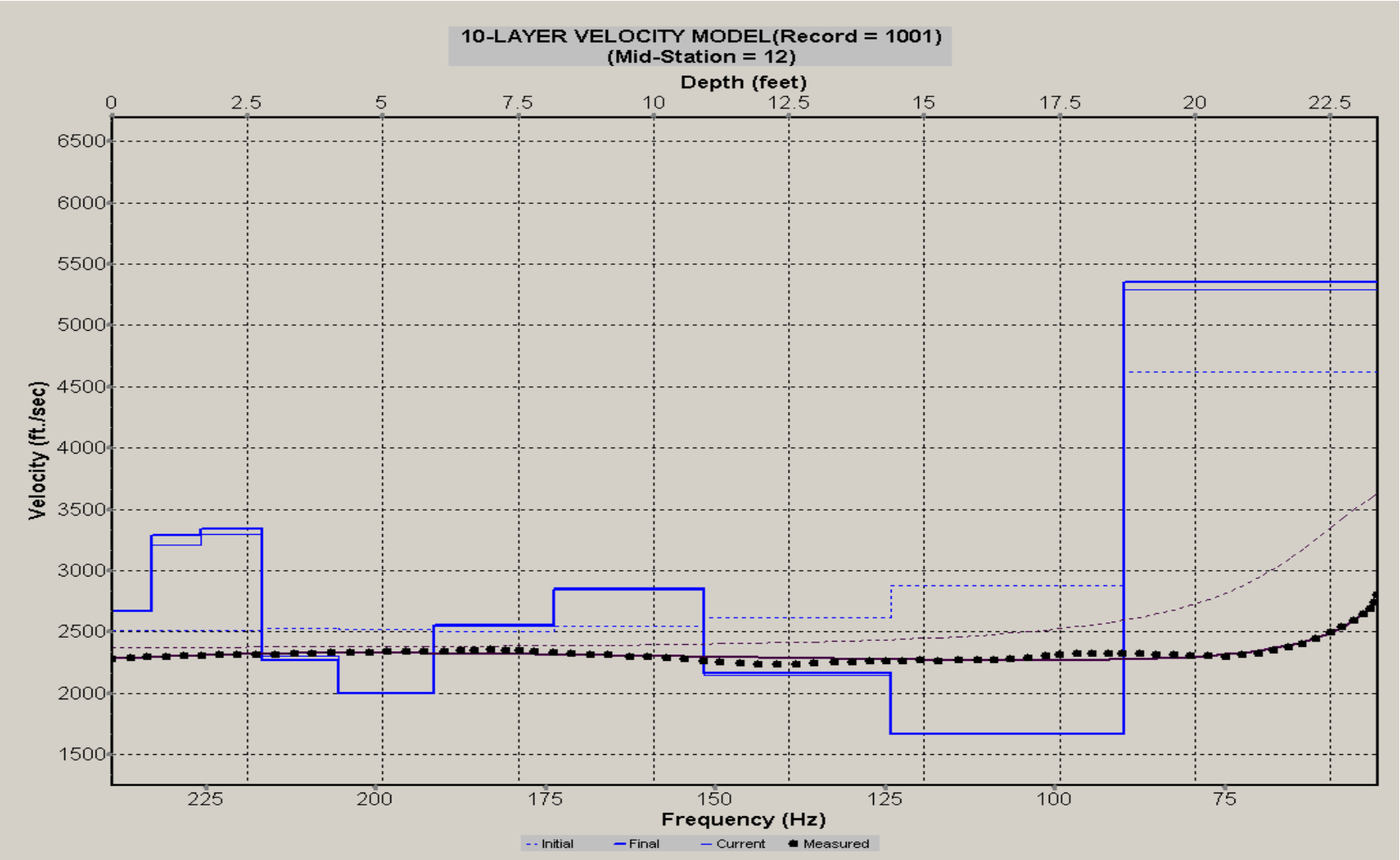

A.183: Velocity Profile Line 1143 used in Post-blast 8 and Post-blast 9

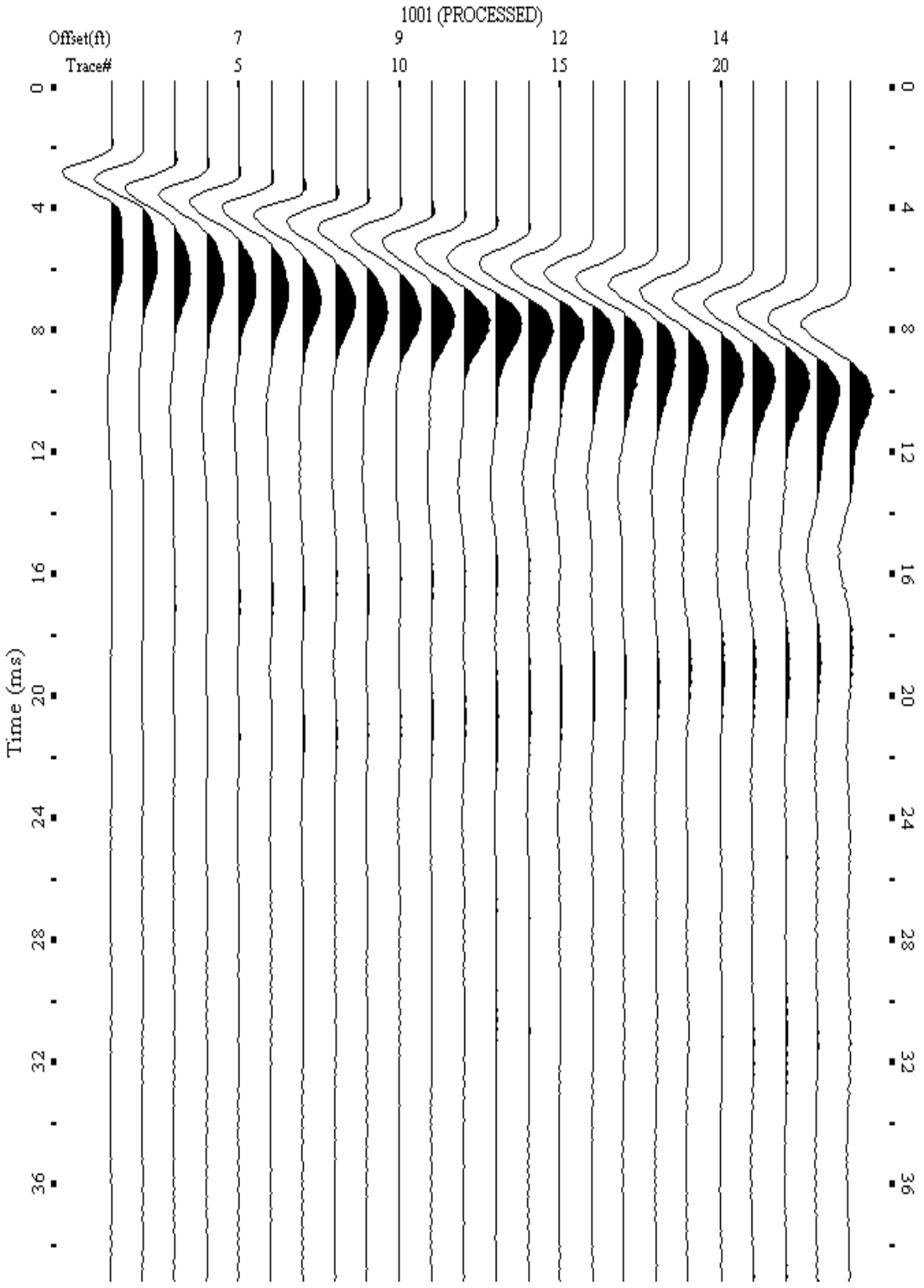

A.184: Shot Gather Line 1144 used in Post-blast 8 and Post-blast 9

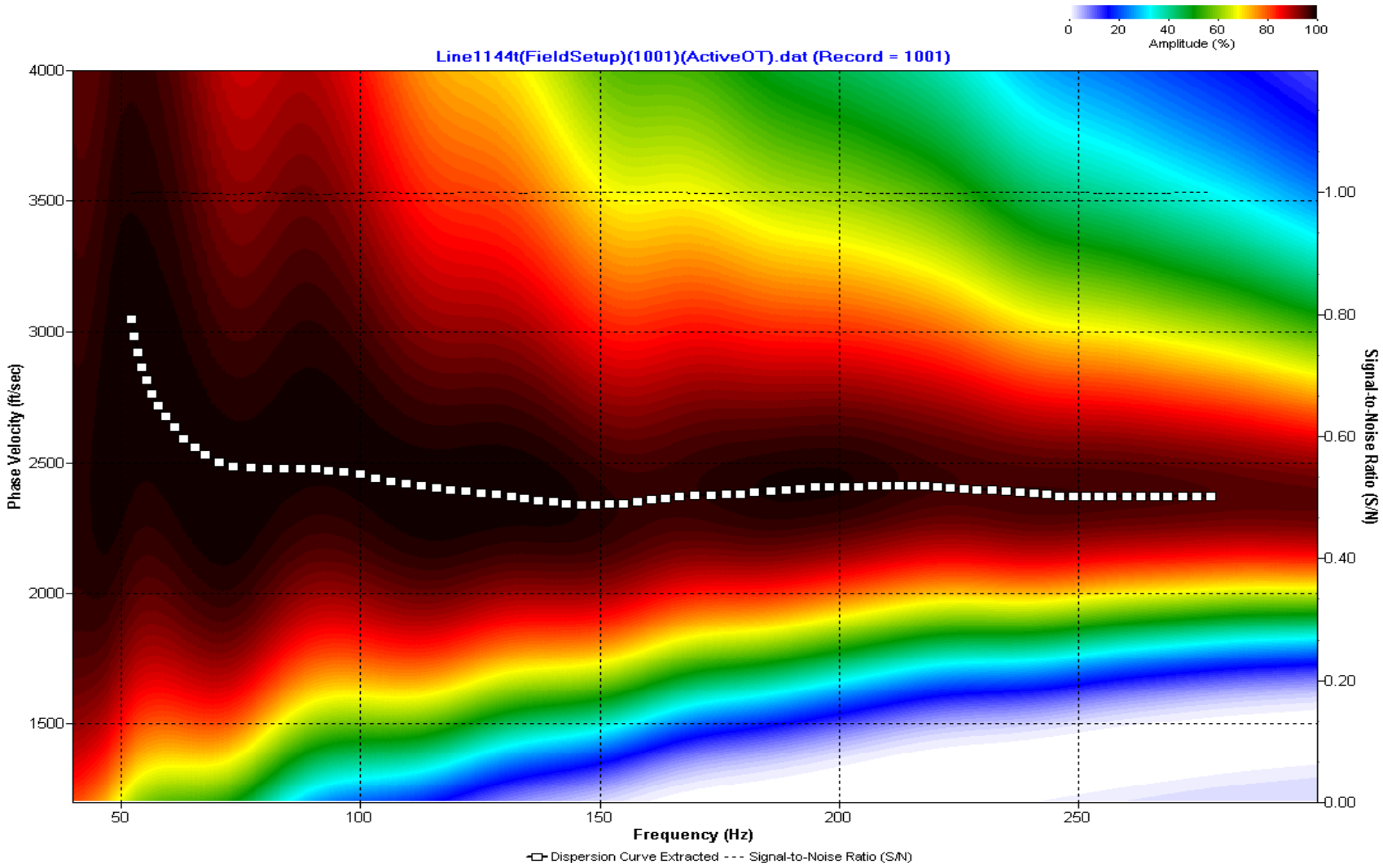

A.185: Dispersion Curve Line 1144 used in Post-blast 8 and Post-blast 9

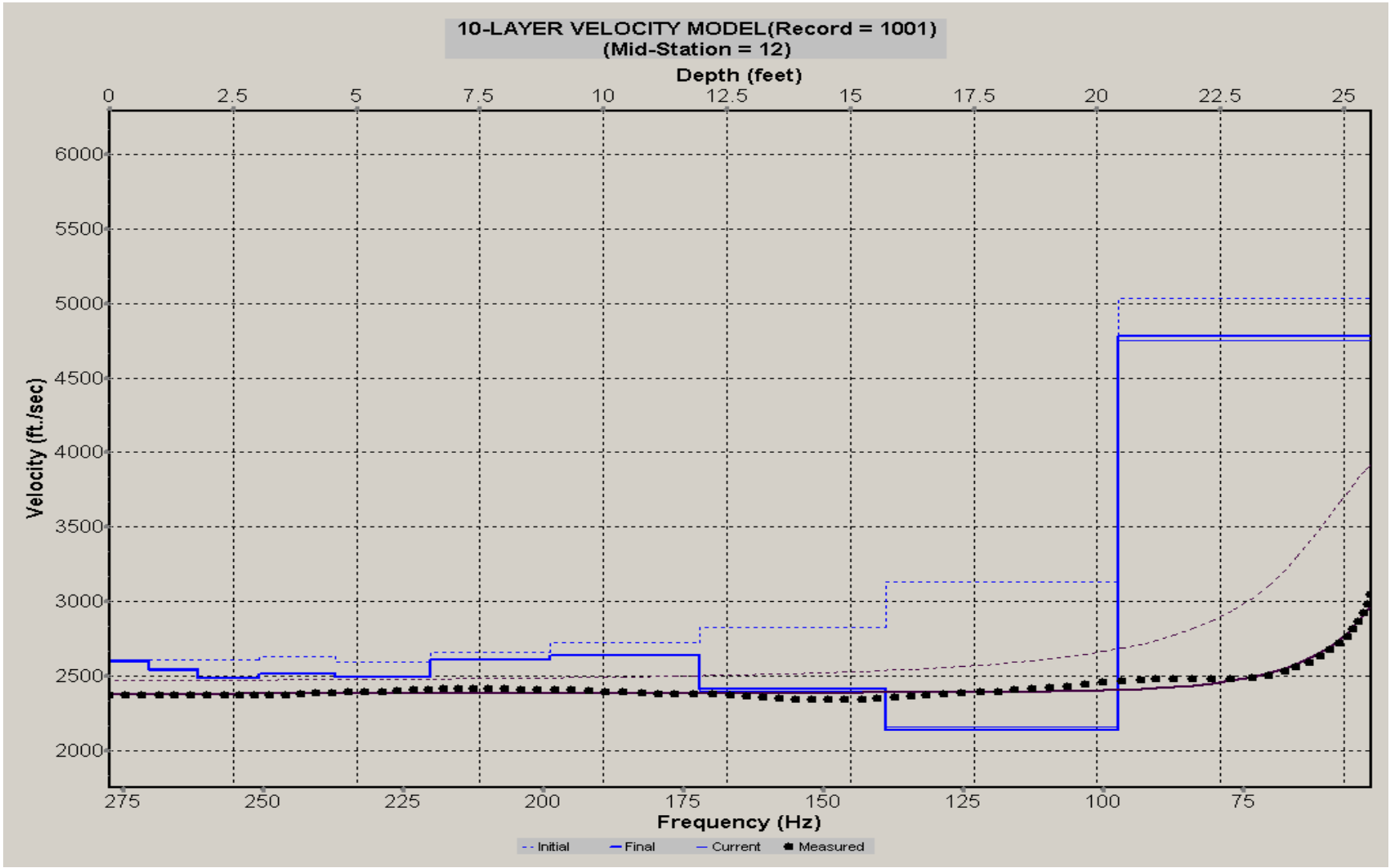

A.186: Velocity Profile Line 1144 used in Post-blast 8 and Post-blast 9

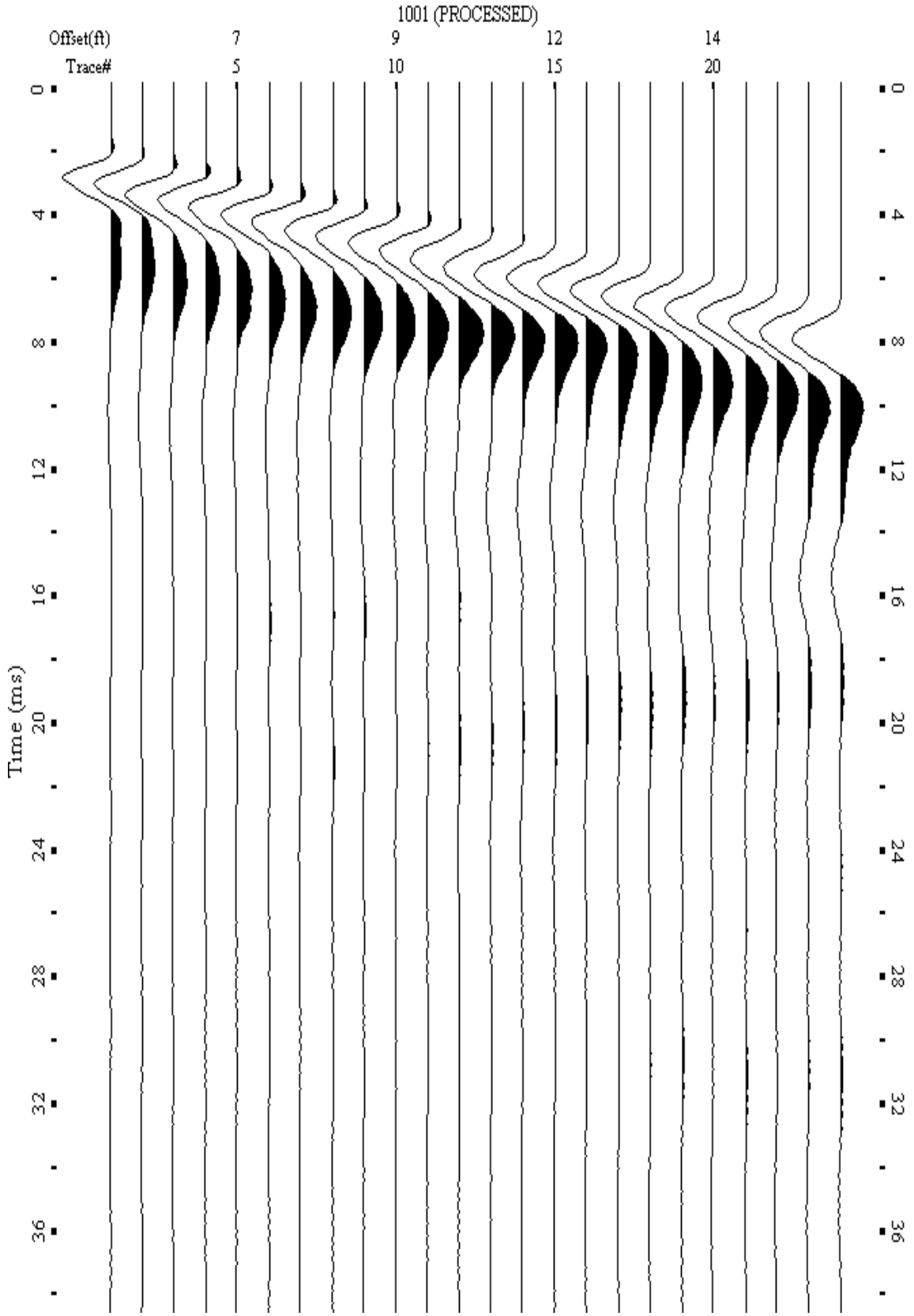

A.187: Shot Gather Line 1145 used in Post-blast 8 and Post-blast 9

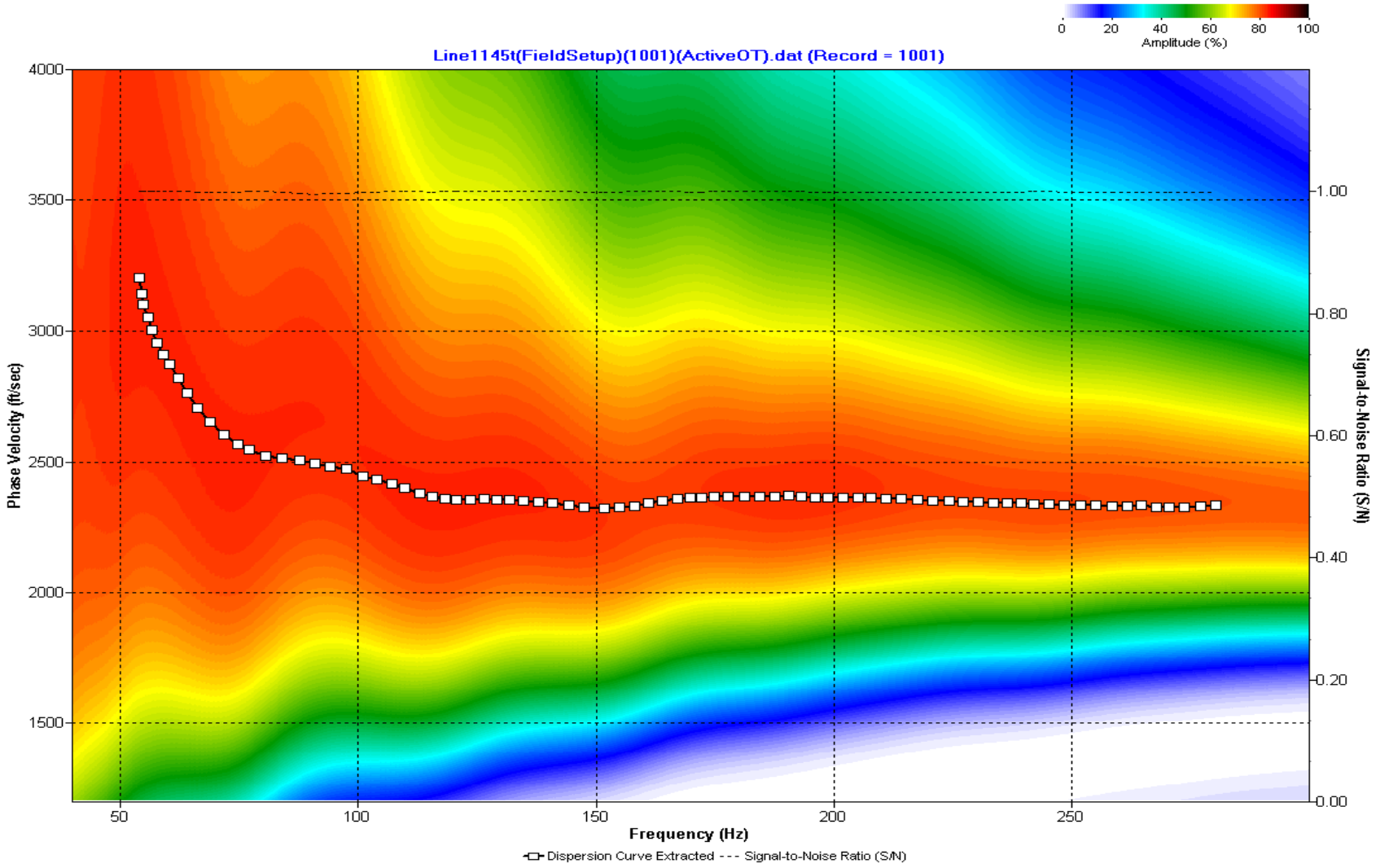

A.188: Dispersion Curve Line 1145 used in Post-blast 8 and Post-blast 9

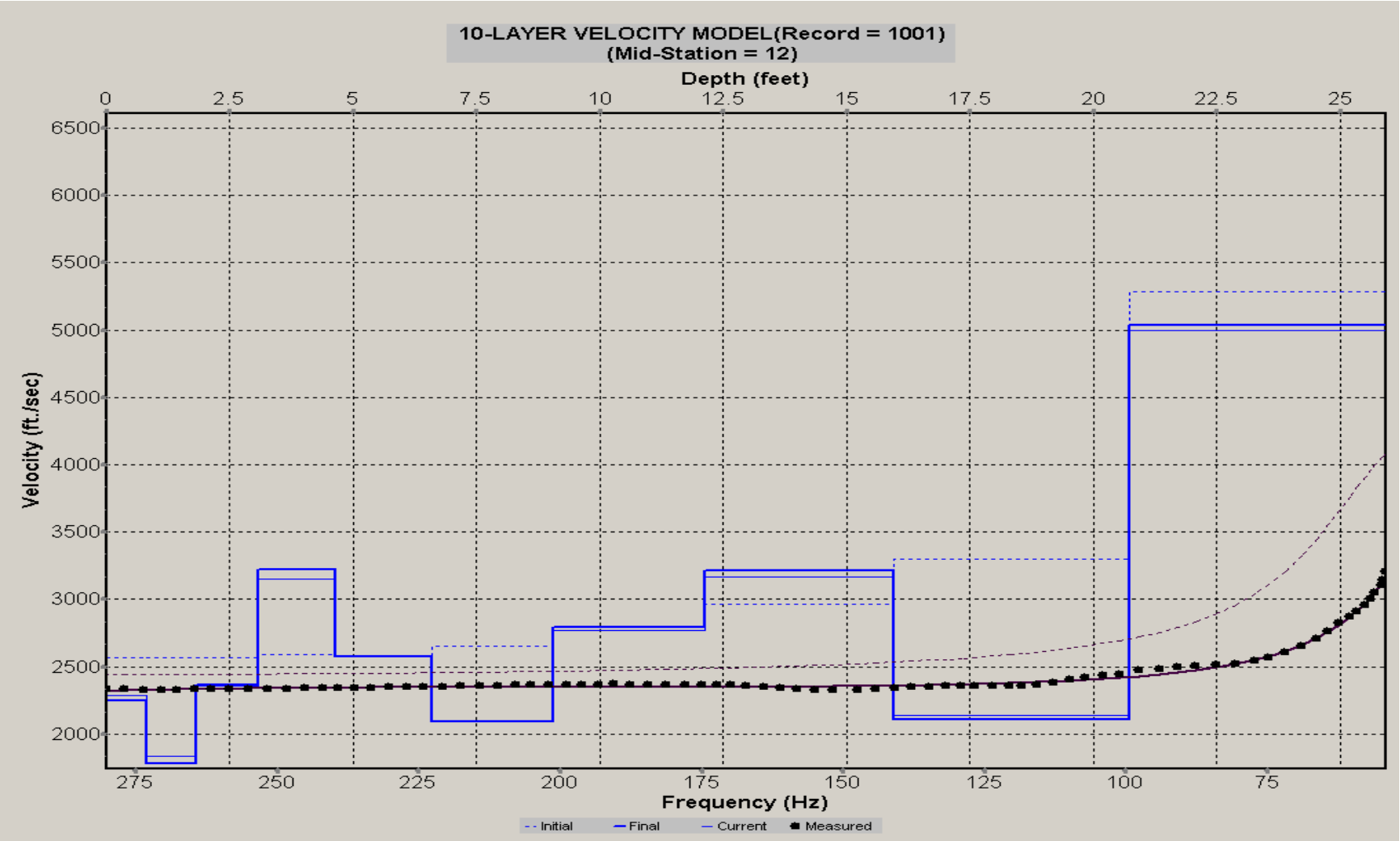

A.189: Velocity Profile Line 1145 used in Post-blast 8 and Post-blast 9

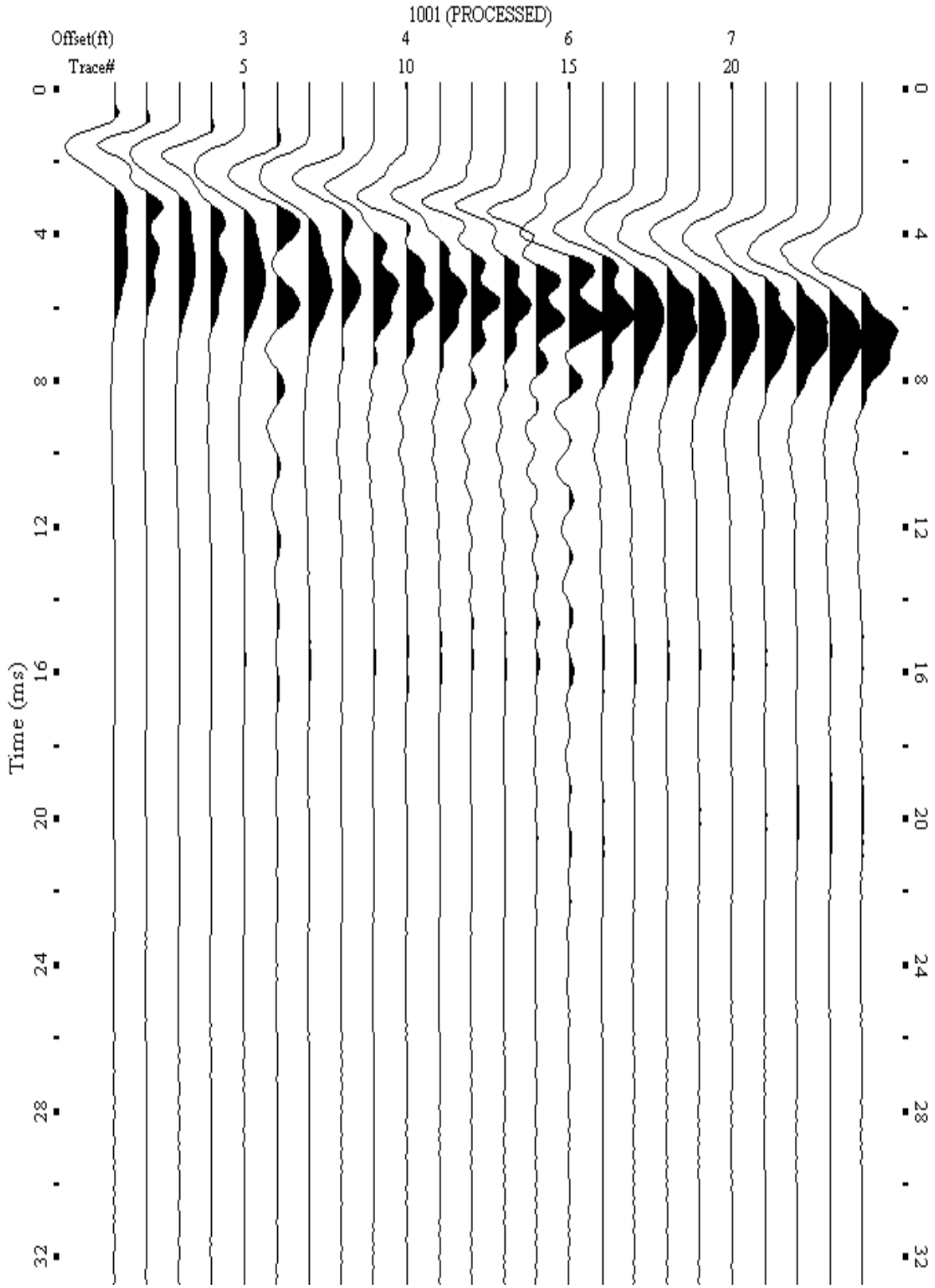

A.190: Shot Gather Line 1146 used in Post-blast 9

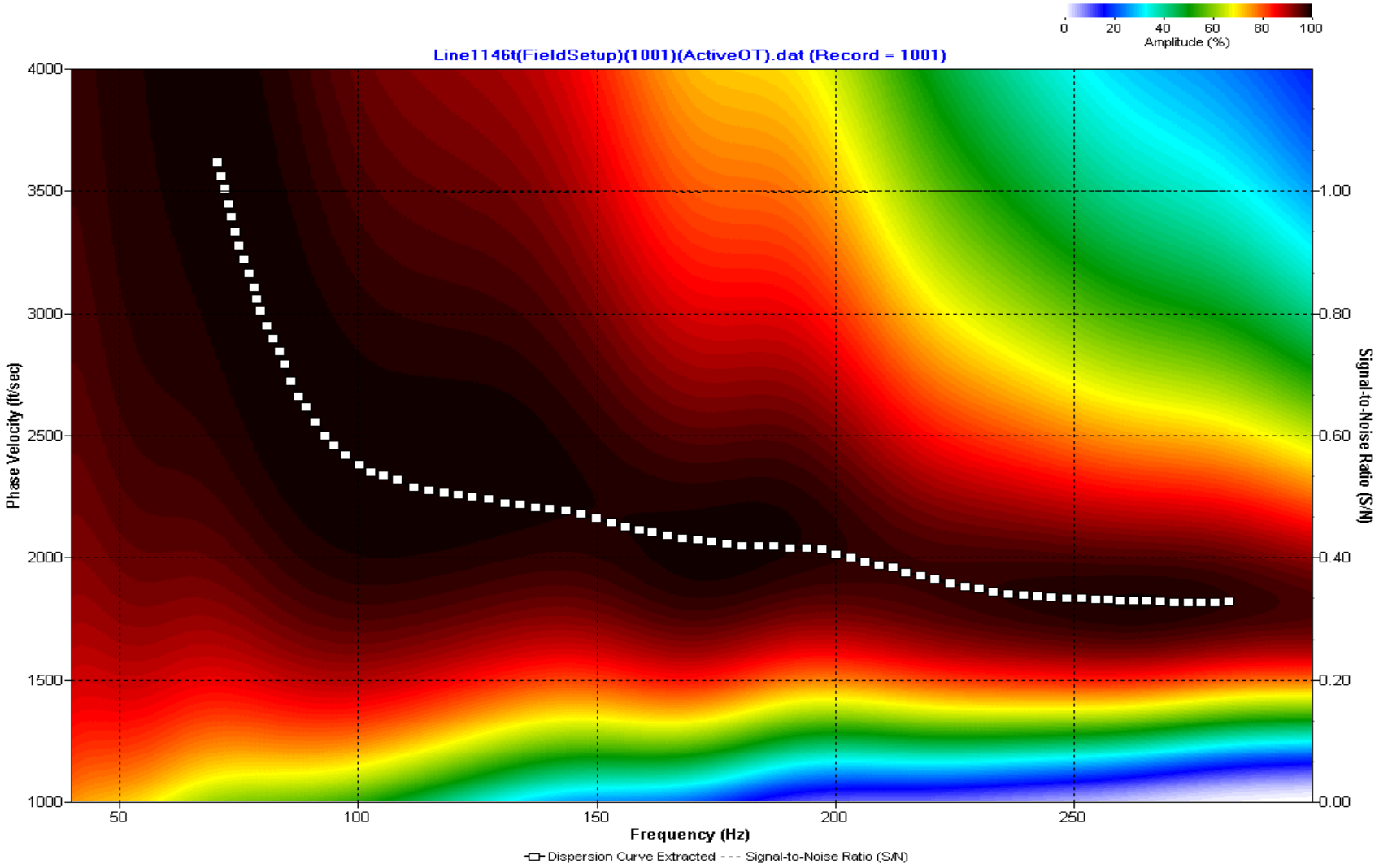

A.191: Dispersion Curve Line 1146 used in Post-blast 9

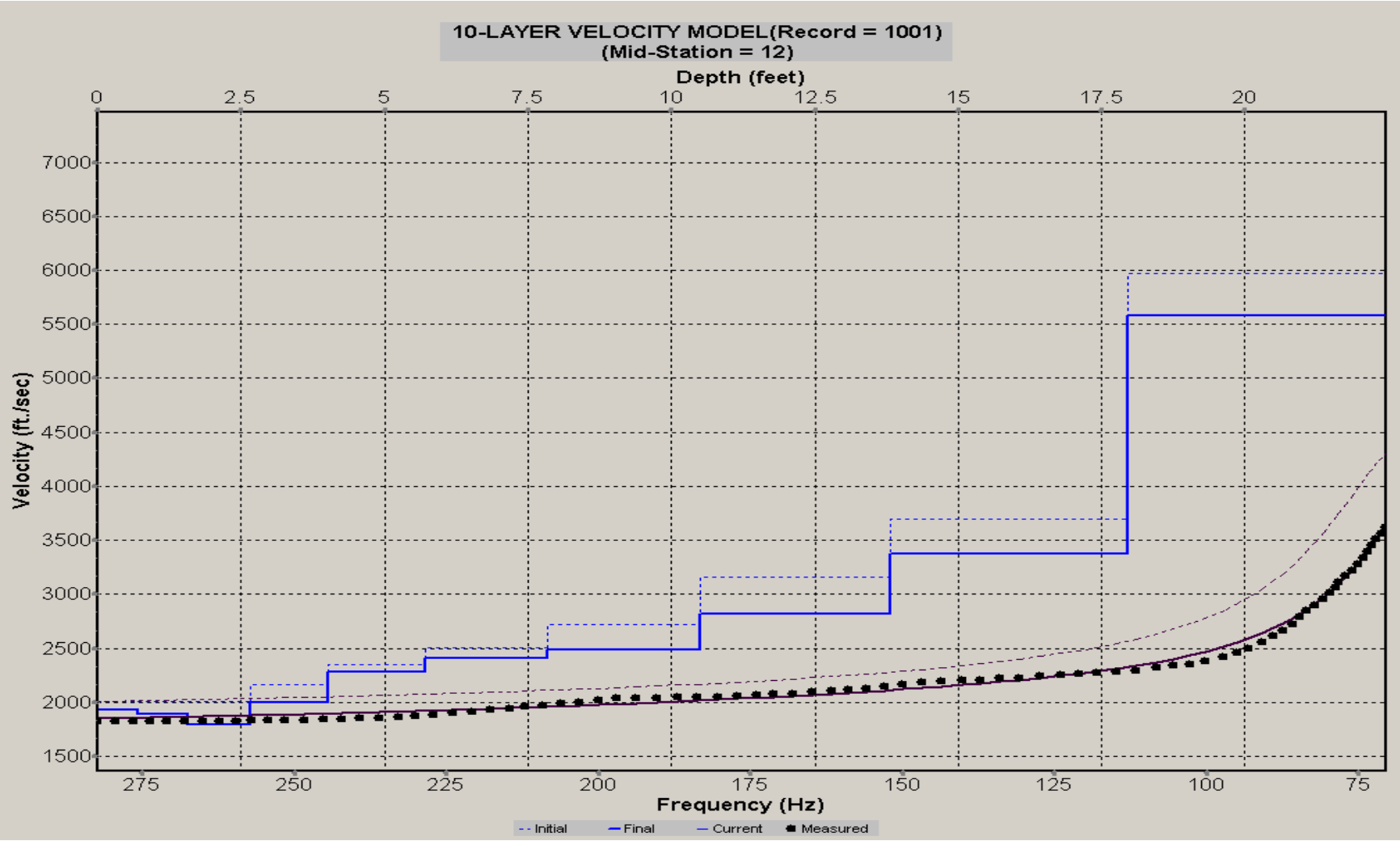

A.192: Velocity Profile Line 1146 used in Post-blast 9

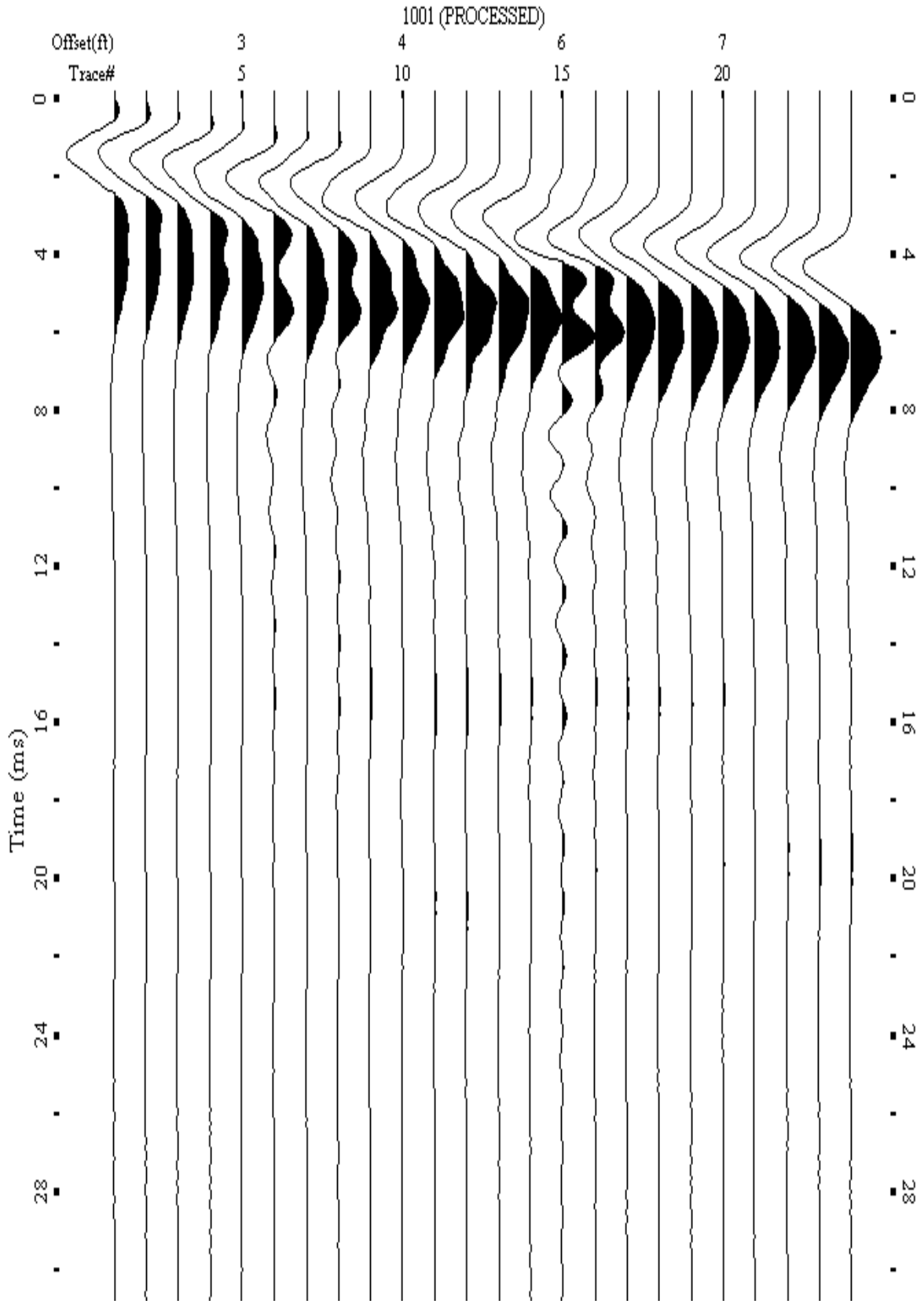

A.193: Shot Gather Line 1147 used in Post-blast 9

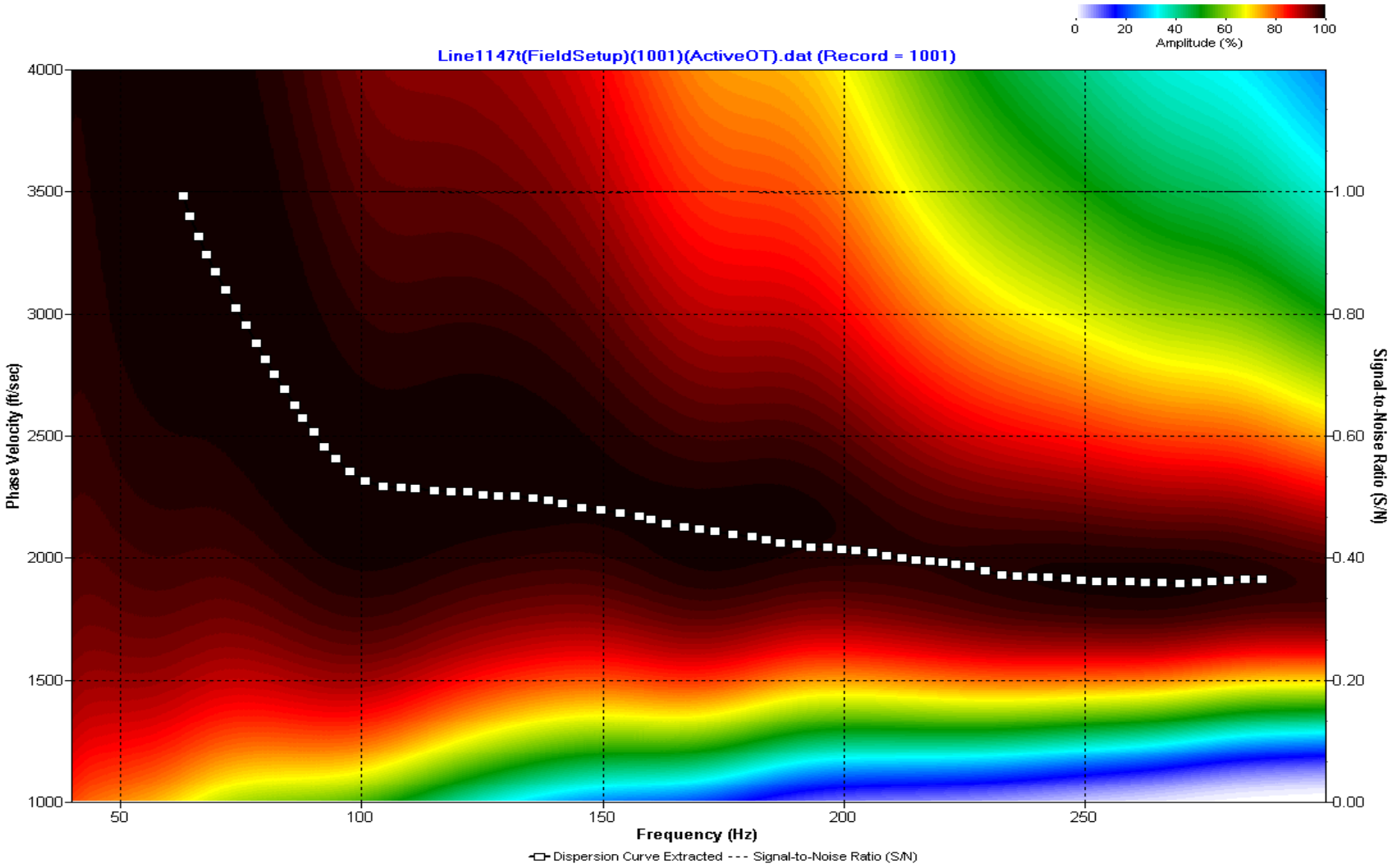

A.194: Dispersion Curve Line 1147 used in Post-blast 9

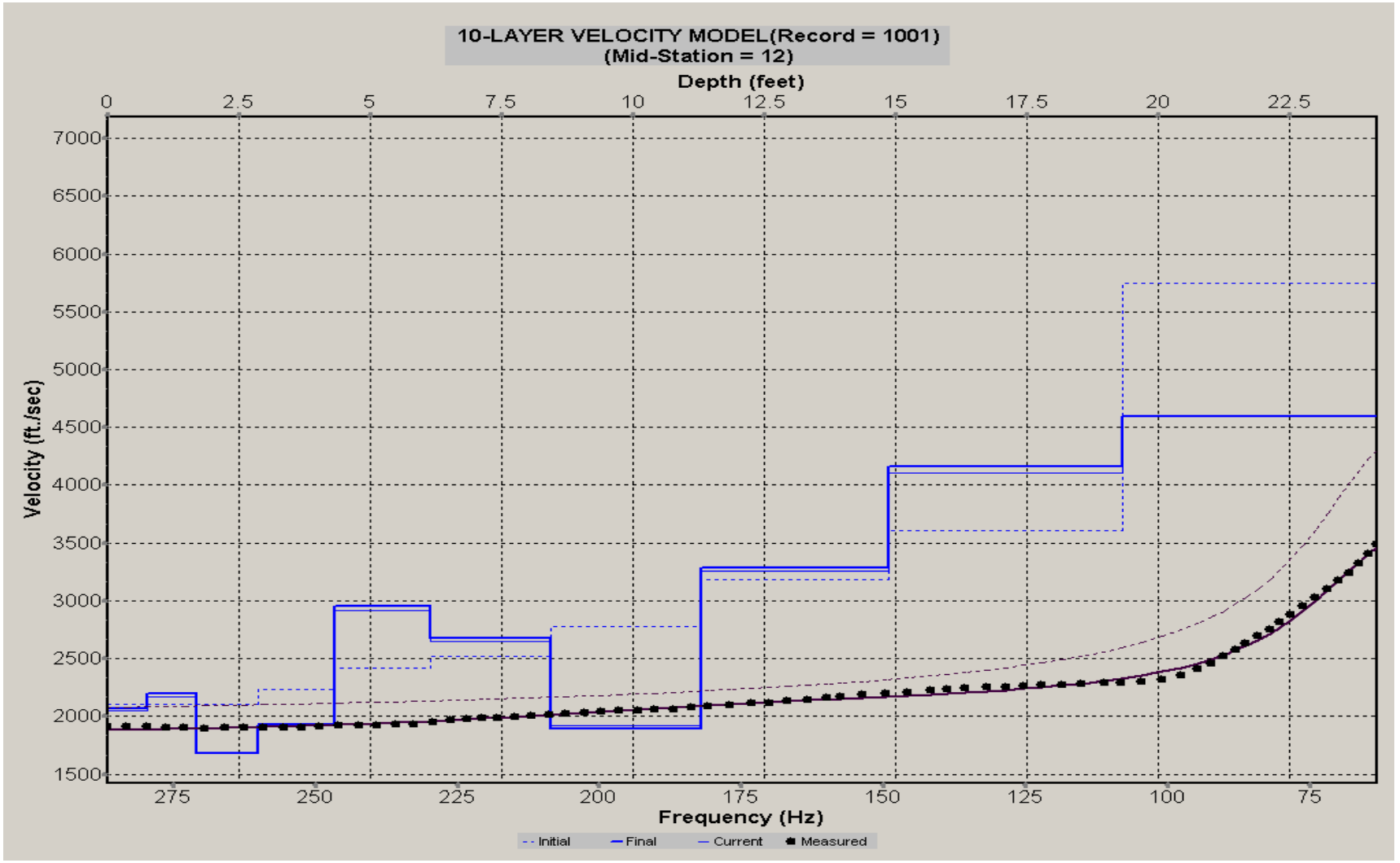

A.195: Velocity Profile Line 1147 used in Post-blast 9

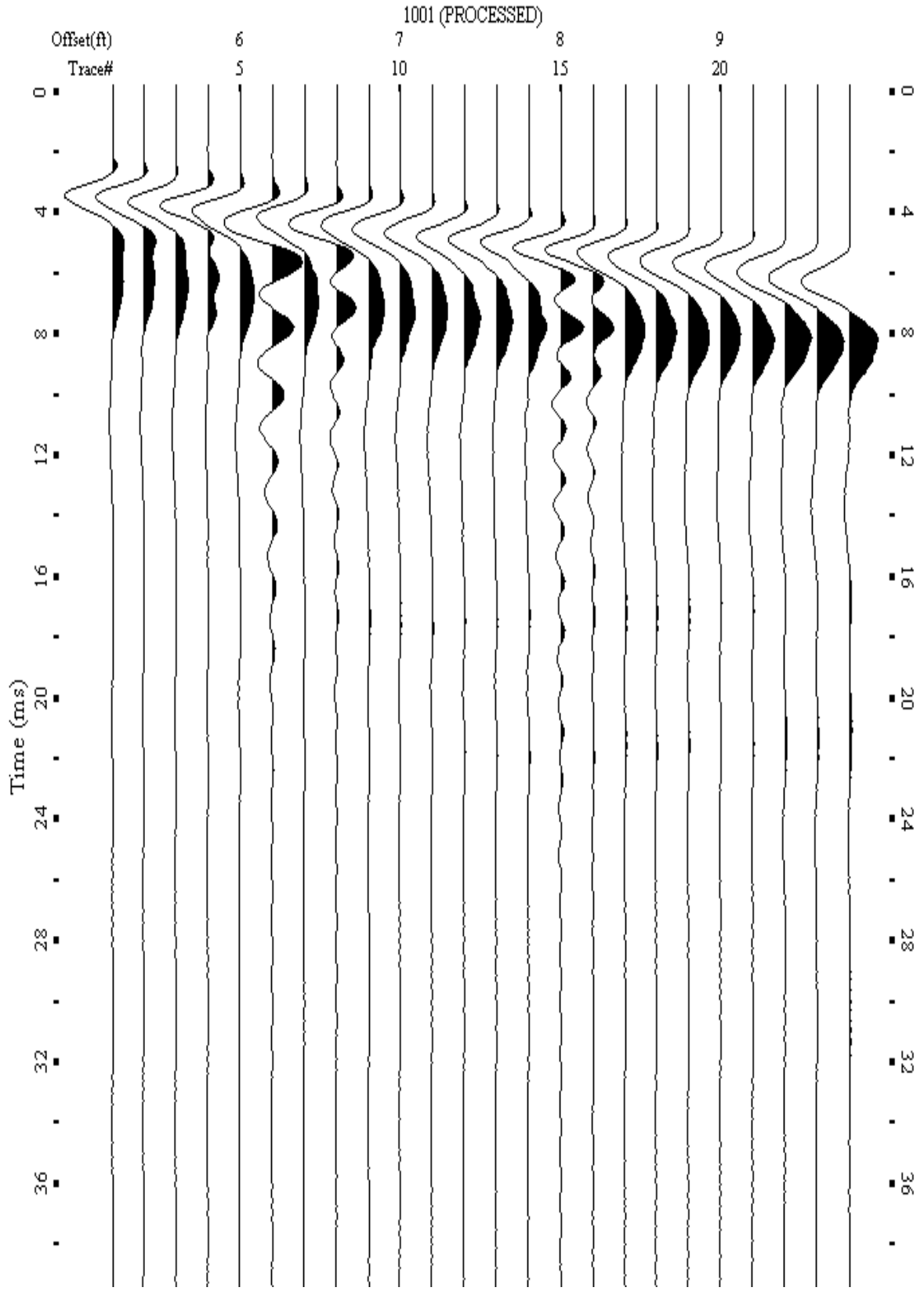

A.196: Shot Gather Line 1148 used in Post-blast 9

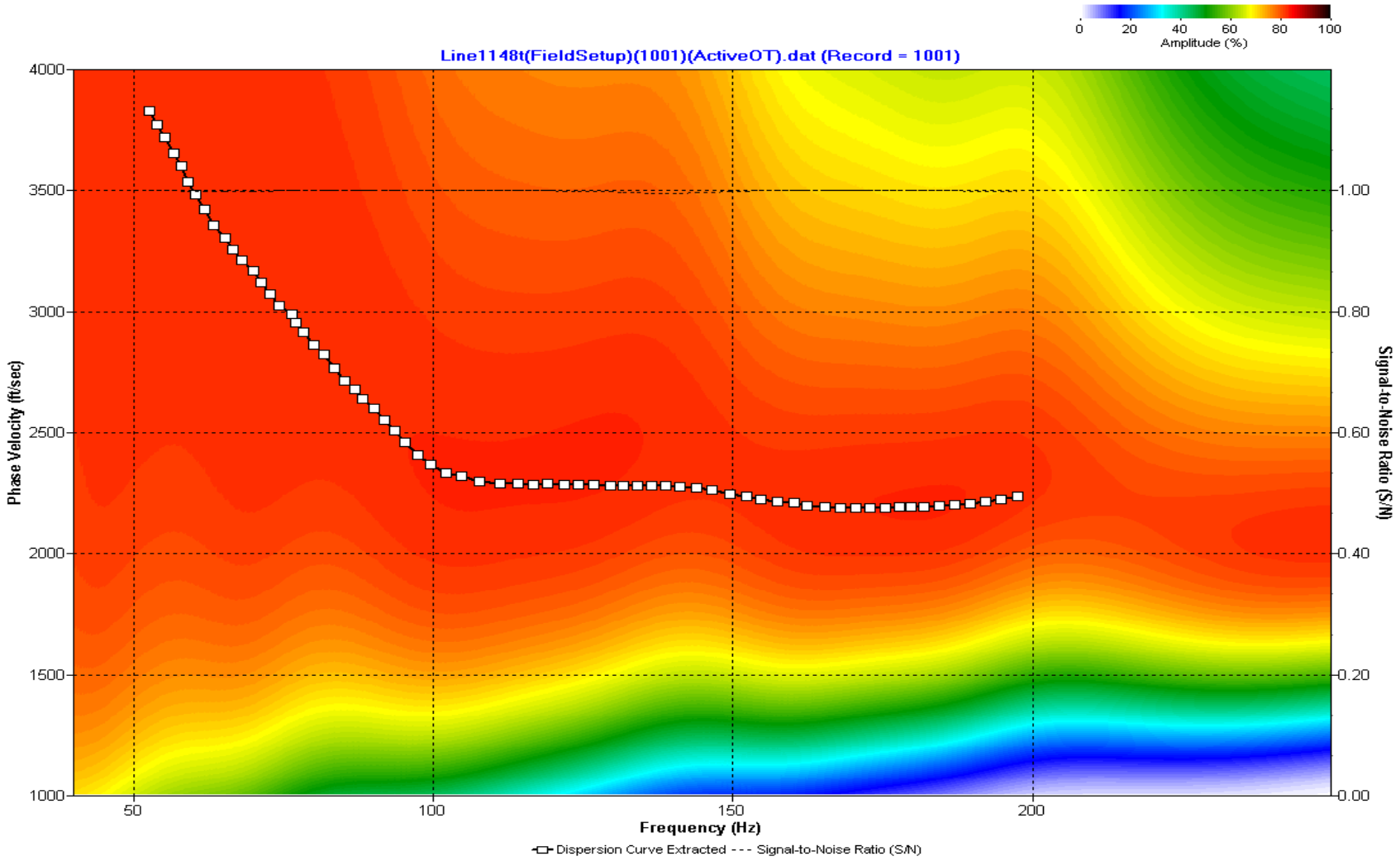

A.197: Dispersion Curve Line 1148 used in Post-blast 9

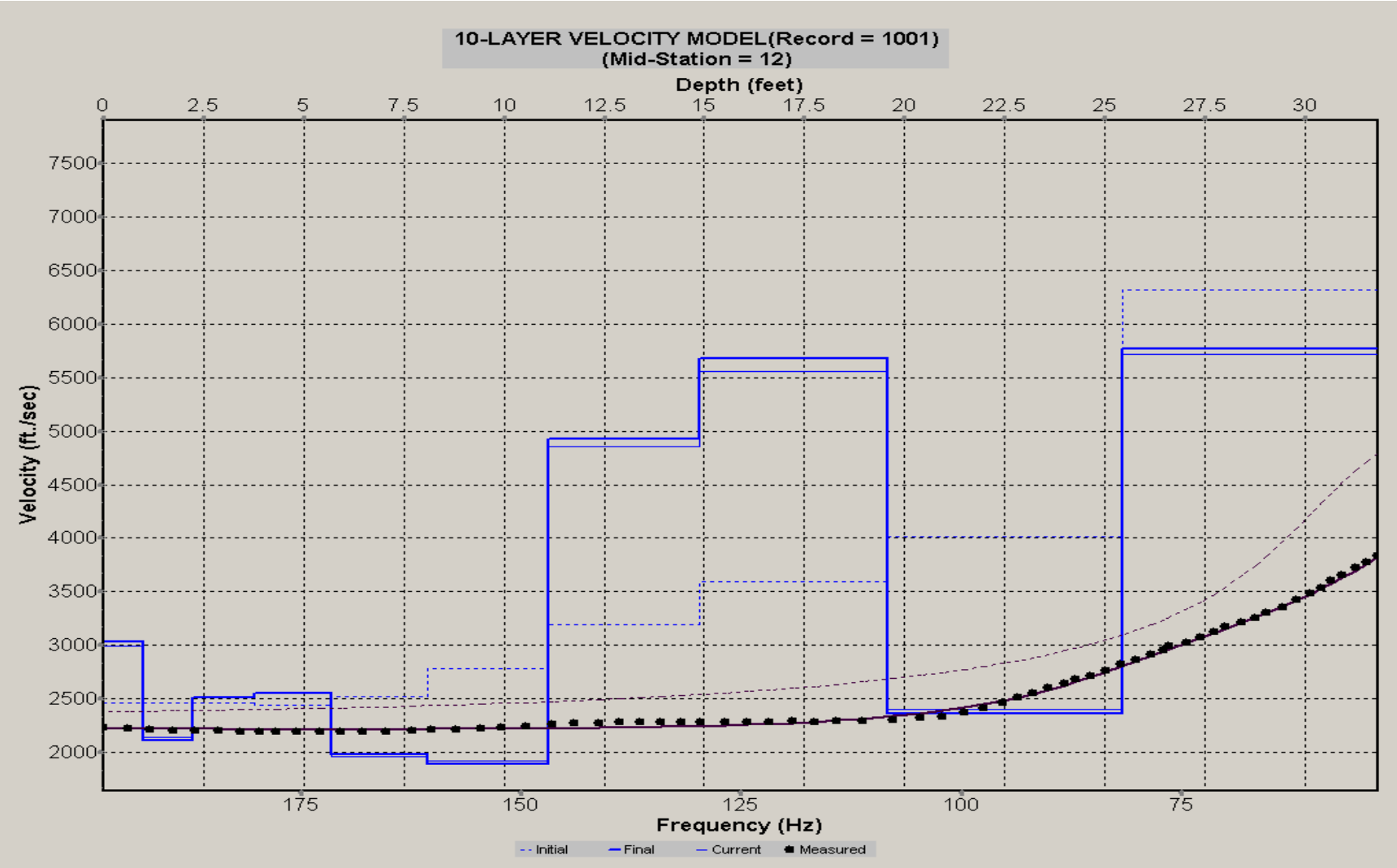

A.198: Velocity Profile Line 1148 used in Post-blast 9

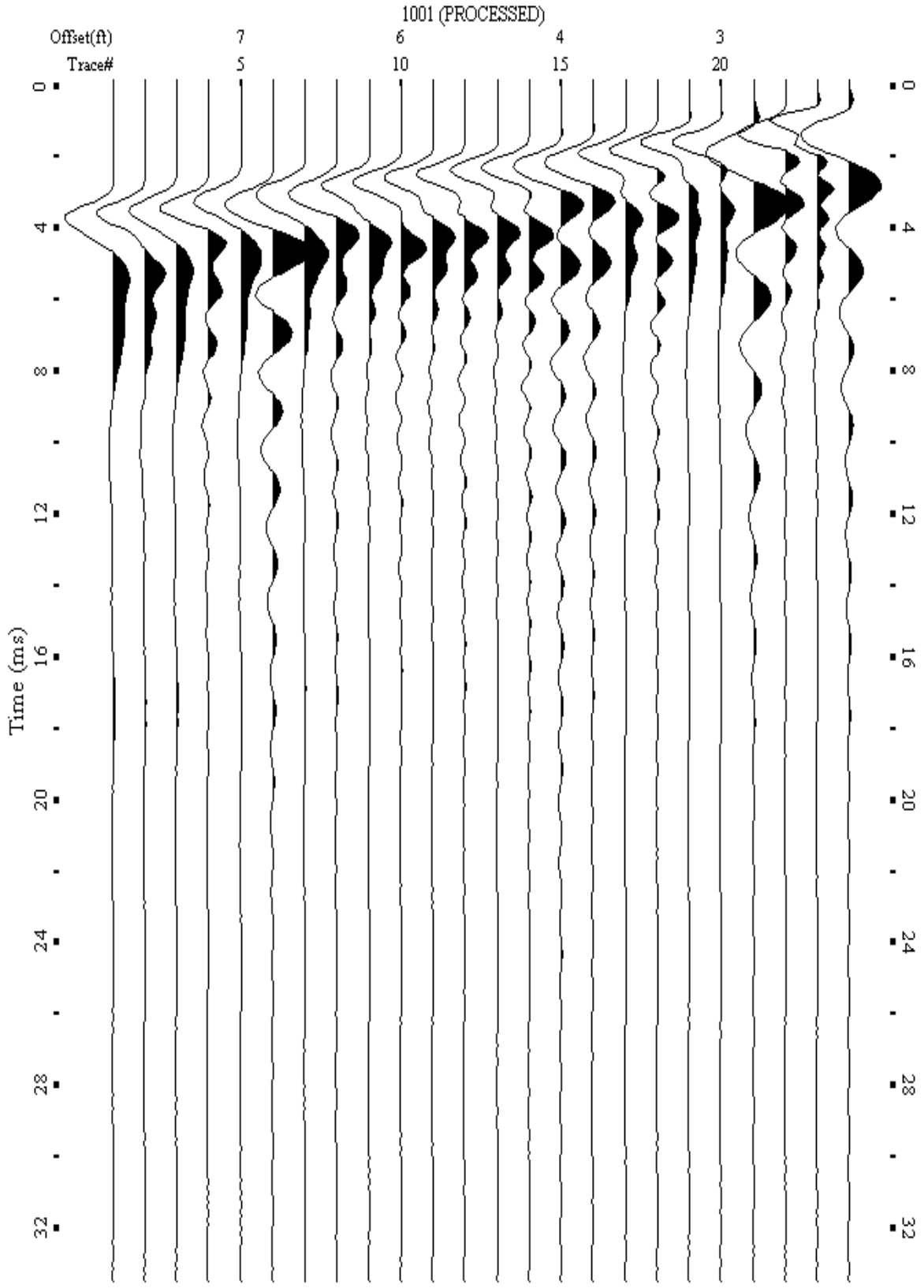

A.199: Shot Gather Line 1150 used in Post-blast 9

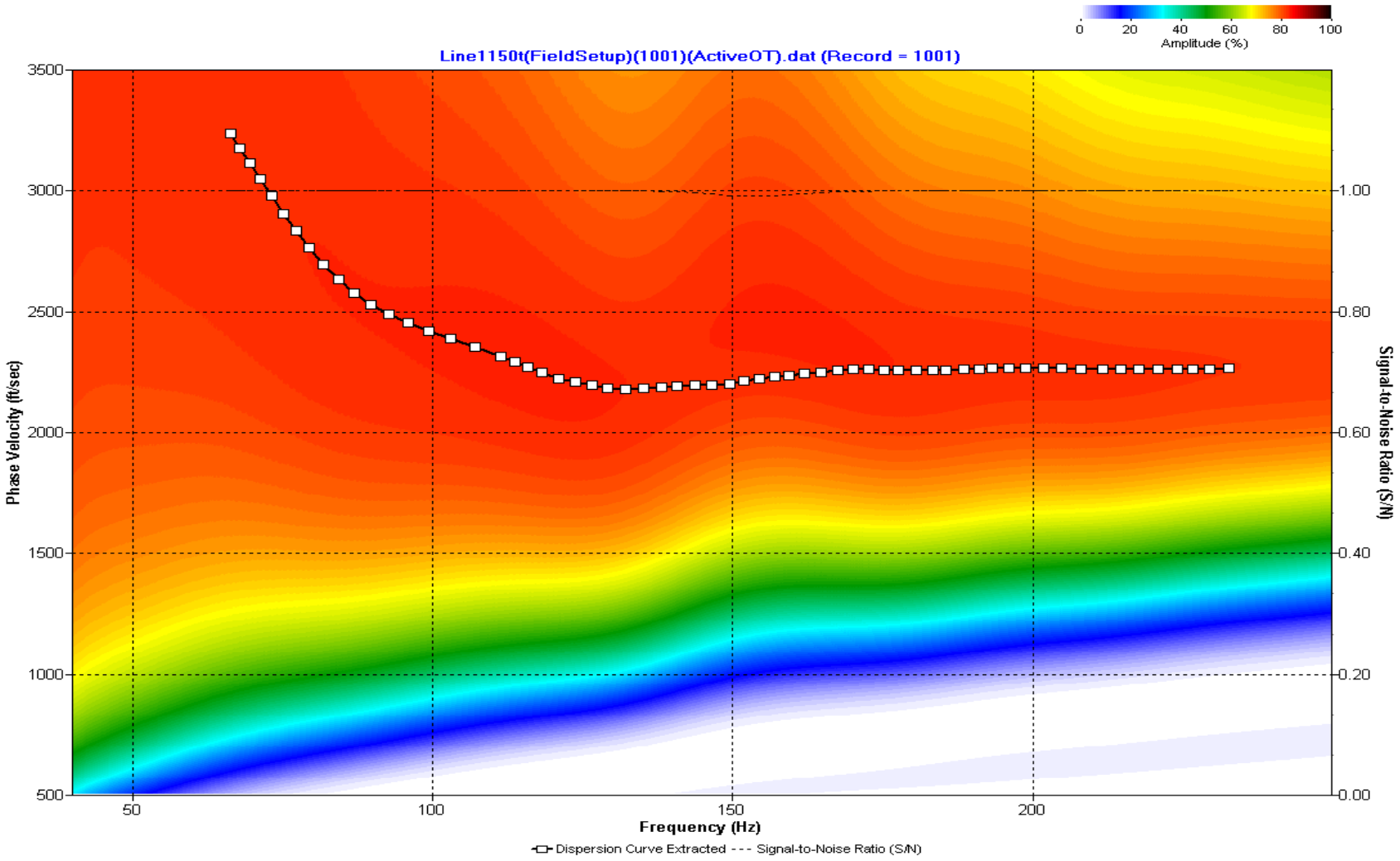

A.200: Dispersion Curve Line 1150 used in Post-blast 9

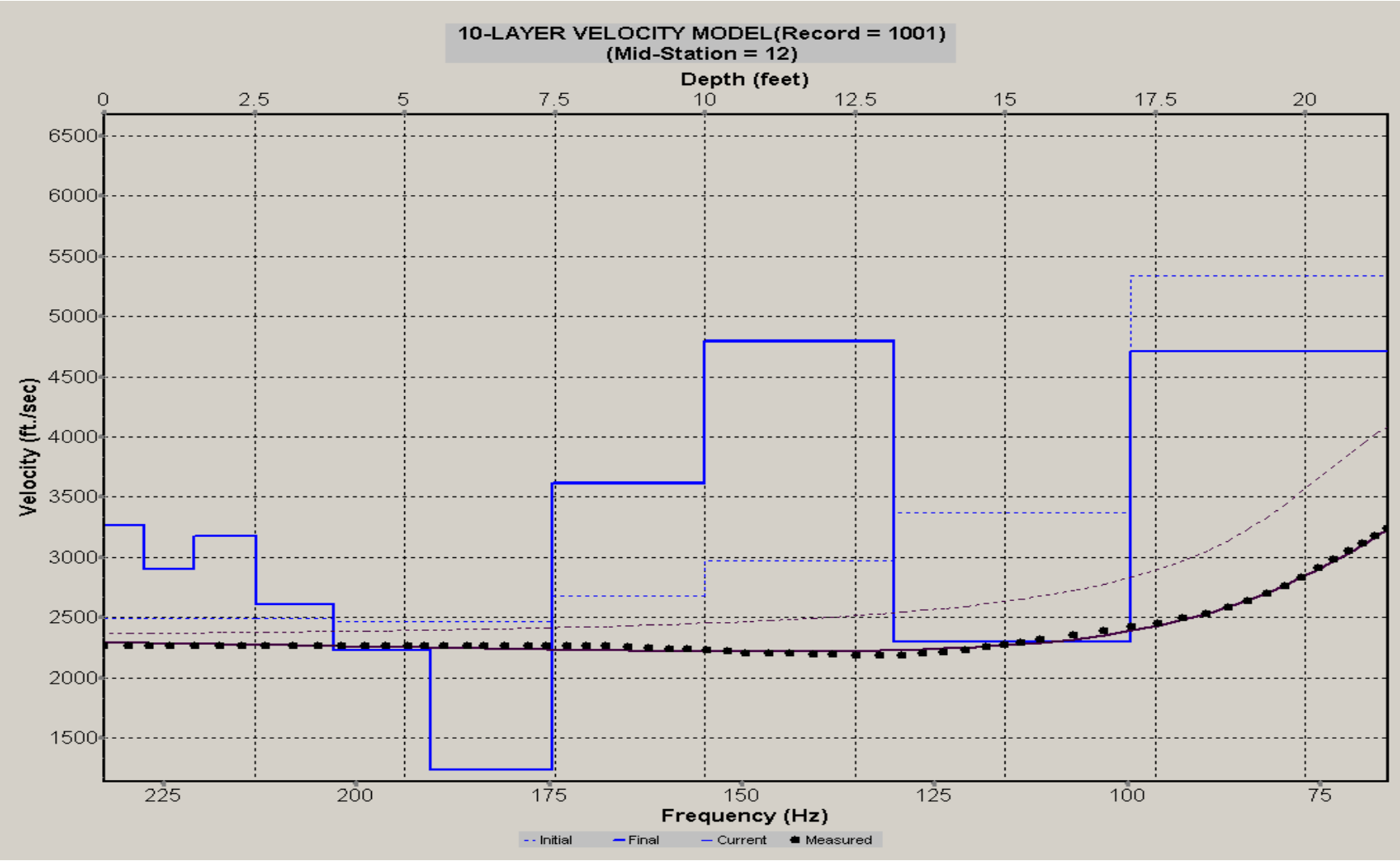

A.201: Velocity Profile Line 1150 used in Post-blast 9

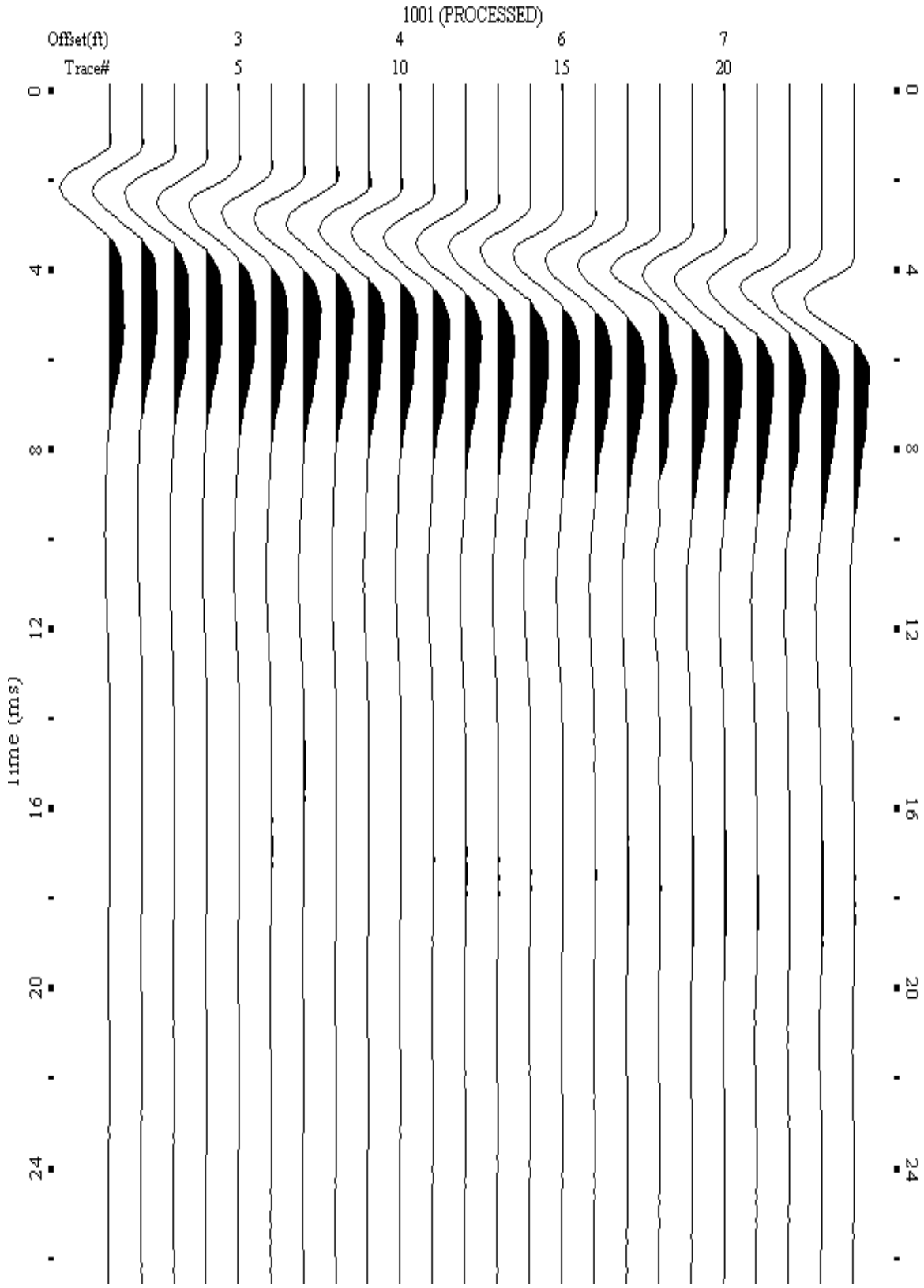

A.202: Shot Gather Line 1154 used in Post-blast 16

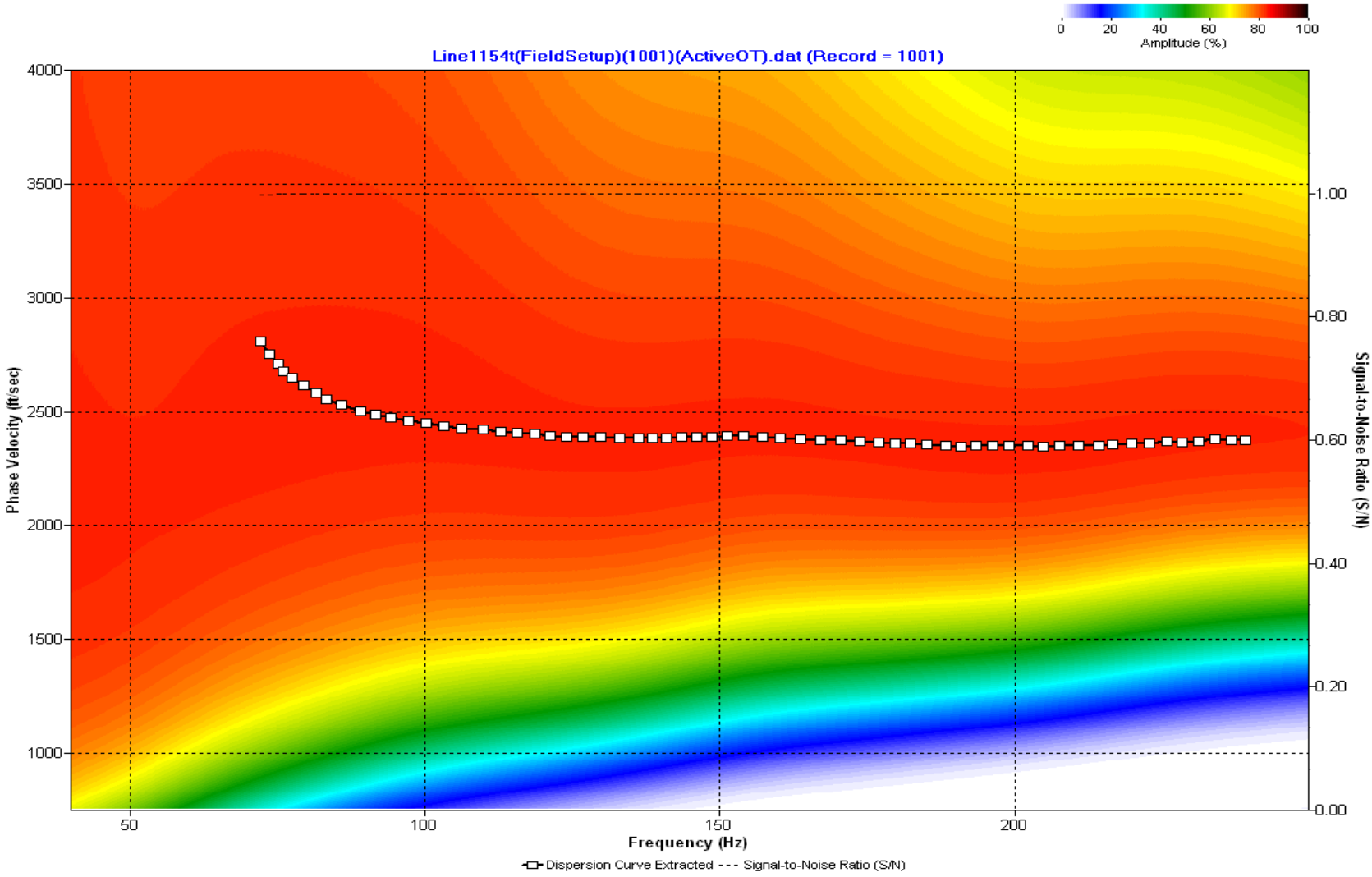

A.203: Dispersion Curve Line 1154 used in Post-blast 16

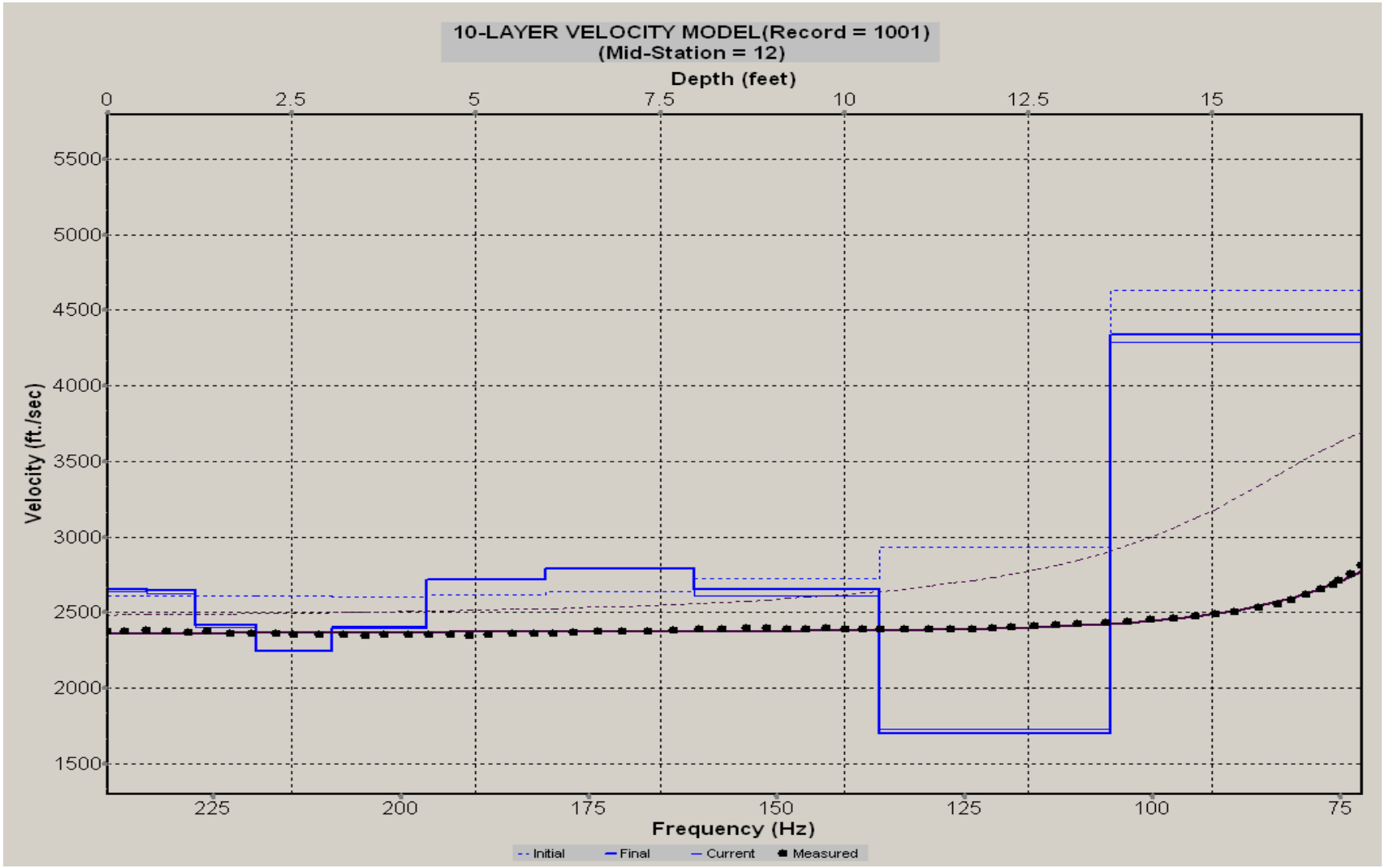

A.204: Velocity Profile Line 1154 used in Post-blast 16

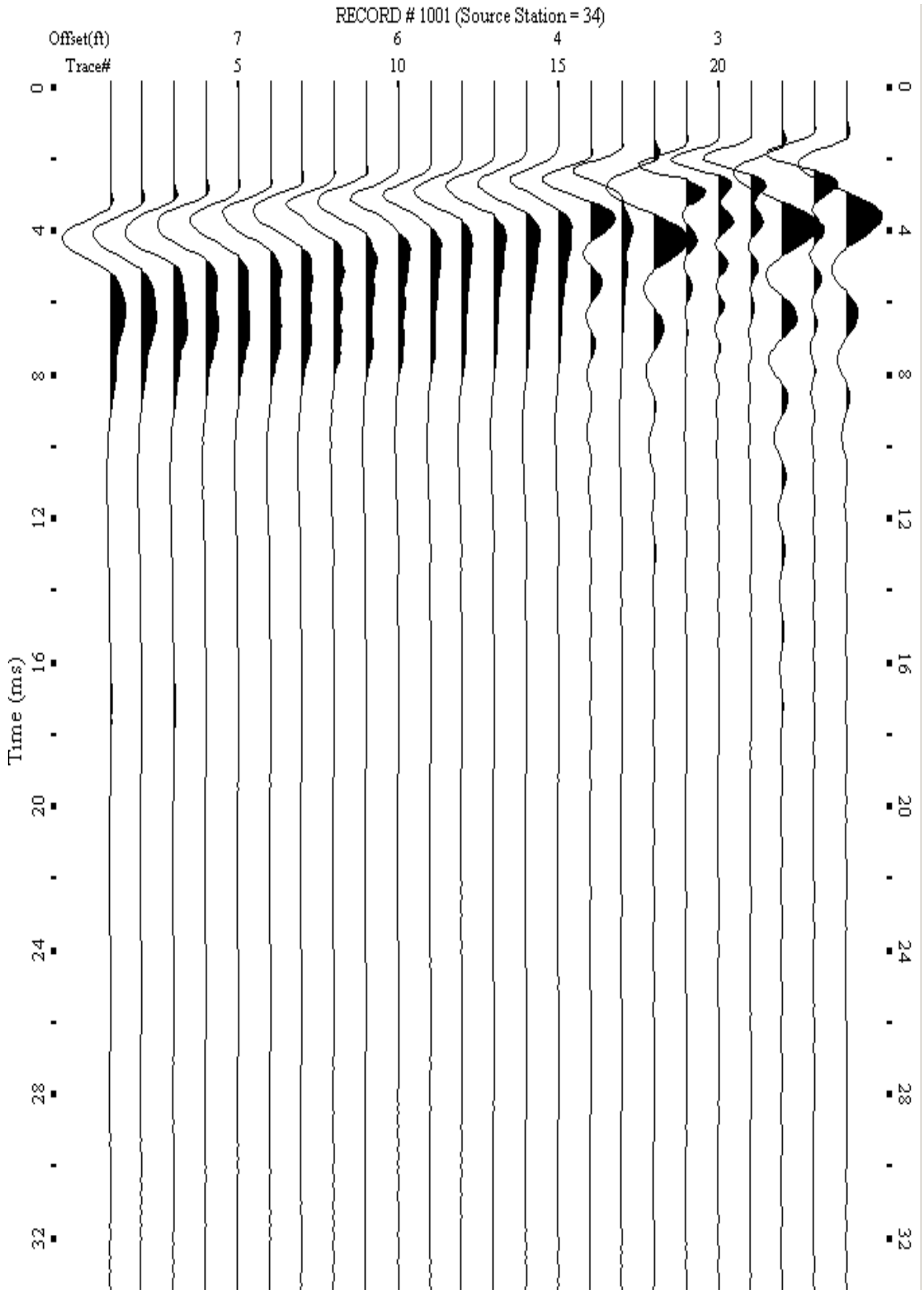

A.205: Shot Gather Line 1158 used in Post-blast 16

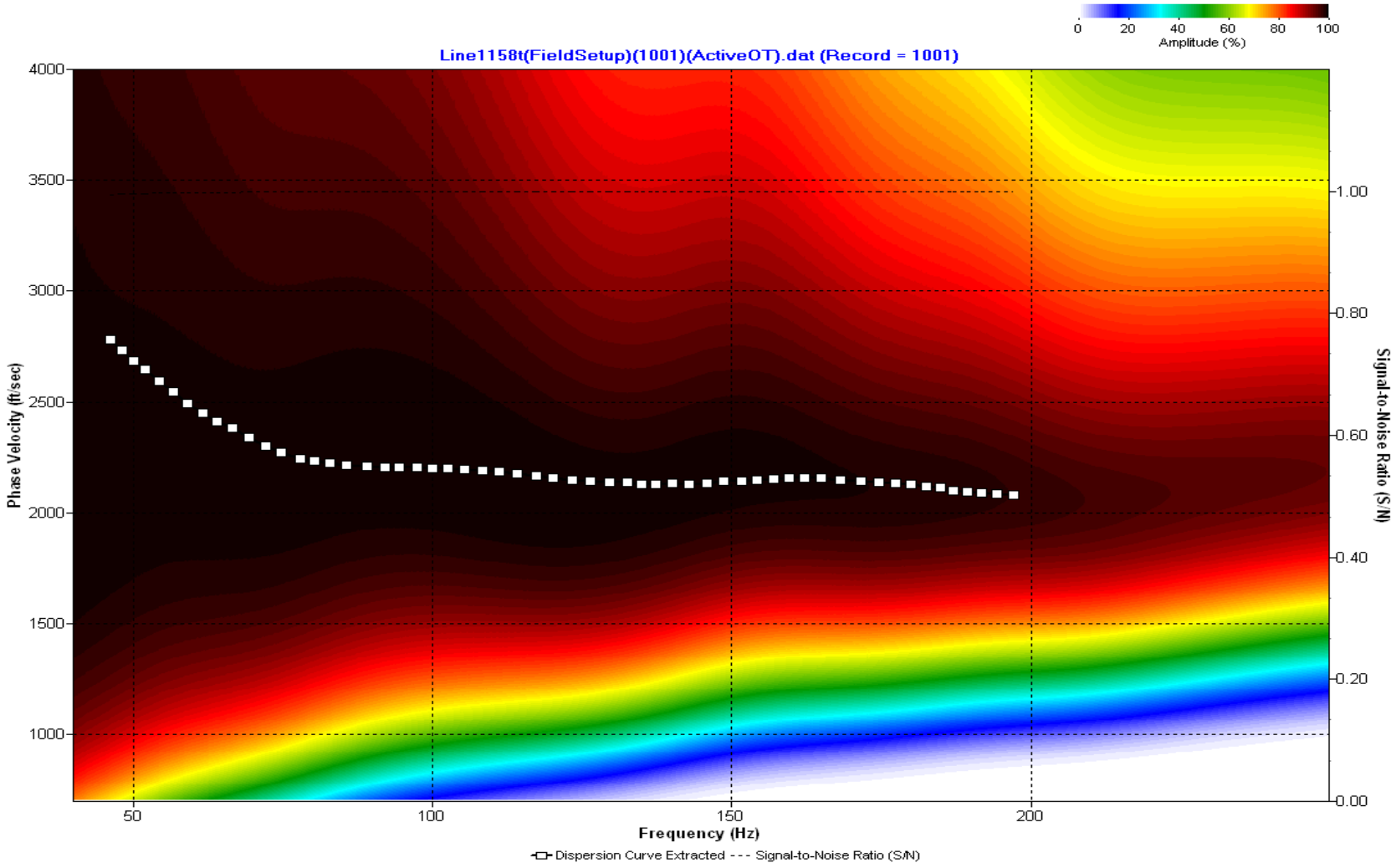

A.206: Dispersion Curve Line 1158 used in Post-blast 16

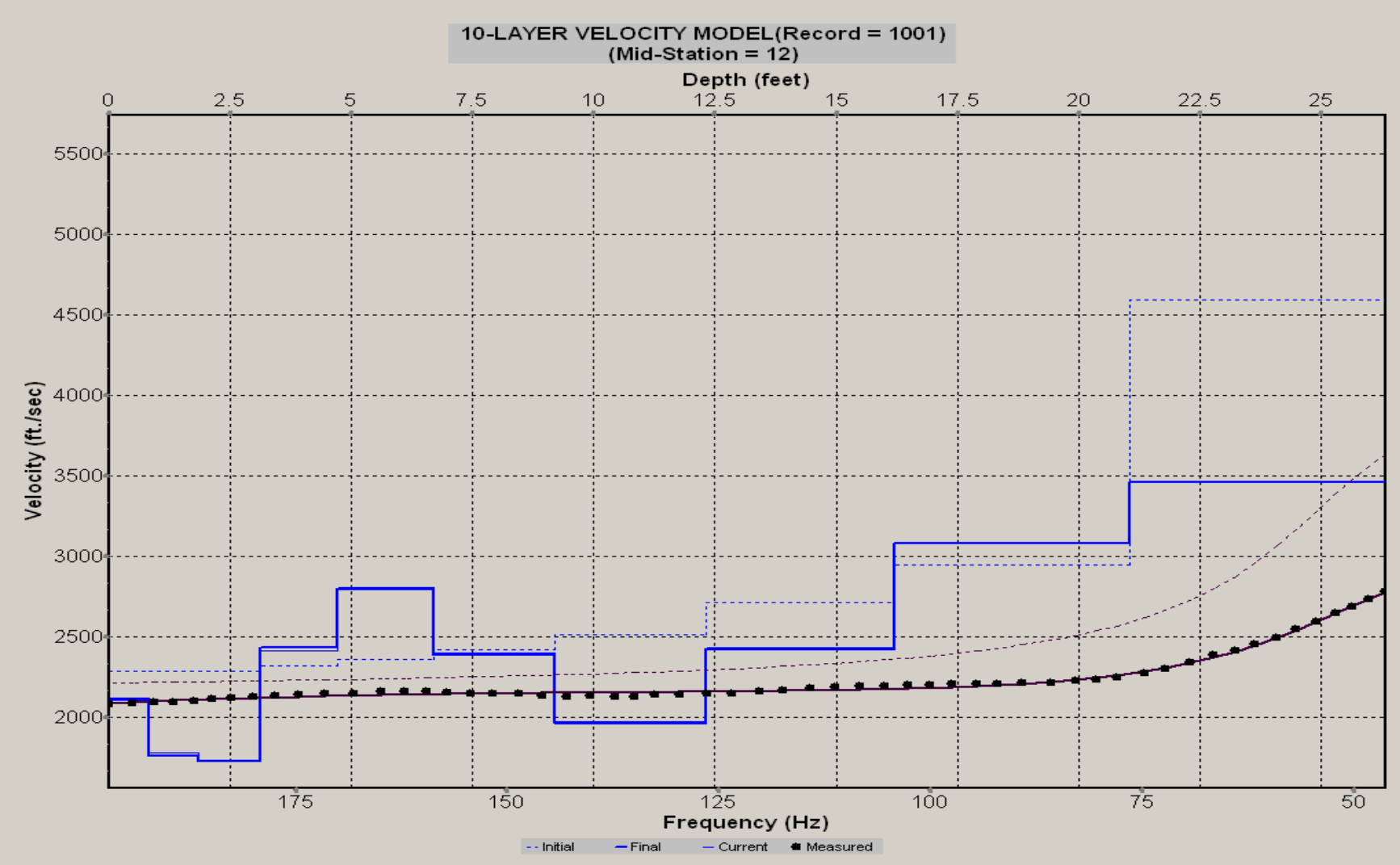

A.207: Velocity Profile Line 1158 used in Post-blast 16

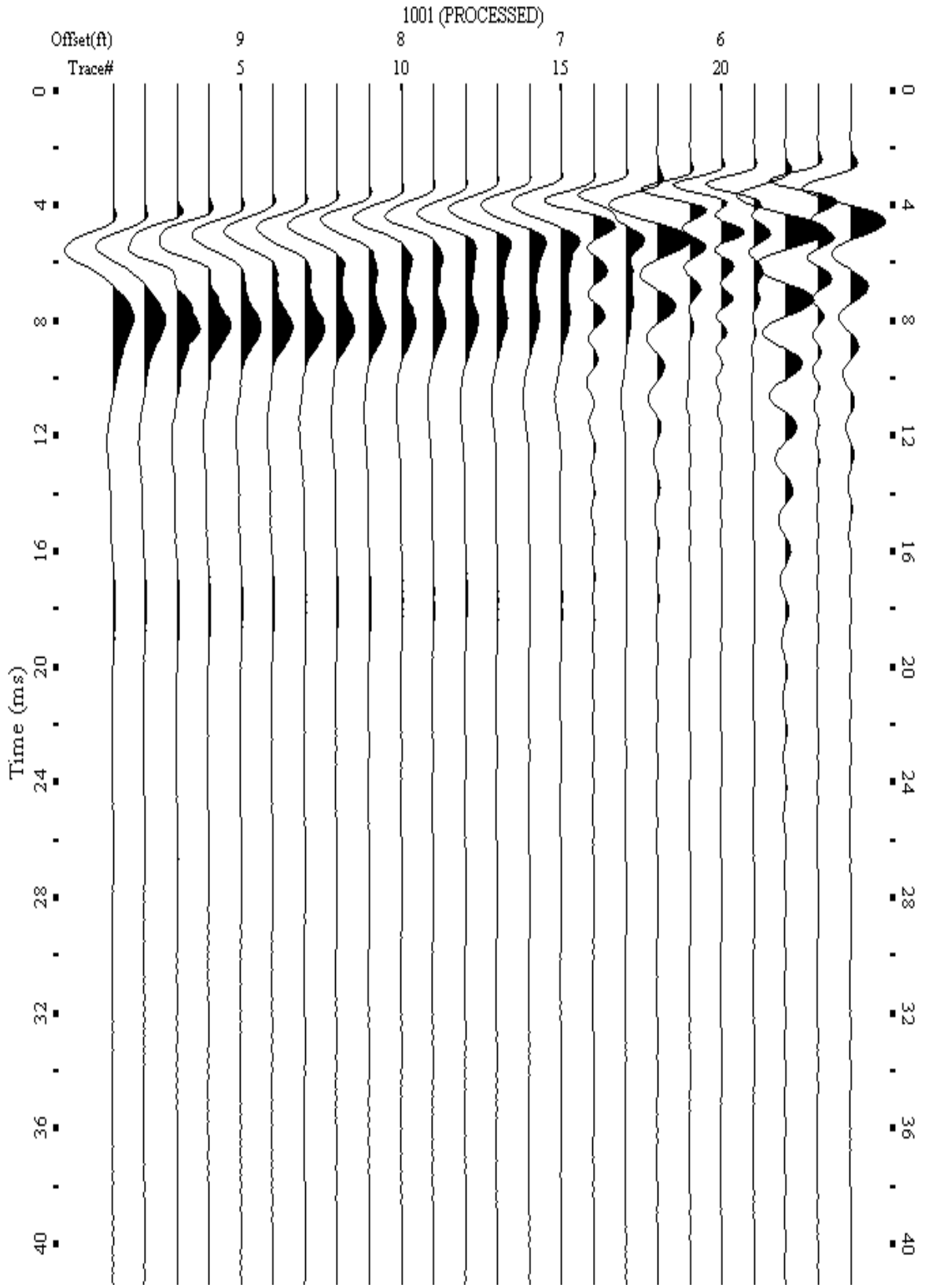

A.208: Shot Gather Line 1160 used in Post-blast 16

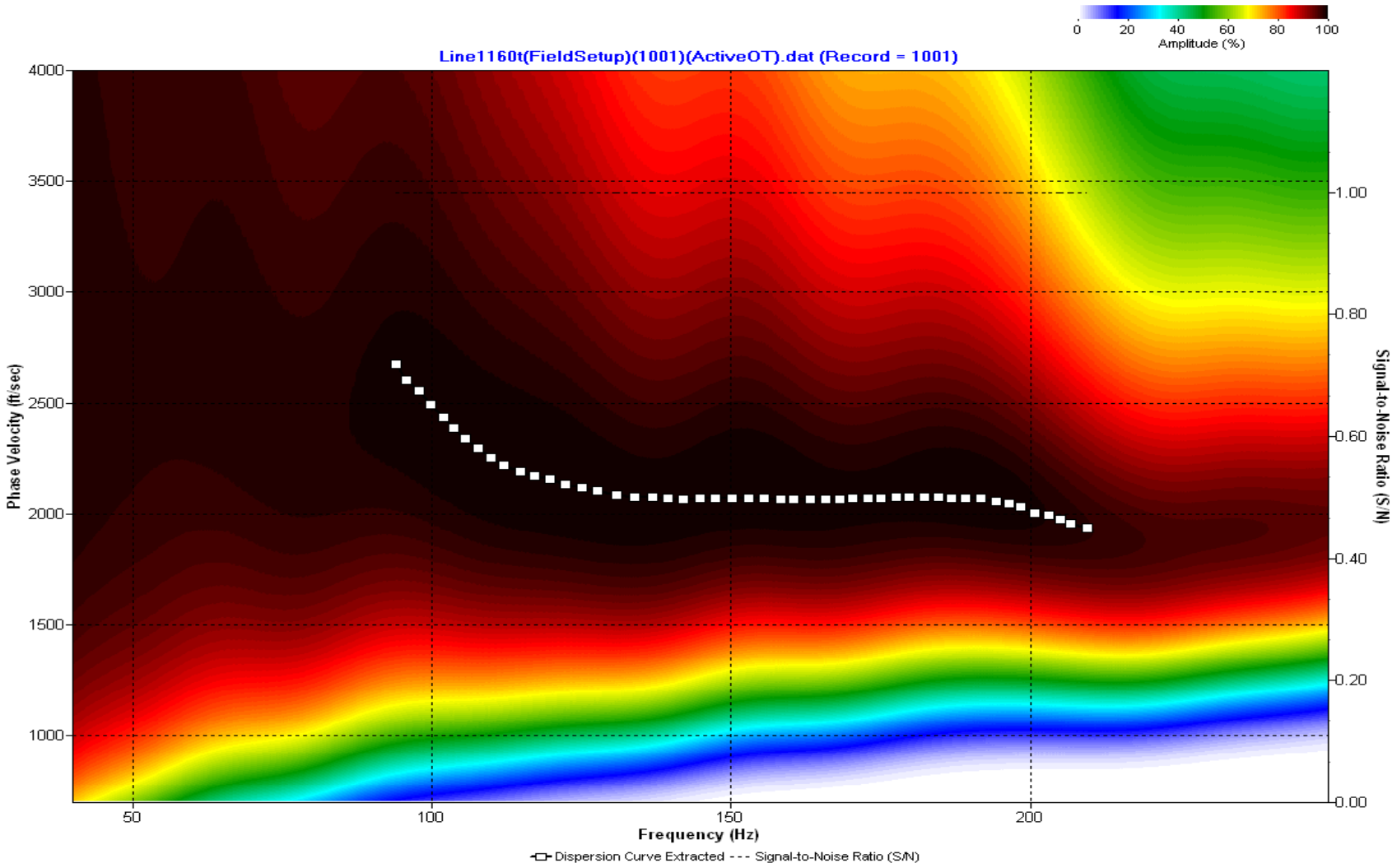

A.209: Dispersion Curve Line 1160 used in Post-blast 16

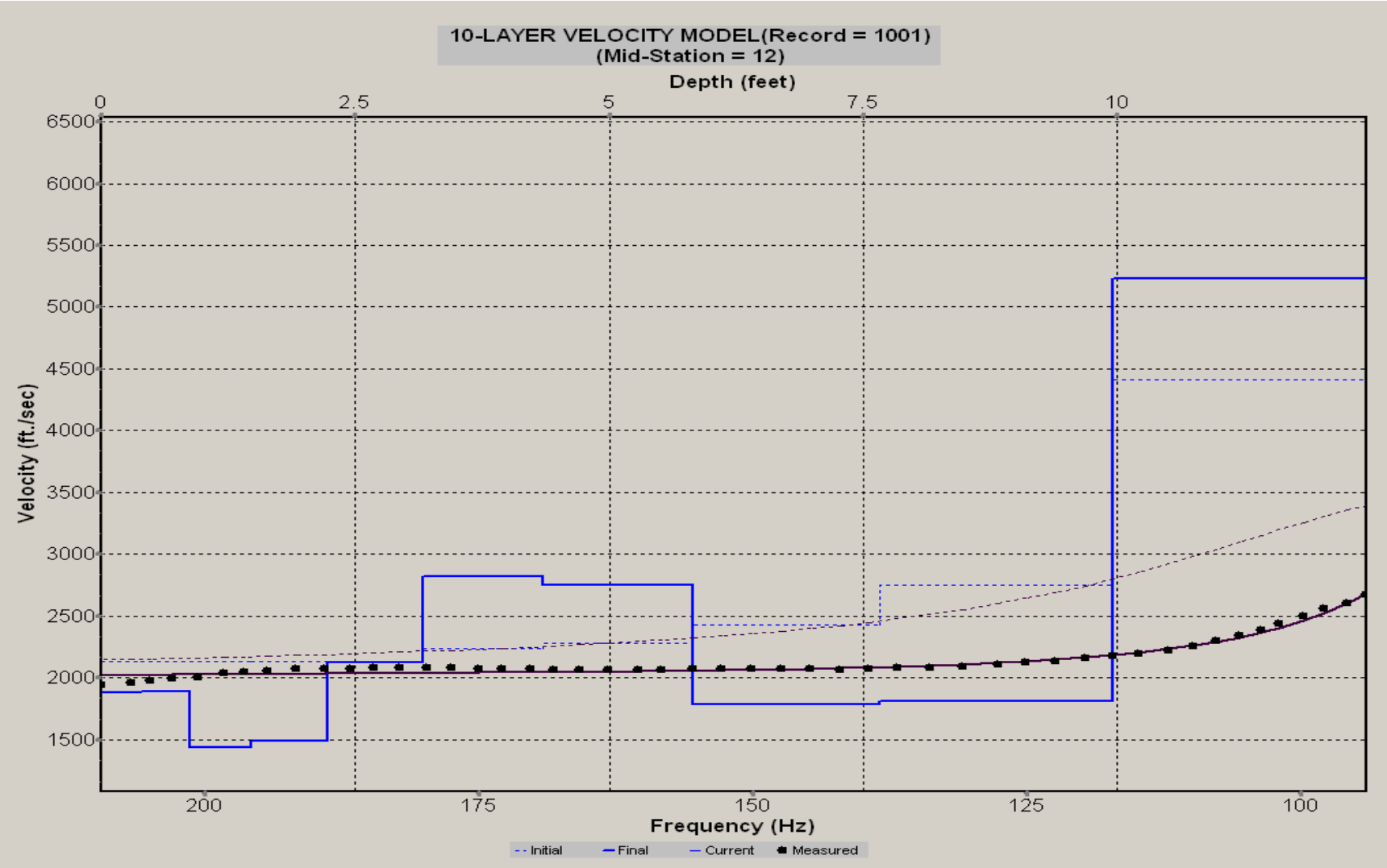

A.210: Velocity Profile Line 1160 used in Post-blast 16

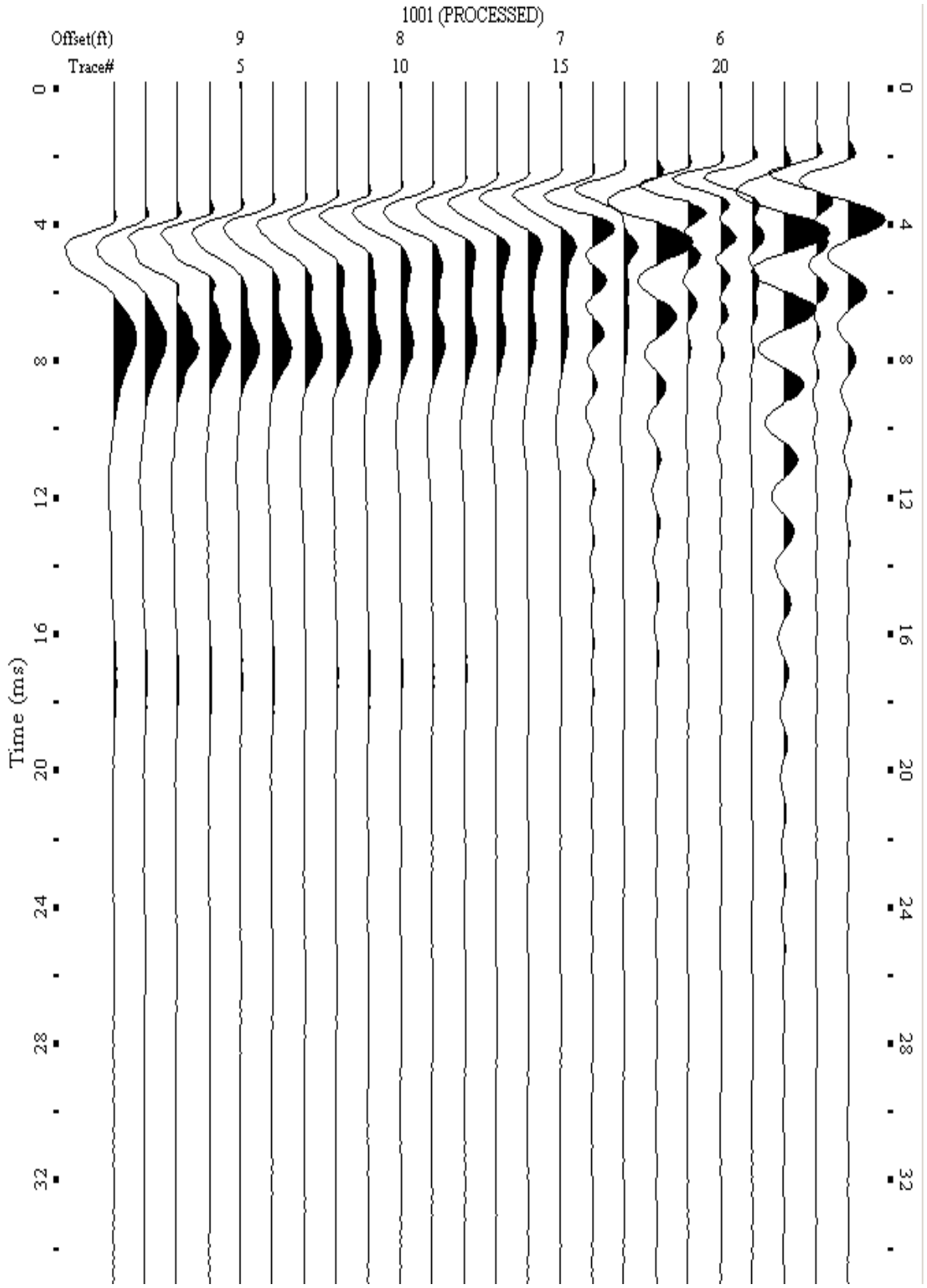

A.211: Shot Gather Line 1161 used in Post-blast 16

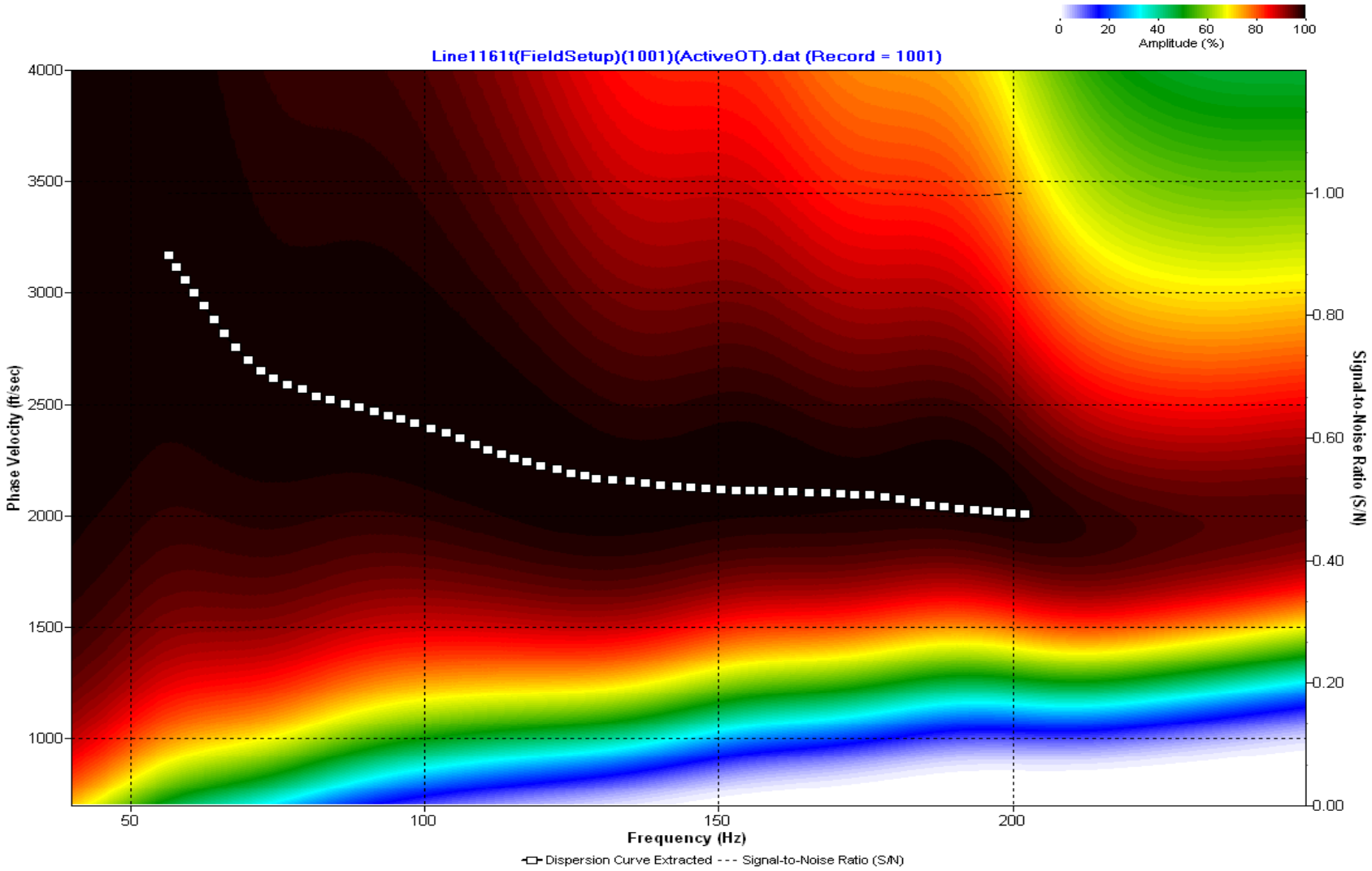

A.212: Dispersion Curve Line 1161 used in Post-blast 16

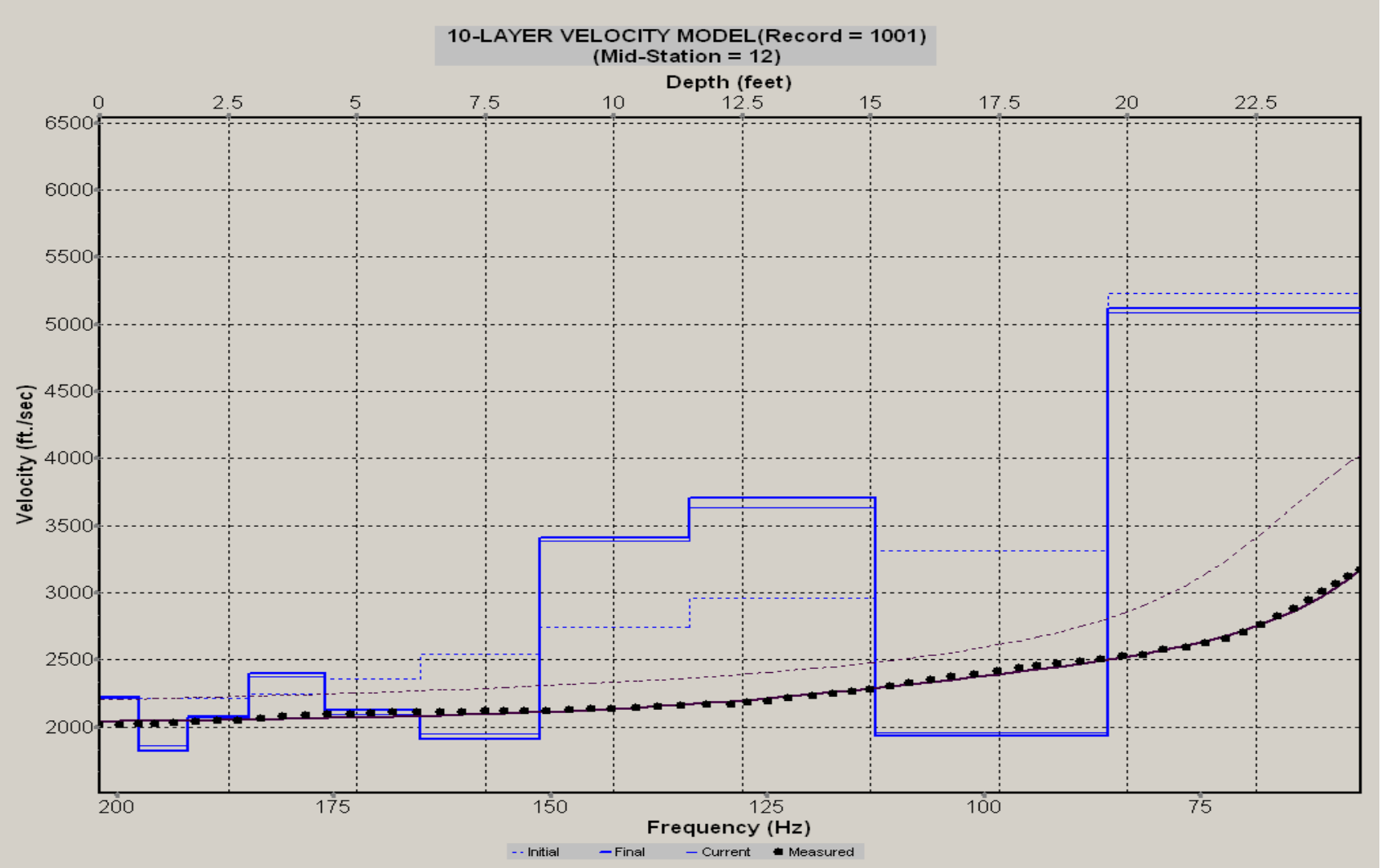

A.213: Velocity Profile Line 1161 used in Post-blast 16

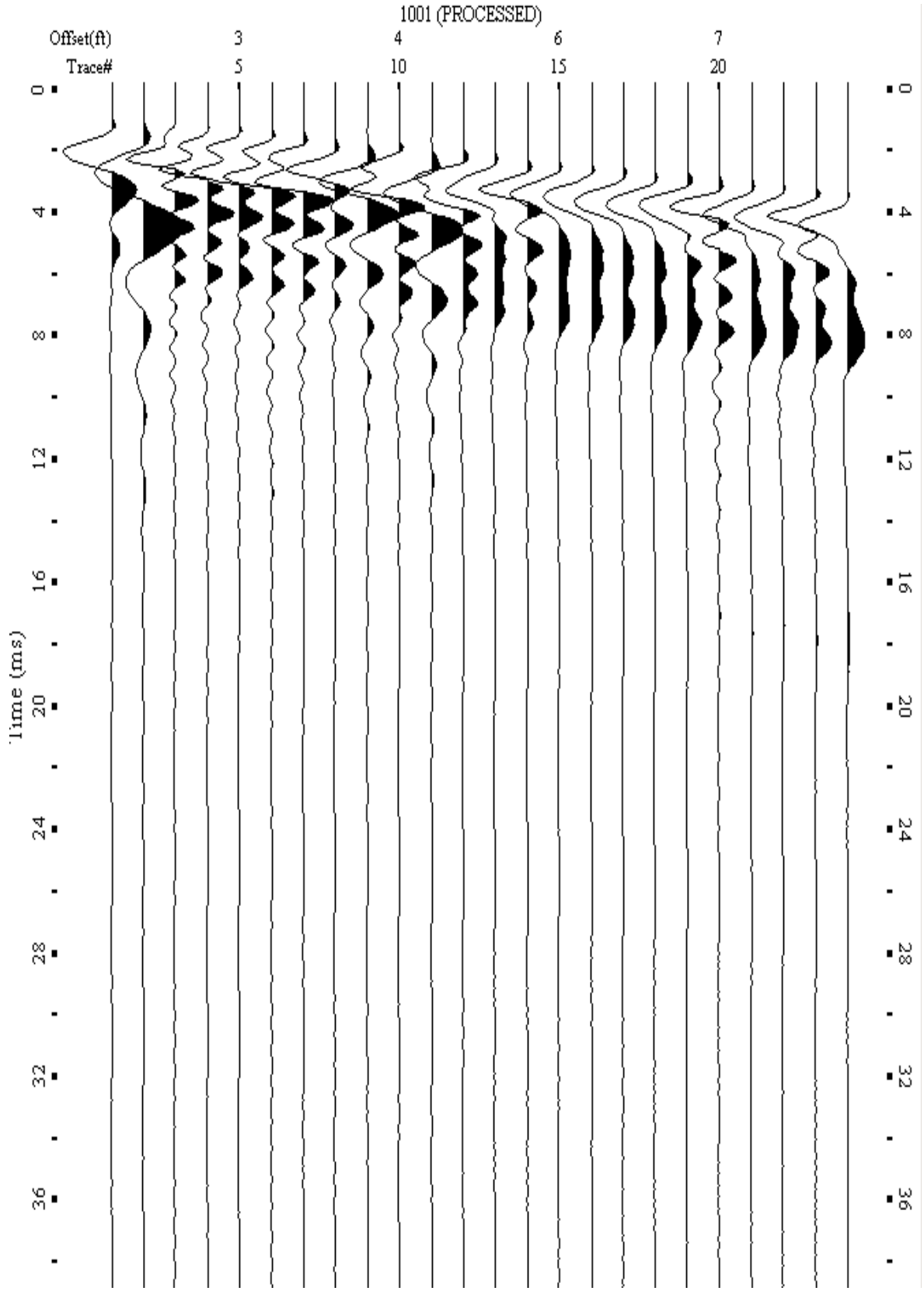

A.214: Shot Gather Line 1163 used in Post-blast 17

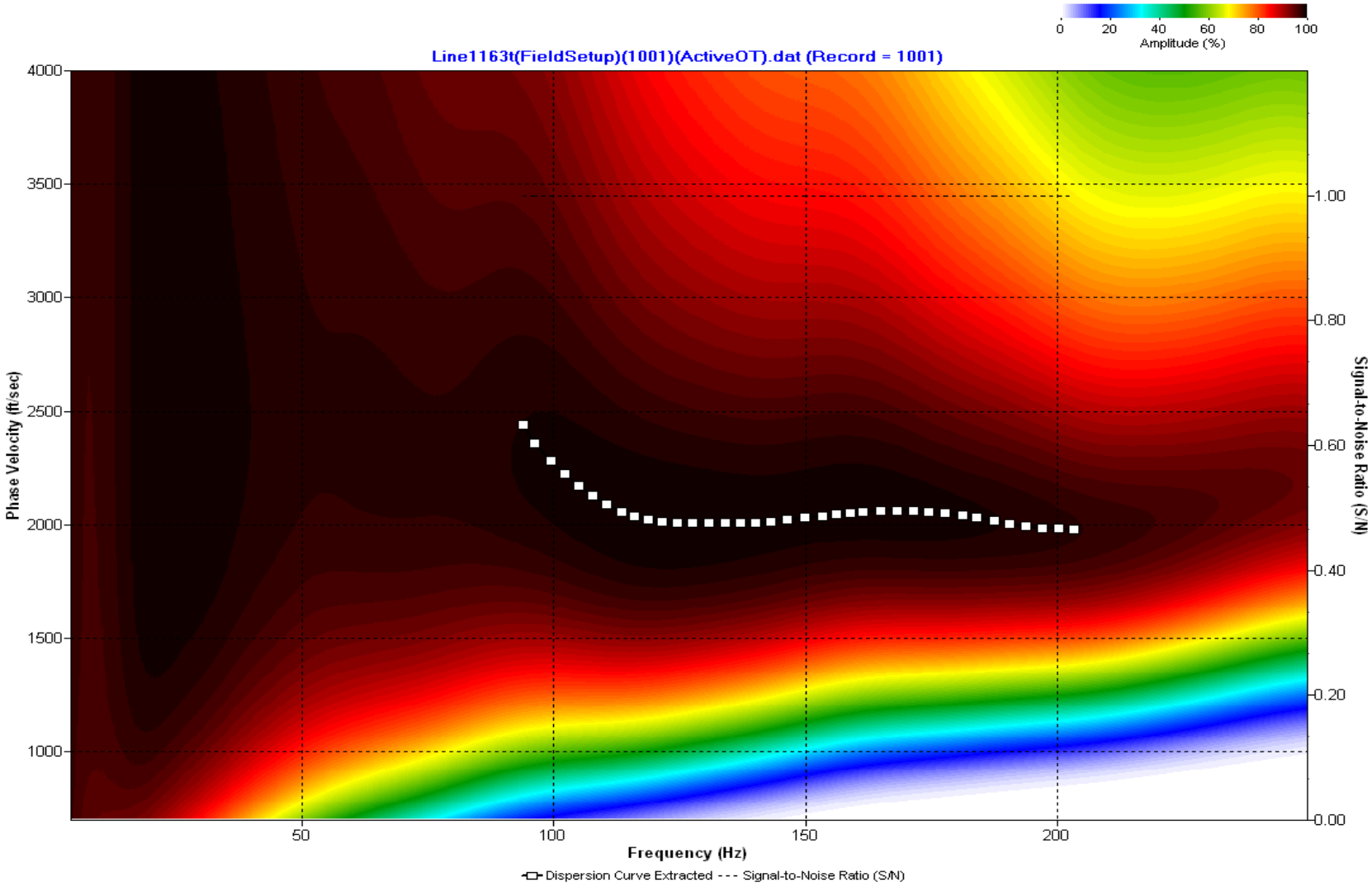

A.215: Dispersion Curve Line 1163 used in Post-blast 17

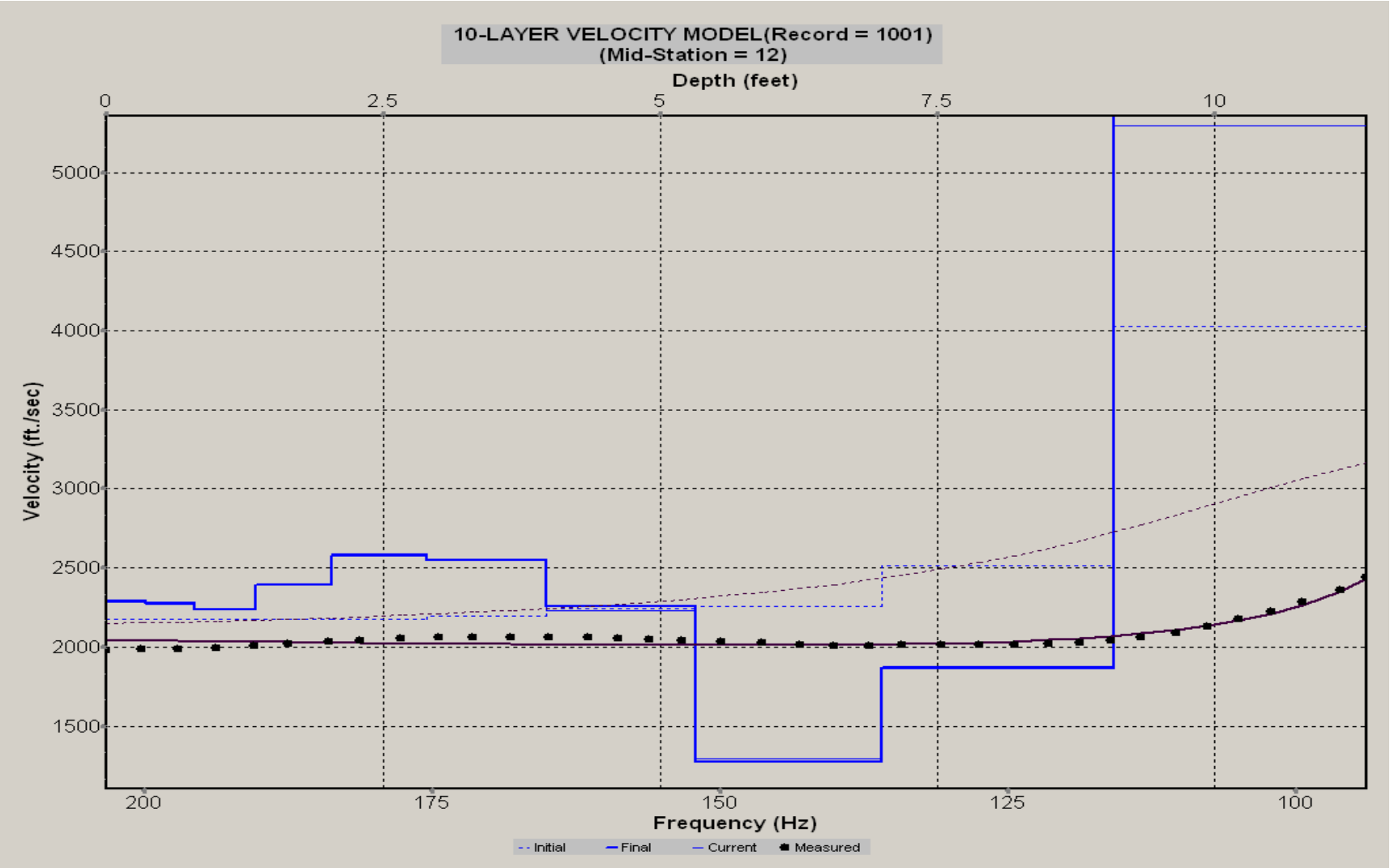

A.216: Velocity Profile Line 1163 used in Post-blast 17

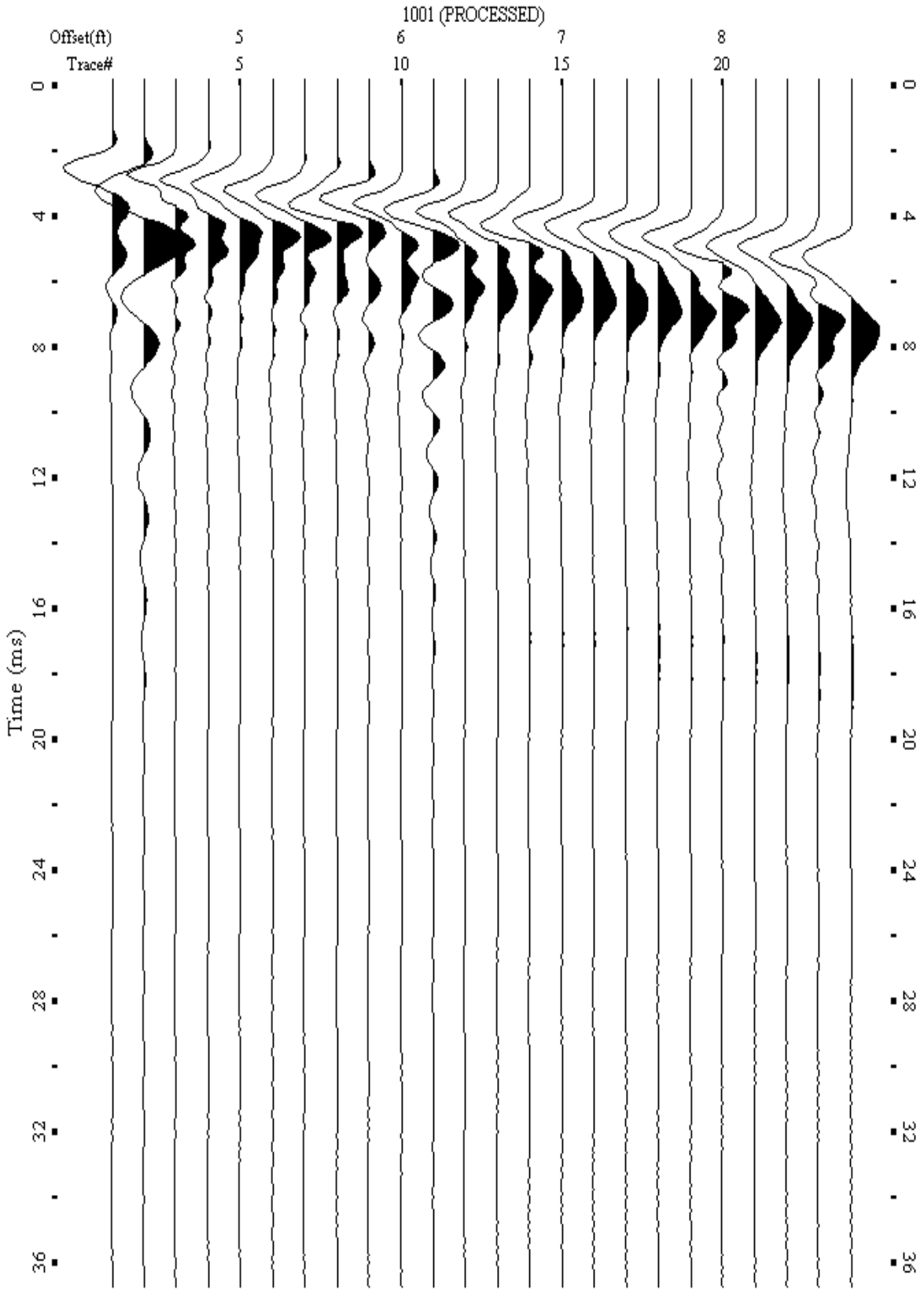

A.217: Shot Gather Line 1164 used in Post-blast 17

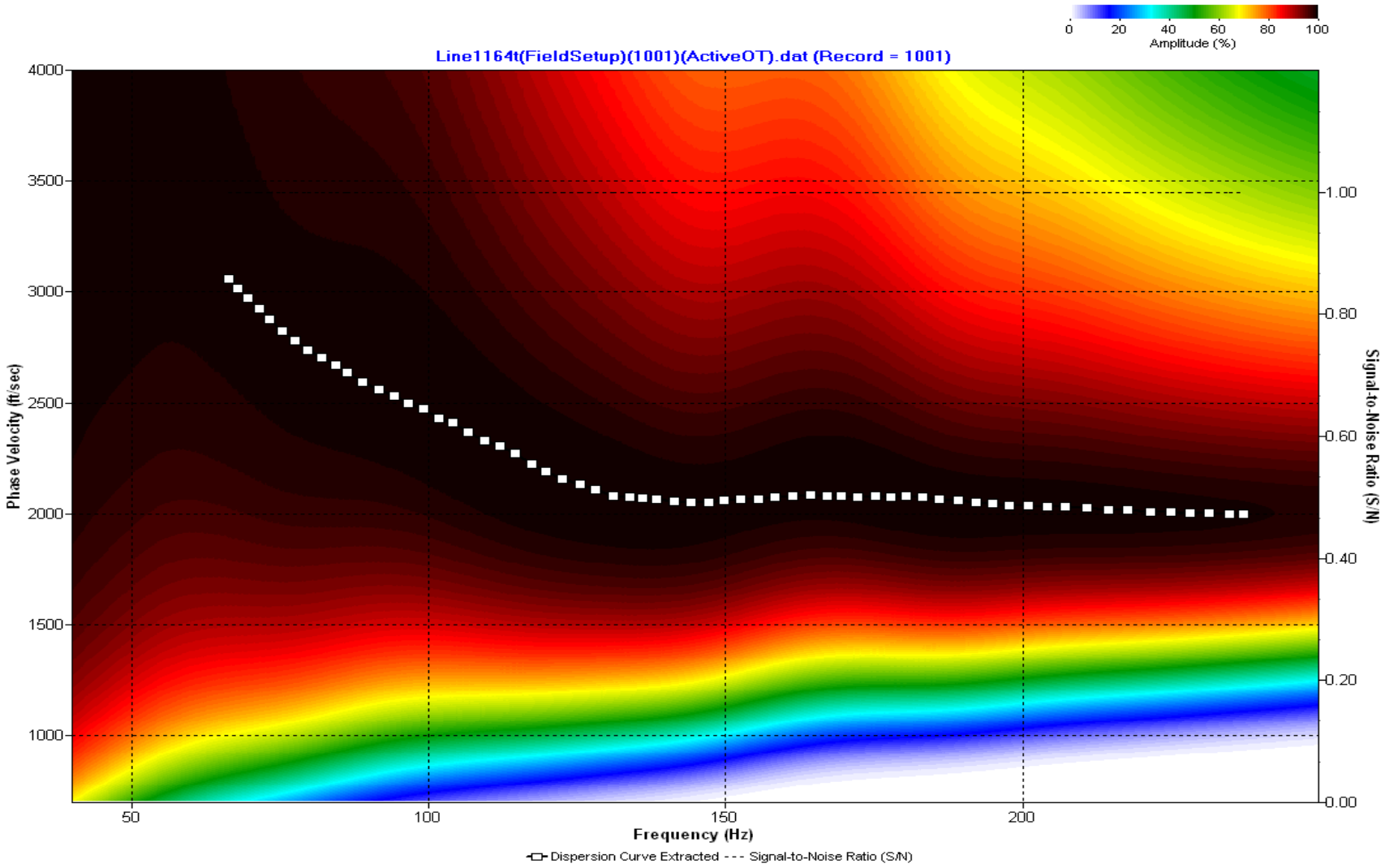

A.218: Dispersion Curve Line 1164 used in Post-blast 17

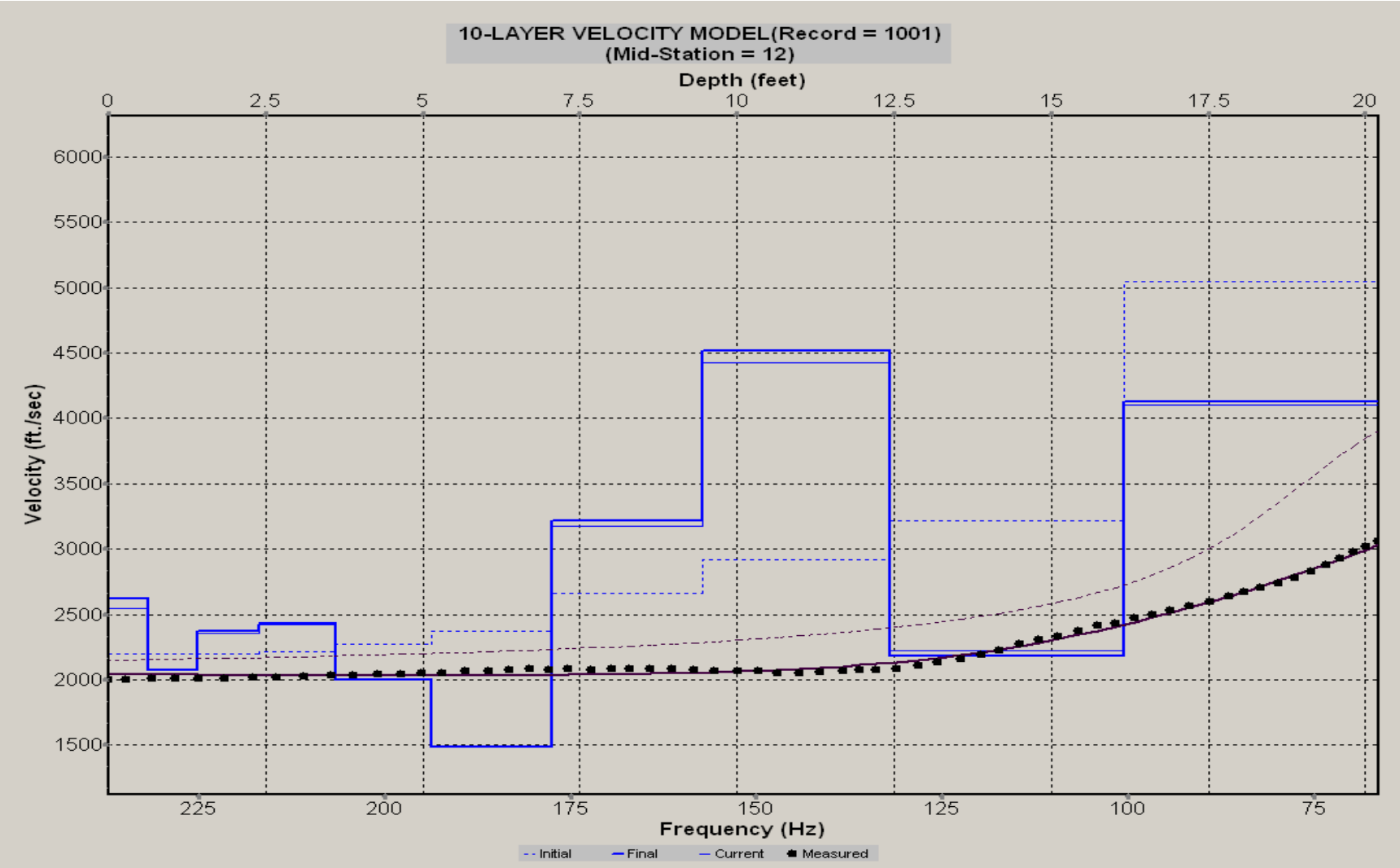

A.219: Velocity Profile Line 1164 used in Post-blast 17

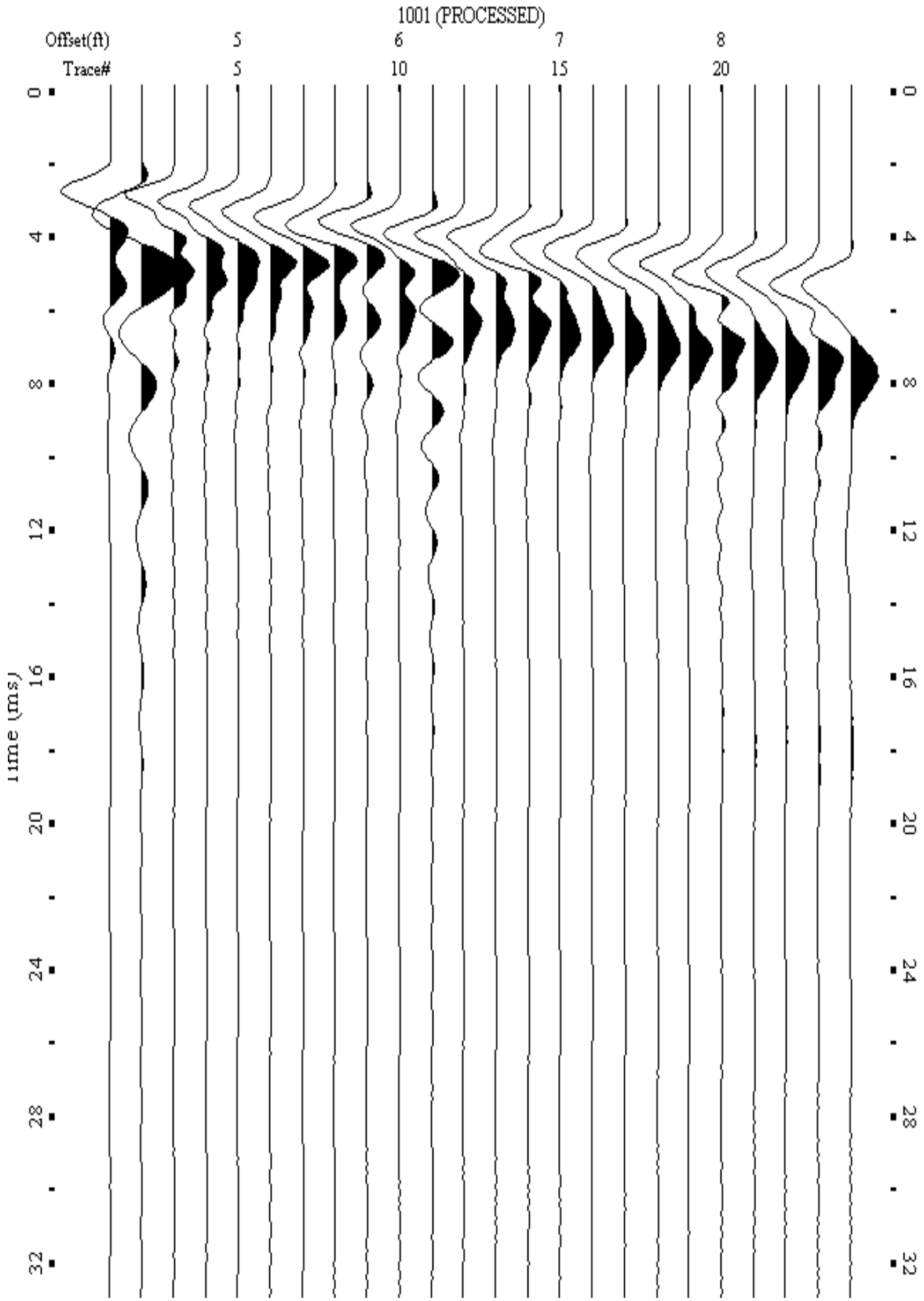

A.220: Shot Gather Line 1165 used in Post-blast 17

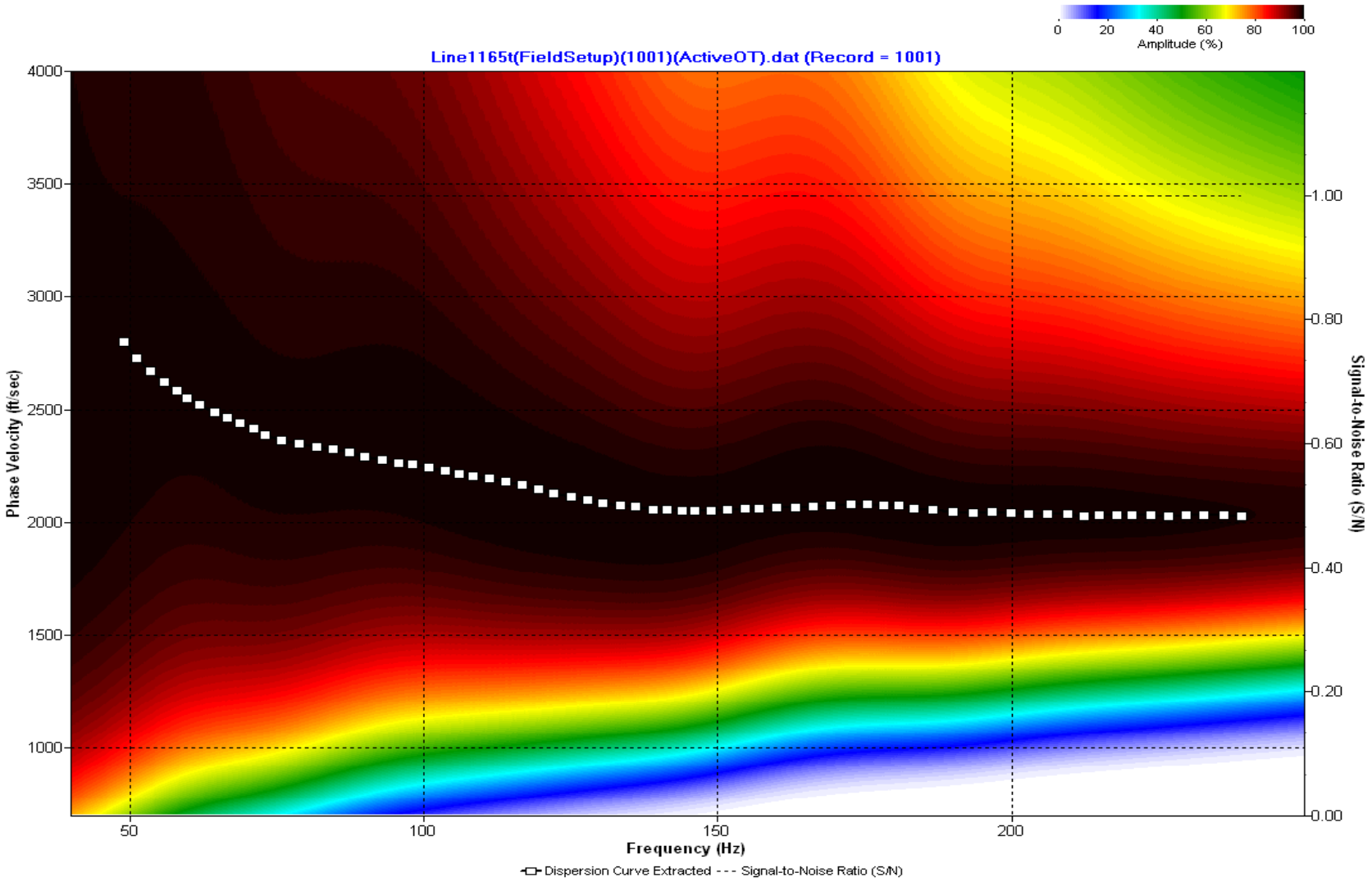

A.221: Dispersion Curve Line 1165 used in Post-blast 17

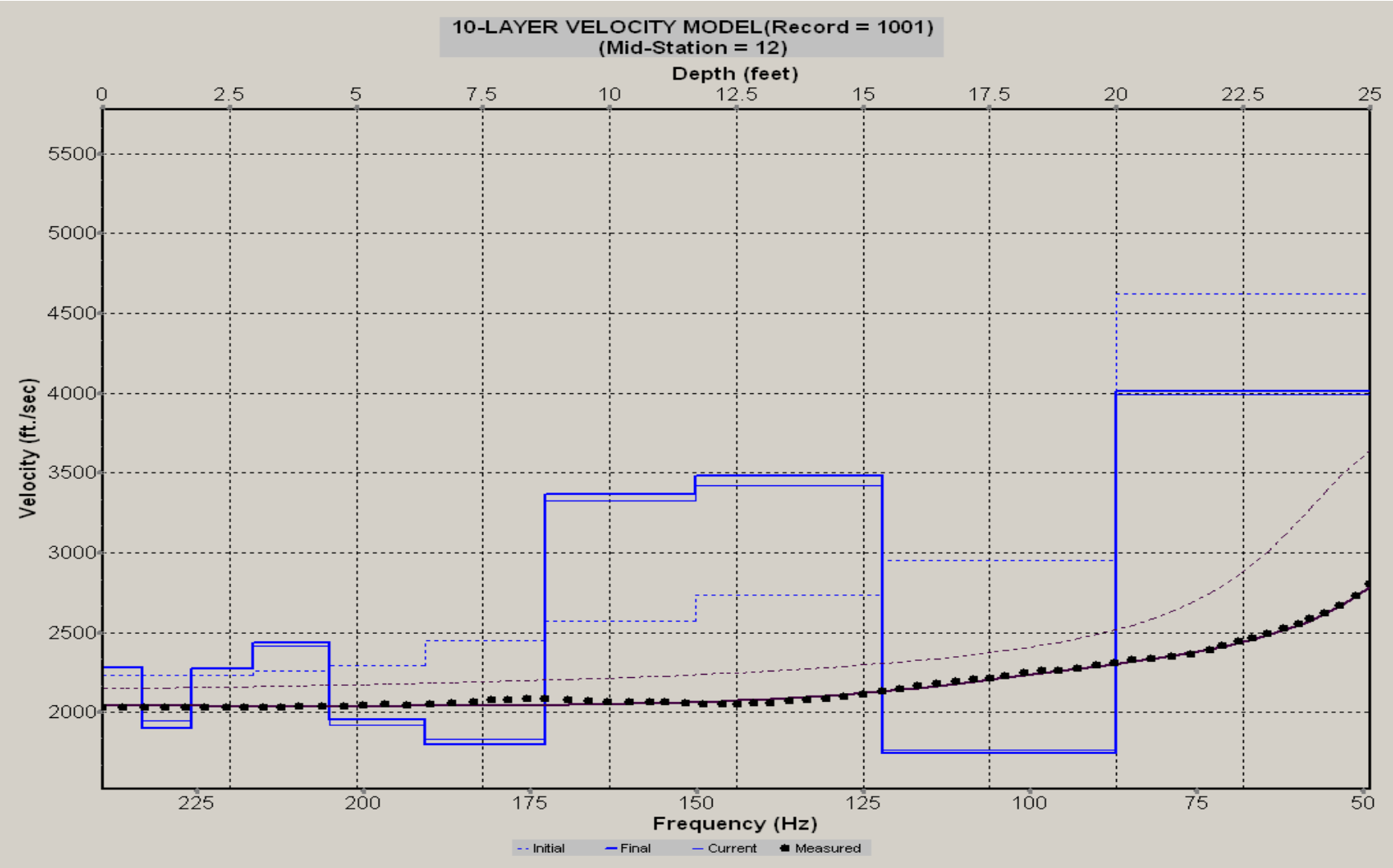

A.222: Velocity Profile Line 1165 used in Post-blast 17

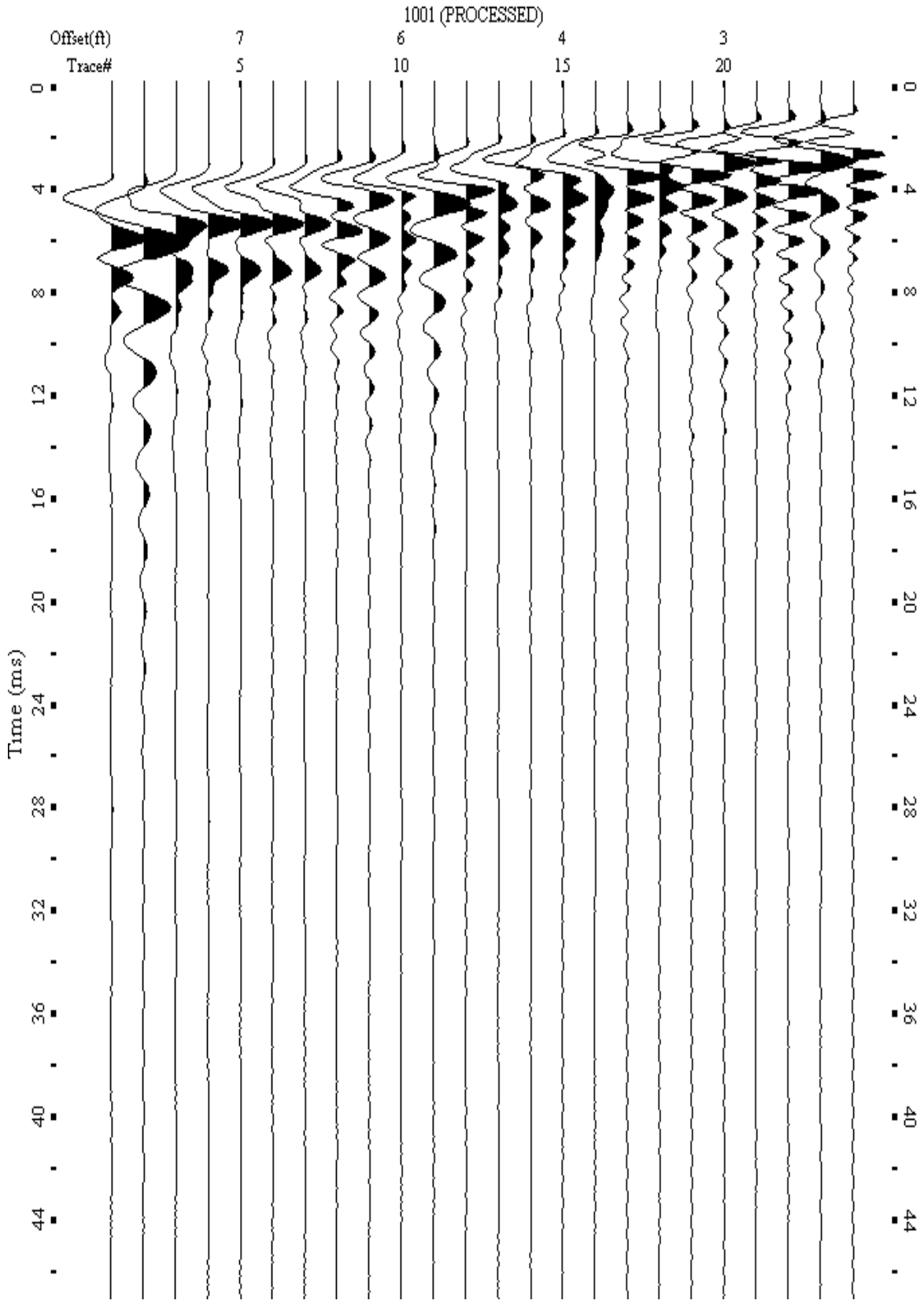

A.223: Shot Gather Line 1167 used in Post-blast 17

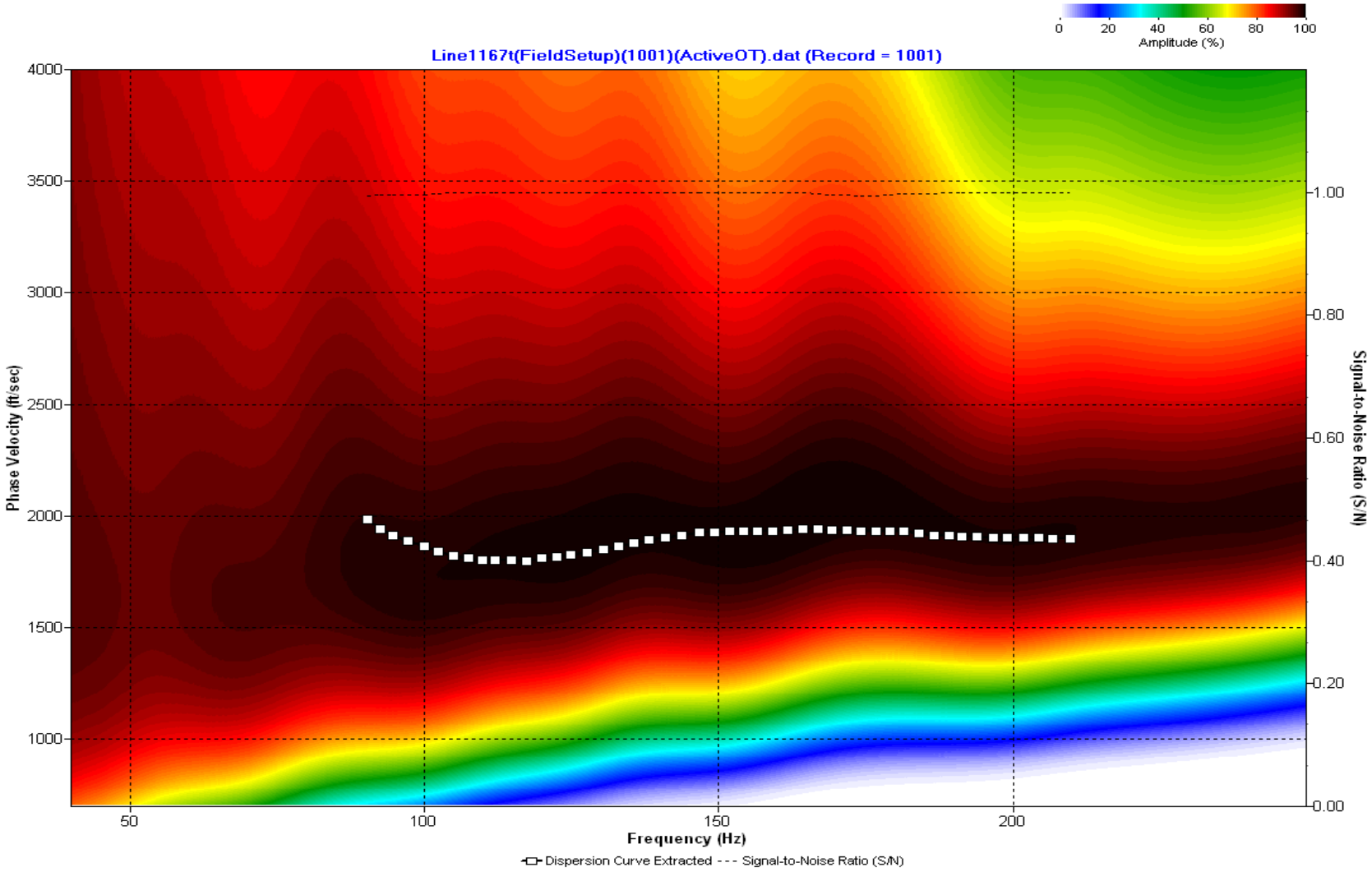

A.224: Dispersion Curve Line 1167 used in Post-blast 17

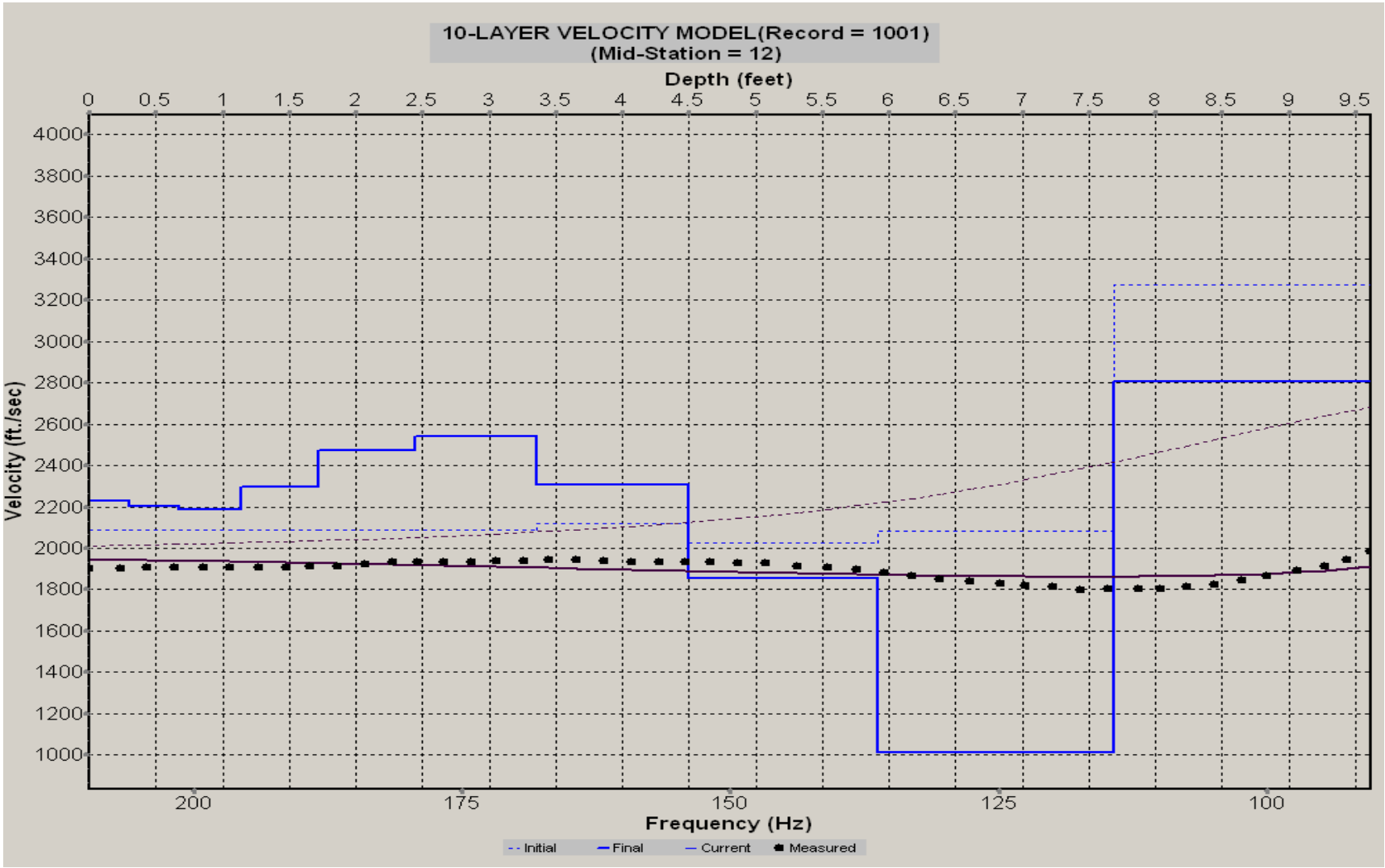

A.225: Velocity Profile Line 1167 used in Post-blast 17

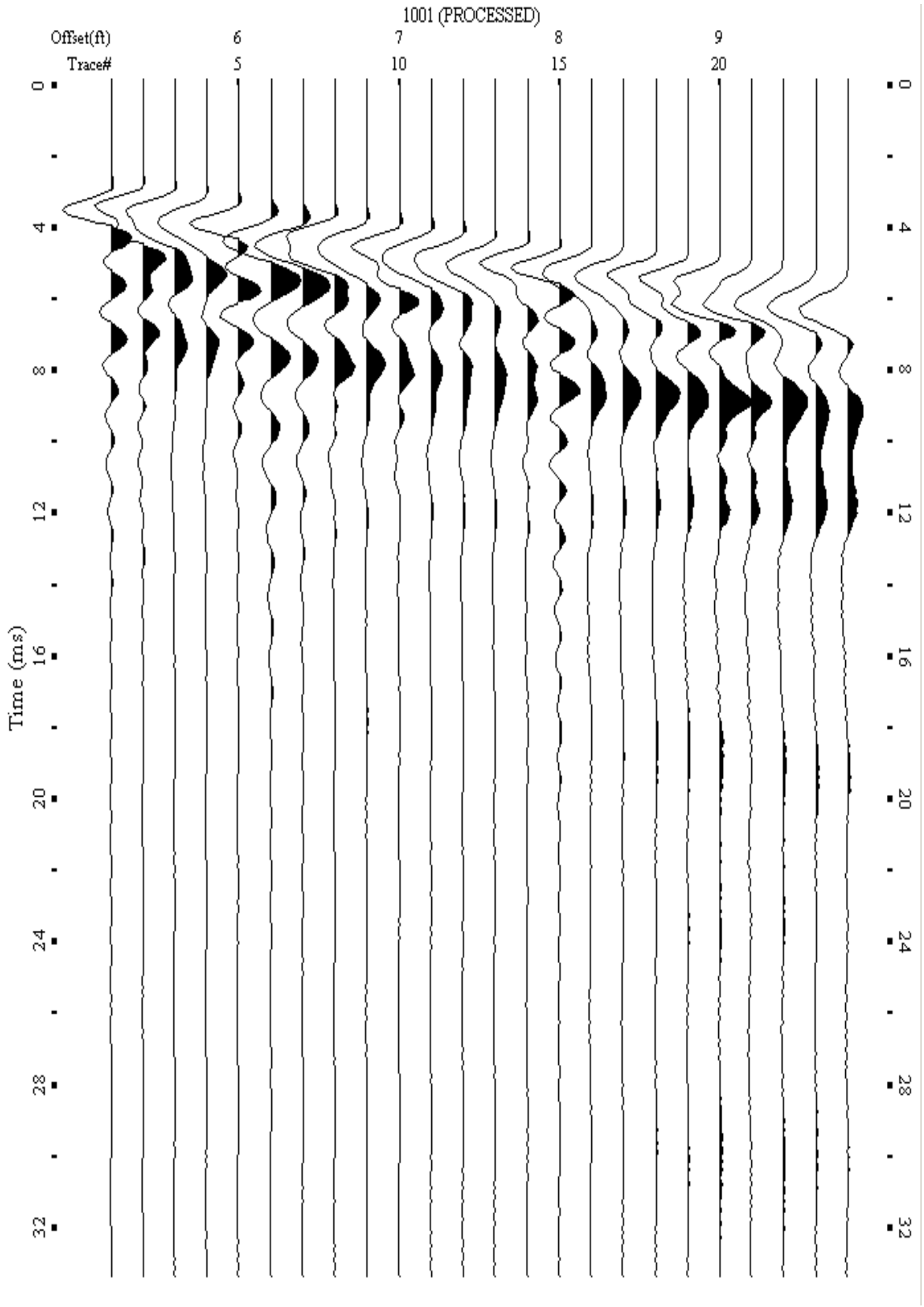

A.226: Shot Gather Line 1172 used in Post-blast 18

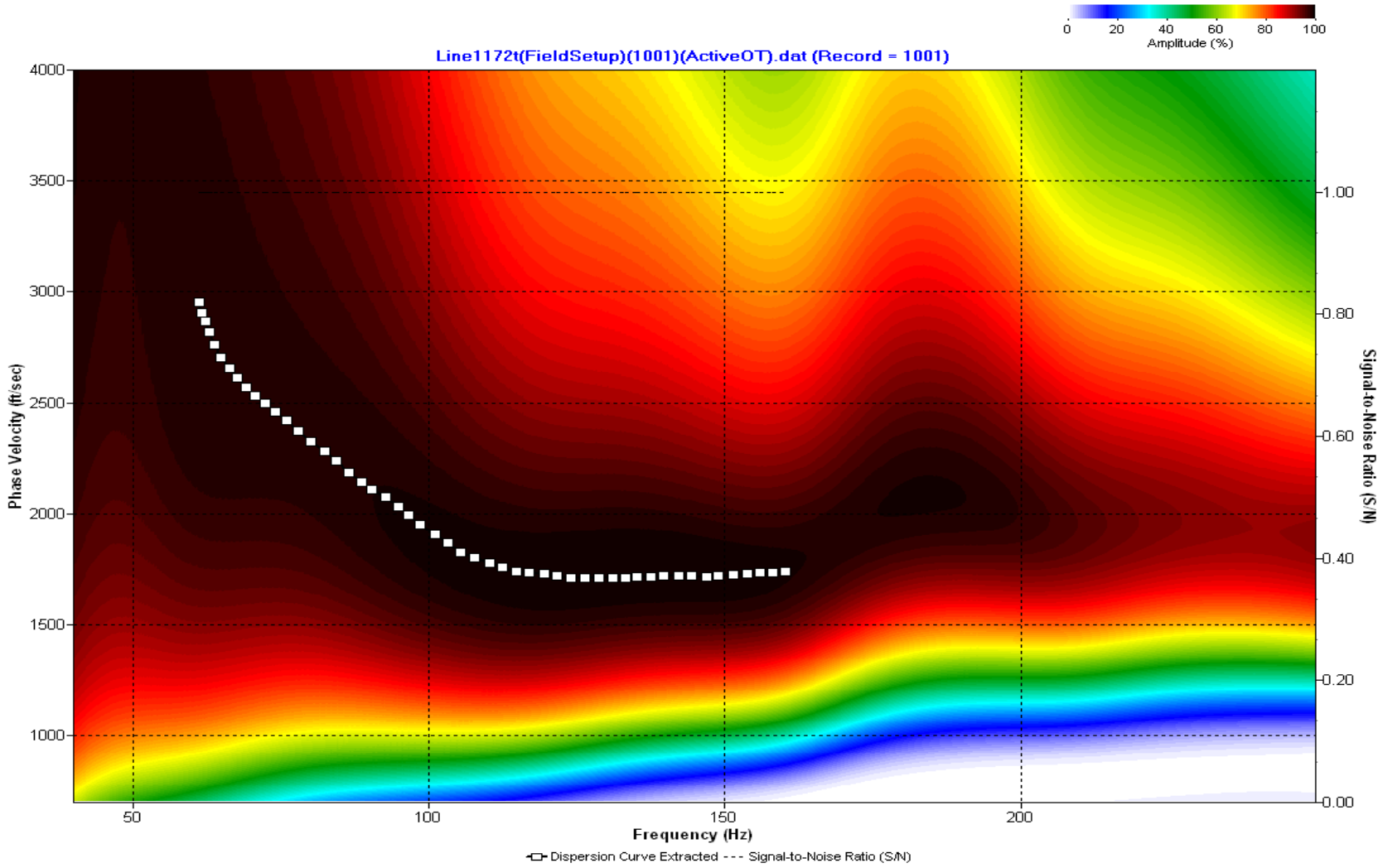

A.227: Dispersion Curve Line 1172 used in Post-blast 18

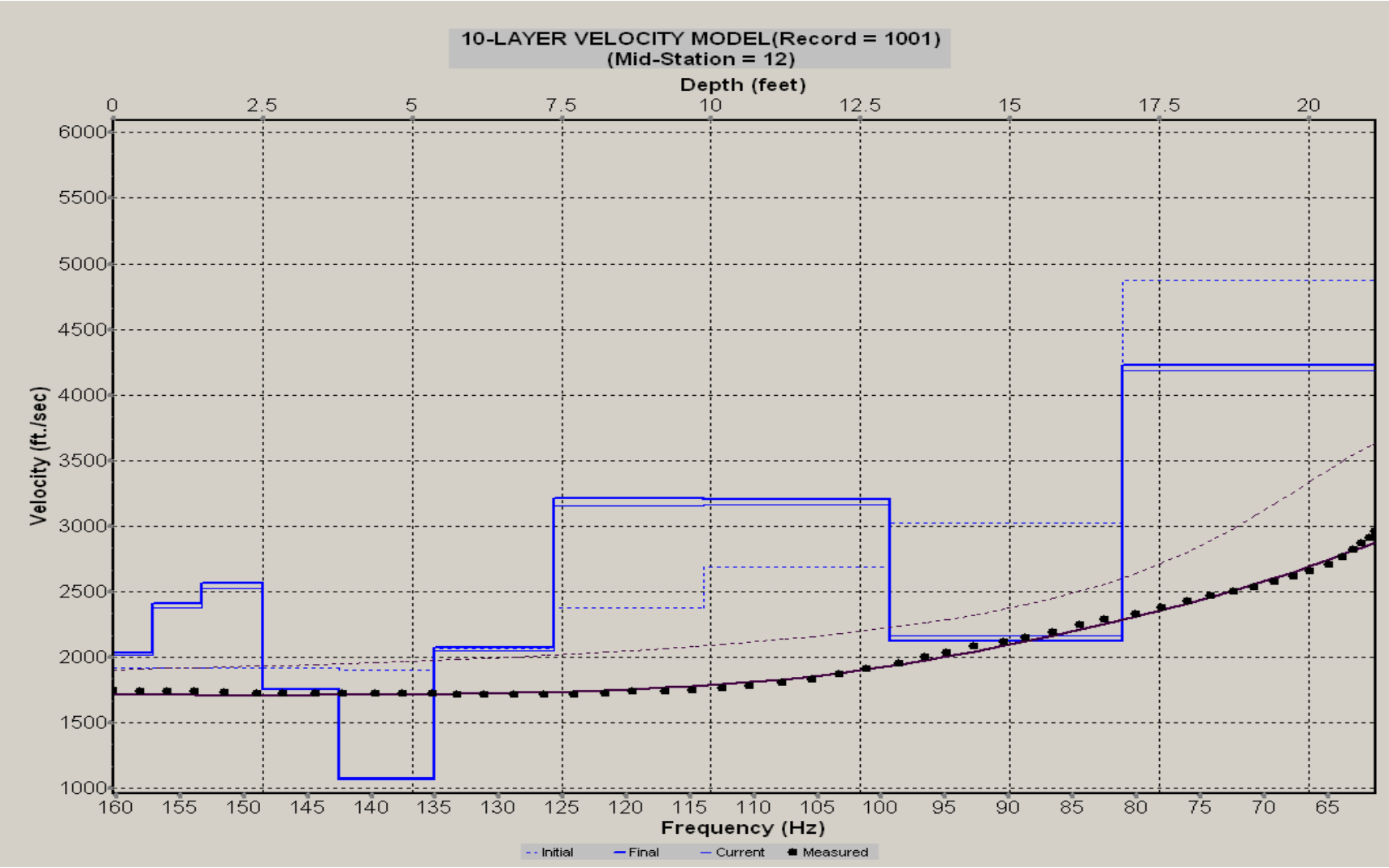

A.228: Velocity Profile Line 1172 used in Post-blast 18

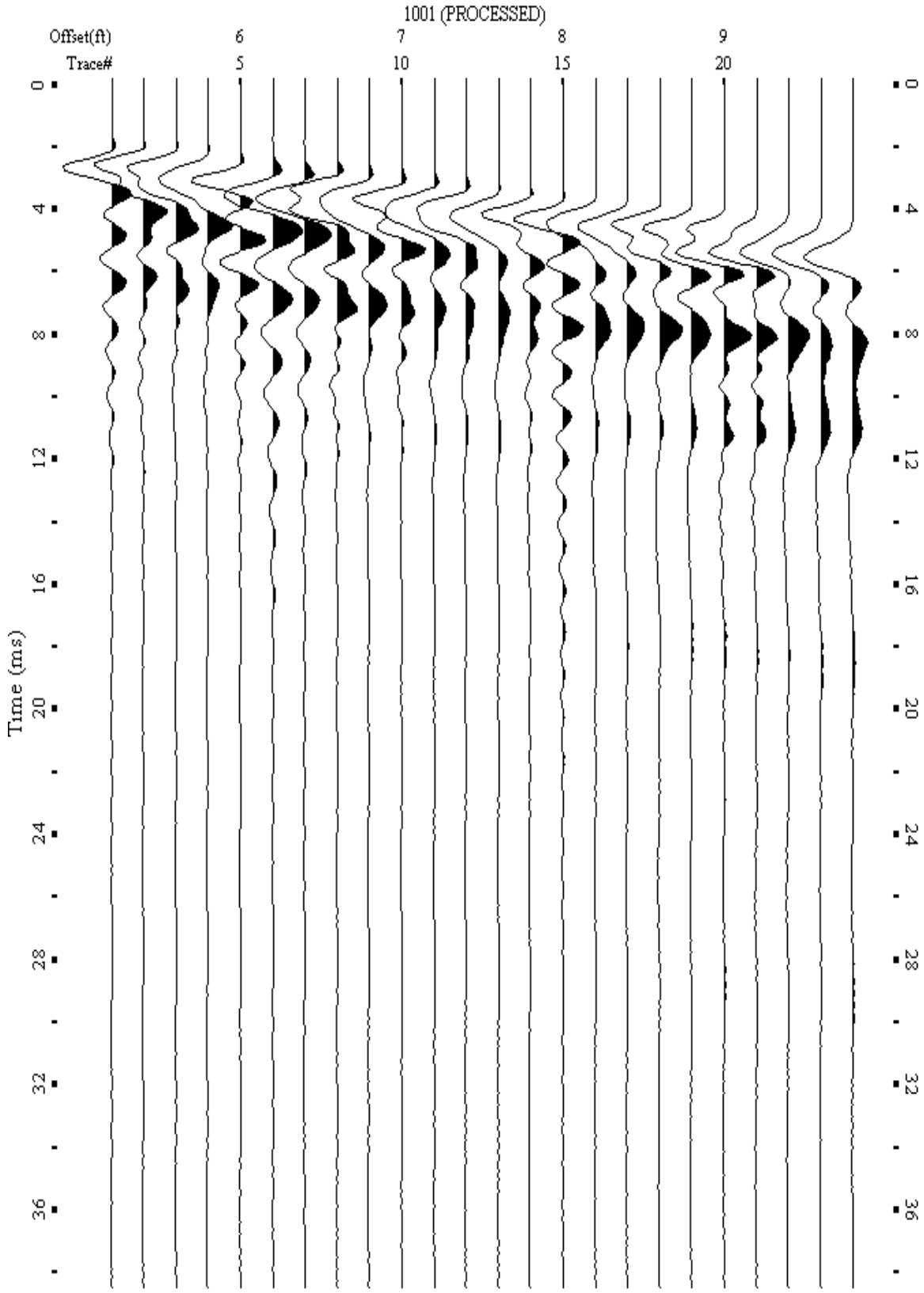

A.229: Shot Gather Line 1173 used in Post-blast 18

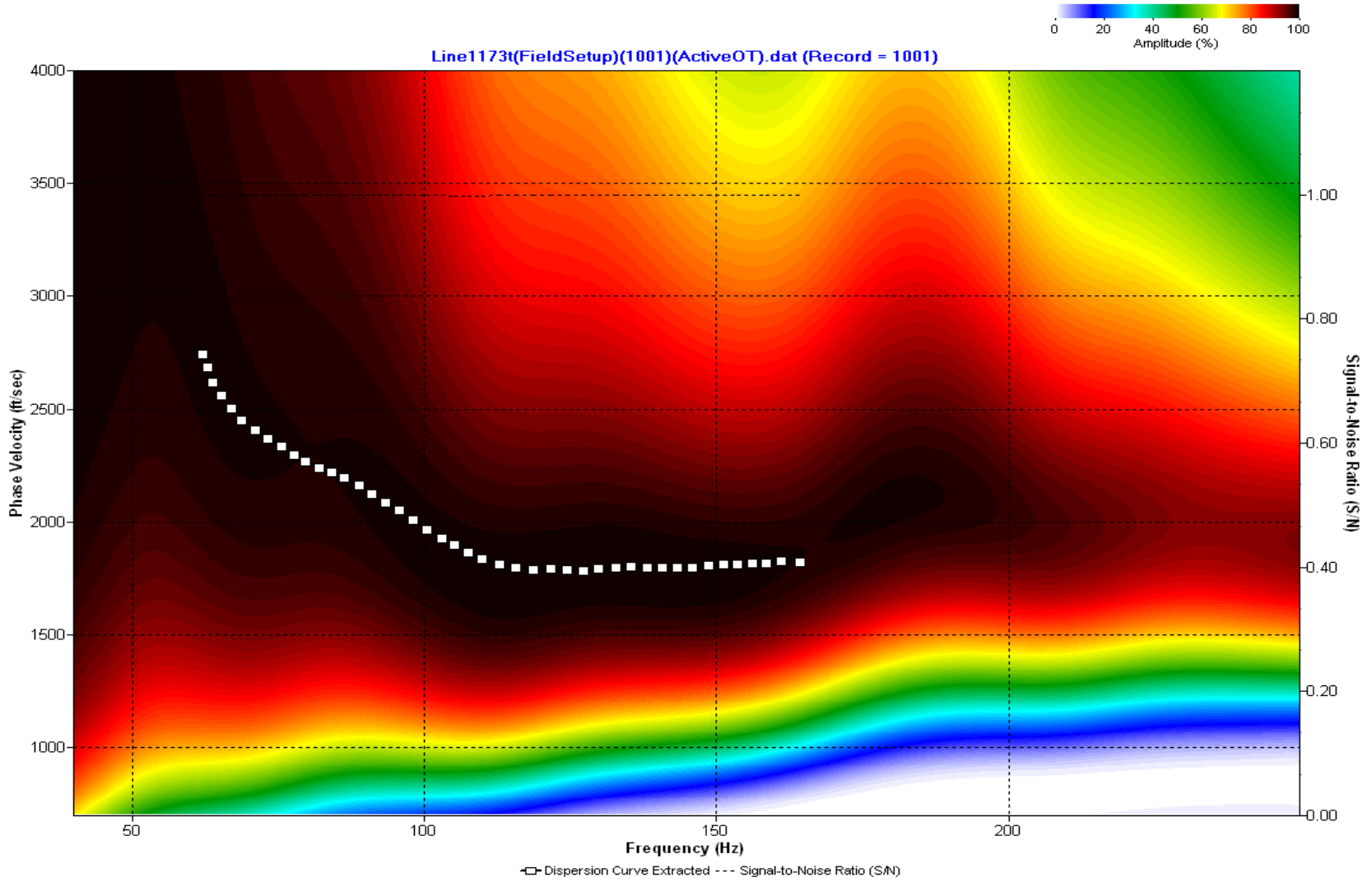

A.230: Dispersion Curve Line 1173 used in Post-blast 18

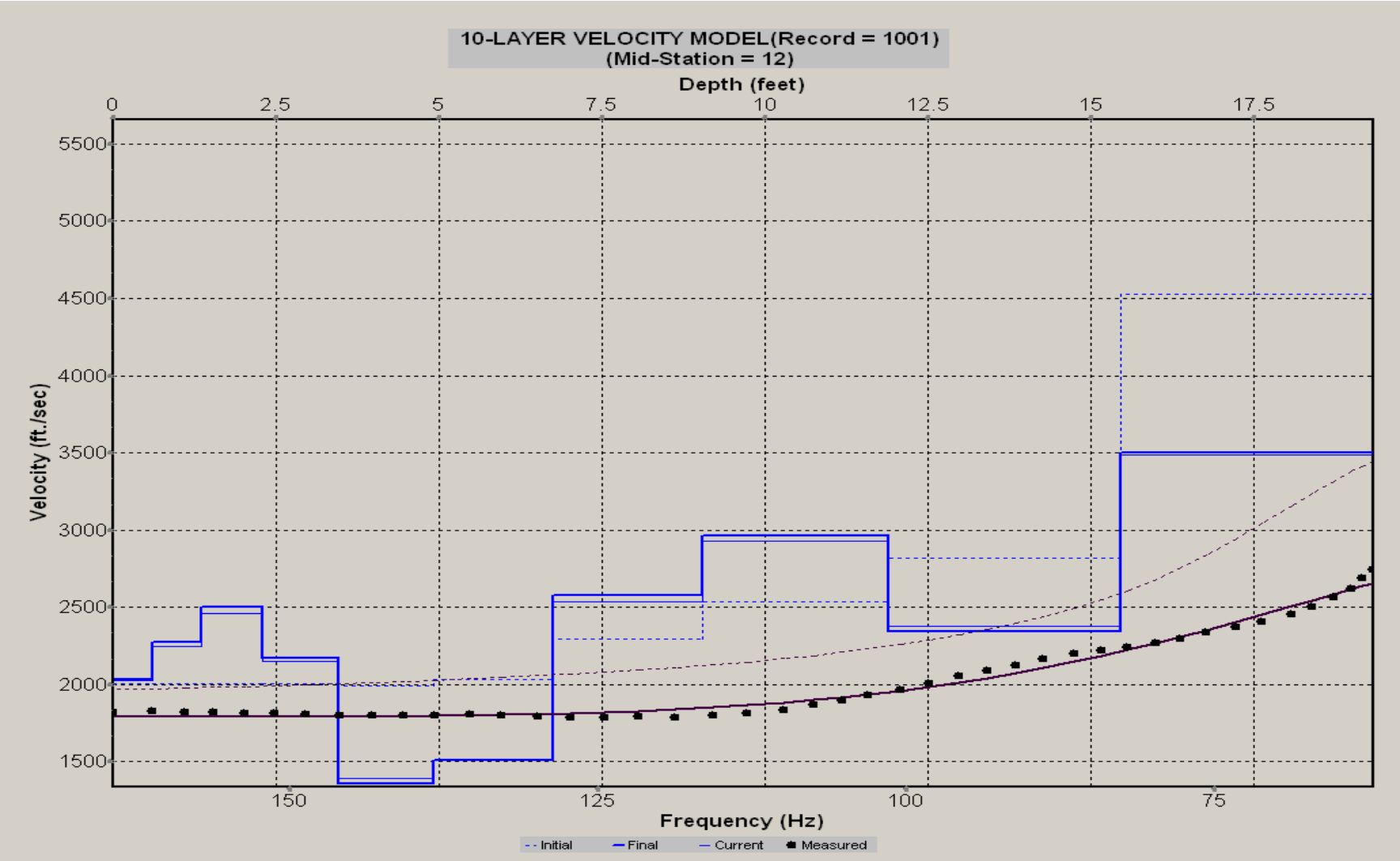

A.231: Velocity Profile Line 1173 used in Post-blast 18

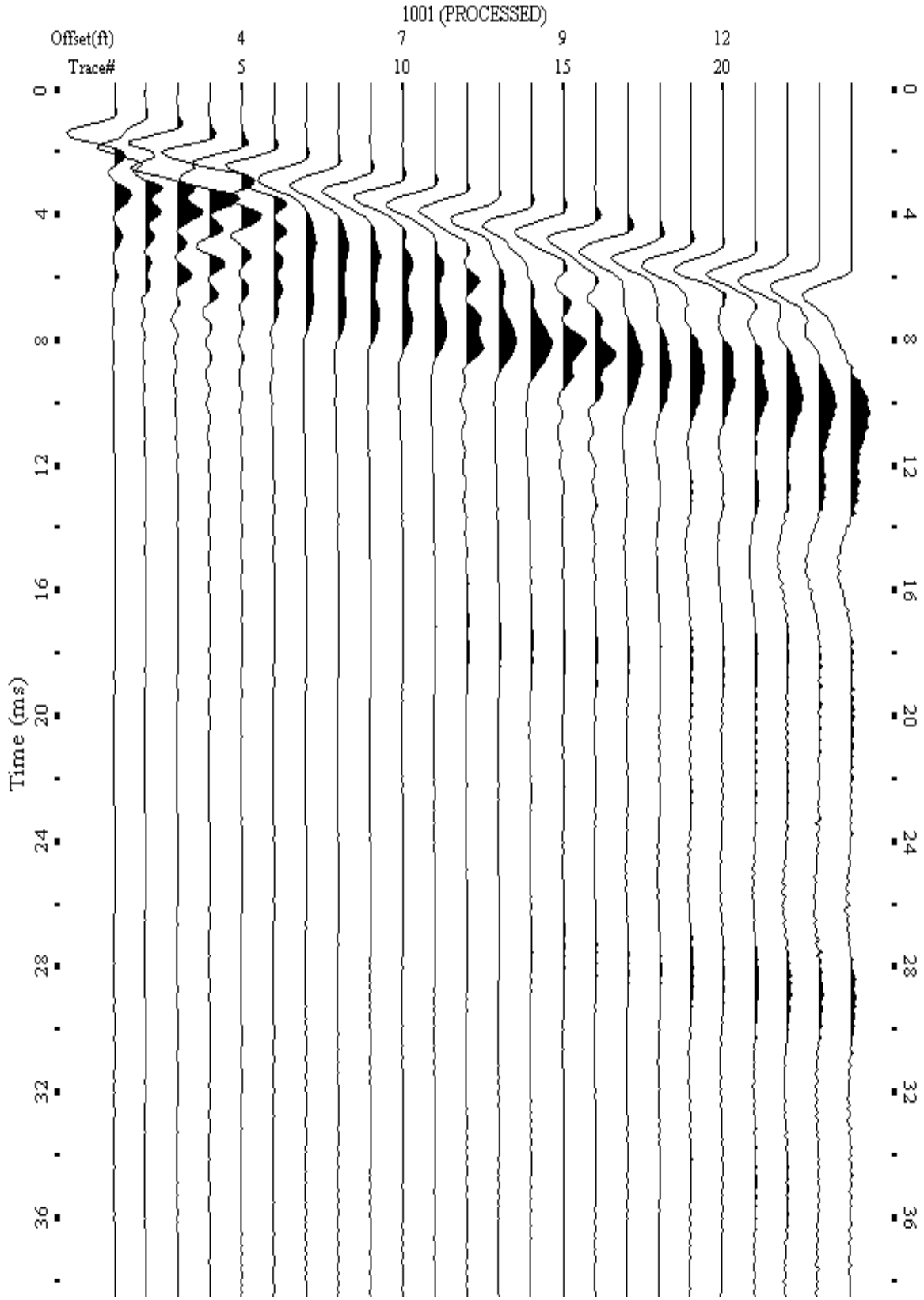

A.232: Shot Gather Line 1174 used in Post-blast 17

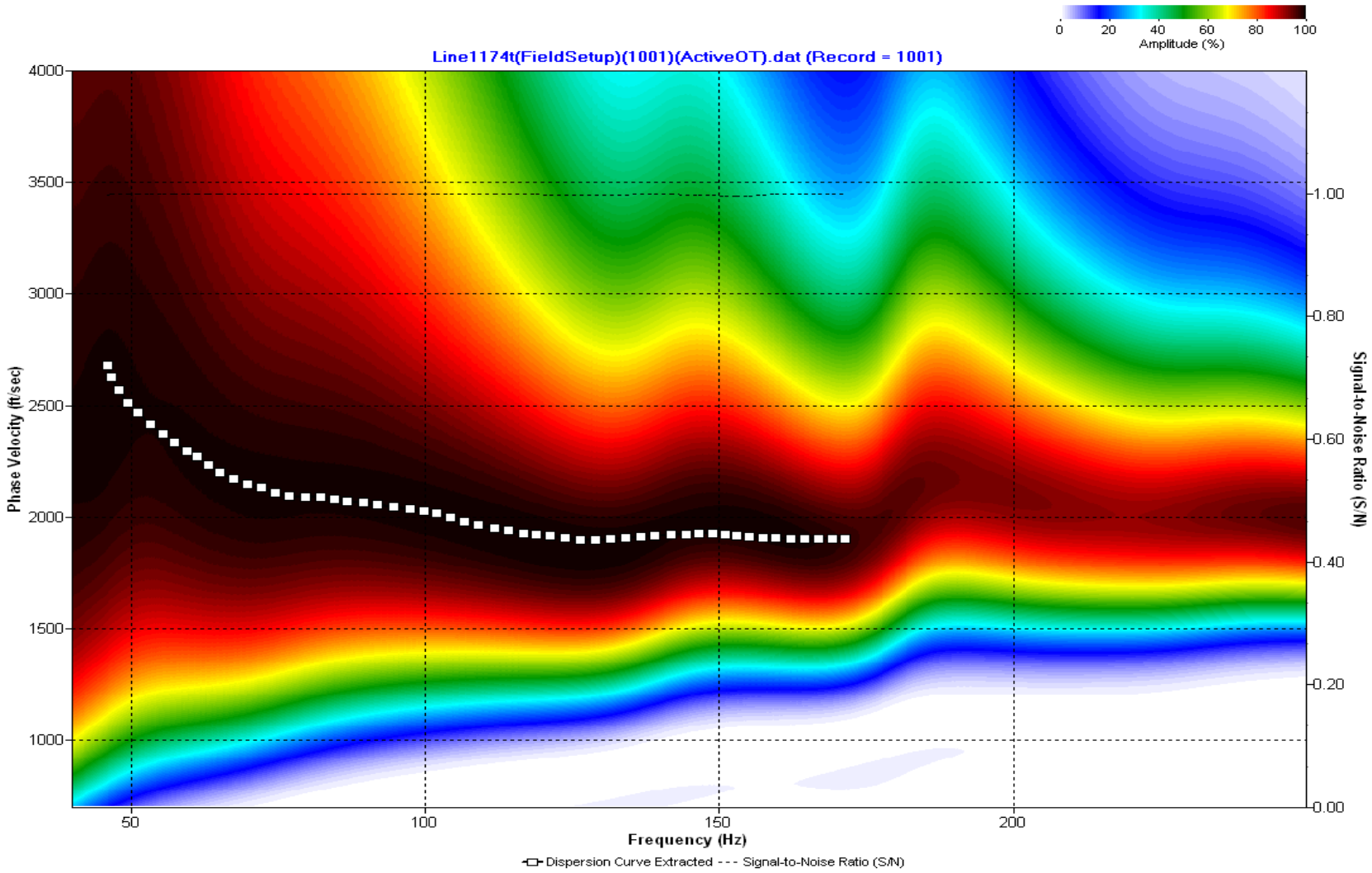

A.233: Dispersion Curve Line 1174 used in Post-blast 17

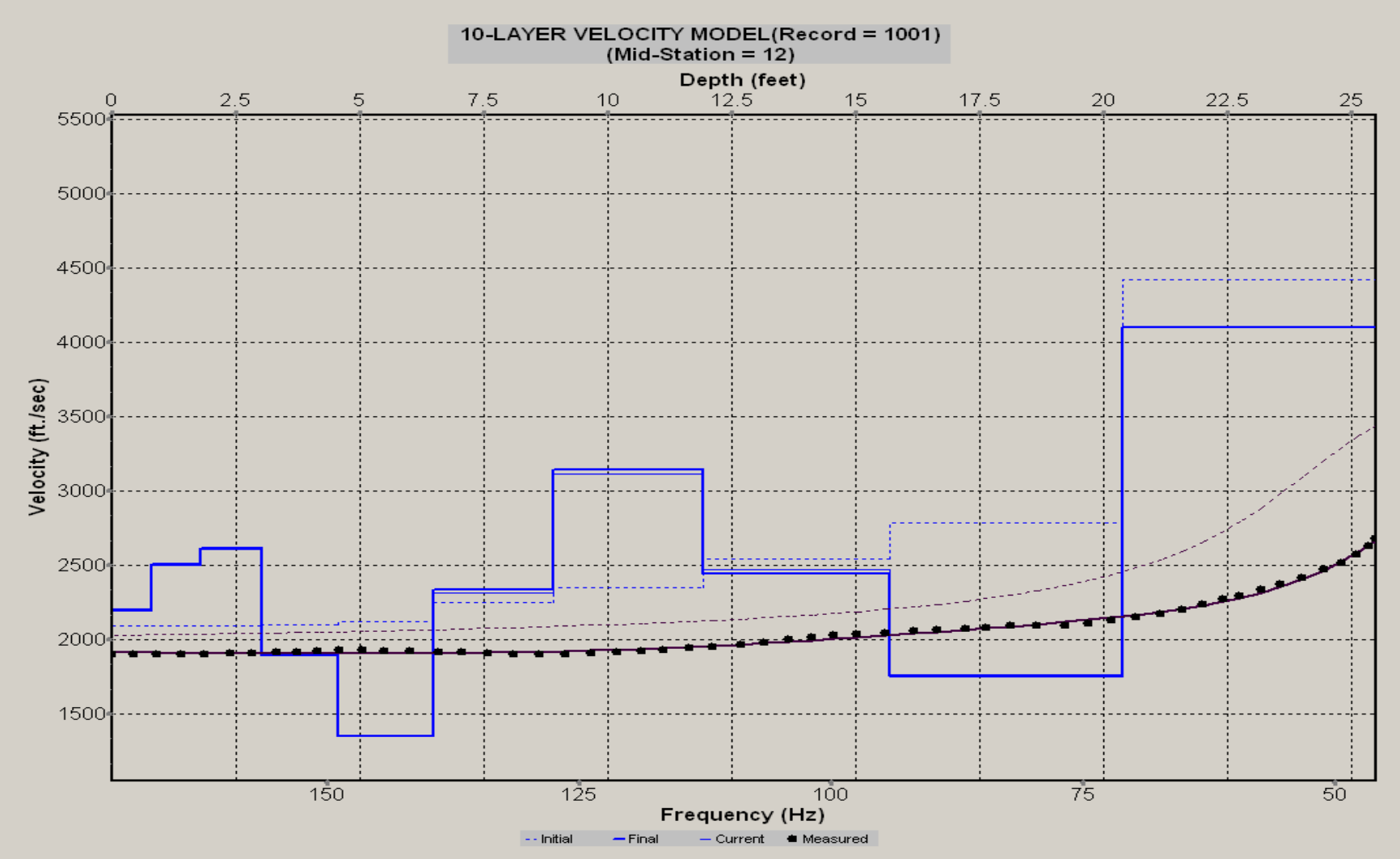

A.234: Velocity Profile Line 1174 used in Post-blast 17

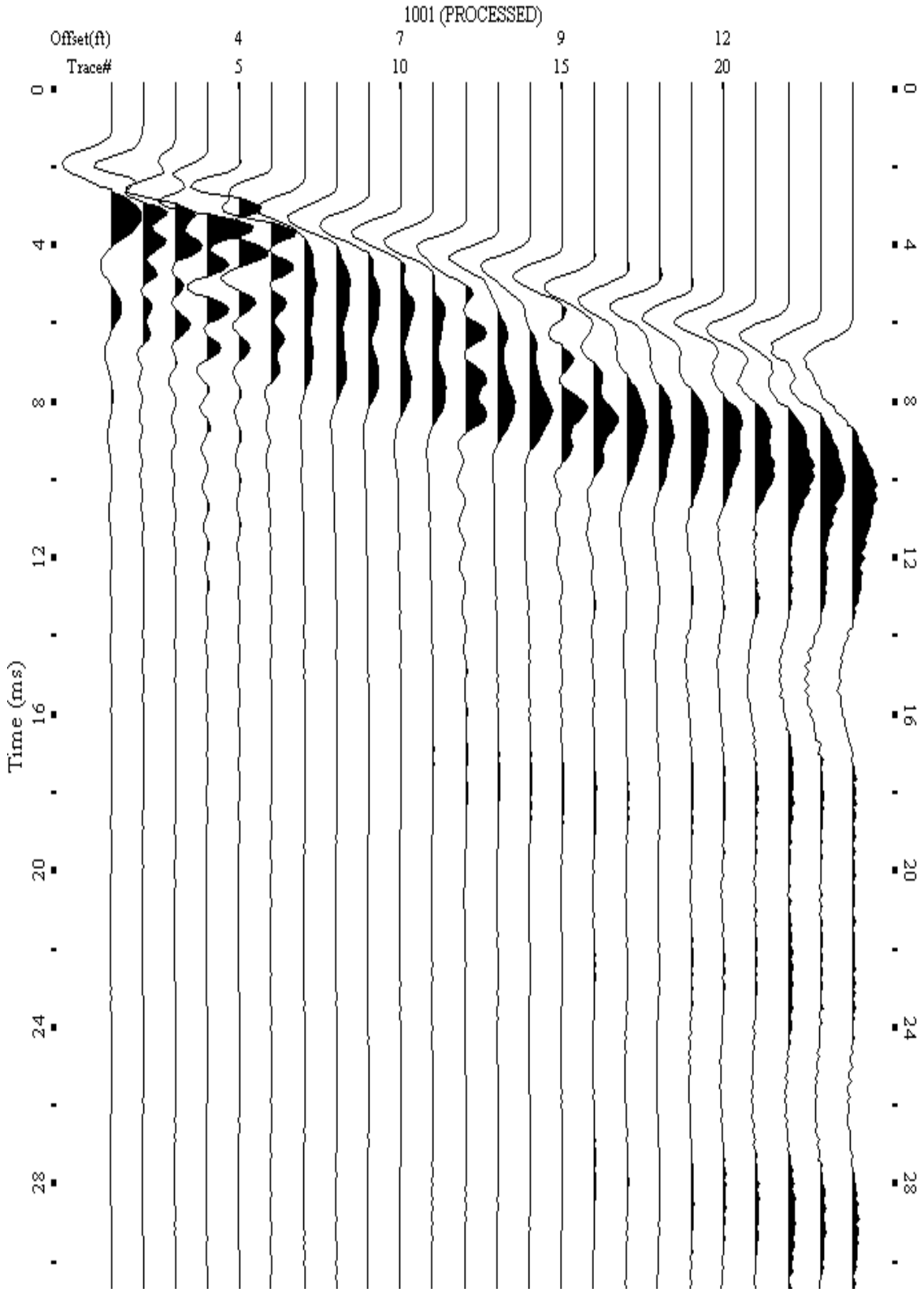

A.235: Shot Gather Line 1175 used in Post-blast 17 and Post-blast 18

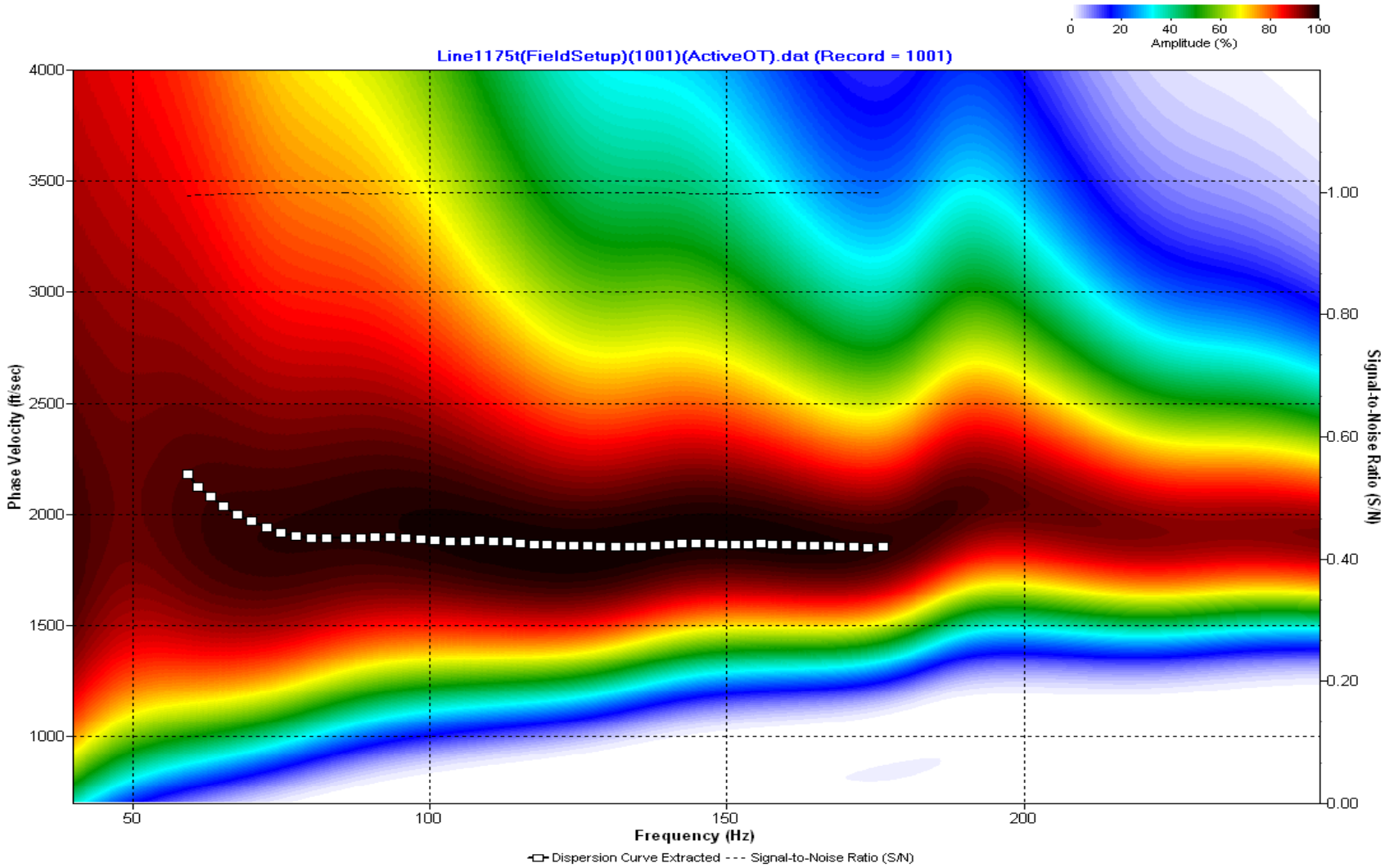

A.236: Dispersion Curve Line 1175 used in Post-blast 17 and Post-blast 18

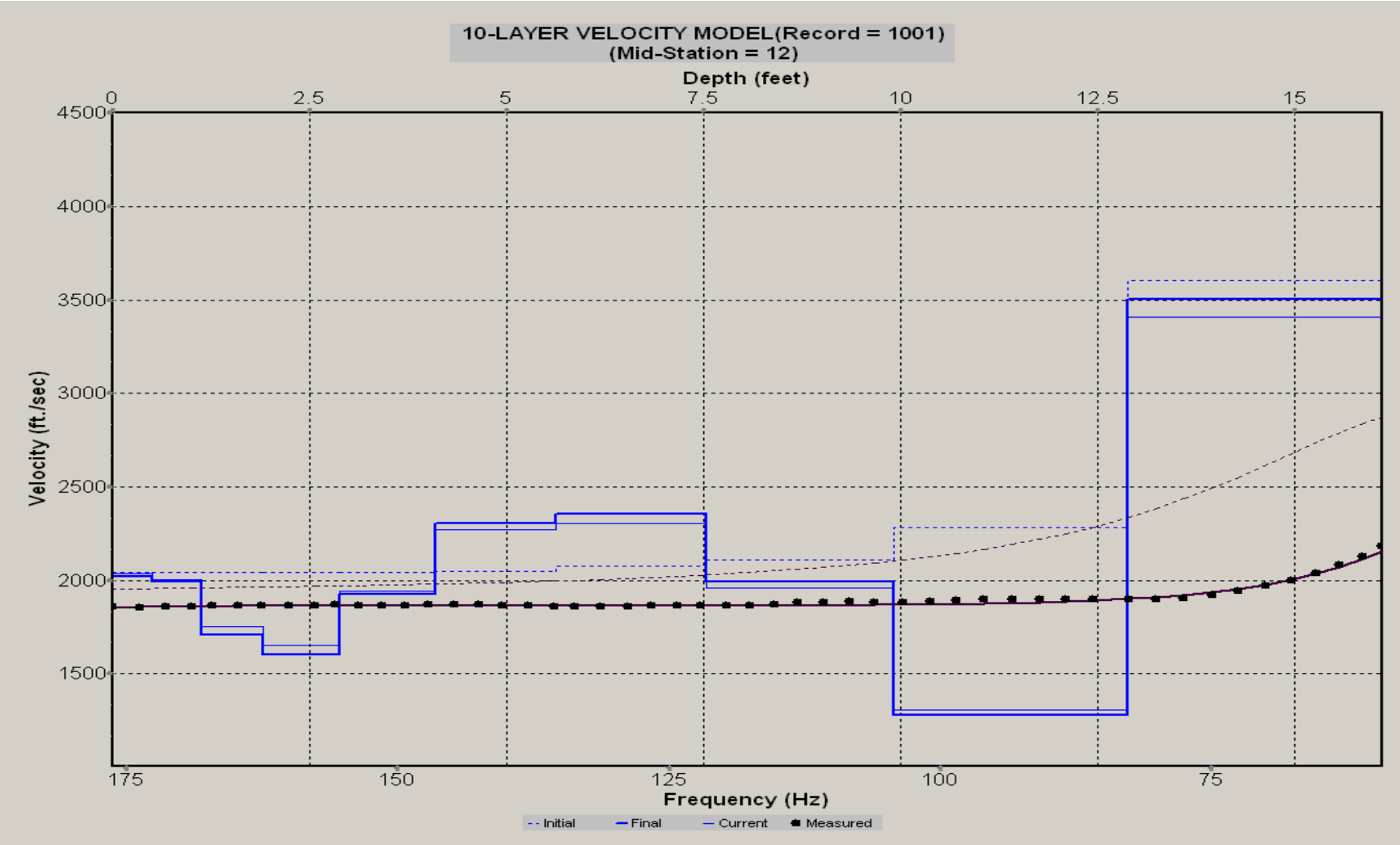

A.237: Velocity Profile Line 1175 used in Post-blast 17 and Post-blast 18

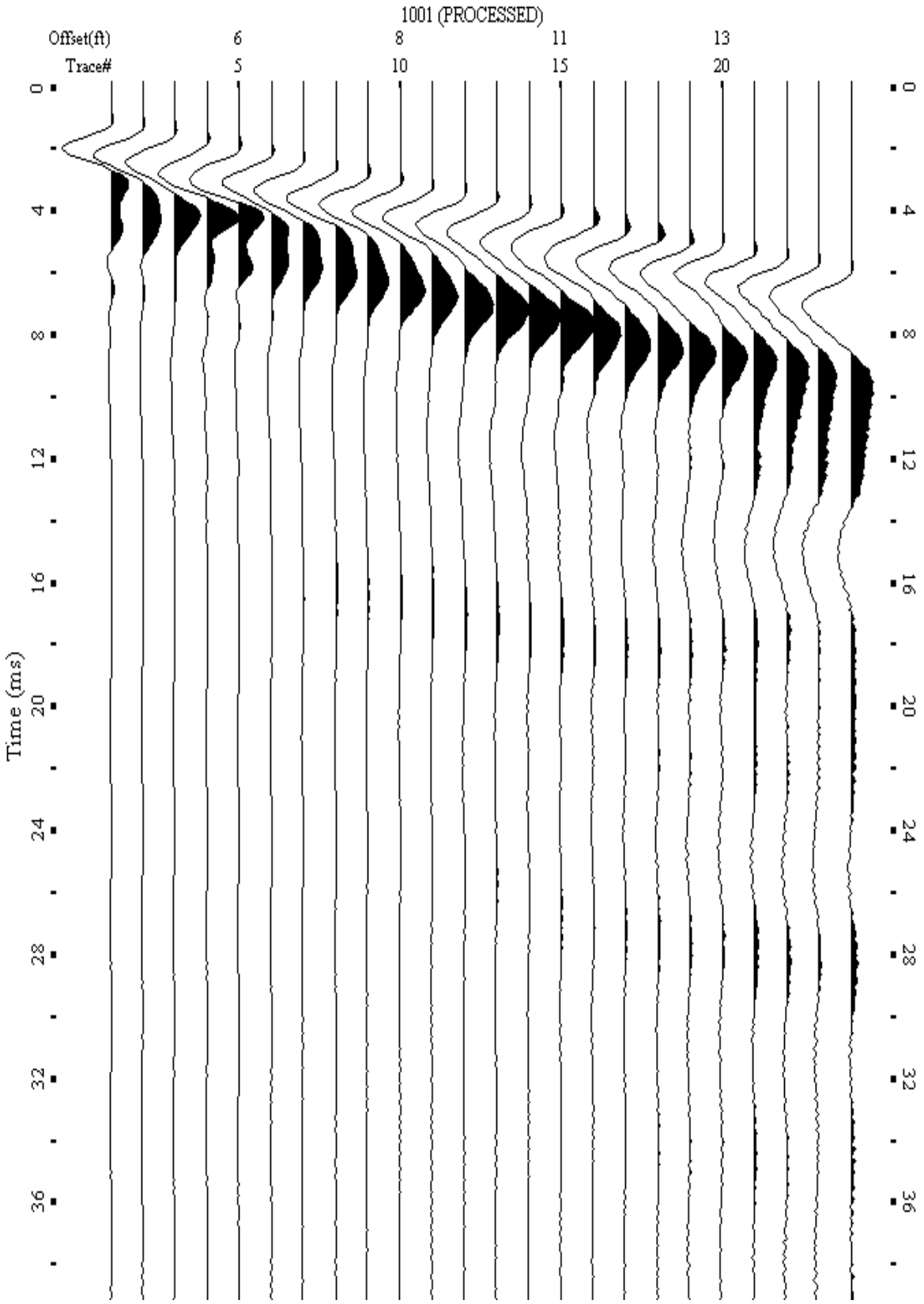

A.238: Shot Gather Line 1177 used in Post-blast 17

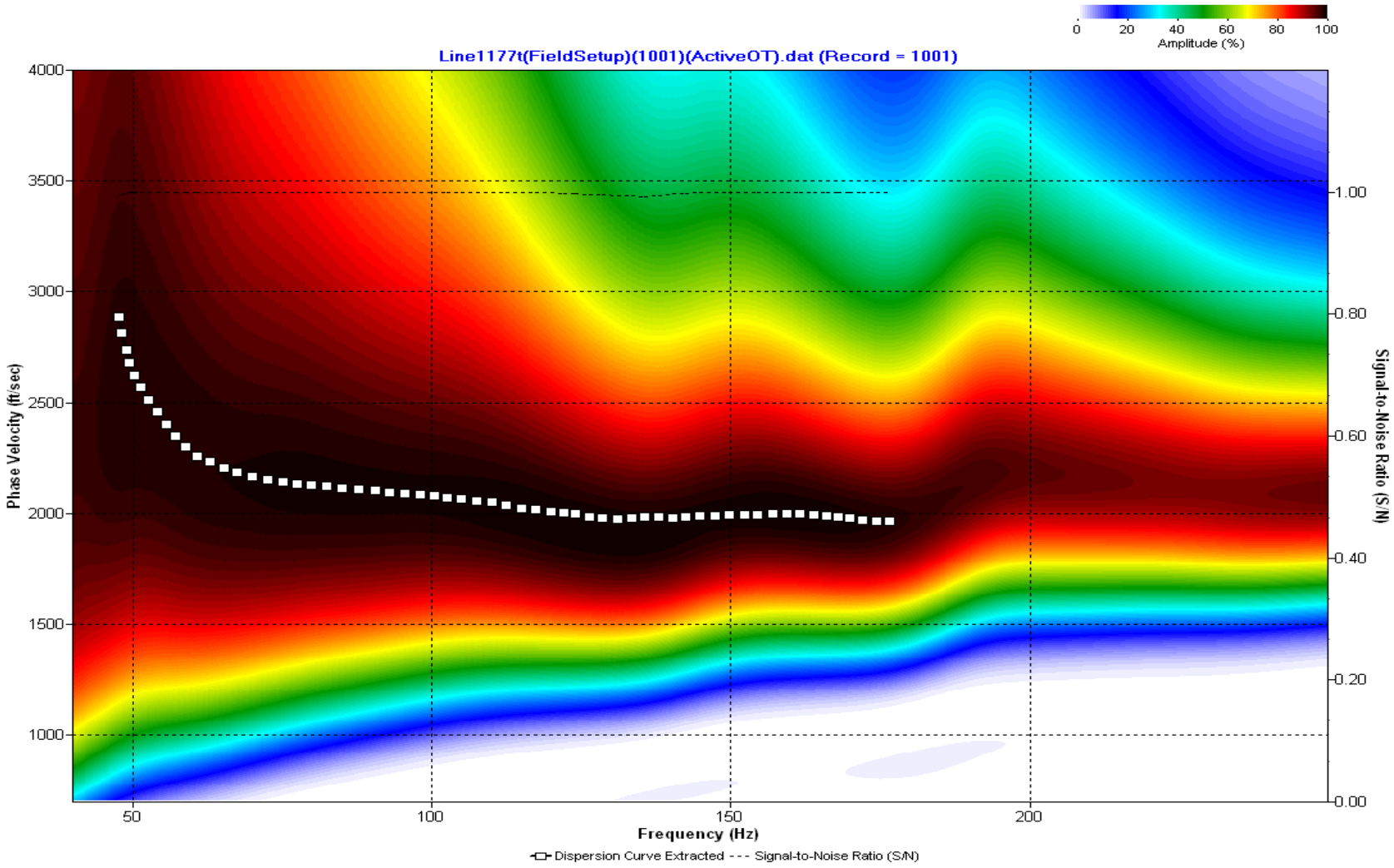

A.239: Dispersion Curve Line 1177 used in Post-blast 17

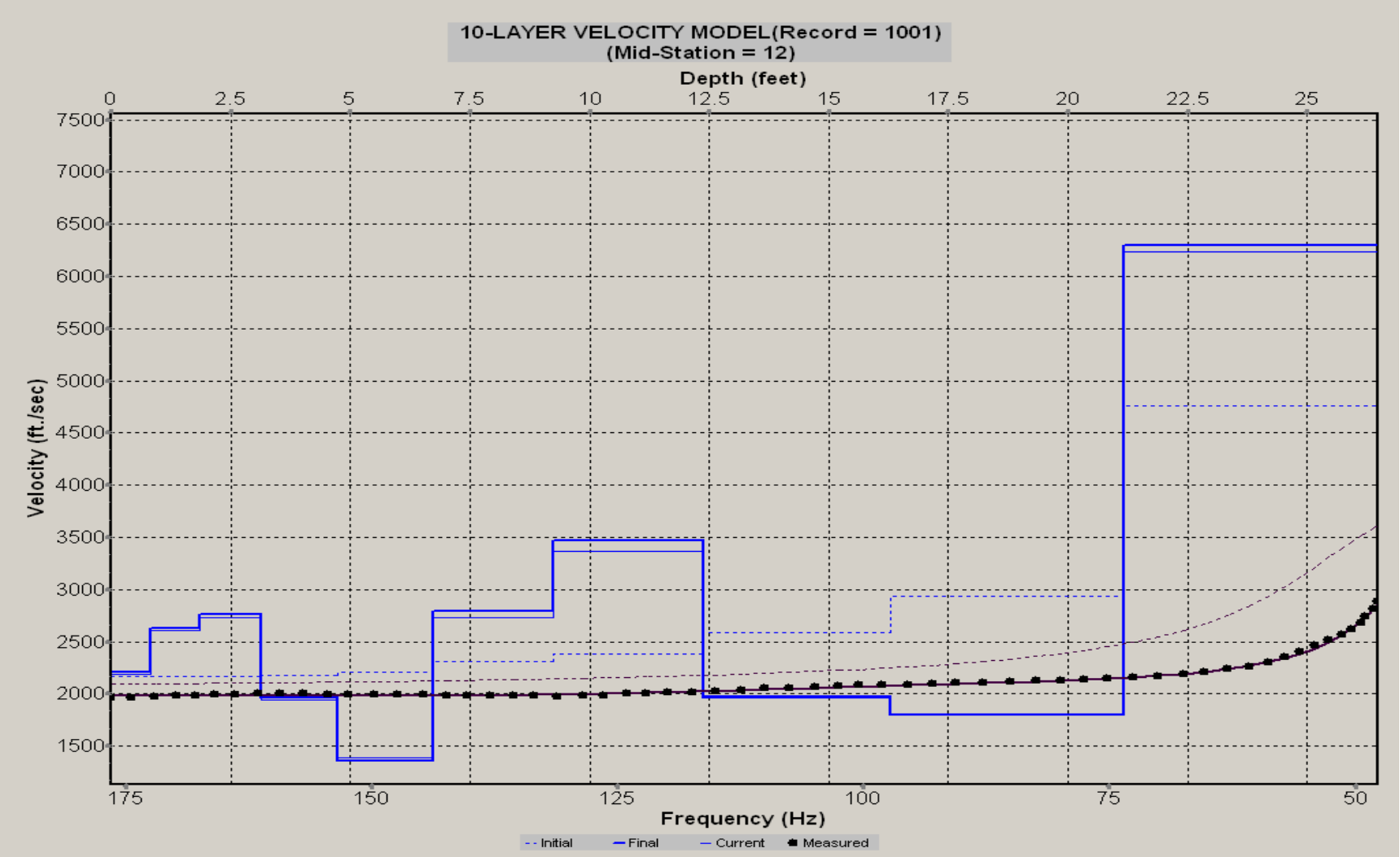

A.240: Velocity Profile Line 1177 used in Post-blast 17

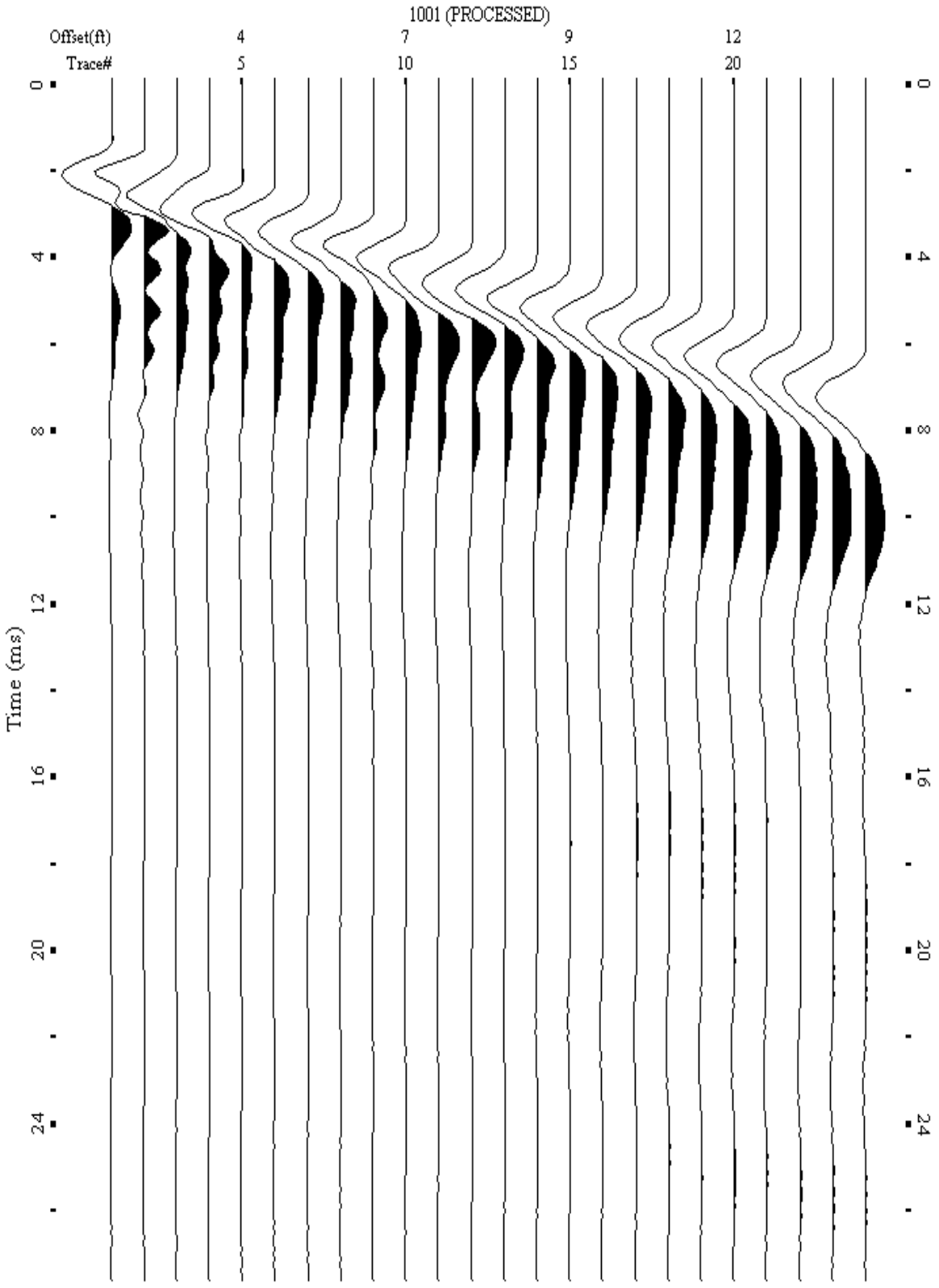

A.241: Shot Gather Line 1178 used in Post-blast 16 and Post-blast 17

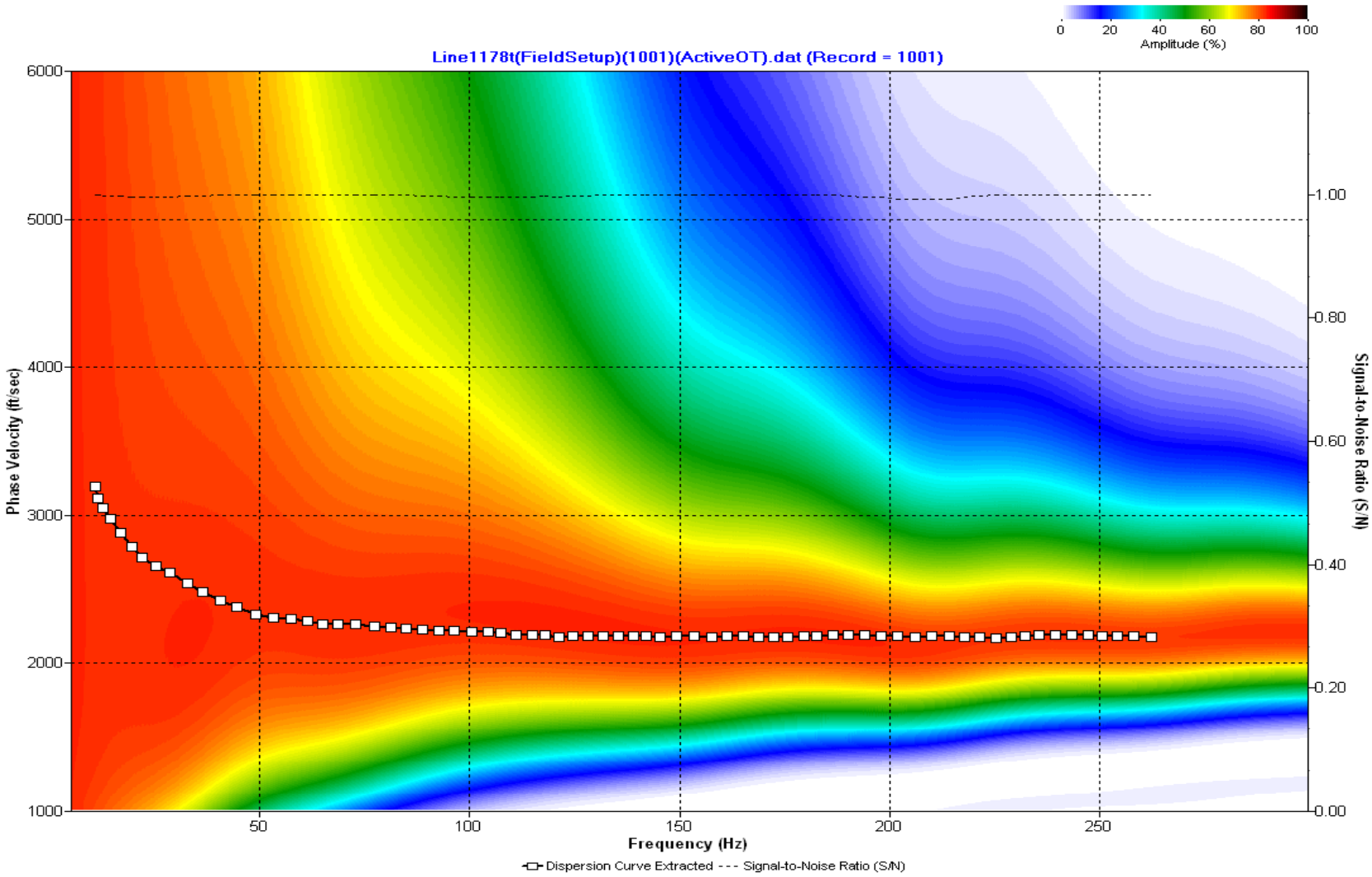

A.242: Dispersion Curve Line 1178 used in Post-blast 16 and Post-blast 17

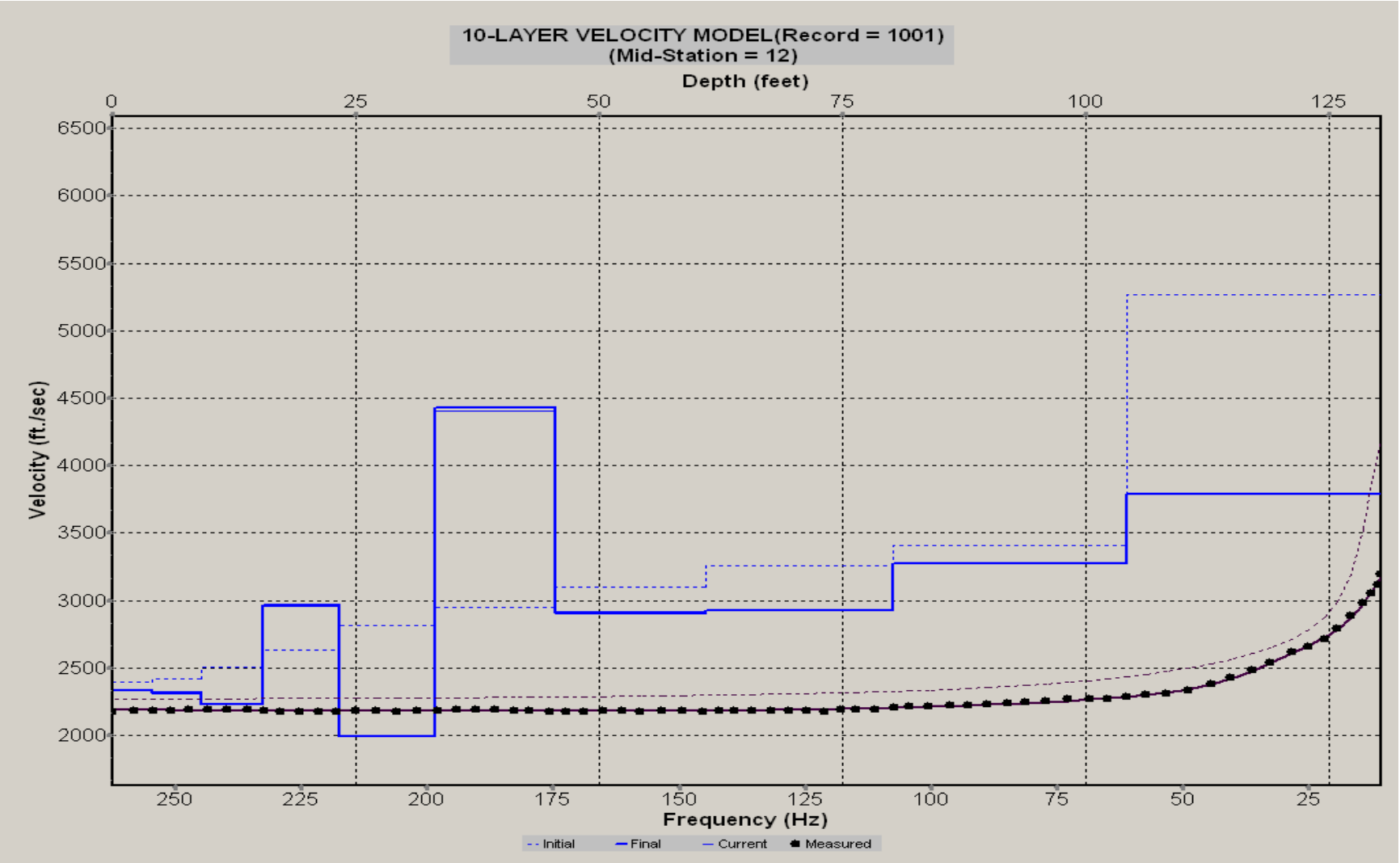

A.243: Velocity Profile Line 1178 used in Post-blast 16 and Post-blast 17

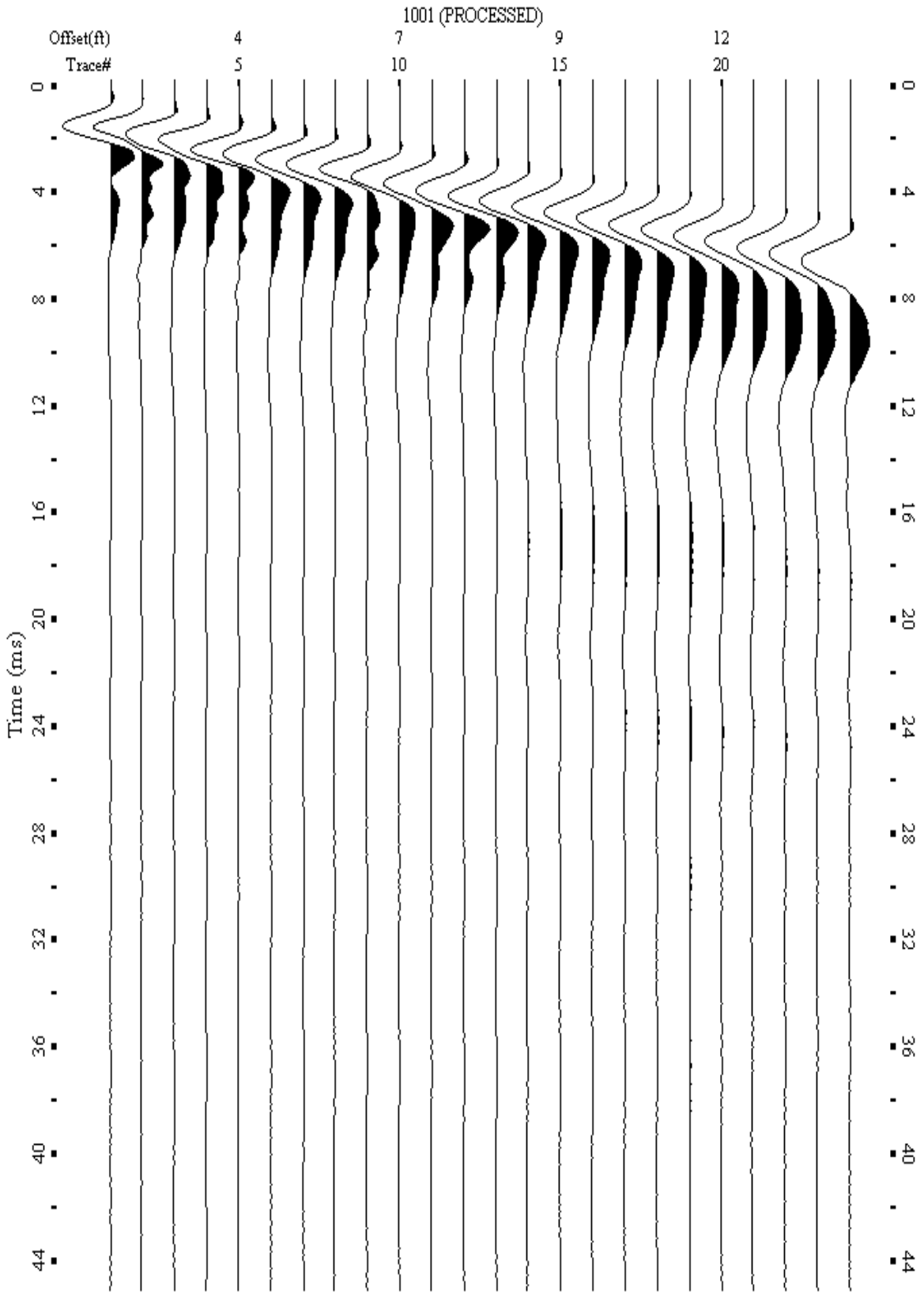

A.244: Shot Gather Line 1179 used in Post-blast 16 and Post-blast 17

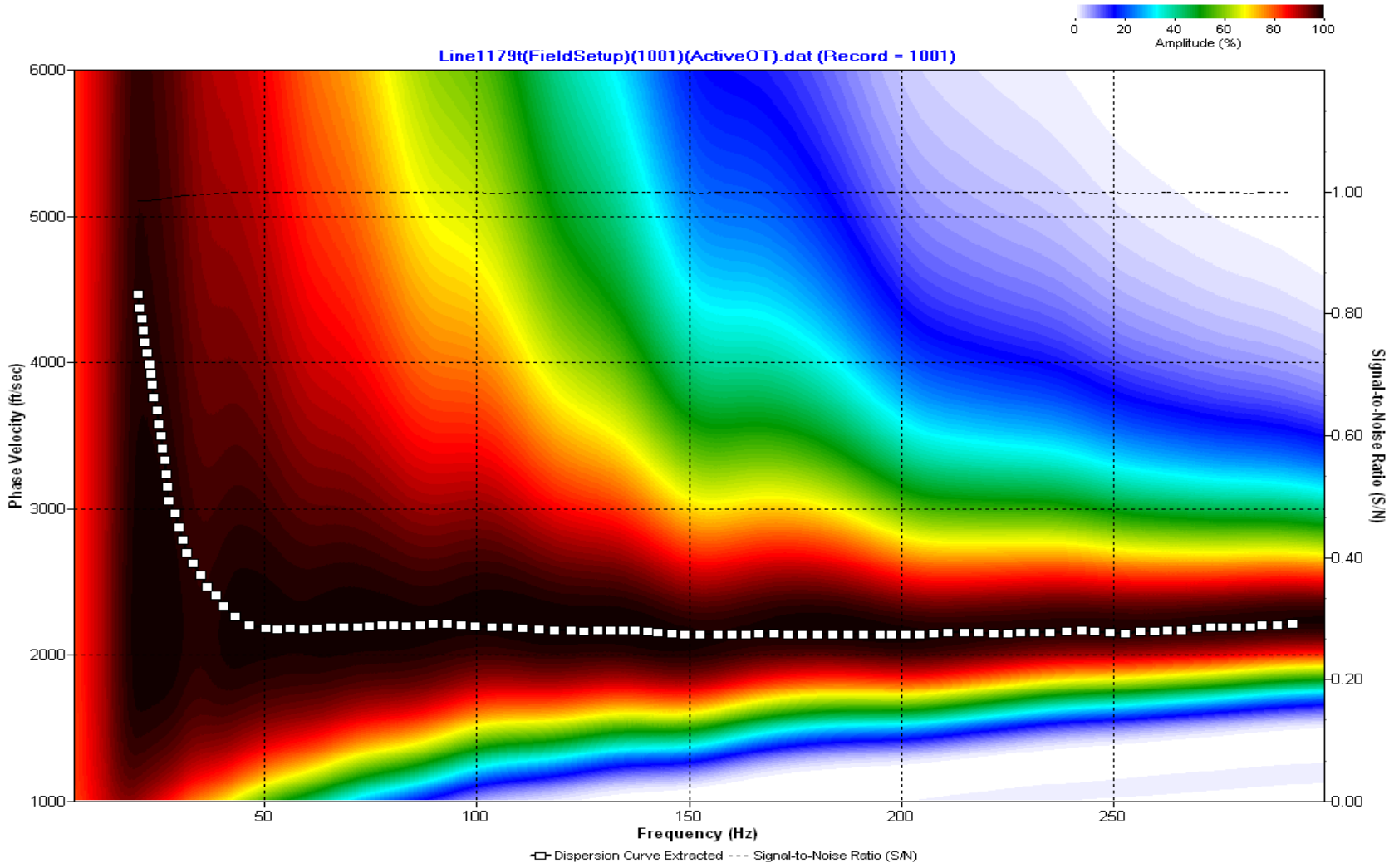

A.245: Dispersion Curve Line 1179 used in Post-blast 16 and Post-blast 17

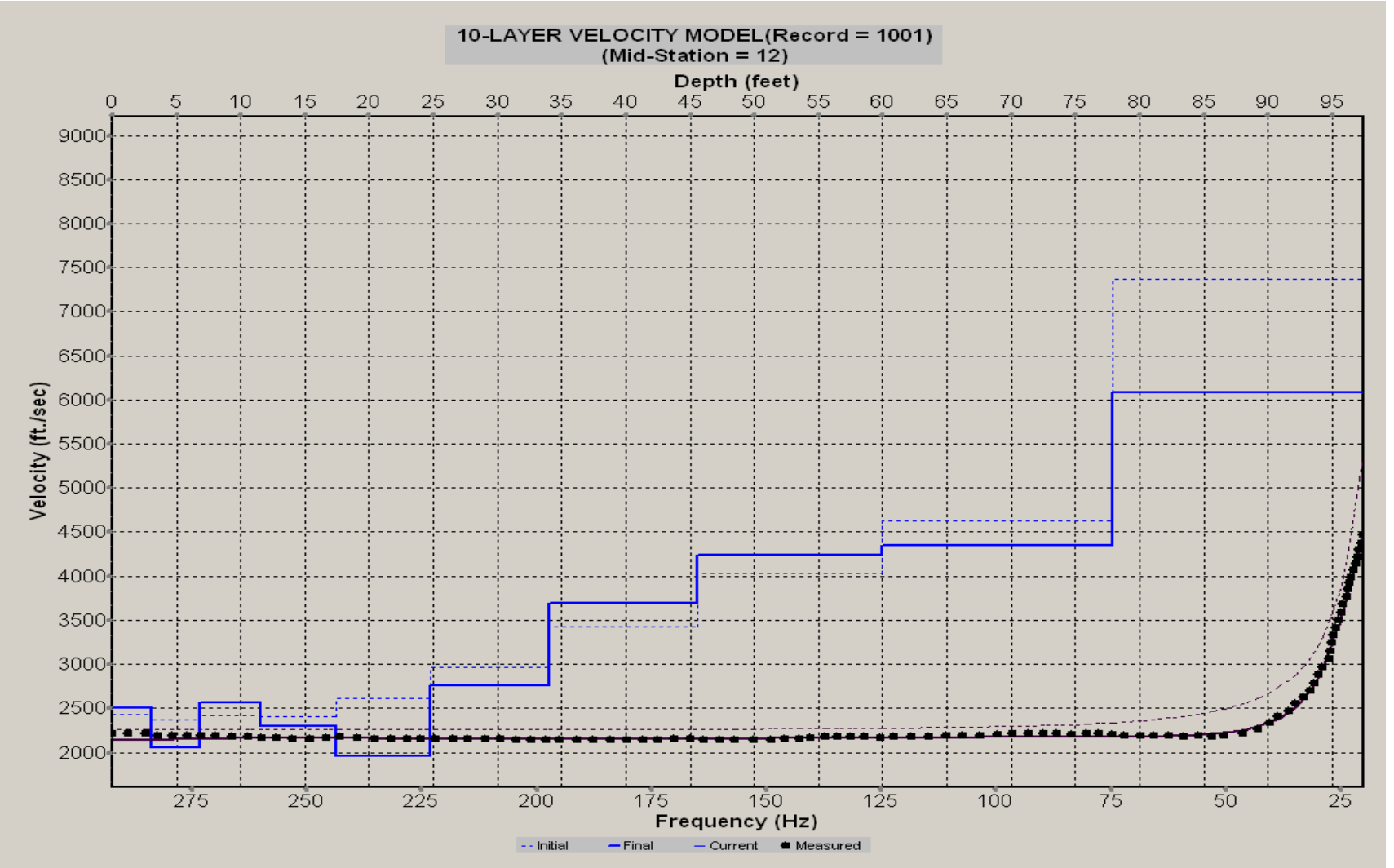

A.246: Velocity Profile Line 1179 used in Post-blast 16 and Post-blast 17

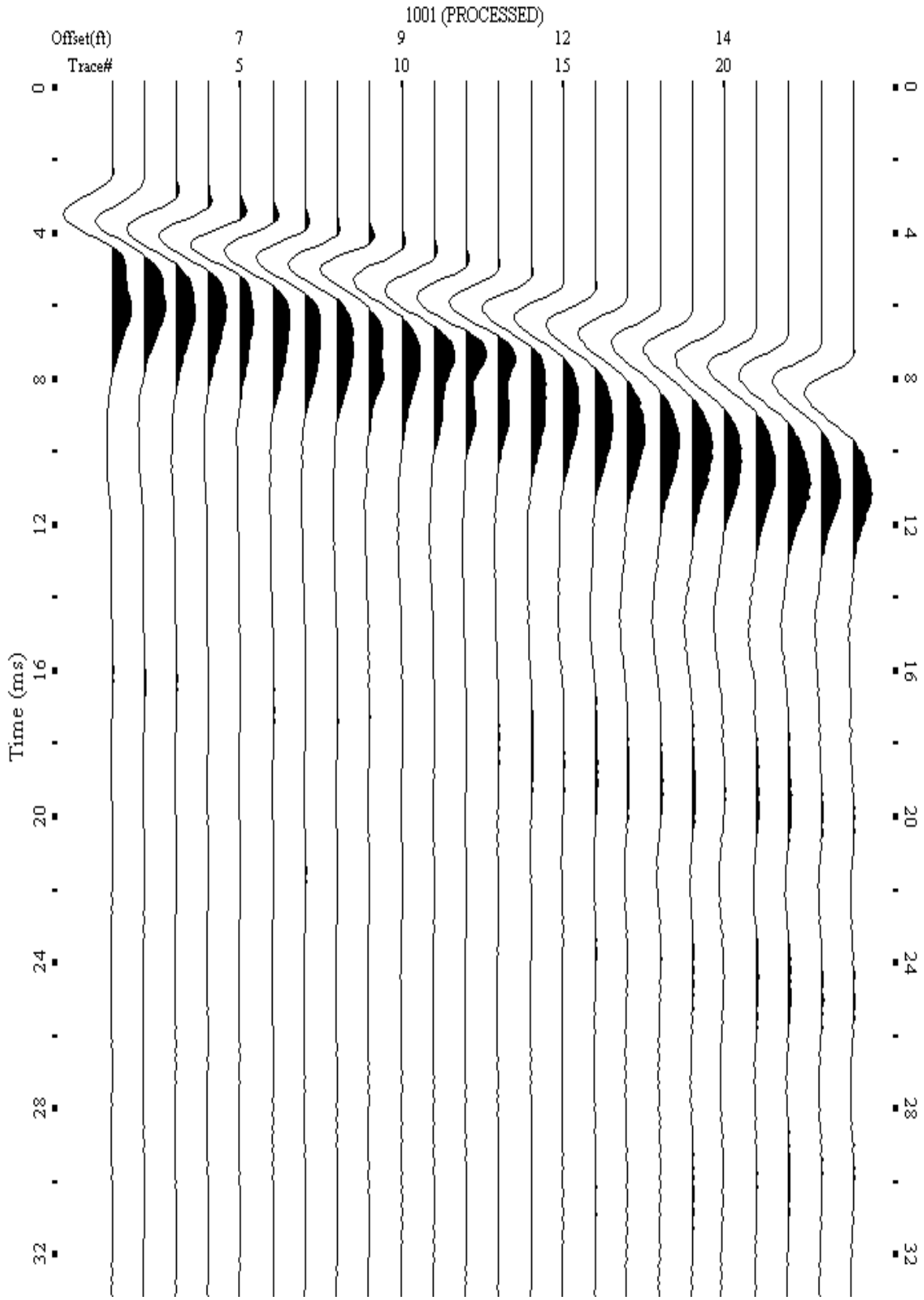

A.247: Shot Gather Line 1180 used in Post-blast 16 and Post-blast 17

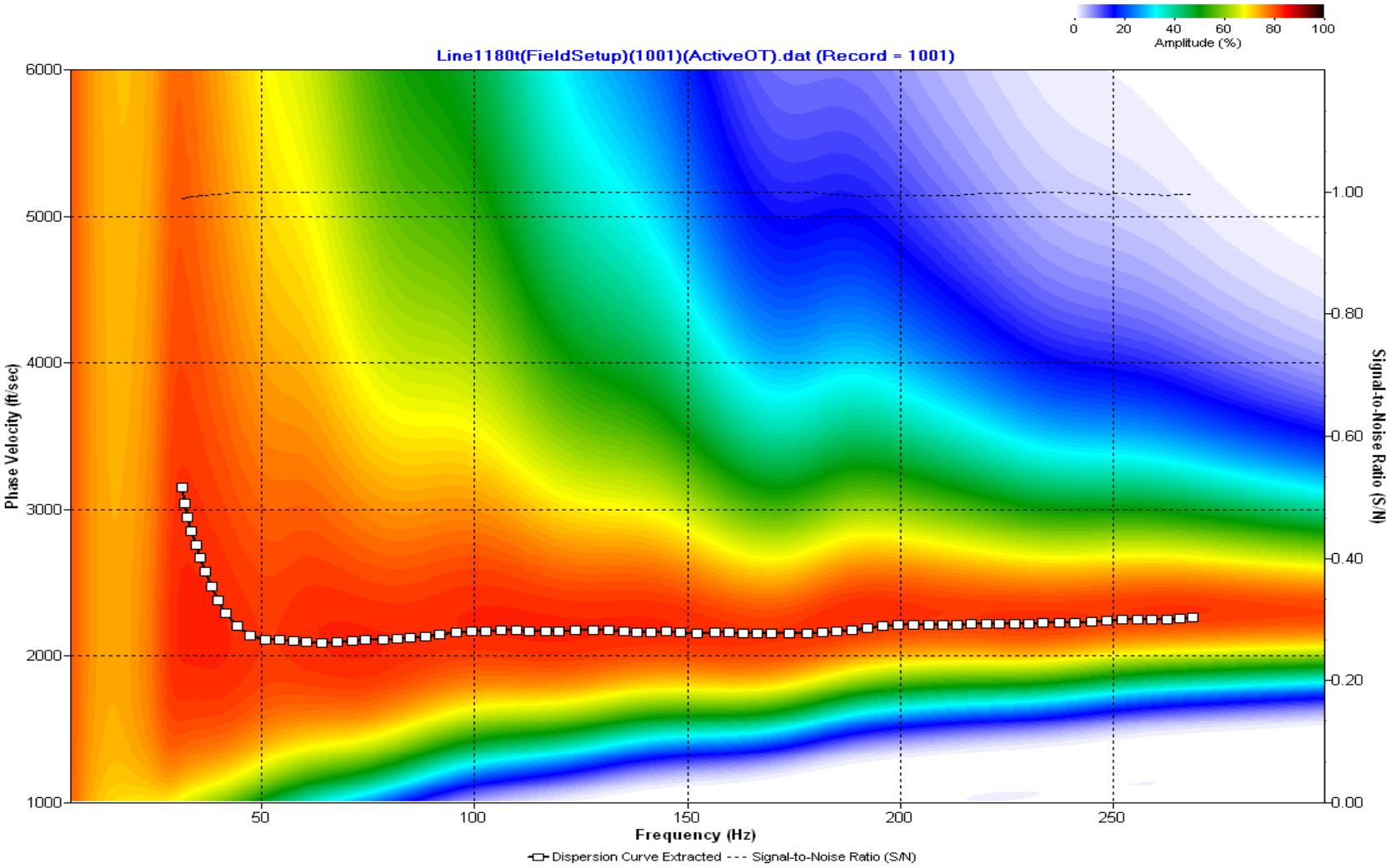

A.248: Dispersion Curve Line 1180 used in Post-blast 16 and Post-blast 17

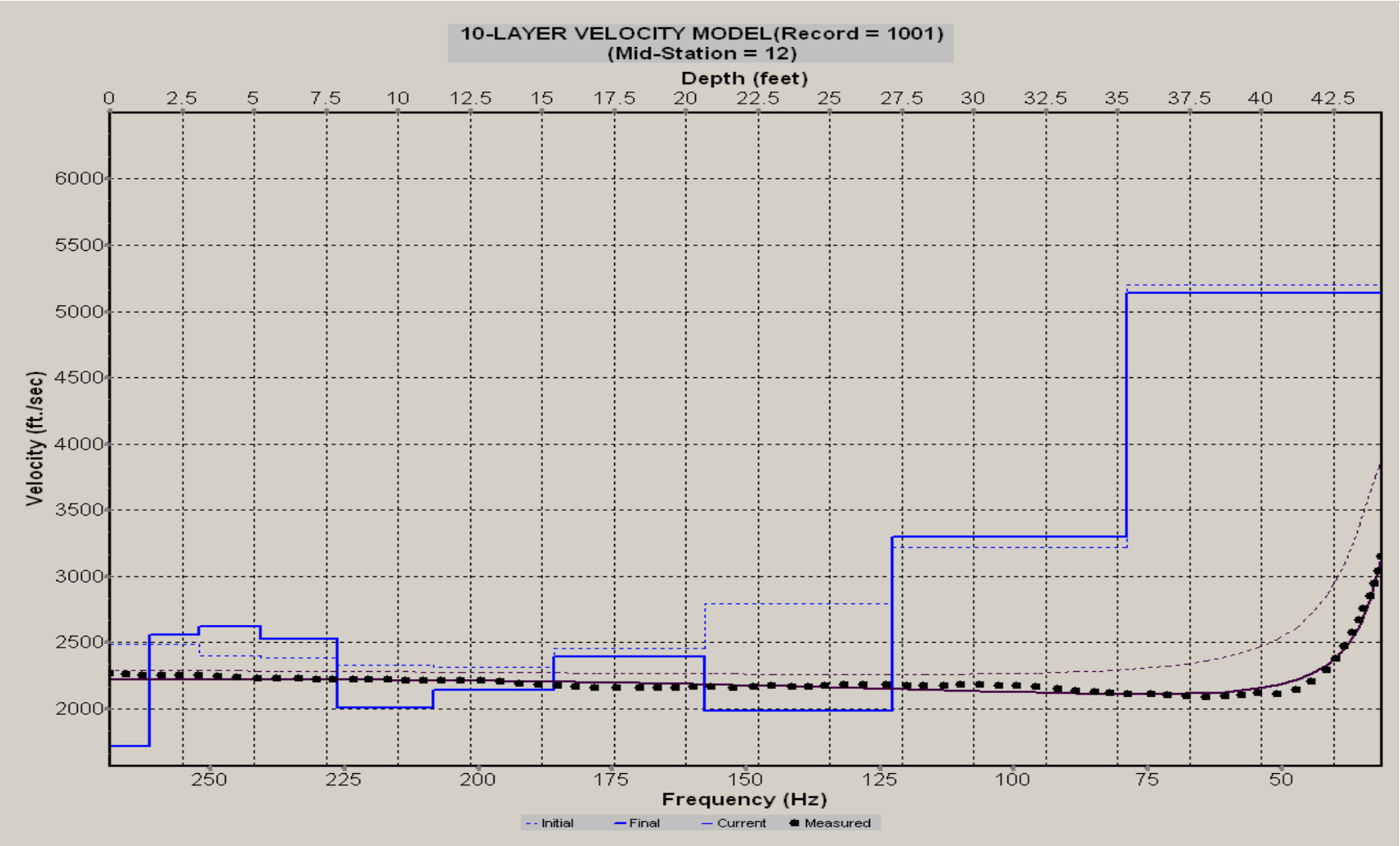

A.249: Velocity Profile Line 1180 used in Post-blast 16 and Post-blast 17

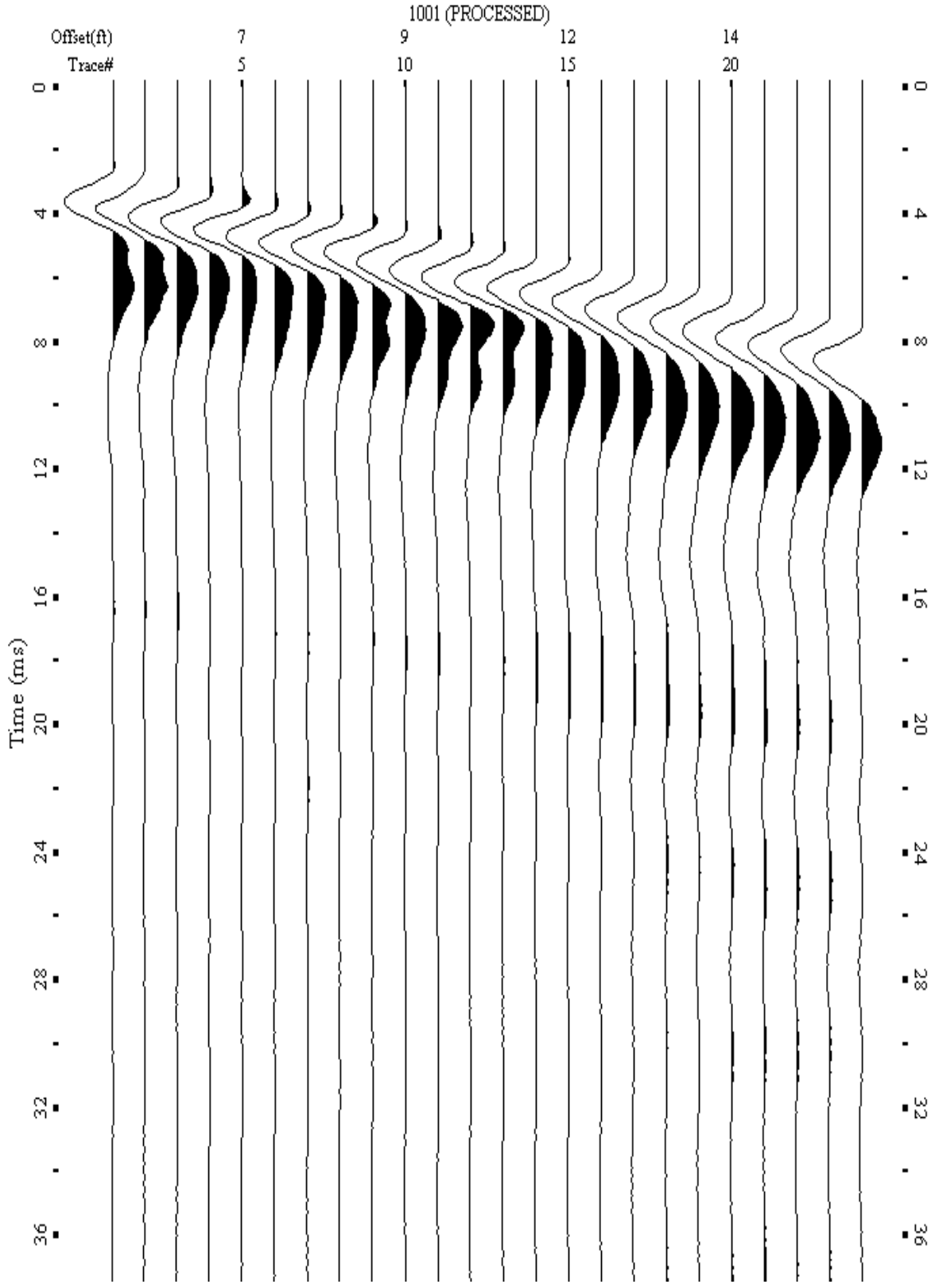

A.250: Shot Gather Line 1181 used in Post-blast 17

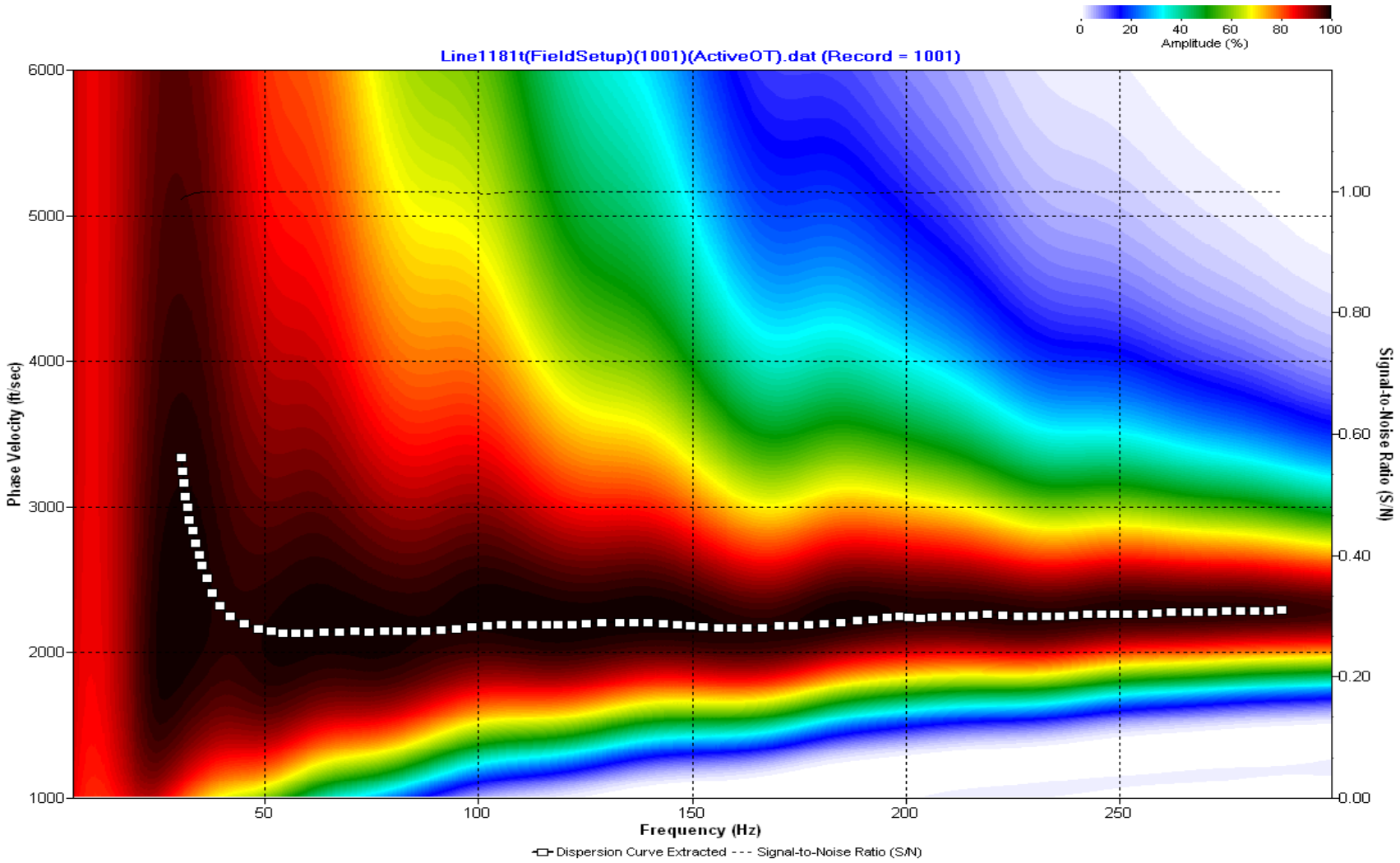

A.251: Dispersion Curve Line 1181 used in Post-blast 17

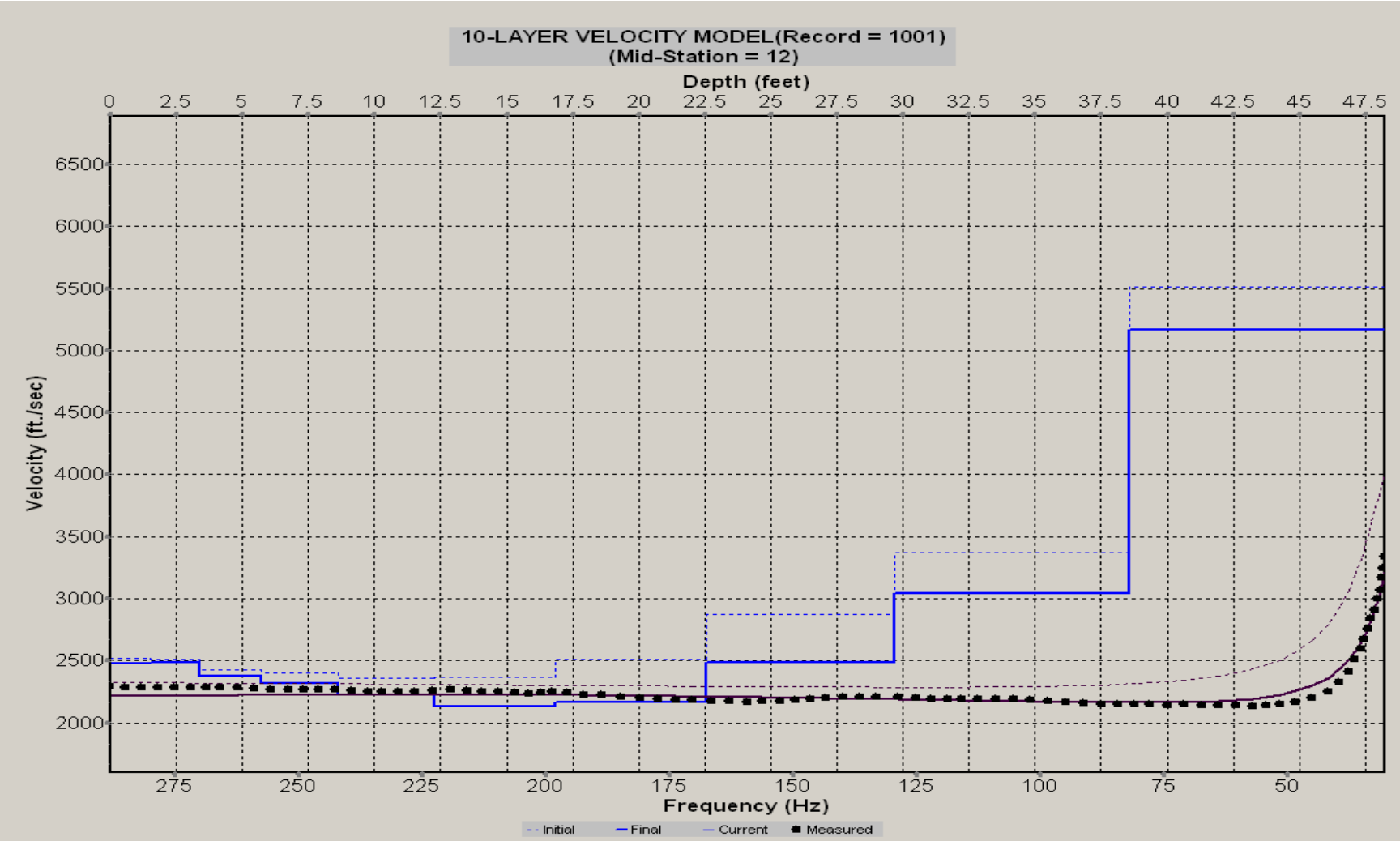

A.252: Velocity Profile Line 1181 used in Post-blast 17

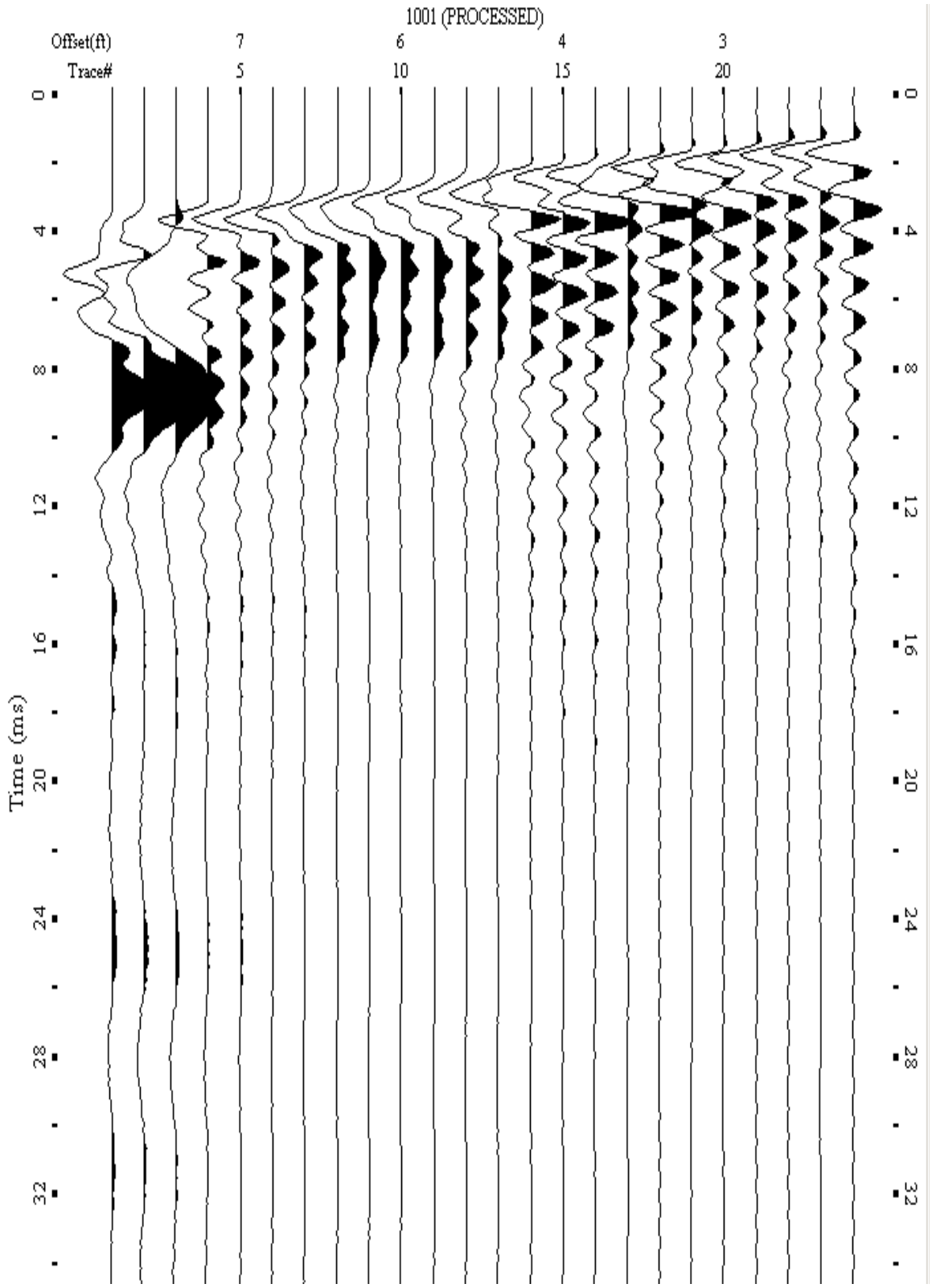

A.253: Shot Gather Line 1186 used in Post-blast 21 and Pre-blast 23

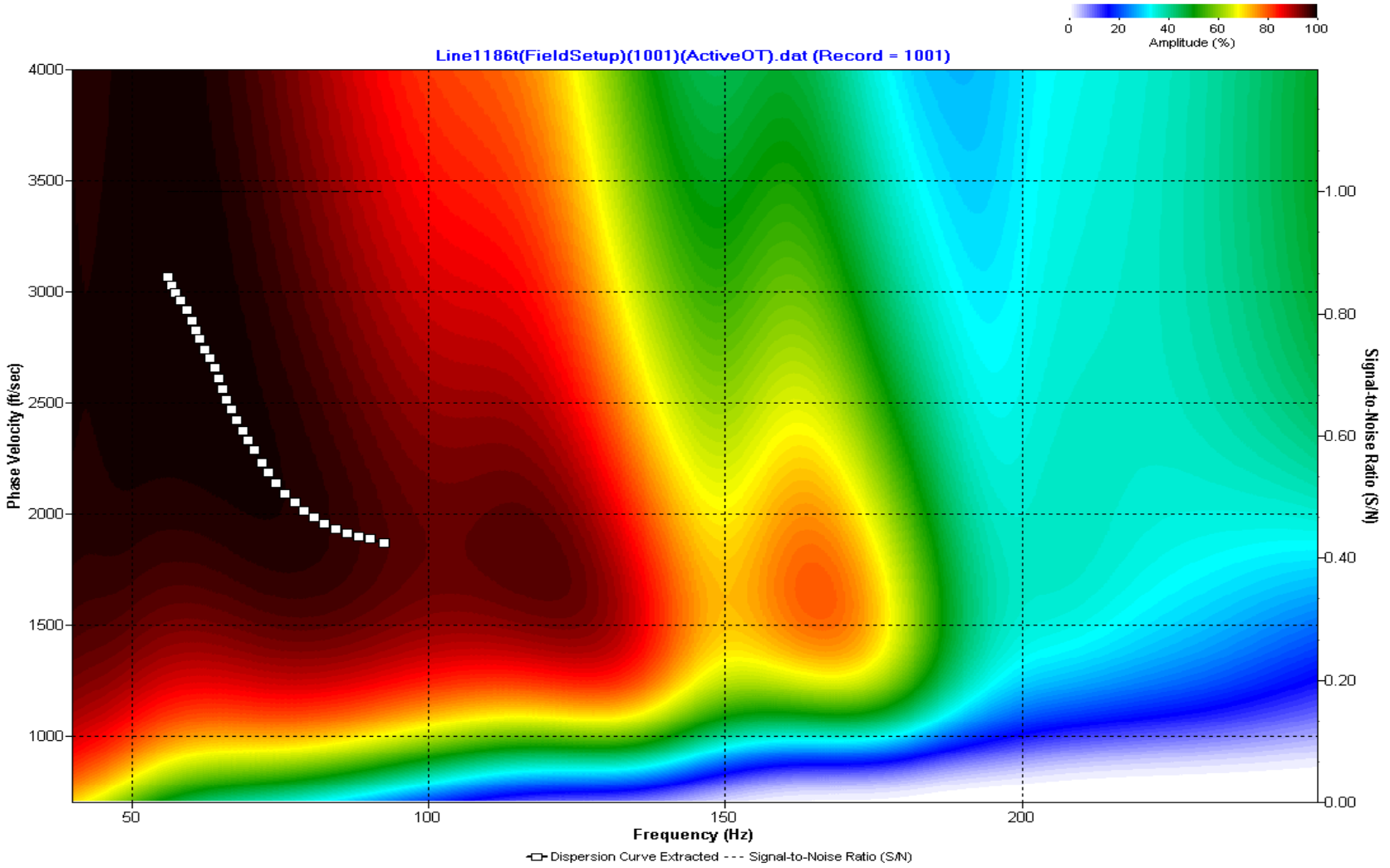

A.254: Dispersion Curve Line 1186 used in Post-blast 21 and Pre-blast 23

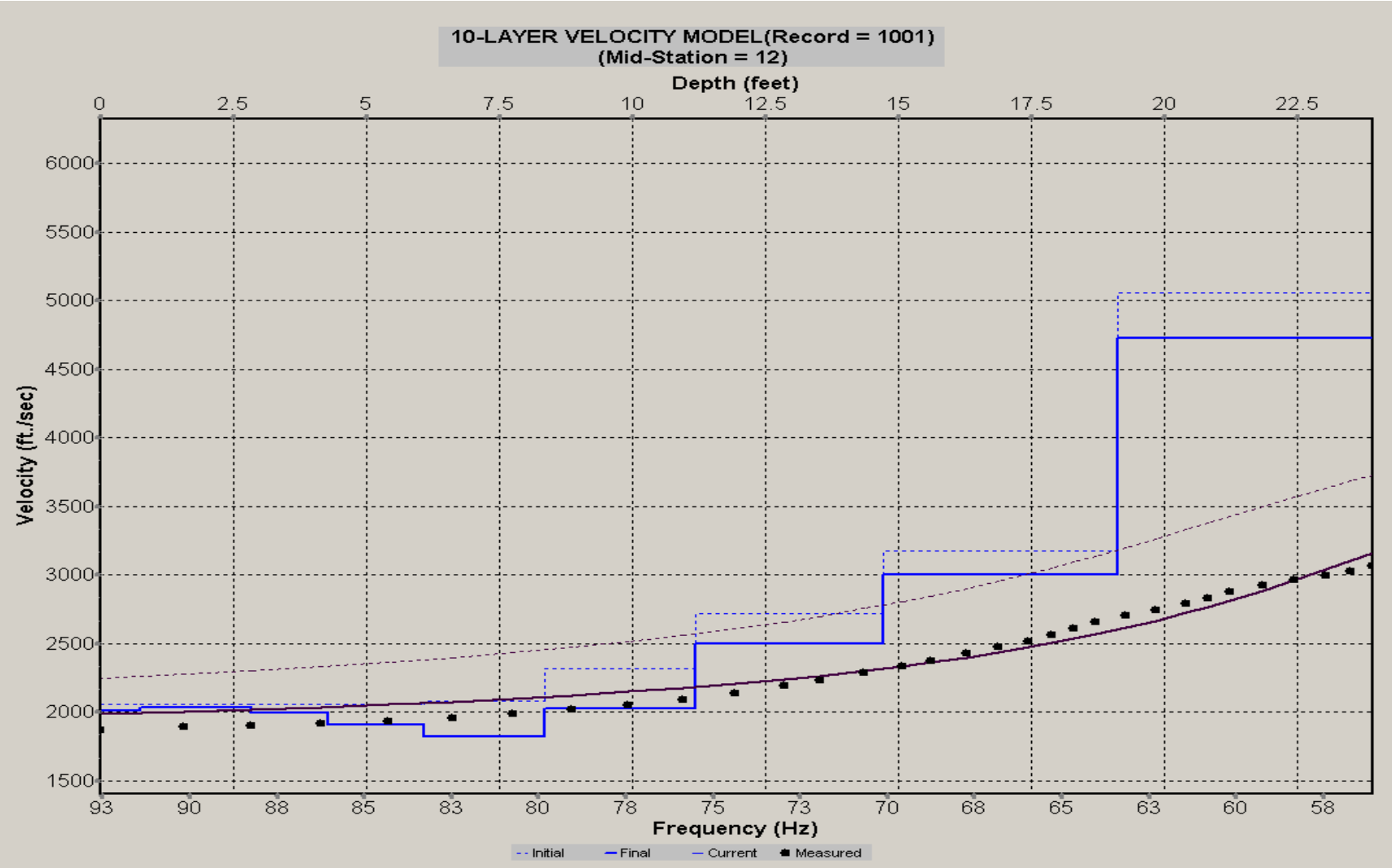

A.255: Velocity Profile Line 1186 used in Post-blast 21 and Pre-blast 23

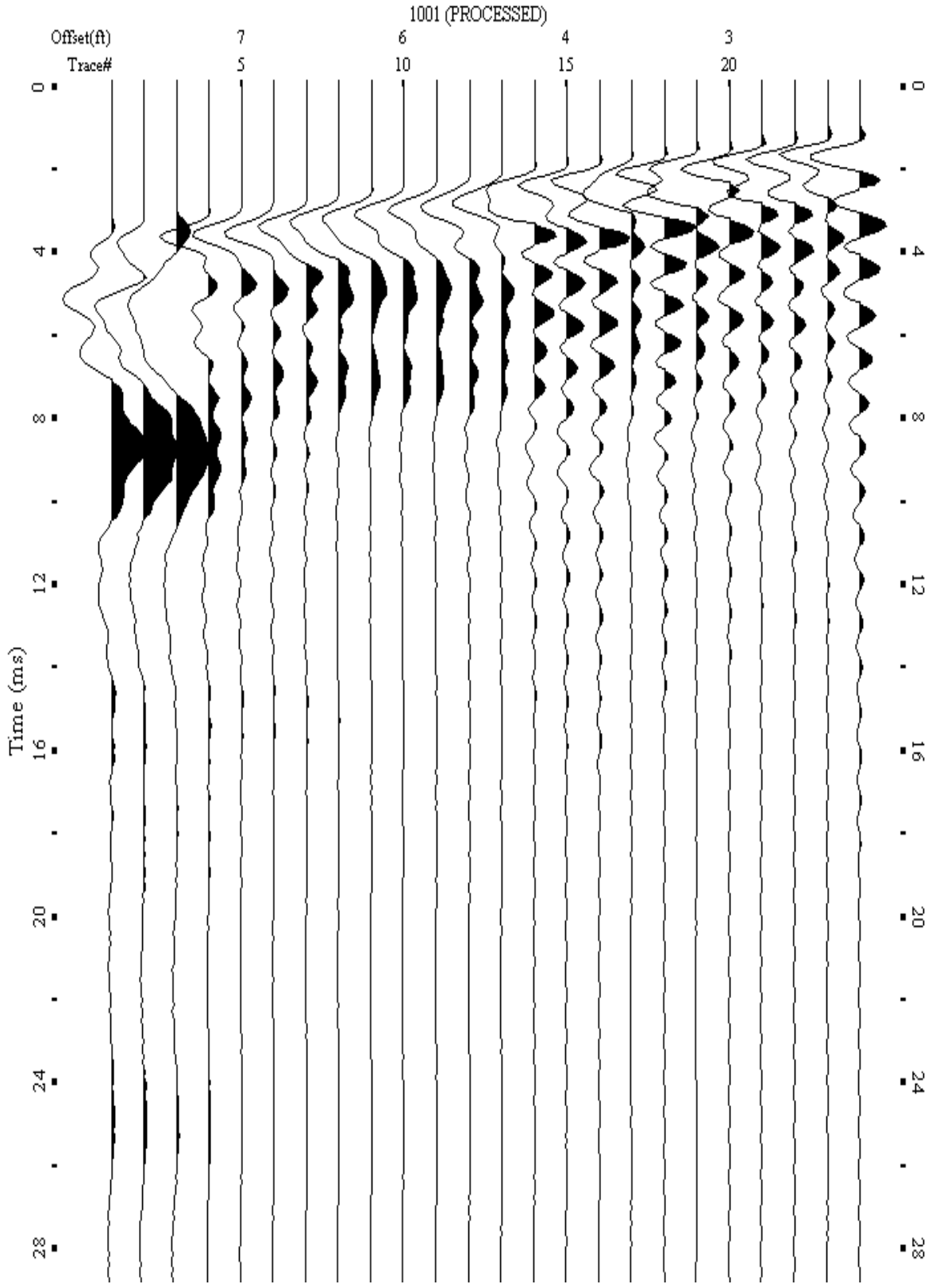

A.256: Shot Gather Line 1187 used in Post-blast 21 and Pre-blast 23

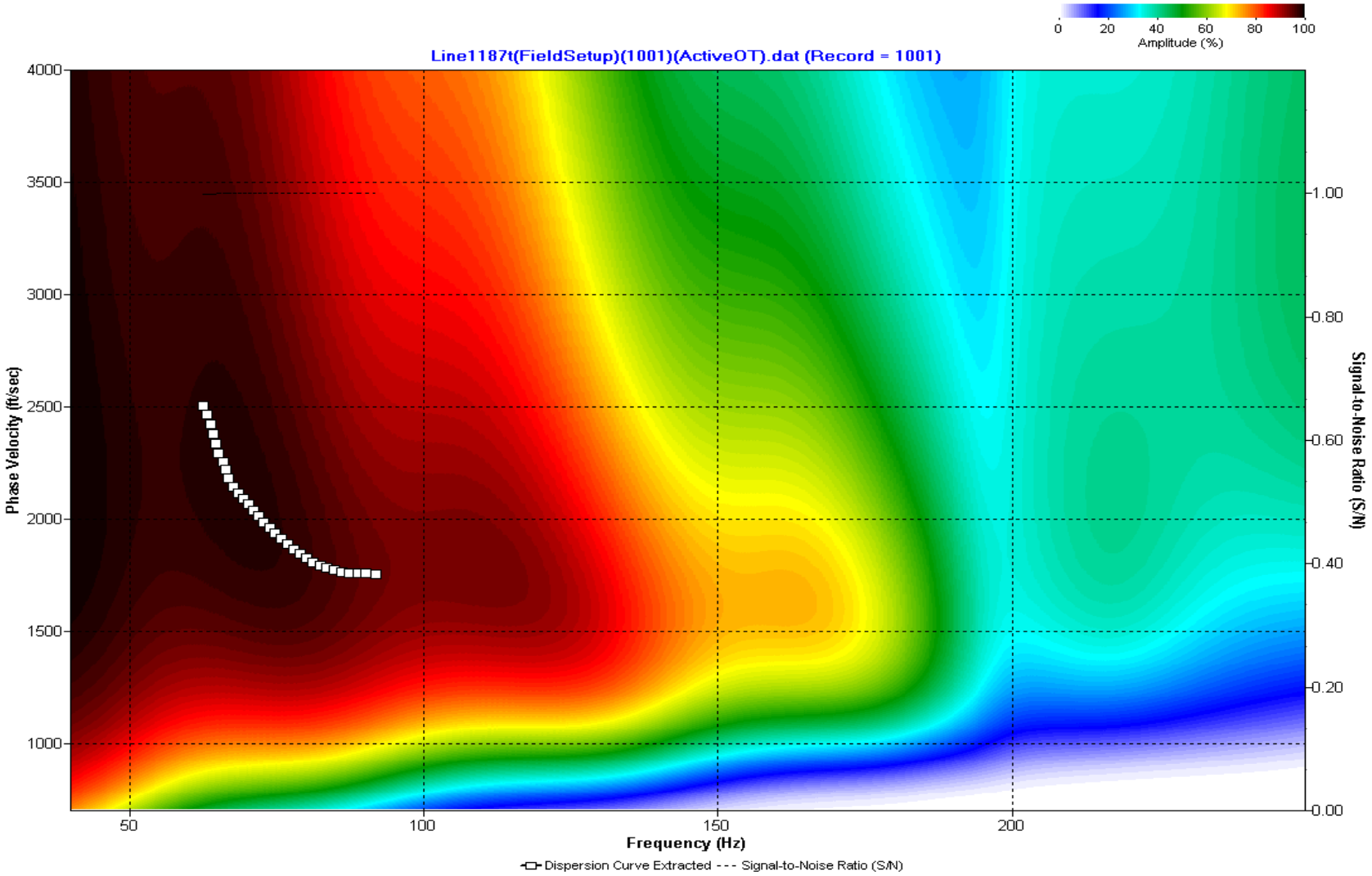

A.257: Dispersion Curve Line 1187 used in Post-blast 21 and Pre-blast 23

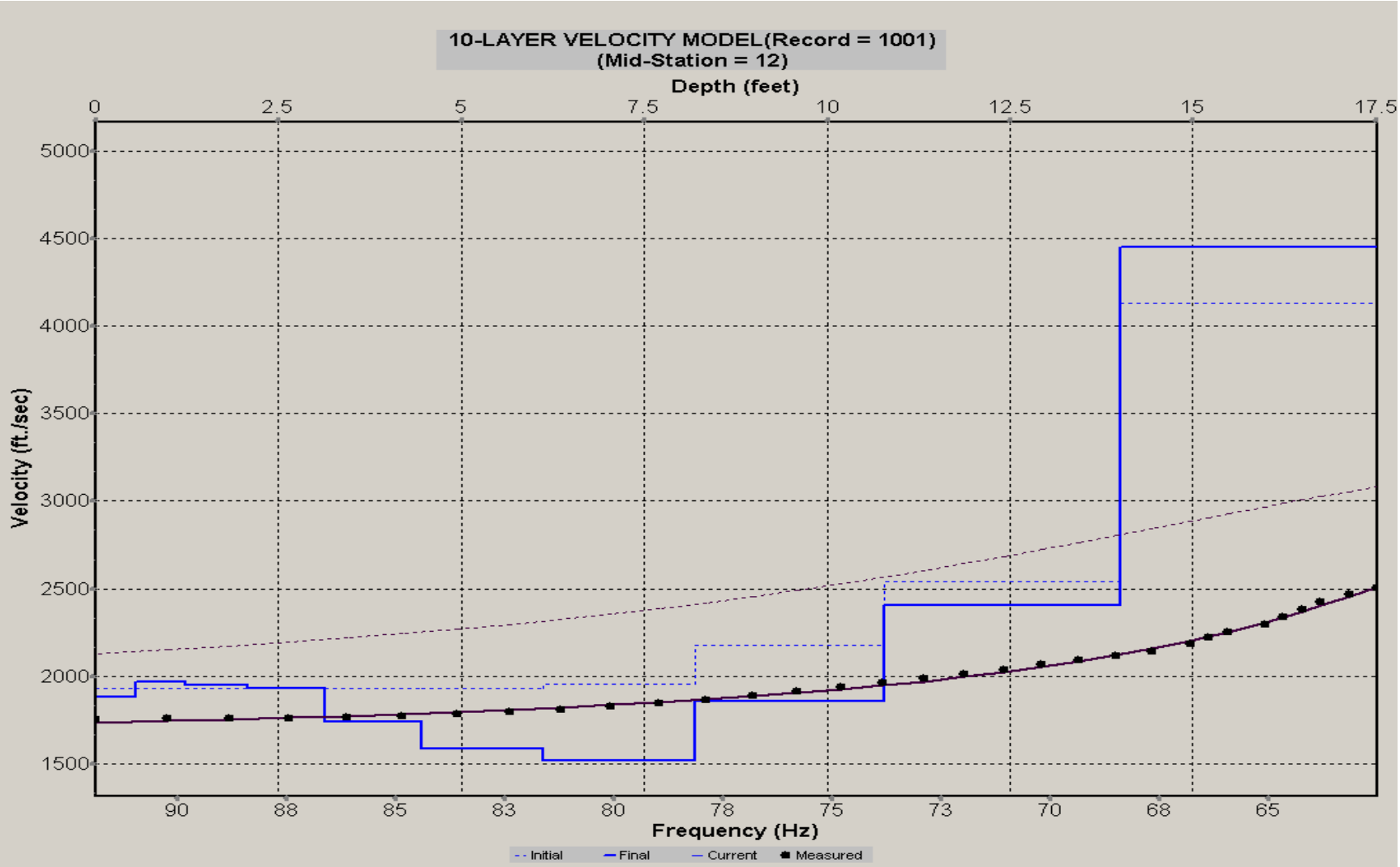

A.258: Velocity Profile Line 1187 used in Post-blast 21 and Pre-blast 23

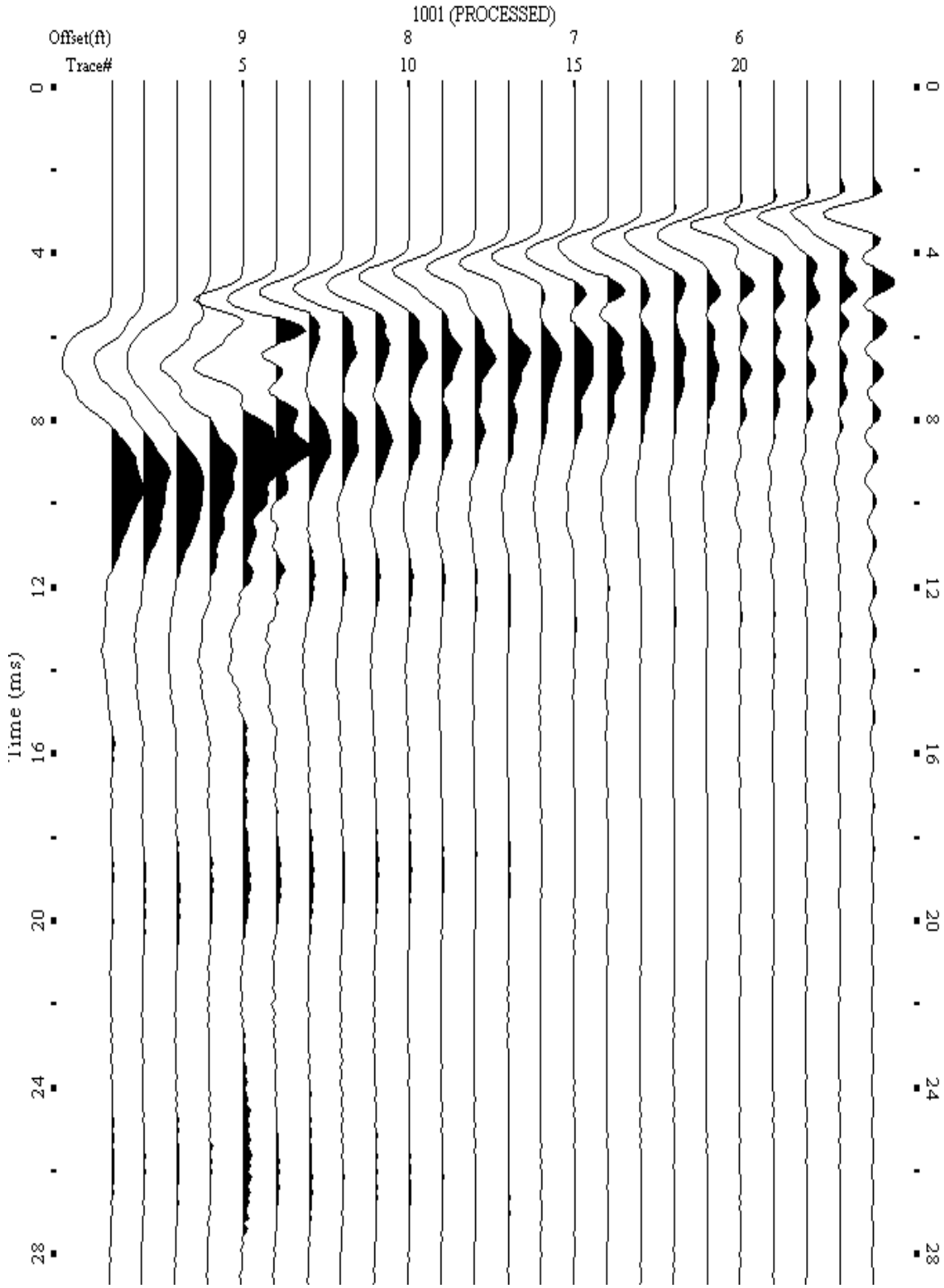

A.259: Shot Gather Line 1188 used in Post-blast 21 and Pre-blast 23

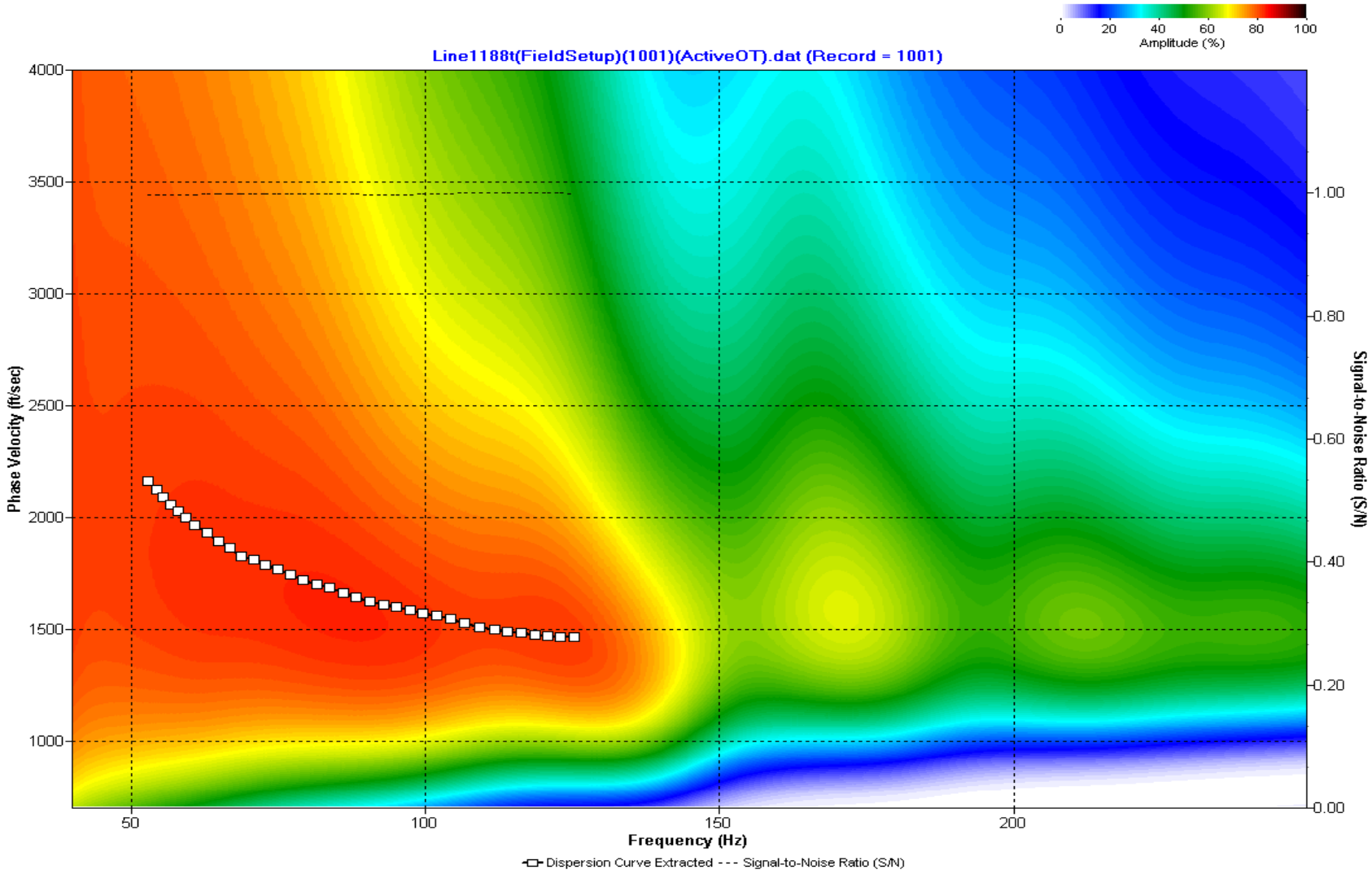

A.260: Dispersion Curve Line 1188 used in Post-blast 21 and Pre-blast 23

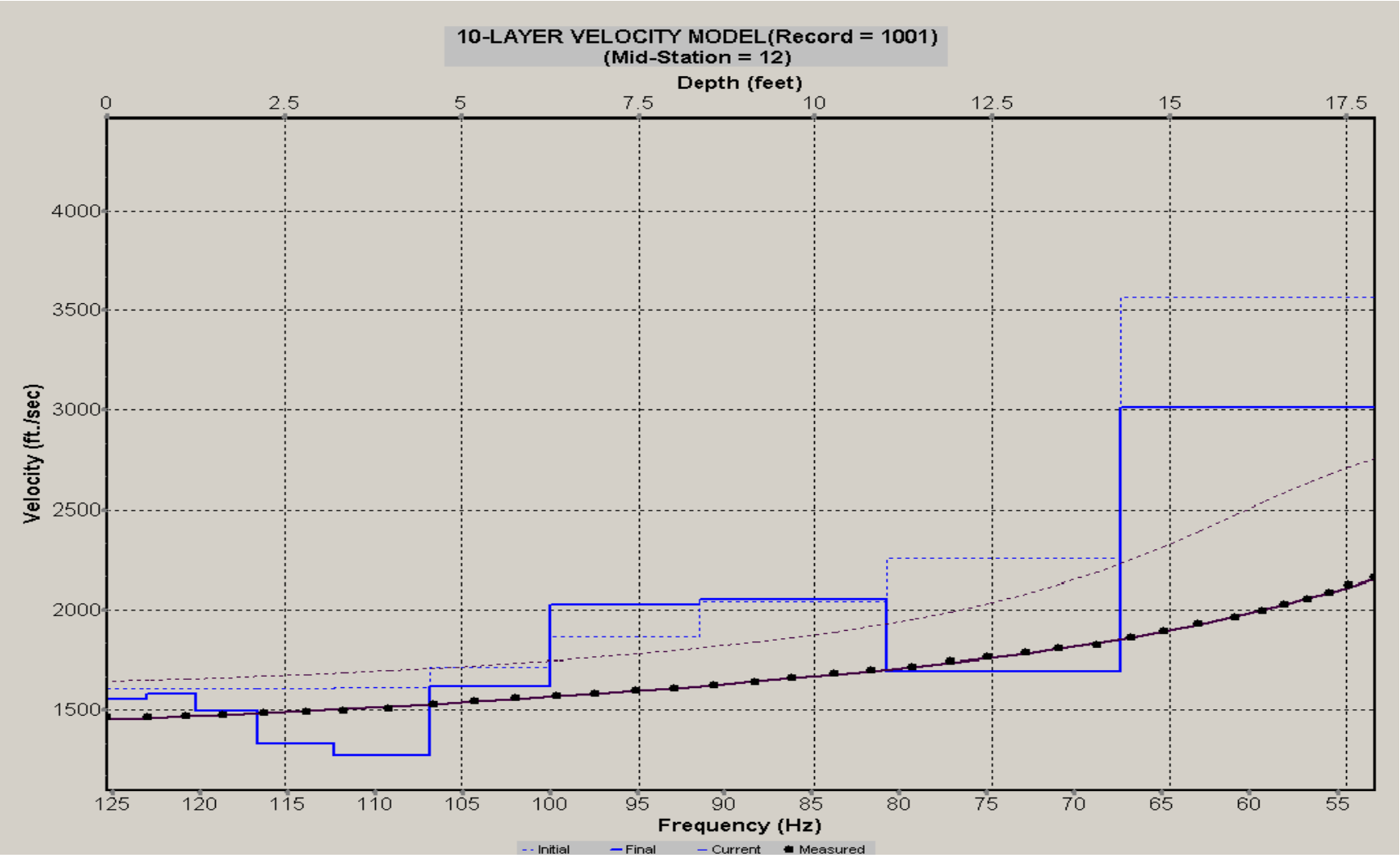

A.261: Velocity Profile Line 1188 used in Post-blast 21 and Pre-blast 23

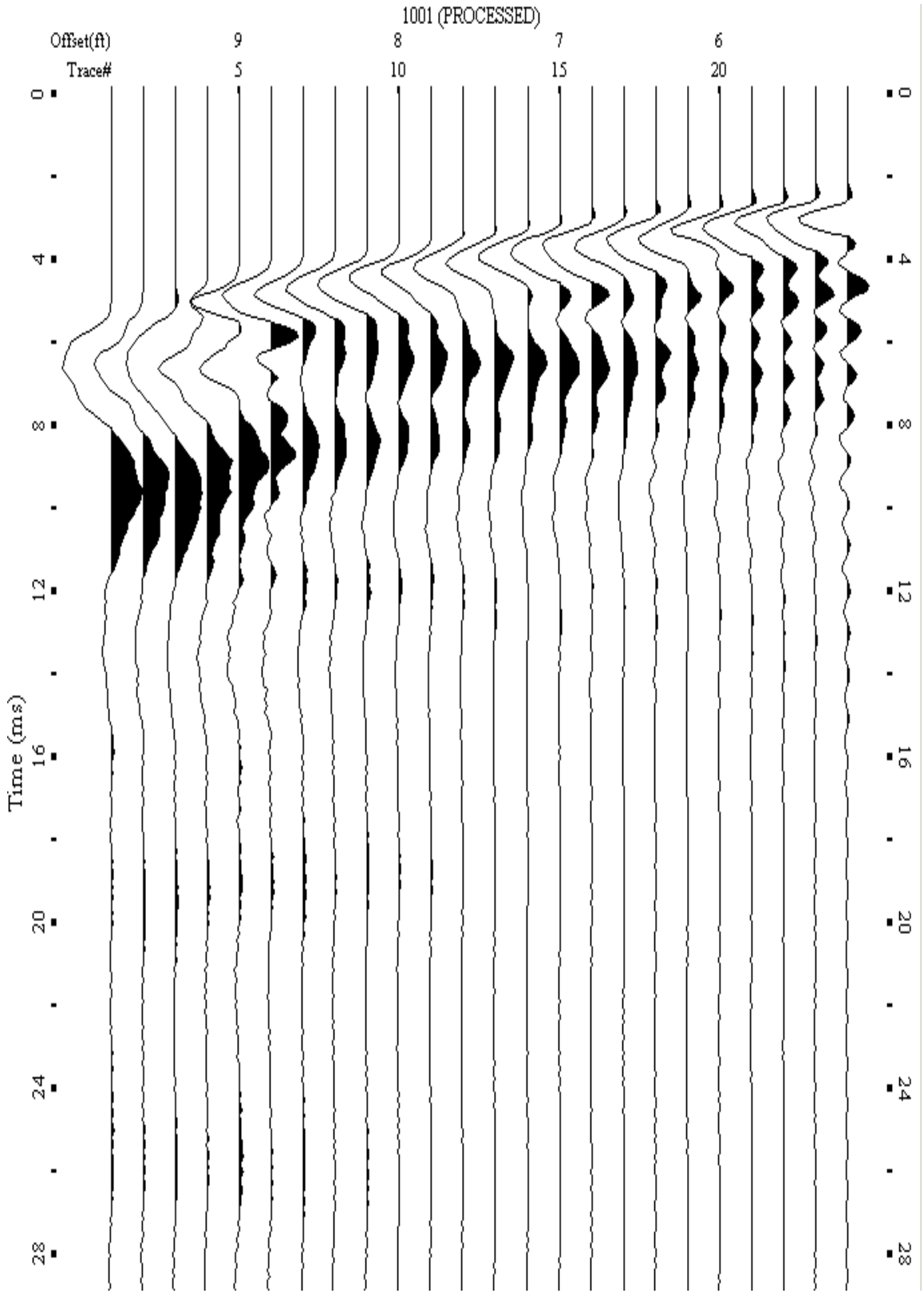

A.262: Shot Gather Line 1189 used in Post-blast 21 and Pre-blast 23

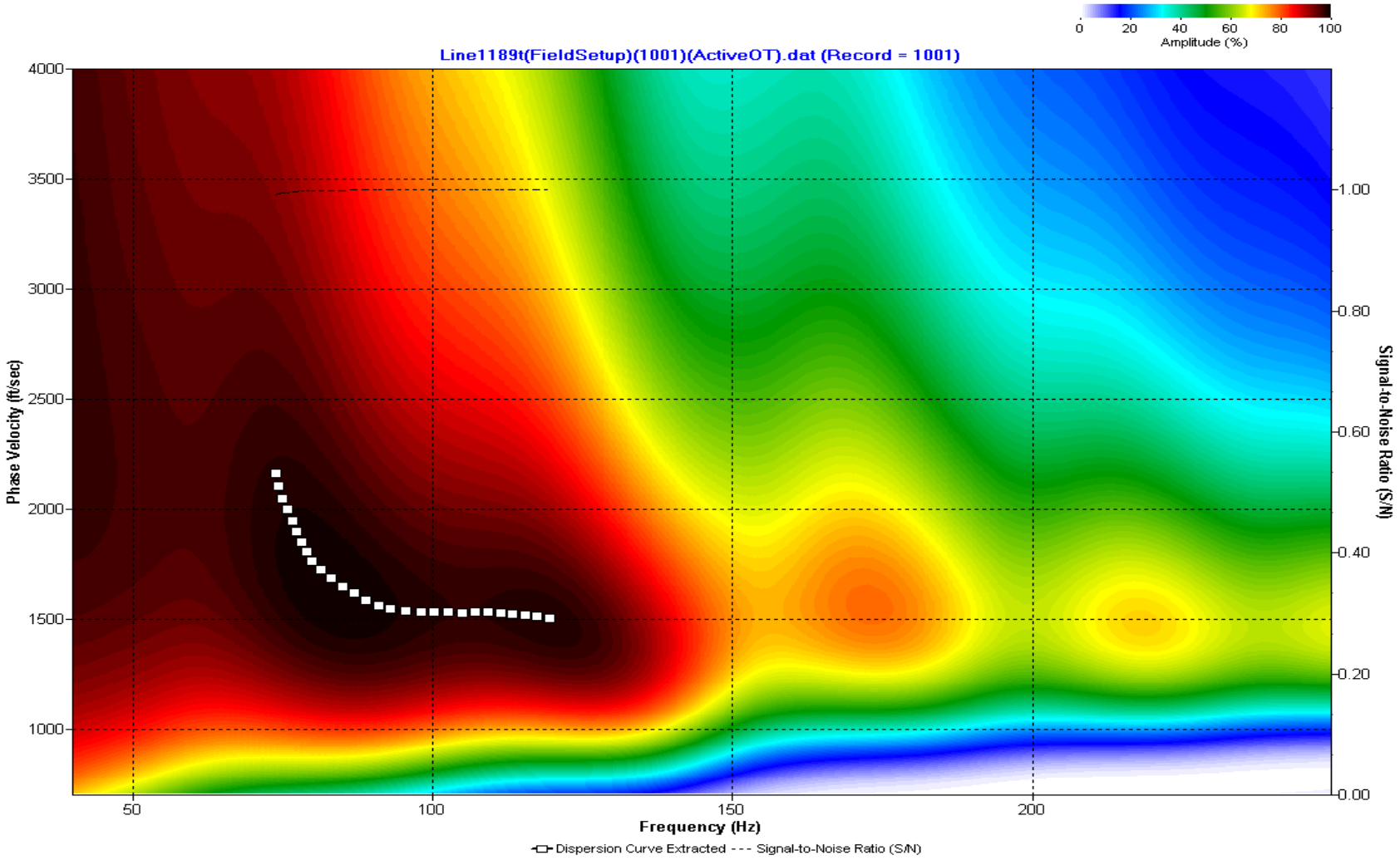

A.263: Dispersion Curve Line 1189 used in Post-blast 21 and Pre-blast 23

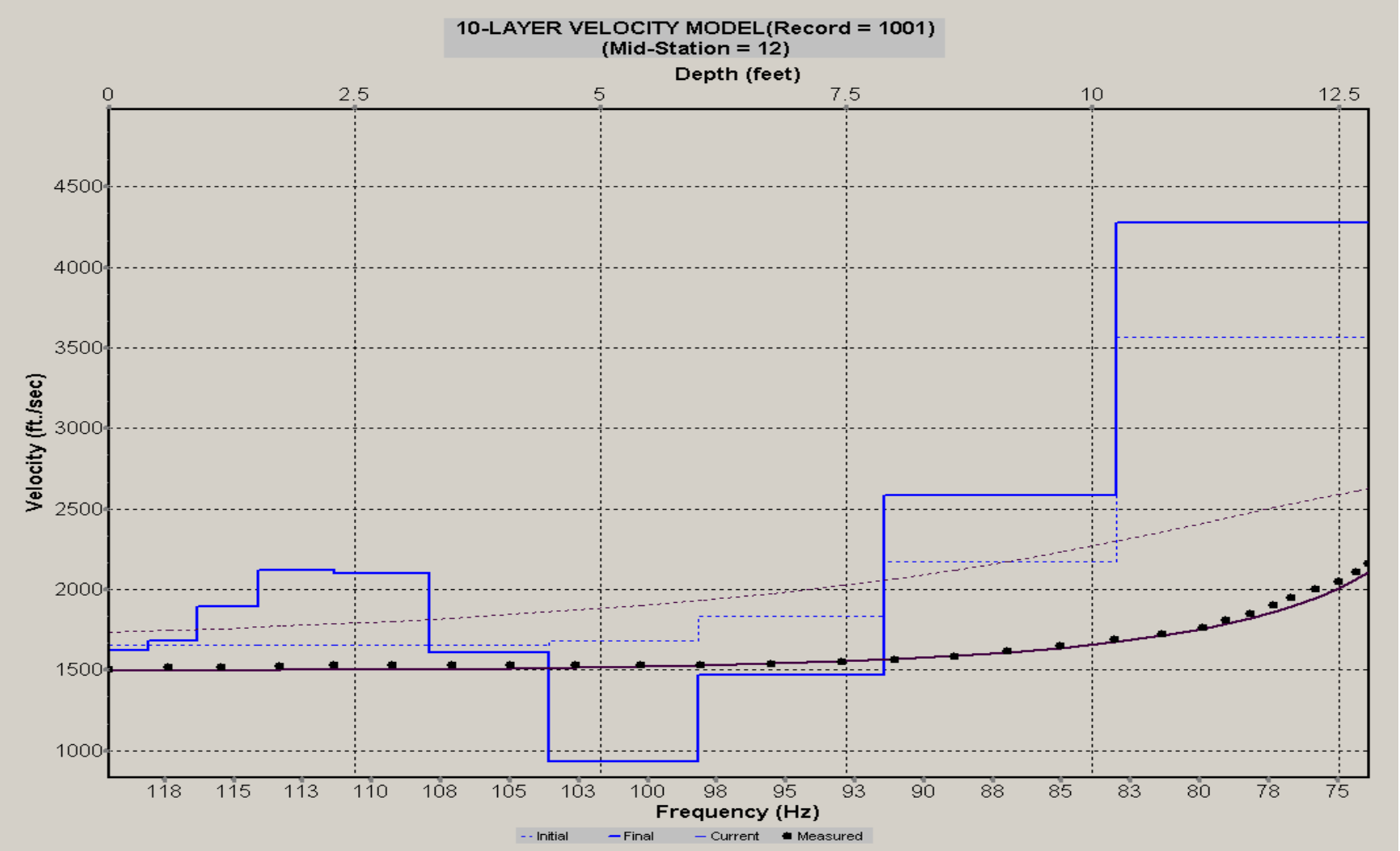

A.264: Velocity Profile Line 1189 used in Post-blast 21 and Pre-blast 23

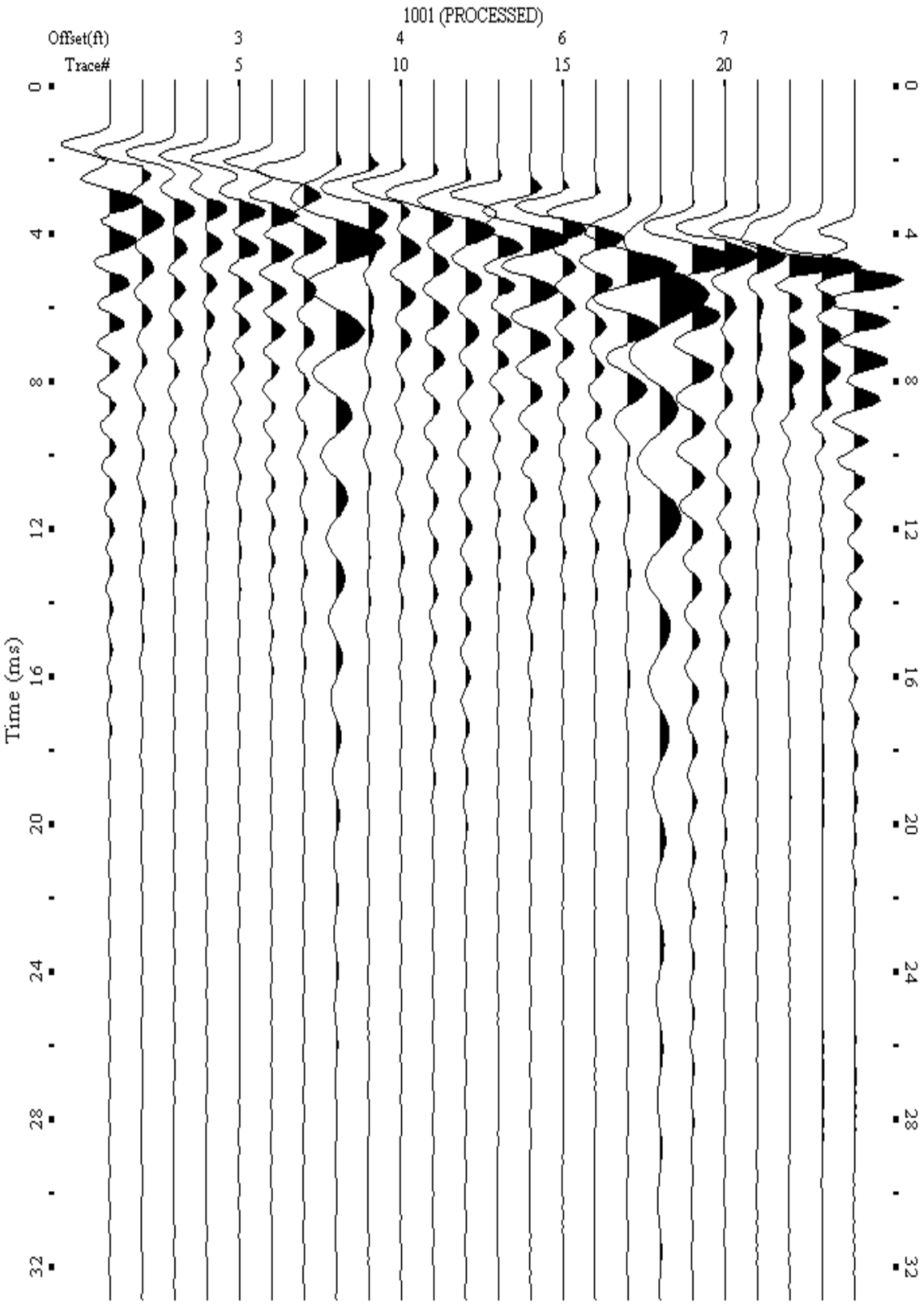

A.265: Shot Gather Line 1198 used in Post-blast 22 and Pre-blast 24

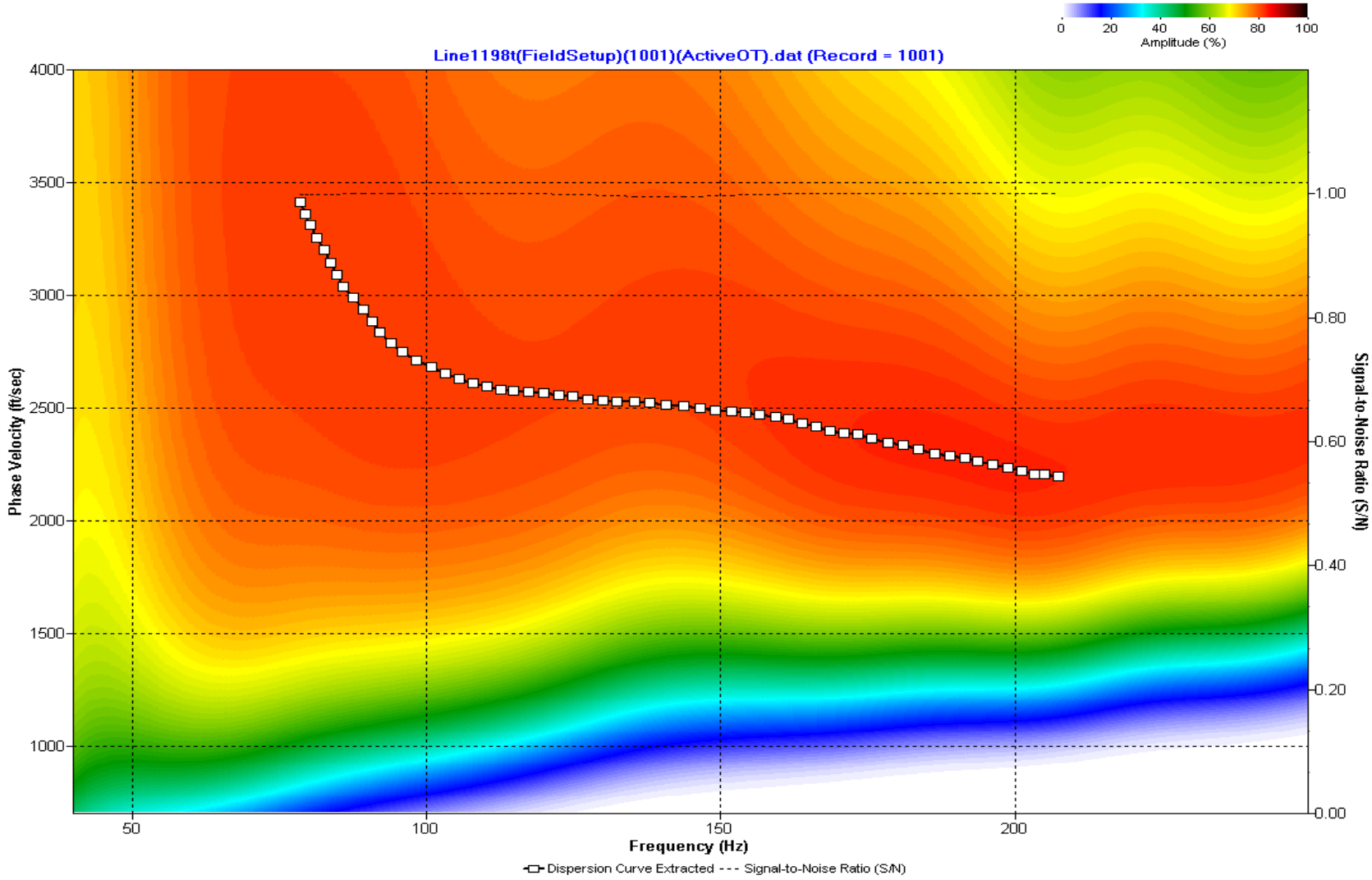

A.266: Dispersion Curve Line 1198 used in Post-blast 22 and Pre-blast 24

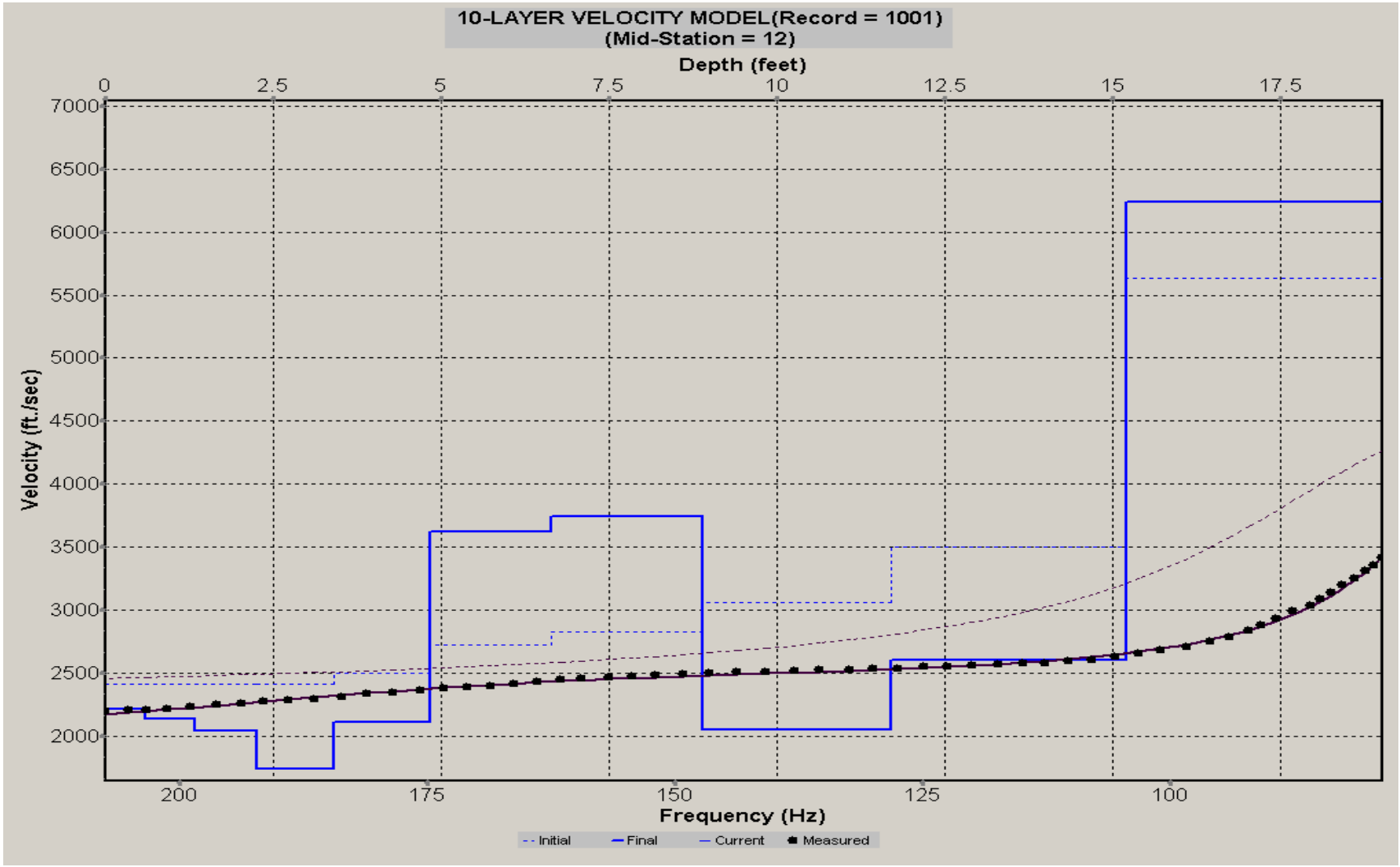

A.267: Velocity Profile Line 1198 used in Post-blast 22 and Pre-blast 24

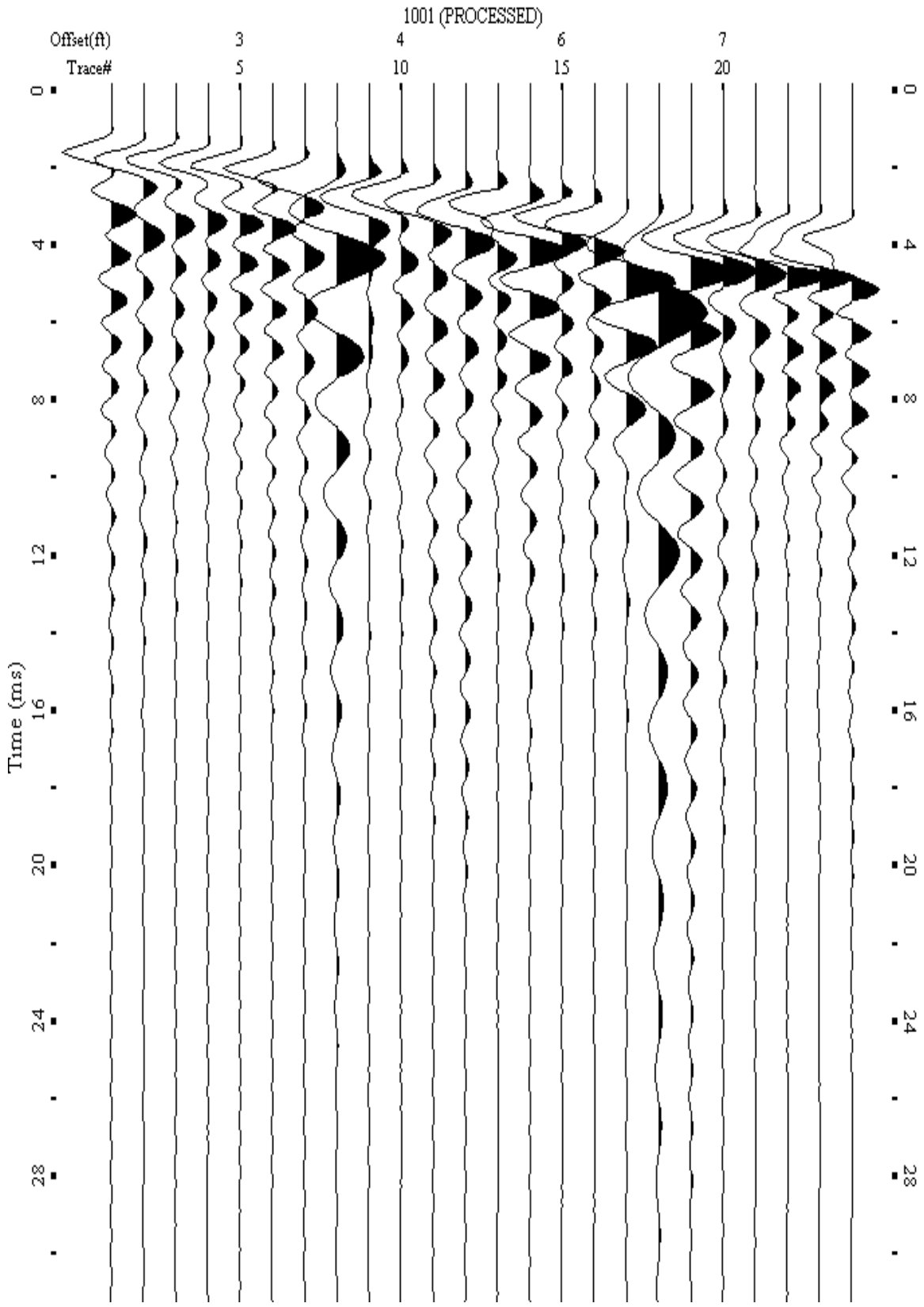

A.268: Shot Gather Line 1199 used in Post-blast 22 and Pre-blast 24

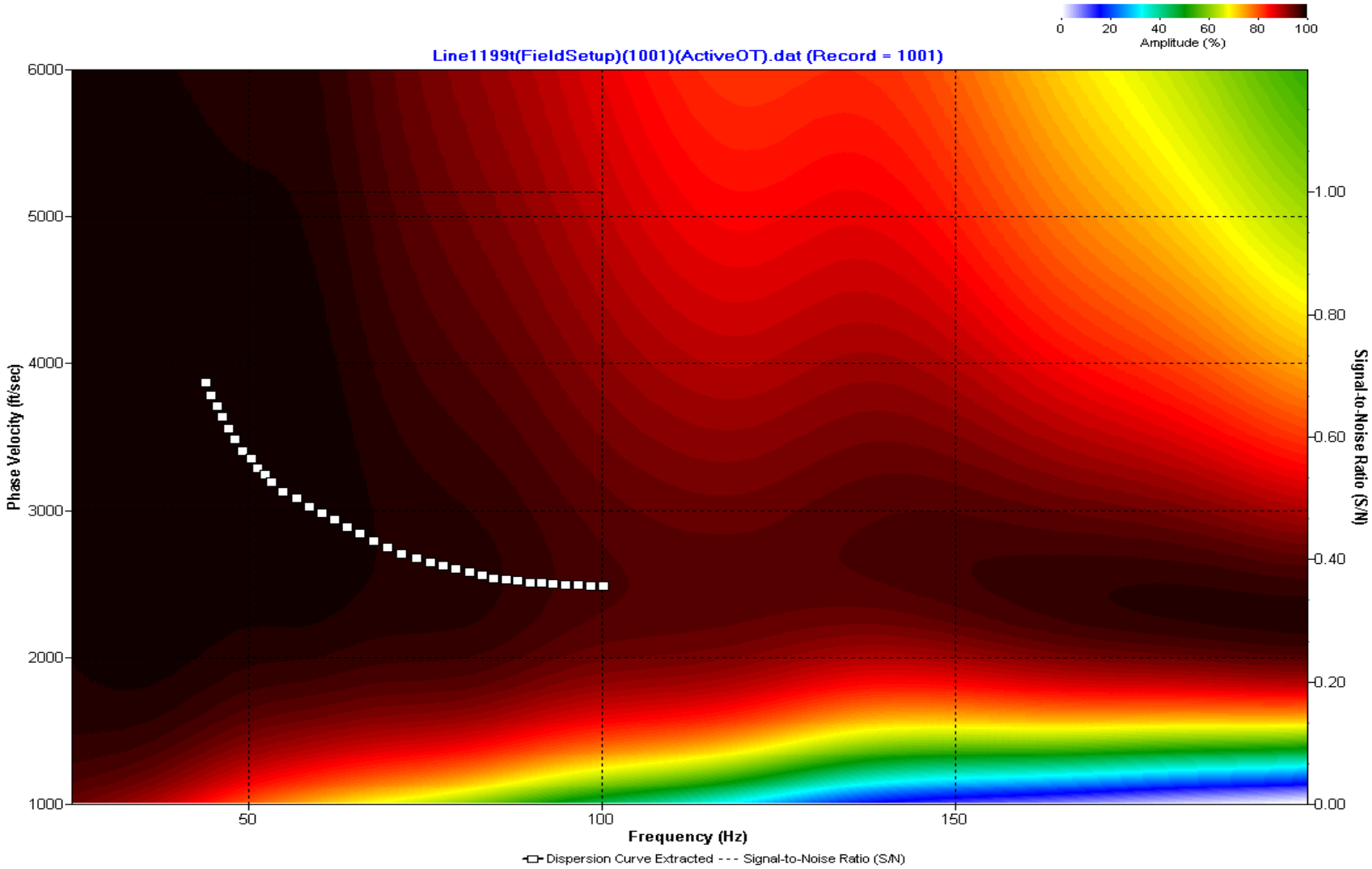

A.269: Dispersion Curve Line 1199 used in Post-blast 22 and Pre-blast 24

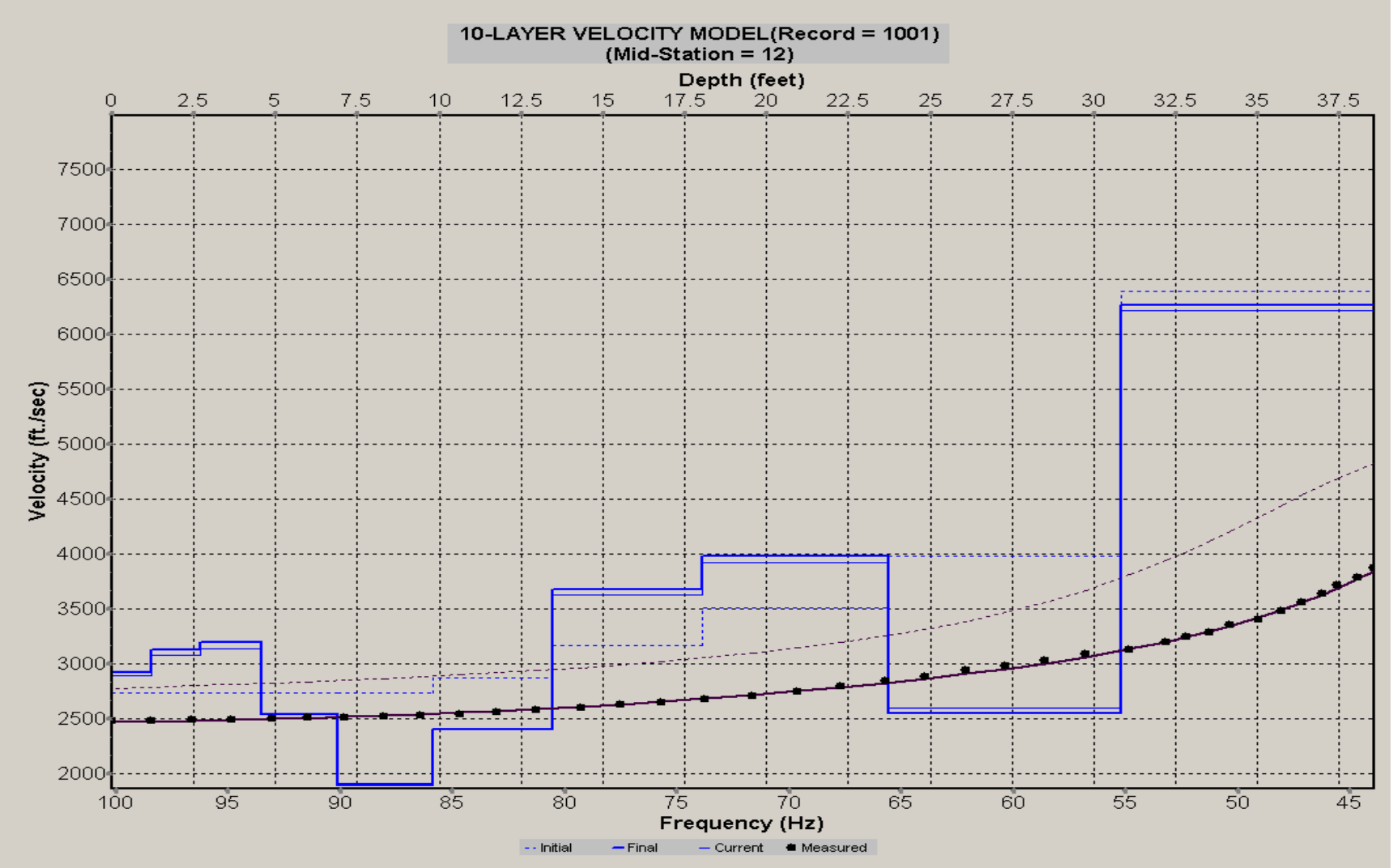

A.270: Velocity Profile Line 1199 used in Post-blast 22 and Pre-blast 24

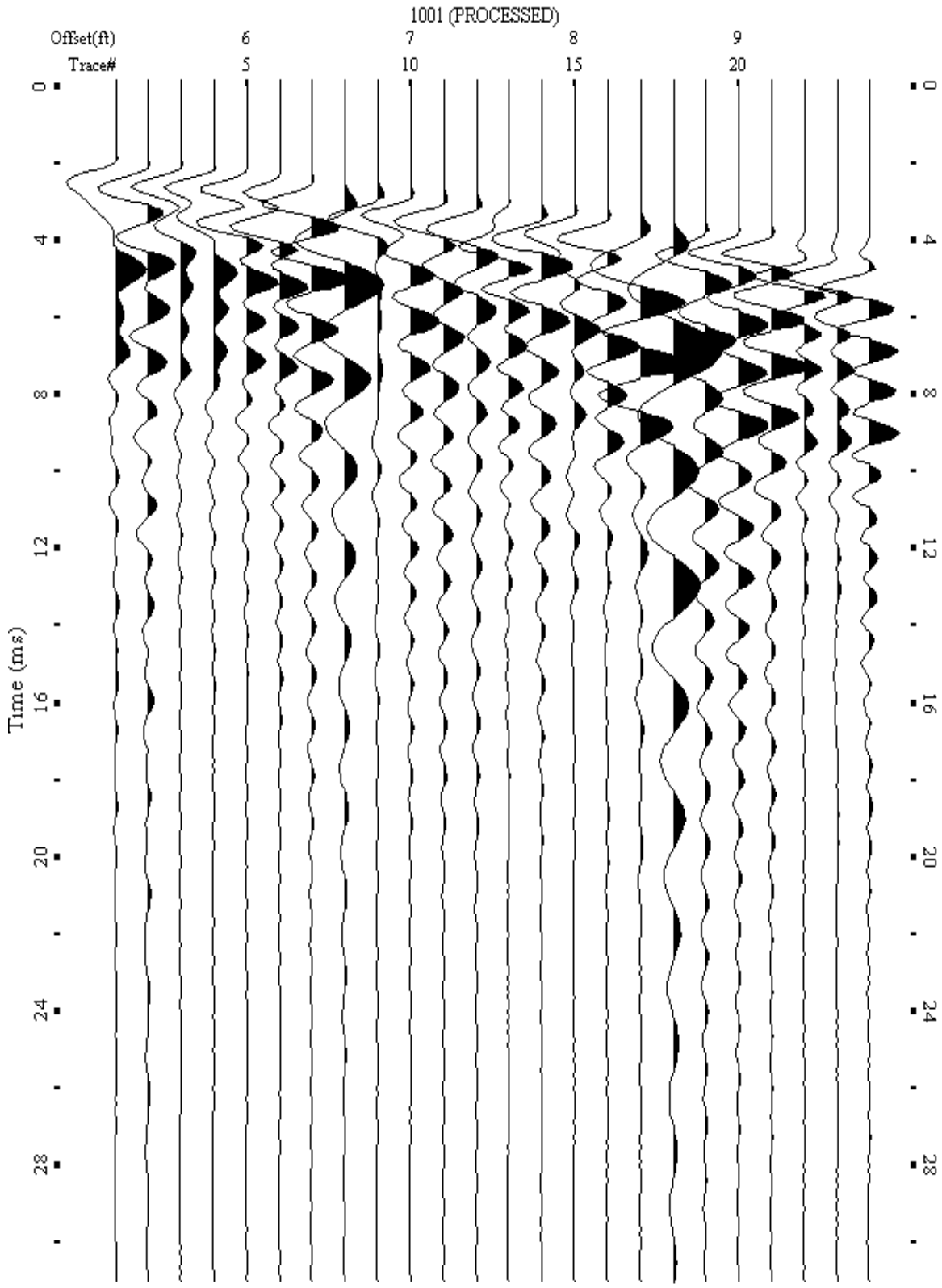

A.271: Shot Gather Line 1200 used in Post-blast 22 and Pre-blast 24

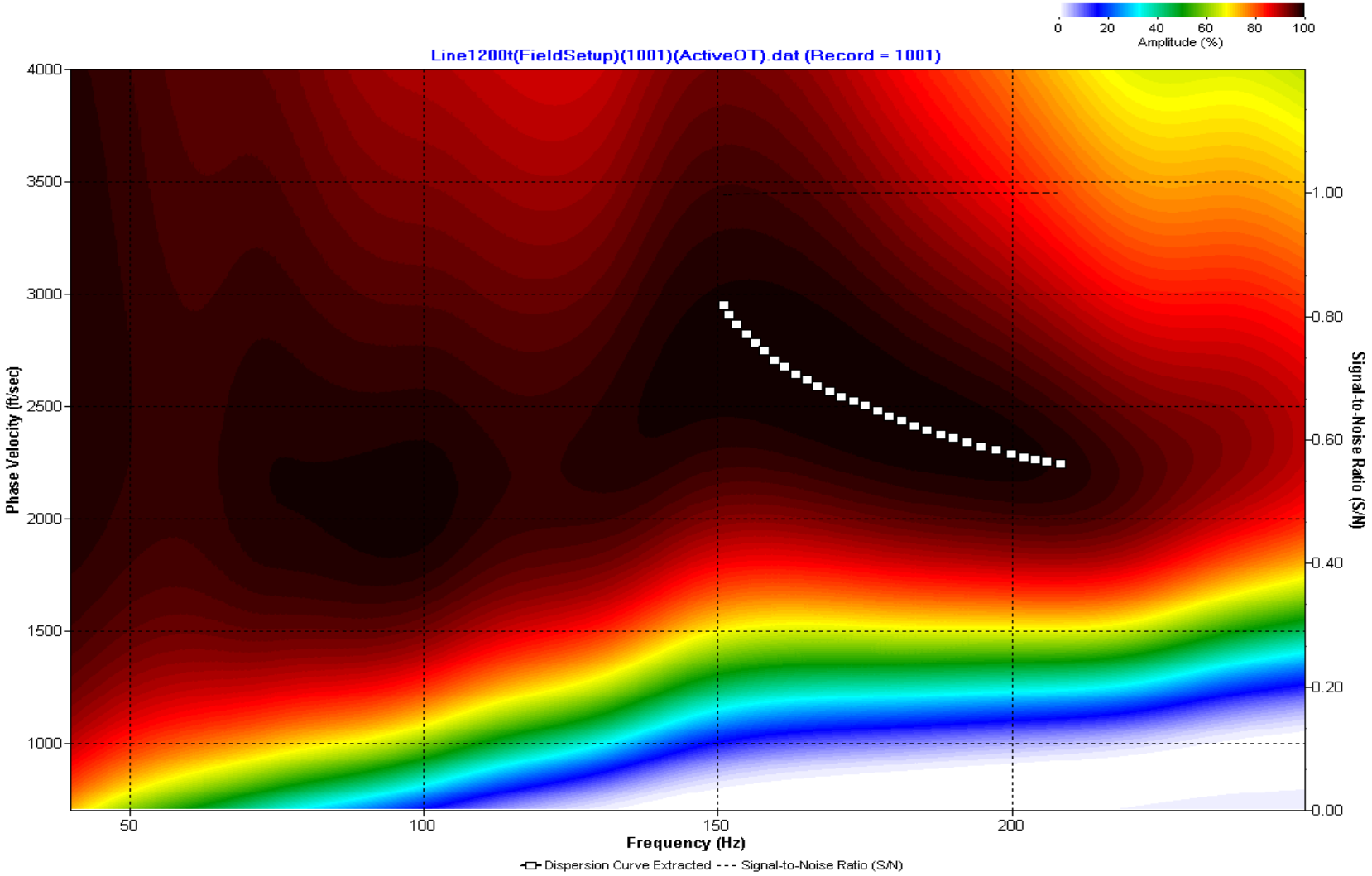

A.272: Dispersion Curve Line 1200 used in Post-blast 22 and Pre-blast 24

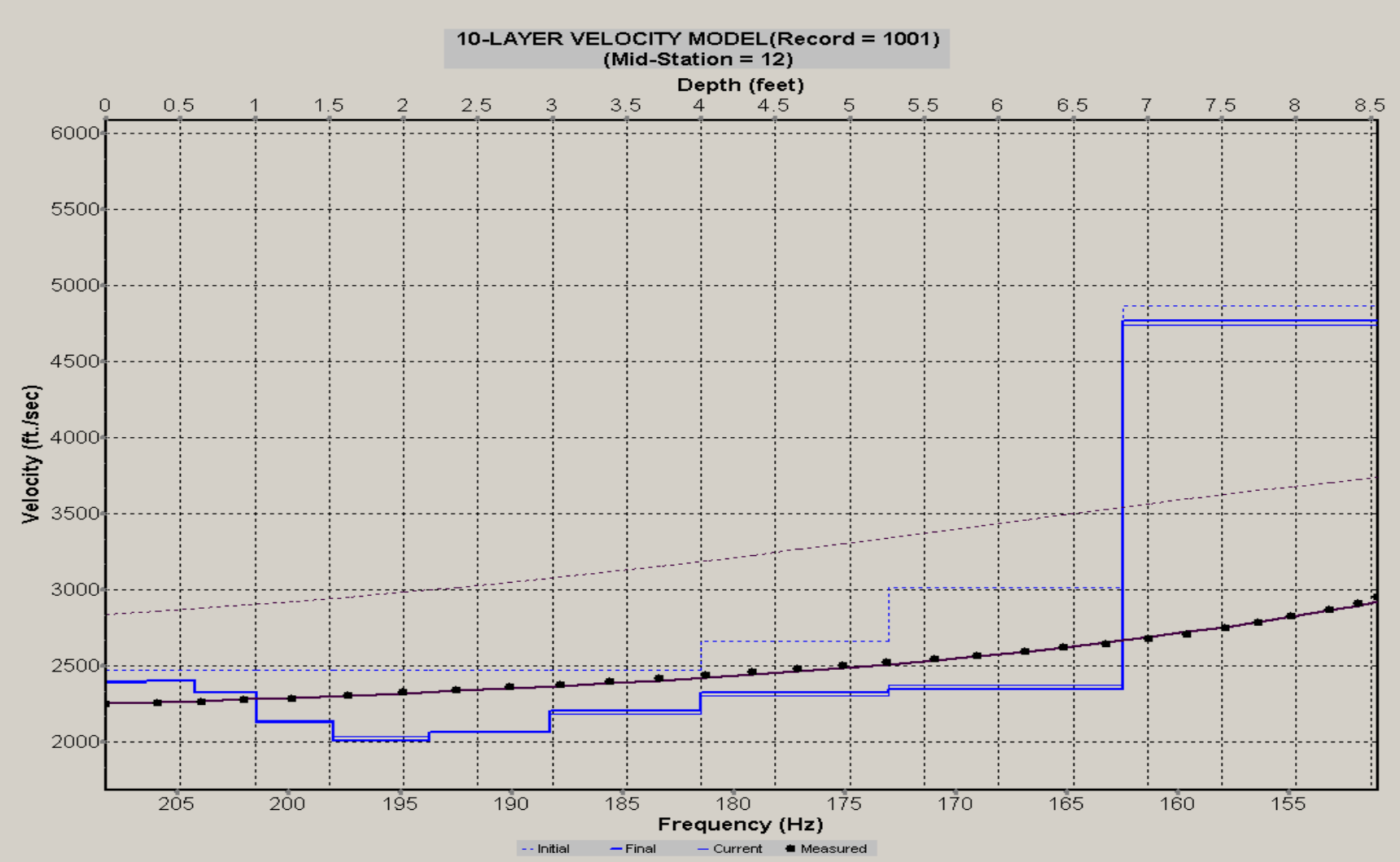

A.273: Velocity Profile Line 1200 used in Post-blast 22 and Pre-blast 24

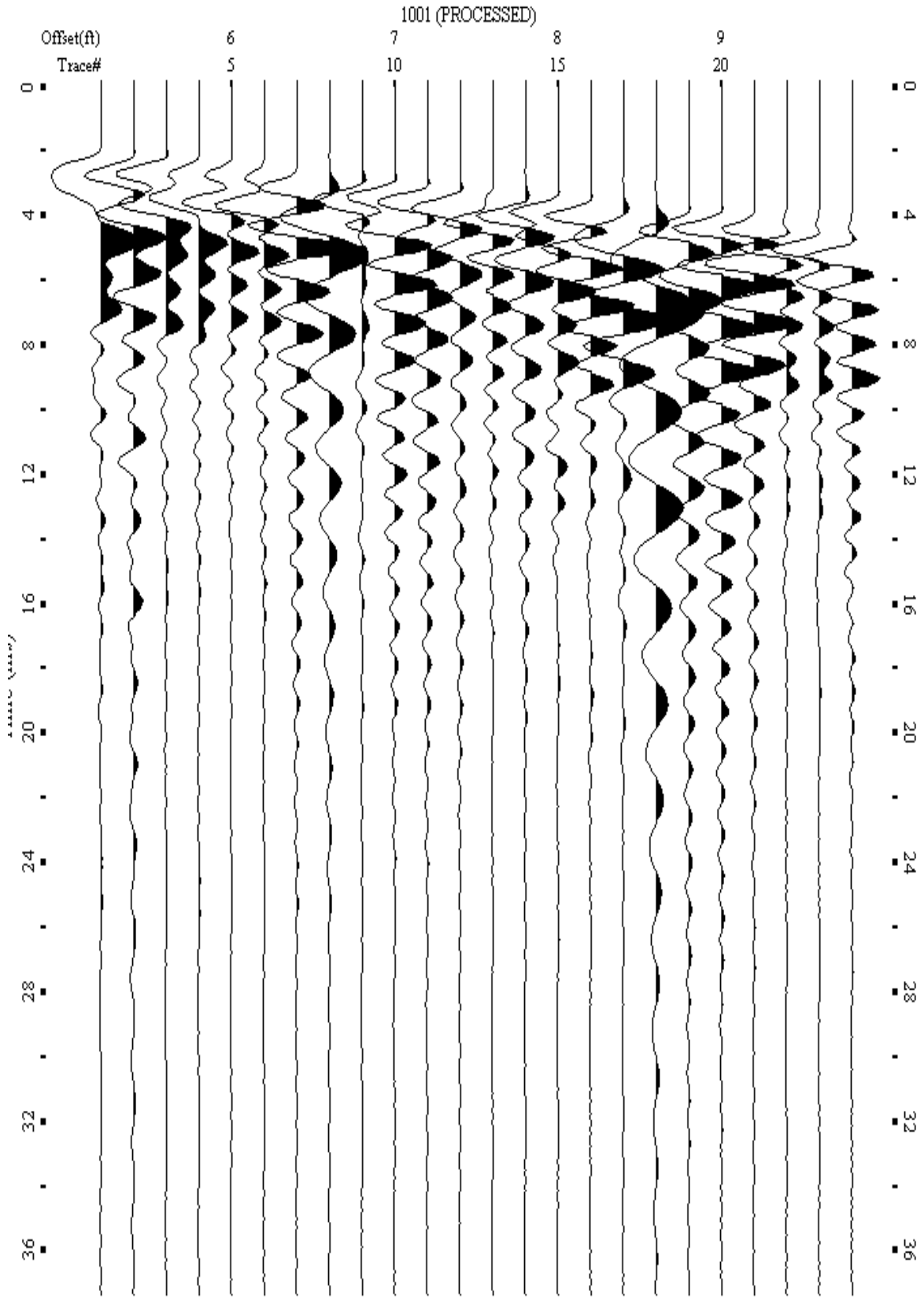

A.274: Shot Gather Line 1201 used in Post-blast 22 and Pre-blast 24

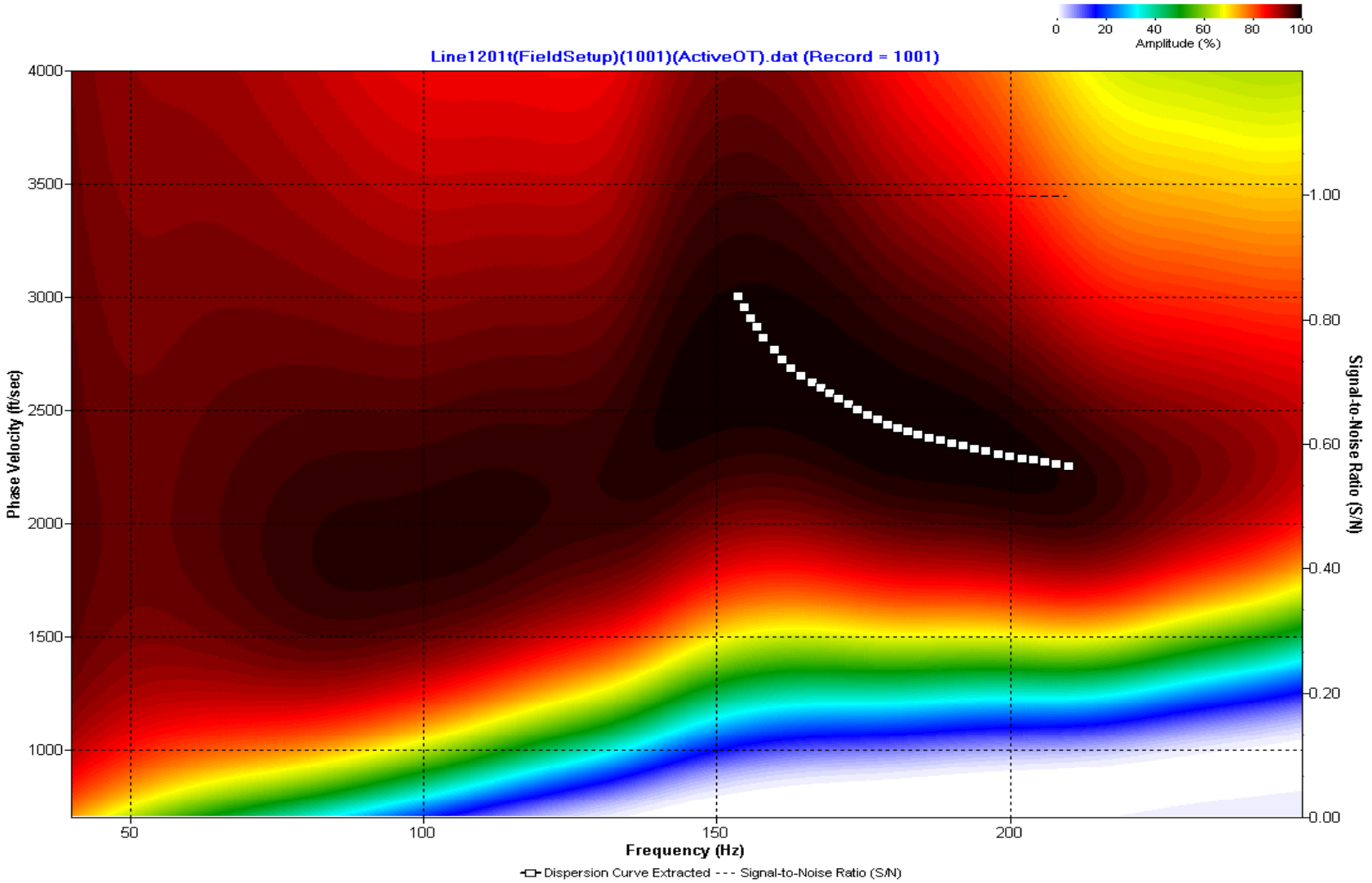

A.275: Dispersion Curve Line 1201 used in Post-blast 22 and Pre-blast 24

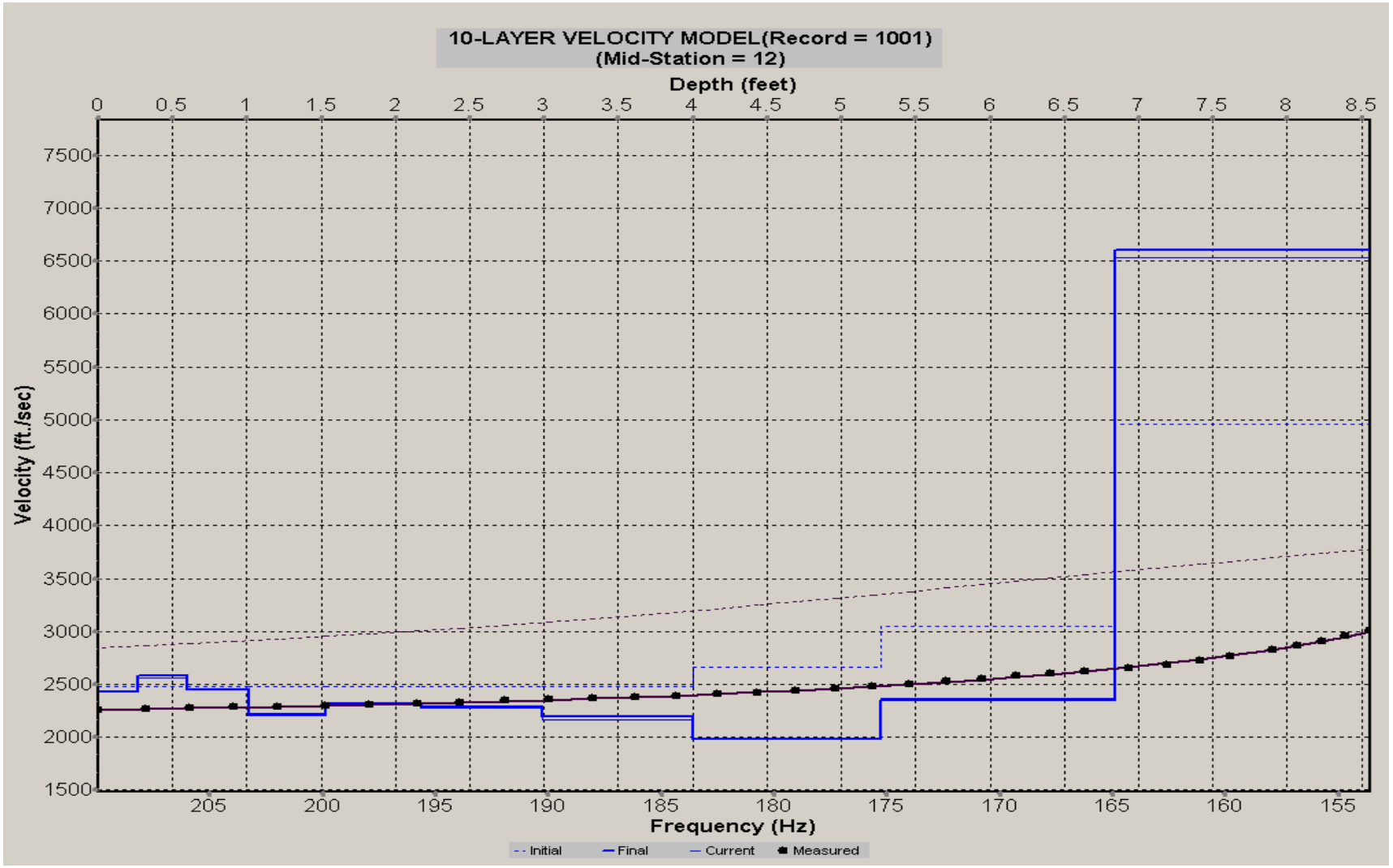

A.276: Velocity Profile Line 1201 used in Post-blast 22 and Pre-blast 24

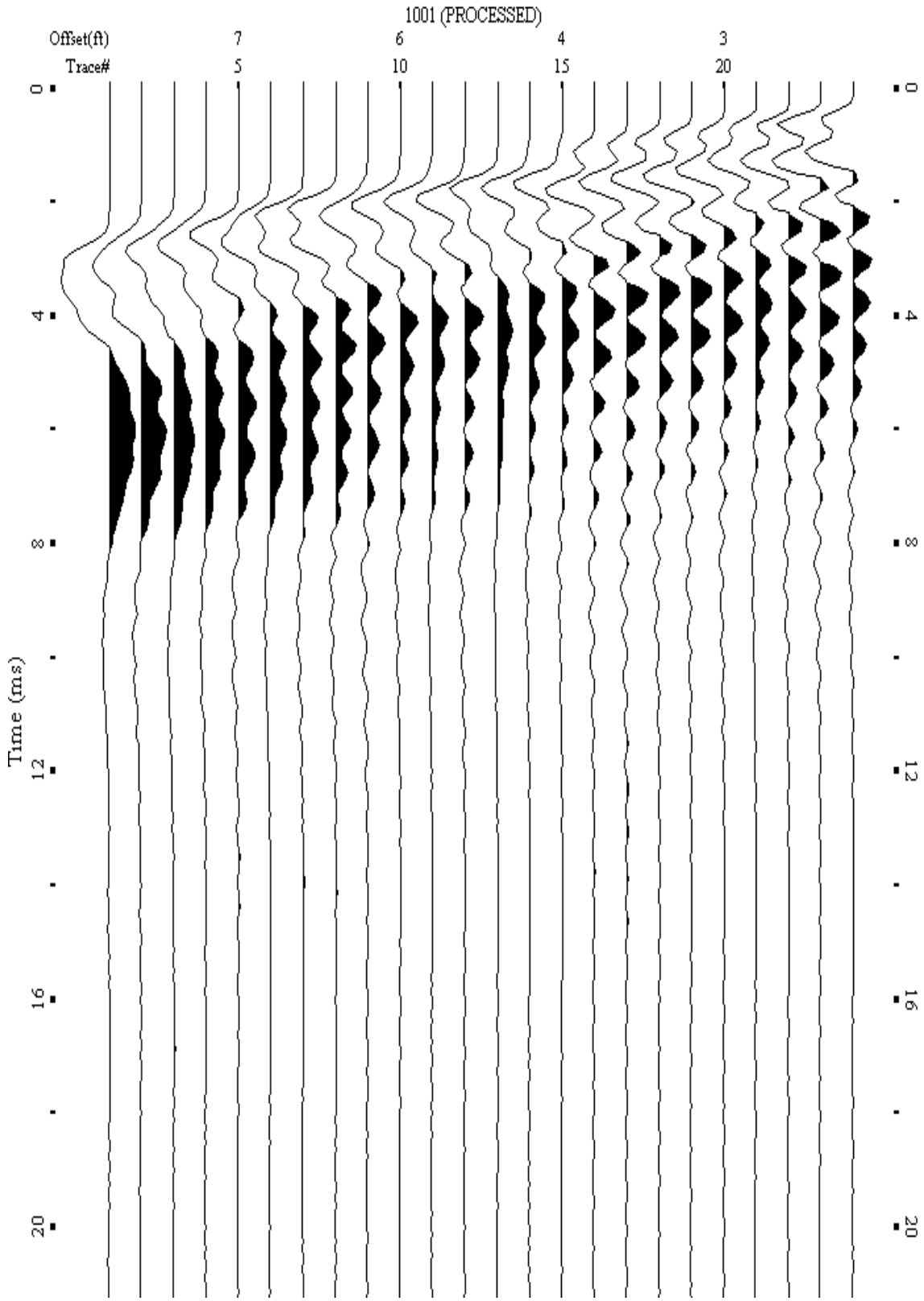

A.277: Shot Gather Line 1202 used in Pre-blast 19, Post-blast 23 and Pre-blast 25

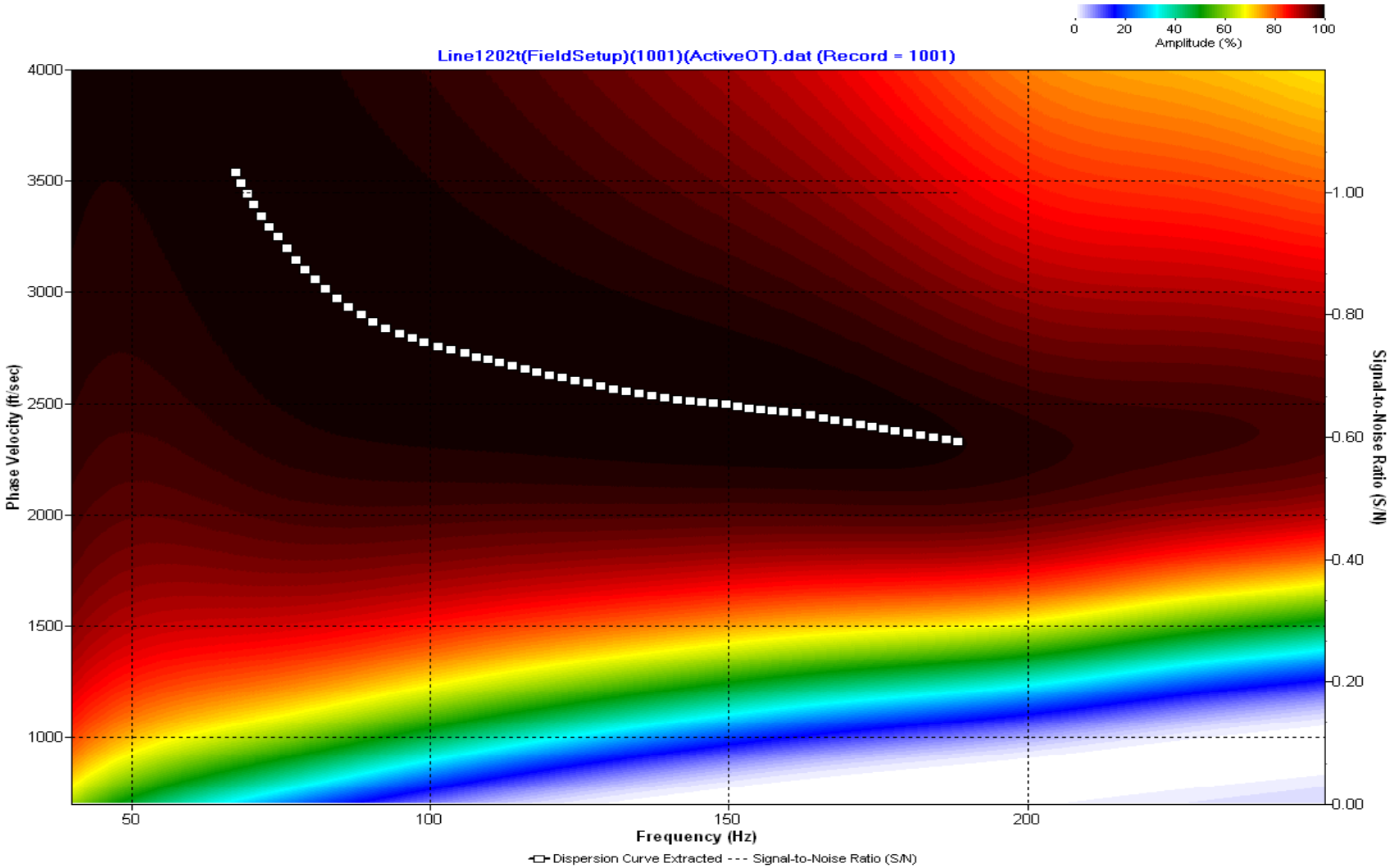

A.278: Dispersion Curve Line 1202 used in Pre-blast 19, Post-blast 23 and Pre-blast 25

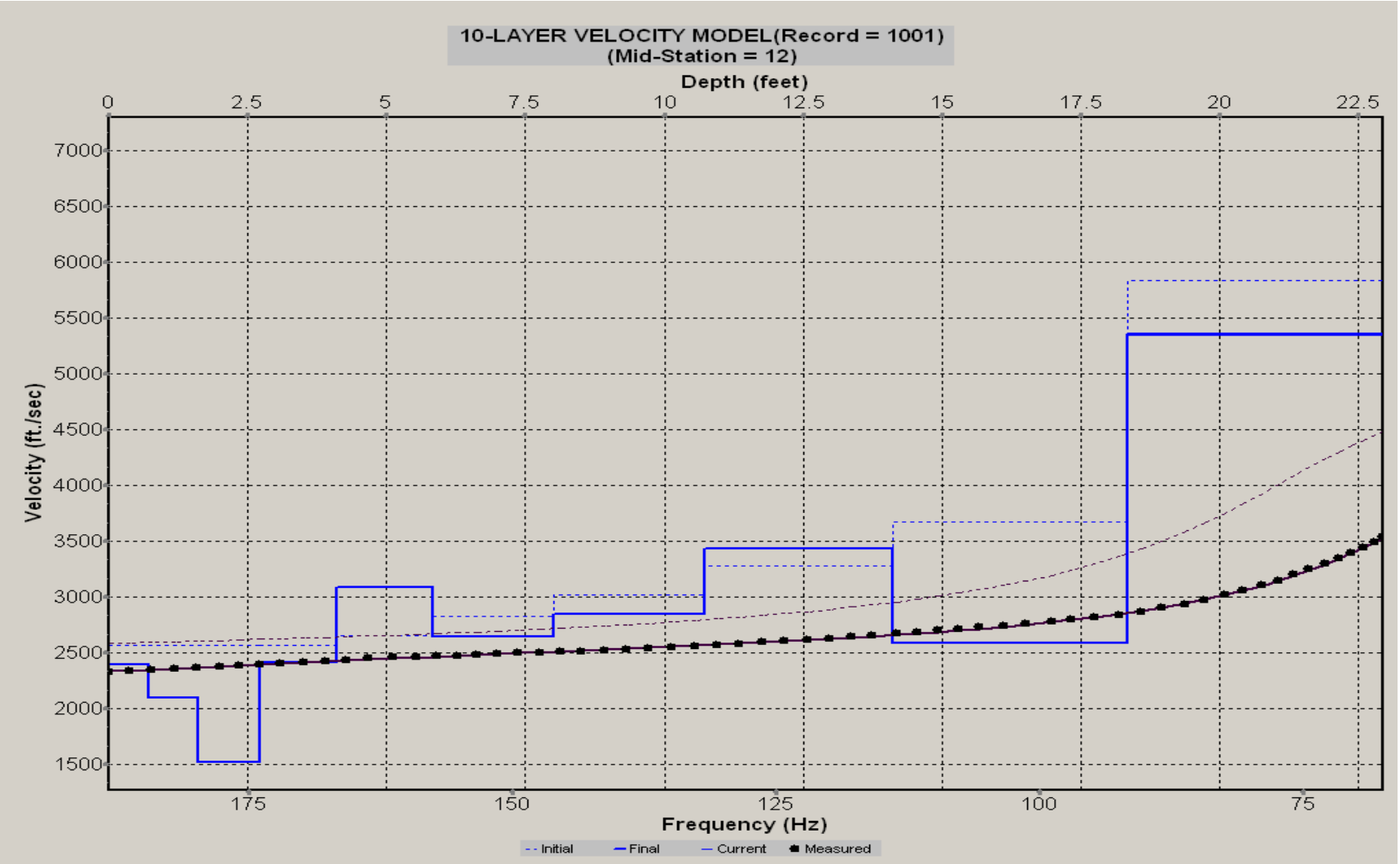

A.279: Velocity Profile Line 1202 used in Pre-blast 19, Post-blast 23 and Pre-blast 25

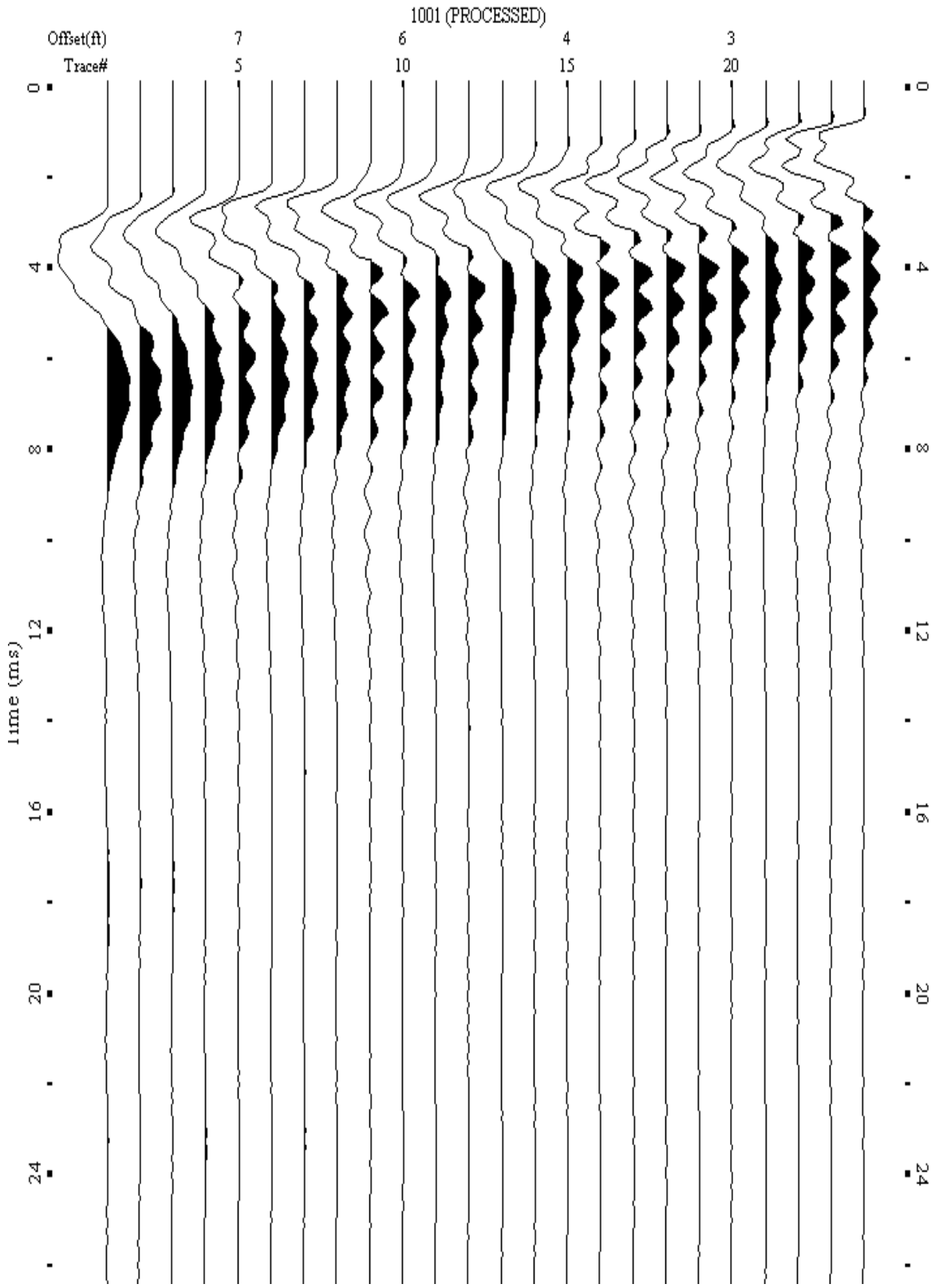

A.280: Shot Gather Line 1203 used in Pre-blast 19, Post-blast 23 and Pre-blast 25

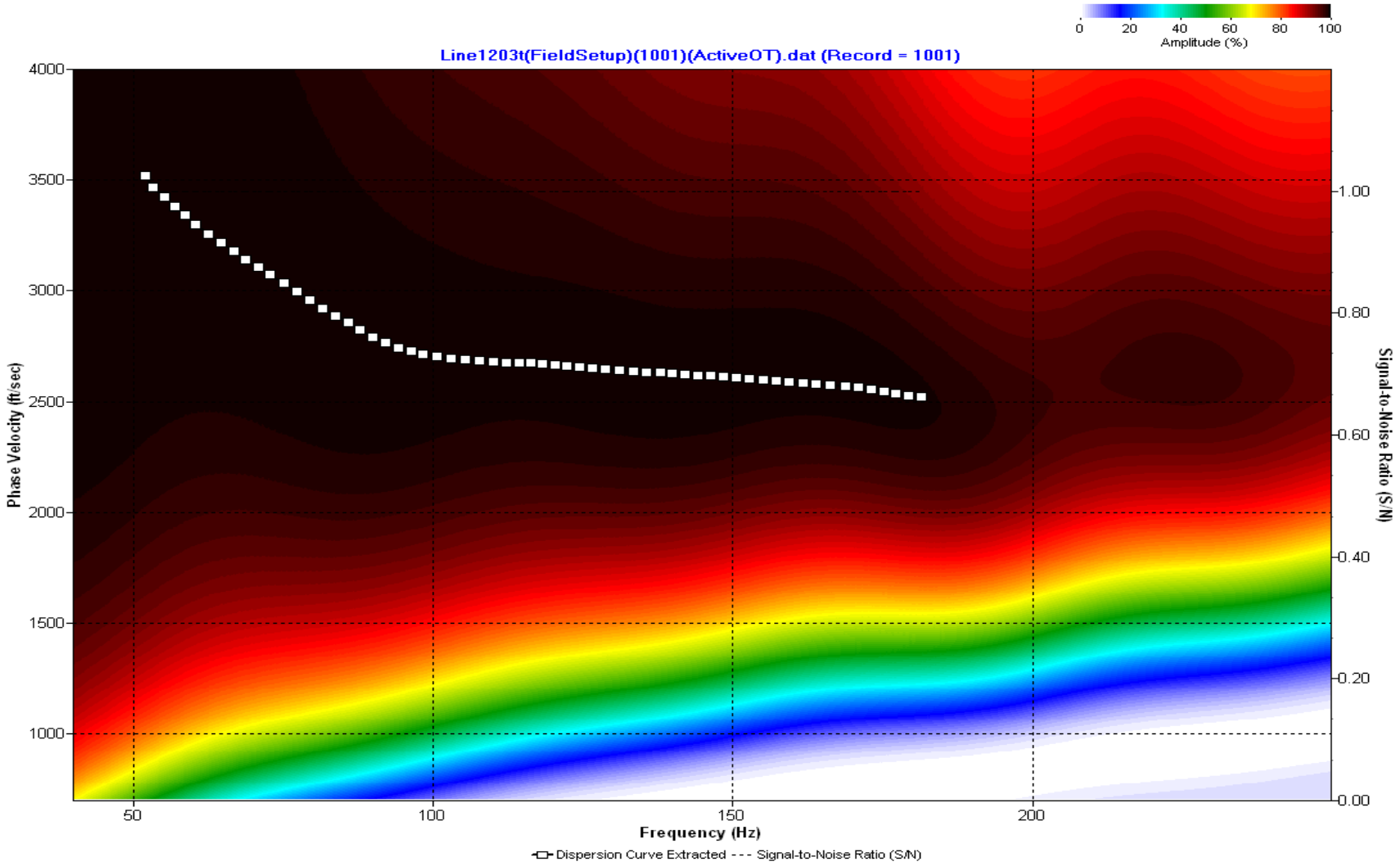

A.281: Dispersion Curve Line 1203 used in Pre-blast 19, Post-blast 23 and Pre-blast 25

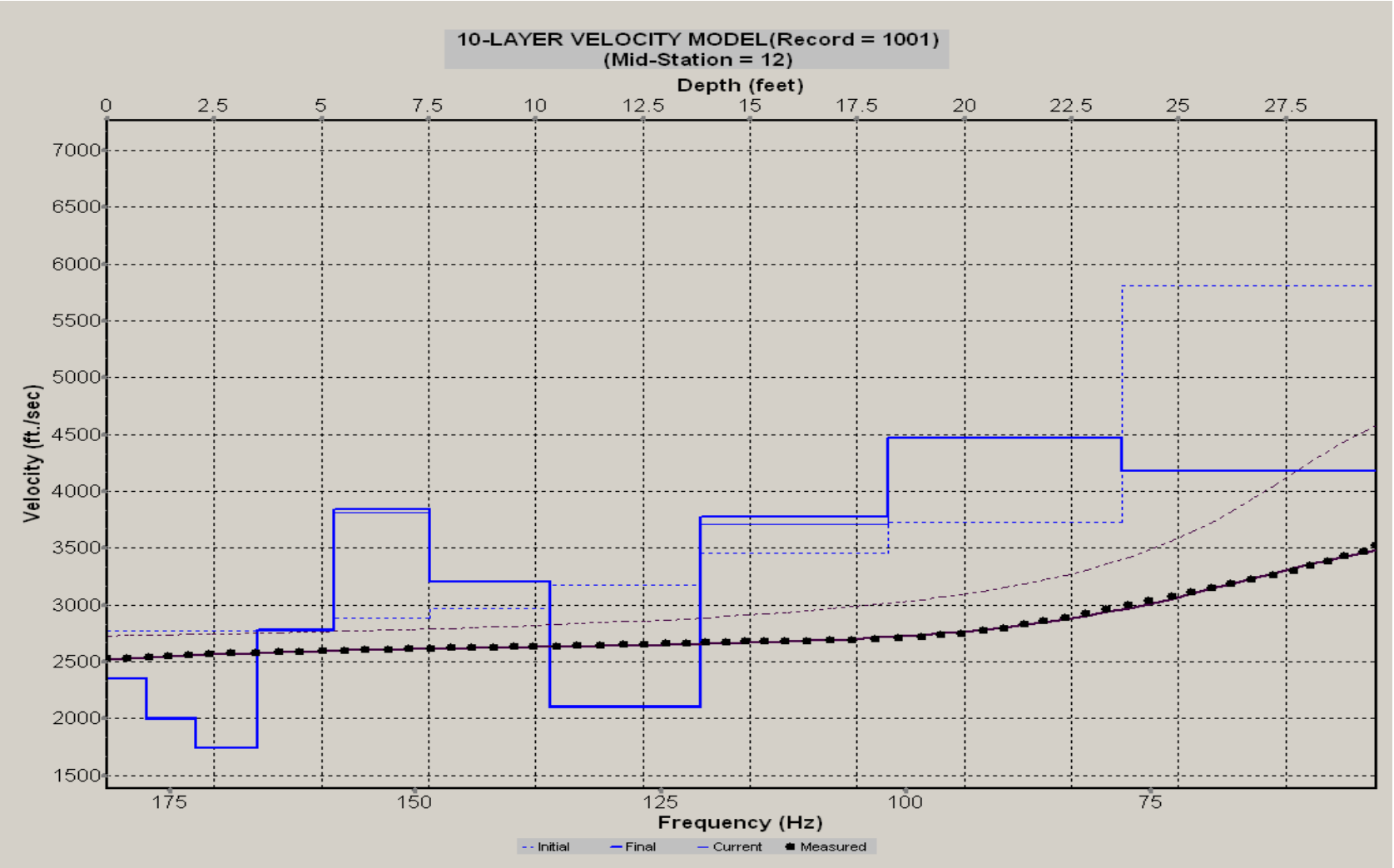

A.282: Velocity Profile Line 1203 used in Pre-blast 19, Post-blast 23 and Pre-blast 25

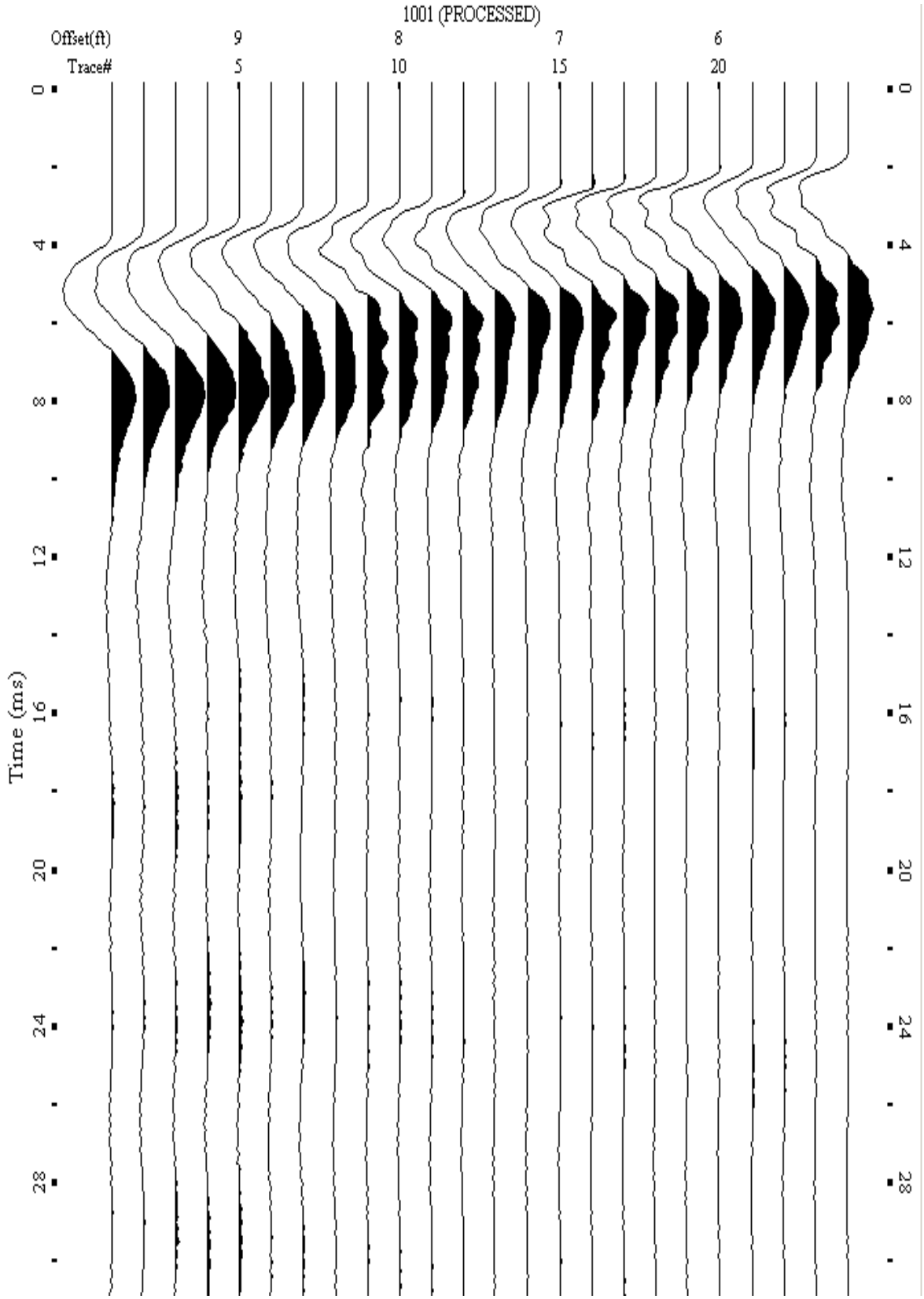

A.283: Shot Gather Line 1204 used in Pre-blast 19, Post-blast 23 and Pre-blast 25

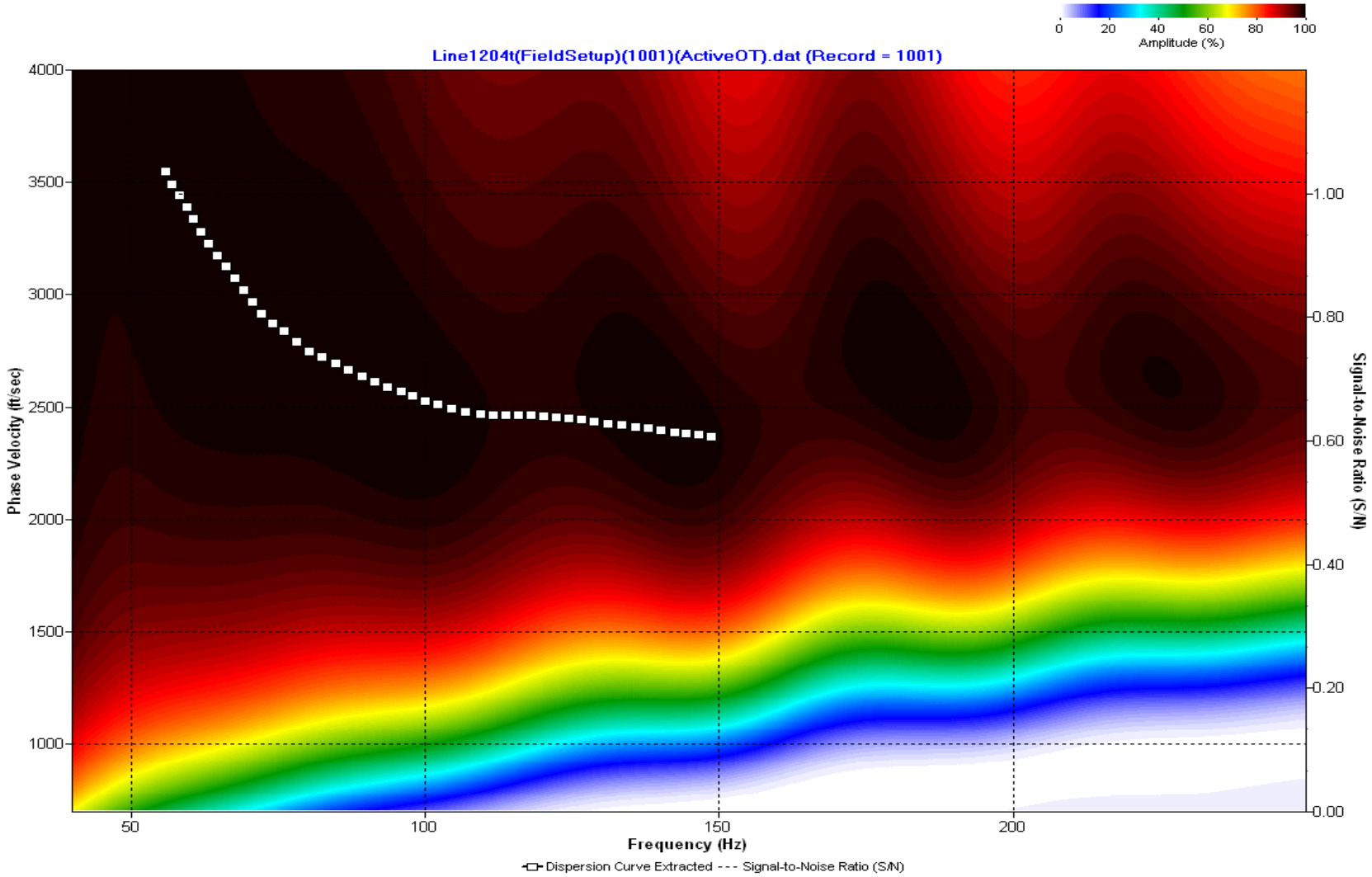

A.284: Dispersion Curve Line 1204 used in Pre-blast 19, Post-blast 23 and Pre-blast 25

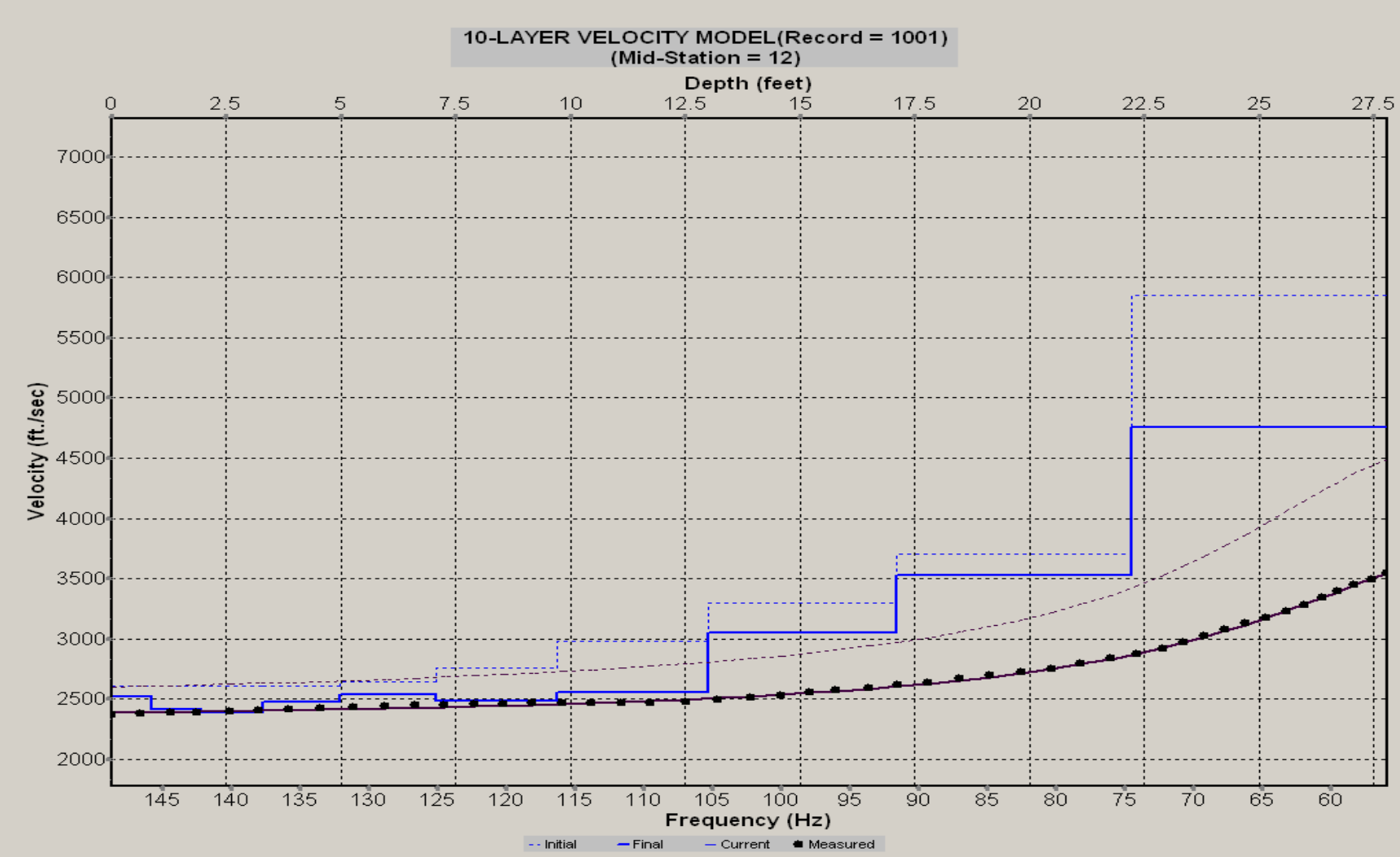

A.285: Velocity Profile Line 1204 used in Pre-blast 19, Post-blast 23 and Pre-blast 25

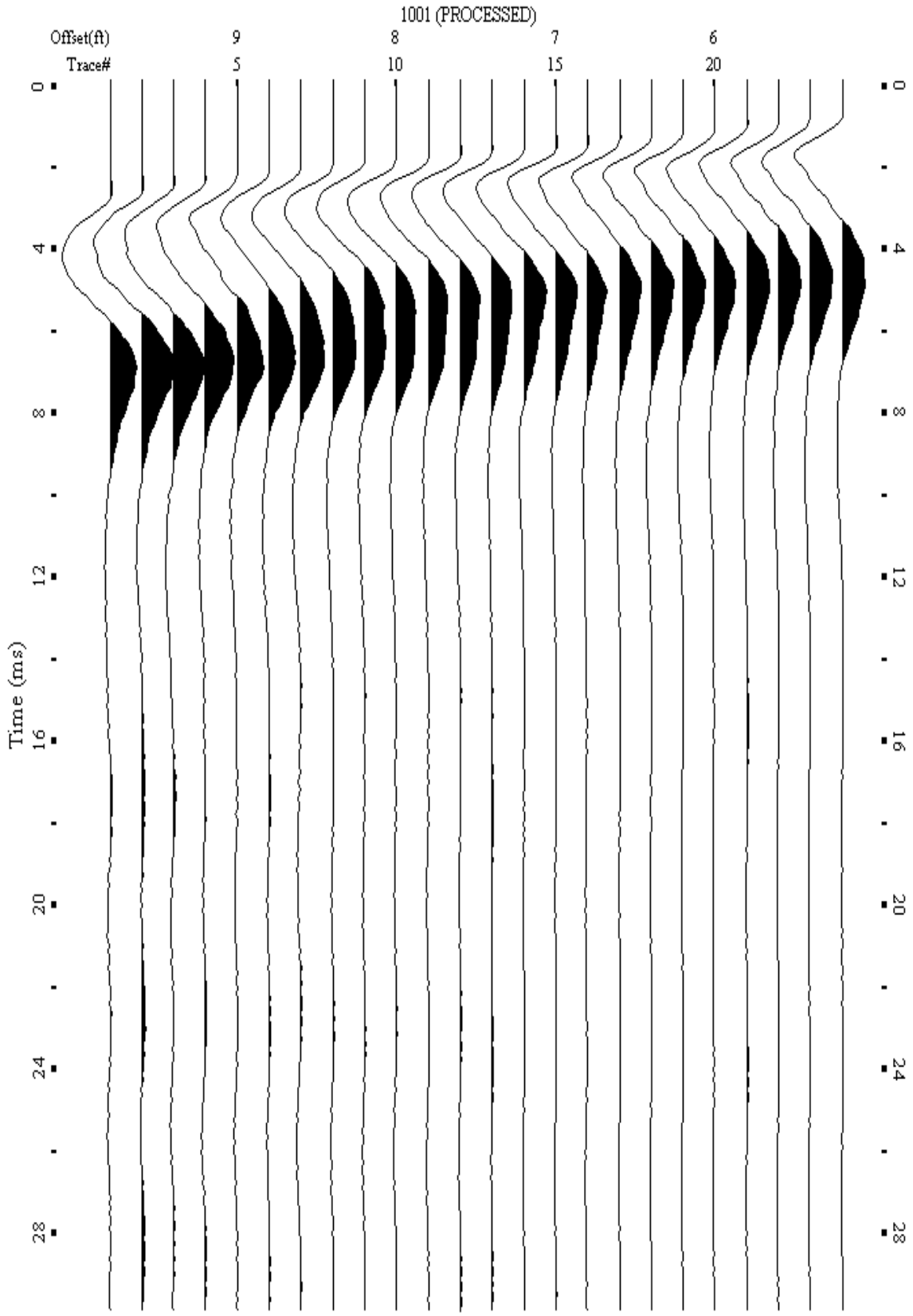

A.286: Shot Gather Line 1205 used in Pre-blast 19, Post-blast 23 and Pre-blast 25

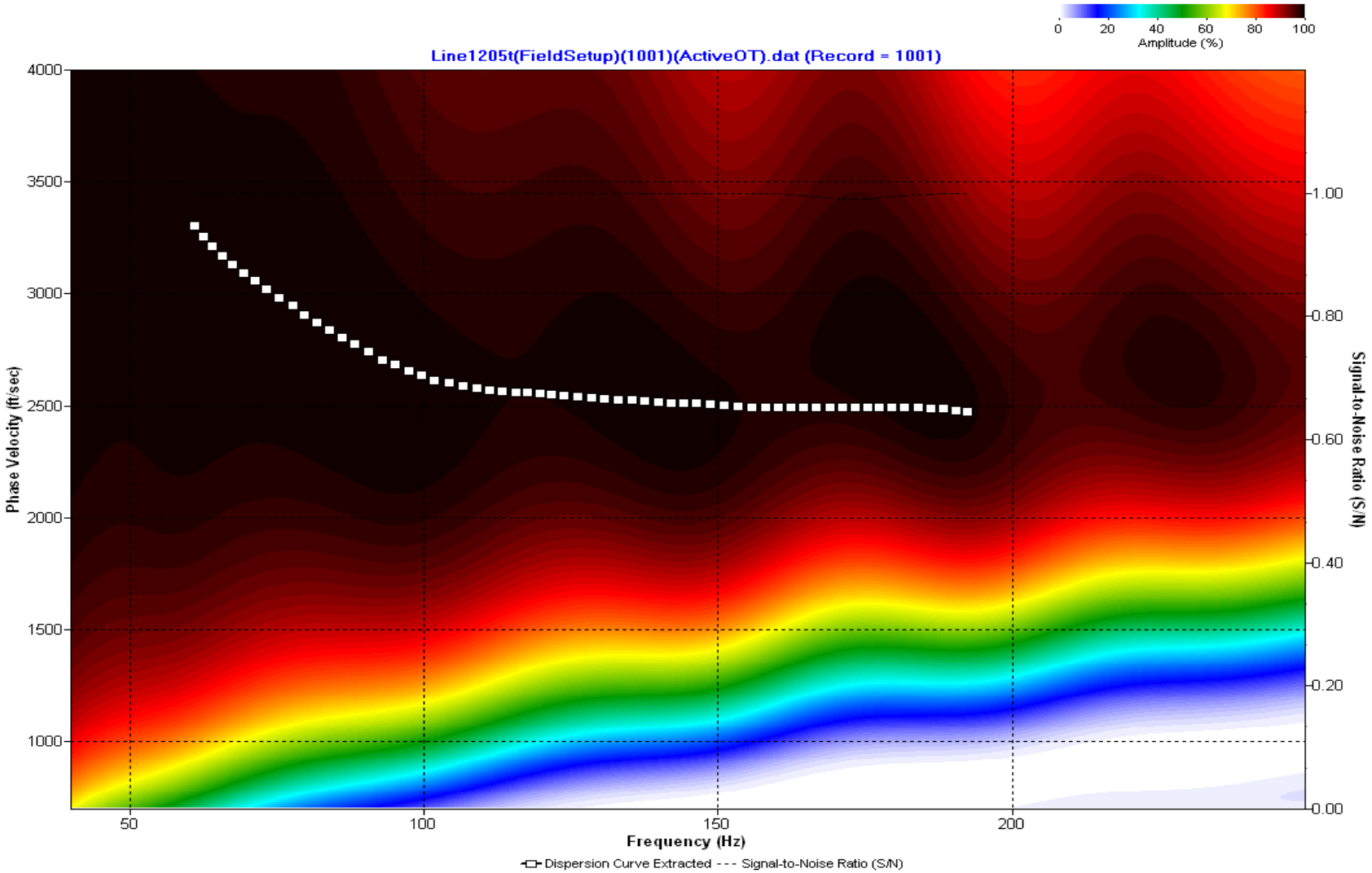

A.285: Dispersion Curve Line 1205 used in Pre-blast 19, Post-blast 23 and Pre-blast 25

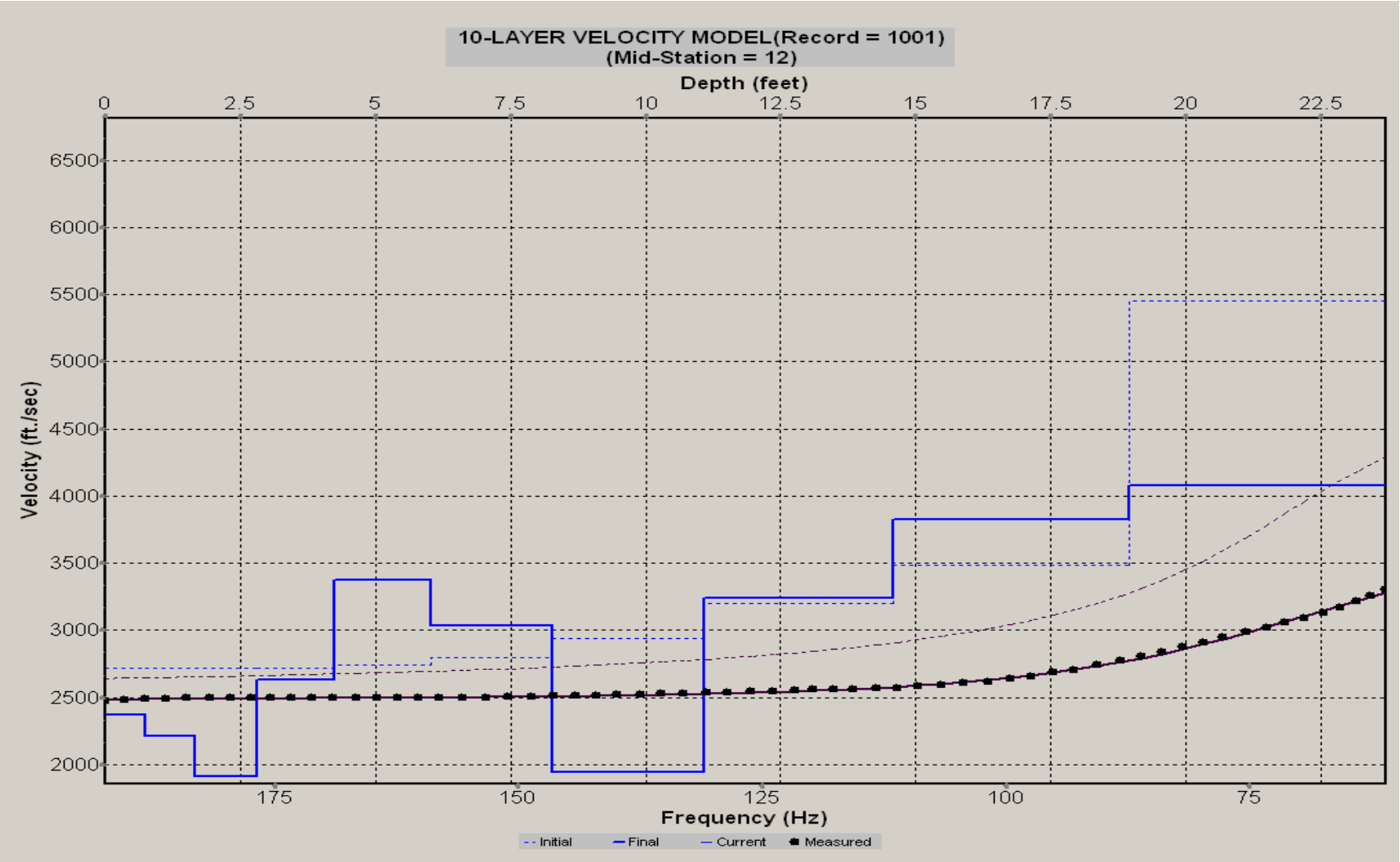

A.286: Velocity Profile Line 1205 used in Pre-blast 19, Post-blast 23 and Pre-blast 25

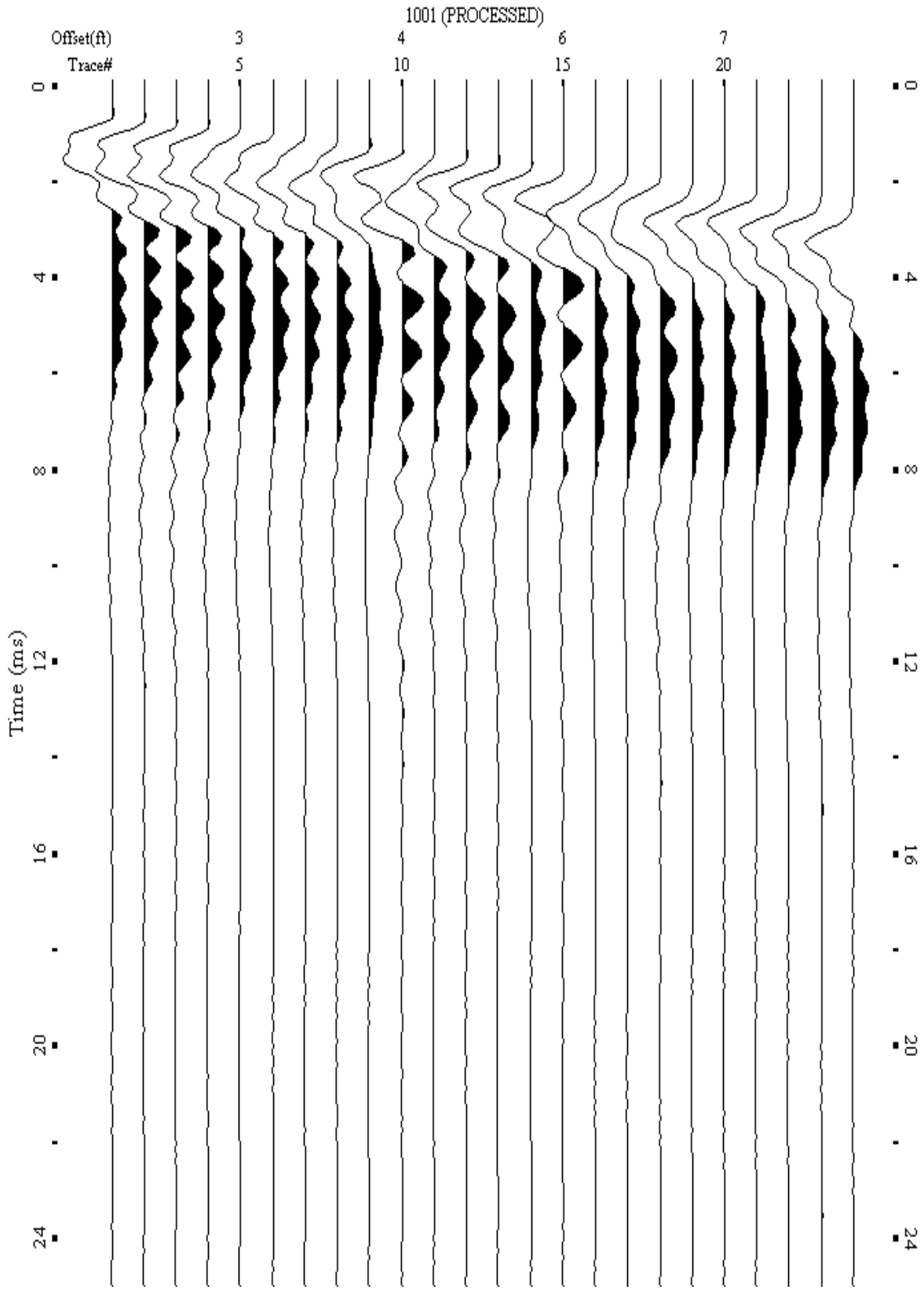

A.286: Shot Gather Line 1206 used in Pre-blast 15, Post-blast 24 and Pre-blast 26

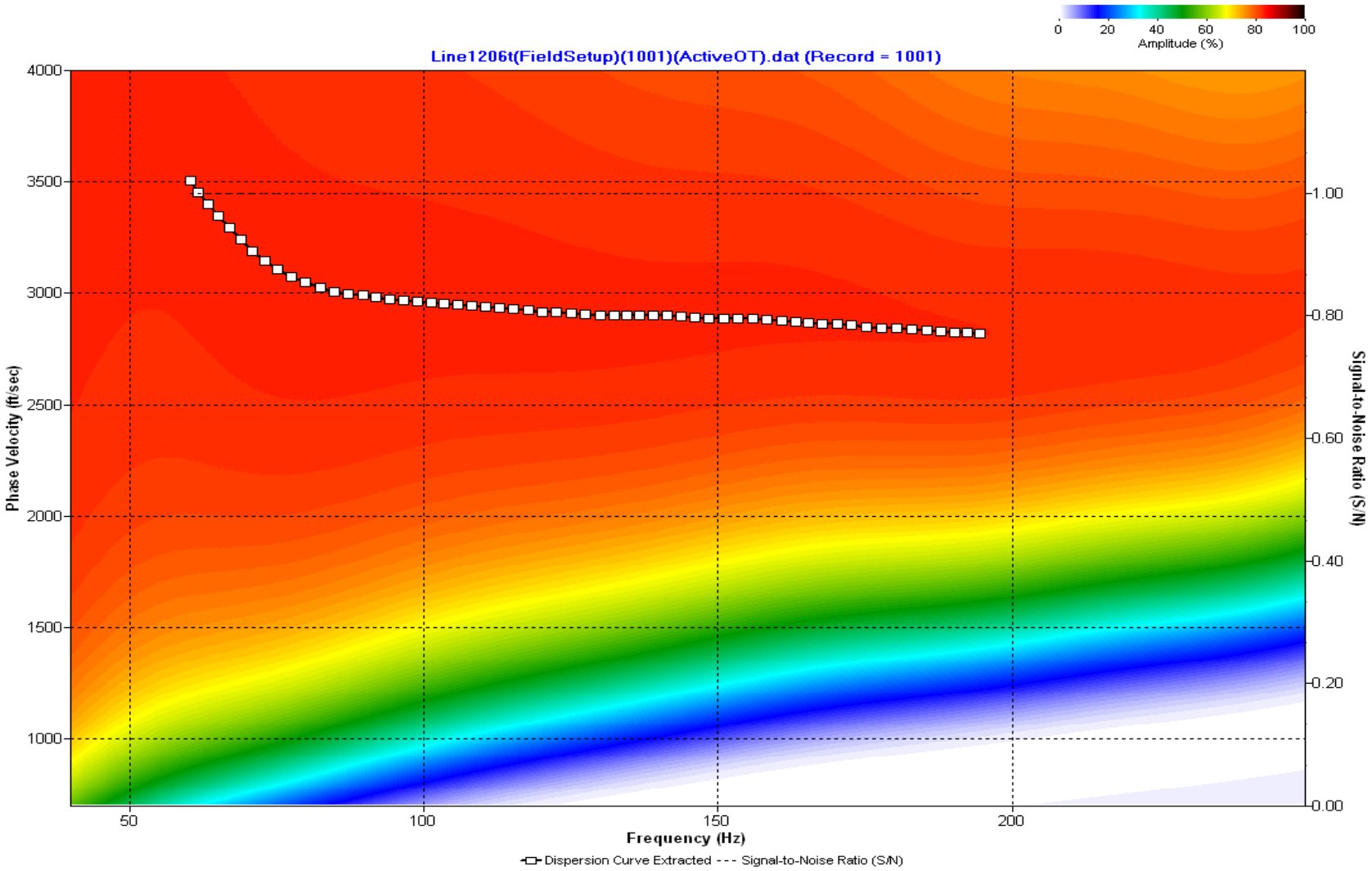

A.290: Dispersion Curve Line 1206 used in Pre-blast 15, Post-blast 24 and Pre-blast 26

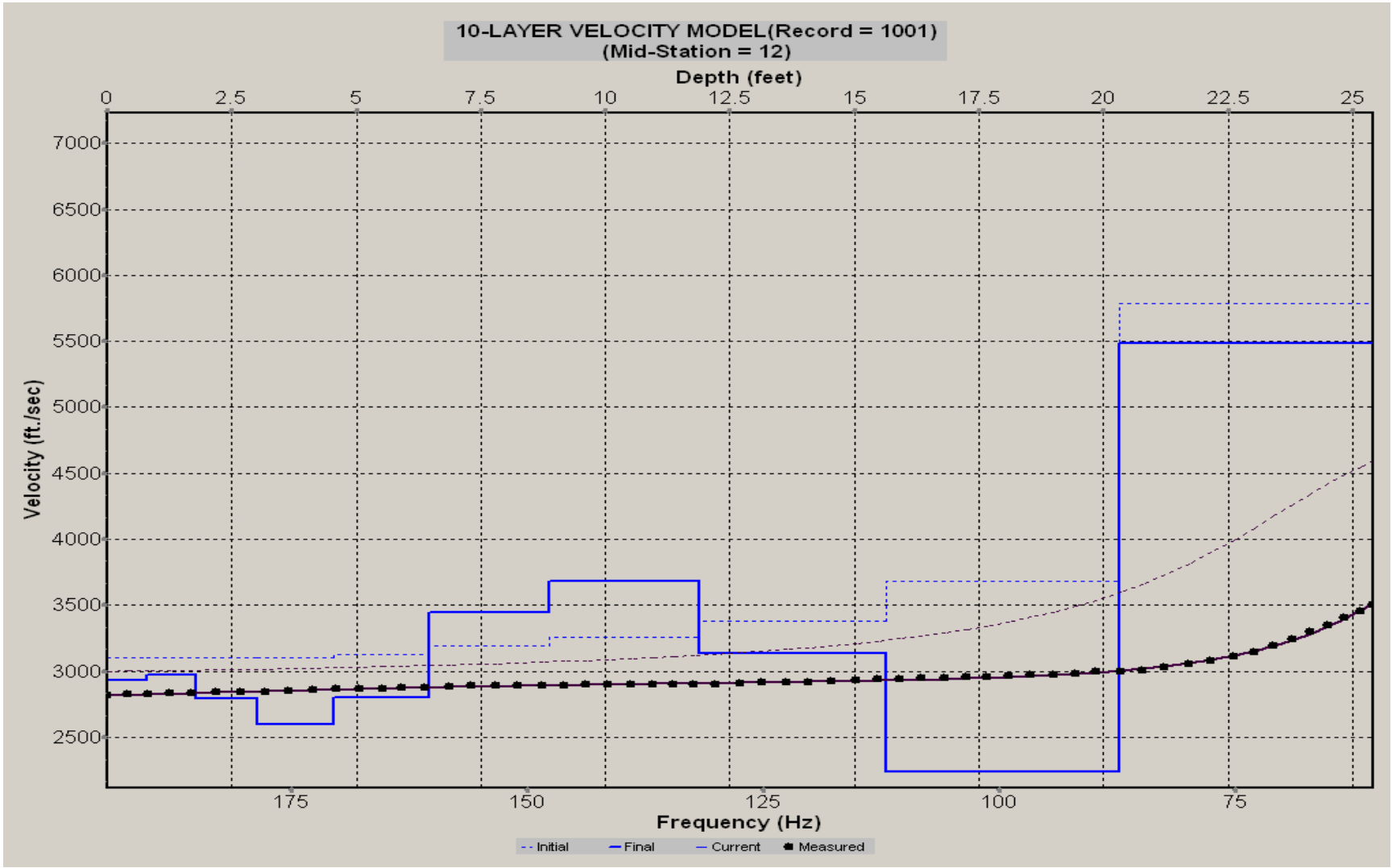

A.291: Velocity Profile Line 1206 used in Pre-blast 15, Post-blast 24 and Pre-blast 26

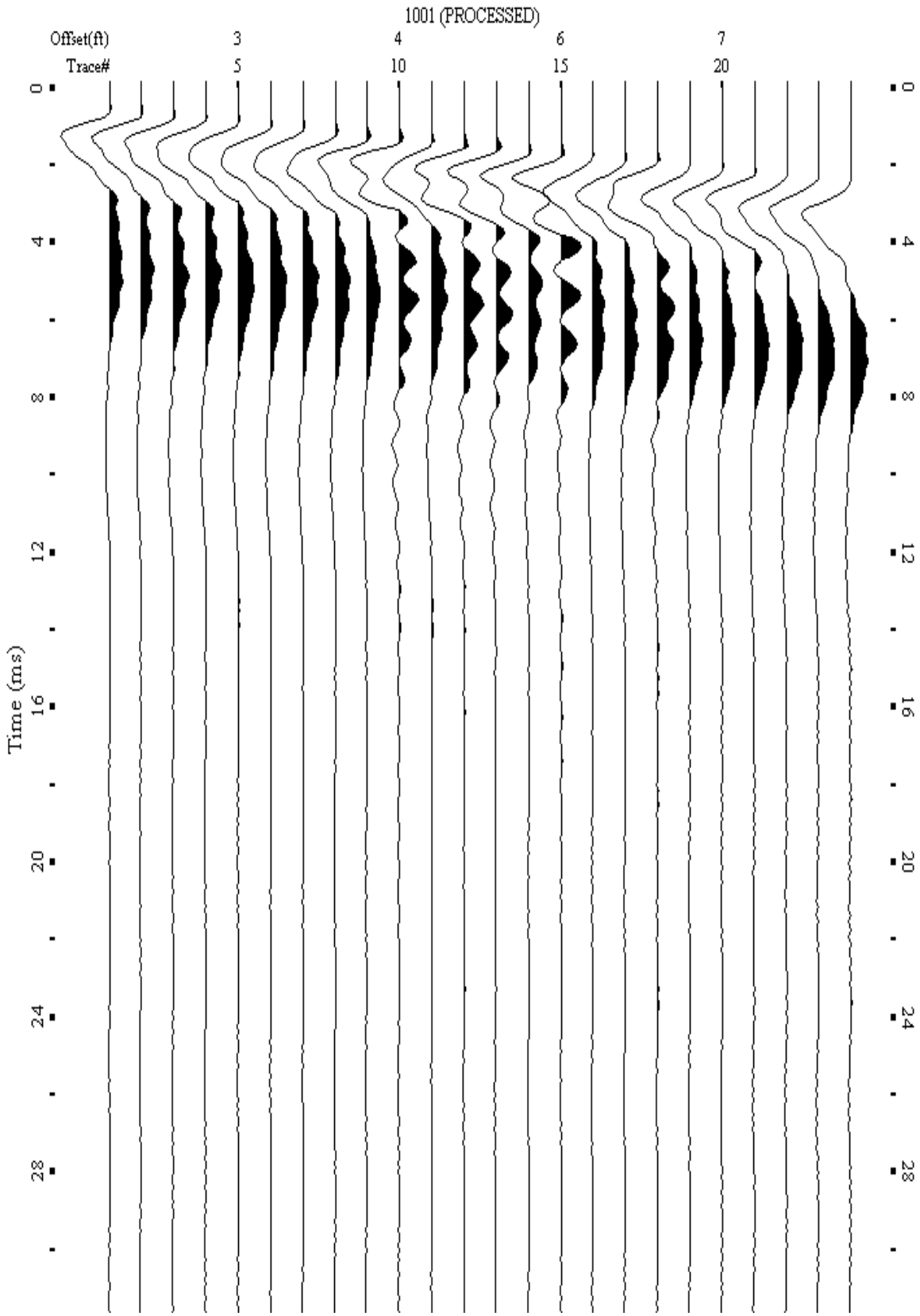

A.292: Shot Gather Line 1207 used in Pre-blast 15, Post-blast 24 and Pre-blast 26

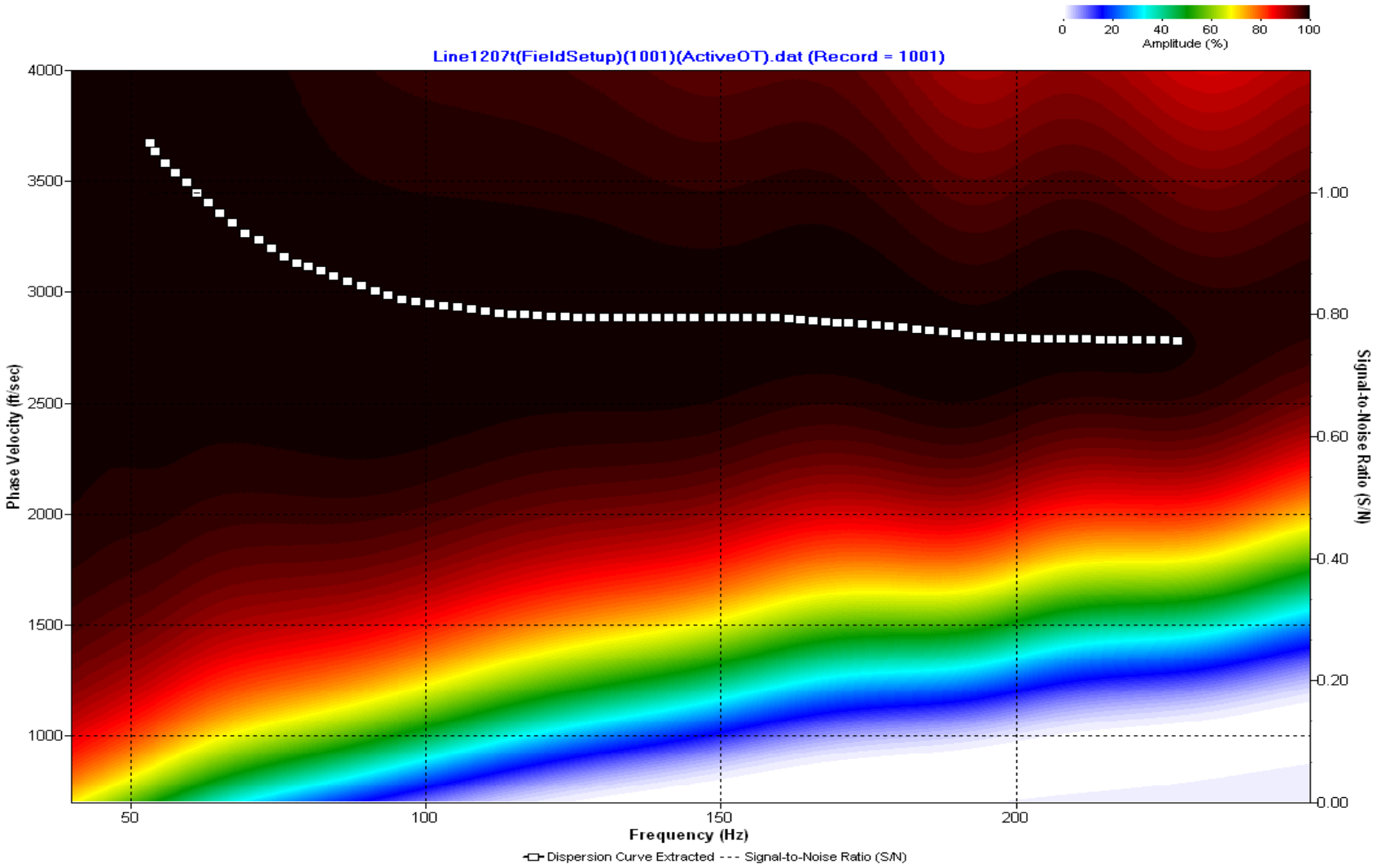

A.293: Dispersion Curve Line 1207 used in Pre-blast 15, Post-blast 24 and Pre-blast 26

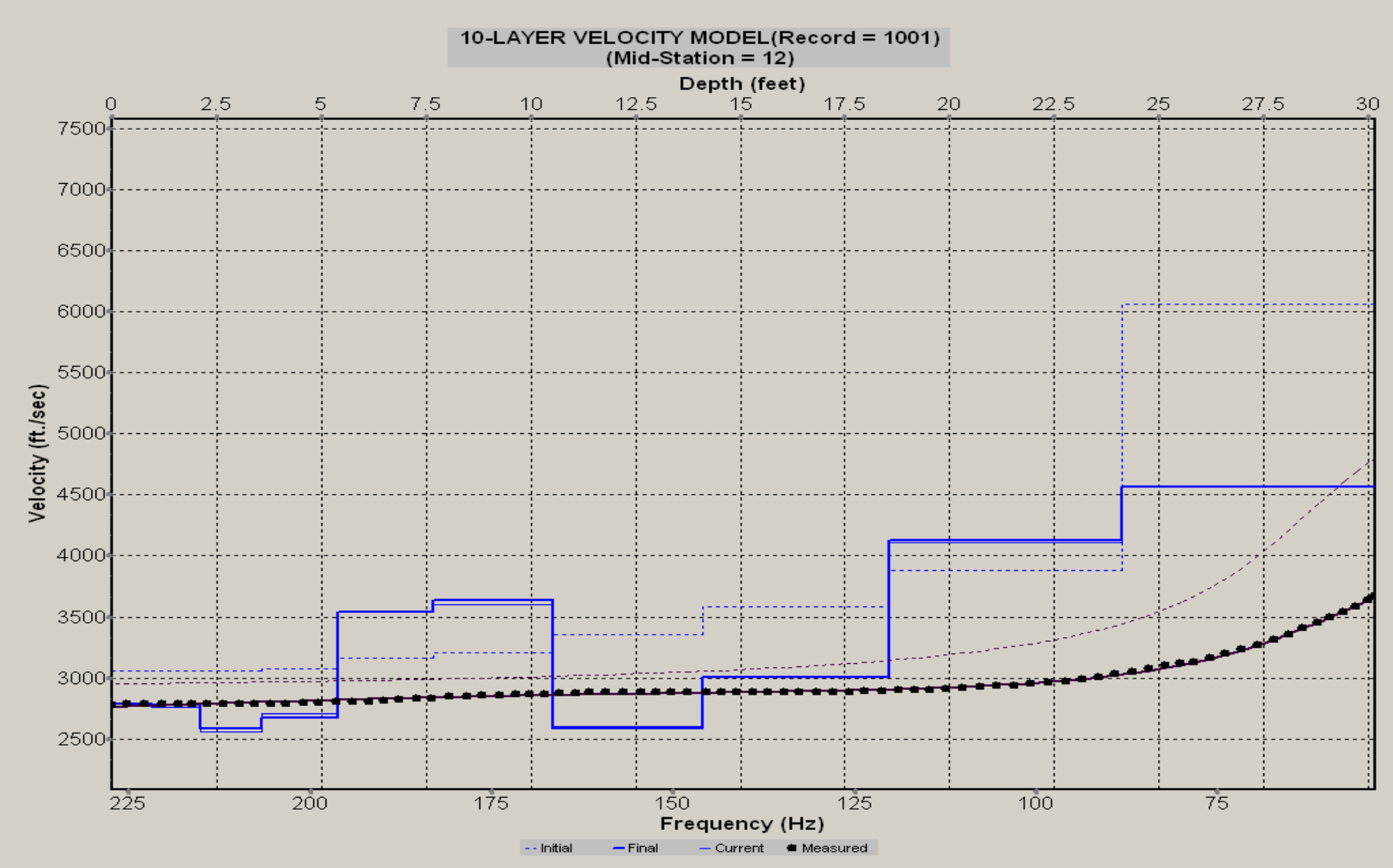

A.294: Velocity Profile Line 1207 used in Pre-blast 15, Post-blast 24 and Pre-blast 26

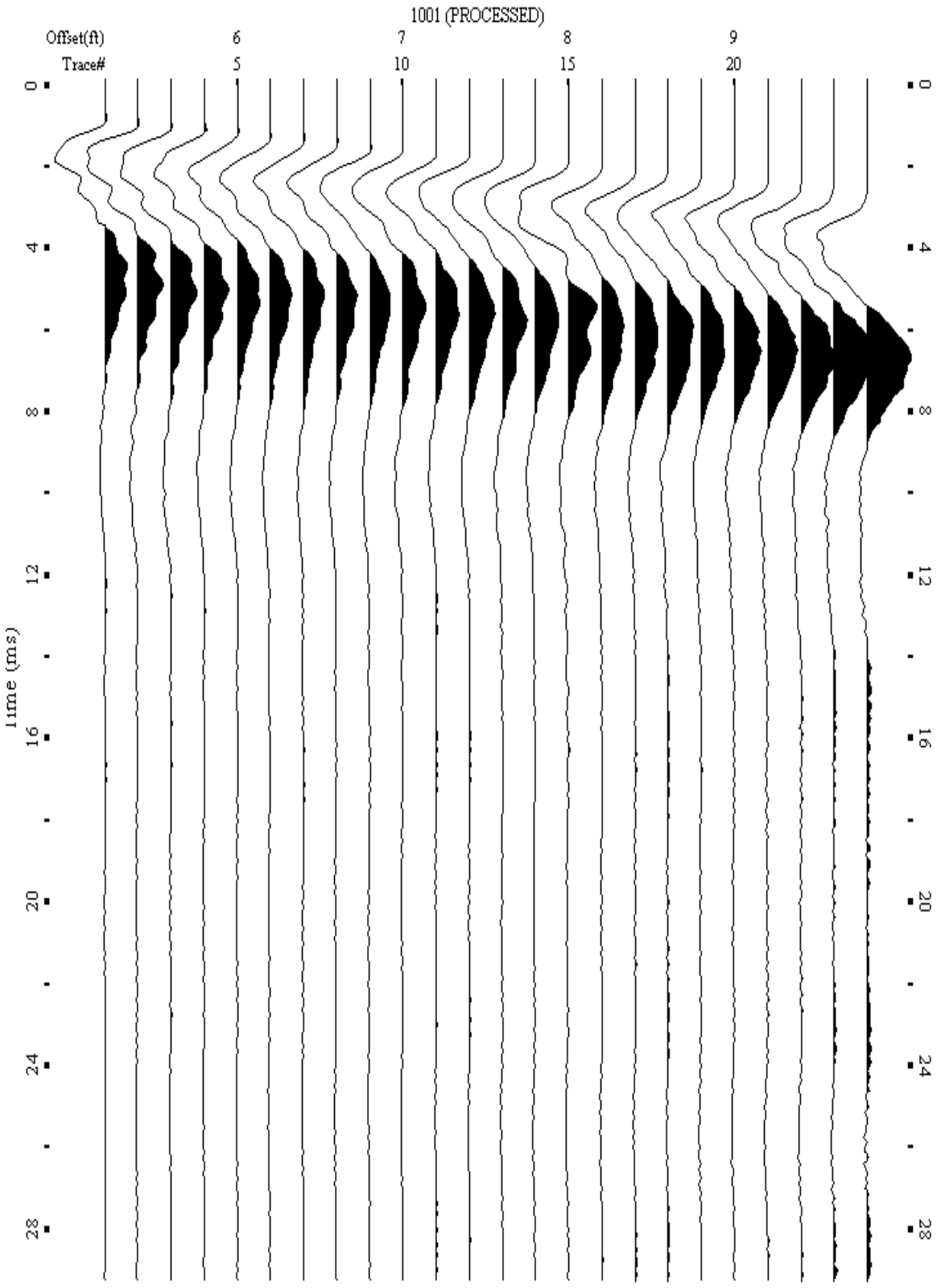

A.295: Shot Gather Line 1208 used in Pre-blast 15, Post-blast 24 and Pre-blast 26

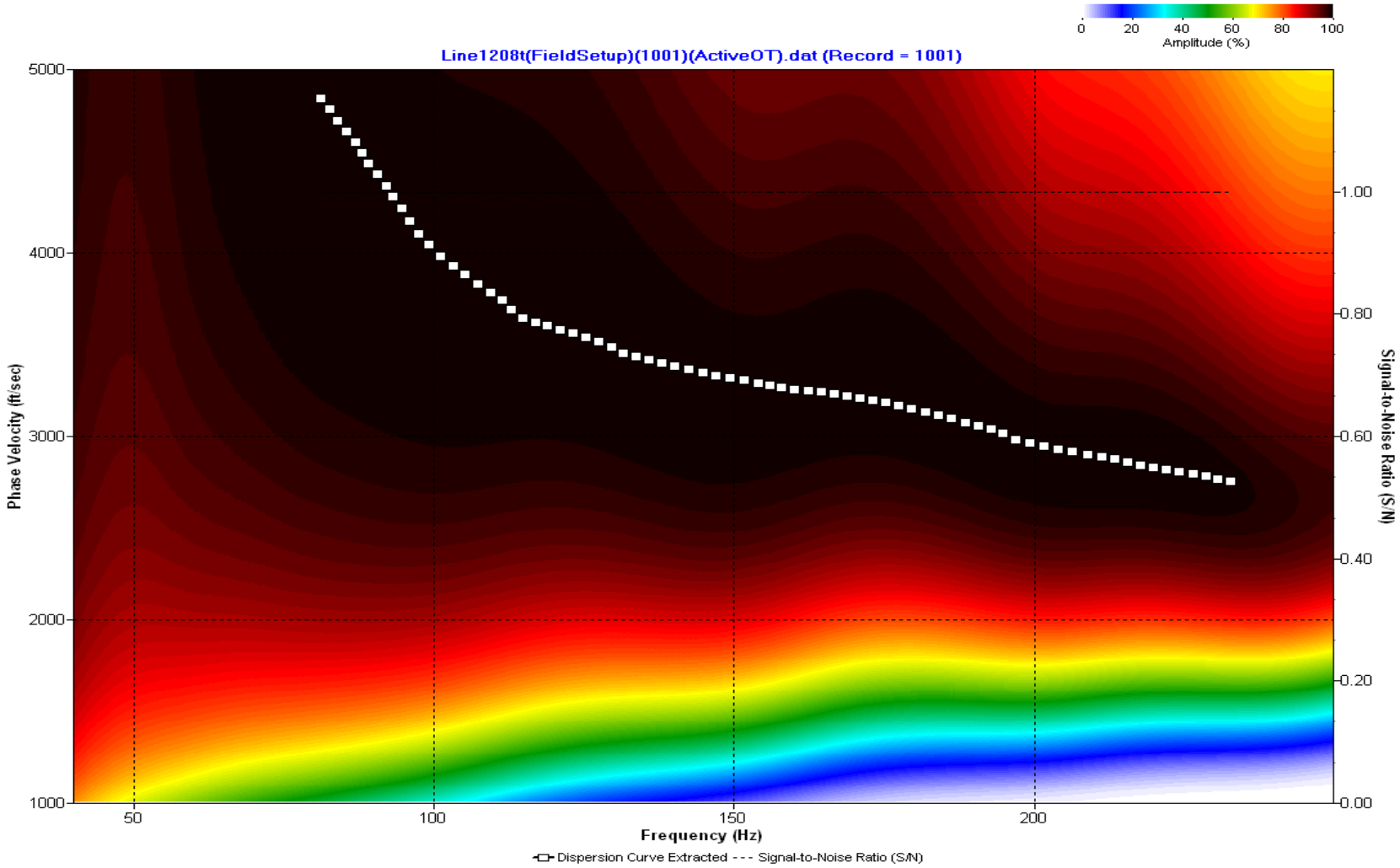

A.296: Dispersion Curve Line 1208 used in Pre-blast 15, Post-blast 24 and Pre-blast 26

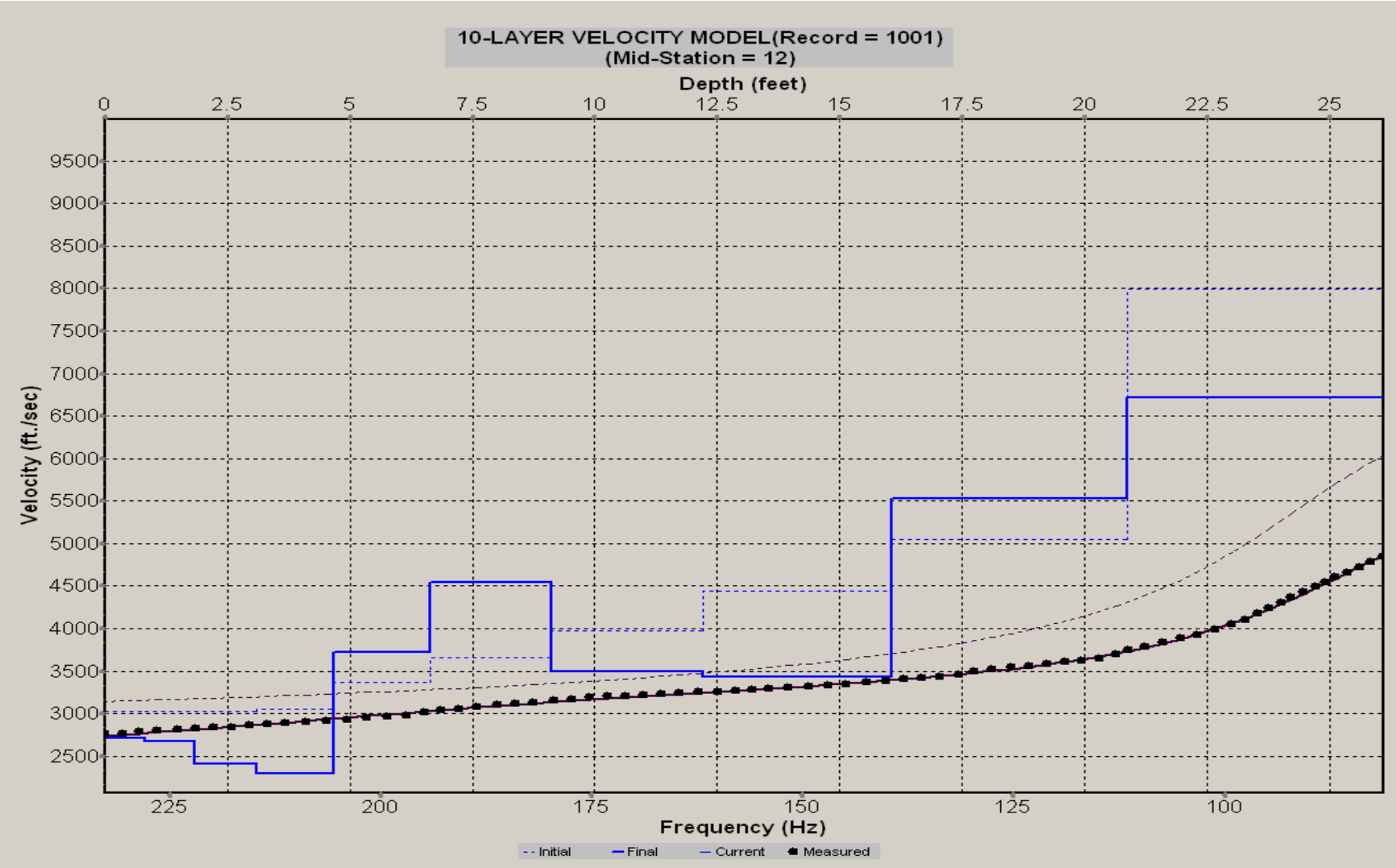

A.297: Velocity Profile Line 1208 used in Pre-blast 15, Post-blast 24 and Pre-blast 26

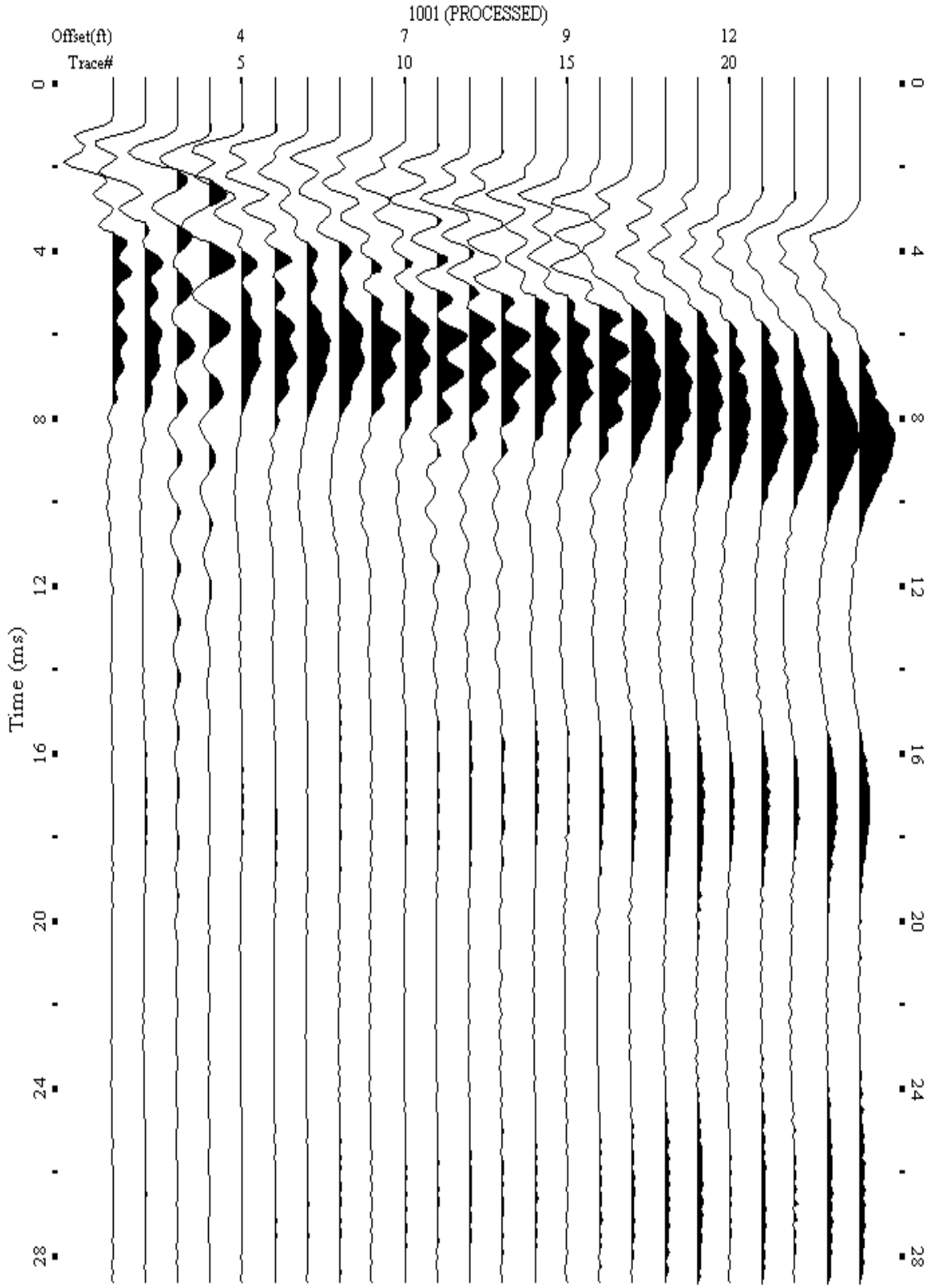

A.298: Shot Gather Line 1214 used in Post-blast 12 and Pre-blast 27

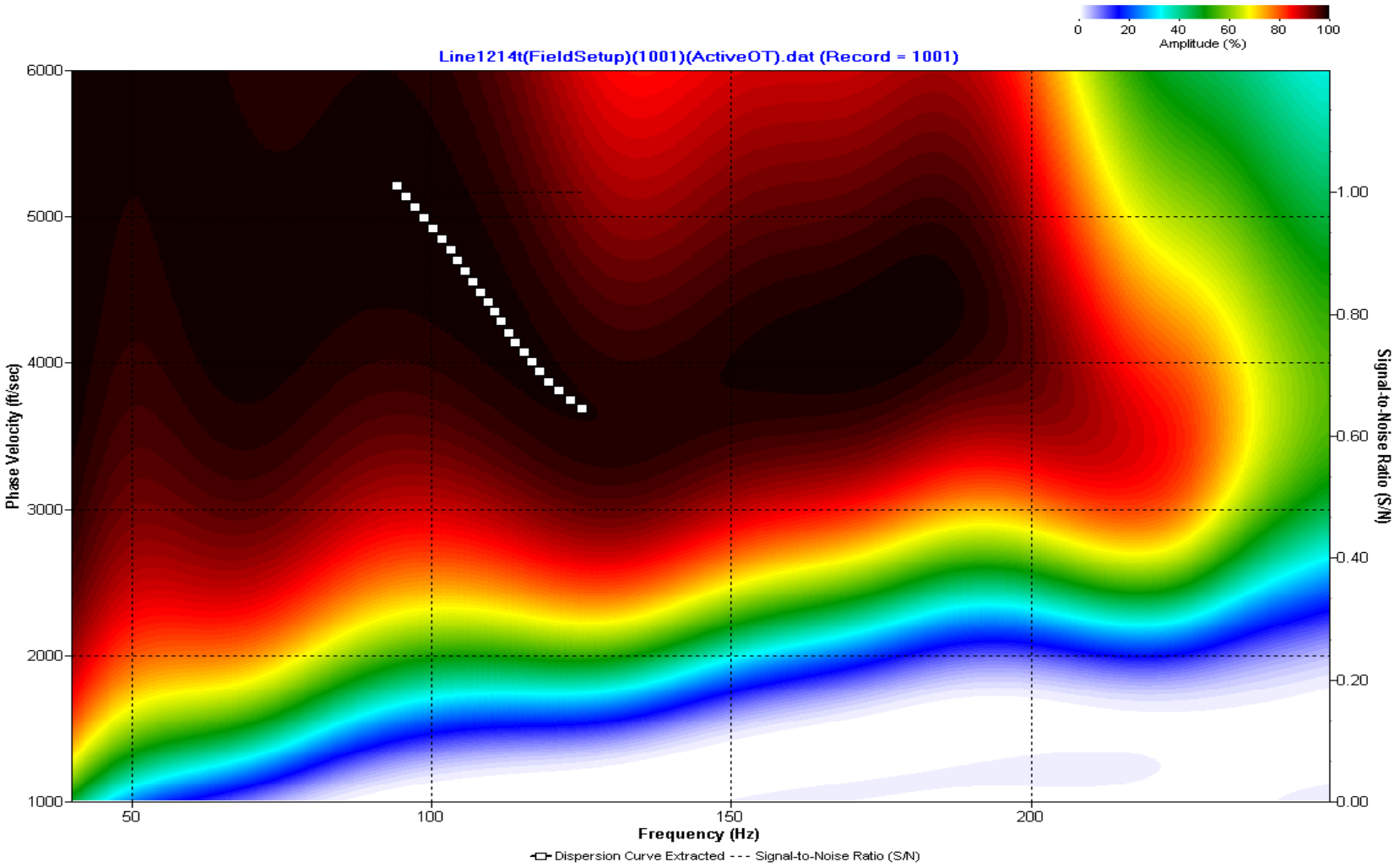

A.299: Dispersion Curve Line 1214 used in Post-blast 12 and Pre-blast 27

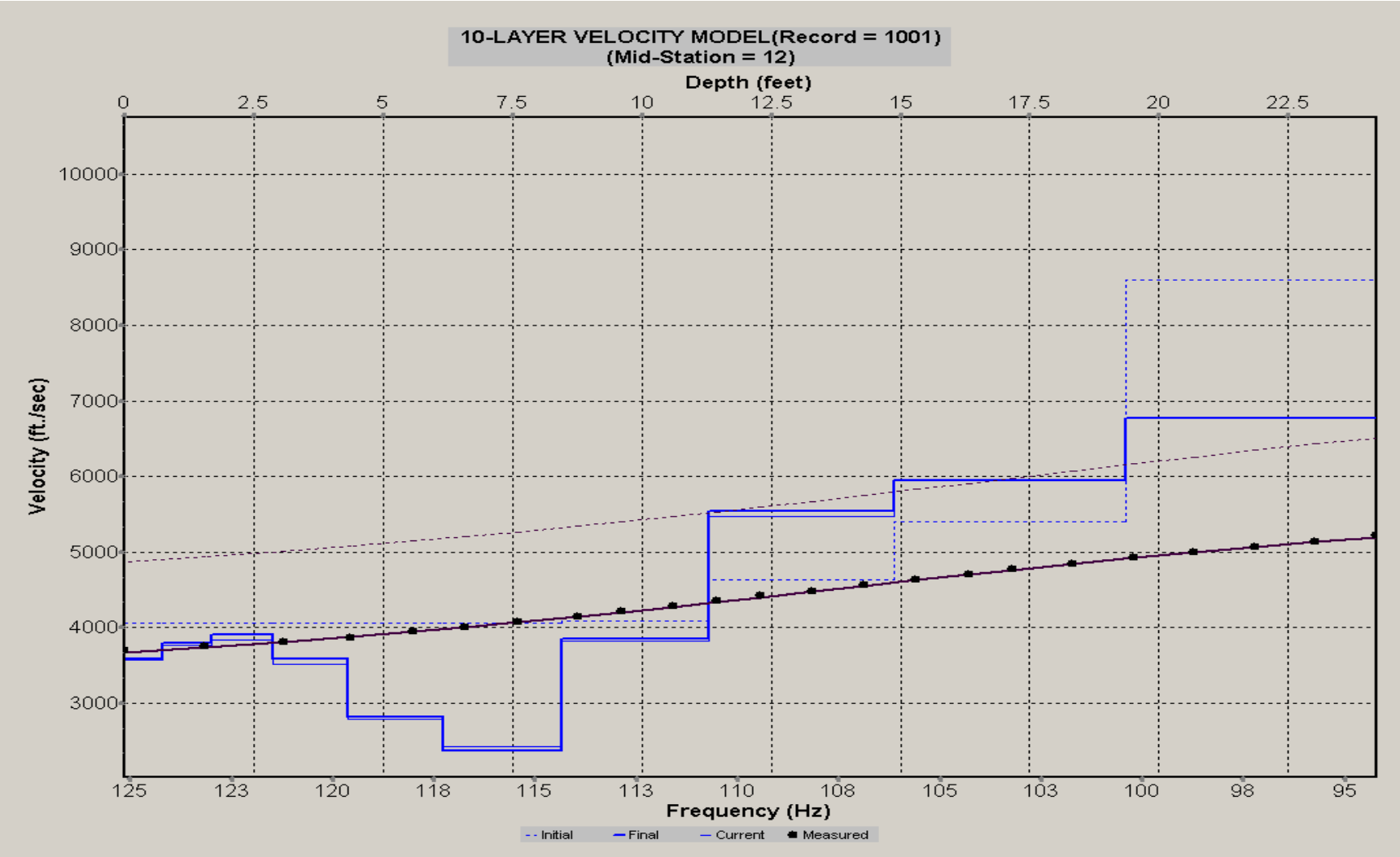

A.300: Velocity Profile Line 1214 used in Post-blast 12 and Pre-blast 27

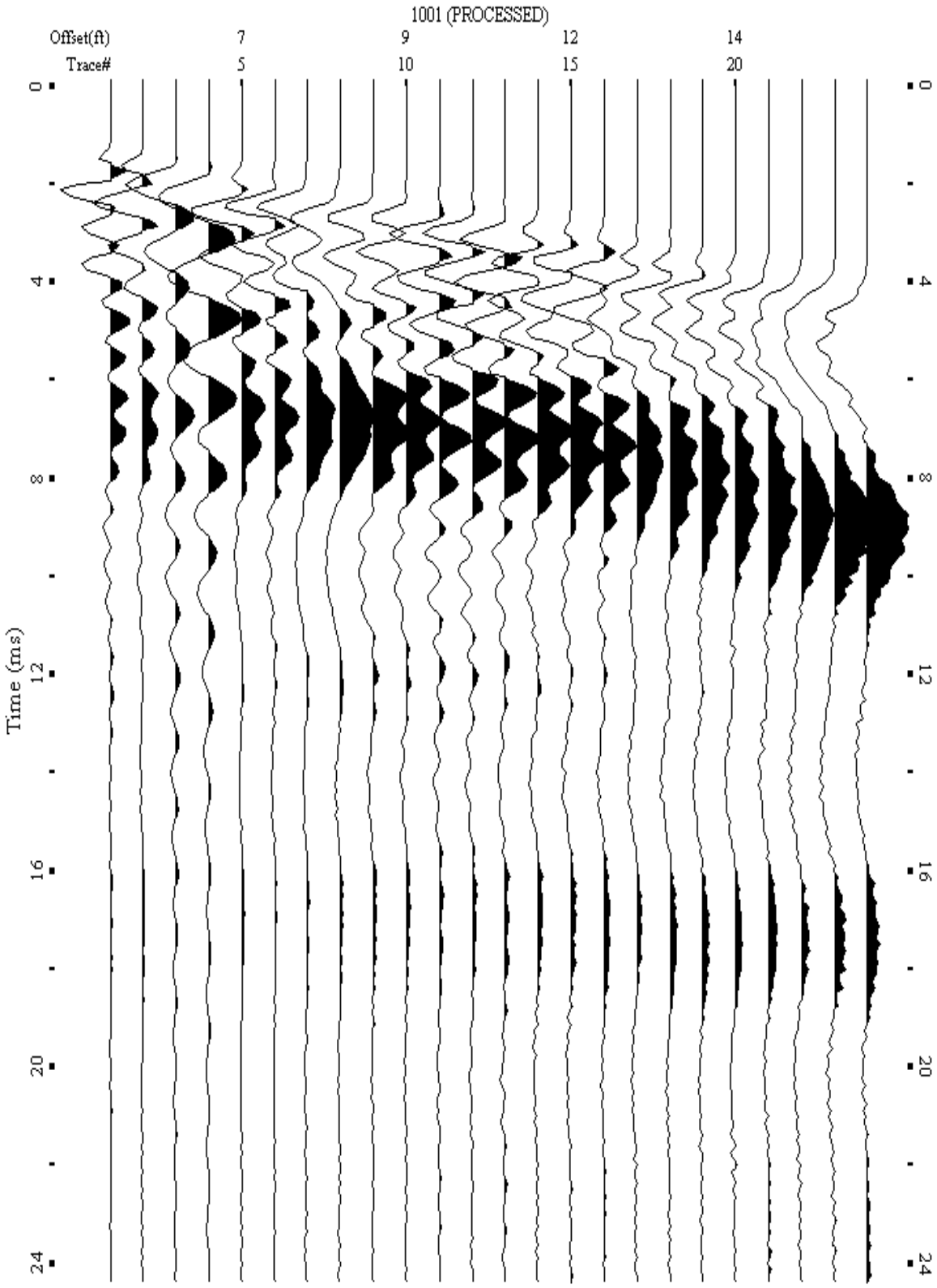

A.301: Shot Gather Line 1216 used in Post-blast 12

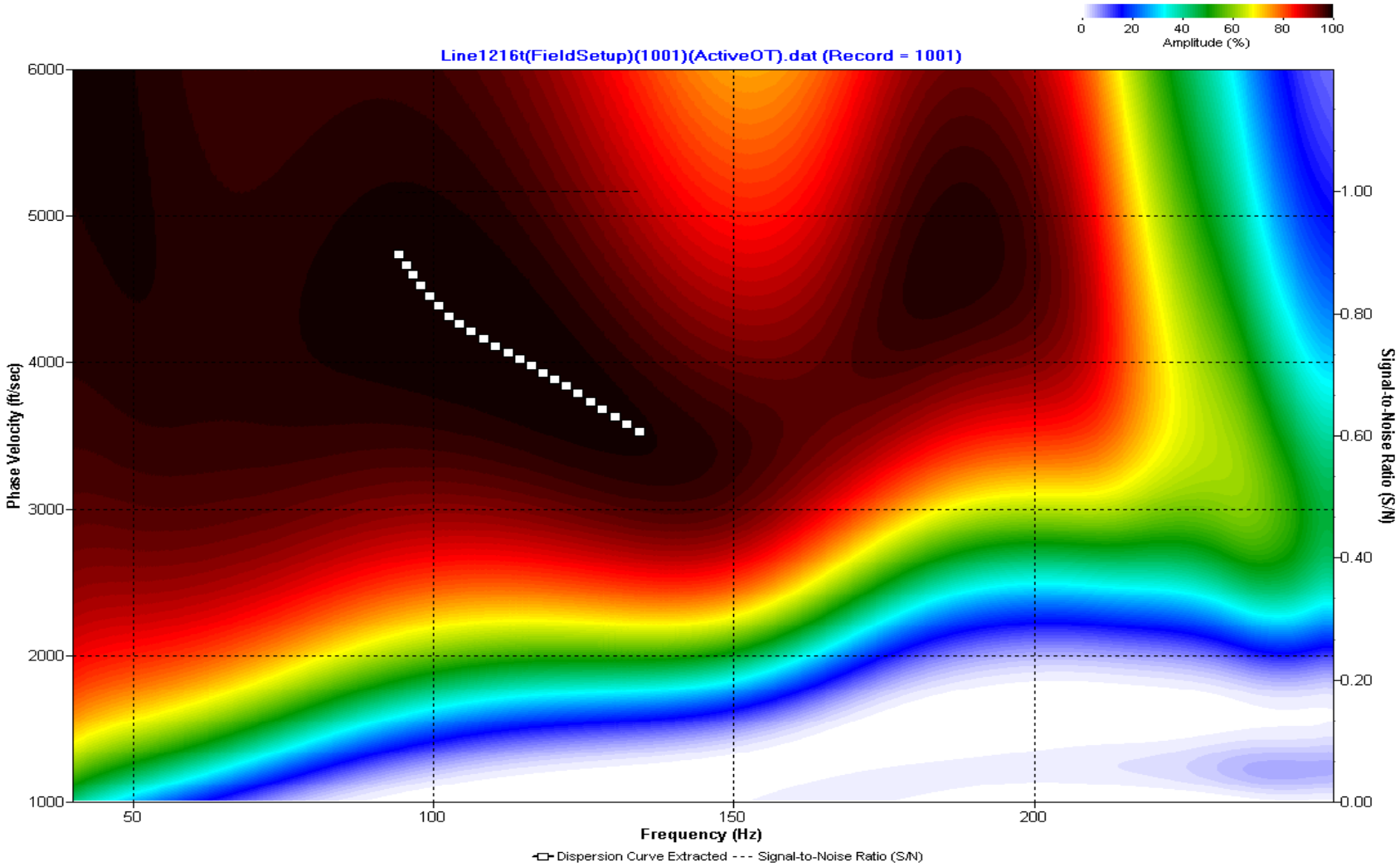

A.302: Dispersion Curve Line 1216 used in Post-blast 12

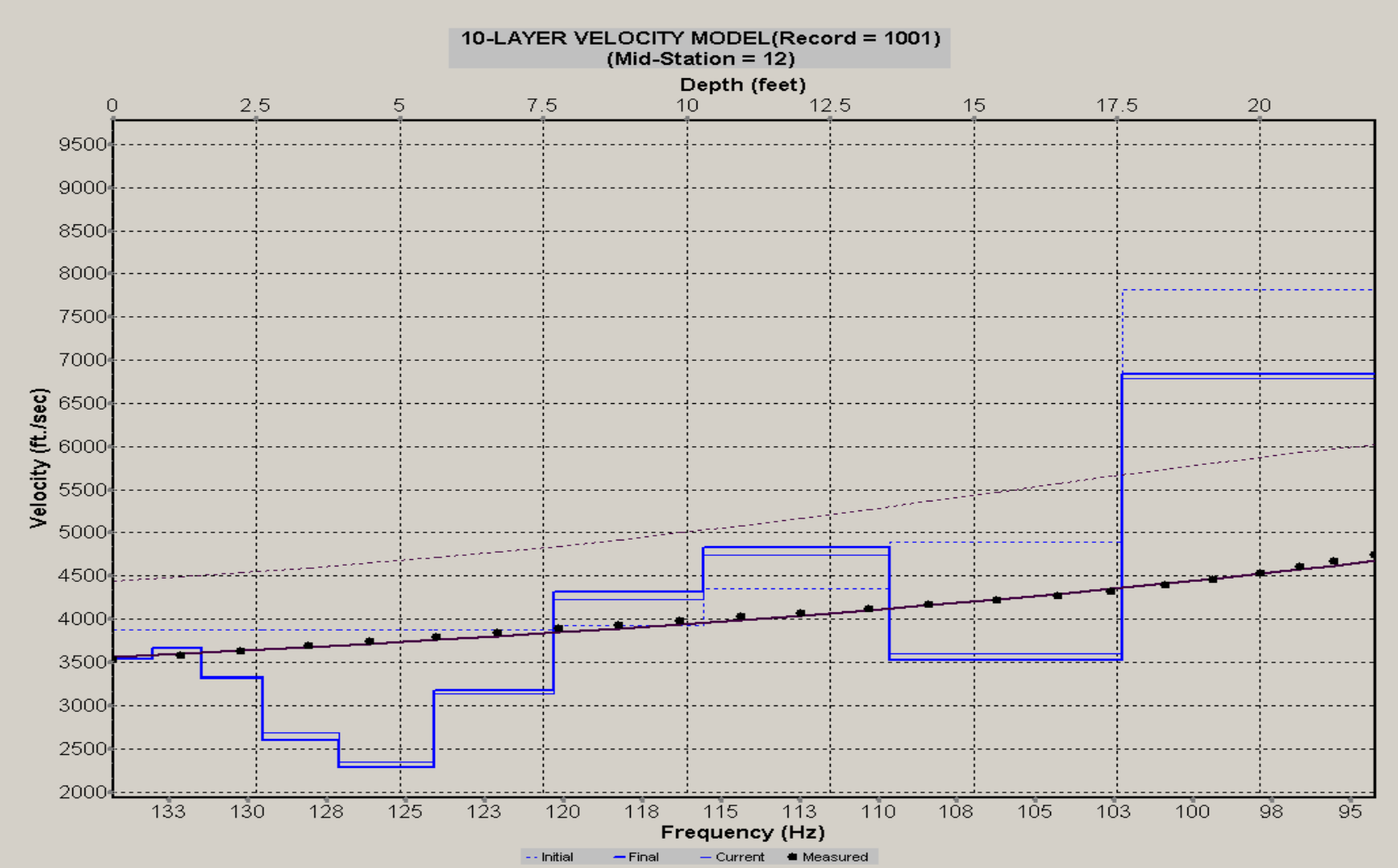

A.304: Velocity Profile Line 1216 used in Post-blast 12

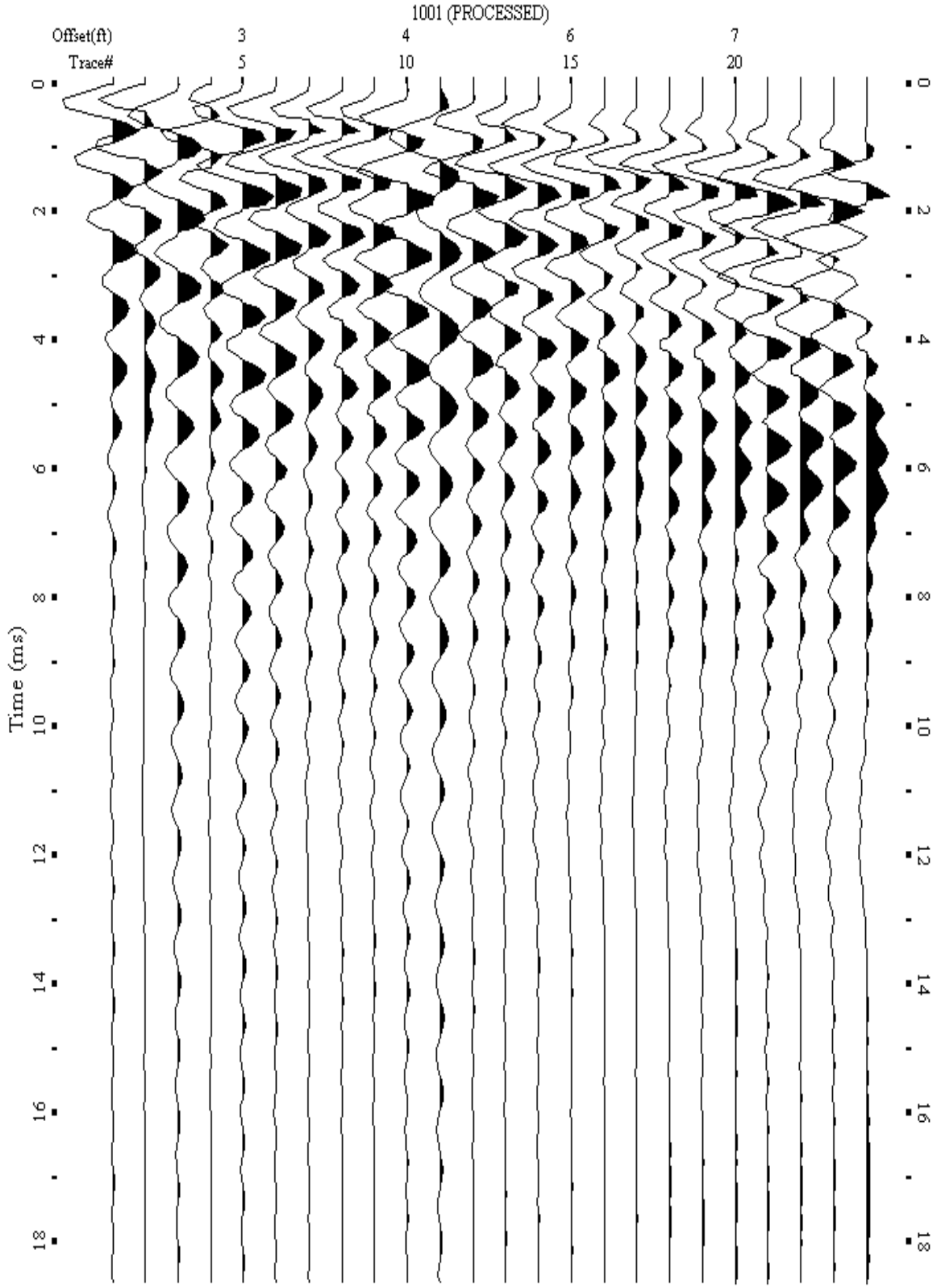

A.304: Shot Gather Line 1219 used in Pre-blast 27

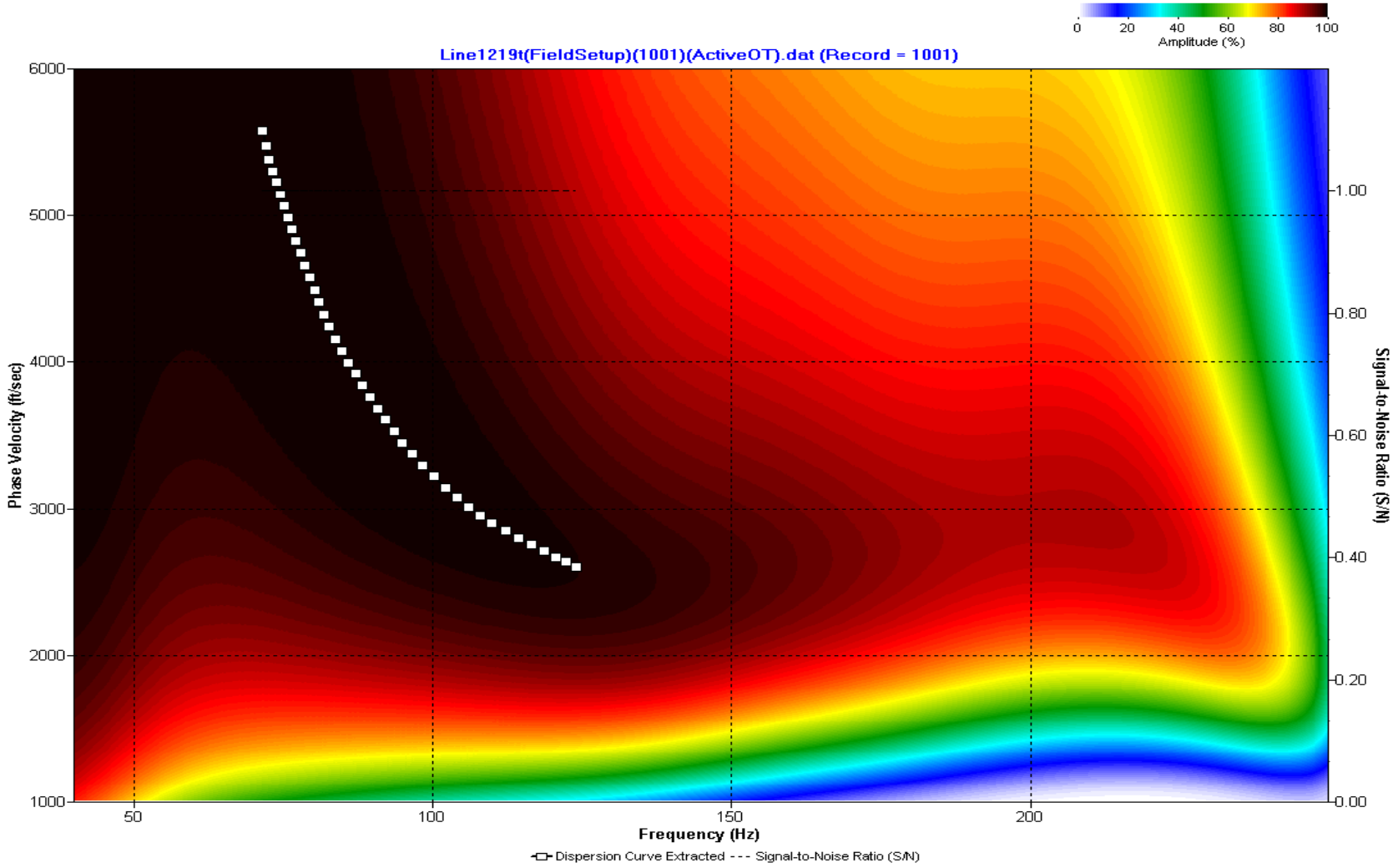

A.305: Dispersion Curve Line 1219 used in Pre-blast 27

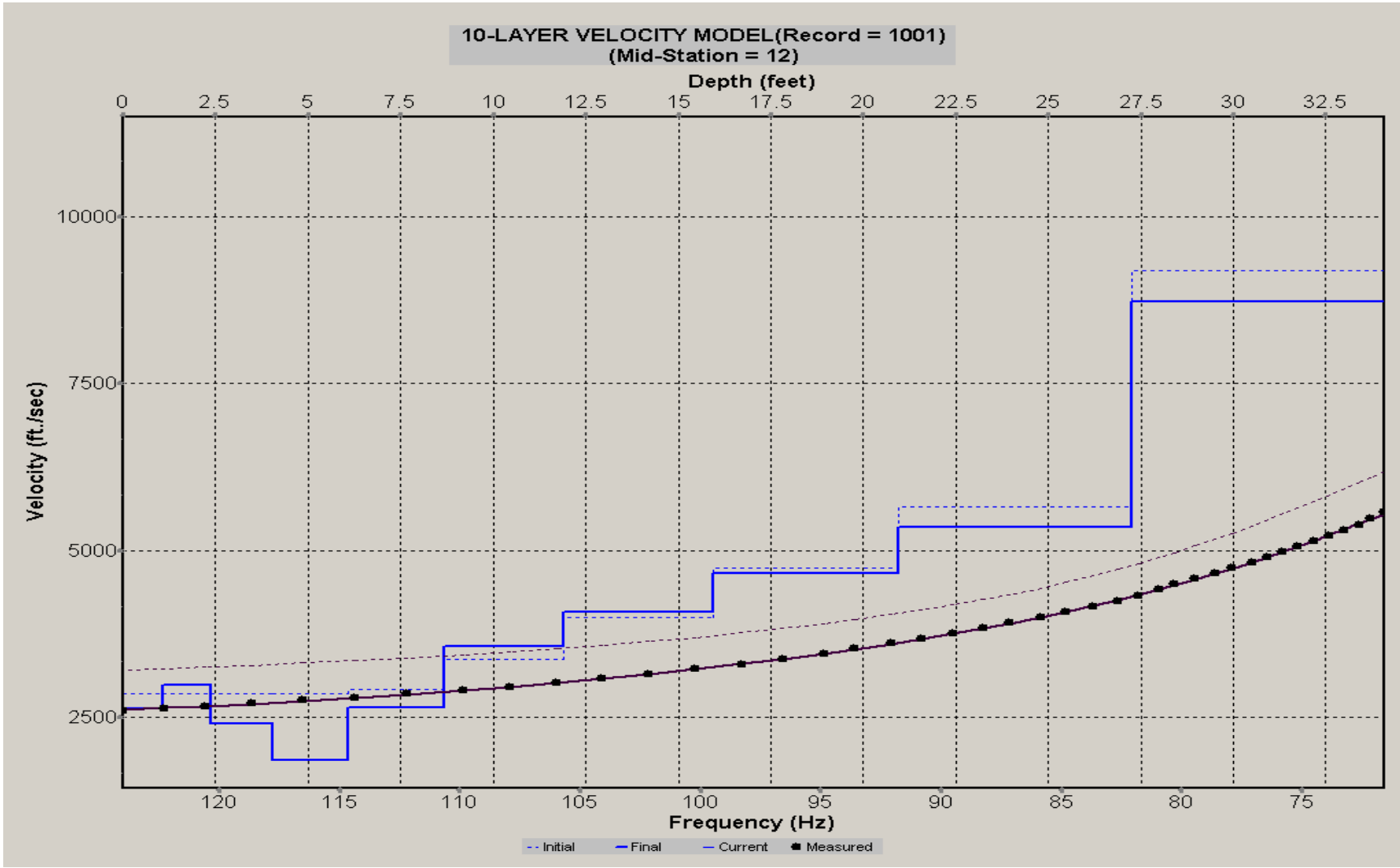

A.306: Velocity Profile Line 1219 used in Pre-blast 27

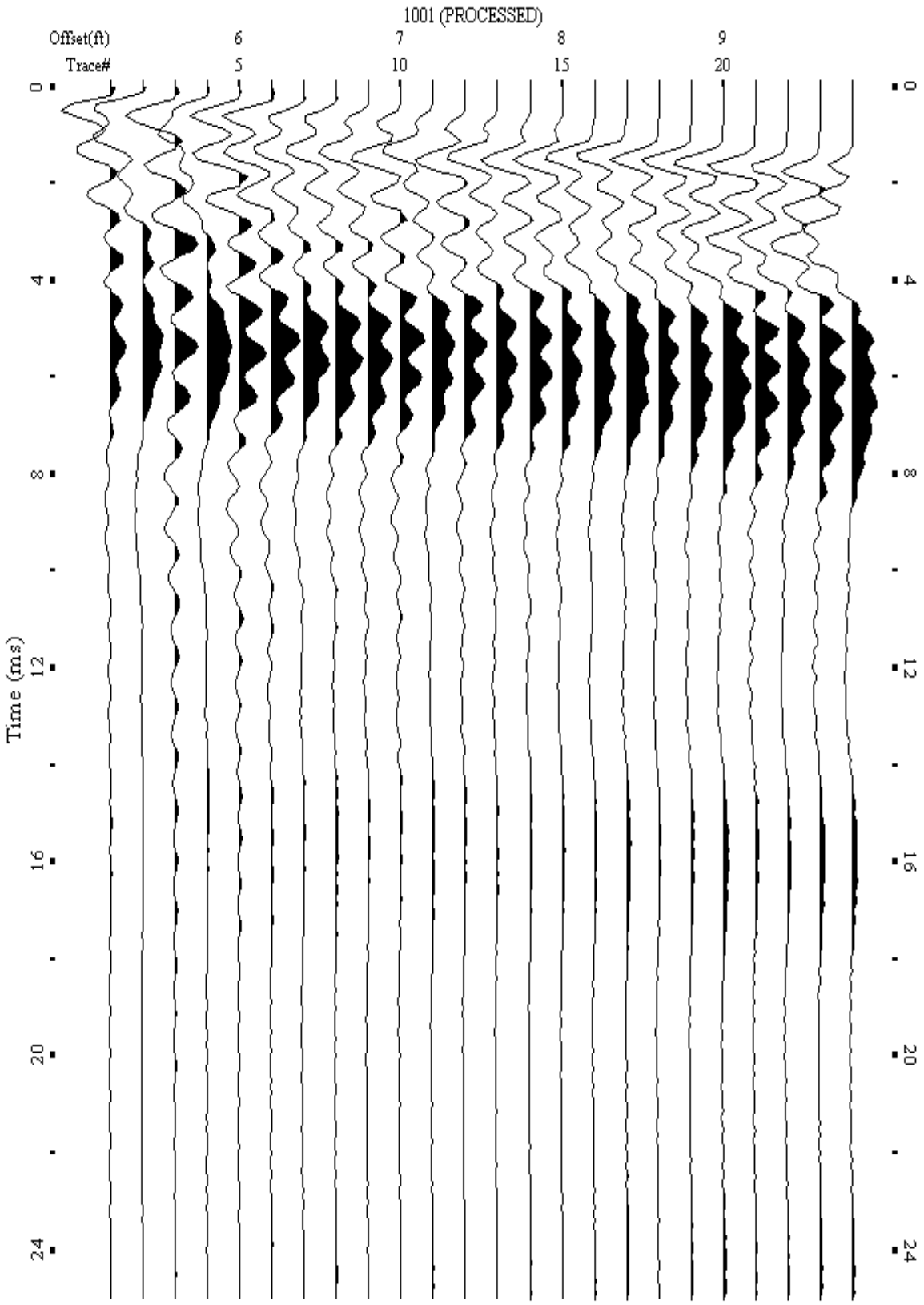

A.307: Shot Gather Line 1221 used in Post-blast 12 and Pre-blast 27

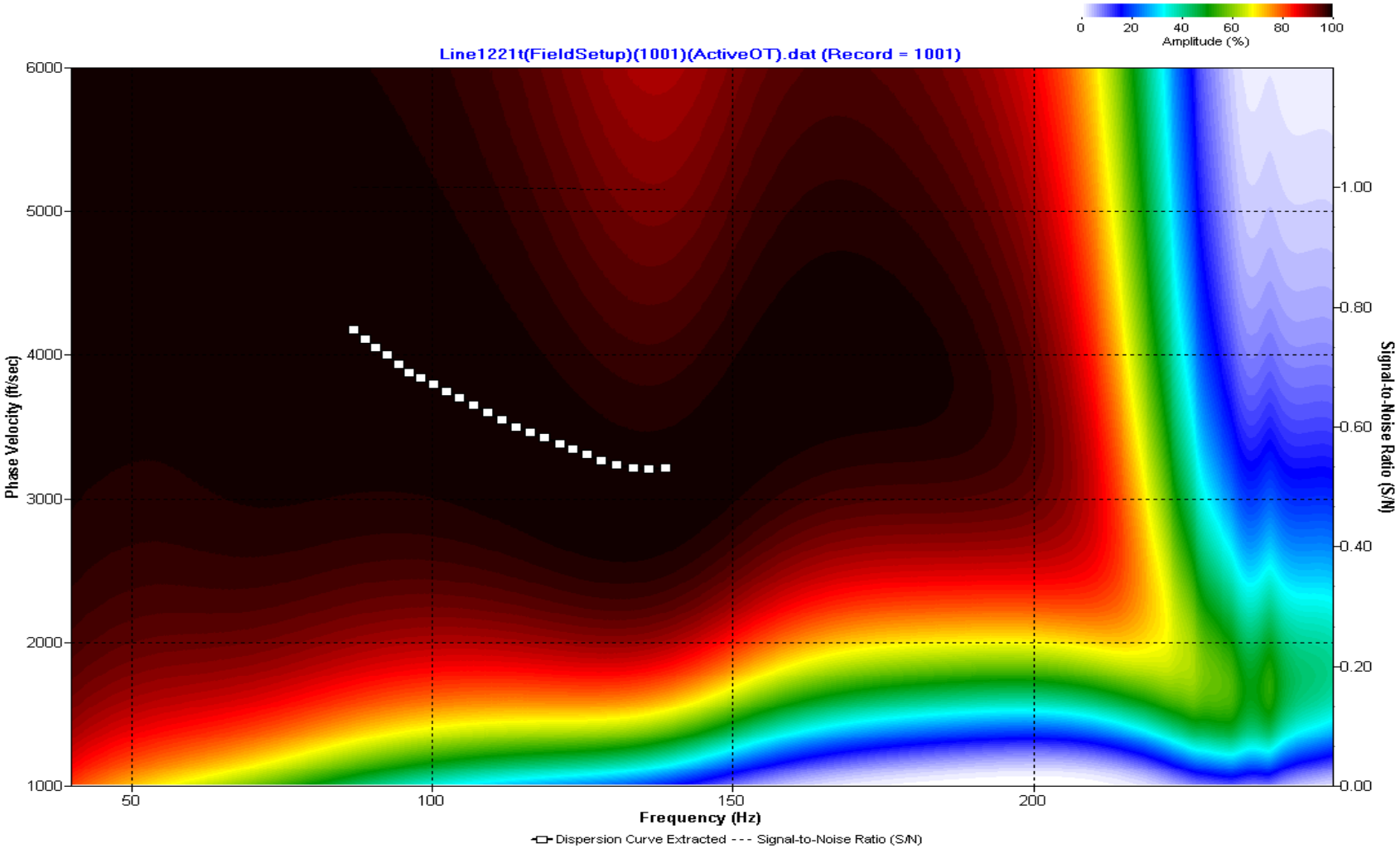

A.308: Dispersion Curve Line 1221 used in Post-blast 12 and Pre-blast 27

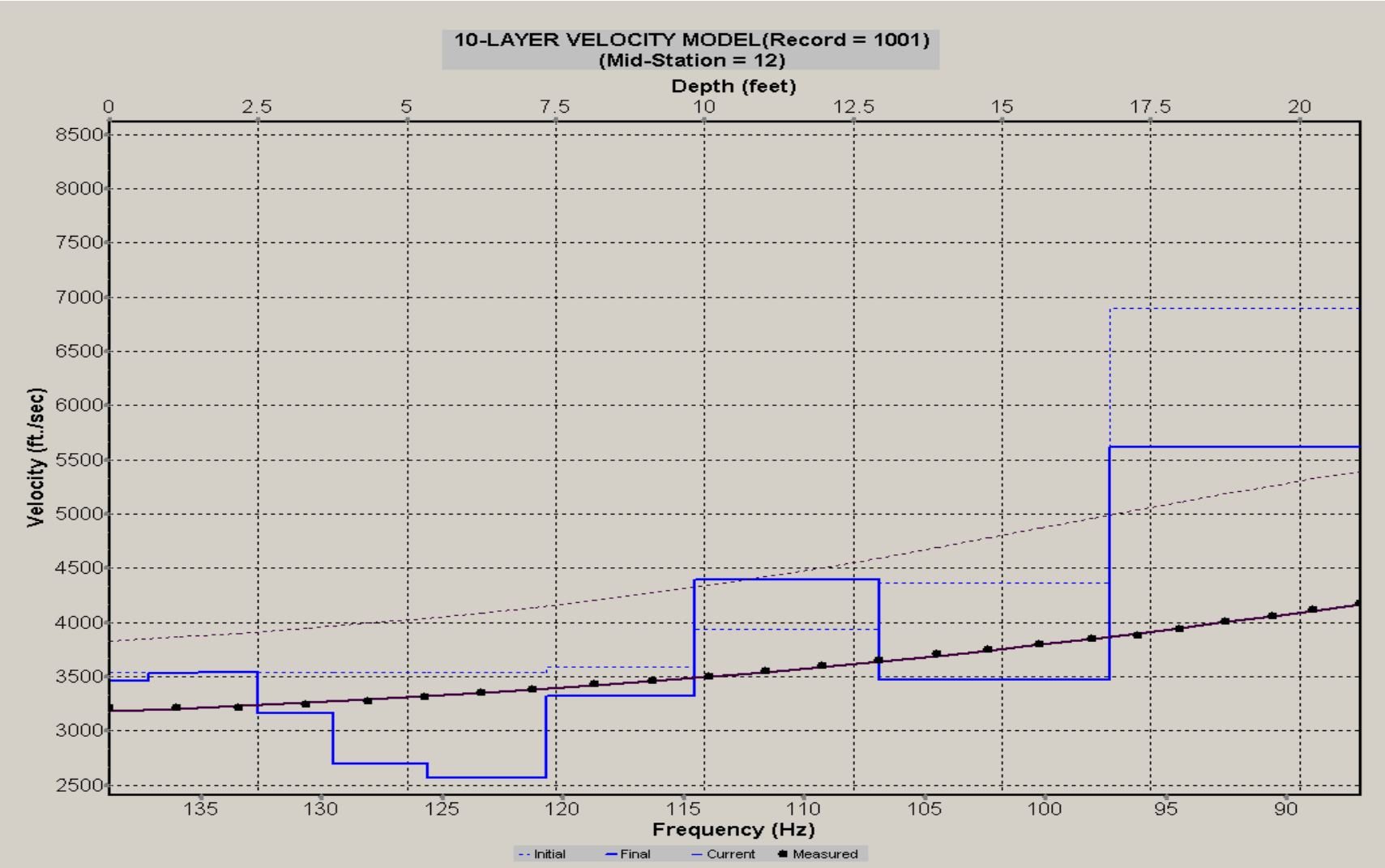

A.309: Velocity Profile Line 1221 used in Post-blast 12 and Pre-blast 27

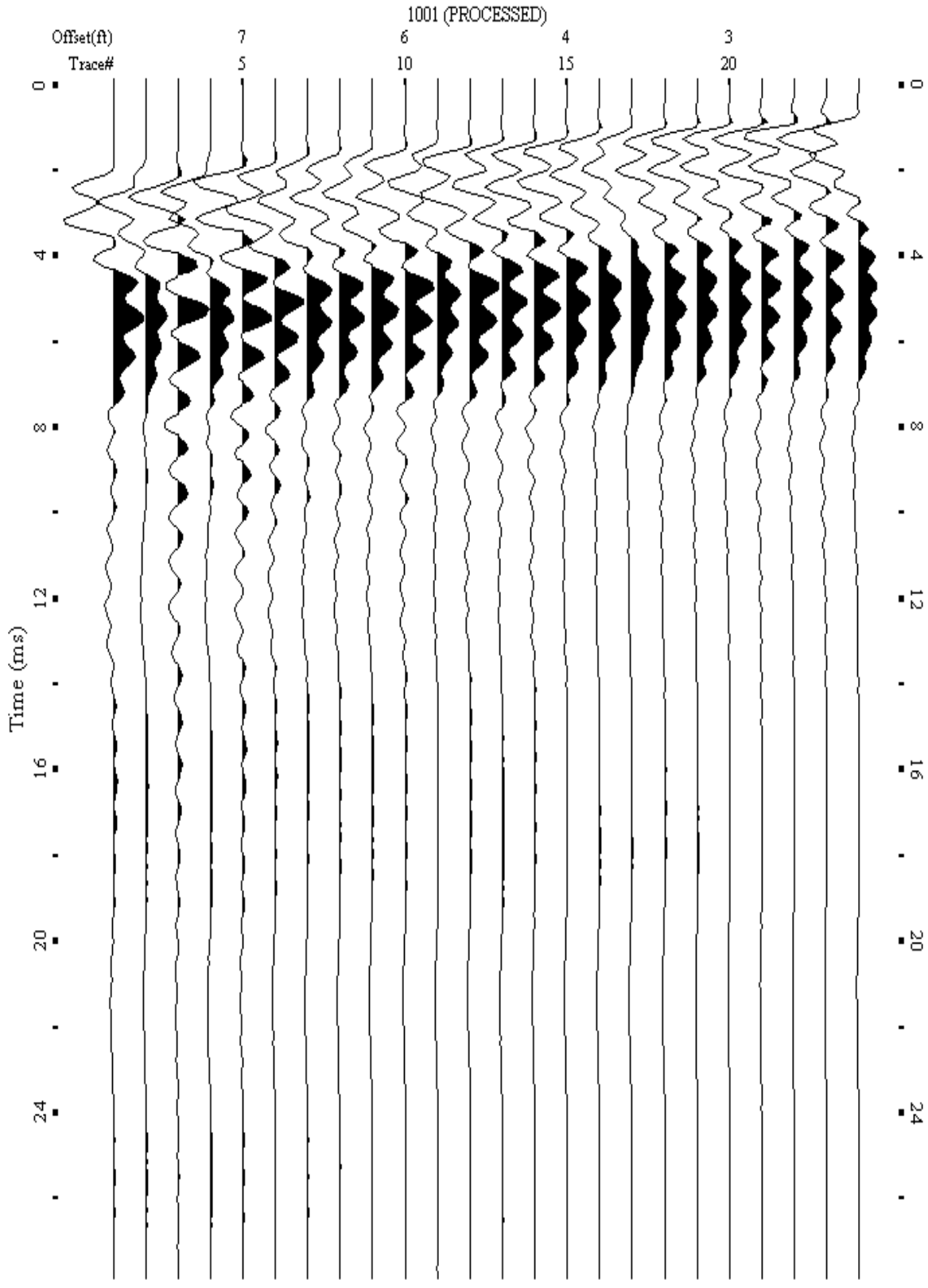

A.310: Shot Gather Line 1222 used in Post-blast 12 and Pre-blast 27

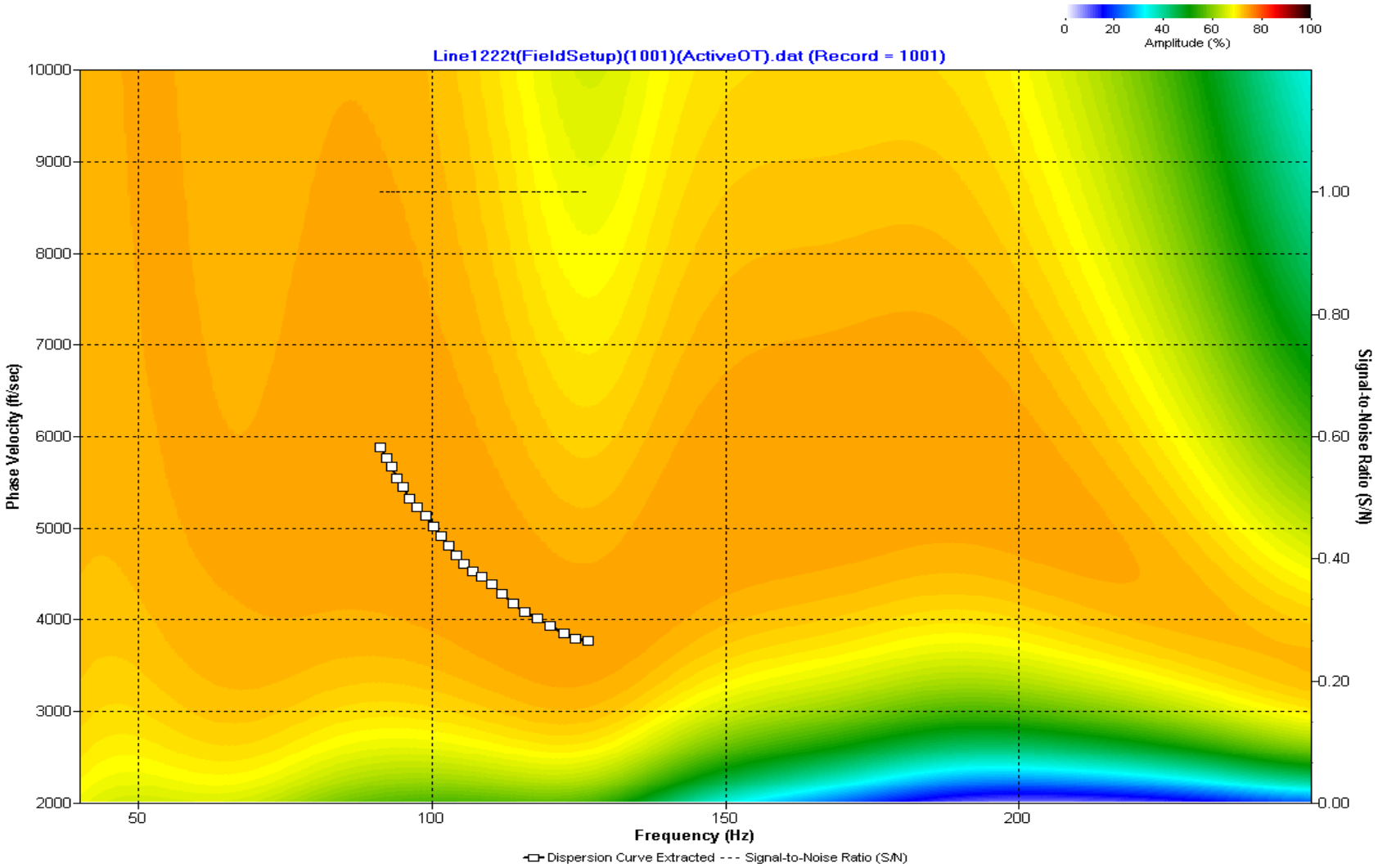

A.311: Dispersion Curve Line 1222 used in Post-blast 12 and Pre-blast 27

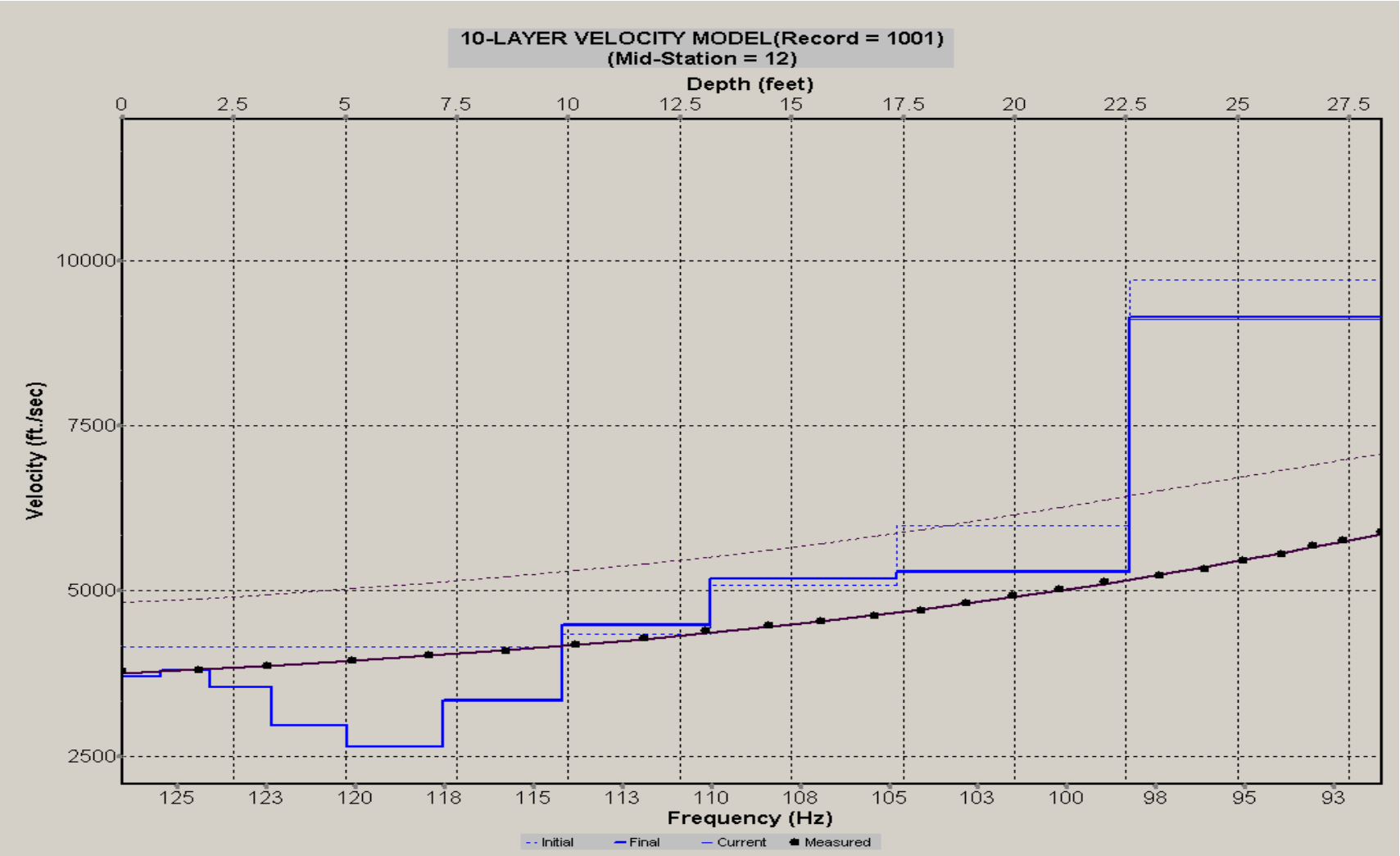

A.312: Velocity Profile Line 1222 used in Post-blast 12 and Pre-blast 27

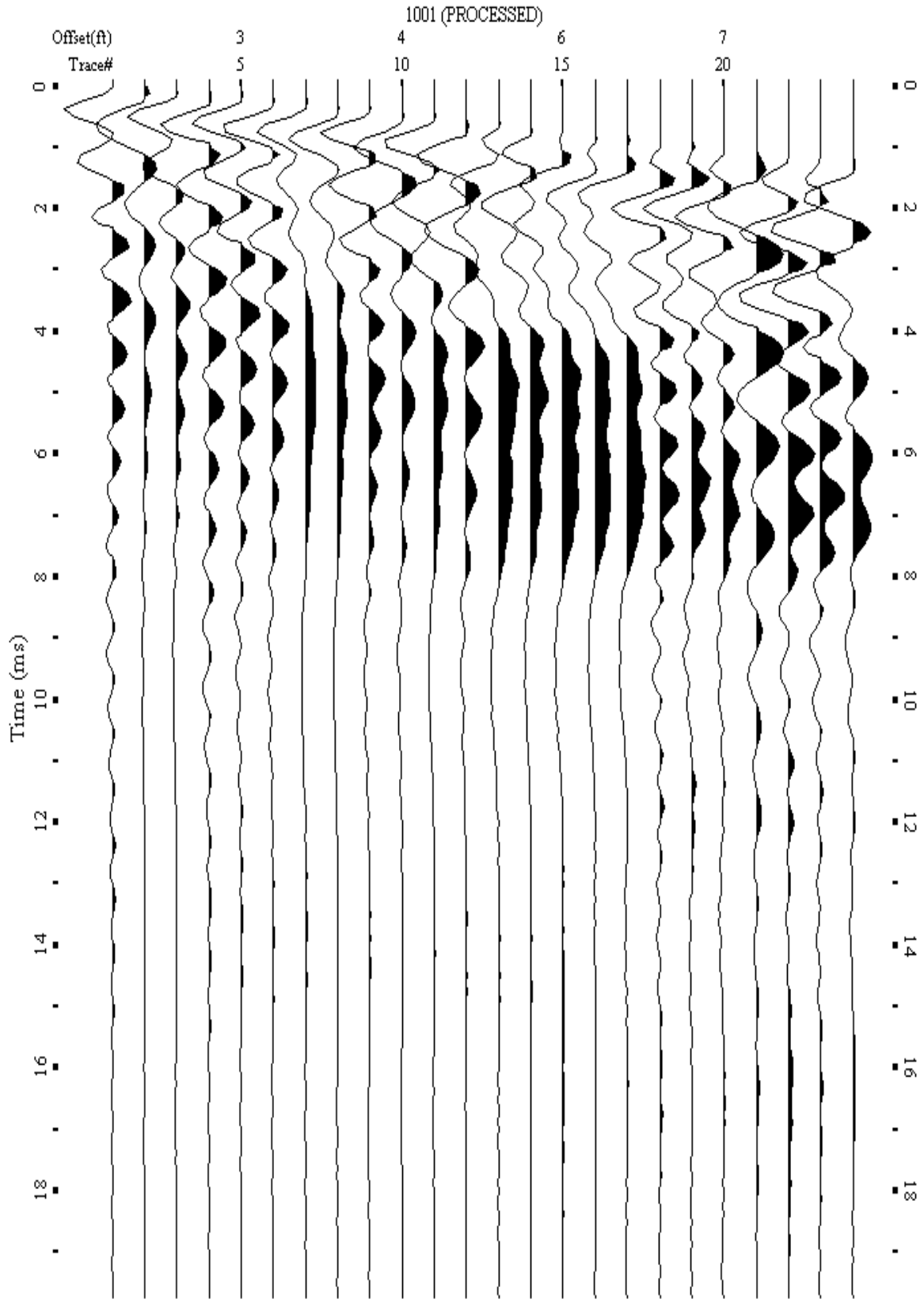

A.313: Shot Gather Line 1224 used in Post-blast 13, Pre-blast 14 and Pre-blast 28

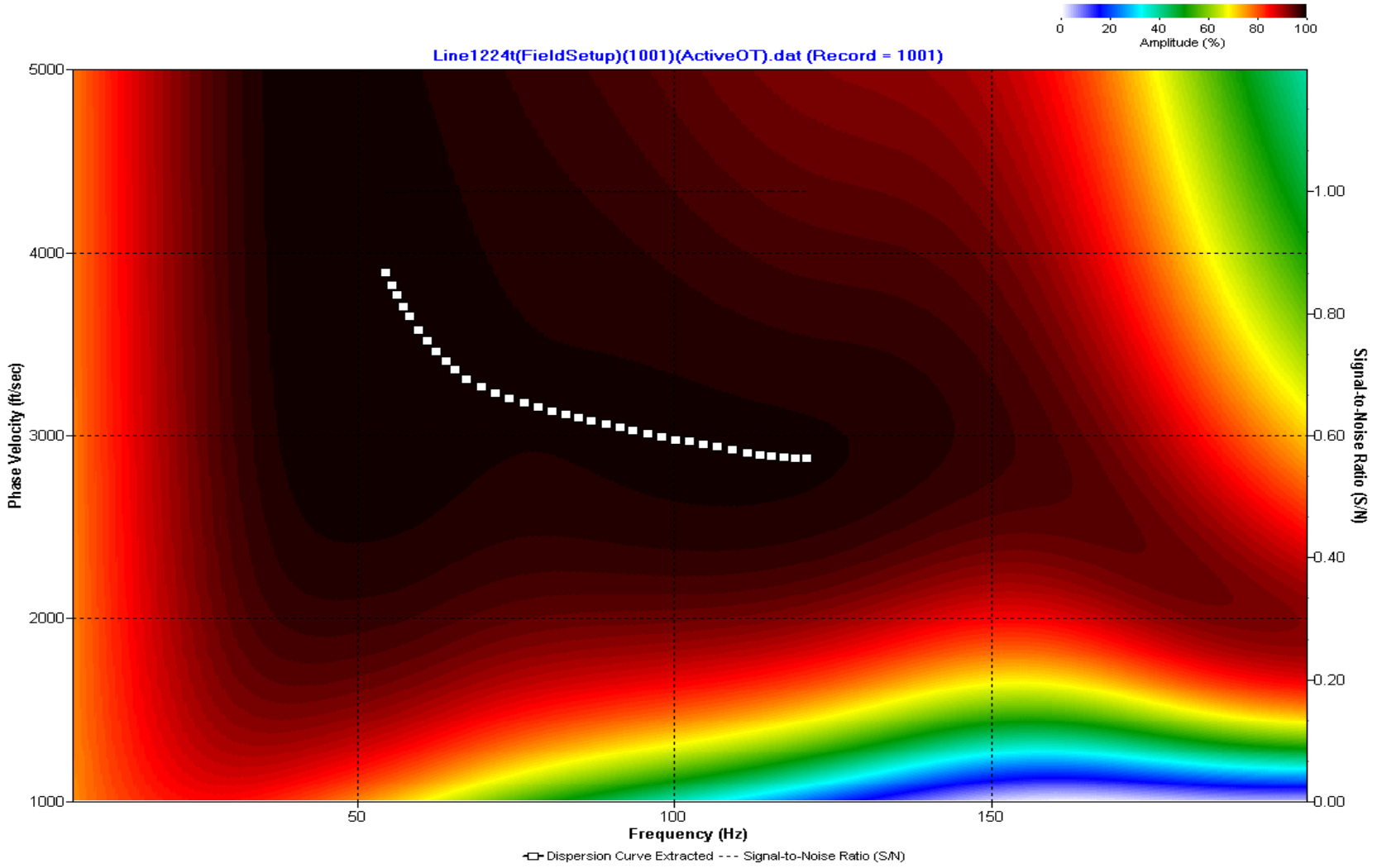

A.314: Dispersion Curve Line 1224 used in Post-blast 13, Pre-blast 14 and Pre-blast 28

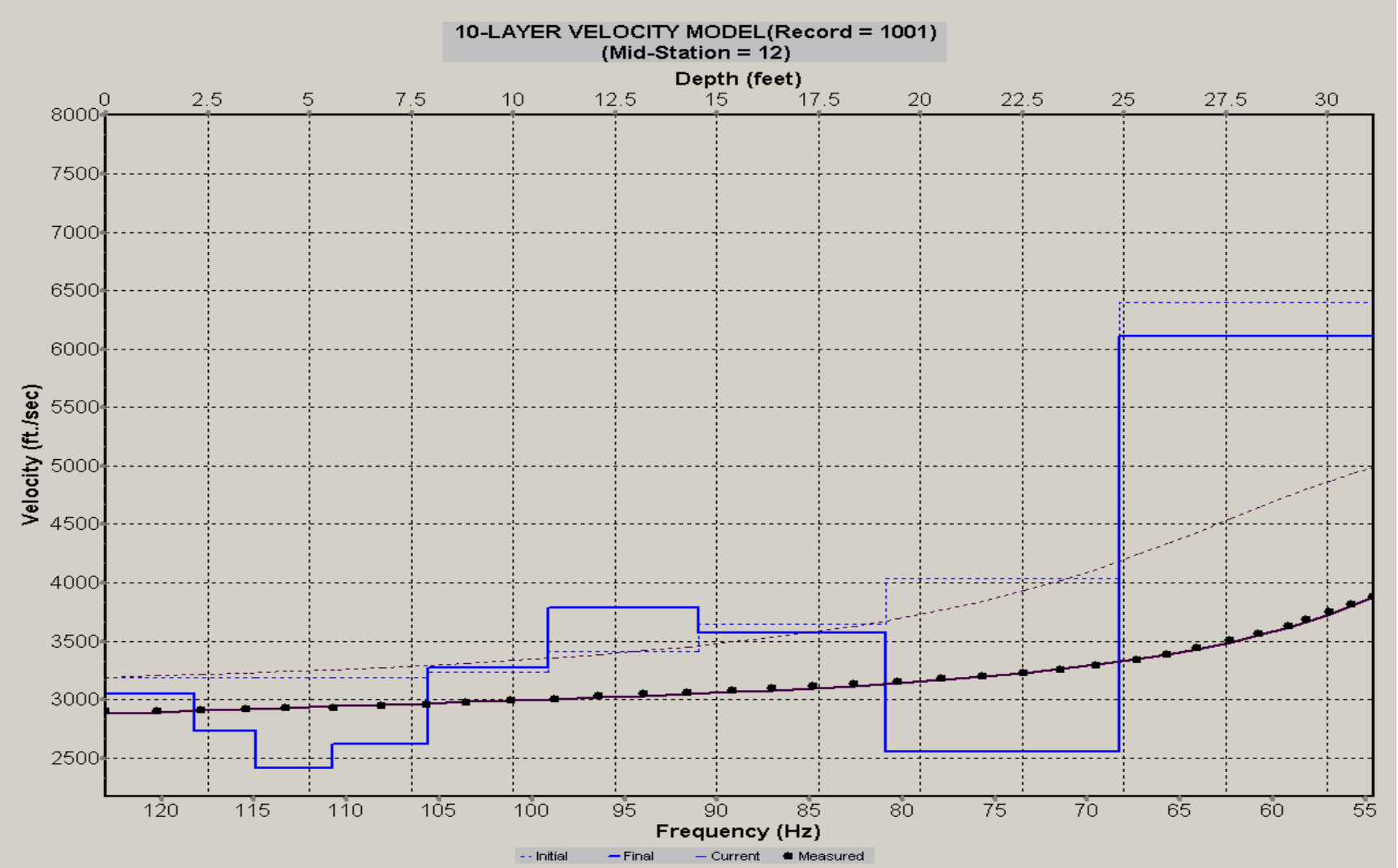

A.315: Velocity Profile Line 1224 used in Post-blast 13, Pre-blast 14 and Pre-blast 28

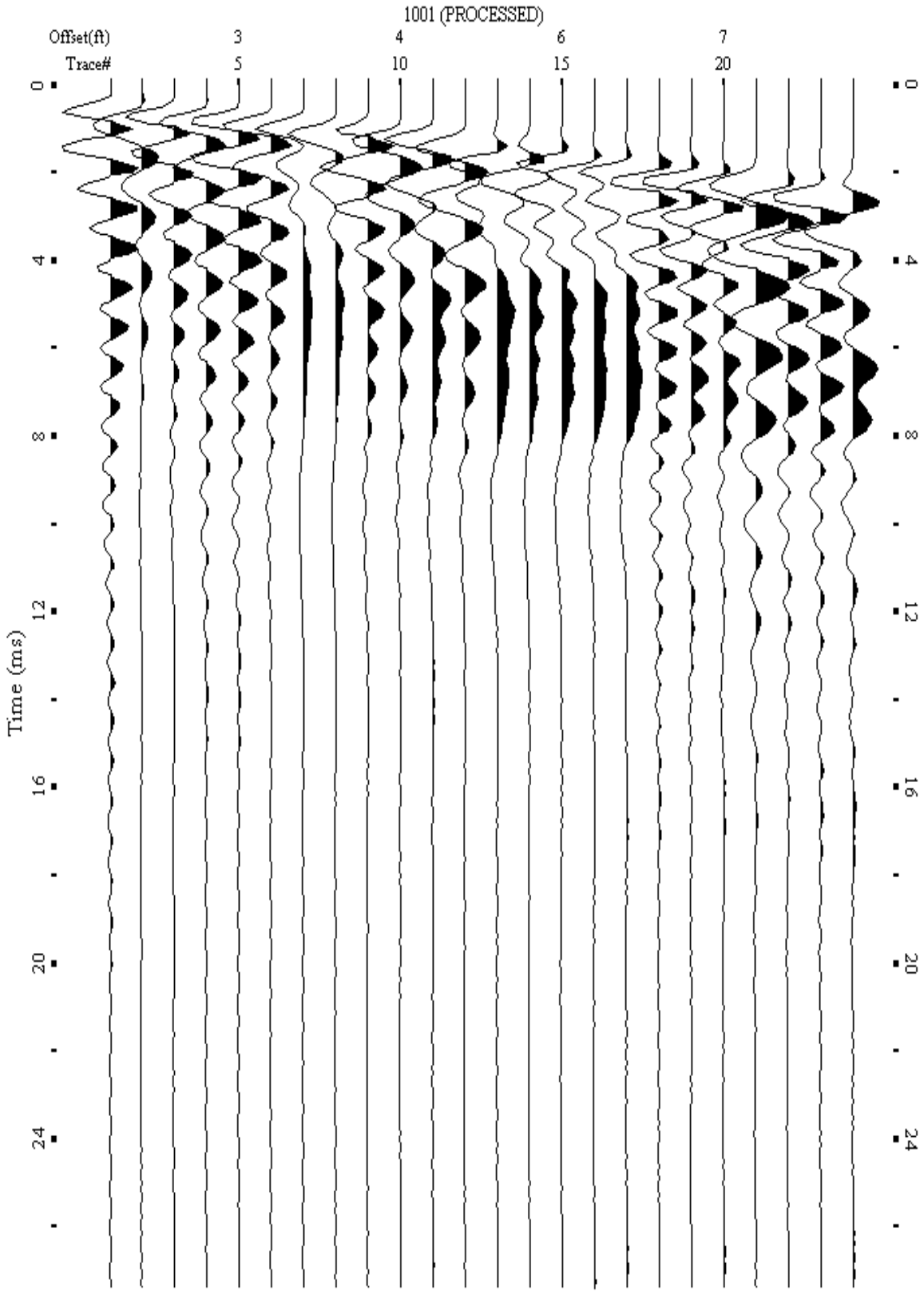

A.316: Shot Gather Line 1225 used in Post-blast 13, Pre-blast 14 and Pre-blast 28

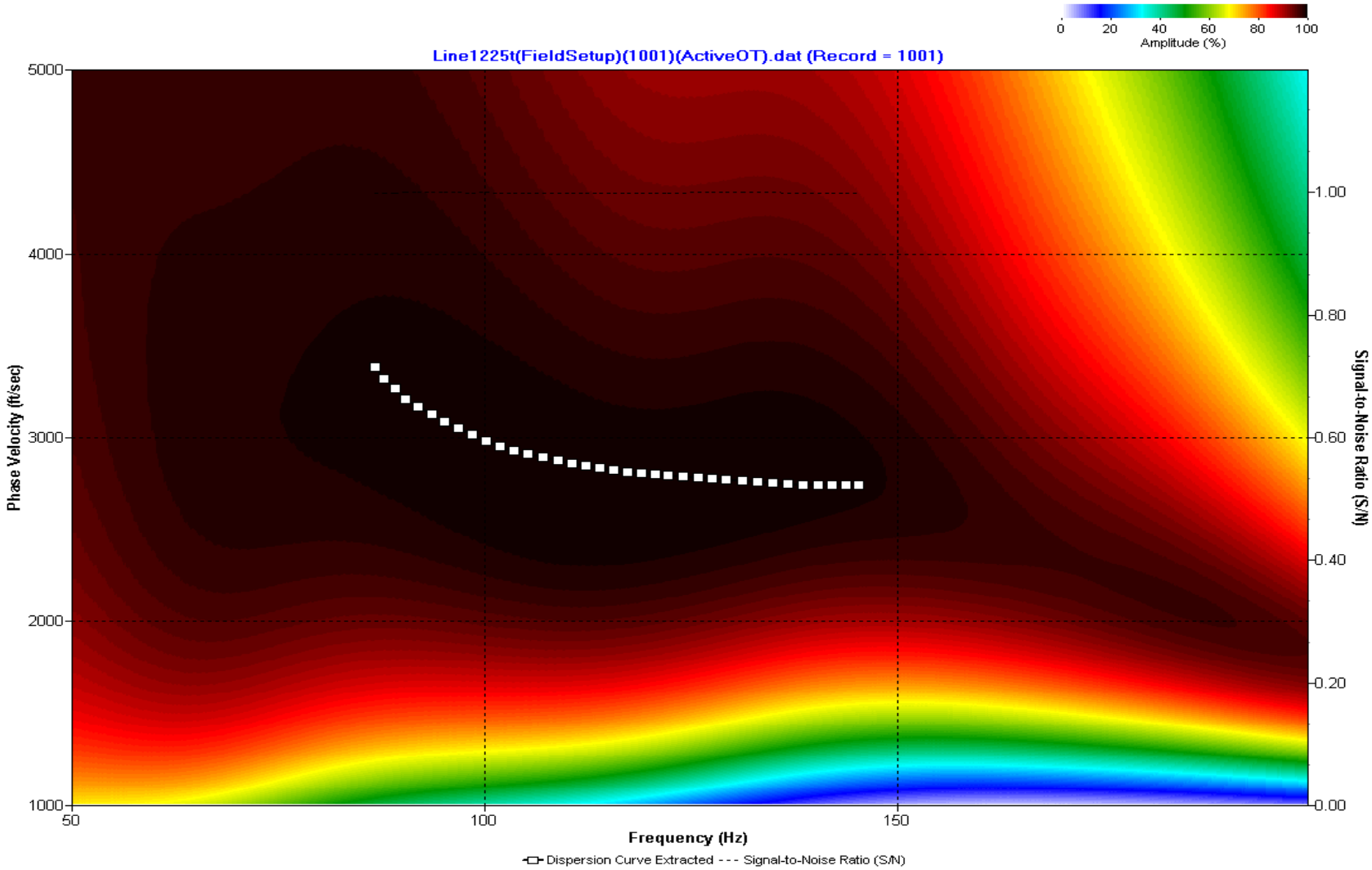

A.317: Dispersion Curve Line 1225 used in Post-blast 13, Pre-blast 14 and Pre-blast 28

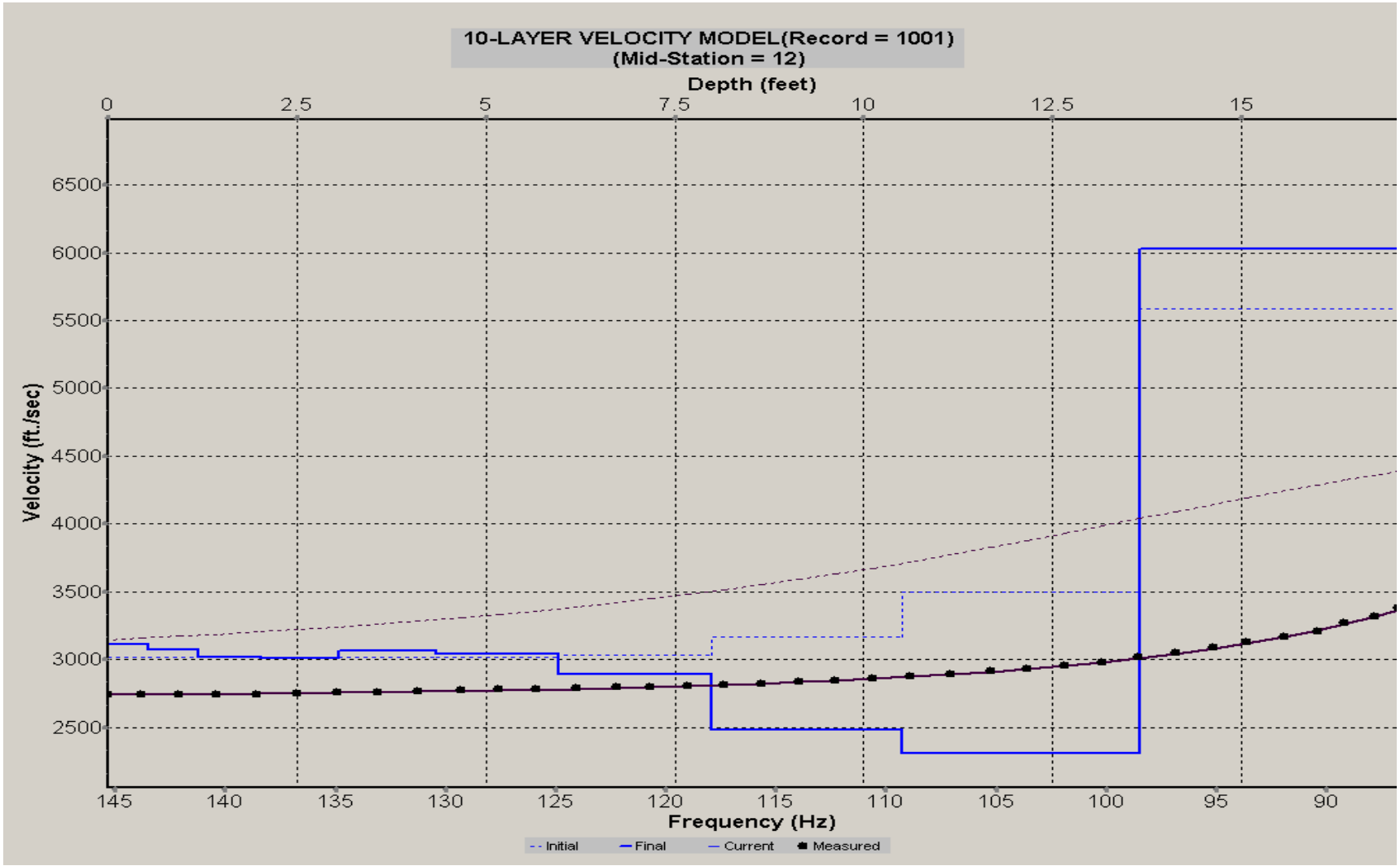

A.318: Velocity Profile Line 1225 used in Post-blast 13, Pre-blast 14 and Pre-blast 28

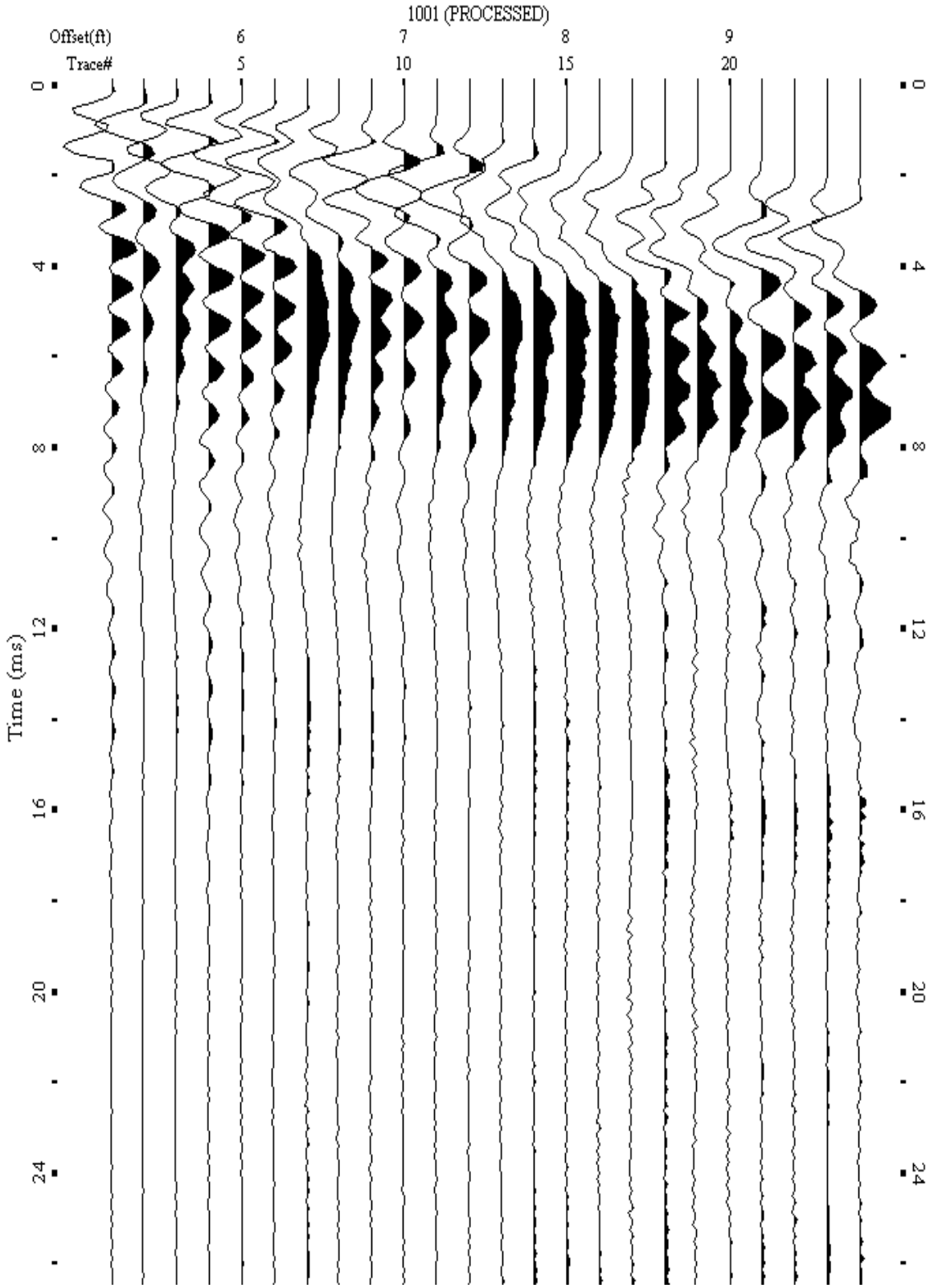

A.319: Shot Gather Line 1227 used in Post-blast 13, Pre-blast 14 and Pre-blast 28

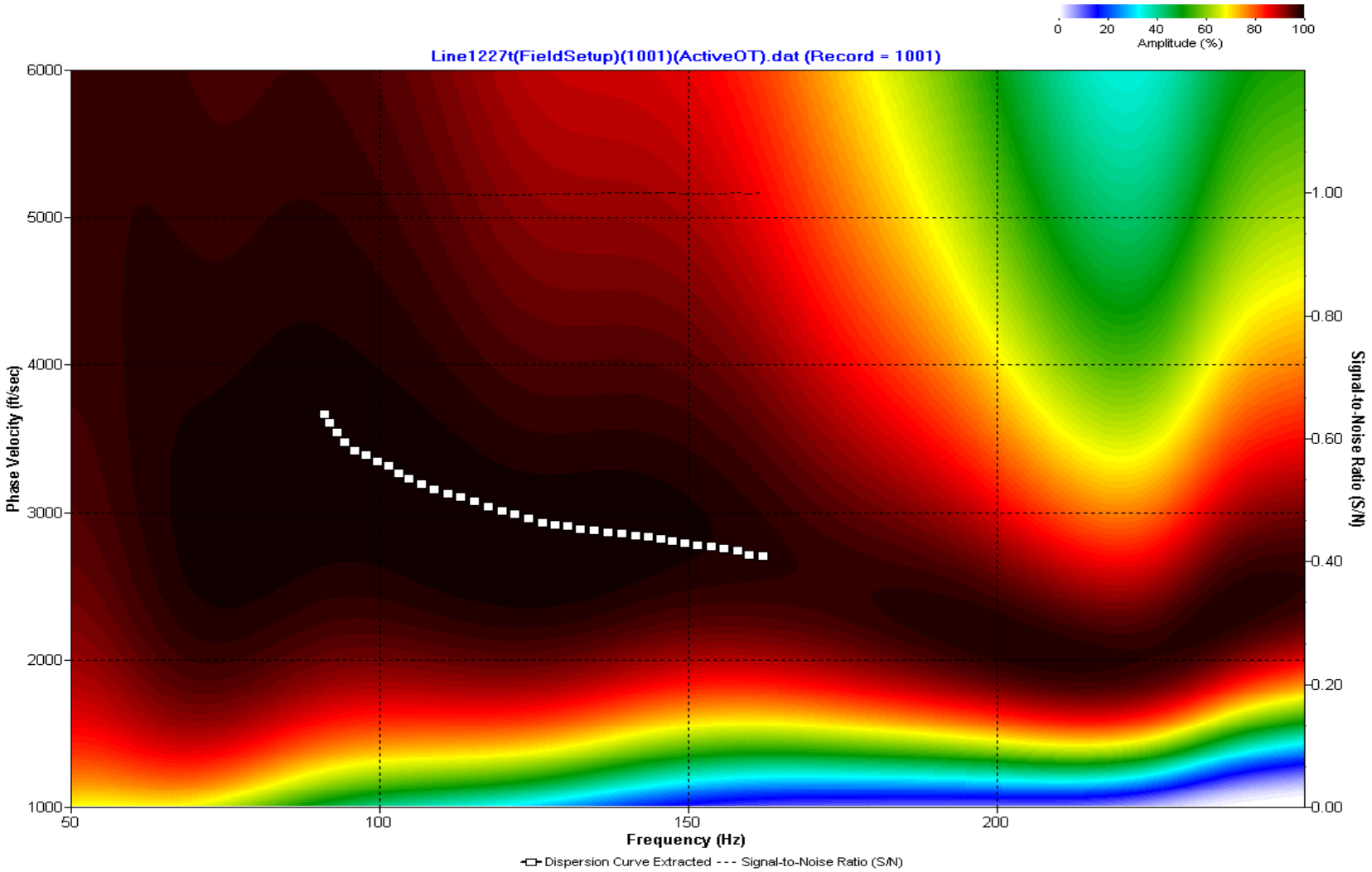

A.320: Dispersion Curve Line 1227 used in Post-blast 13, Pre-blast 14 and Pre-blast 28

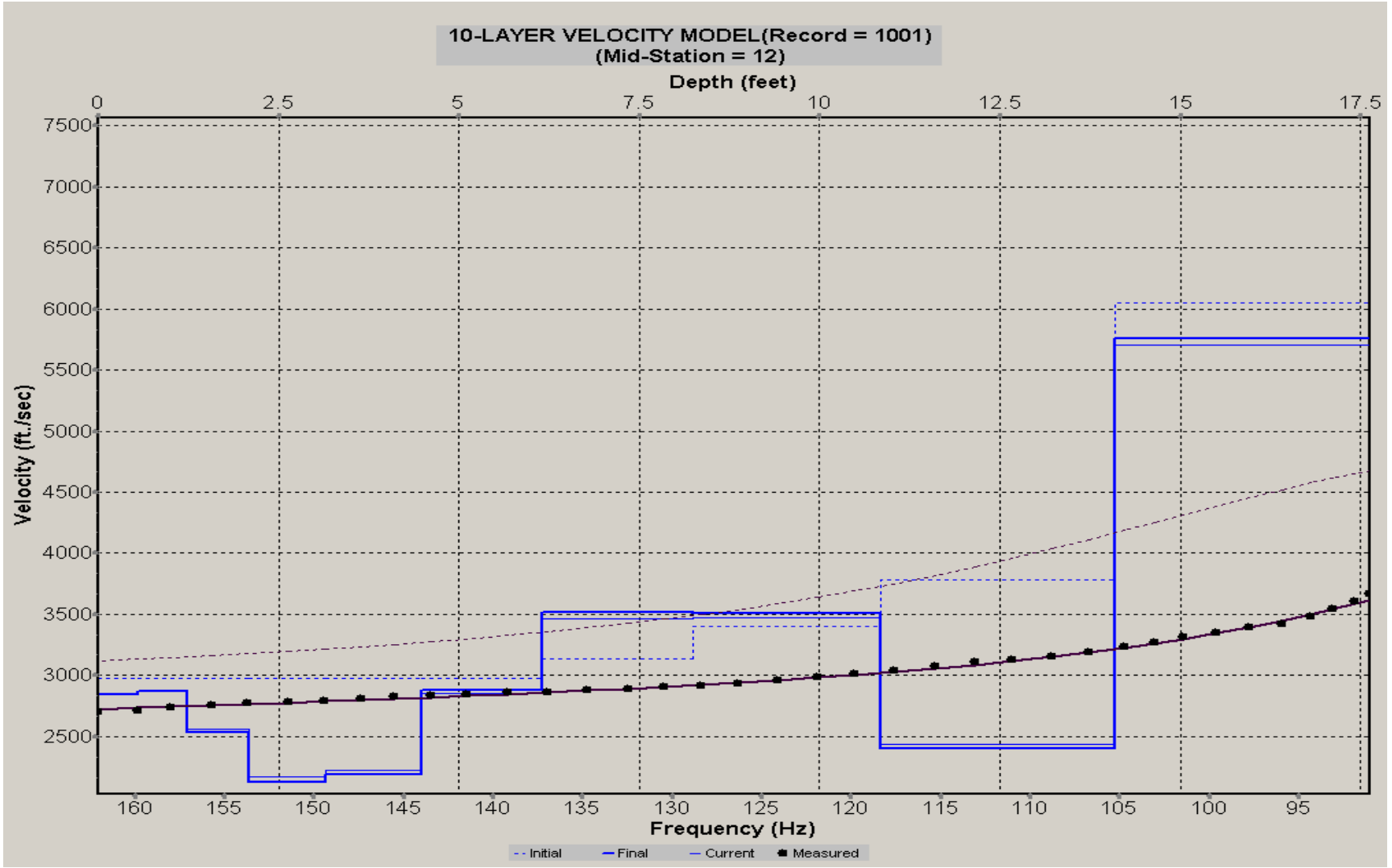

A.321: Velocity Profile Line 1227 used in Post-blast 13, Pre-blast 14 and Pre-blast 28

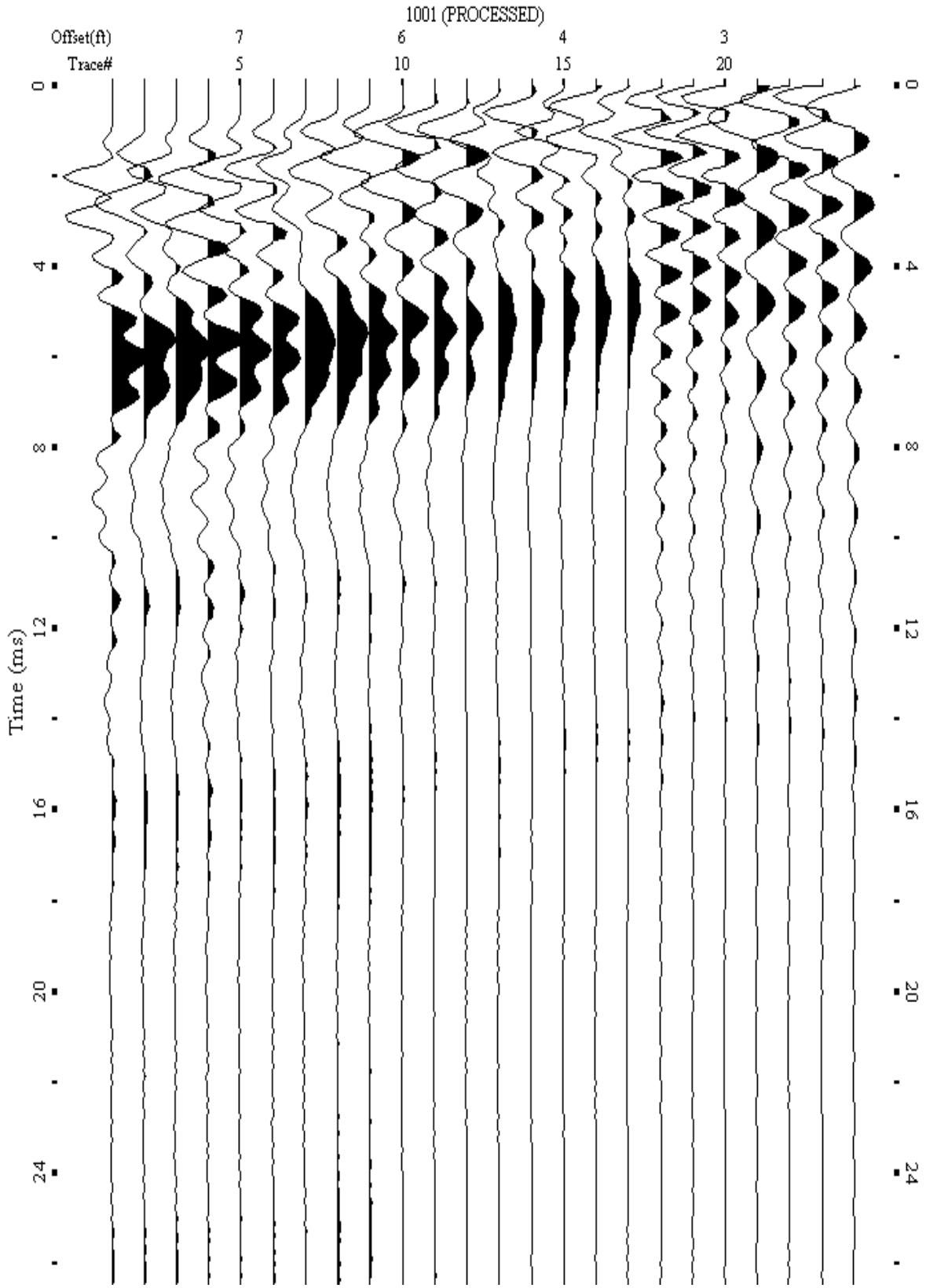

A.322: Shot Gather Line 1228 used in Post-blast 13, Pre-blast 14 and Pre-blast 28

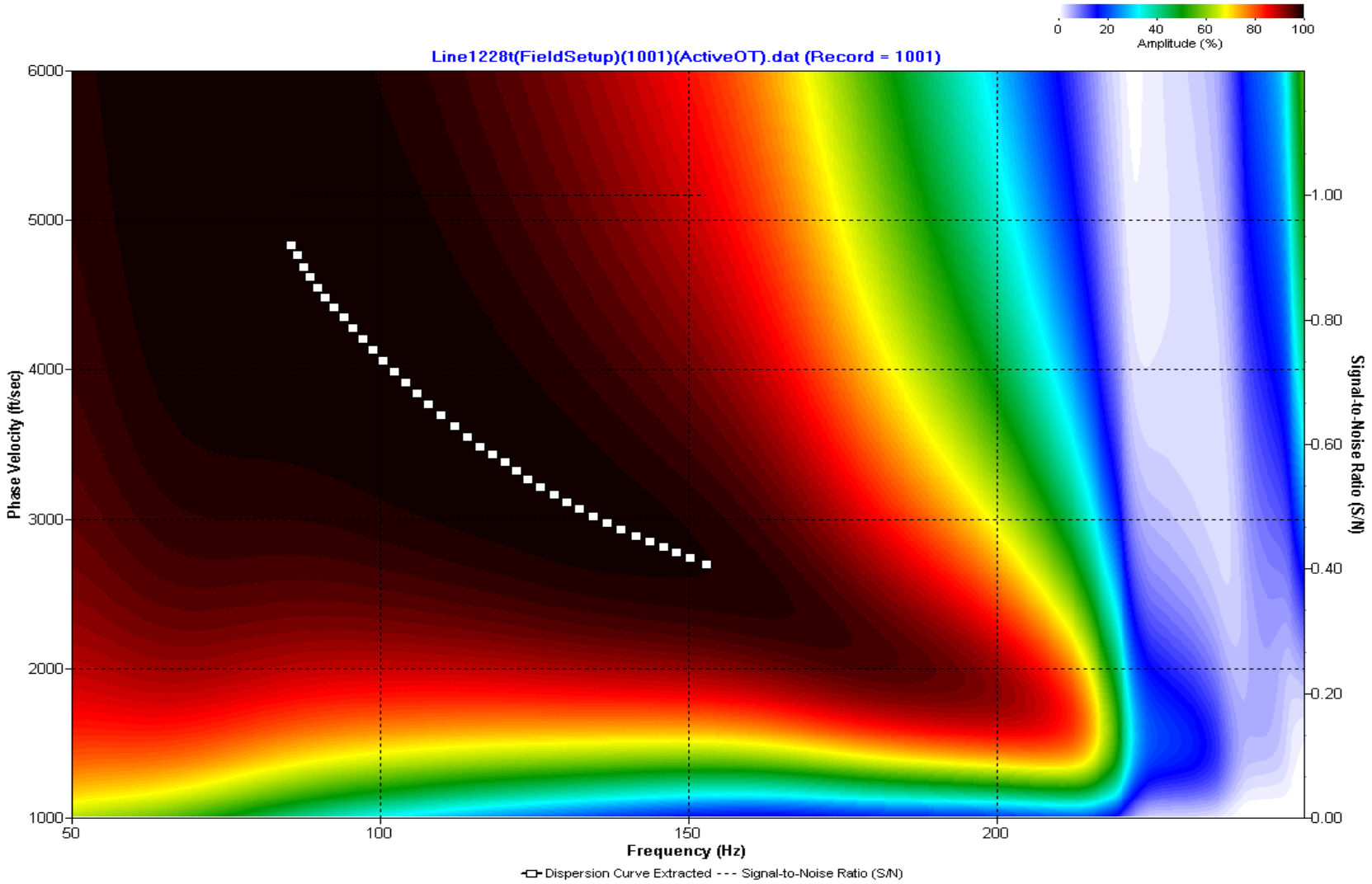

A.323: Dispersion Curve Line 1228 used in Post-blast 13, Pre-blast 14 and Pre-blast 28

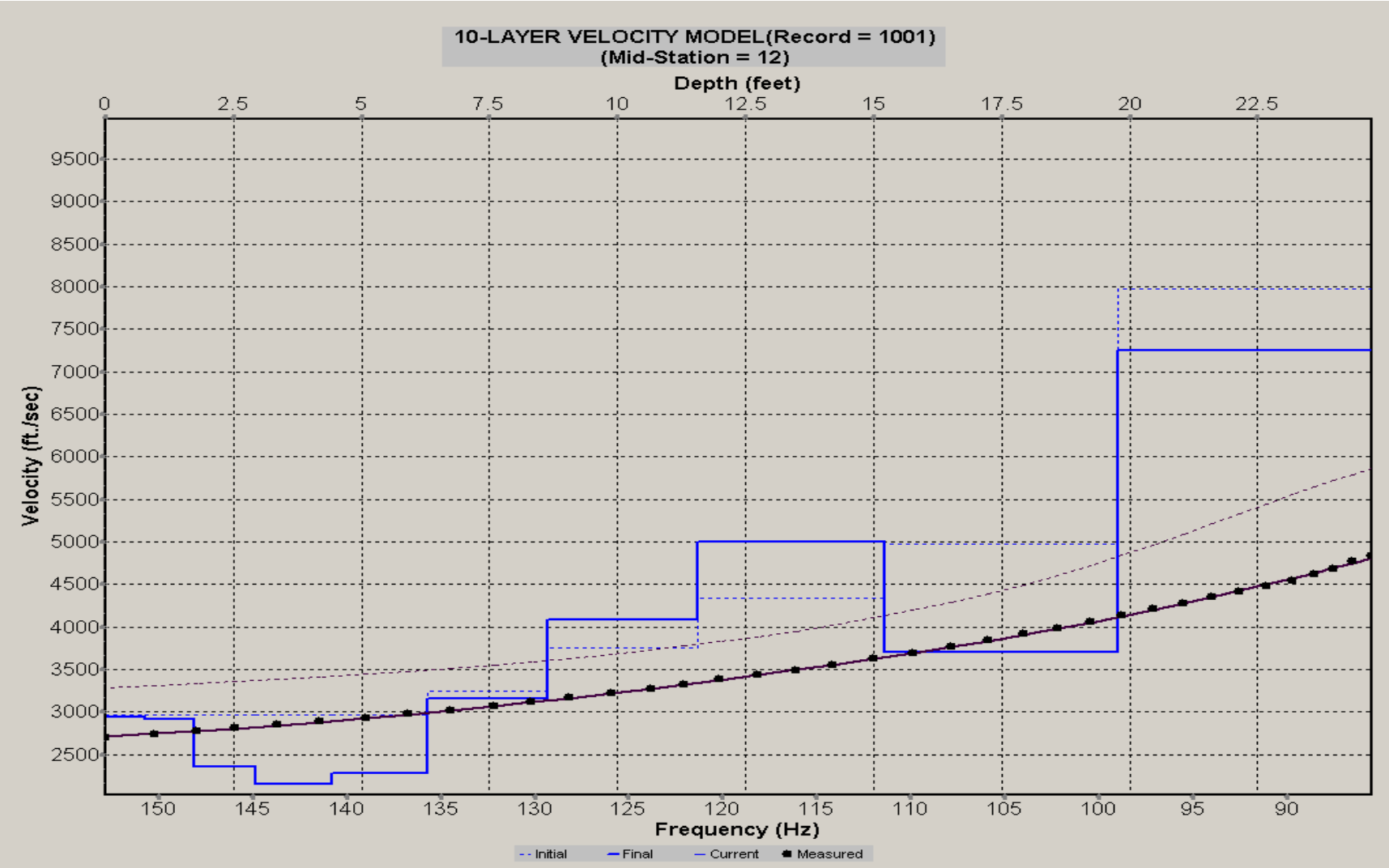

A.324: Velocity Profile Line 1228 used in Post-blast 13, Pre-blast 14 and Pre-blast 28

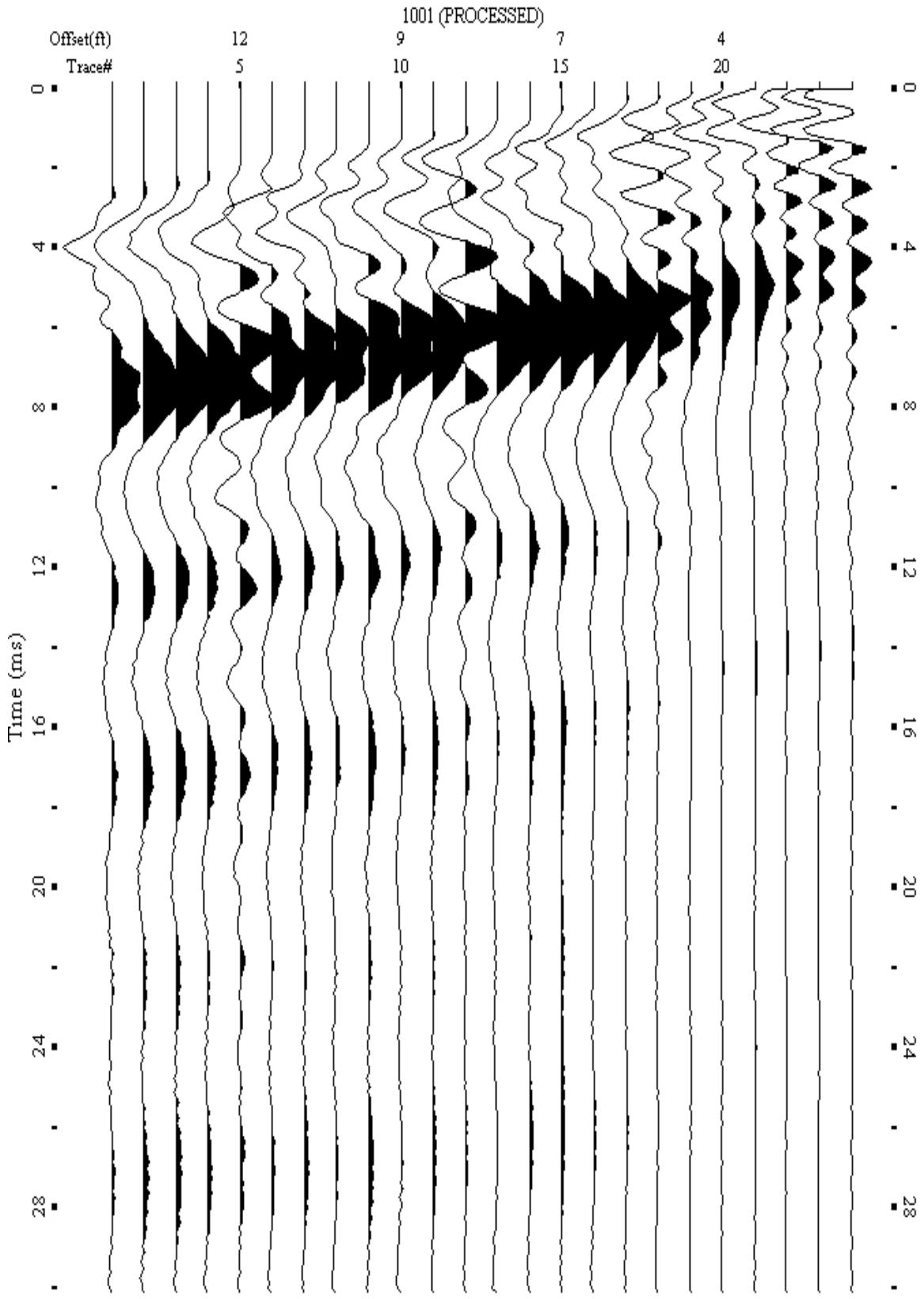

A.325: Shot Gather Line 1237 used in Post-blast 13, Post-blast 14 and Pre-blast 29

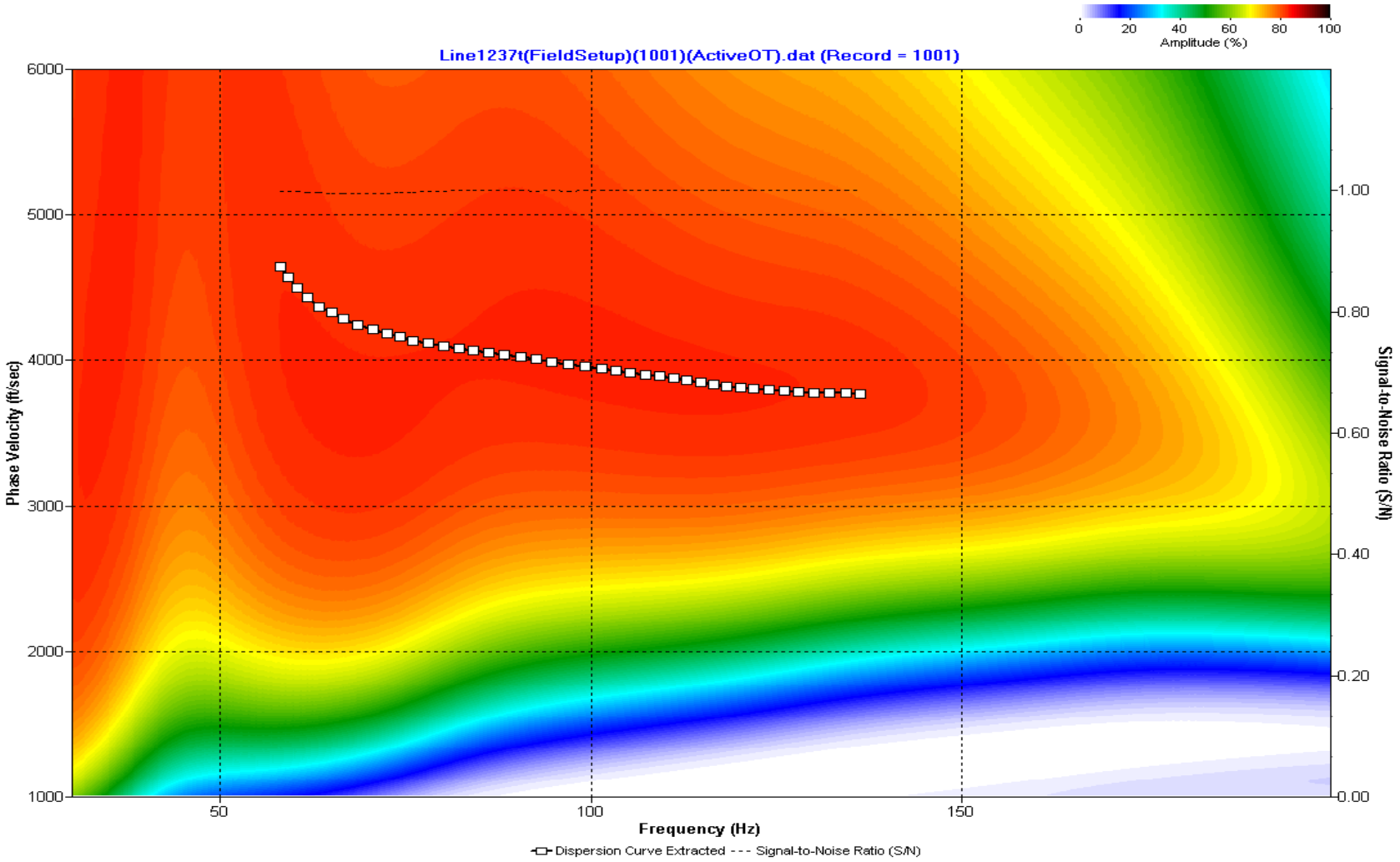

A.326: Dispersion Curve Line 1237 used in Post-blast 13, Post-blast 14 and Pre-blast 29

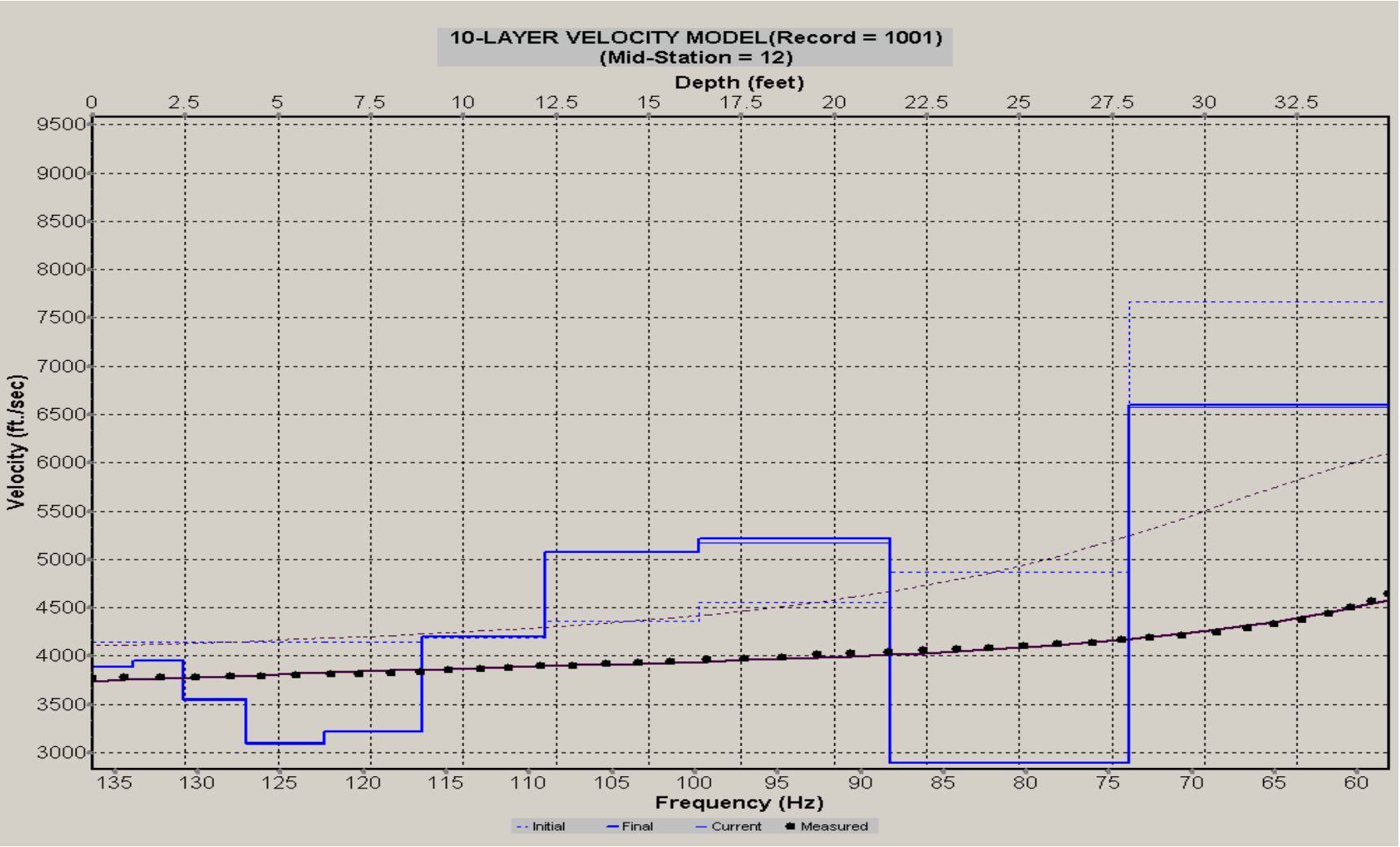

A.327: Velocity Profile Line 1237 used in Post-blast 13, Post-blast 14 and Pre-blast 29

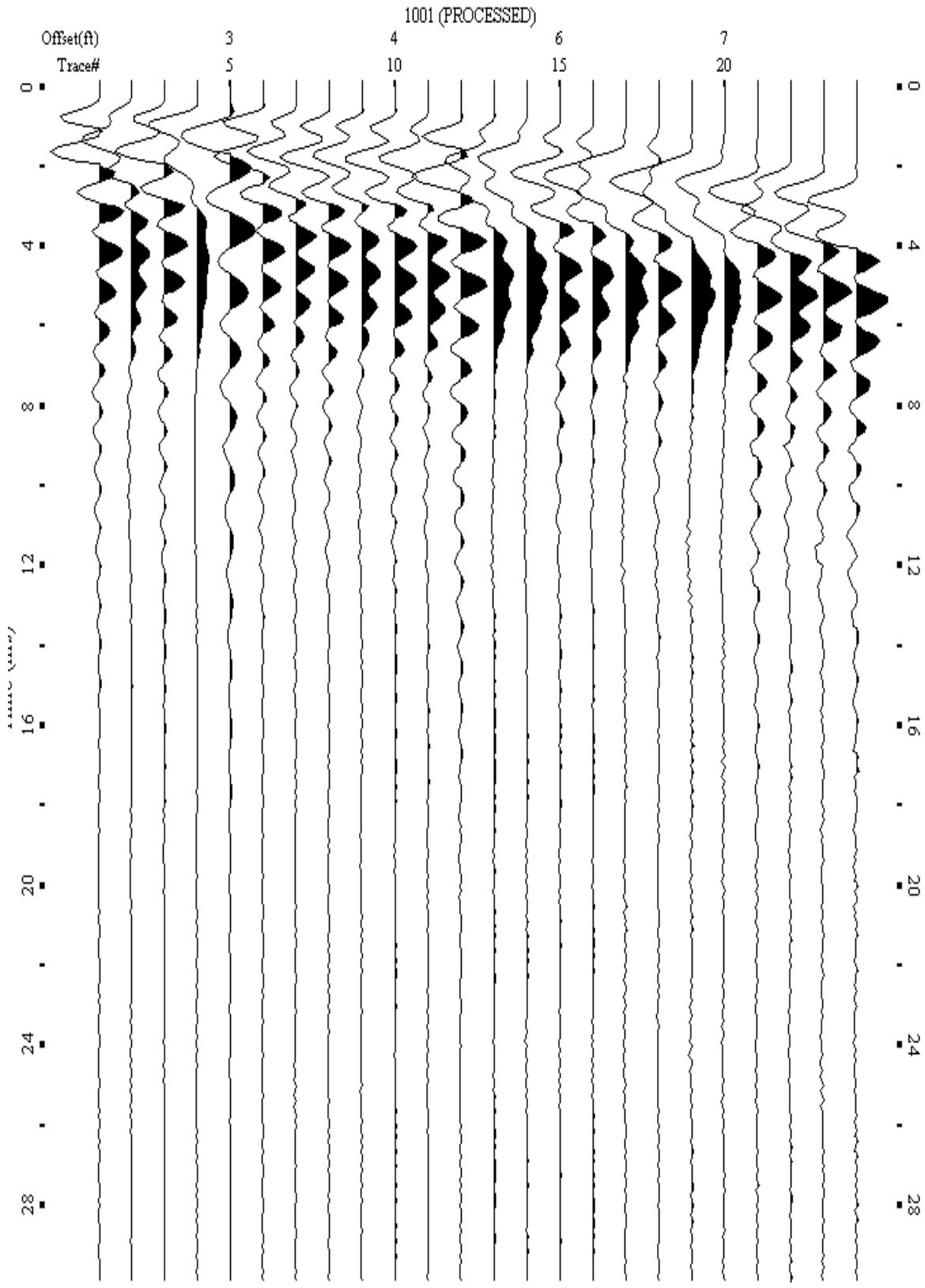

A.328: Shot Gather Line 1240 used in Post-blast 14

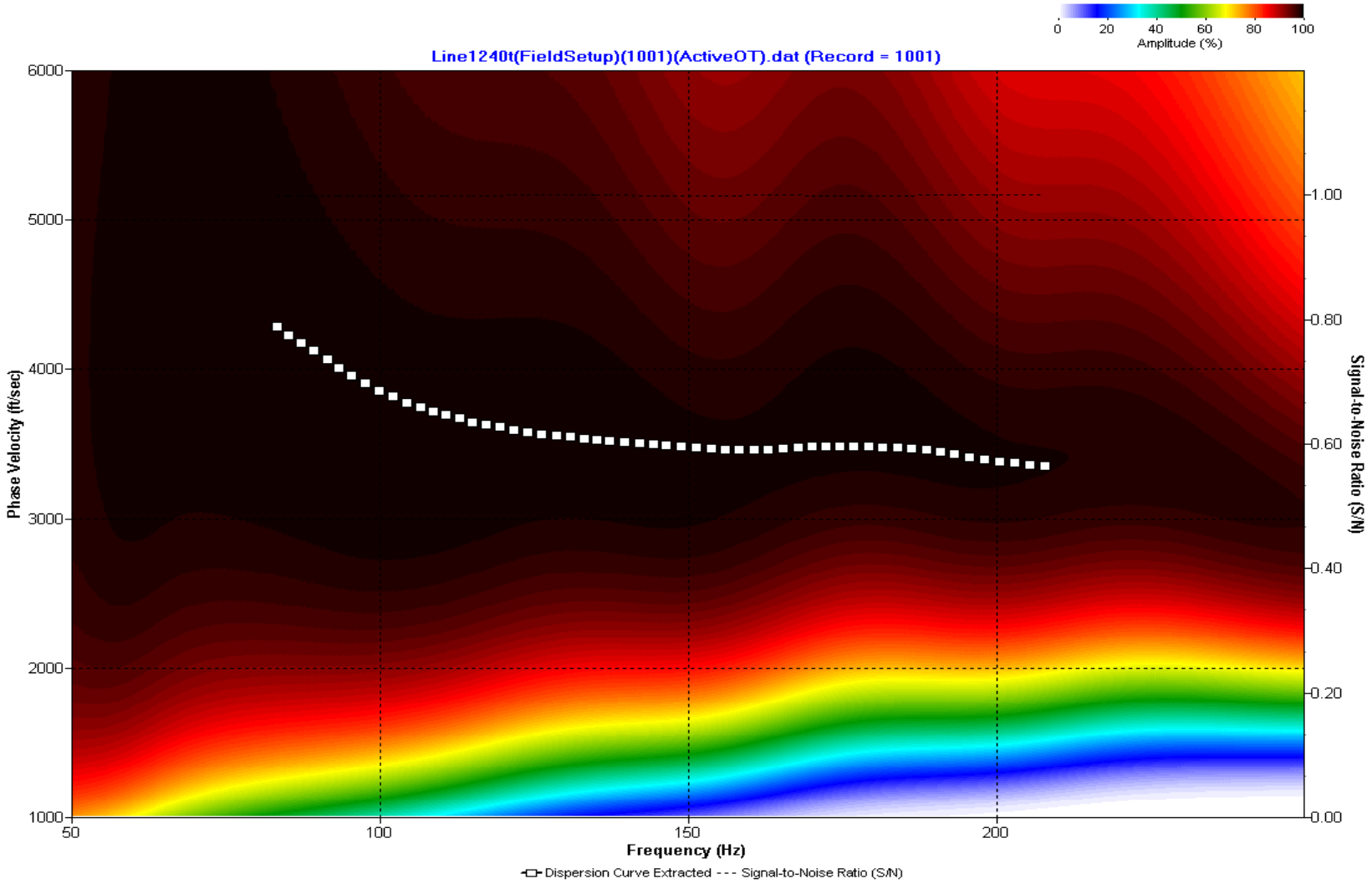

A.329: Dispersion Curve Line 1240 used in Post-blast 14

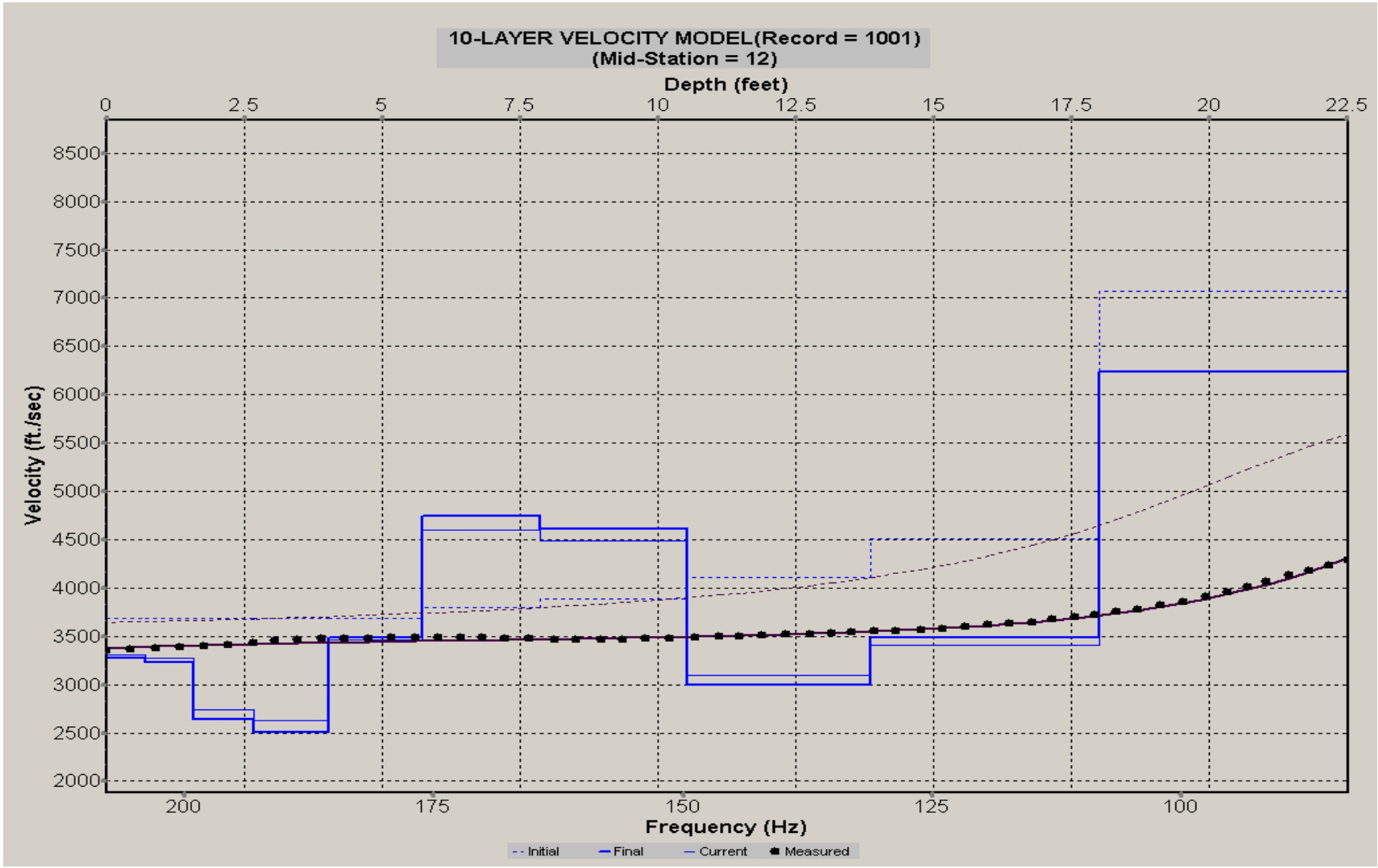

A.330: Velocity Profile Line 1240 used in Post-blast 14

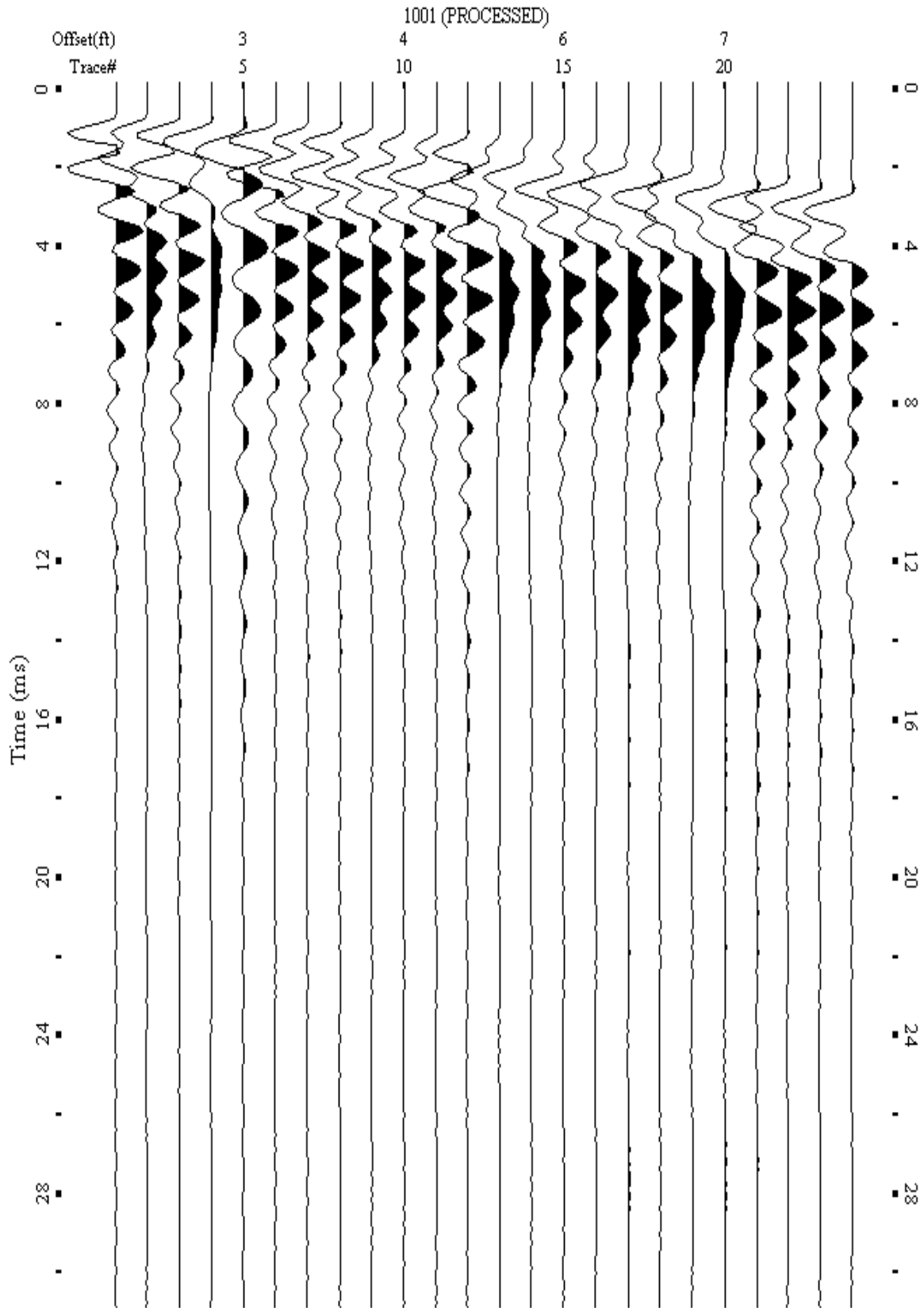

A.331: Shot Gather Line 1241 used in Post-blast 14 and Pre-blast 29

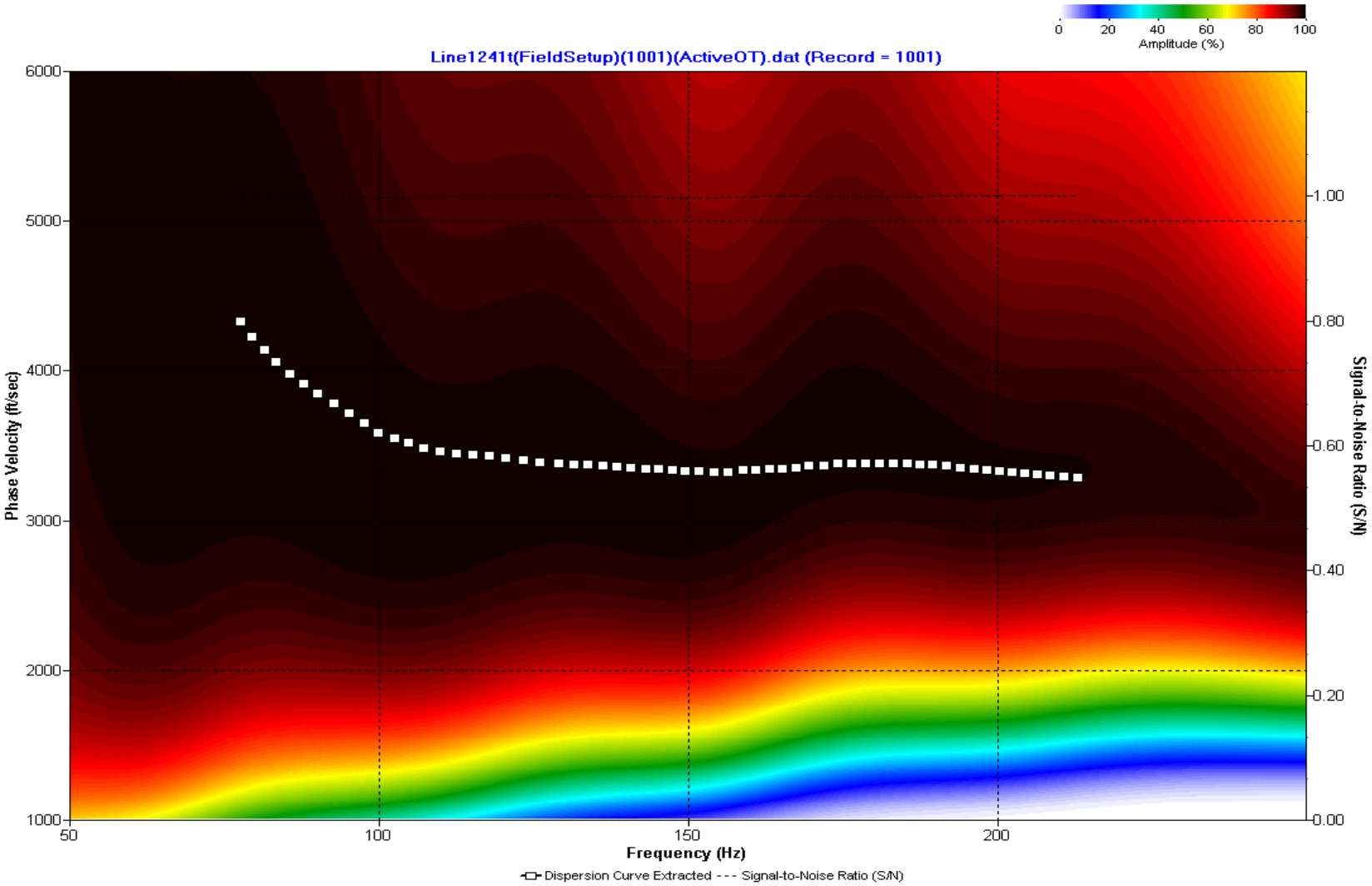

A.332: Dispersion Curve Line 1241 used in Post-blast 14 and Pre-blast 29

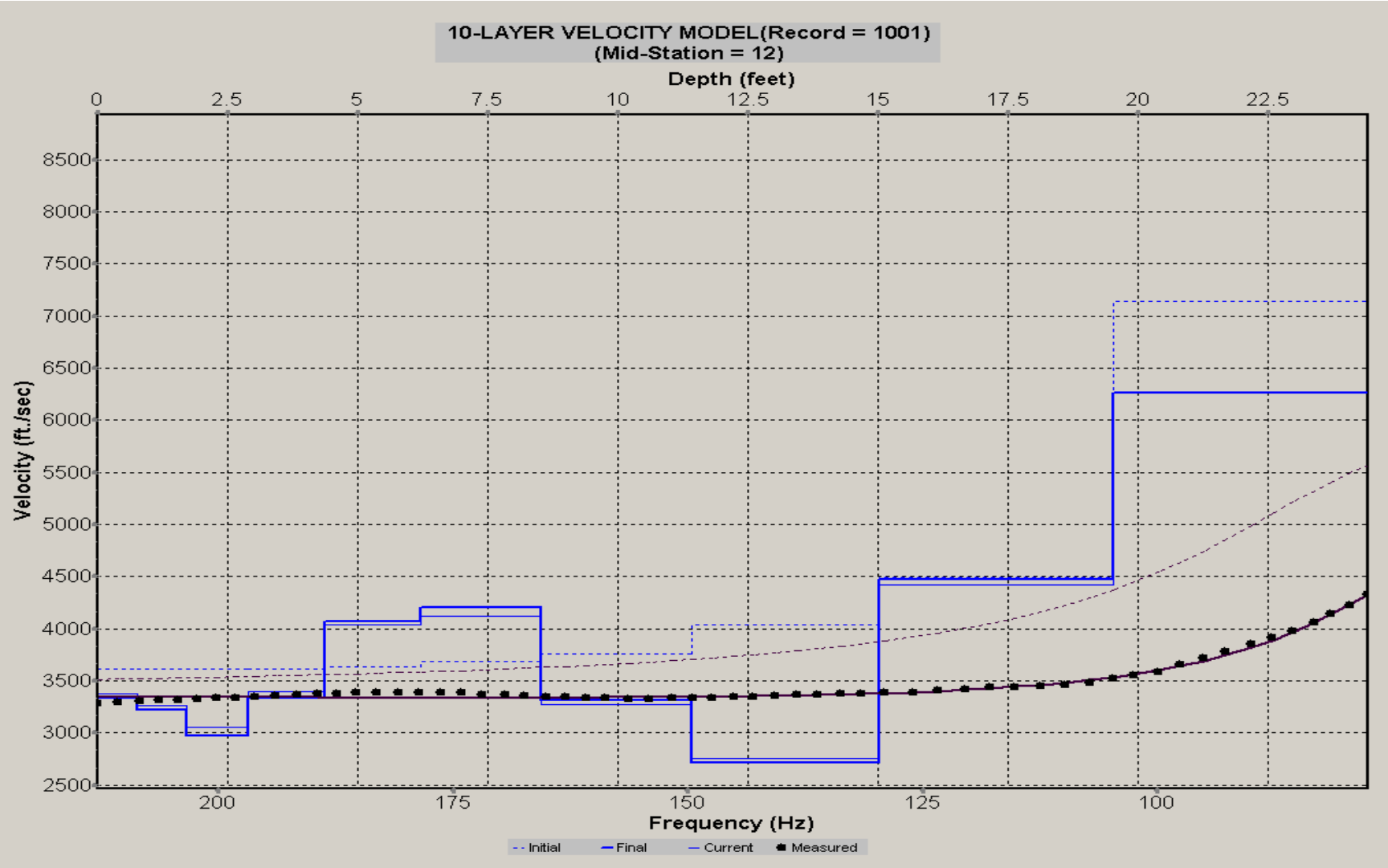

A.333: Velocity Profile Line 1241 used in Post-blast 14 and Pre-blast 29

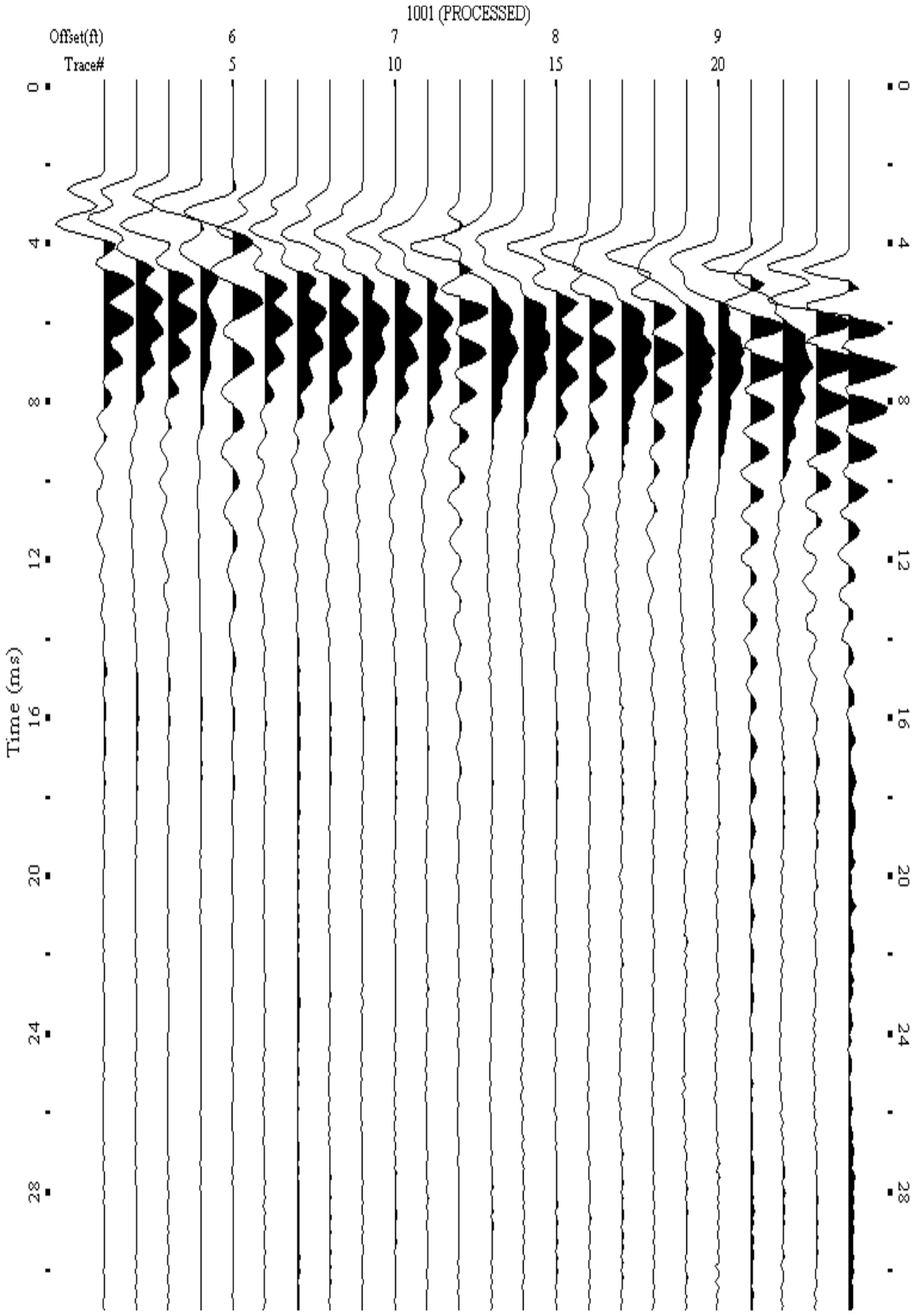

A.334: Shot Gather Line 1243 used in Post-blast 14 and Pre-blast 29

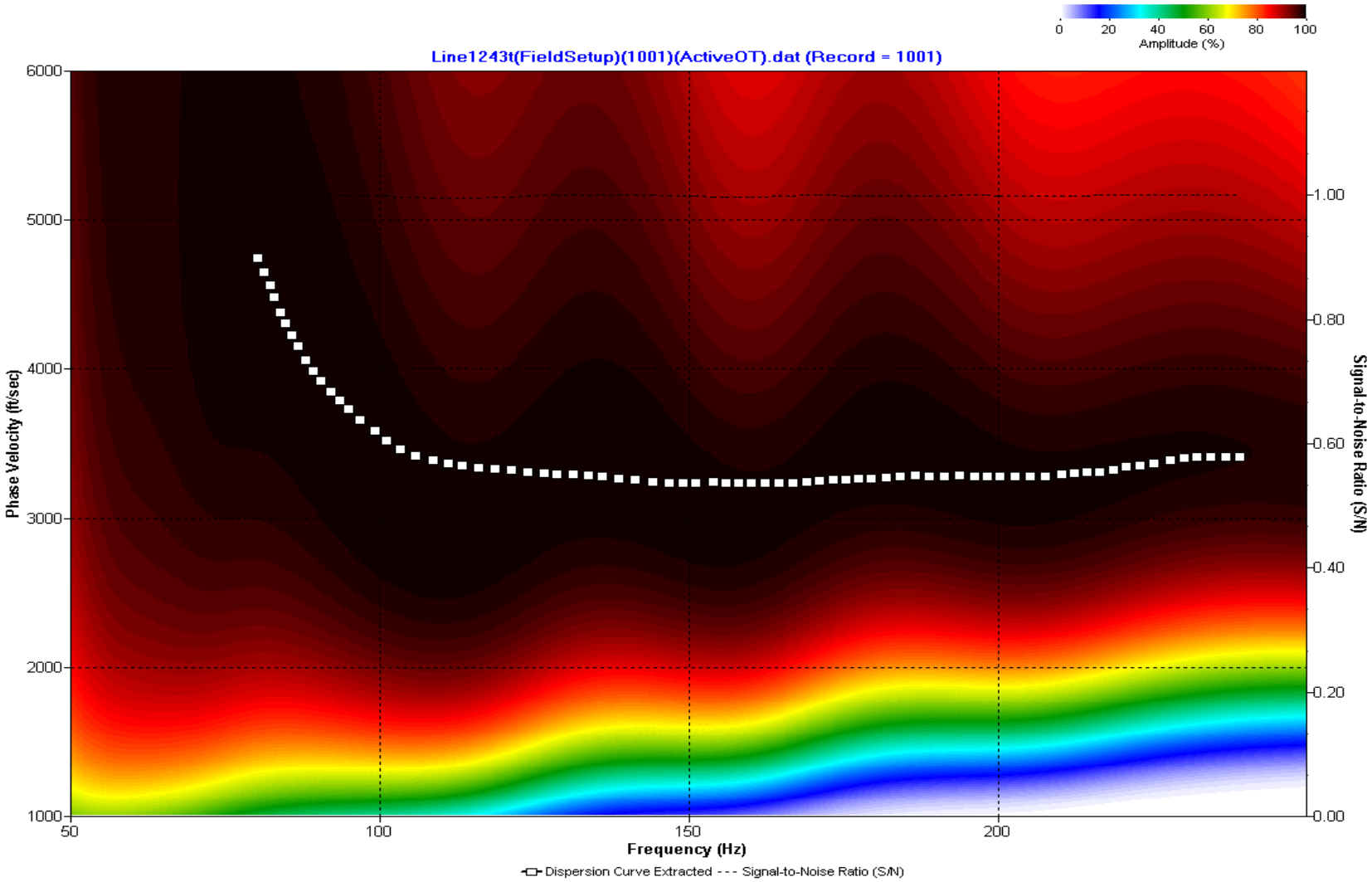

A.335: Dispersion Curve Line 1243 used in Post-blast 14 and Pre-blast 29

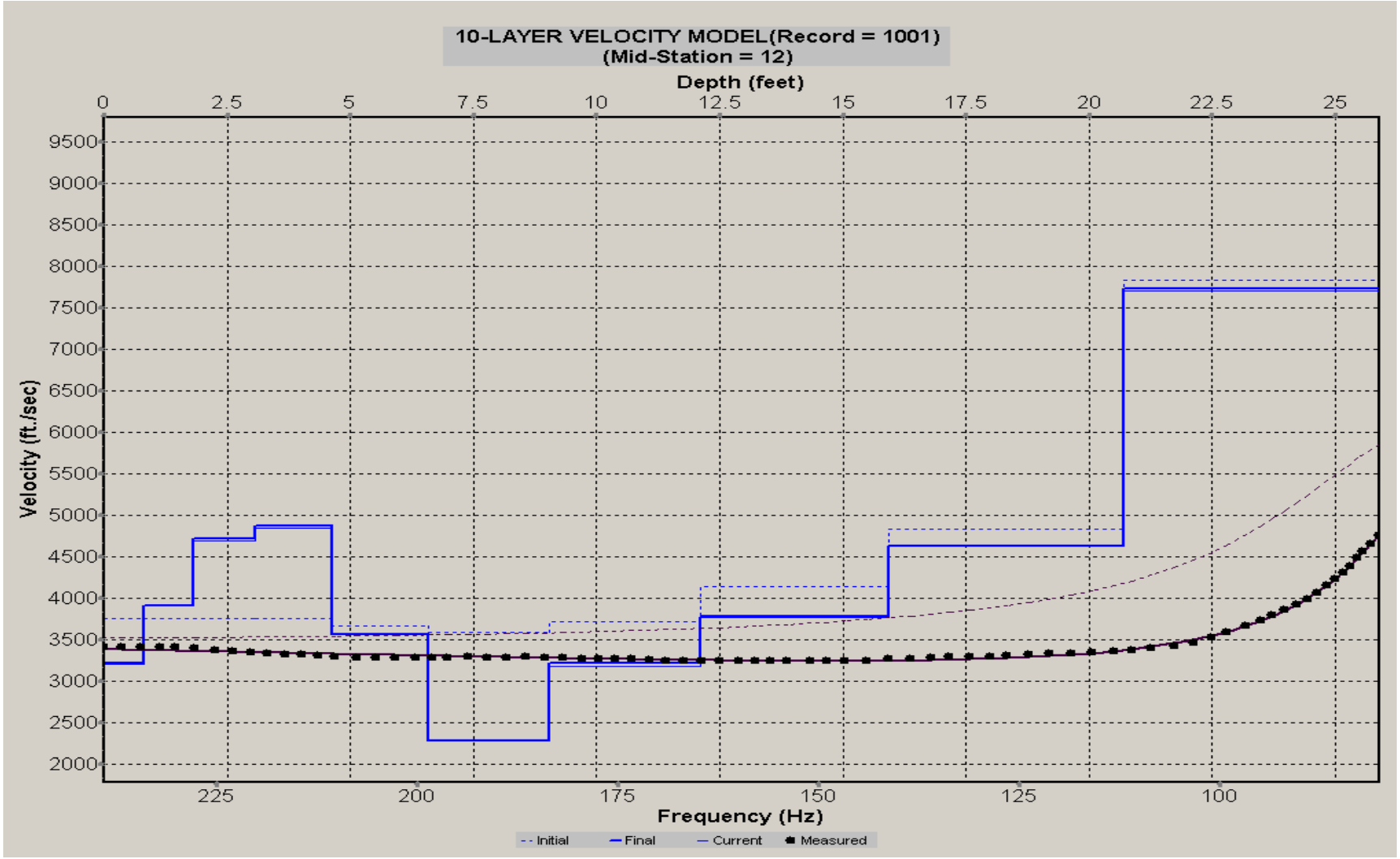

A.336: Velocity Profile Line 1243 used in Post-blast 14 and Pre-blast 29

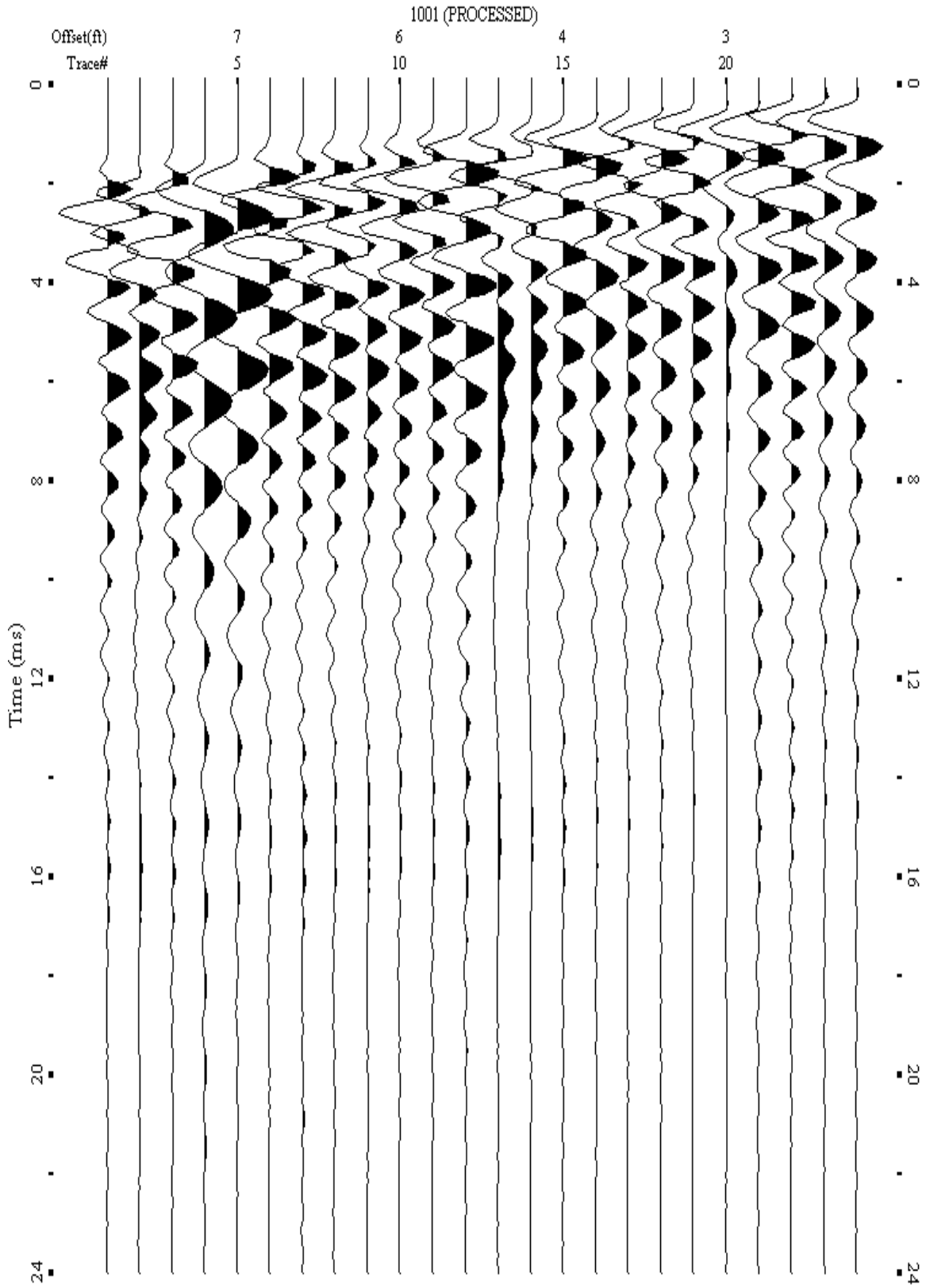

A.337: Shot Gather Line 1245 used in Post-blast 14

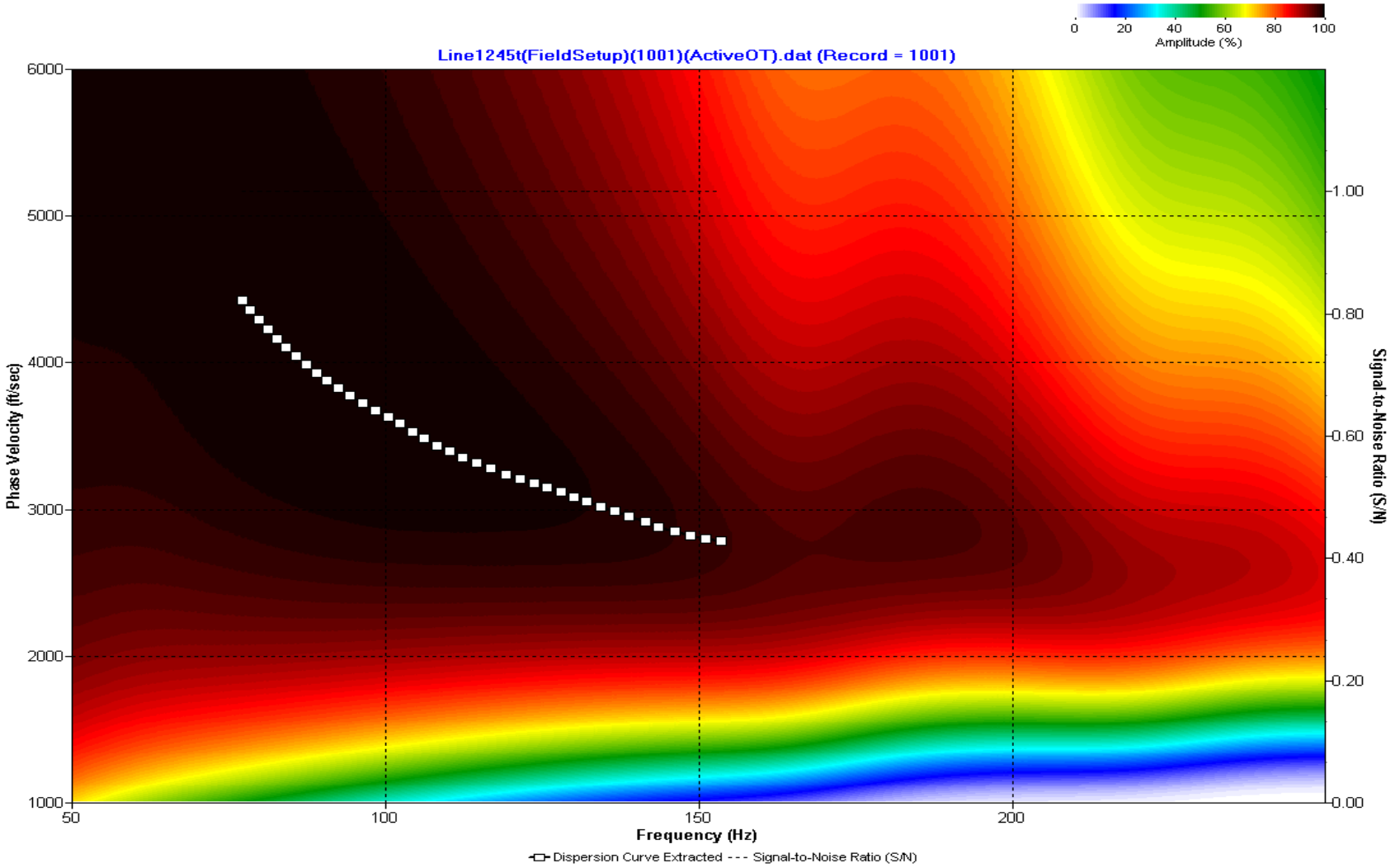

A.338: Dispersion Curve Line 1245 used in Post-blast 14

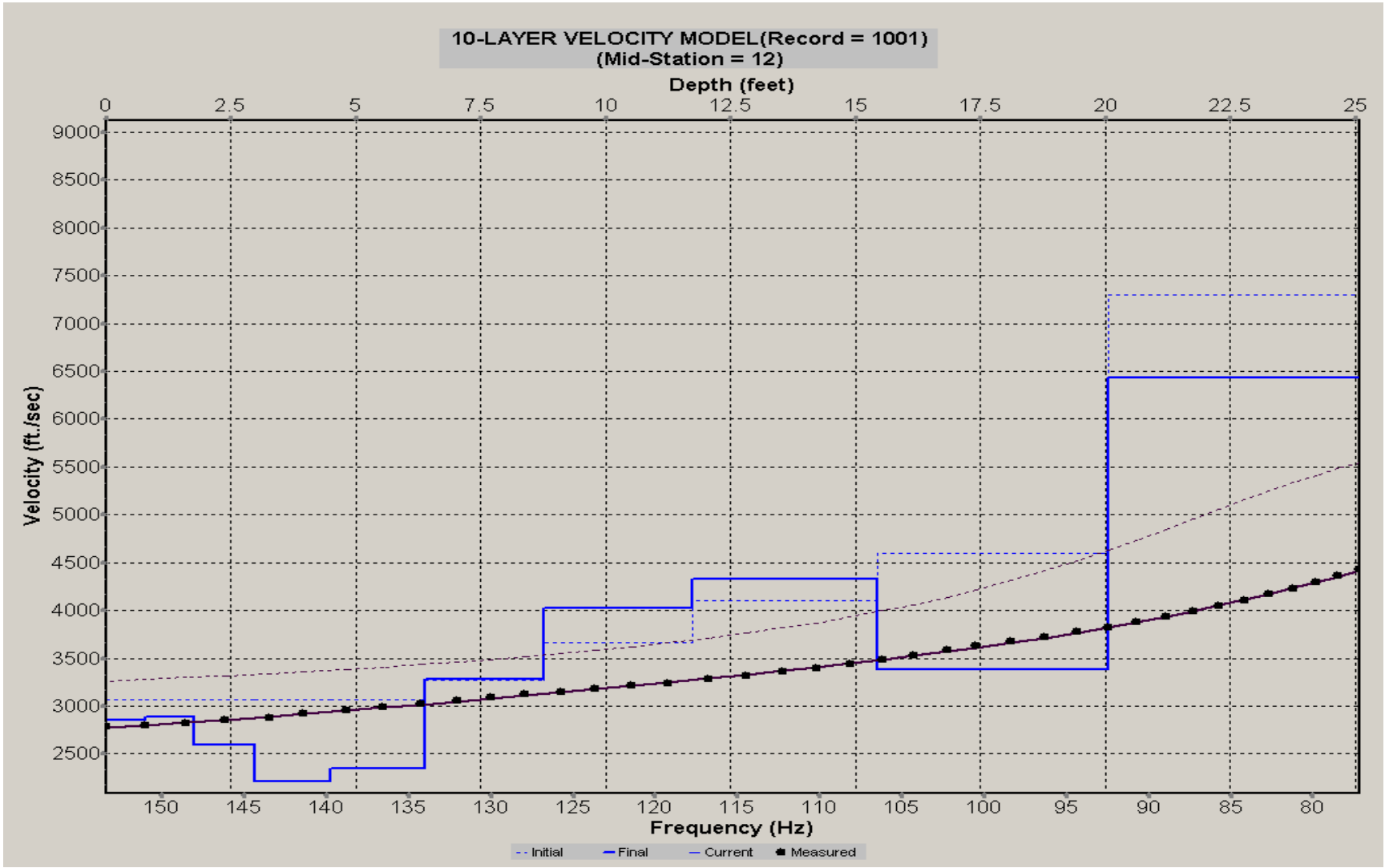

A.339: Velocity Profile Line 1245 used in Post-blast 14

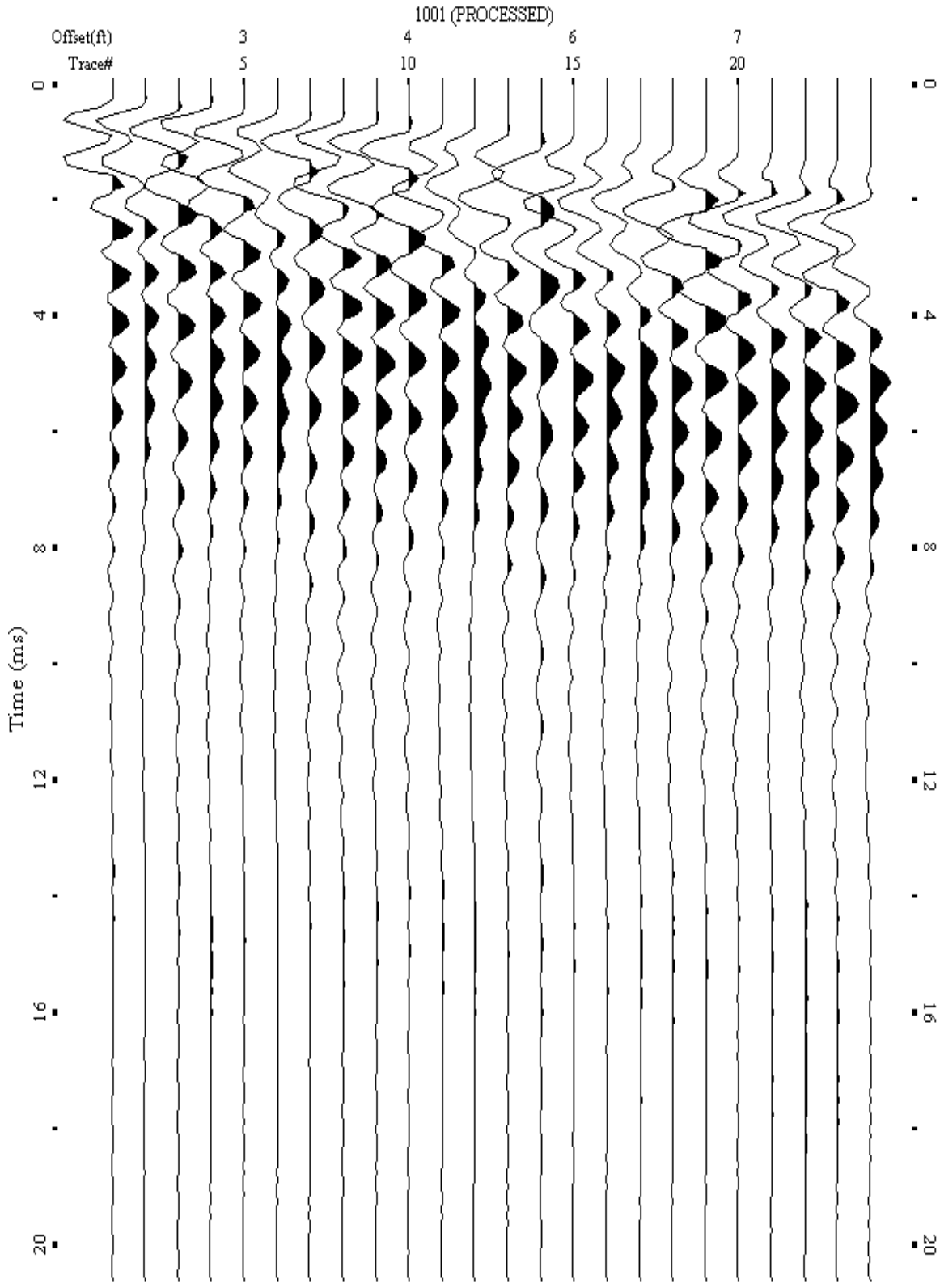

A.340: Shot Gather Line 1248 used in Post-blast 15 and Pre-blast 29

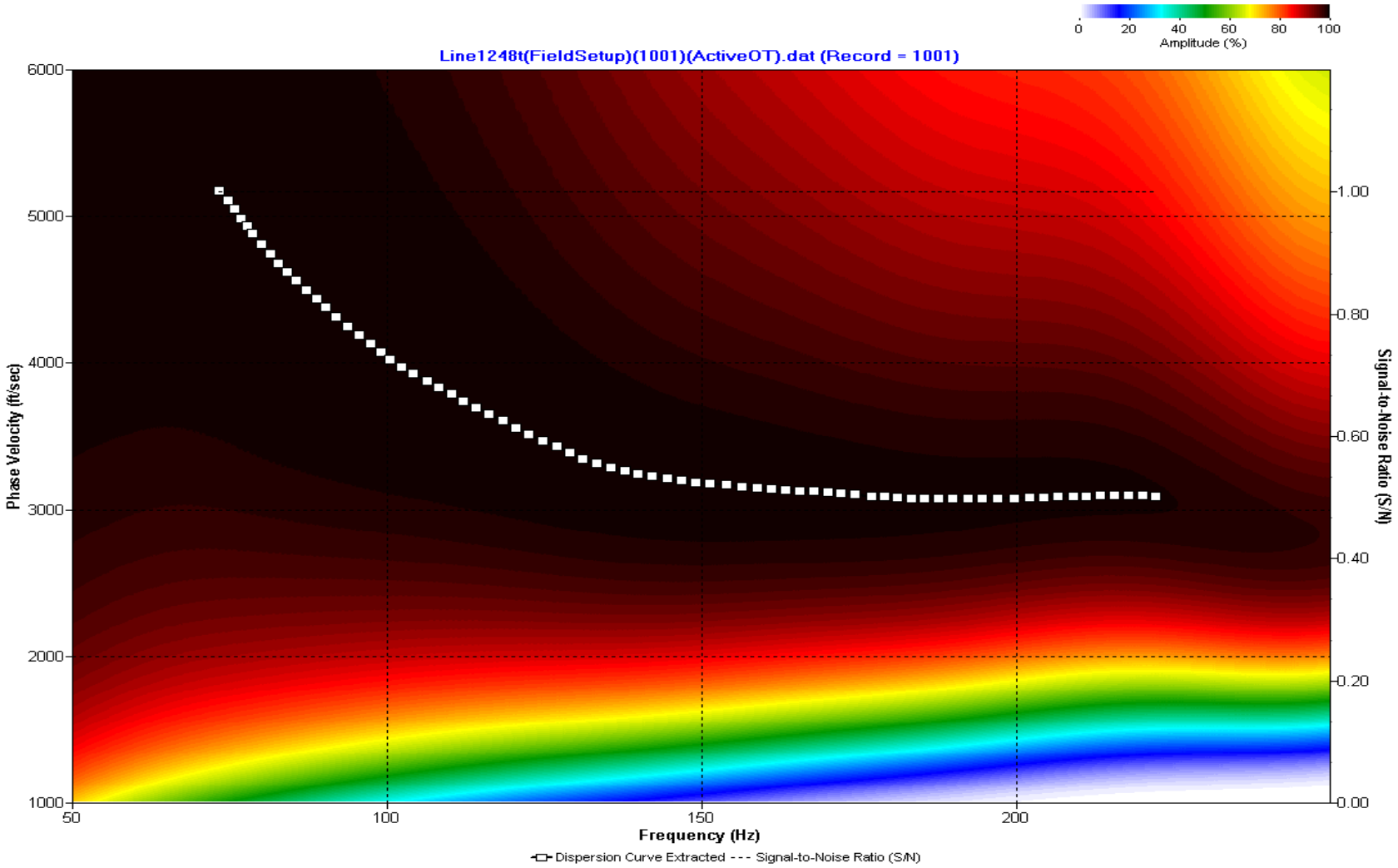

A.341: Dispersion Curve Line 1248 used in Post-blast 15 and Pre-blast 29

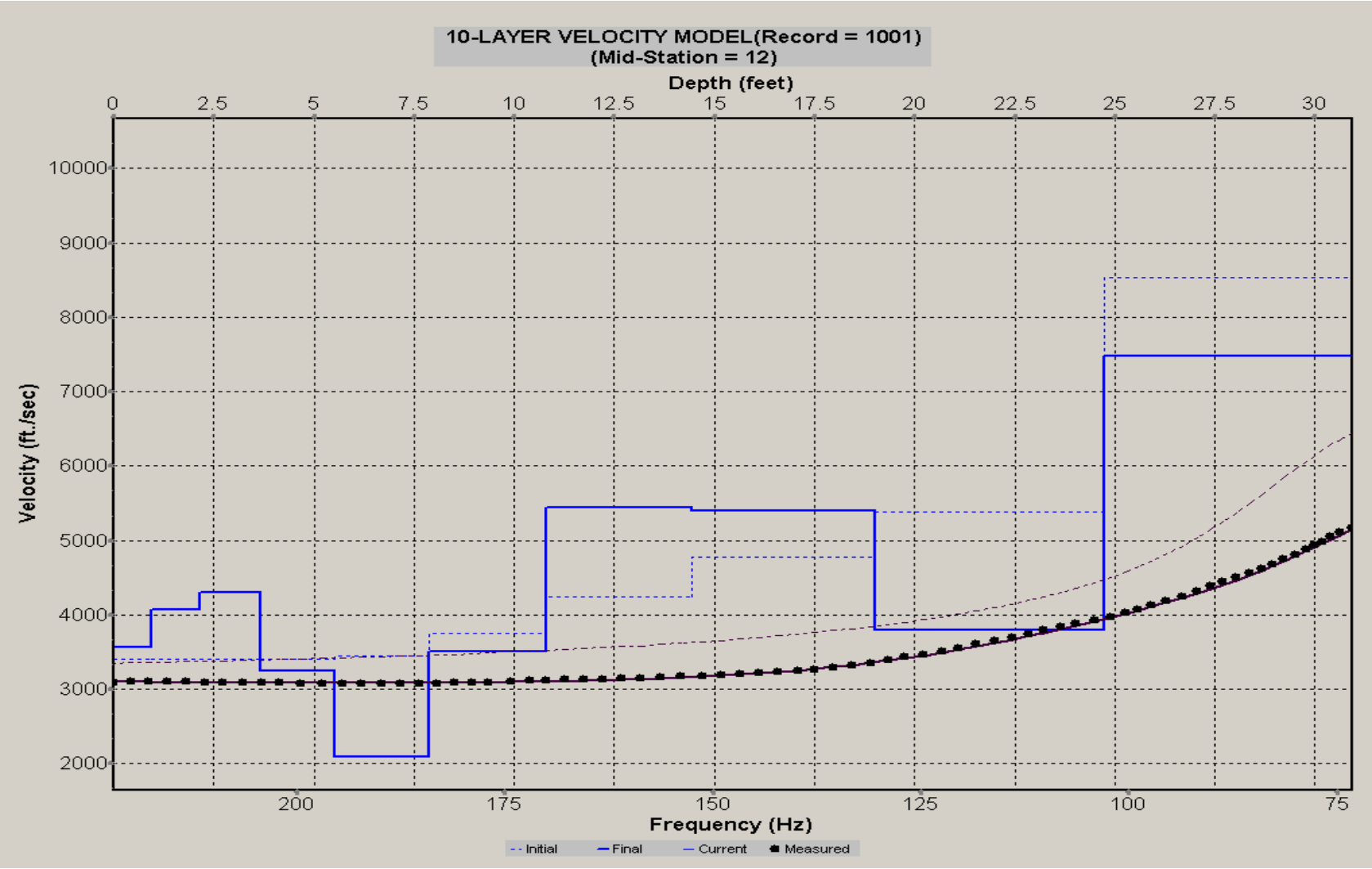

A.342: Velocity Profile Line 1248 used in Post-blast 15 and Pre-blast 29

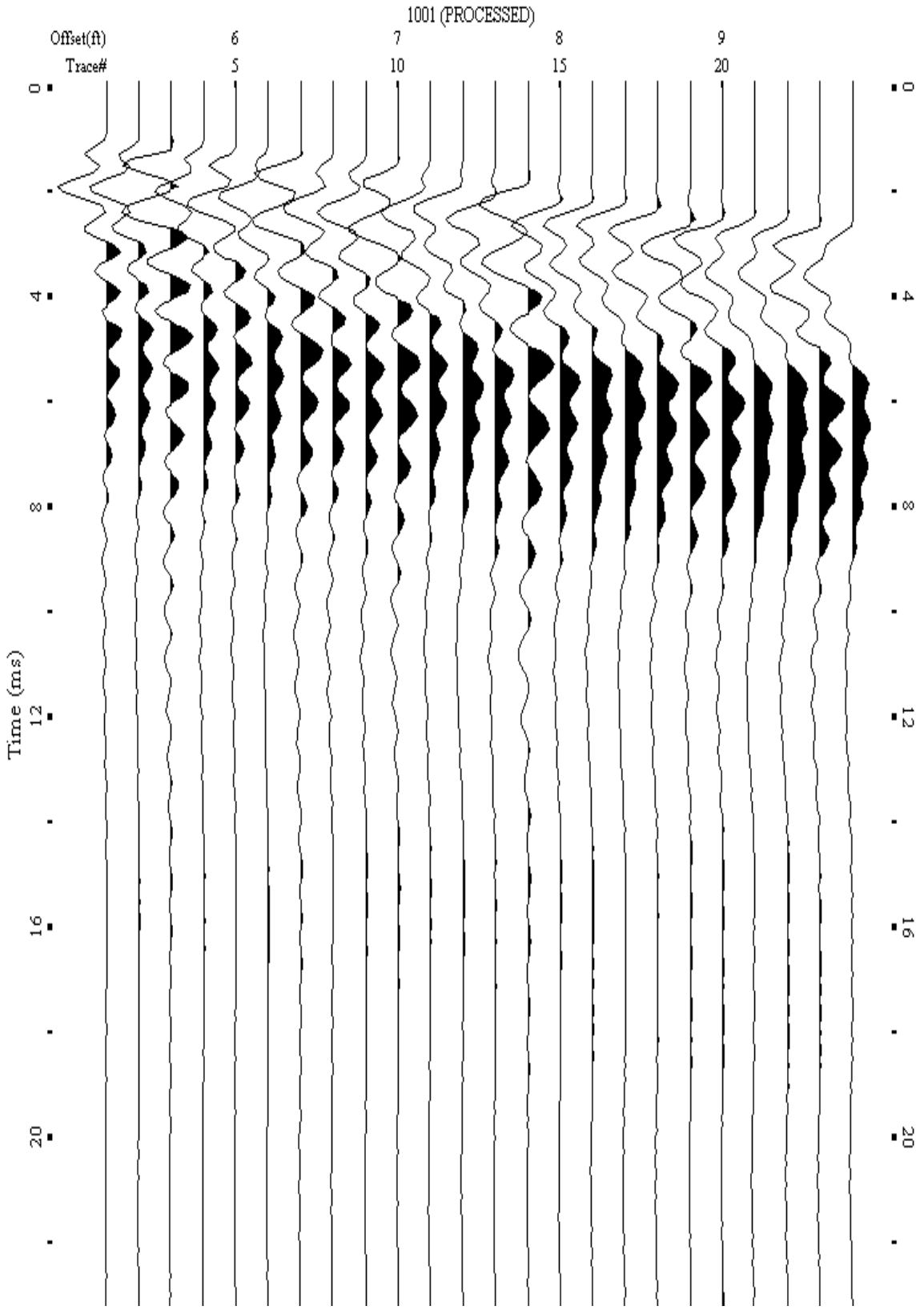

A.343: Shot Gather Line 1250 used in Post-blast 15 and Pre-blast 29

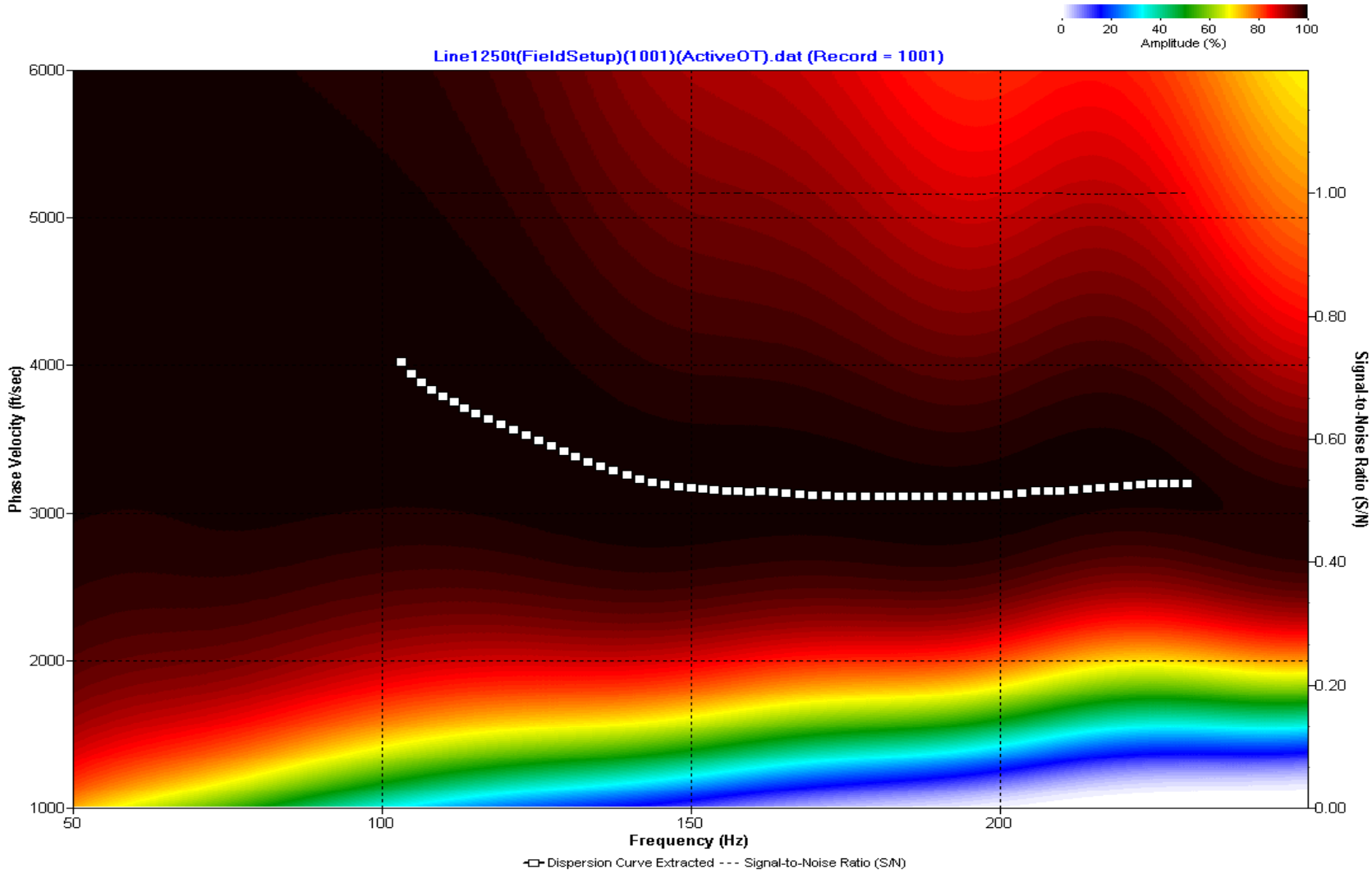

A.344: Dispersion Curve Line 1250 used in Post-blast 15 and Pre-blast 29

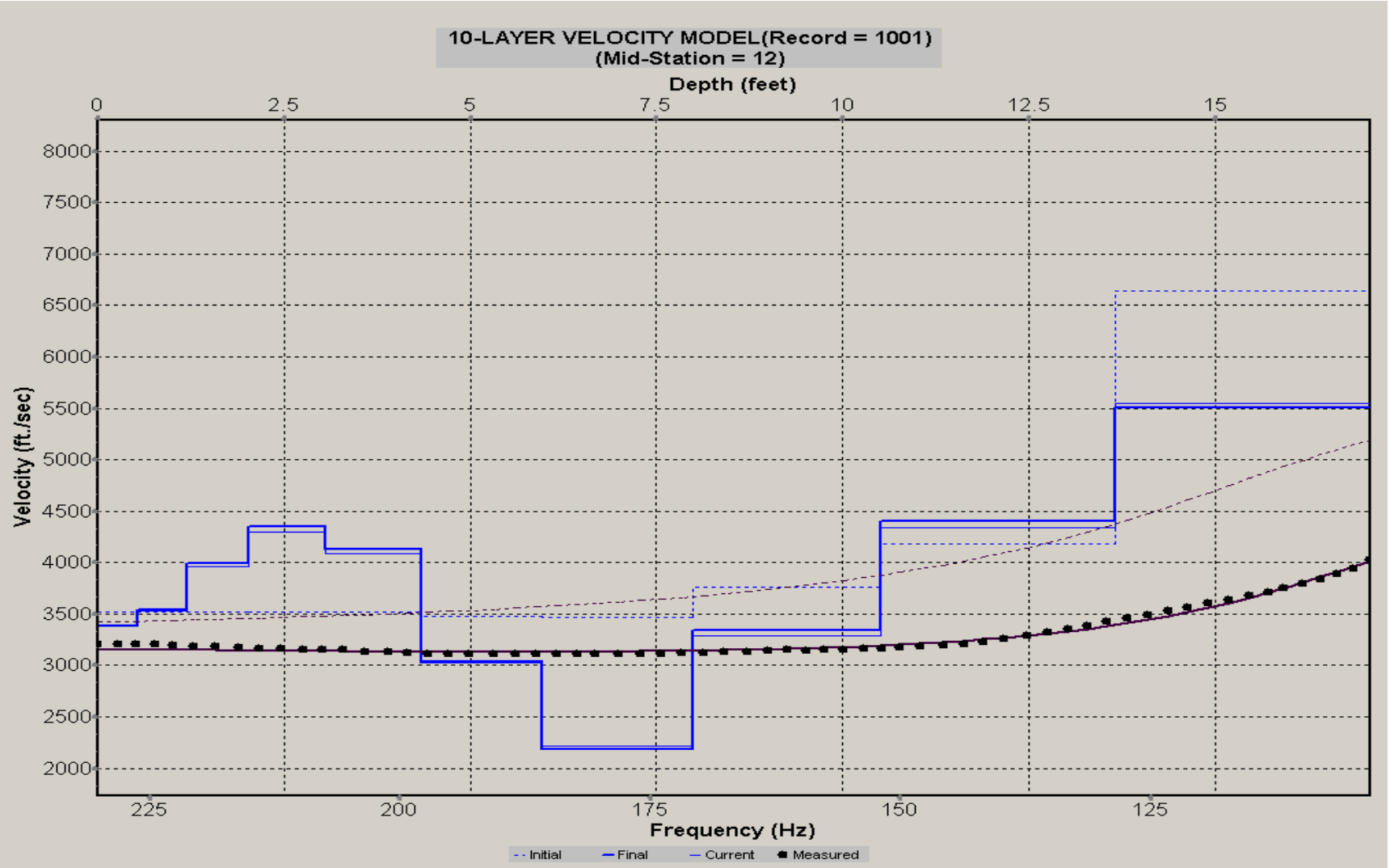

A.345: Velocity Profile Line 1250 used in Post-blast 15 and Pre-blast 29

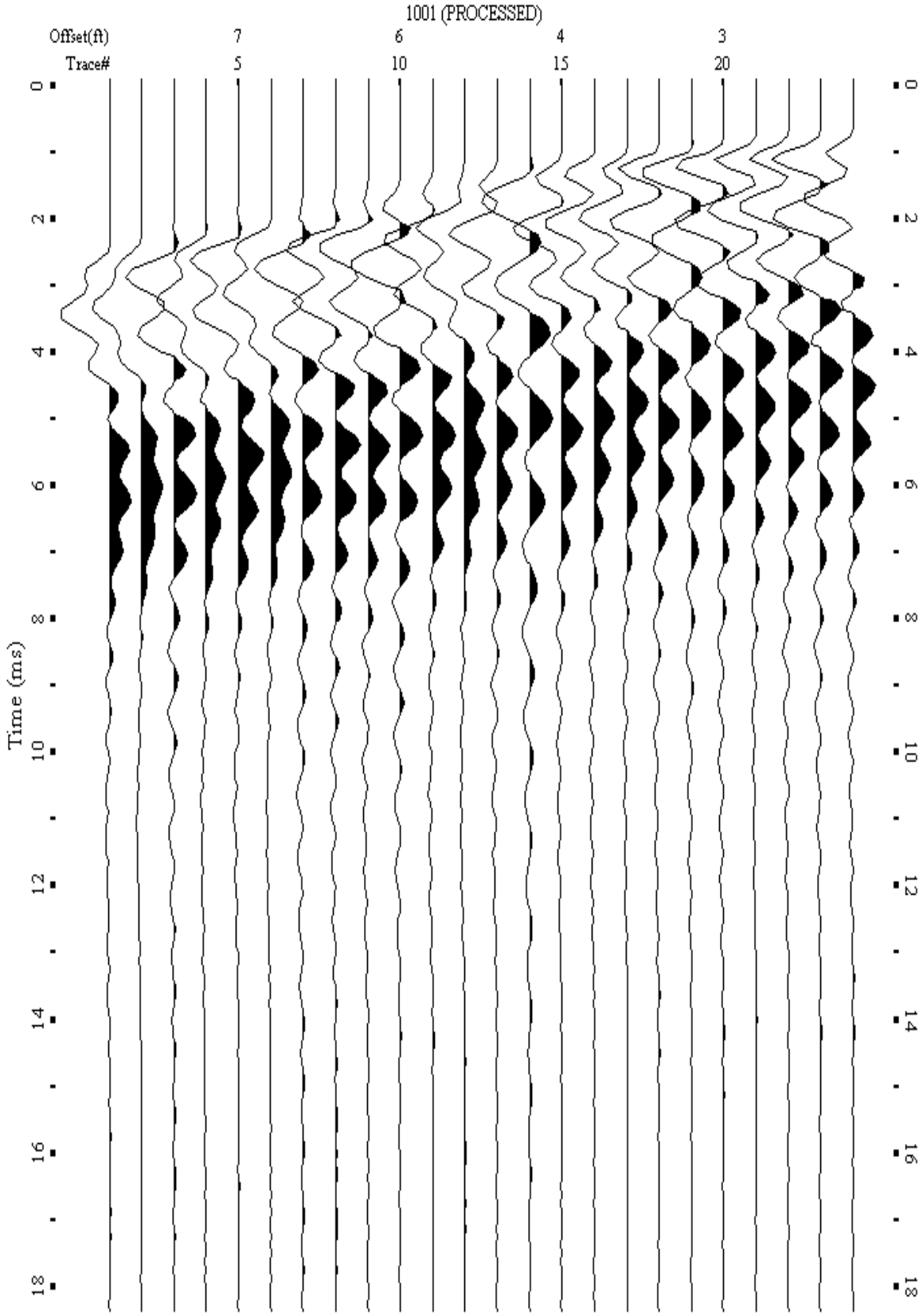

A.346: Shot Gather Line 1252 used in Post-blast 15 and Pre-blast 29

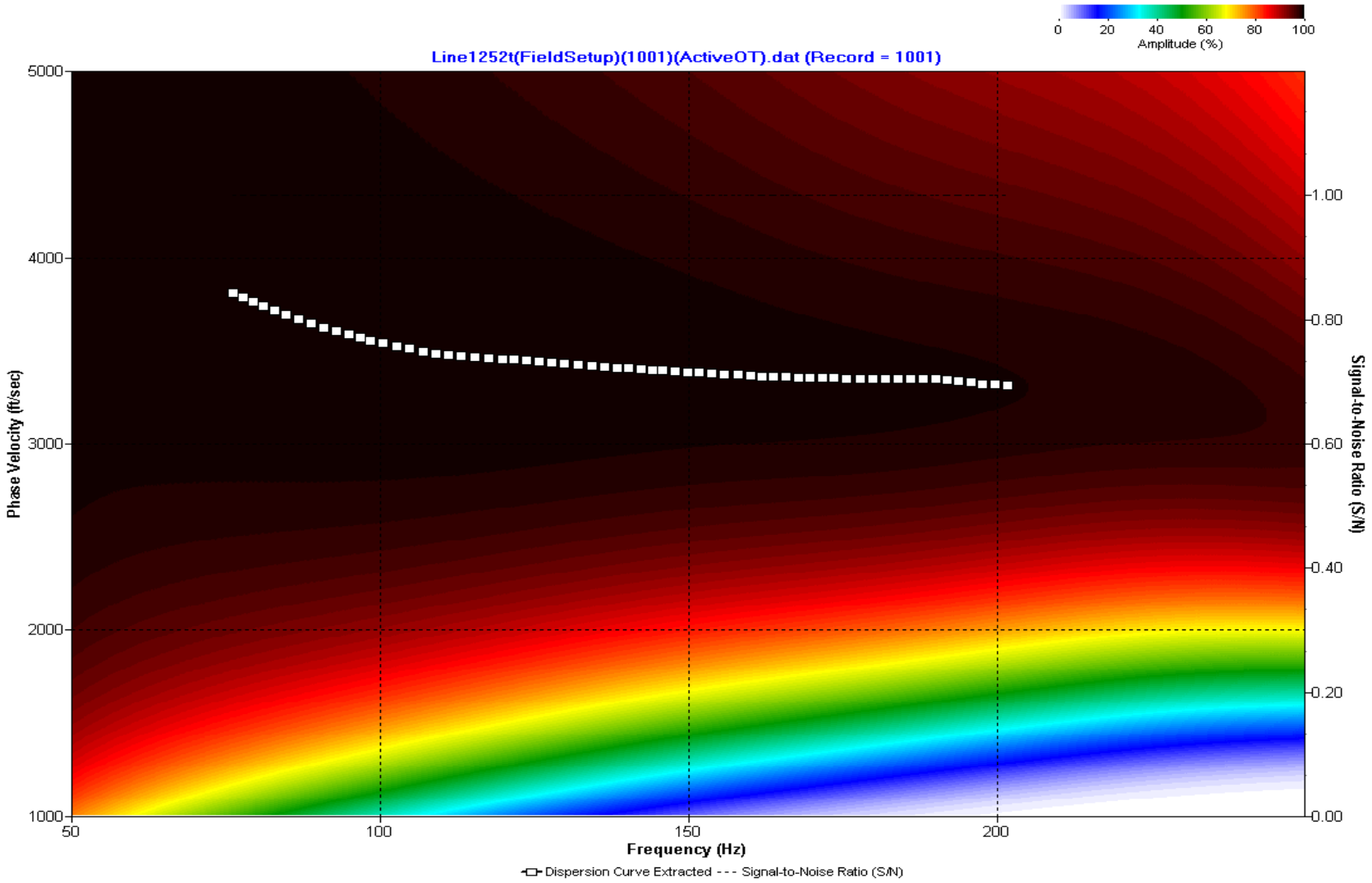

A.347: Dispersion Curve Line 1252 used in Post-blast 15 and Pre-blast 29

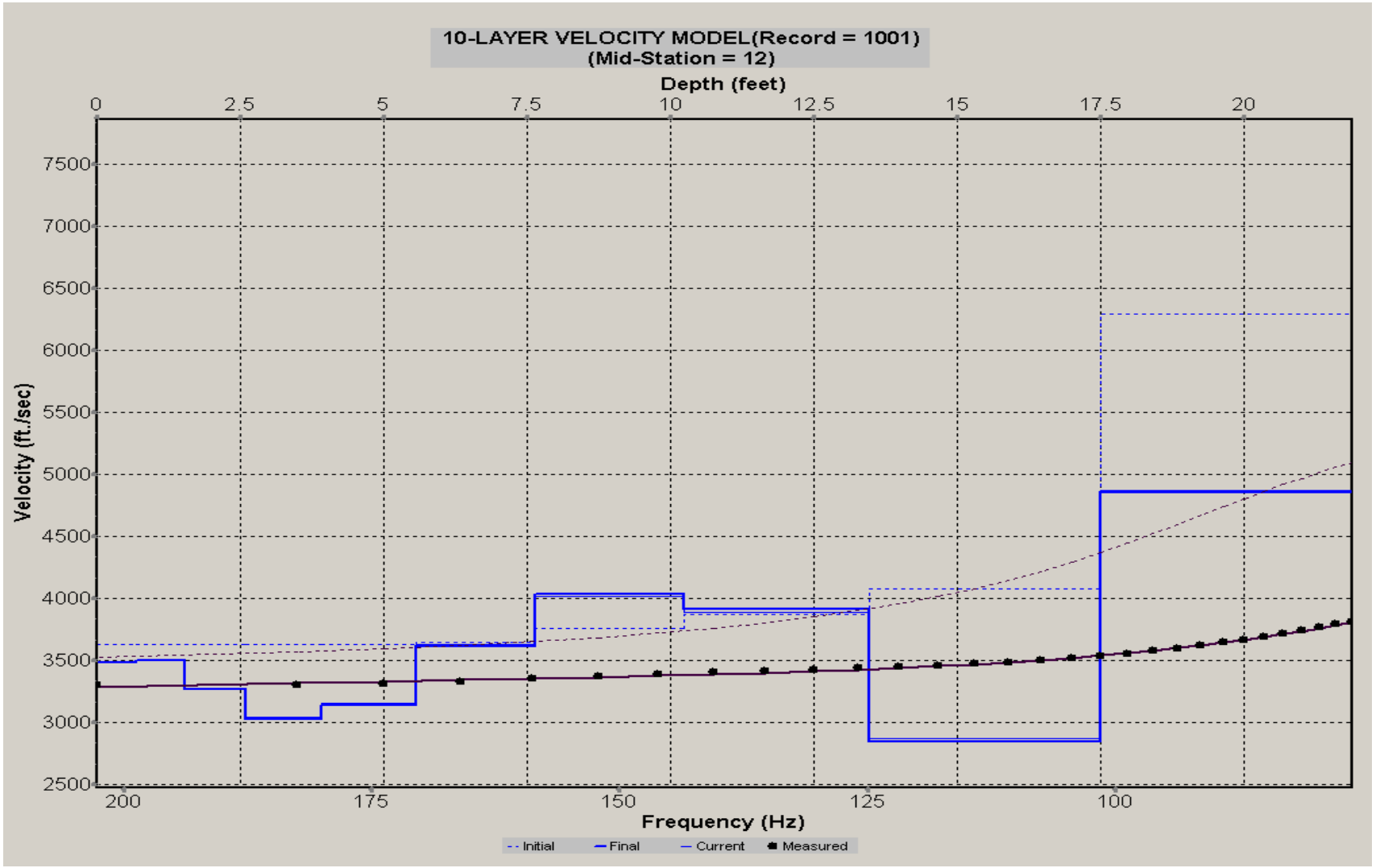

A.348: Velocity Profile Line 1252 used in Post-blast 15 and Pre-blast 29

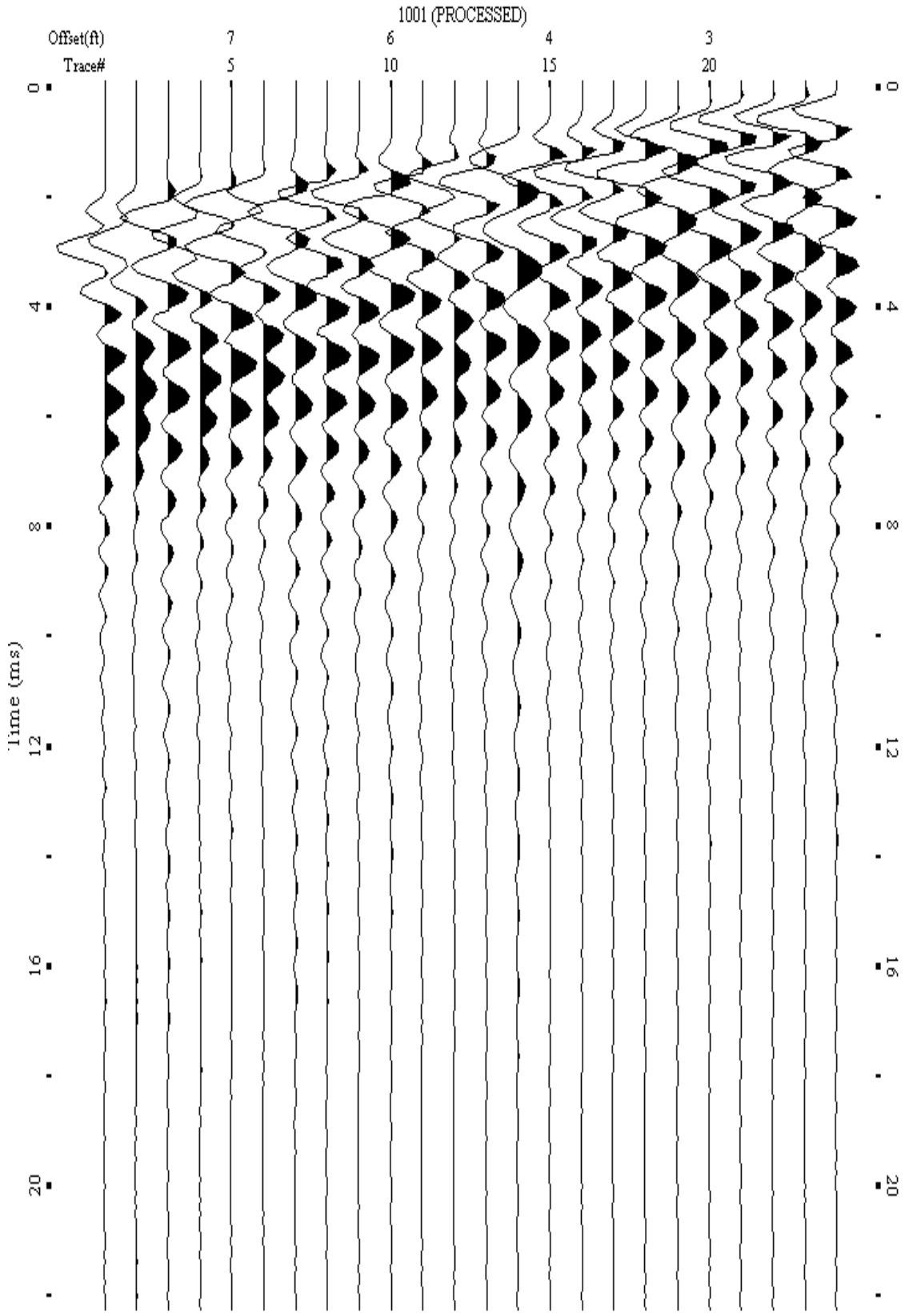

A.349: Shot Gather Line 1253 used in Post-blast 15 and Pre-blast 29

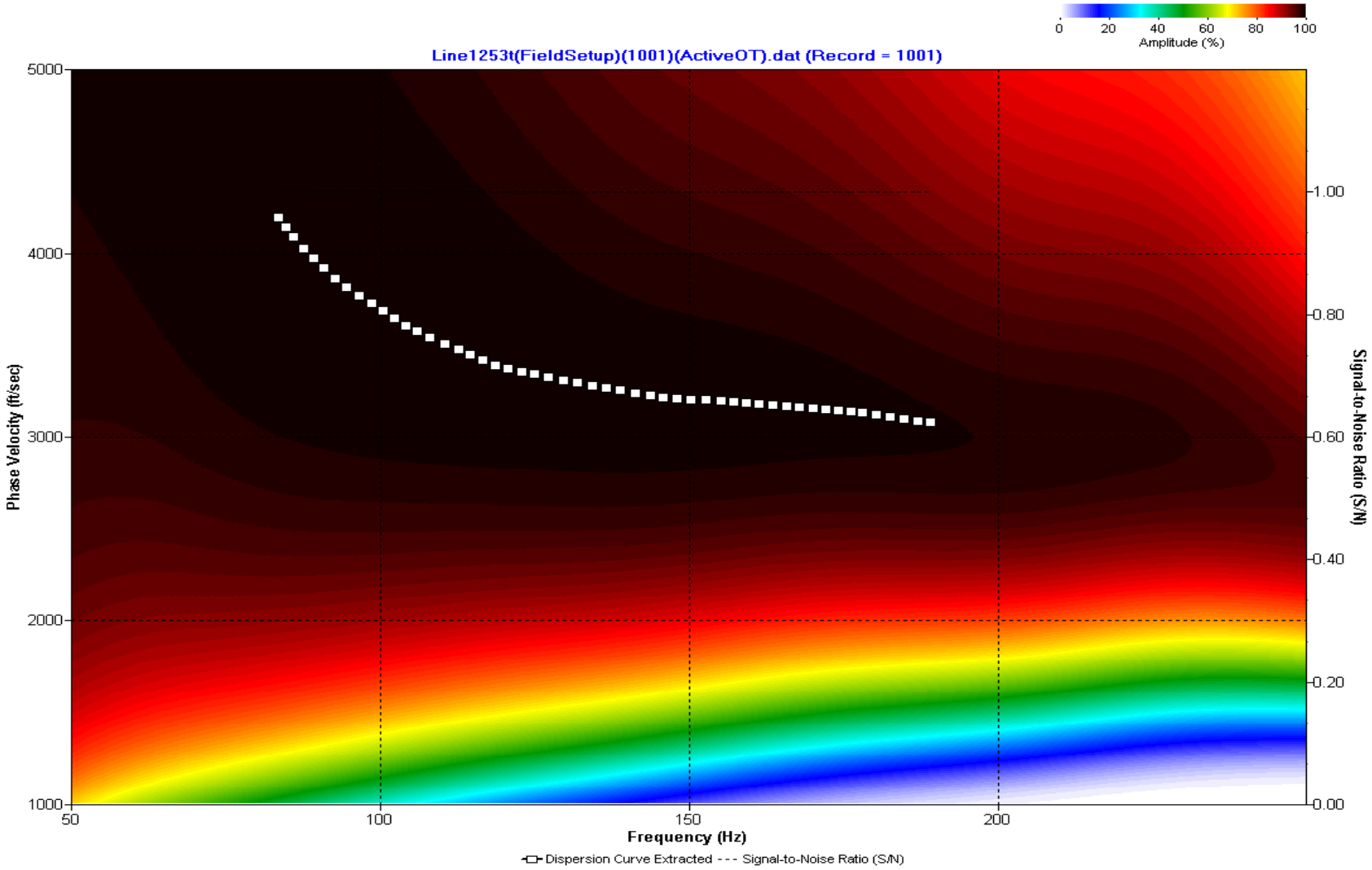

A.350: Dispersion Curve Line 1253 used in Post-blast 15 and Pre-blast 29

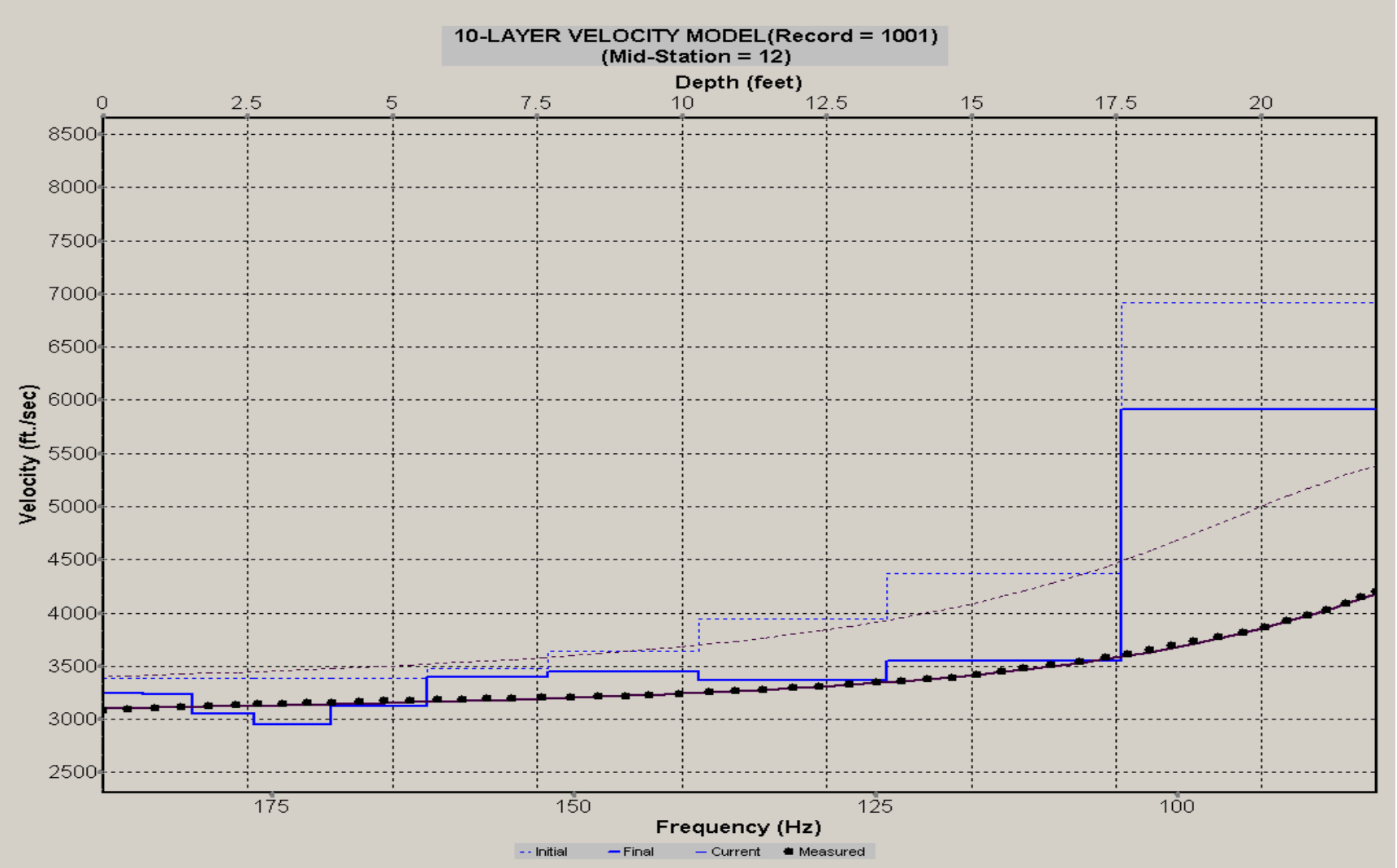

A.351: Velocity Profile Line 1253 used in Post-blast 15 and Pre-blast 29

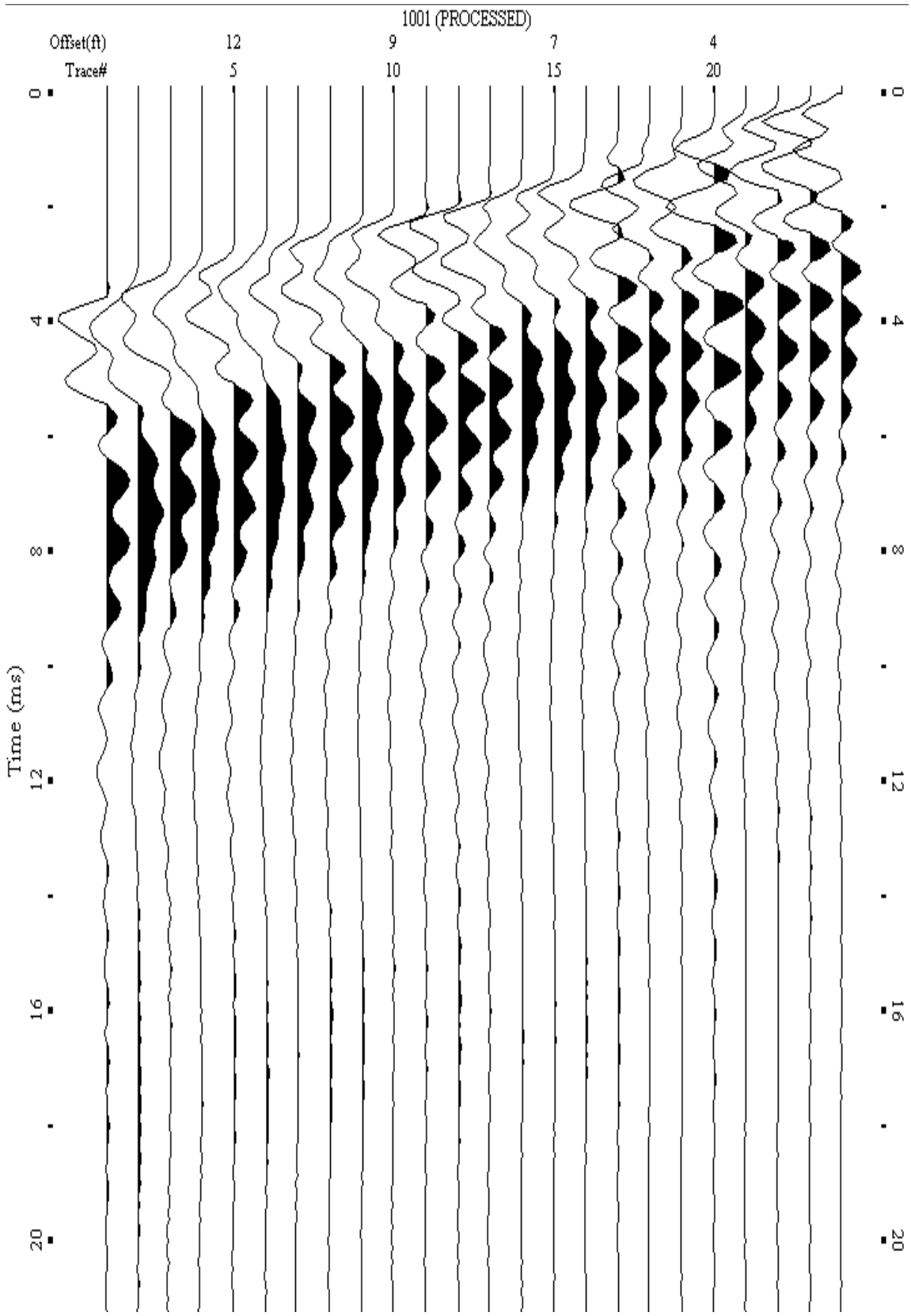

A.352: Shot Gather Line 1257 used in Pre-blast 12, Pre-blast 29 and Pre-blast 30

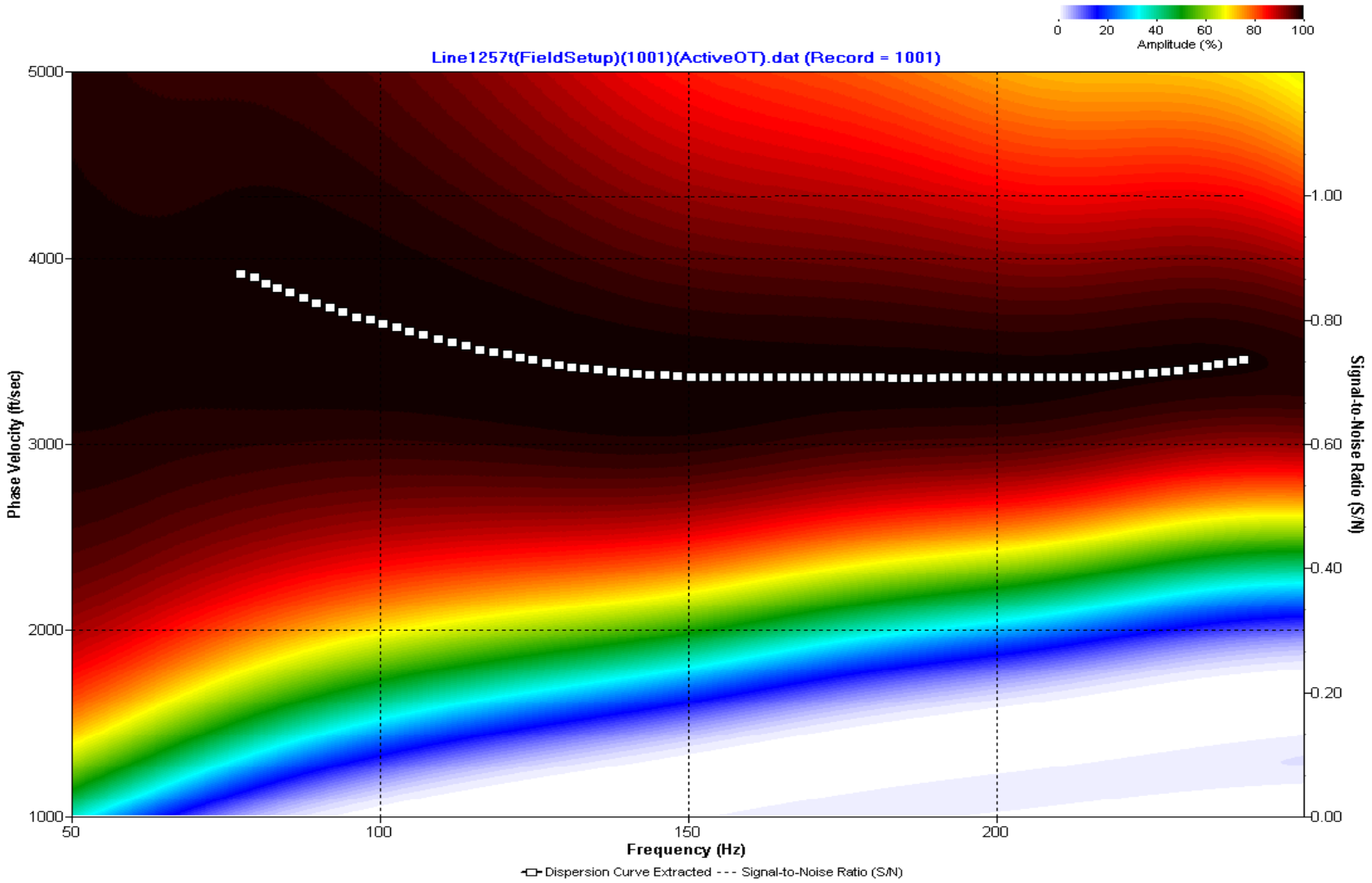

A.353: Dispersion Curve Line 1257 used in Pre-blast 12, Pre-blast 29 and Pre-blast 30

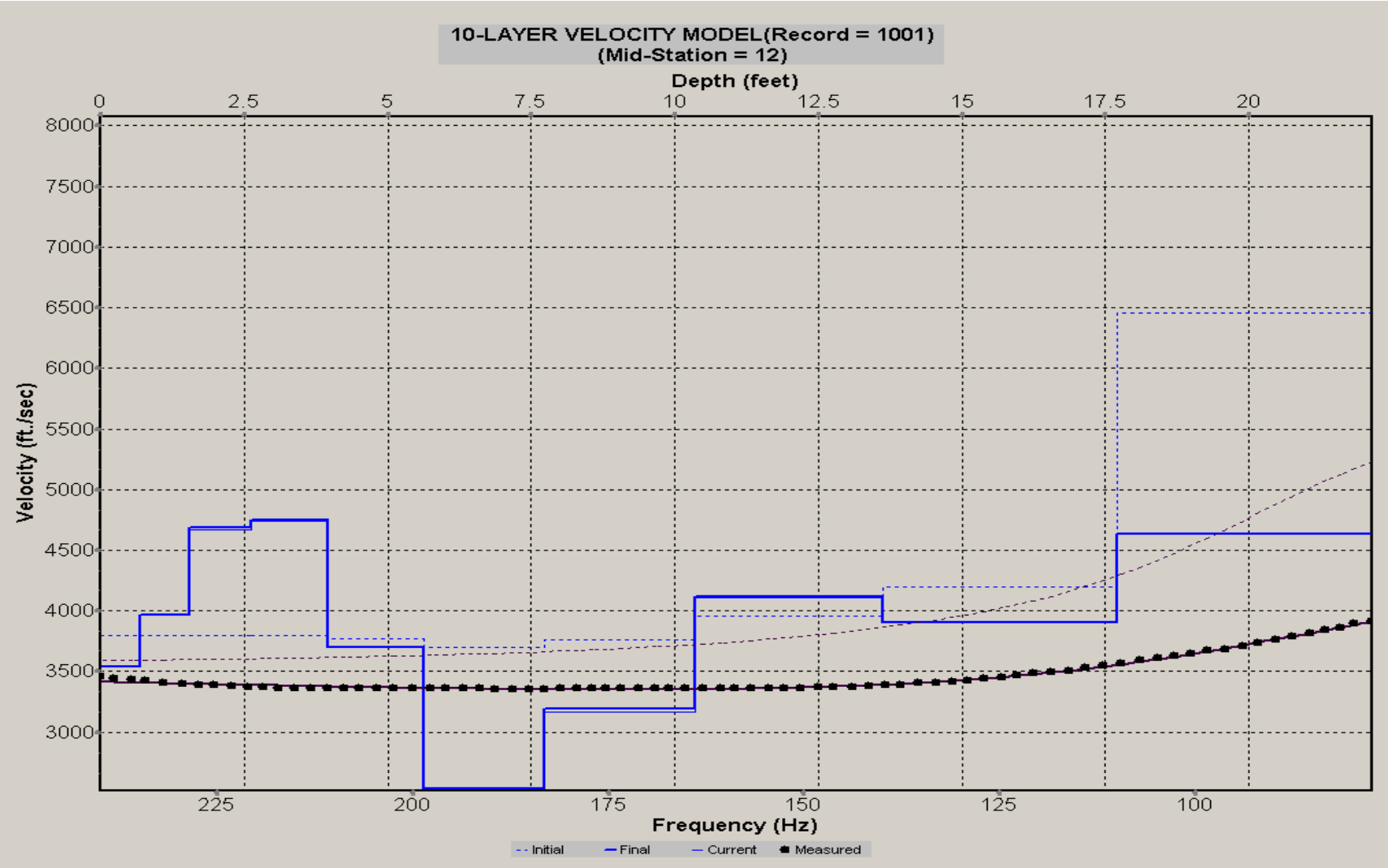

A.354: Velocity Profile Line 1257 used in Pre-blast 12, Pre-blast 29 and Pre-blast 30

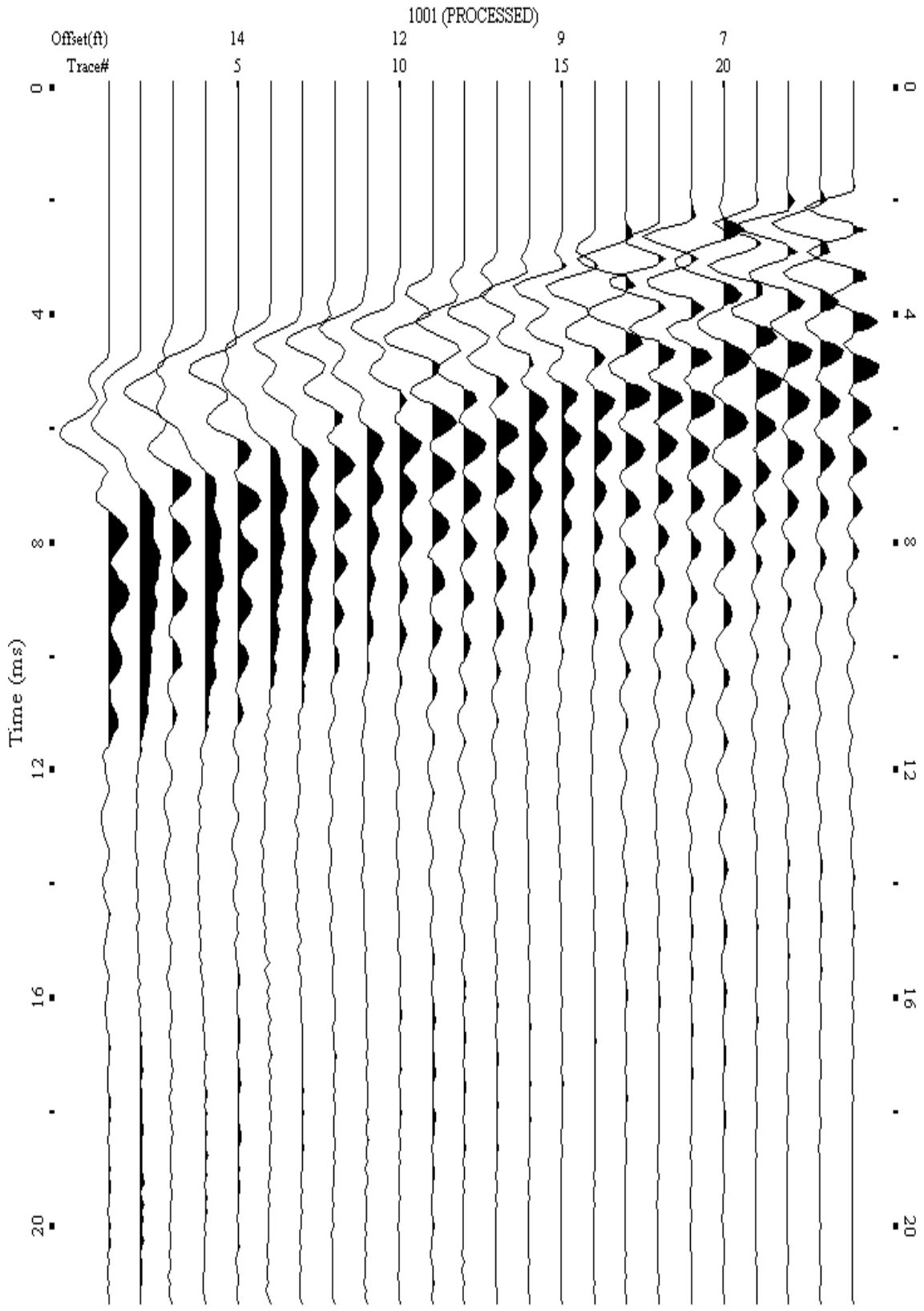

A.355: Shot Gather Line 1258 used in Pre-blast 12, Pre-blast 29 and Pre-blast 30

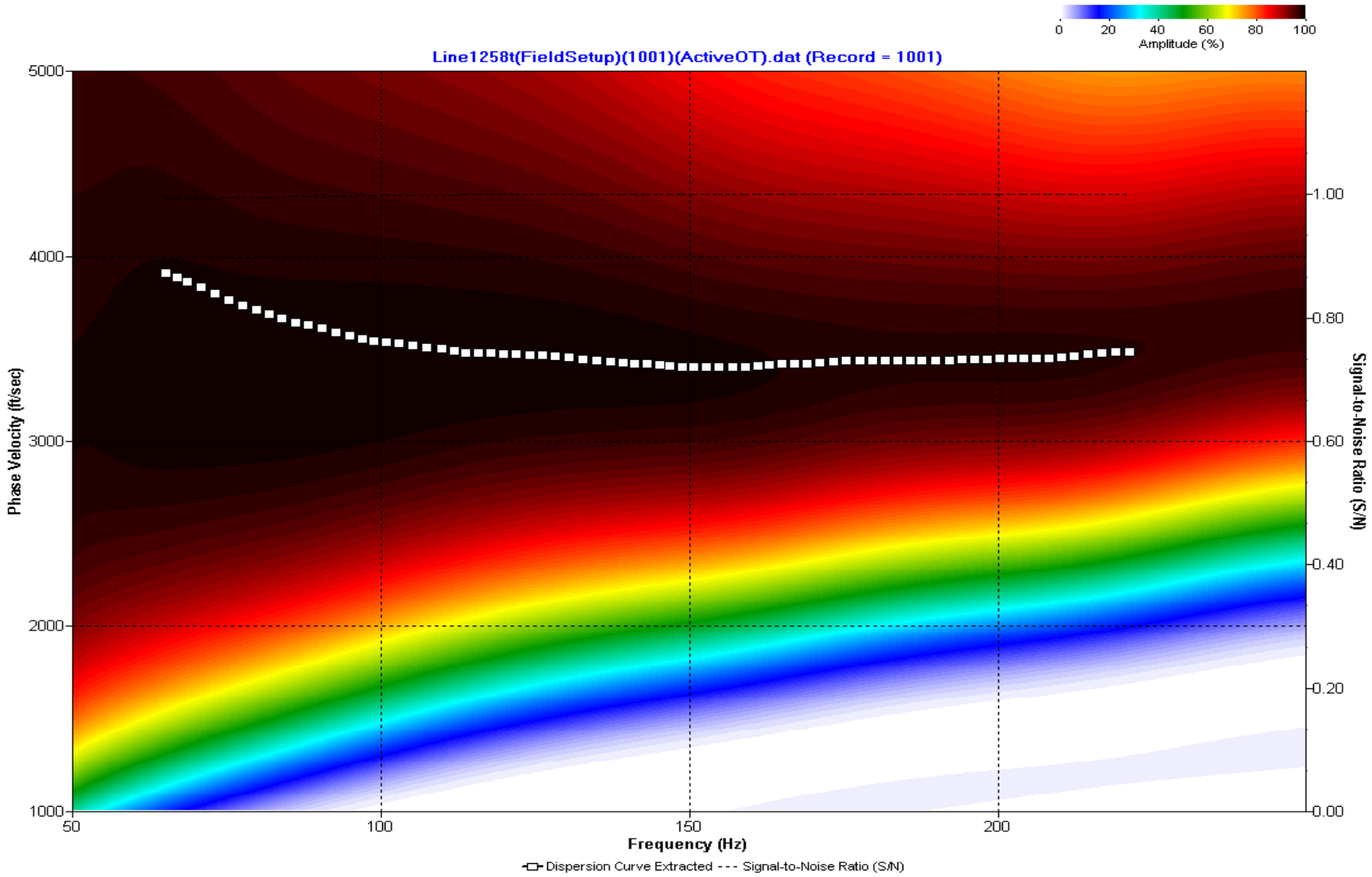

A.356: Dispersion Curve Line 1258 used in Pre-blast 12, Pre-blast 29 and Pre-blast 30

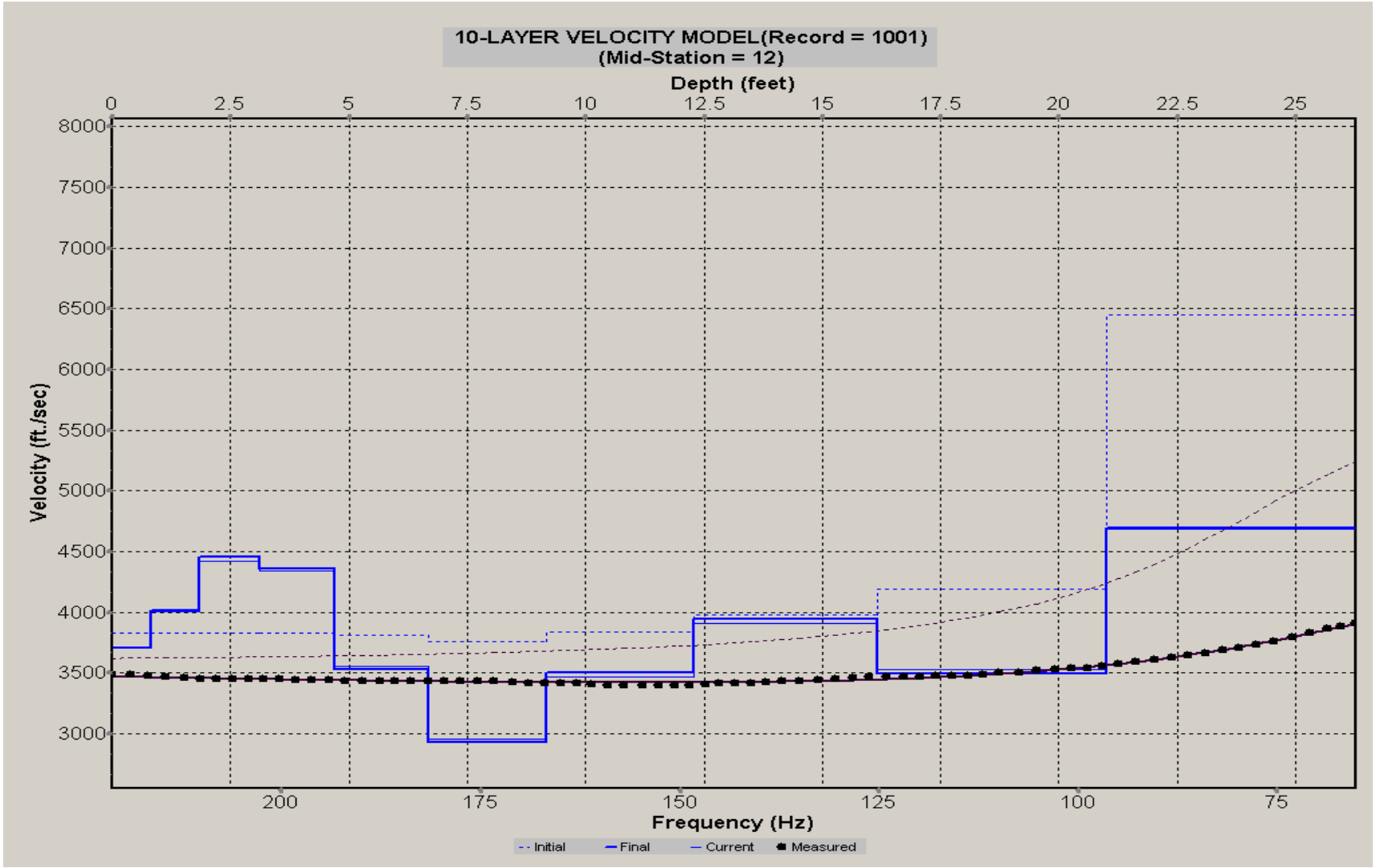

A.357: Velocity Profile Line 1258 used in Pre-blast 12, Pre-blast 29 and Pre-blast 30

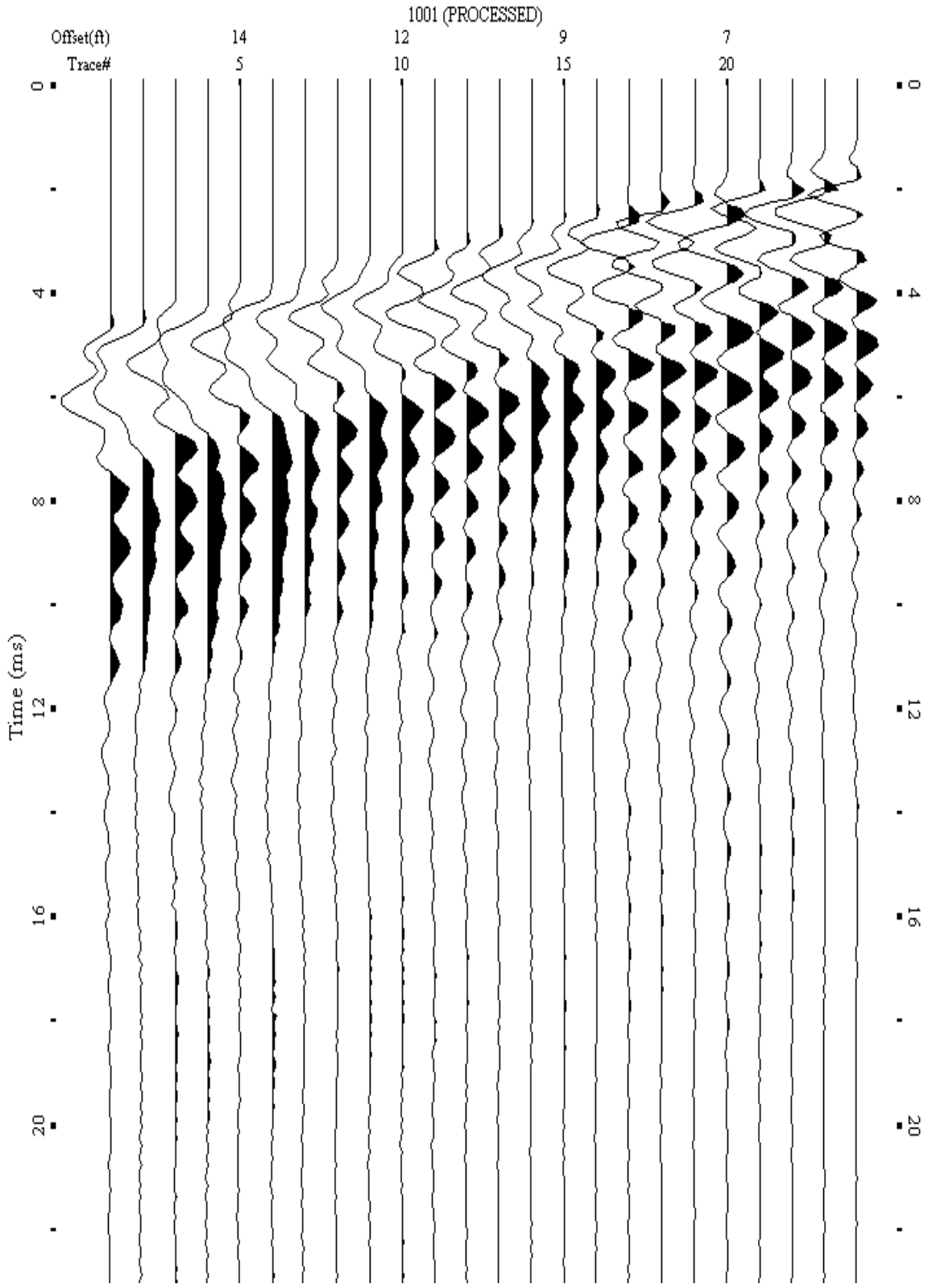

A.358: Shot Gather Line 1259 used in Pre-blast 12, Post-blast 15, Pre-blast 29 and Pre-blast 30

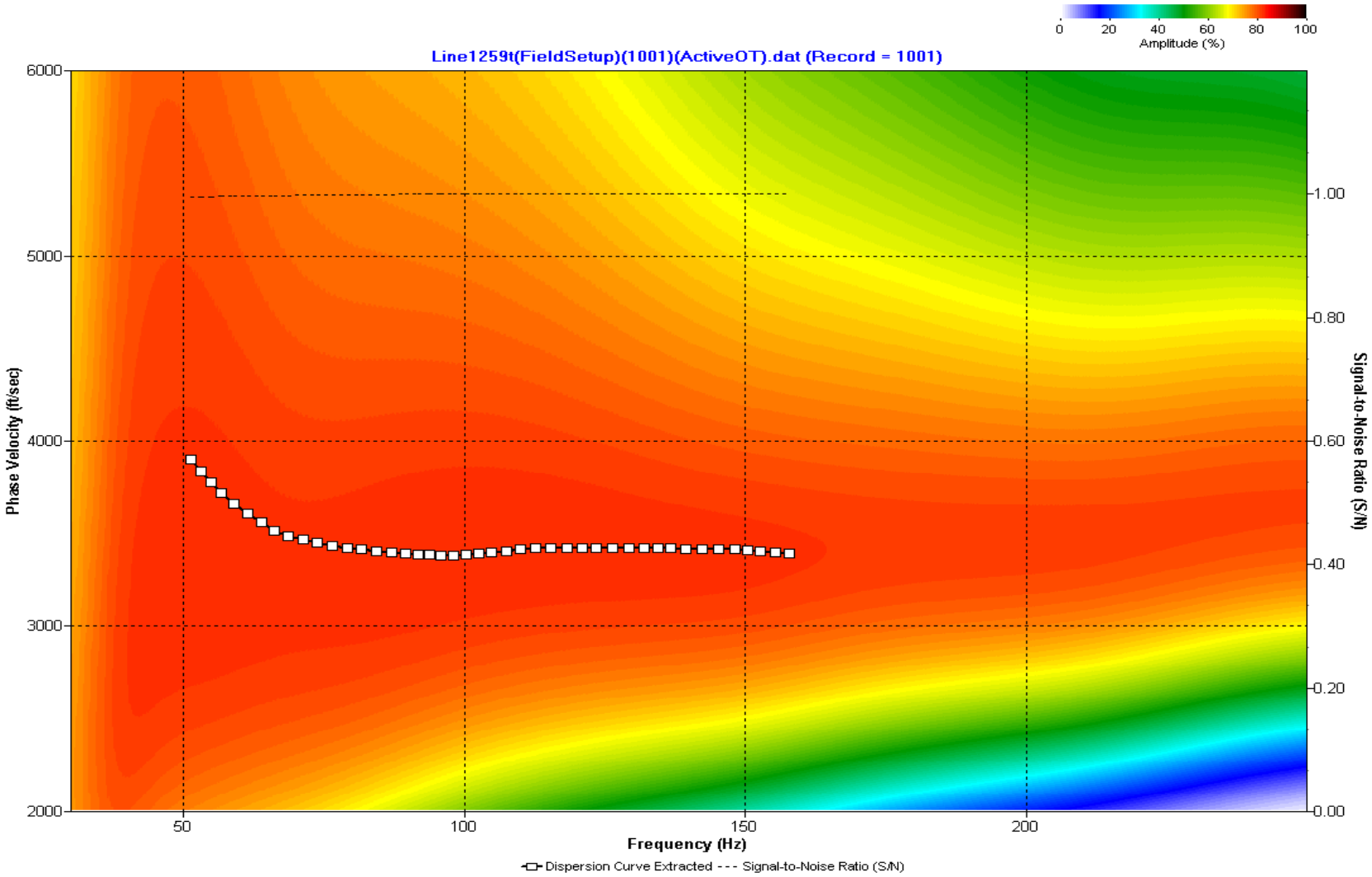

A.359: Dispersion Curve Line 1259 used in Pre-blast 12, Post-blast 15, Pre-blast 29 and Pre-blast 30

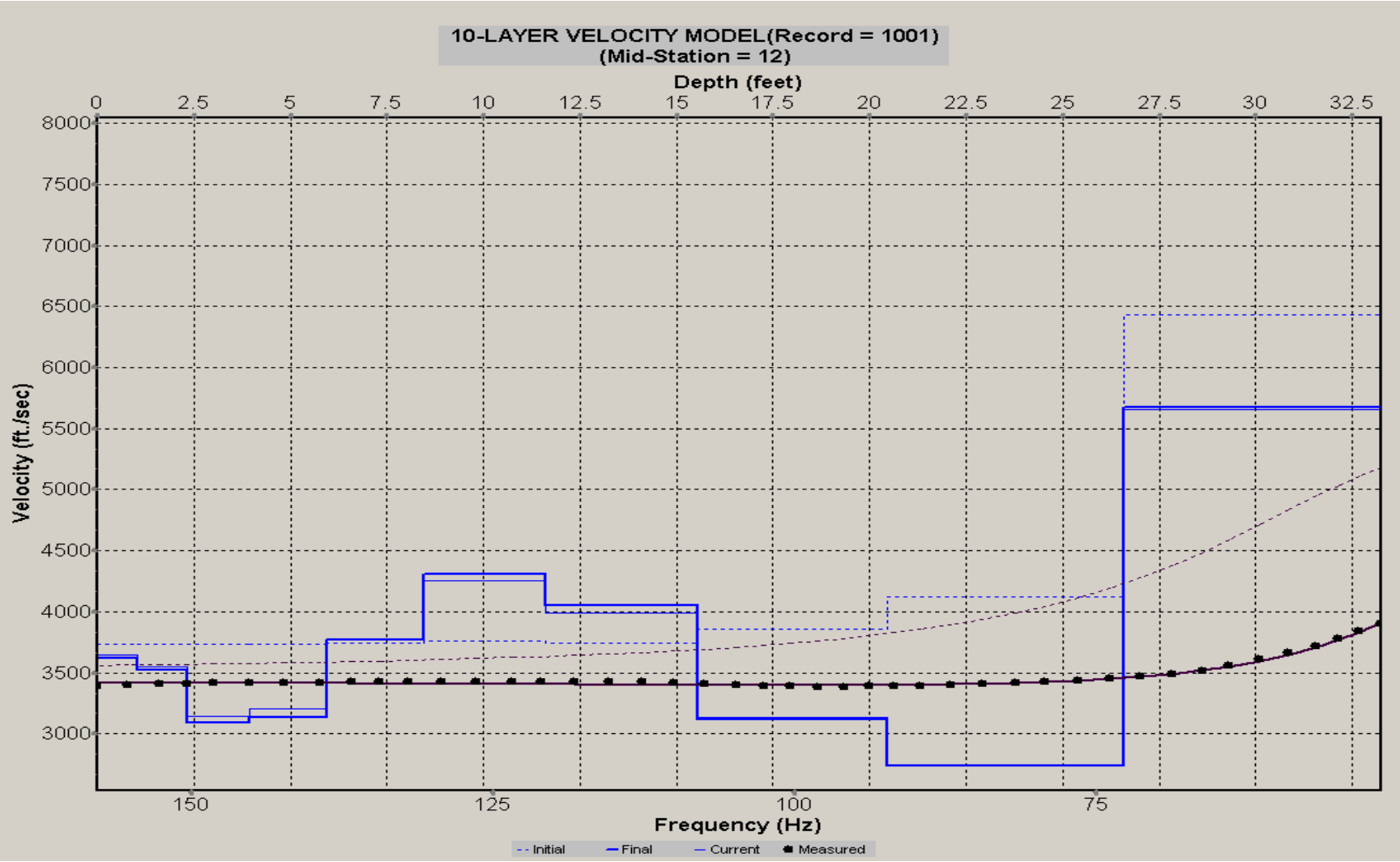

A.360: Velocity Profile Line 1259 used in Pre-blast 12, Post-blast 15, Pre-blast 29 and Pre-blast 30

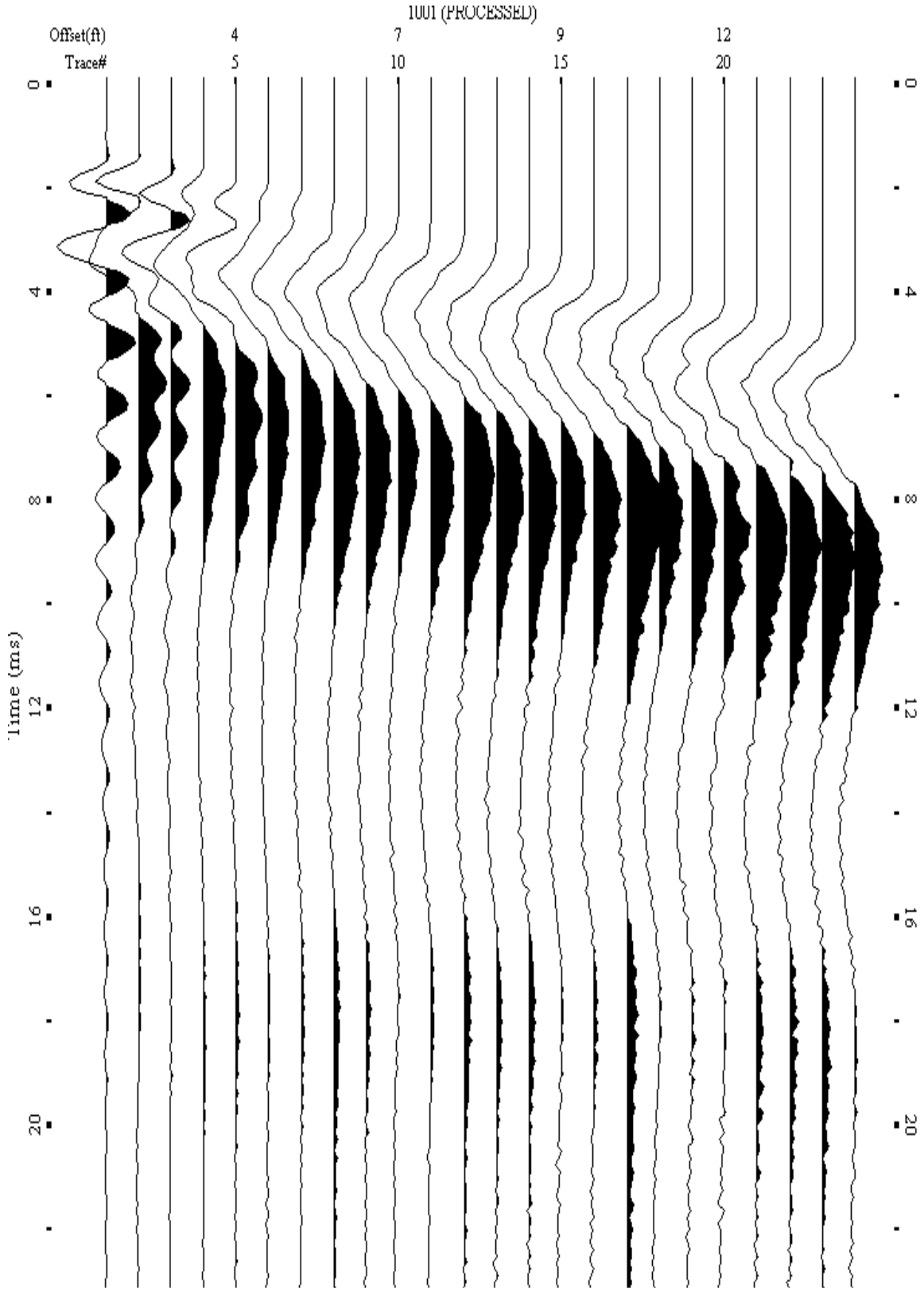

A.361: Shot Gather Line 1260 used in Pre-blast 12, Post-blast 15, Pre-blast 29 and Pre-blast 30

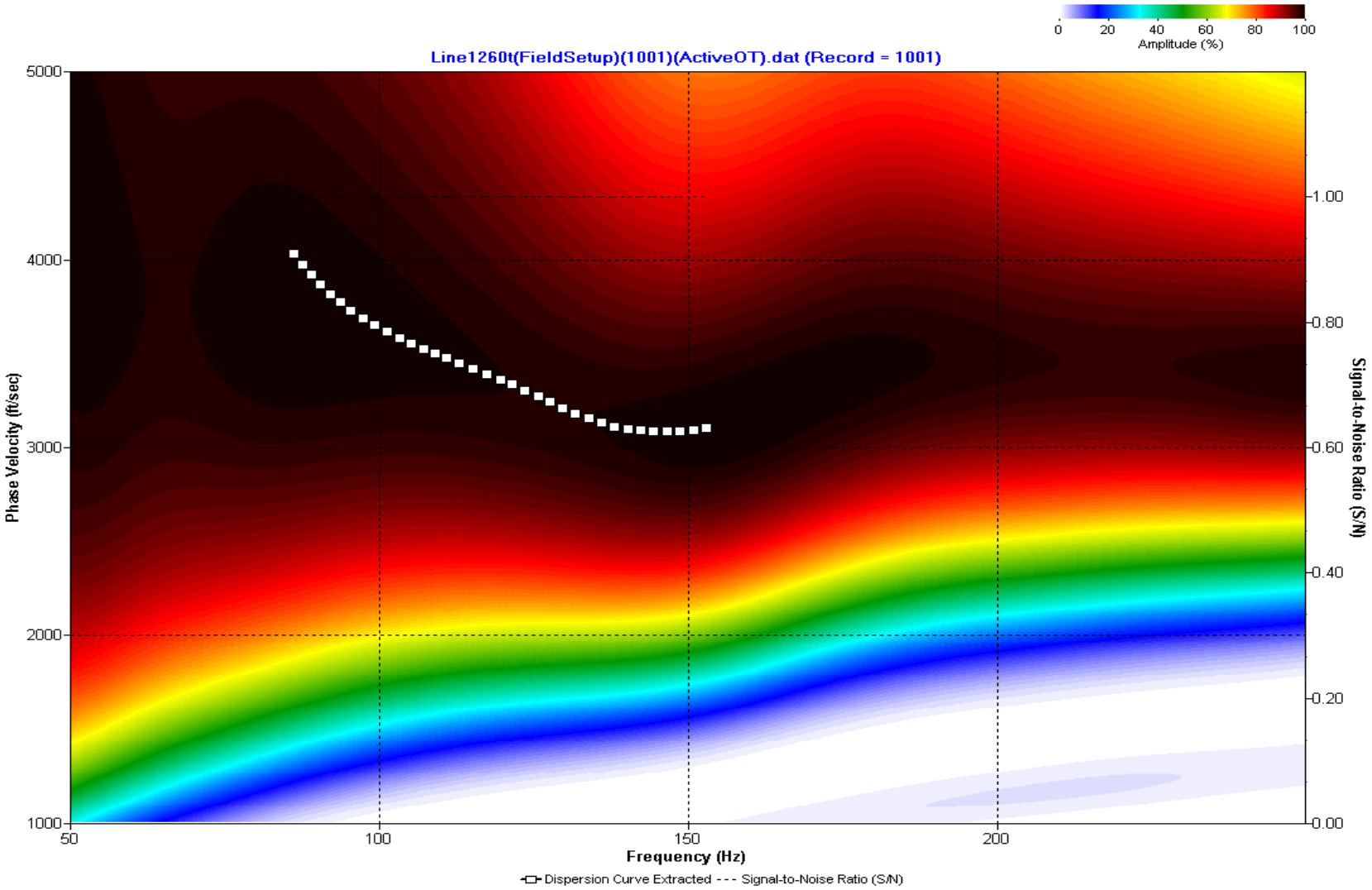

A.362: Dispersion Curve Line 1260 used in Pre-blast 12, Post-blast 15, Pre-blast 29 and Pre-blast 30

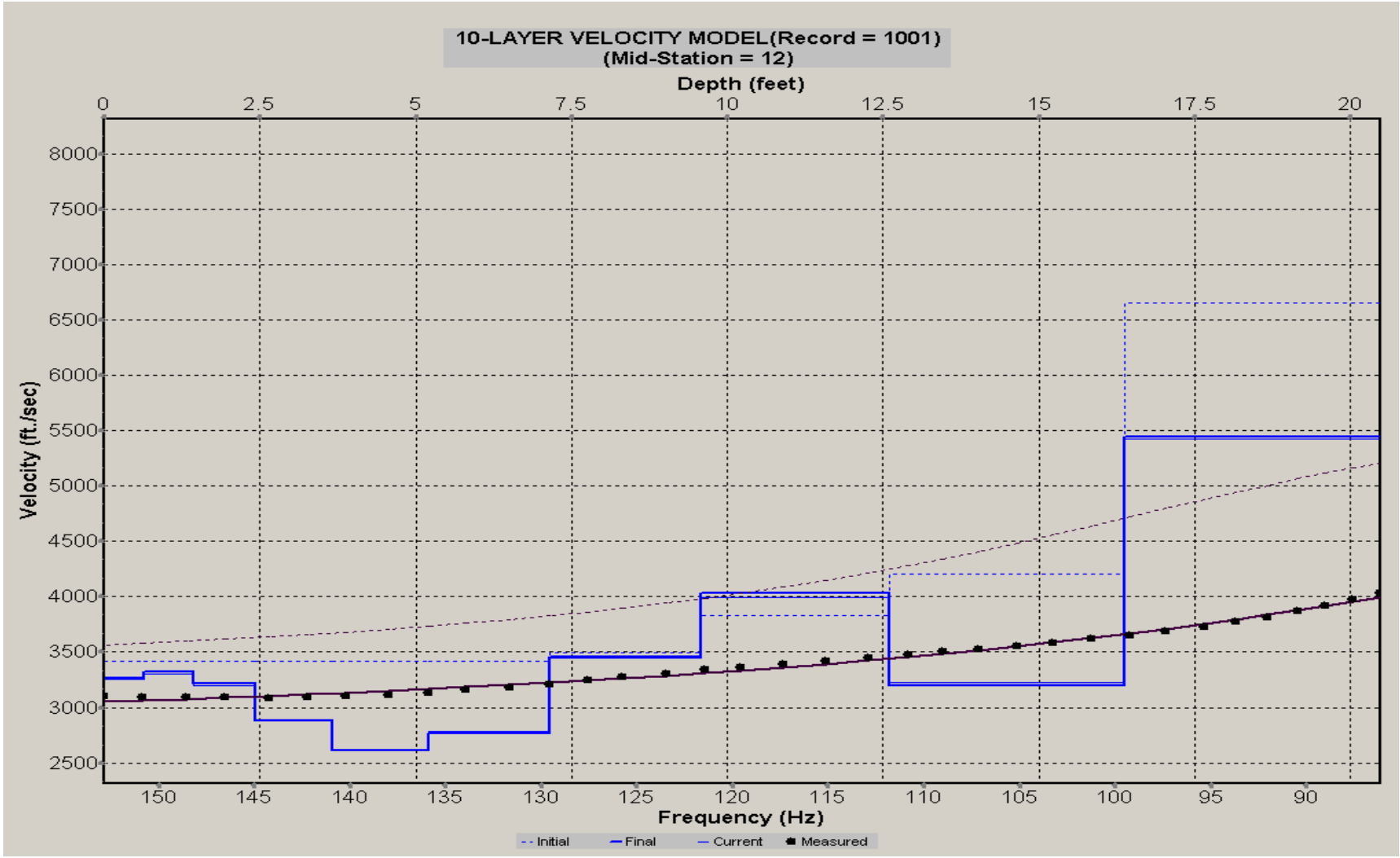

A.363: Velocity Profile Line 1260 used in Pre-blast 12, Post-blast 15, Pre-blast 29 and Pre-blast 30

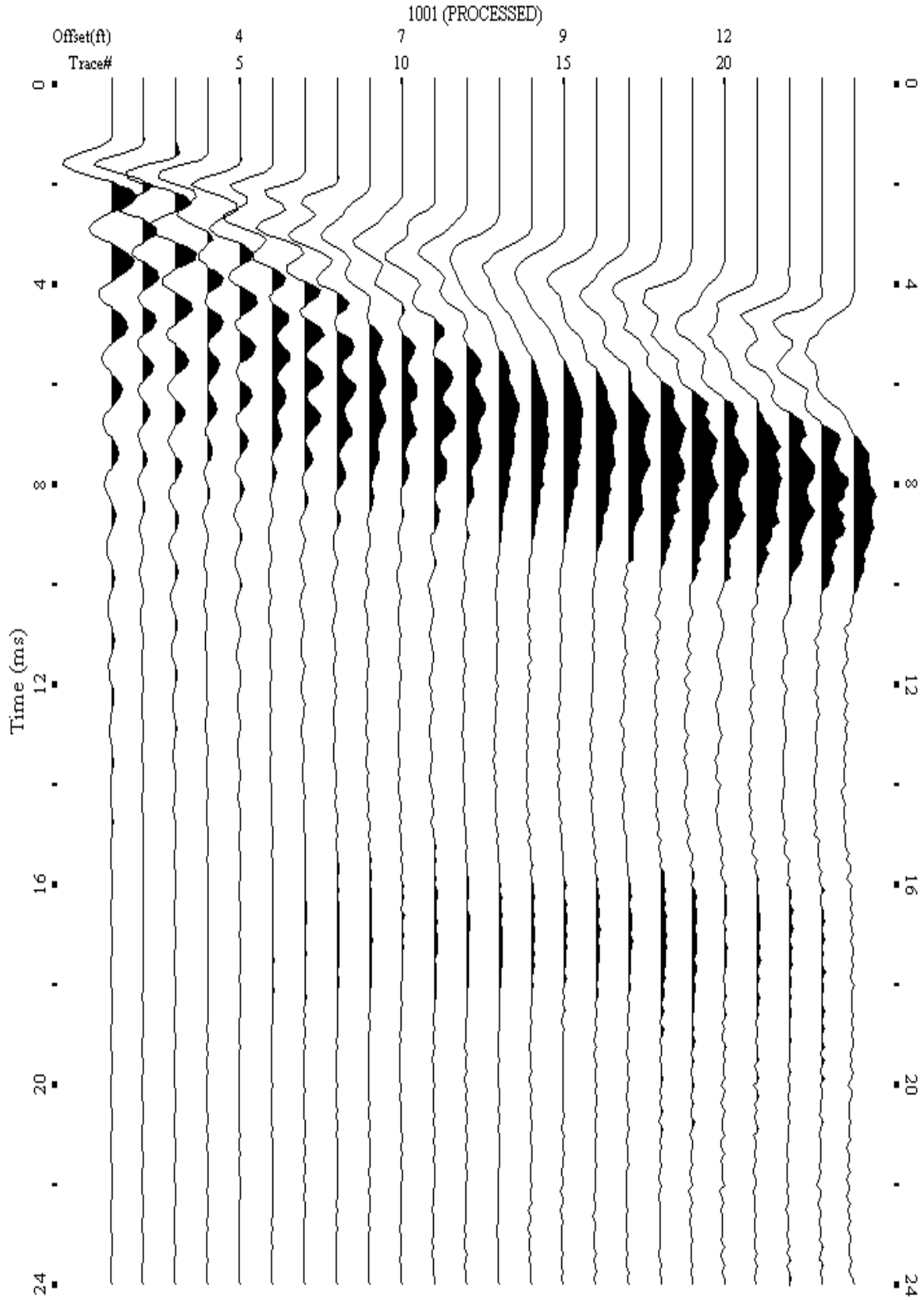

A.364: Shot Gather Line 1261 used in Post-blast 15 and Pre-blast 29

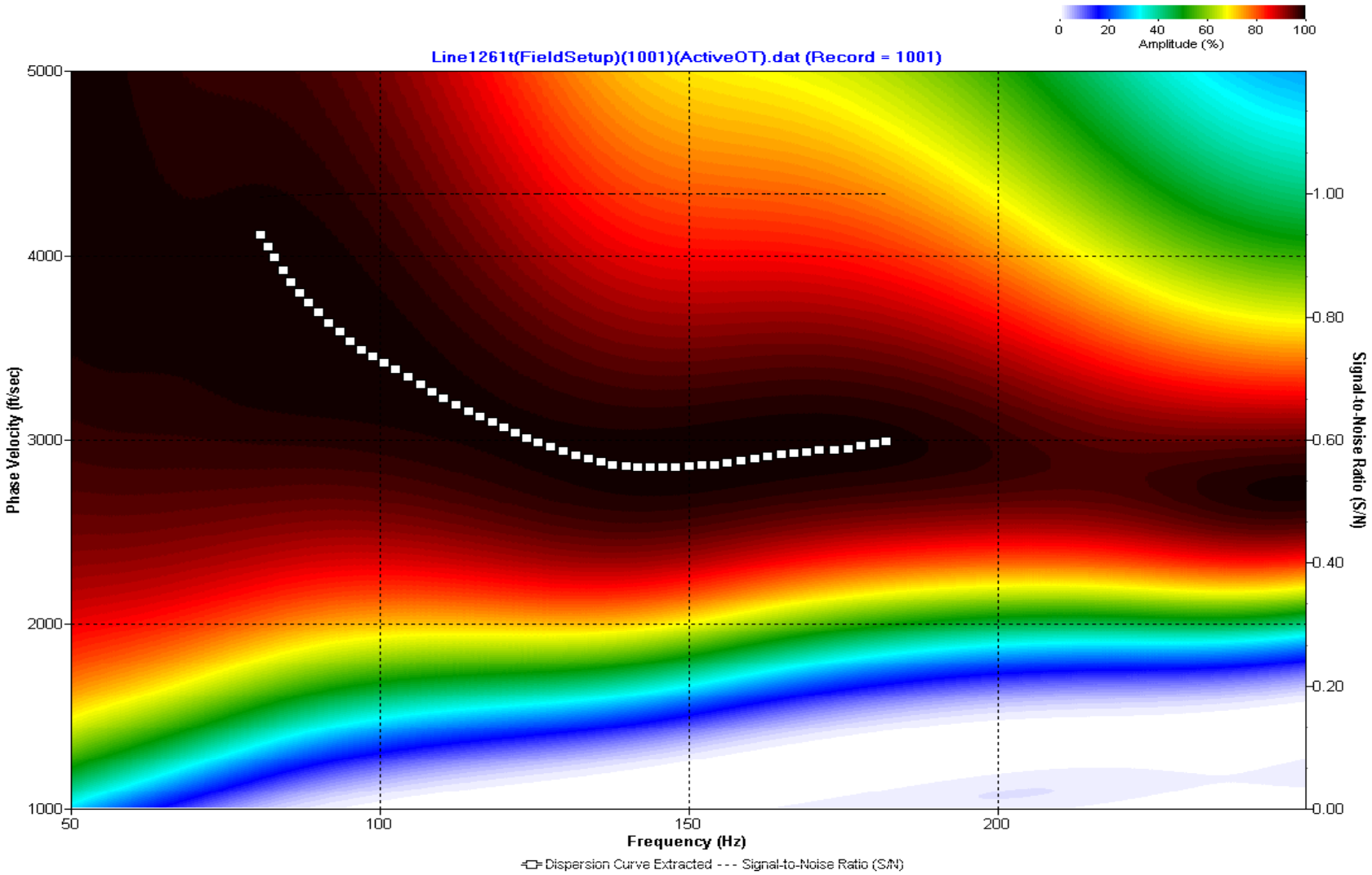

A.365: Dispersion Curve Line 1261 used in Post-blast 15 and Pre-blast 29

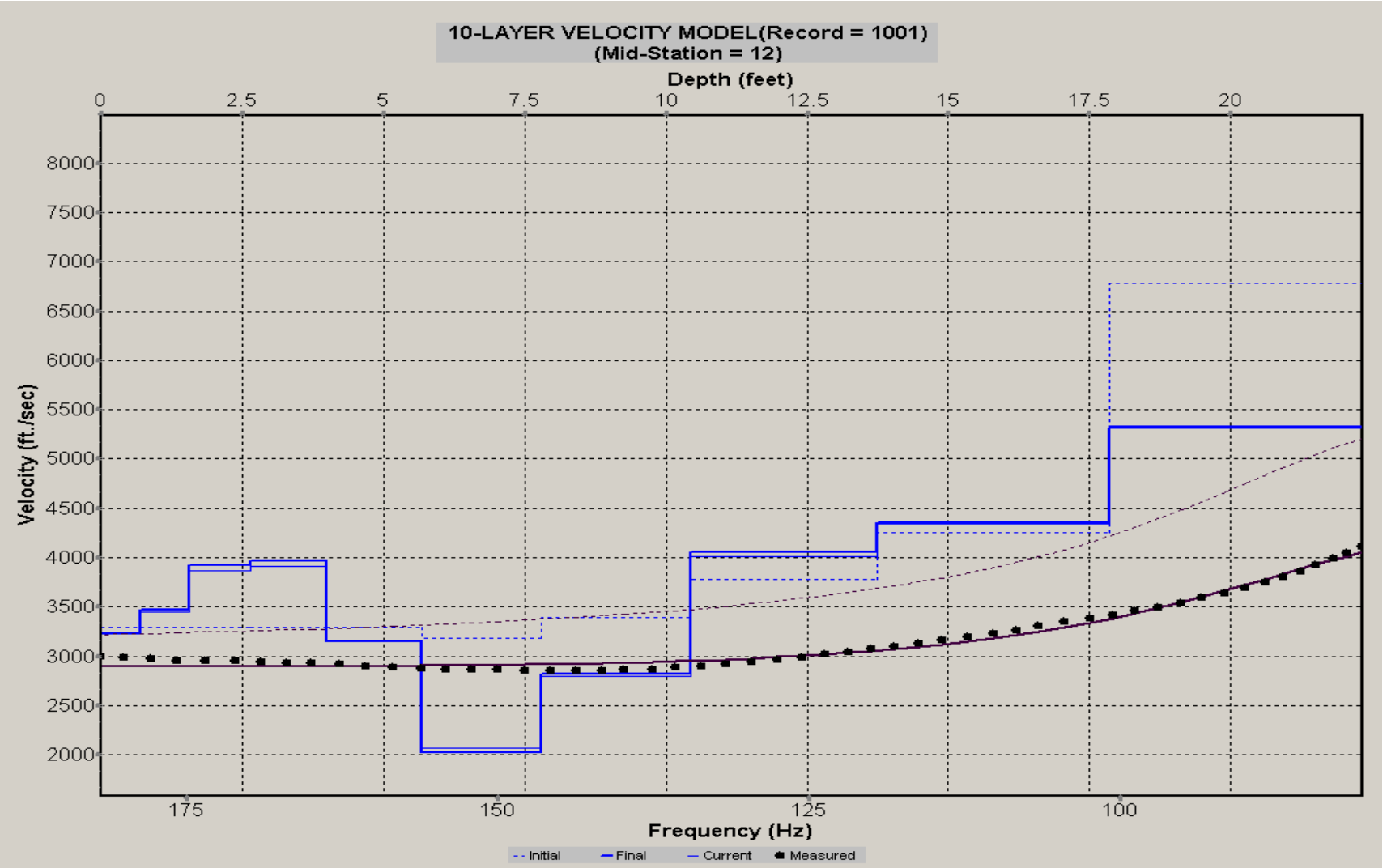

A.366: Velocity Profile Line 1261 used in Post-blast 15 and Pre-blast 29

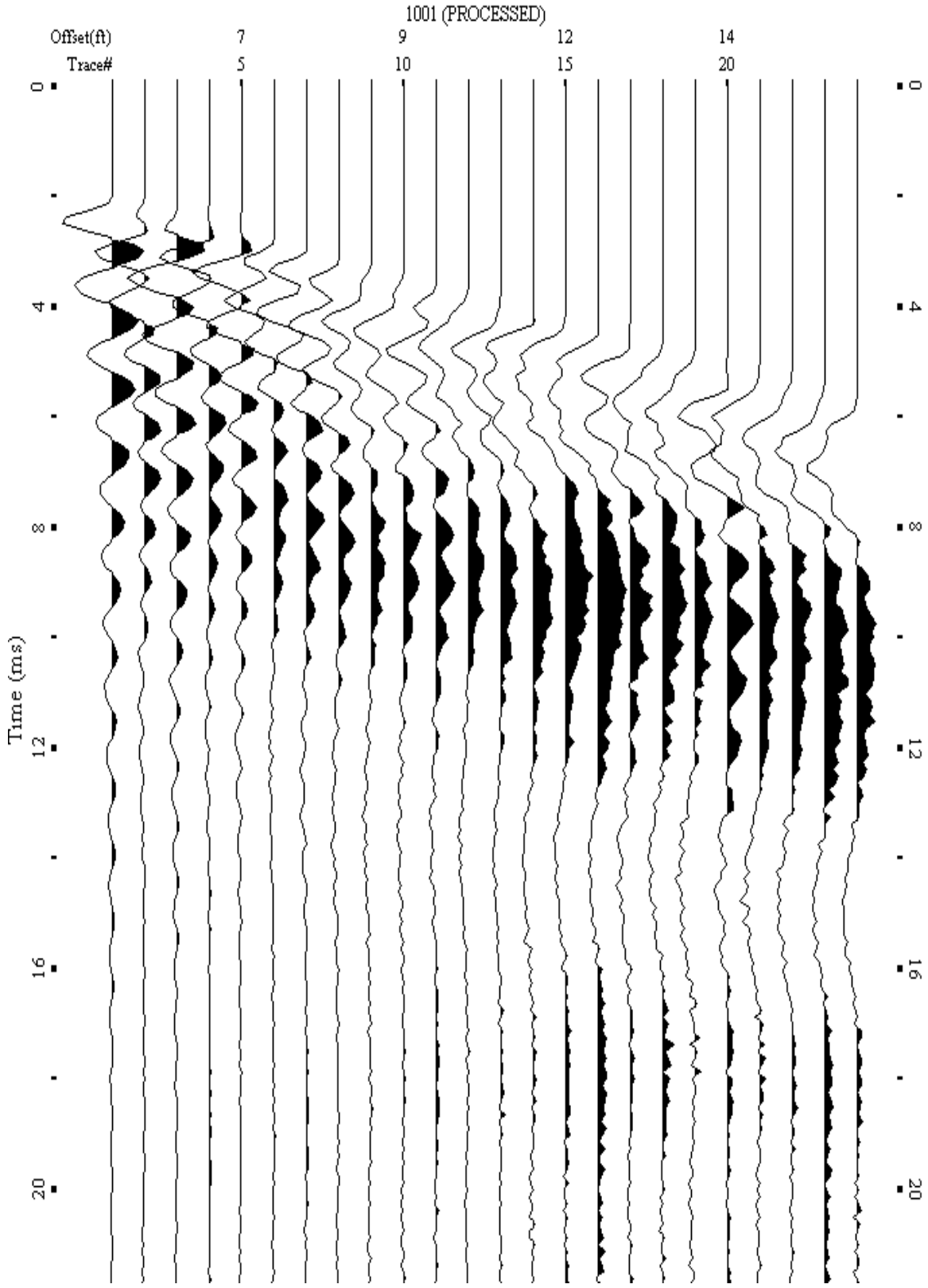

A.367: Shot Gather Line 1262 used in Pre-blast 12, Post-blast 15, Pre-blast 29 and Pre-blast 30

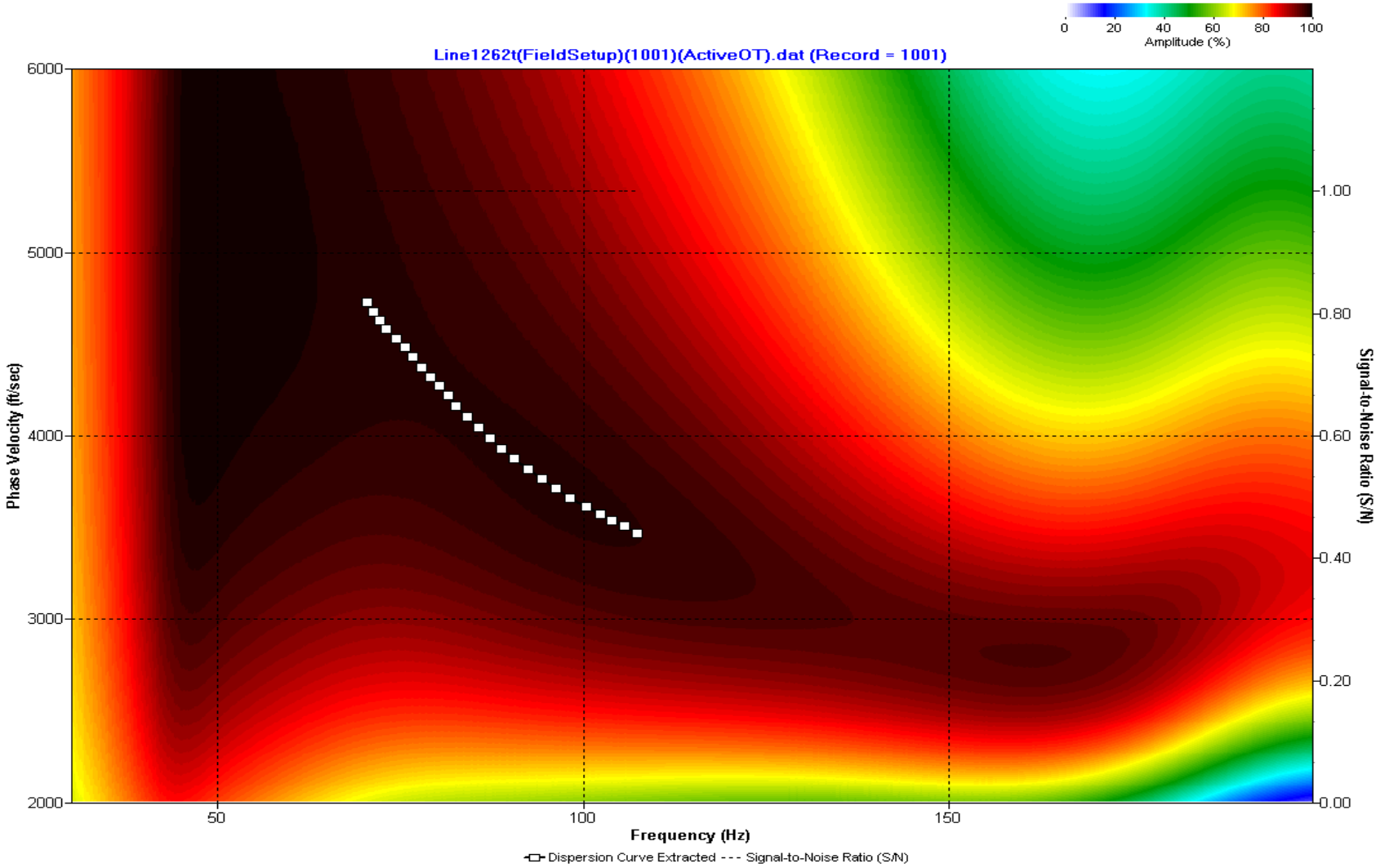

A.368: Dispersion Curve Line 1262 used in Pre-blast 12, Post-blast 15, Pre-blast 29 and Pre-blast 30

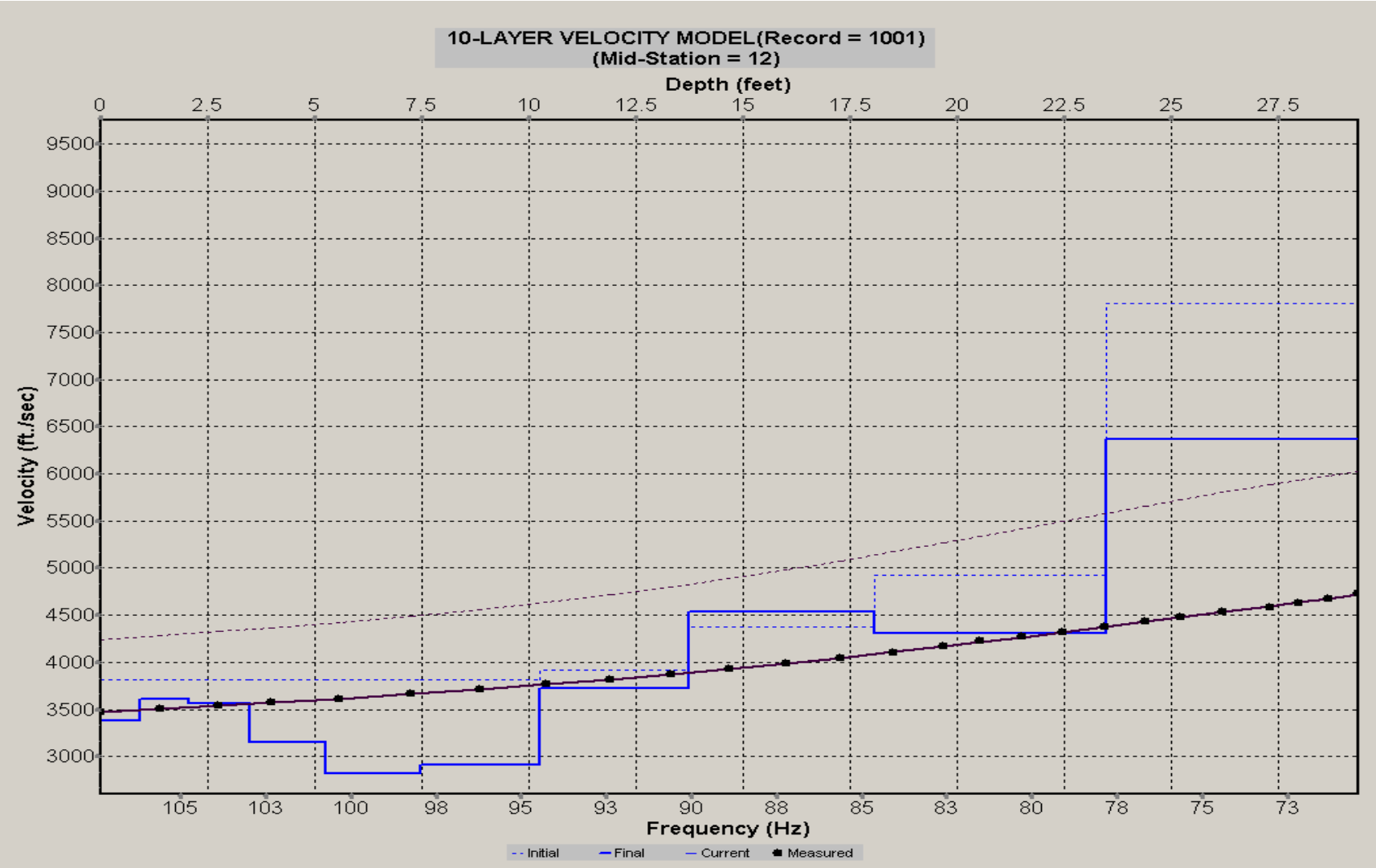

A.369: Velocity Profile Line 1262 used in Pre-blast 12, Post-blast 15, Pre-blast 29 and Pre-blast 30

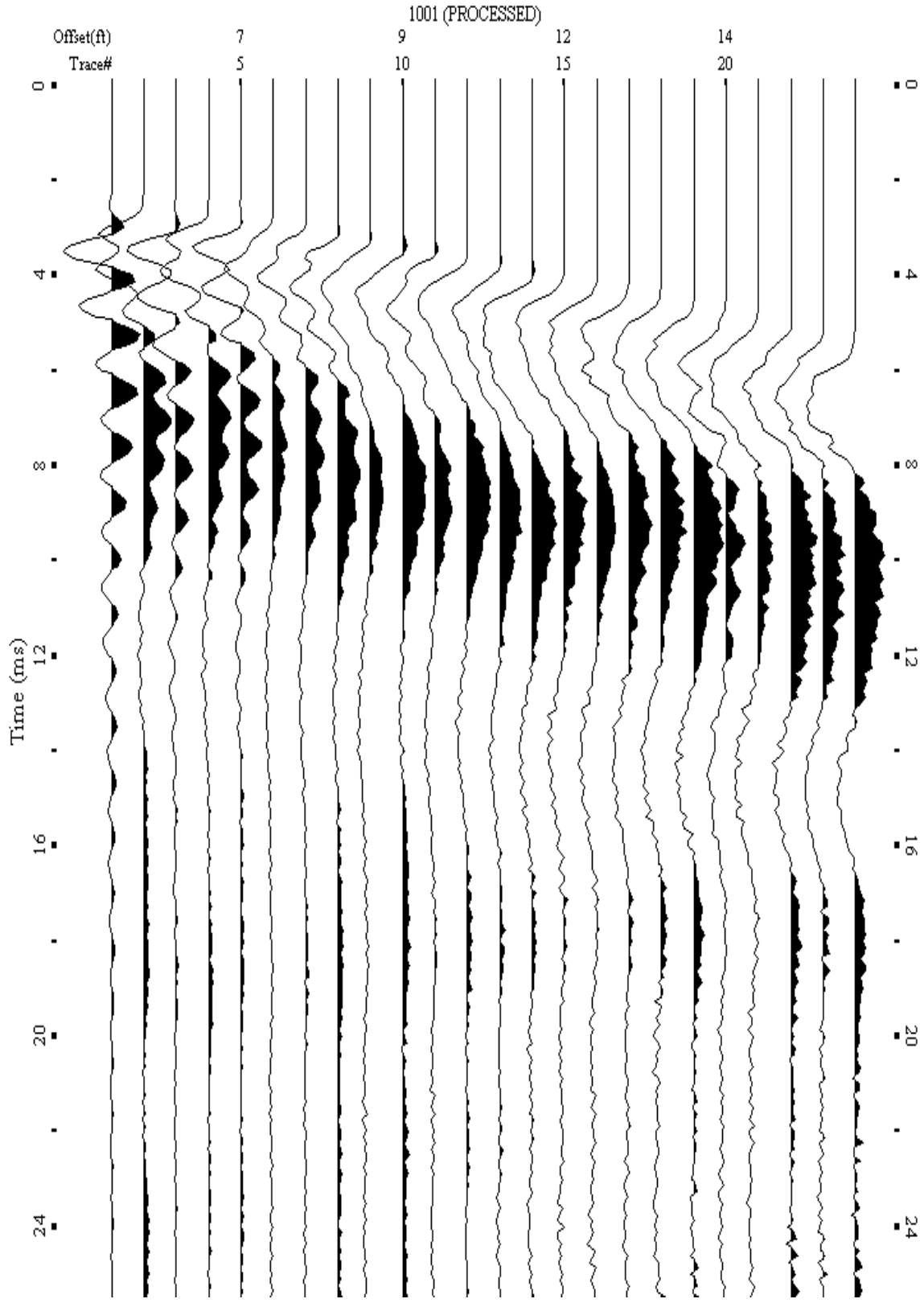

A.370: Shot Gather Line 1263 used in Post-blast 25

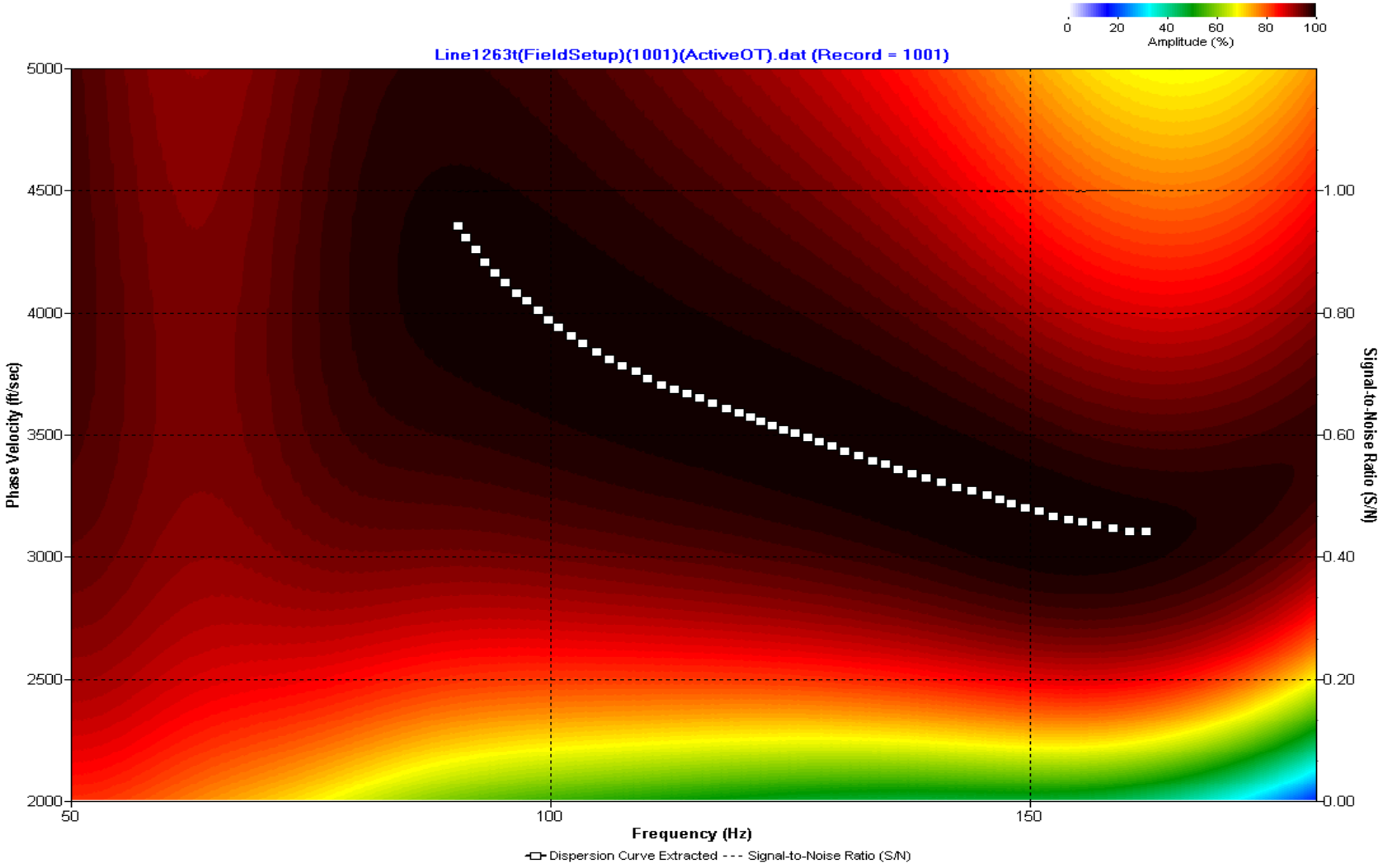

A.371: Dispersion Curve Line 1263 used in Post-blast 25

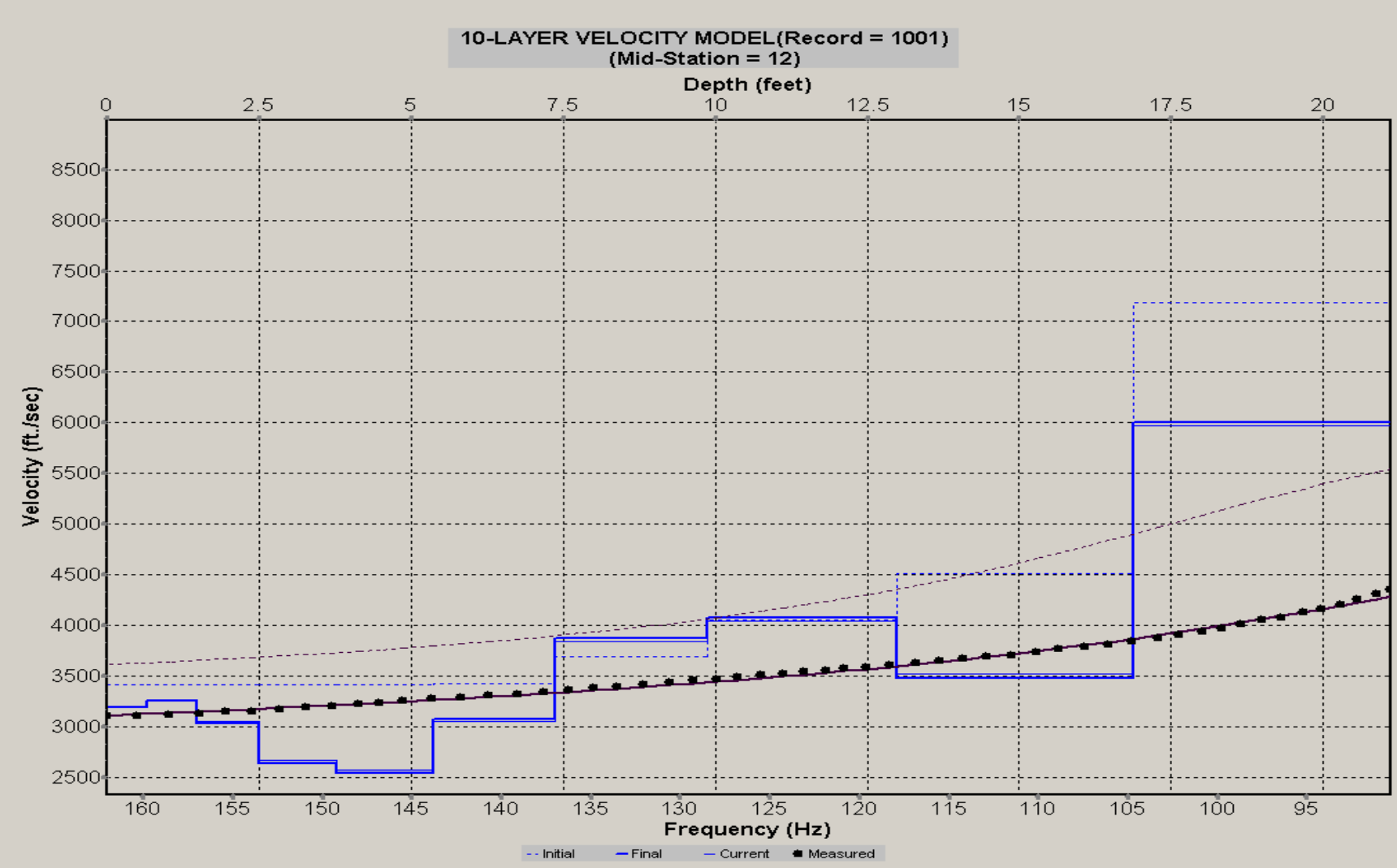

A.372: Velocity Profile Line 1263 used in Post-blast 25

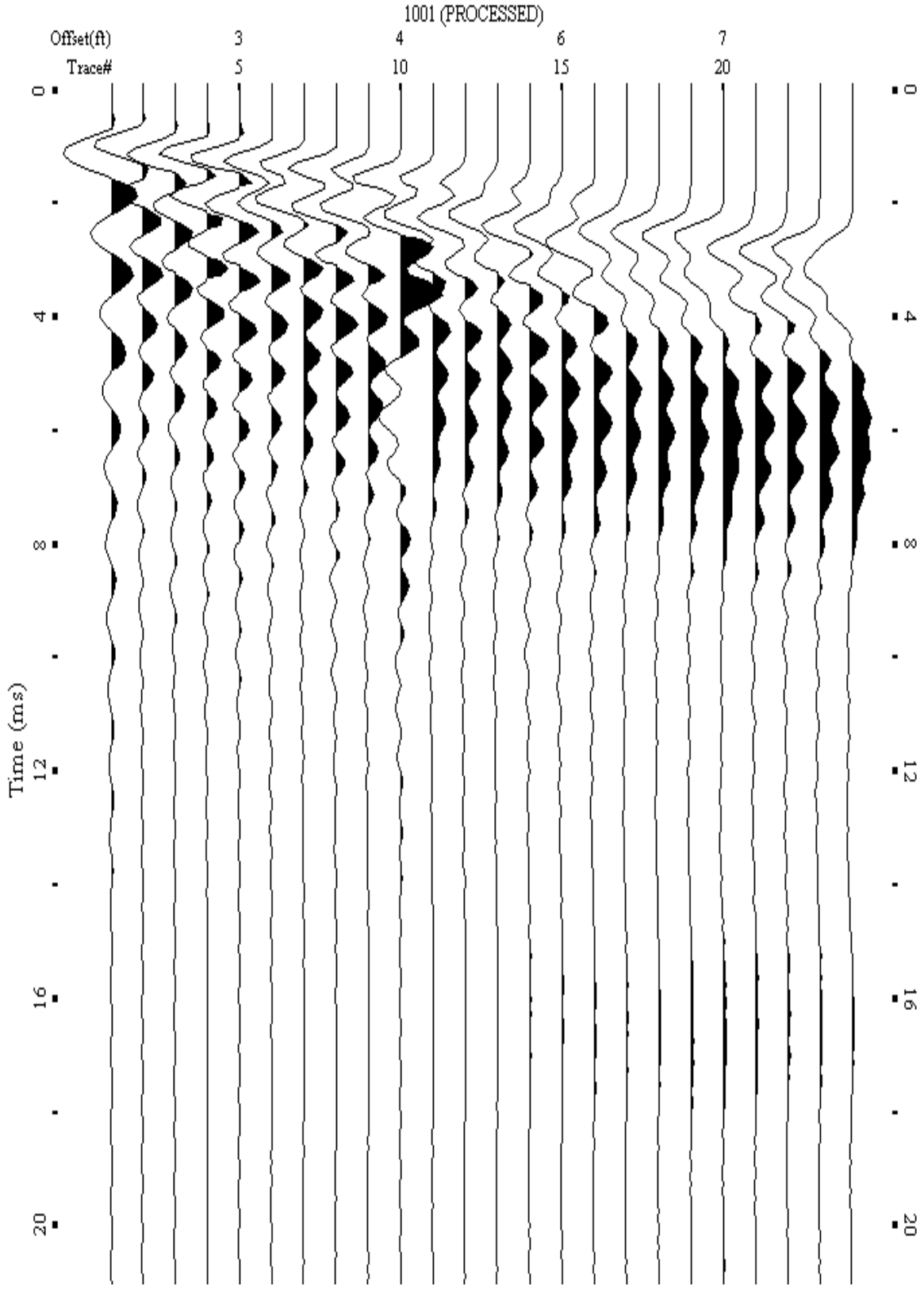

A.373: Shot Gather Line 1264 used in Post-blast 25

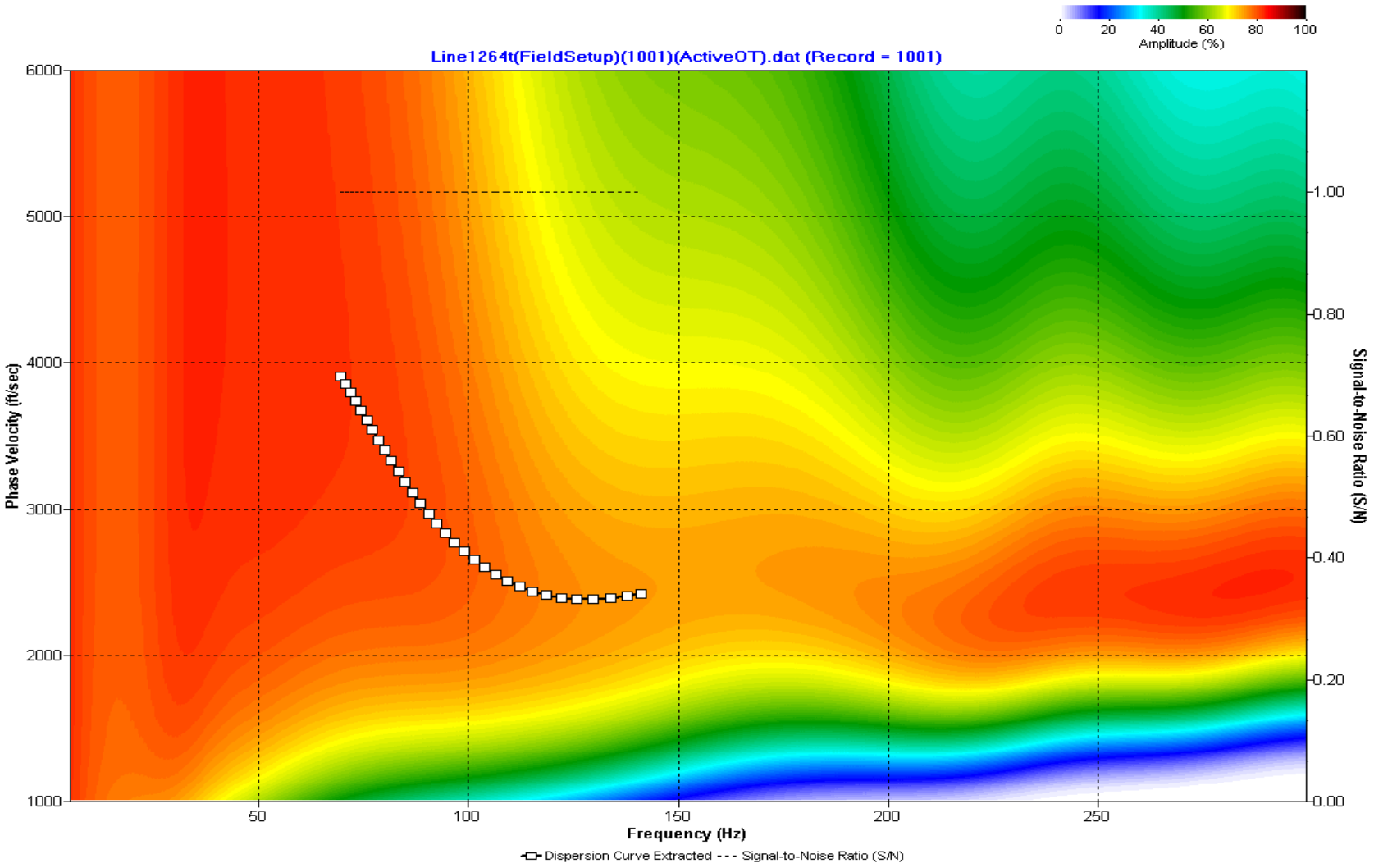

A.374: Dispersion Curve Line 1264 used in Post-blast 25

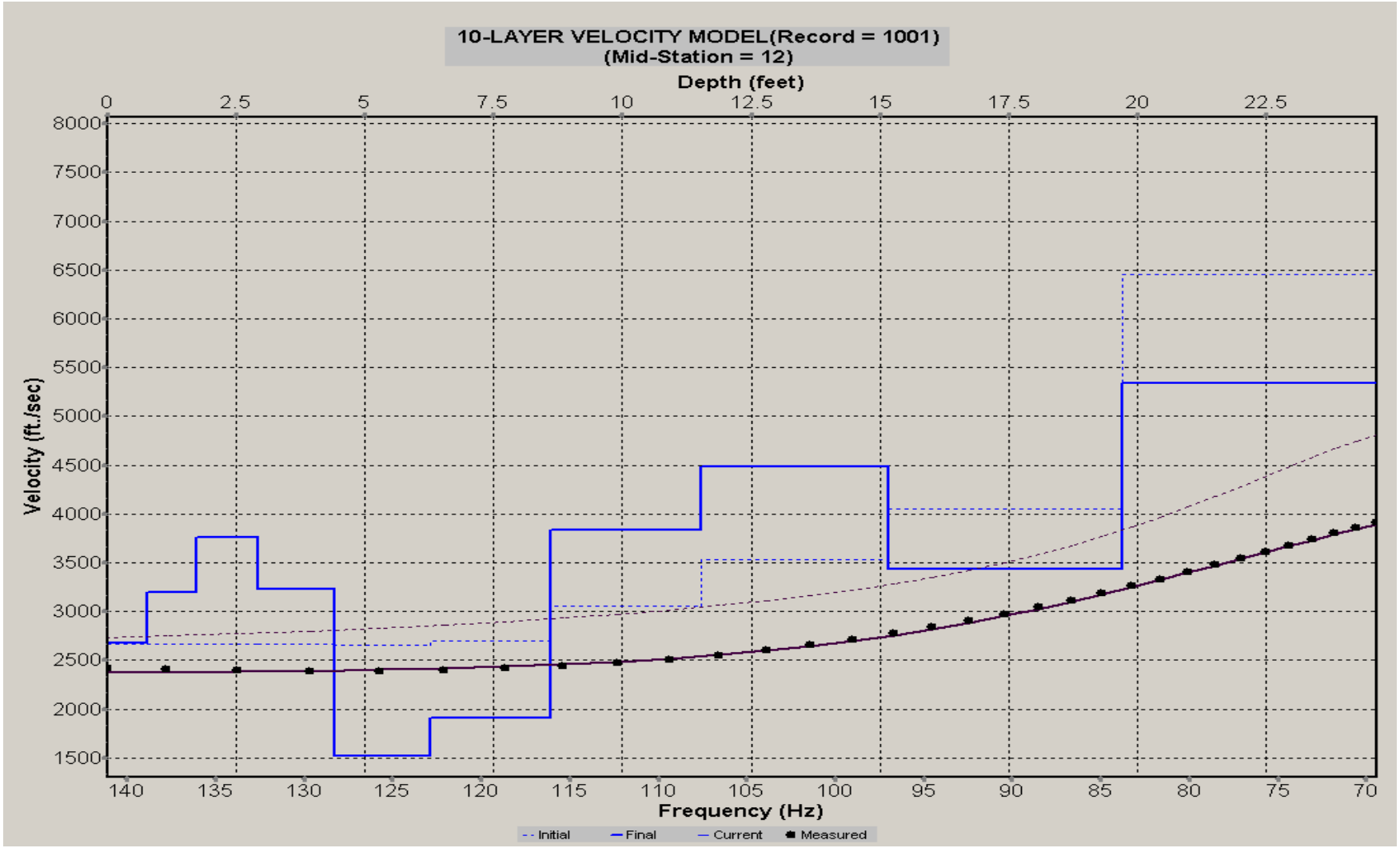

A.375: Velocity Profile Line 1264 used in Post-blast 25

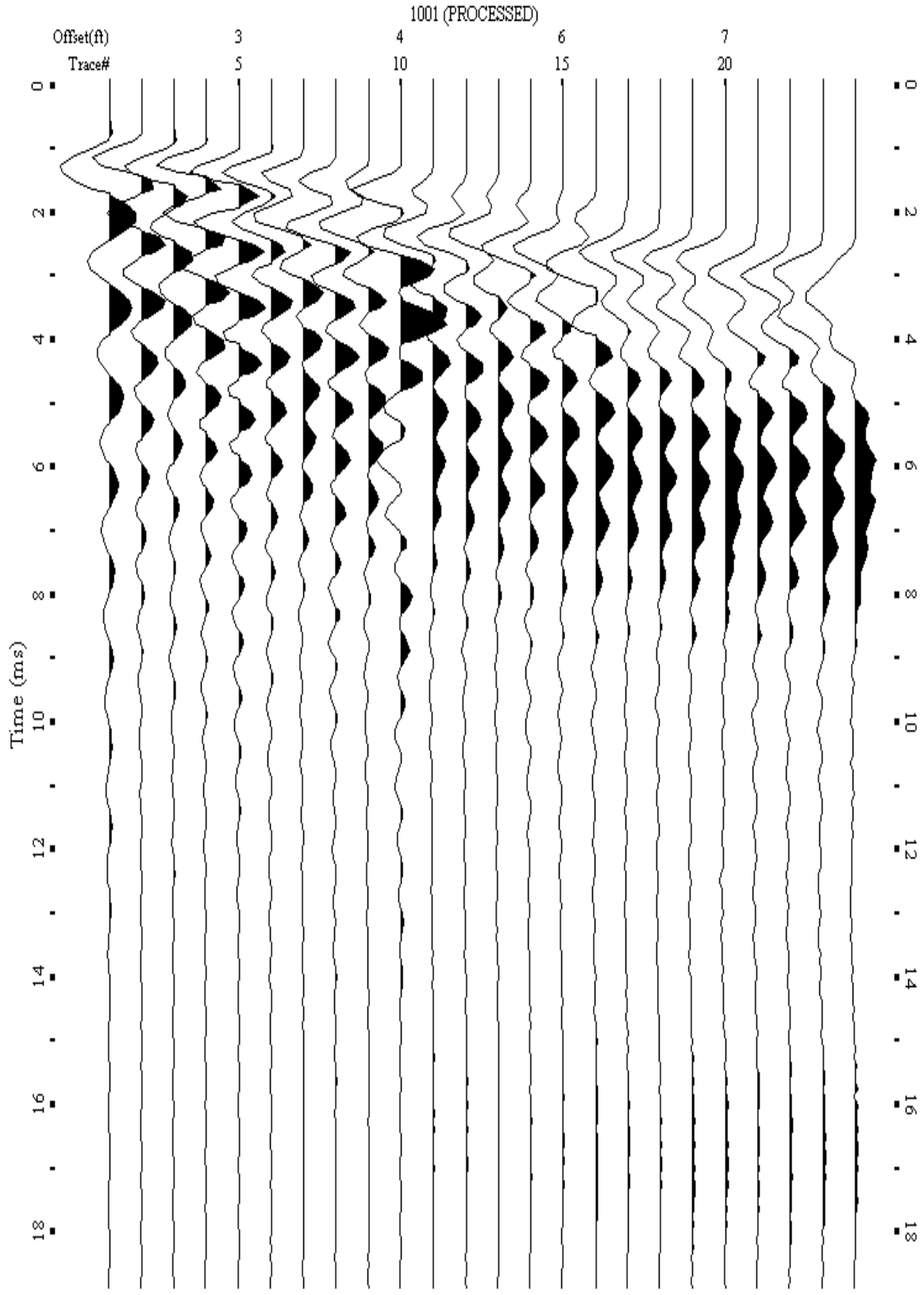

A.376: Shot Gather Line 1265 used in Post-blast 25

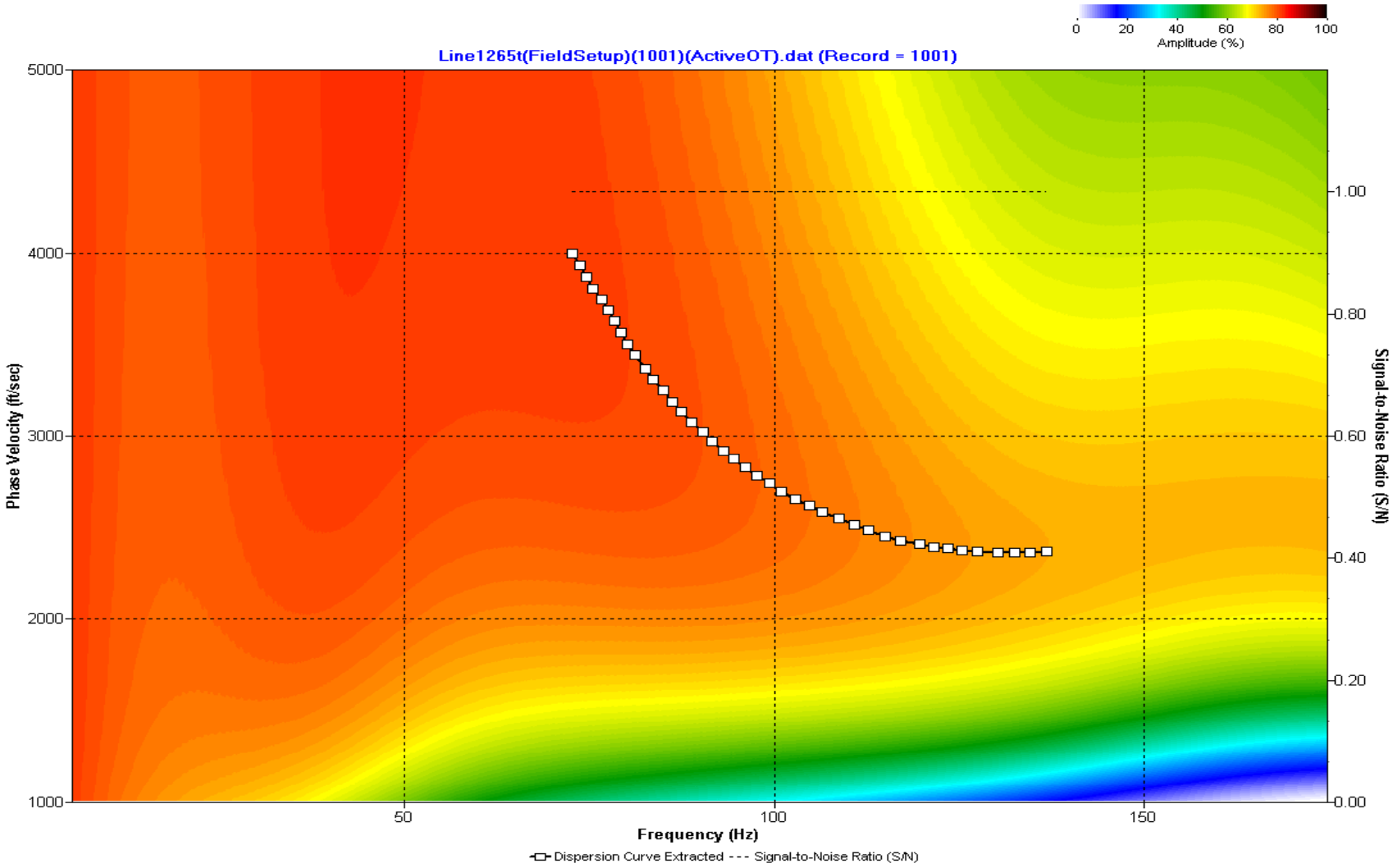

A.377: Dispersion Curve Line 1265 used in Post-blast 25

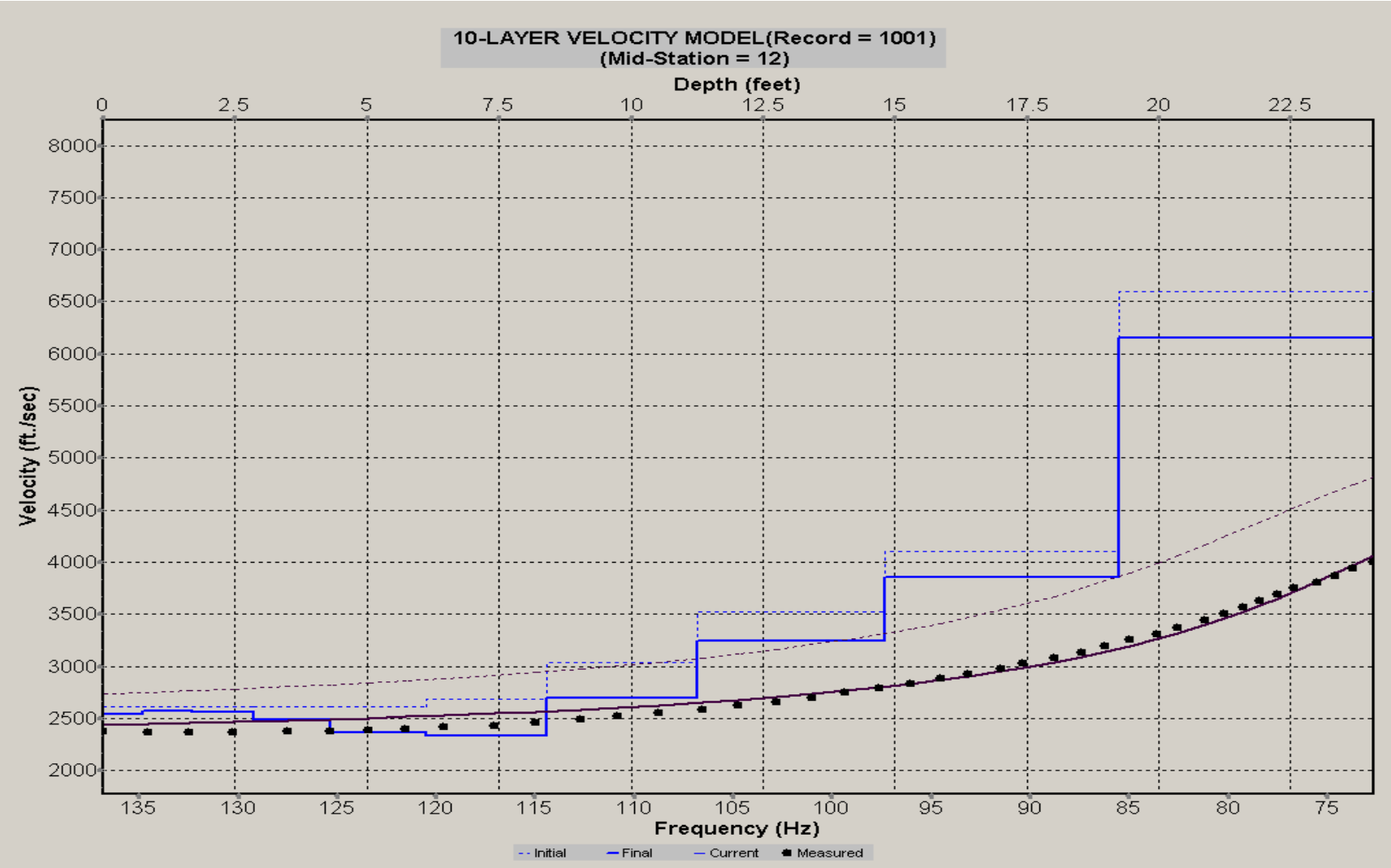

A.378: Velocity Profile Line 1265 used in Post-blast 25

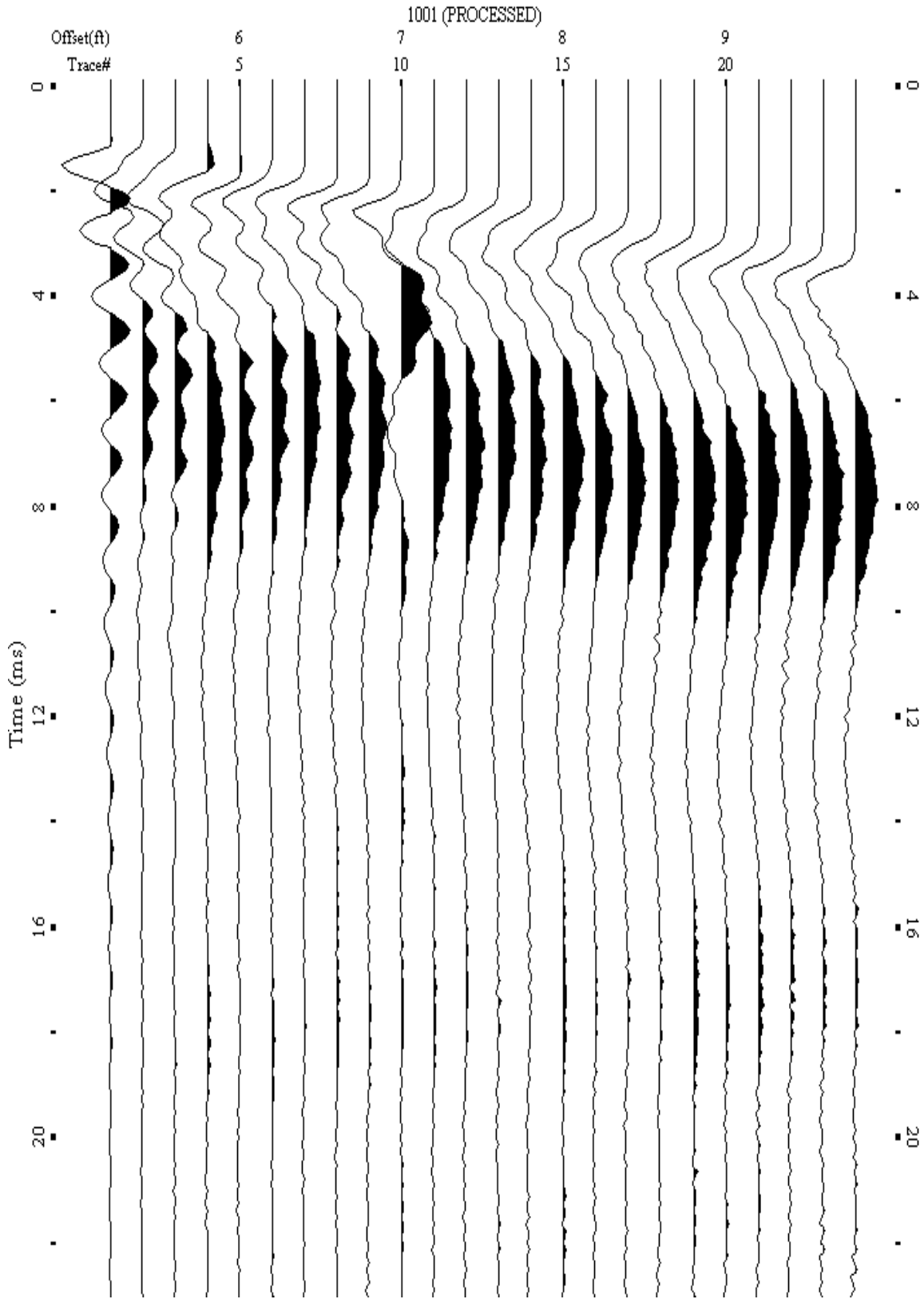

A.379: Shot Gather Line 1266 used in Post-blast 25

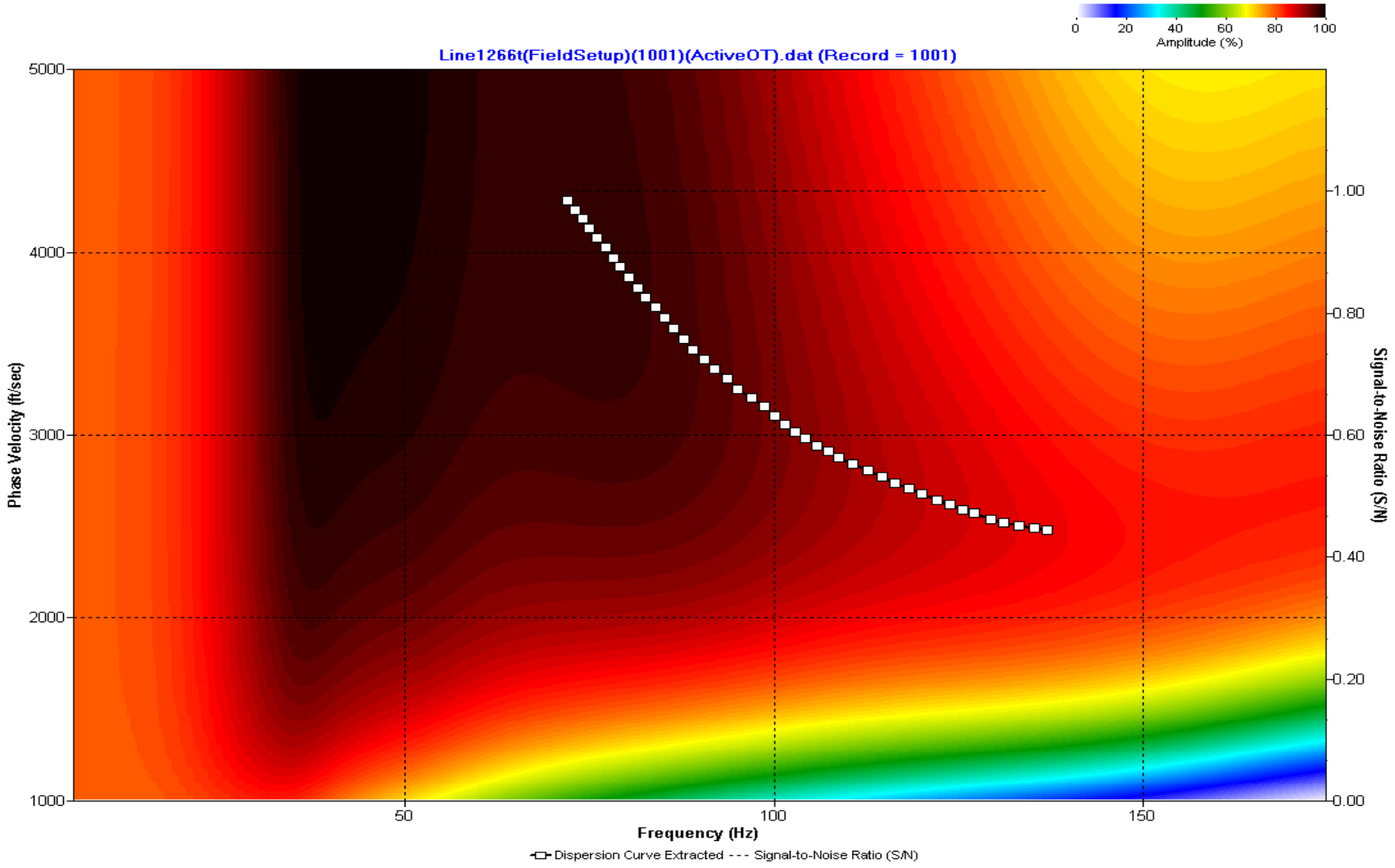

A.380: Dispersion Curve Line 1266 used in Post-blast 25

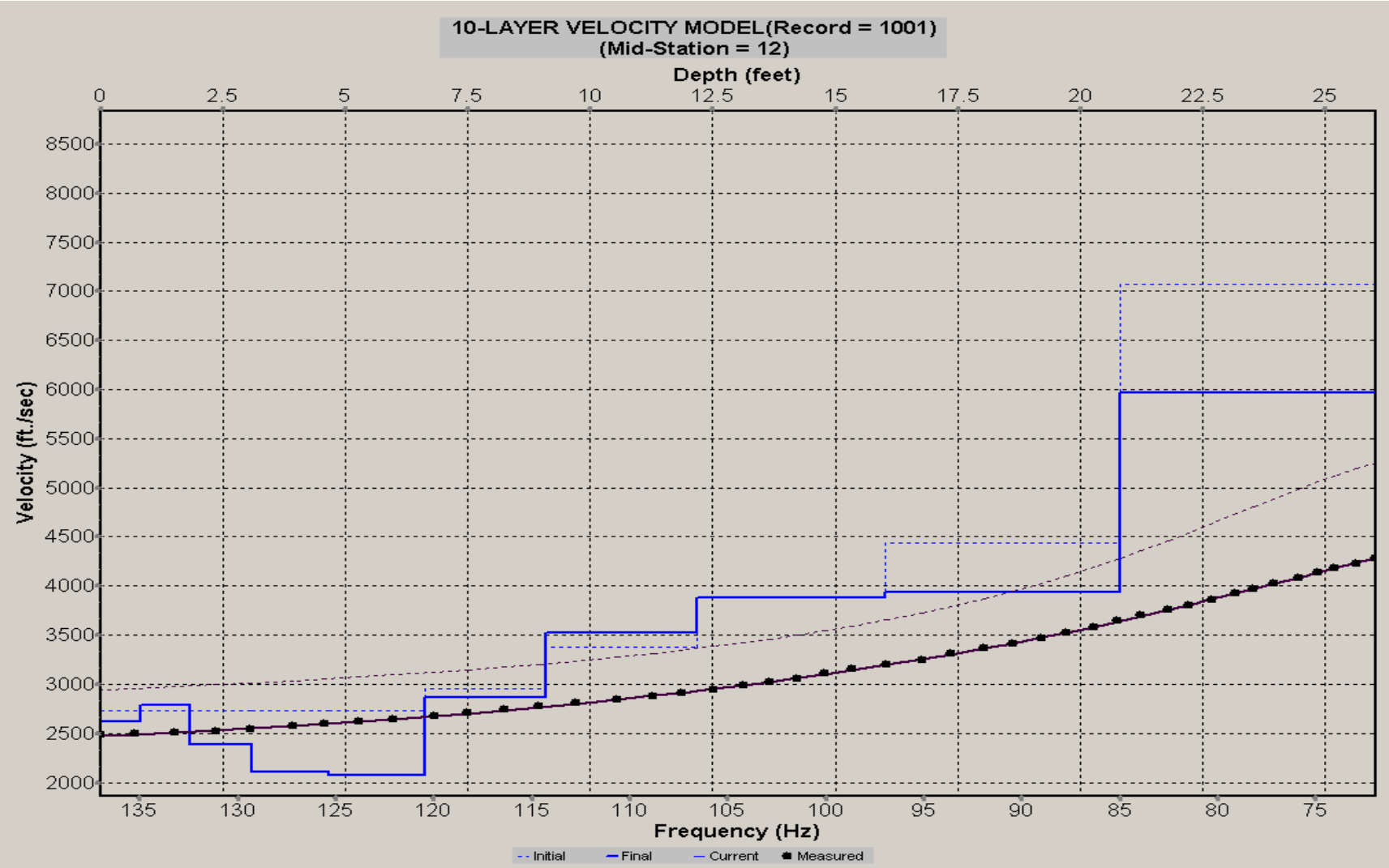

A.381: Velocity Profile Line 1266 used in Post-blast 25

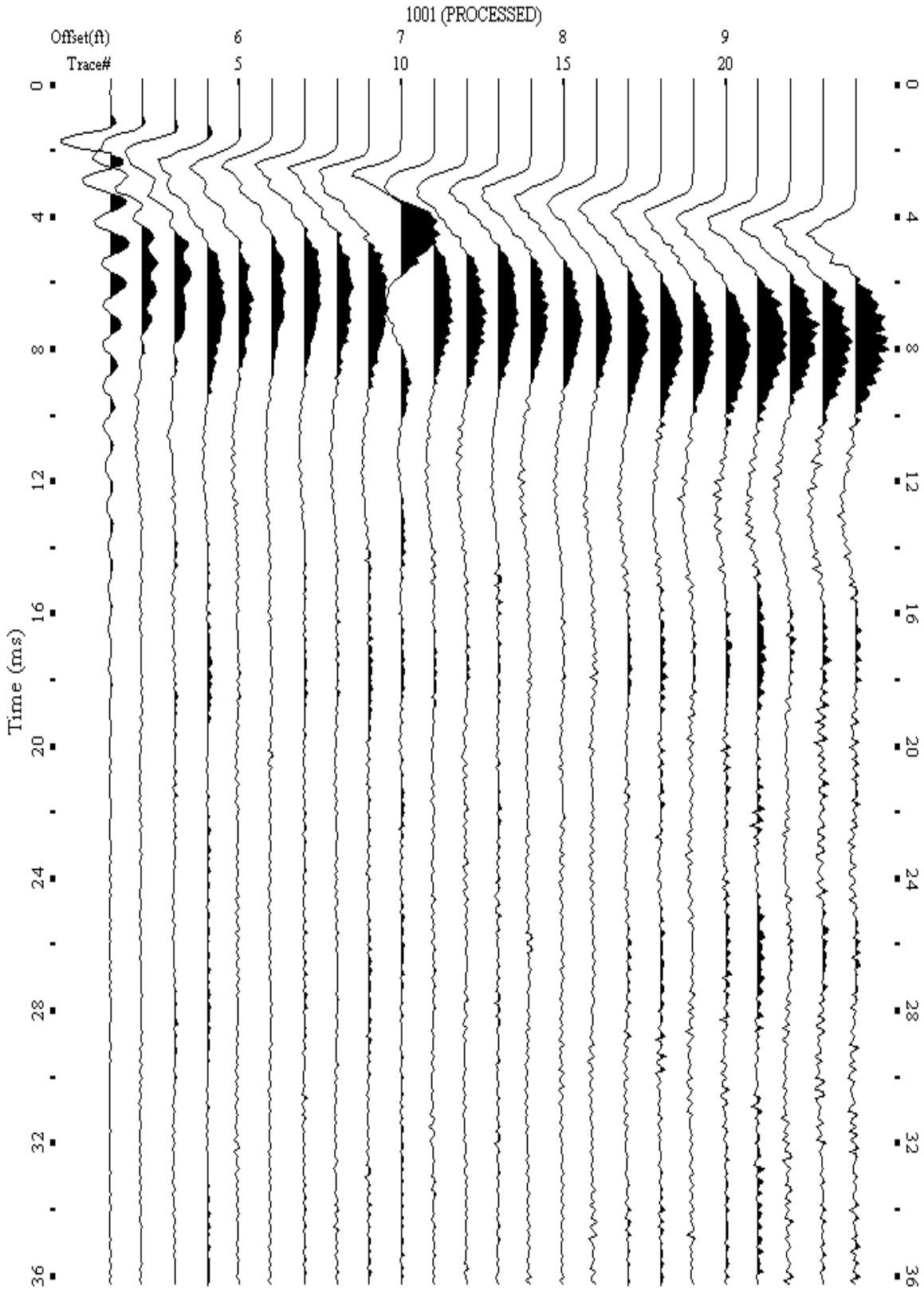

A.382: Shot Gather Line 1267 used in Post-blast 25

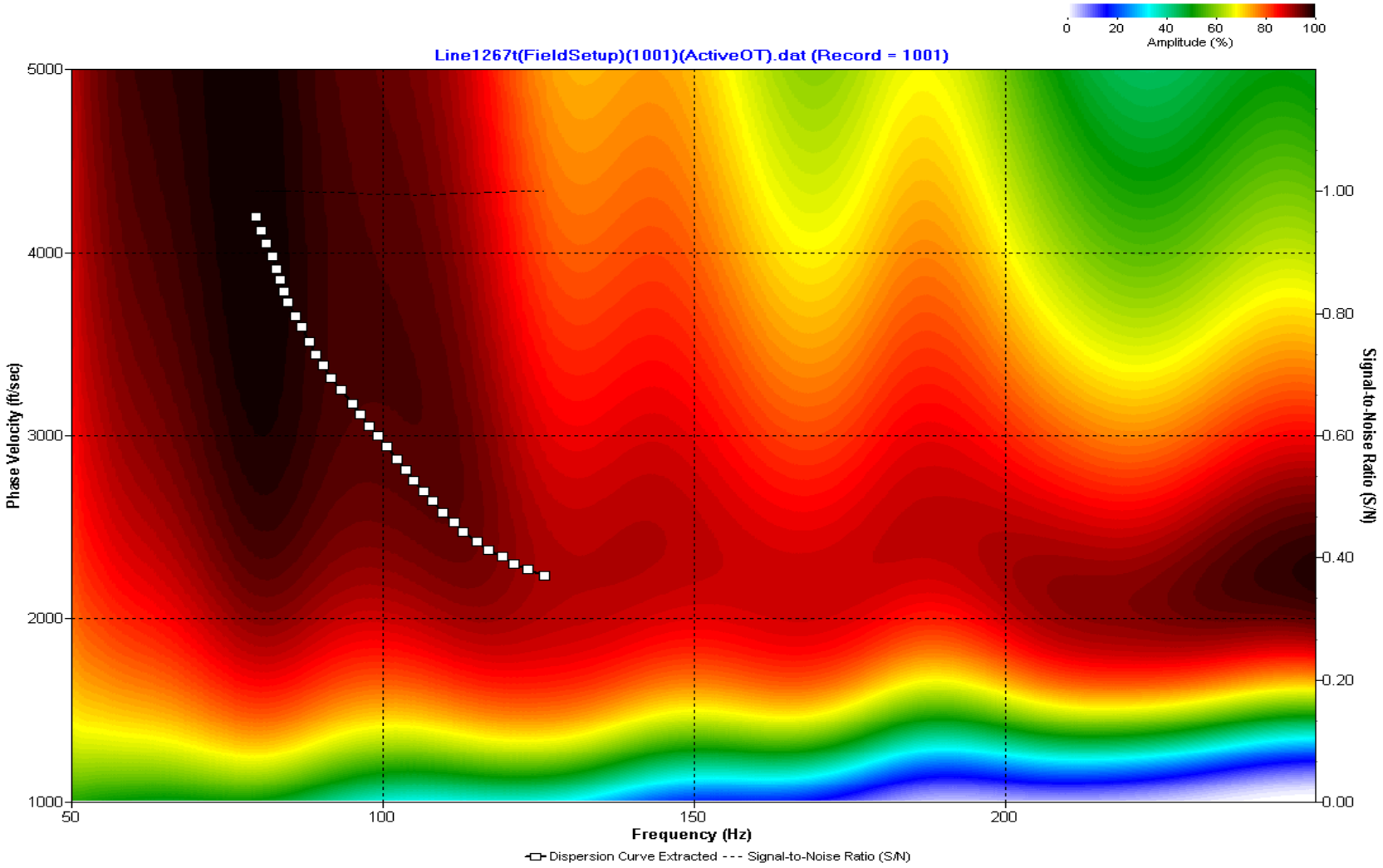

A.383: Dispersion Curve Line 1267 used in Post-blast 25

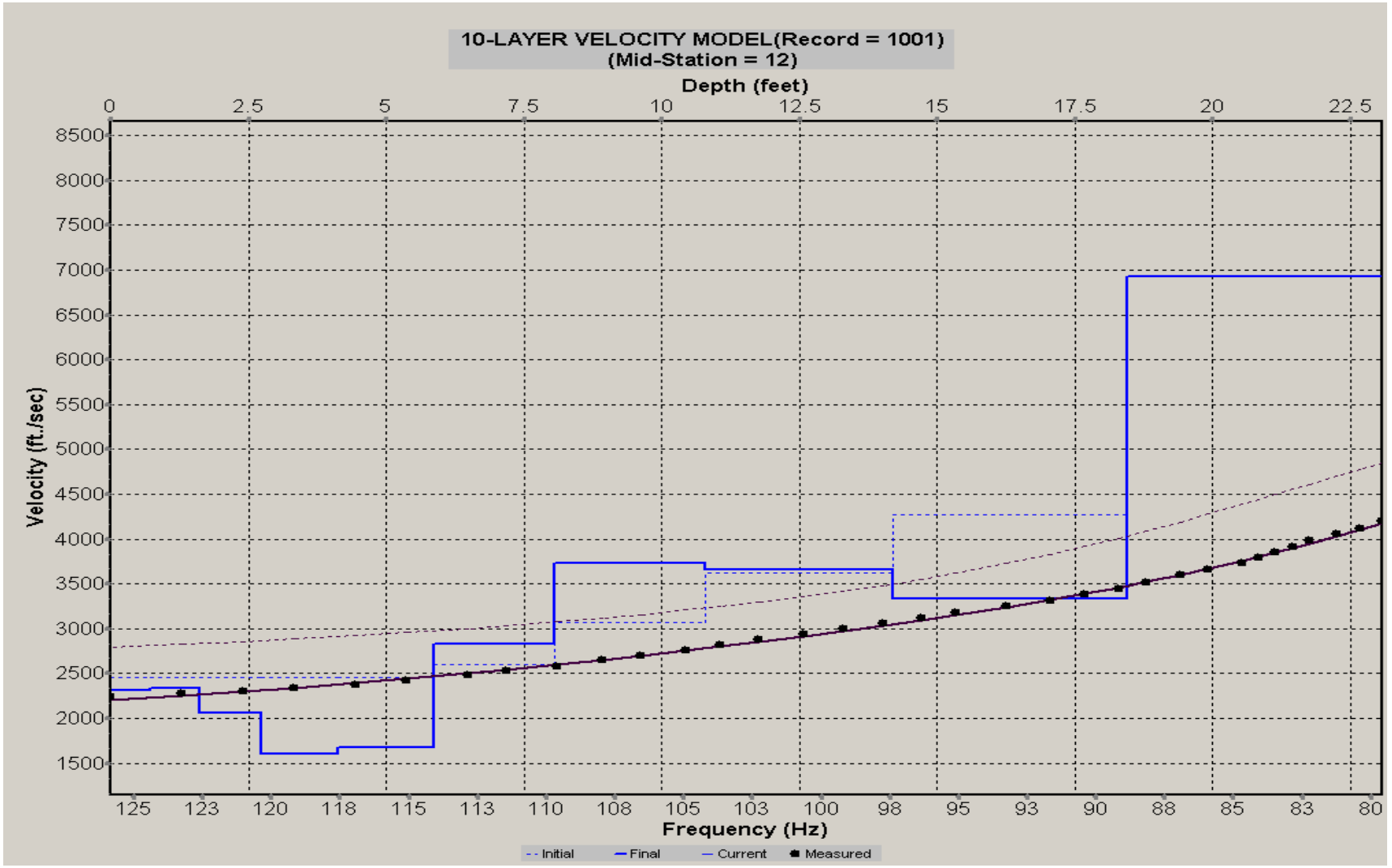

A.384: Velocity Profile Line 1267 used in Post-blast 25

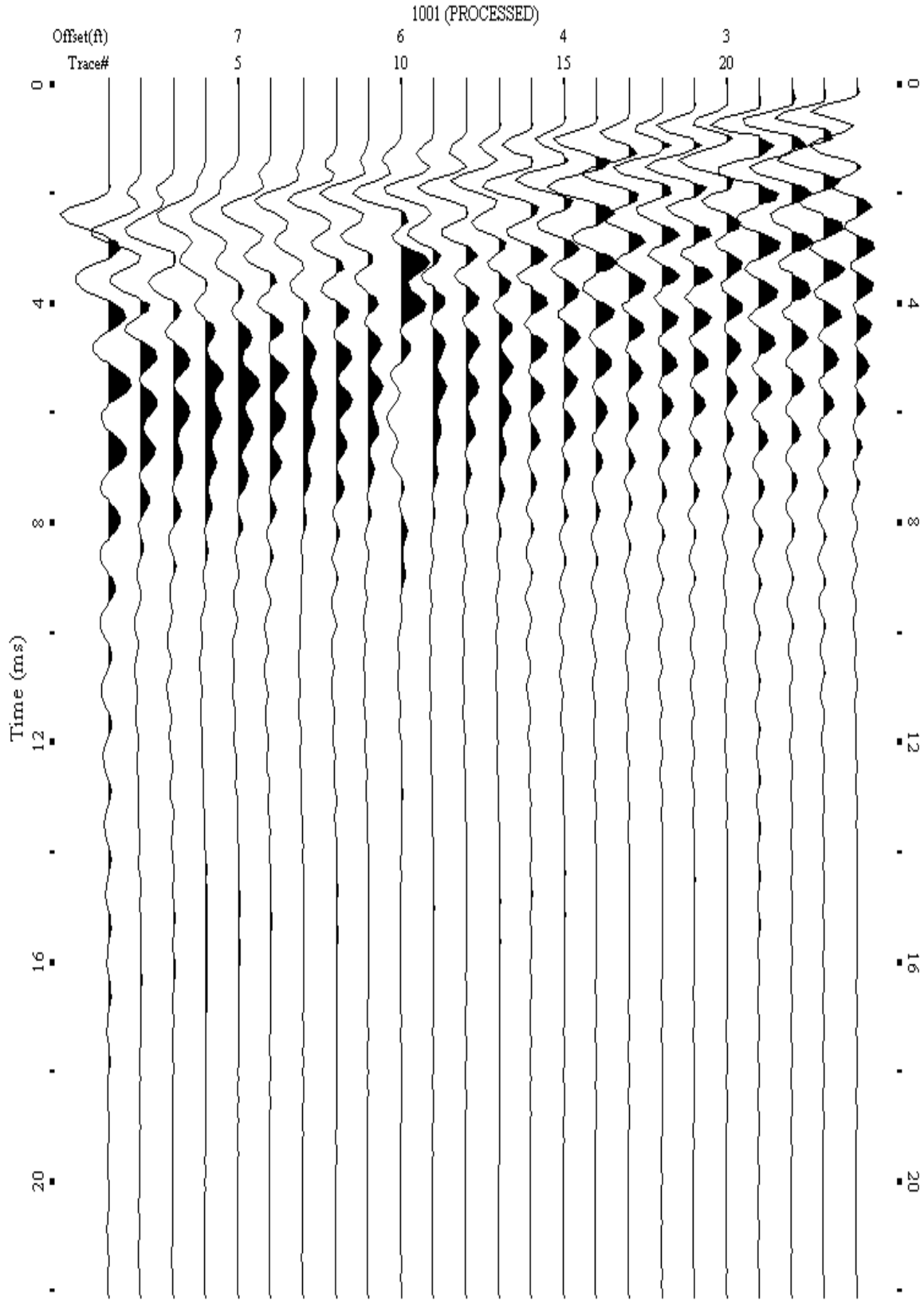

A.385: Shot Gather Line 1268 used in Pre-blast 12, Pre-blast 30

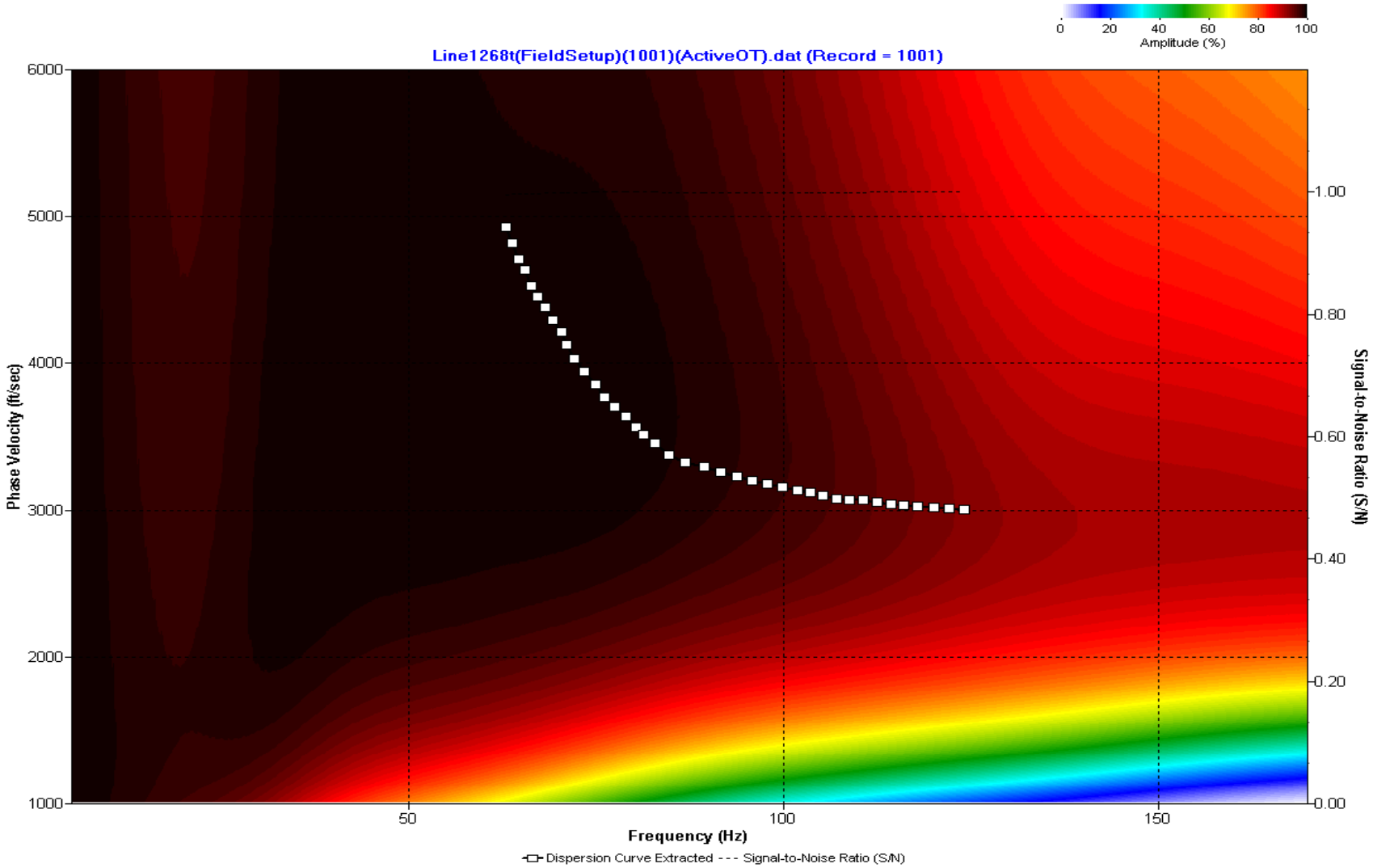

A.386: Dispersion Curve Line 1268 used in Pre-blast 12, Pre-blast 30

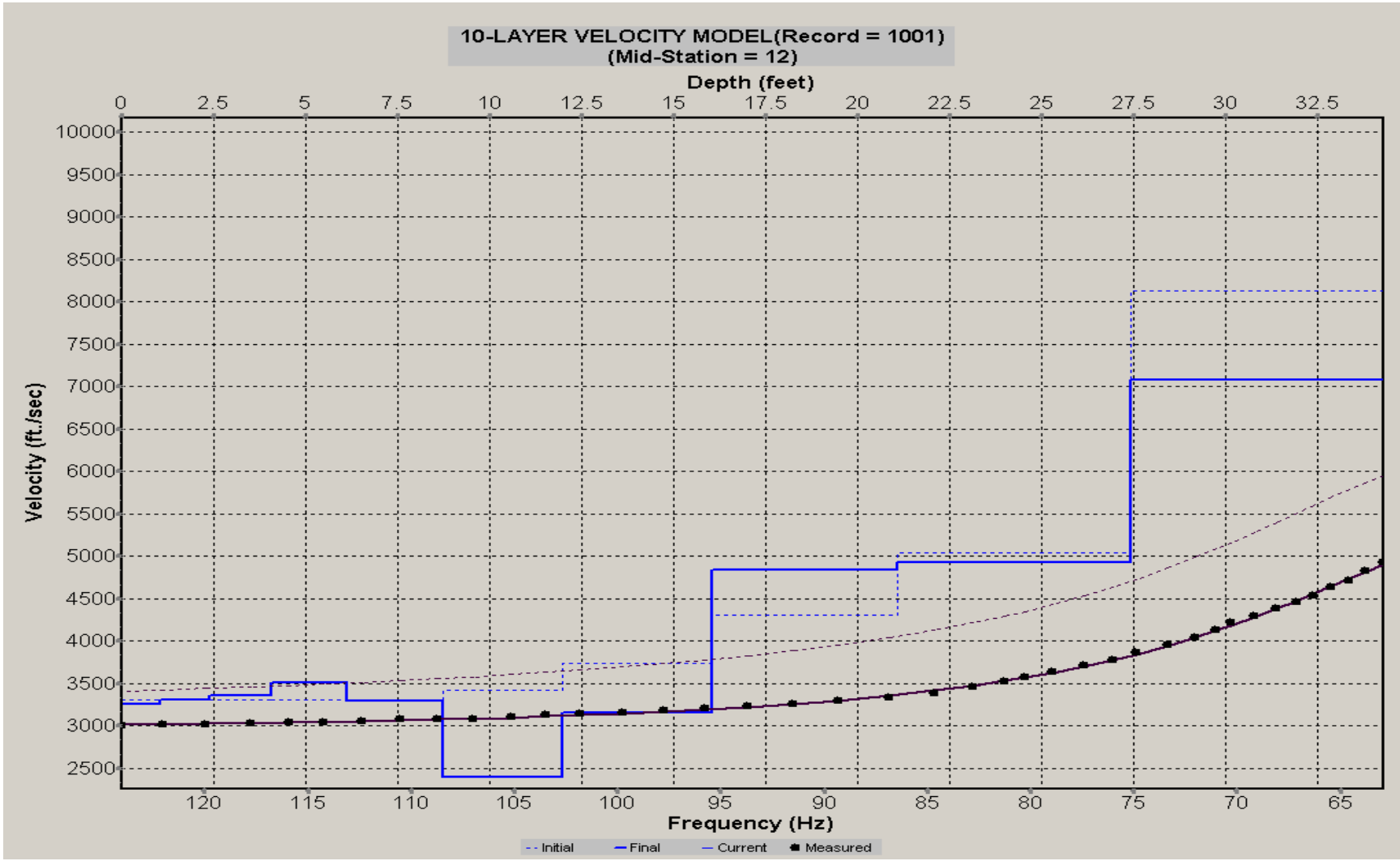

A.387: Velocity Profile Line 1268 used in Pre-blast 12, Pre-blast 30

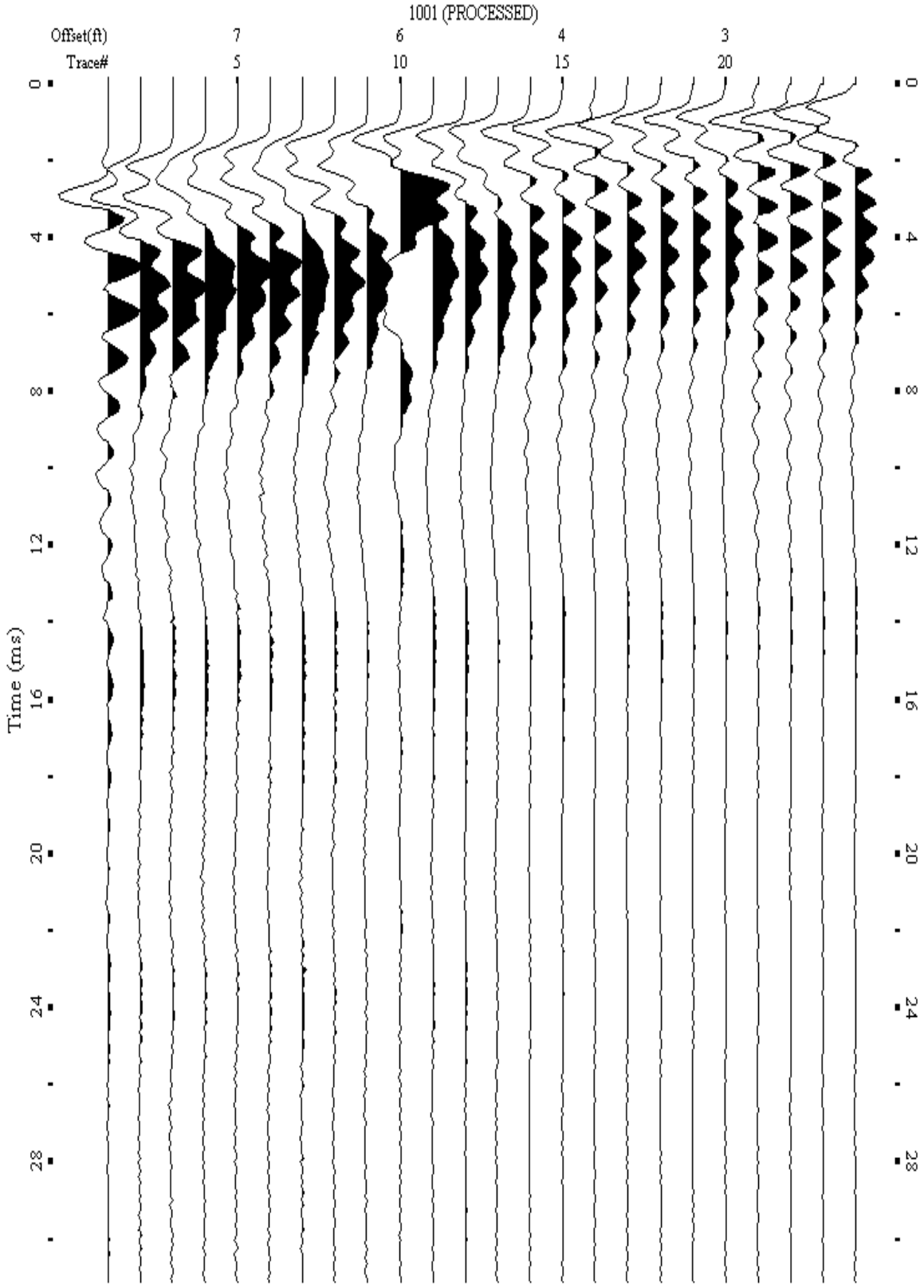

A.388: Shot Gather Line 1269 used in Pre-blast 12, Pre-blast 30

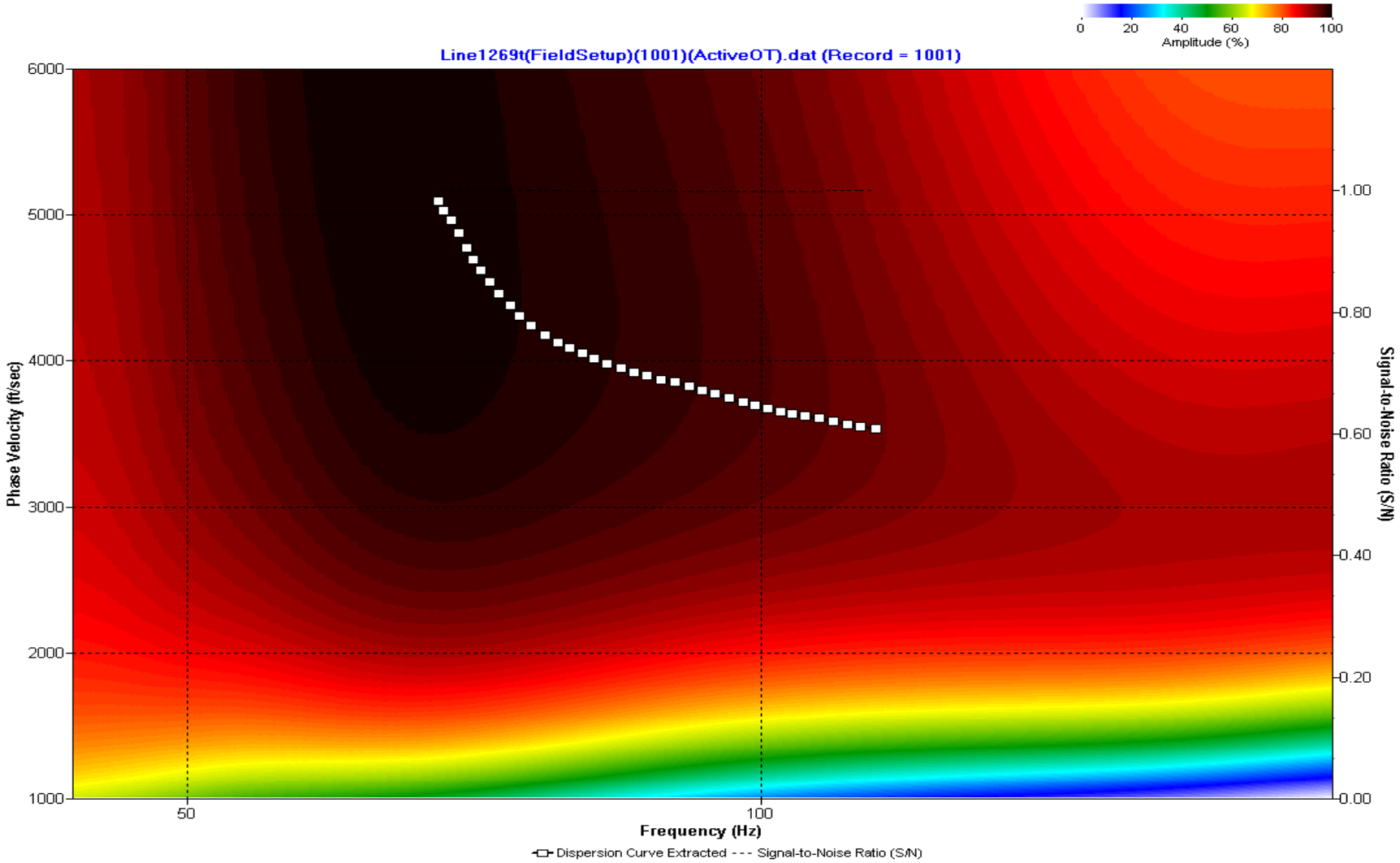

A.389: Dispersion Curve Line 1269 used in Pre-blast 12, Pre-blast 30

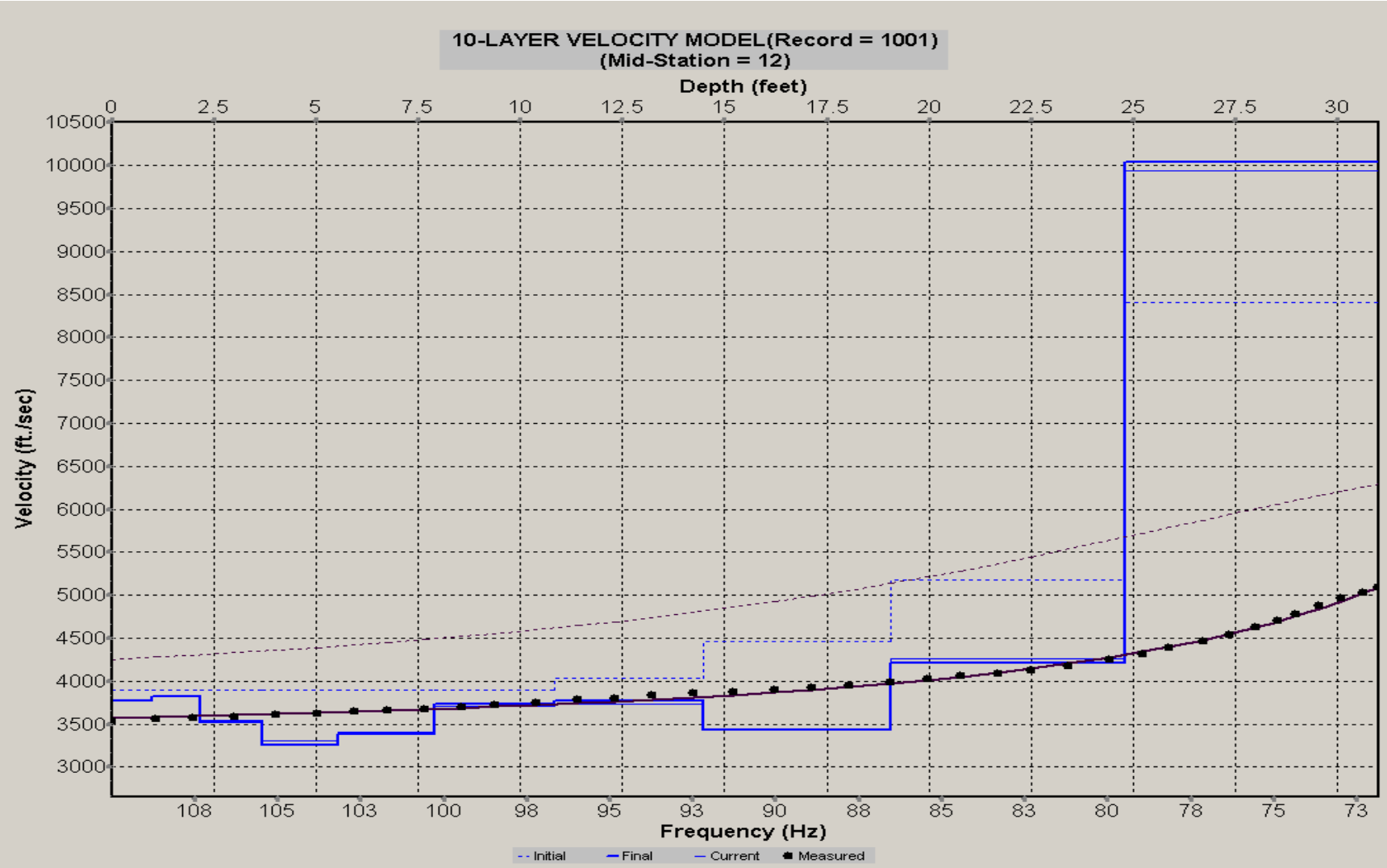

A.390: Velocity Profile Line 1269 used in Pre-blast 12, Pre-blast 30

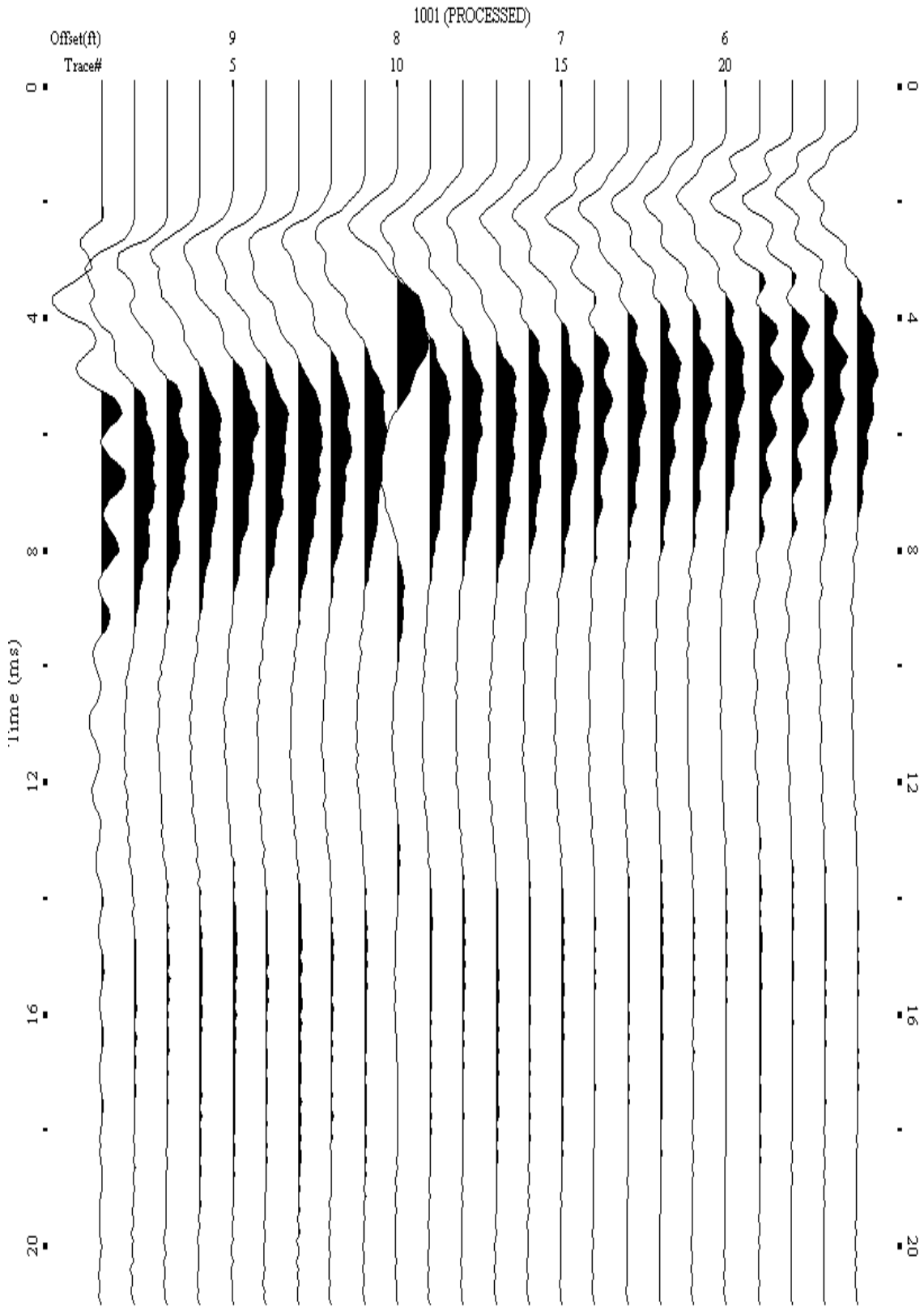

A.391: Shot Gather Line 1270 used in Pre-blast 12, Pre-blast 30

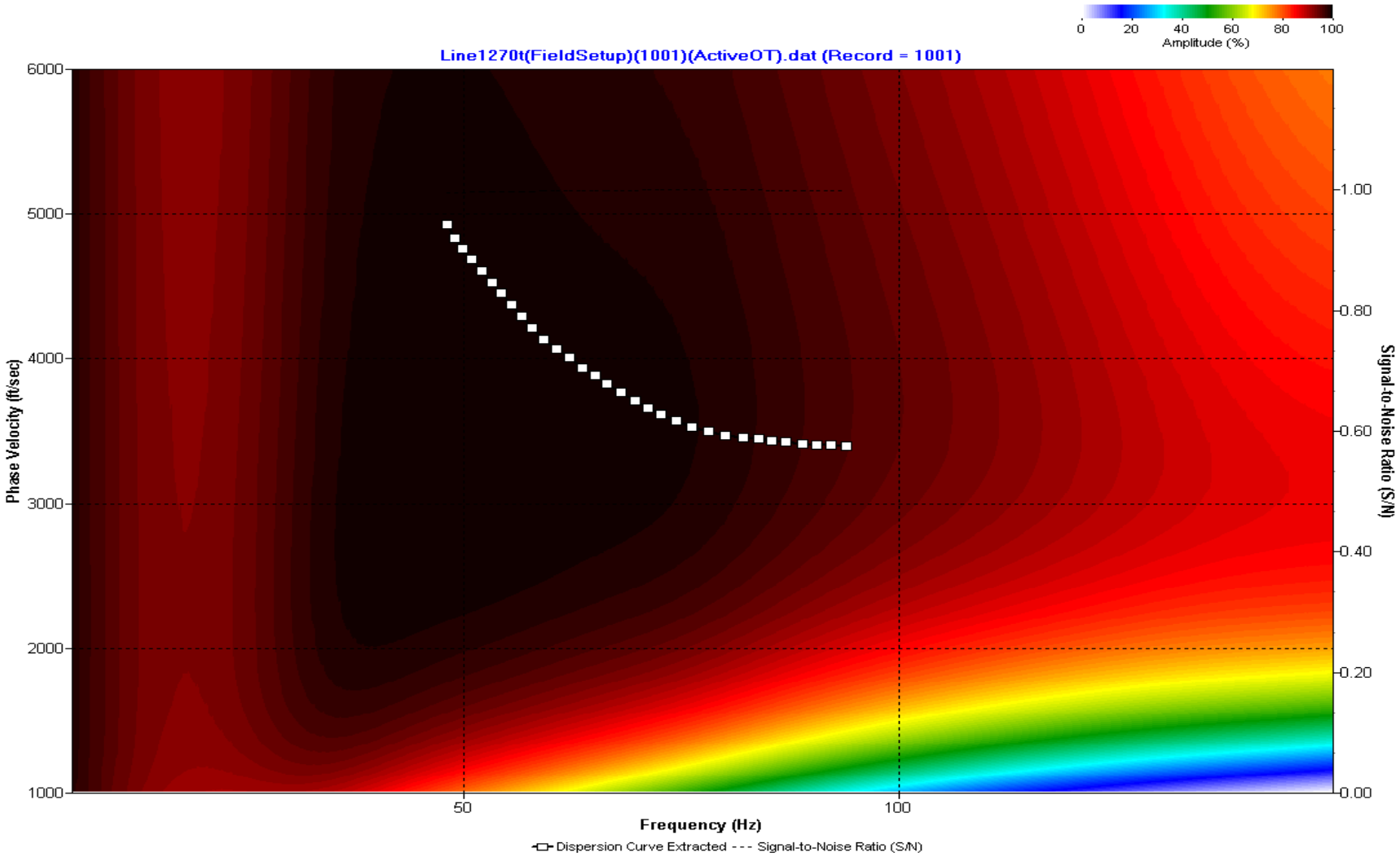

A.392: Dispersion Curve Line 1270 used in Pre-blast 12, Pre-blast 30

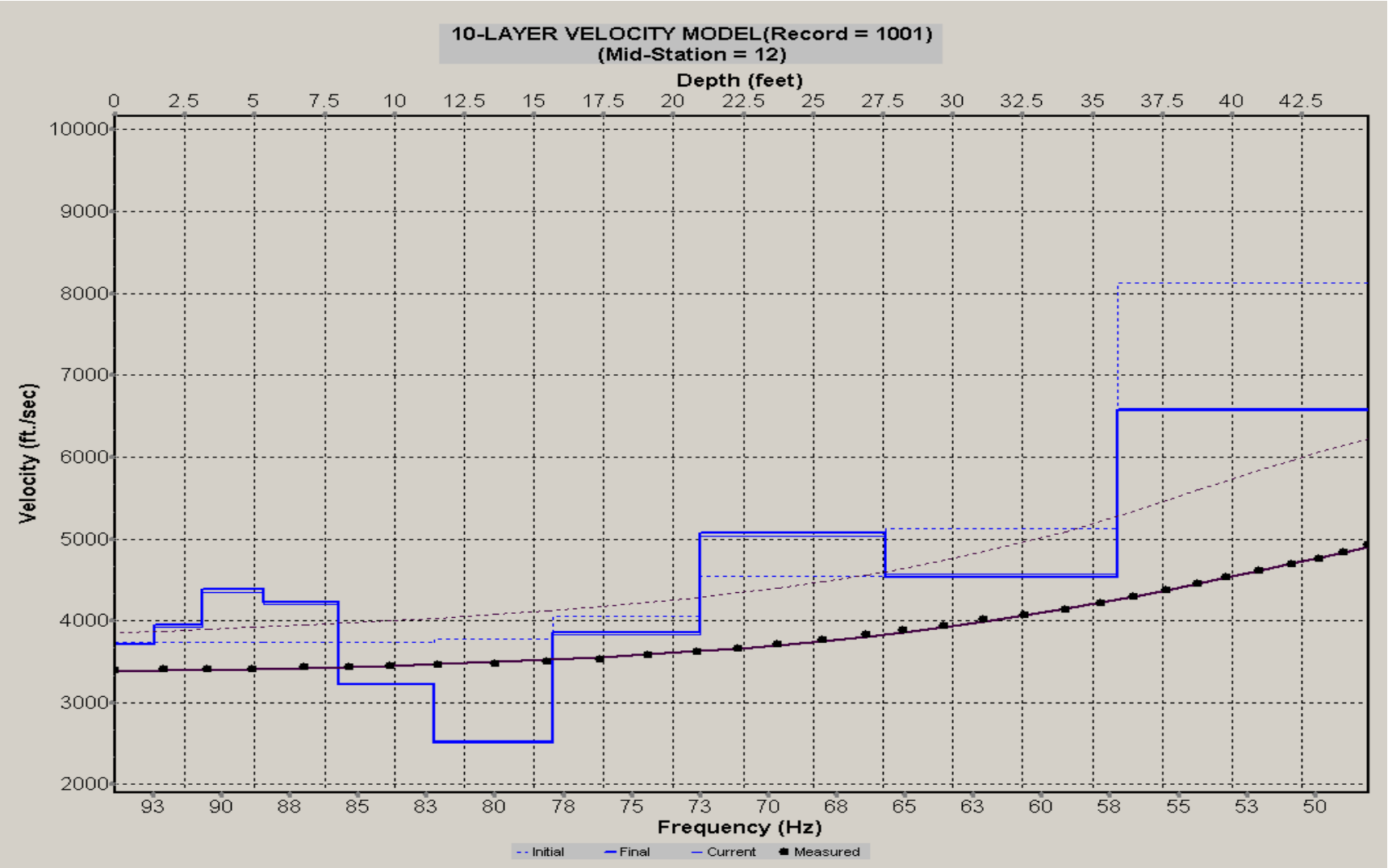

A.393: Velocity Profile Line 1270 used in Pre-blast 12, Pre-blast 30

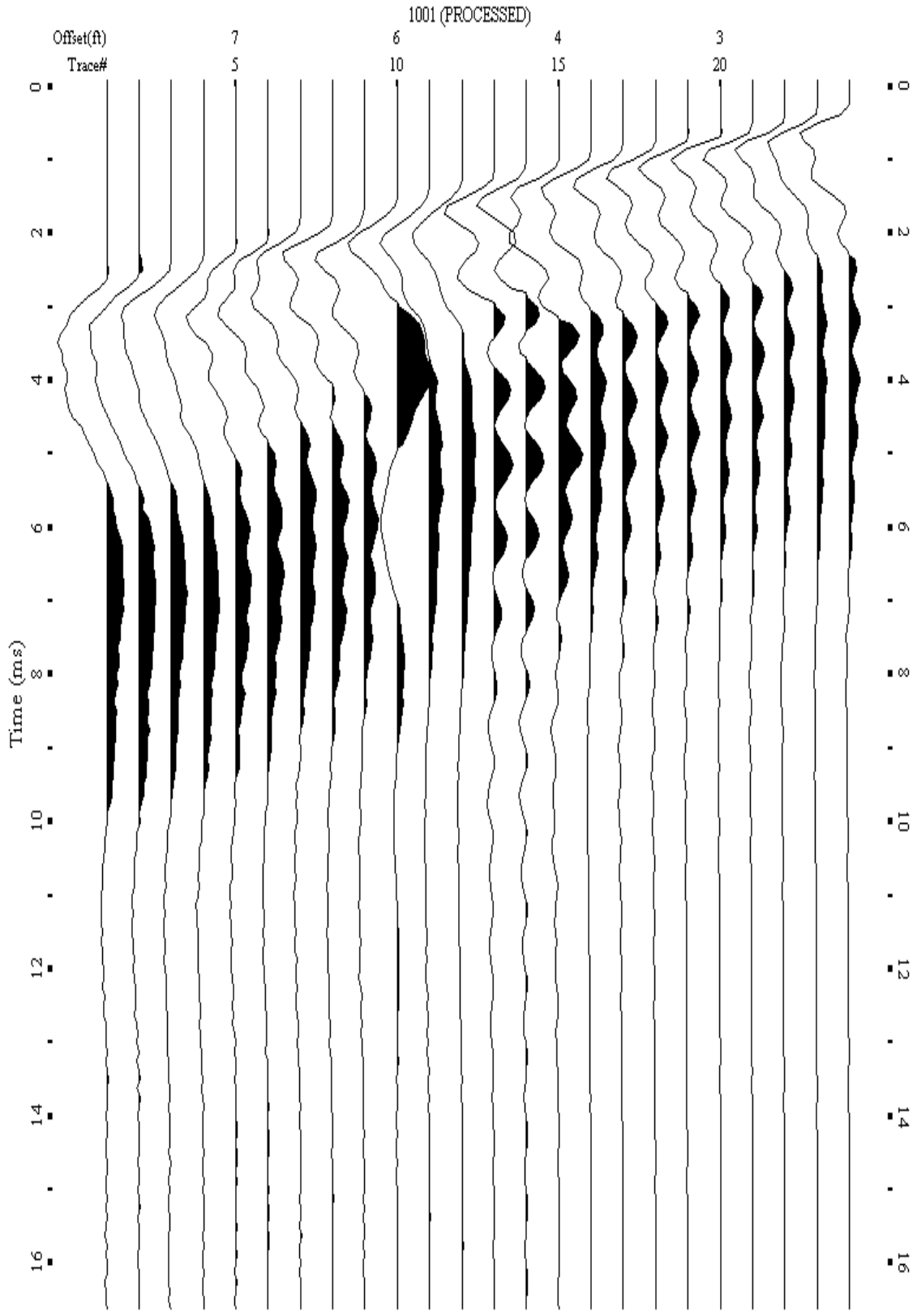

A.394: Shot Gather Line 1273 used in Pre-blast 35

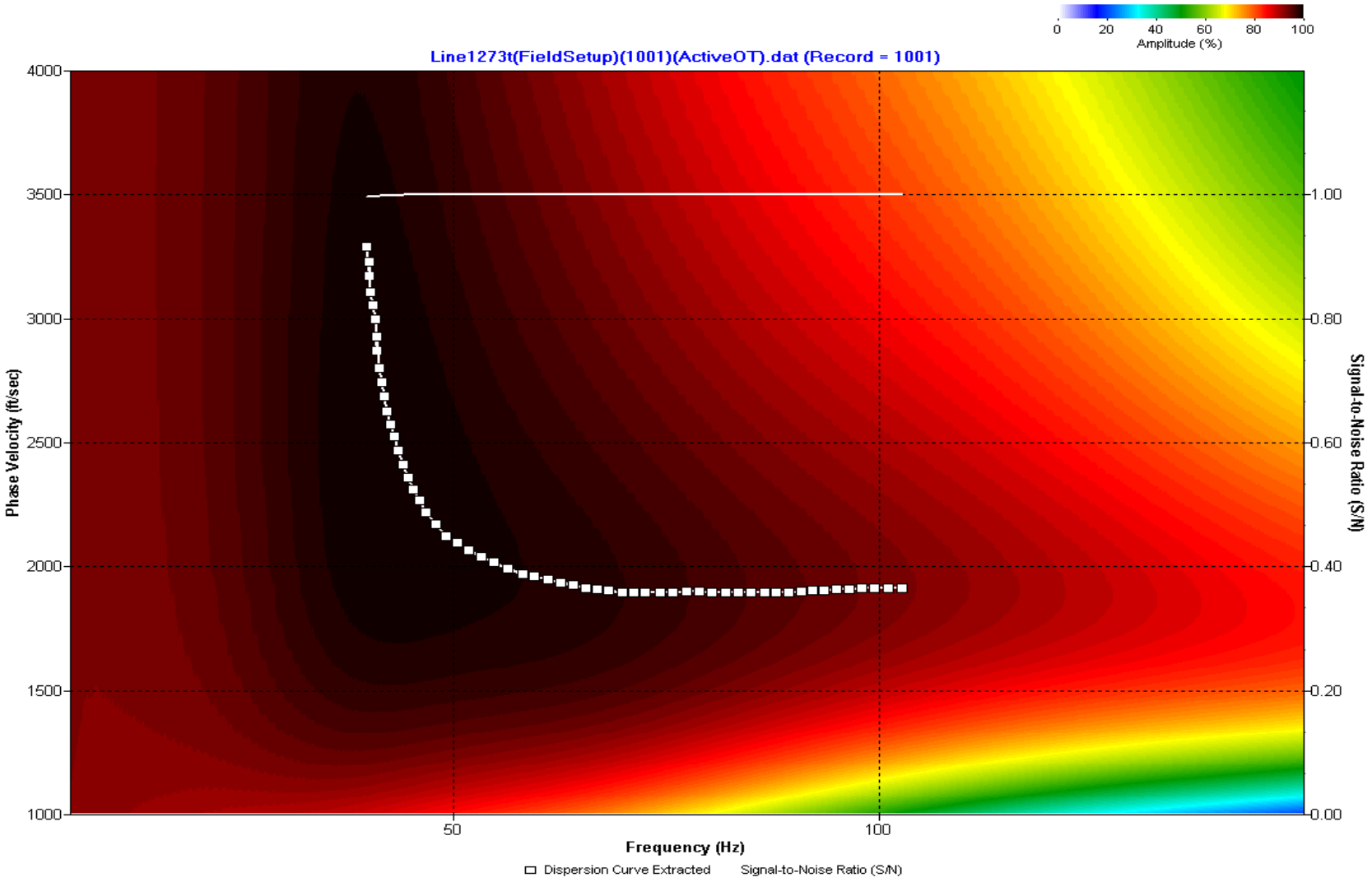

A.395: Dispersion Curve Line 1273 used in Pre-blast 35

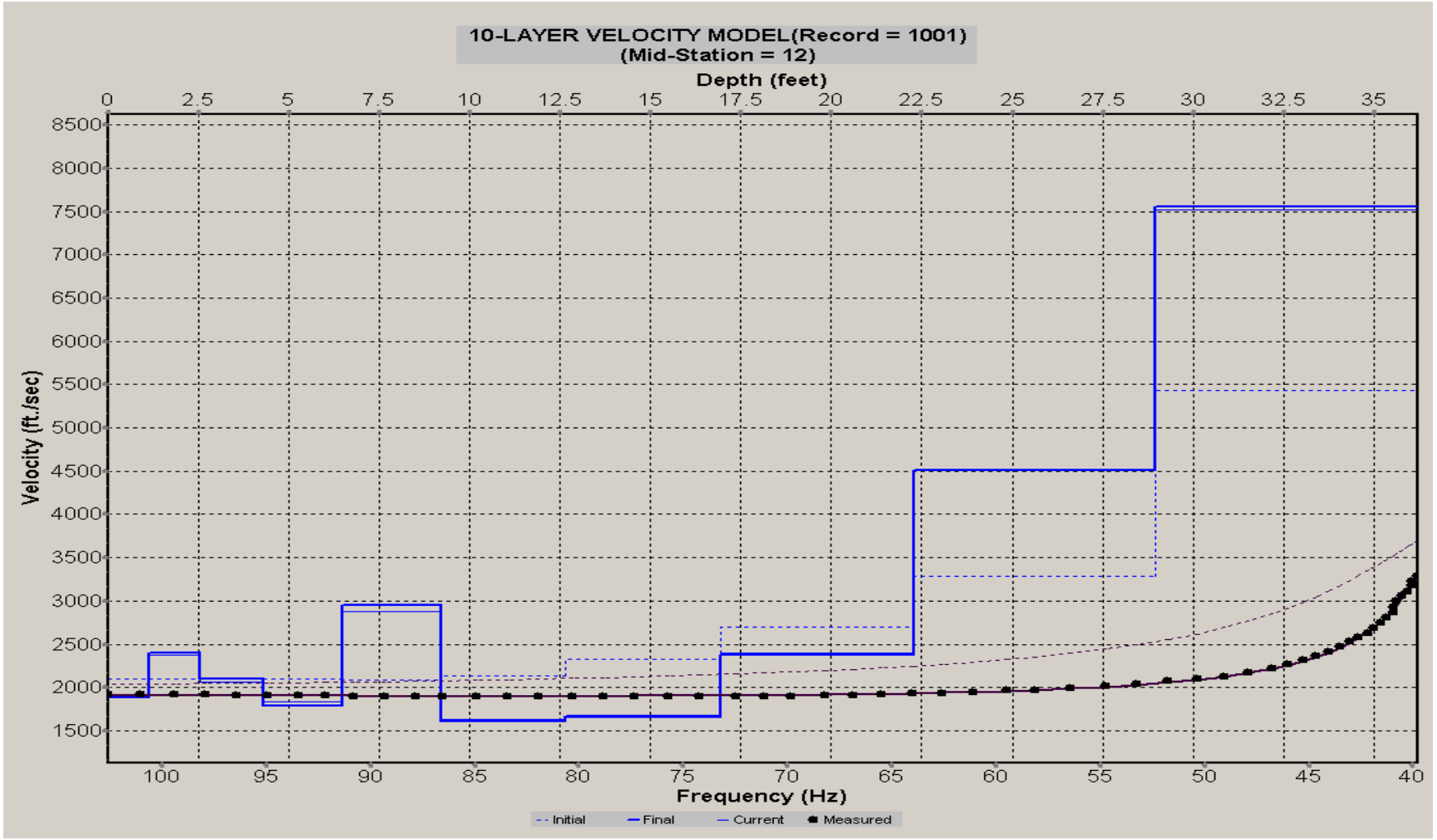

A.396: Velocity Profile Line 1273 used in Pre-blast 35

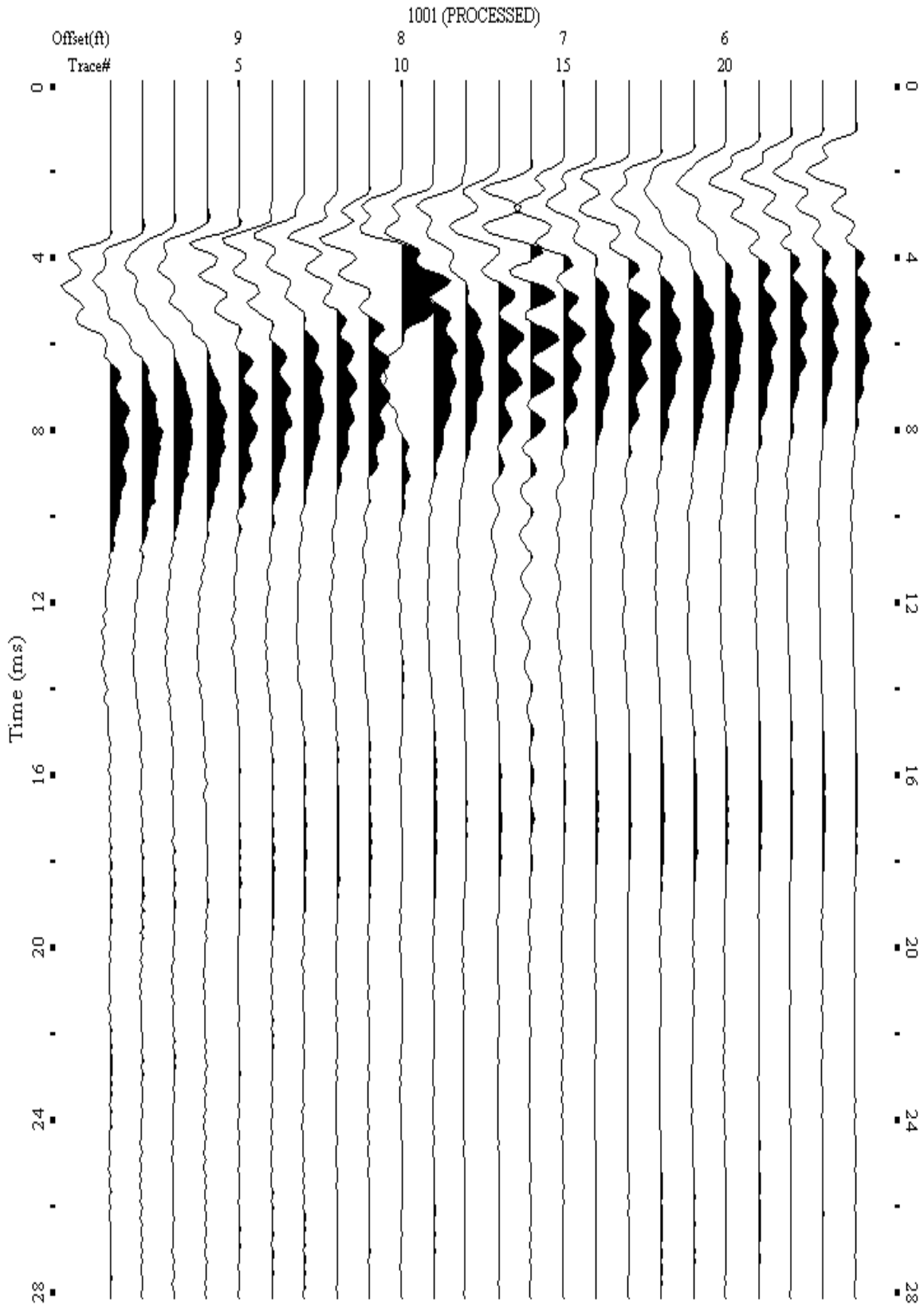

A.397: Shot Gather Line 1274 used in Pre-blast 35

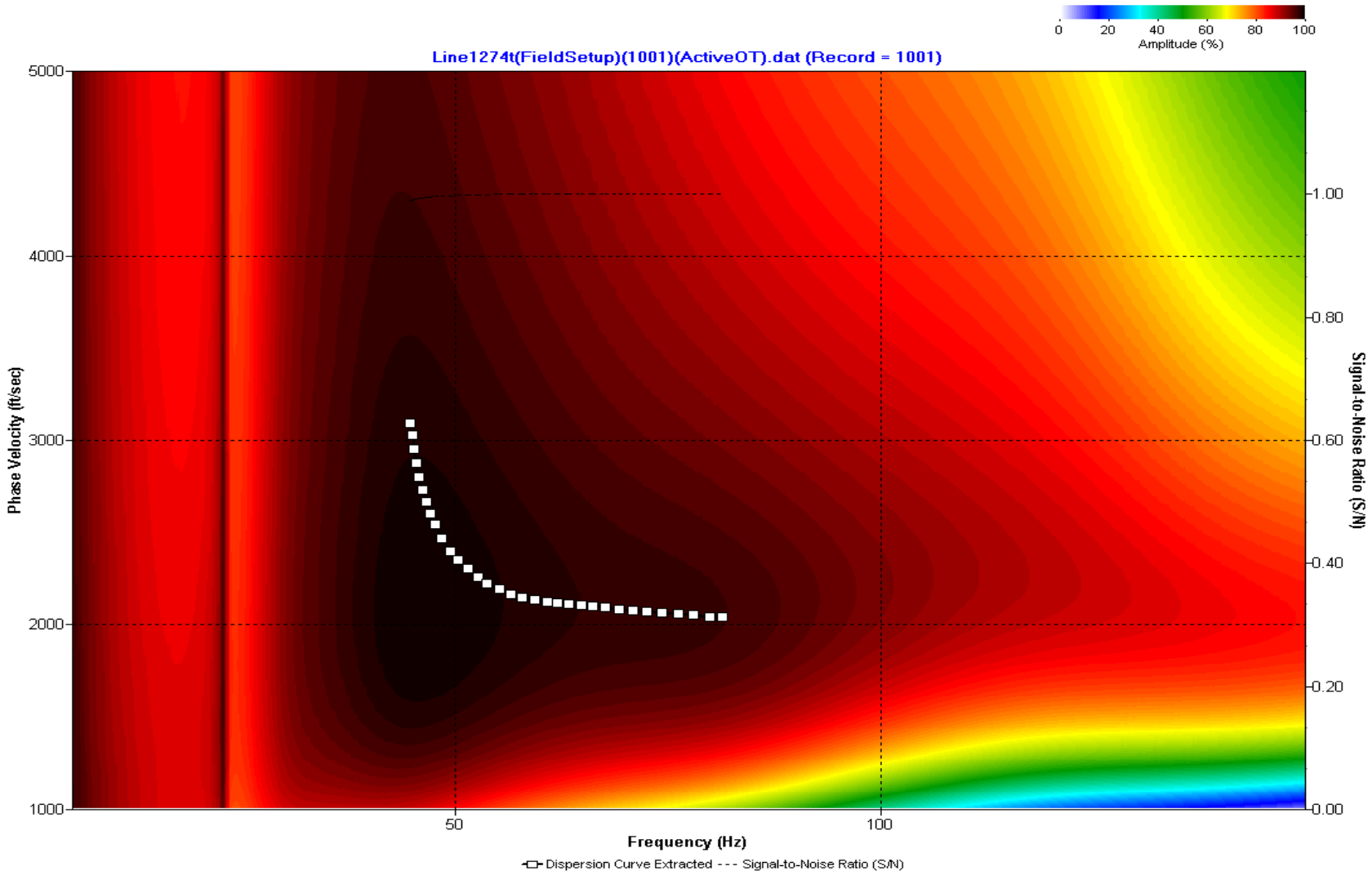

A.398: Dispersion Curve Line 1274 used in Pre-blast 35

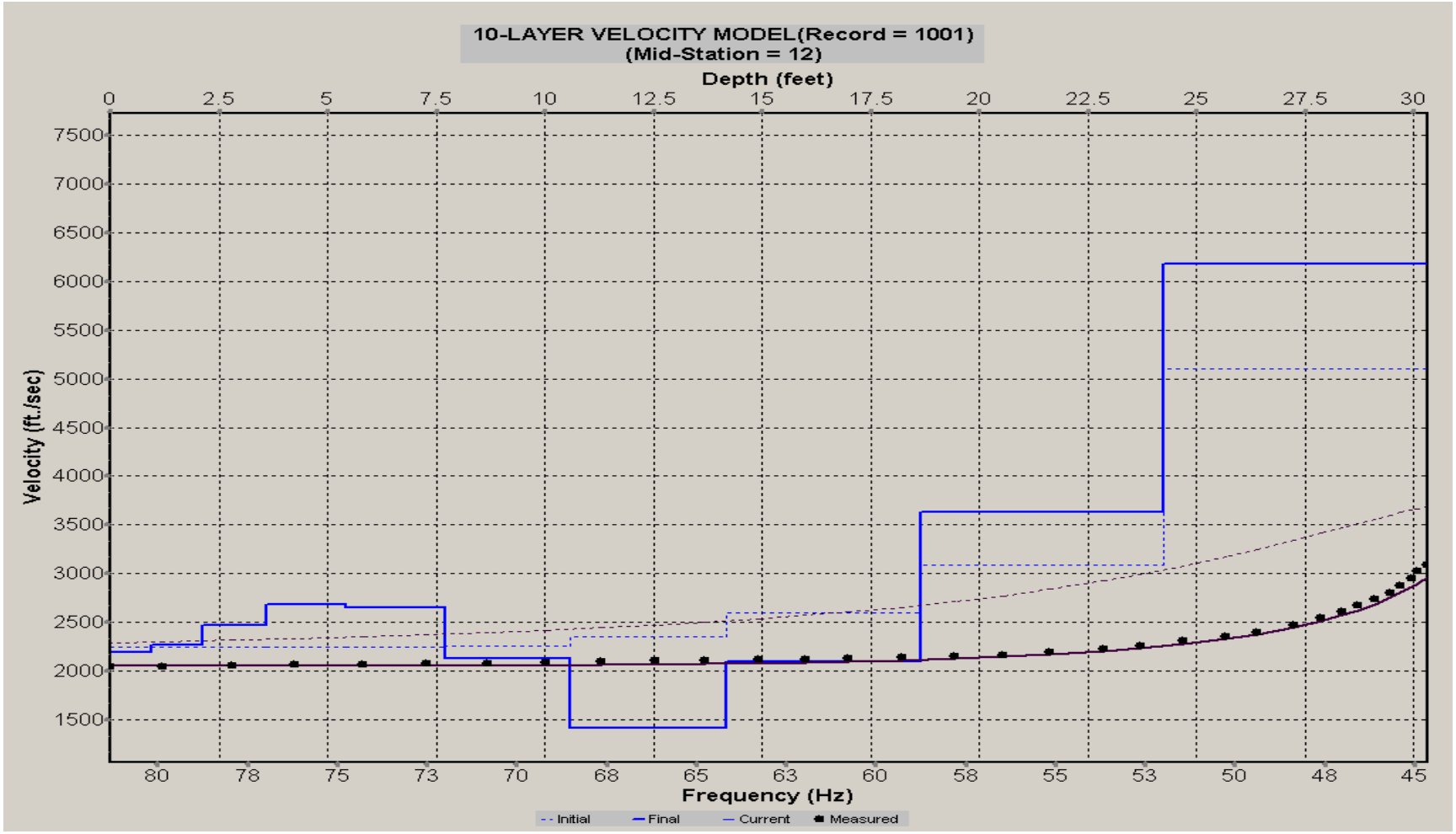

A.399: Velocity Profile Line 1274 used in Pre-blast 35

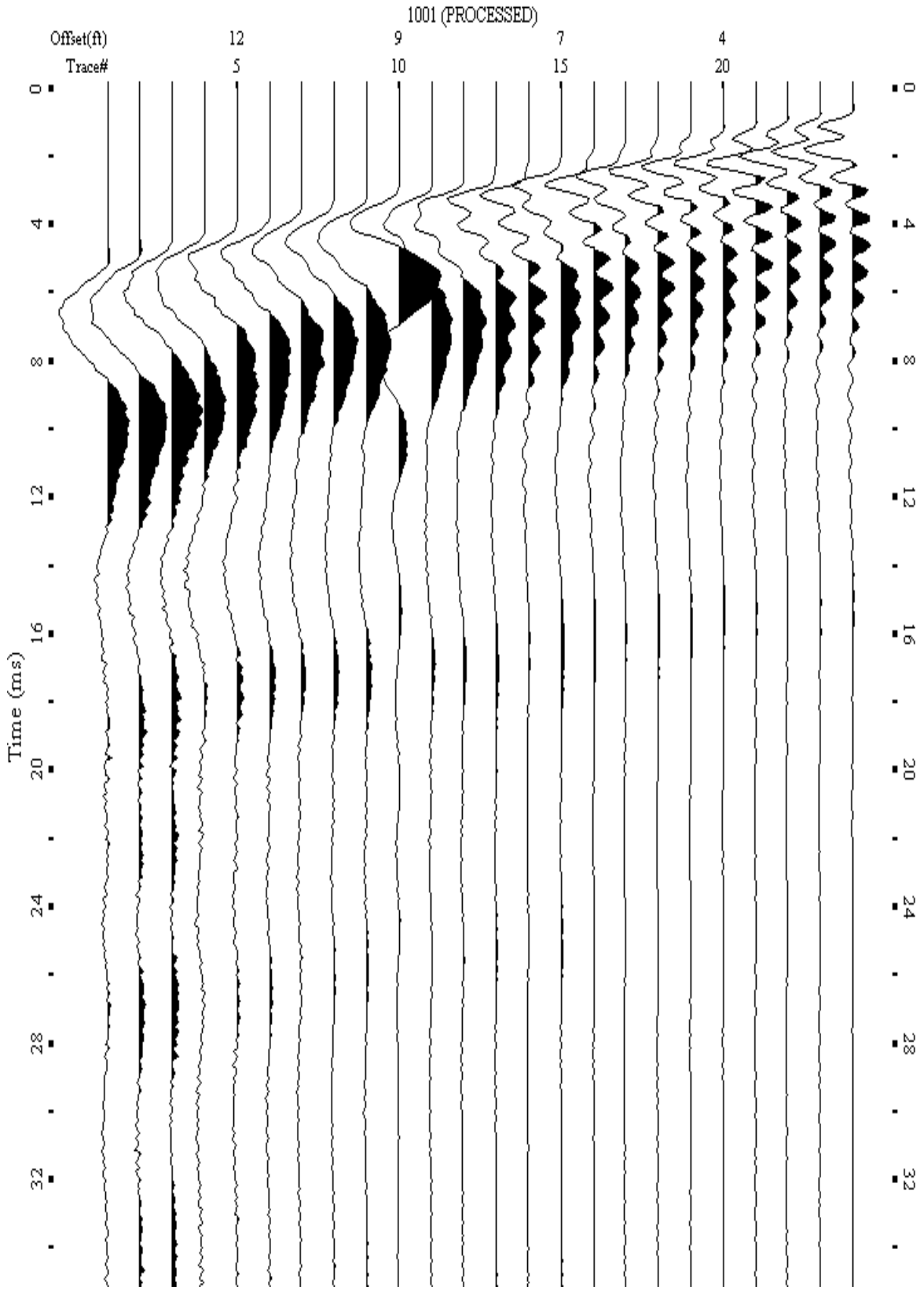

A.400: Shot Gather Line 1276 used in Post-blast 25 and Pre-blast 35

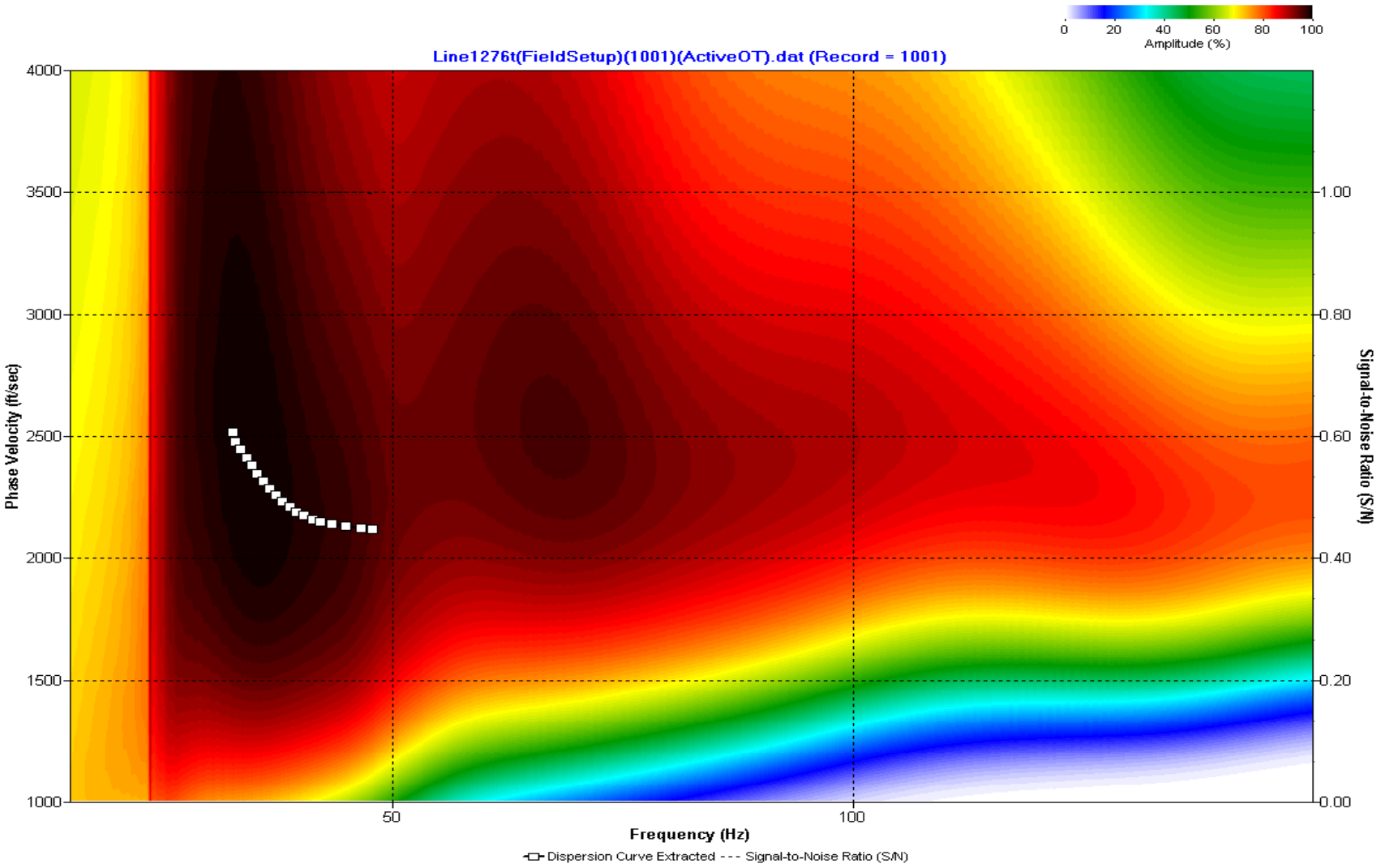

A.401: Dispersion Curve Line 1276 used in Post-blast 25 and Pre-blast 35

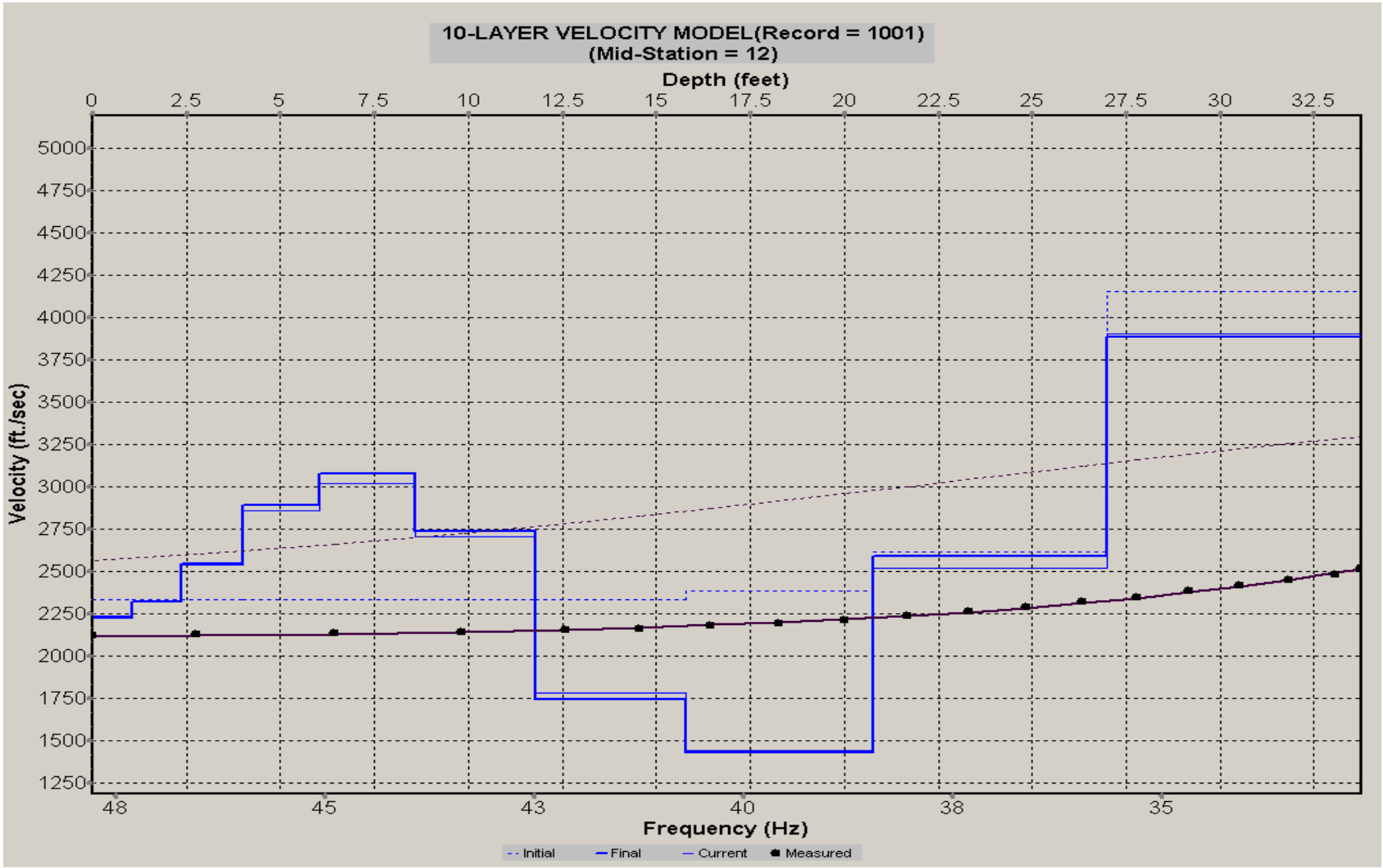

A.402: Velocity Profile Line 1276 used in Post-blast 25 and Pre-blast 35

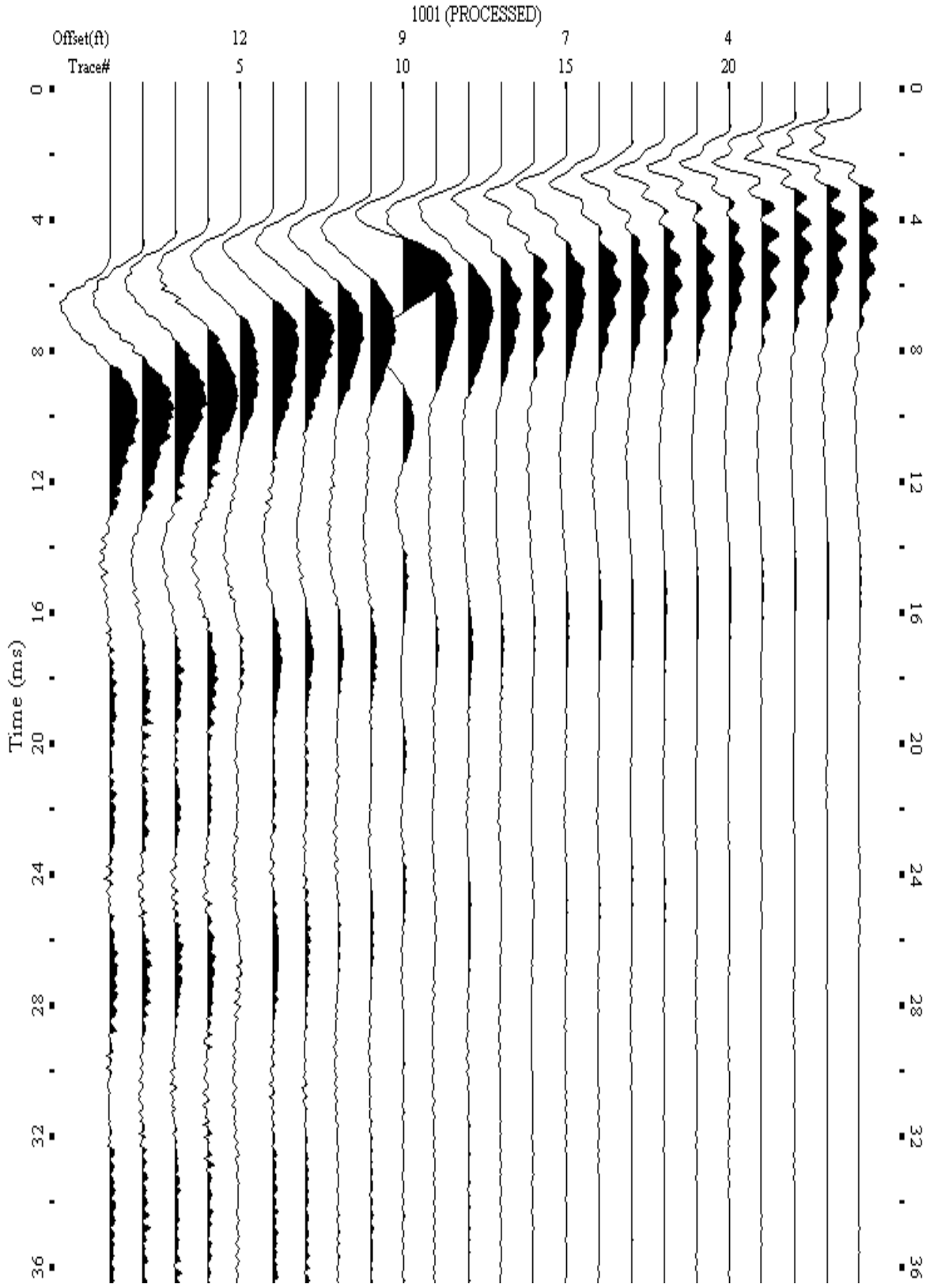

A.403: Shot Gather Line 1277 used in Post-blast 25 and Pre-blast 35

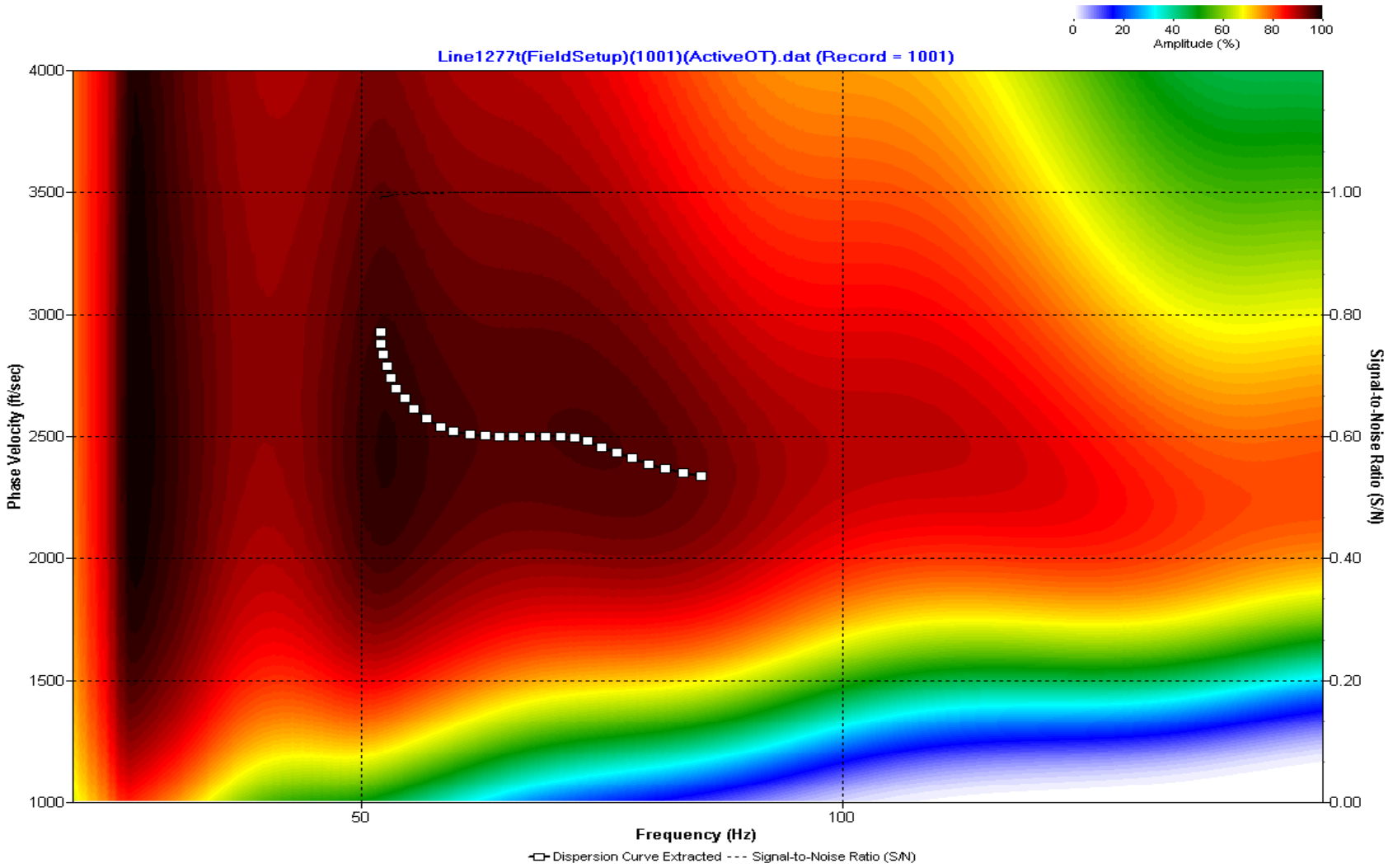

A.404: Dispersion Curve Line 1277 used in Post-blast 25 and Pre-blast 35

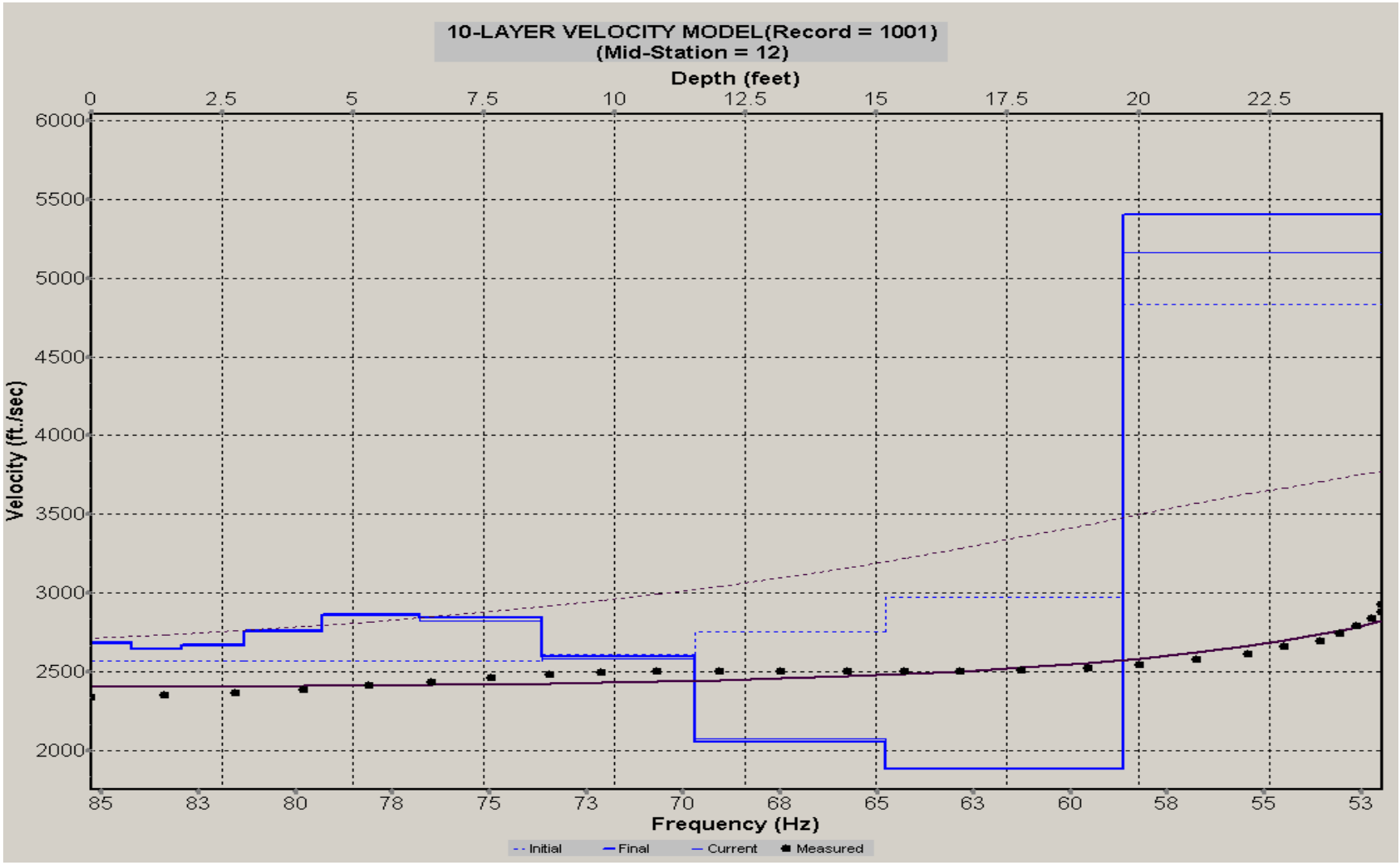

A.405: Velocity Profile Line 1277 used in Post-blast 25 and Pre-blast 35

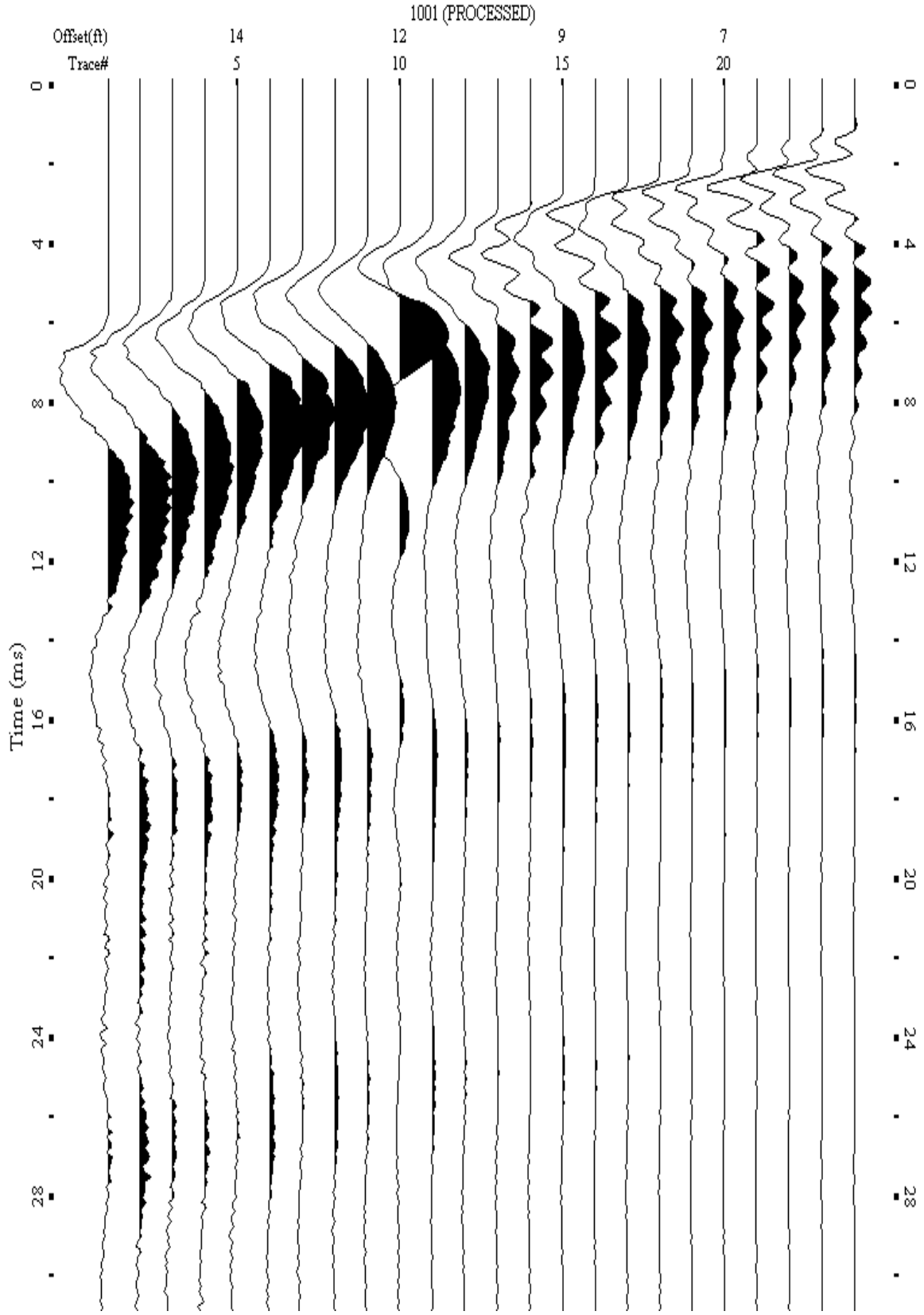

A.406: Shot Gather Line 1278 used in Pre-blast 12 and Post-blast 26

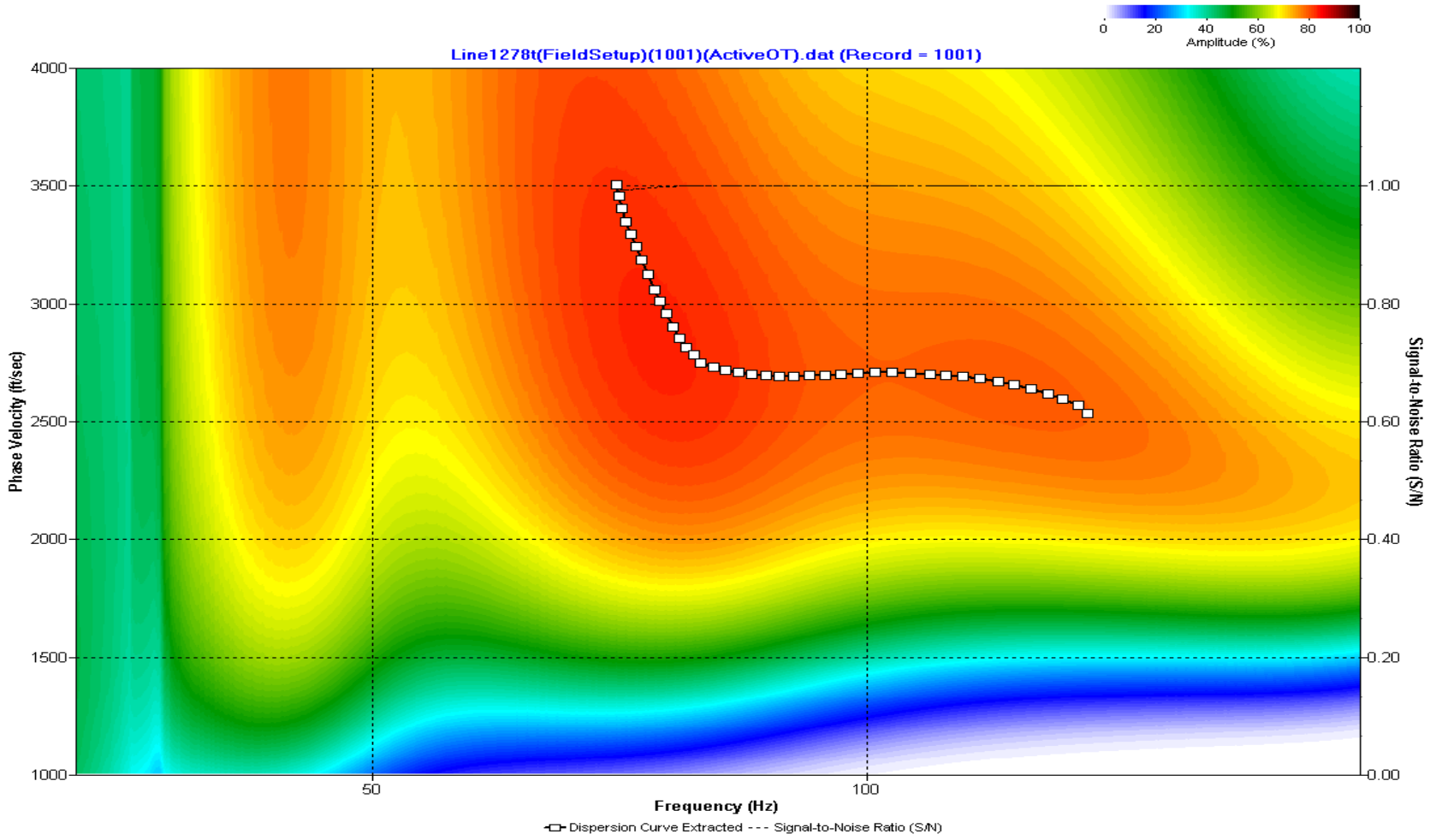

A.407: Dispersion Curve Line 1278 used in Pre-blast 12 and Post-blast 26

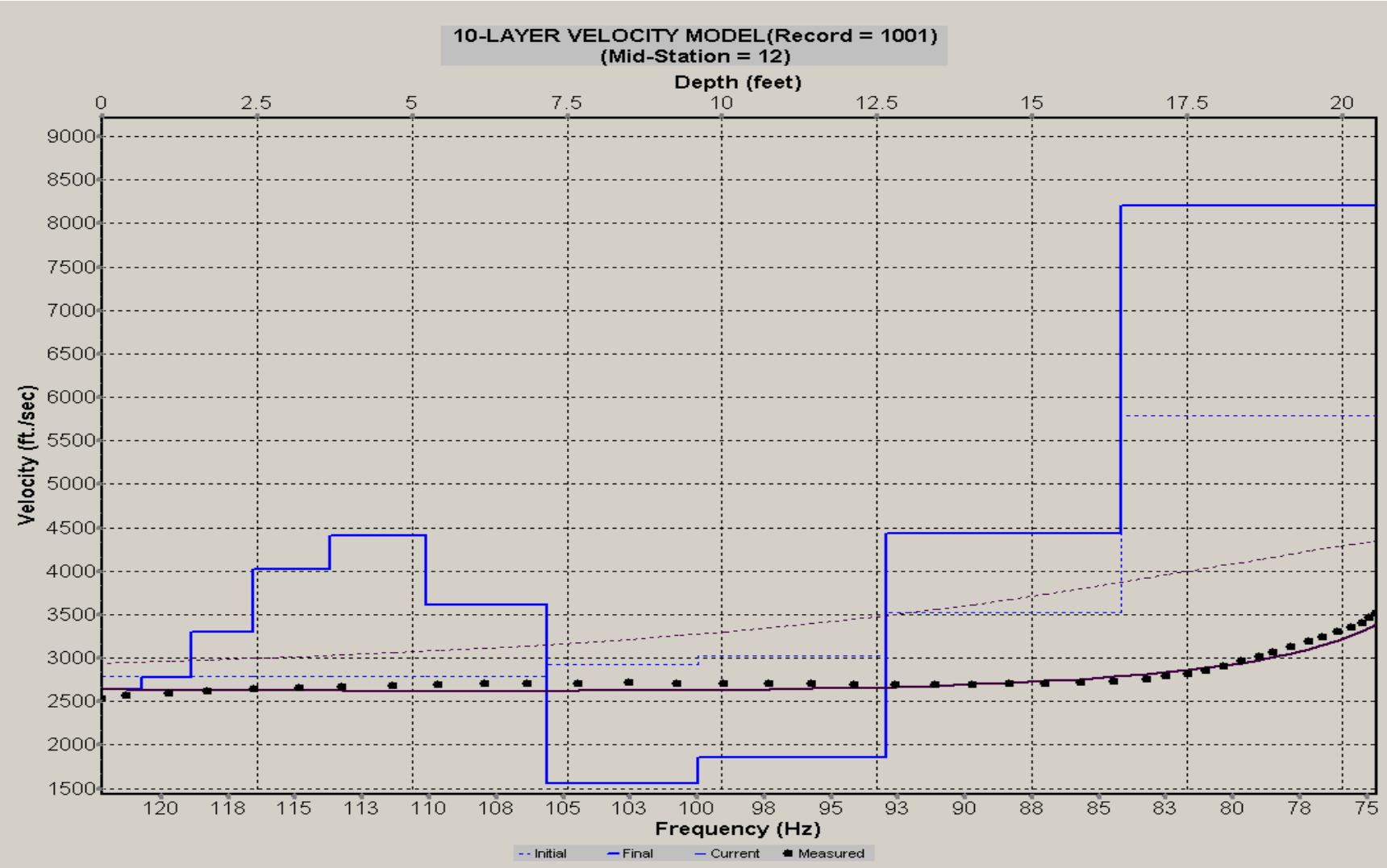

A.408: Velocity Profile Line 1278 used in Pre-blast 12 and Post-blast 26

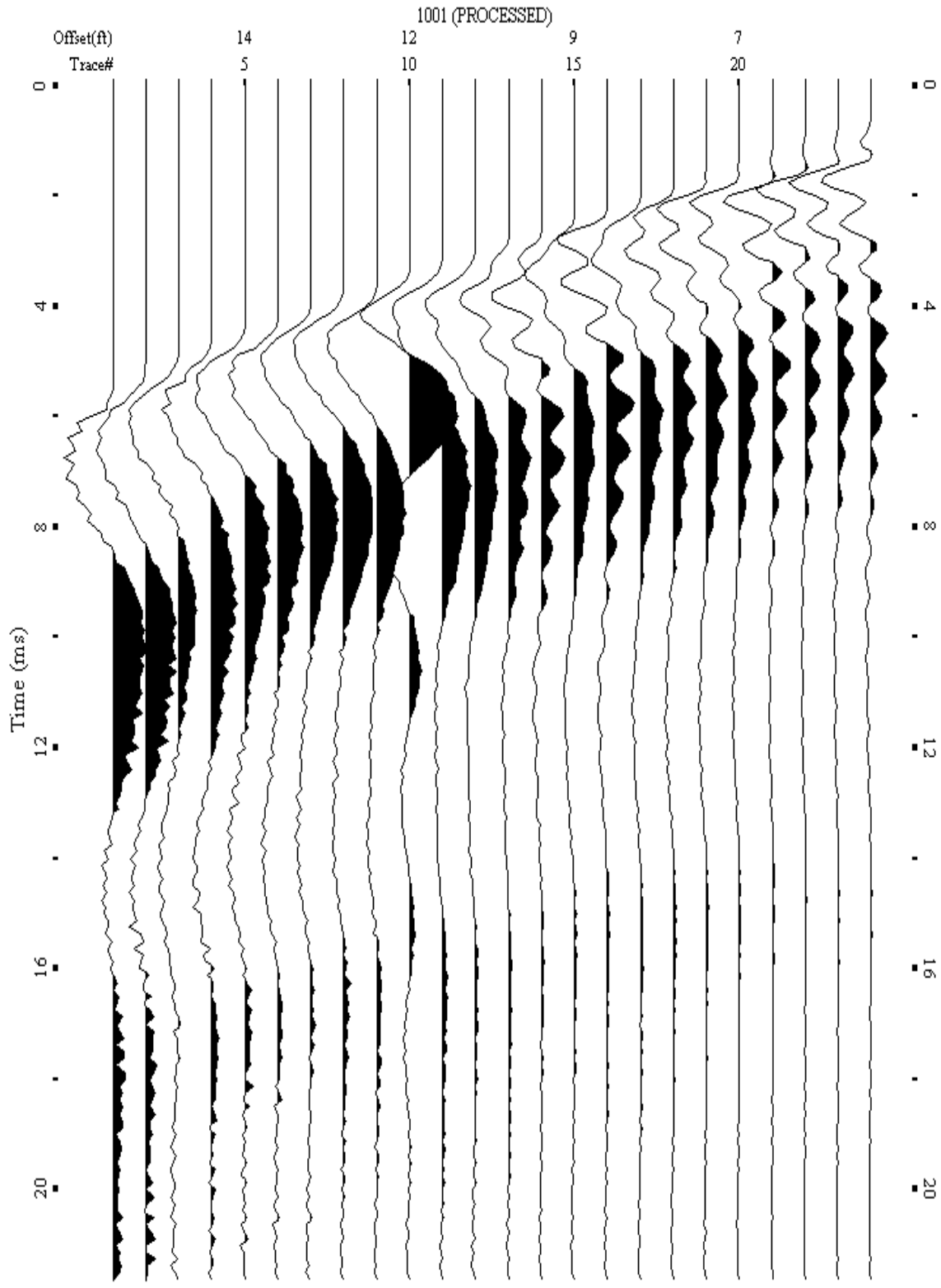

A.409: Shot Gather Line 1279 used in Pre-blast 12, Post-blast 26, Pre-blast 30 and Pre-blast 35

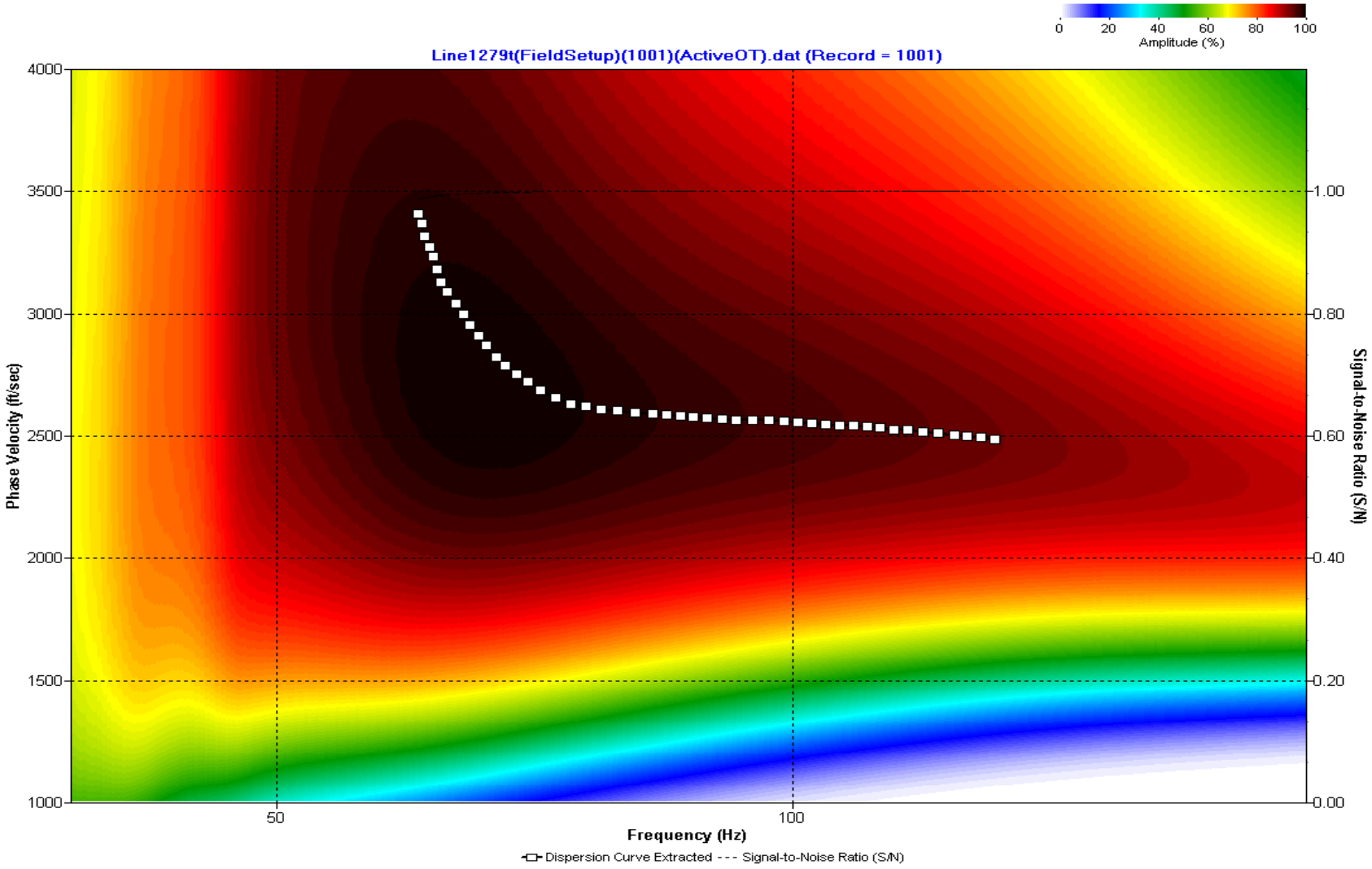

A.410: Dispersion Curve Line 1279 used in Pre-blast 12, Post-blast 26, Pre-blast 30, and Pre-blast 35

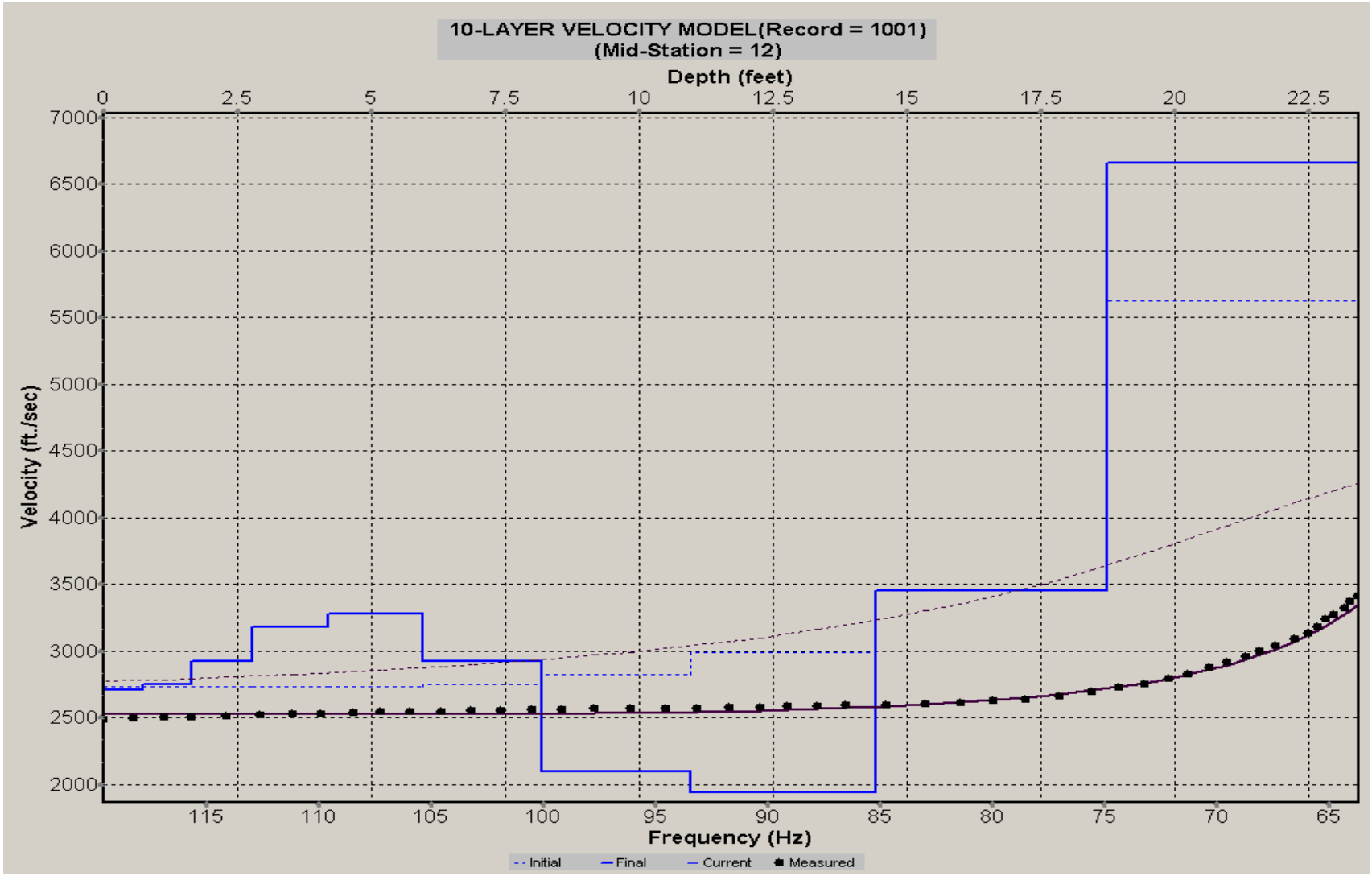

A.411: Velocity Profile Line 1279 used in Pre-blast 12, Post-blast 26, Pre-blast 30 and Pre-blast 35

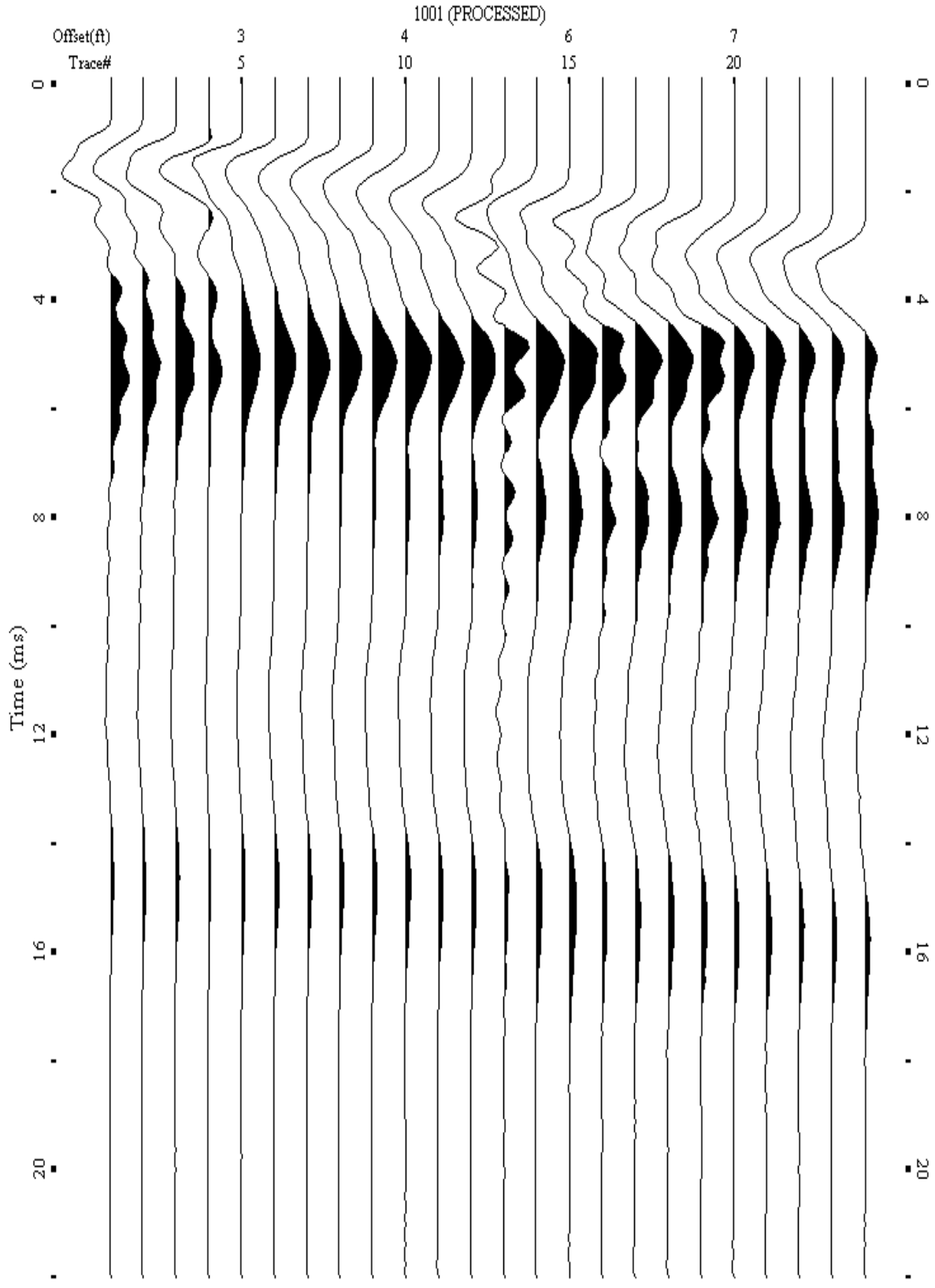

A.412: Shot Gather Line 1280 used in Post-blast 20

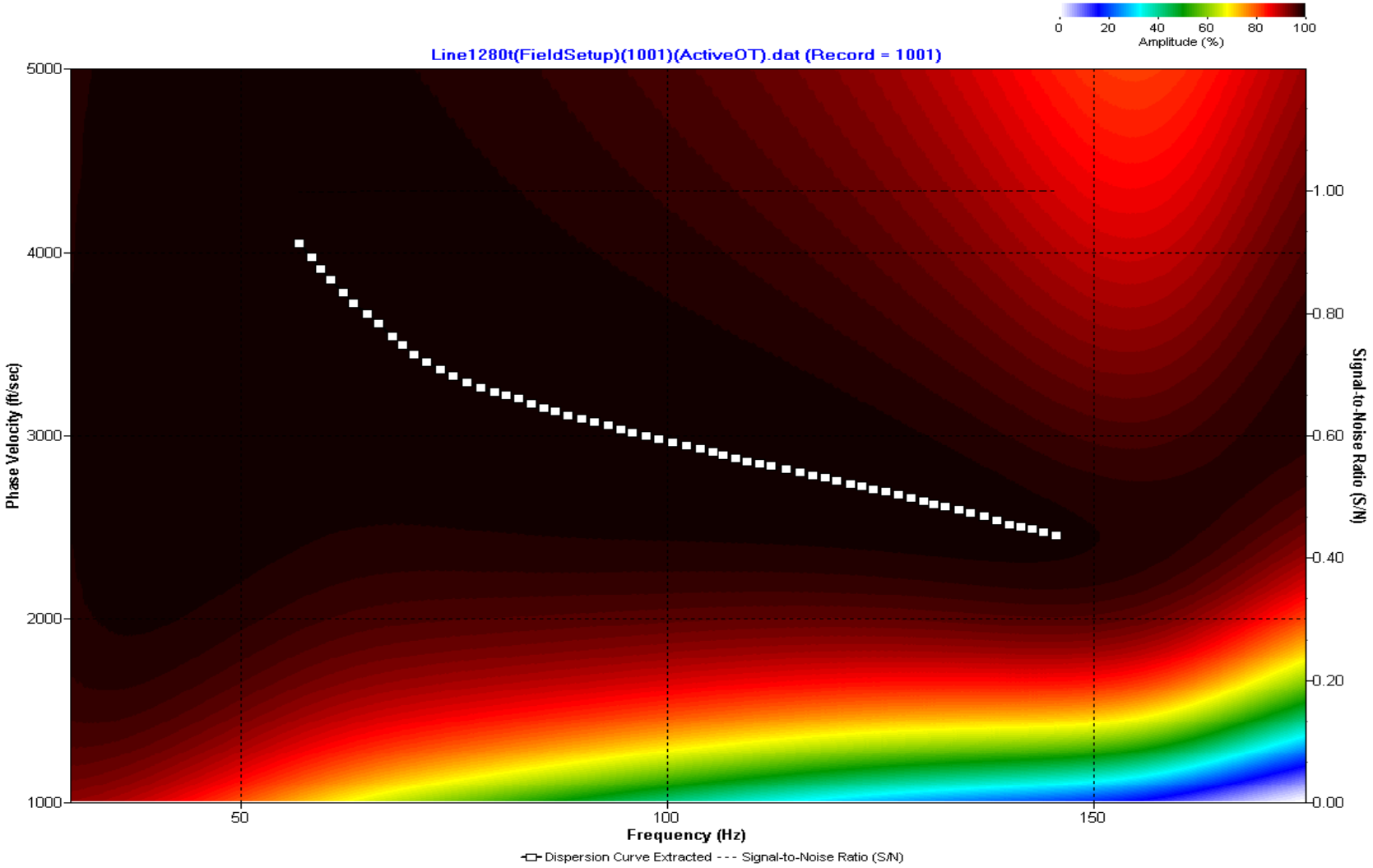

A.413: Dispersion Curve Line 1280 used in Post-blast 20

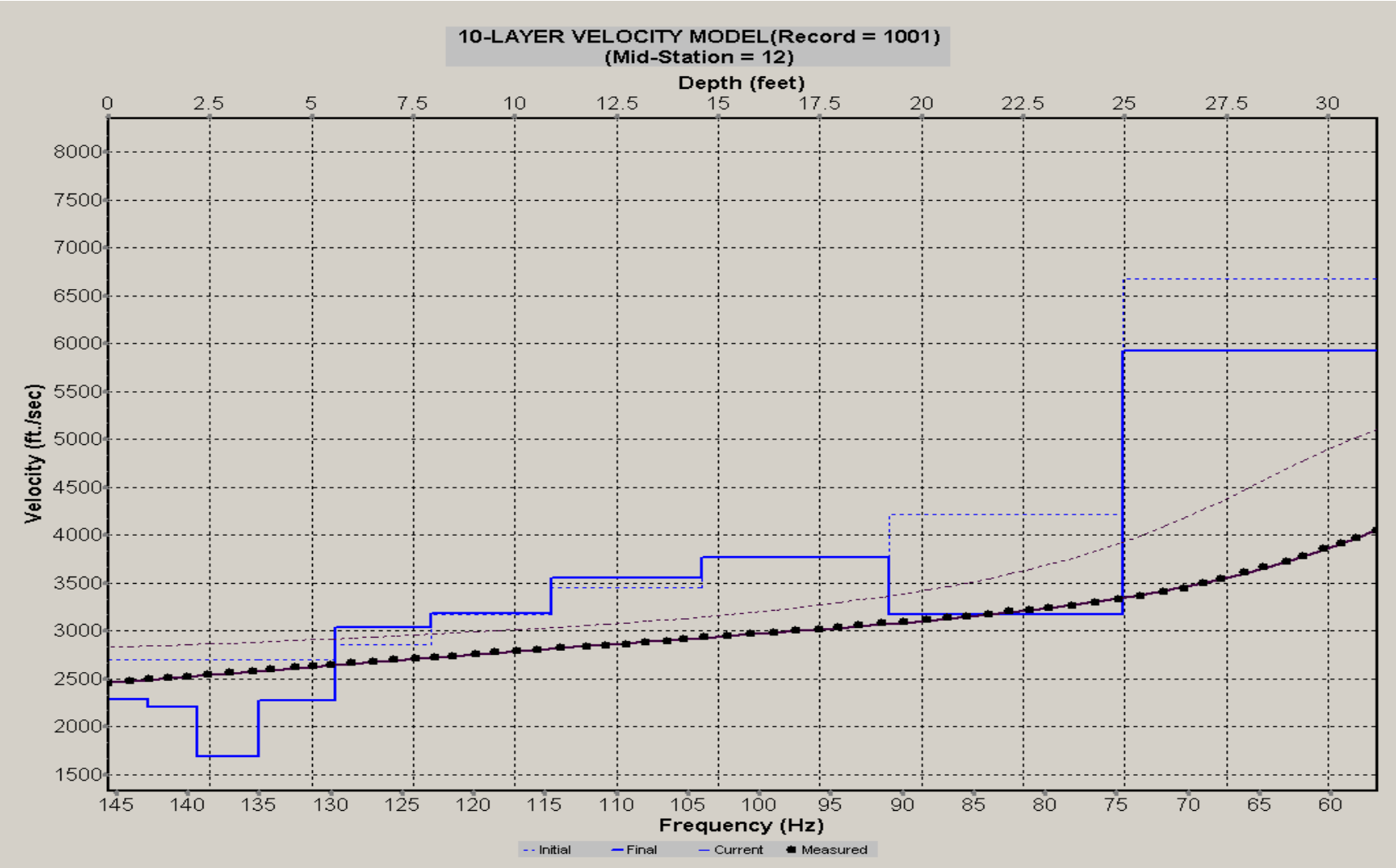

A.414: Velocity Profile Line 1280 used in Post-blast 20

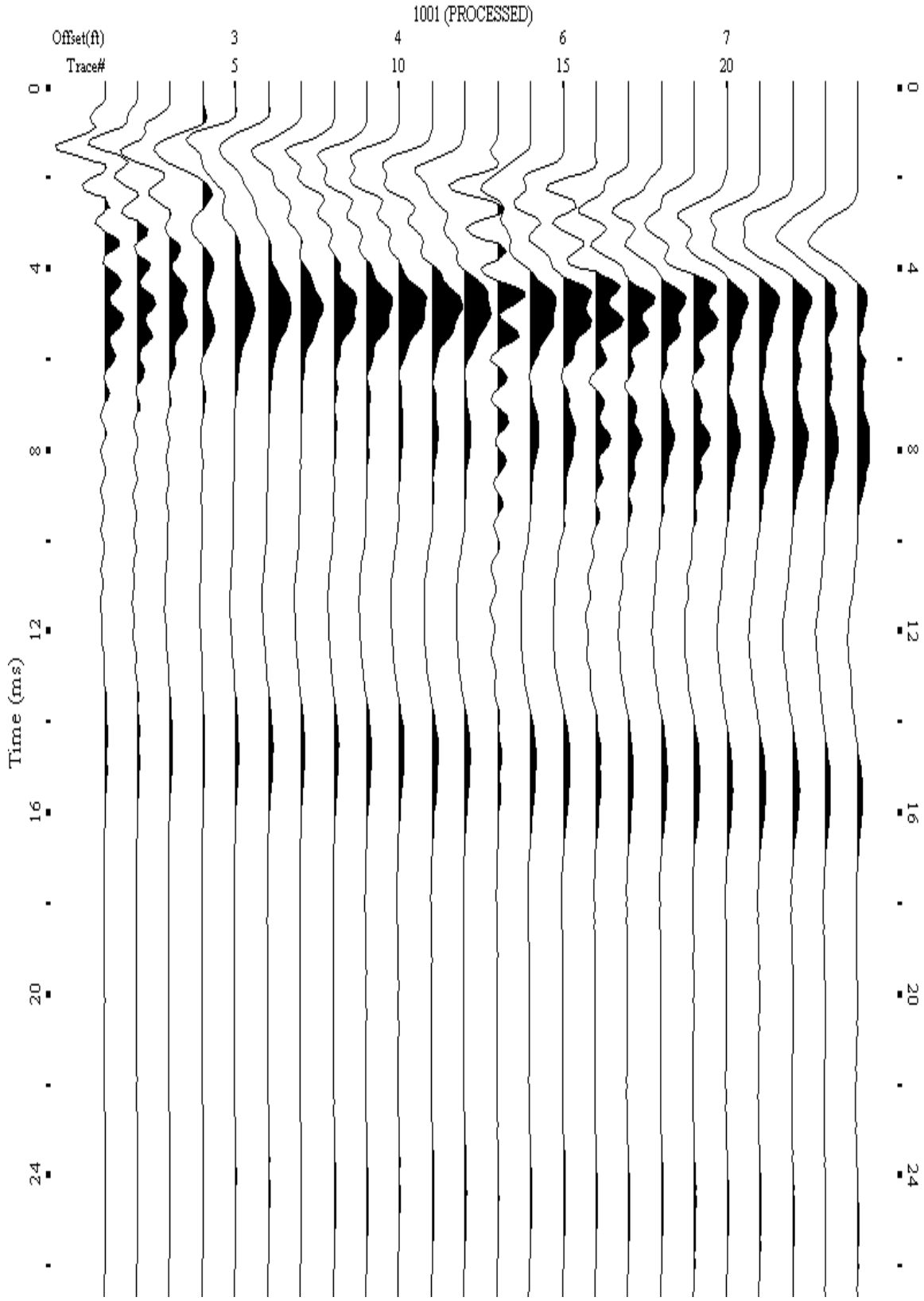

A.415: Shot Gather Line 1281 used in Post-blast 20

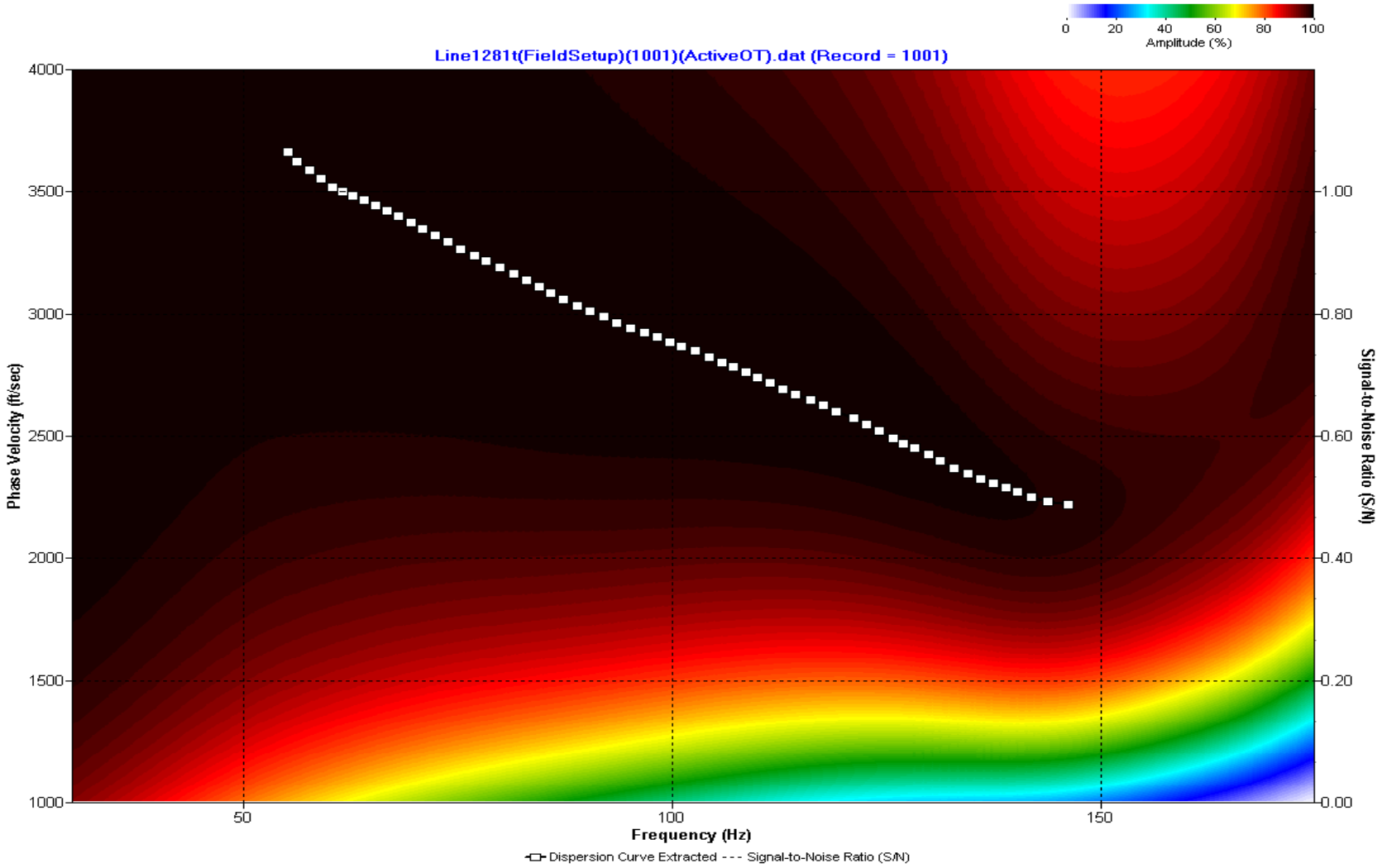

A.416: Dispersion Curve Line 1281 used in Post-blast 20

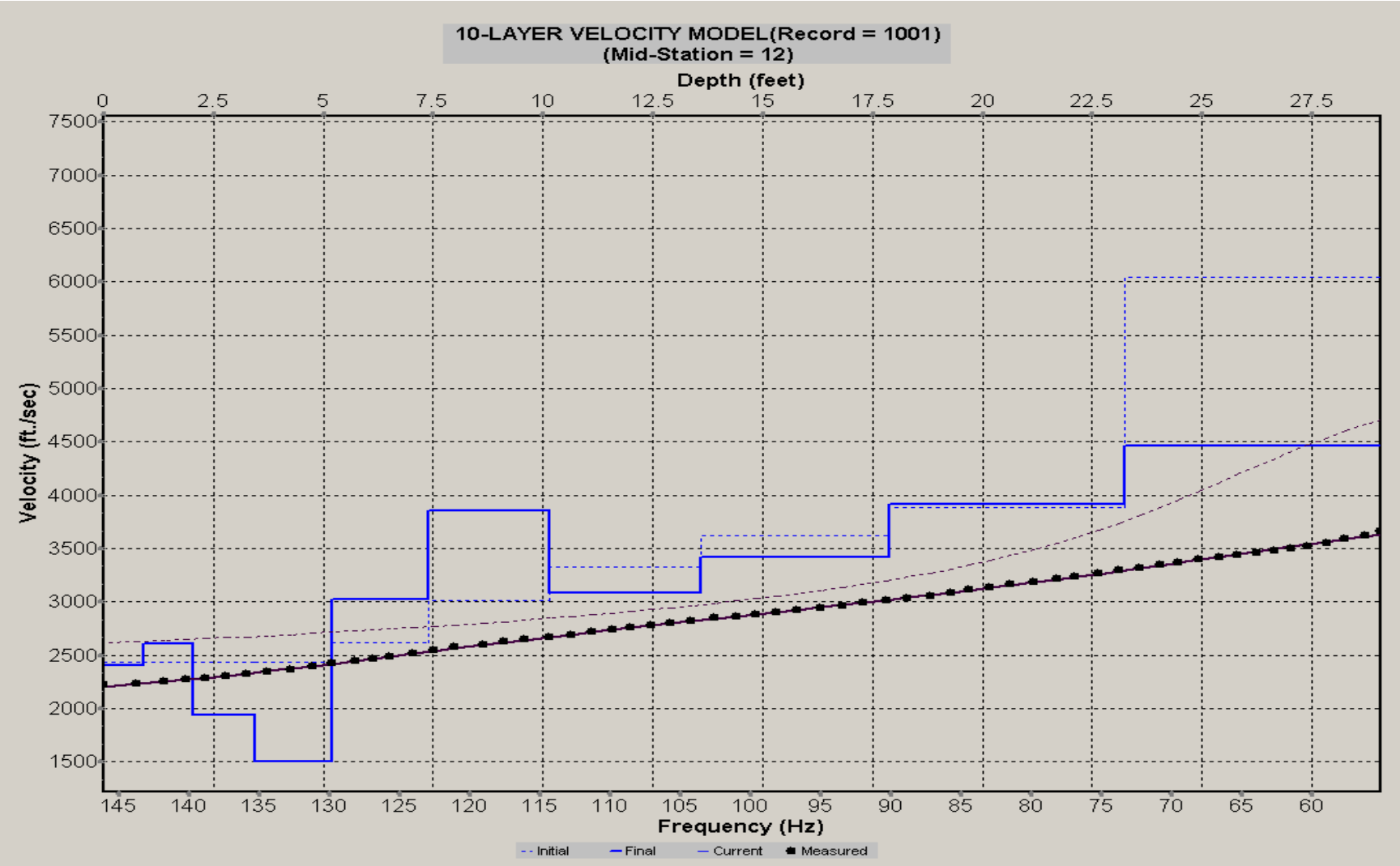

A.417: Velocity Profile Line 1281 used in Post-blast 20

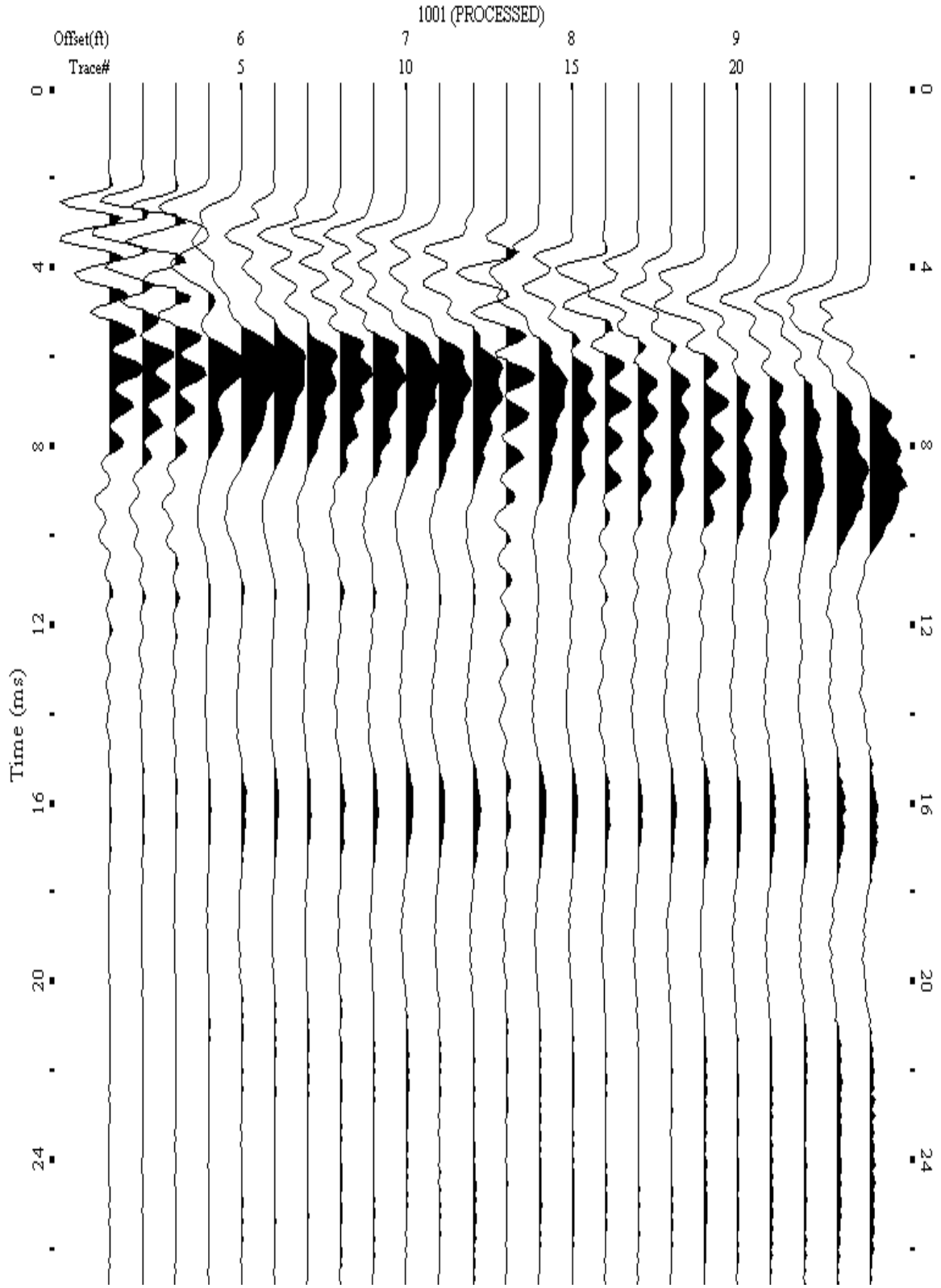

A.418: Shot Gather Line 1282 used in Post-blast 20 and Pre-blast 27

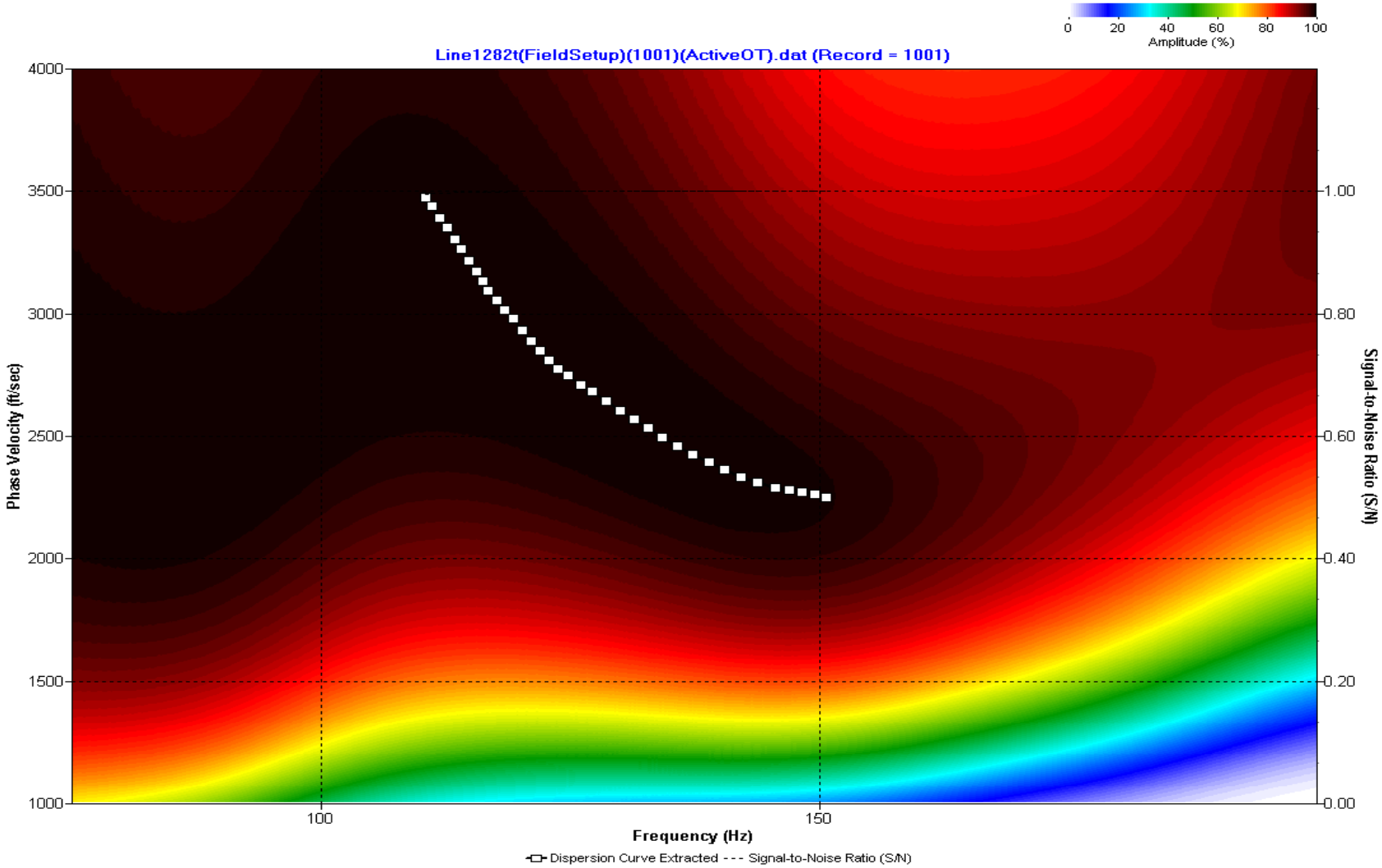

A.419: Dispersion Curve Line 1282 used in Post-blast 20 and Pre-blast 27

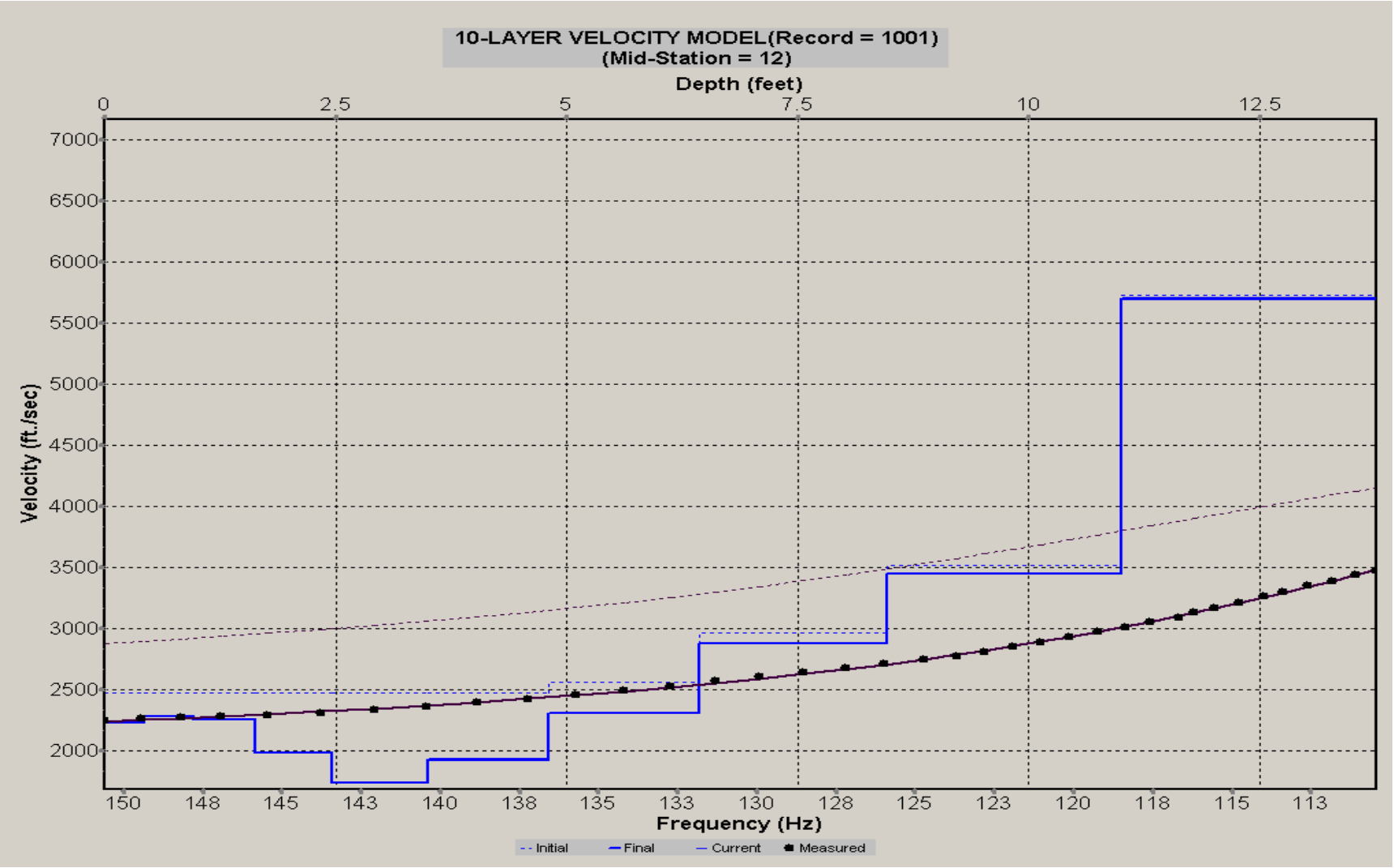

A.420: Velocity Profile Line 1282 used in Post-blast 20 and Pre-blast 27

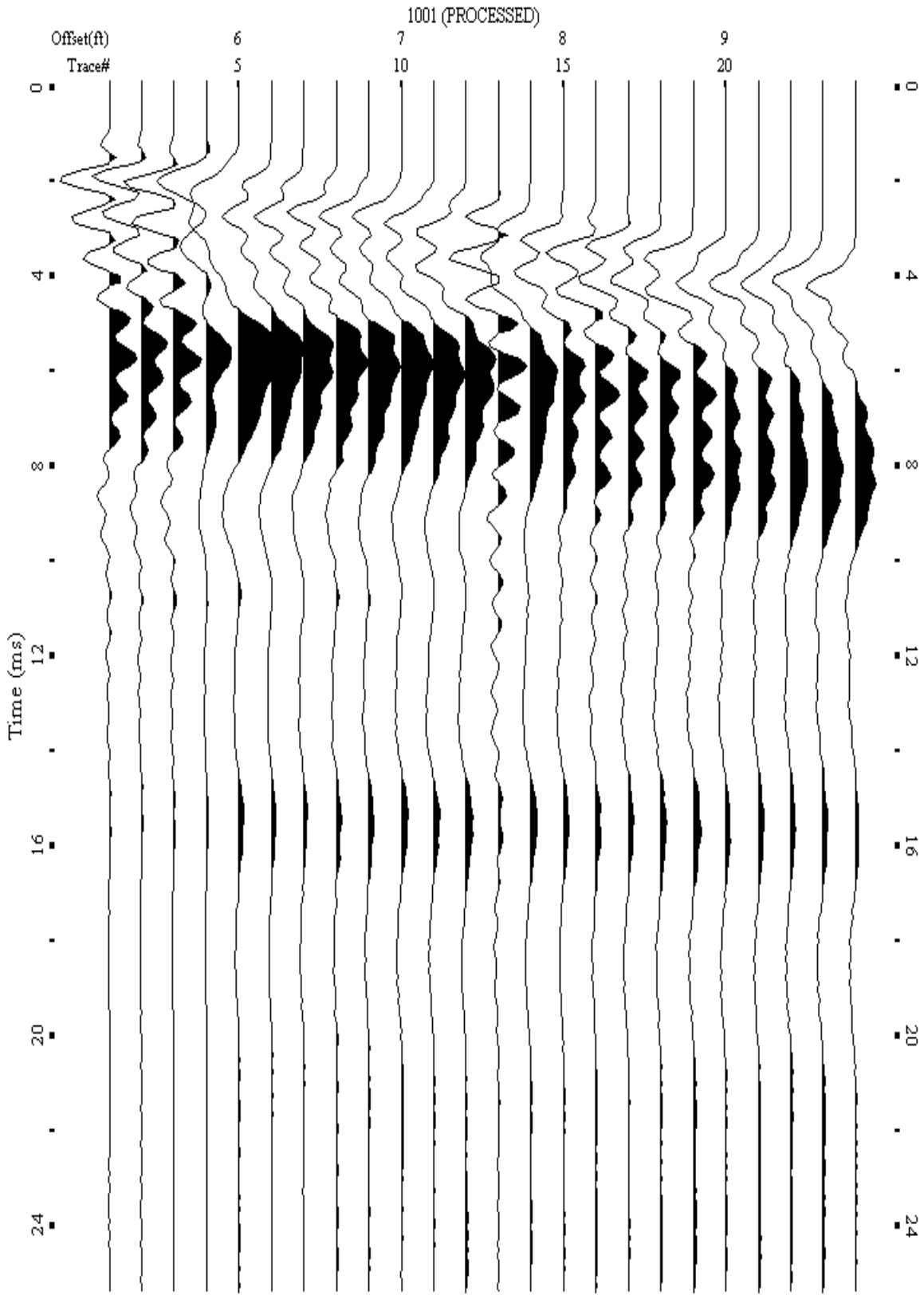

A.421: Shot Gather Line 1283 used in Post-blast 20 and Pre-blast 27

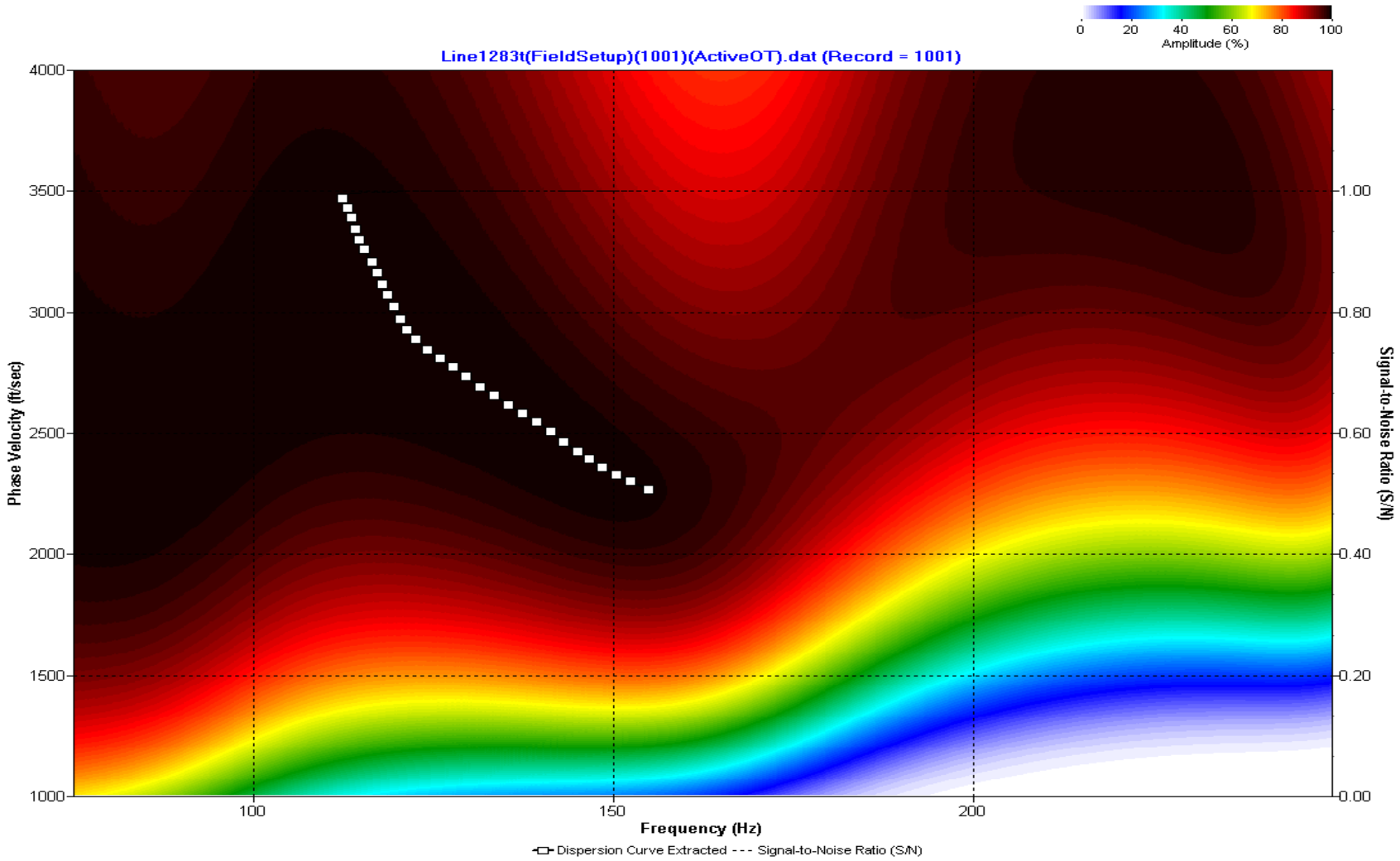

A.422: Dispersion Curve Line 1283 used in Post-blast 20 and Pre-blast 27

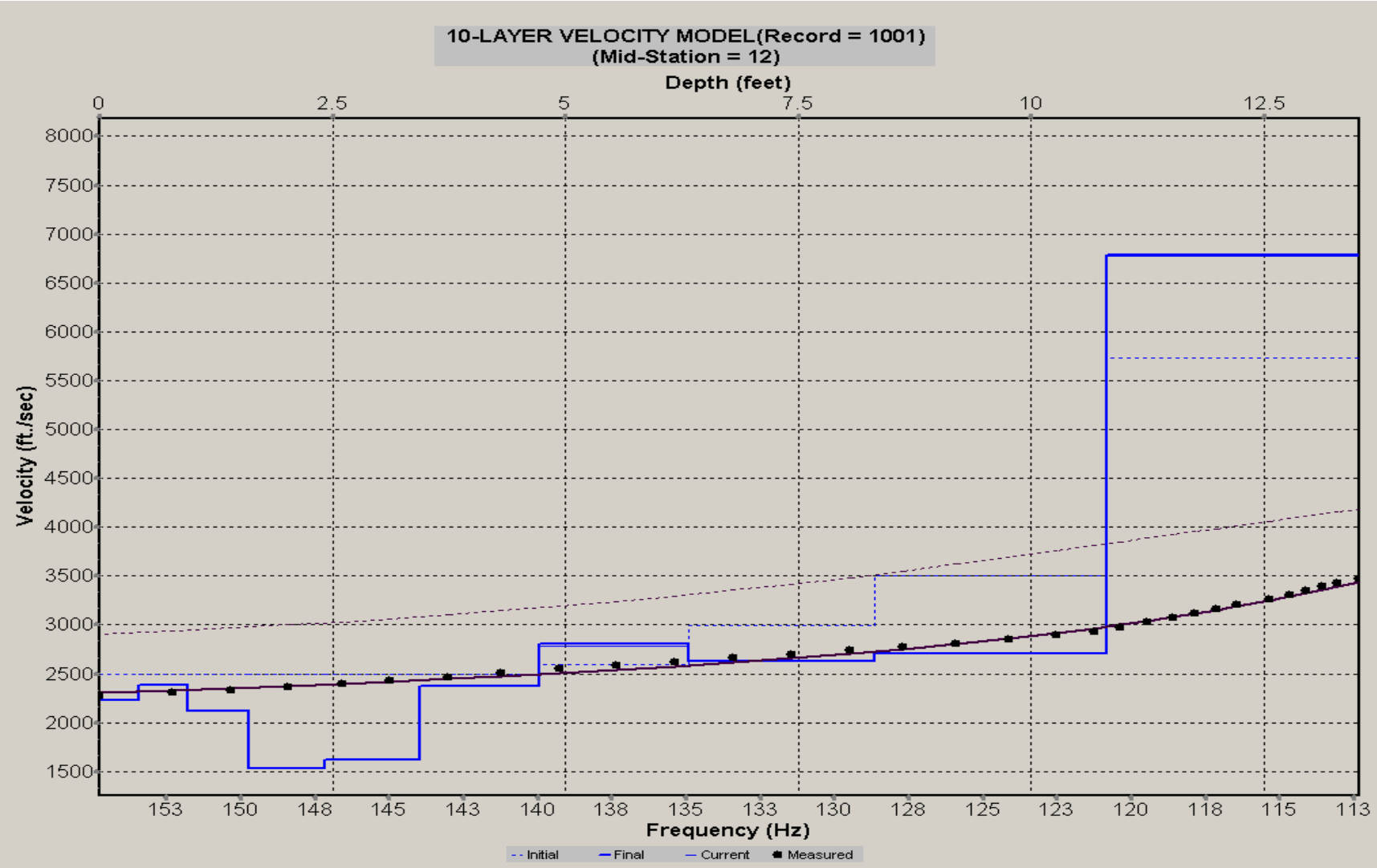

A.423: Velocity Profile Line 1283 used in Post-blast 20 and Pre-blast 27

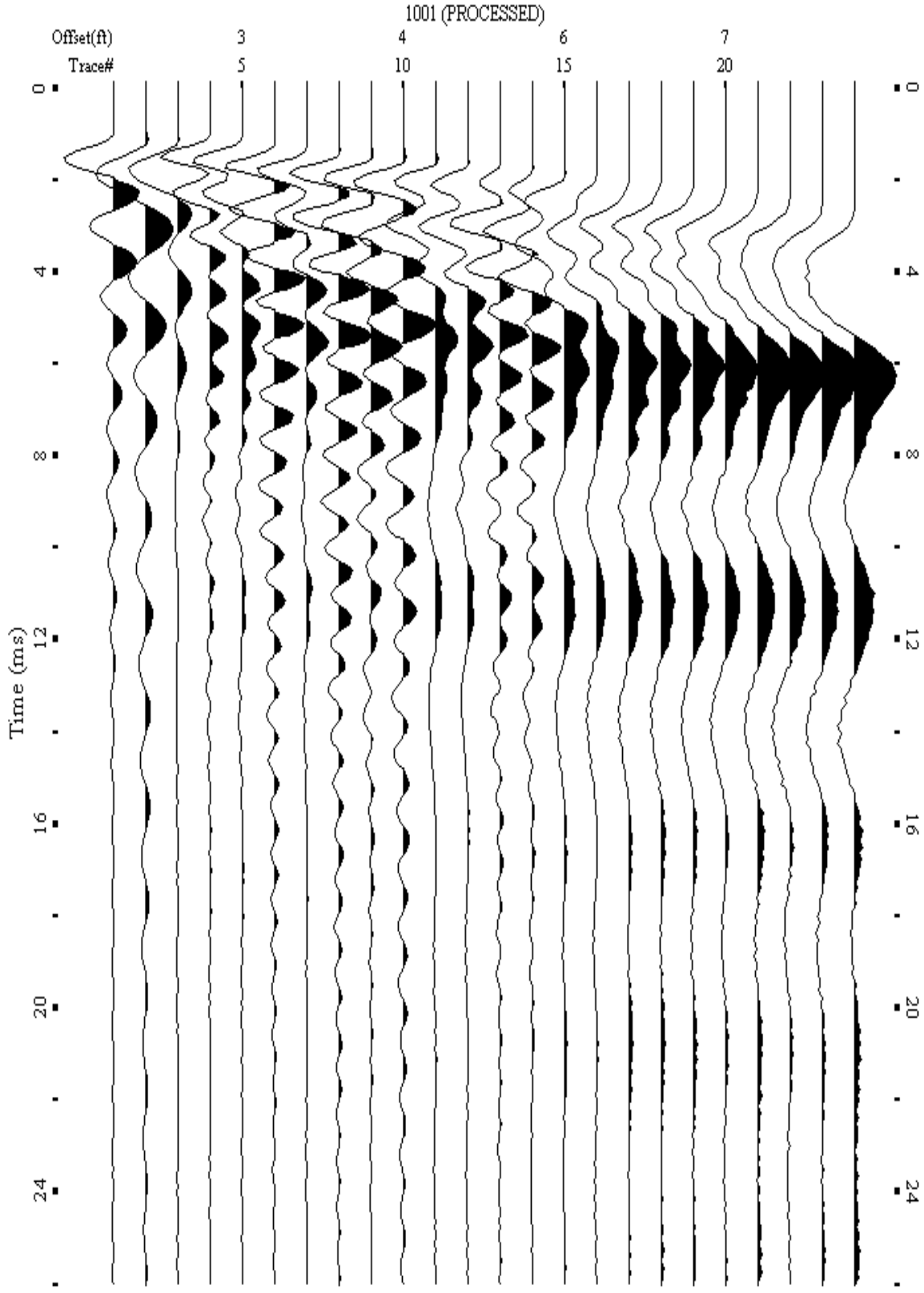

A.424: Shot Gather Line 1286 used in Pre-blast 14 and Pre-blast 28

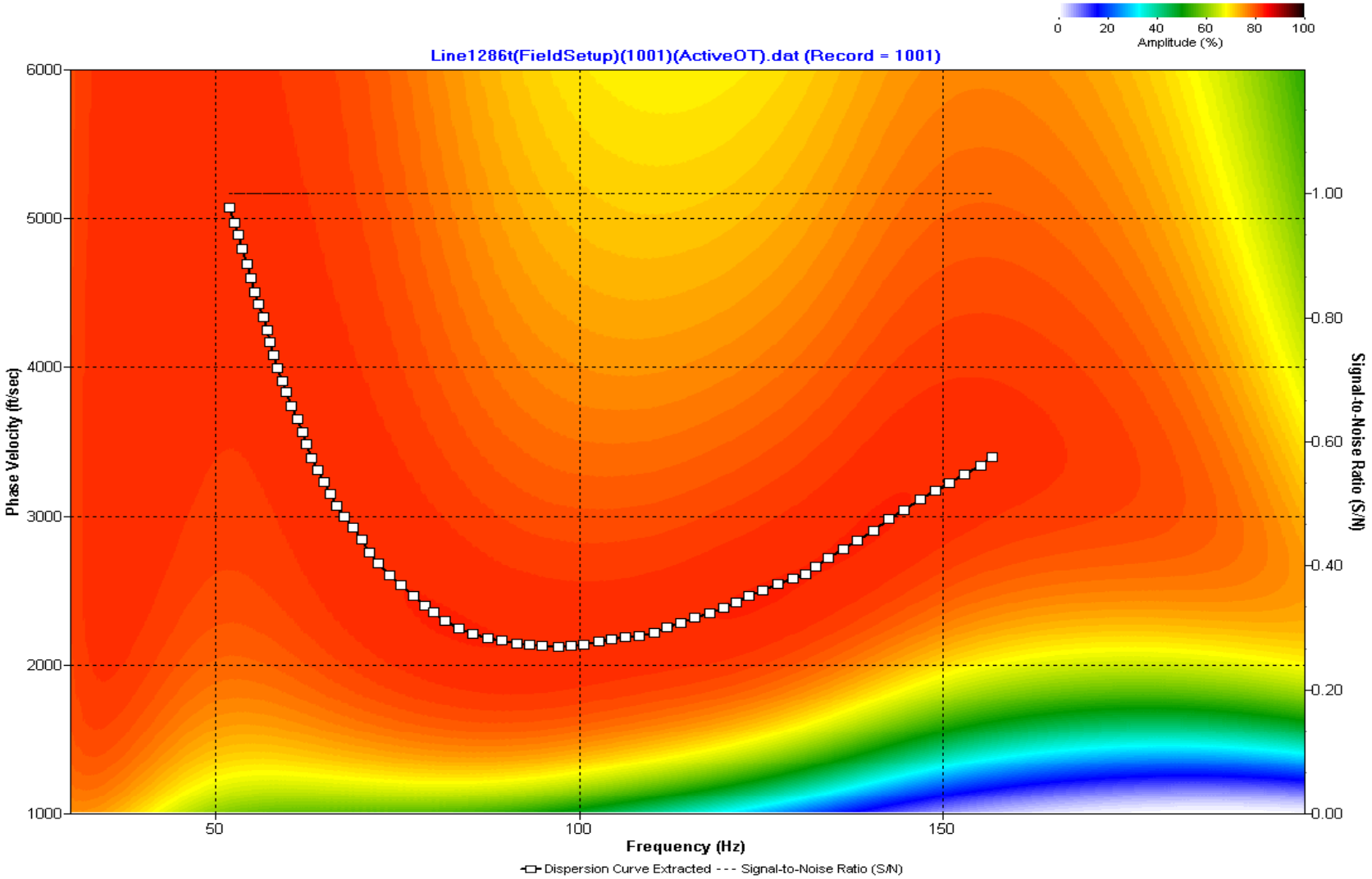

A.425: Dispersion Curve Line 1286 used in Pre-blast 14 and Pre-blast 28

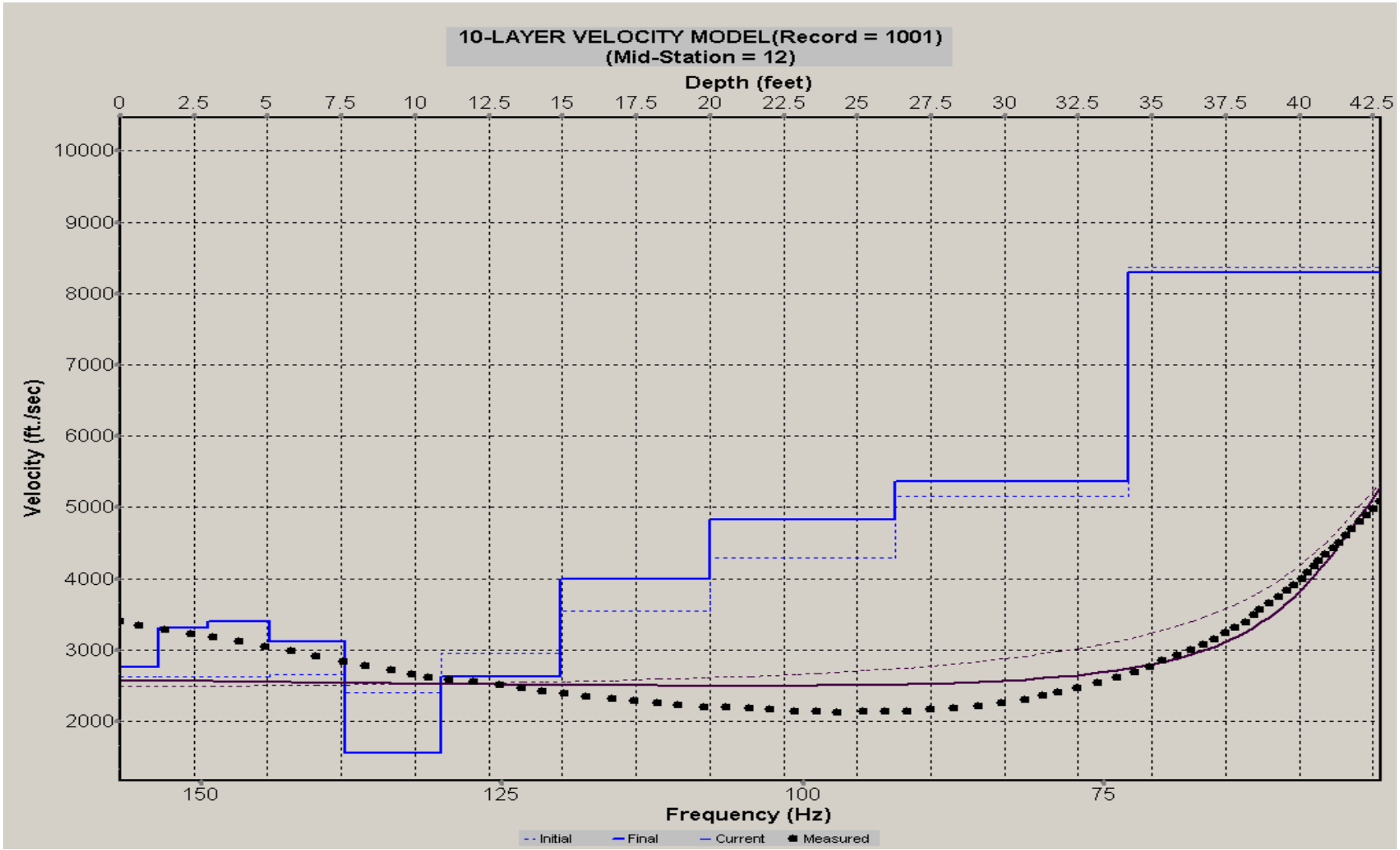

A.426: Velocity Profile Line 1286 used in Pre-blast 14 and Pre-blast 28

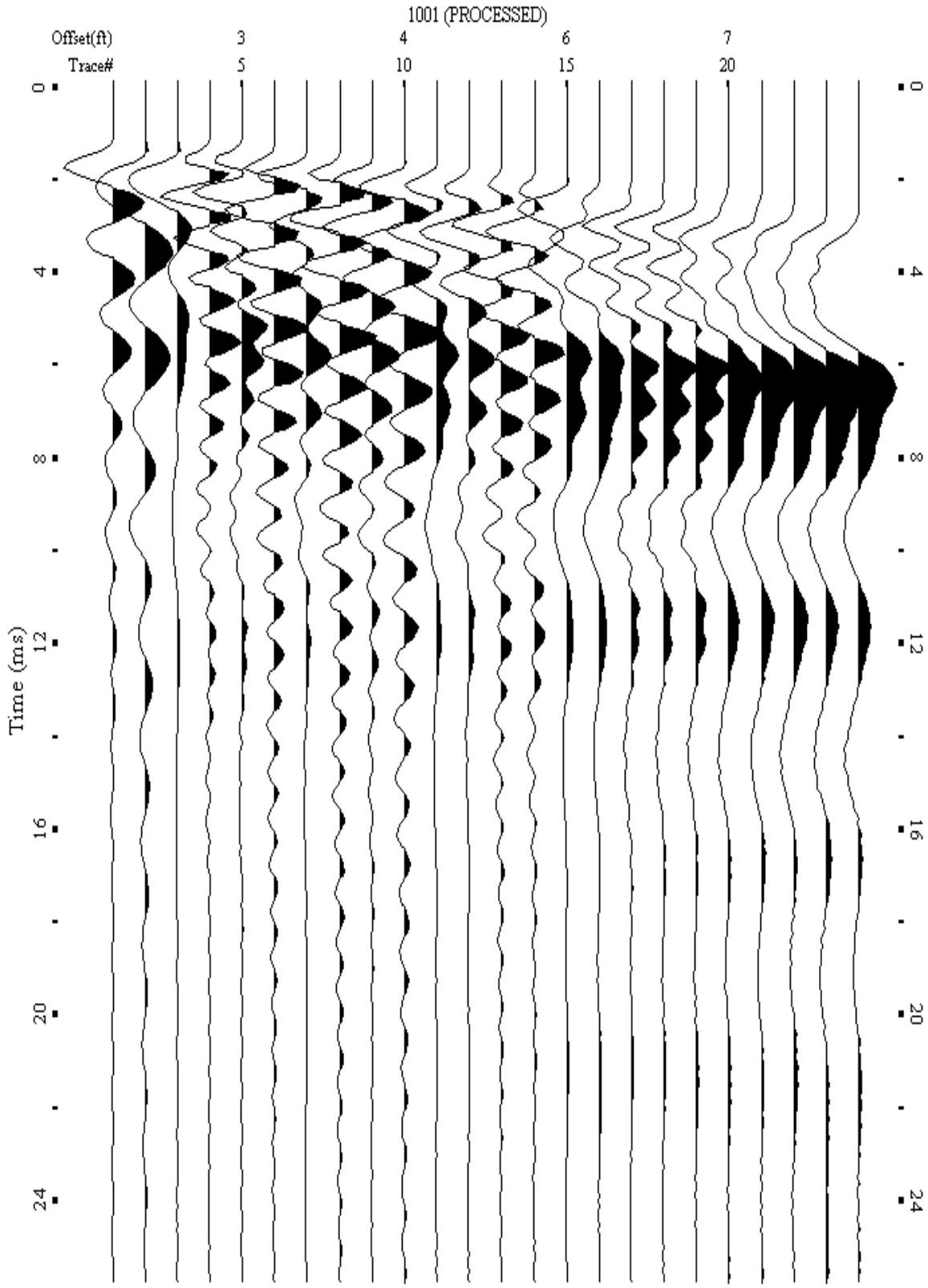

A.427: Shot Gather Line 1287 used in Post-blast 19 and Pre-blast 28

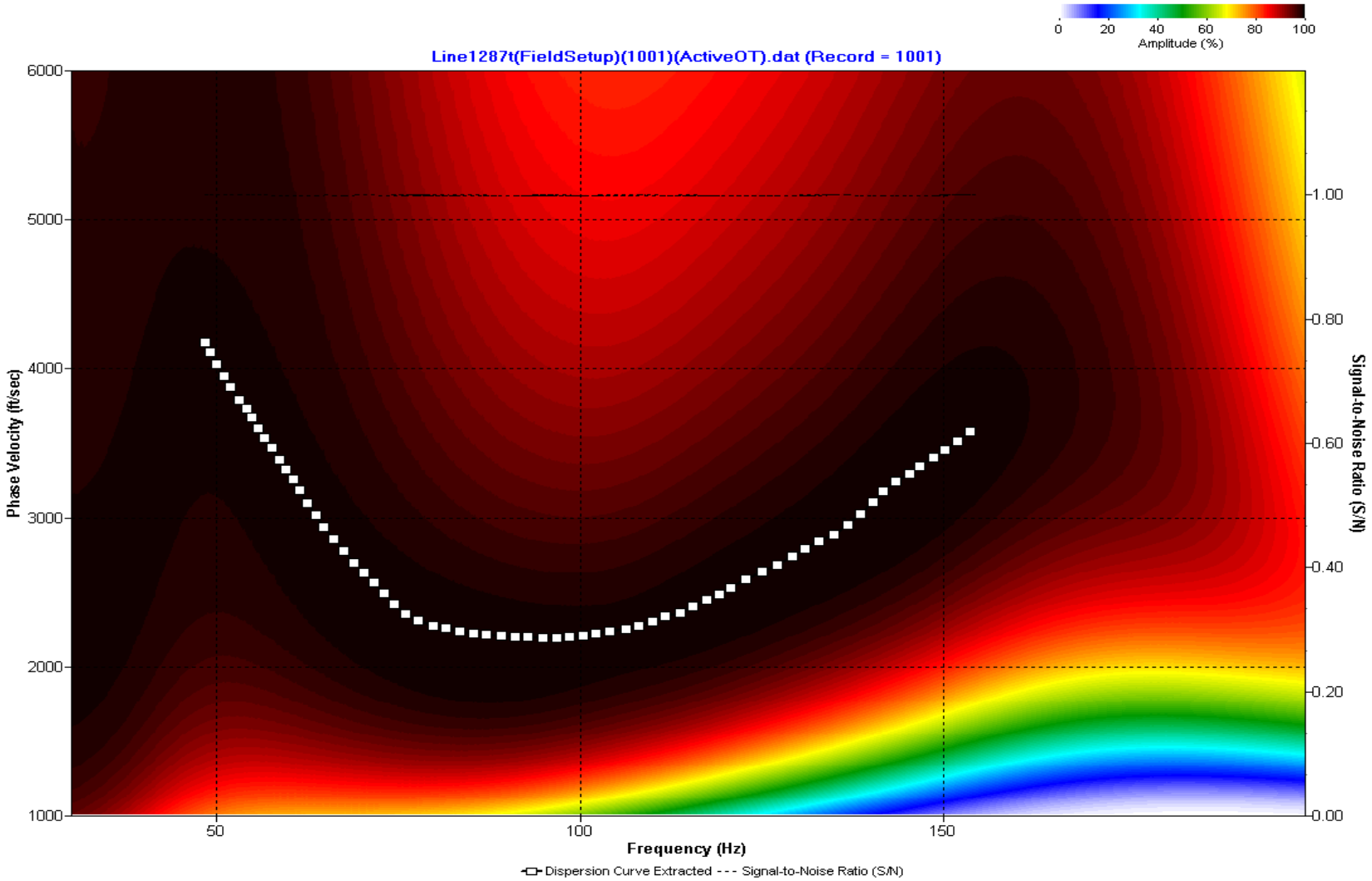

A.428: Dispersion Curve Line 1287 used in Post-blast 19 and Pre-blast 28

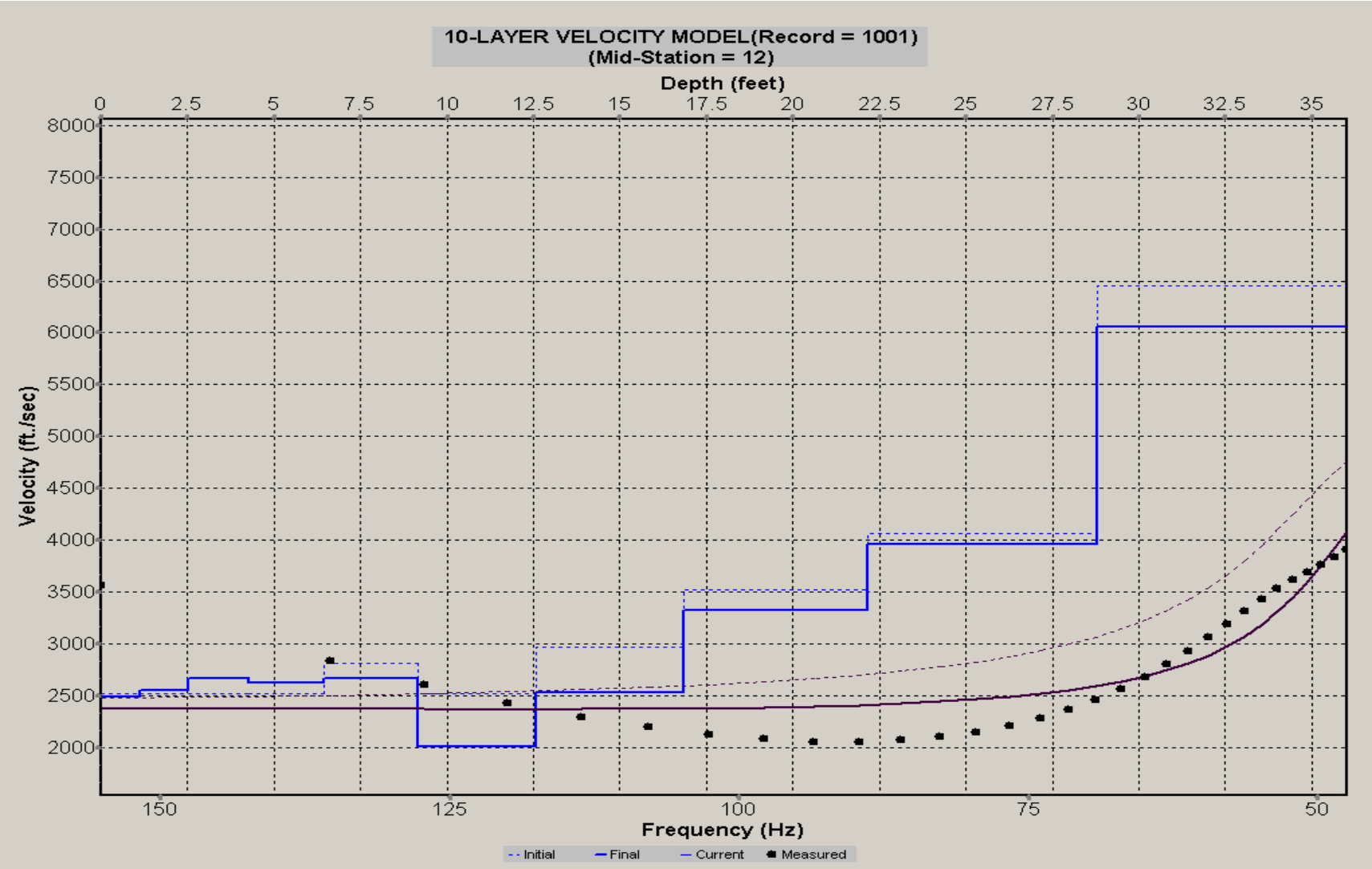

A.429: Velocity Profile Line 1287 used in Post-blast 19 and Pre-blast 28

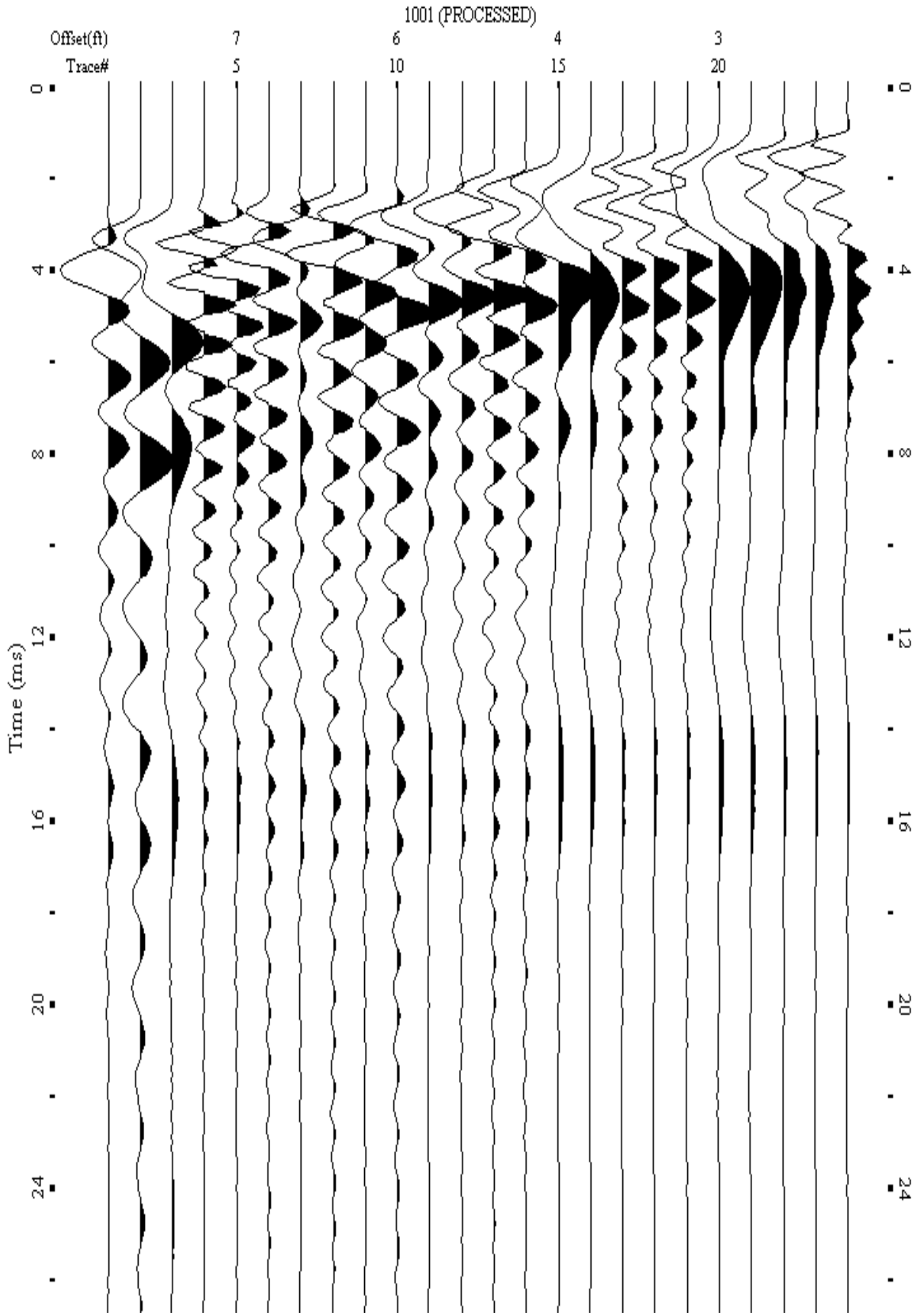

A.430: Shot Gather Line 1290 used in Post-blast 19

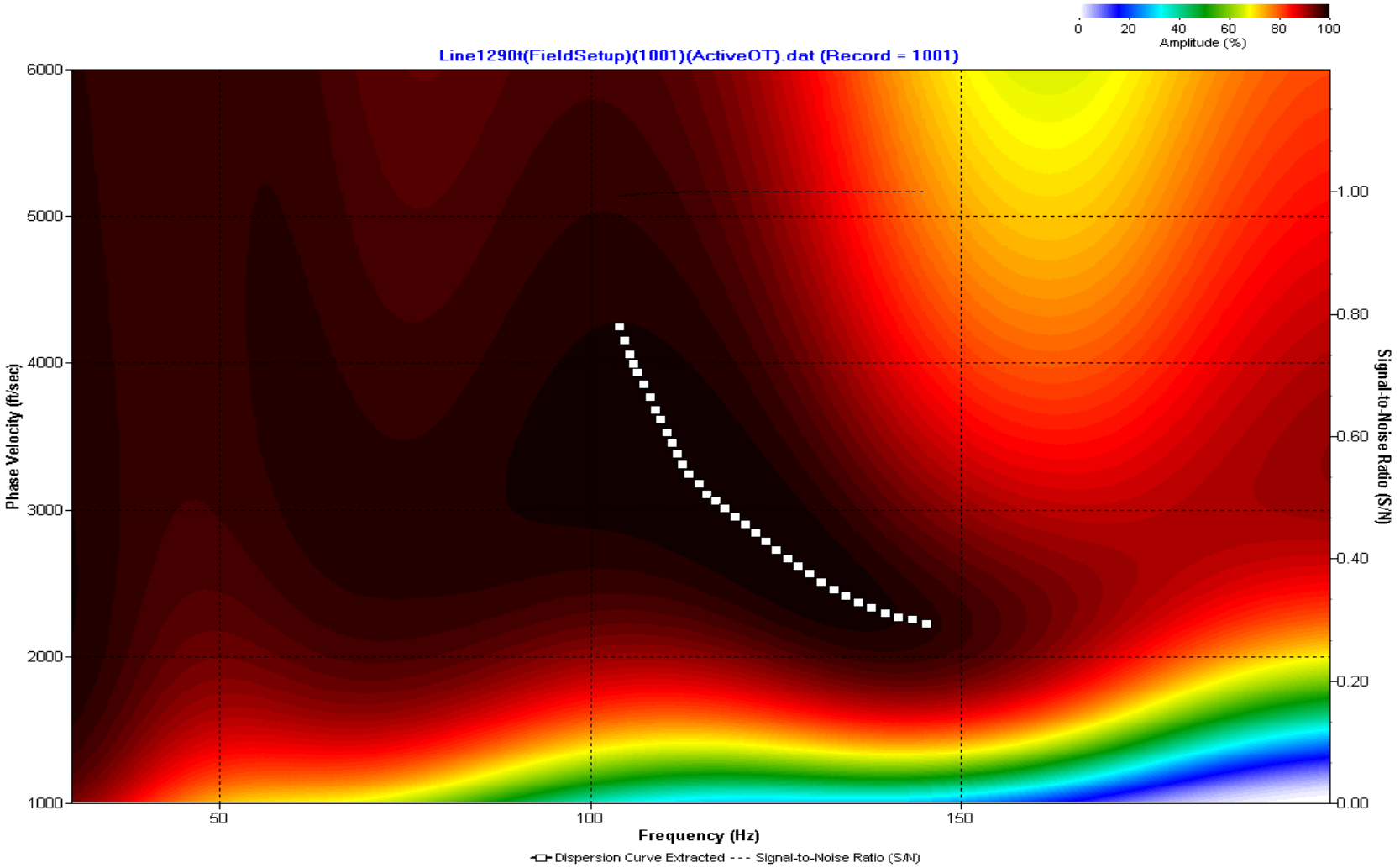

A.431: Dispersion Curve Line 1290 used in Post-blast 19

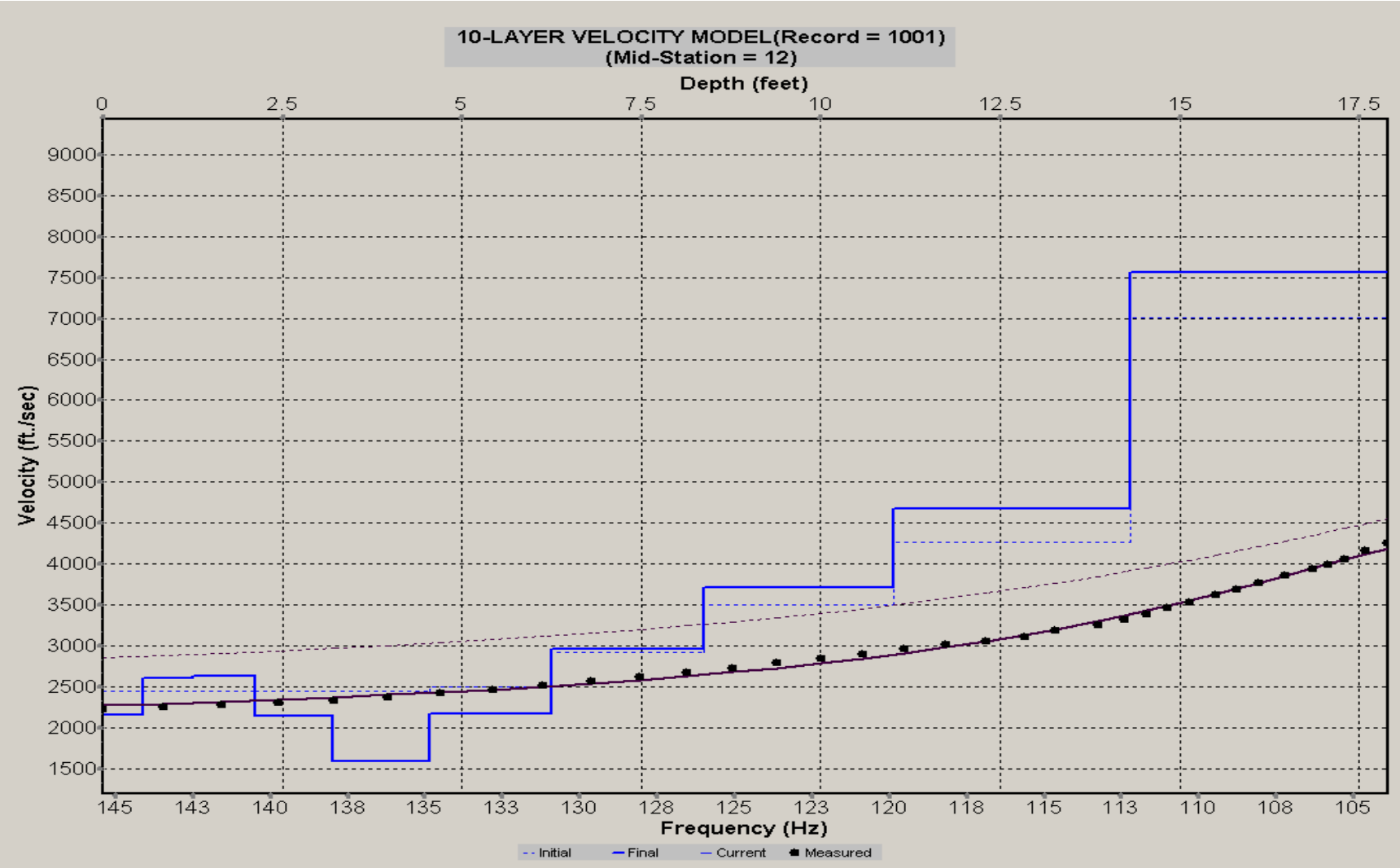

A.432: Velocity Profile Line 1290 used in Post-blast 19

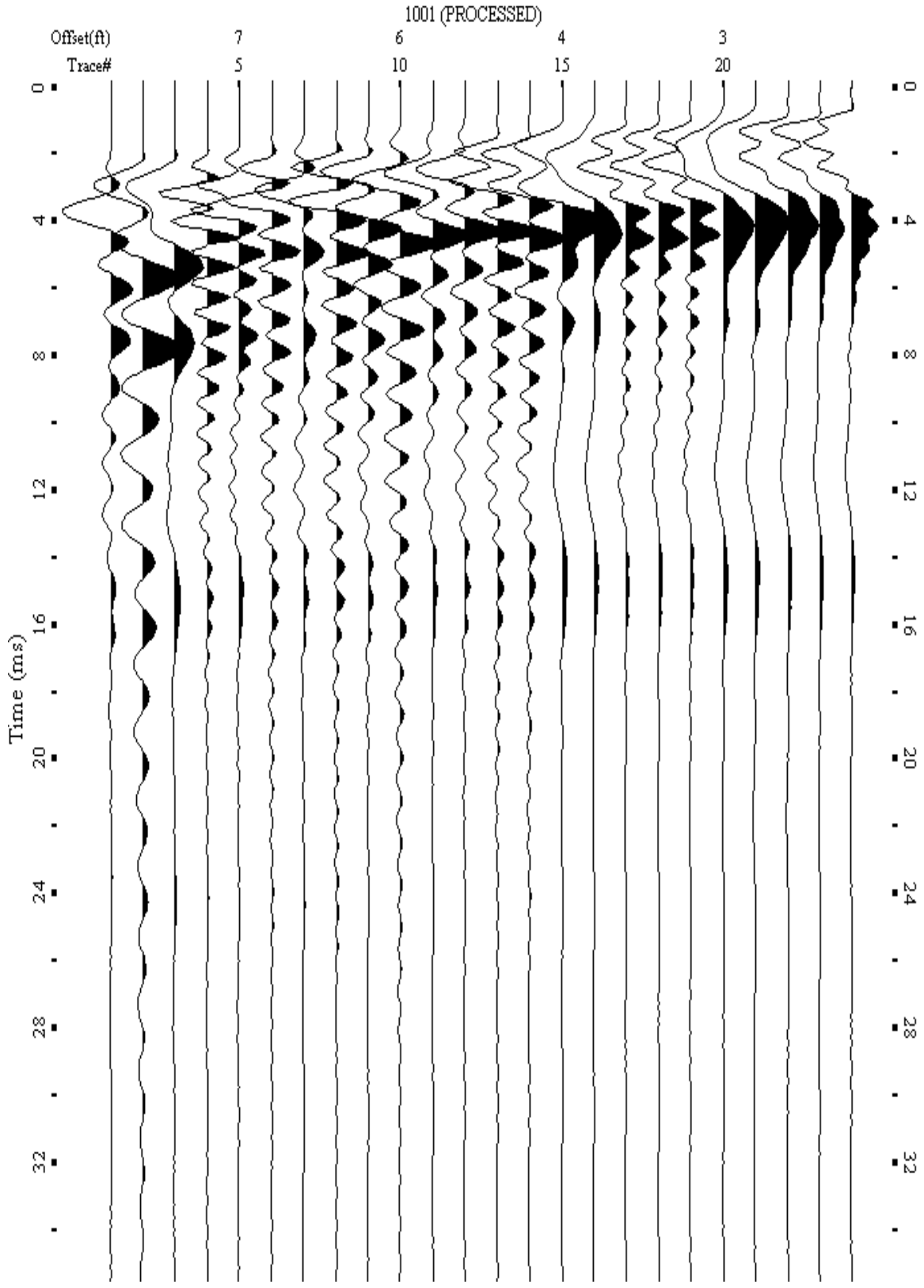

A.433: Shot Gather Line 1291 used in Post-blast 19 and Pre-blast 28

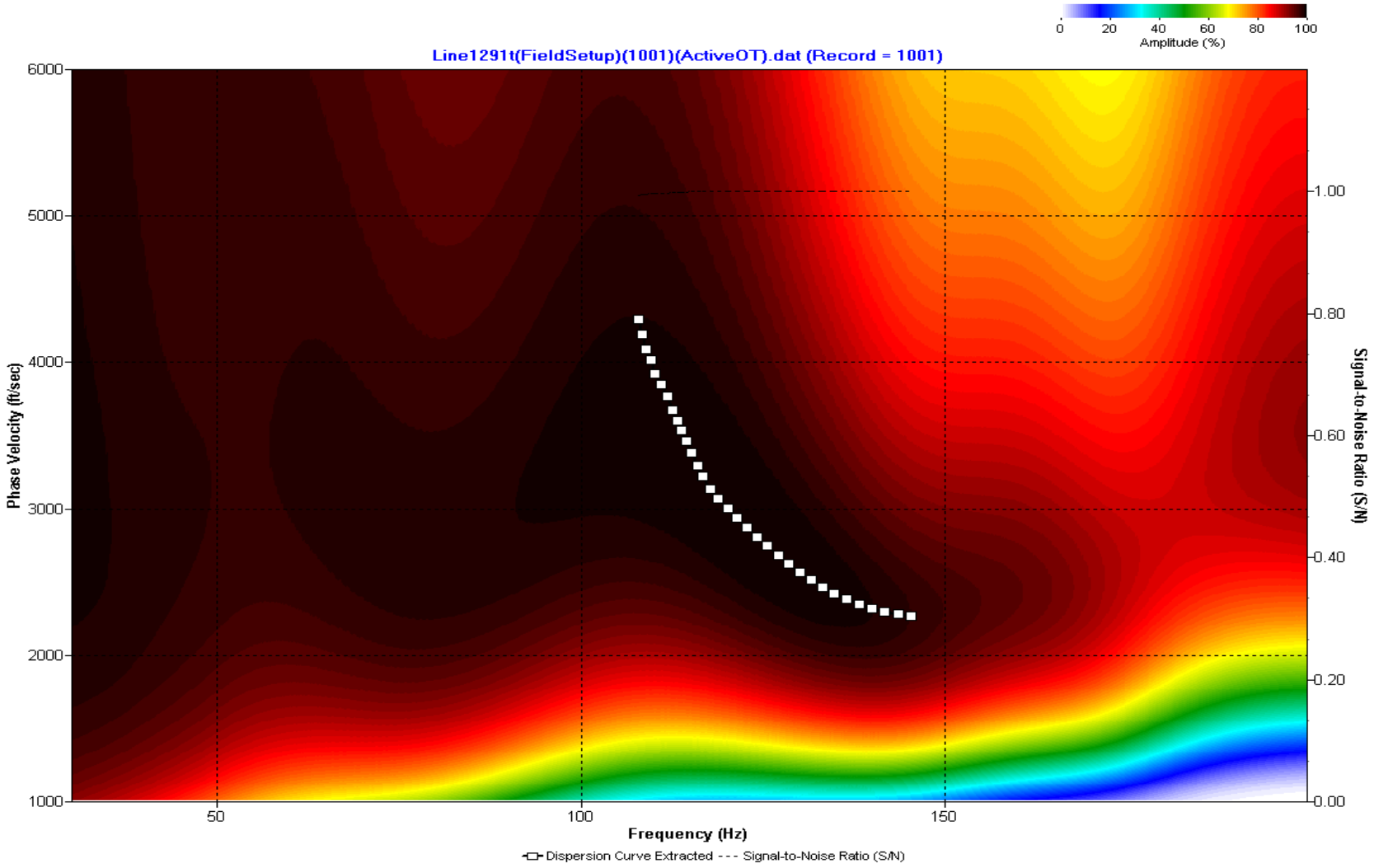

A.434: Dispersion Curve Line 1291 used in Post-blast 19 and Pre-blast 28

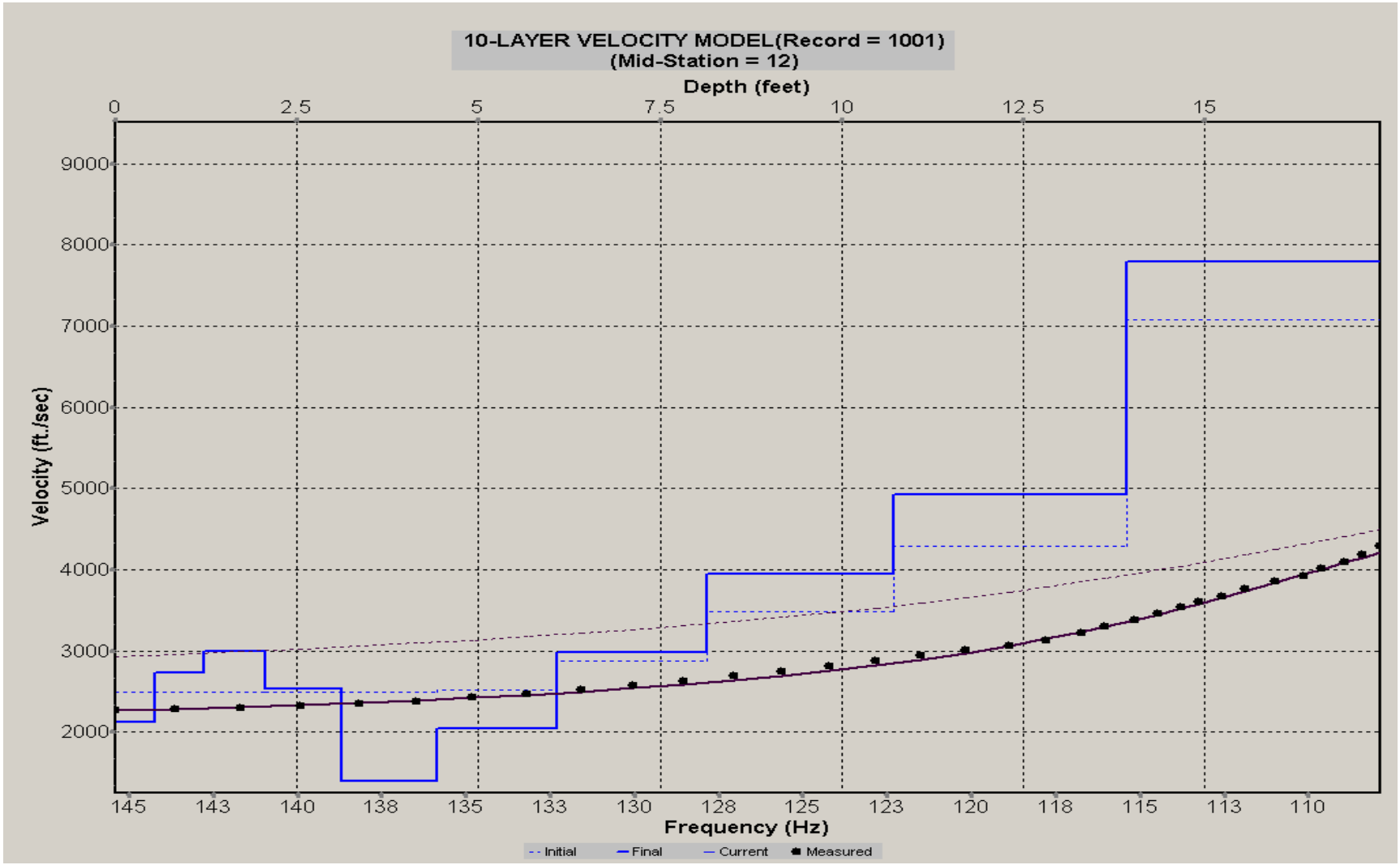

A.435: Velocity Profile Line 1291 used in Post-blast 19 and Pre-blast 28

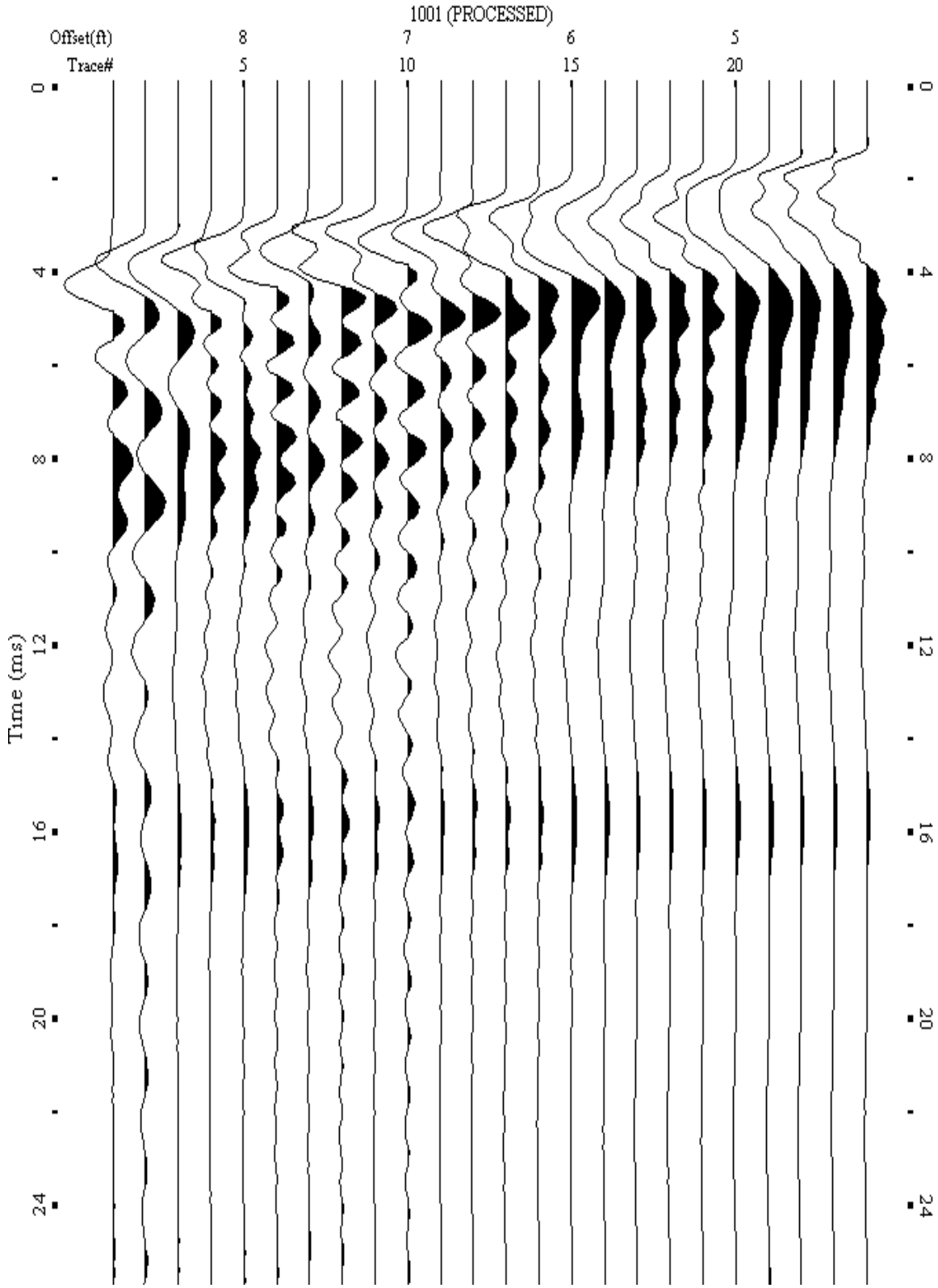

A.436: Shot Gather Line 1292 used in Pre-blast 14, Post-blast 19 and Pre-blast 28

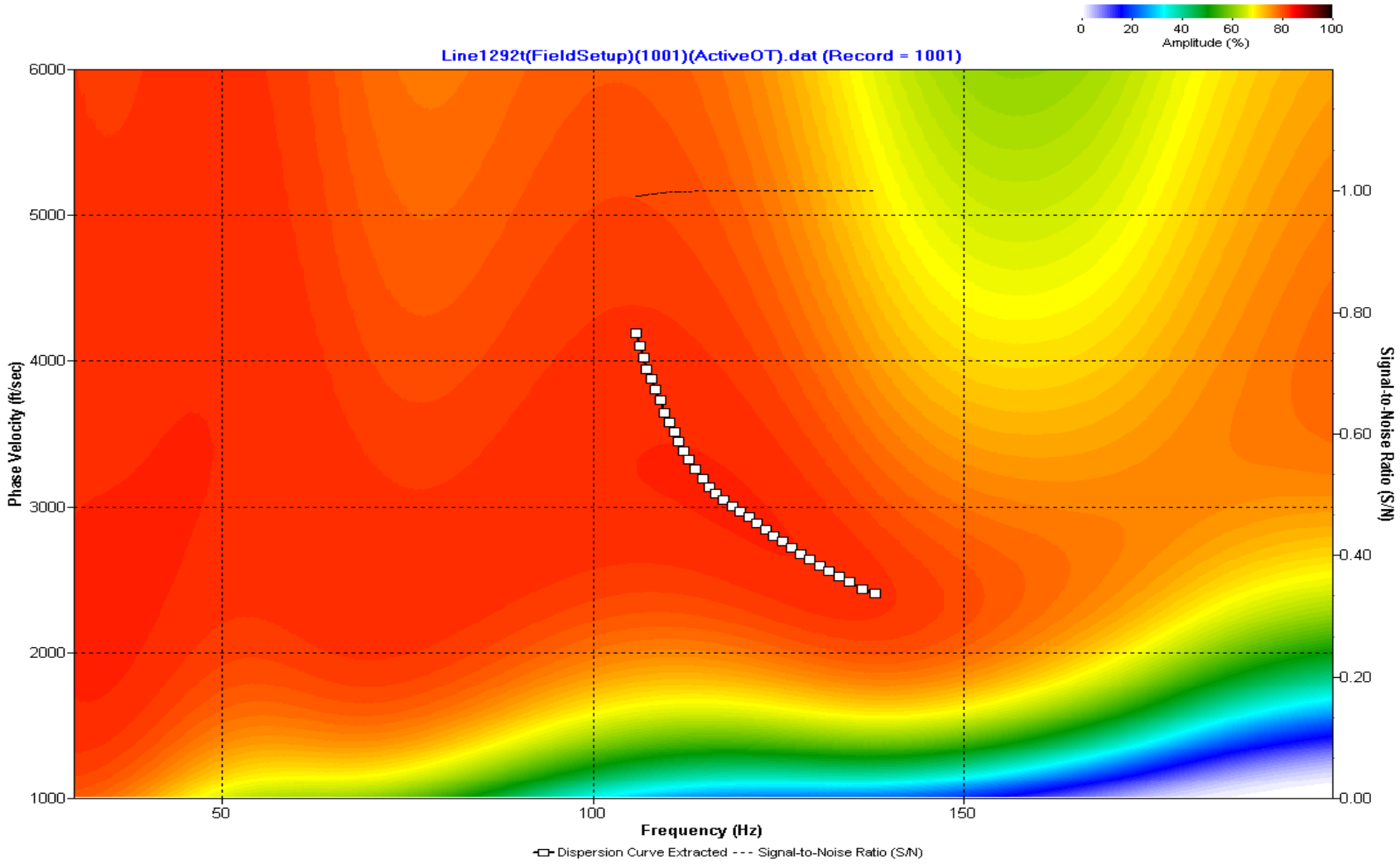

A.437: Dispersion Curve Line 1292 used in Pre-blast 14, Post-blast 19 and Pre-blast 28

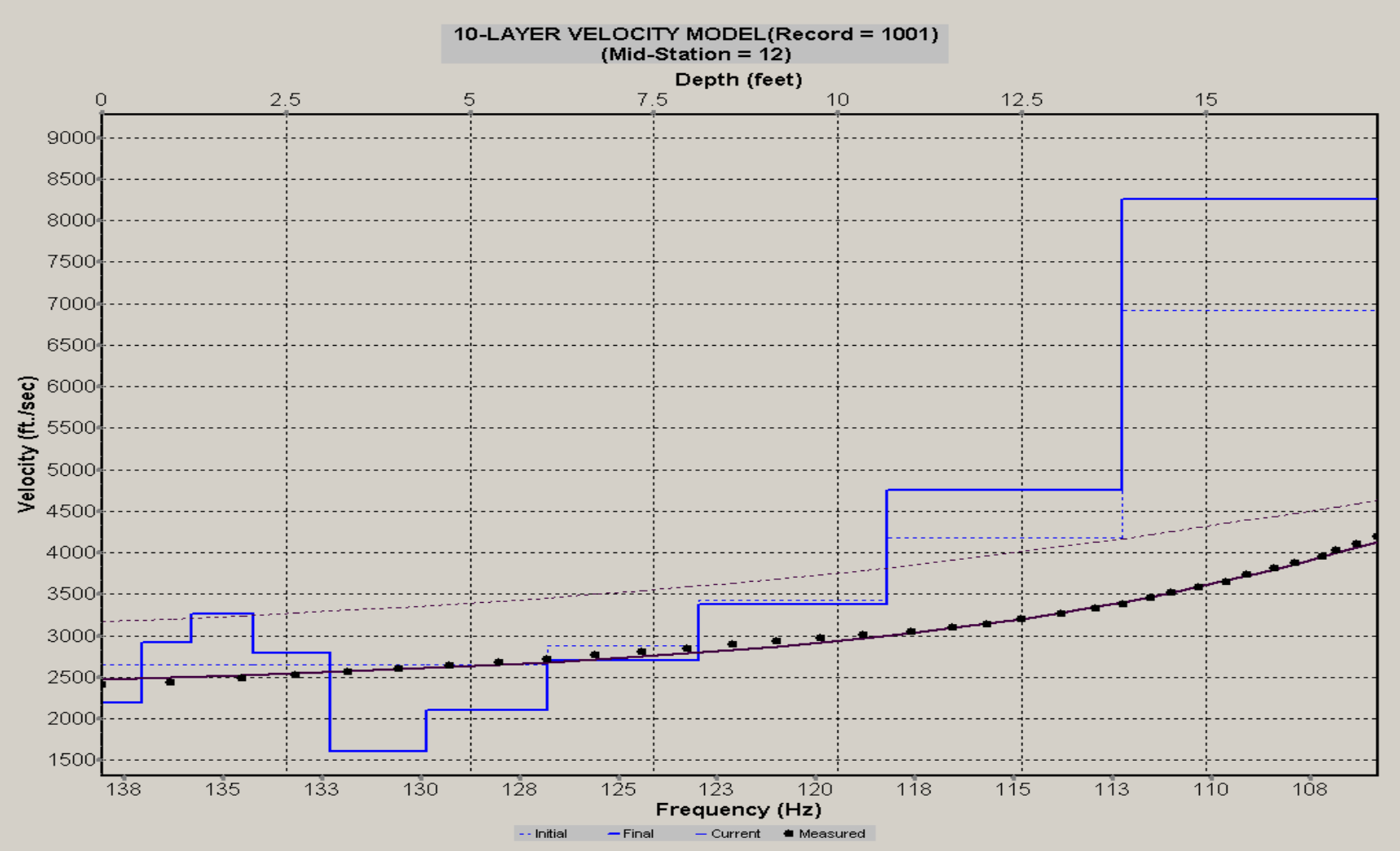

A.438: Velocity Profile Line 1292 used in Pre-blast 14, Post-blast 19 and Pre-blast 28

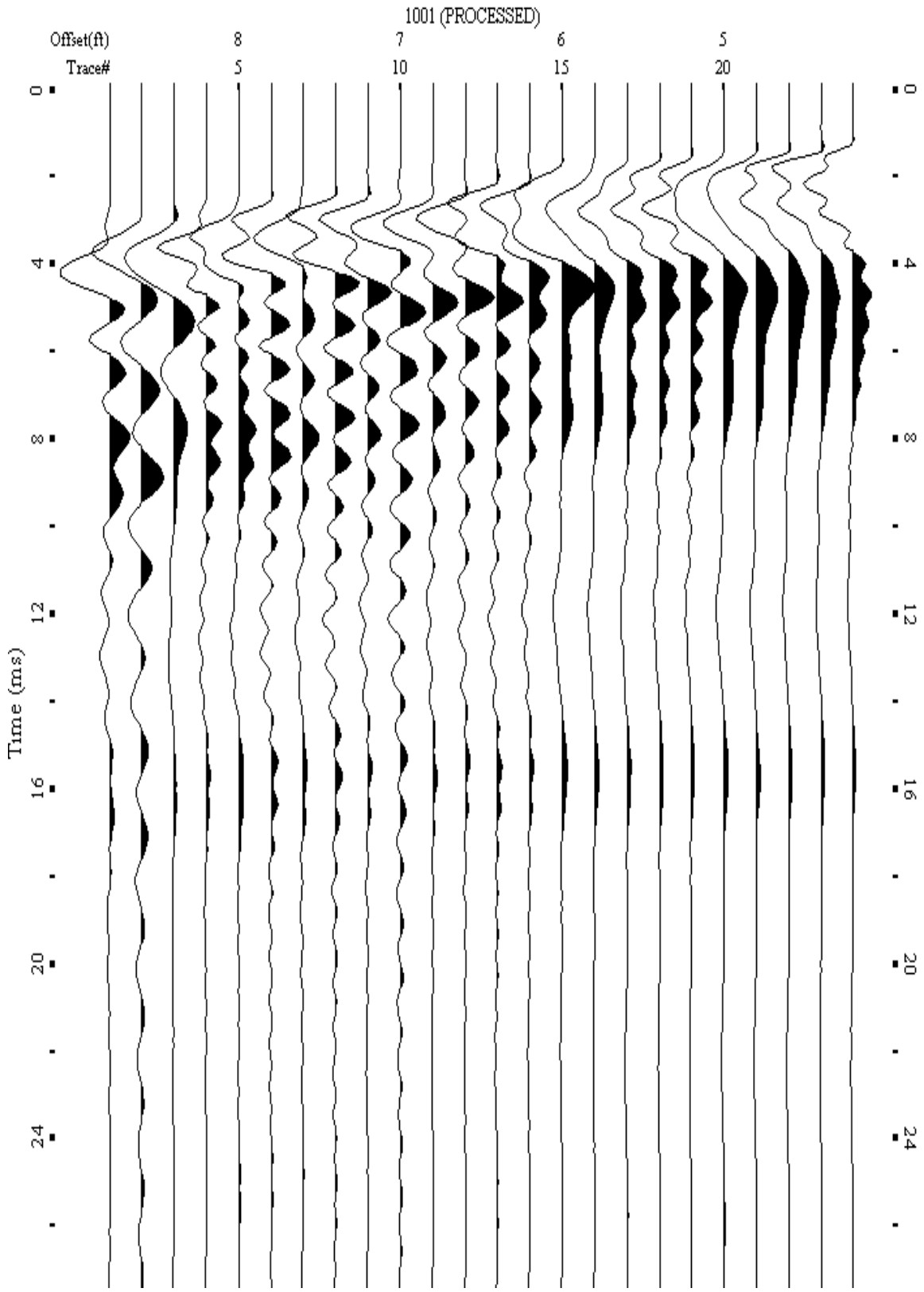

A.439: Shot Gather Line 1293 used in Pre-blast 14, Post-blast 19 and Pre-blast 28

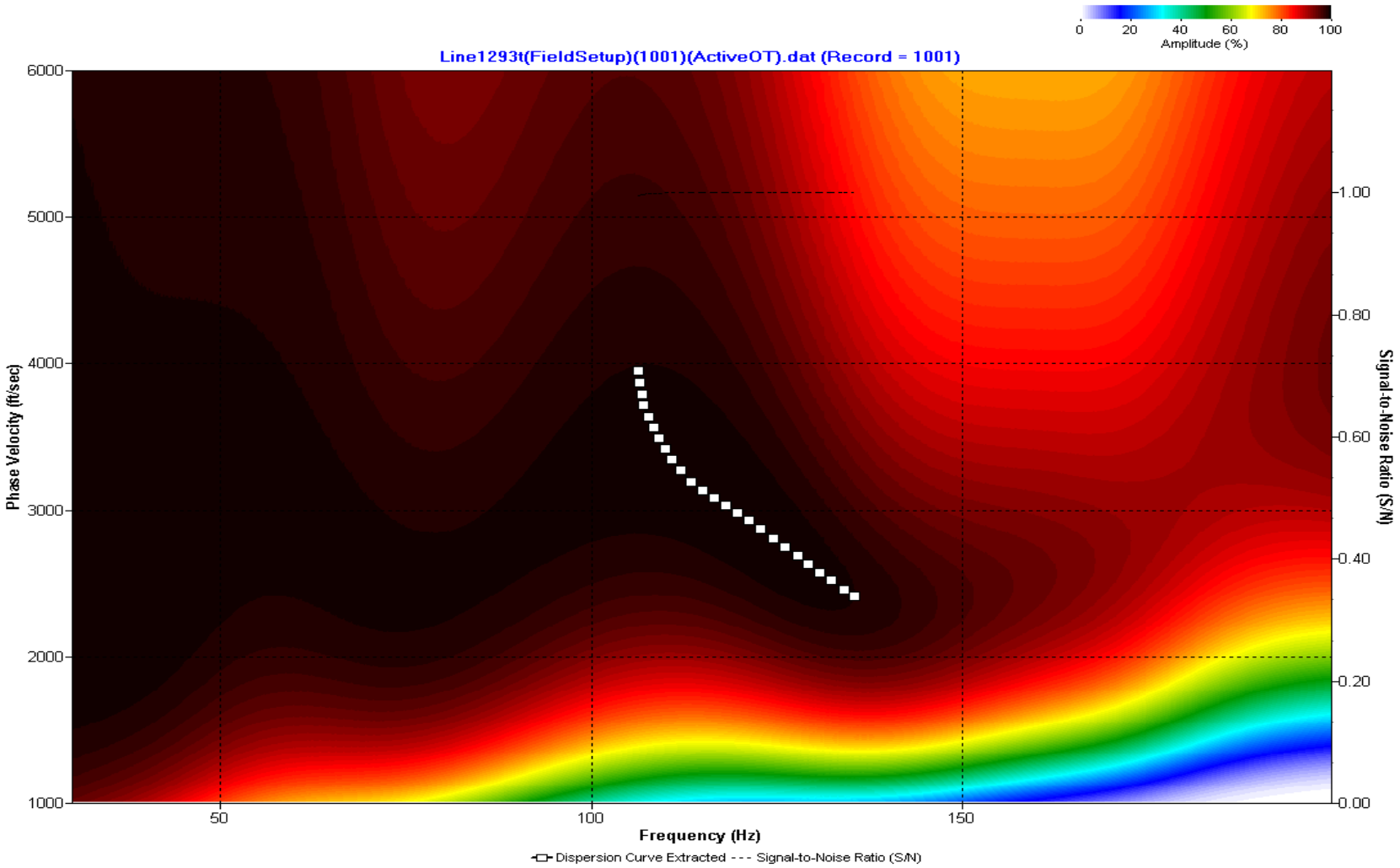

A.440: Dispersion Curve Line 1293 used in Pre-blast 14, Post-blast 19 and Pre-blast 28

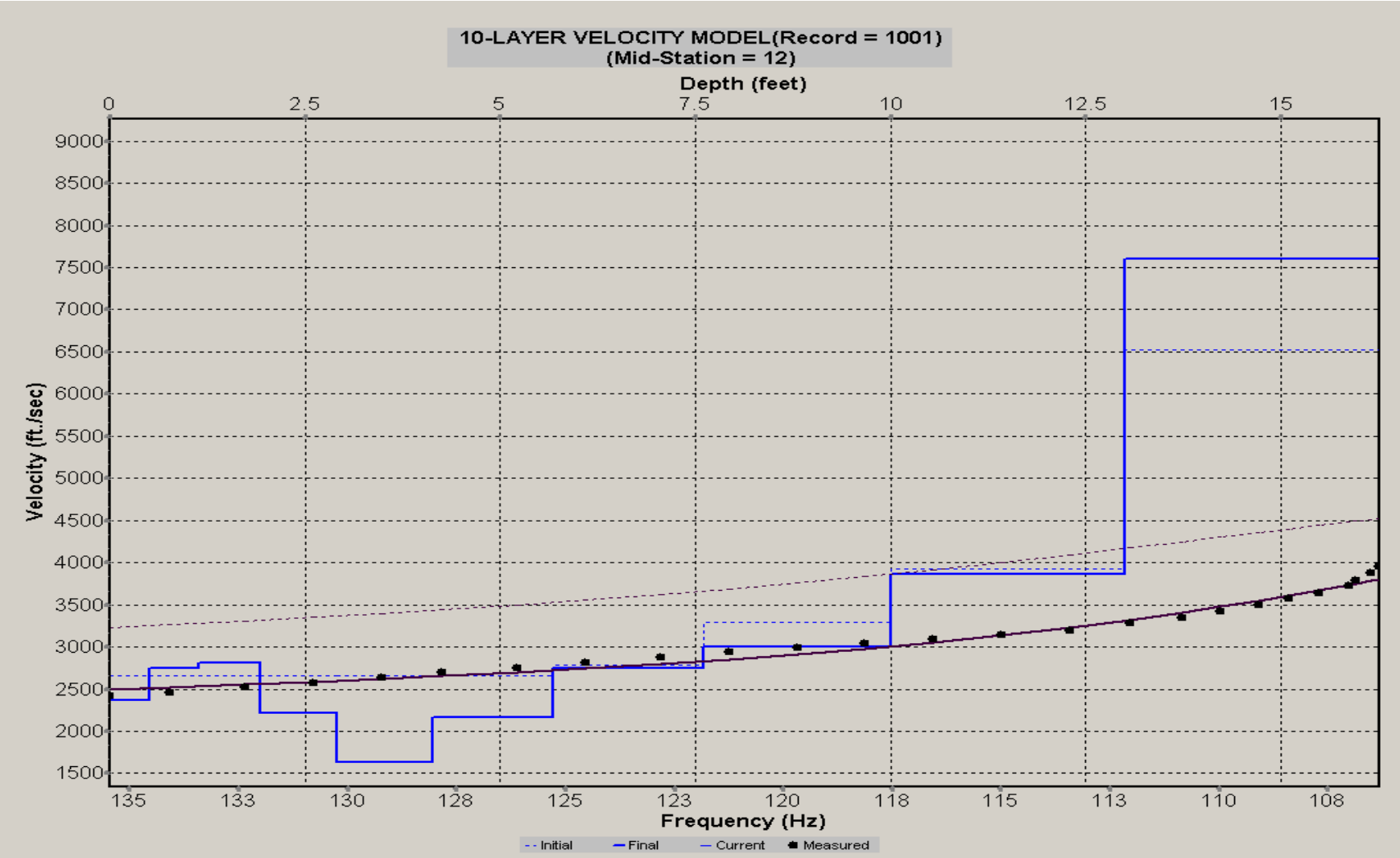

A.441: Velocity Profile Line 1293 used in Pre-blast 14, Post-blast 19 and Pre-blast 28

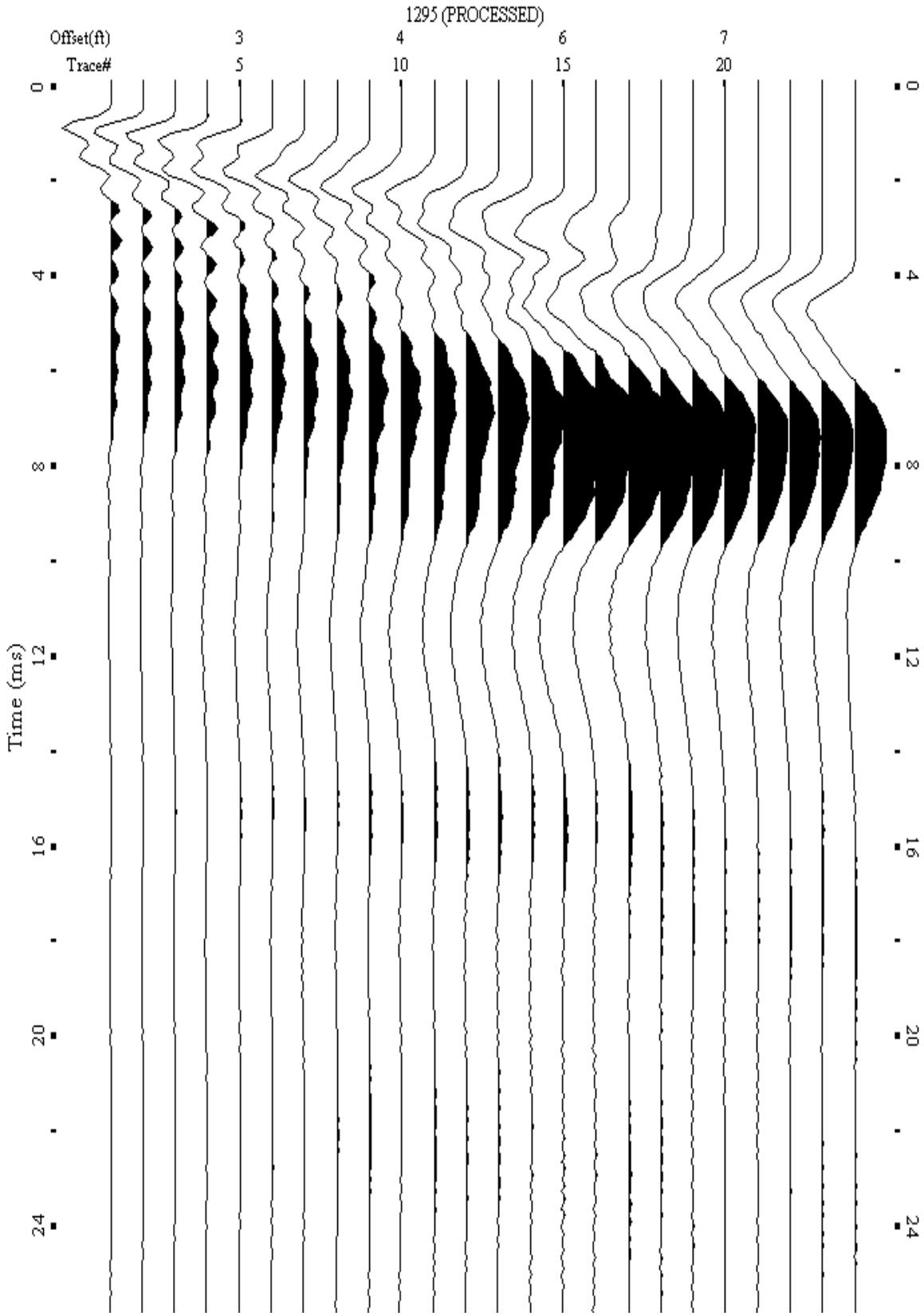

A.442: Shot Gather Line 1295 used in Post-blast 11

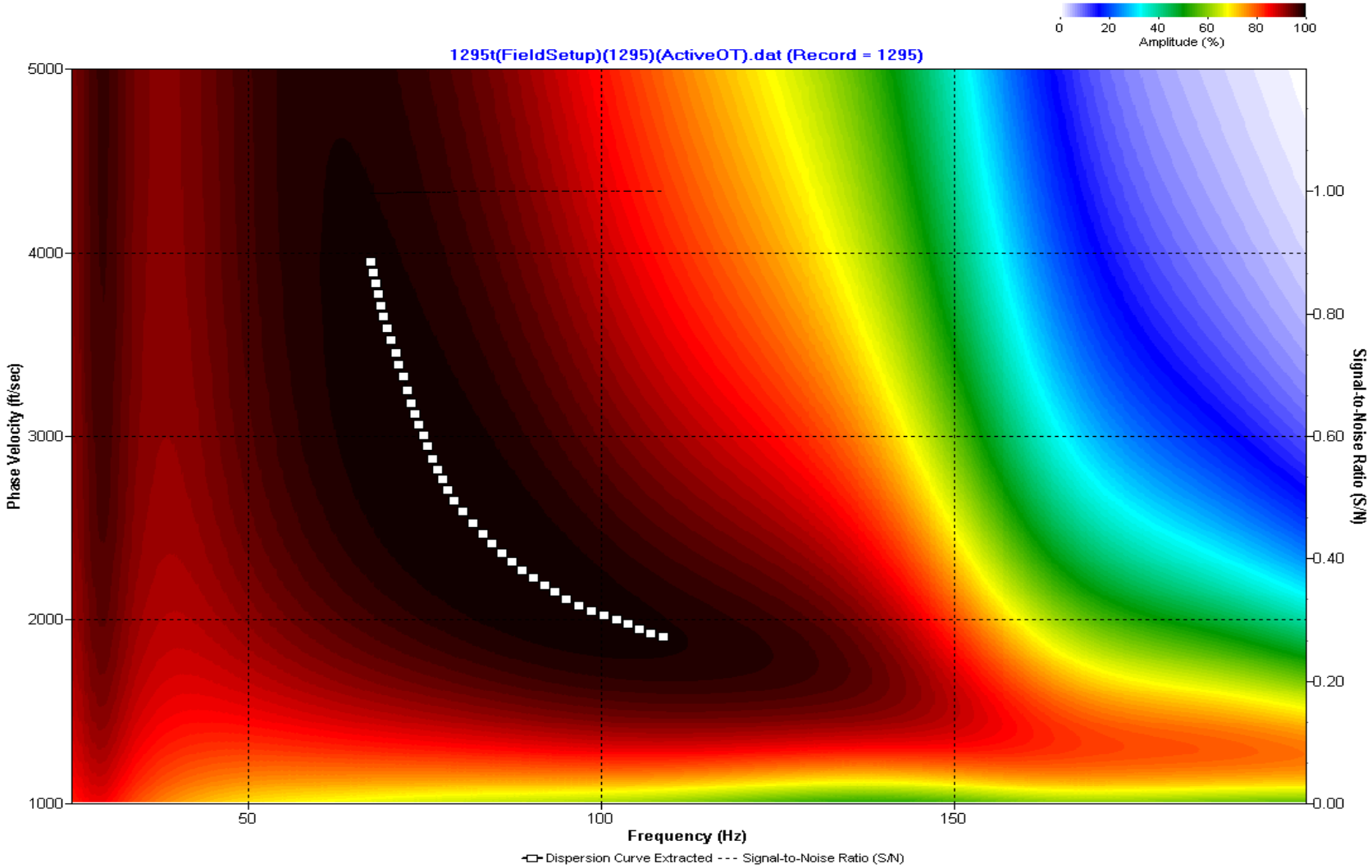

A.443: Dispersion Curve Line 1295 used in Post-blast 11

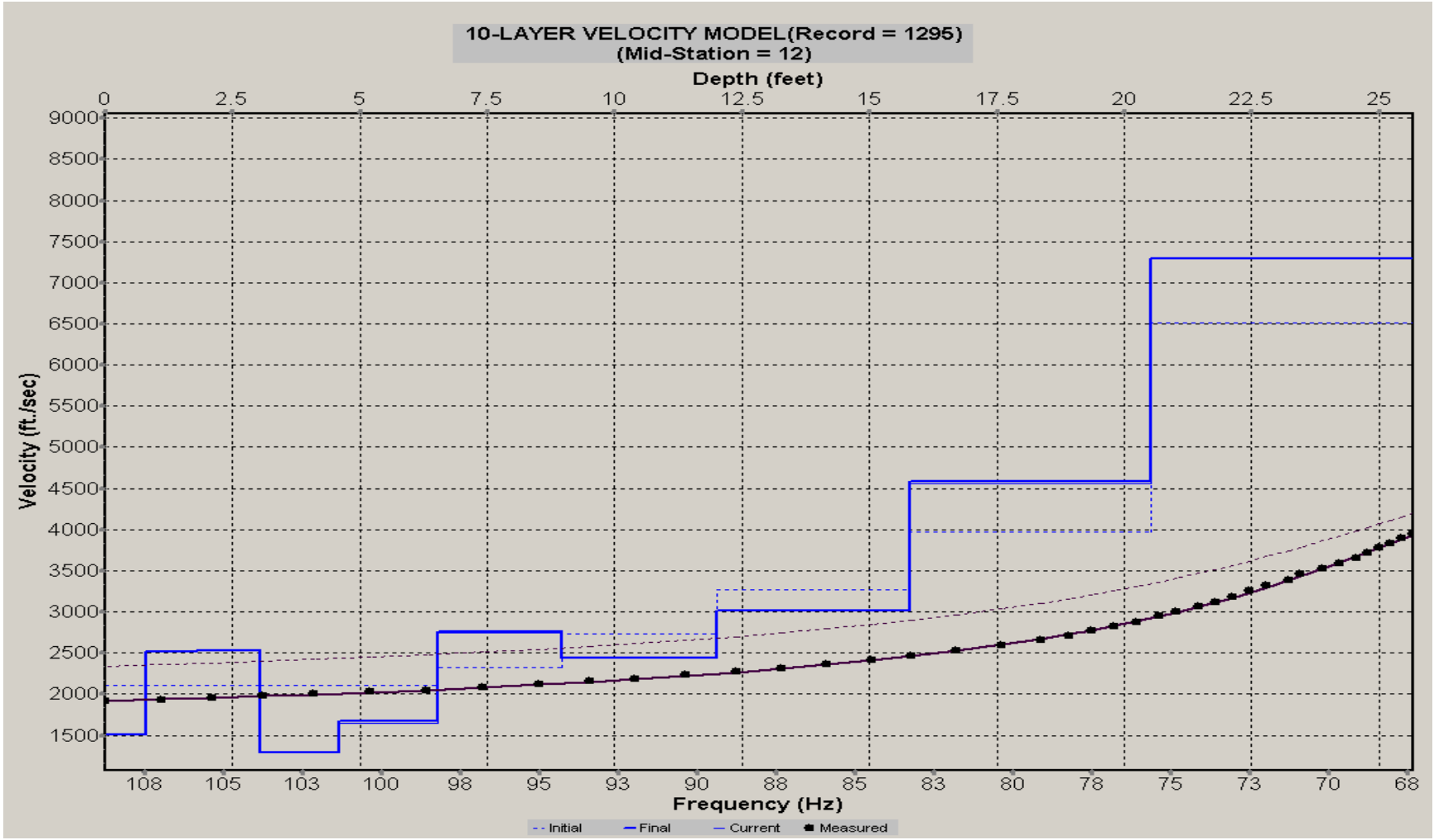

A.444: Velocity Profile Line 1295 used in Post-blast 11

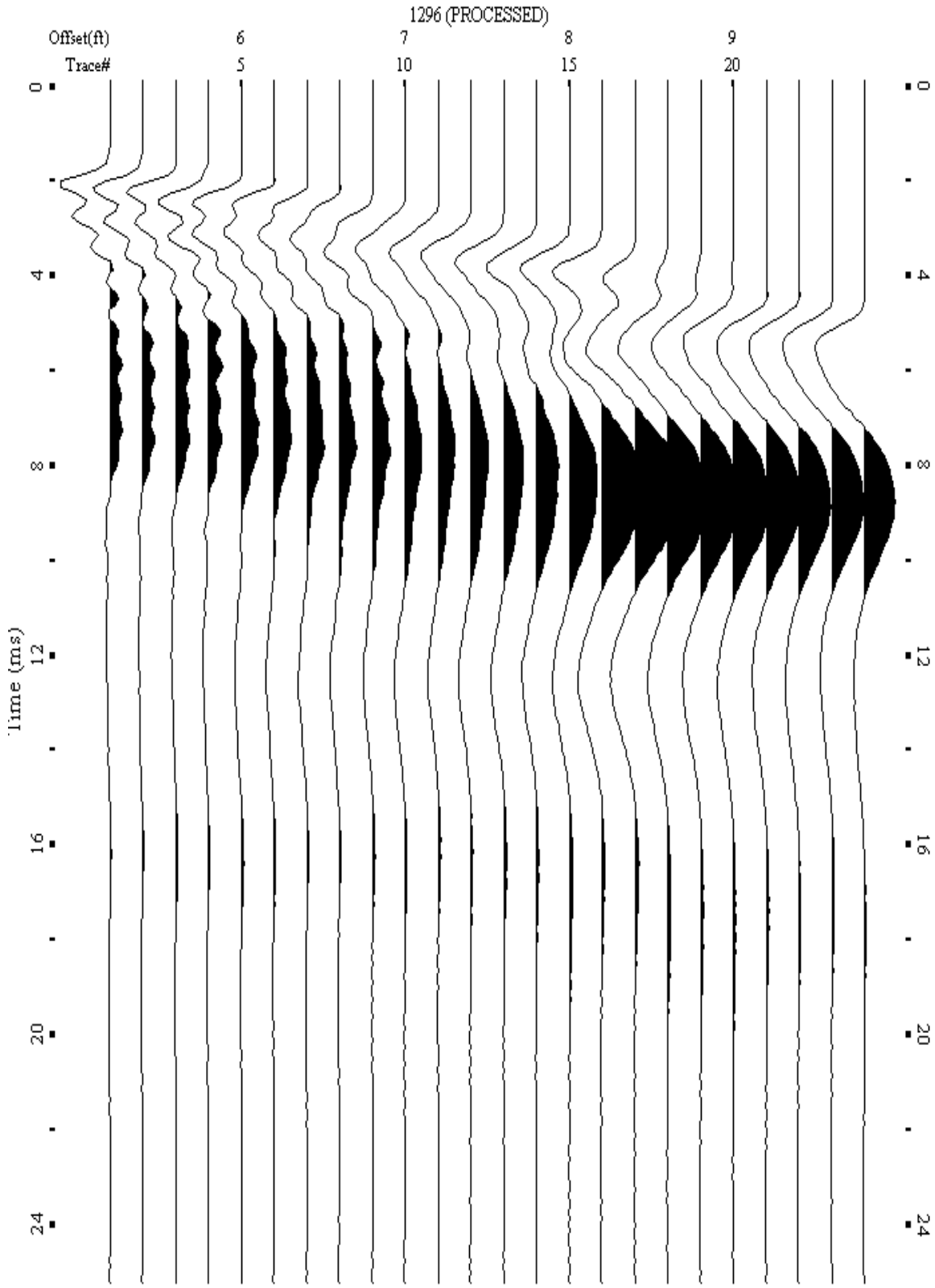

A.445: Shot Gather Line 1296 used in Post-blast 11

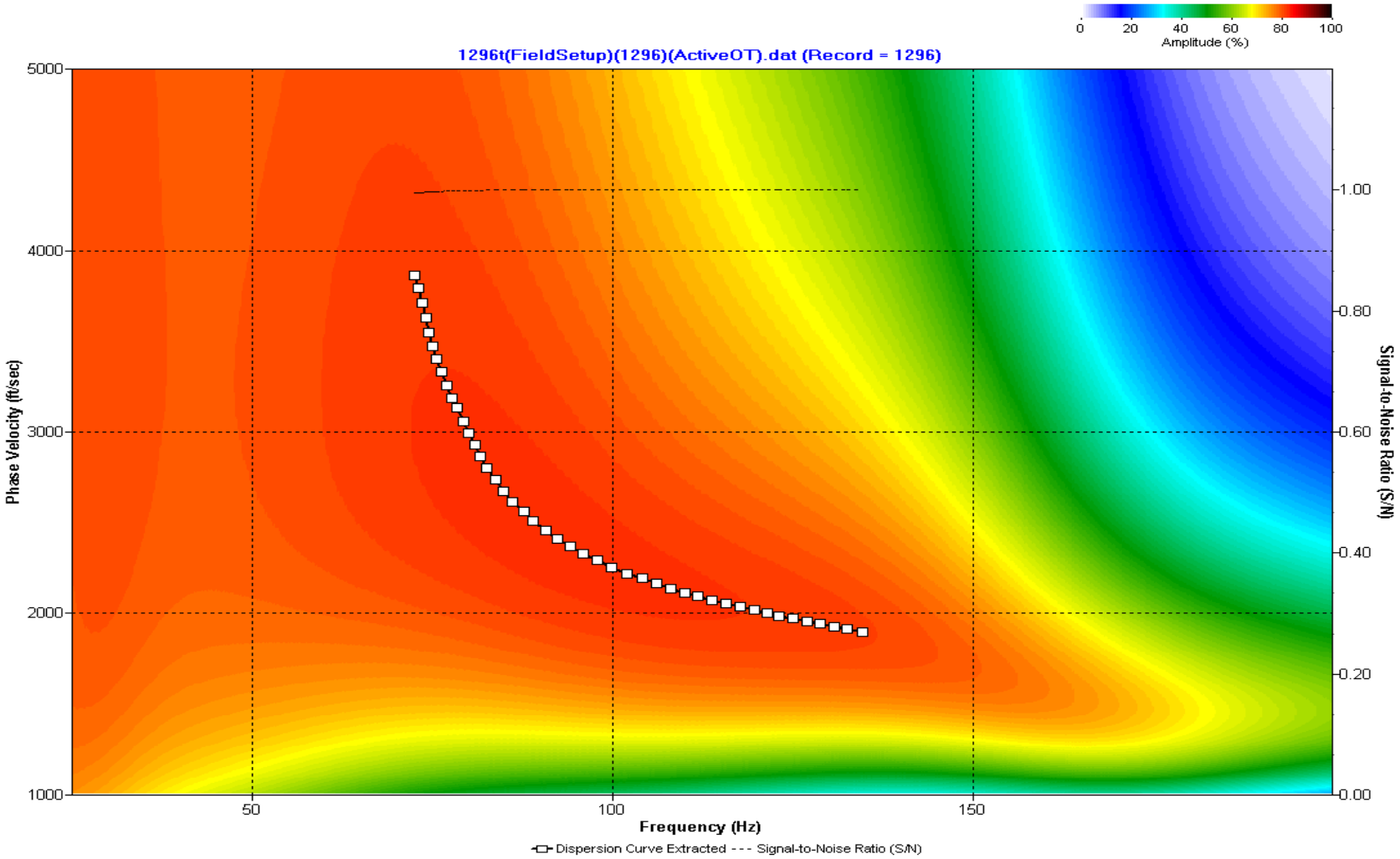

A.446: Dispersion Curve Line 1296 used in Post-blast 11

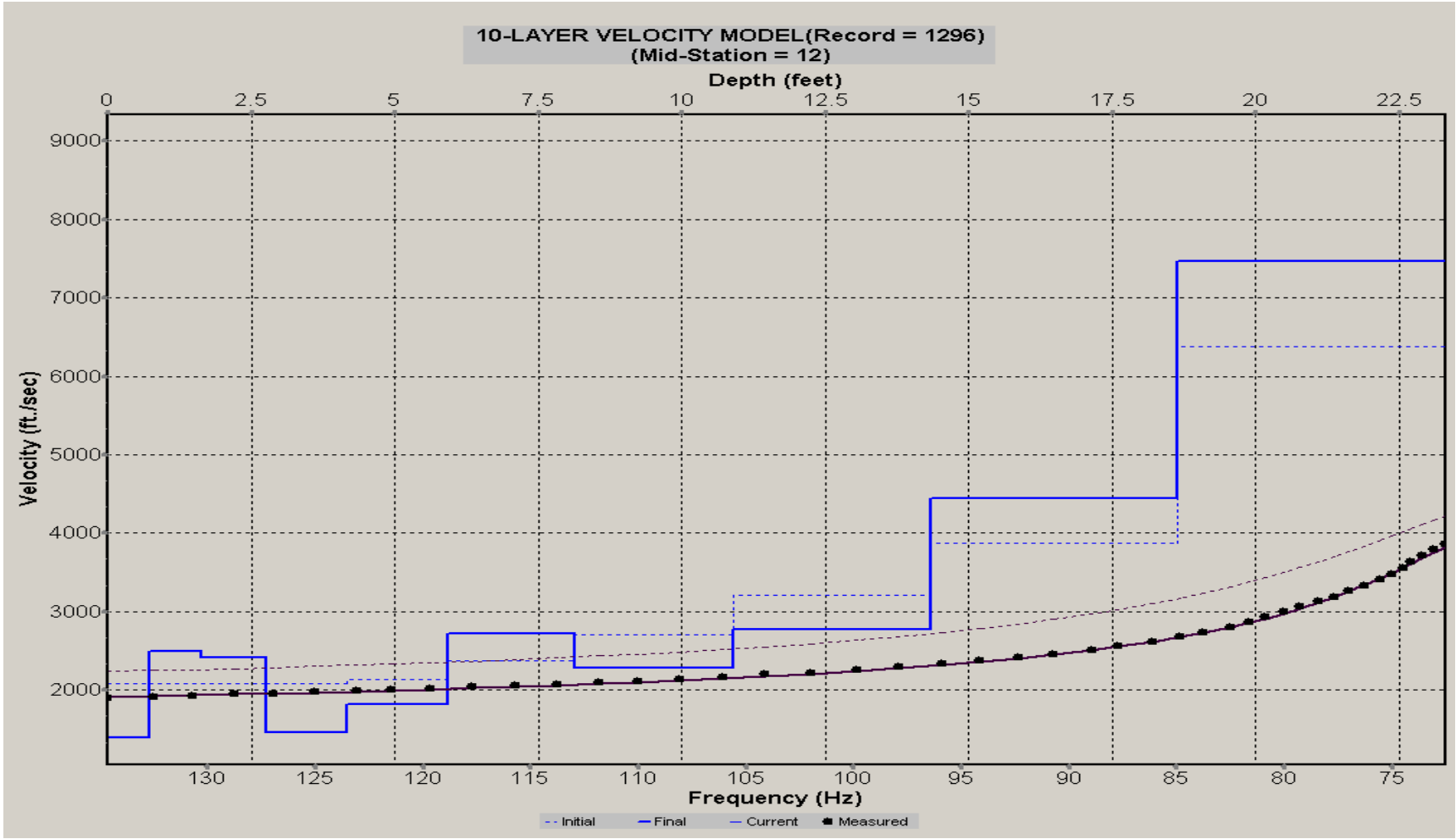

A.447: Velocity Profile Line 1296 used in Post-blast 11

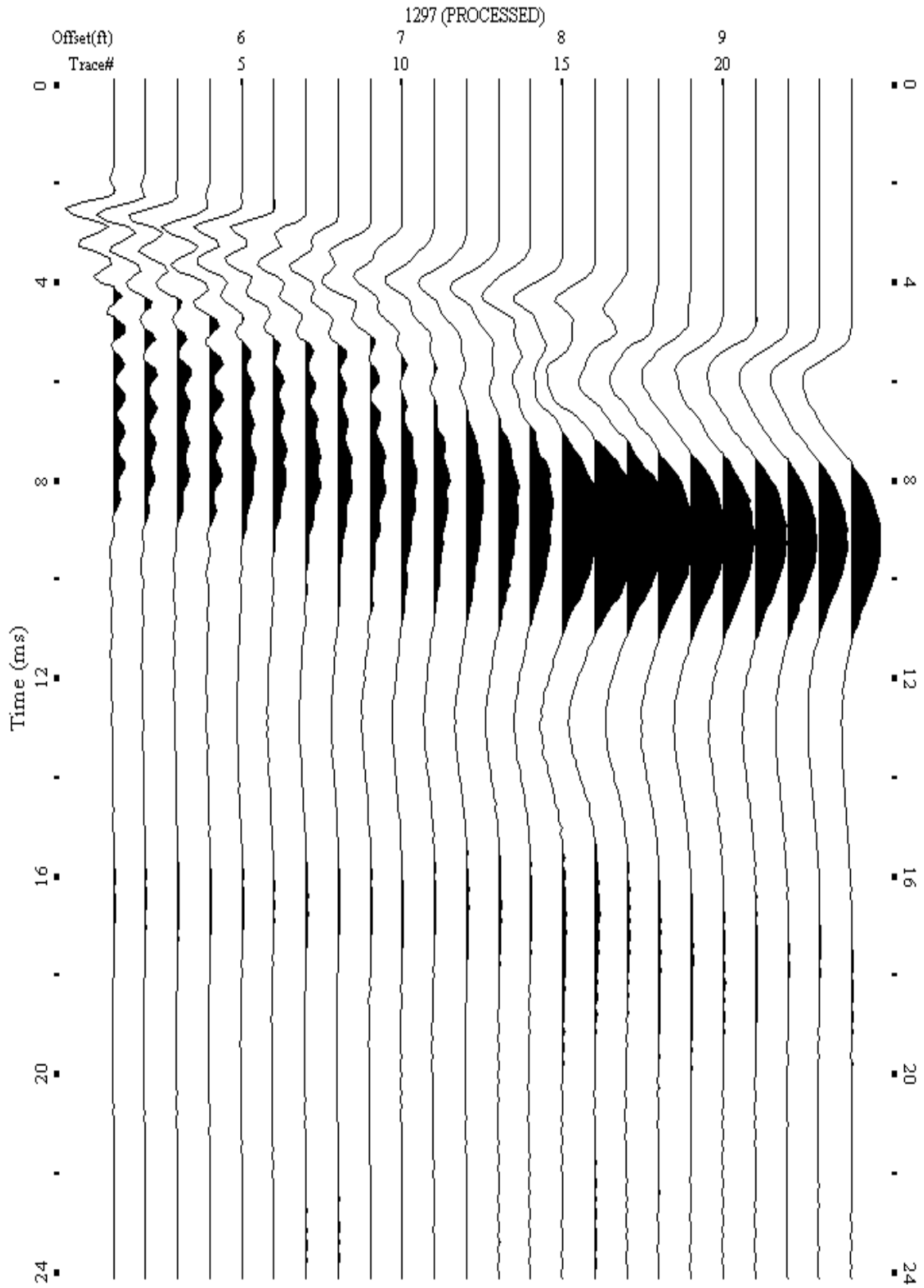

A.448: Shot Gather Line 1297 used in Post-blast 11

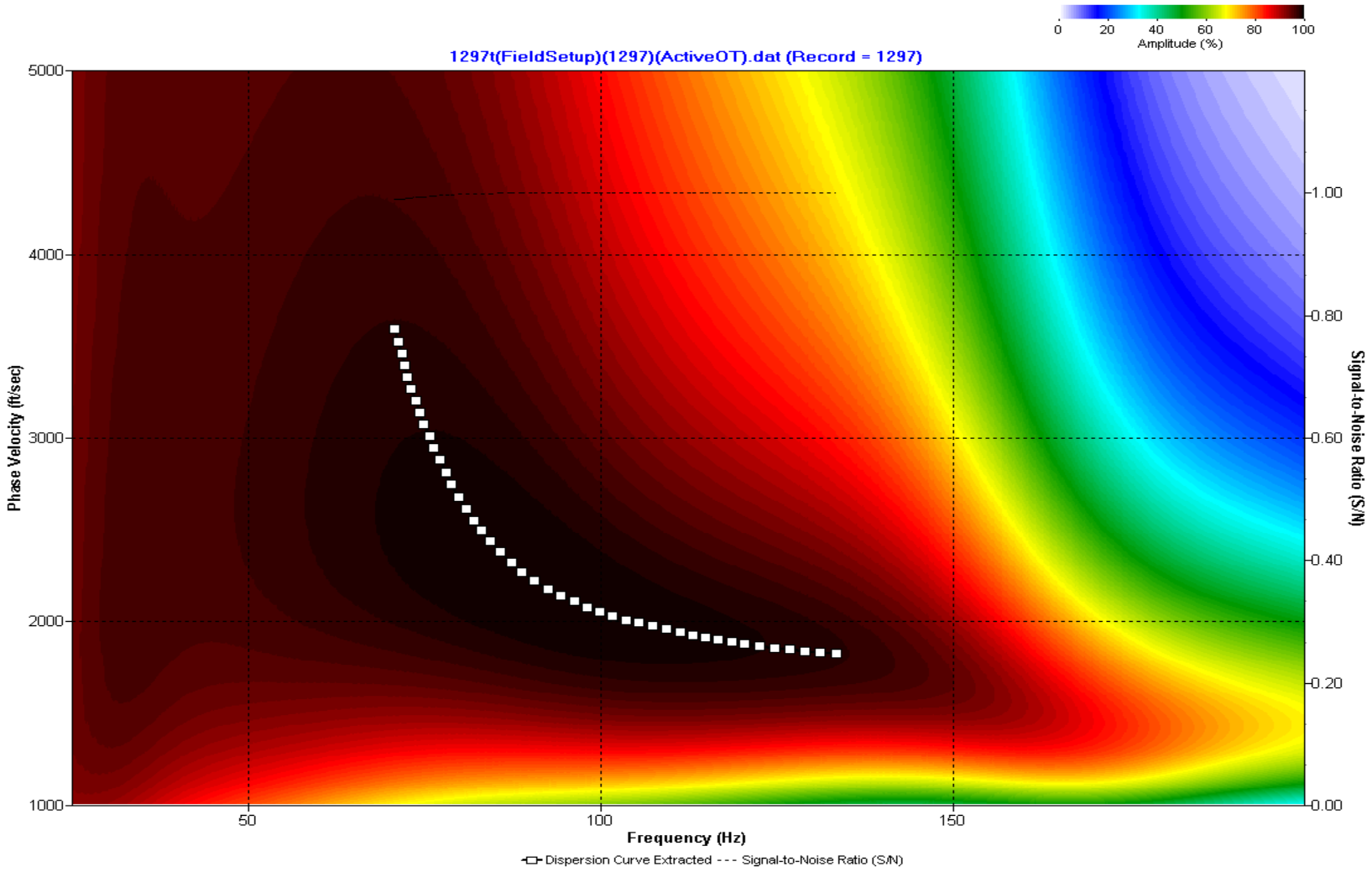

A.449: Dispersion Curve Line 1297 used in Post-blast 11

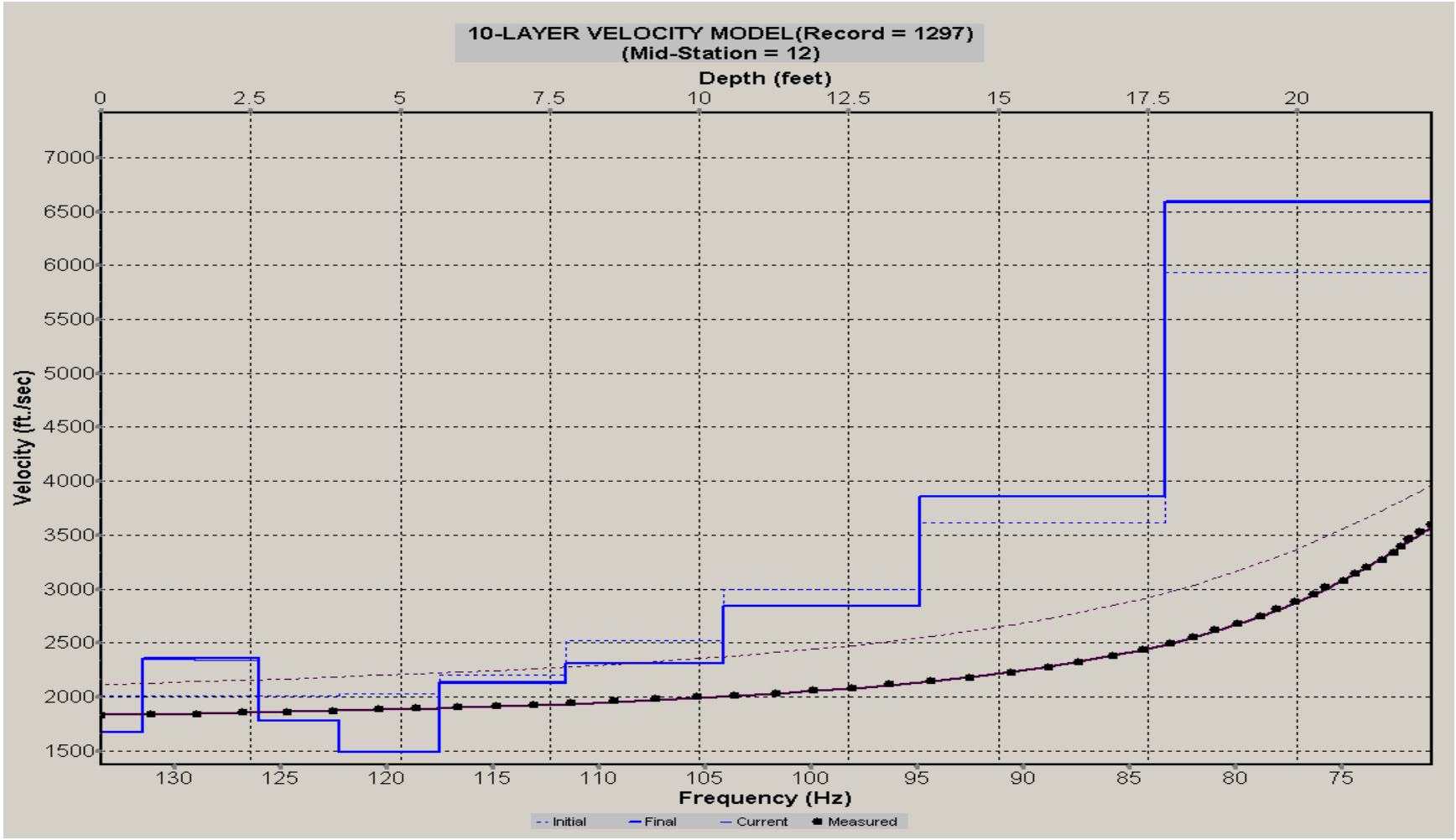

A.450: Velocity Profile Line 1297 used in Post-blast 11

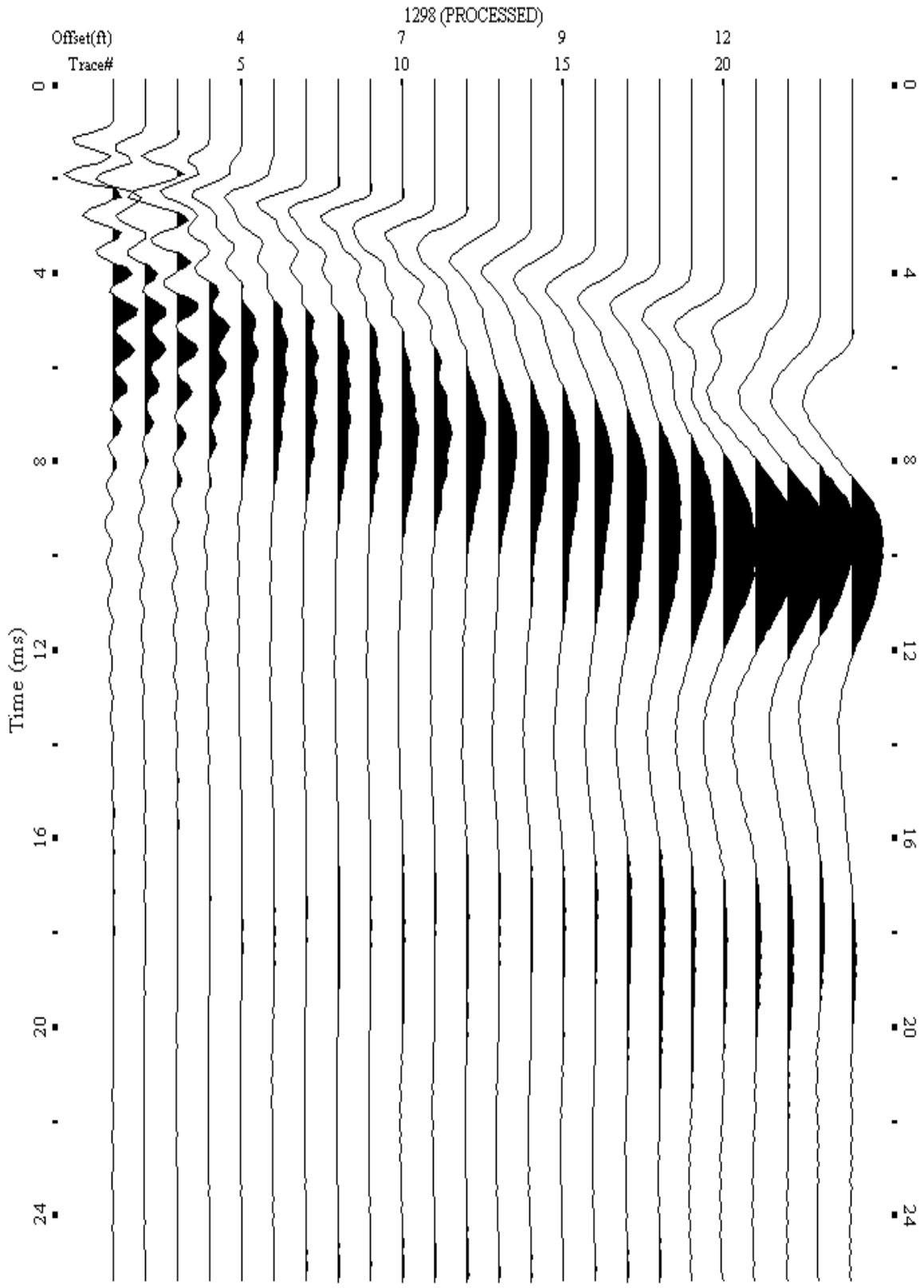

A.451: Shot Gather Line 1298 used in Post-blast 11 and Post-blast 27

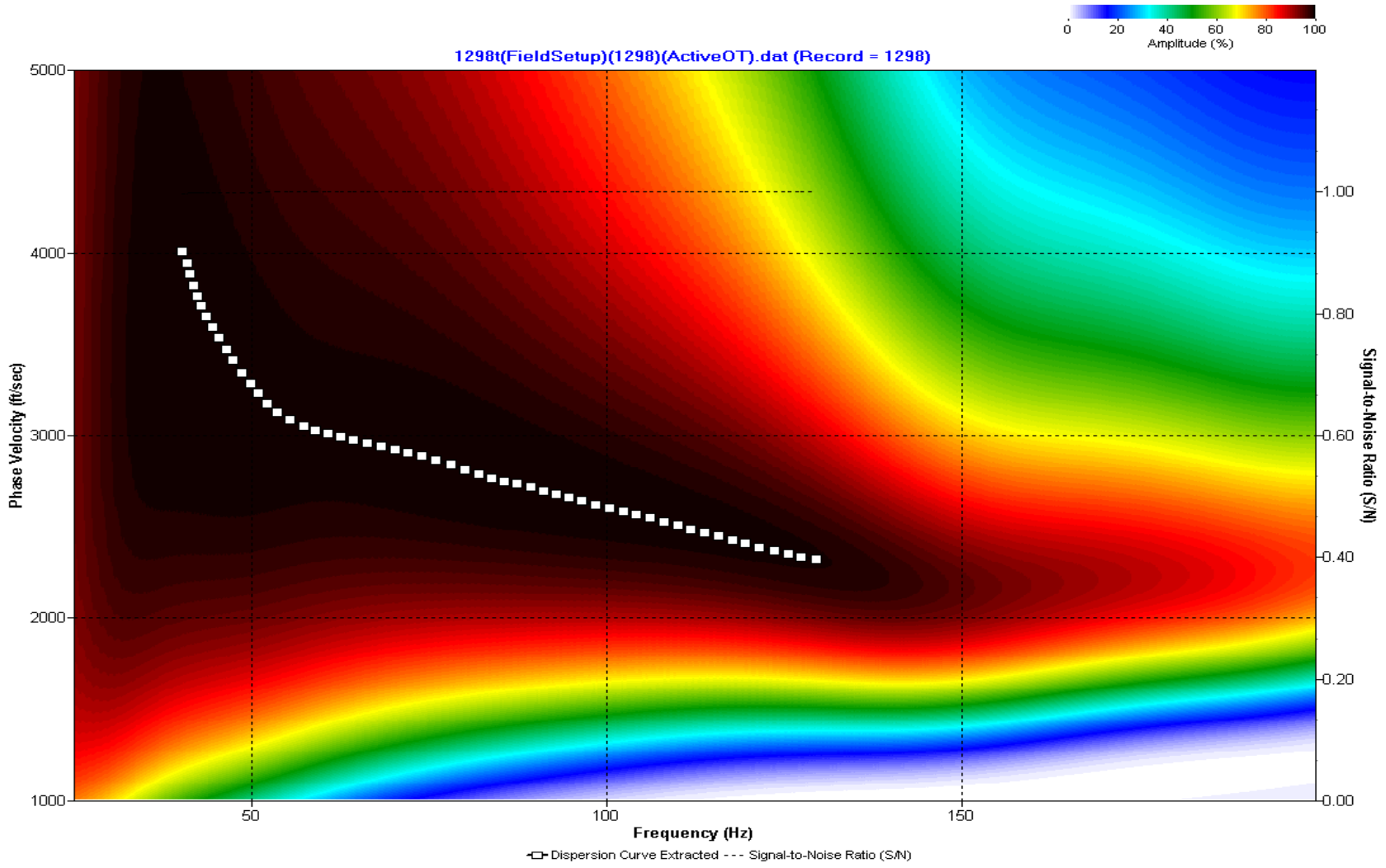

A.452: Dispersion Curve Line 1298 used in Post-blast 11 and Post-blast 27

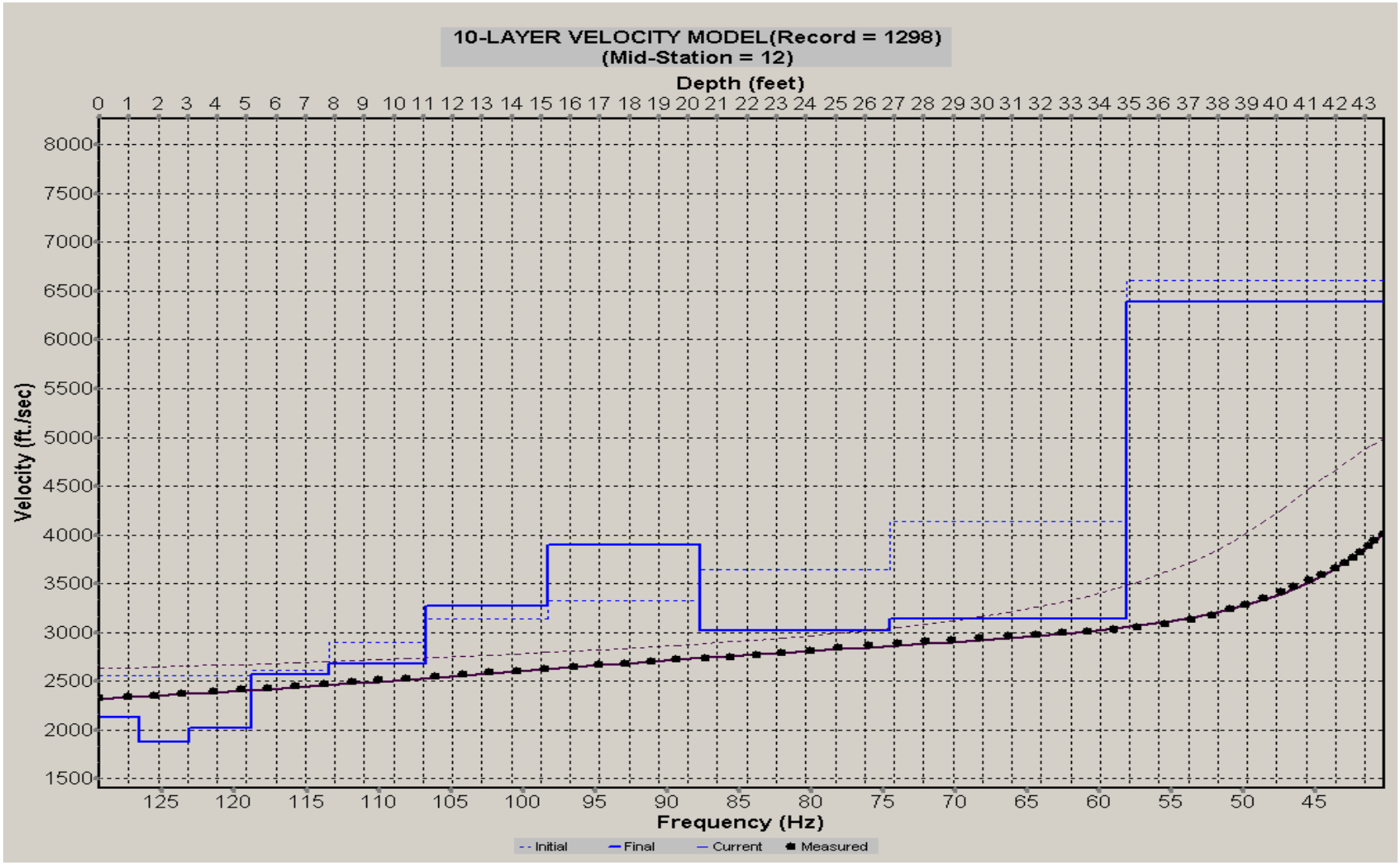

A.453: Velocity Profile Line 1298 used in Post-blast 11 and Post-blast 27

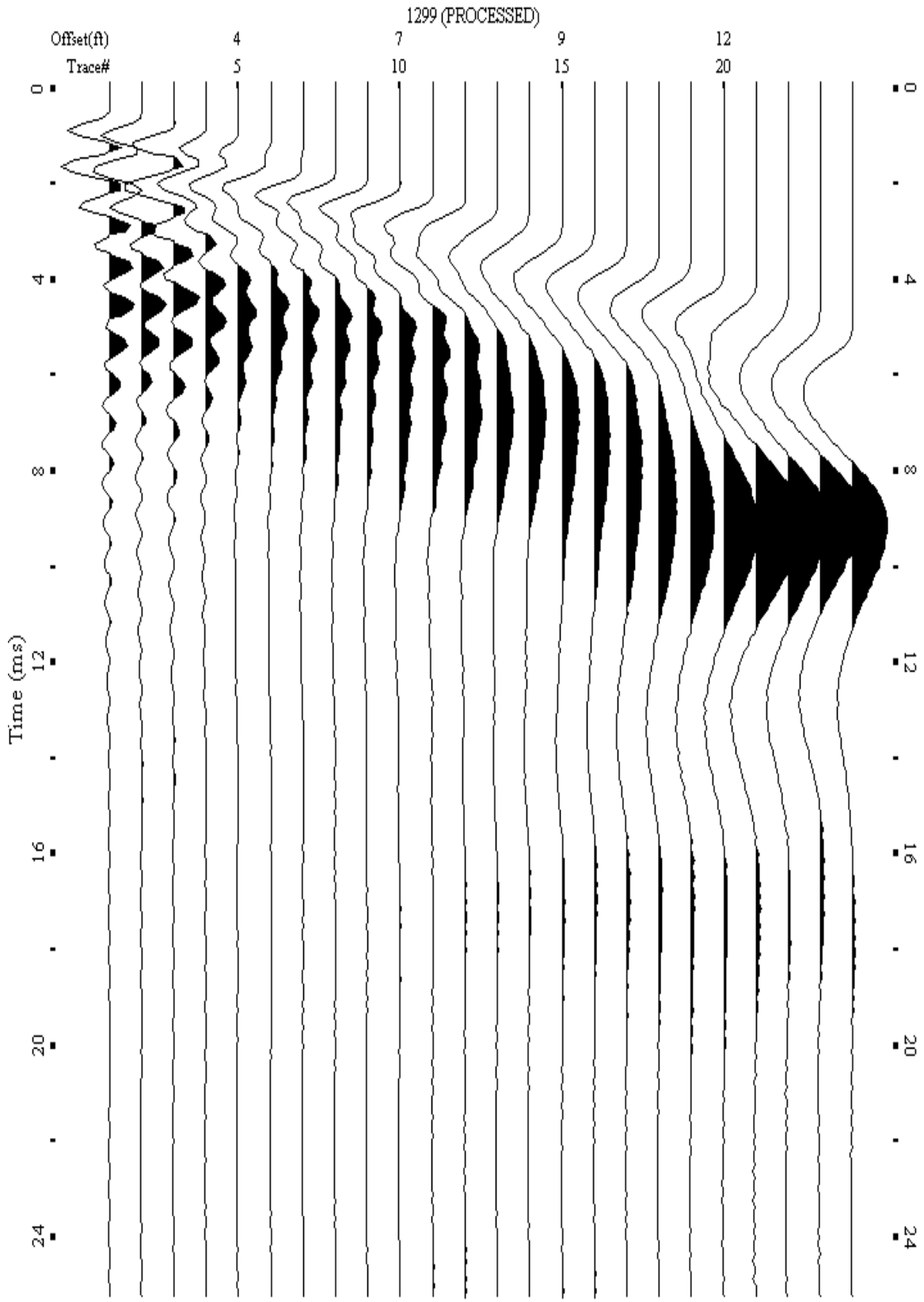

A.454: Shot Gather Line 1299 used in Post-blast 11, Post-blast 27 and Pre-blast 31

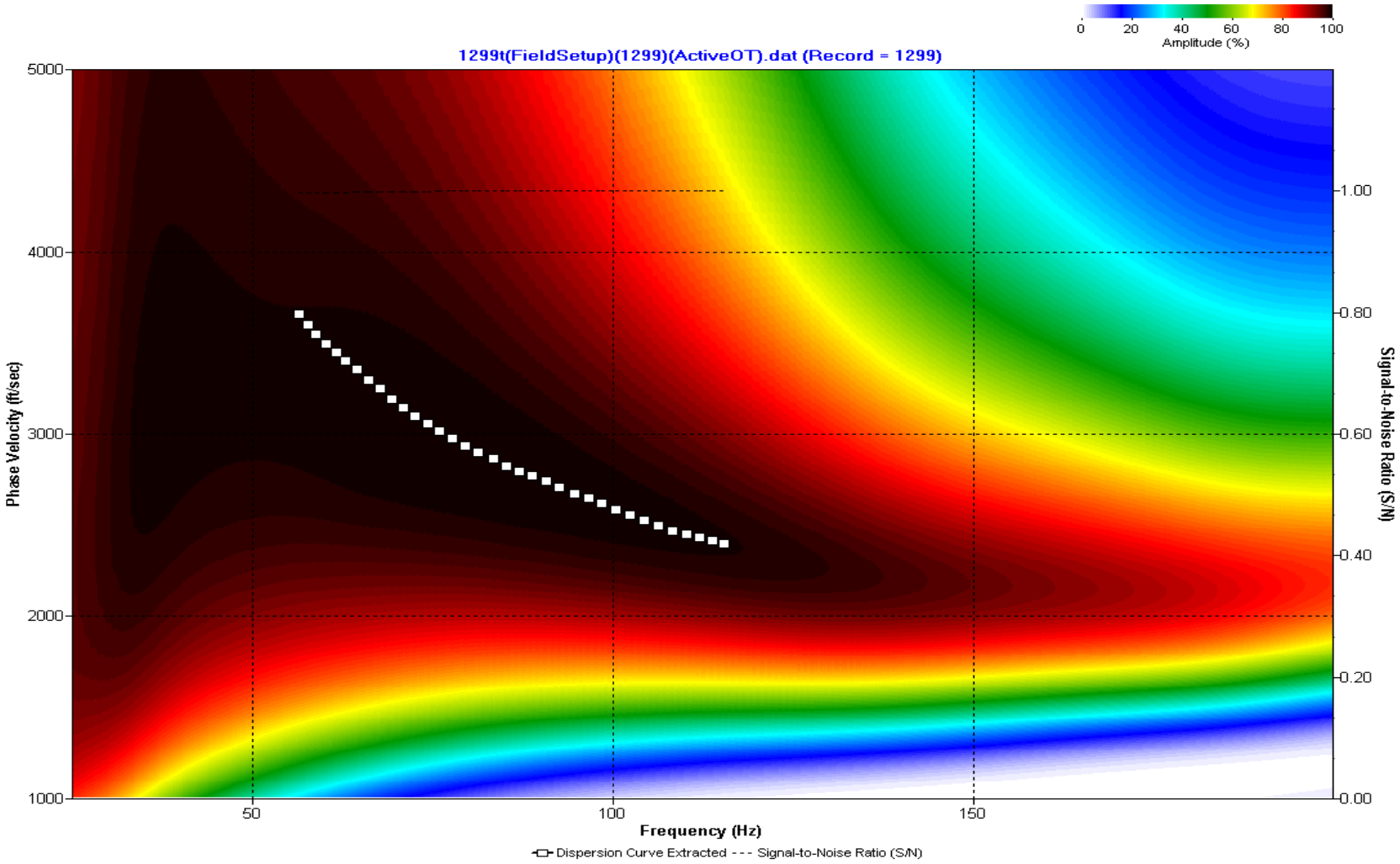

A.455: Dispersion Curve Line 1299 used in Post-blast 11, Post-blast 27 and Pre-blast 31

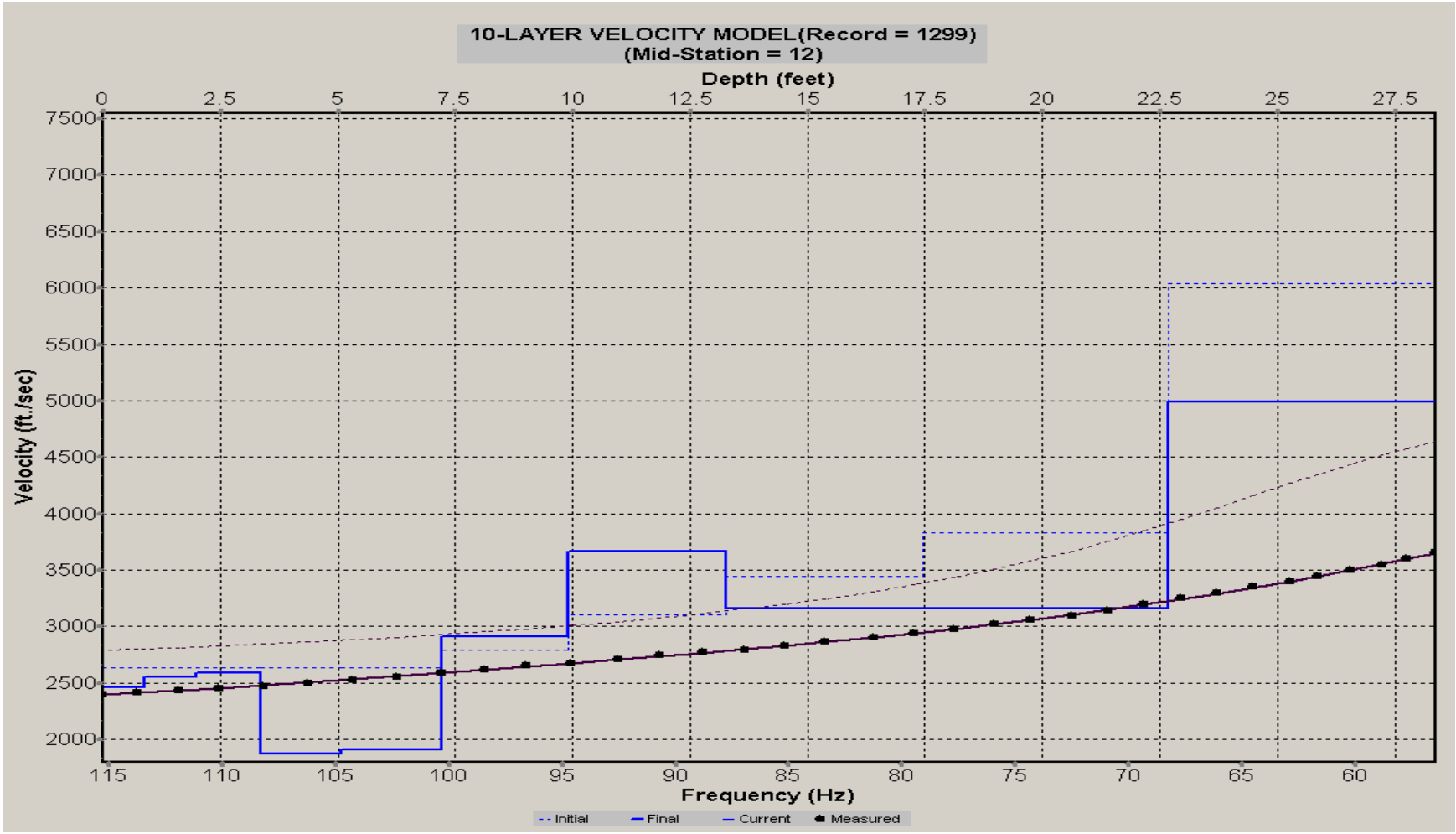

A.456: Velocity Profile Line 1299 used in Post-blast 11, Post-blast 27 and Pre-blast 31

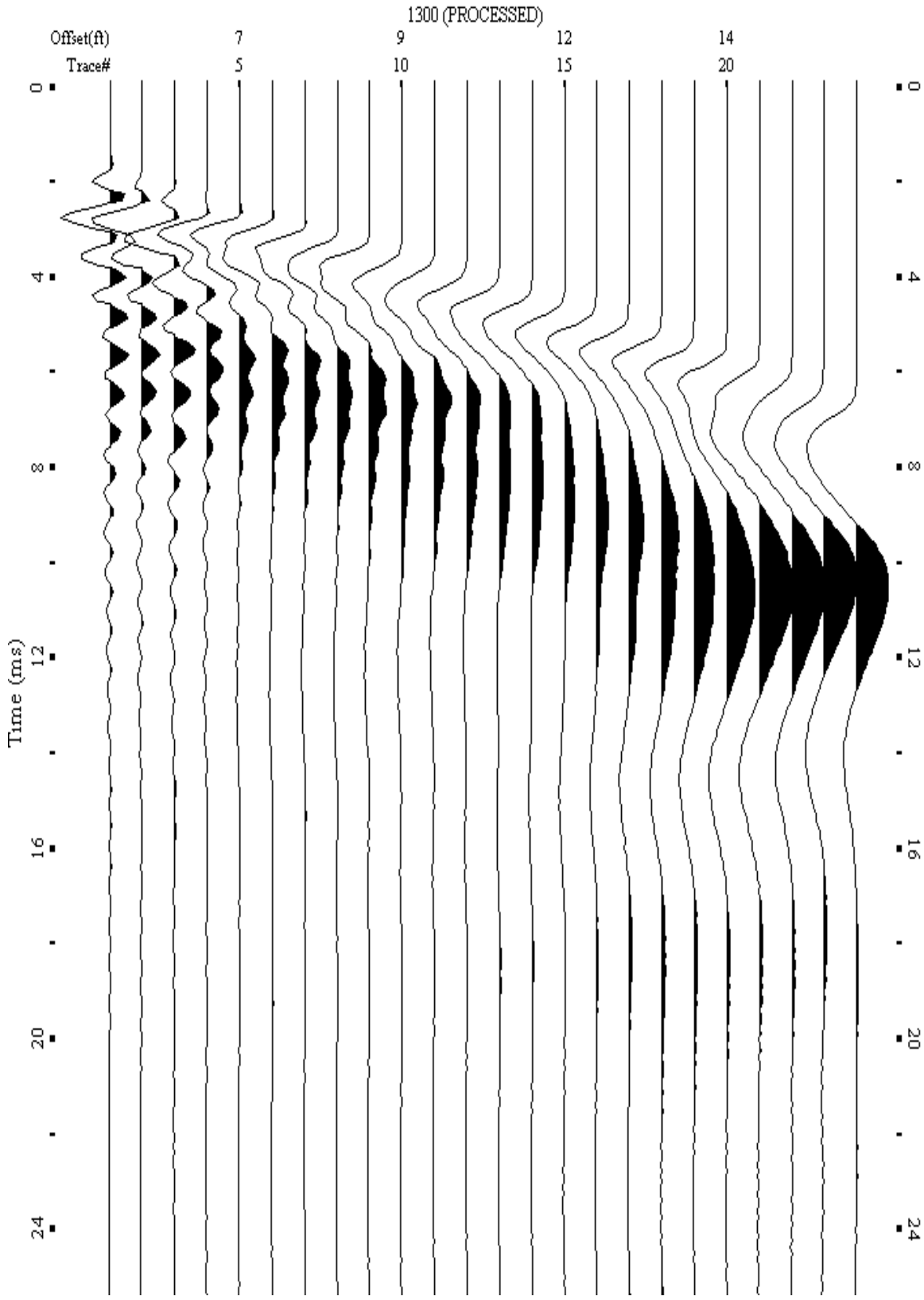

A.457: Shot Gather Line 1300 used in Post-blast 11, Post-blast 27 and Pre-blast 31

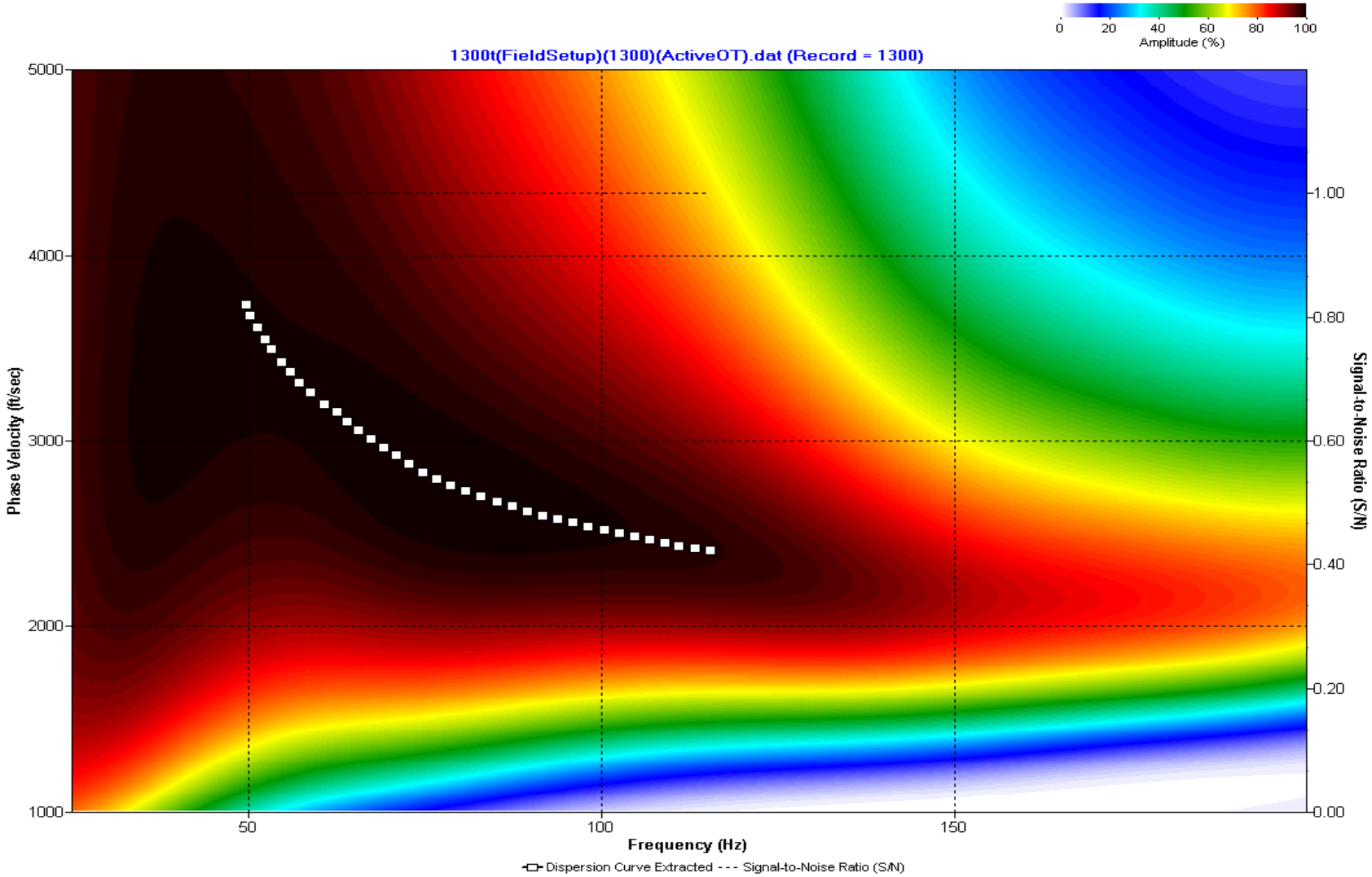

A.458: Dispersion Curve Line 1300 used in Post-blast 11, Post-blast 27 and Pre-blast 31

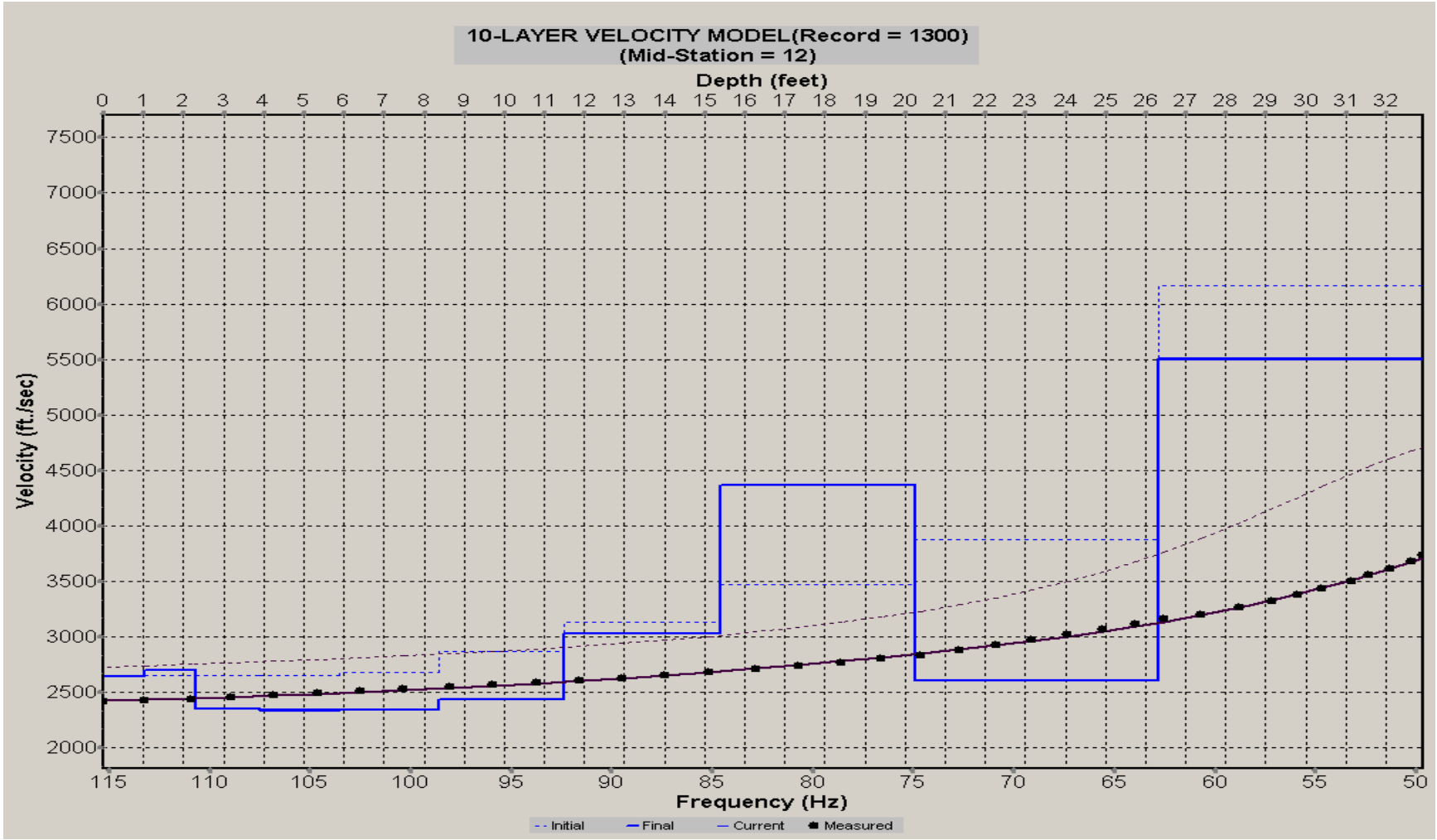

A.459: Velocity Profile Line 1300 used in Post-blast 11, Post-blast 27 and Pre-blast 31

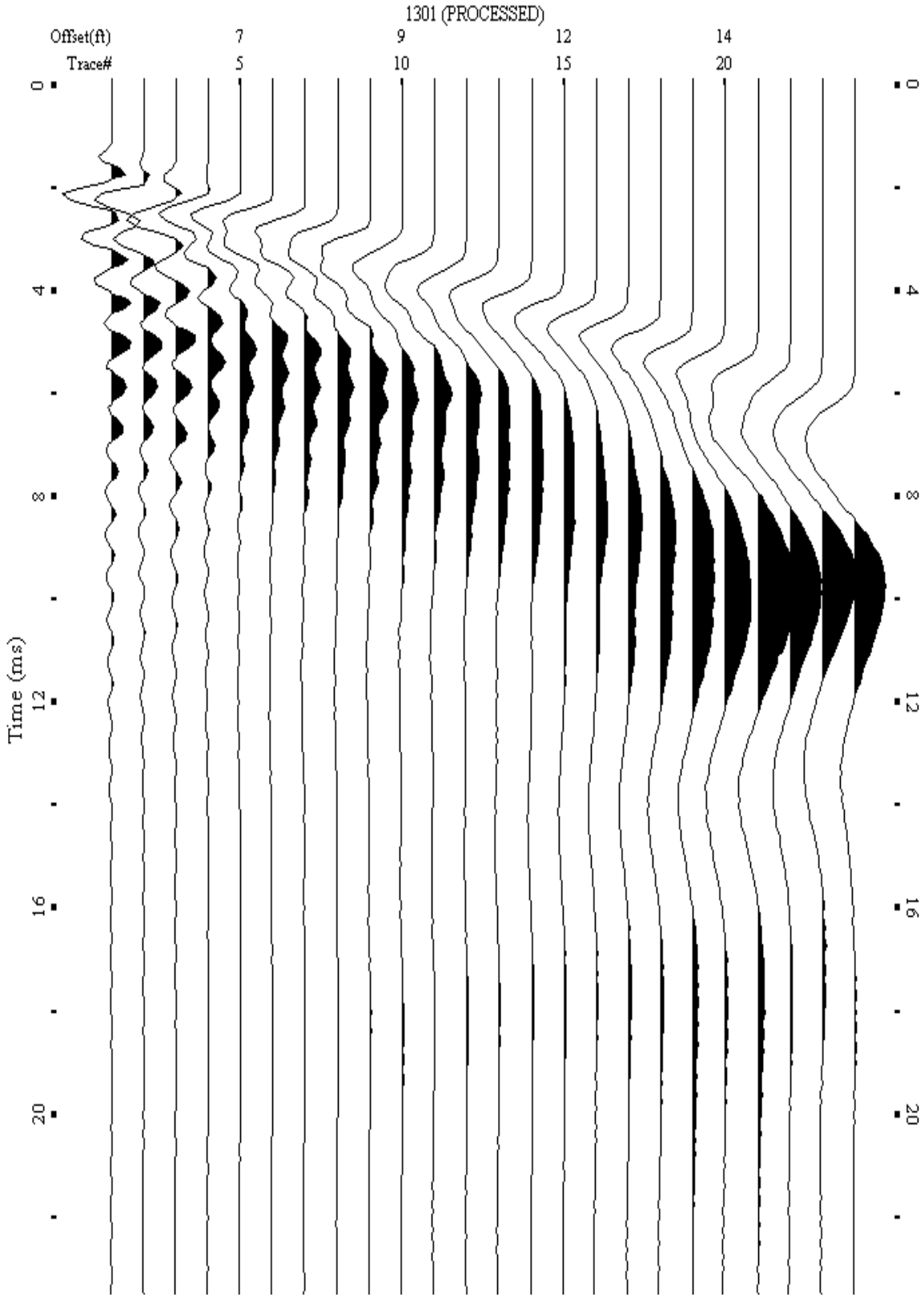

A.460: Shot Gather Line 1301 used in Post-blast 11, Post-blast 27 and Pre-blast 31

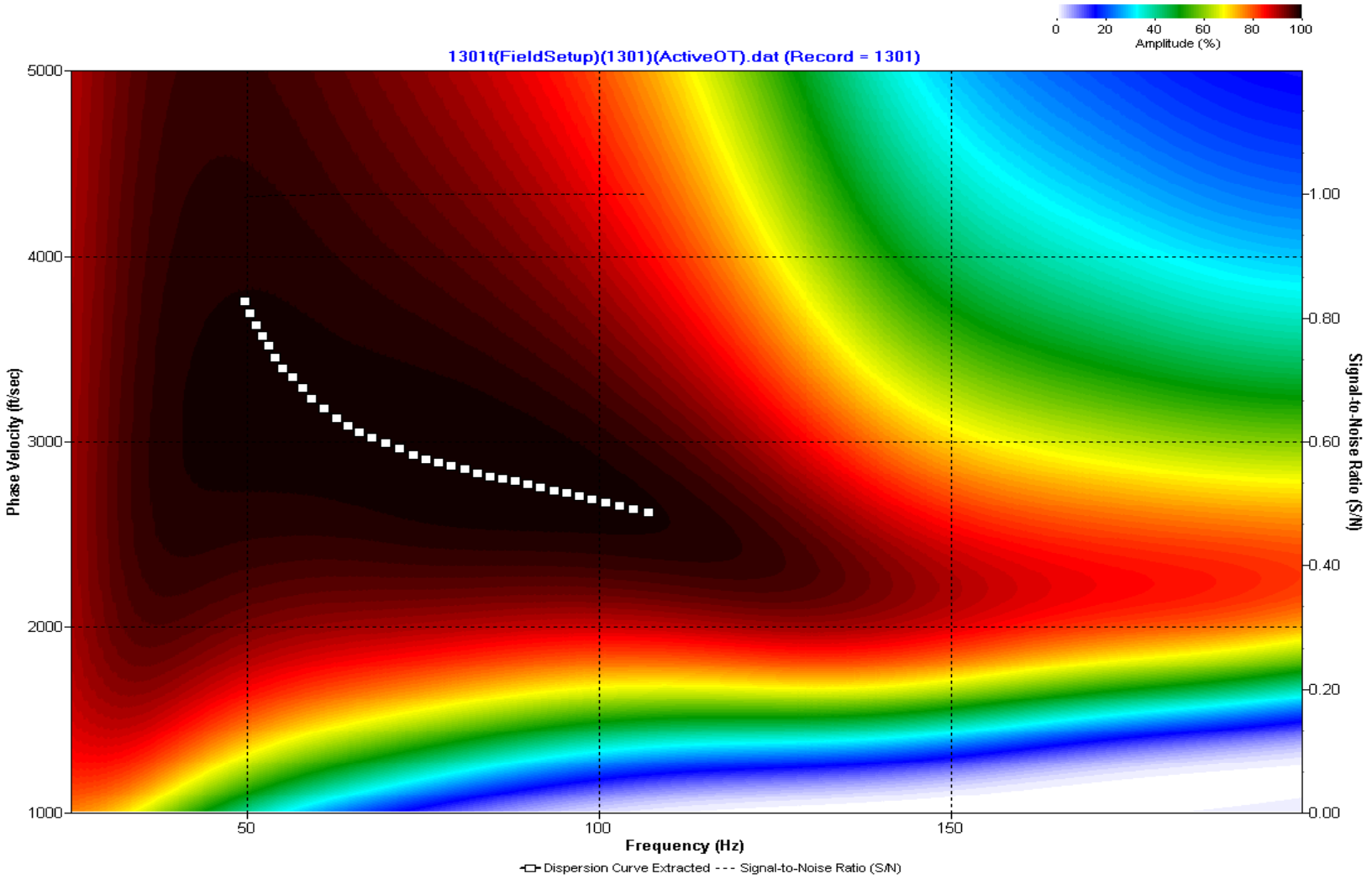

A.461: Dispersion Curve Line 1301 used in Post-blast 11, Post-blast 27 and Pre-blast 31

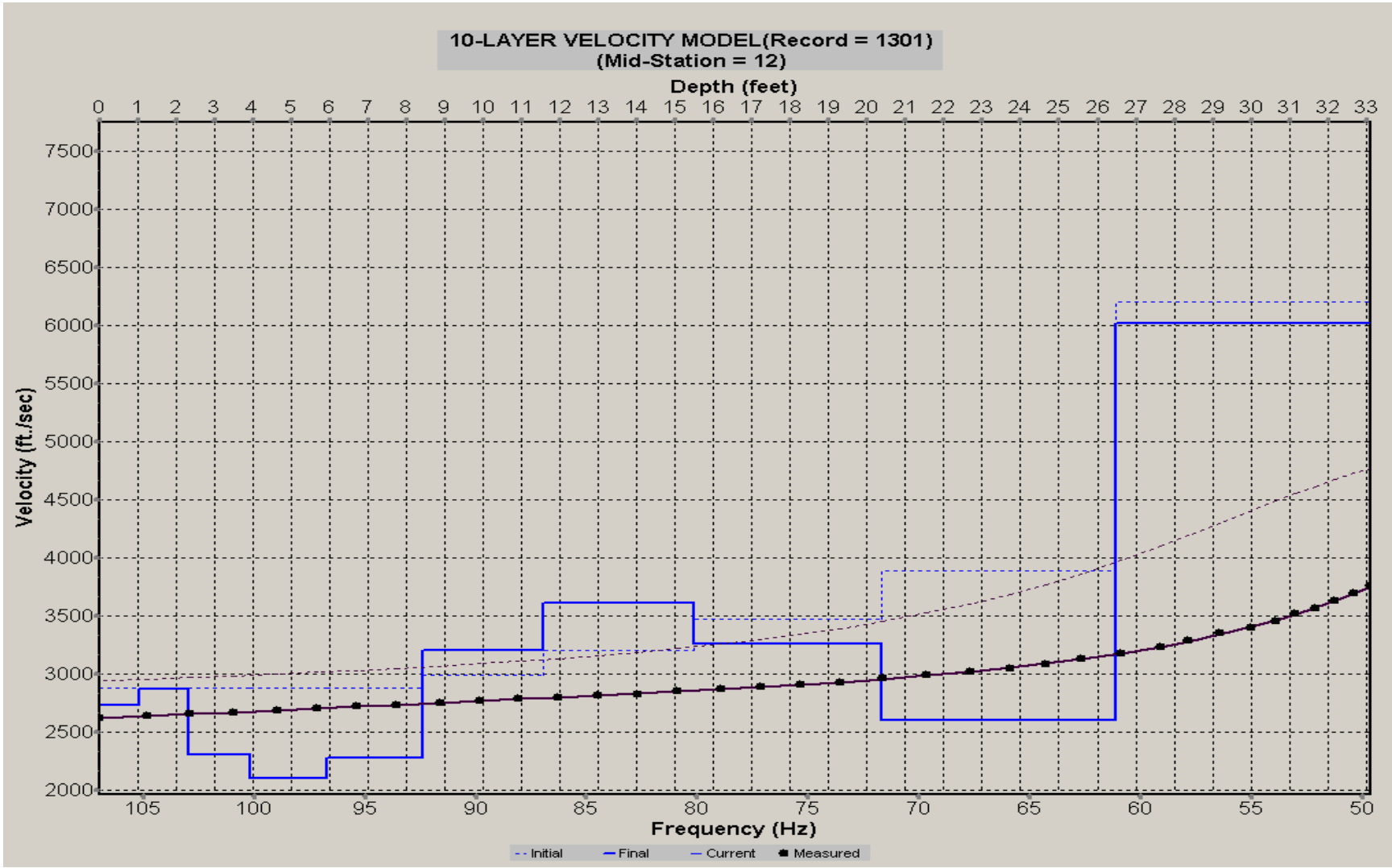

A.462: Velocity Profile Line 1301 used in Post-blast 11, Post-blast 27 and Pre-blast 31

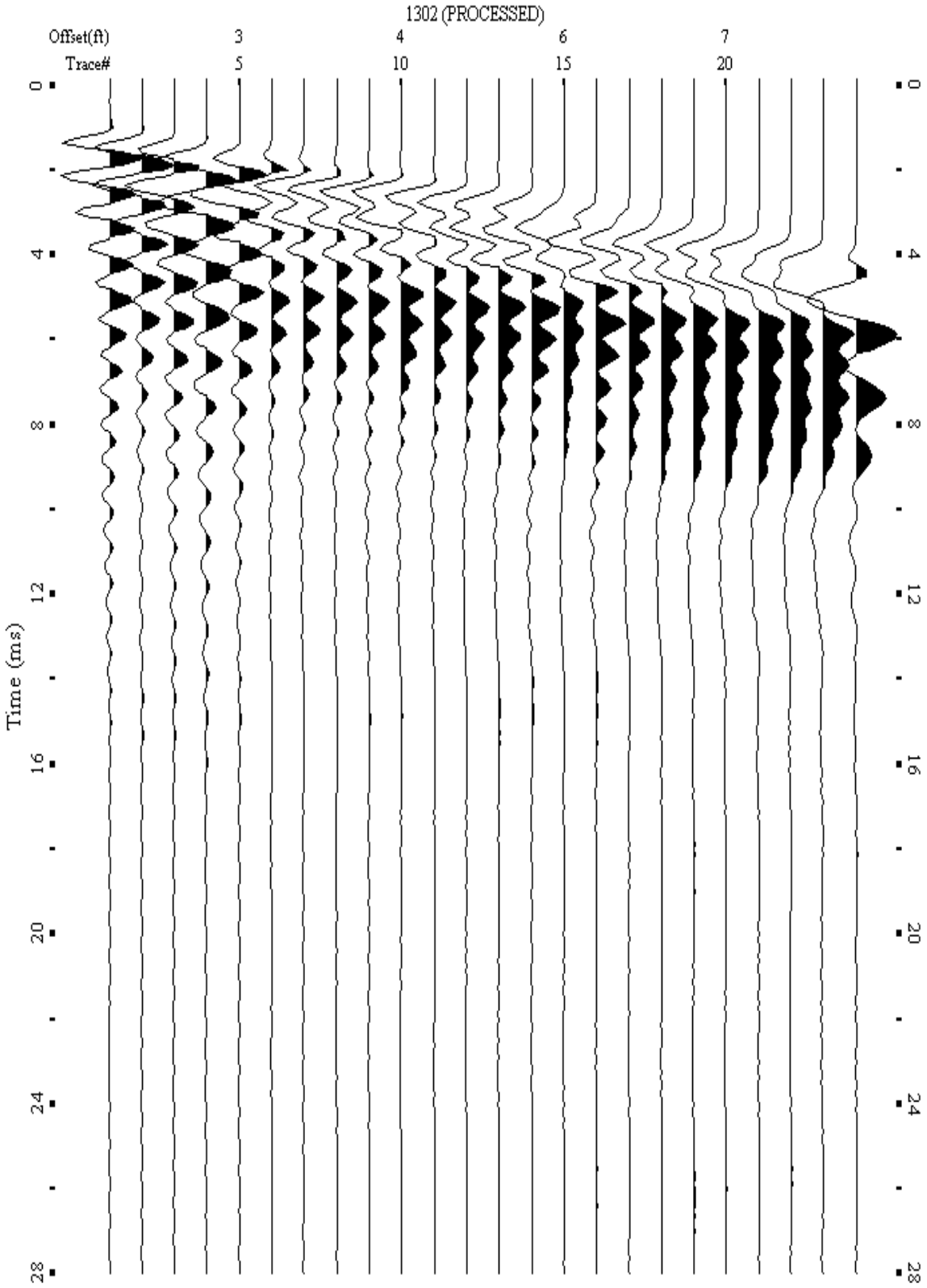

A.463: Shot Gather Line 1302 used in Post-blast 27

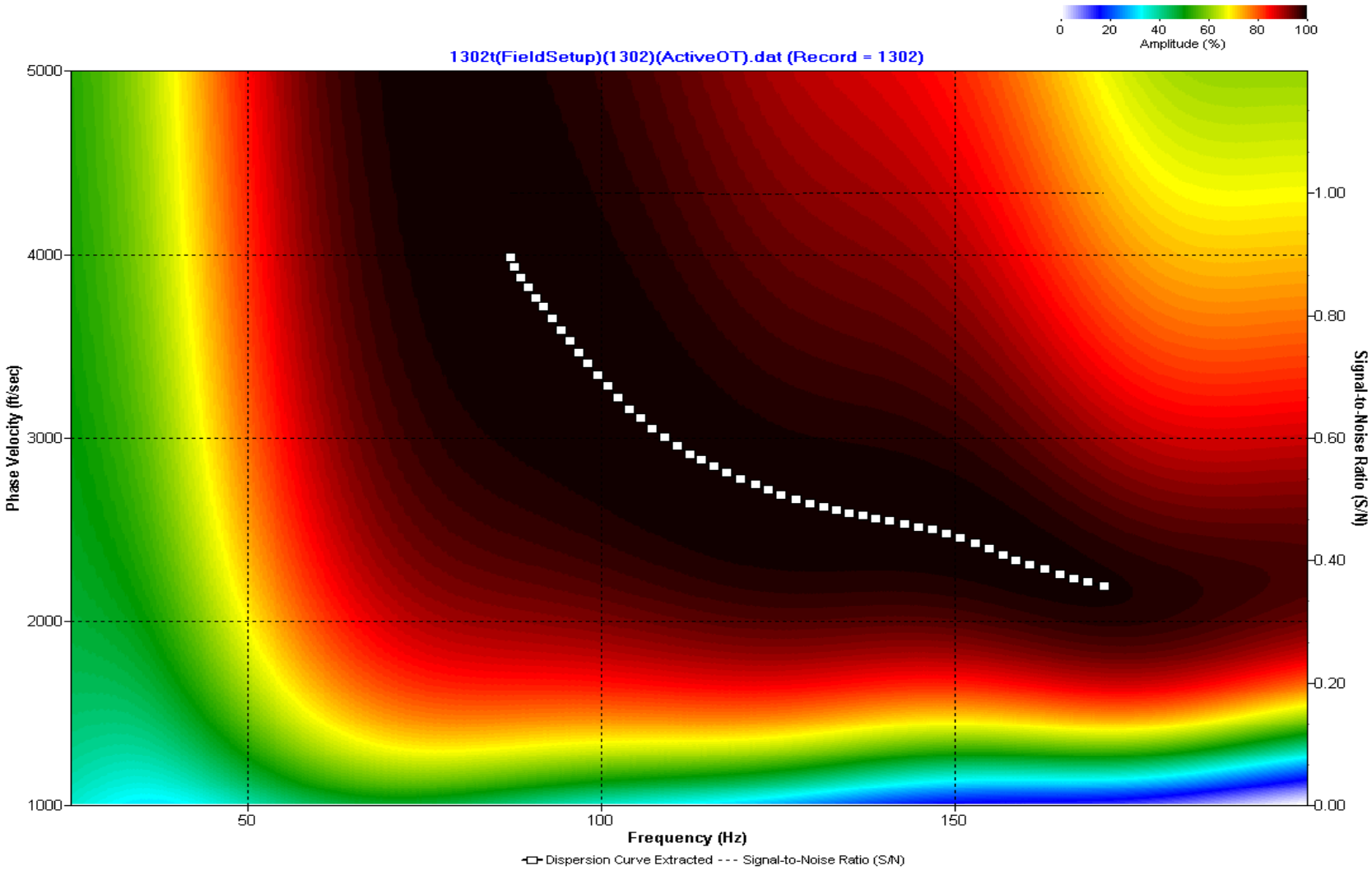

A.464: Dispersion Curve Line 1302 used in Post-blast 27

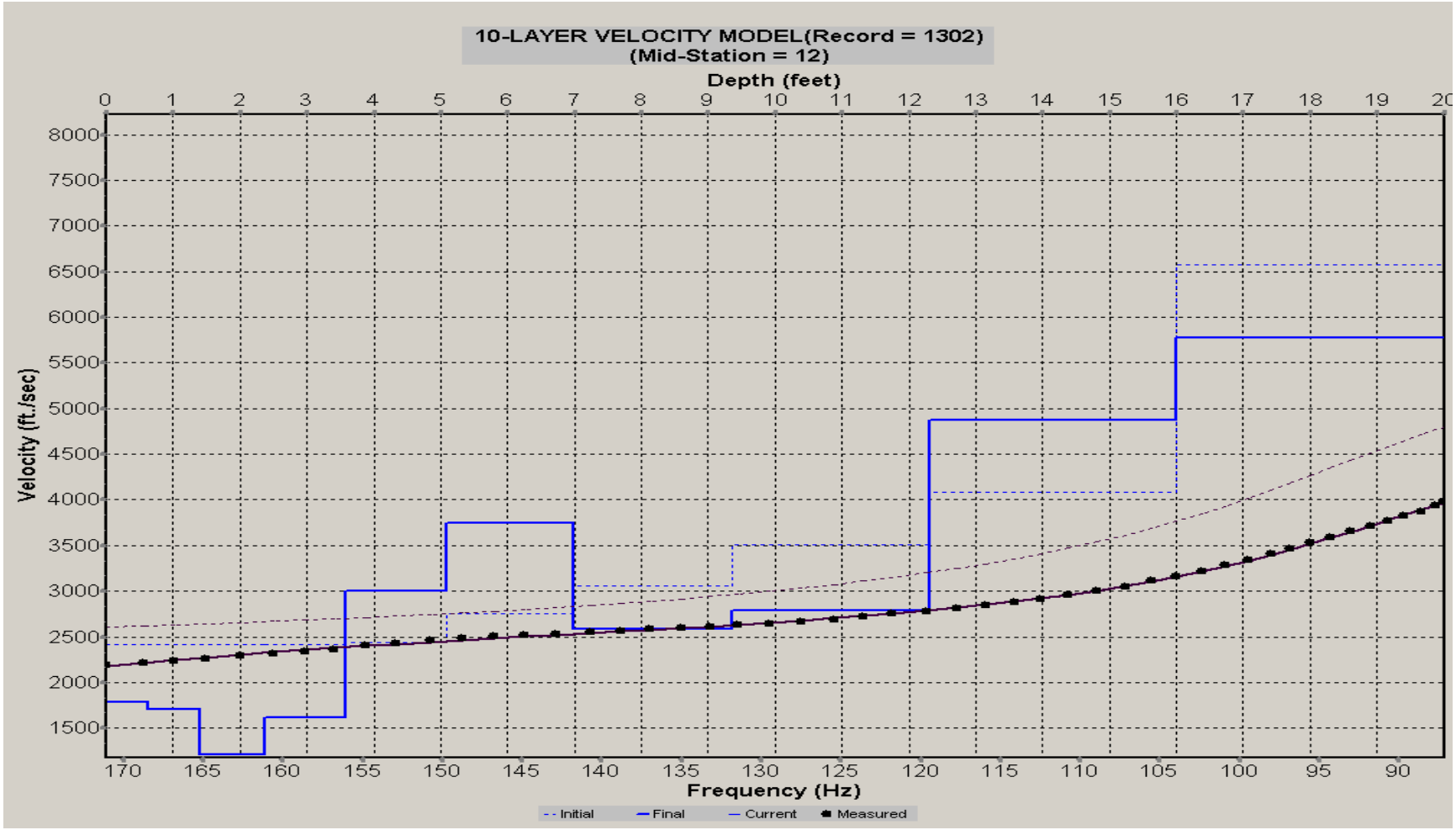

A.465: Velocity Profile Line 1302 used in Post-blast 27

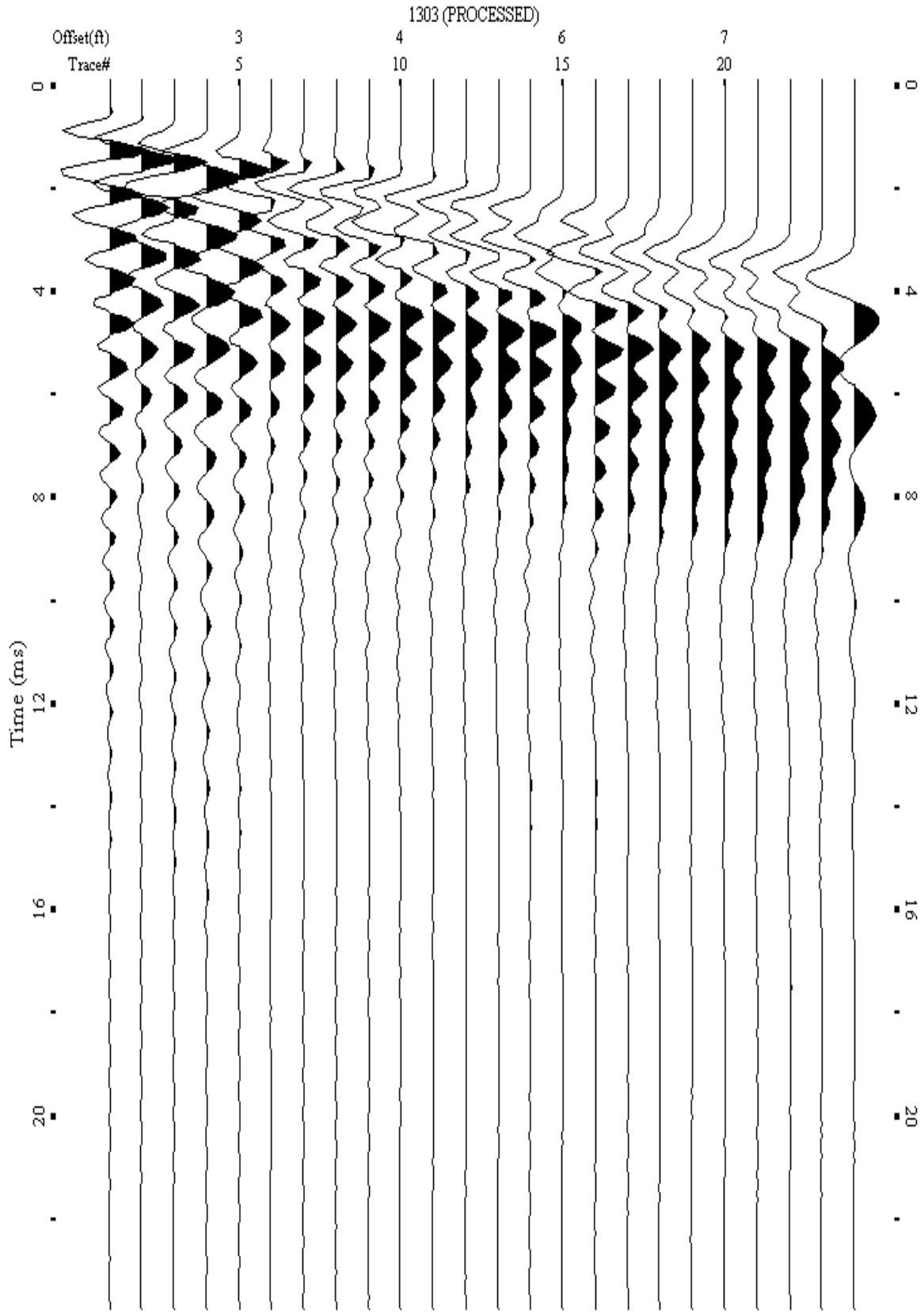

A.466: Shot Gather Line 1303 used in Pre-blast 31

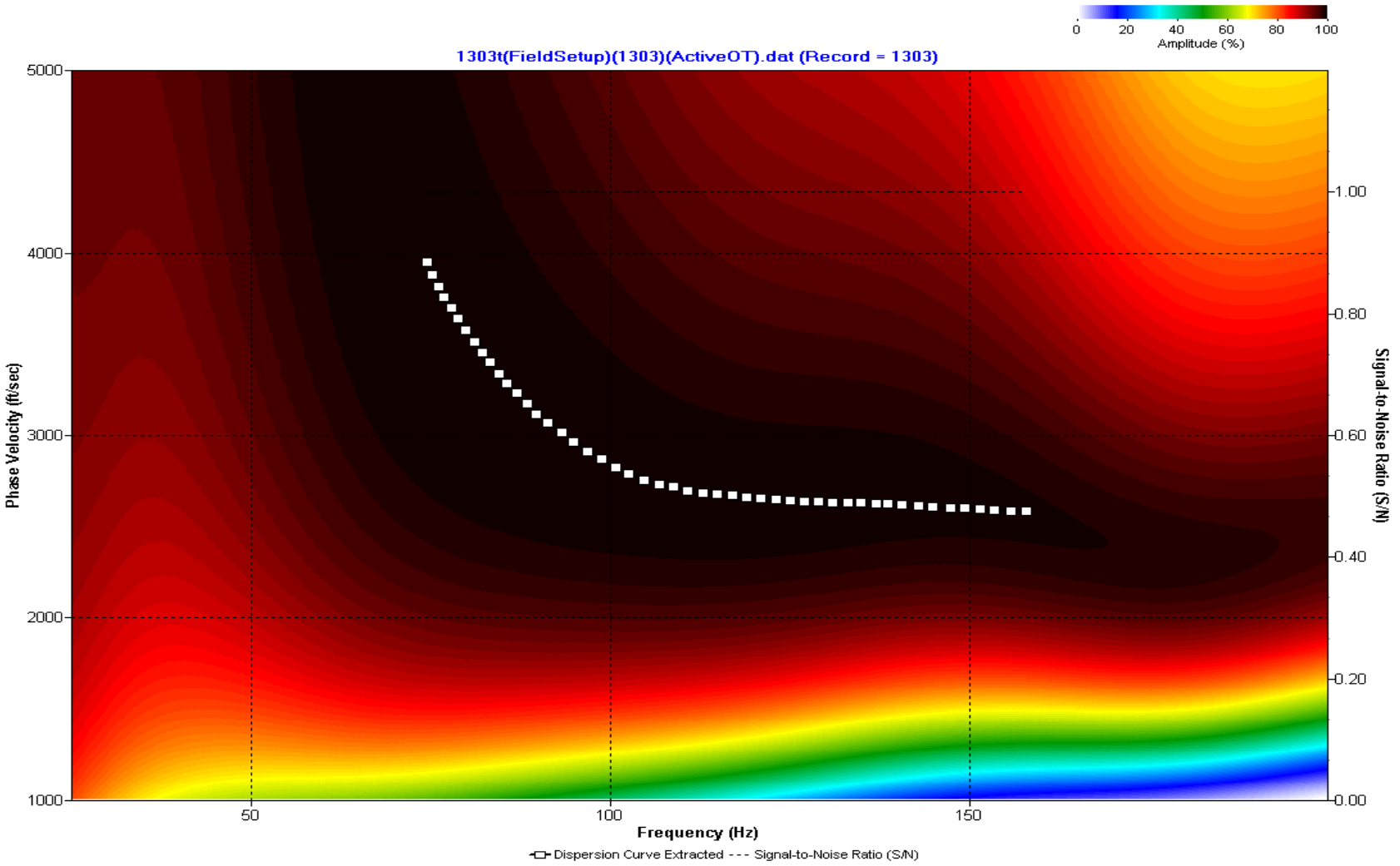

A.467: Dispersion Curve Line 1303 used in Pre-blast 31

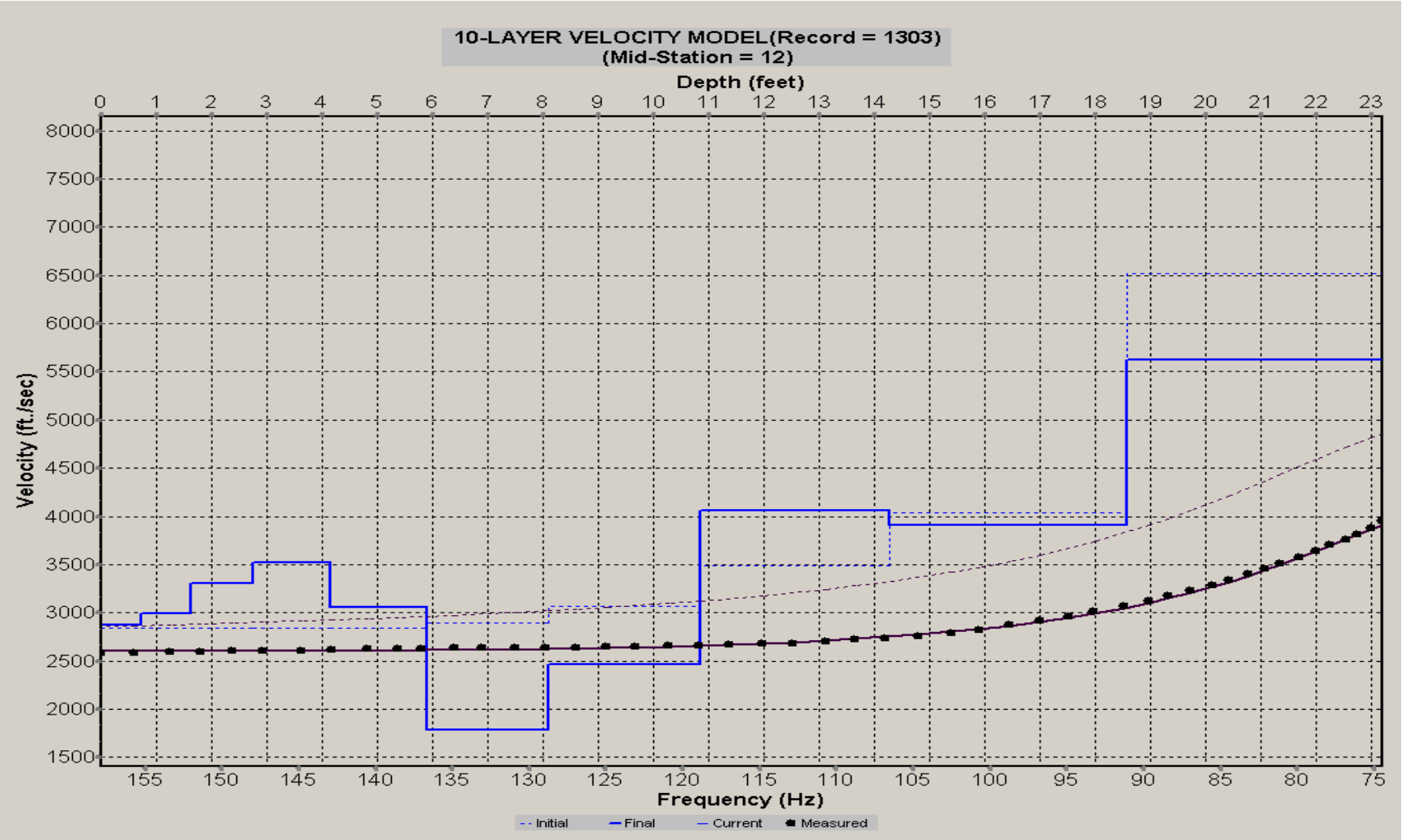

A.468: Velocity Profile Line 1303 used in Pre-blast 31

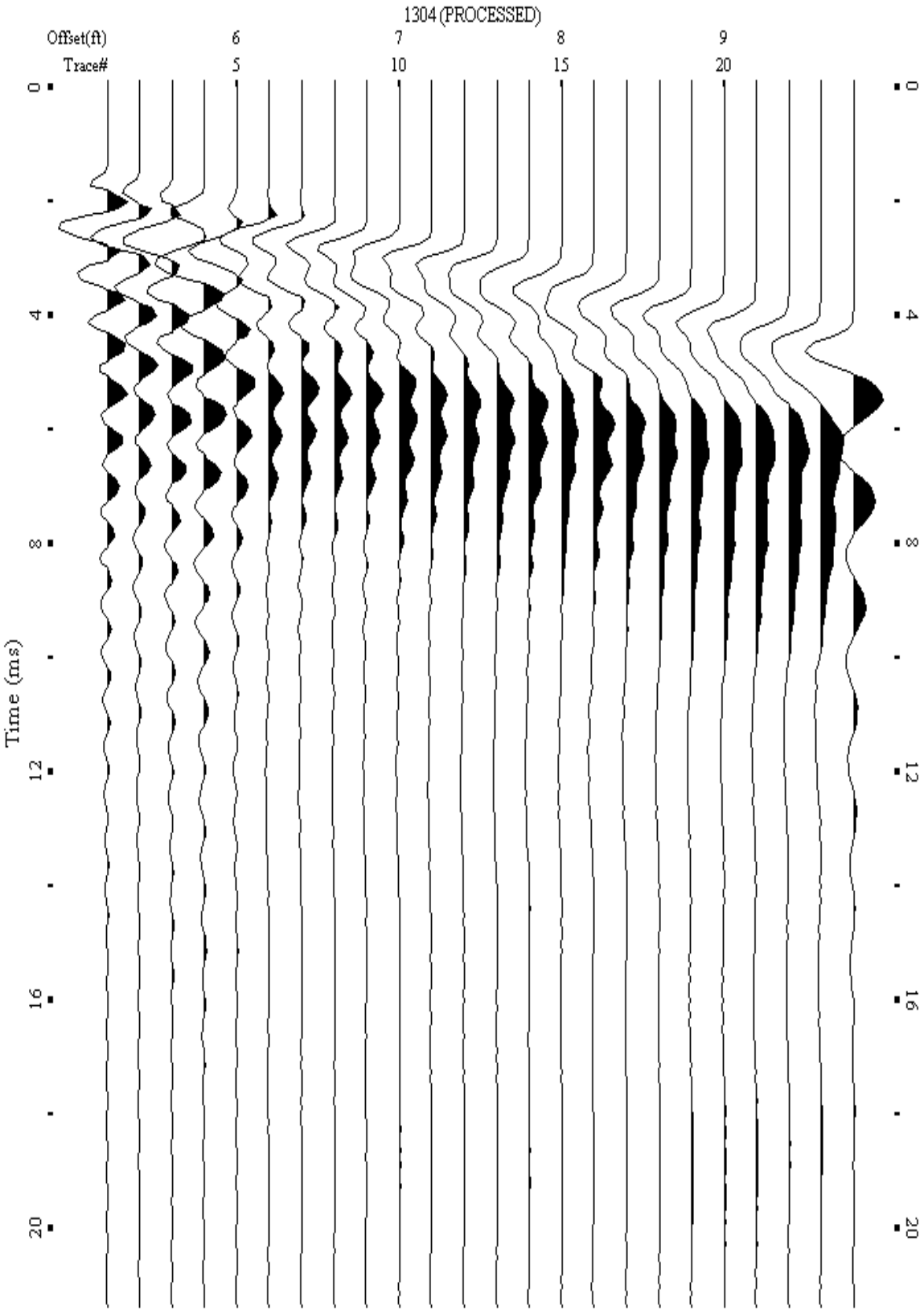

A.469: Shot Gather Line 1304 used in Pre-blast 31

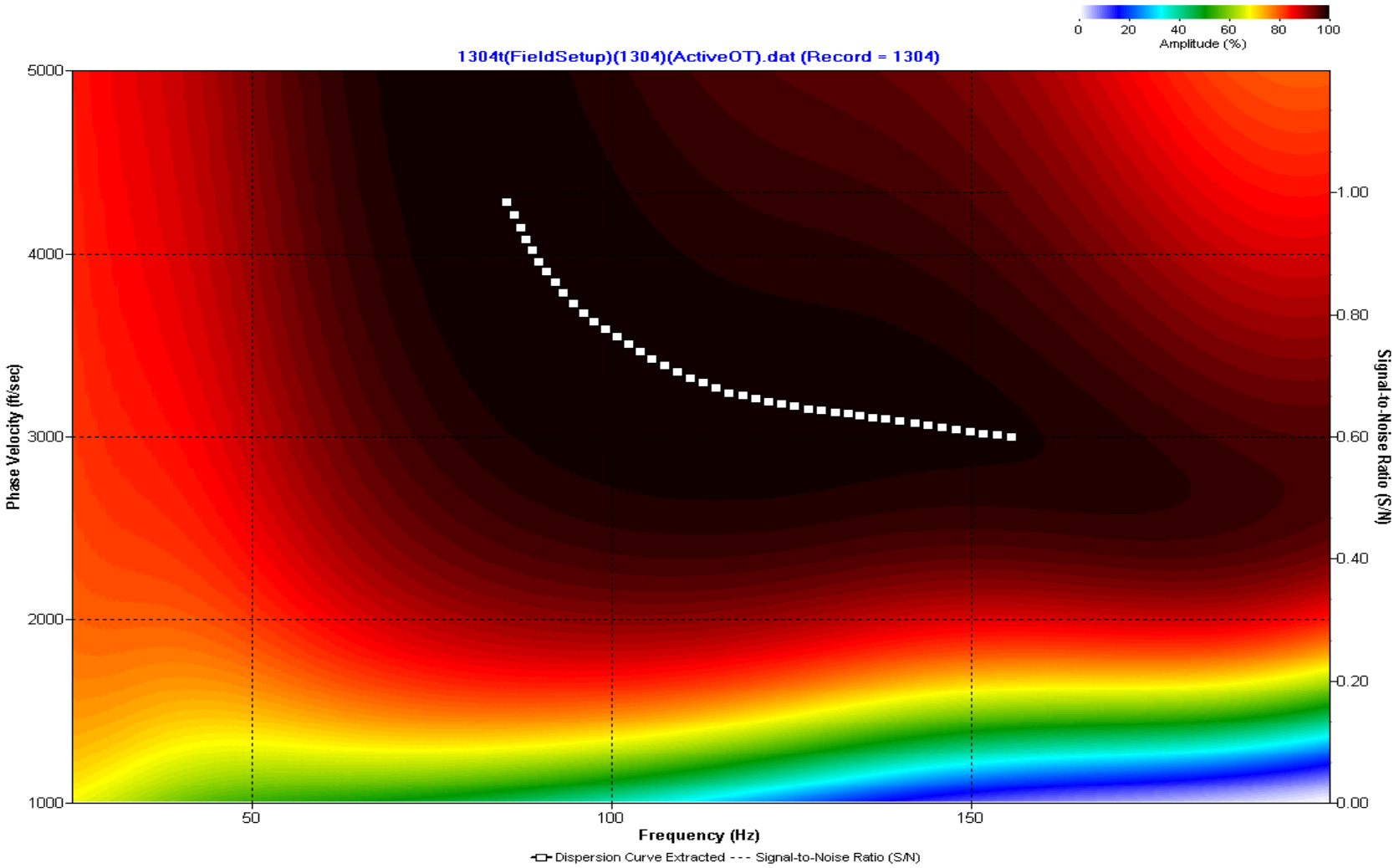

A.470: Dispersion Curve Line 1304 used in Pre-blast 31

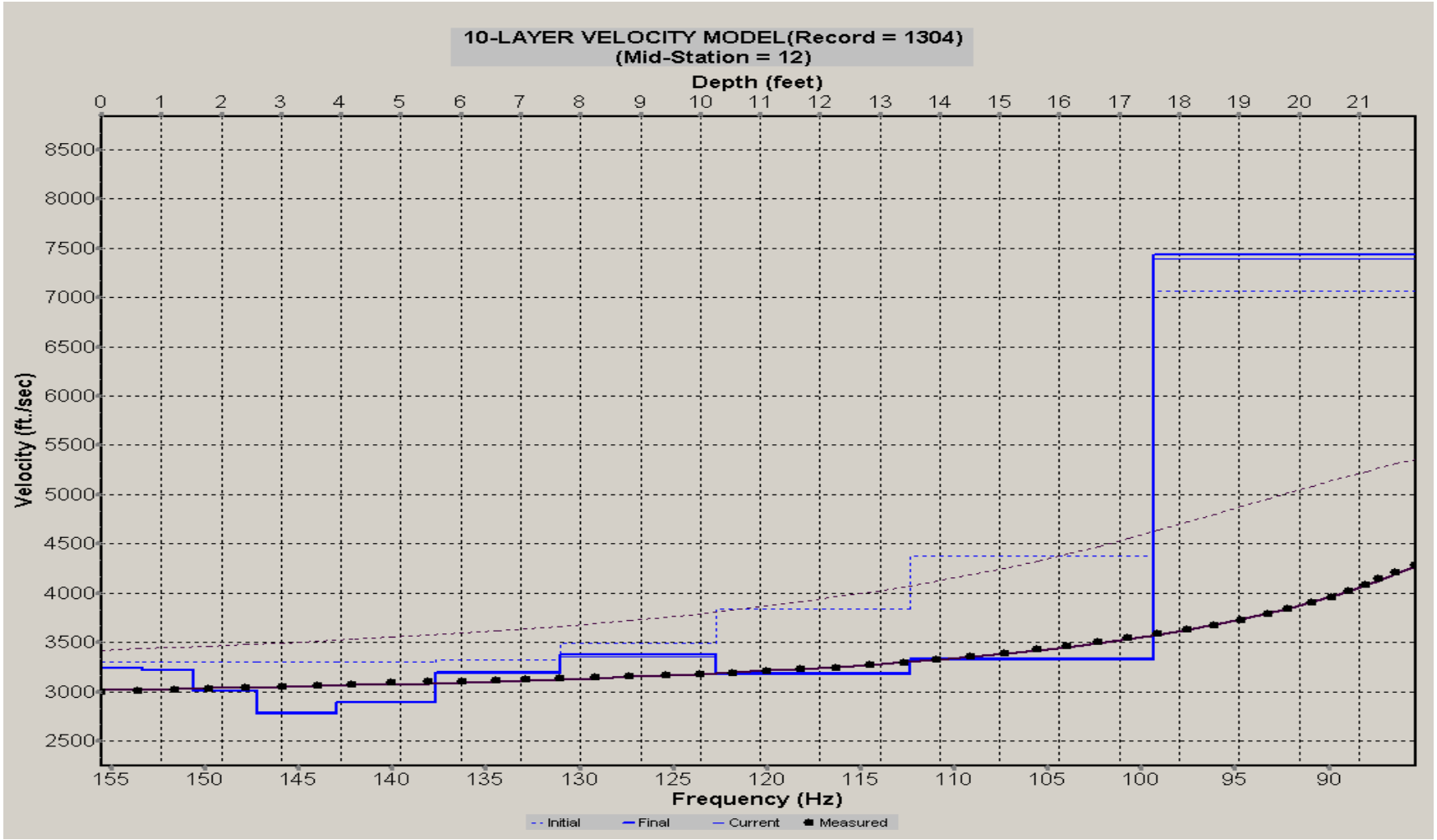

A.471: Velocity Profile Line 1304 used in Pre-blast 31

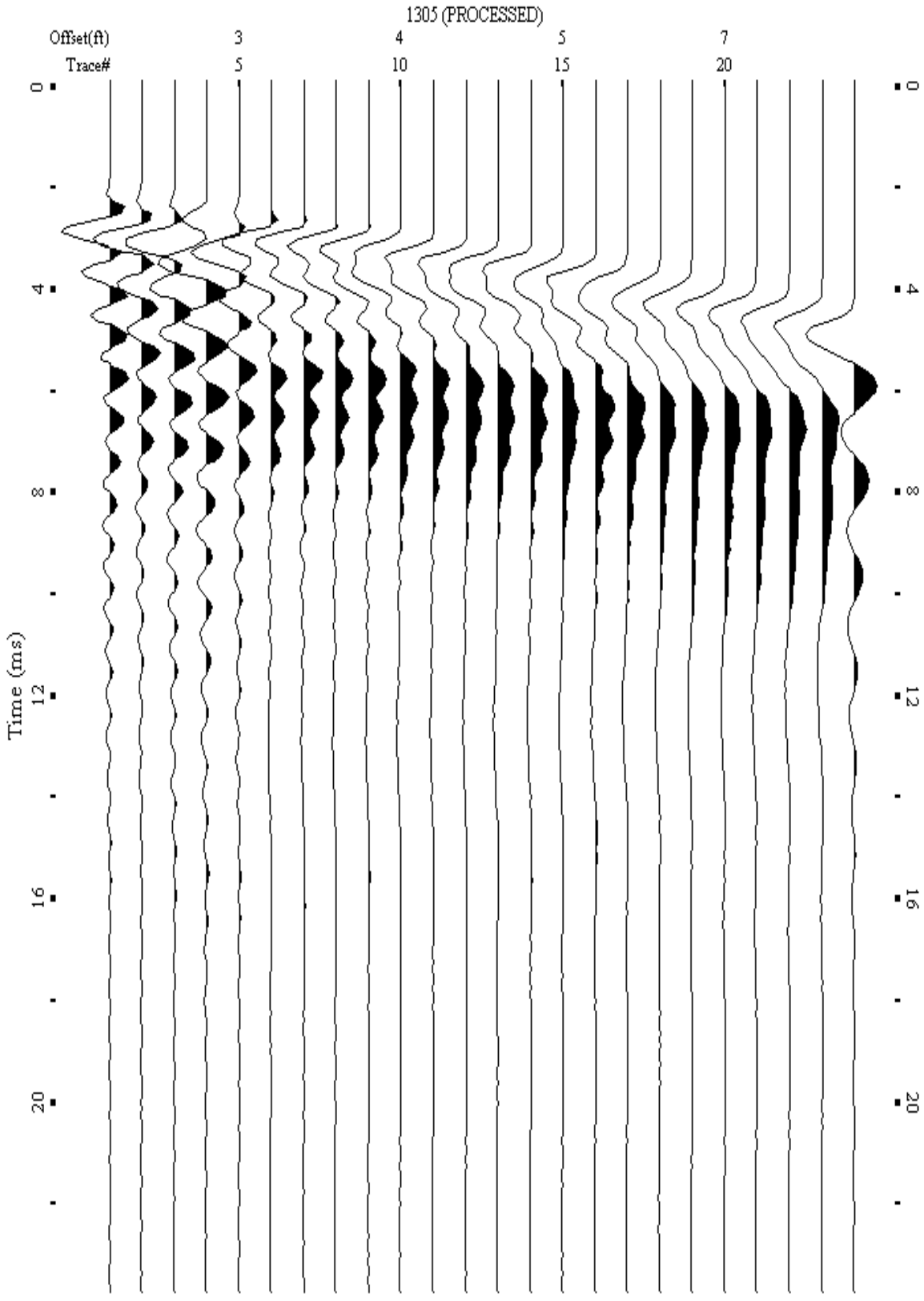

A.472: Shot Gather Line 1305 used in Post-blast 27 and Pre-blast 31

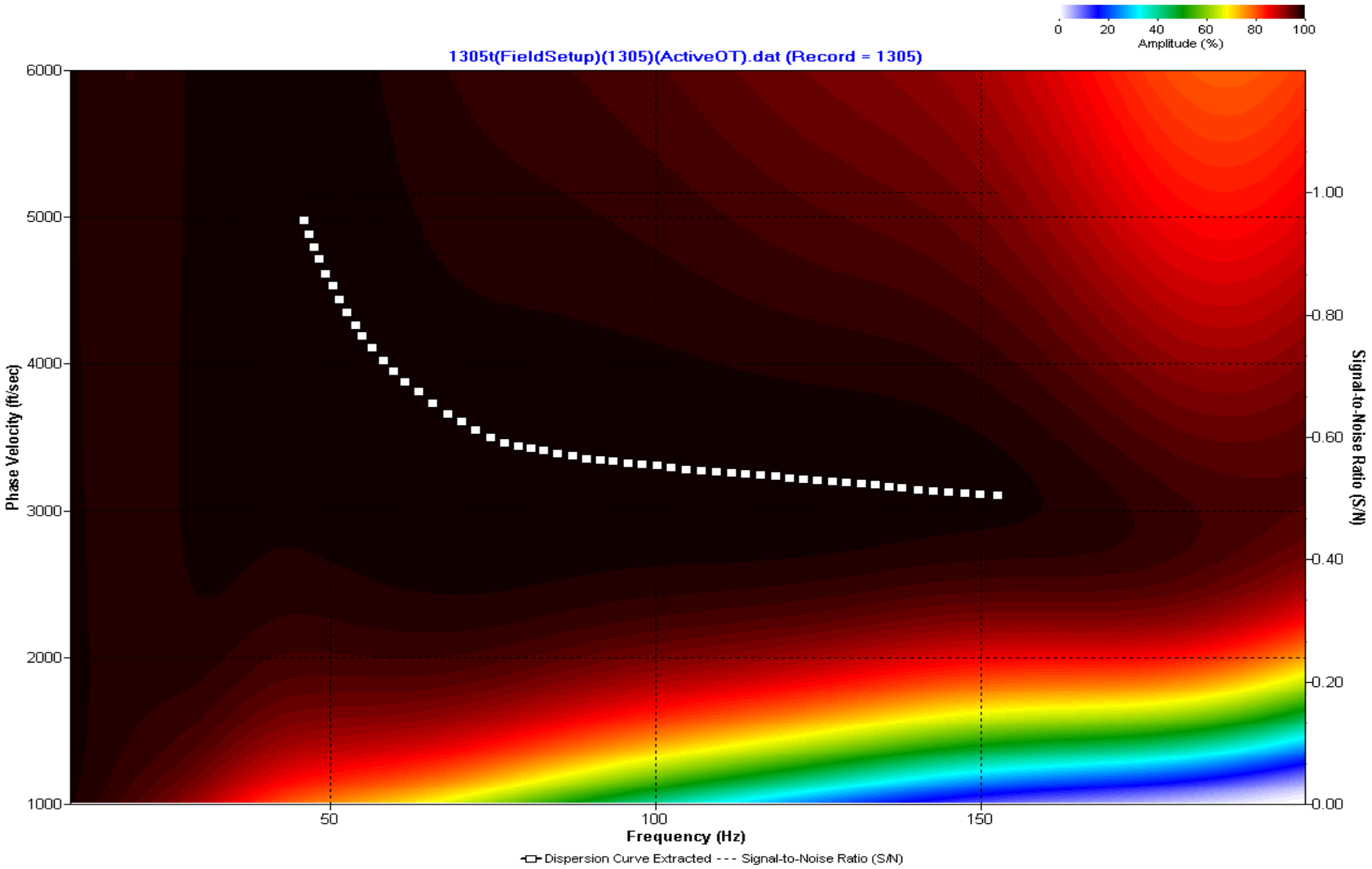

A.473: Dispersion Curve Line 1305 used in Post-blast 27 and Pre-blast 31

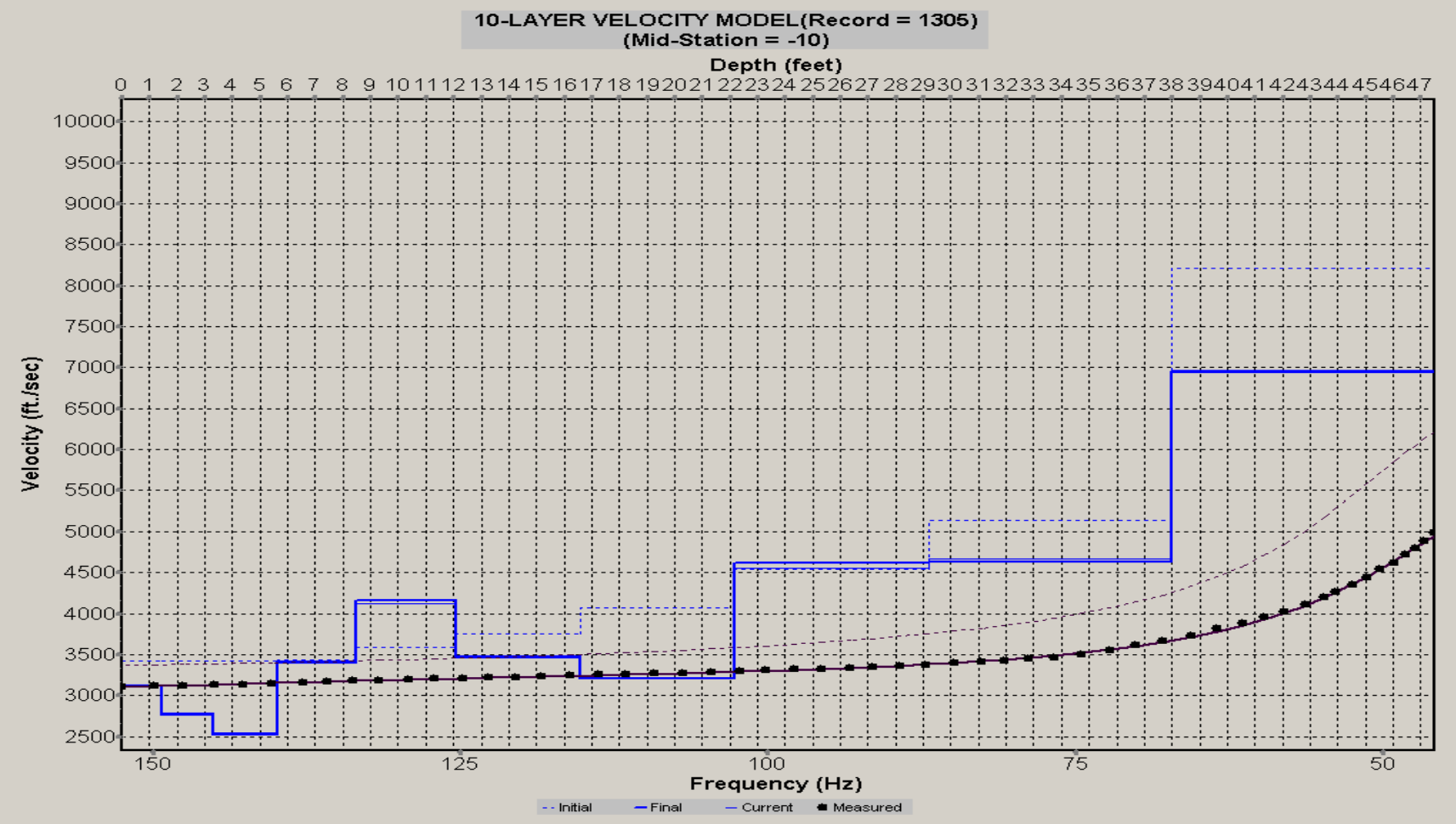

A.474: Velocity Profile Line 1305 used in Post-blast 27 and Pre-blast 31

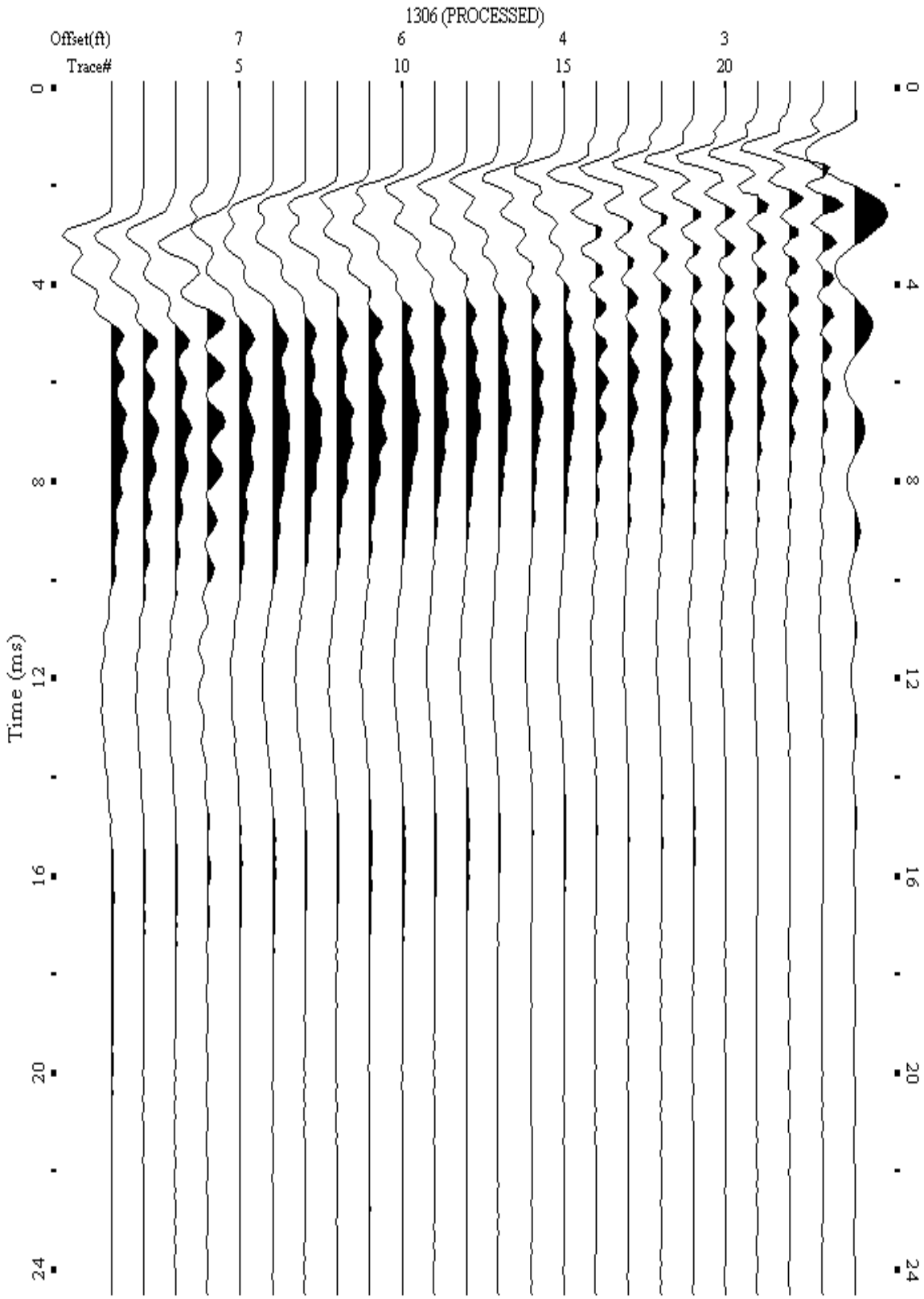

A.475: Shot Gather Line 1306 used in Post-blast 27 and Pre-blast 31

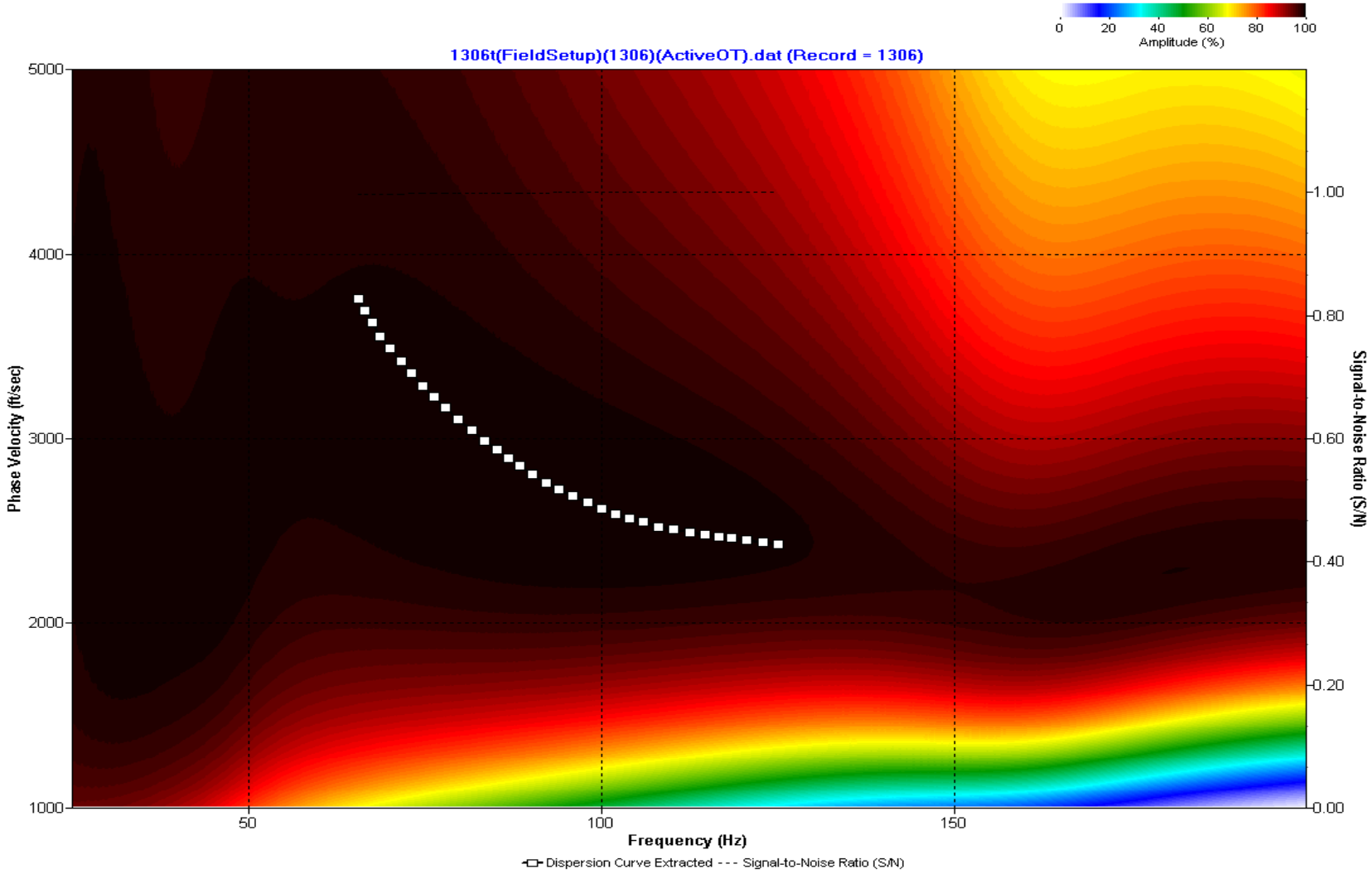

A.476: Dispersion Curve Line 1306 used in Post-blast 27 and Pre-blast 31

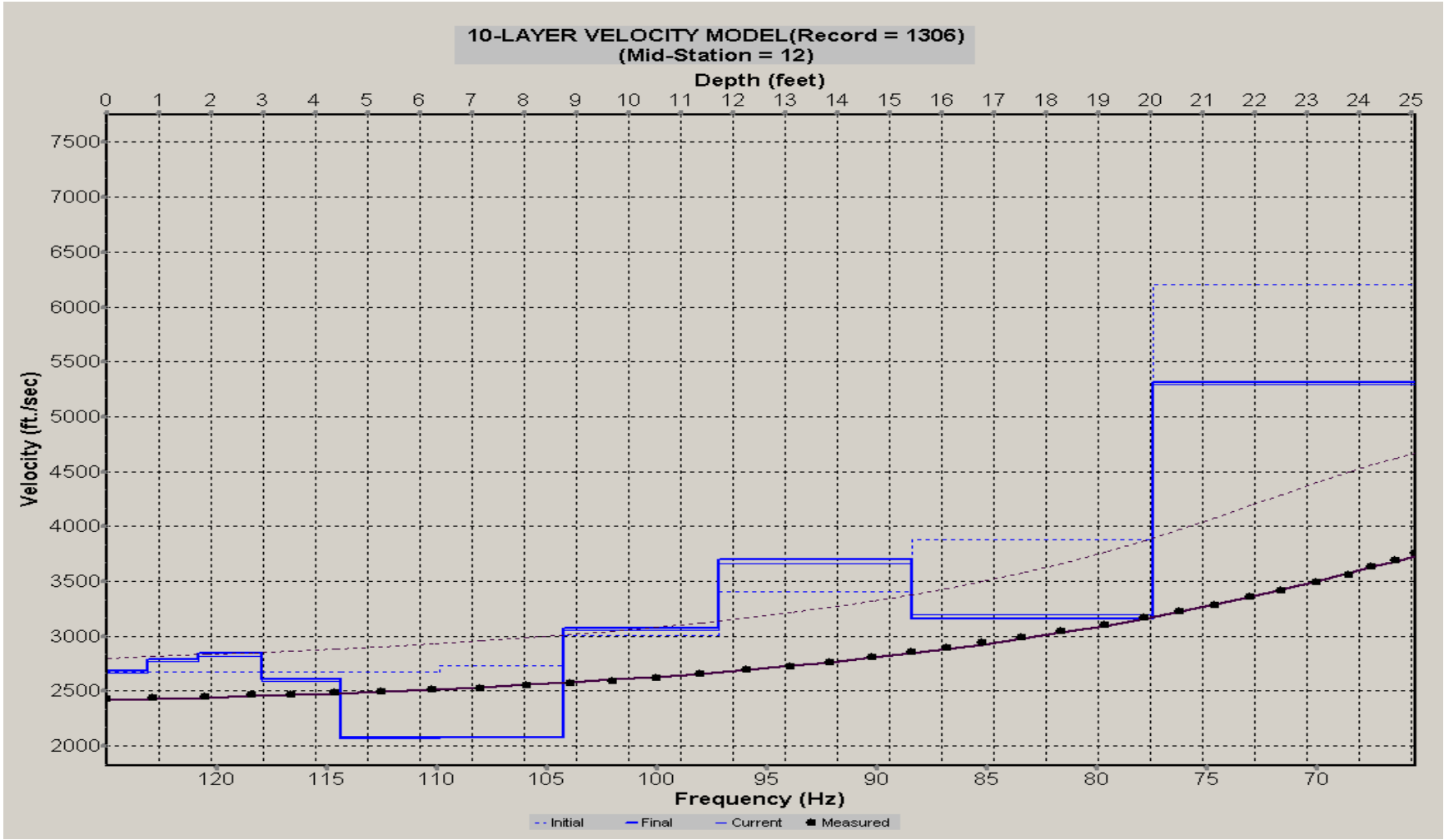

A.477: Velocity Profile Line 1306 used in Post-blast 27 and Pre-blast 31

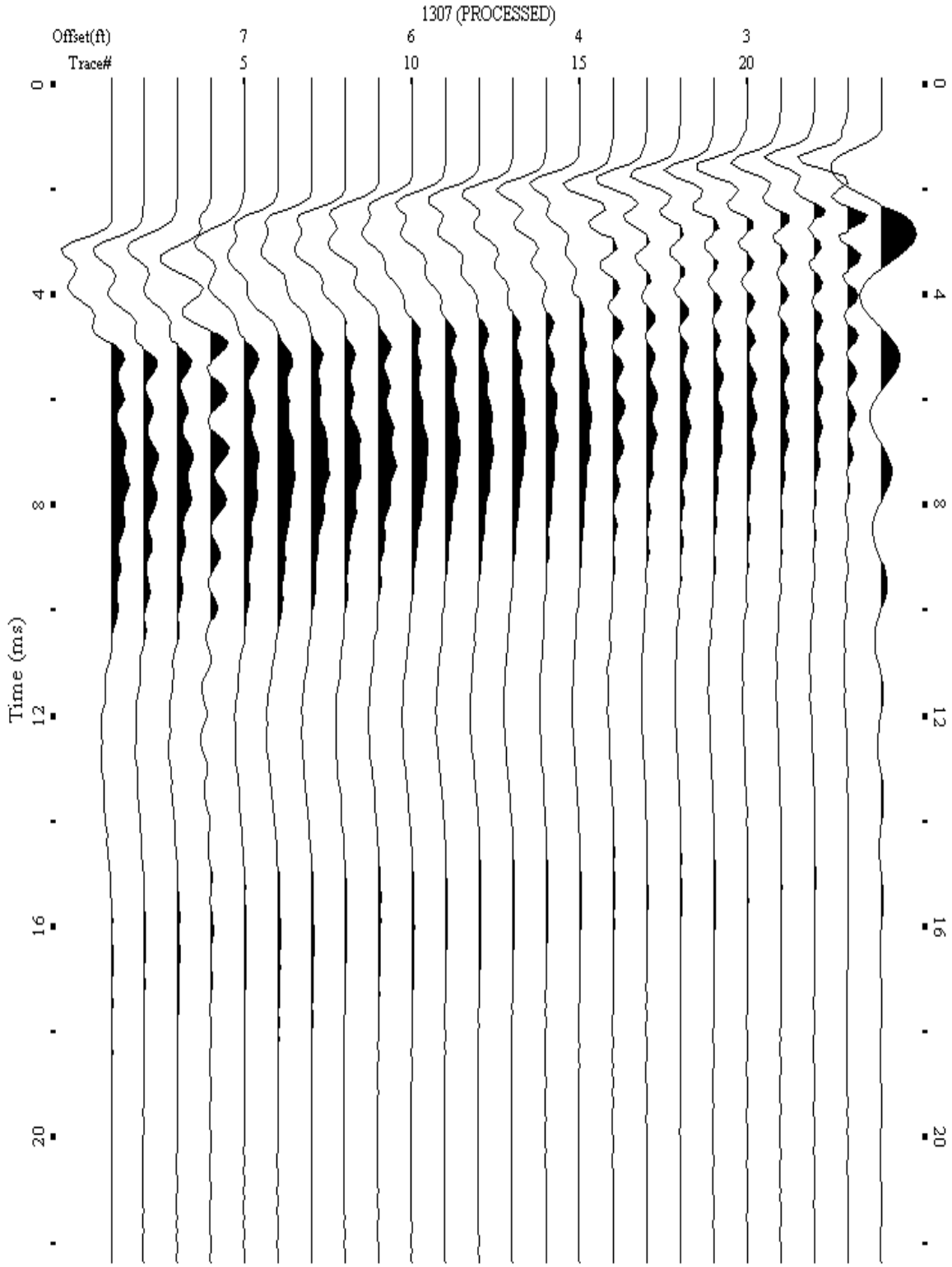

A.478: Shot Gather Line 1307 used in Post-blast 27 and Pre-blast 31

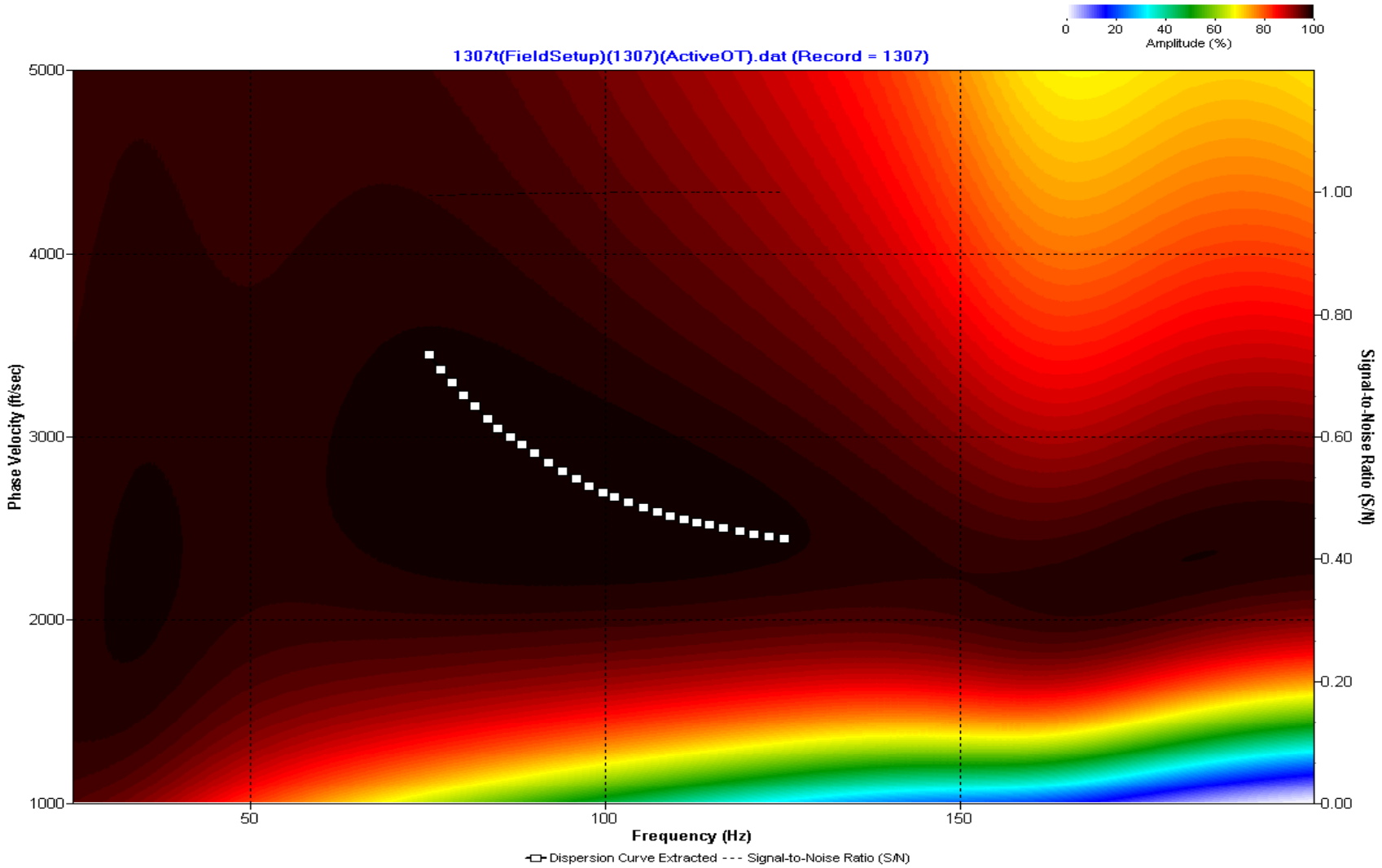

A.479: Dispersion Curve Line 1307 used in Post-blast 27 and Pre-blast 31

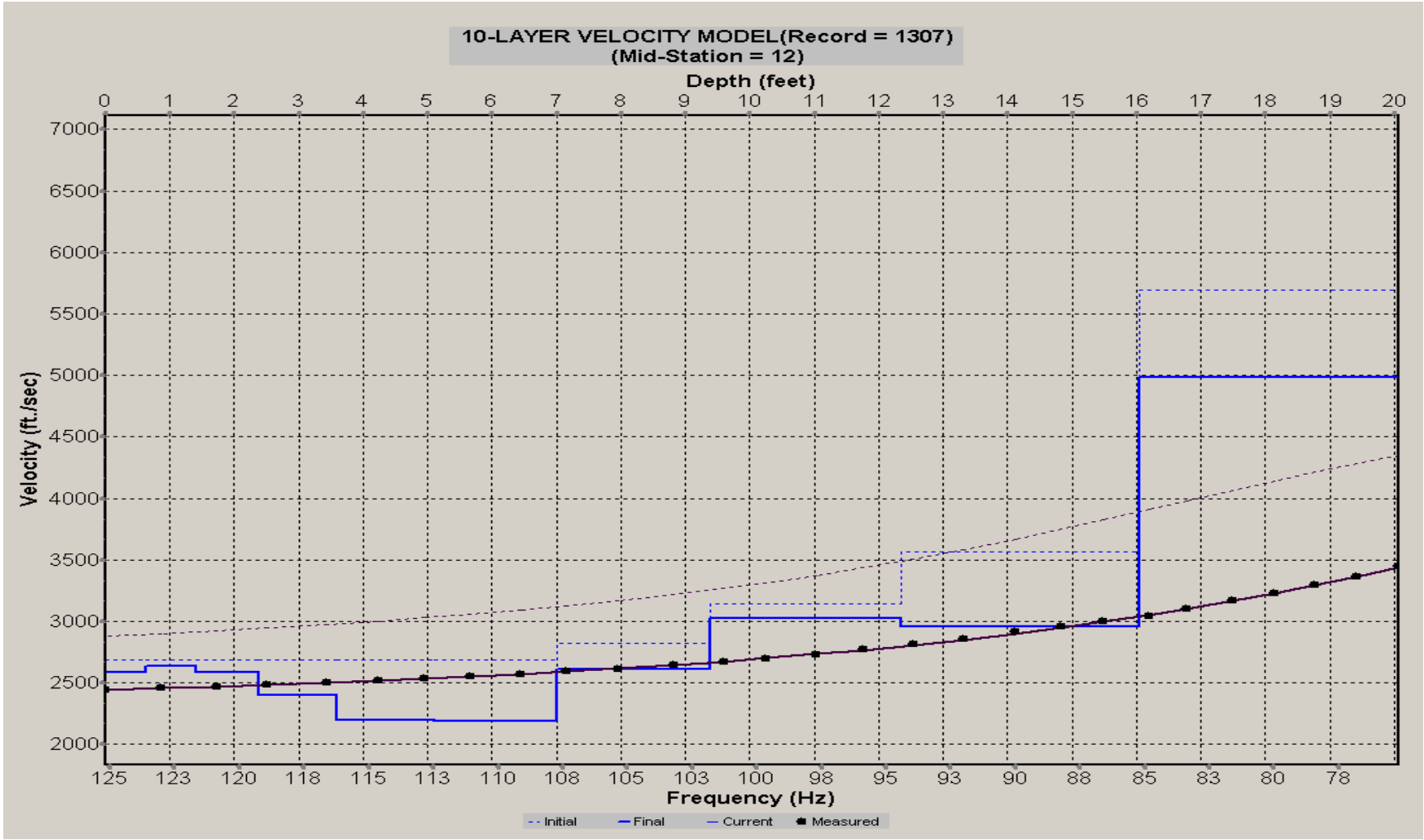

A.480: Velocity Profile Line 1307 used in Post-blast 27 and Pre-blast 31

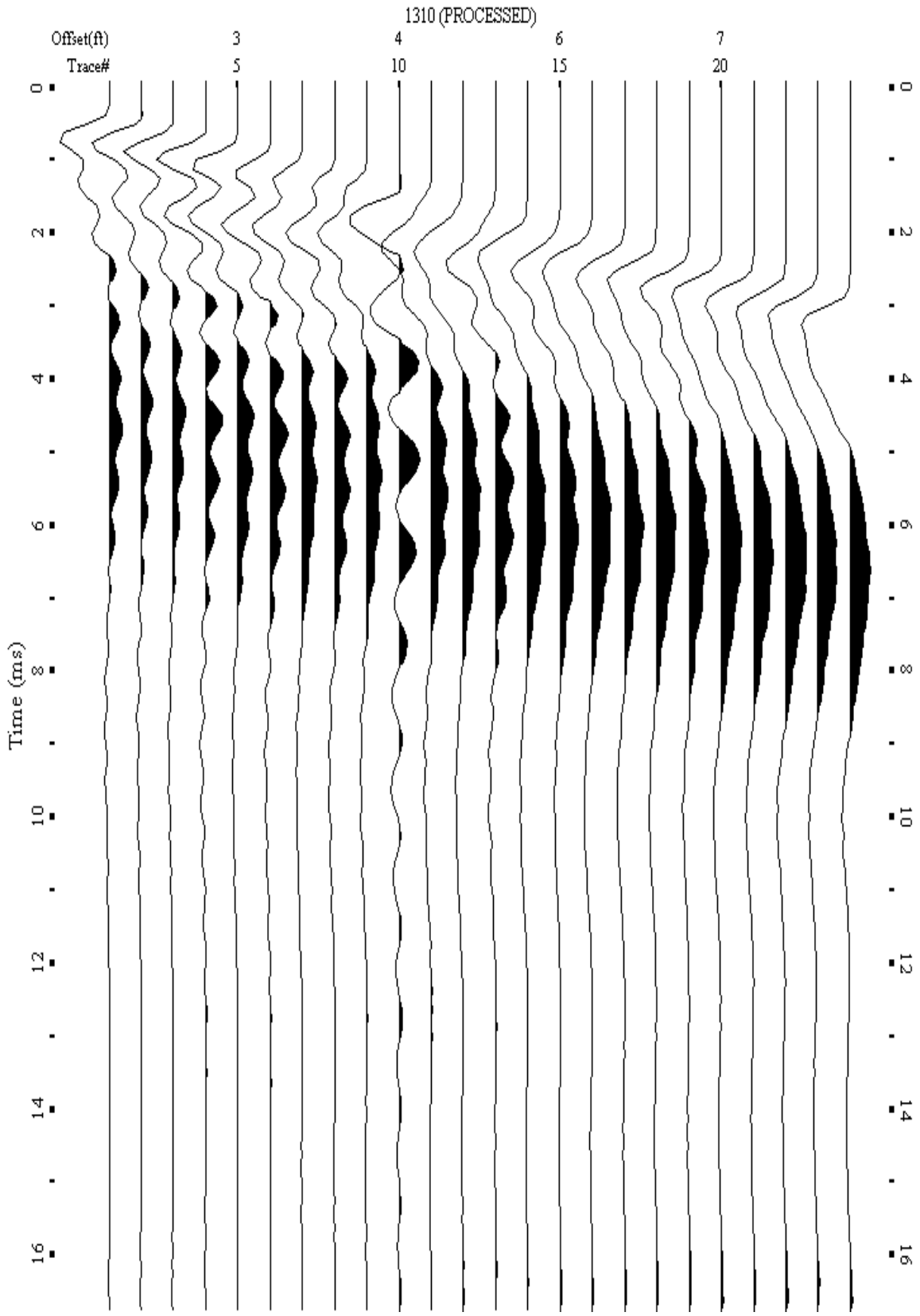

A.481: Shot Gather Line 1310 used in Pre-blast 13, Post-blast 28 and Pre-blast 32

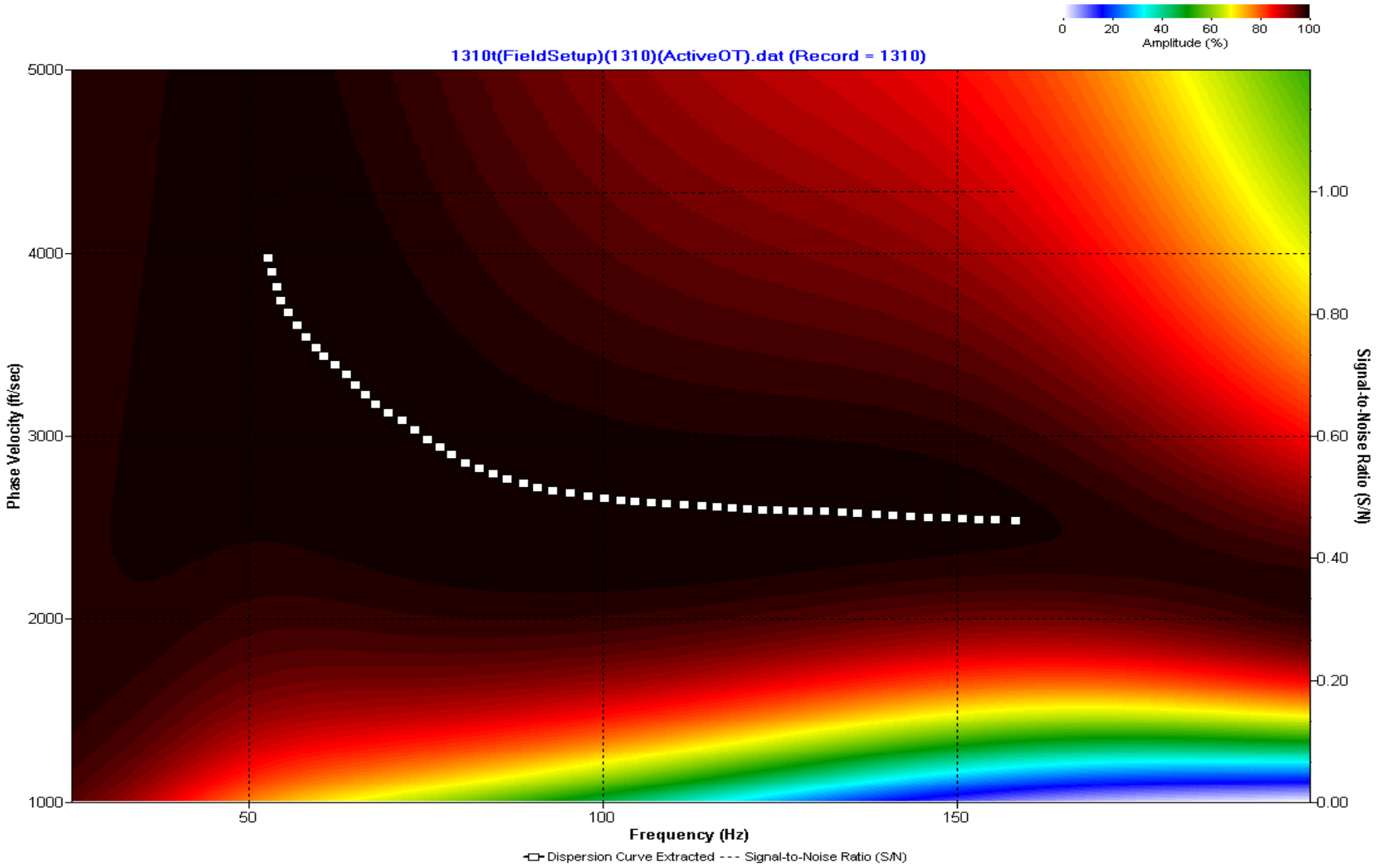

A.482: Dispersion Curve Line 1310 used in Pre-blast 13, Post-blast 28 and Pre-blast 32

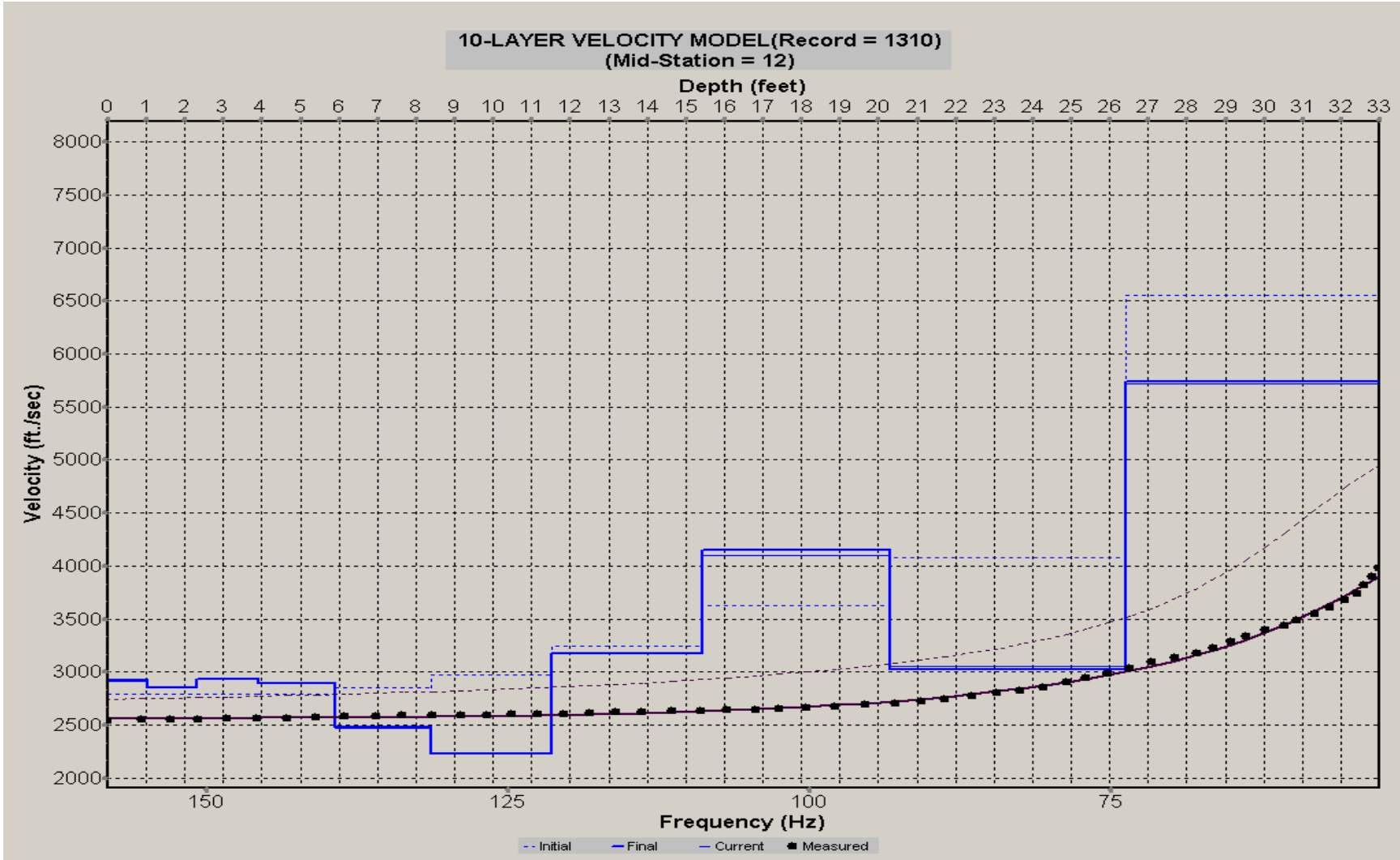

A.483: Velocity Profile Line 1310 used in Pre-blast 13, Post-blast 28 and Pre-blast 32

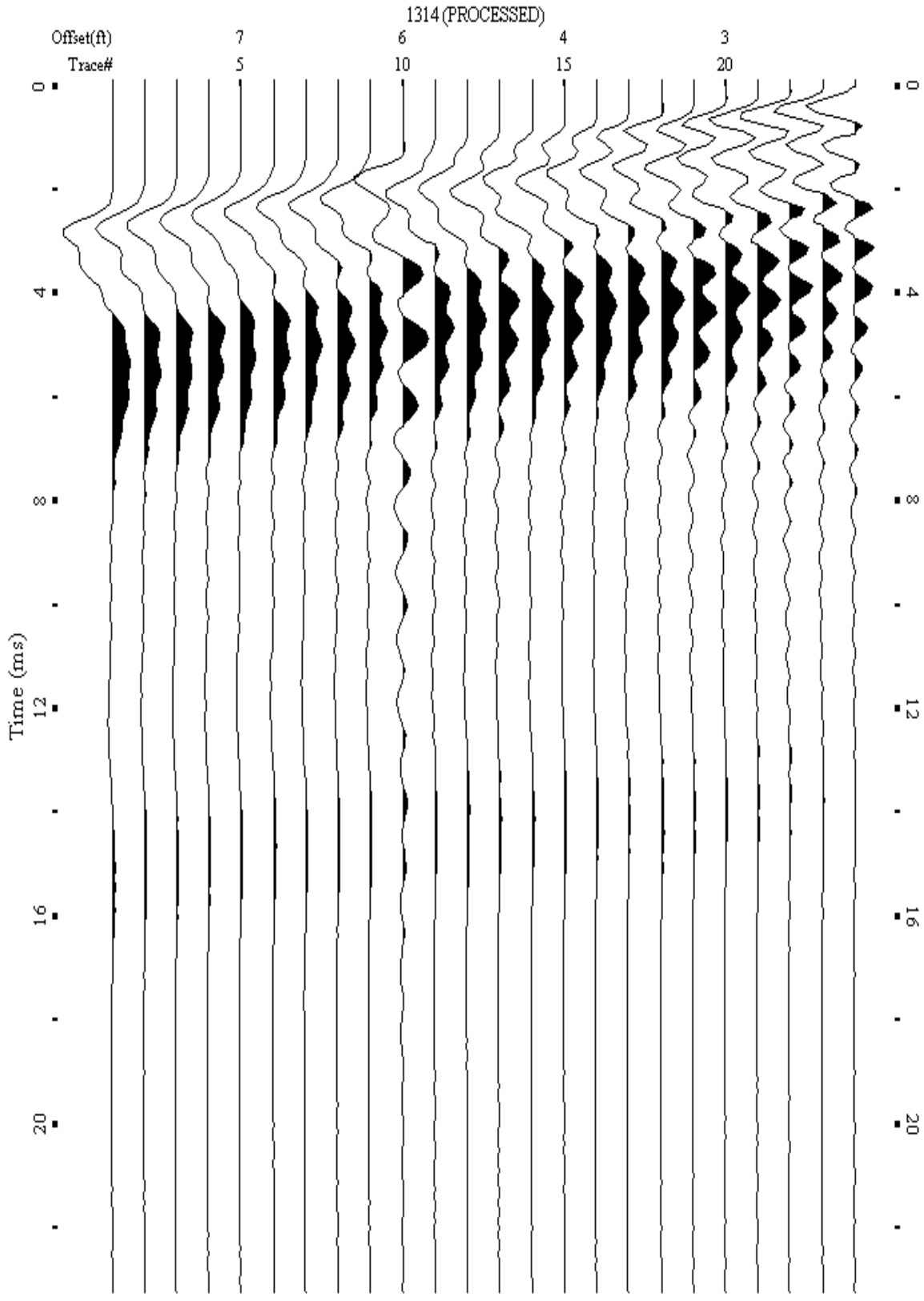

A.484: Shot Gather Line 1314 used in Pre-blast 14

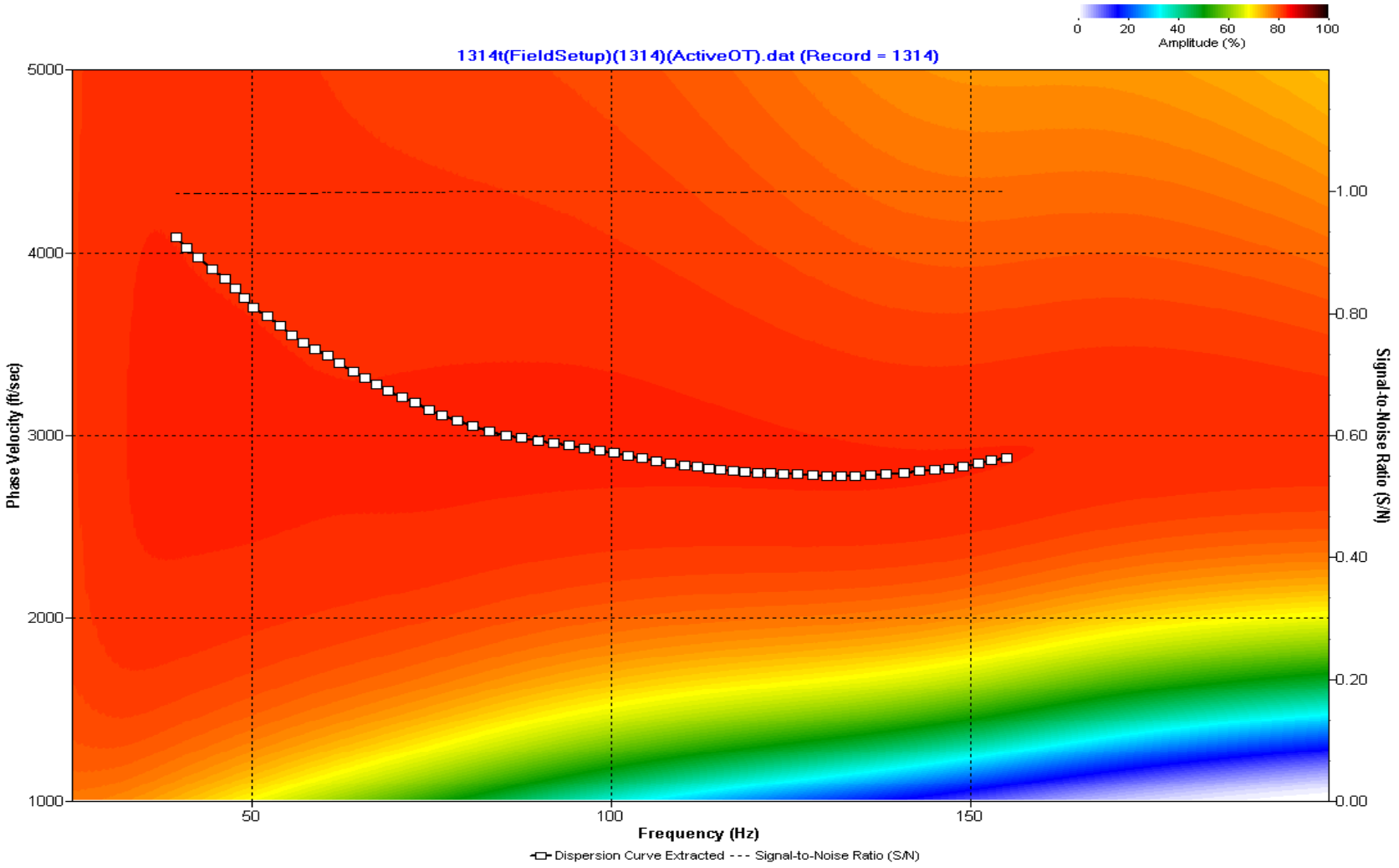

A.485: Dispersion Curve Line 1314 used in Pre-blast 14

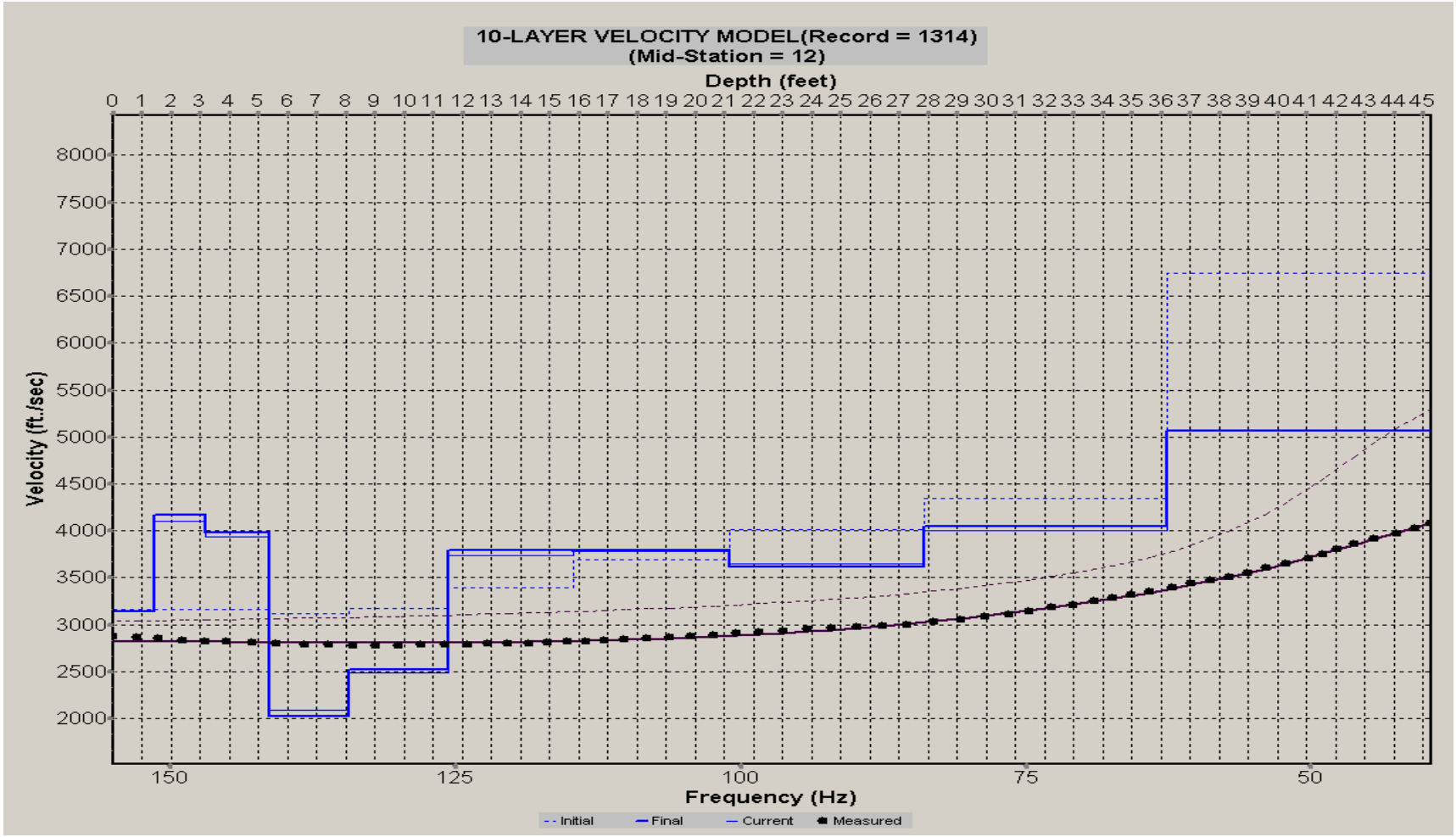

A.486: Velocity Profile Line 1314 used in Pre-blast 14

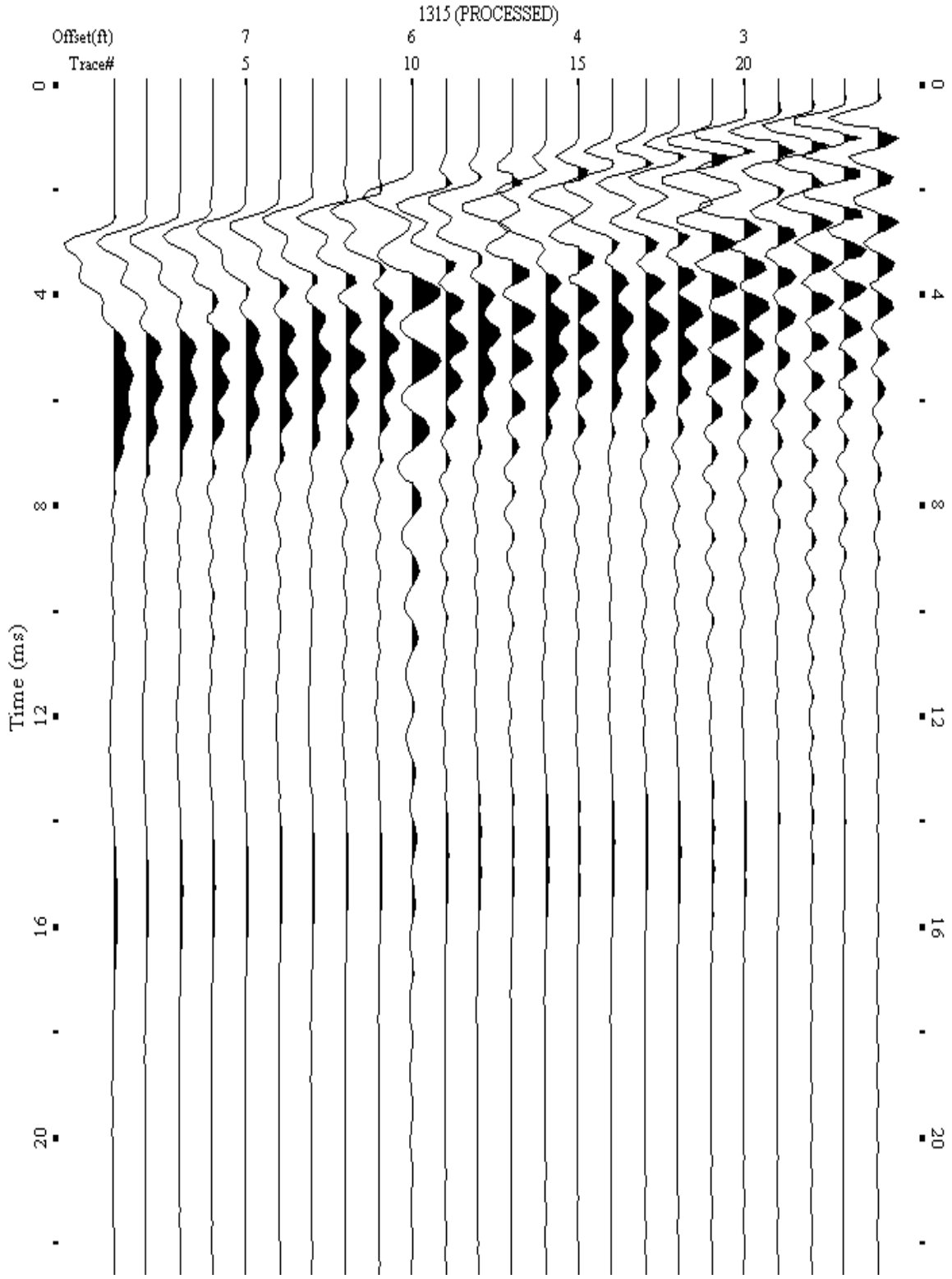

A.487: Shot Gather Line 1315 used in Pre-blast 13, Post-blast 28 and Pre-blast 32

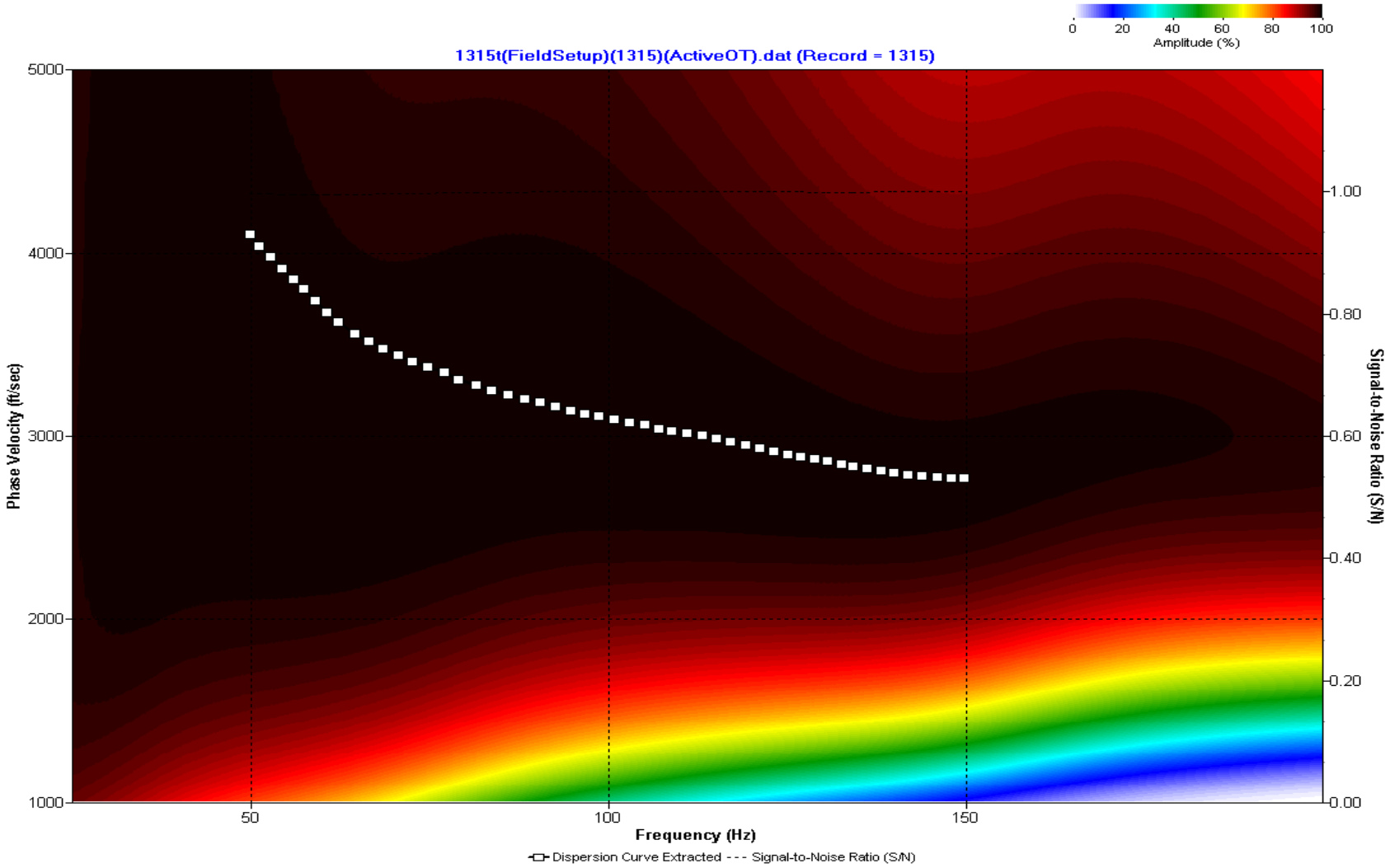

A.488: Dispersion Curve Line 1315 used in Pre-blast 13, Post-blast 28 and Pre-blast 32

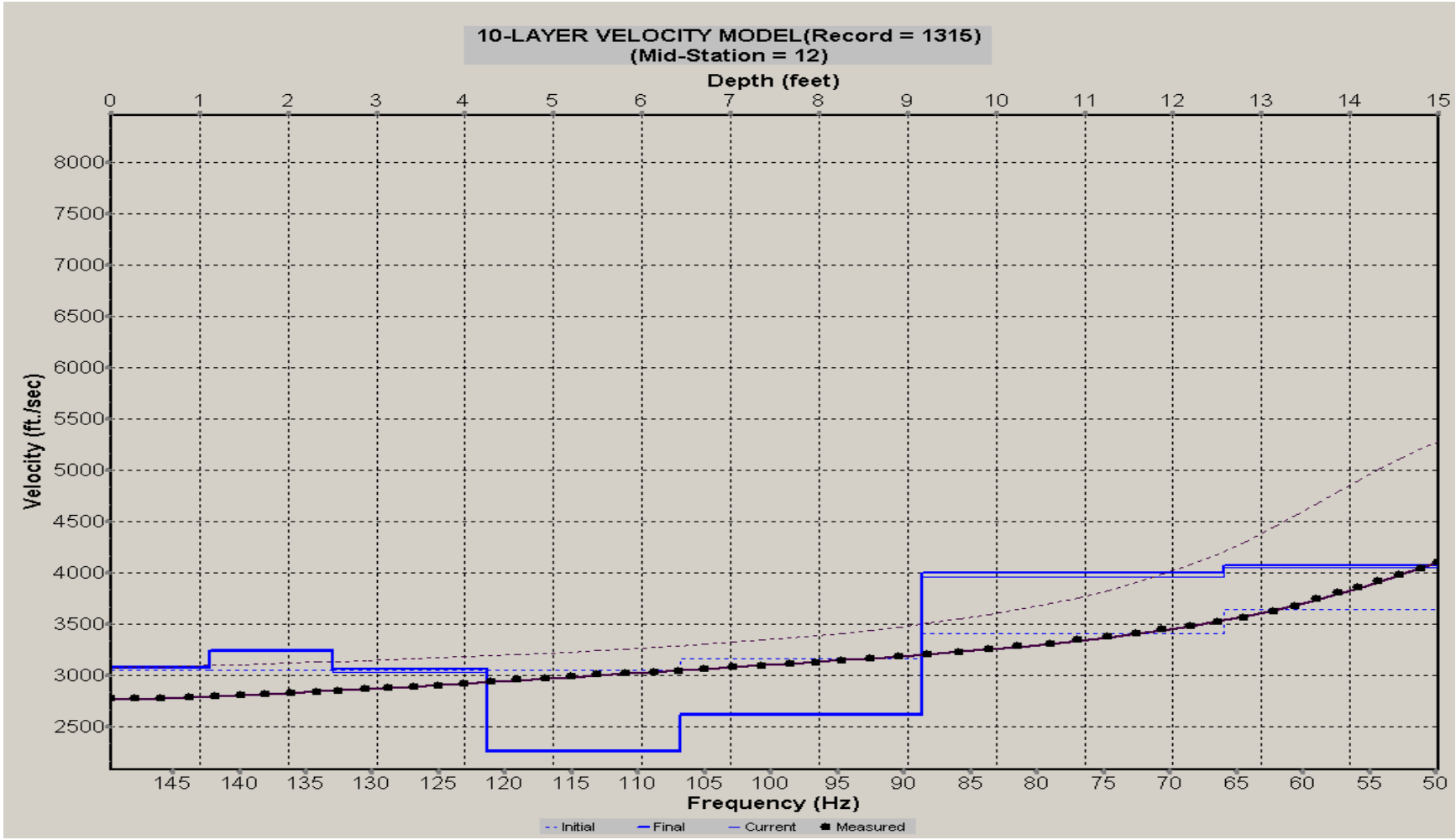

A.489: Velocity Profile Line 1315 used in Pre-blast 13, Post-blast 28 and Pre-blast 32

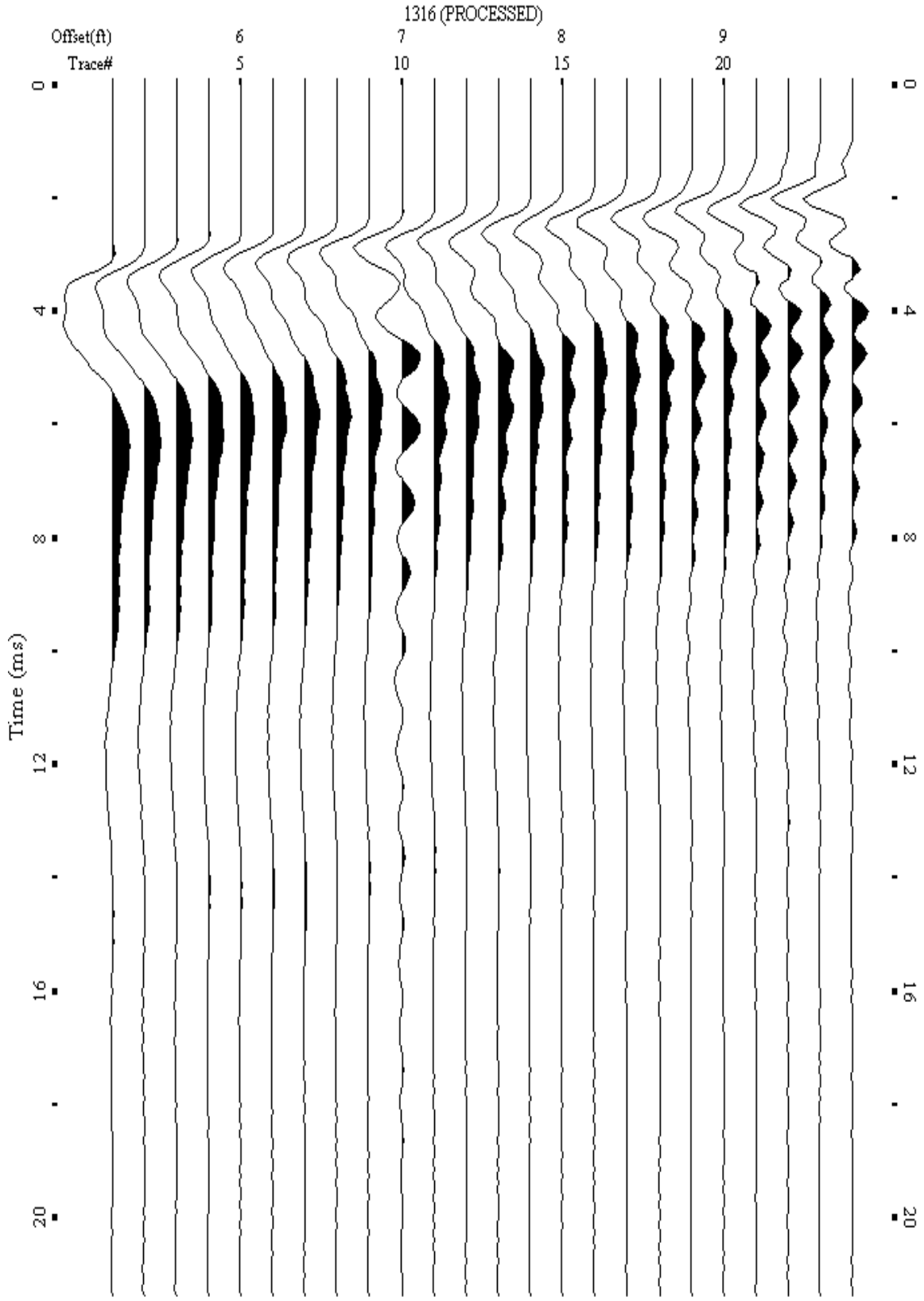

A.490: Shot Gather Line 1316 used in Pre-blast 13, Post-blast 28 and Pre-blast 32

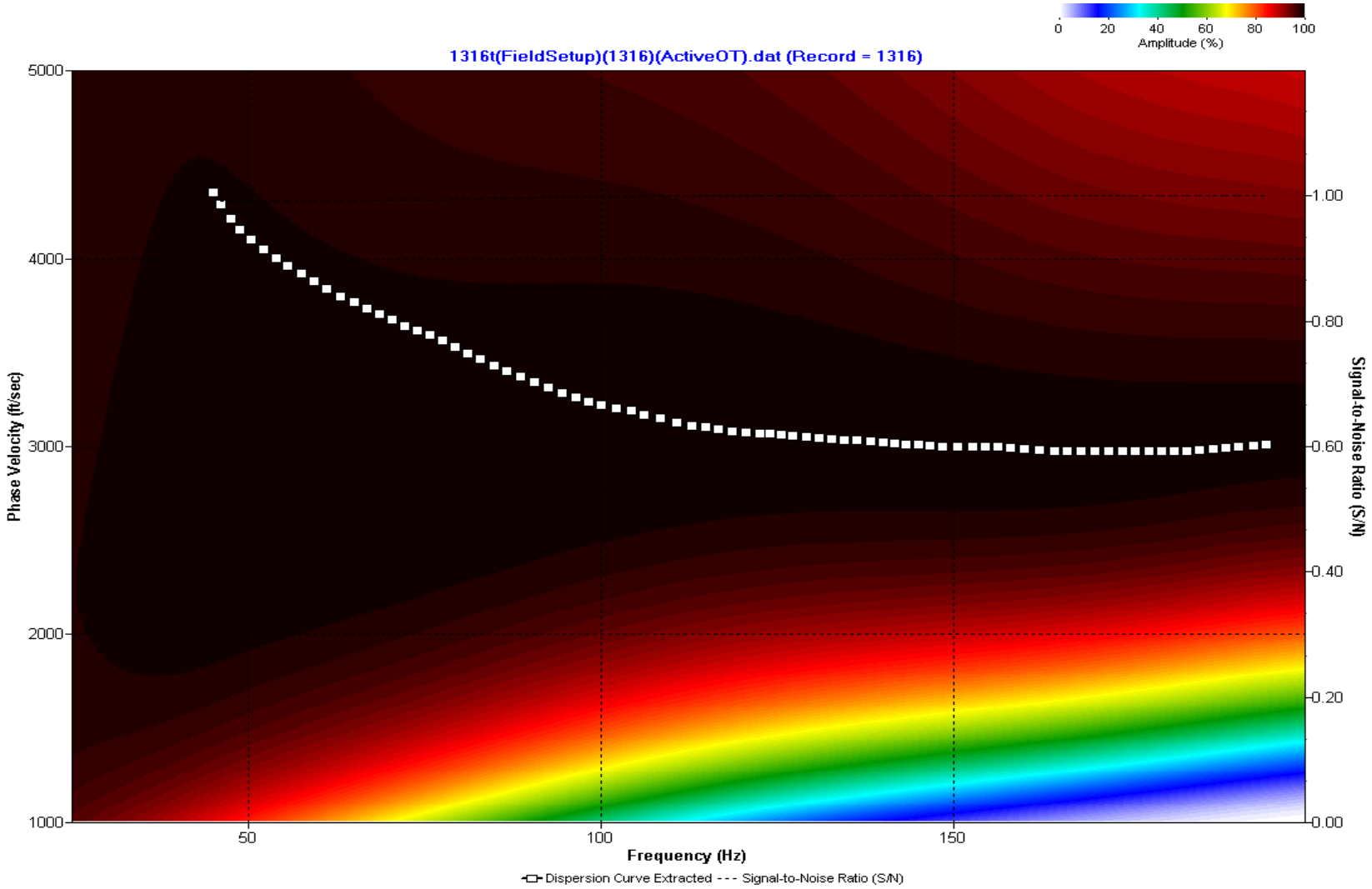

A.491: Dispersion Curve Line 1316 used in Pre-blast 13, Post-blast 28 and Pre-blast 32

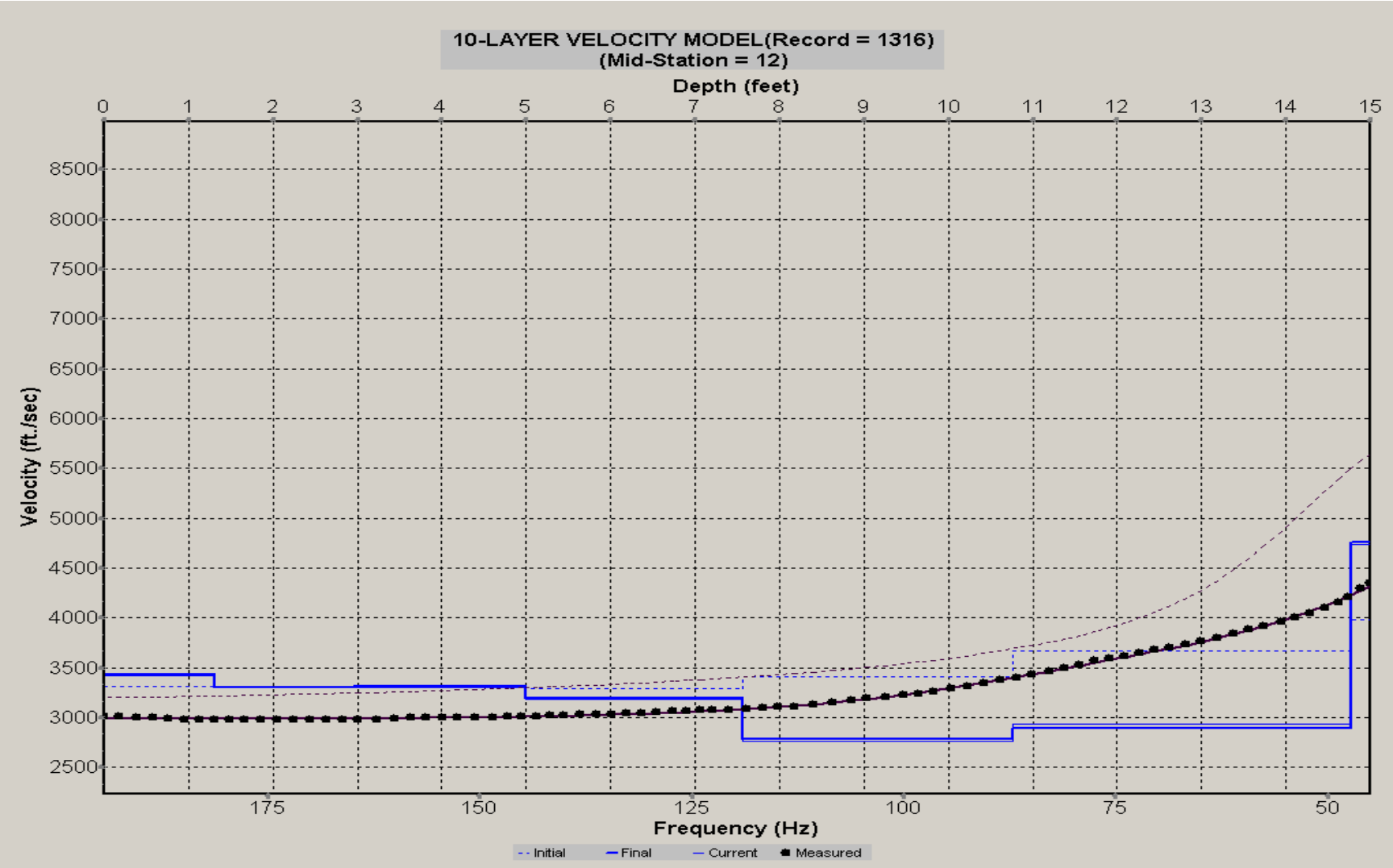

A.492: Velocity Profile Line 1316 used in Pre-blast 13, Post-blast 28 and Pre-blast 32

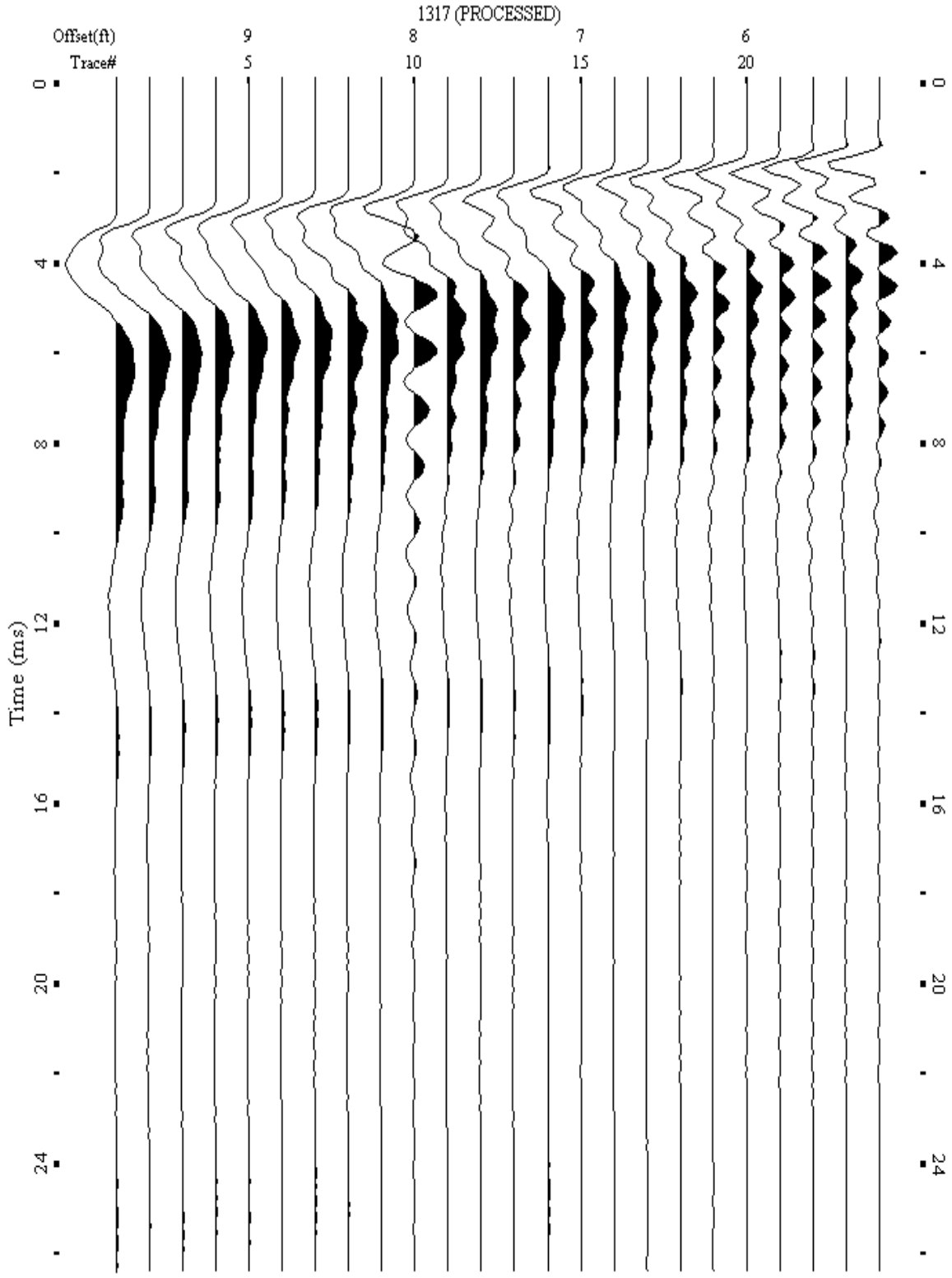

A.493: Shot Gather Line 1317 used in Pre-blast 13, Post-blast 28 and Pre-blast 32

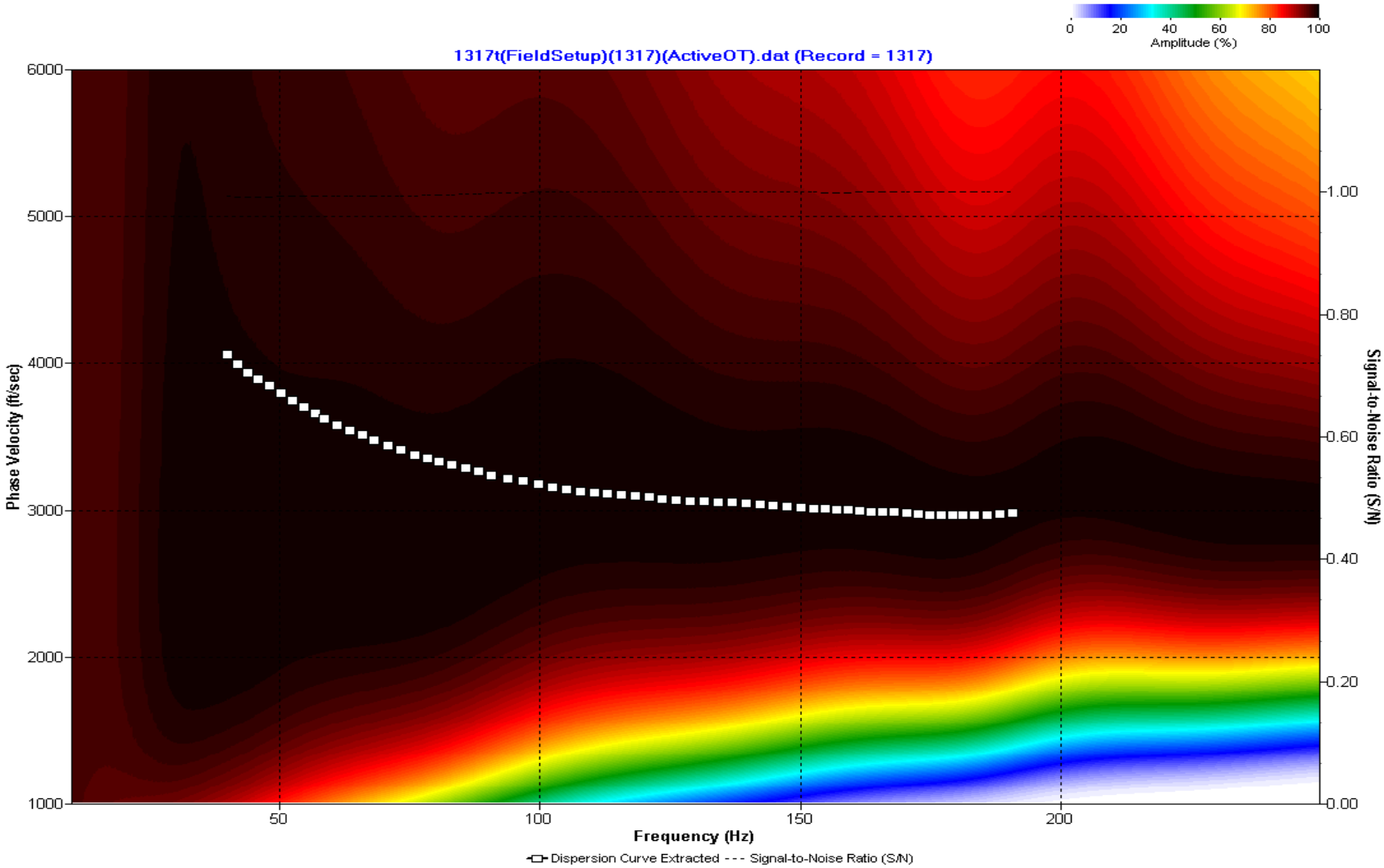

A.494: Dispersion Curve Line 1317 used in Pre-blast 13, Post-blast 28 and Pre-blast 32

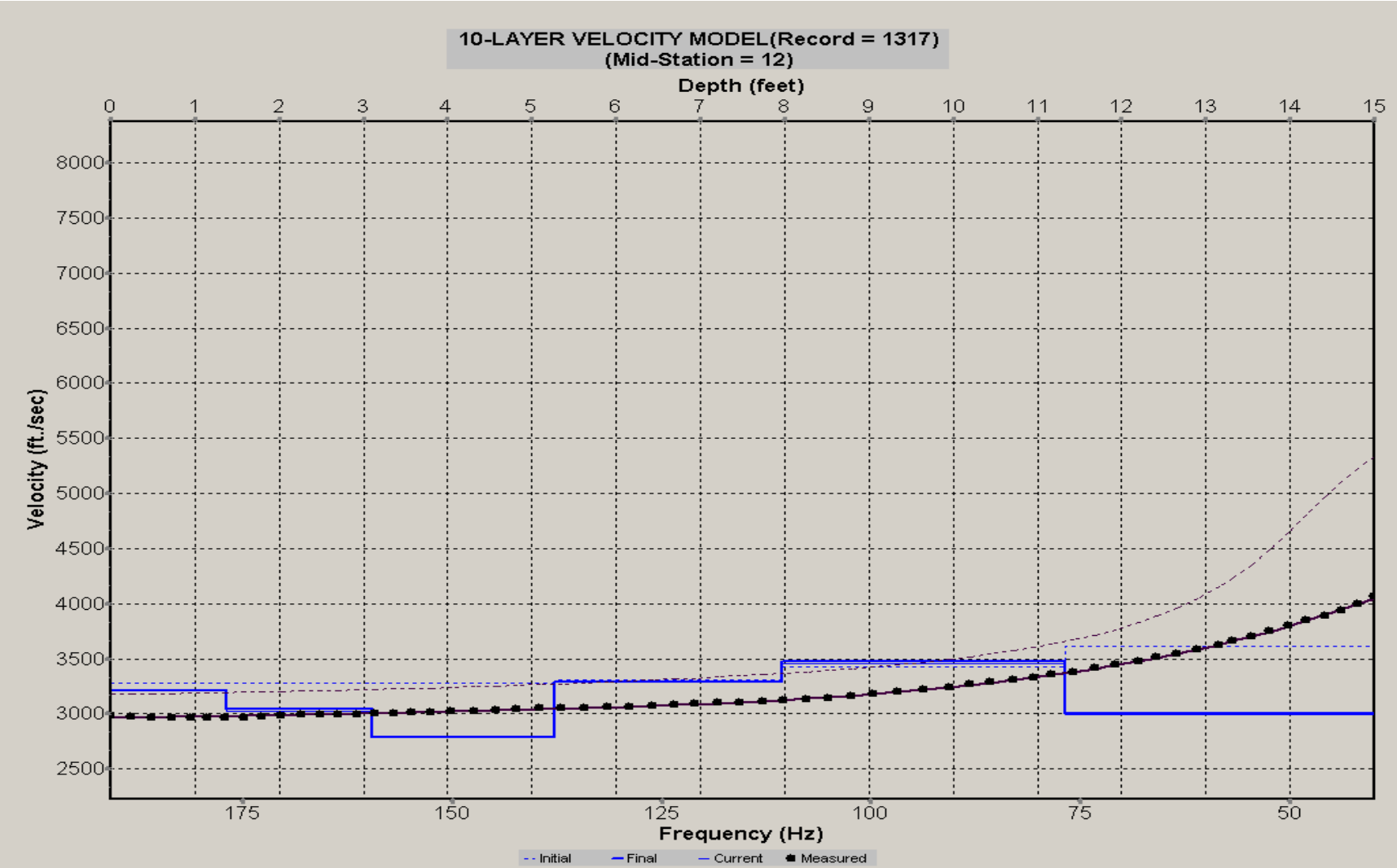

A.495: Velocity Profile Line 1317 used in Pre-blast 13, Post-blast 28 and Pre-blast 32

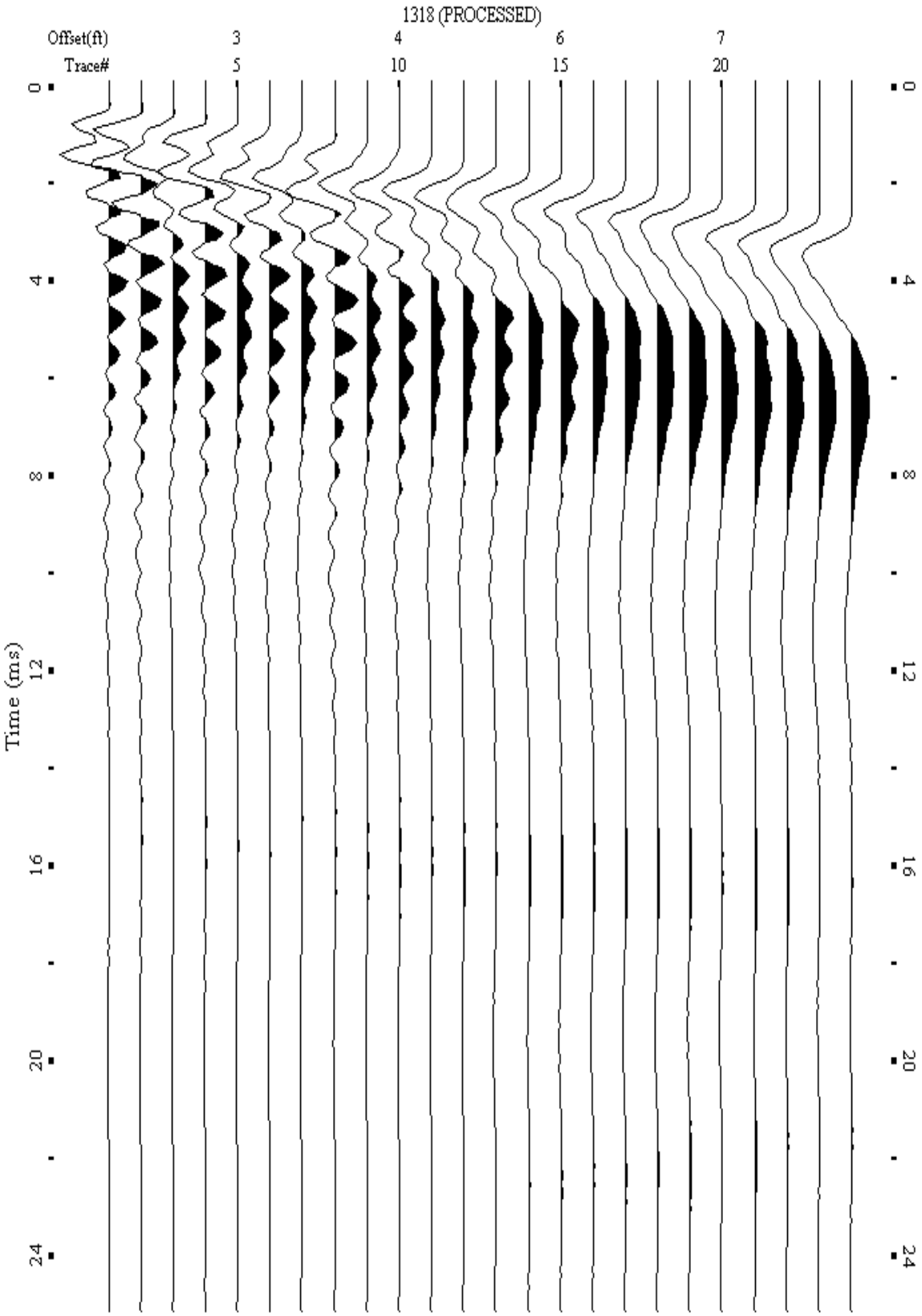

A.496: Shot Gather Line 1318 used in Pre-blast 33

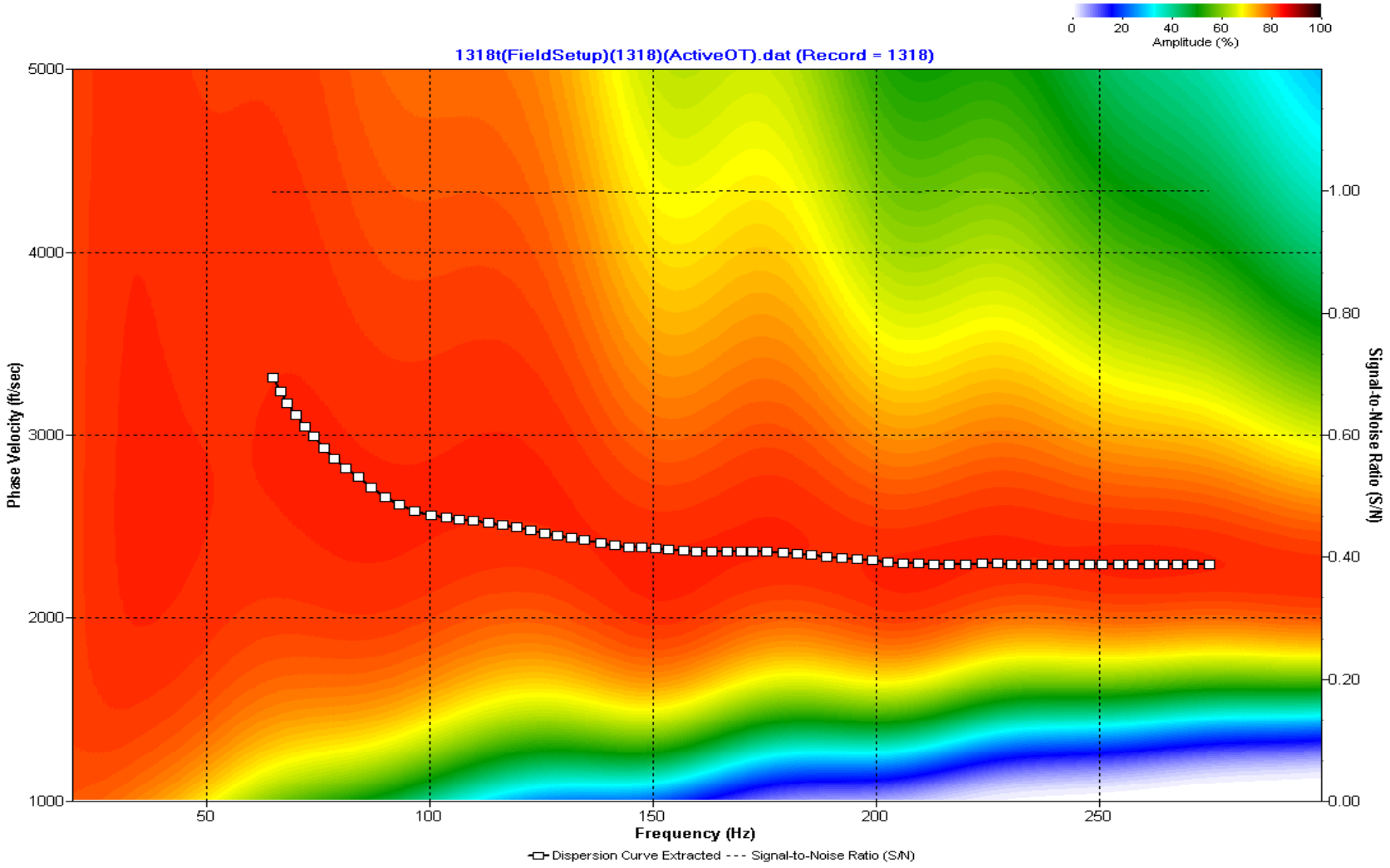

A.497: Dispersion Curve Line 1318 used in Pre-blast 33

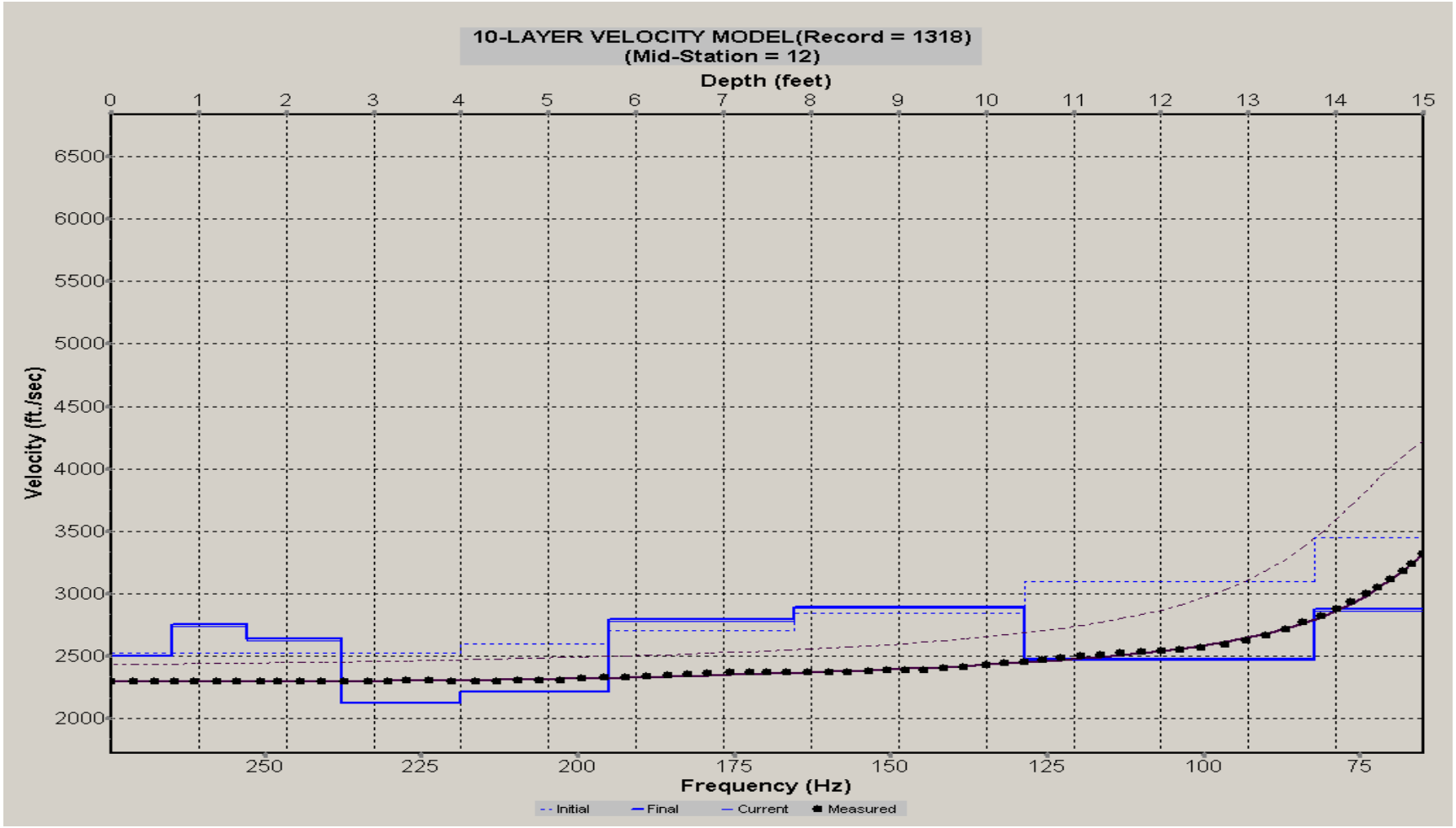

A.498: Velocity Profile Line 1318 used in Pre-blast 33

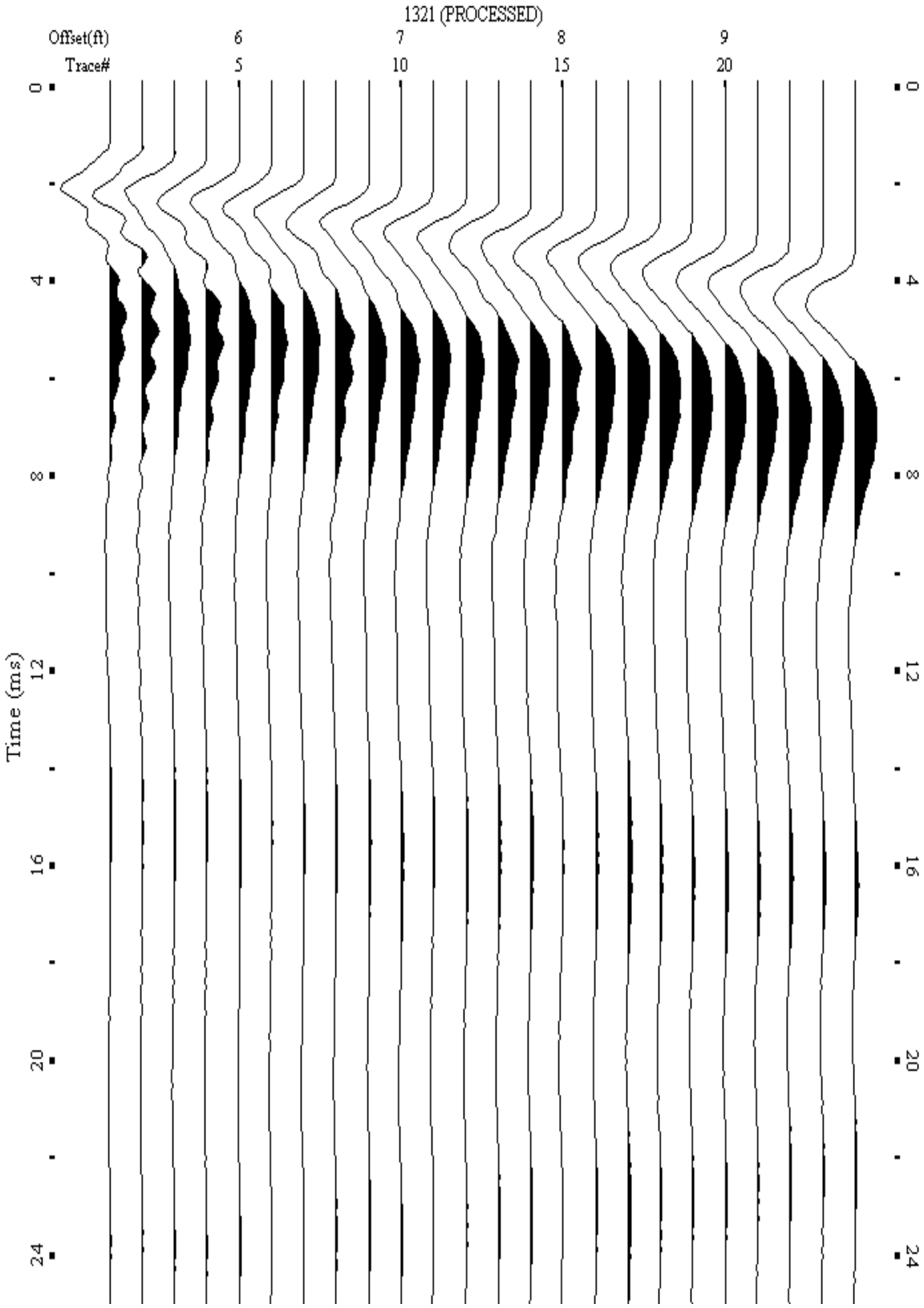

A.499: Shot Gather Line 1321 used in Pre-blast 33

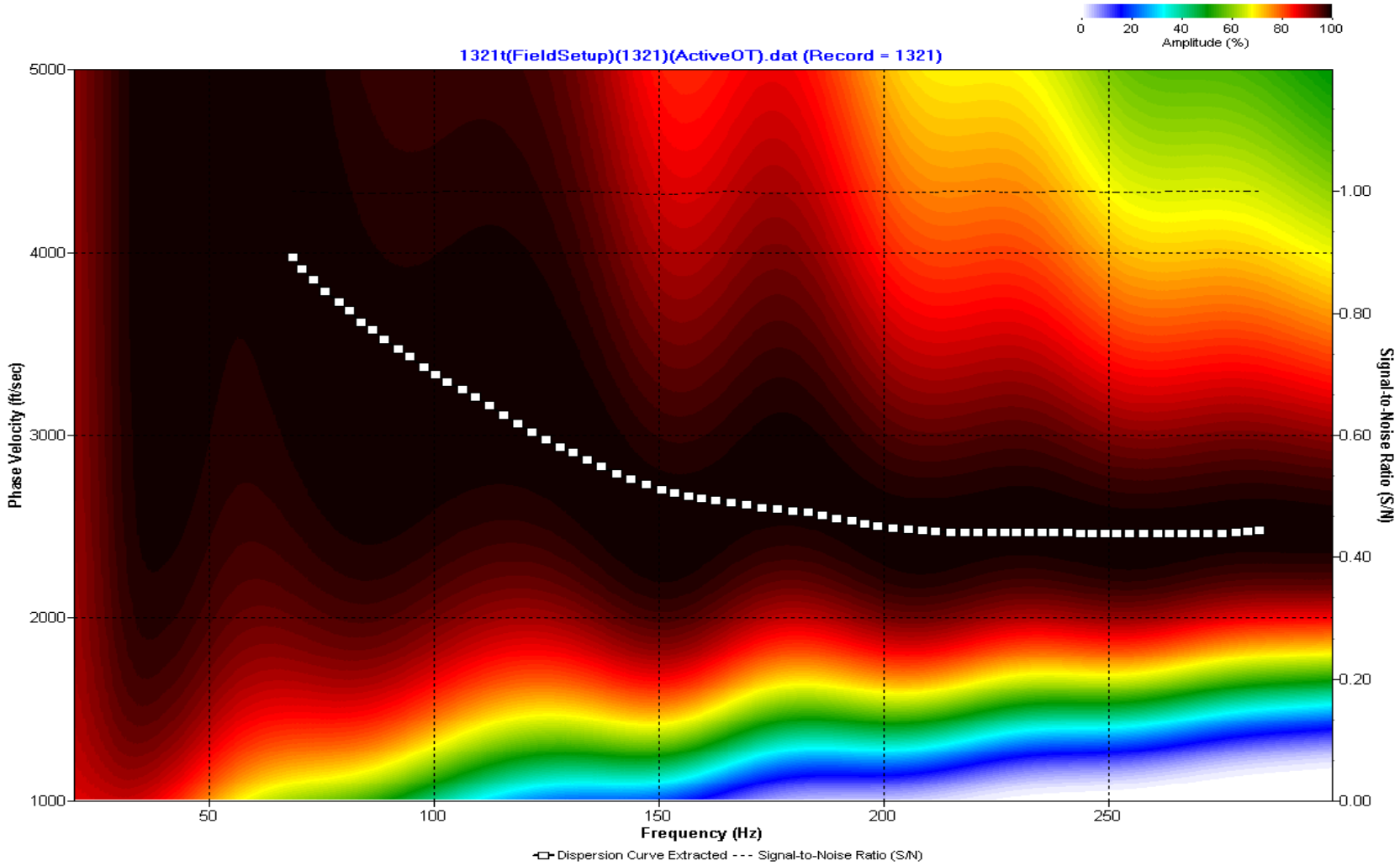

A.500: Dispersion Curve Line 1321 used in Pre-blast 33

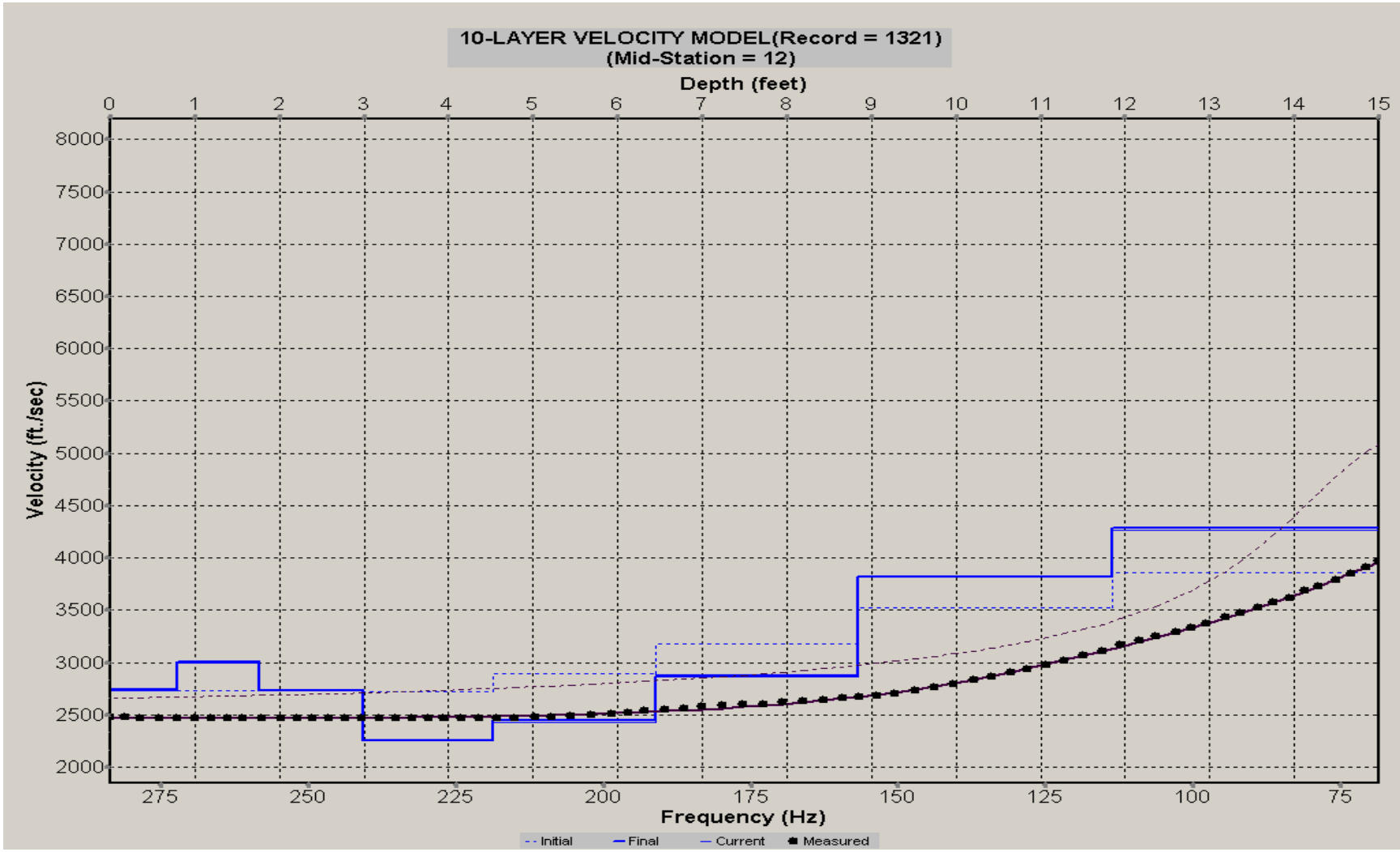

A.501: Velocity Profile Line 1321 used in Pre-blast 33

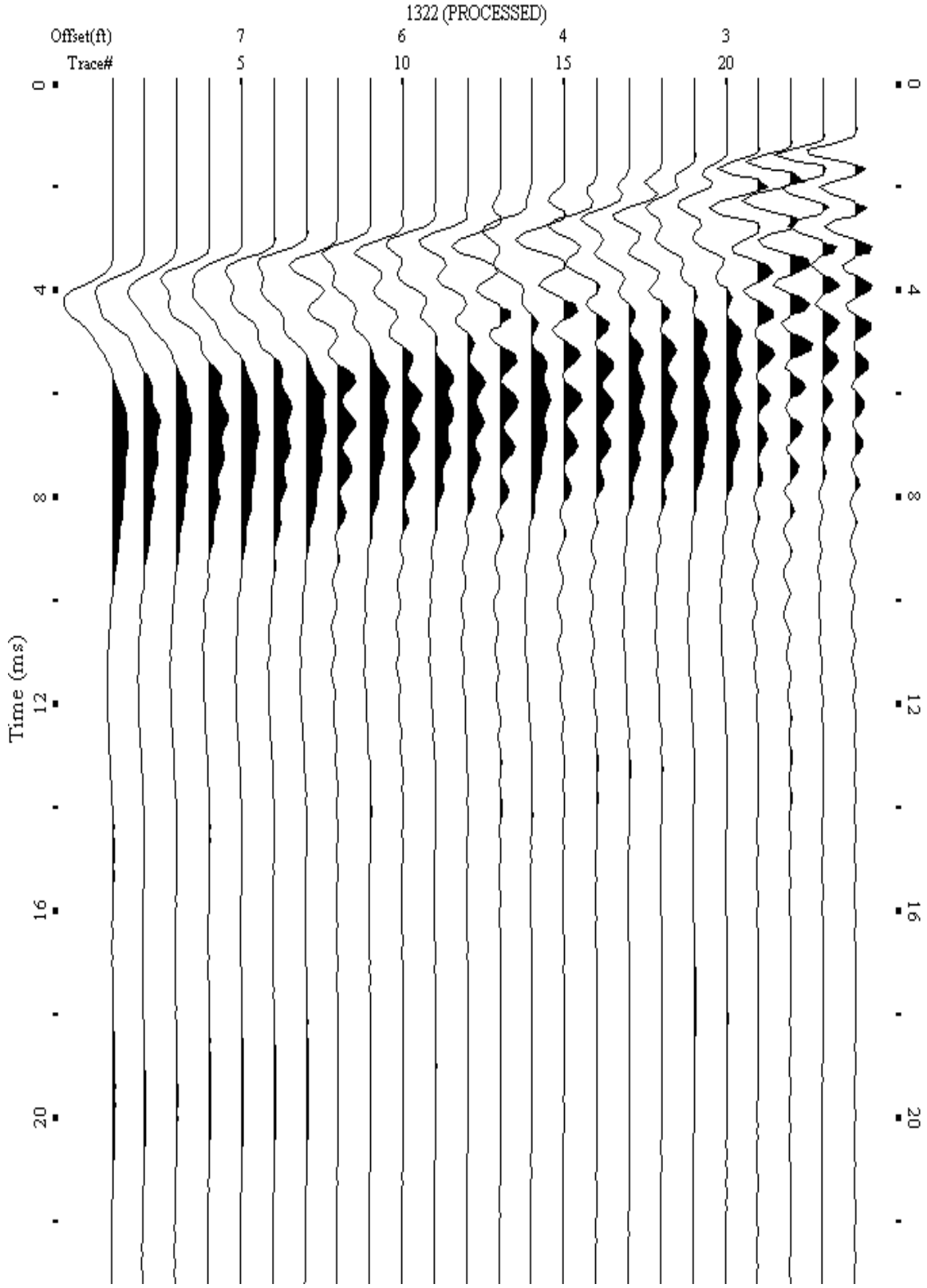

A.502: Shot Gather Line 1322 used in Post-blast 29 and Pre-blast 33

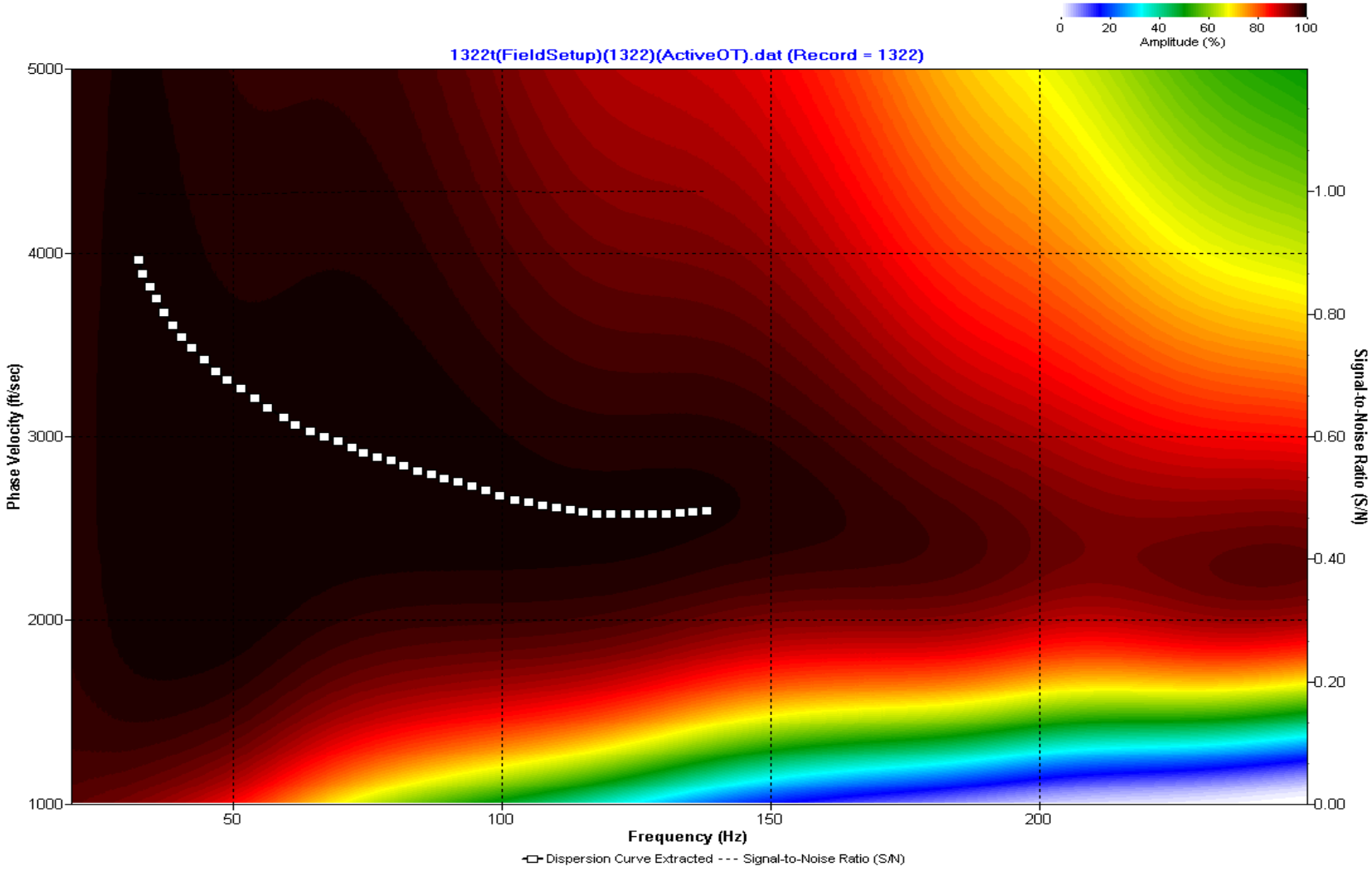

A.503: Dispersion Curve Line 1322 used in Post-blast 29 and Pre-blast 33

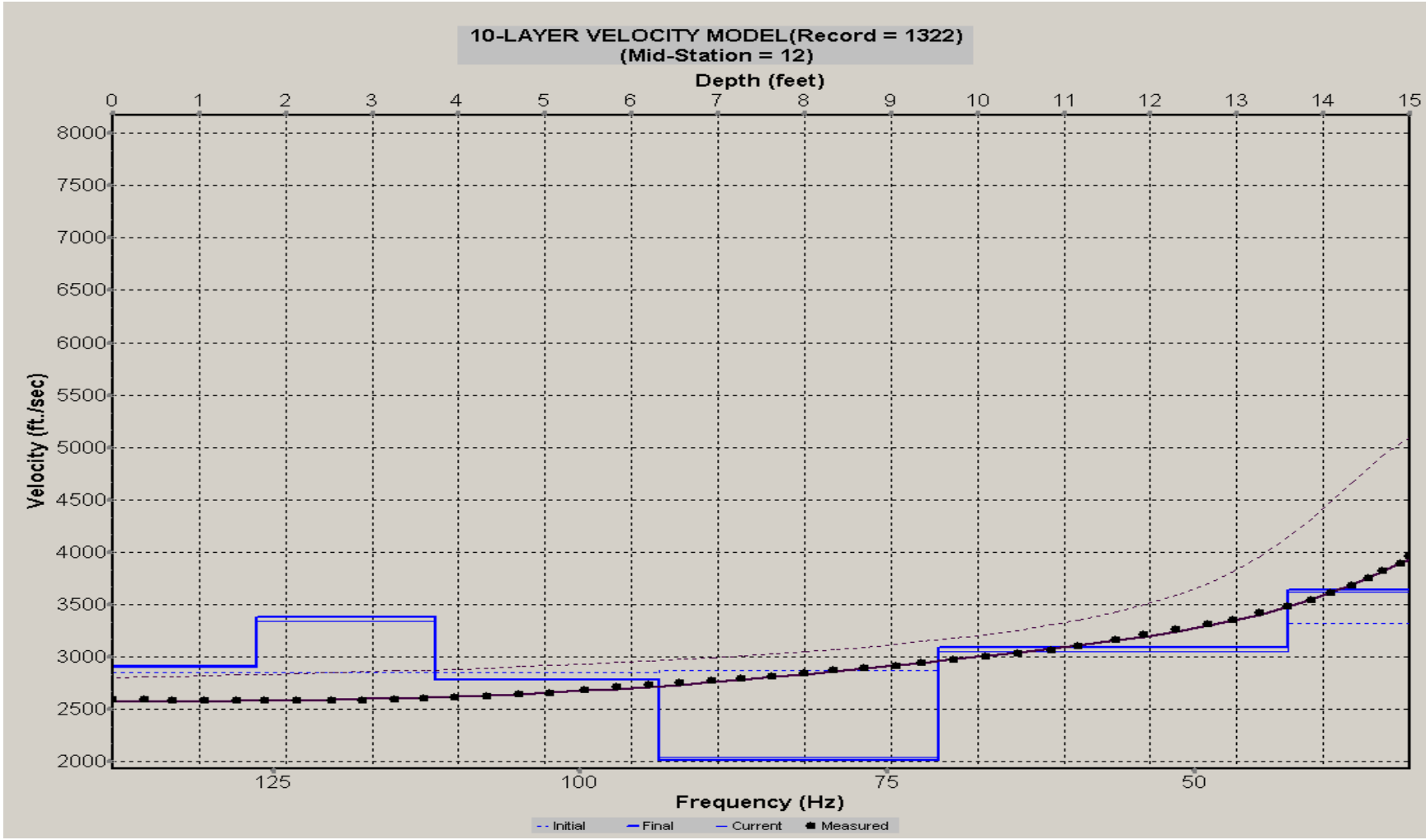

A.504: Velocity Profile Line 1322 used in Post-blast 29 and Pre-blast 33

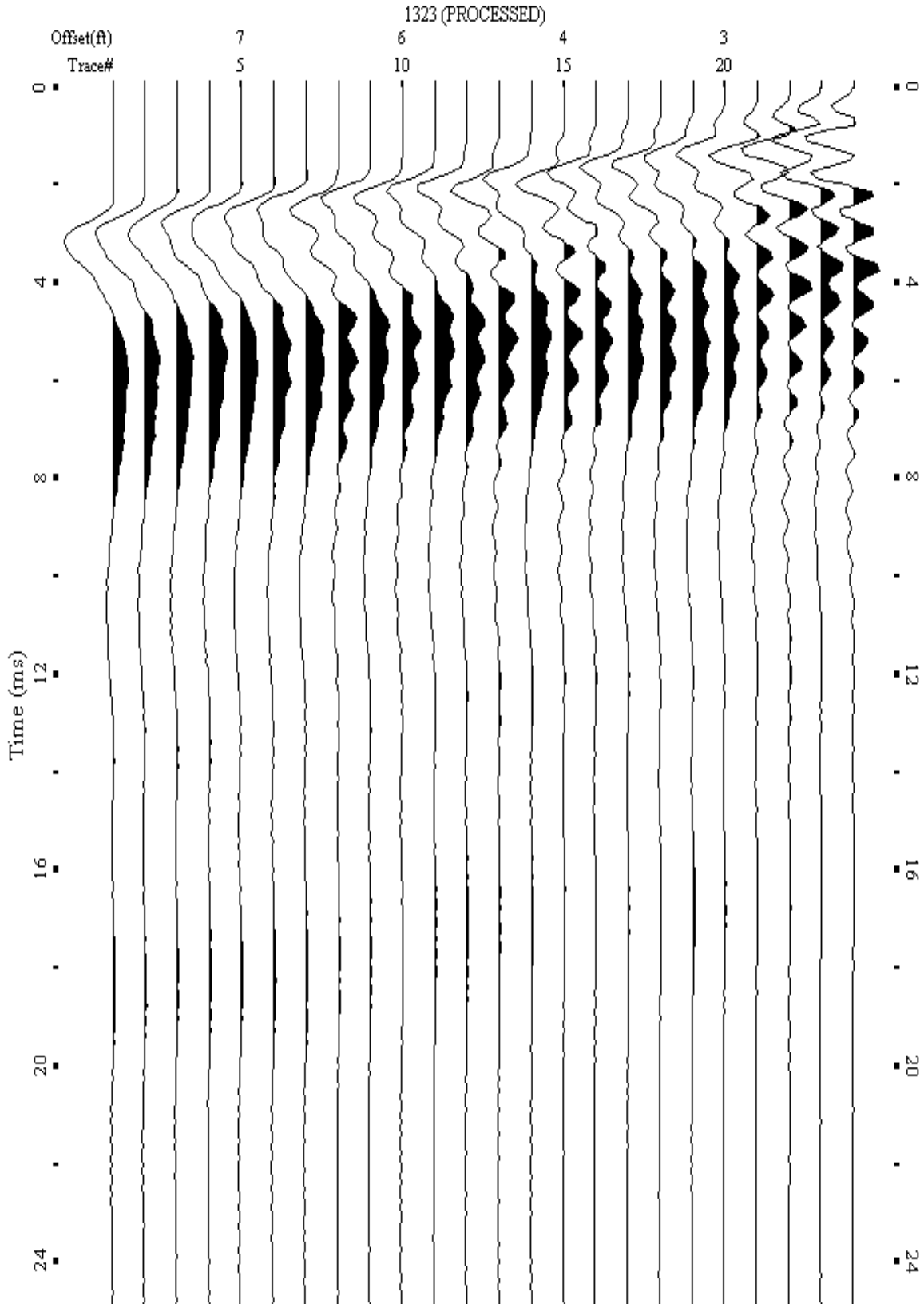

A.505: Shot Gather Line 1323 used in Post-blast 29 and Pre-blast 33

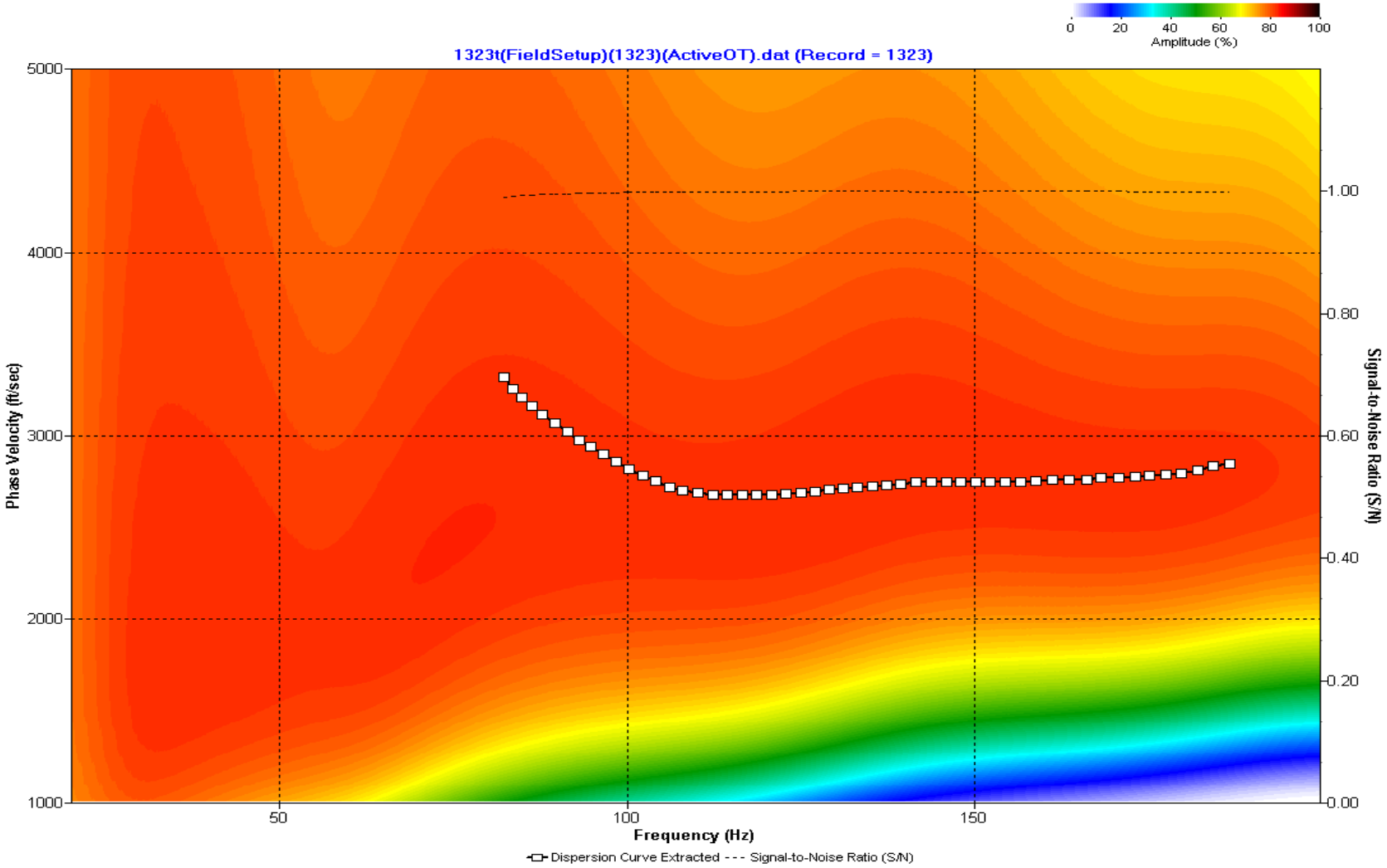

A.506: Dispersion Curve Line 1323 used in Post-blast 29 and Pre-blast 33

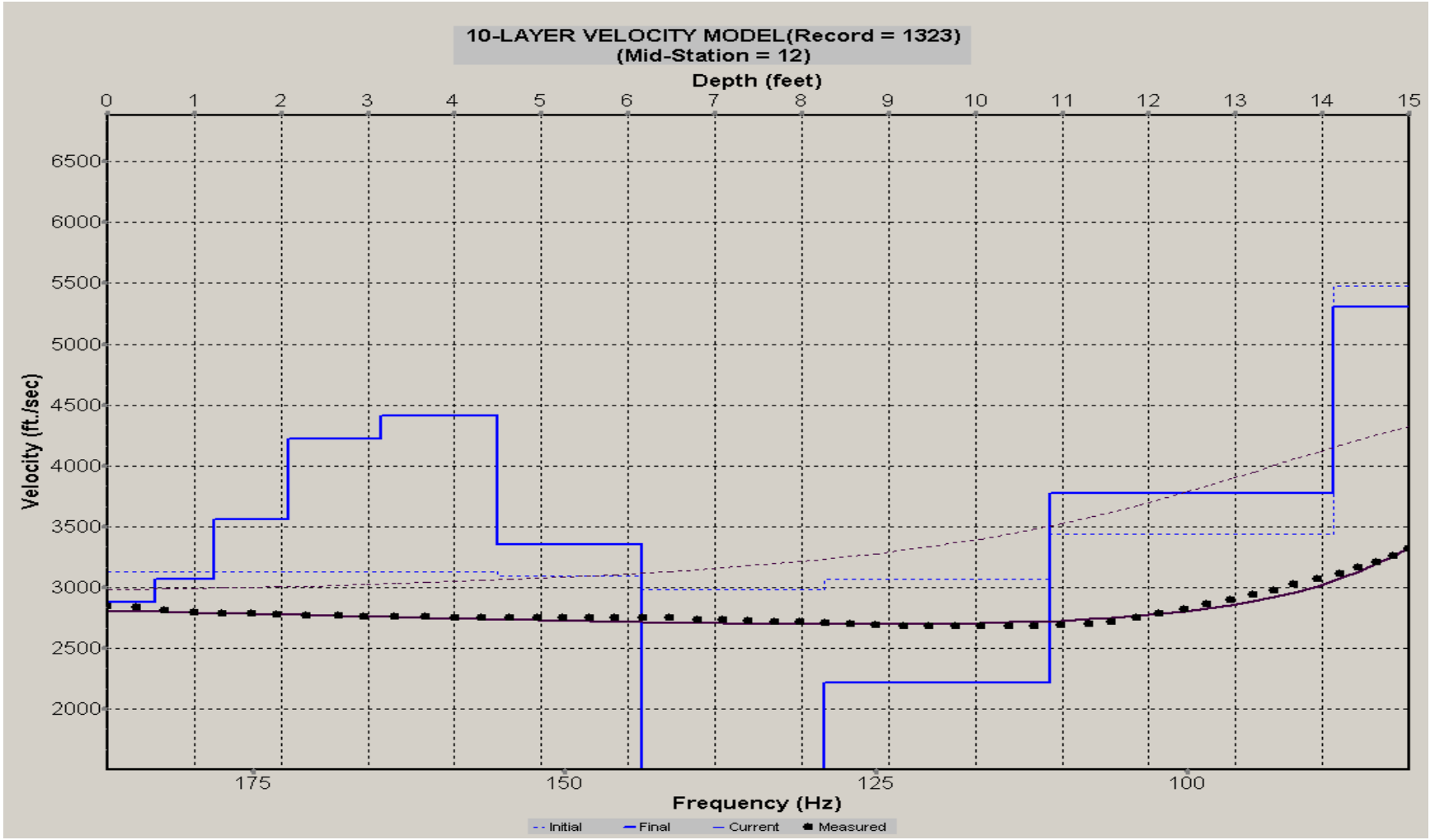

A.507: Velocity Profile Line 1323 used in Post-blast 29 and Pre-blast 33

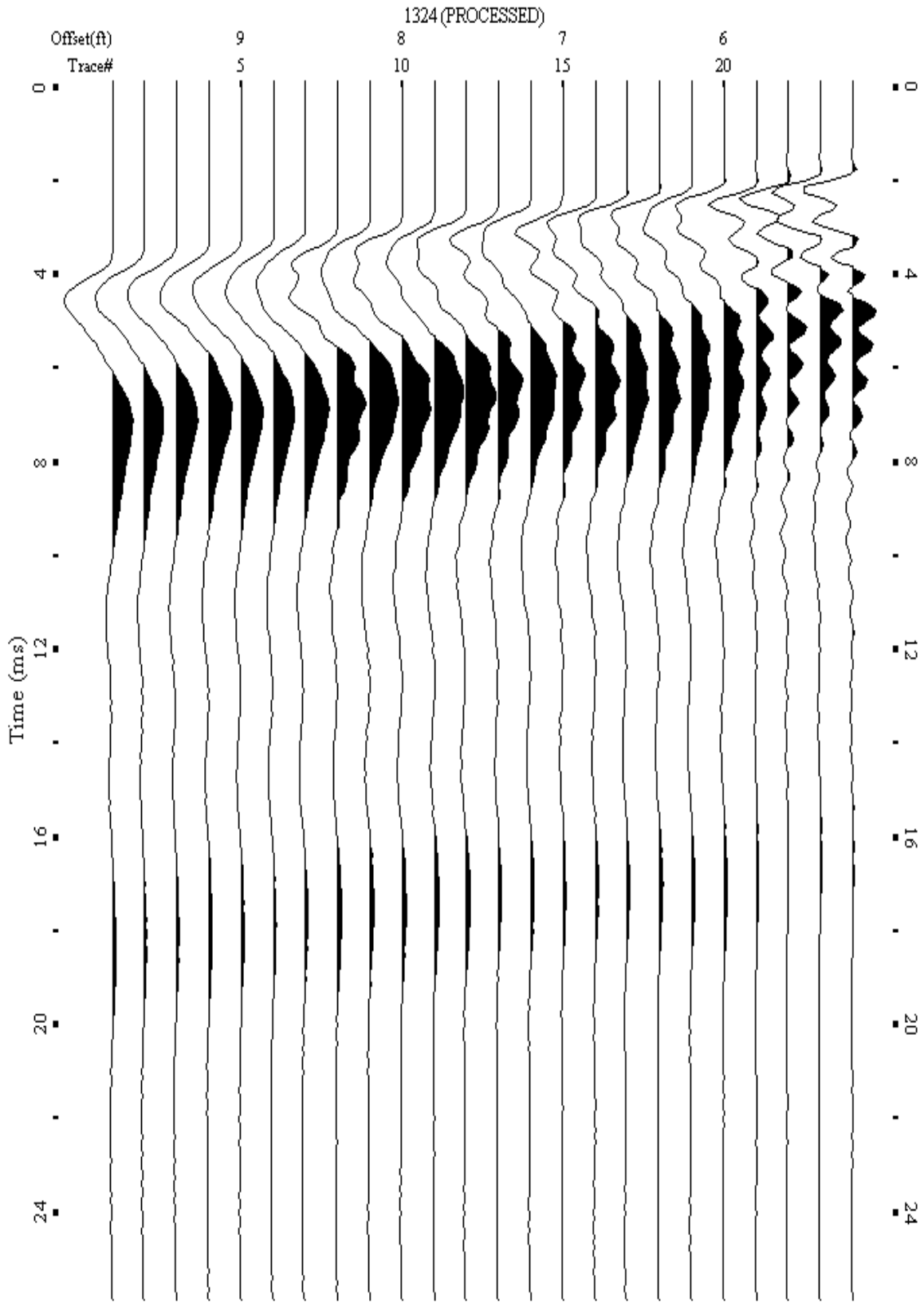

A.508: Shot Gather Line 1324 used in Post-blast 29 and Pre-blast 33

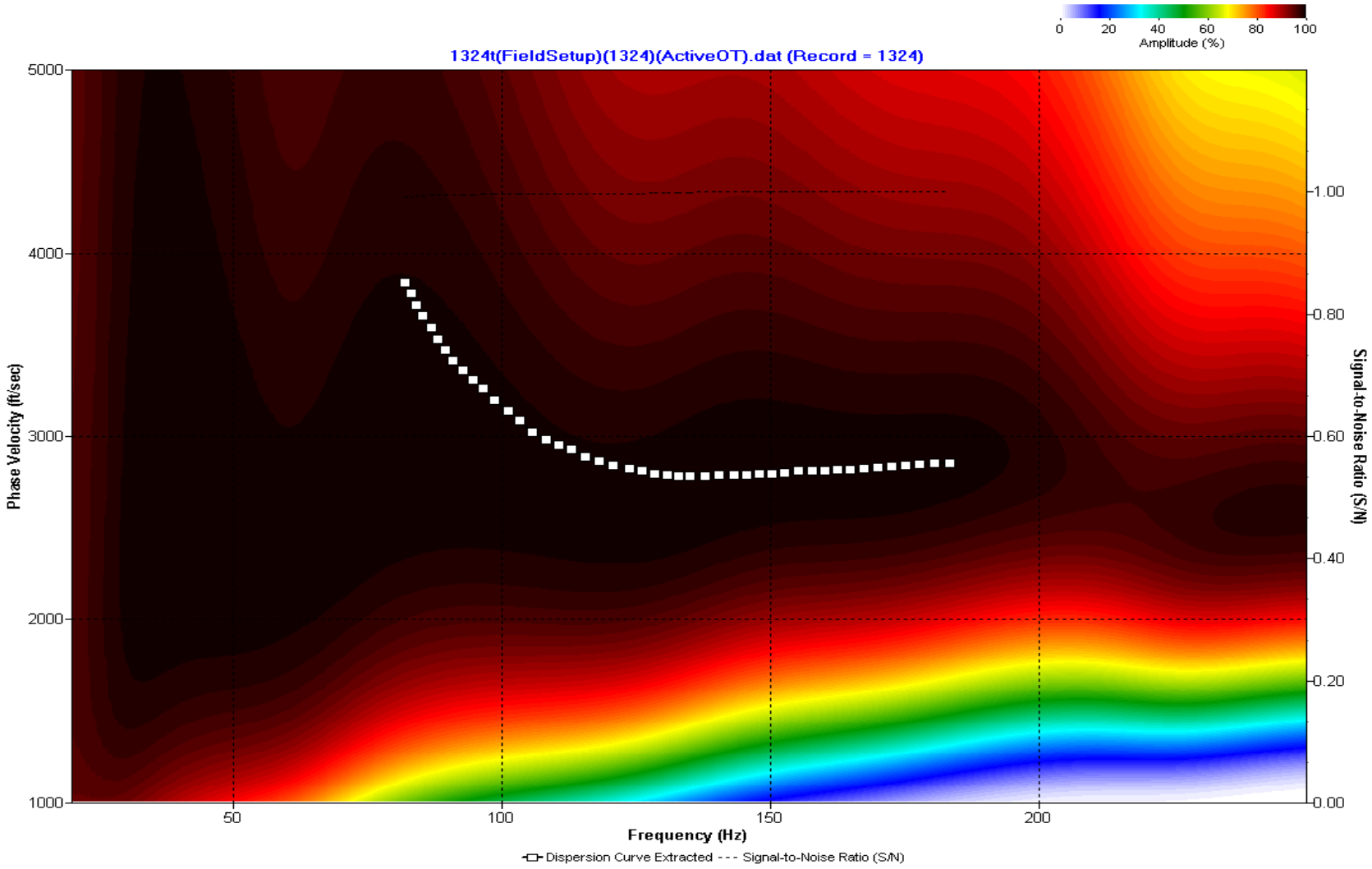

A.509: Dispersion Curve Line 1324 used in Post-blast 29 and Pre-blast 33

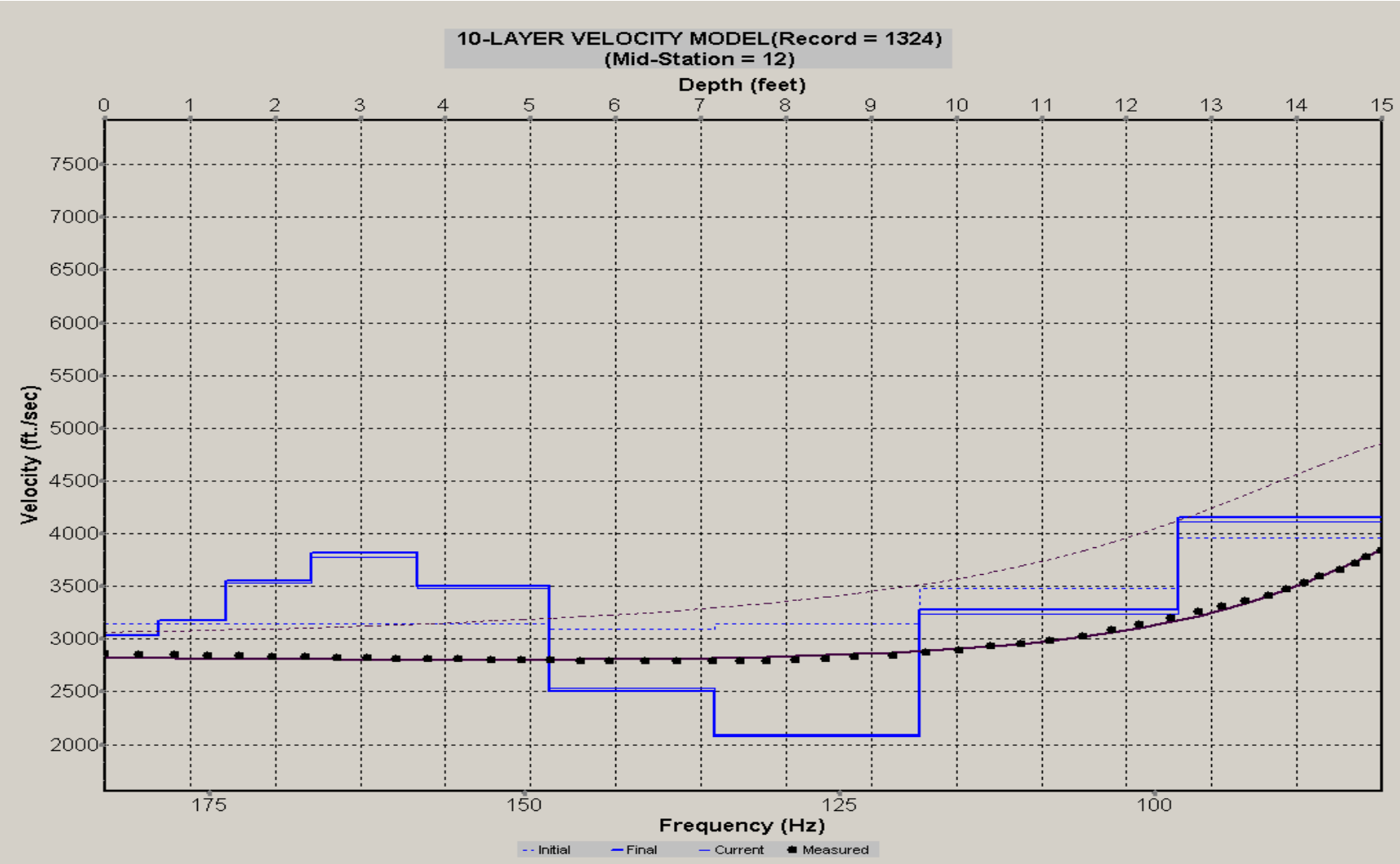

A.510: Velocity Profile Line 1324 used in Post-blast 29 and Pre-blast 33

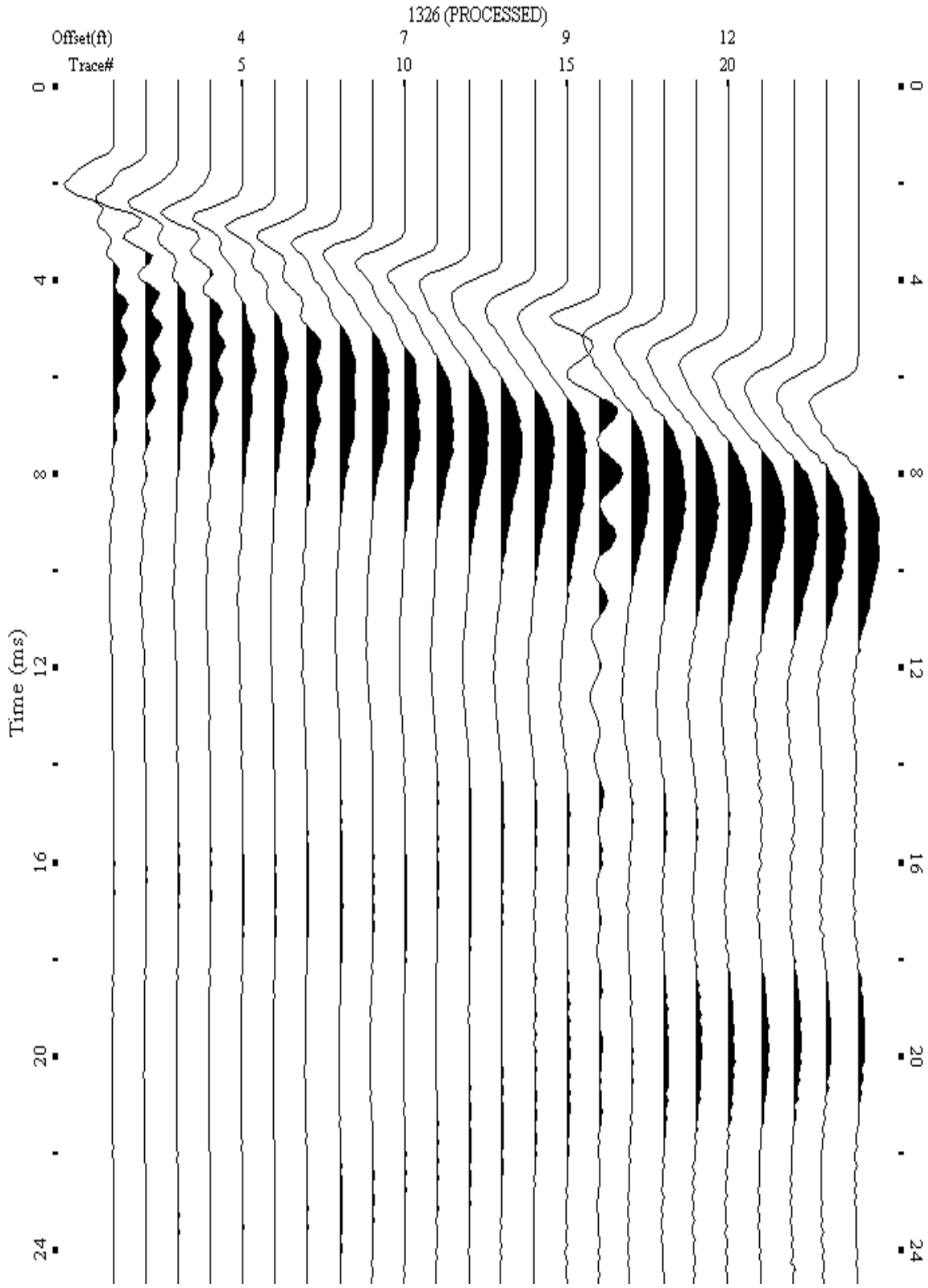

A.511: Shot Gather Line 1326 used in Pre-blast 13, Post-blast 28, Post-blast 29, Pre-blast 32, and Pre-blast 33

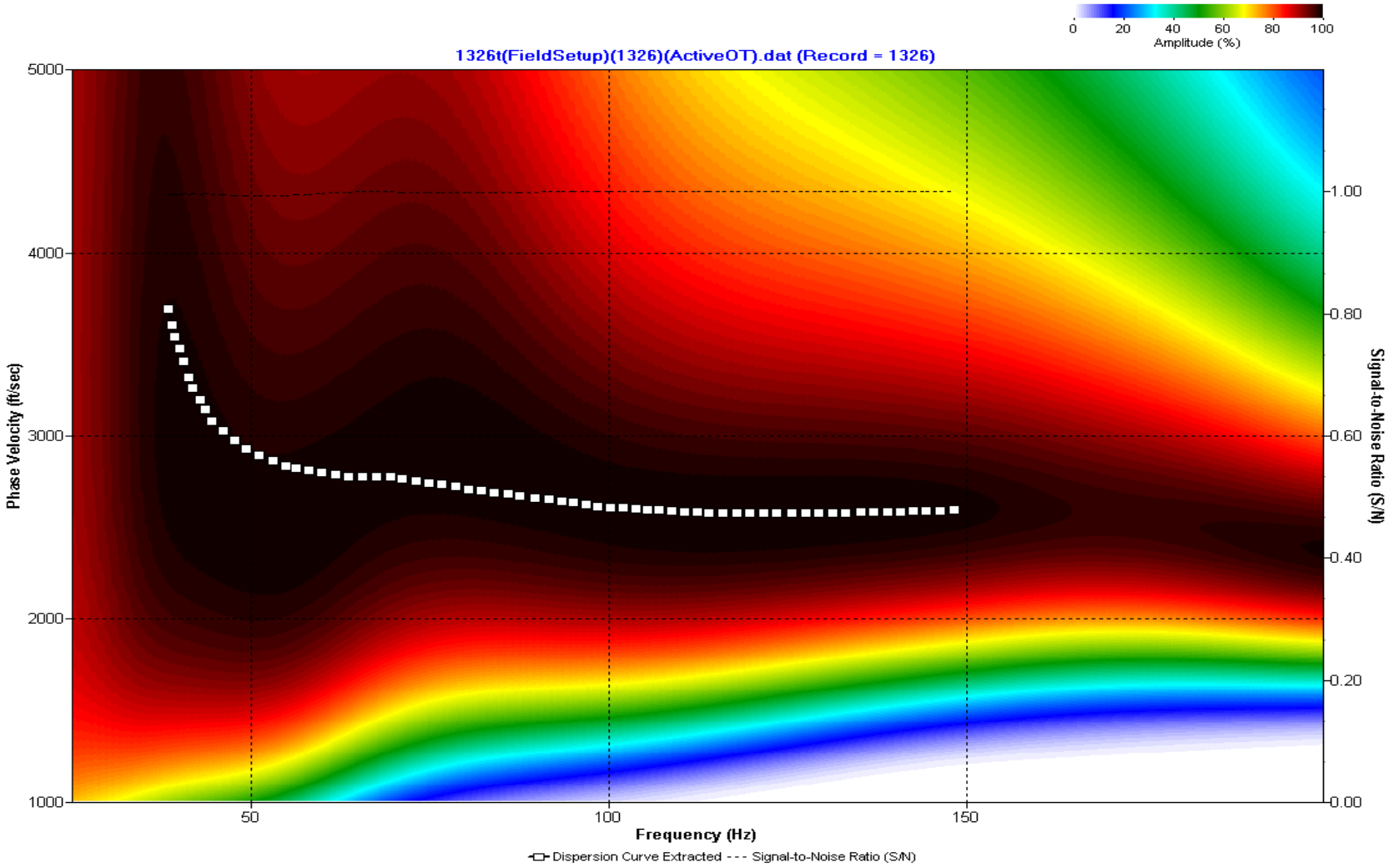

A.512: Dispersion Curve Line 1326 used in Pre-blast 13, Post-blast 28, Post-blast 29, Pre-blast 32, and Pre-blast 33

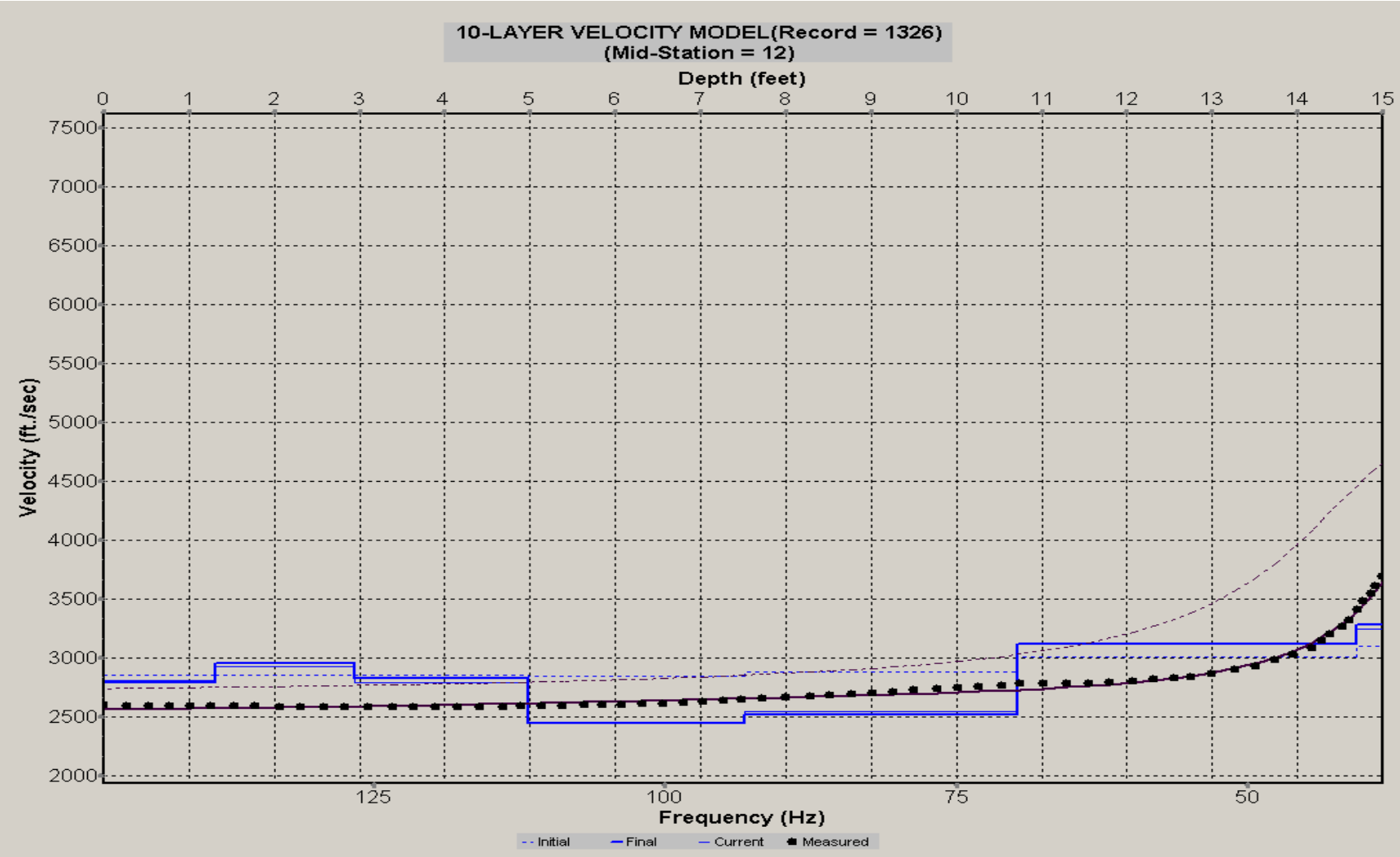

A.513: Velocity Profile Line 1326 used in Pre-blast 13, Post-blast 28, Post-blast 29, Pre-blast 32, and Pre-blast 33

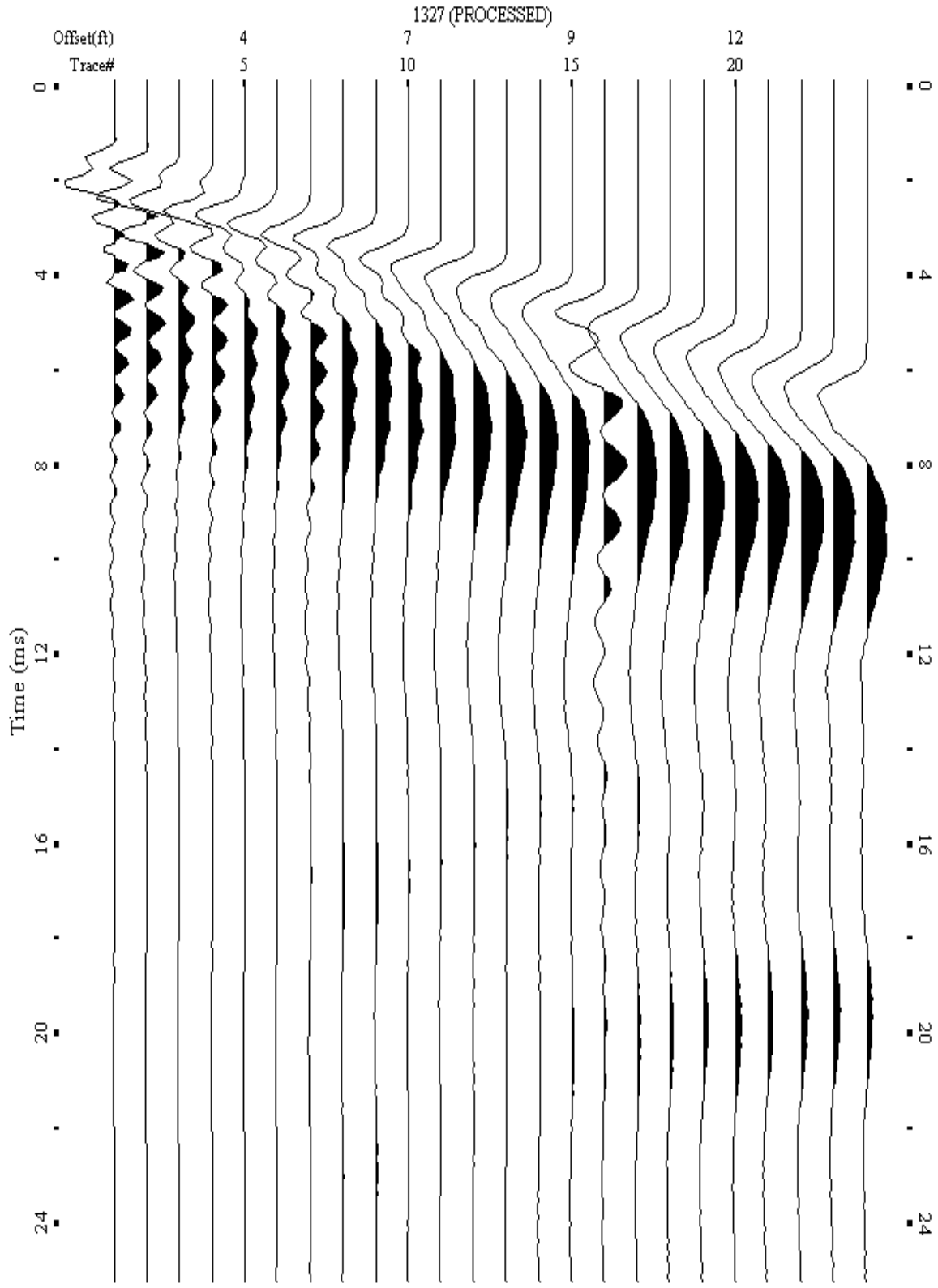

A.514: Shot Gather Line 1327 used in Pre-blast 13, Post-blast 29, Pre-blast 32, and Pre-blast 33

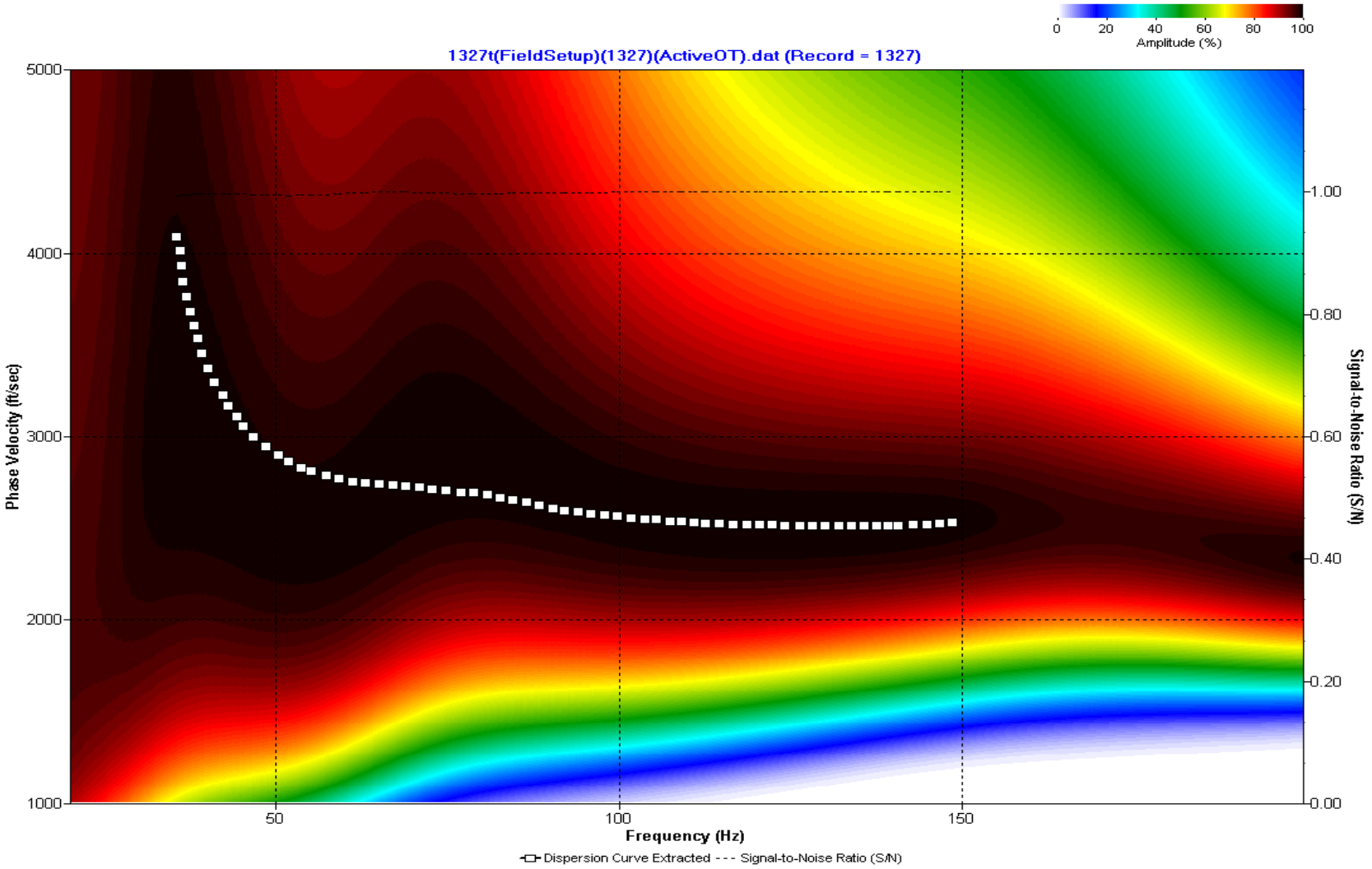

A.515: Dispersion Curve Line 1327 used in Pre-blast 13, Post-blast 29, Pre-blast 32, and Pre-blast 33

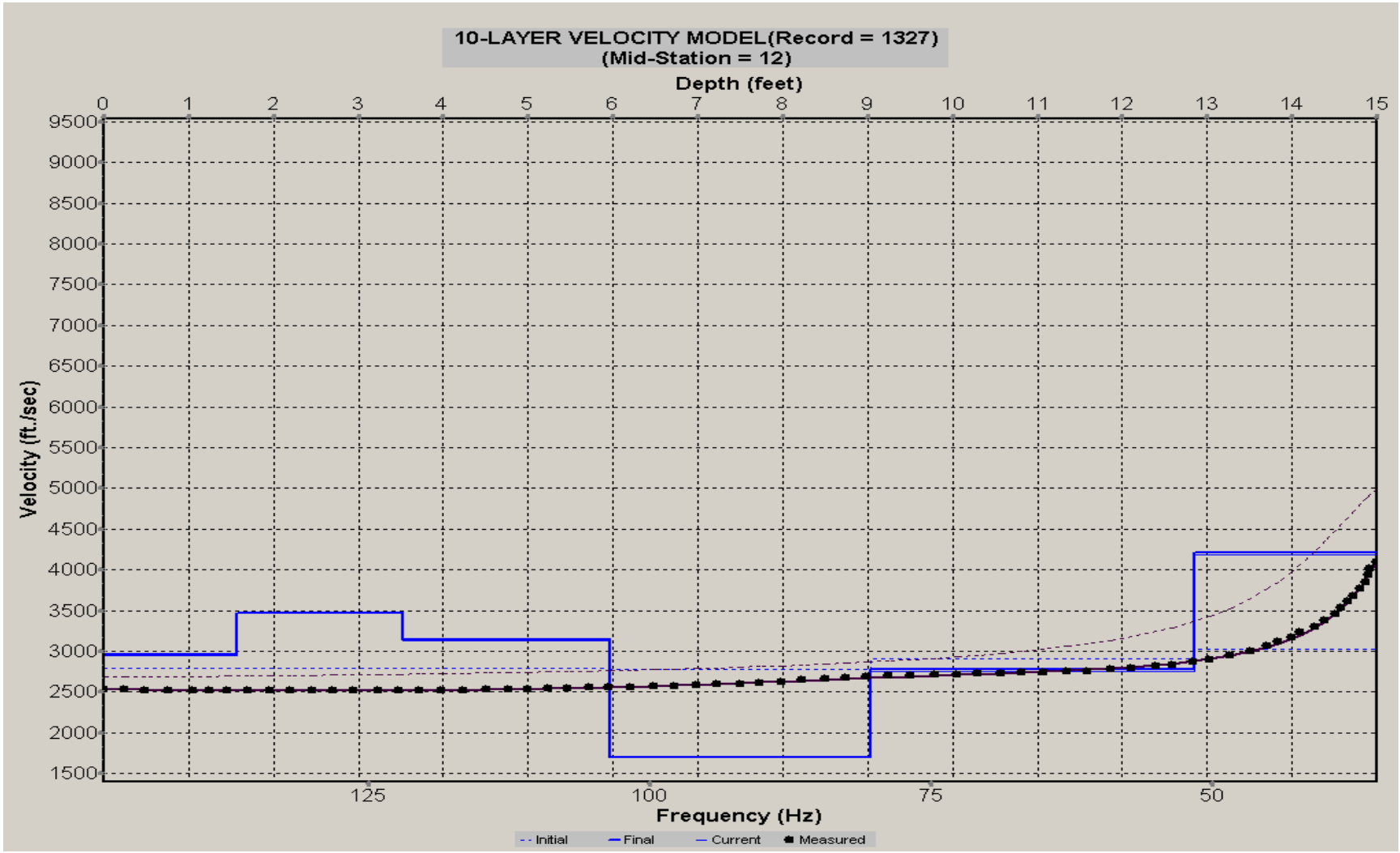

A.516: Velocity Profile Line 1327 used in Pre-blast 13, Post-blast 29, Pre-blast 32, and Pre-blast 33

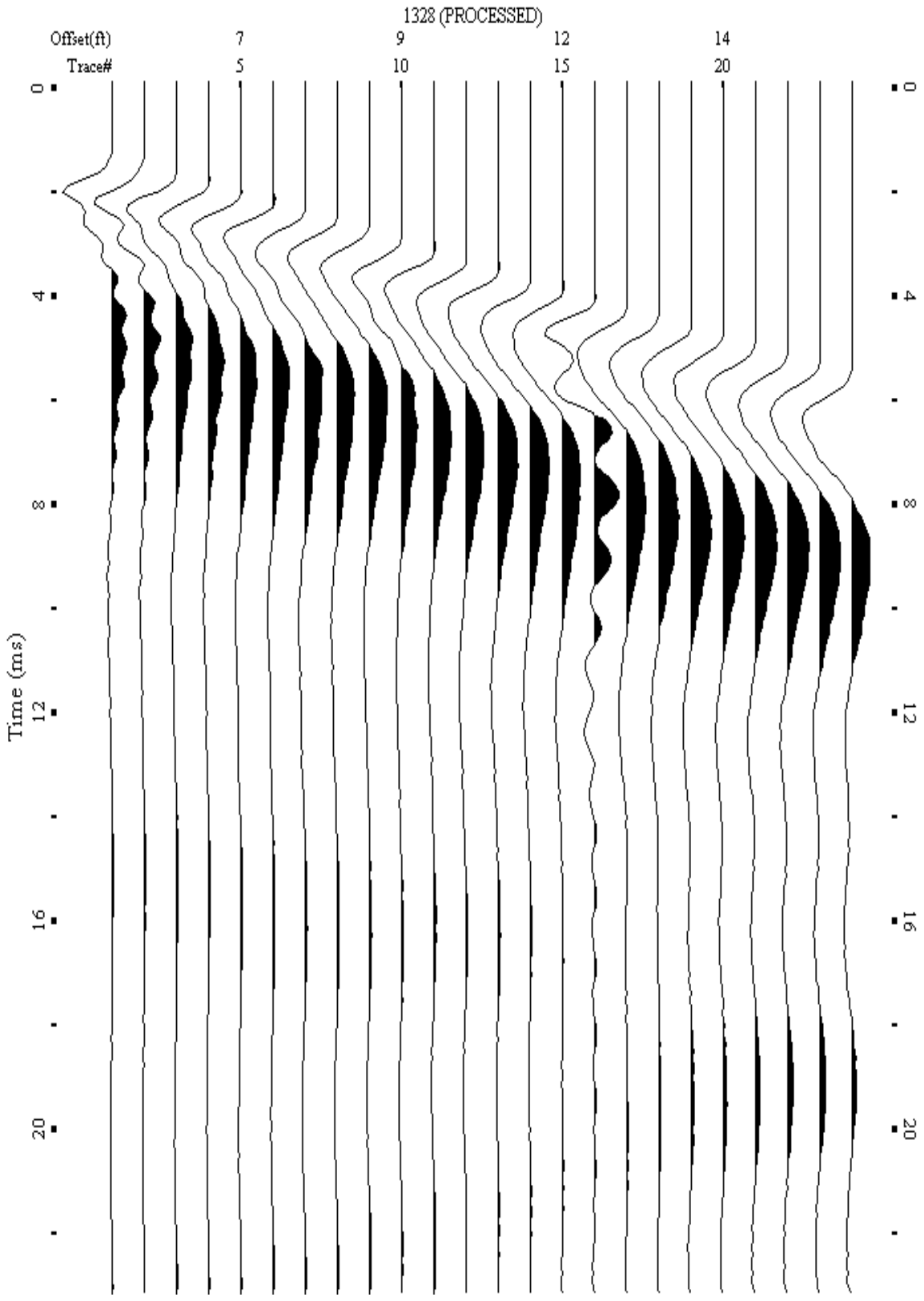

A.517: Shot Gather Line 1328 used in Pre-blast 13, Post-blast 28, Post-blast 29, Pre-blast 32, and Pre-blast 33

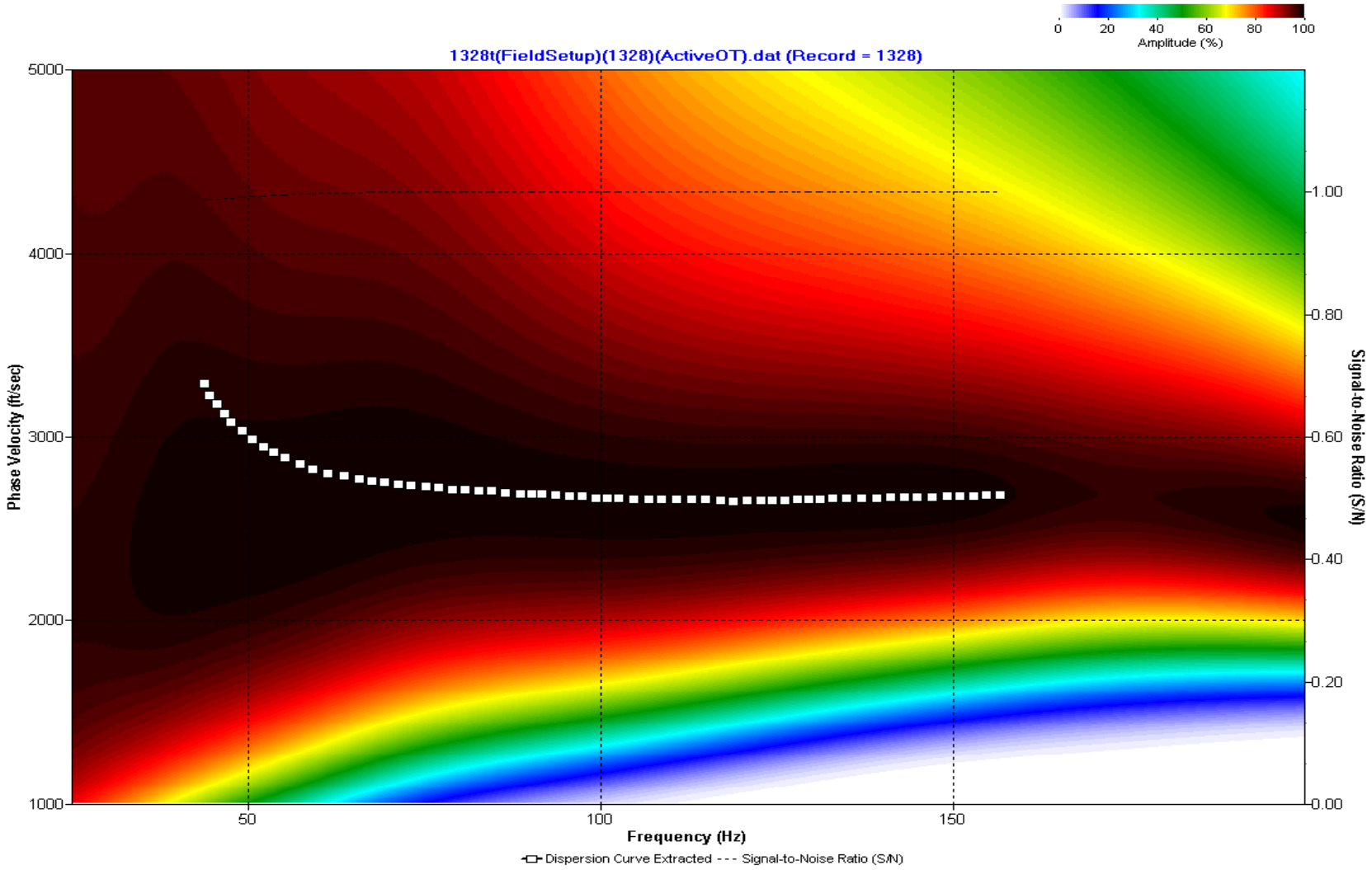

A.518: Dispersion Curve Line 1328 used in Pre-blast 13, Post-blast 28, Post-blast 29, Pre-blast 32, and Pre-blast 33

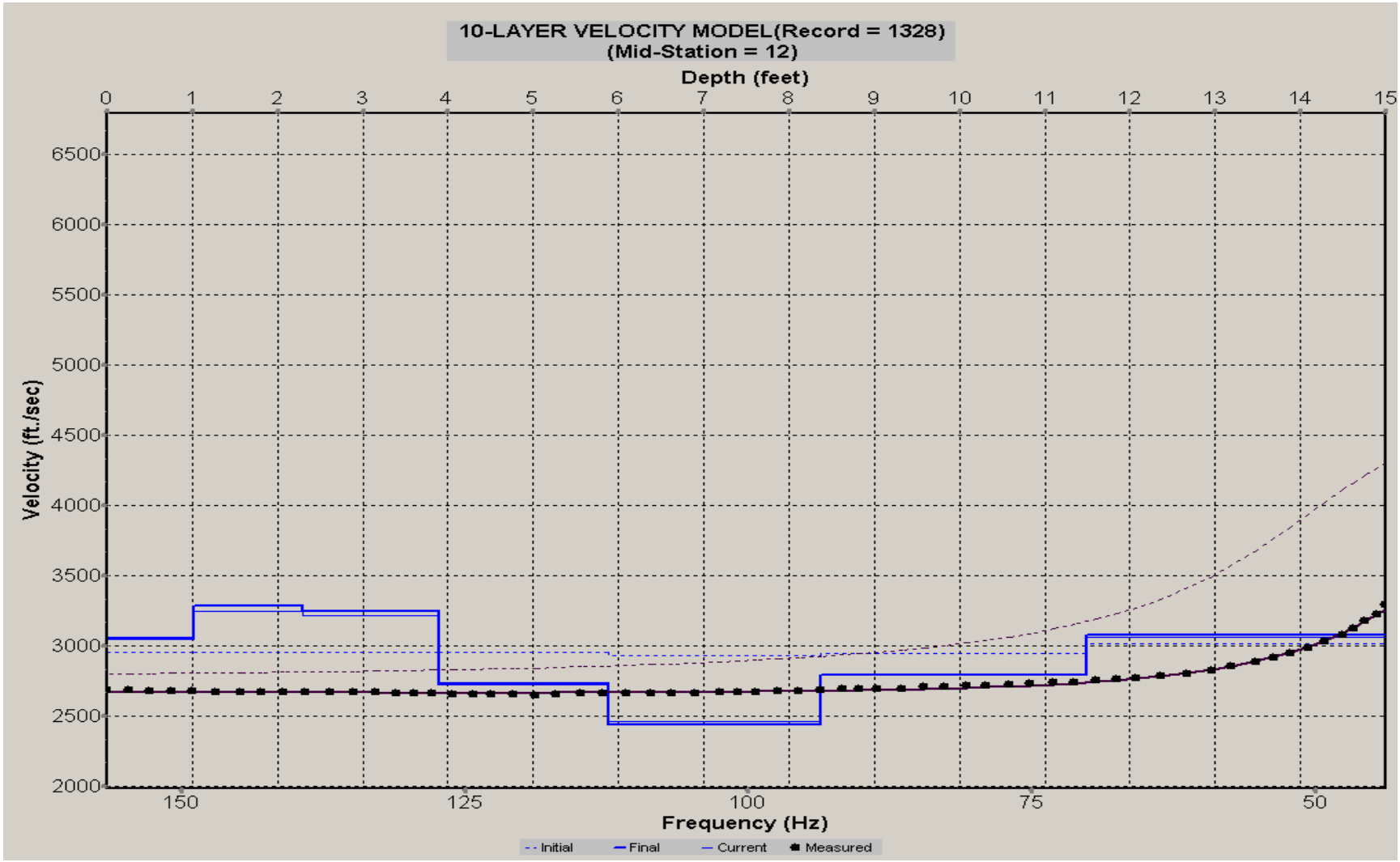

A.519: Velocity Profile Line 1328 used in Pre-blast 13, Post-blast 28, Post-blast 29, Pre-blast 32, and Pre-blast 33

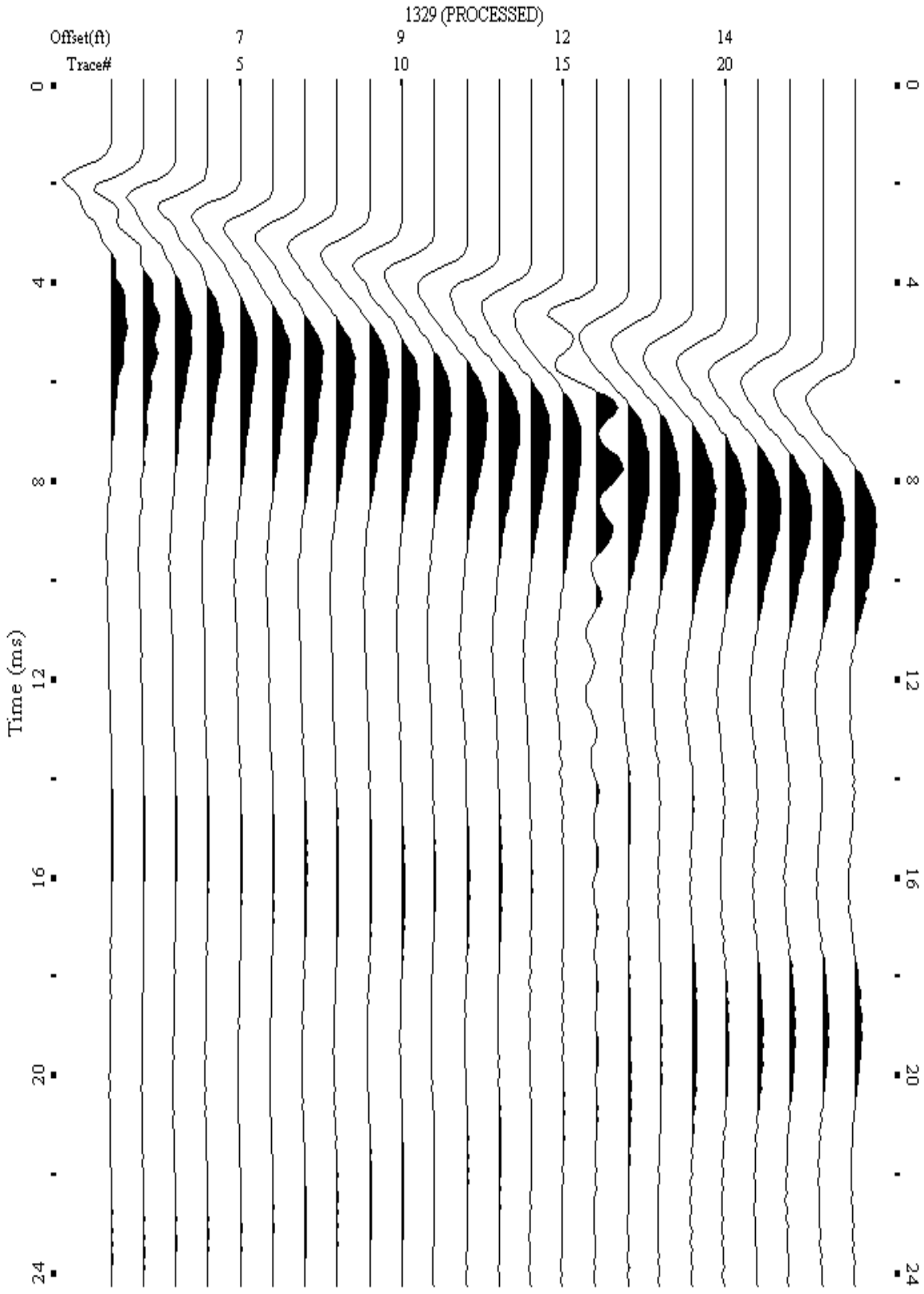

A.520: Shot Gather Line 1329 used in Post-blast 29

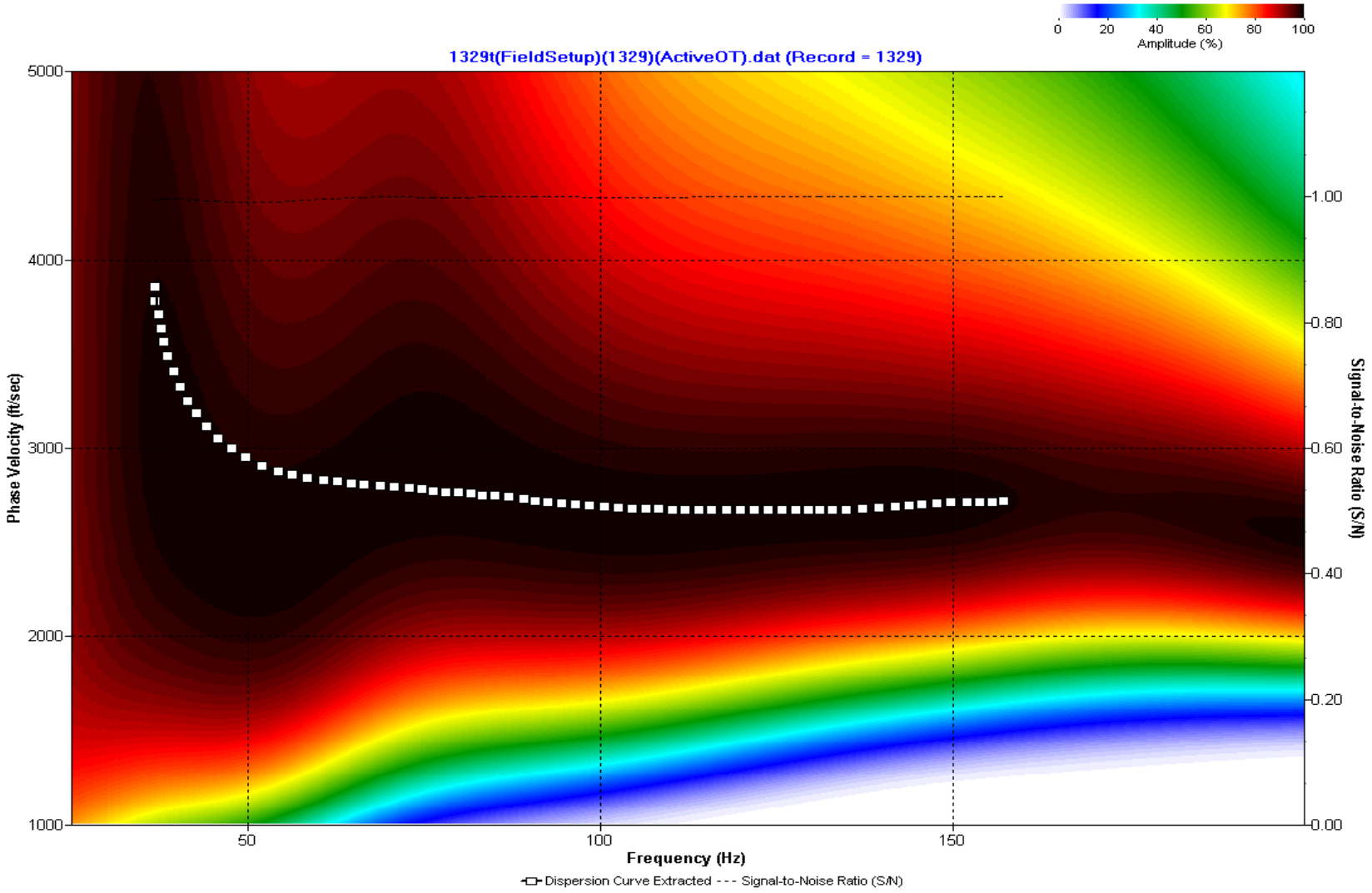

A.521: Dispersion Curve Line 1329 used in Post-blast 29

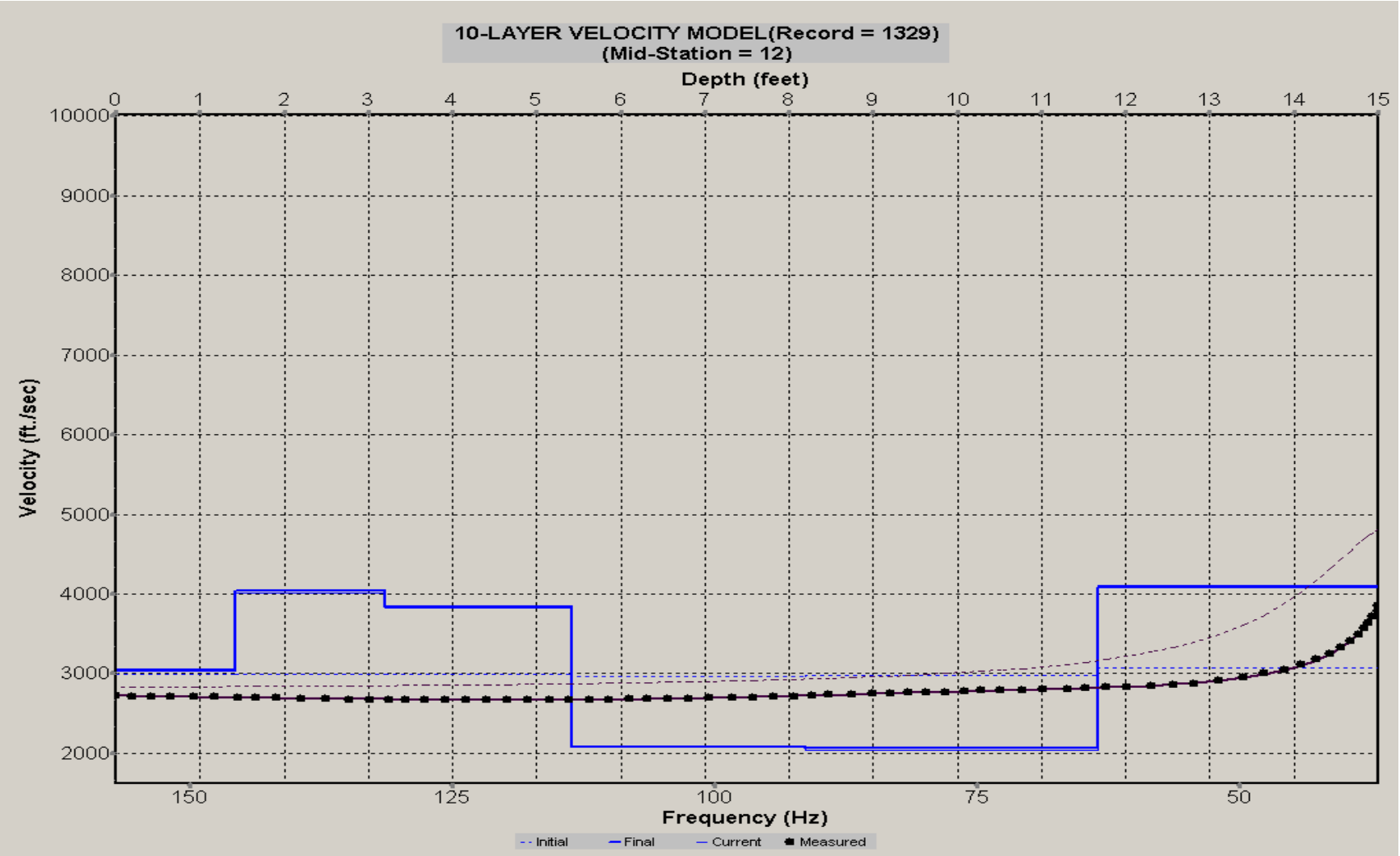

A.522: Velocity Profile Line 1329 used in Post-blast 29

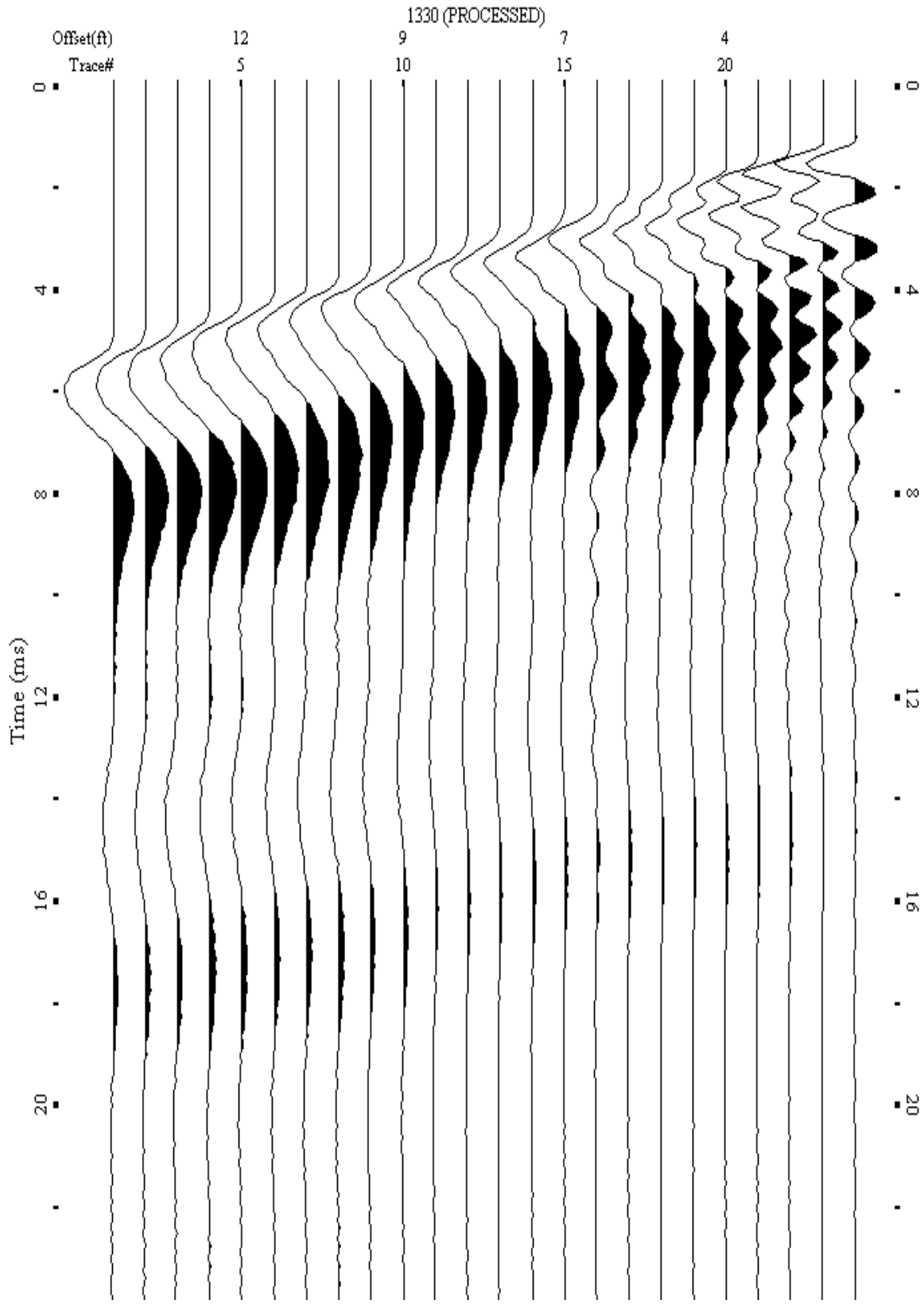

A.523: Shot Gather Line 1330 used in Post-blast 28

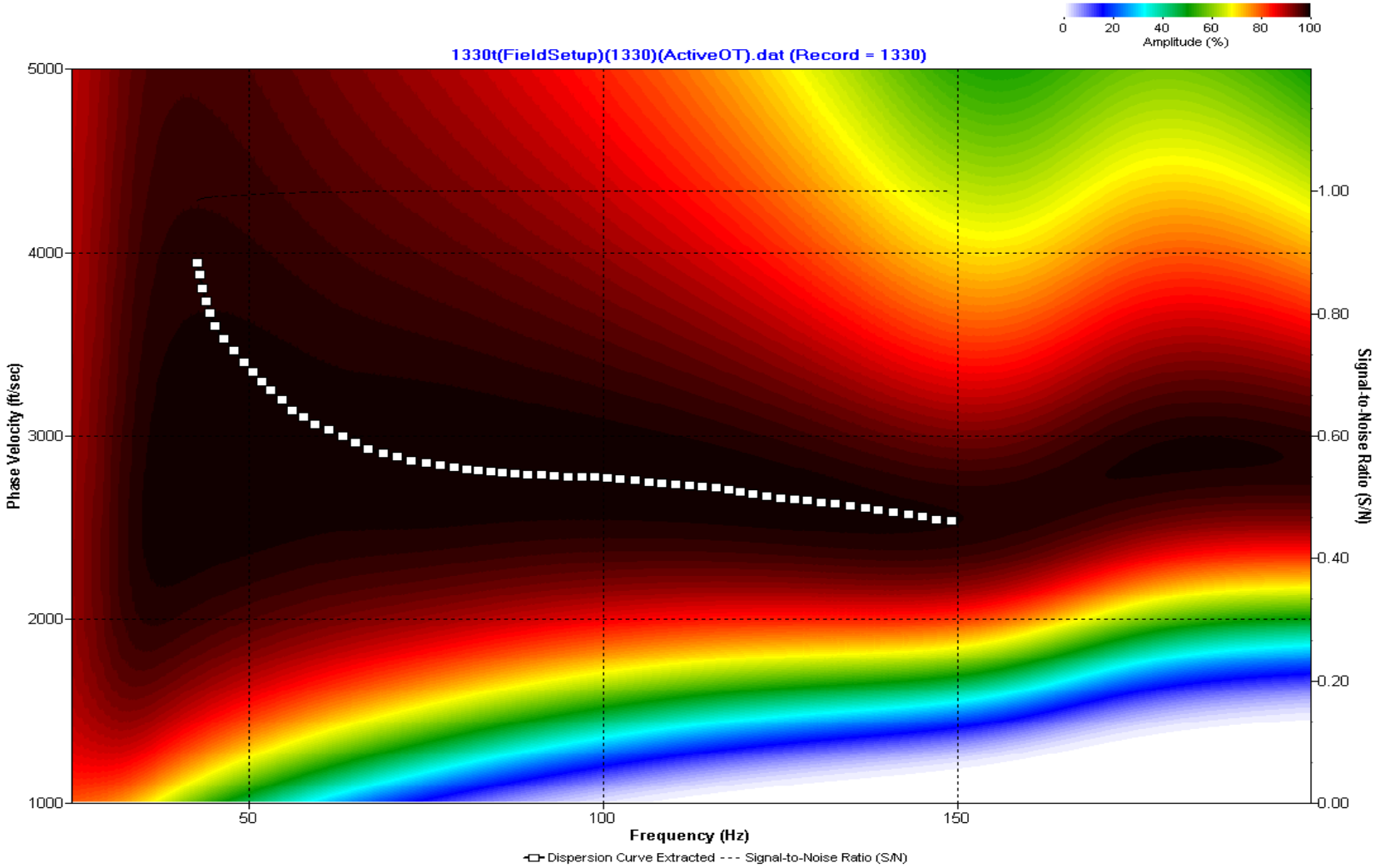

A.524: Dispersion Curve Line 1330 used in Post-blast 28

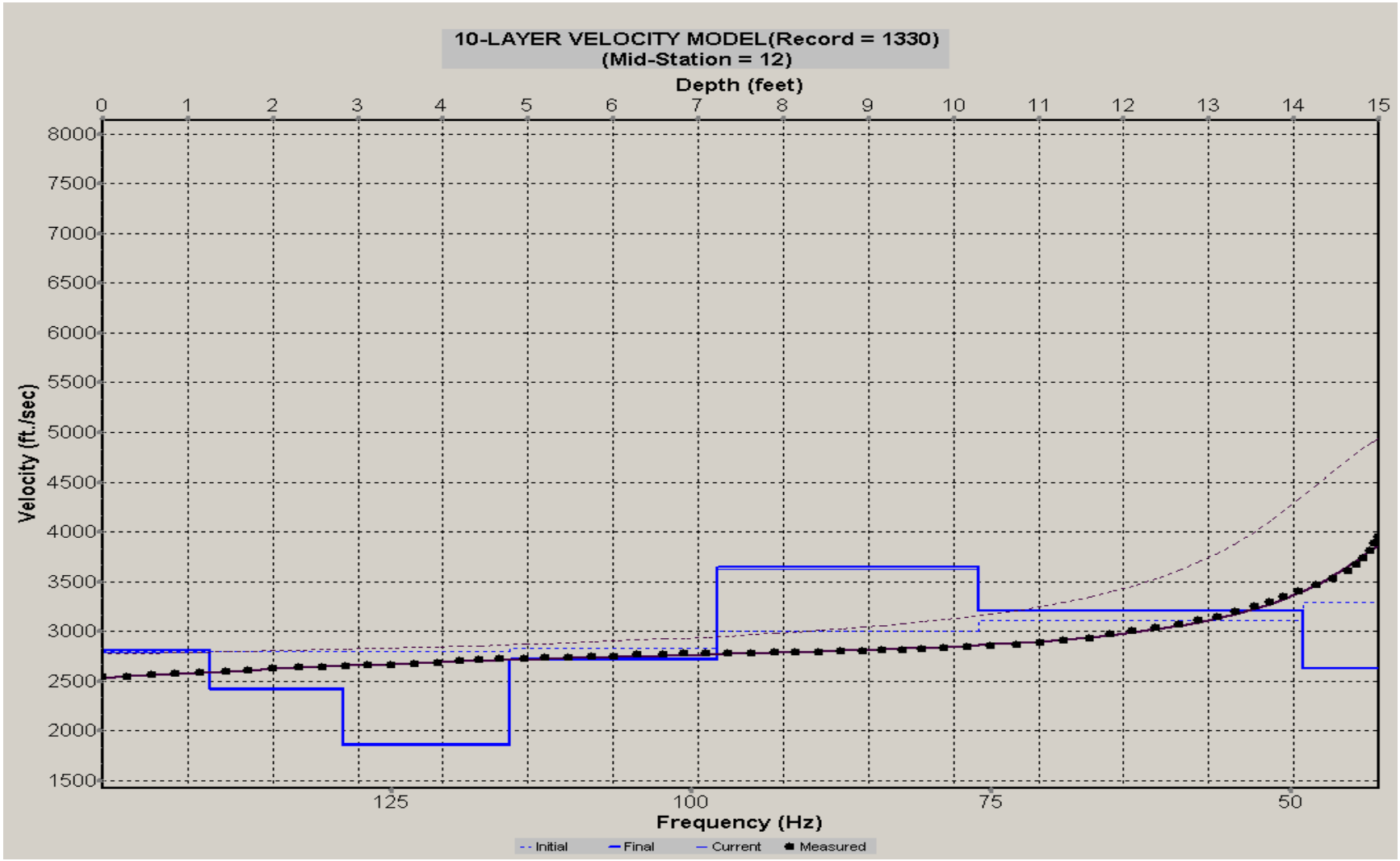

A.525: Velocity Profile Line 1330 used in Post-blast 28

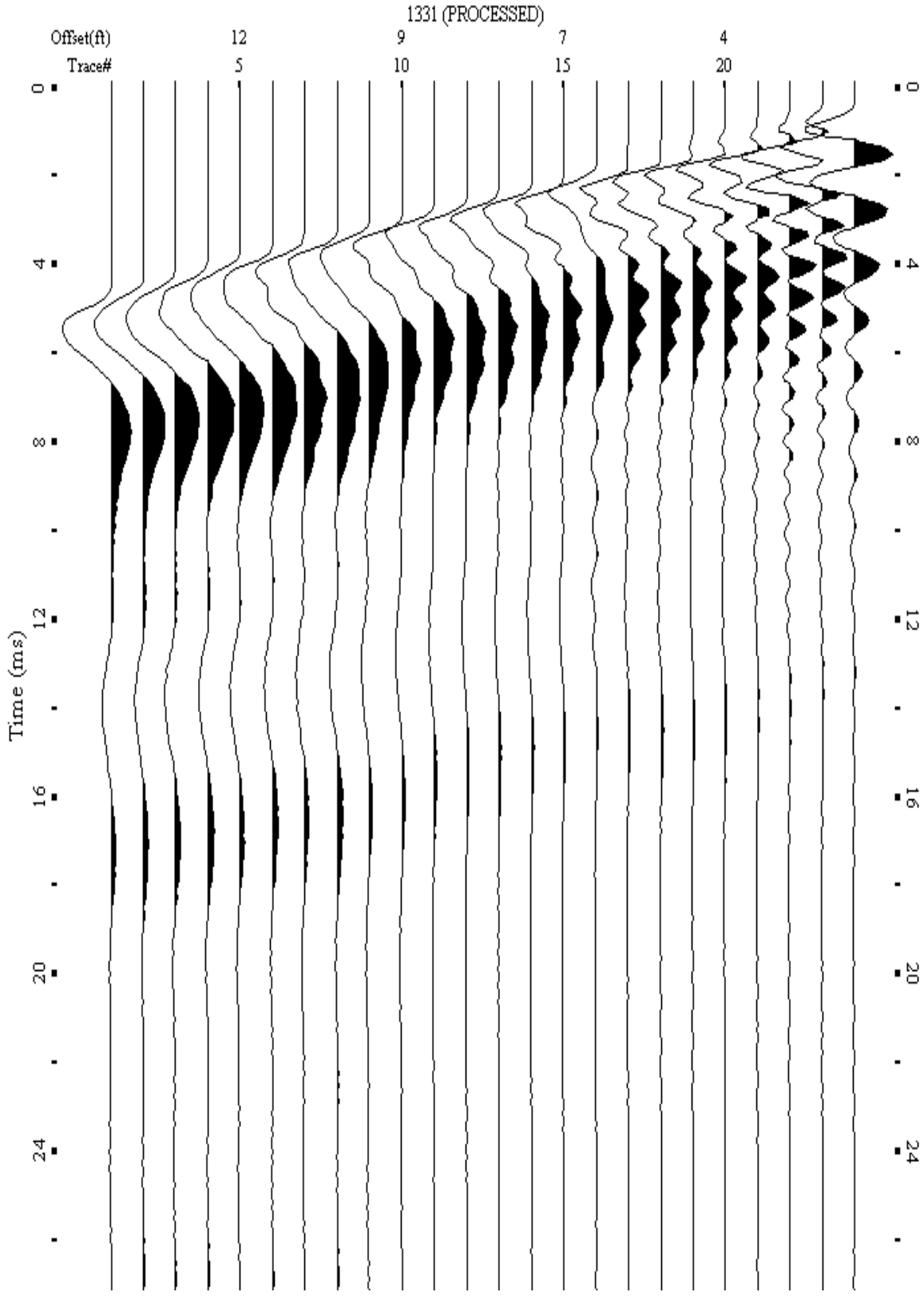

A.526: Shot Gather Line 1331 used in Pre-blast 13, Post-blast 28, Pre-blast 32, and Pre-blast 33

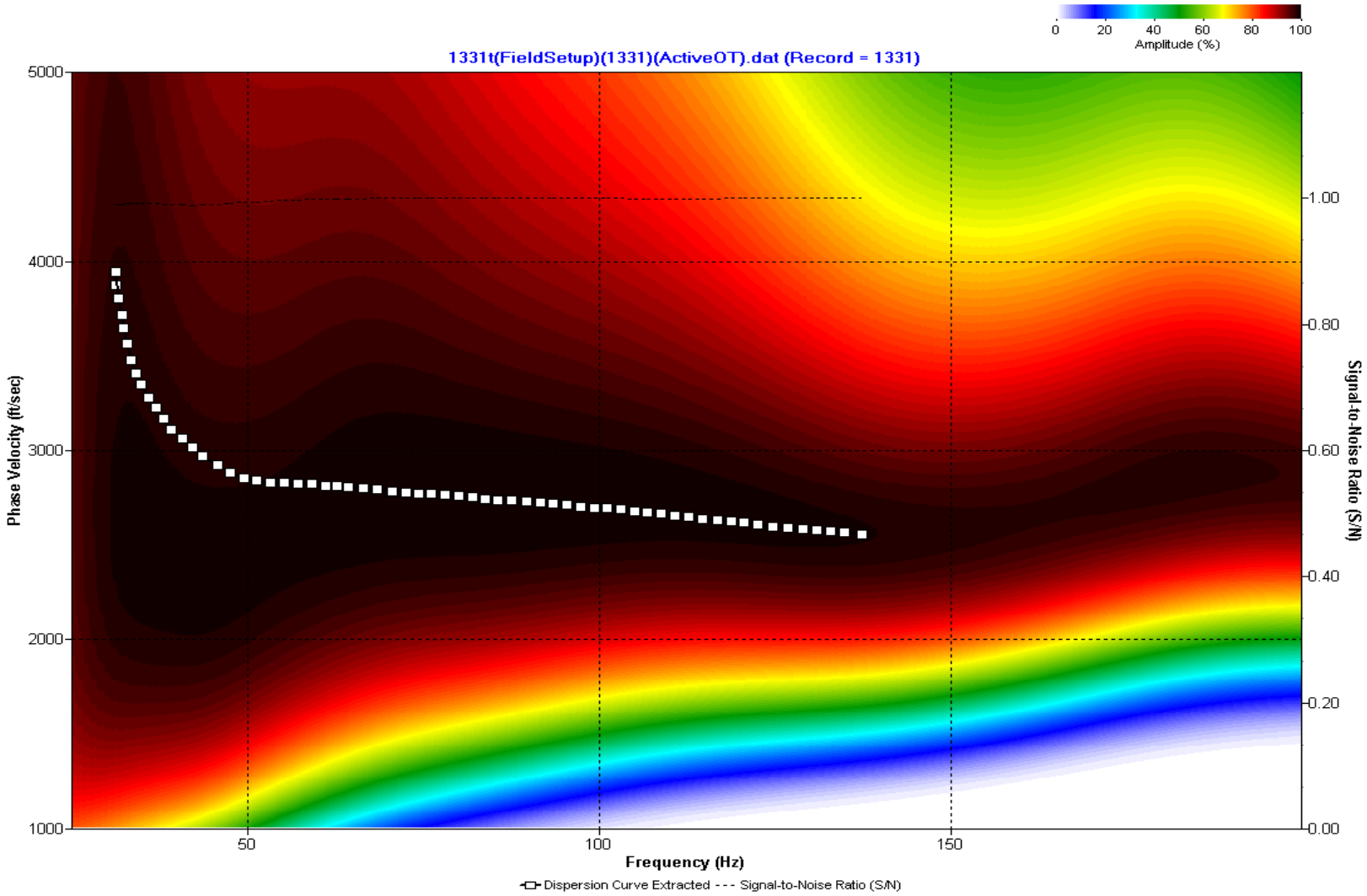

A.527: Dispersion Curve Line 1331 used in Pre-blast 13, Post-blast 28, Pre-blast 32, and Pre-blast 33

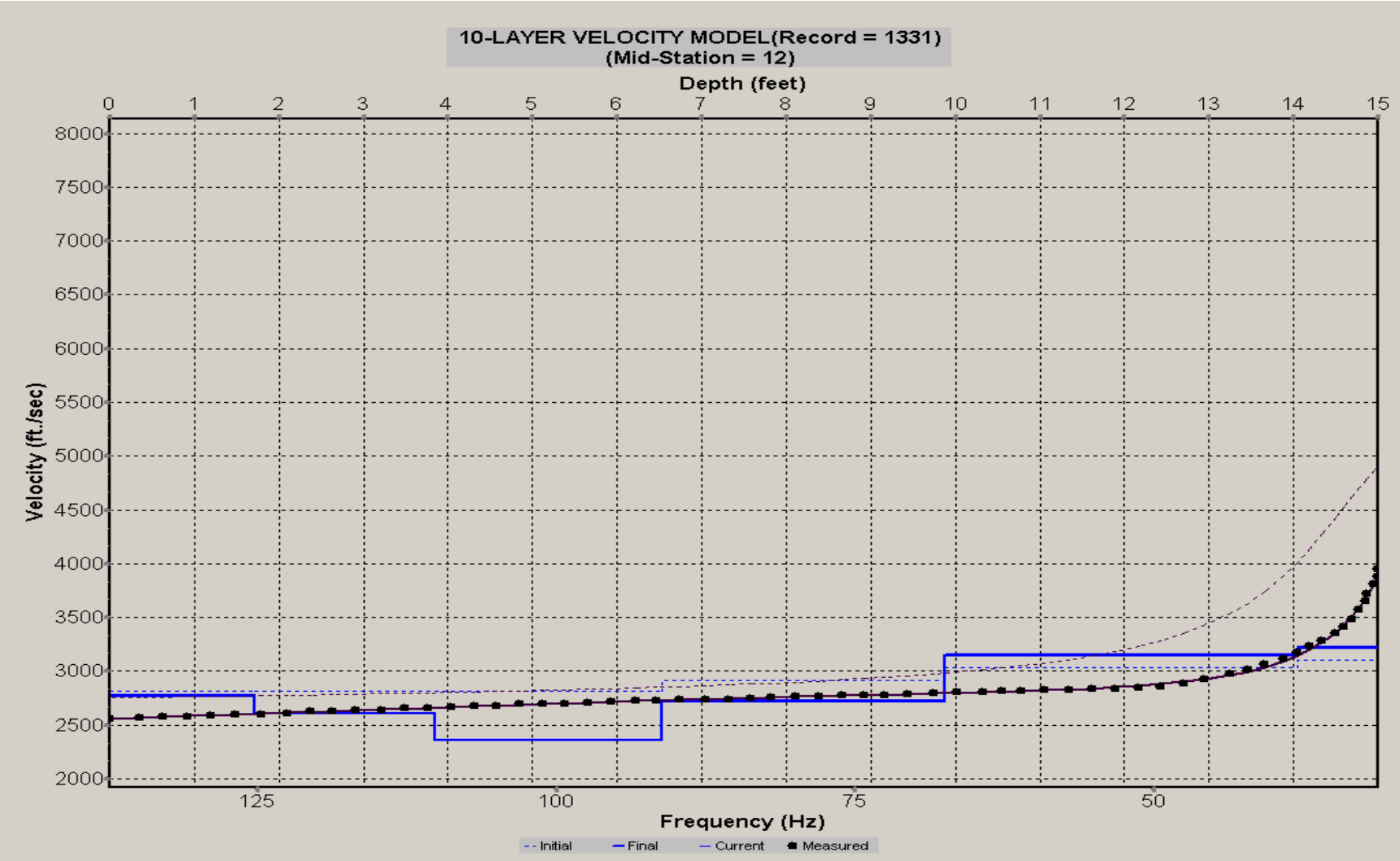

A.528: Velocity Profile Line 1331 used in Pre-blast 13, Post-blast 28, Pre-blast 32, and Pre-blast 33

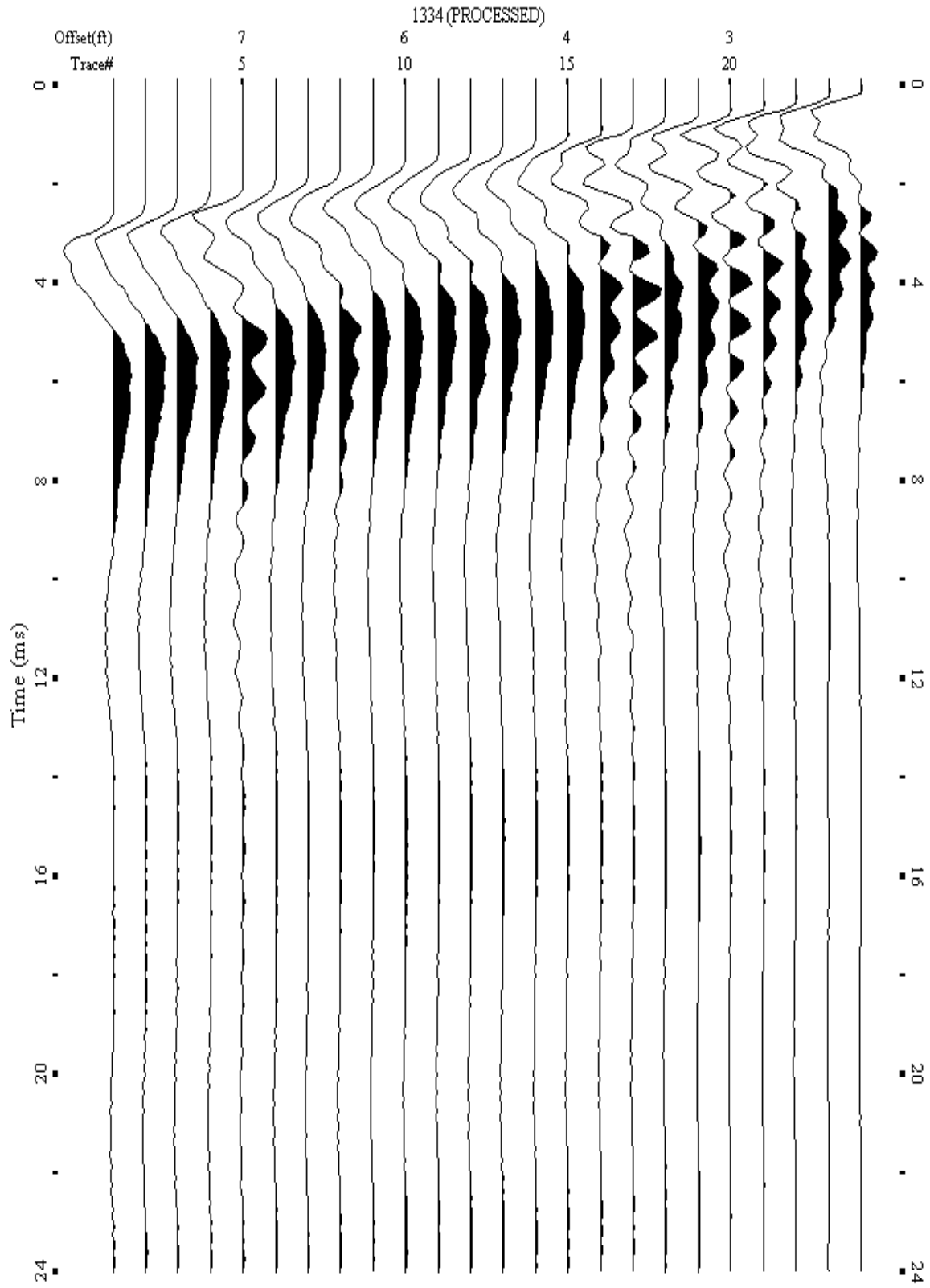

A.529: Shot Gather Line 1334 used in Pre-blast 34

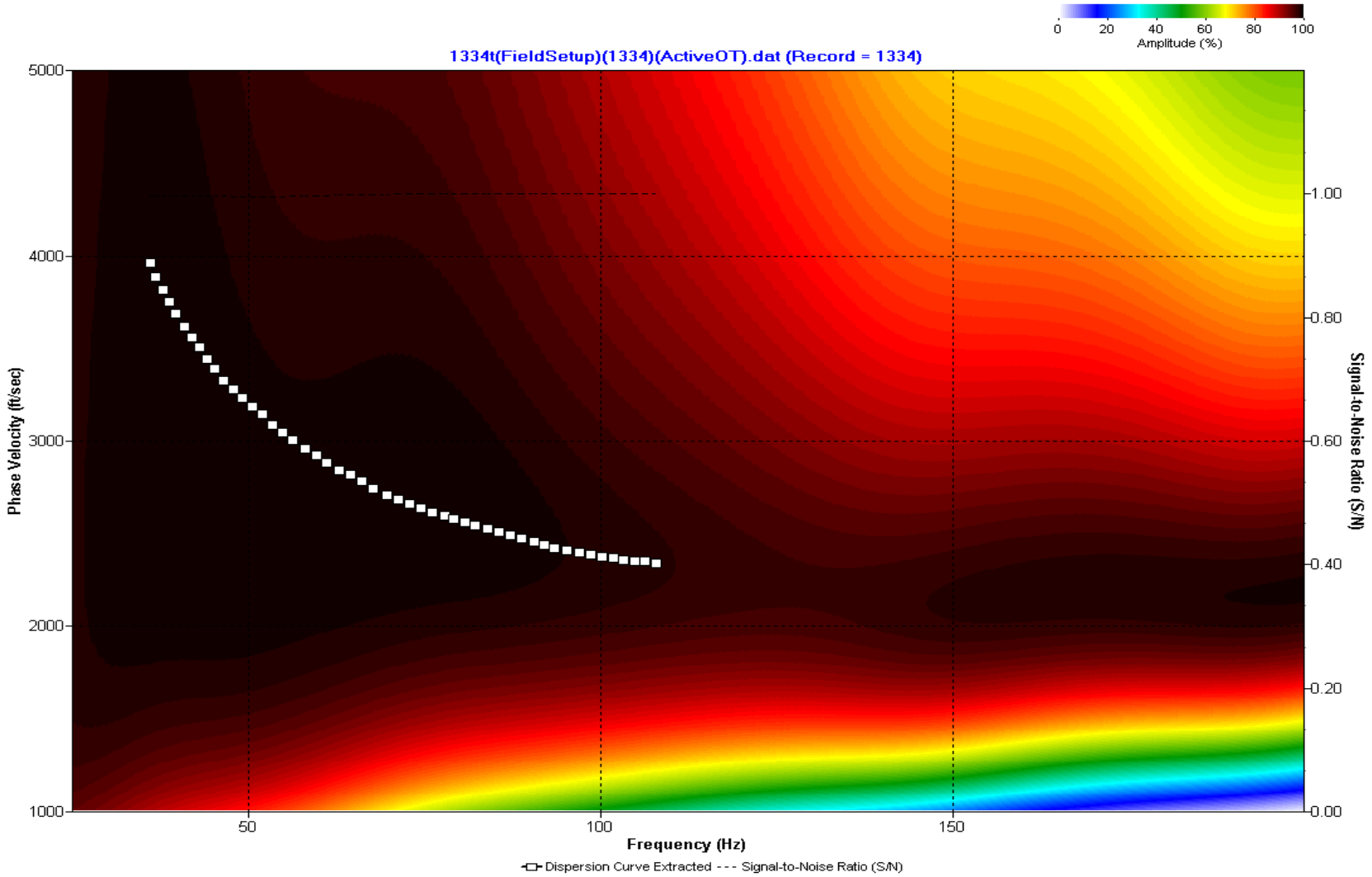

A.530: Dispersion Curve Line 1334 used in Pre-blast 34

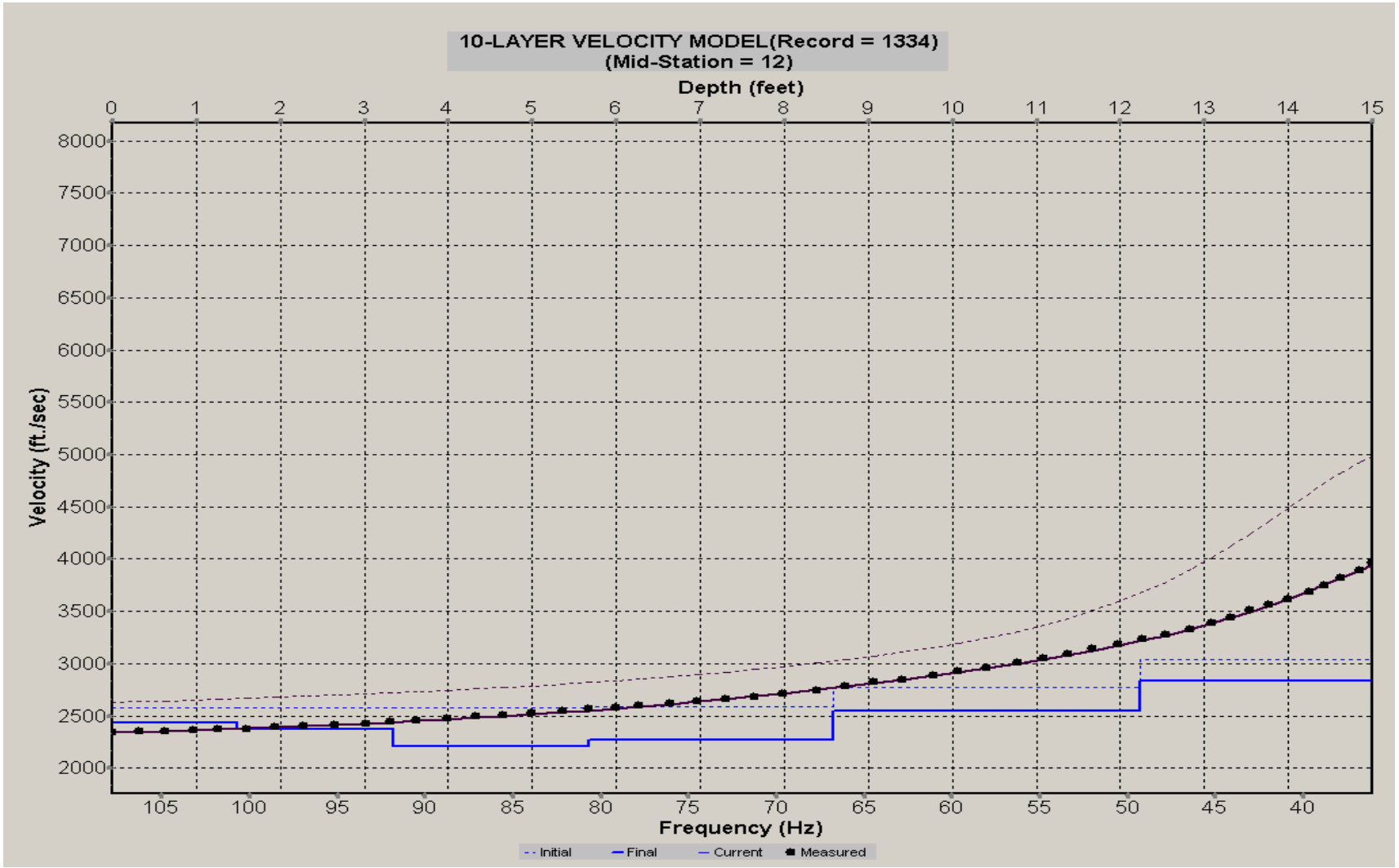

A.531: Velocity Profile Line 1334 used in Pre-blast 34

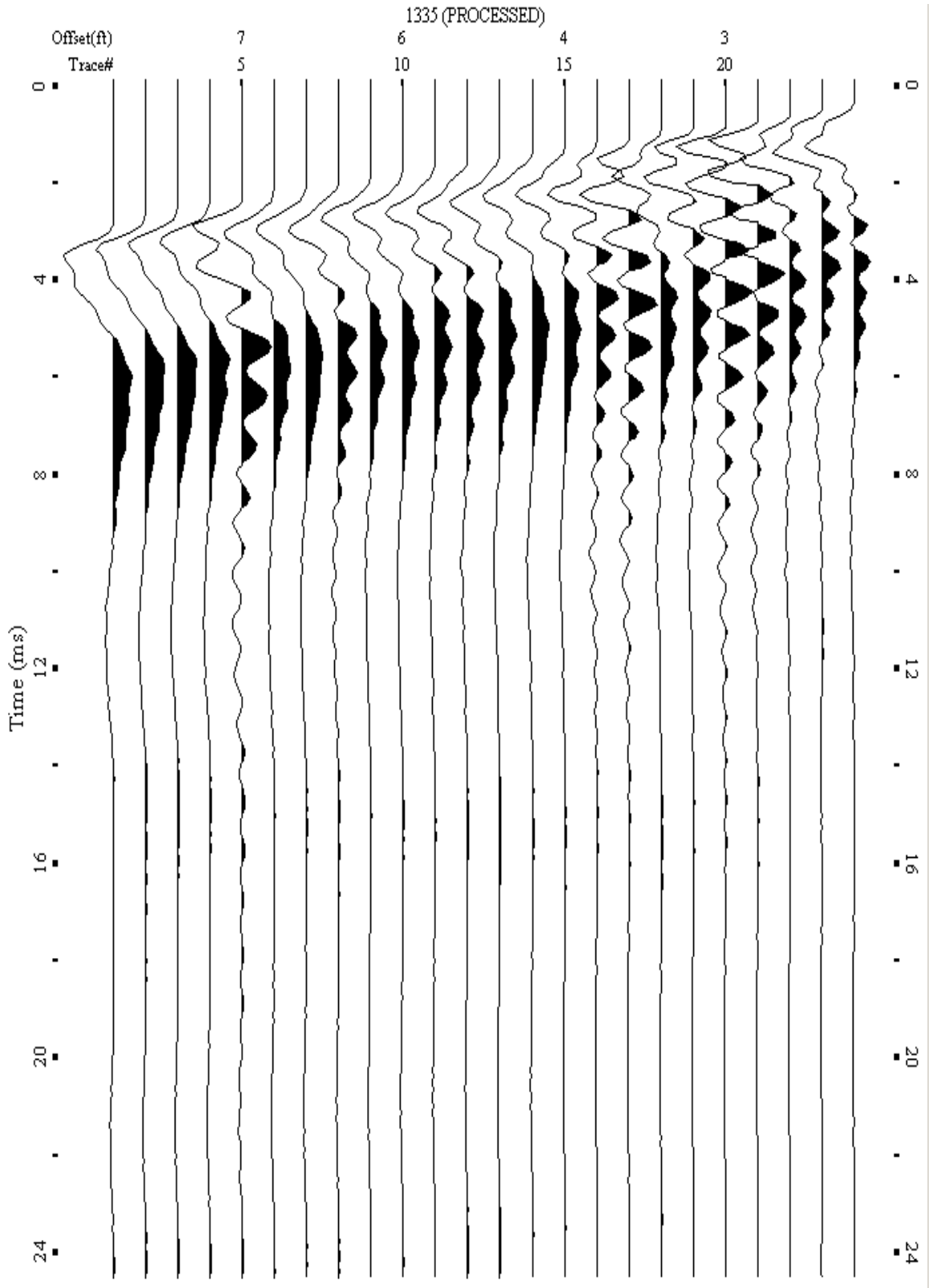

A.532: Shot Gather Line 1335 used in Pre-blast 34

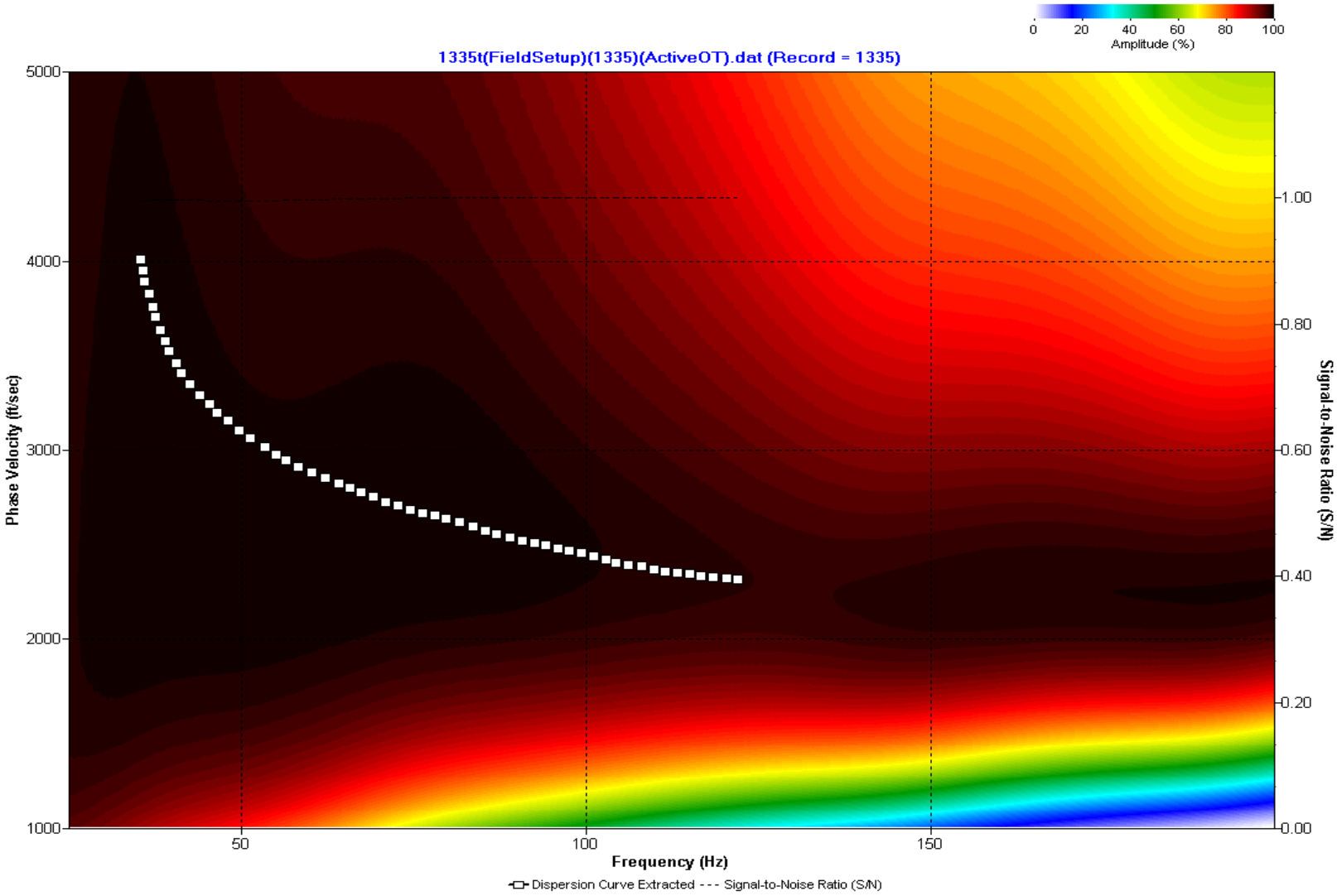

A.533: Dispersion Curve Line 1335 used in Pre-blast 34

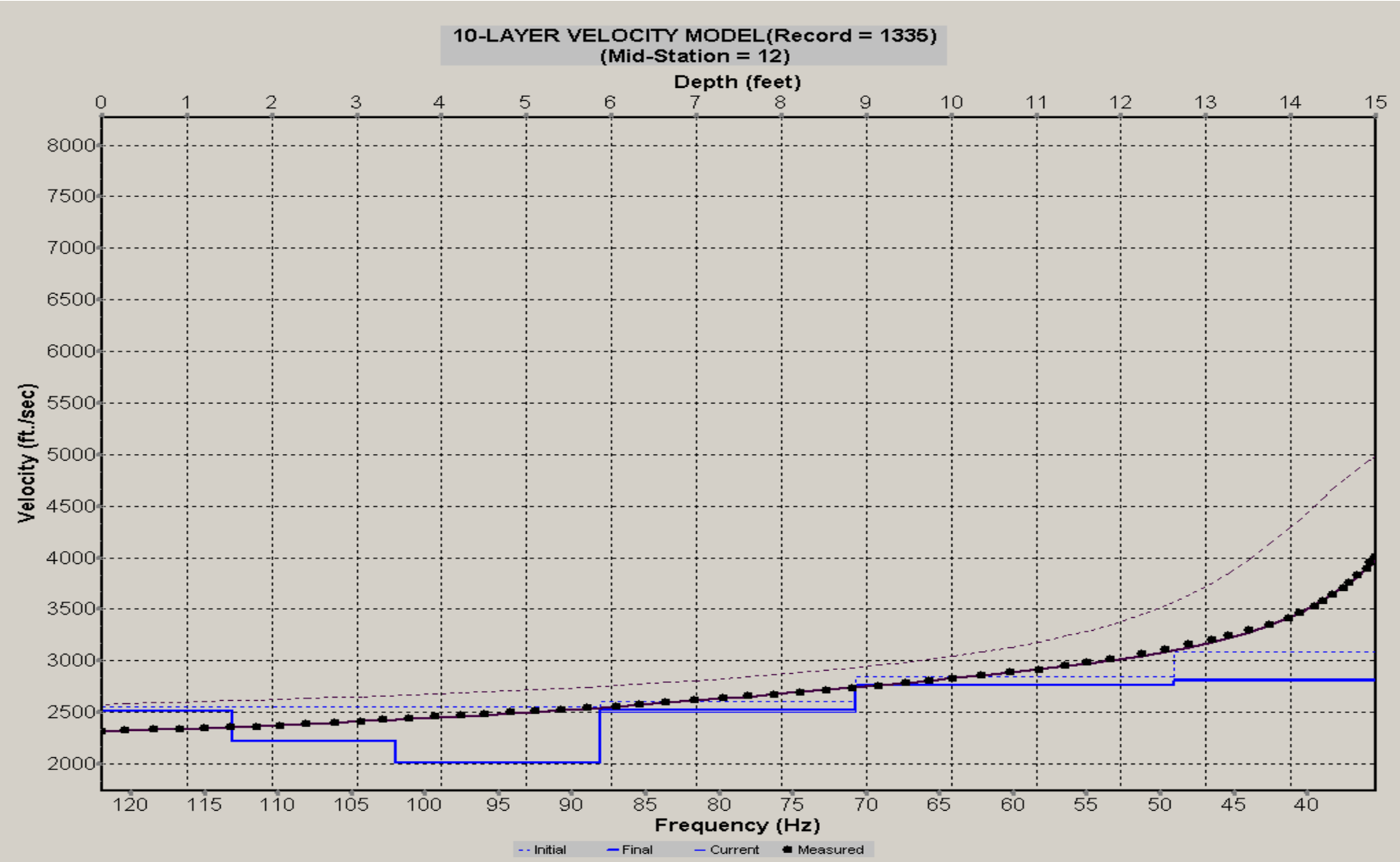

A.534: Velocity Profile Line 1335 used in Pre-blast 34

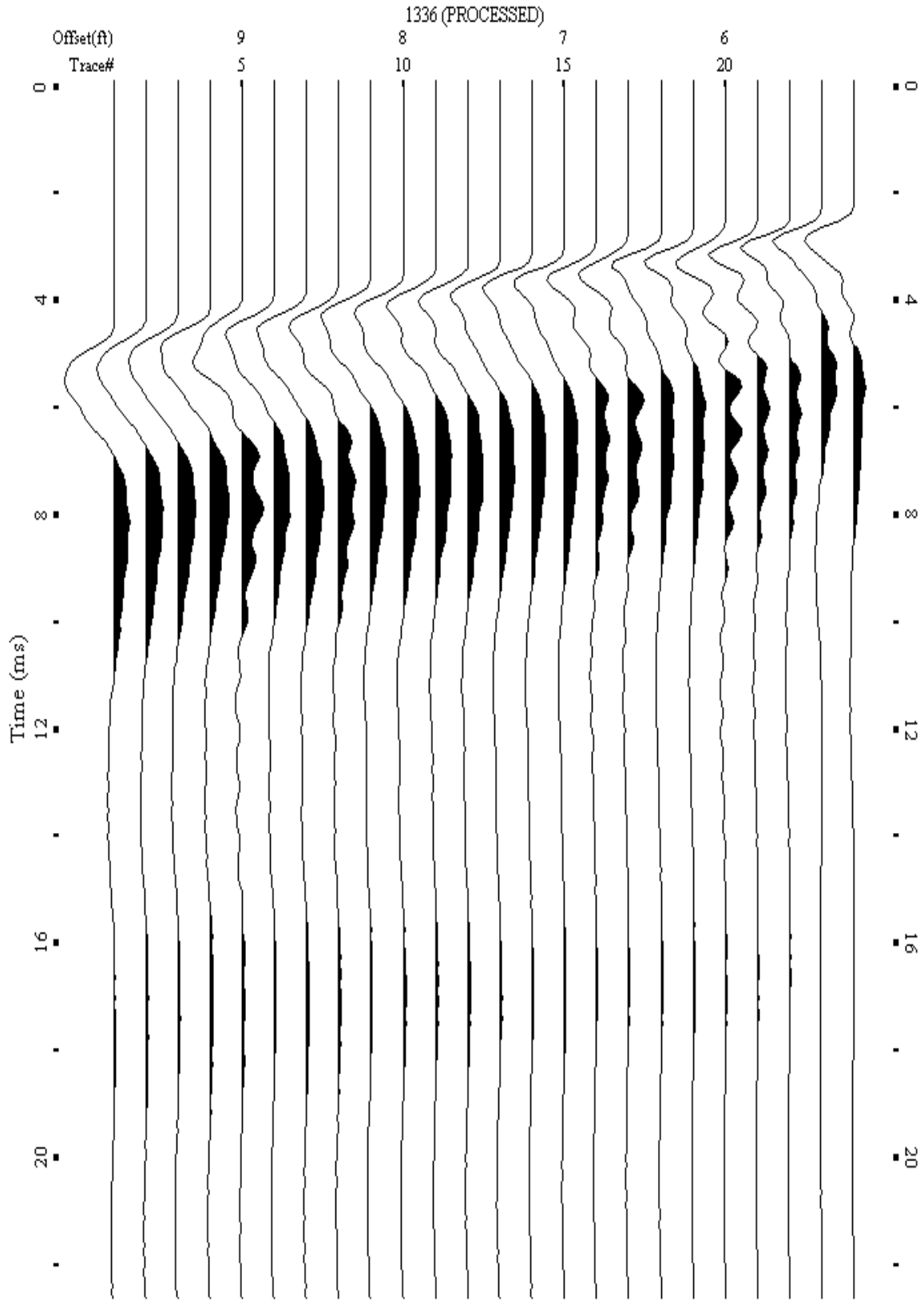

A.535: Shot Gather Line 1336 used in Post-blast 30 and Pre-blast 34

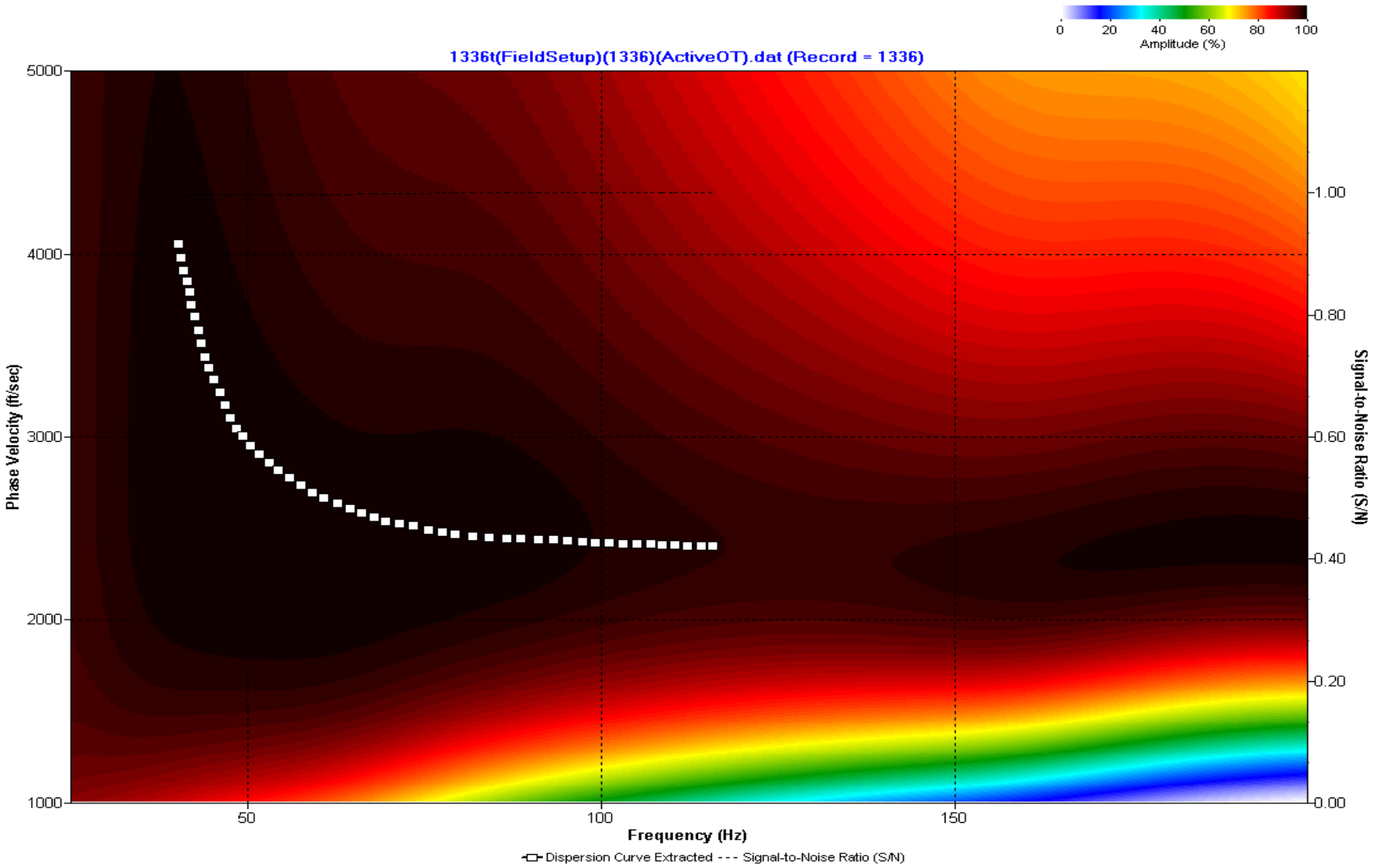

A.536: Dispersion Curve Line 1336 used in Post-blast 30 and Pre-blast 34

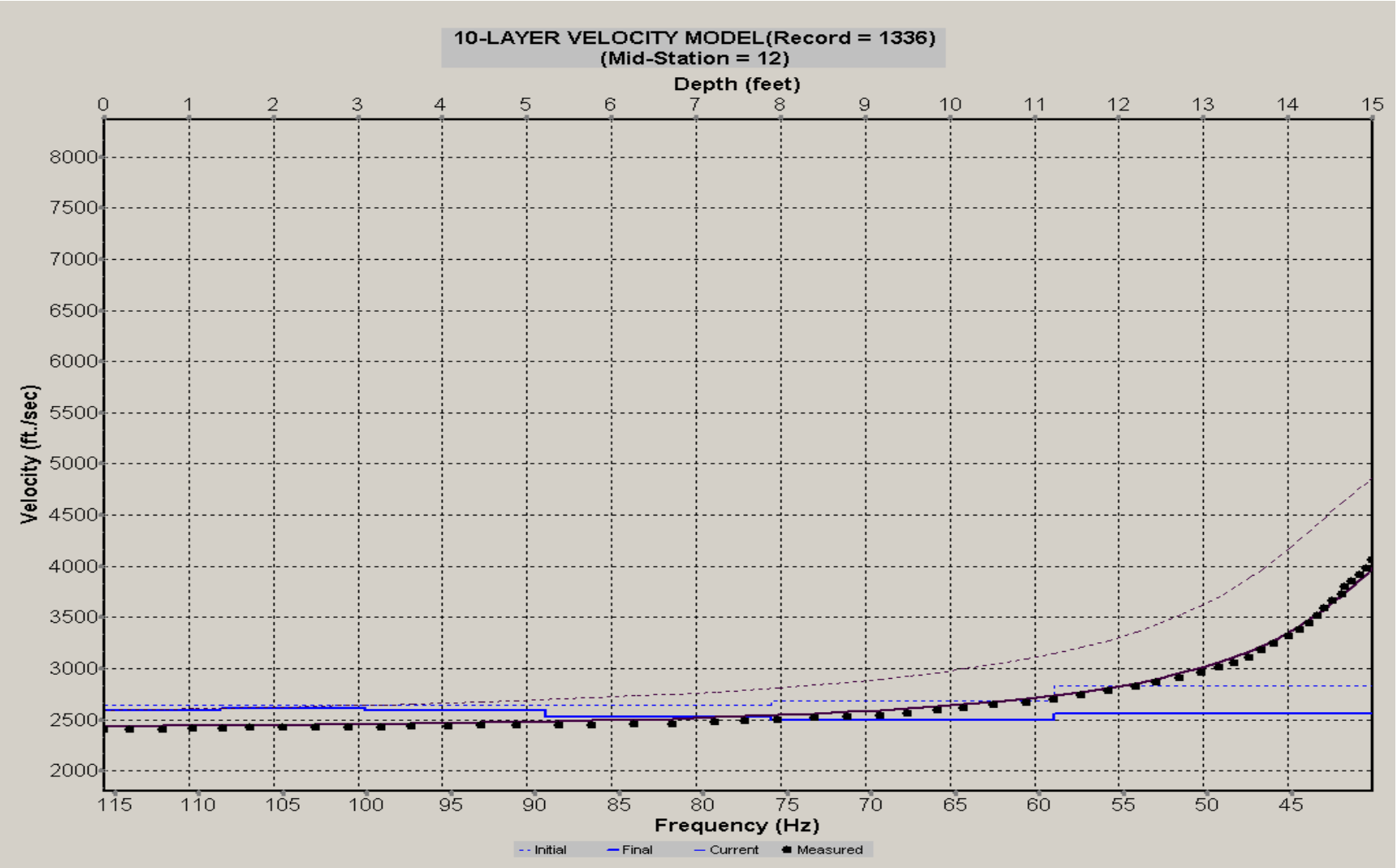

A.537: Velocity Profile Line 1336 used in Post-blast 30 and Pre-blast 34

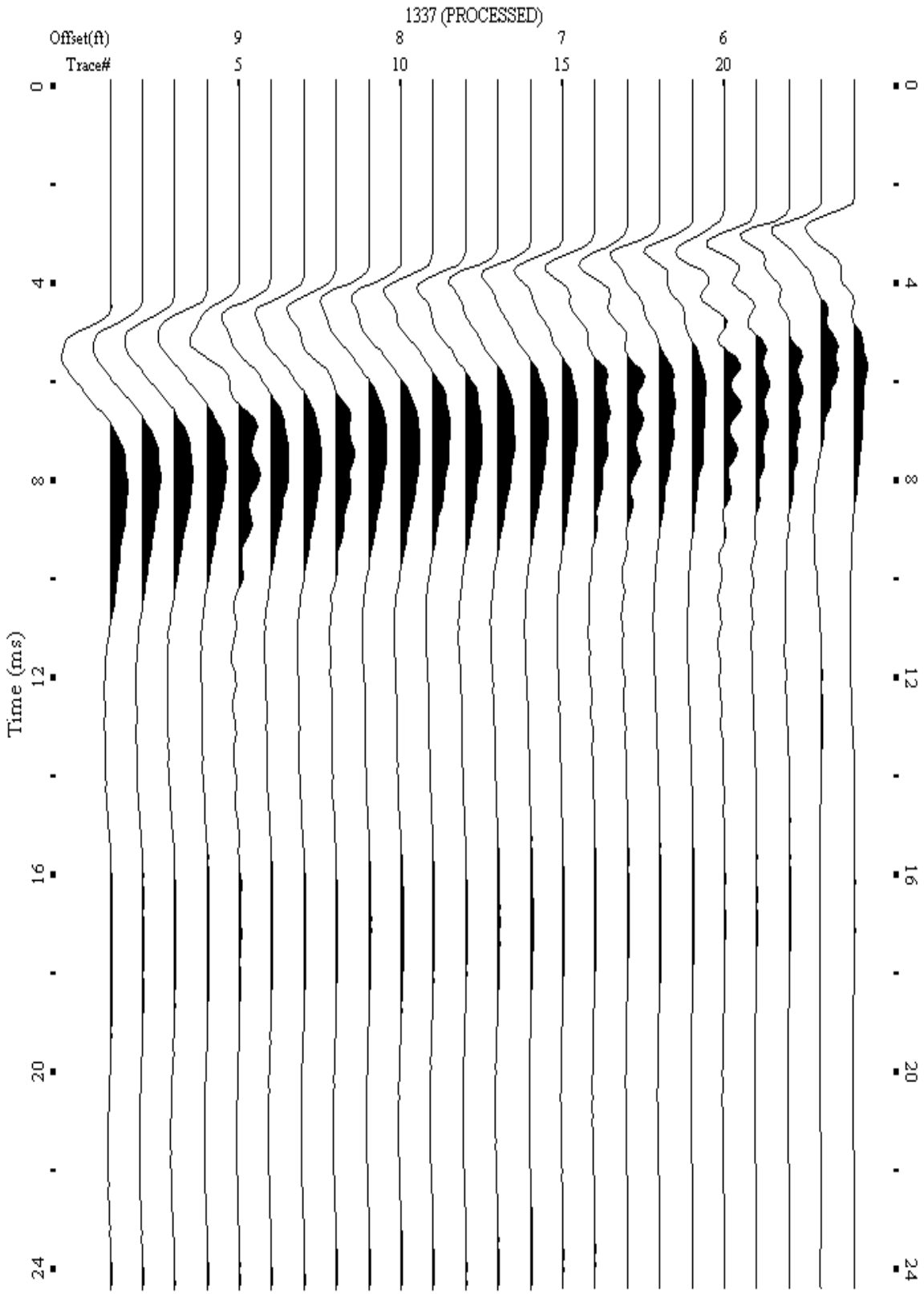

A.538: Shot Gather Line 1337 used in Post-blast 30 and Pre-blast 34

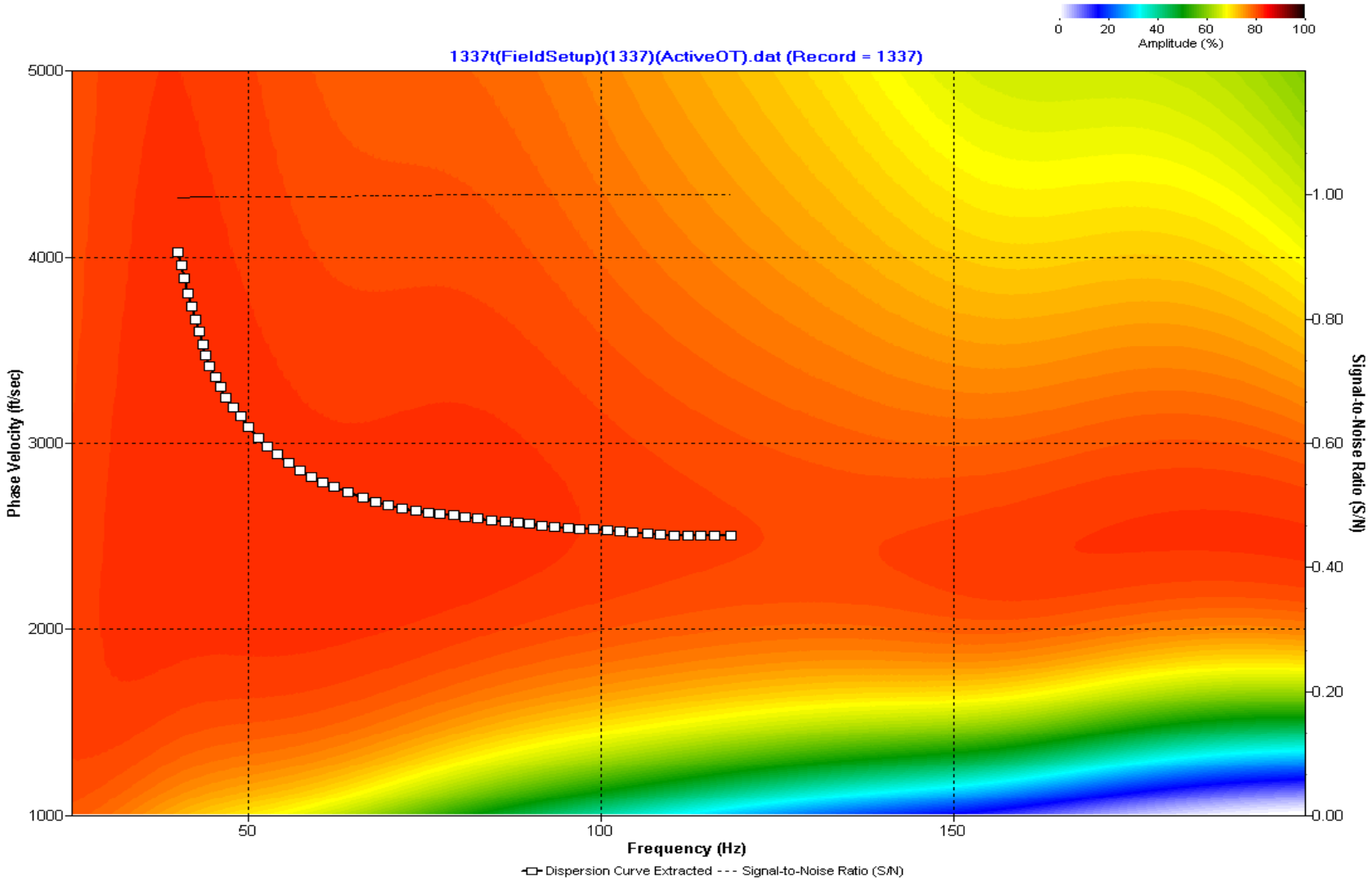

A.539: Dispersion Curve Line 1337 used in Post-blast 30 and Pre-blast 34

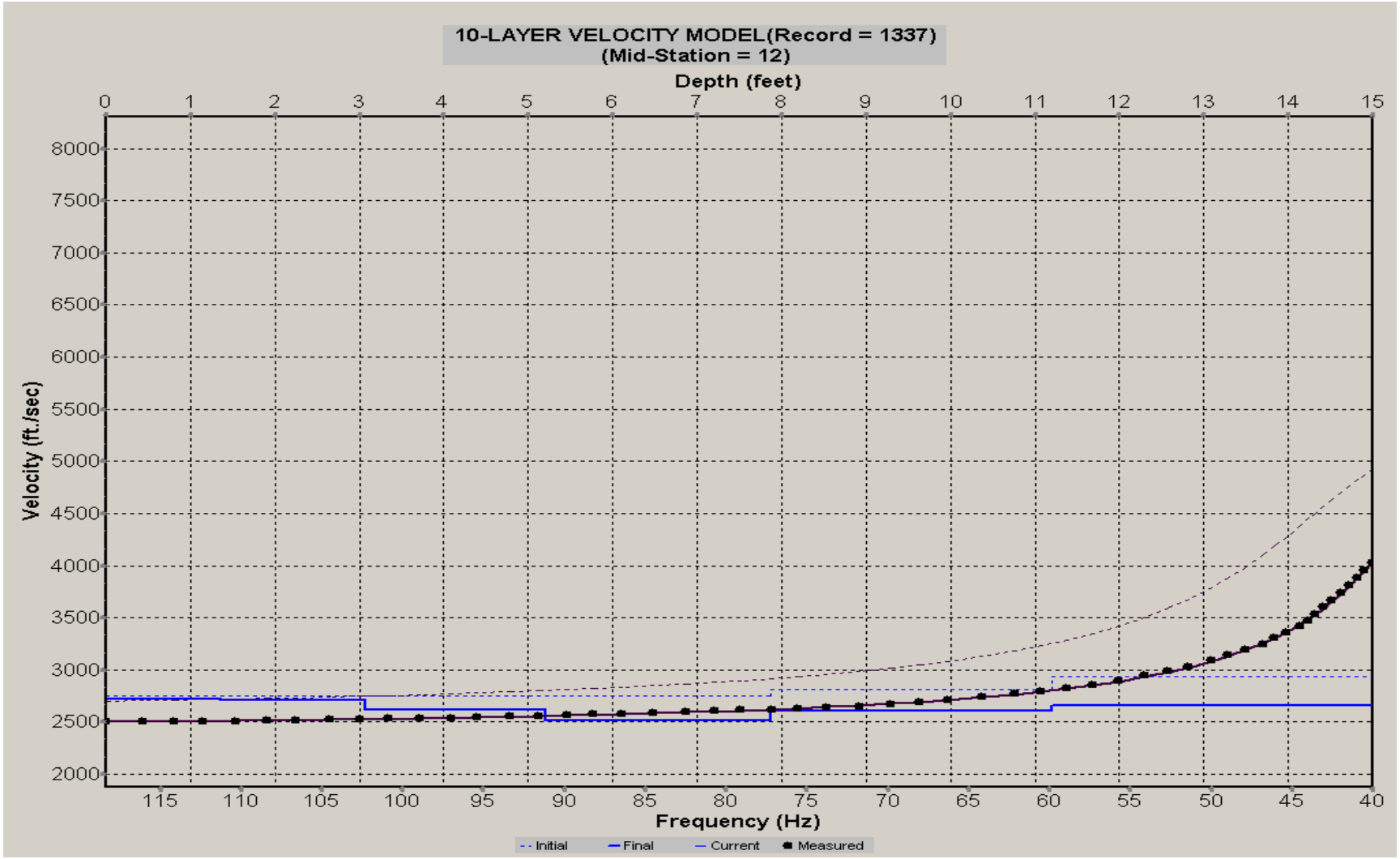

A.540: Velocity Profile Line 1337 used in Post-blast 30 and Pre-blast 34

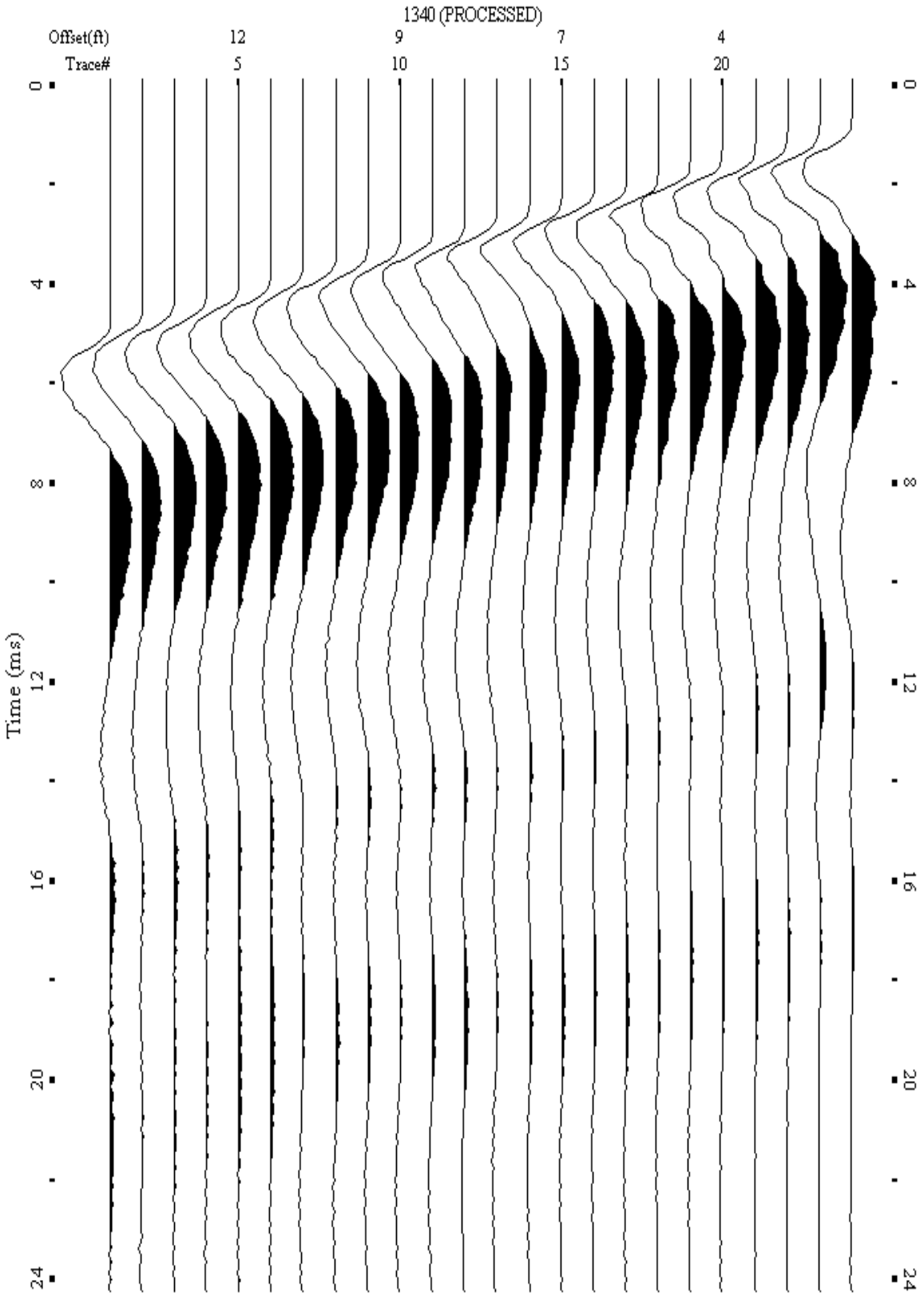

A.541: Shot Gather Line 1340 used in Post-blast 29, Post-blast 30 and Pre-blast 33

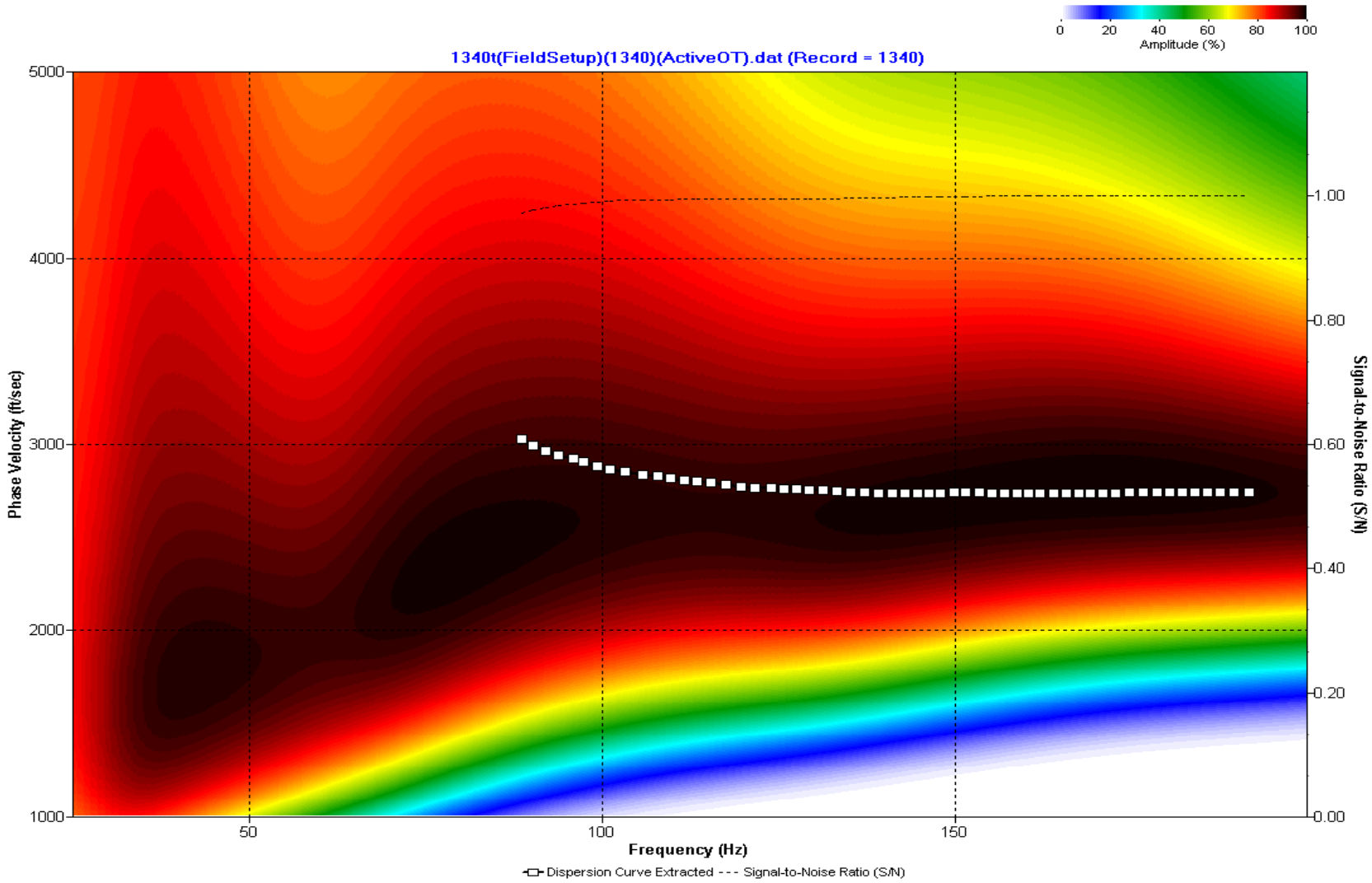

A.542: Dispersion Curve Line 1340 used in Post-blast 29, Post-blast 30 and Pre-blast 33

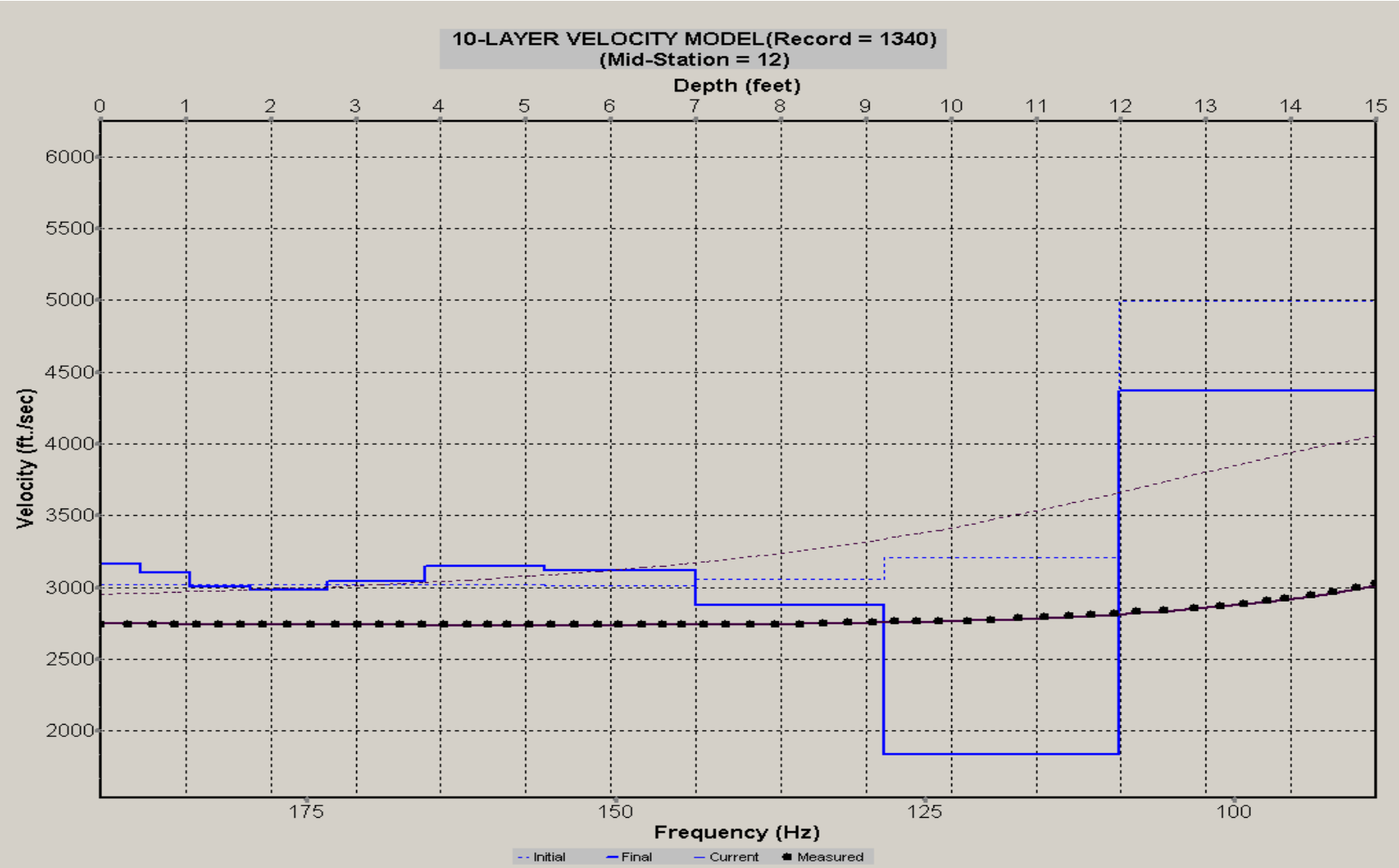

A.543: Velocity Profile Line 1340 used in Post-blast 29, Post-blast 30 and Pre-blast 33

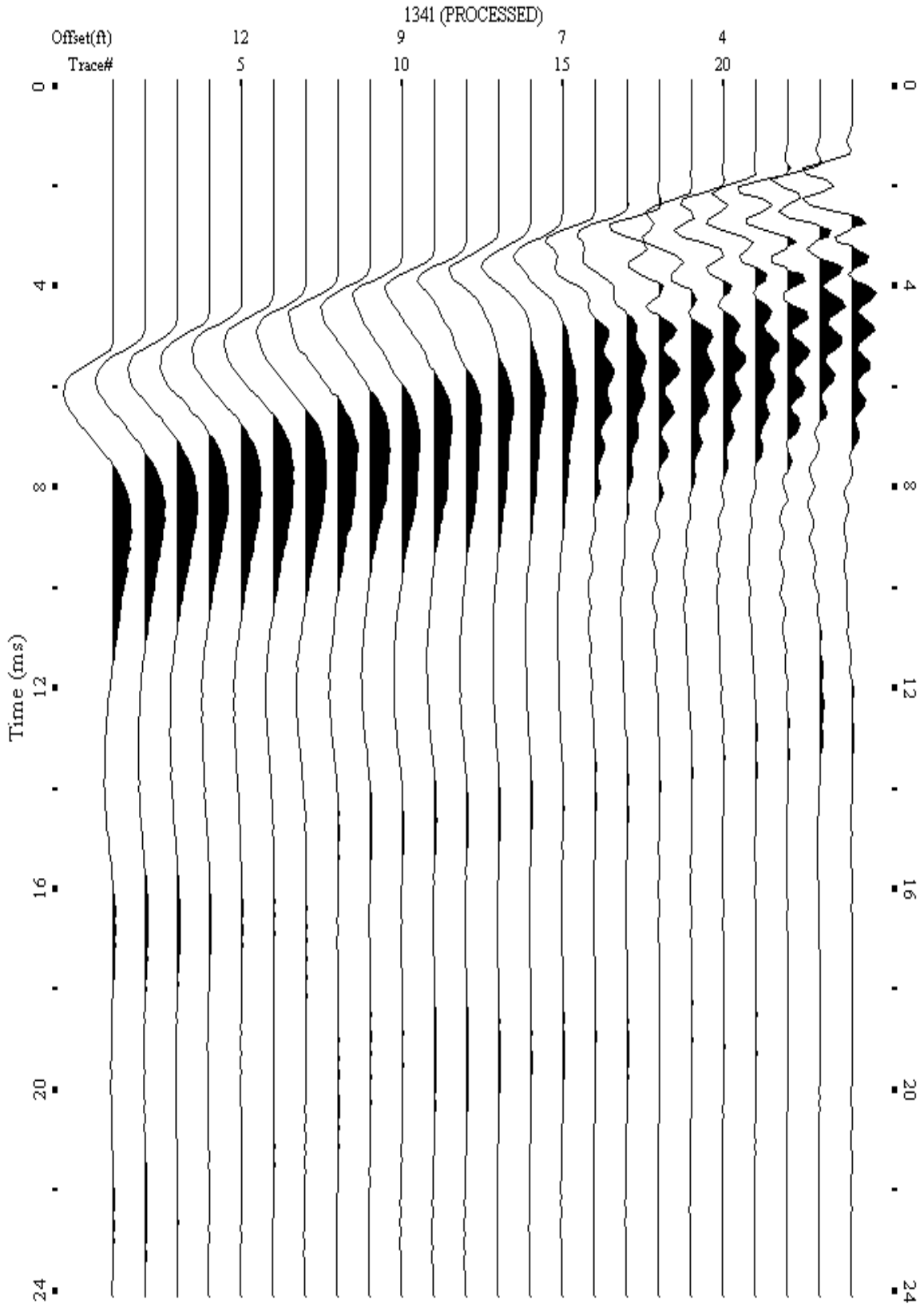

A.544: Shot Gather Line 1341 used in Post-blast 29, Post-blast 30 and Pre-blast 33

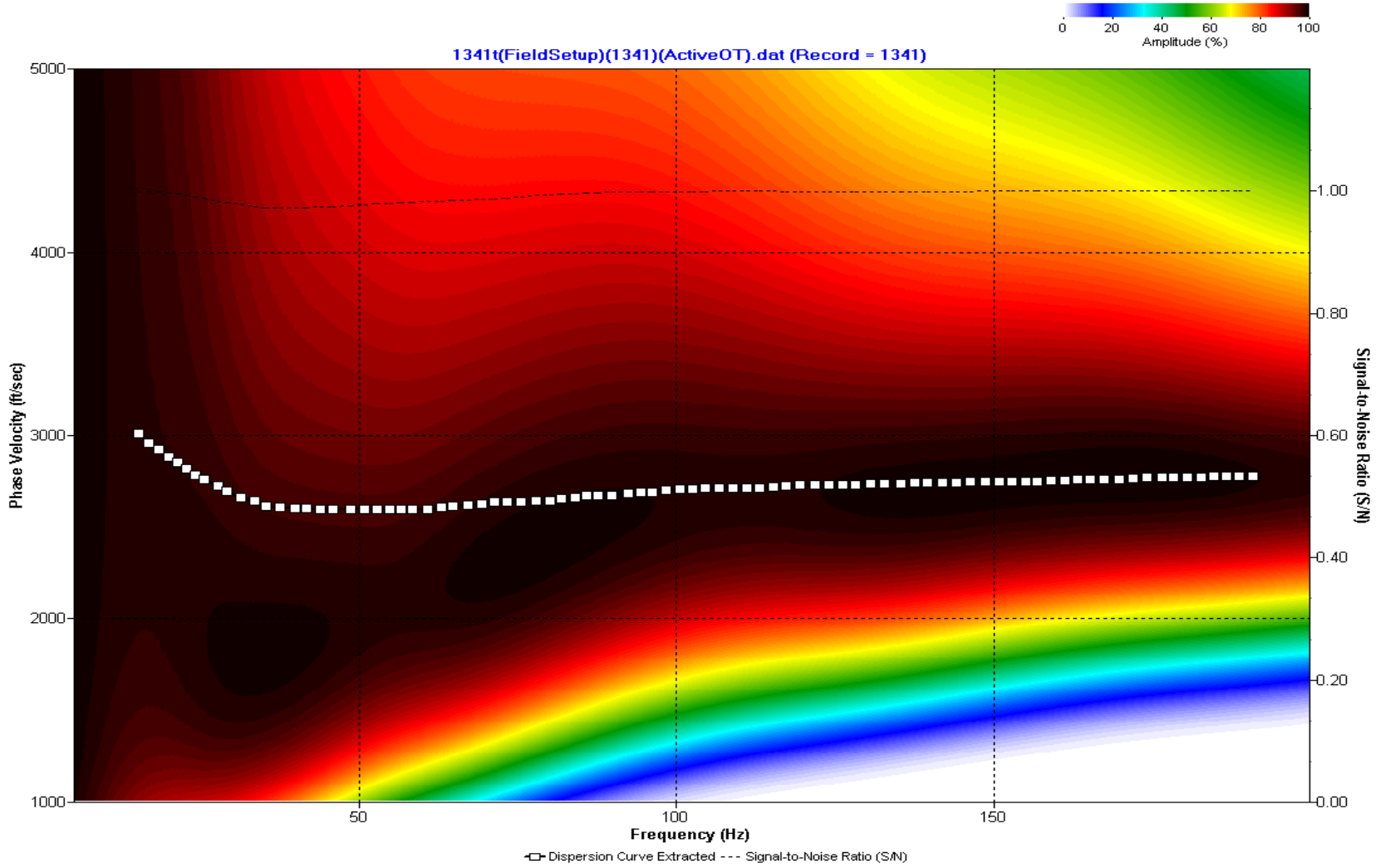

A.545: Dispersion Curve Line 1341 used in Post-blast 29, Post-blast 30 and Pre-blast 33

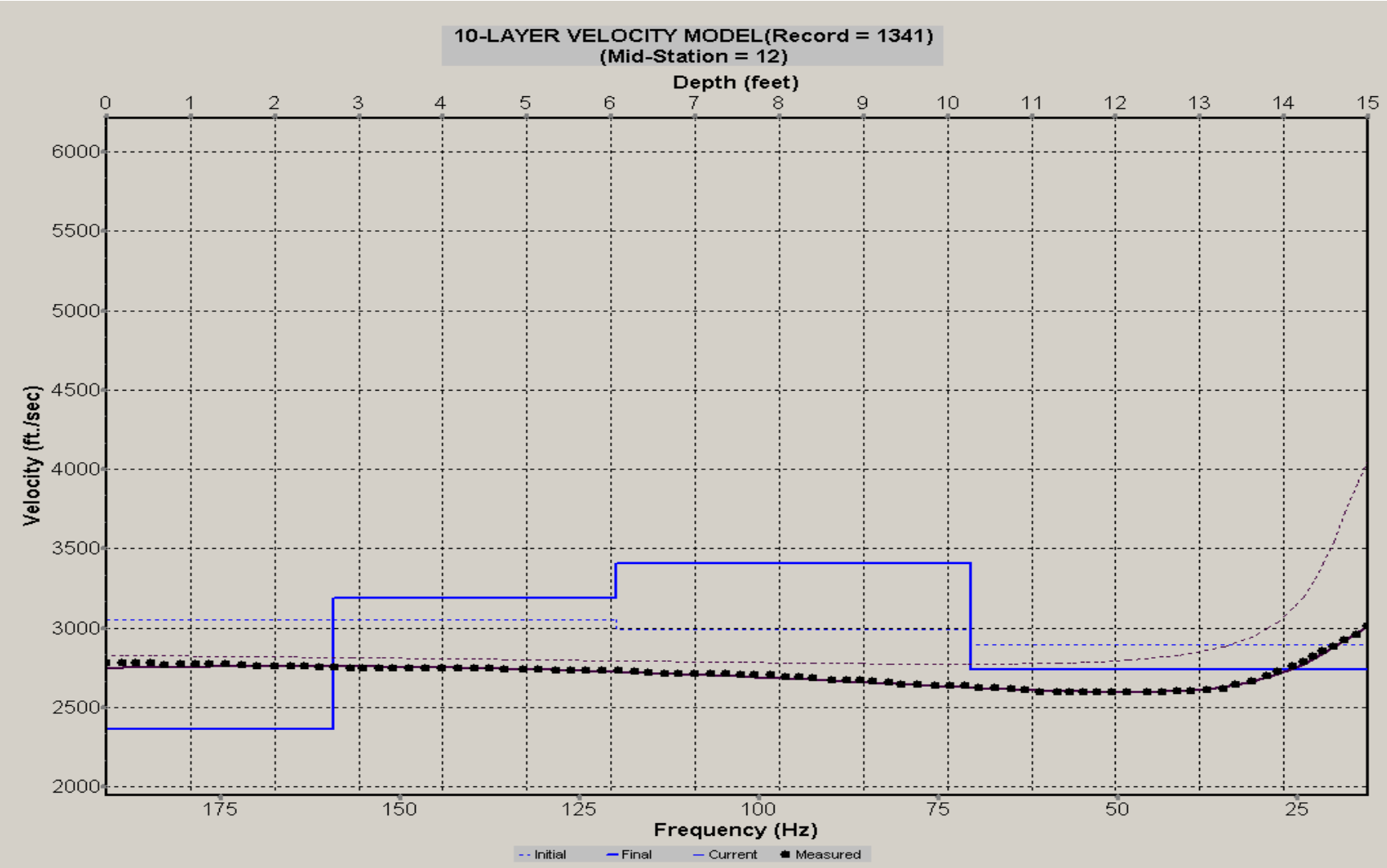

A.546: Velocity Profile Line 1341 used in Post-blast 29, Post-blast 30 and Pre-blast 33

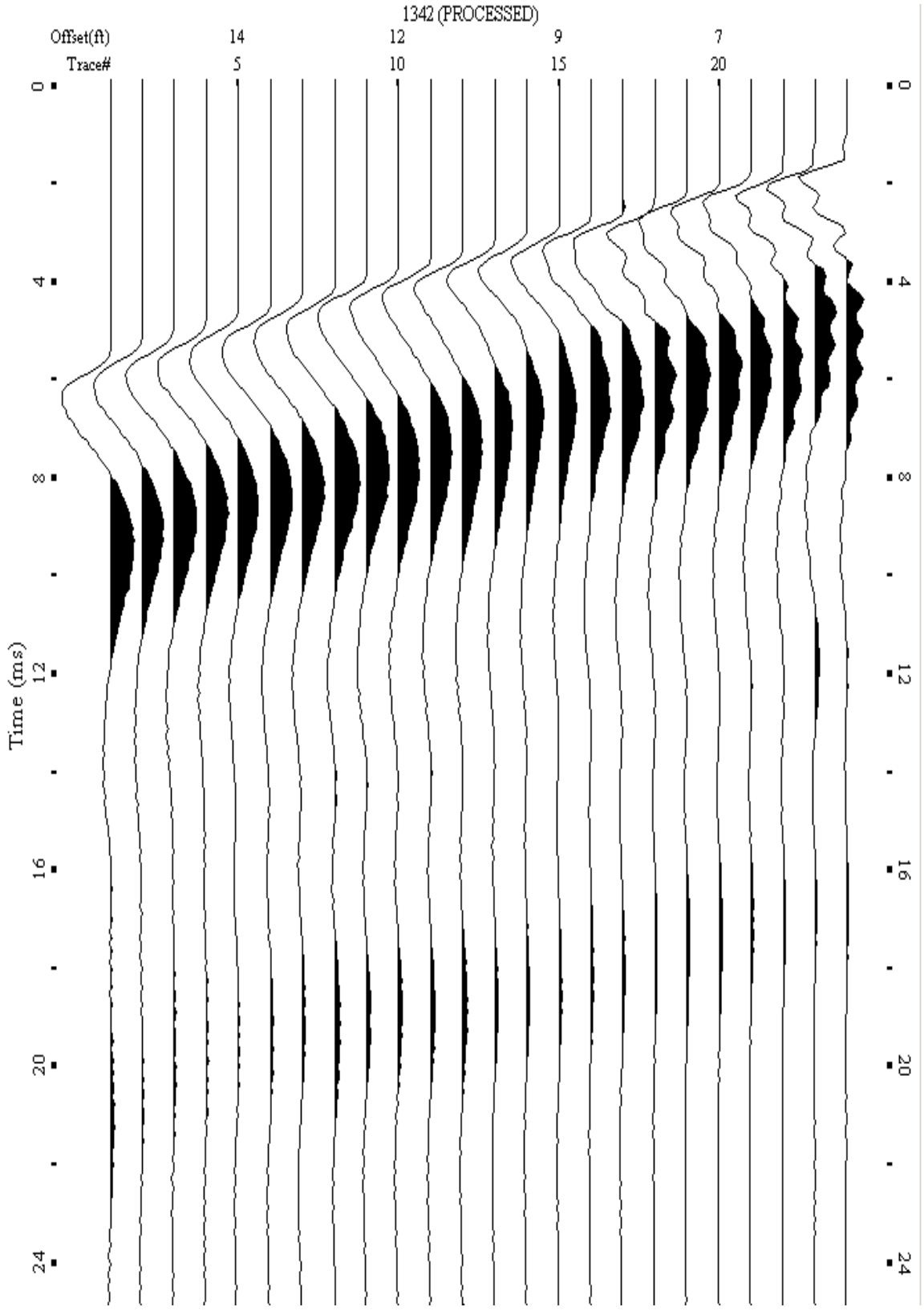

A.547: Shot Gather Line 1342 used in Post-blast 29 and Pre-blast 33

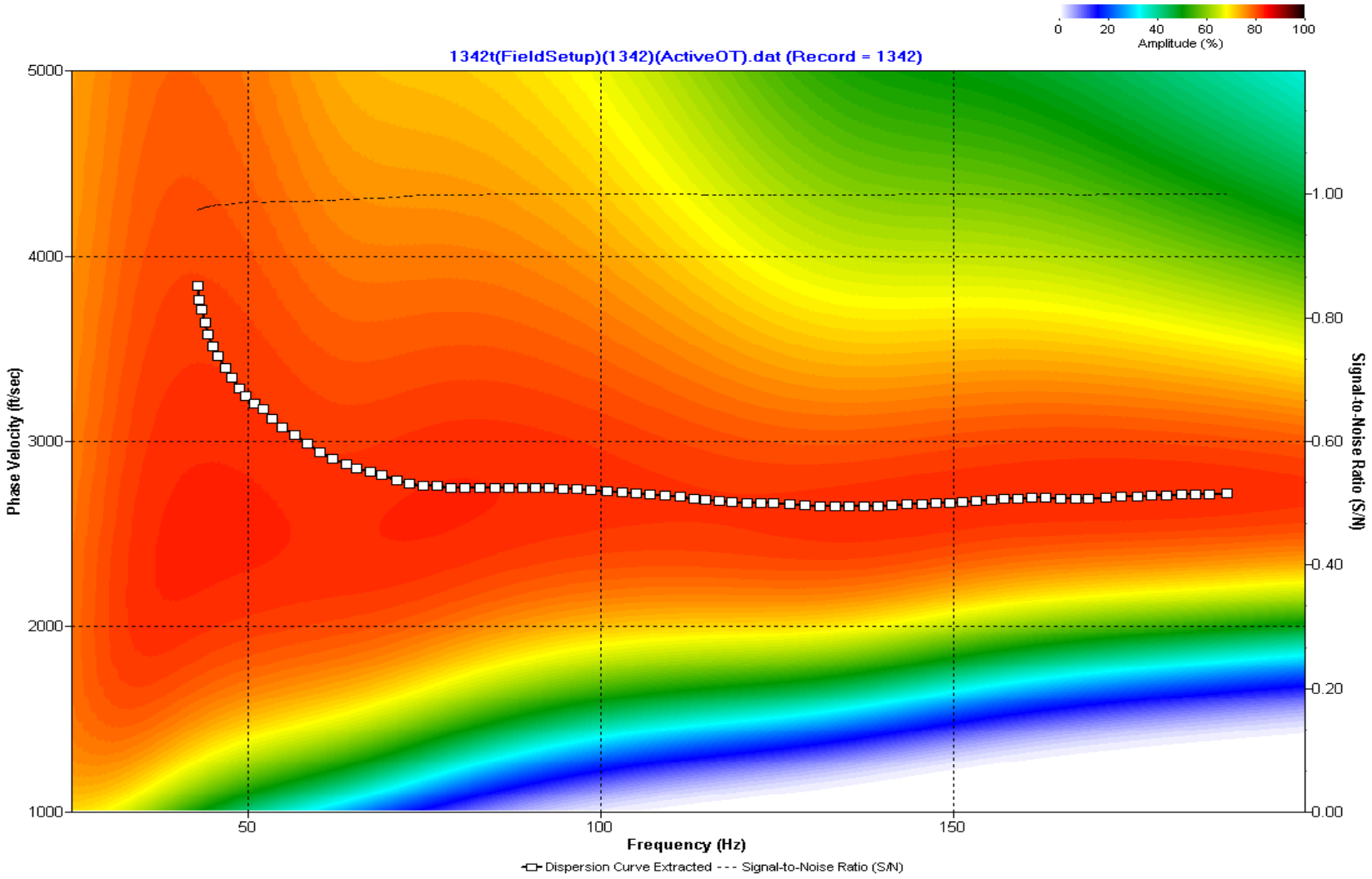

A.548: Dispersion Curve Line 1342 used in Post-blast 29 and Pre-blast 33

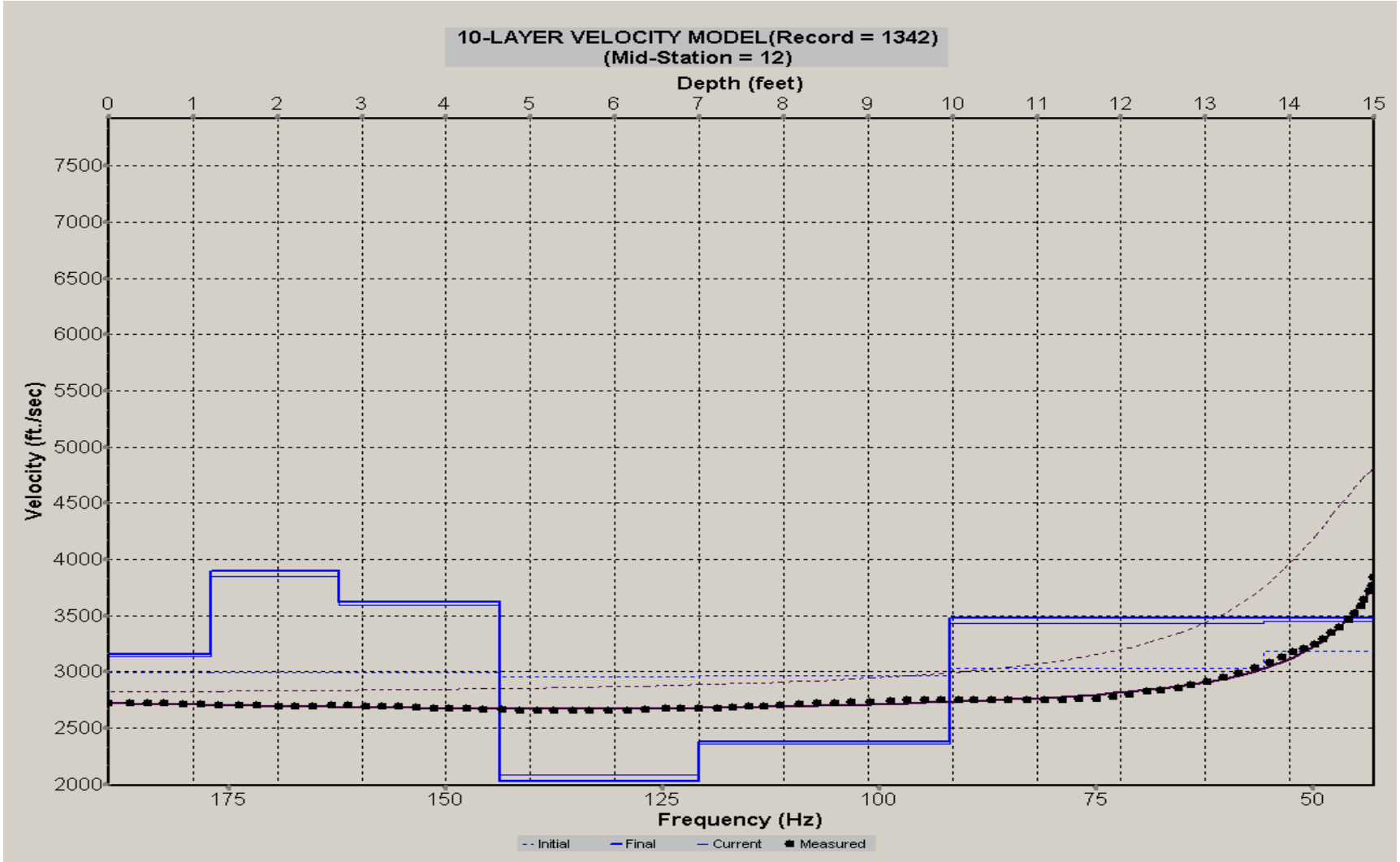

A.549: Velocity Profile Line 1342 used in Post-blast 29 and Pre-blast 33

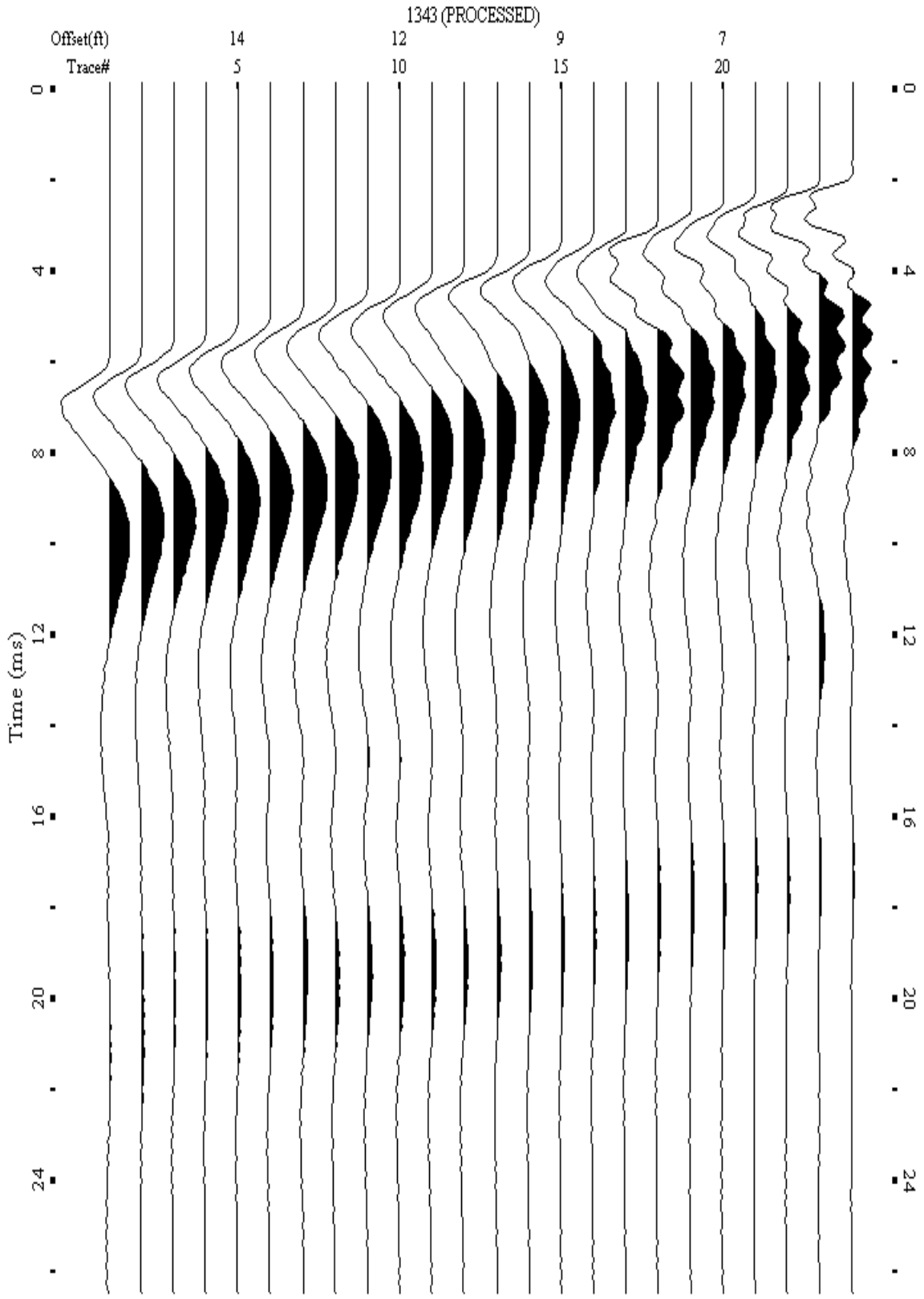

A.550: Shot Gather Line 1343 used in Post-blast 29, Pre-blast 33 and Pre-blast 34

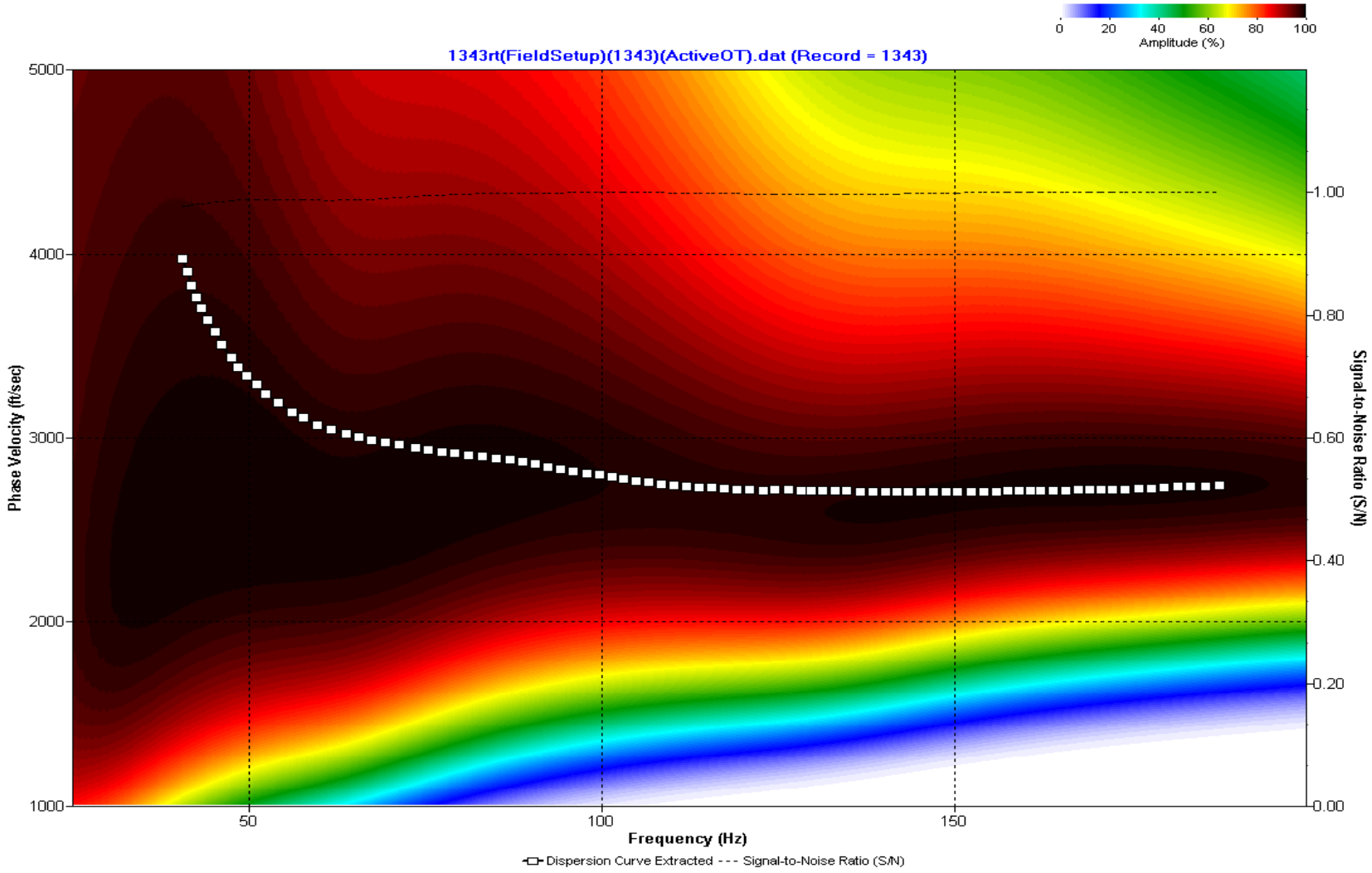

A.551: Dispersion Curve Line 1343 used in Post-blast 29, Pre-blast 33 and Pre-blast 34

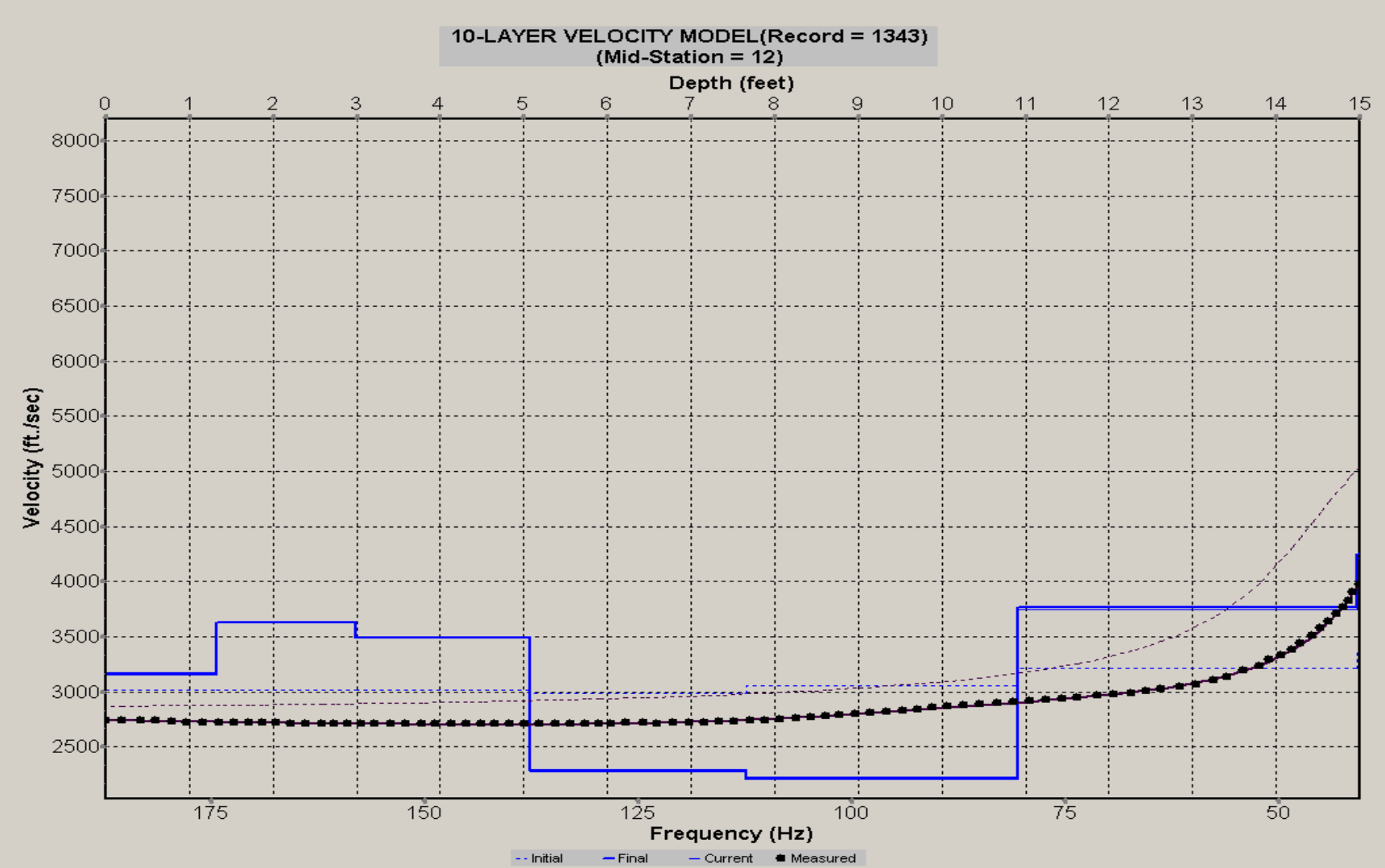

A.552: Velocity Profile Line 1343 used in Post-blast 29, Pre-blast 33 and Pre-blast 34

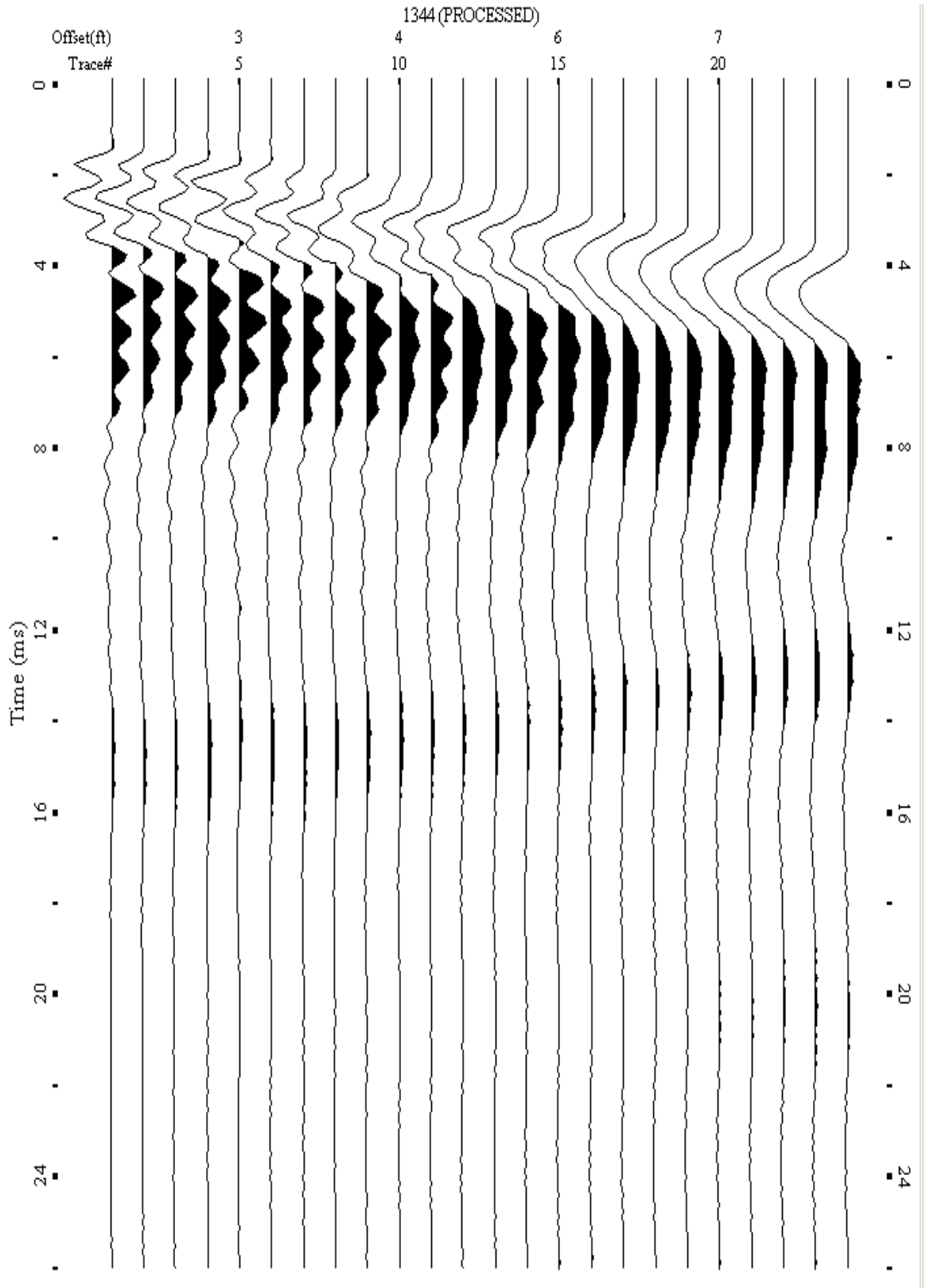

A.553: Shot Gather Line 1344 used in Post-blast 31

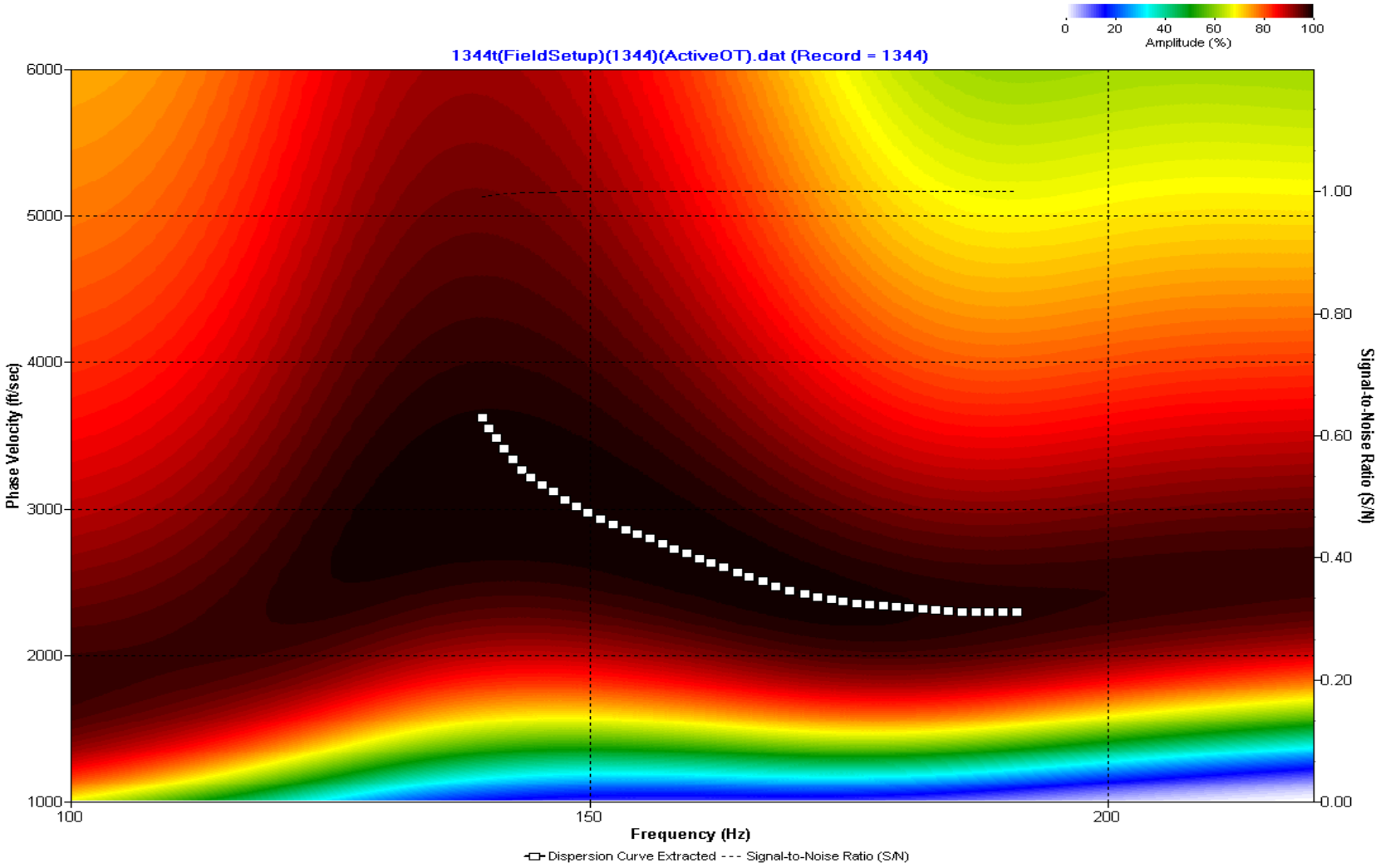

A.554: Dispersion Curve Line 1344 used in Post-blast 31

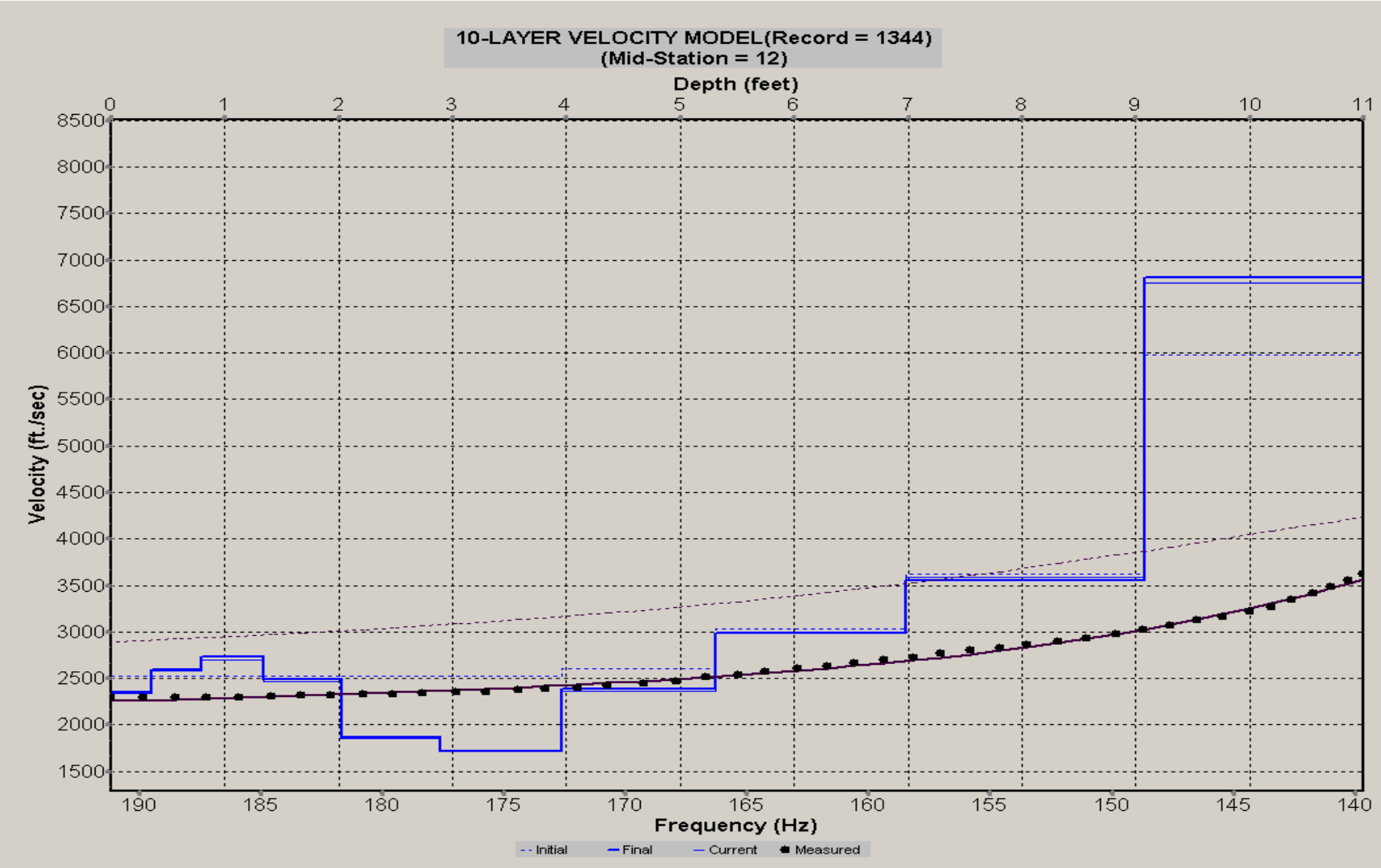

A.555: Velocity Profile Line 1344 used in Post-blast 31

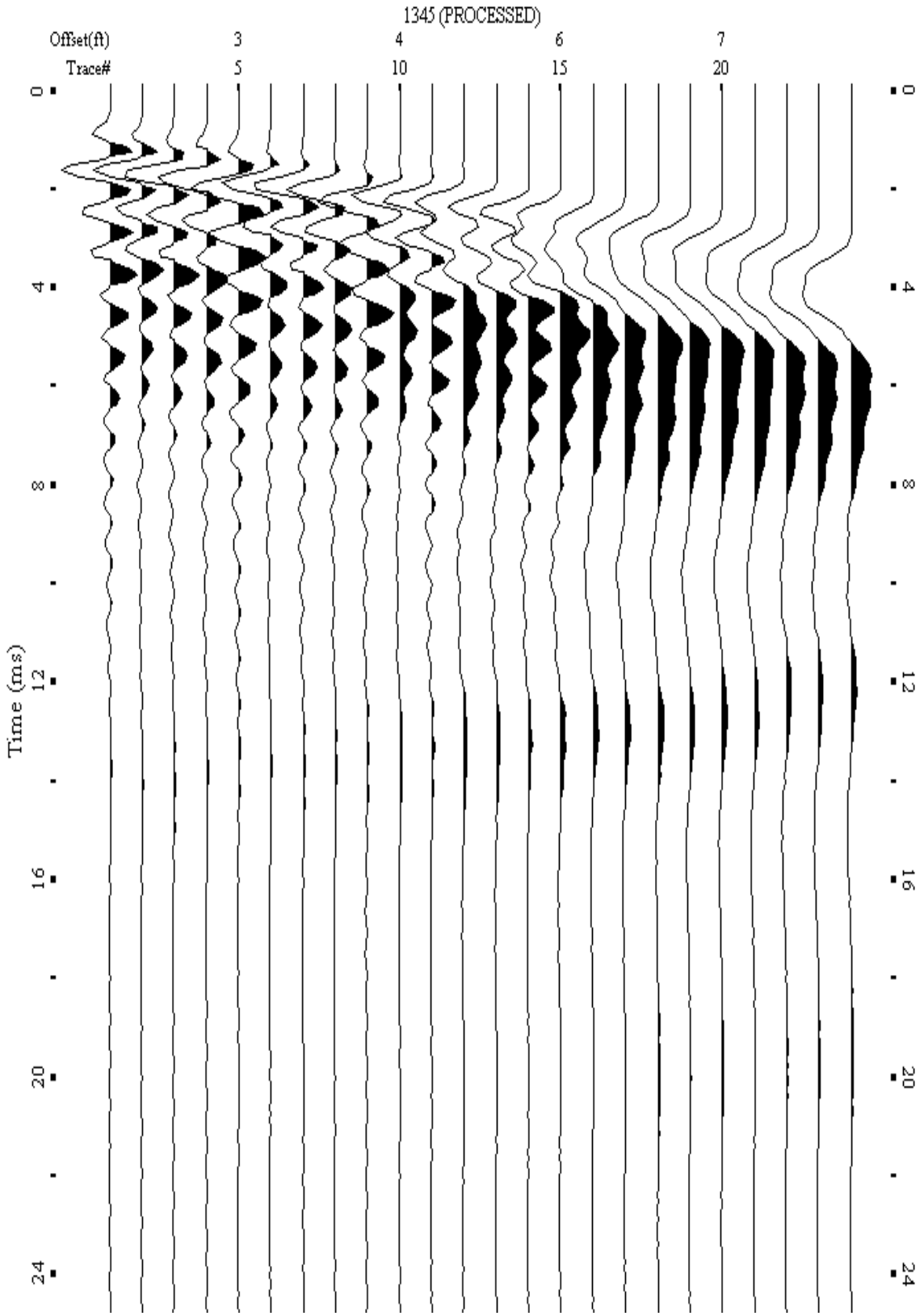

A.556: Shot Gather Line 1345 used in Post-blast 31

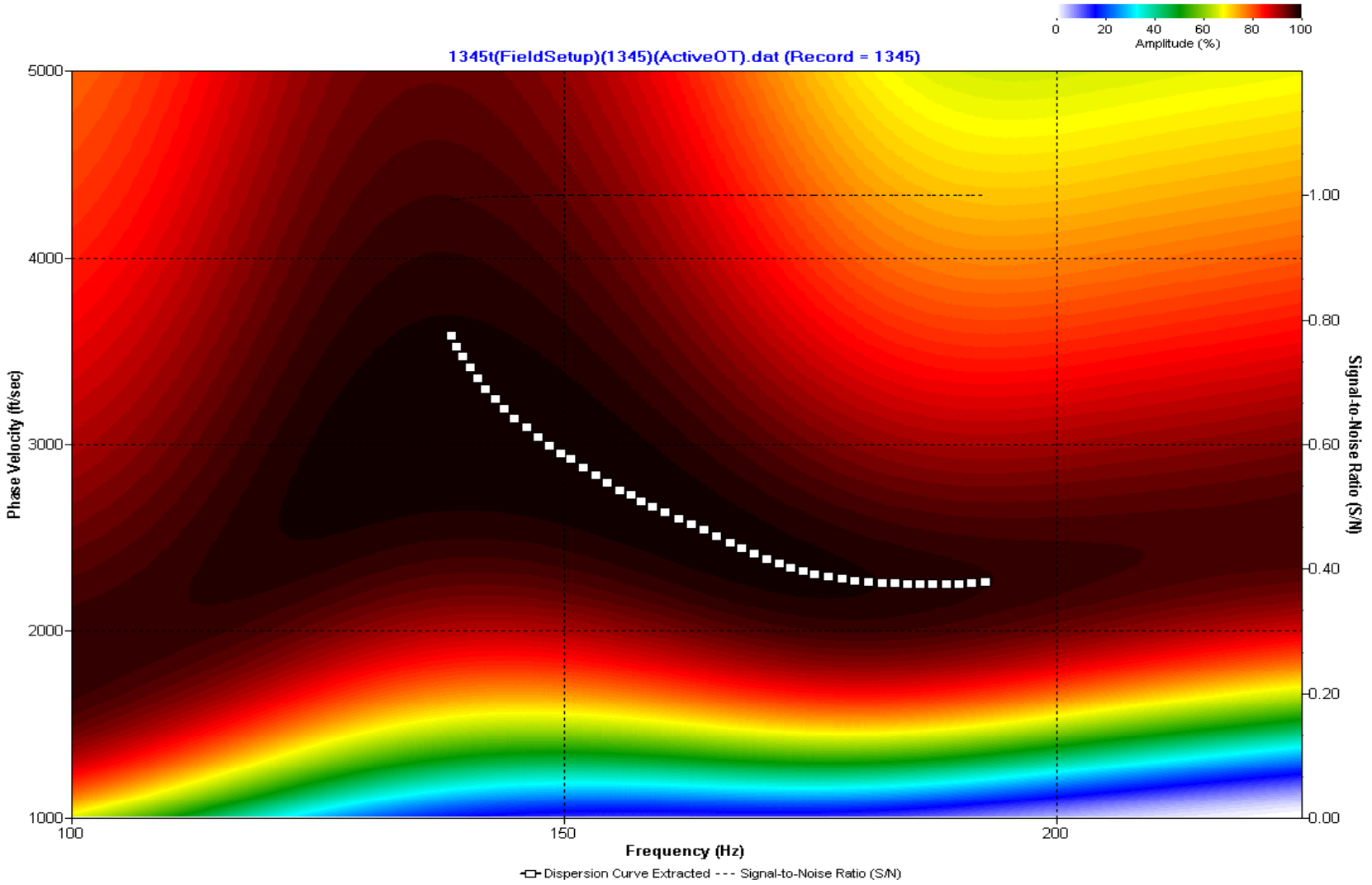

A.557: Dispersion Curve Line 1345 used in Post-blast 31

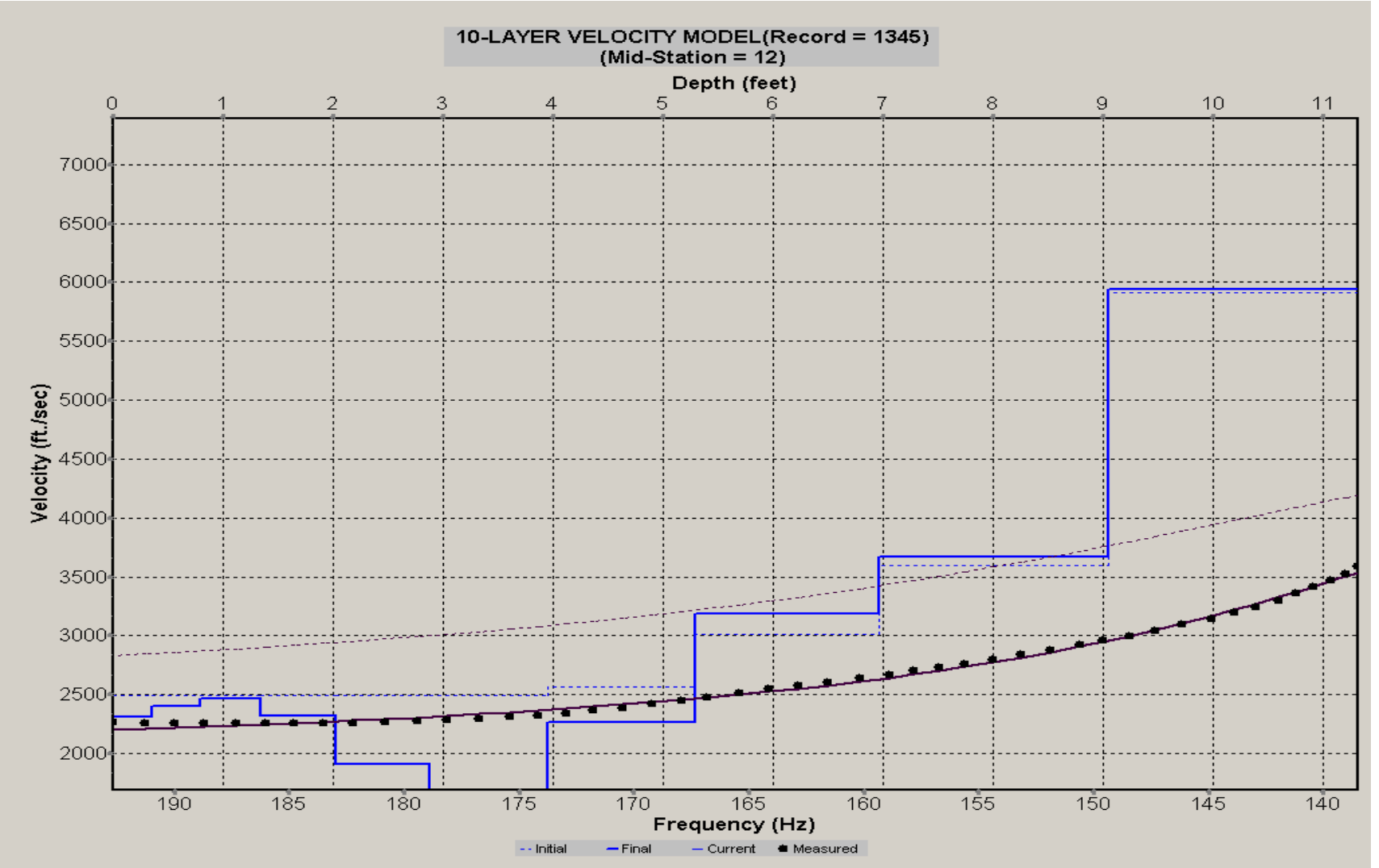

A.558: Velocity Profile Line 1345 used in Post-blast 31

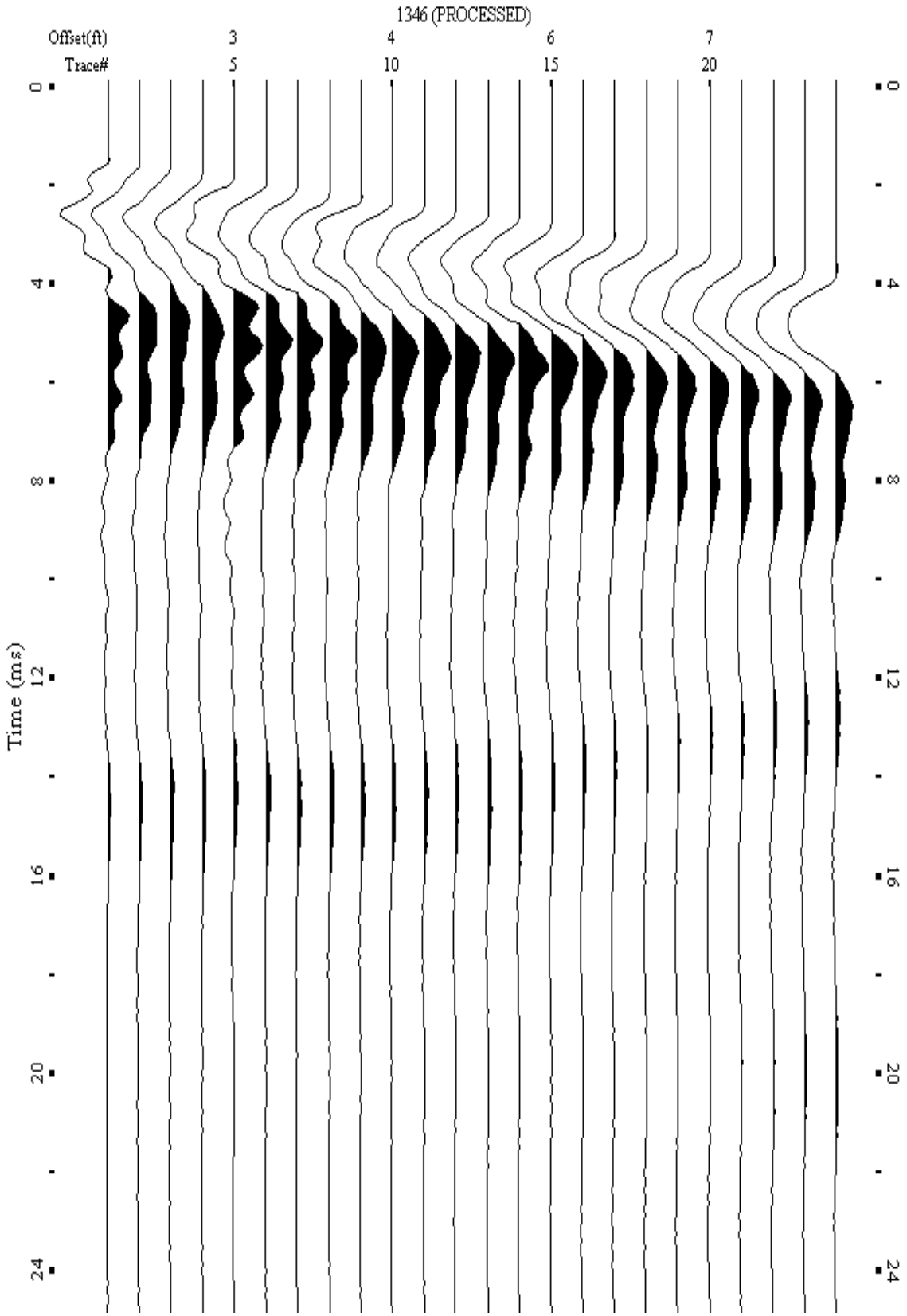

A.559: Shot Gather Line 1346 used in Post-blast 31

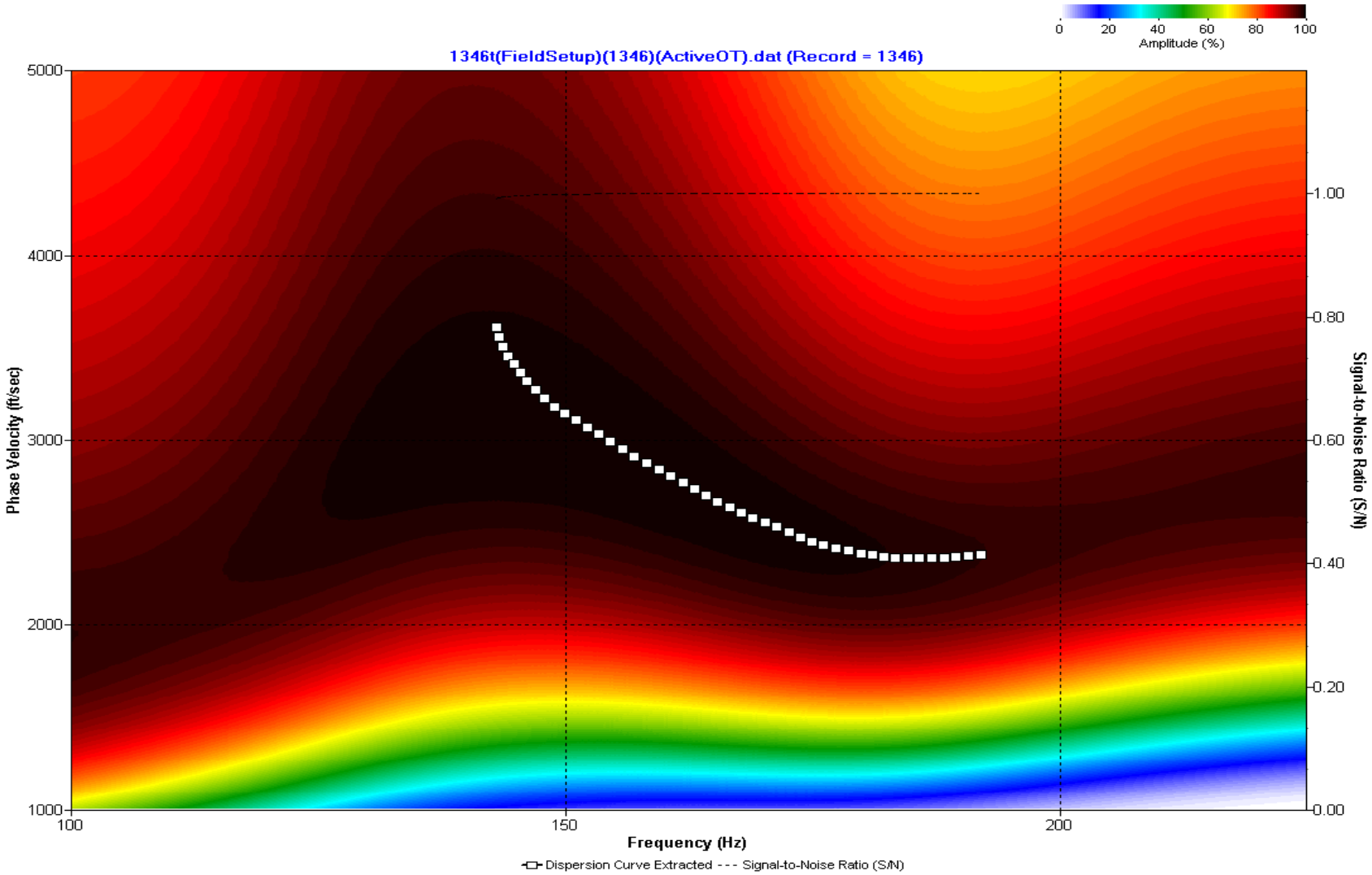

A.560: Dispersion Curve Line 1346 used in Post-blast 31

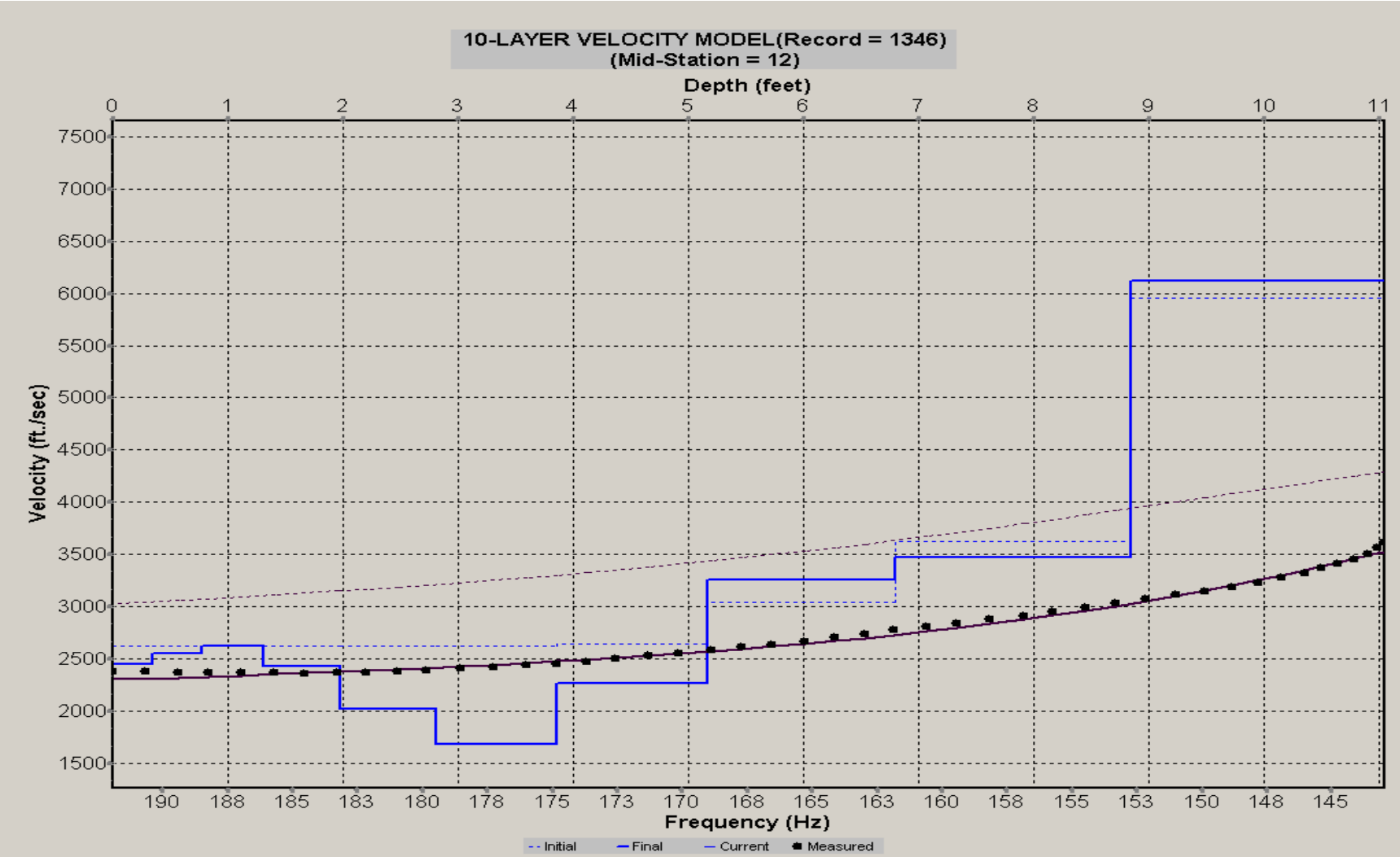

A.561: Velocity Profile Line 1346 used in Post-blast 31

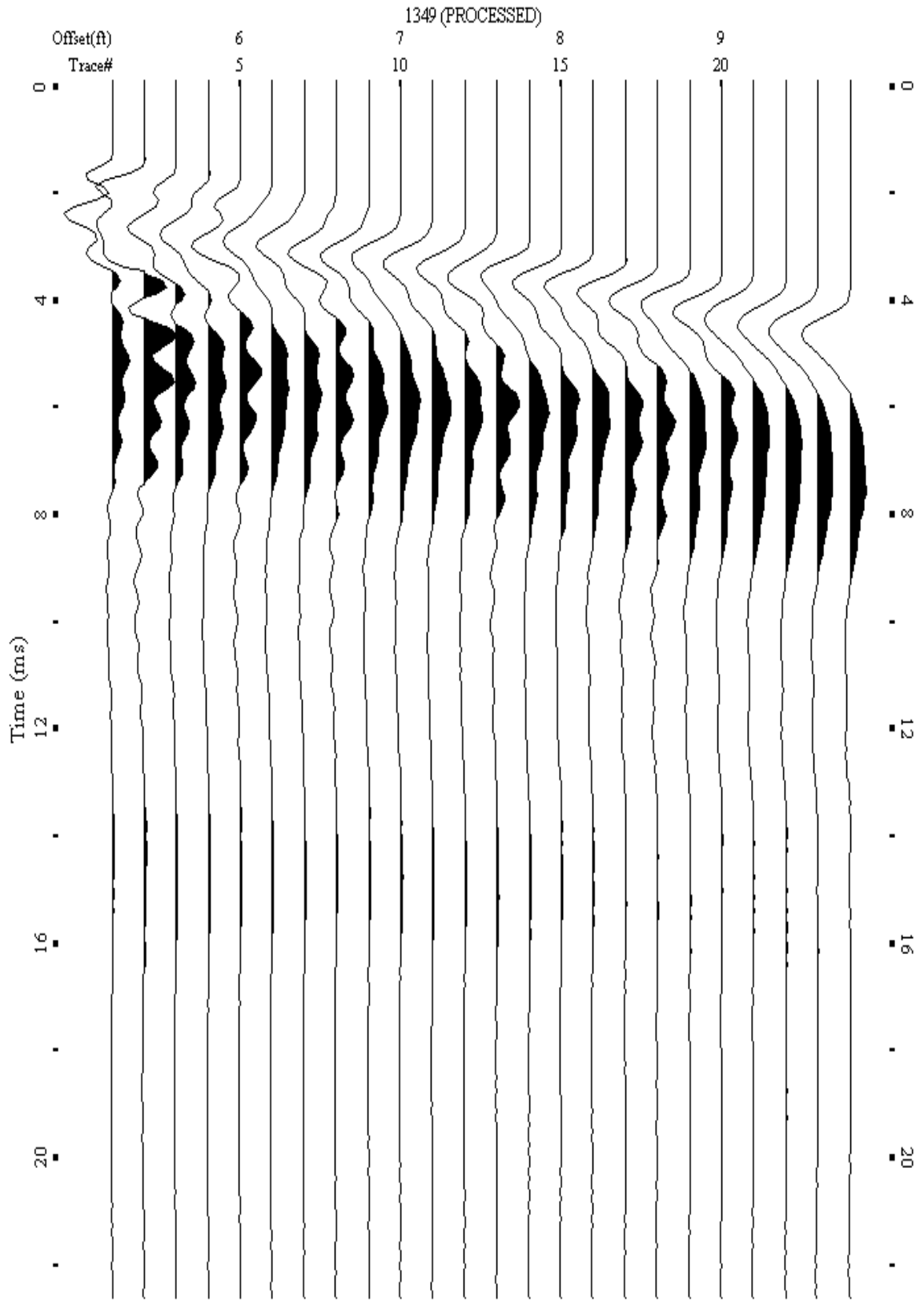

A.562: Shot Gather Line 1349 used in Post-blast 32

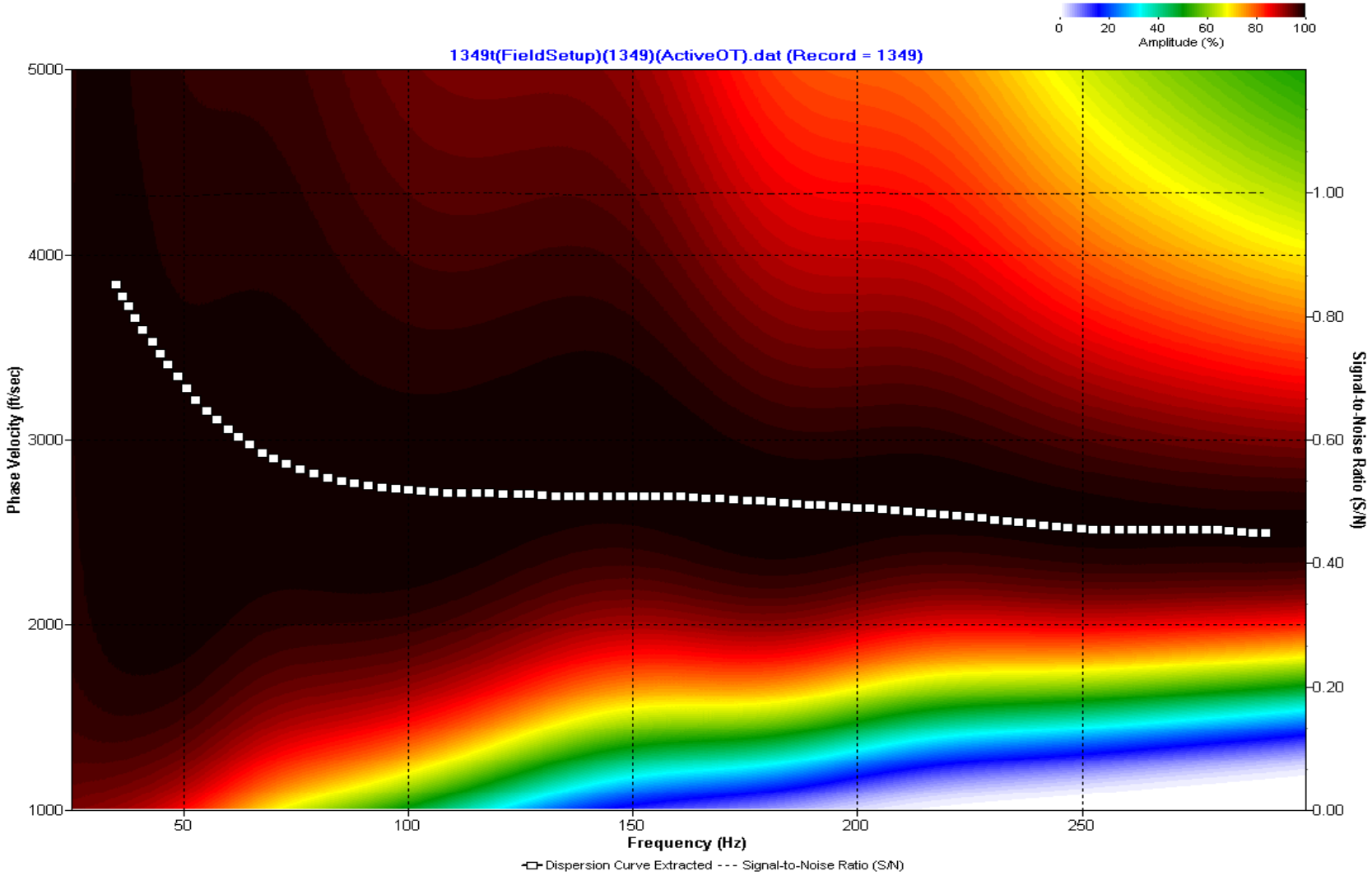

A.563: Dispersion Curve Line 1349 used in Post-blast 32

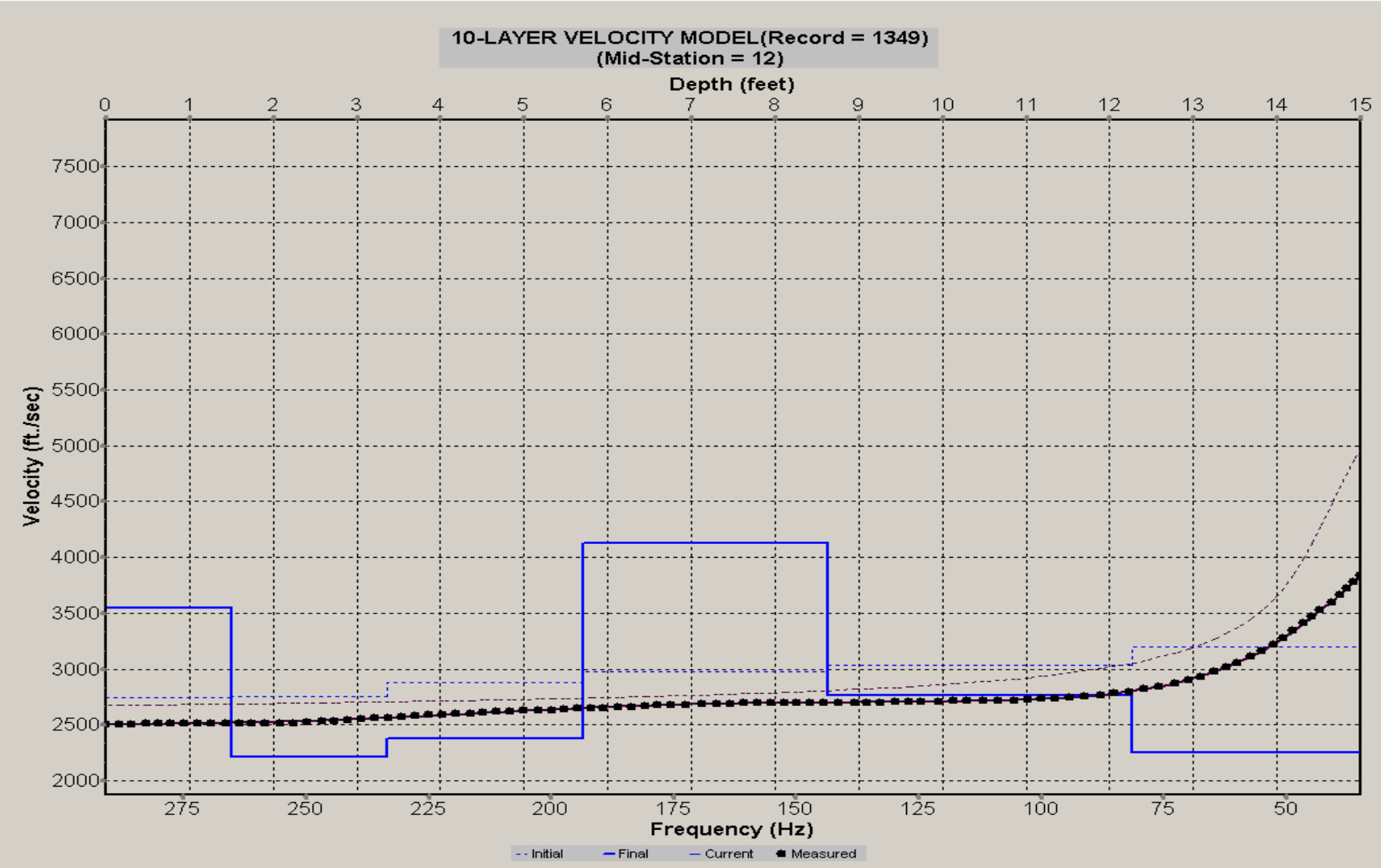

A.564: Velocity Profile Line 1349 used in Post-blast 32

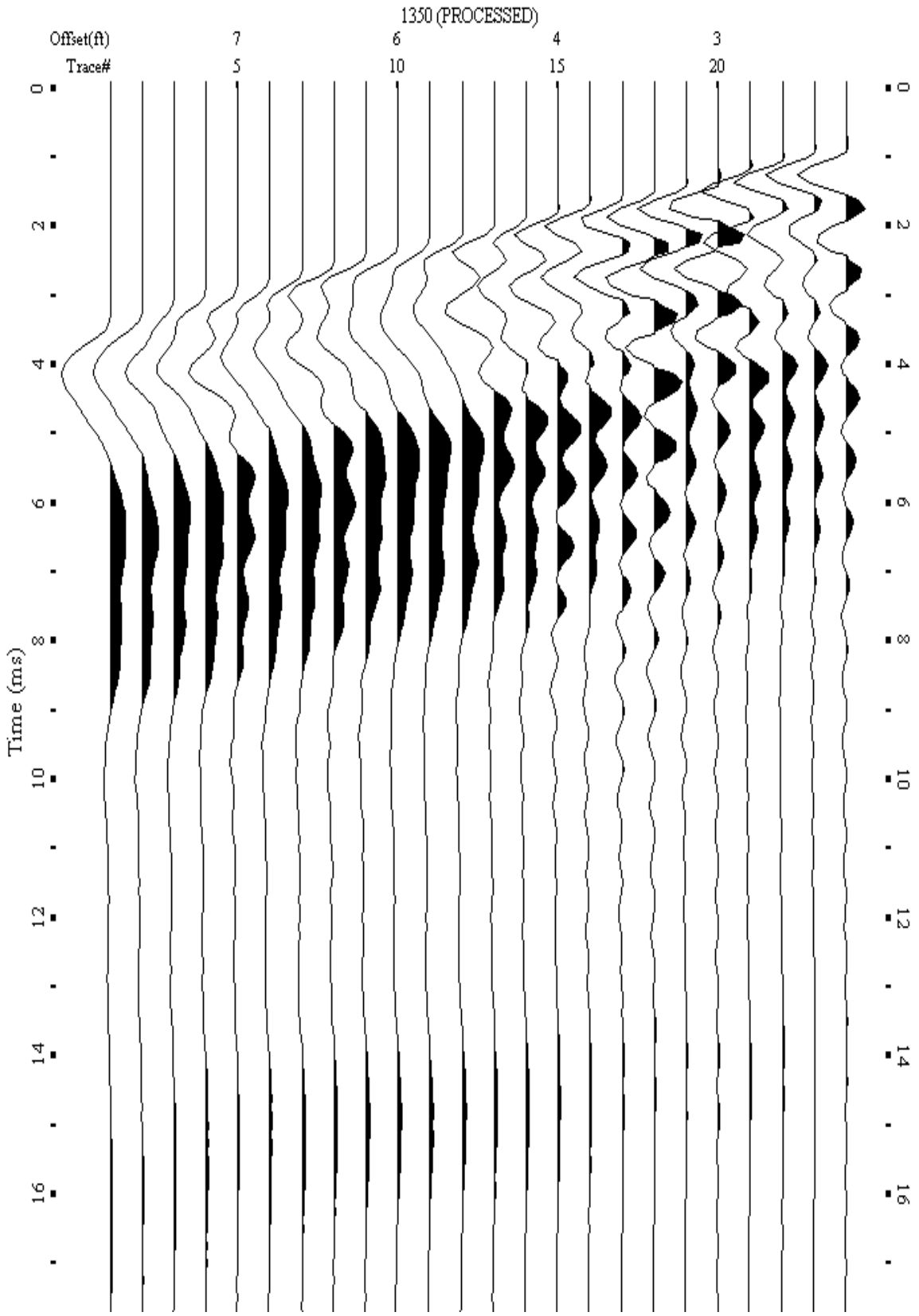

A.565: Shot Gather Line 1350 used in Post-blast 32

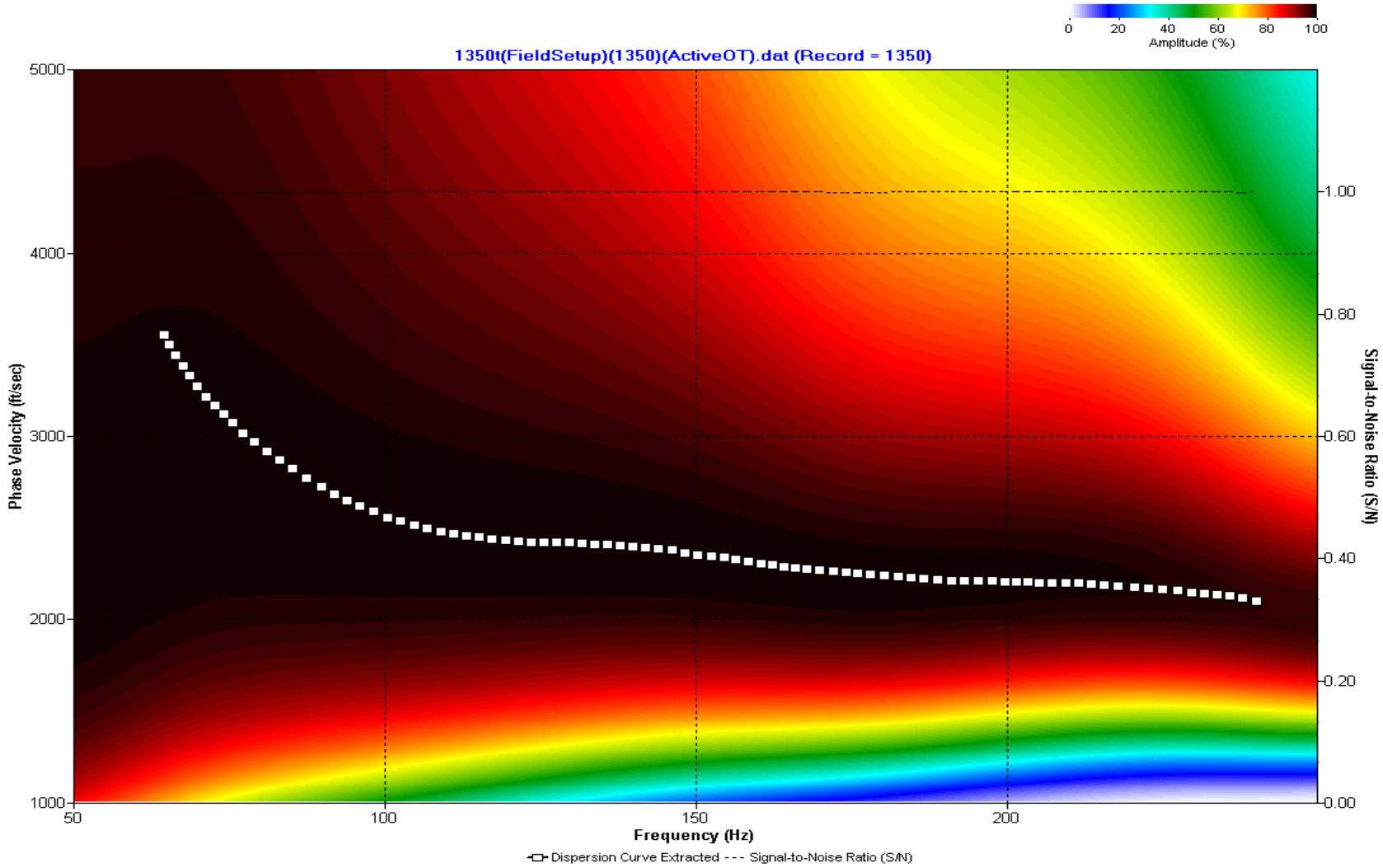

A.566: Dispersion Curve Line 1350 used in Post-blast 32

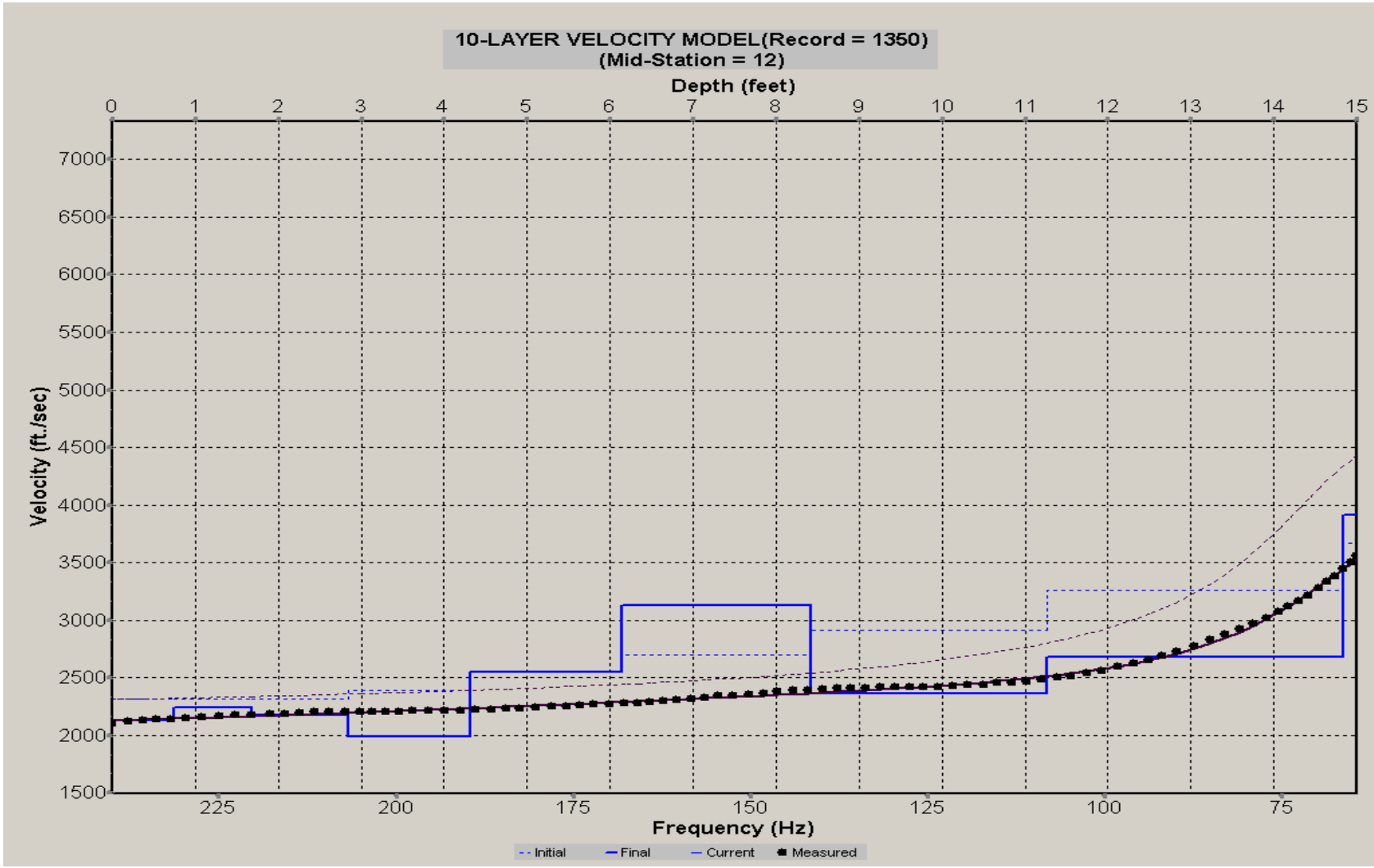

A.567: Velocity Profile Line 1350 used in Post-blast 32

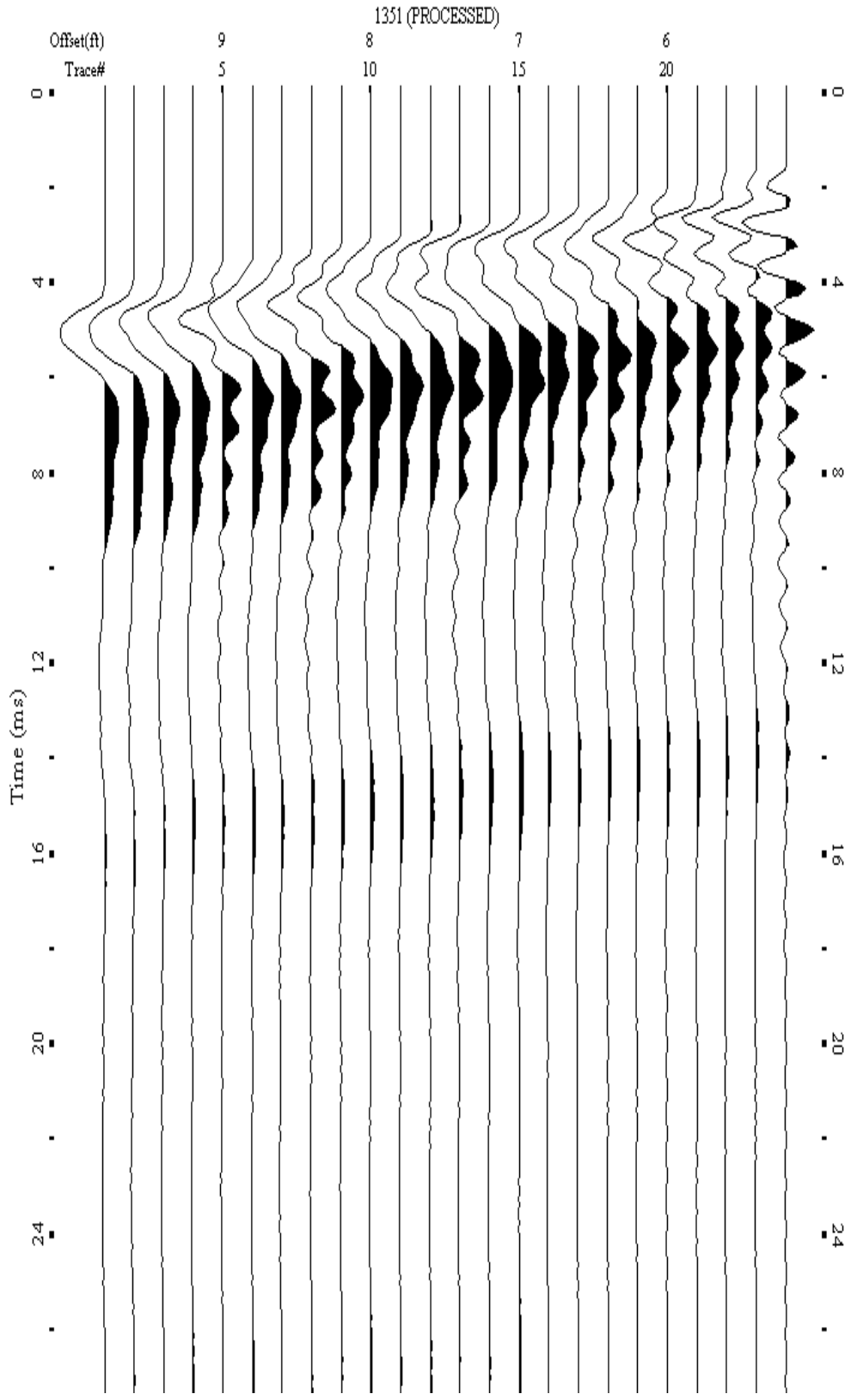

A.568: Shot Gather Line 1351 used in Post-blast 32

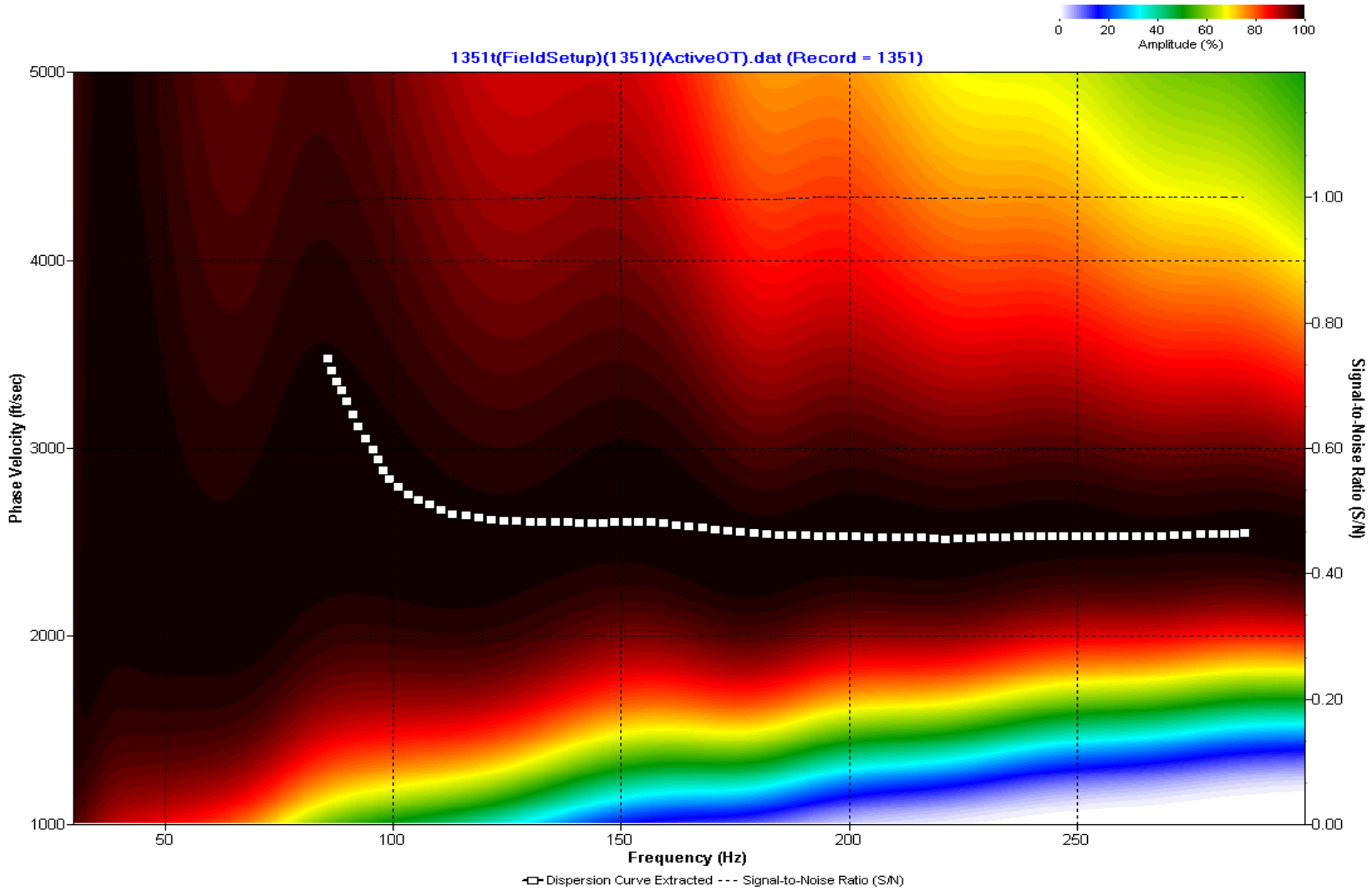

A.569: Dispersion Curve Line 1351 used in Post-blast 32

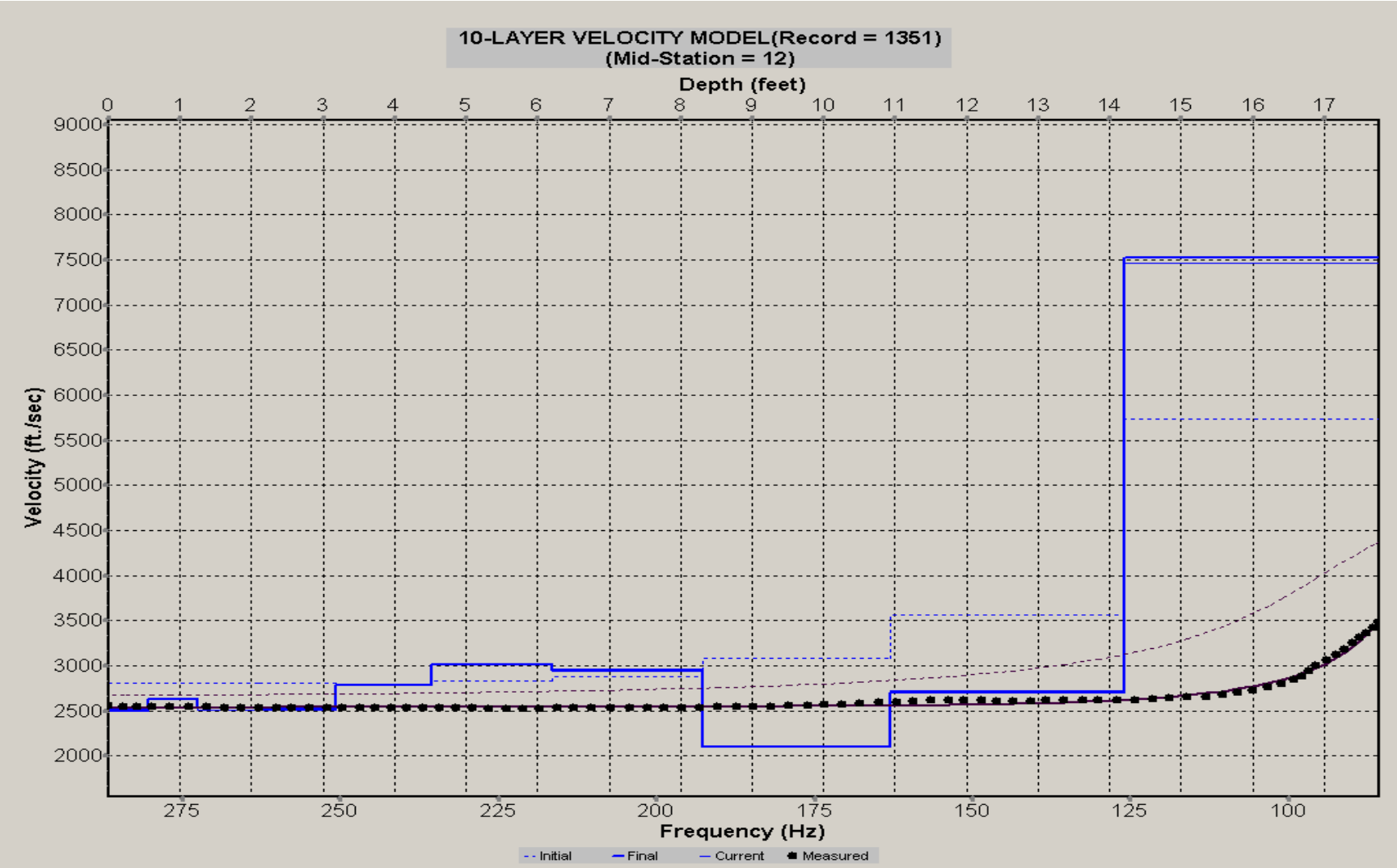

A.570: Velocity Profile Line 1351 used in Post-blast 32

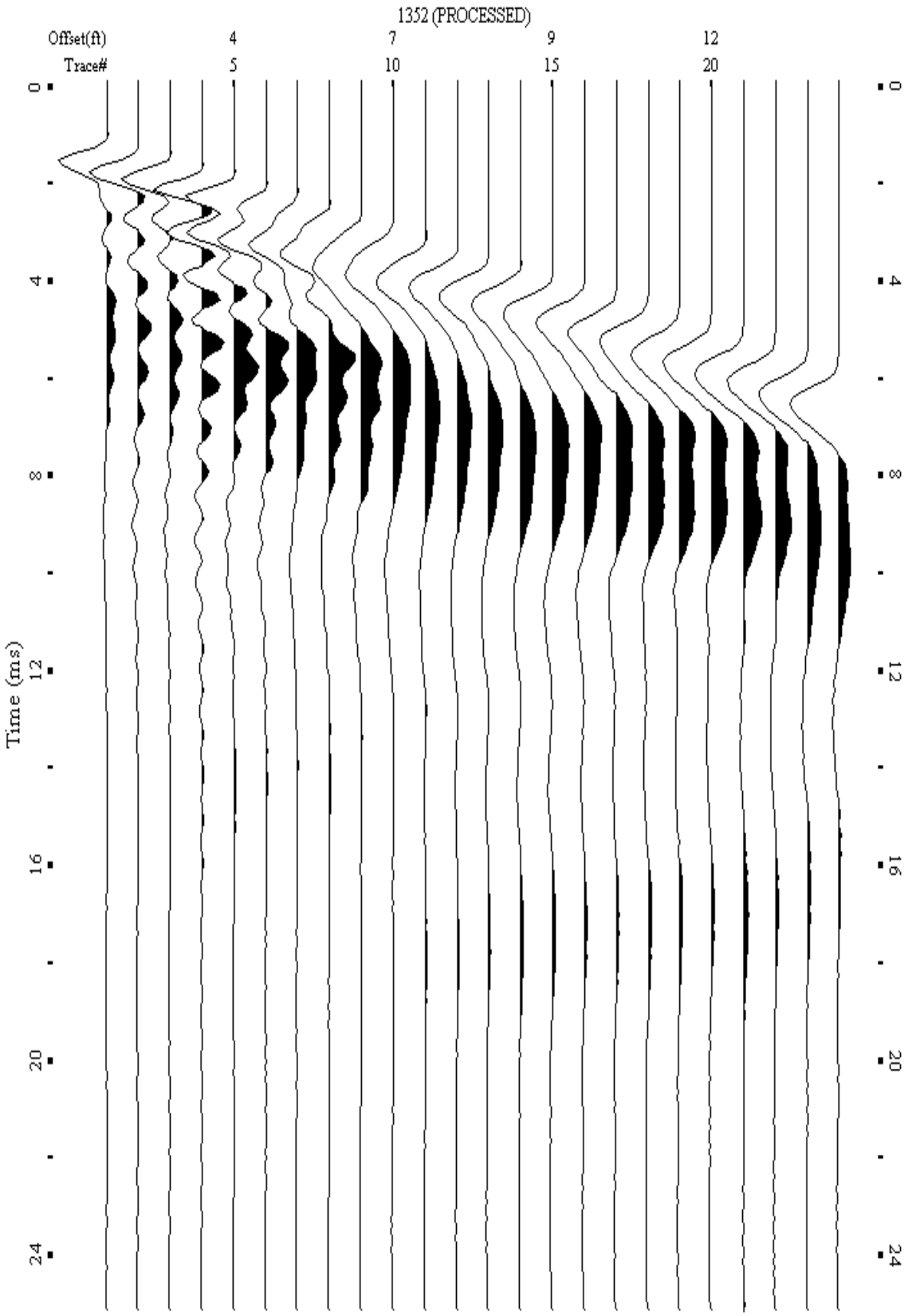

A.571: Shot Gather Line 1352 used in Post-blast 31 and Post-blast 32

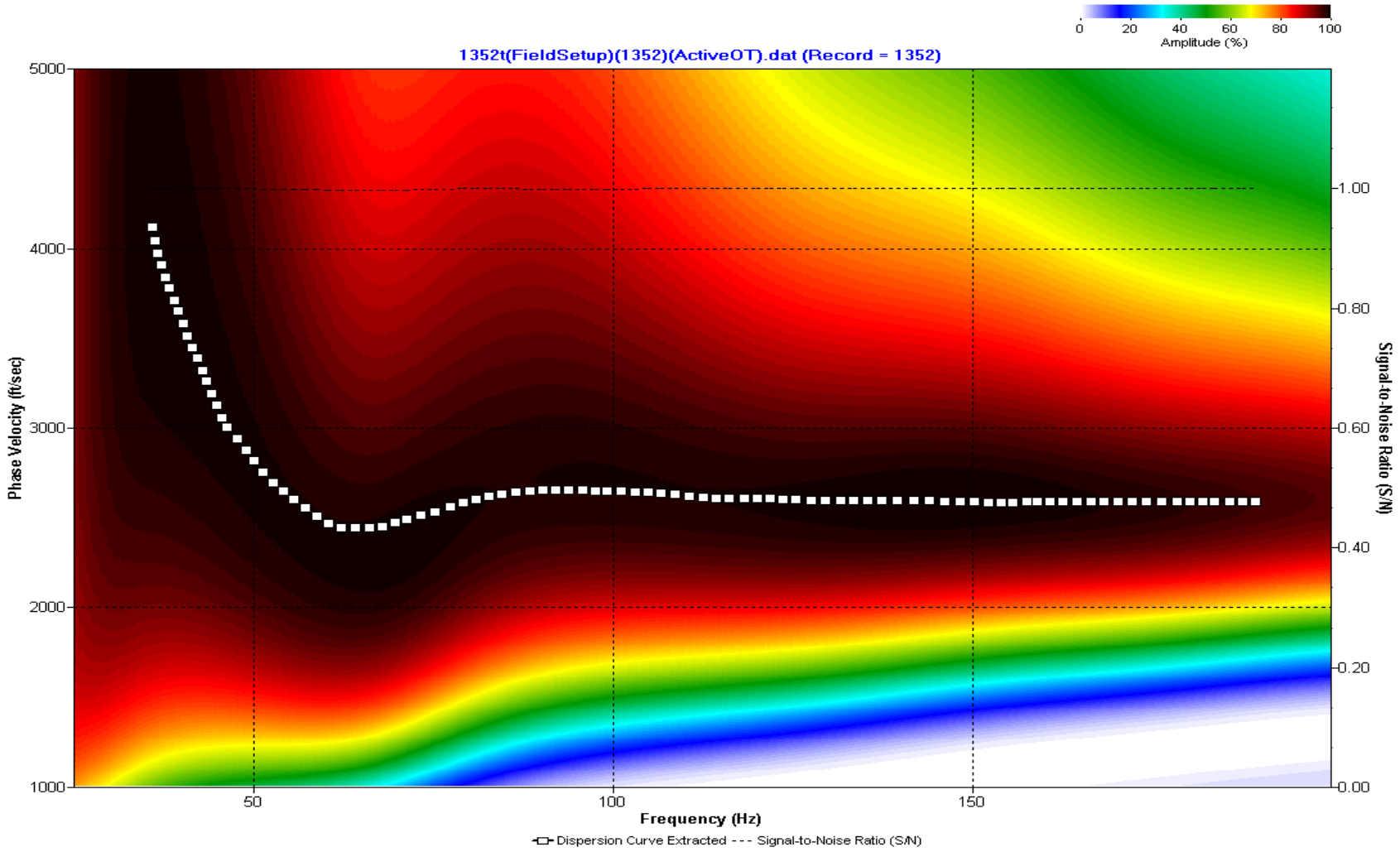

A.572: Dispersion Curve Line 1352 used in Post-blast 31 and Post-blast 32

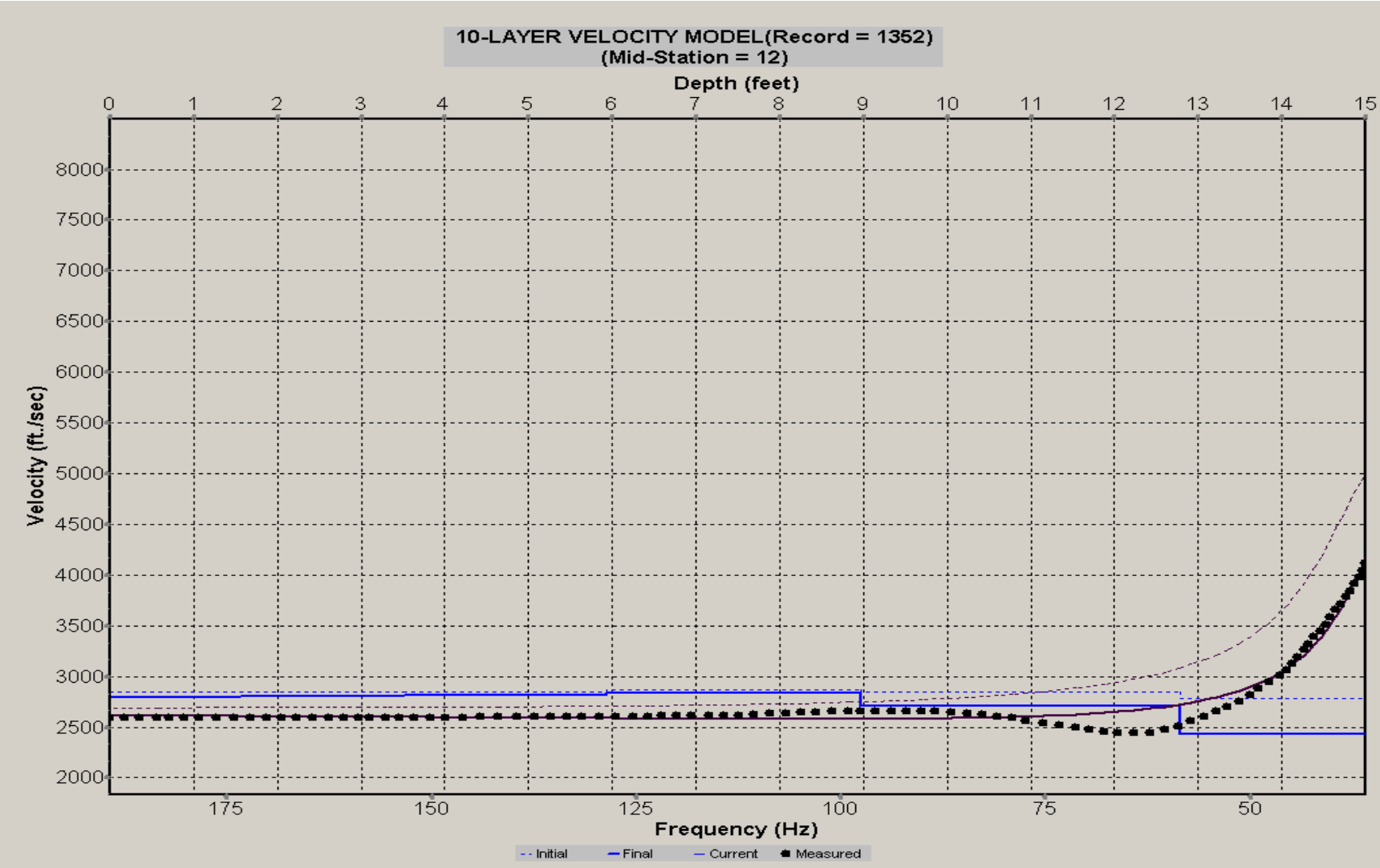

A.573: Velocity Profile Line 1352 used in Post-blast 31 and Post-blast 32

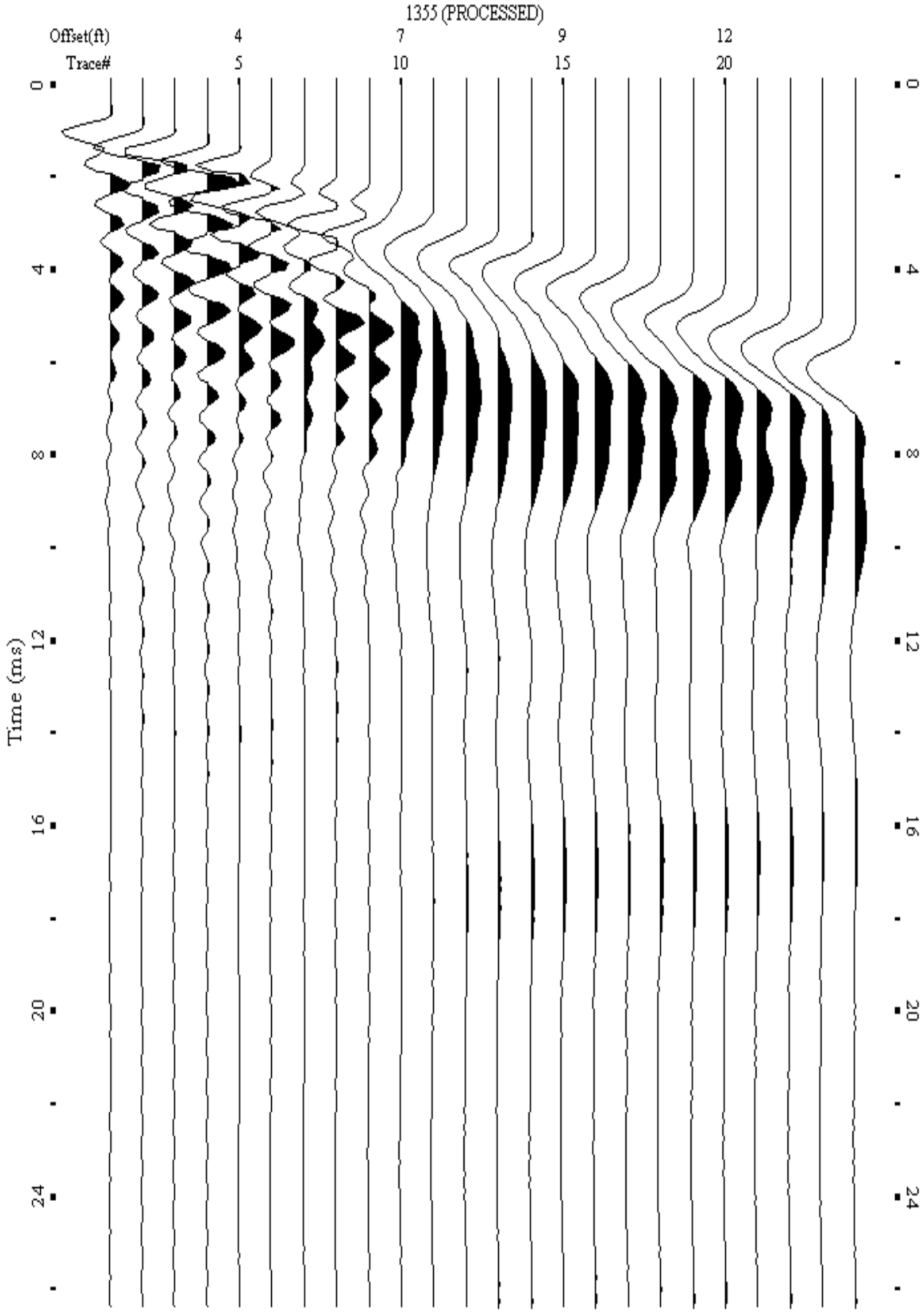

A.574: Shot Gather Line 1355 used in Post-blast 31 and Post-blast 32

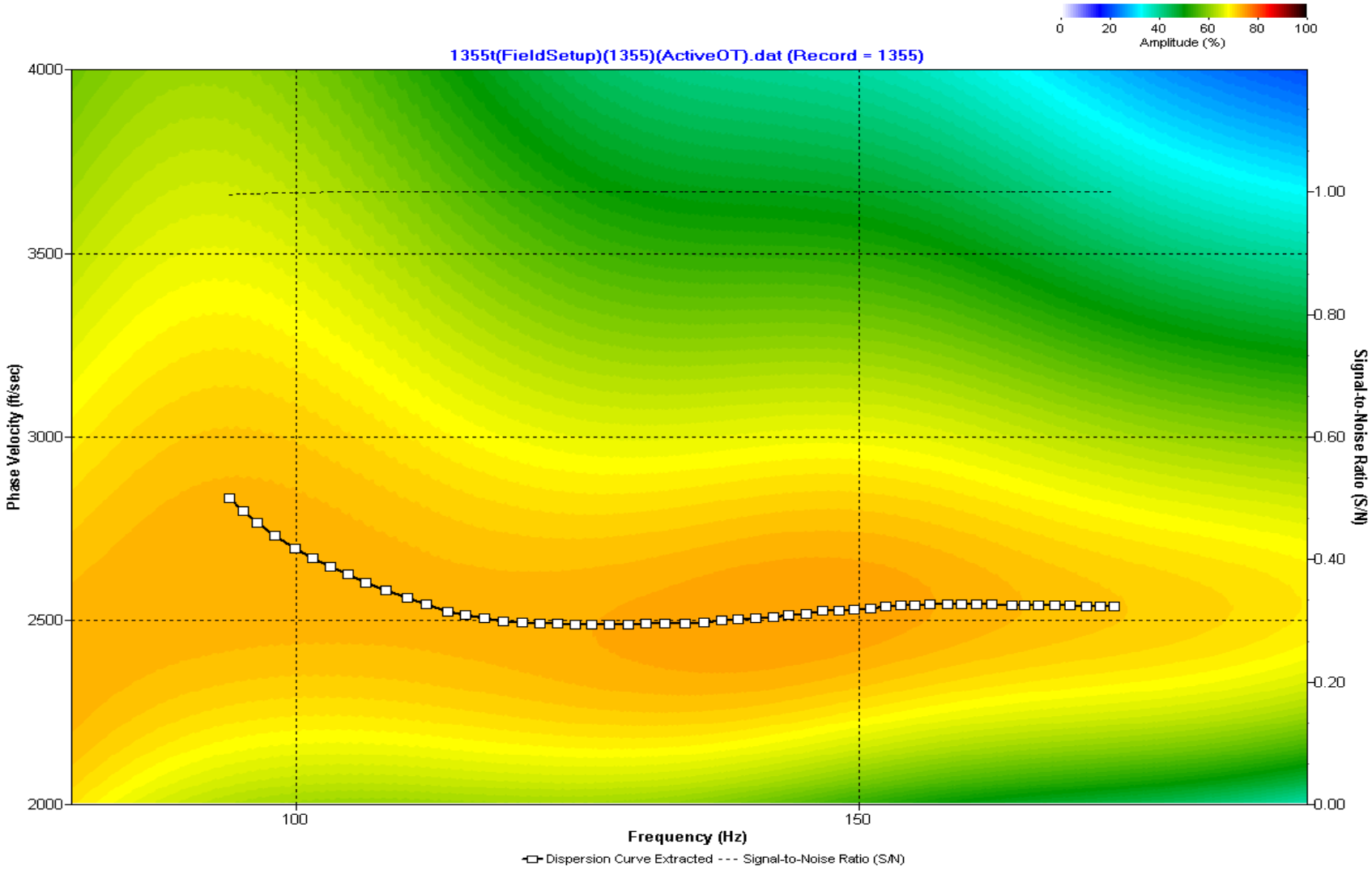

A.575: Dispersion Curve Line 1355 used in Post-blast 31 and Post-blast 32

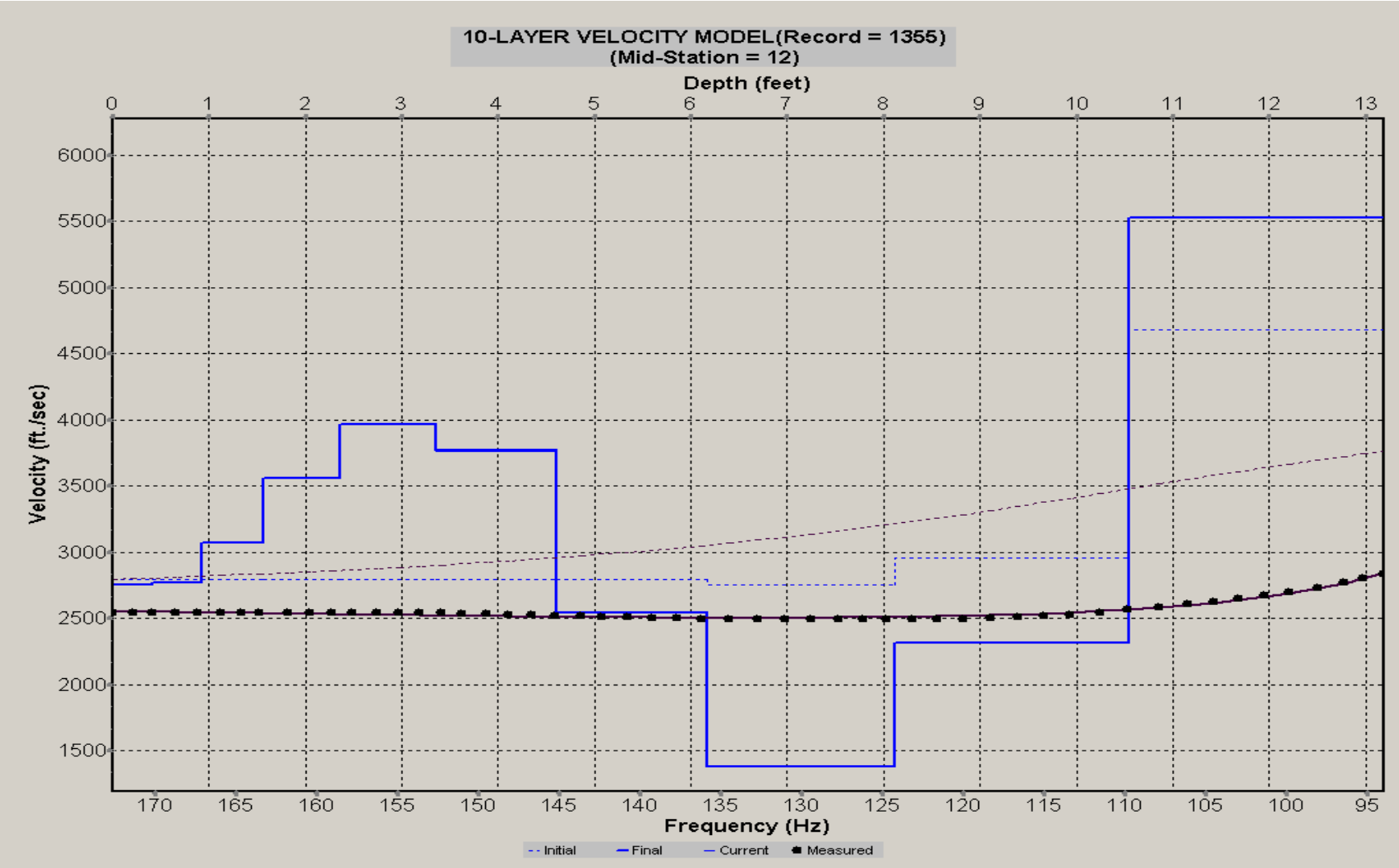

A.576: Velocity Profile Line 1355 used in Post-blast 31 and Post-blast 32

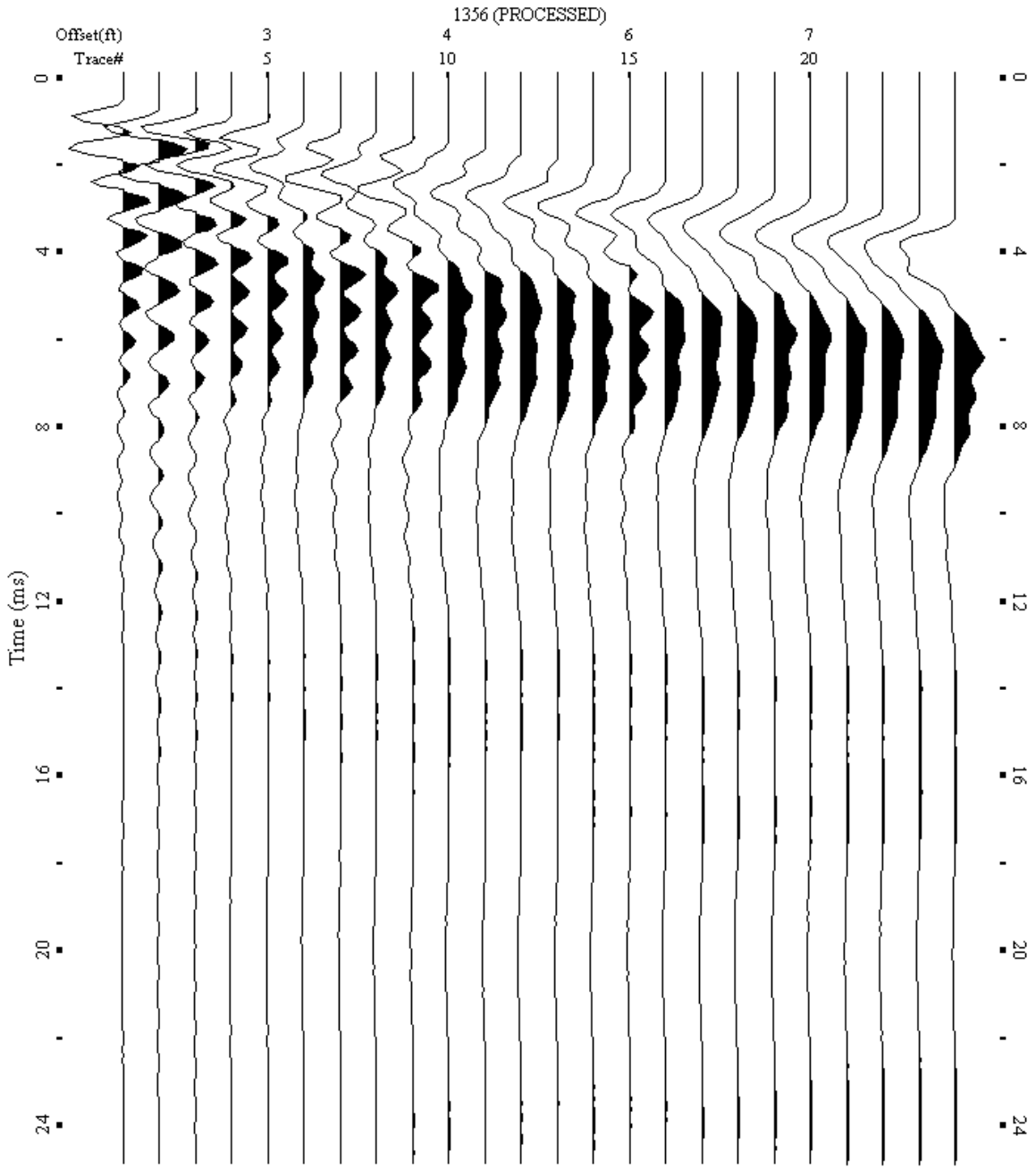

A.577: Shot Gather Line 1356 used in Post-blast 33

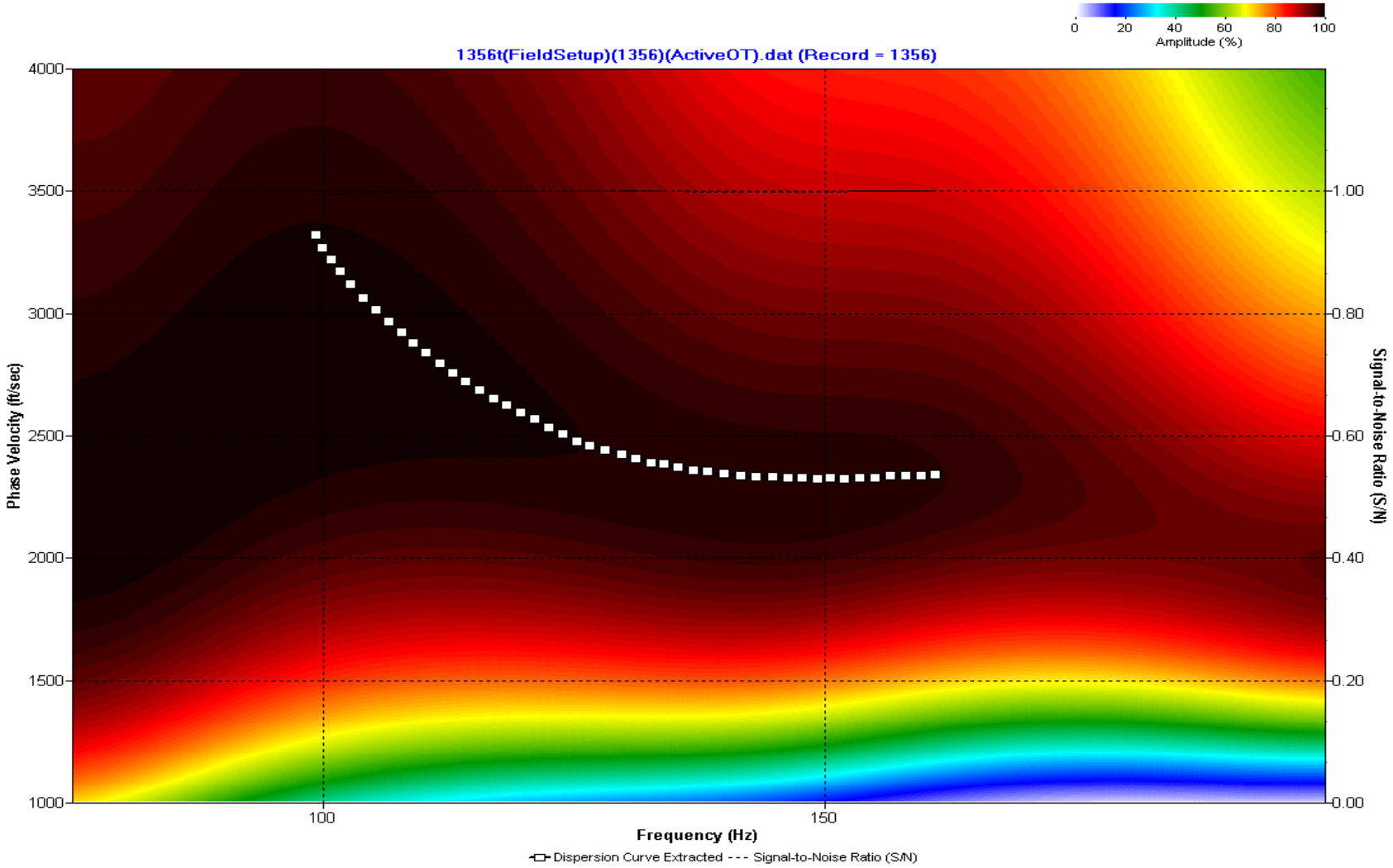

A.578: Dispersion Curve Line 1356 used in Post-blast 33

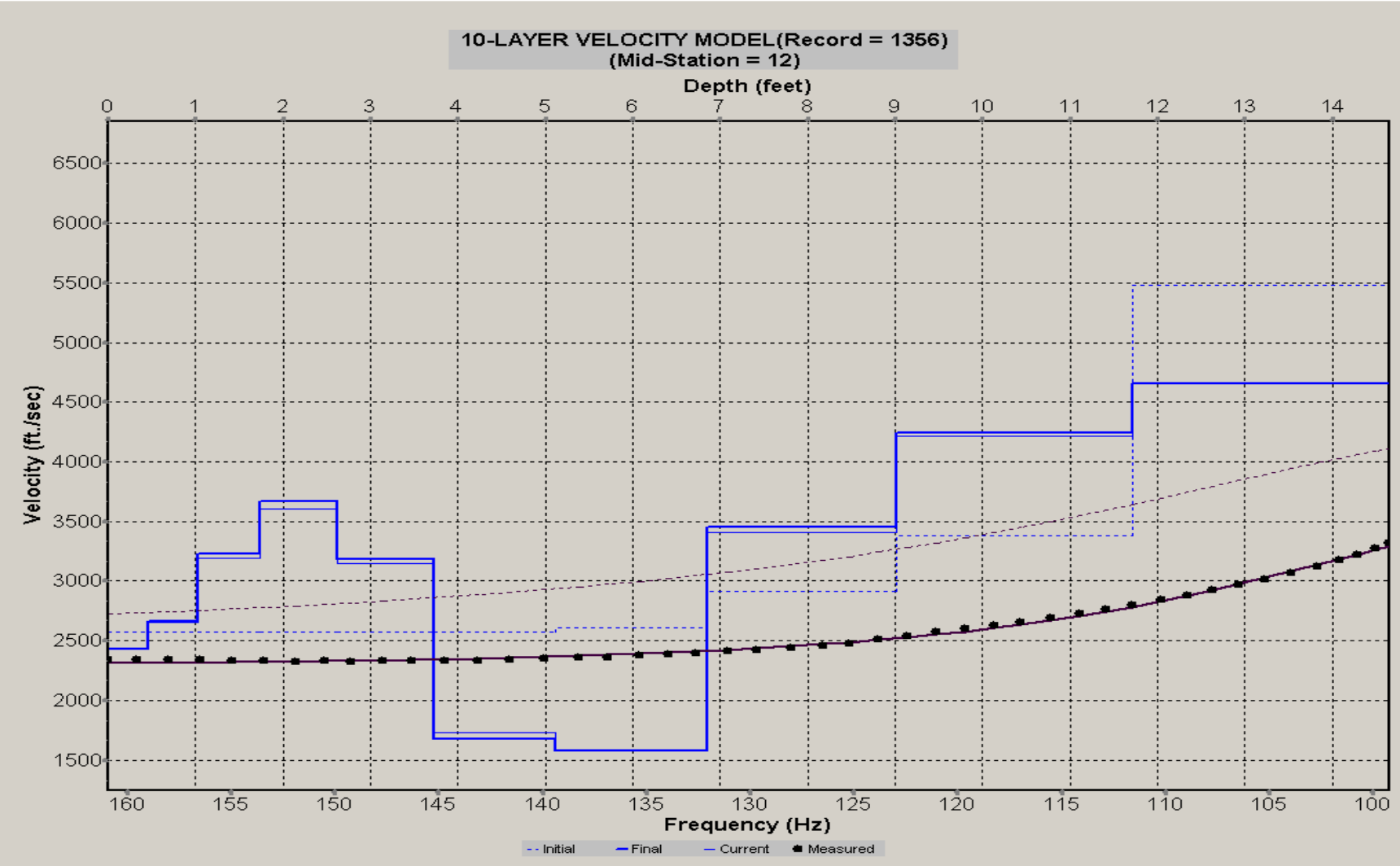

A.579: Velocity Profile Line 1356 used in Post-blast 33

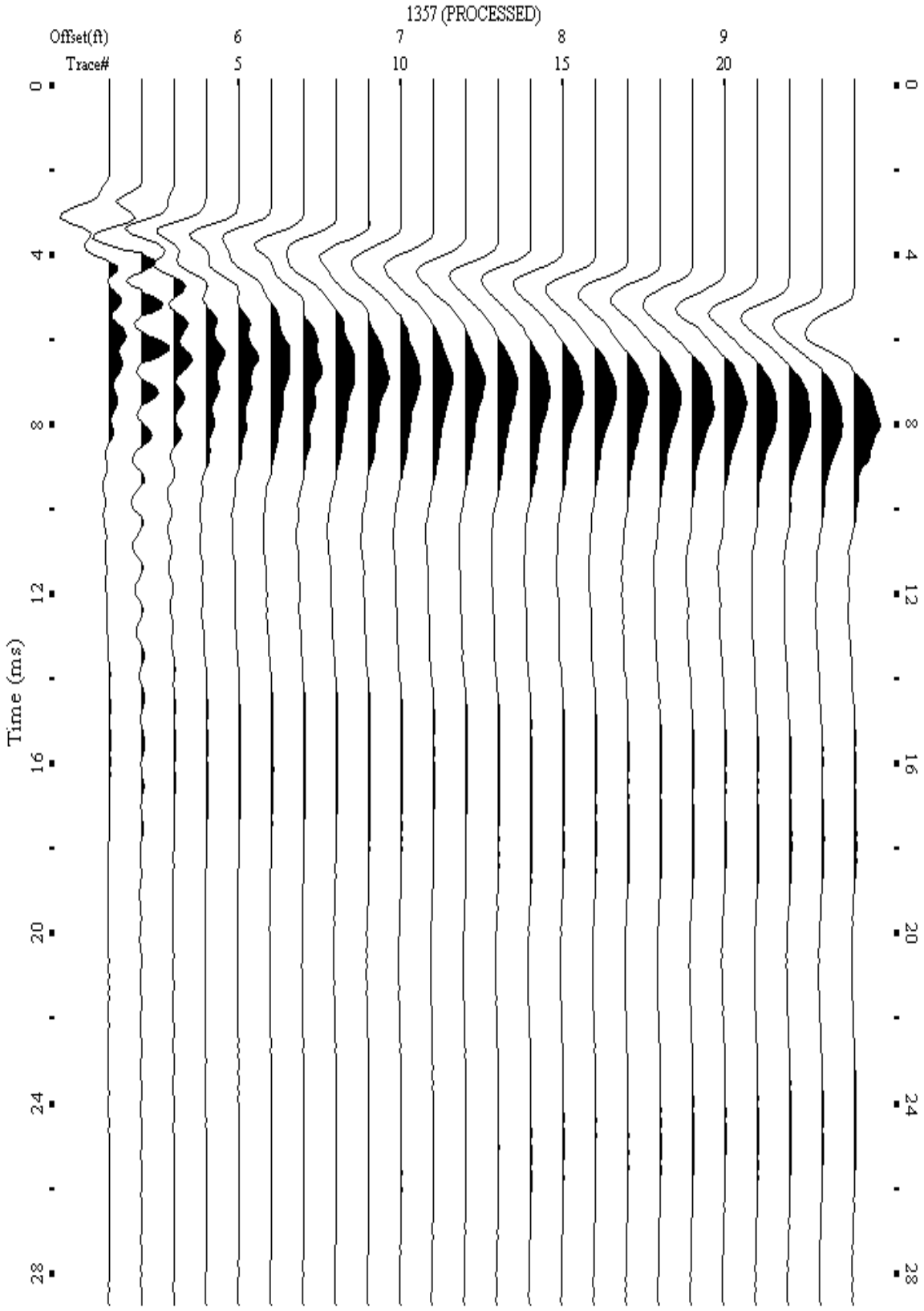

A.580: Shot Gather Line 1357 used in Post-blast 33

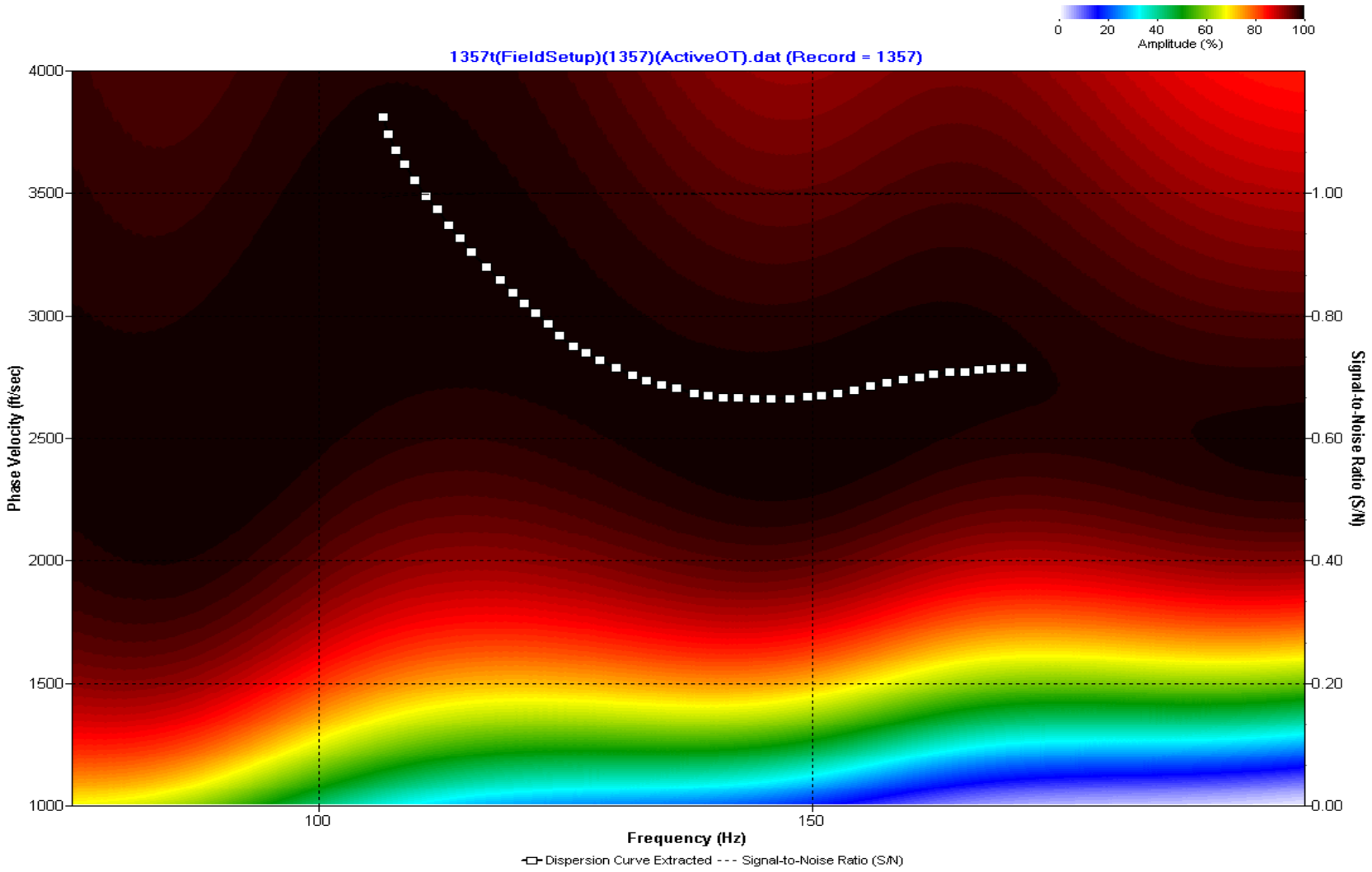

A.581: Dispersion Curve Line 1357 used in Post-blast 33

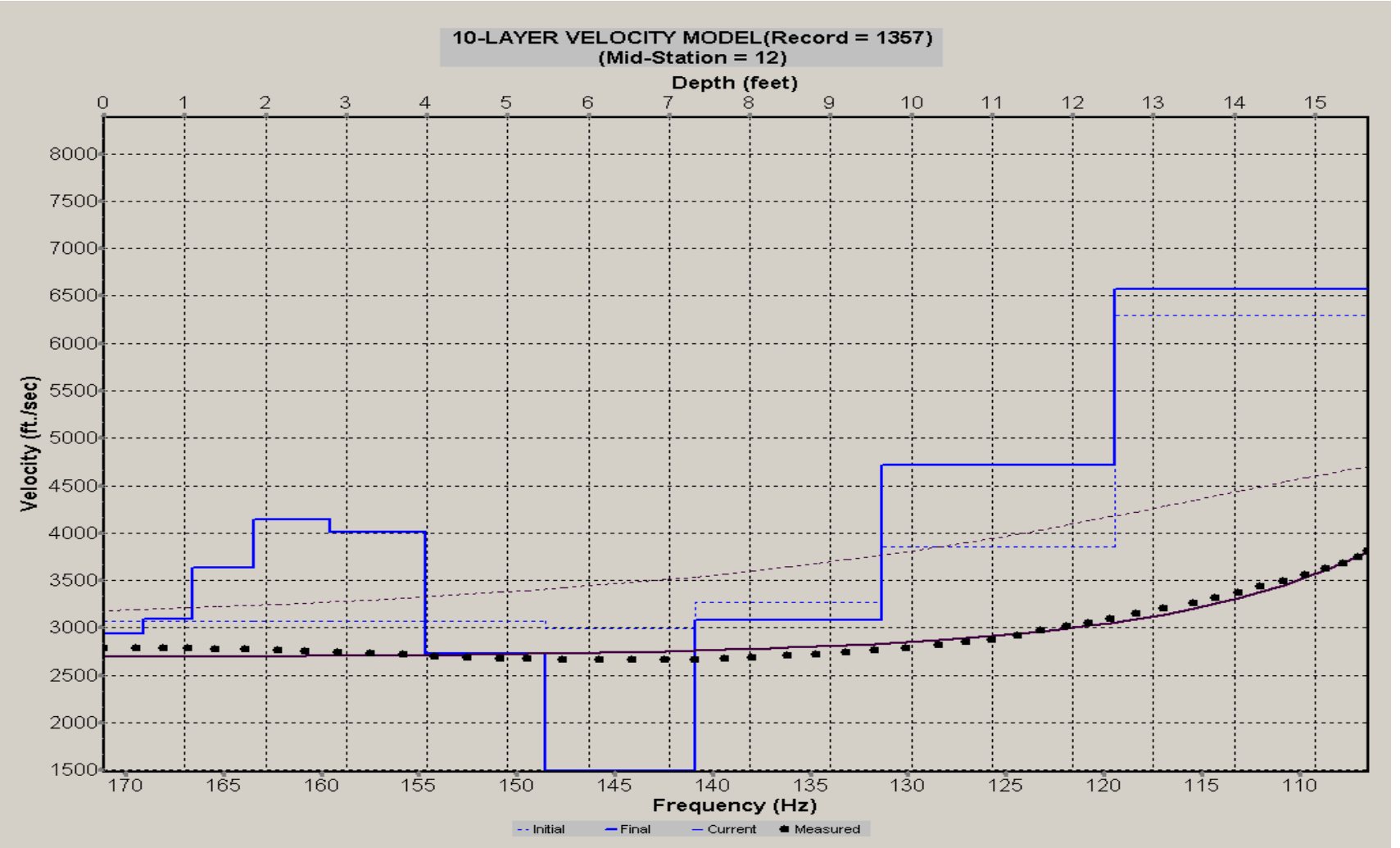

A.582: Velocity Profile Line 1357 used in Post-blast 33

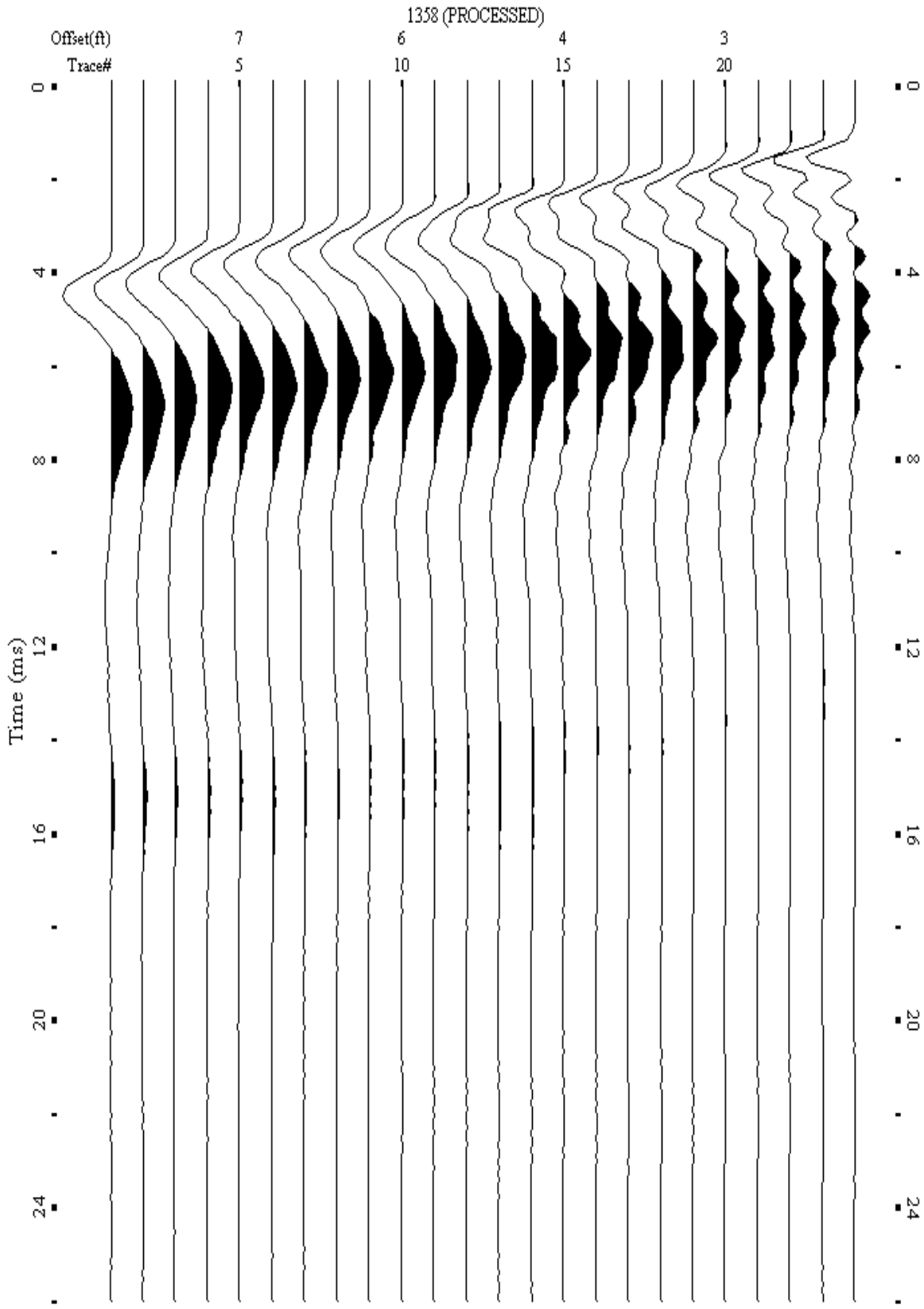

A.583: Shot Gather Line 1358 used in Post-blast 33

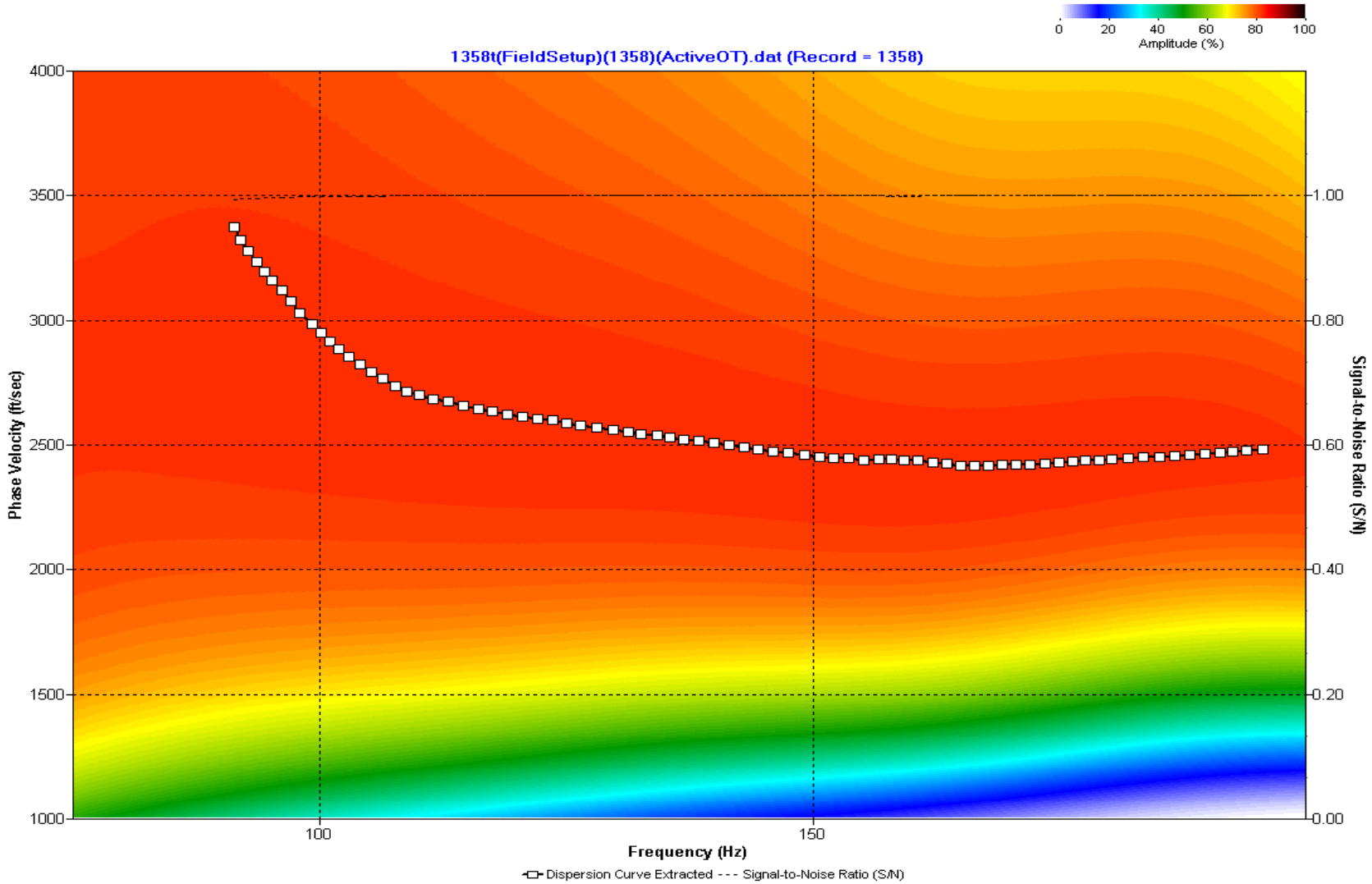

A.584: Dispersion Curve Line 1358 used in Post-blast 33

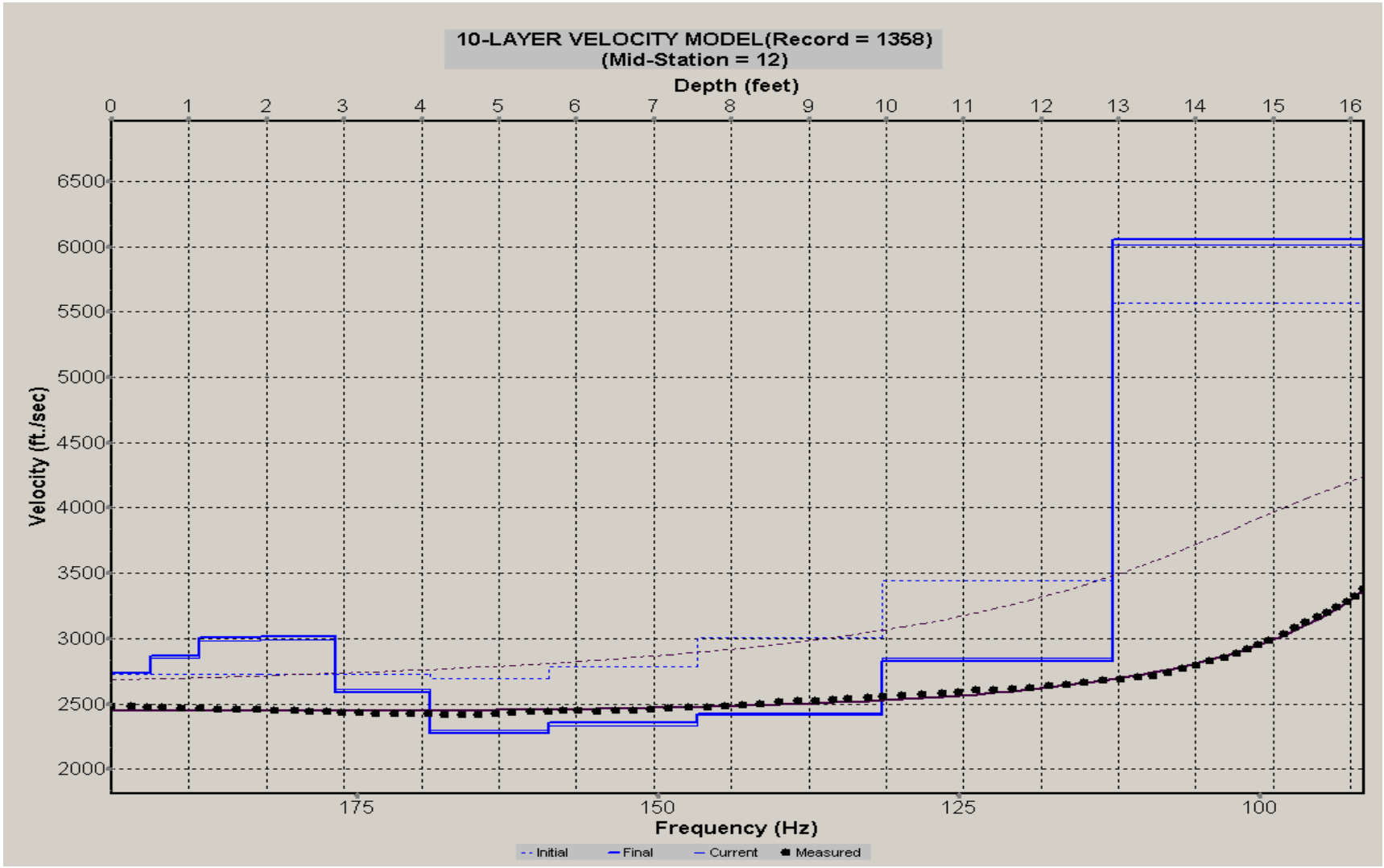

A.585: Velocity Profile Line 1358 used in Post-blast 33

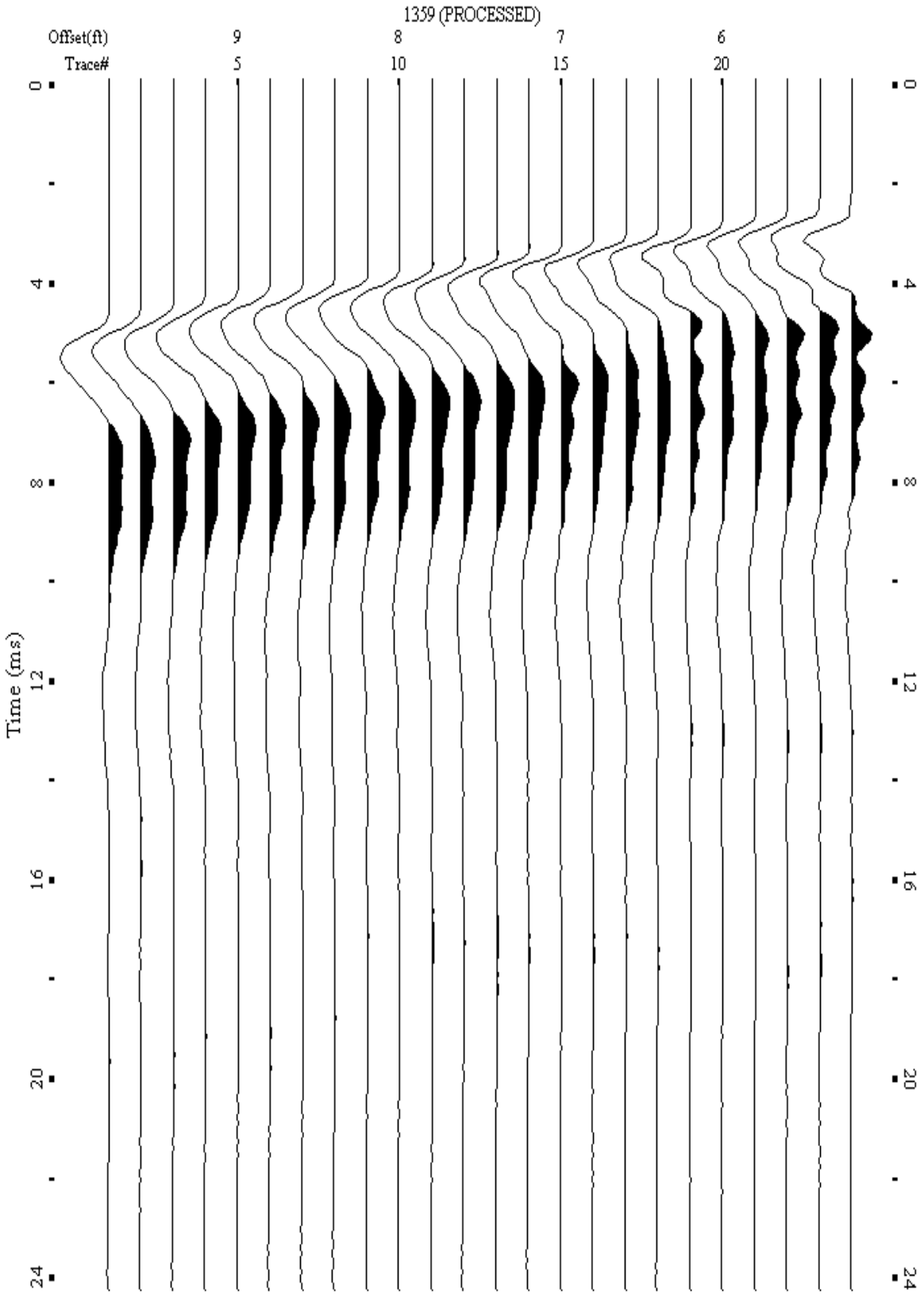

A.586: Shot Gather Line 1359 used in Post-blast 33

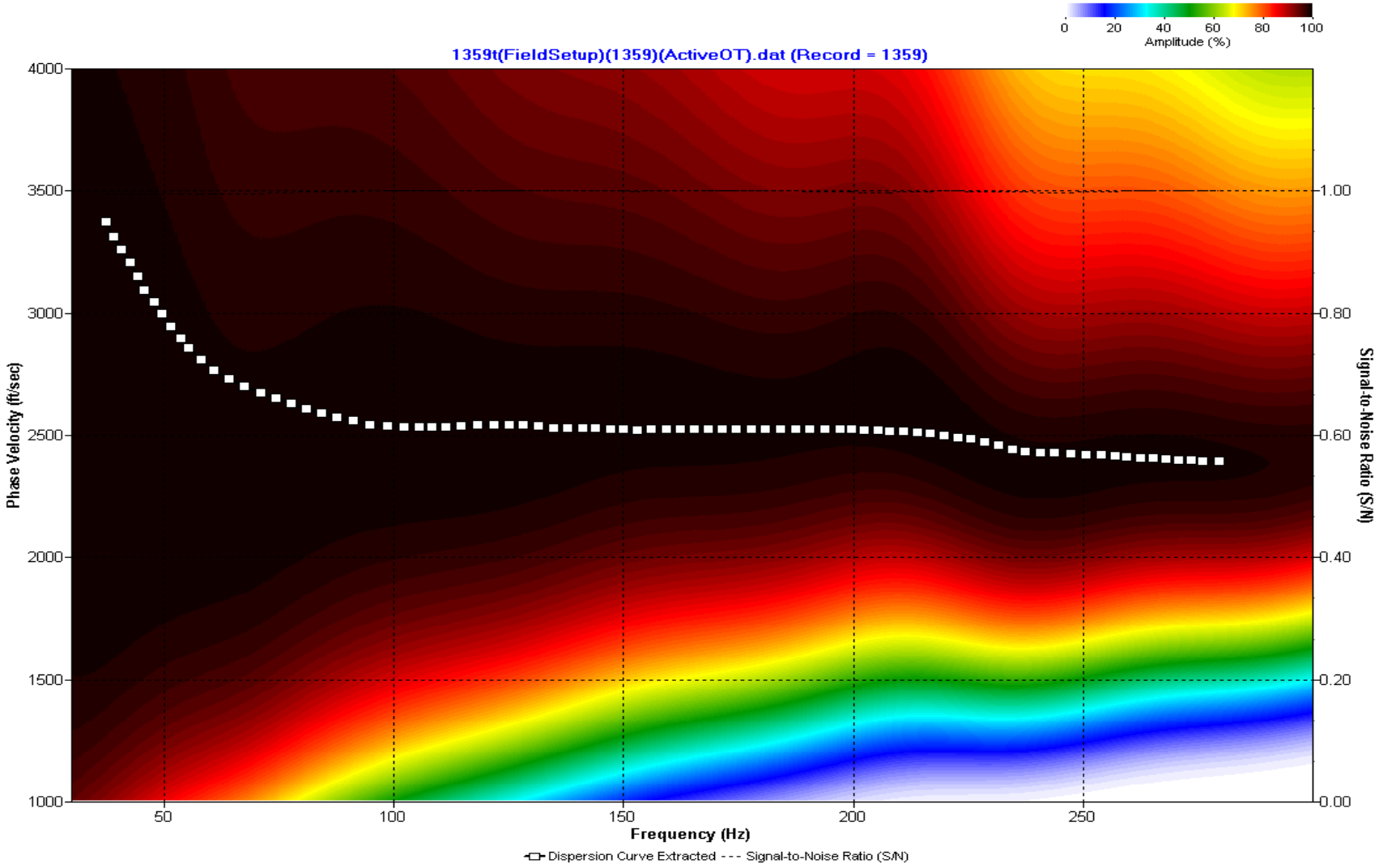

A.587: Dispersion Curve Line 1359 used in Post-blast 33

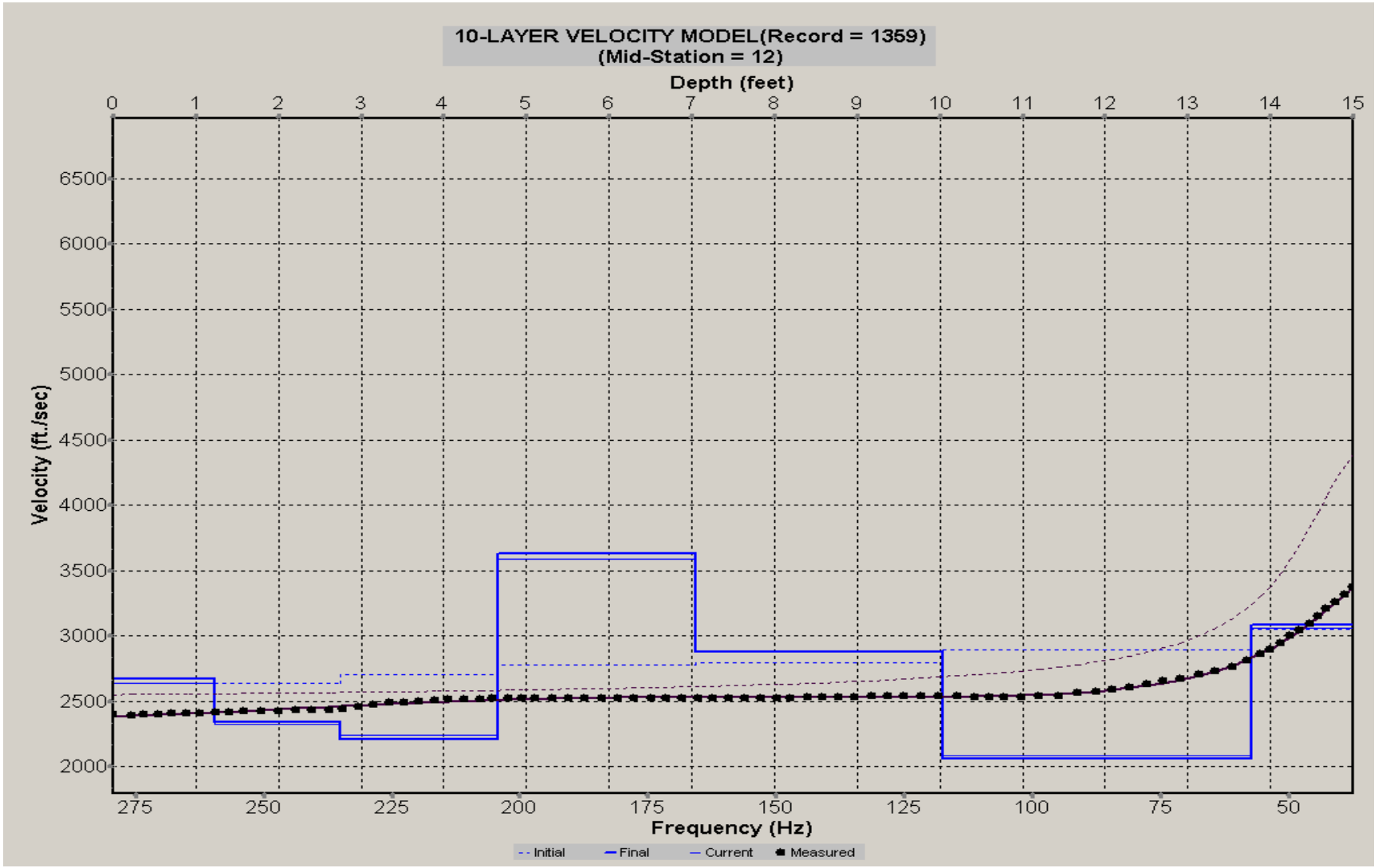

A.588: Velocity Profile Line 1359 used in Post-blast 33

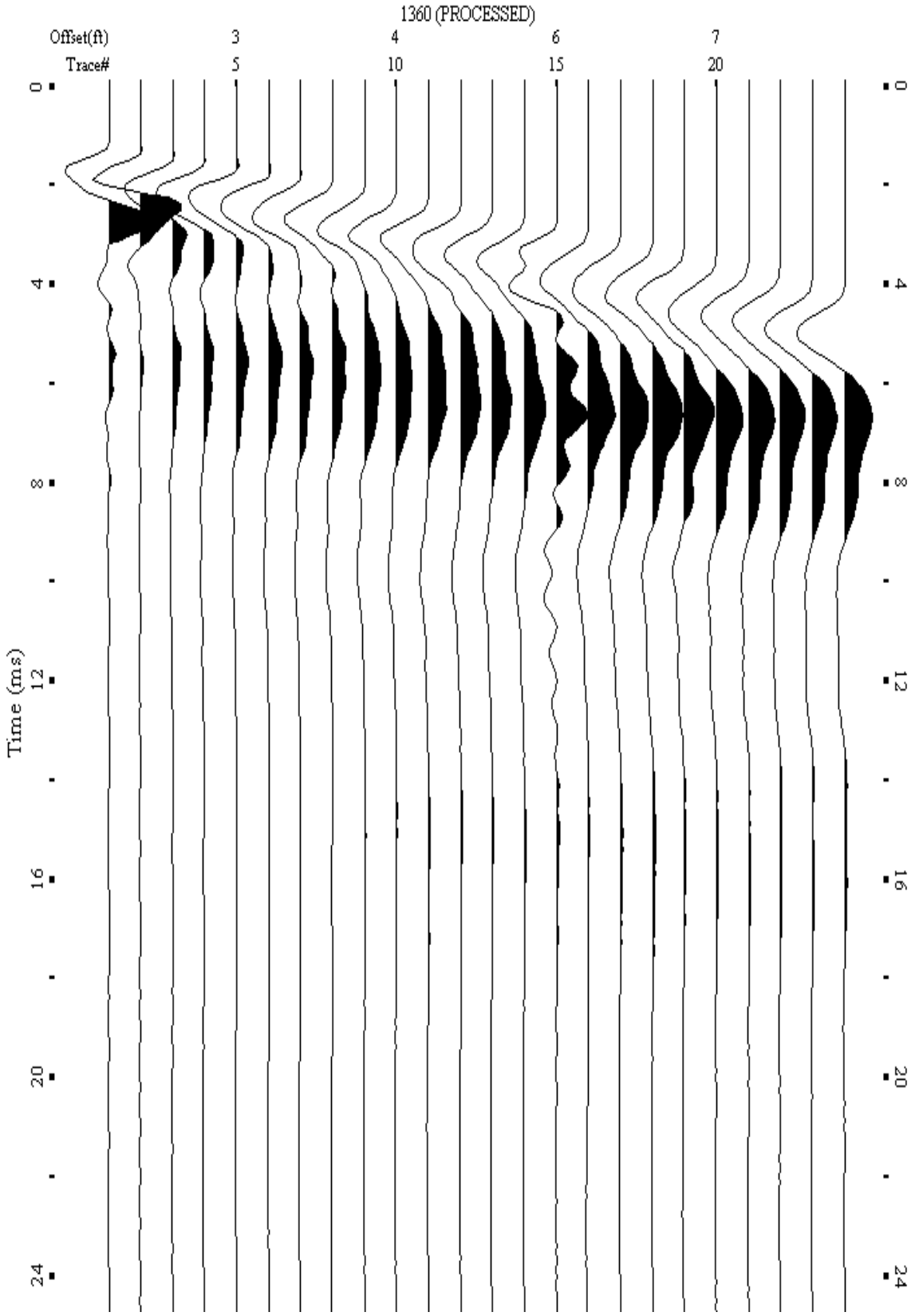

A.589: Shot Gather Line 1360 used in Post-blast 34

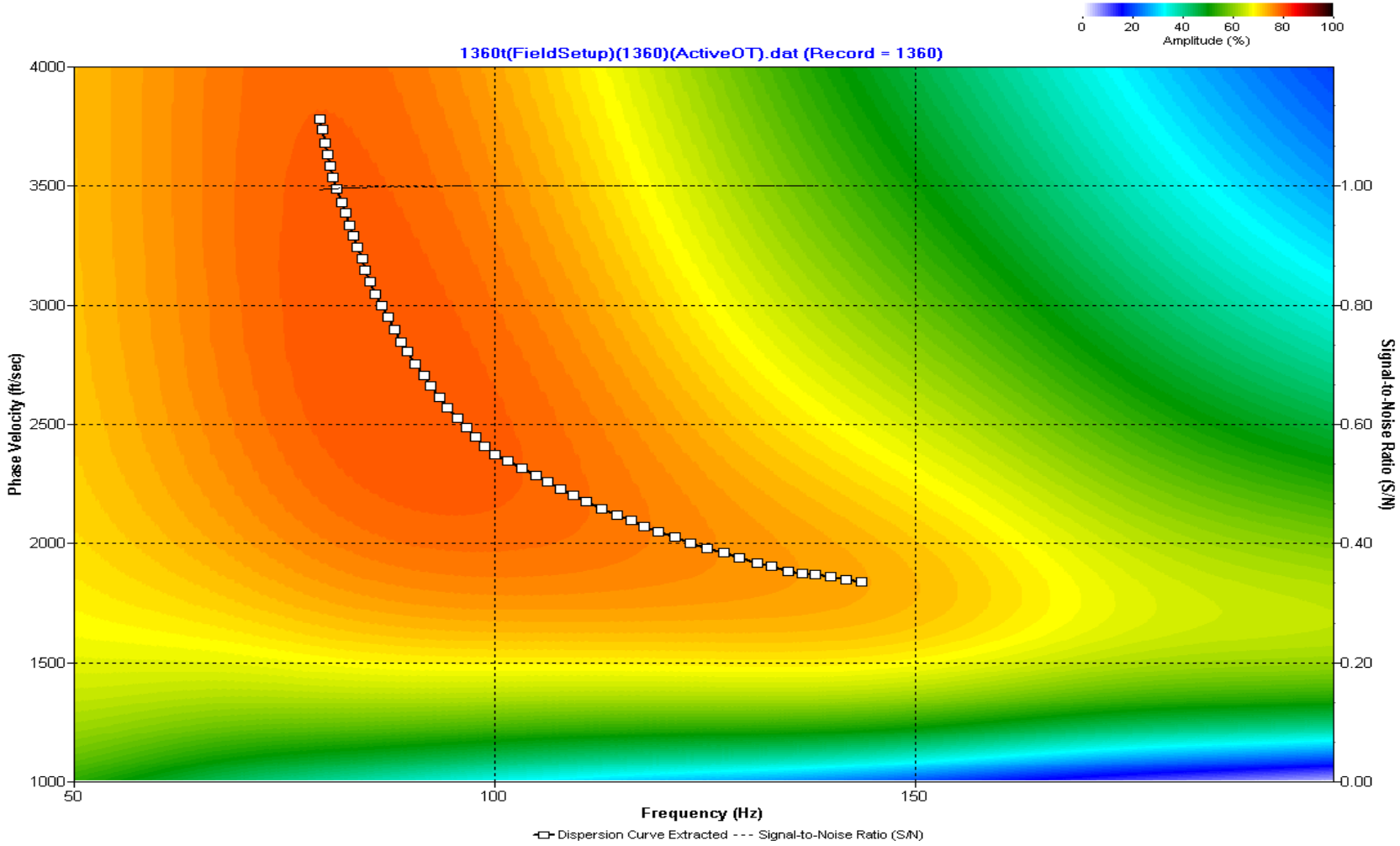

A.590: Dispersion Curve Line 1360 used in Post-blast 34

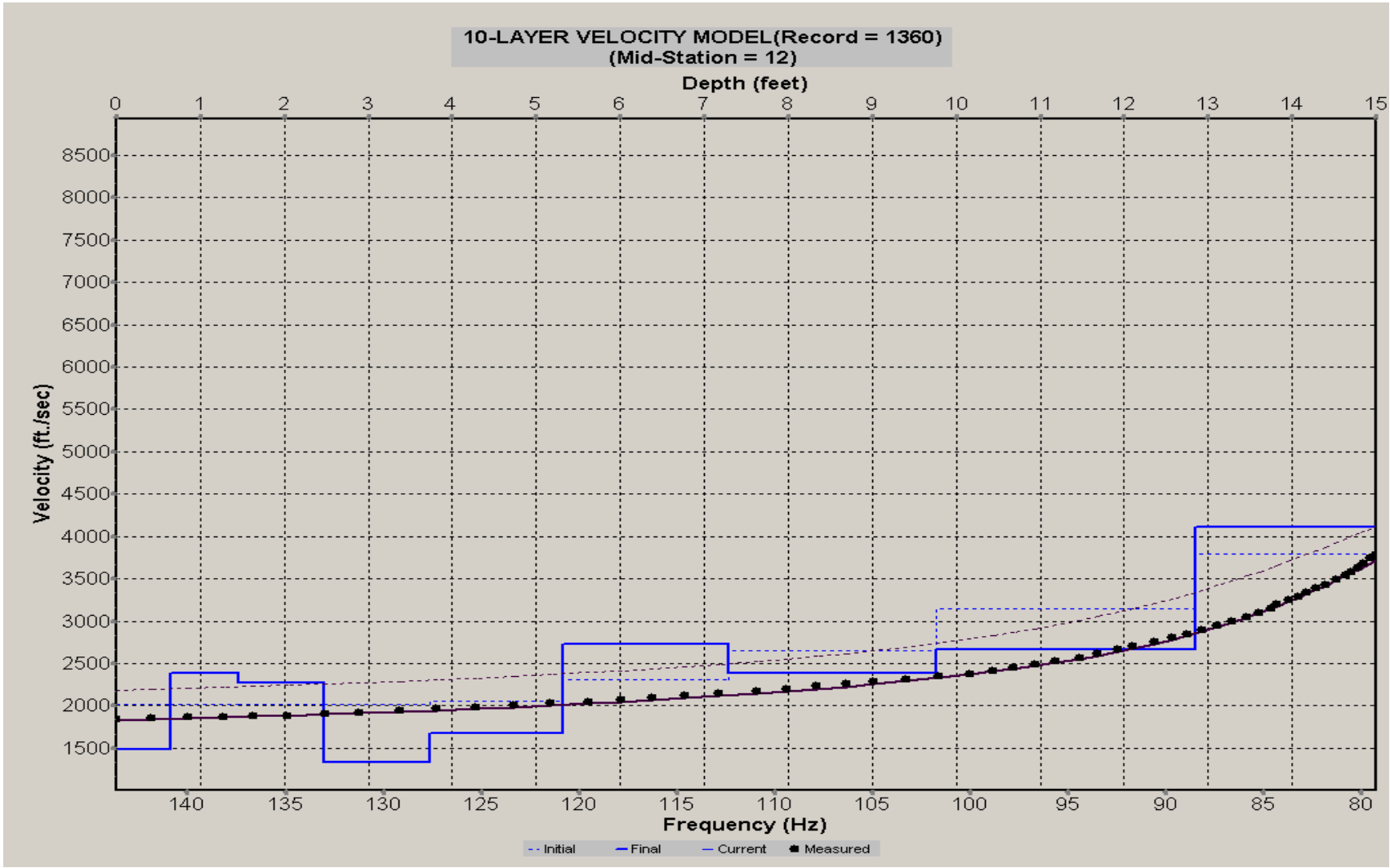

A.591: Velocity Profile Line 1360 used in Post-blast 34

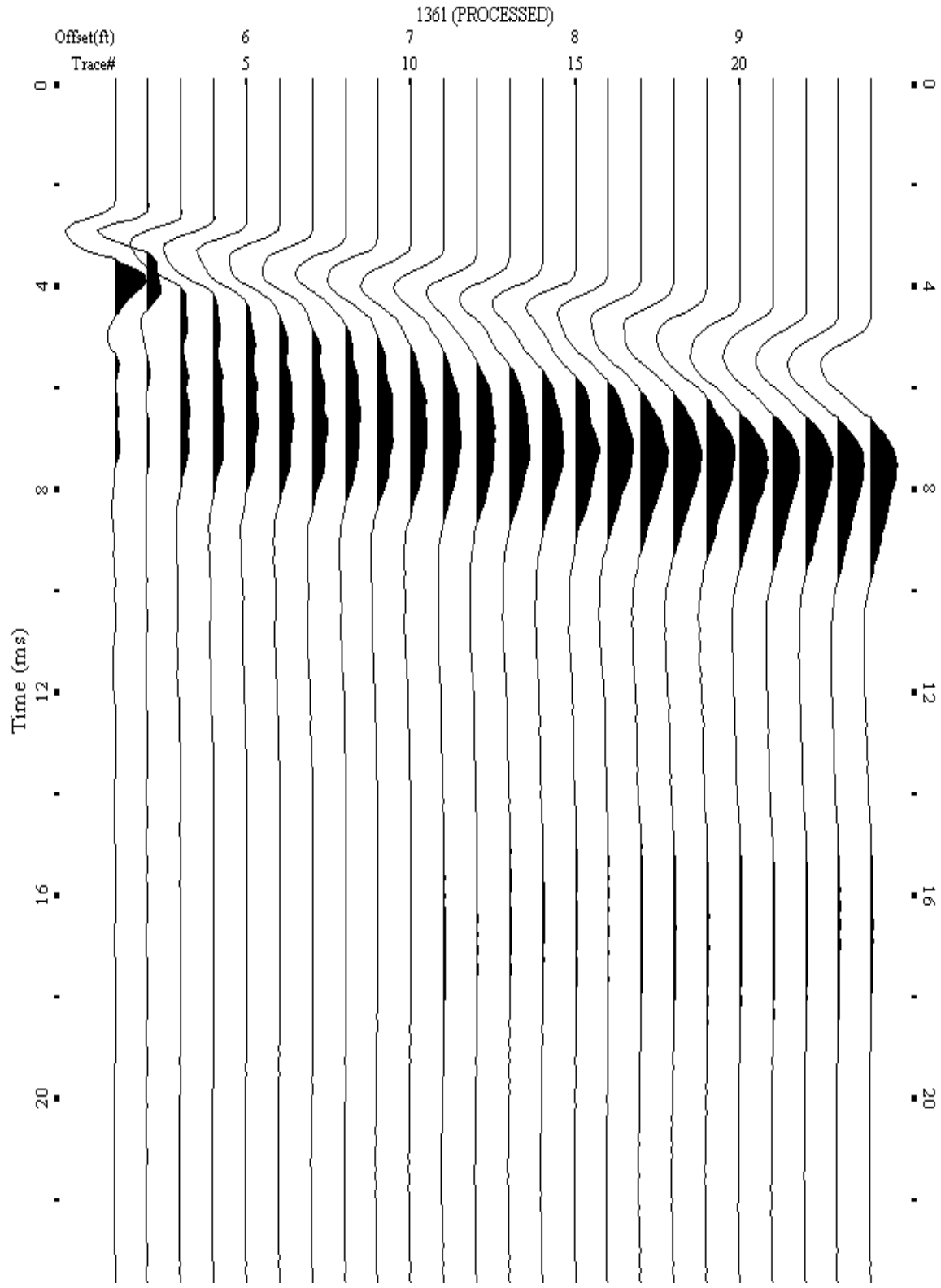

A.592: Shot Gather Line 1361 used in Post-blast 34

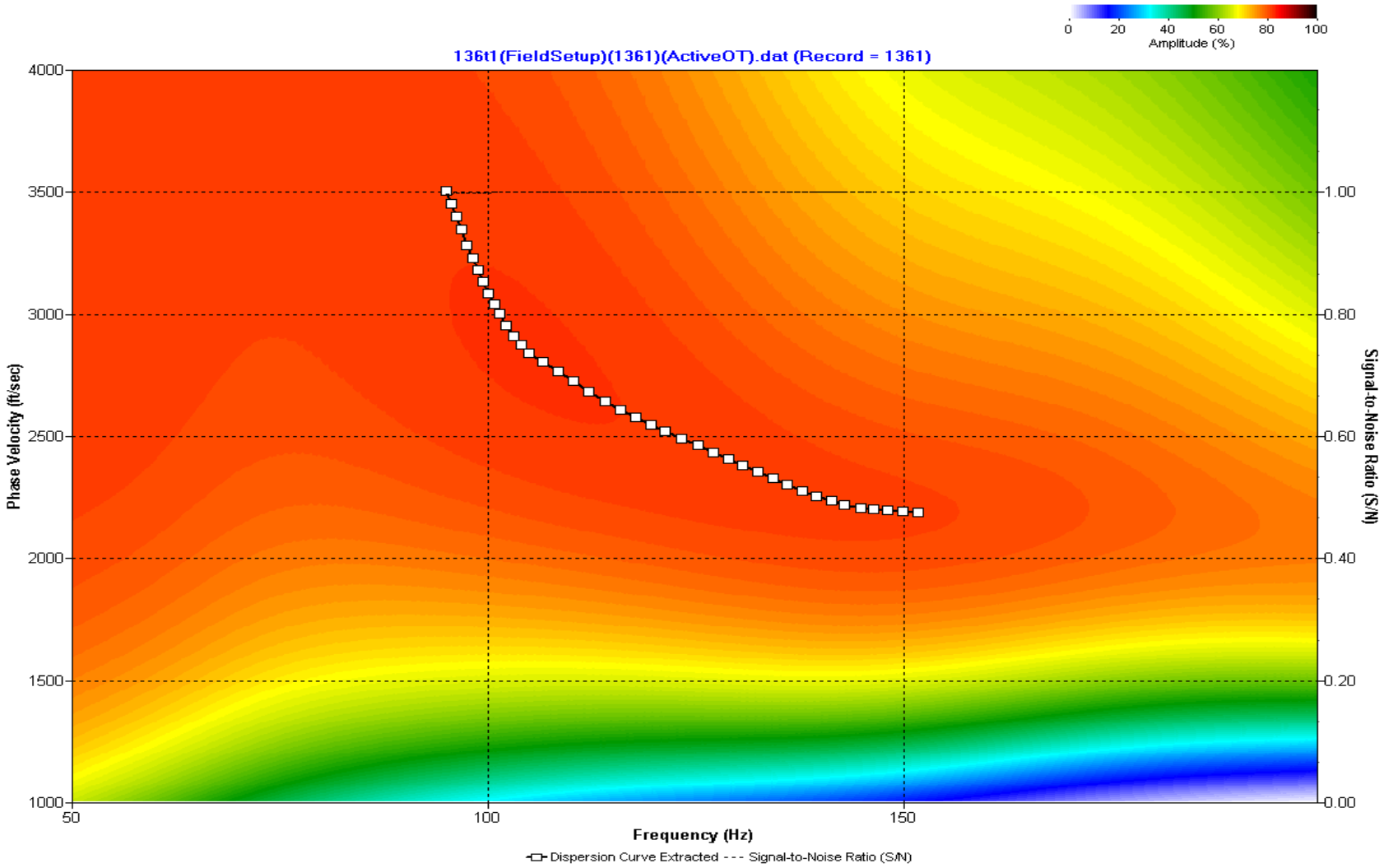

A.593: Dispersion Curve Line 1361 used in Post-blast 34

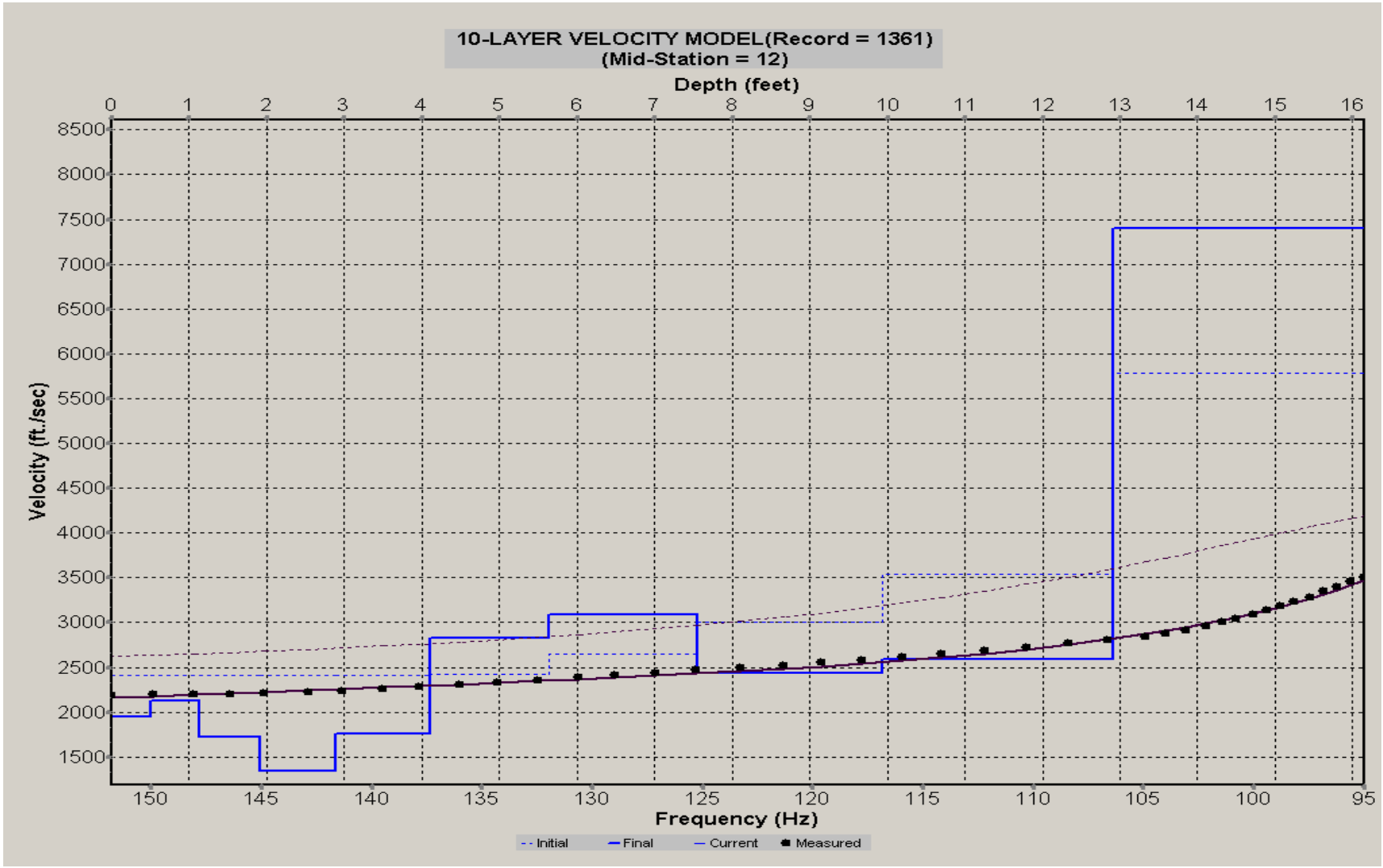

A.594: Velocity Profile Line 1361 used in Post-blast 34

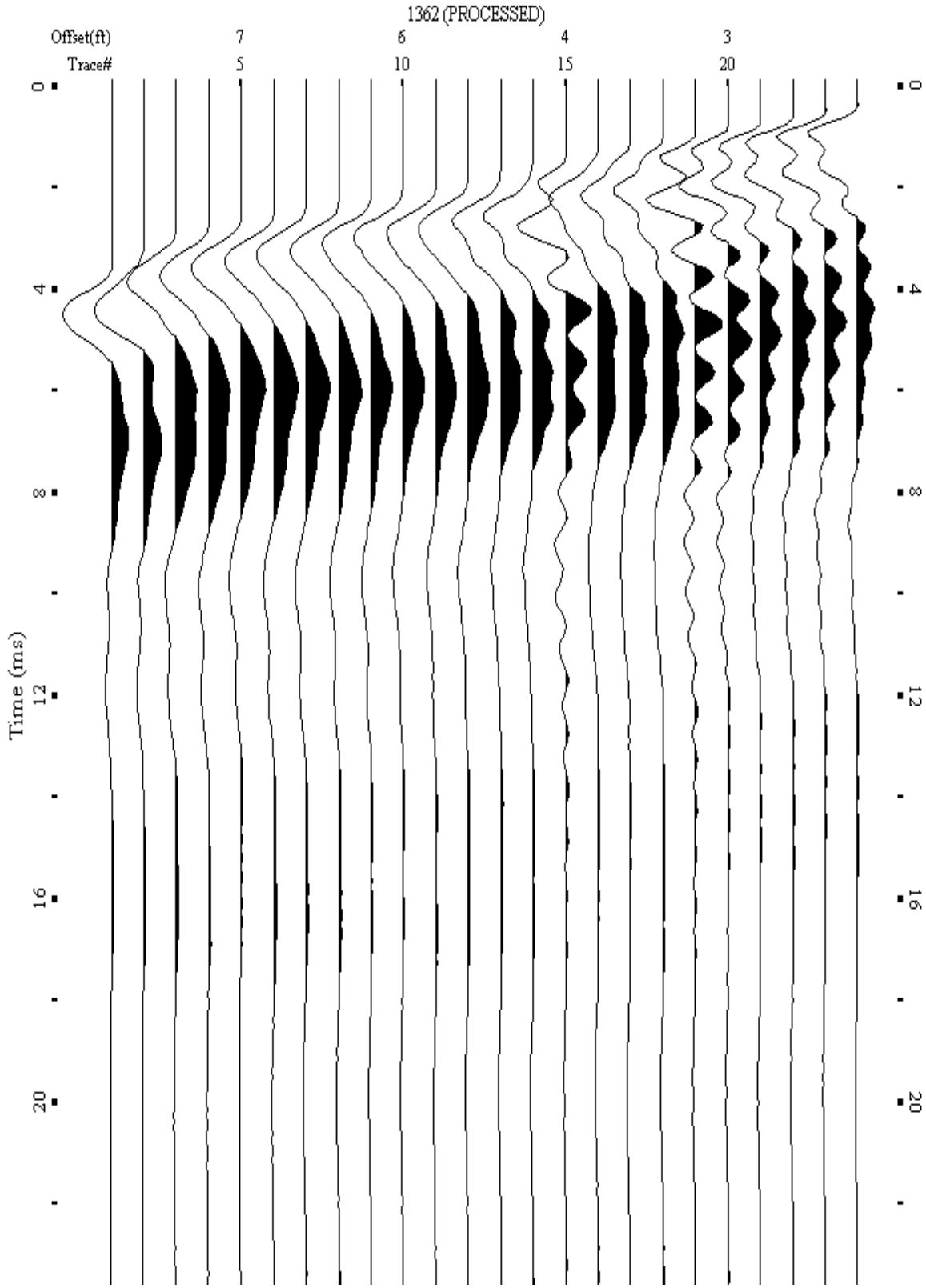

A.595: Shot Gather Line 1362 used in Post-blast 34

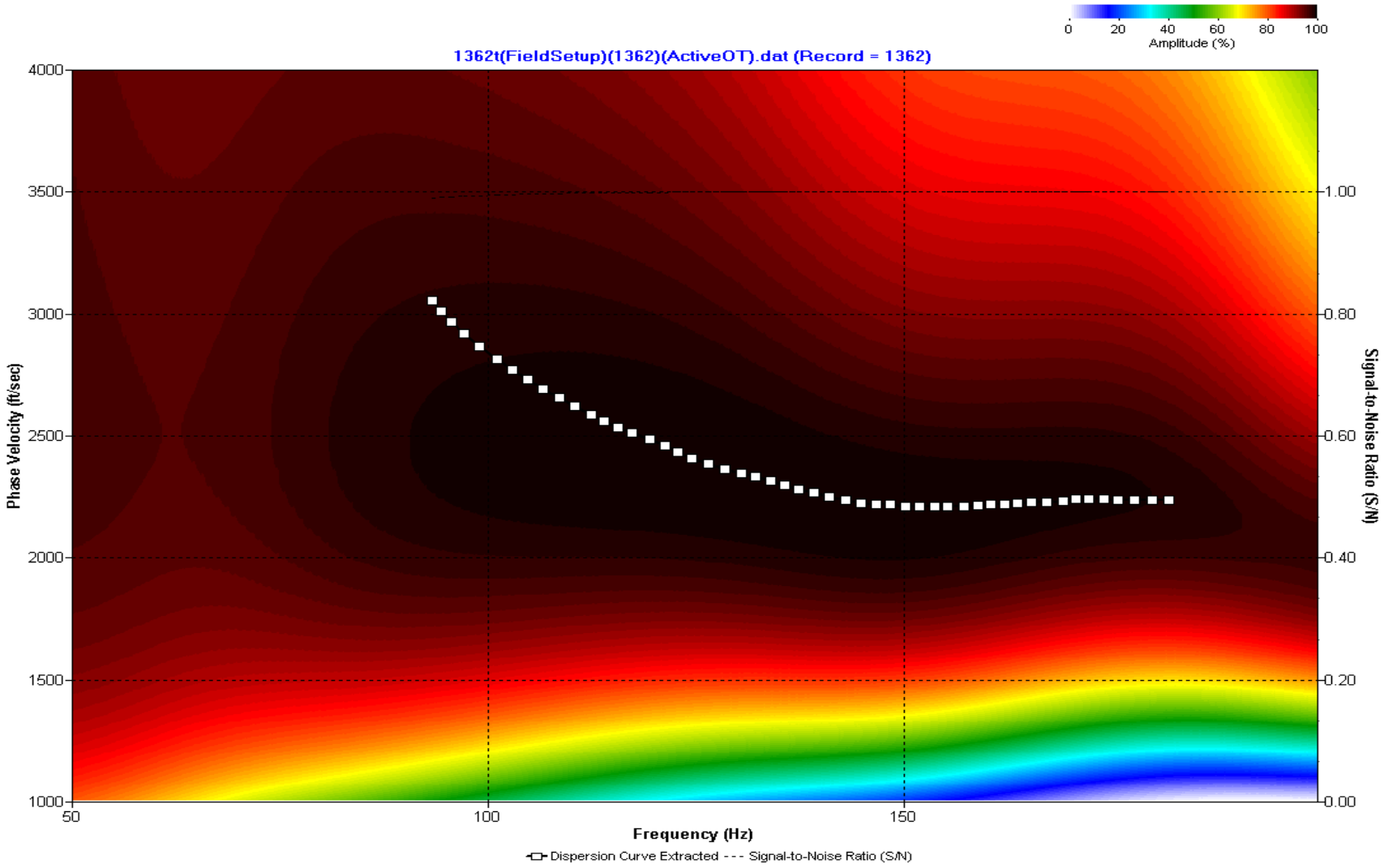

A.596: Dispersion Curve Line 1362 used in Post-blast 34

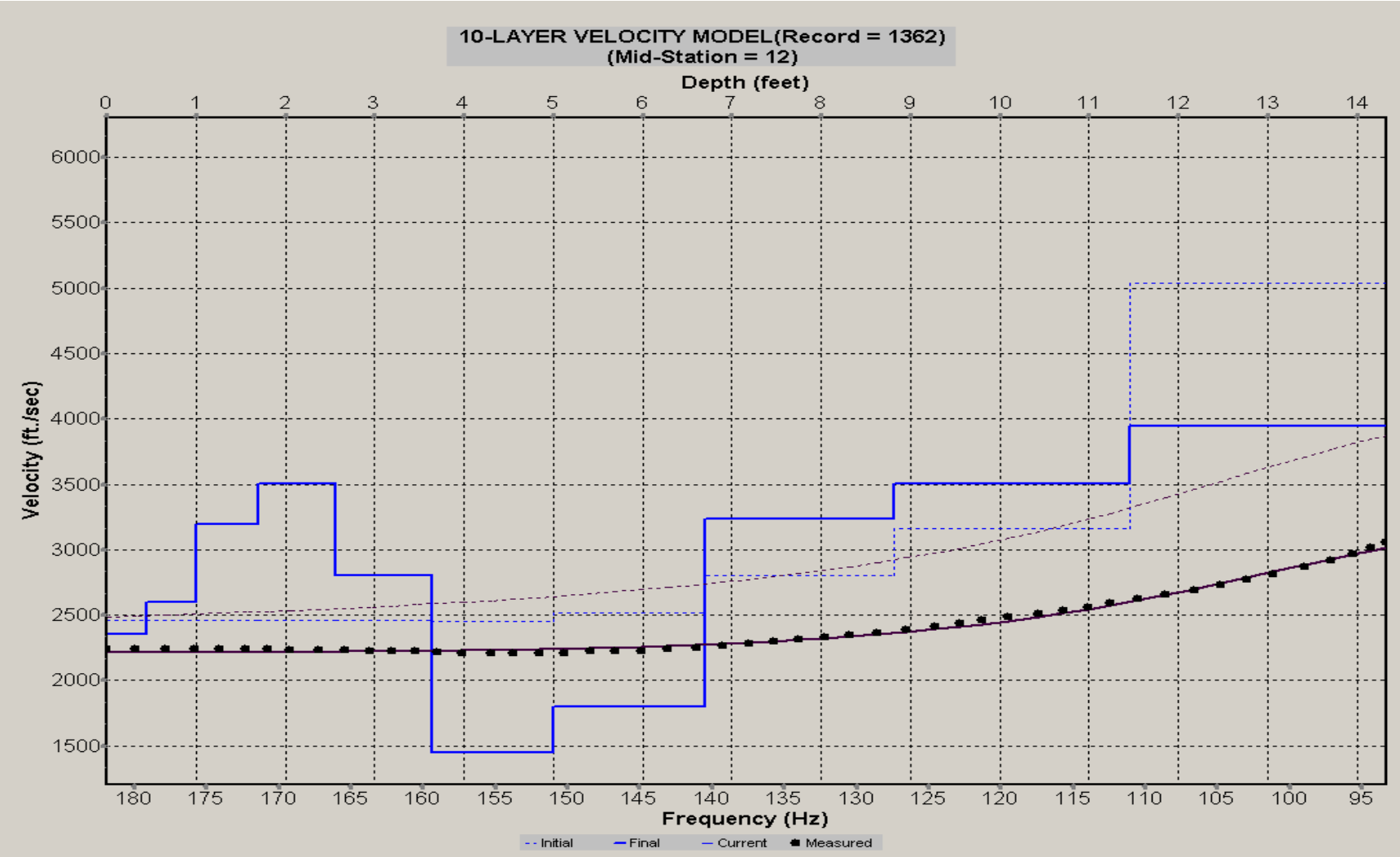

A.597: Velocity Profile Line 1362 used in Post-blast 34

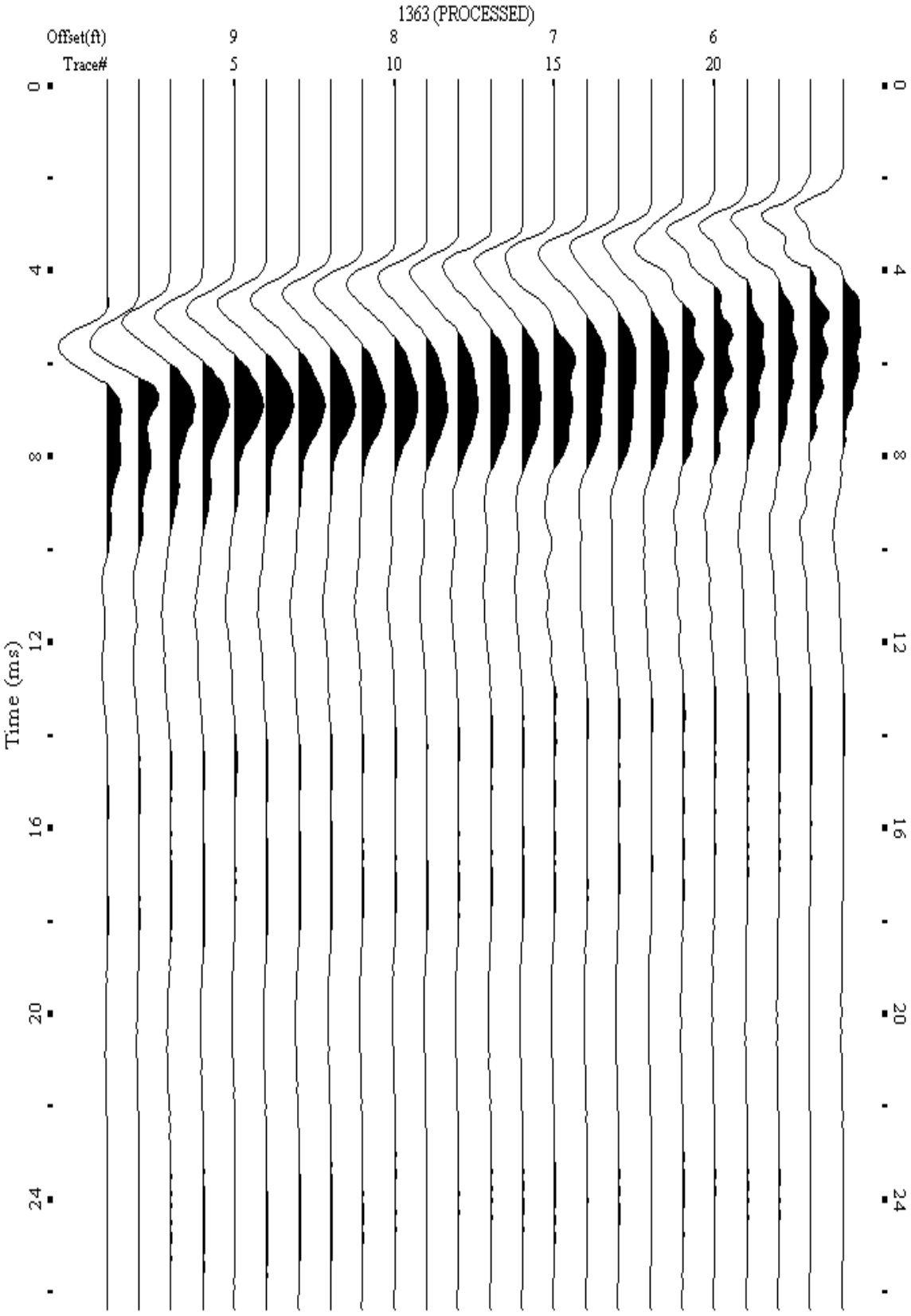

A.598: Shot Gather Line 1363 used in Post-blast 34

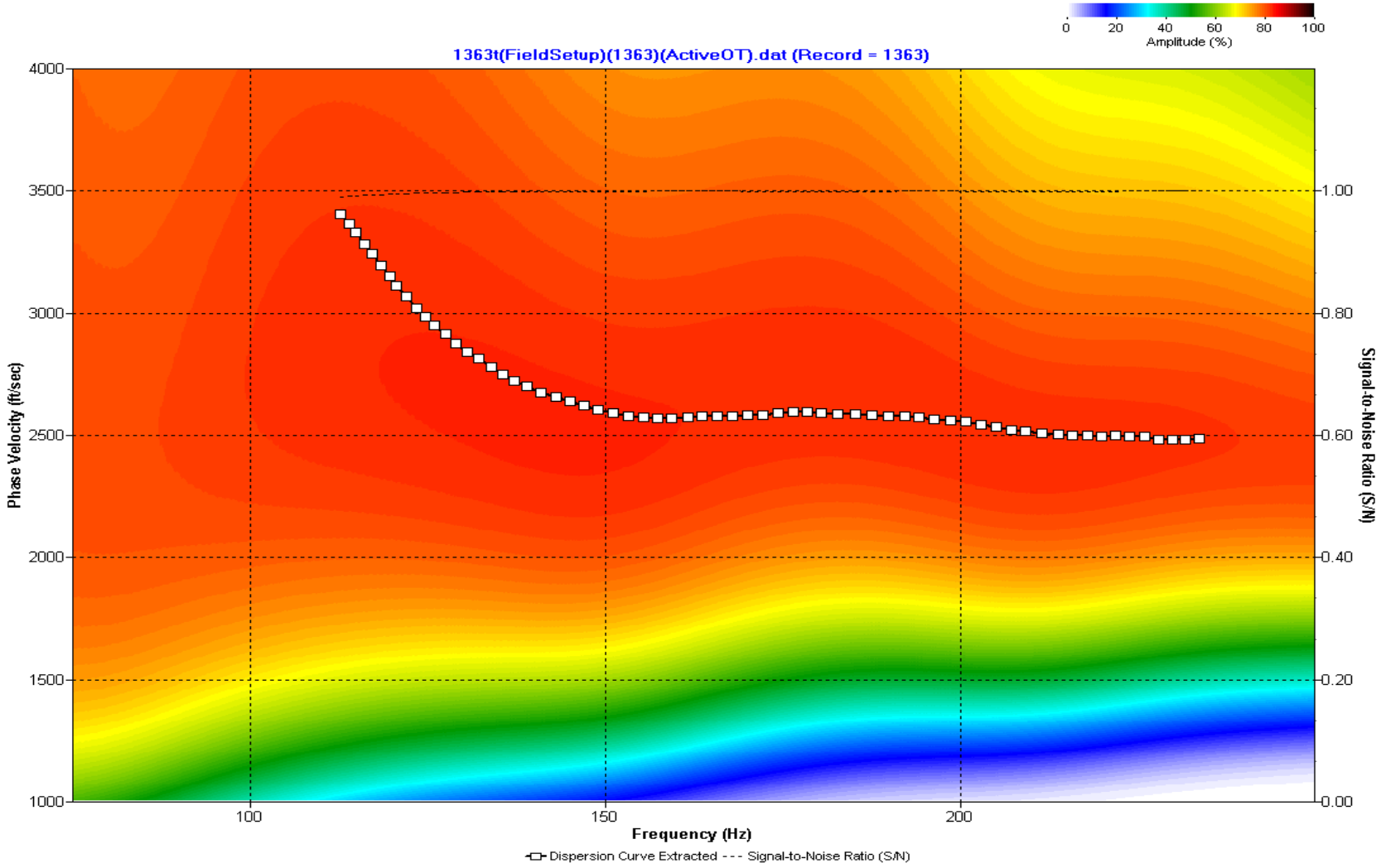

A.599: Dispersion Curve Line 1363 used in Post-blast 34

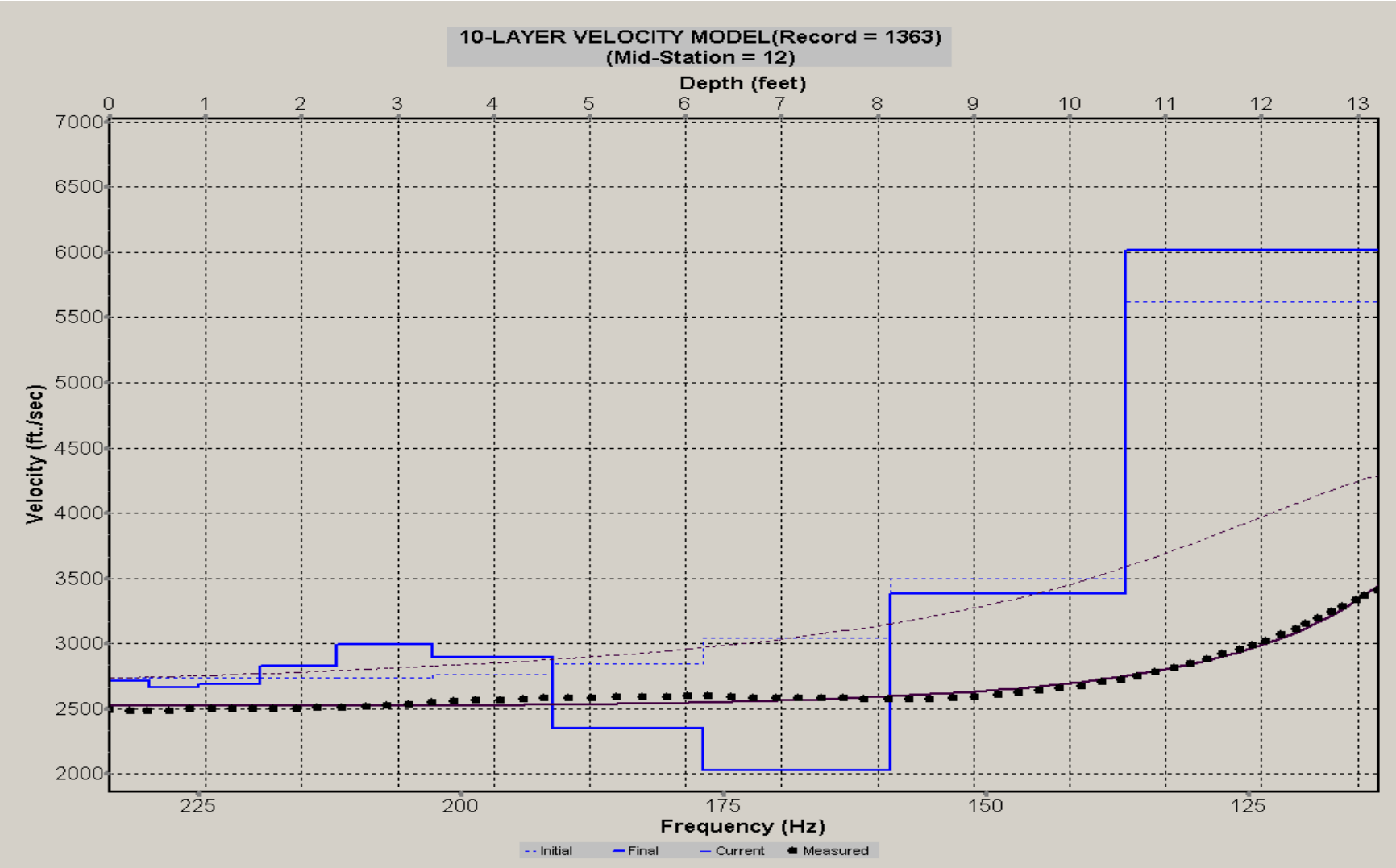

A.600: Velocity Profile Line 1363 used in Post-blast 34

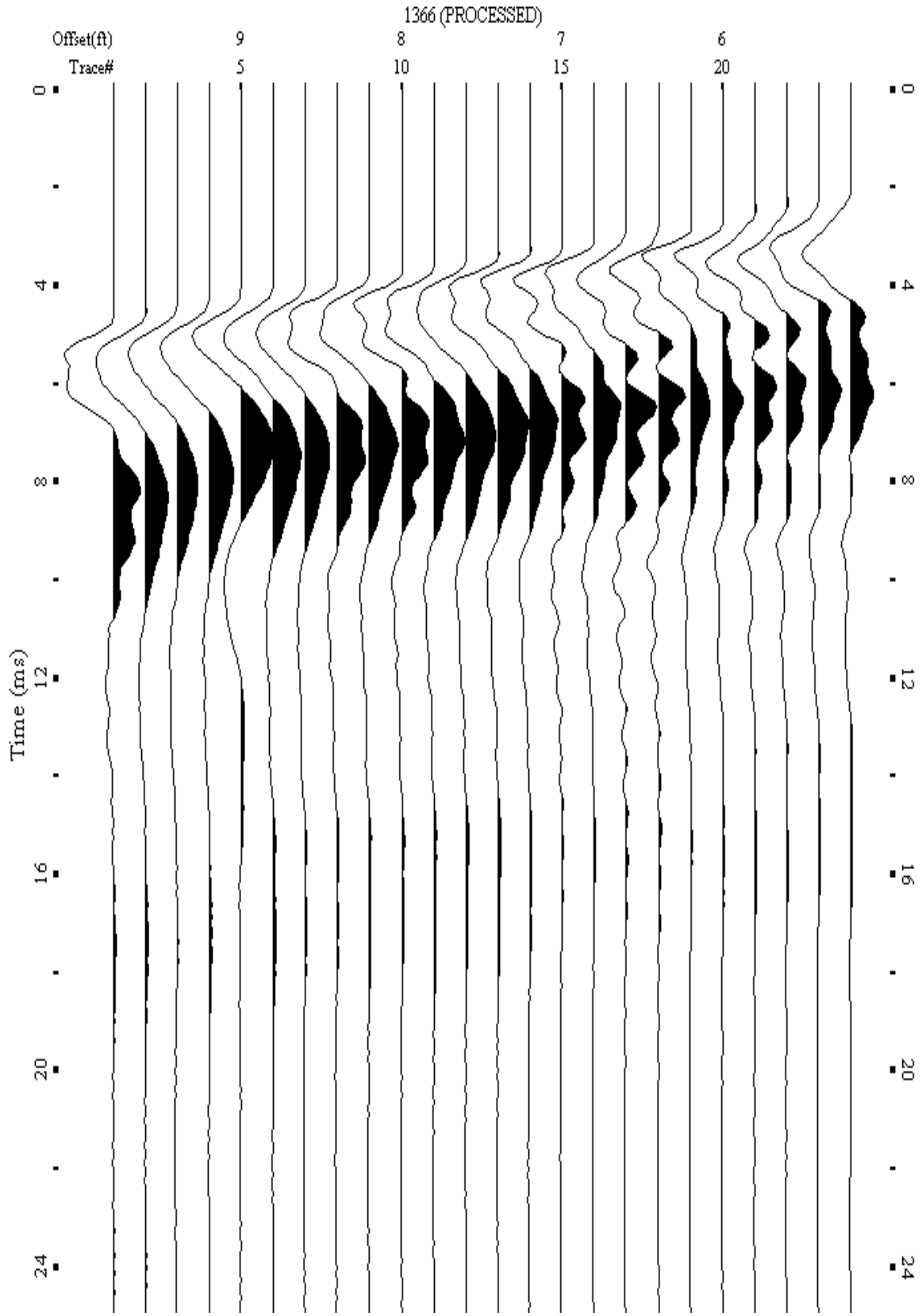

A.601 Shot Gather Line 1366 used in Post-blast 35

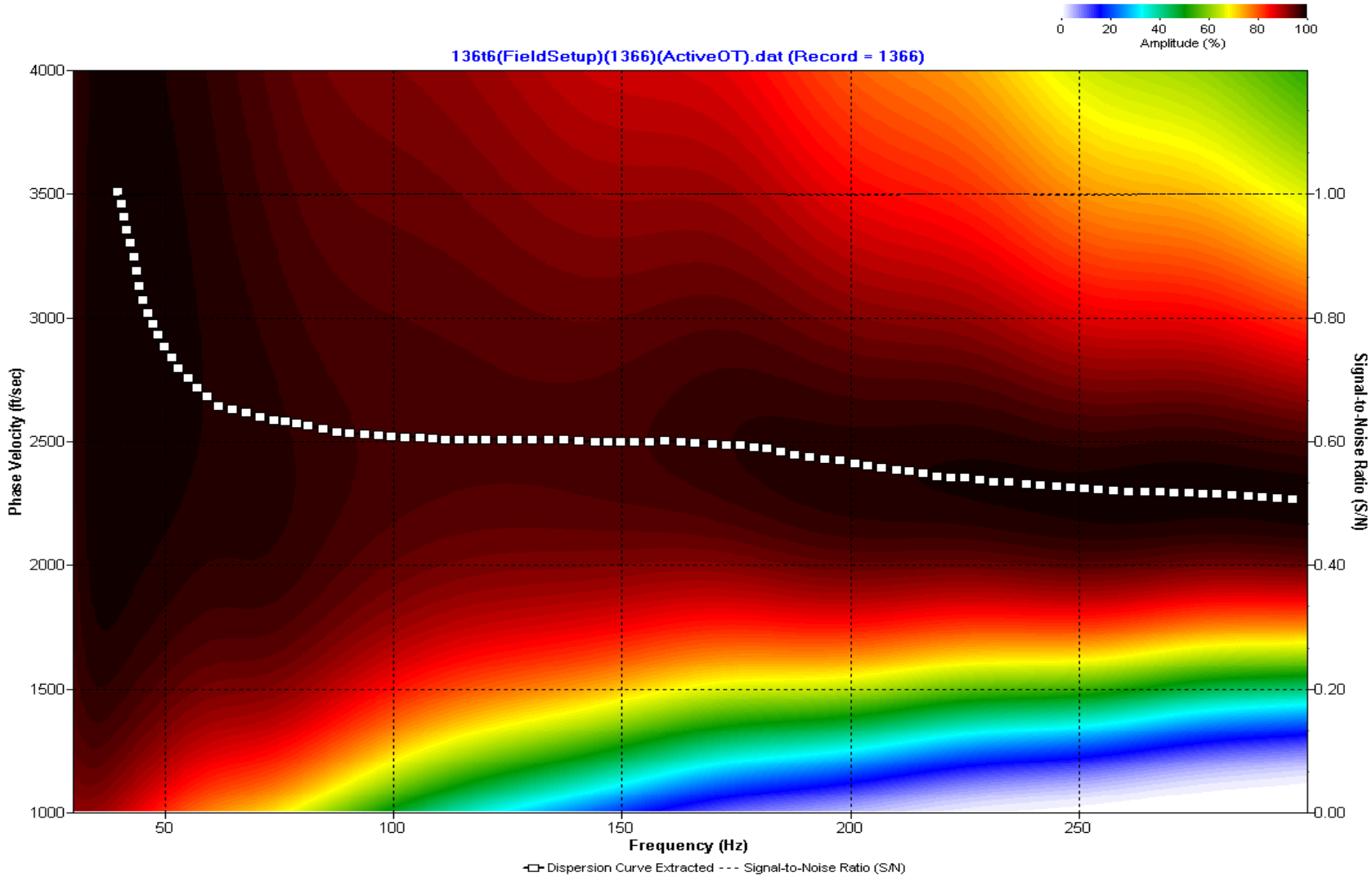

A.602: Dispersion Curve Line 1366 used in Post-blast 35

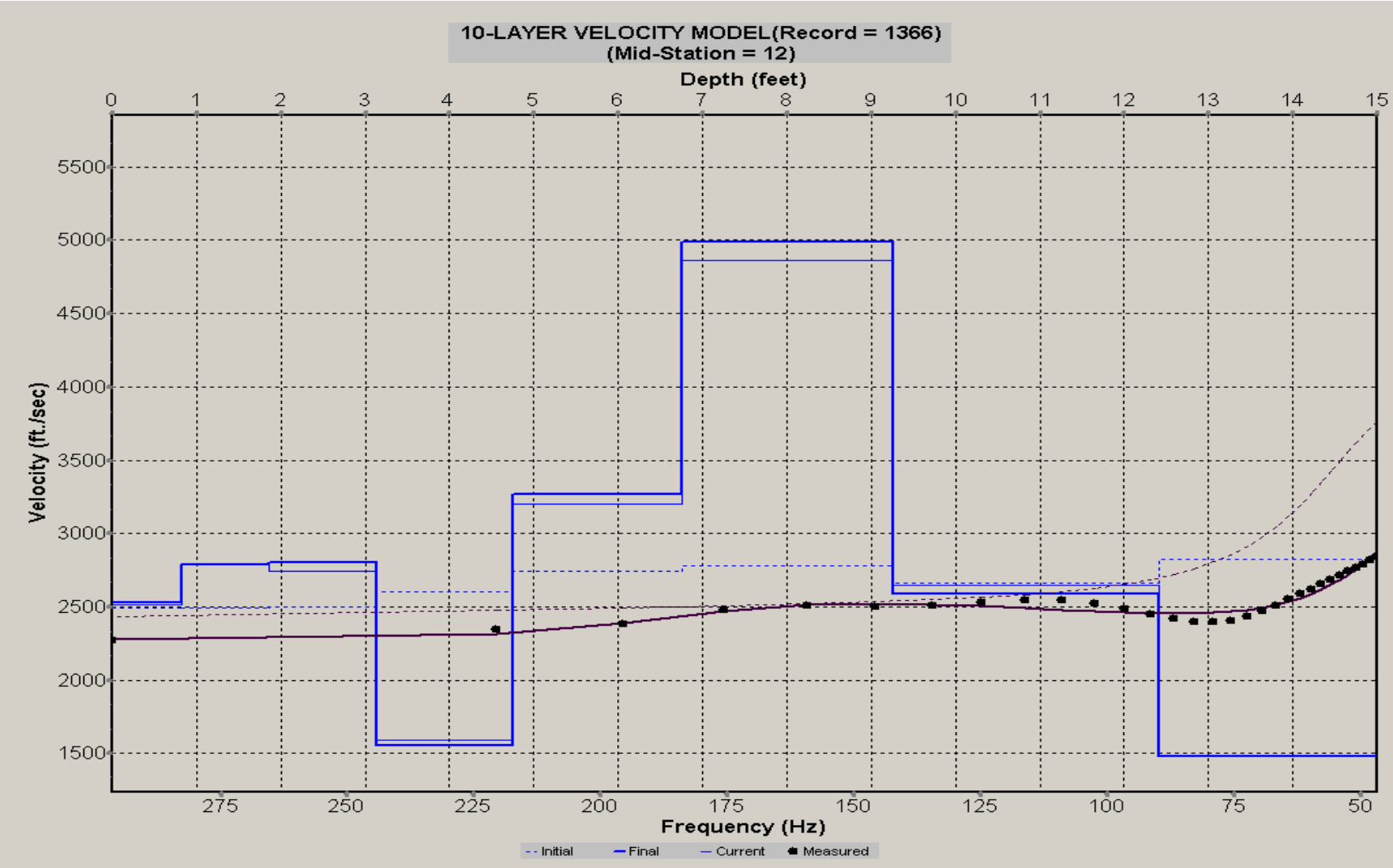

A.603: Velocity Profile Line 1366 used in Post-blast 35

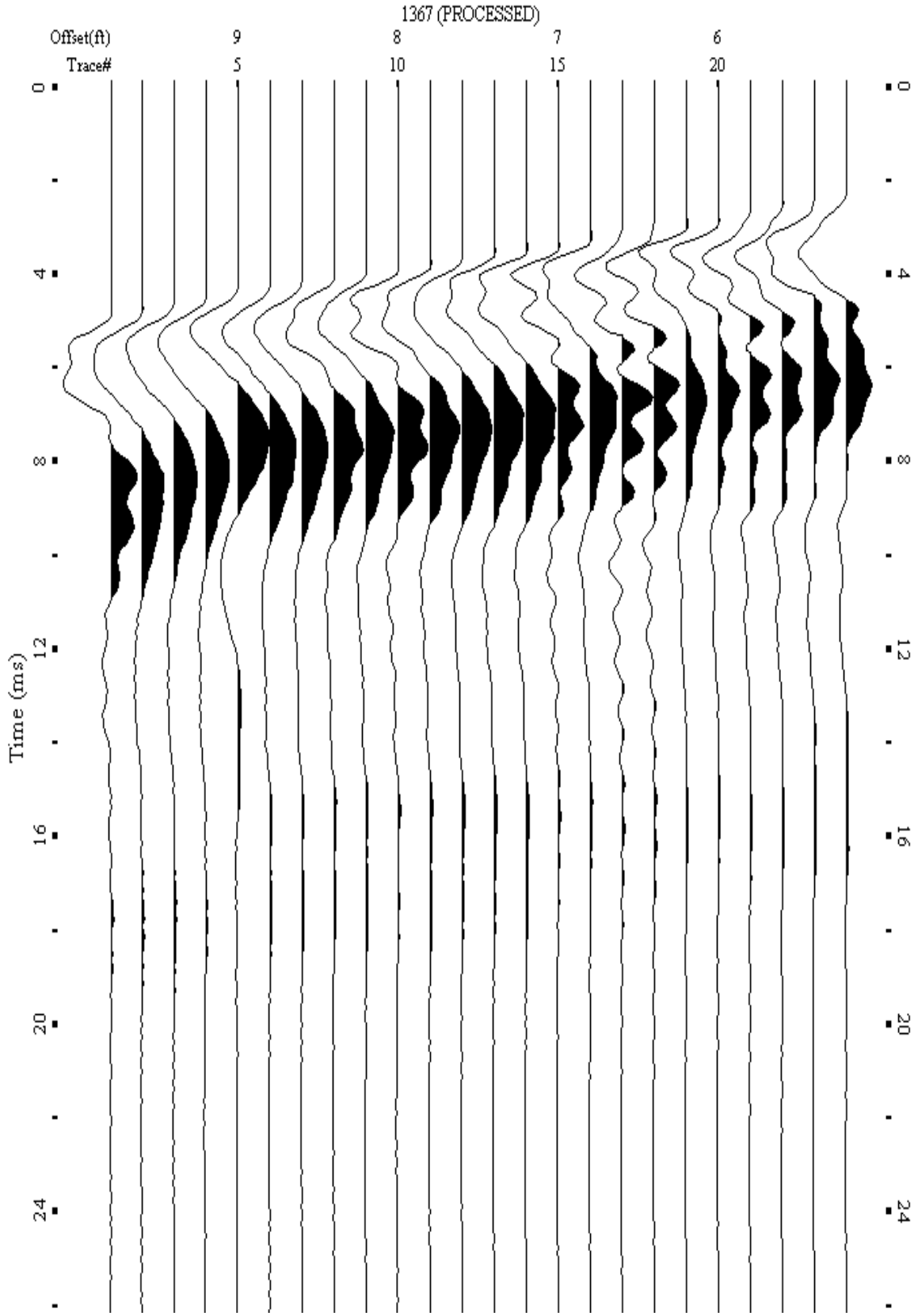

A.604 Shot Gather Line 1367 used in Post-blast 35

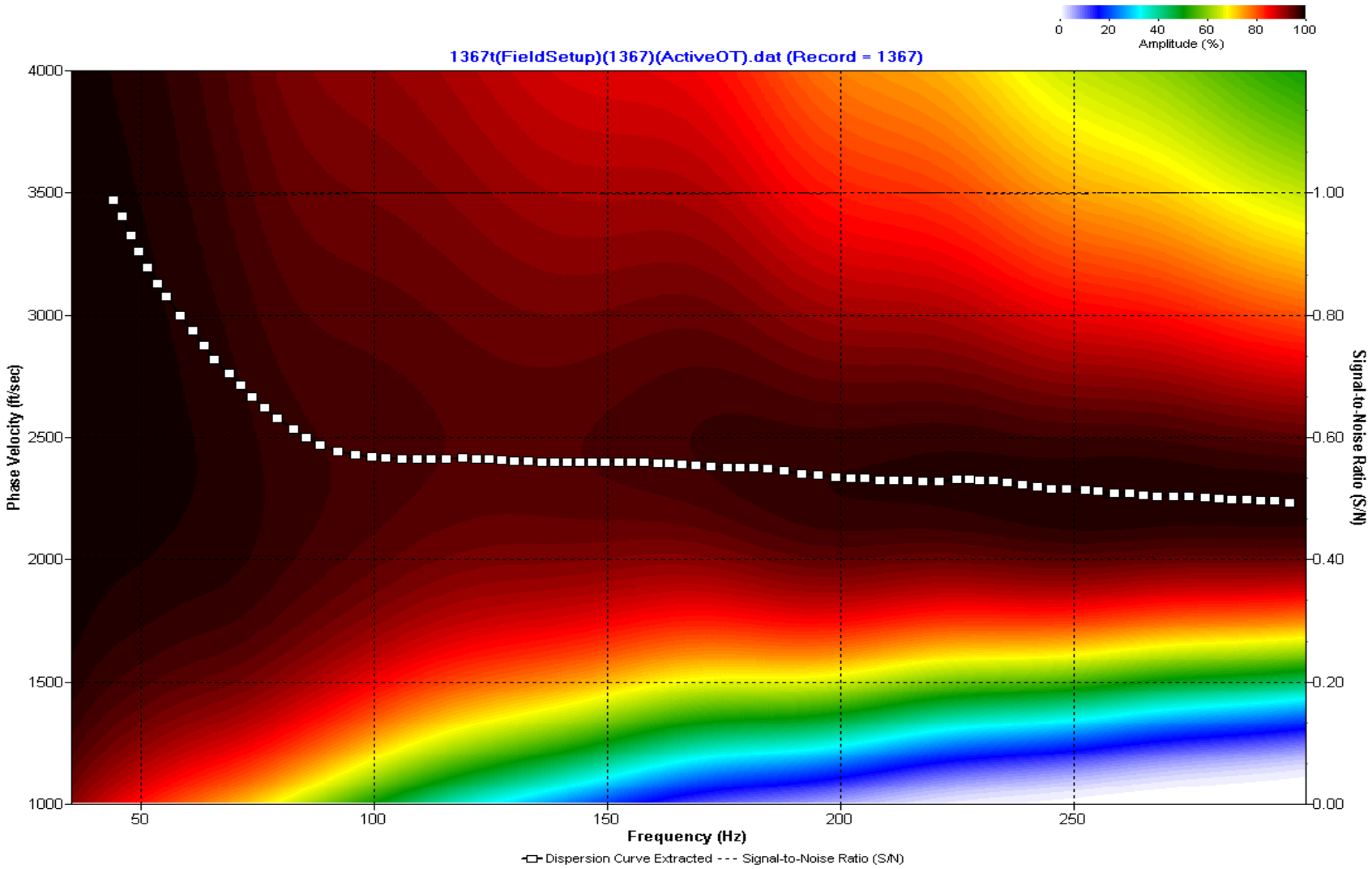

A.605: Dispersion Curve Line 1367 used in Post-blast 35

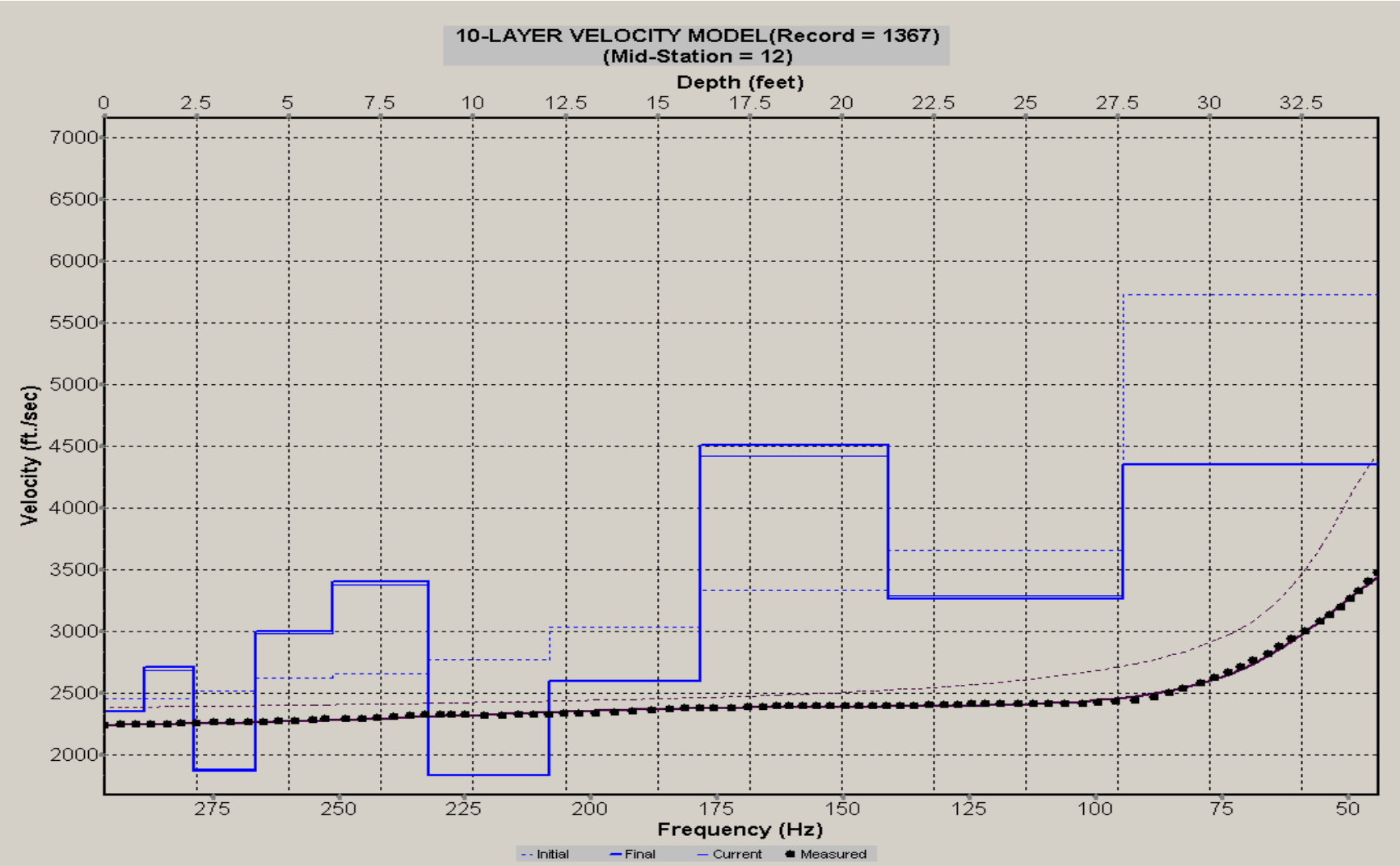

A.606: Velocity Profile Line 1367 used in Post-blast 35

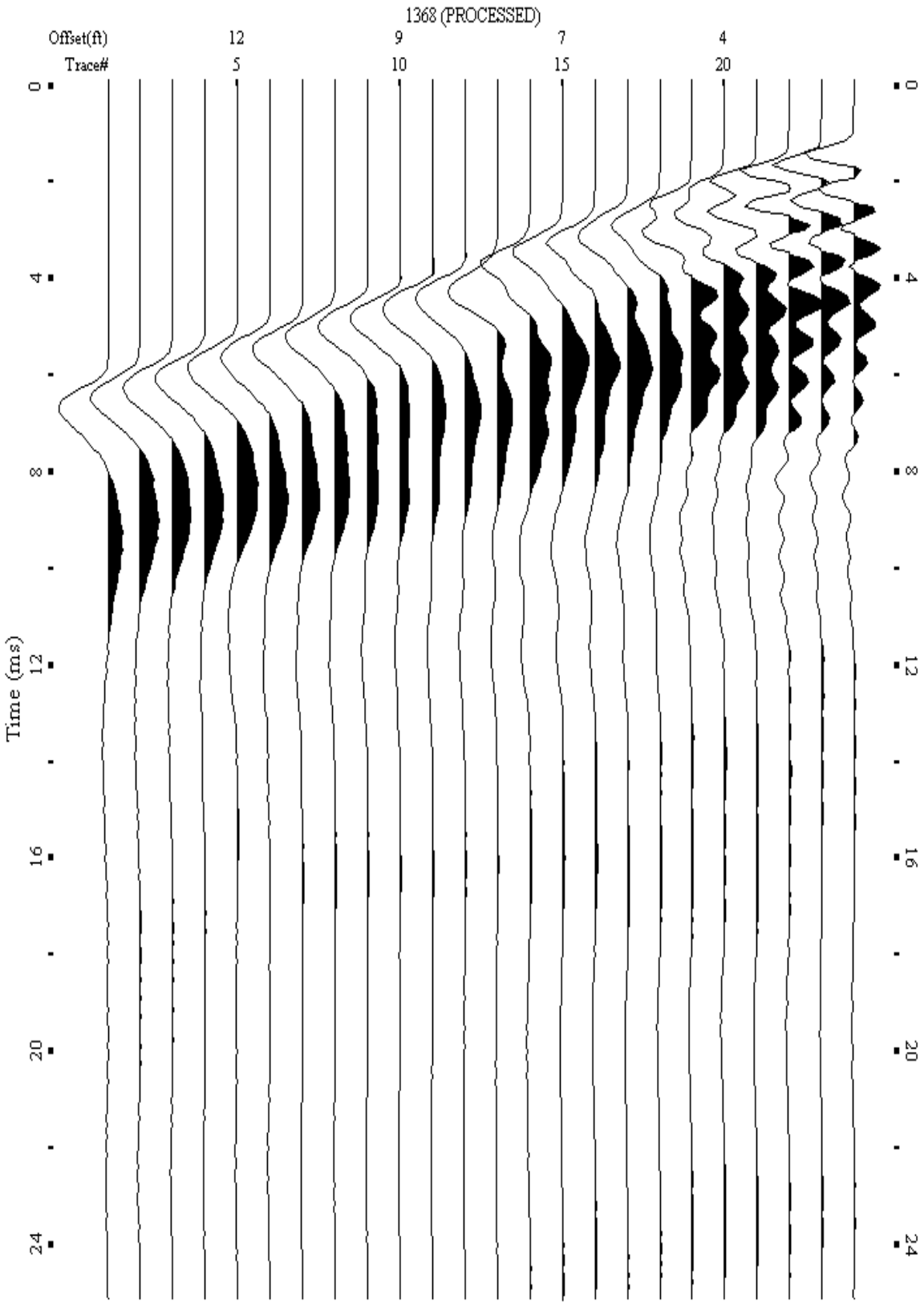

A.607 Shot Gather Line 1368 used in Post-blast 34

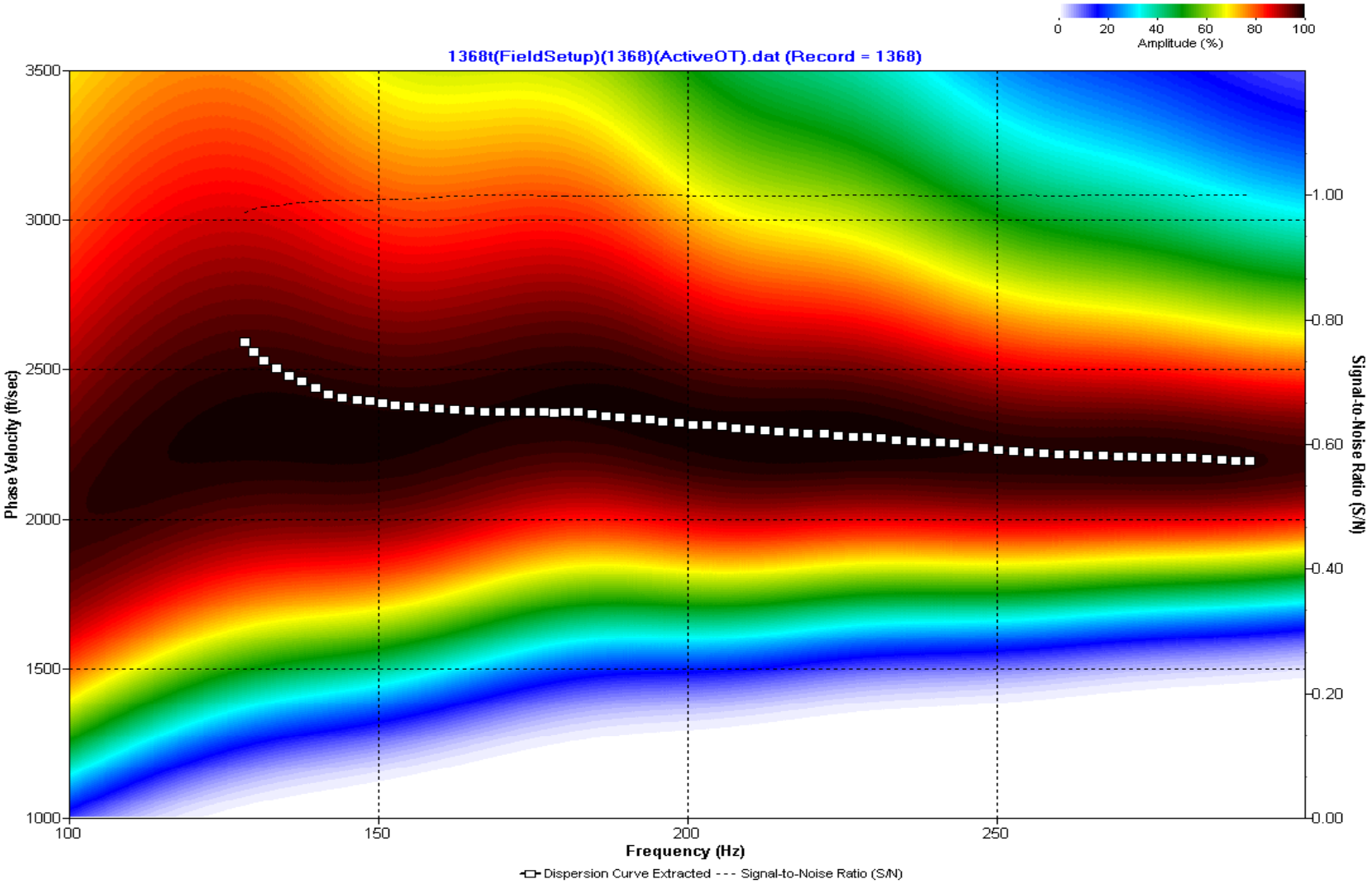

A.608: Dispersion Curve Line 1368 used in Post-blast 34

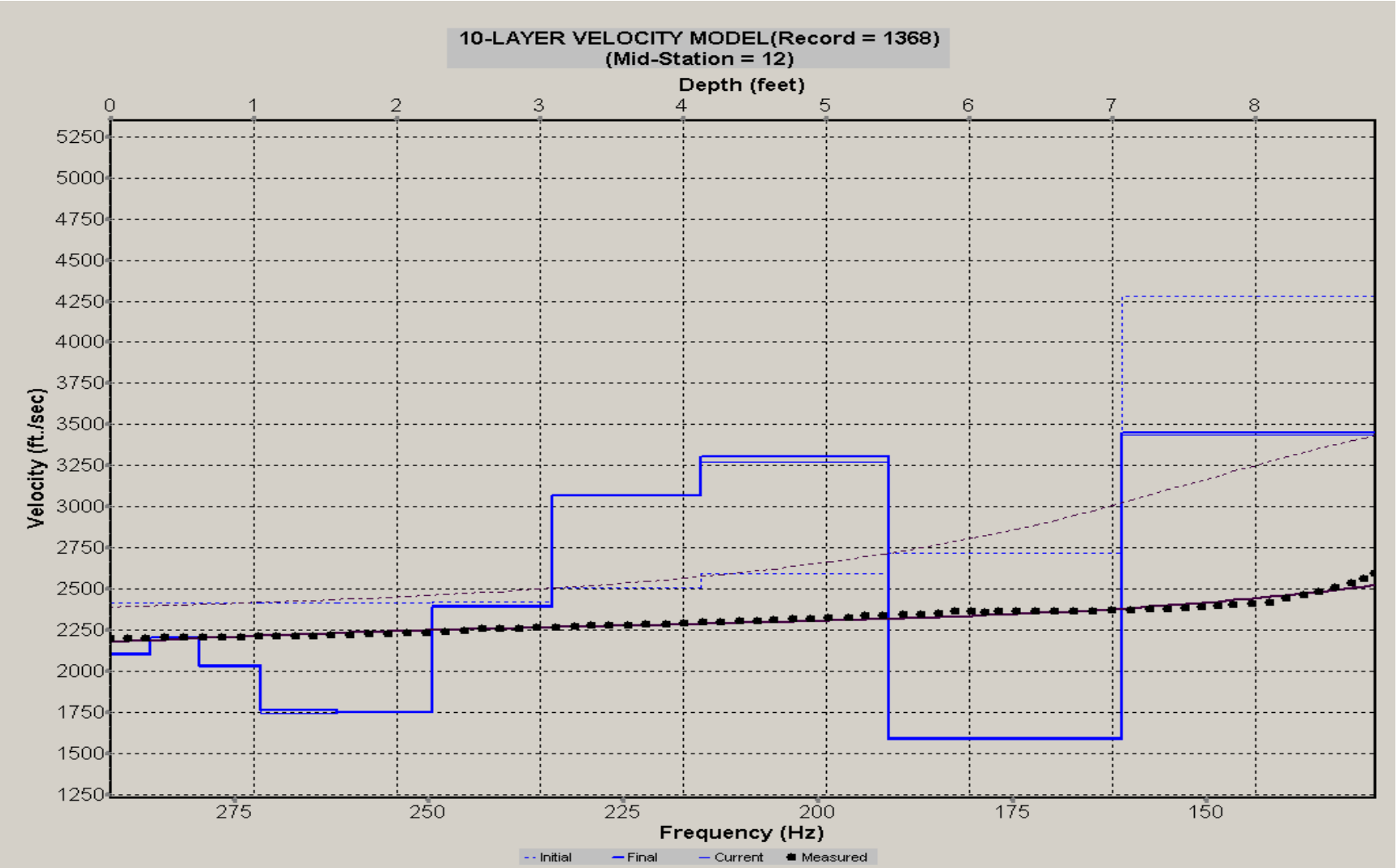

A.609: Velocity Profile Line 1368 used in Post-blast 34

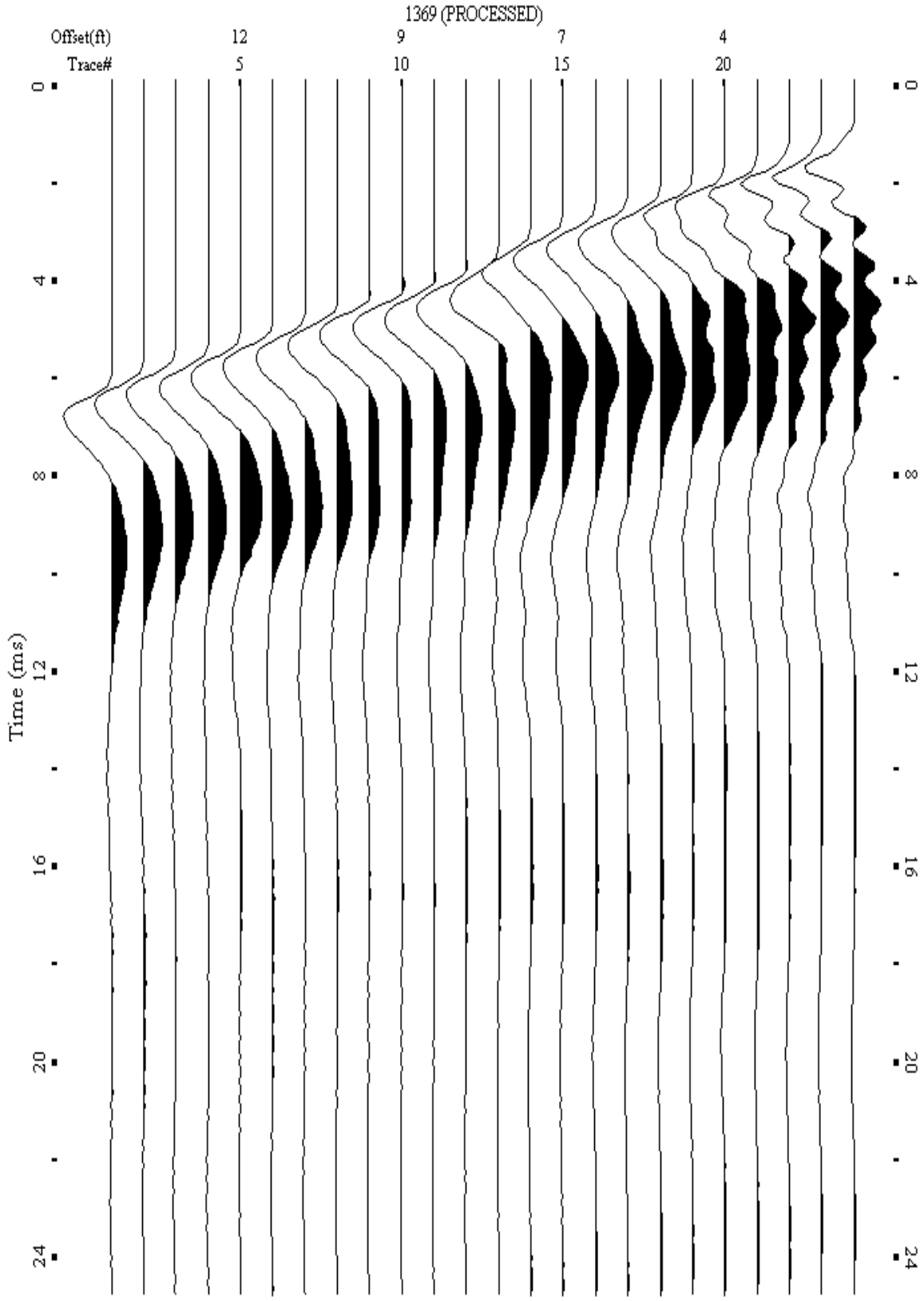

A.610 Shot Gather Line 1369 used in Post-blast 34 and Post-blast 35

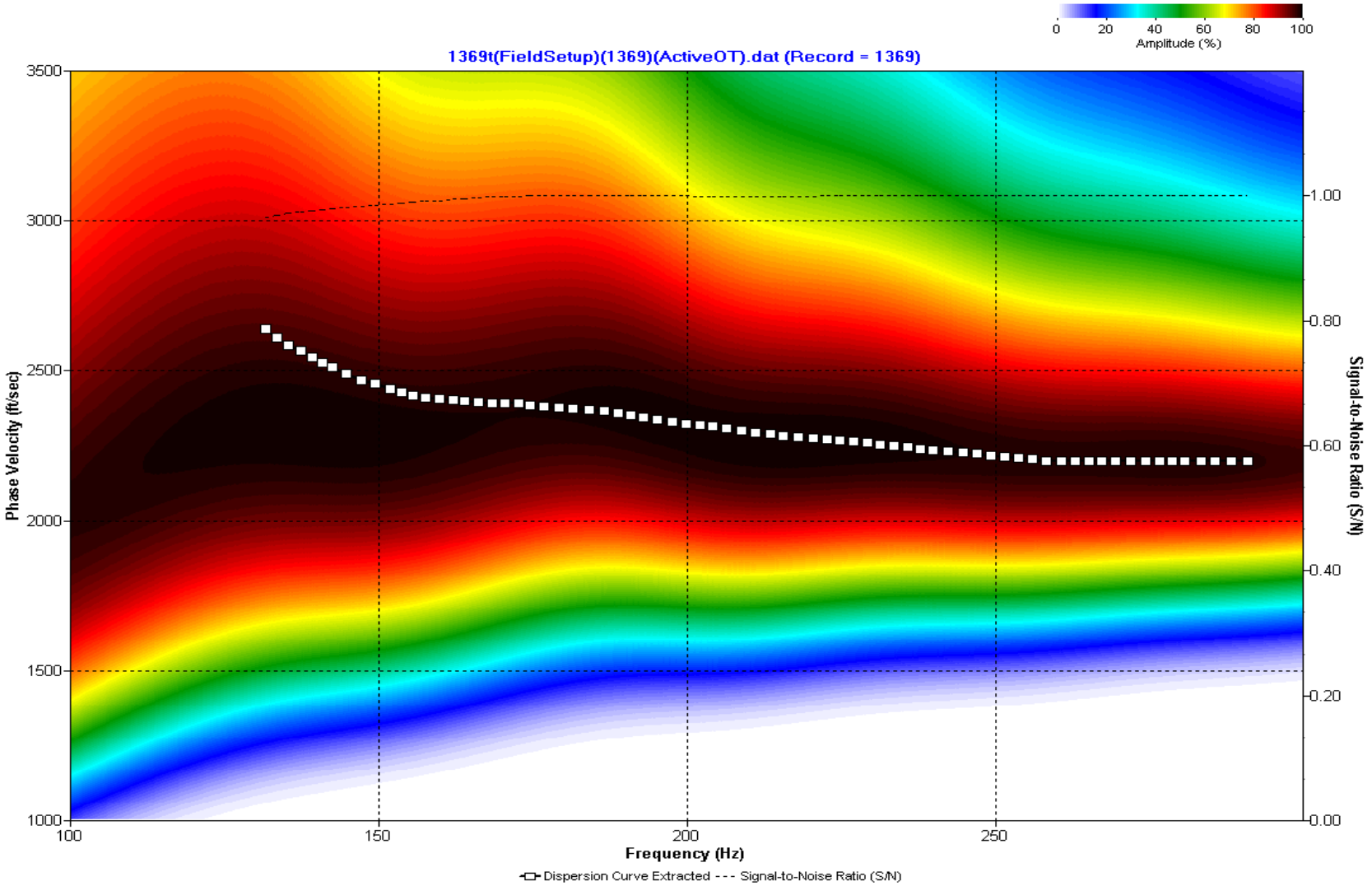

A.611: Dispersion Curve Line 1369 used in Post-blast 34 and Post-blast 35

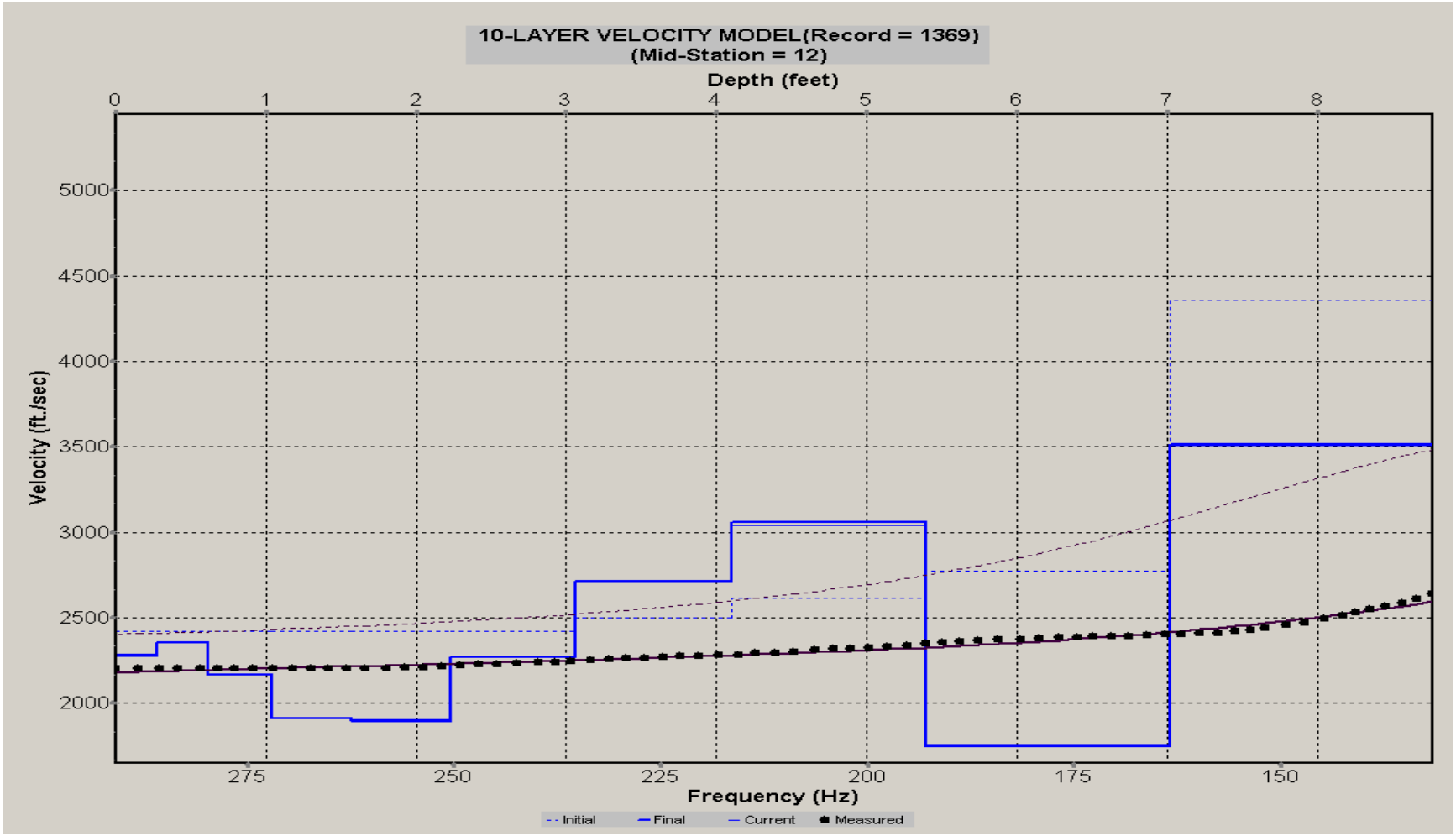

A.612: Velocity Profile Line 1369 used in Post-blast 34 and Post-blast 35

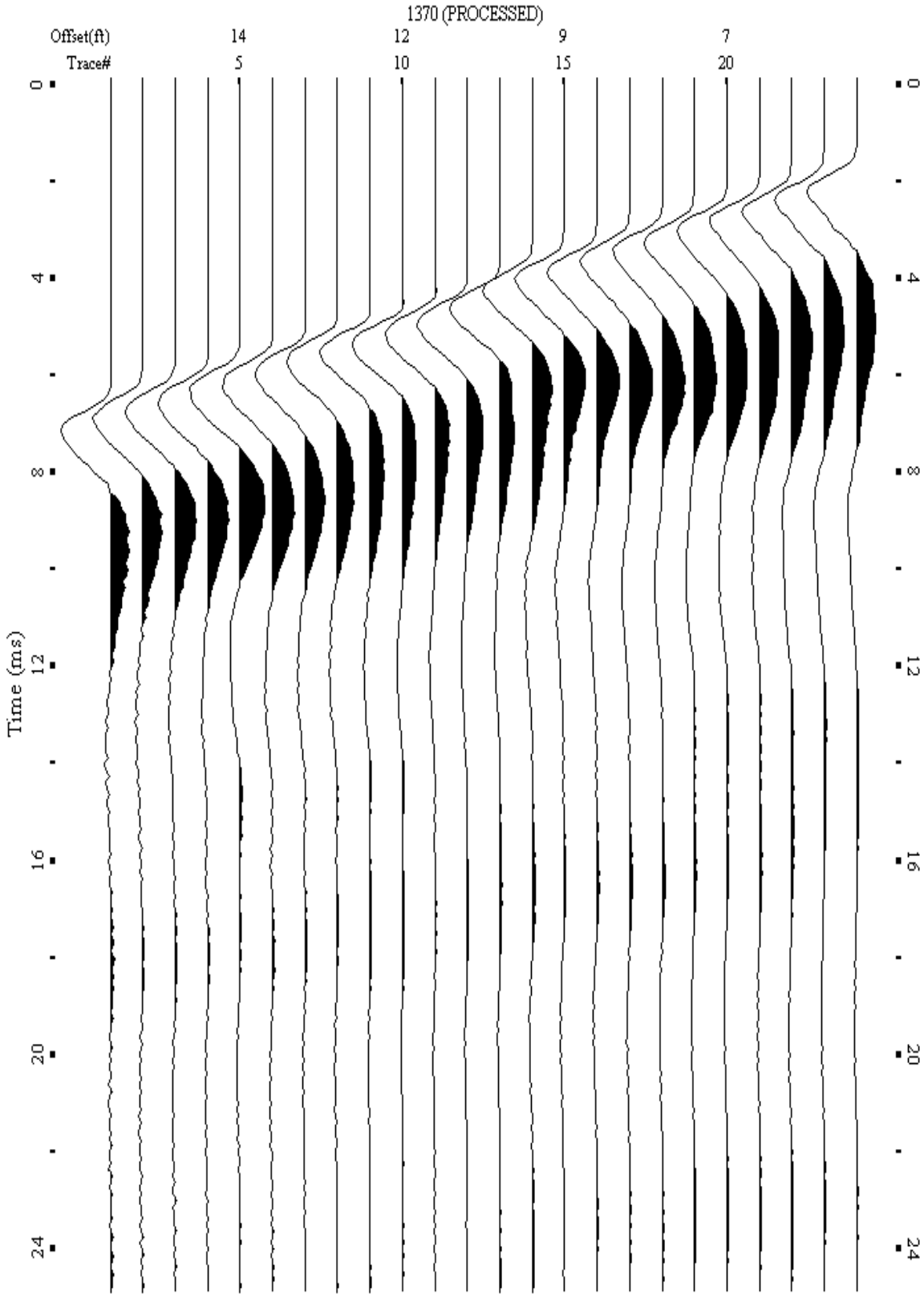

A.613 Shot Gather Line 1370 used in Post-blast 34 and Post-blast 35

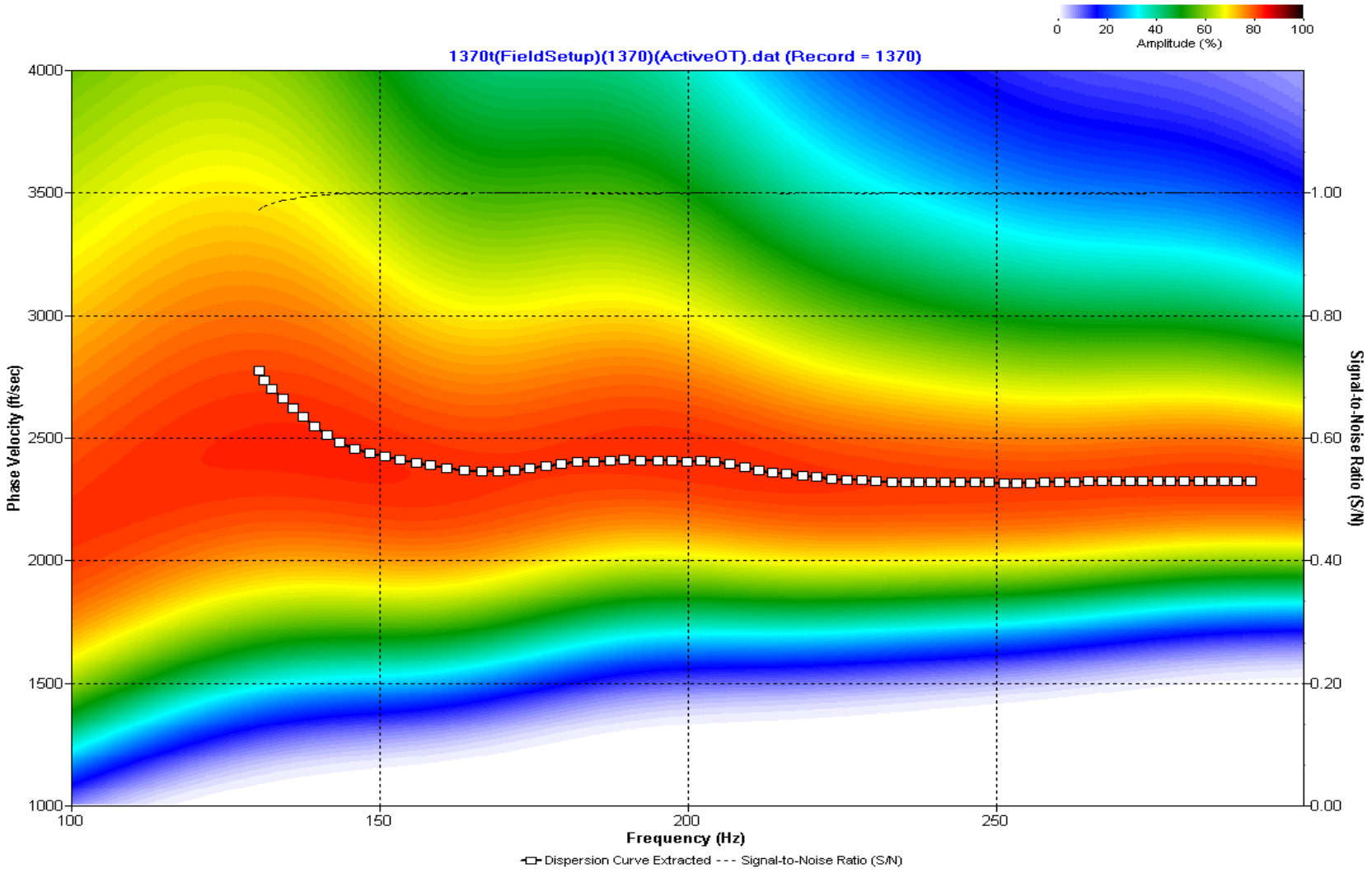

A.614: Dispersion Curve Line 1370 used in Post-blast 34 and Post-blast 35

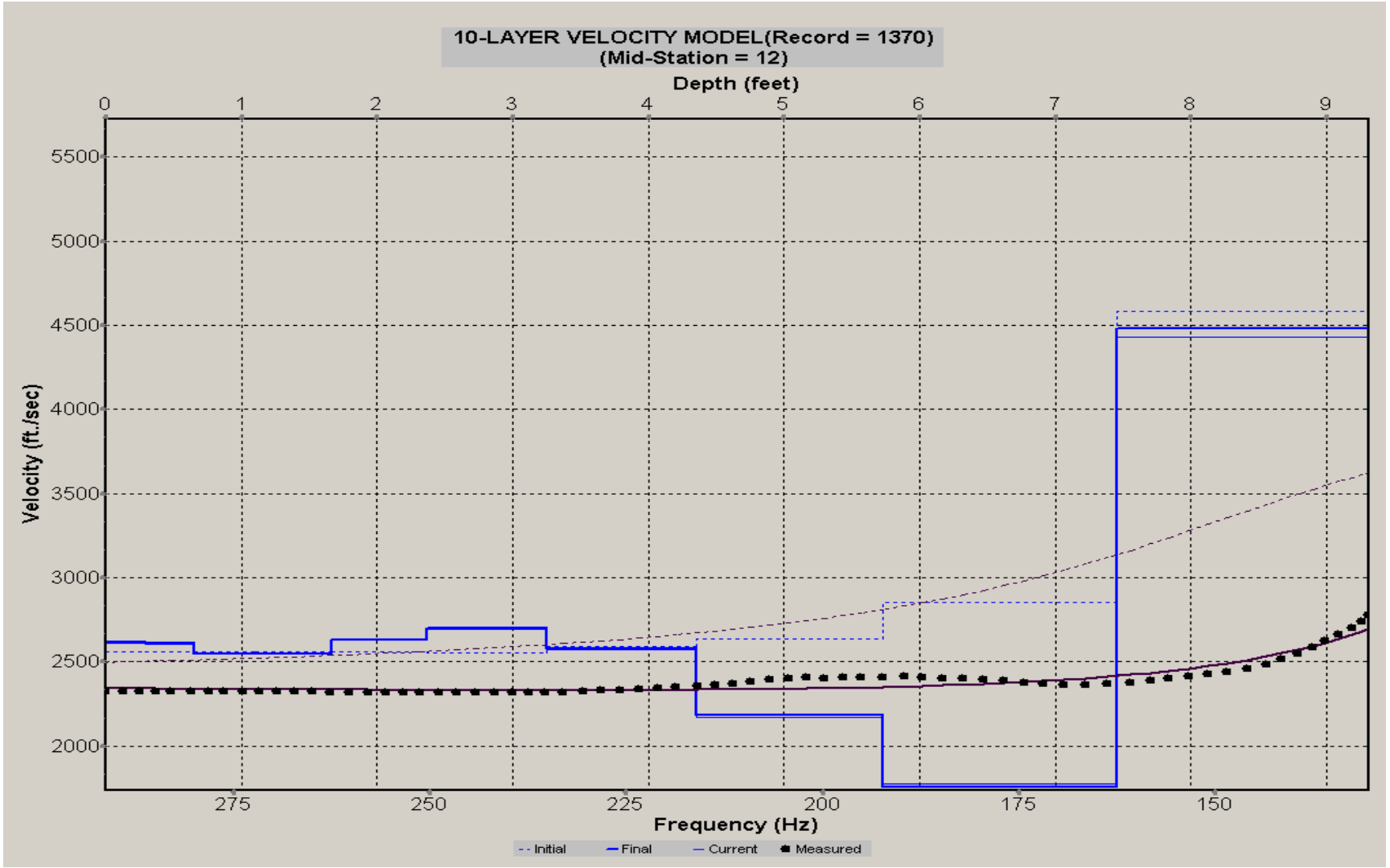

A.615: Velocity Profile Line 1370 used in Post-blast 34 and Post-blast 35

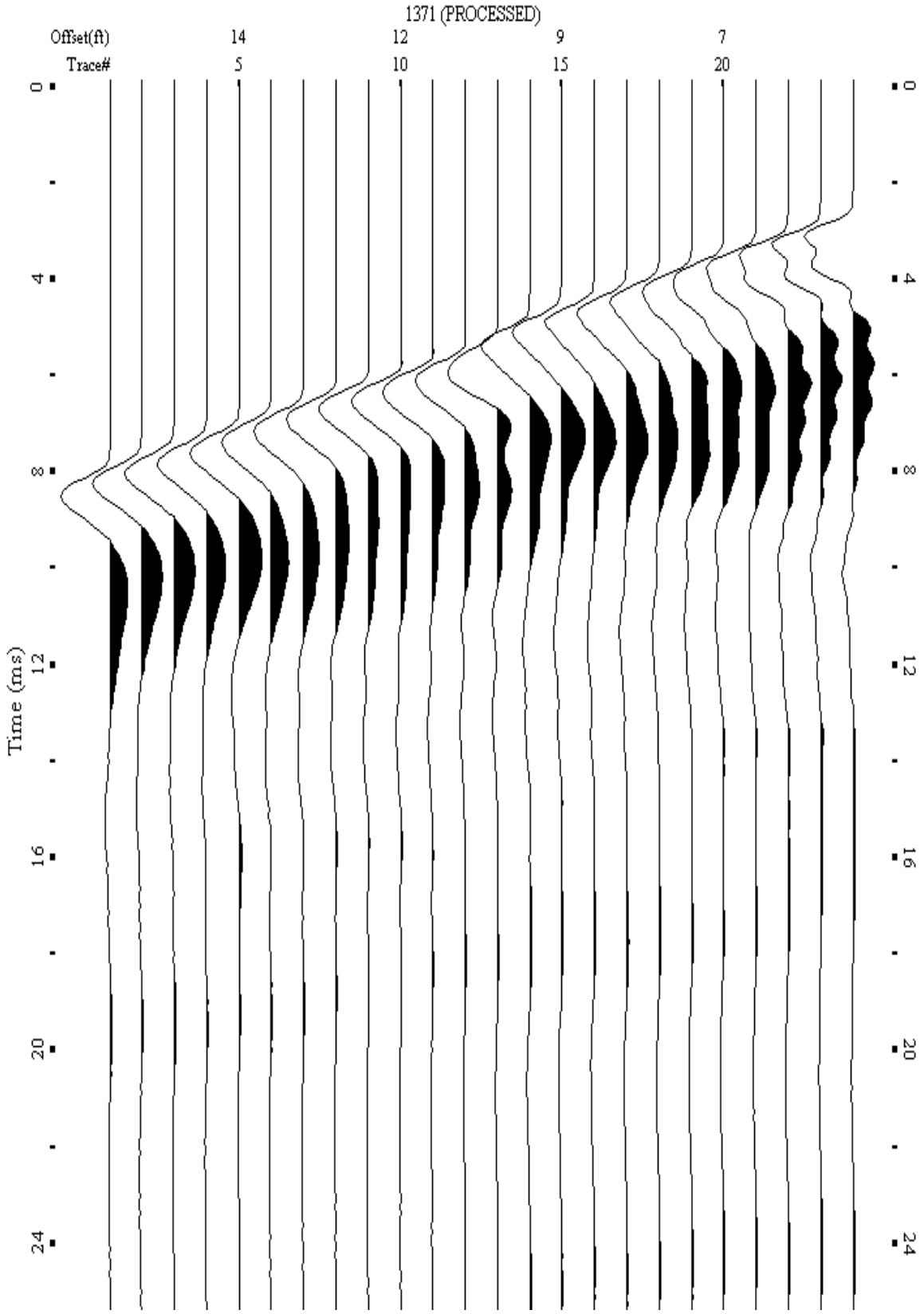

A.616 Shot Gather Line 1371 used in Post-blast 34 and Post-blast 35

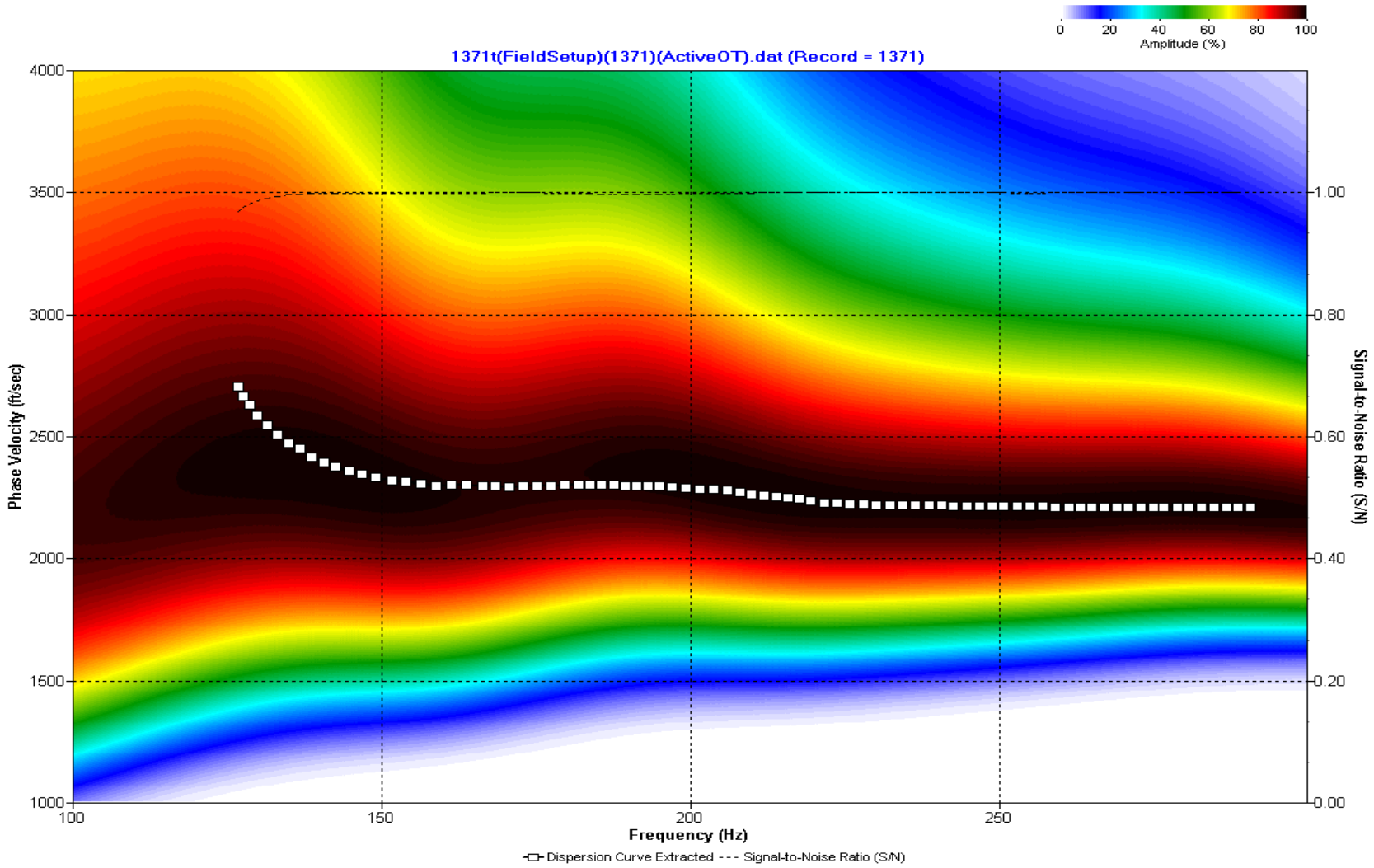

A.617: Dispersion Curve Line 1371 used in Post-blast 34 and Post-blast 35

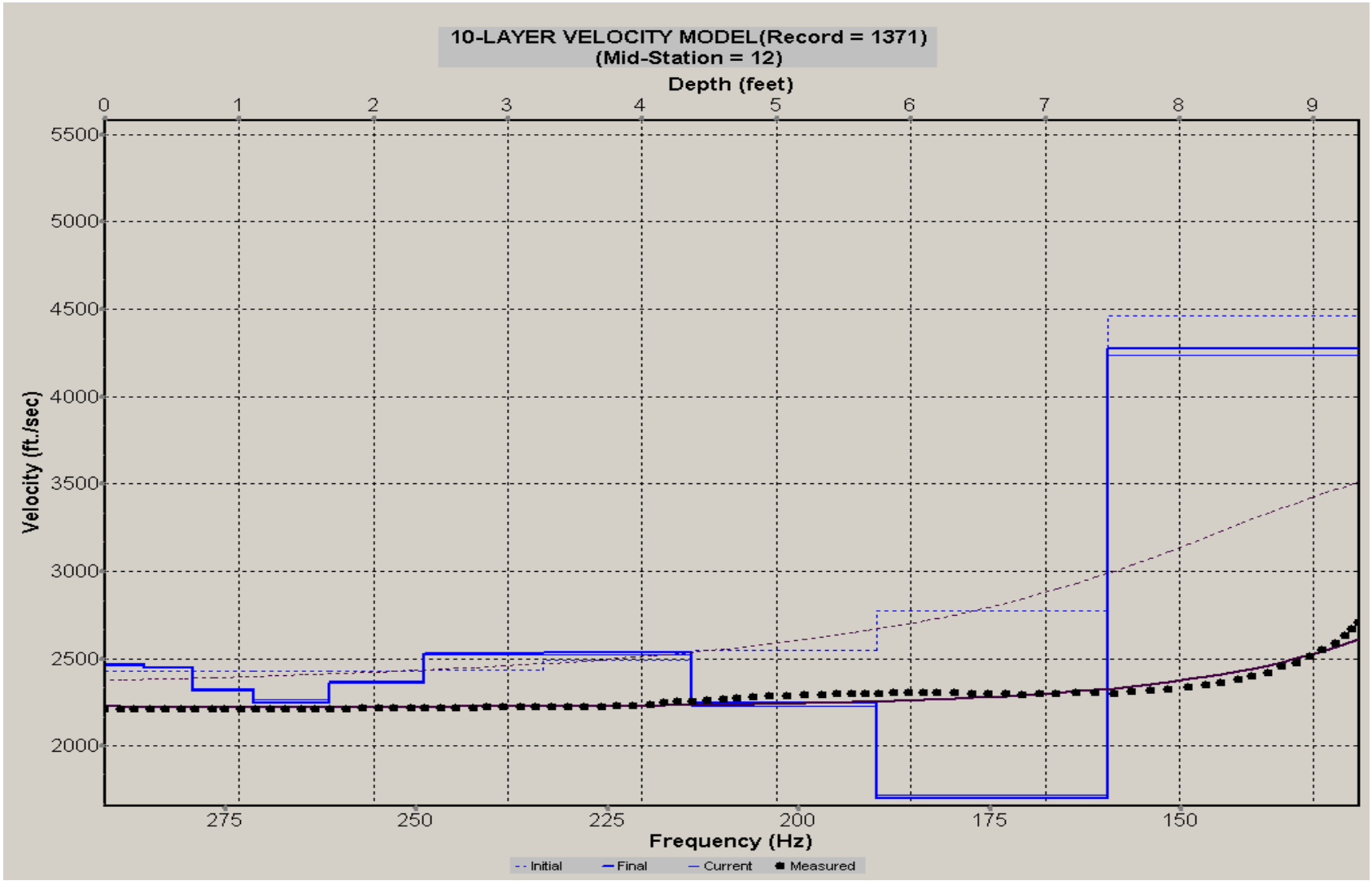

A.618: Velocity Profile Line 1371 used in Post-blast 34 and Post-blast 35

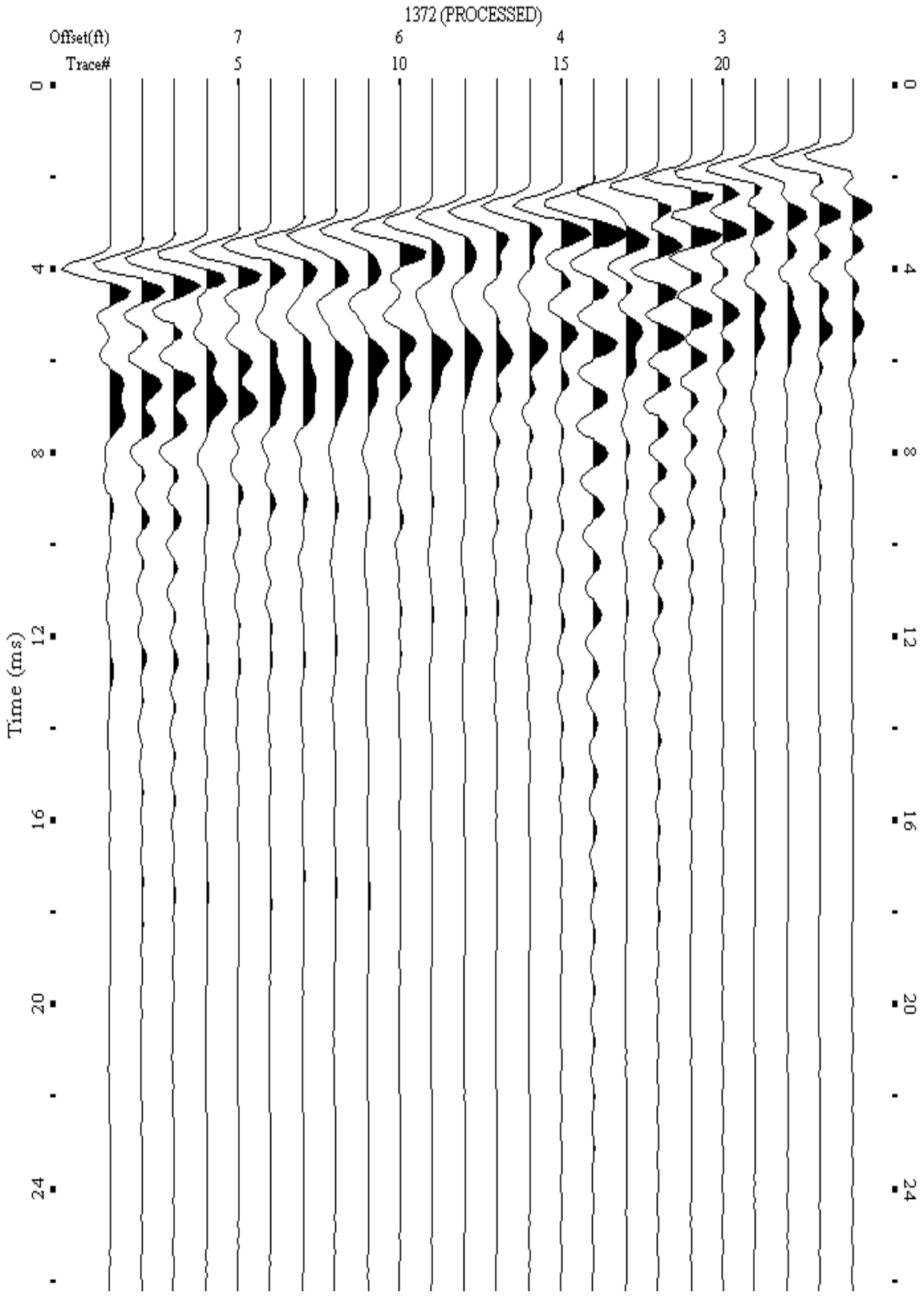

A.619 Shot Gather Line 1372 used in Pre-blast 40

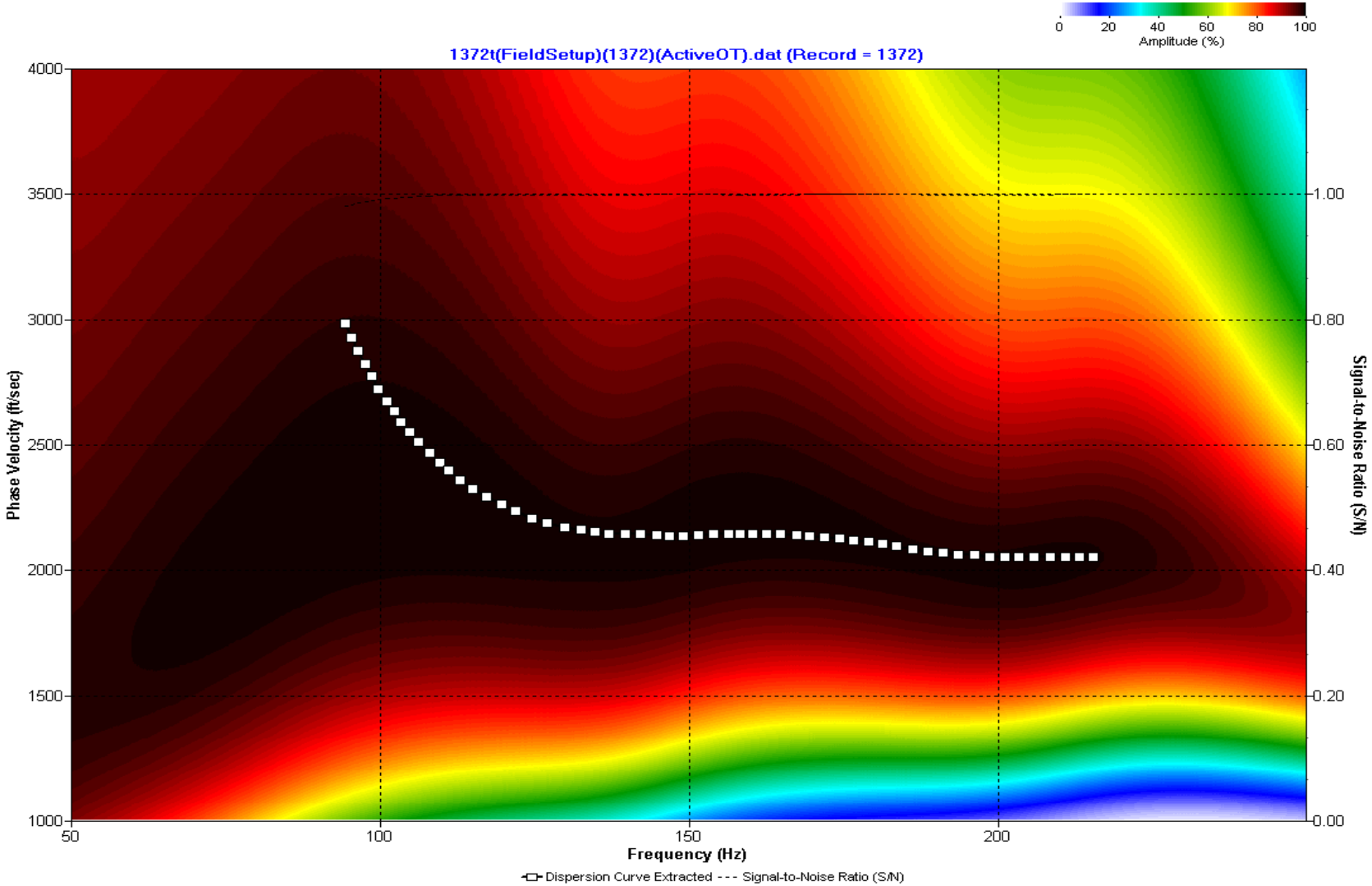

A.620: Dispersion Curve Line 1372 used in Pre-blast 40

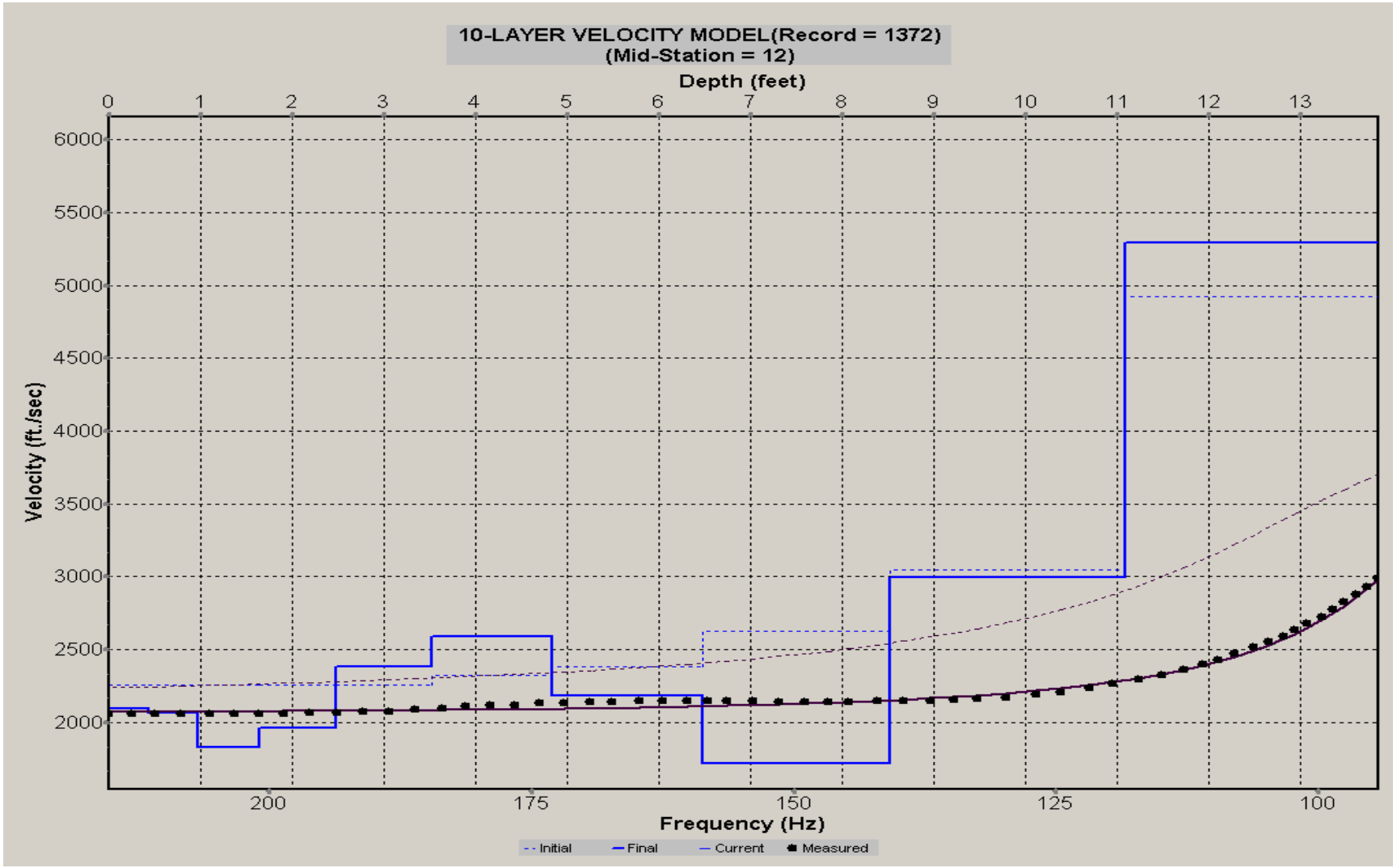

A.621: Velocity Profile Line 1372 used in Pre-blast 40

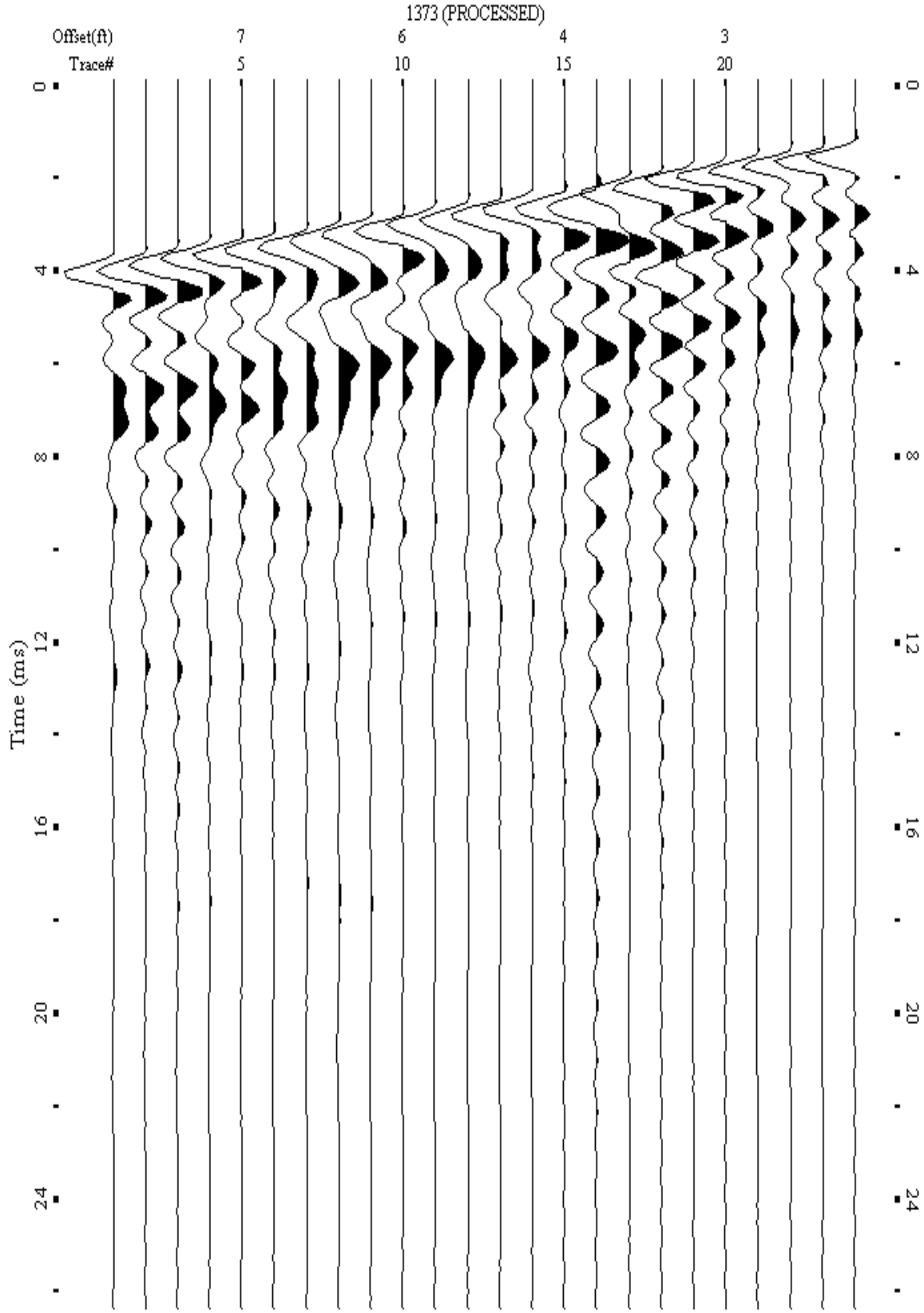

A.622 Shot Gather Line 1373 used in Pre-blast 40

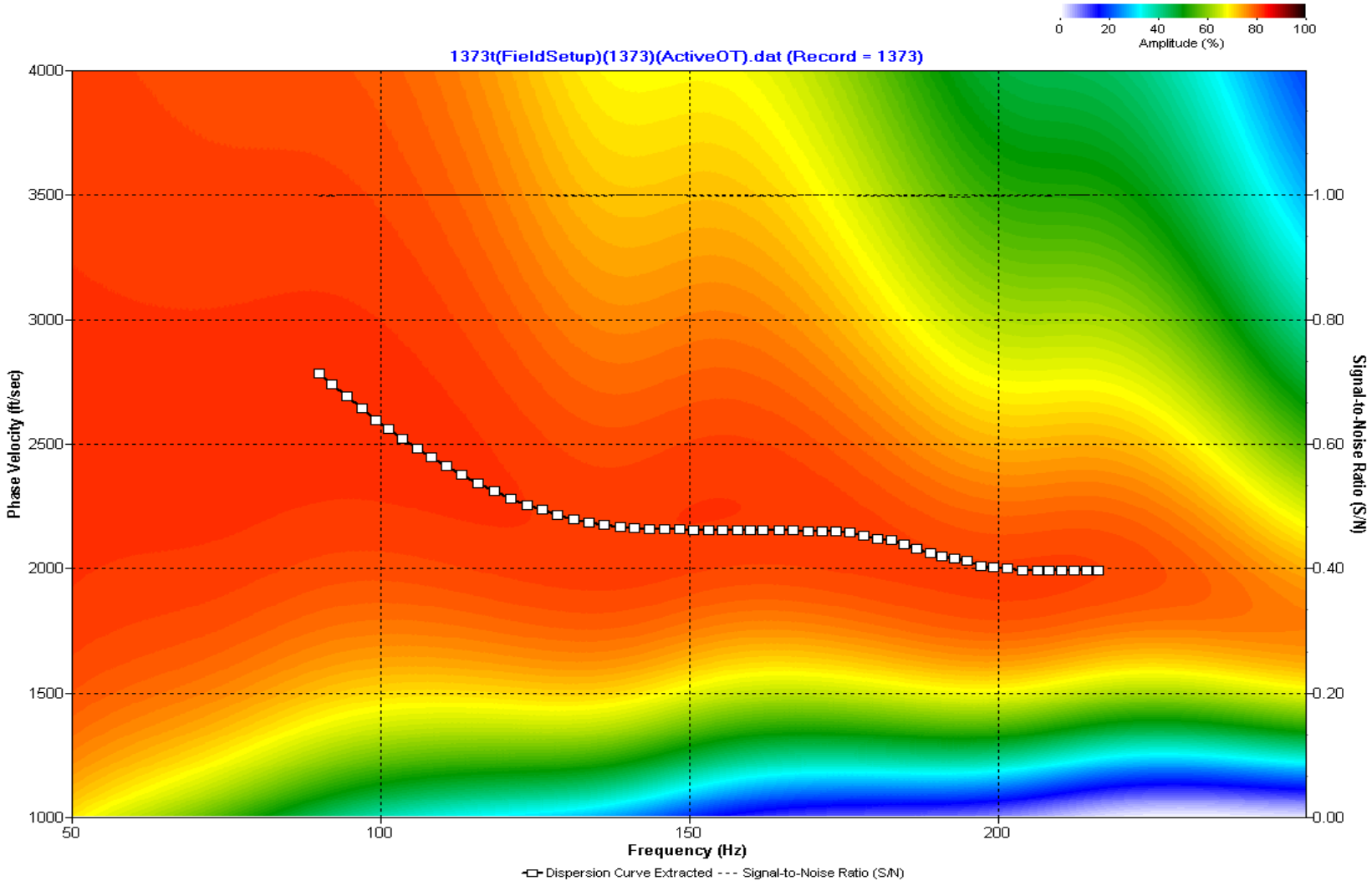

A.623: Dispersion Curve Line 1373 used in Pre-blast 40

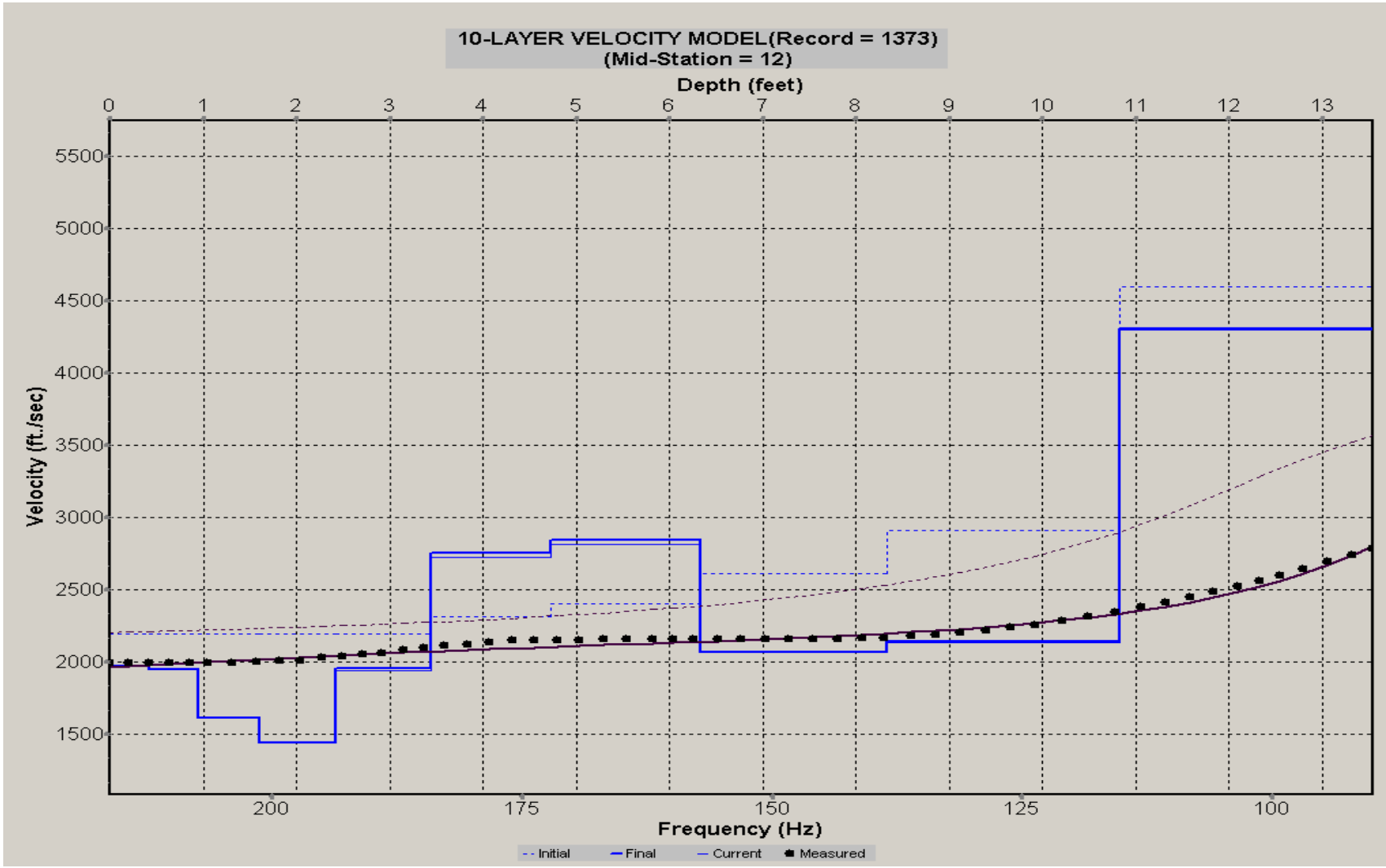

A.624: Velocity Profile Line 1373 used in Pre-blast 40

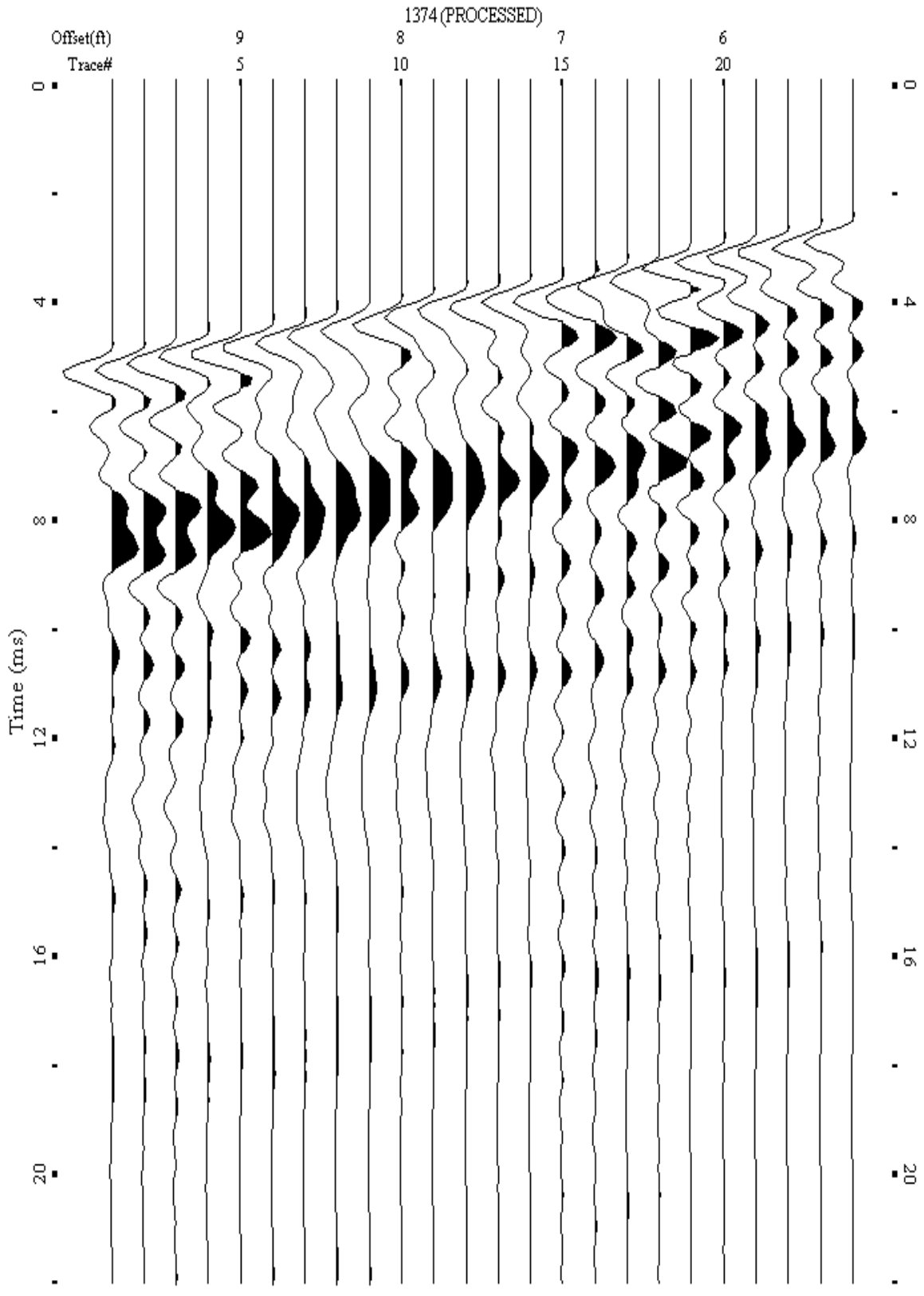

A.625 Shot Gather Line 1374 used in Pre-blast 40

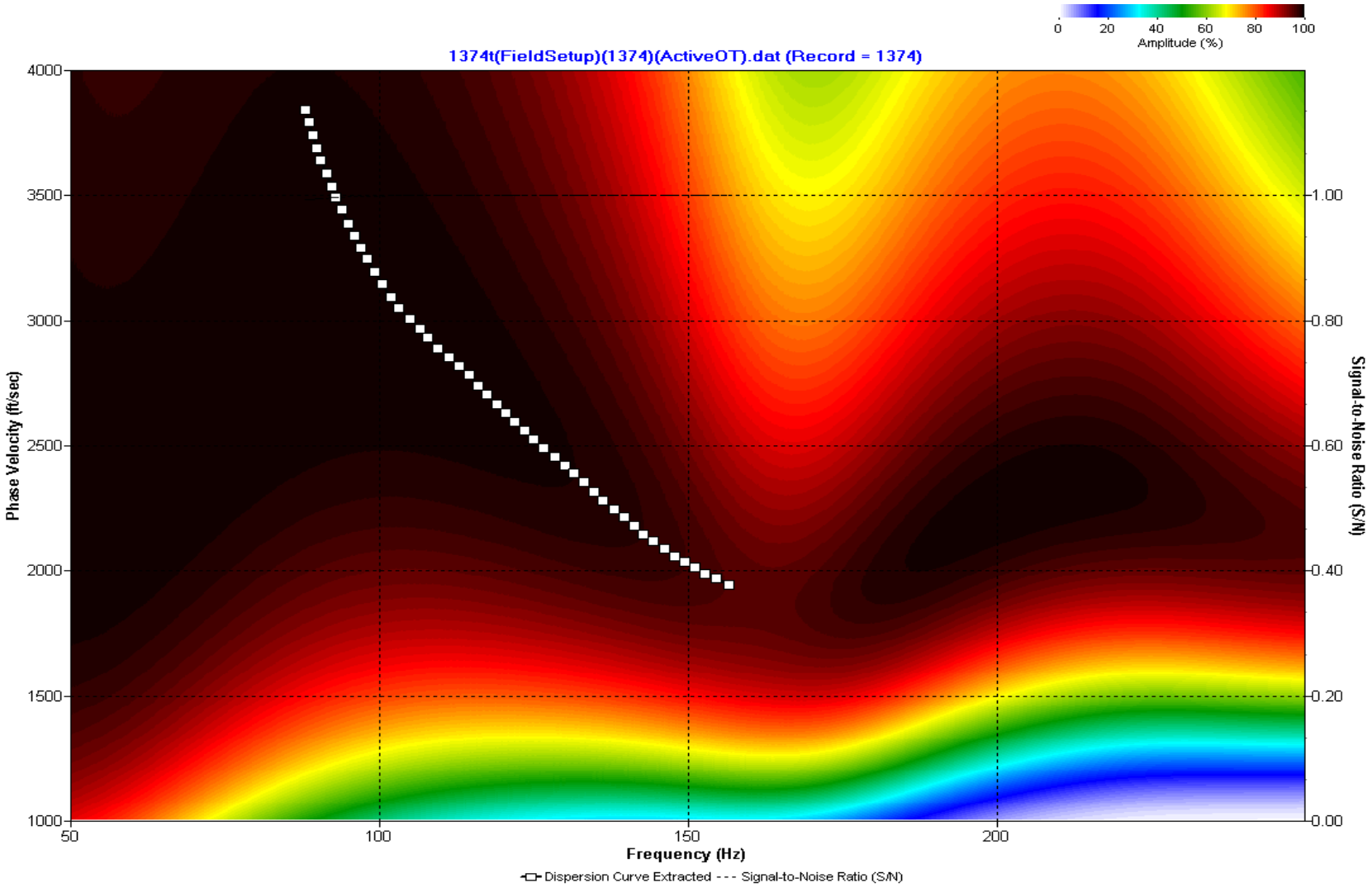

A.626: Dispersion Curve Line 1374 used in Pre-blast 40

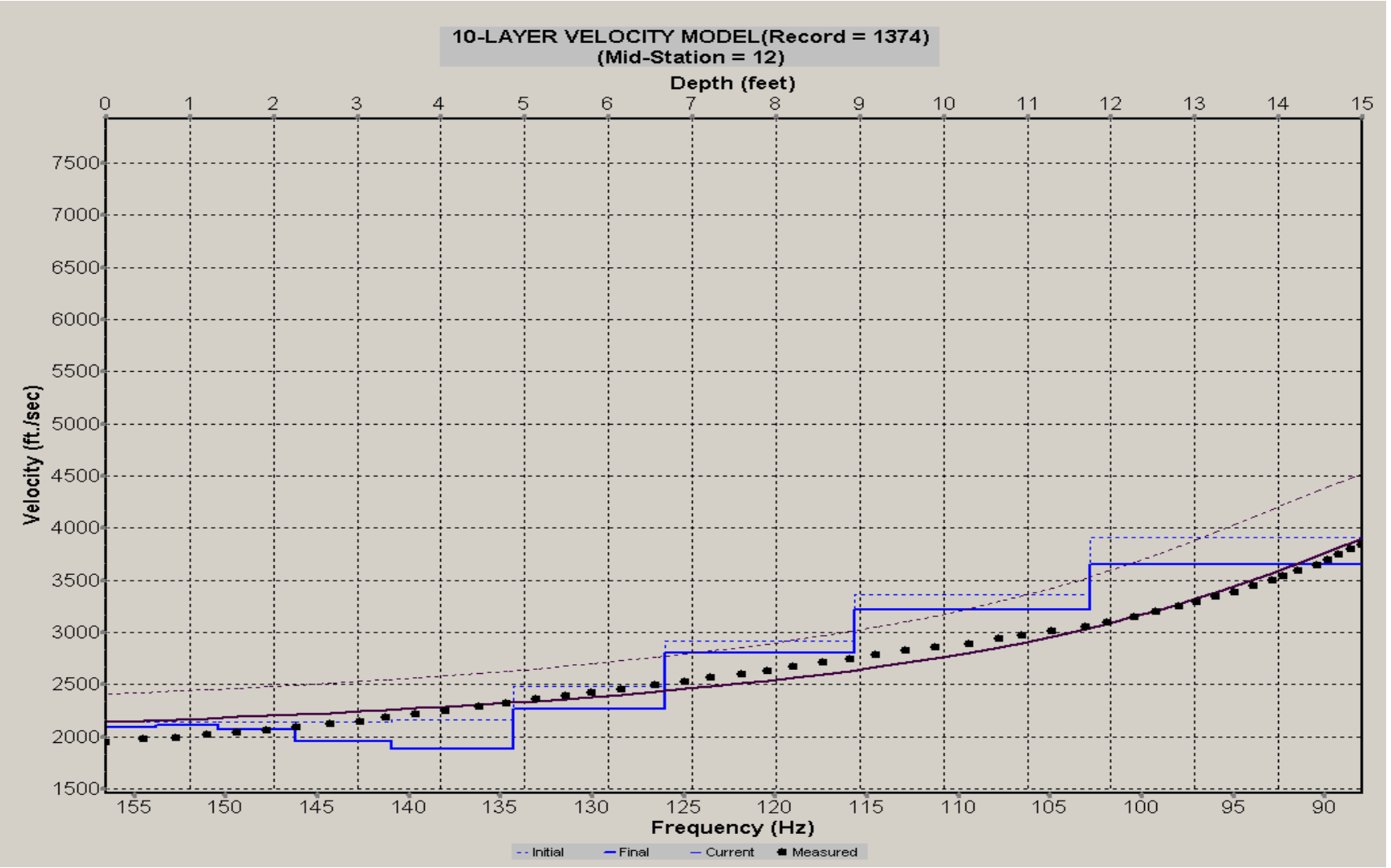

A.627: Velocity Profile Line 1374 used in Pre-blast 40

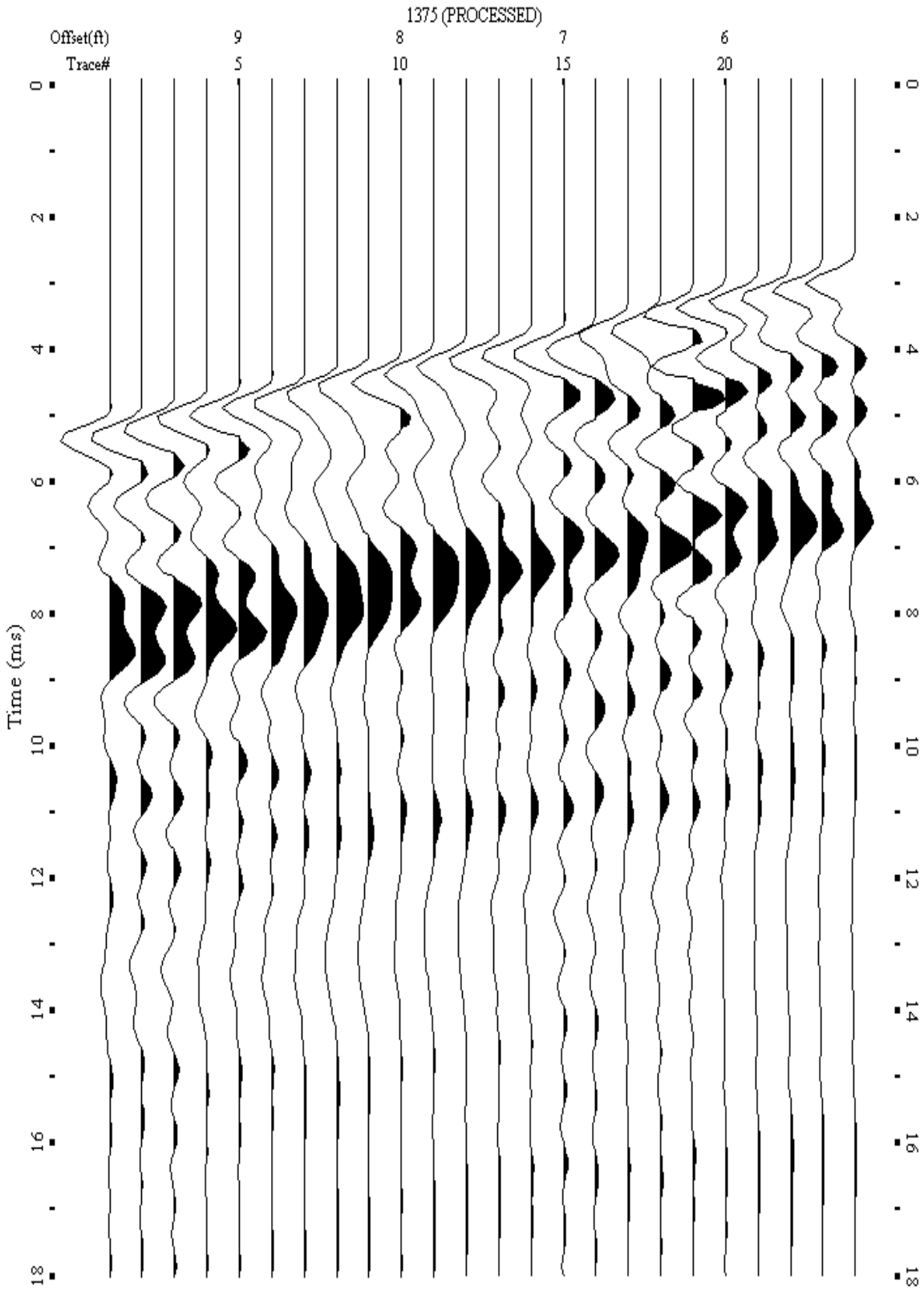

A.628 Shot Gather Line 1375 used in Pre-blast 40

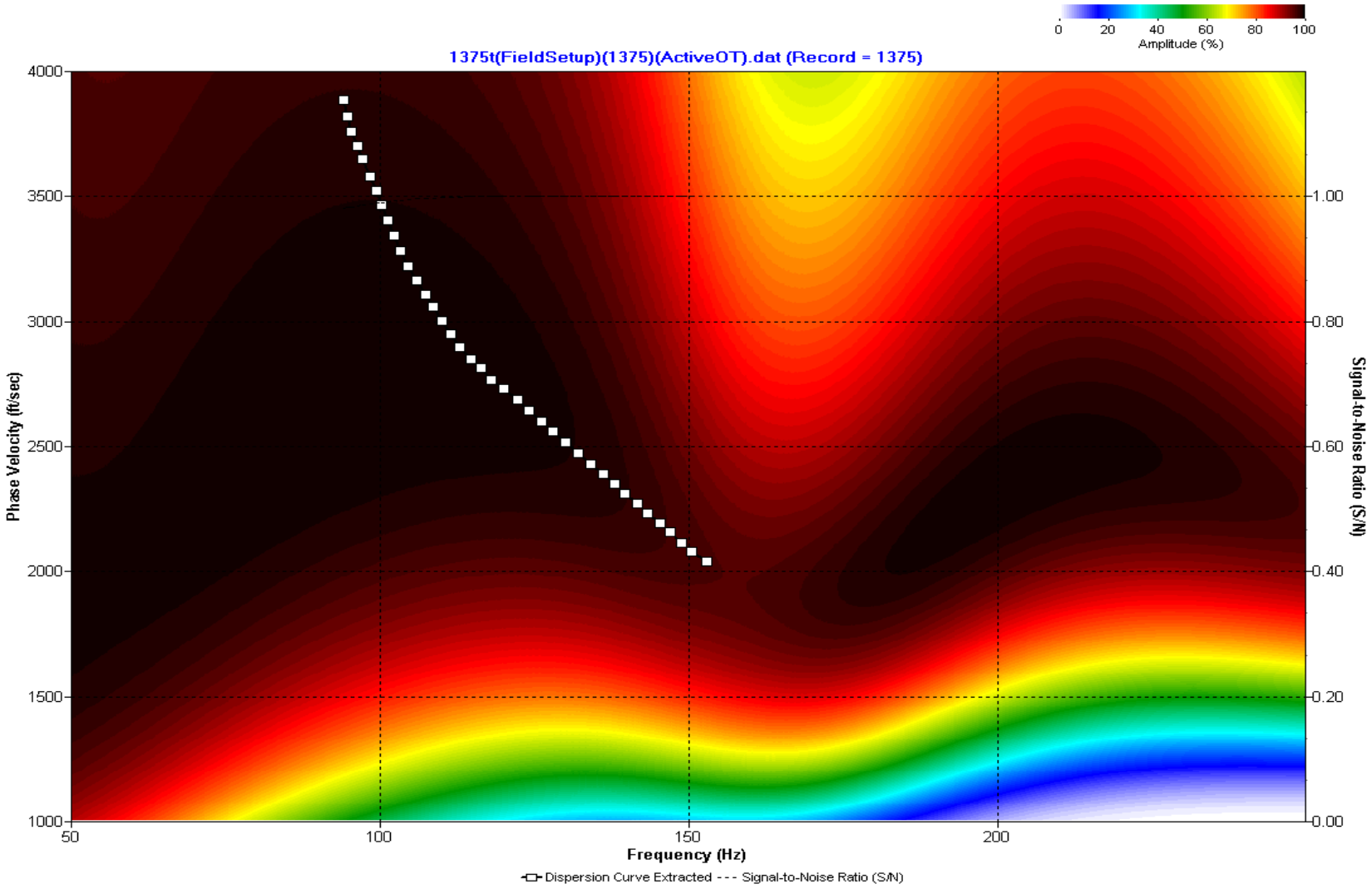

A.629: Dispersion Curve Line 1375 used in Pre-blast 40

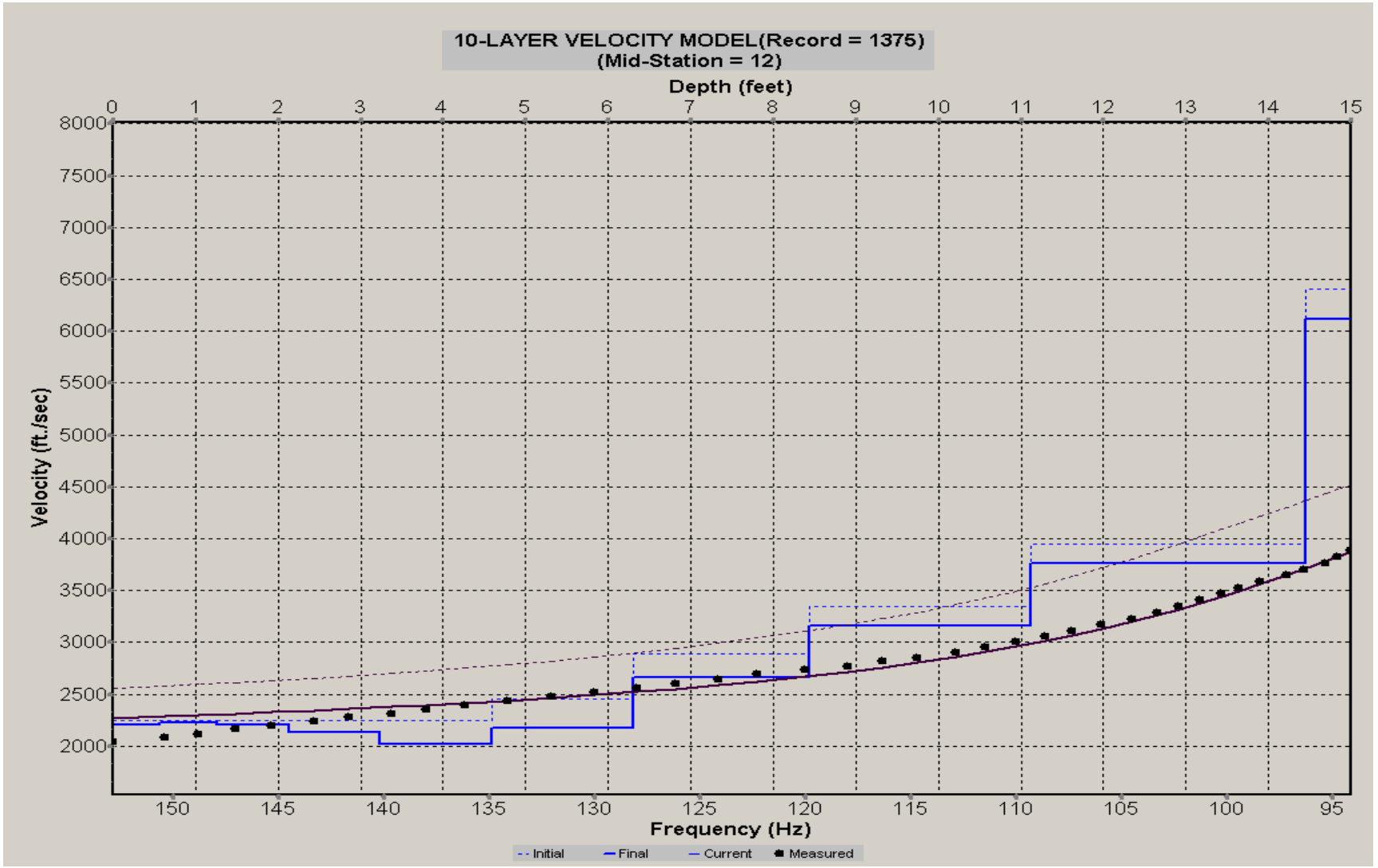

A.630: Velocity Profile Line 1375 used in Pre-blast 40

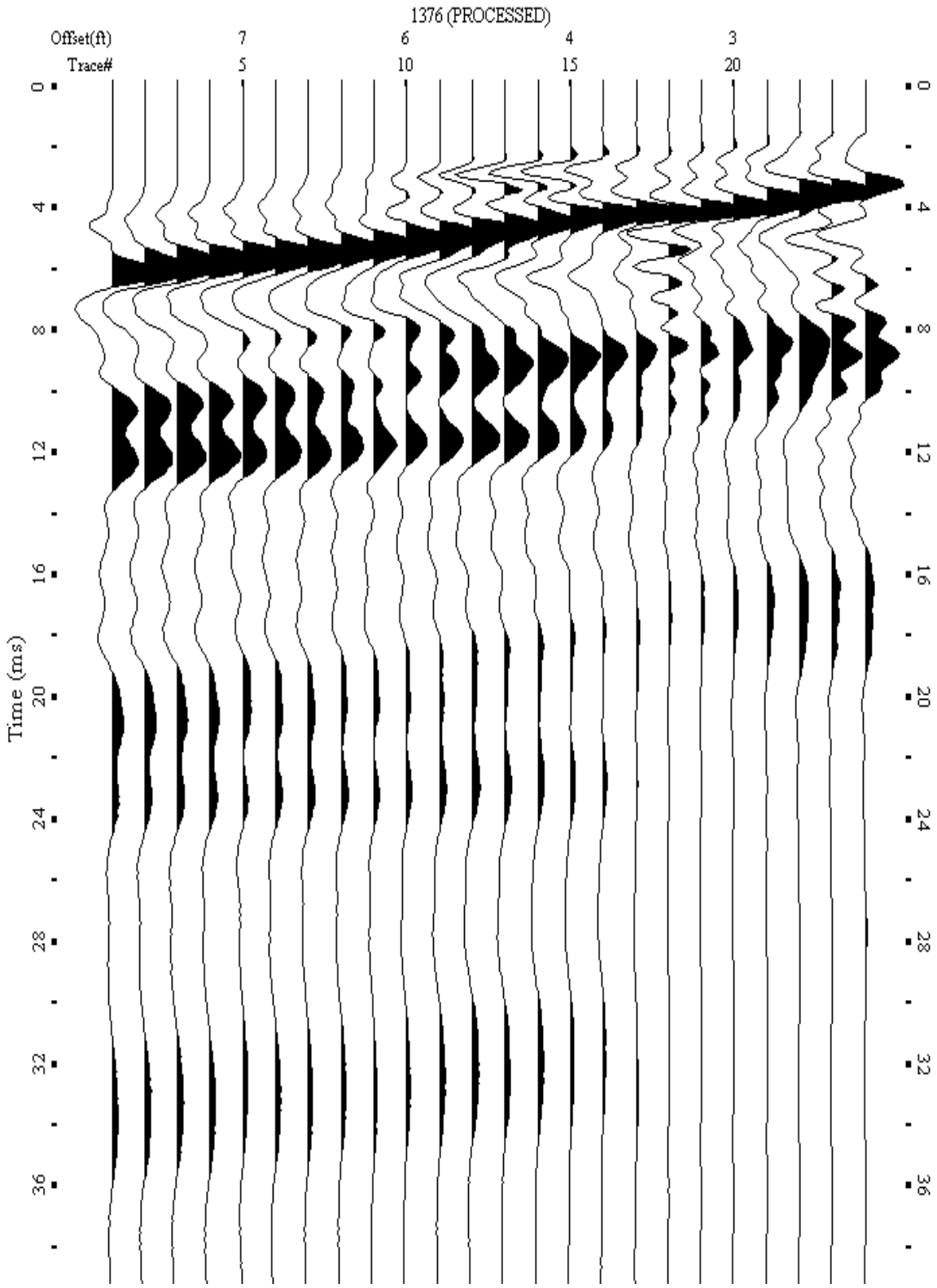

A.631: Shot Gather Line 1376 used in Pre-blast 11, Pre-blast 20, and Pre-blast 39

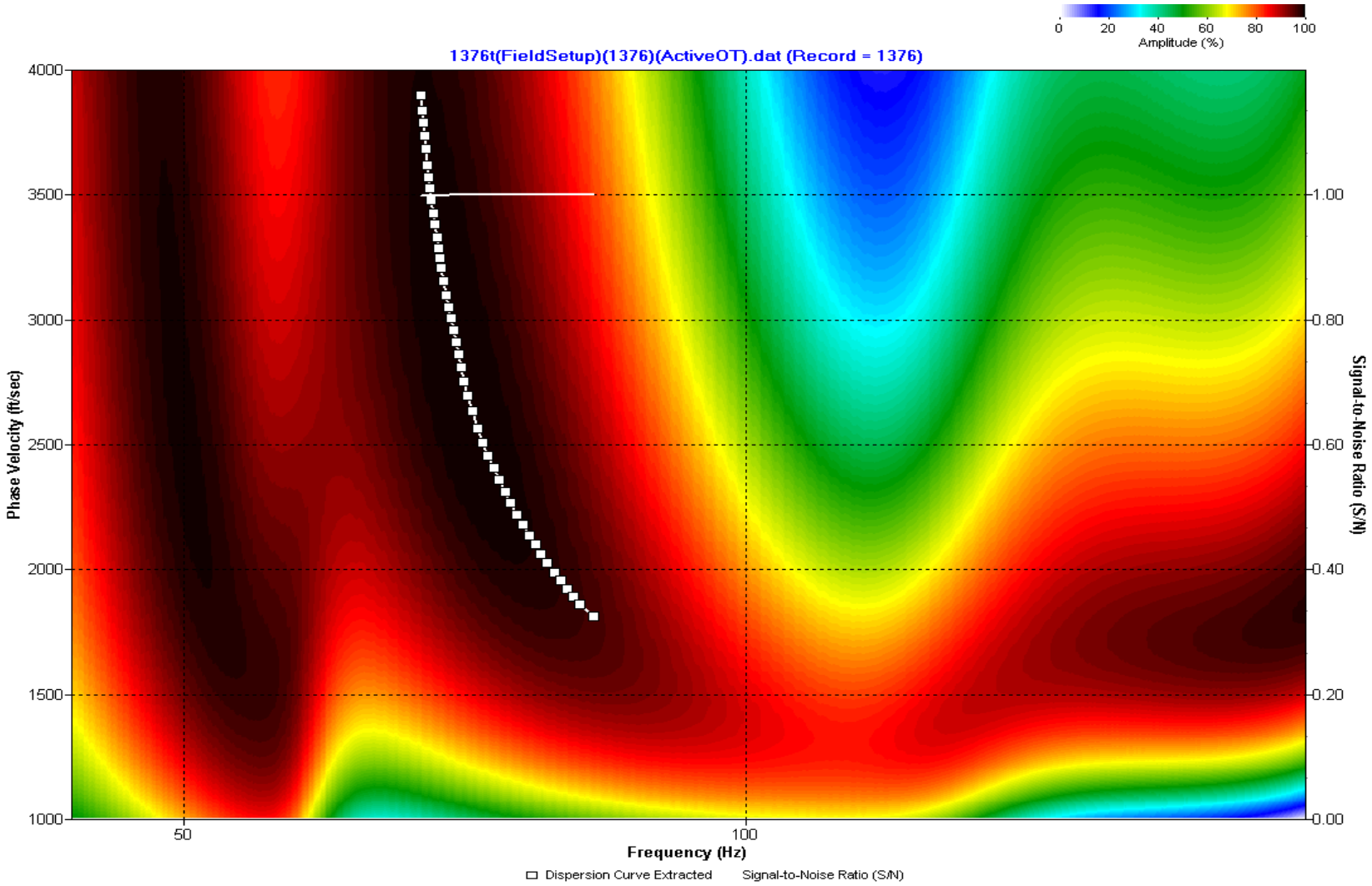

A.632: Dispersion Curve Line 1376 used in Pre-blast 11, Pre-blast 20, and Pre-blast 39

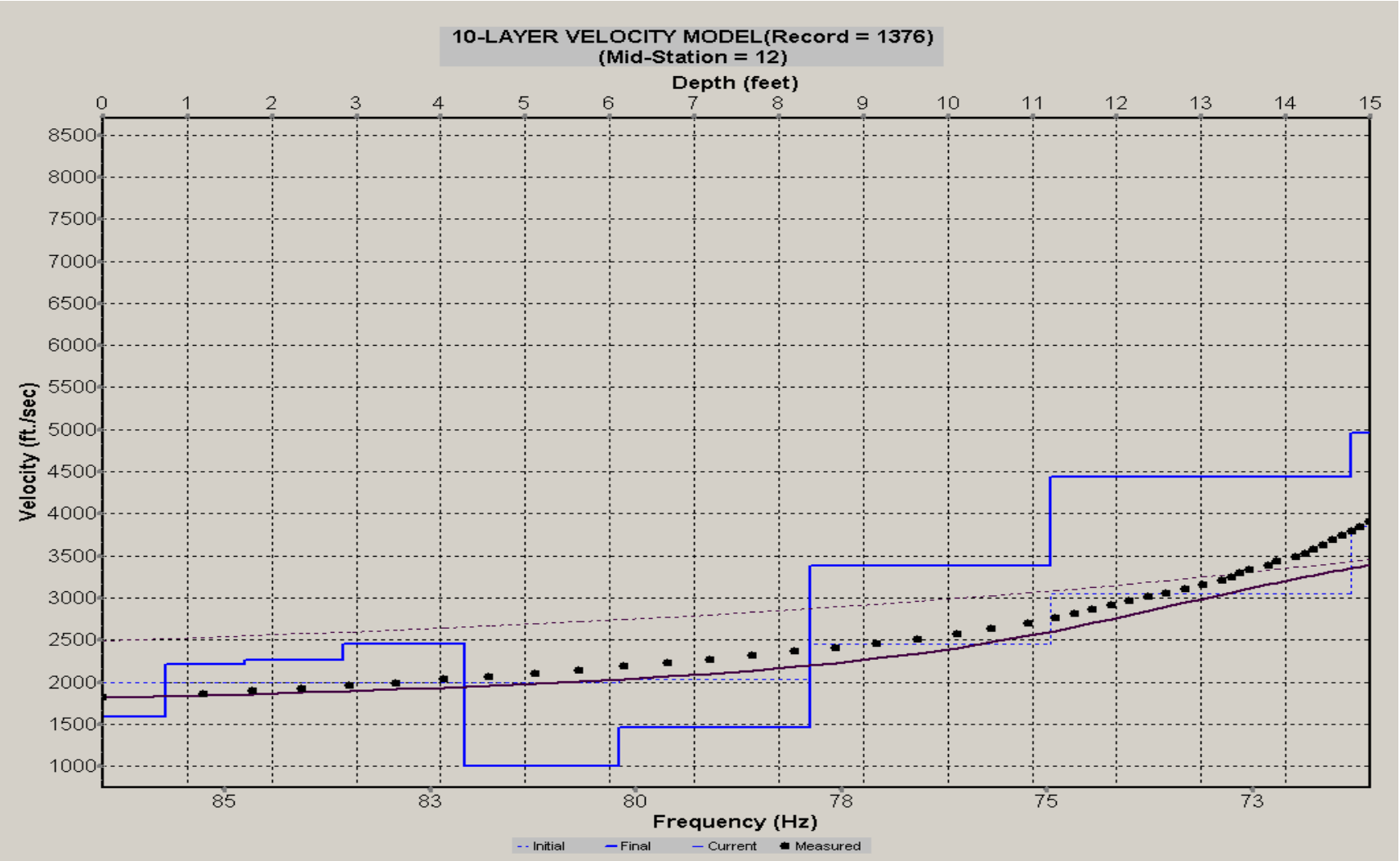

A.633: Velocity Profile Line 1376 used in Pre-blast 11, Pre-blast 20, and Pre-blast 39

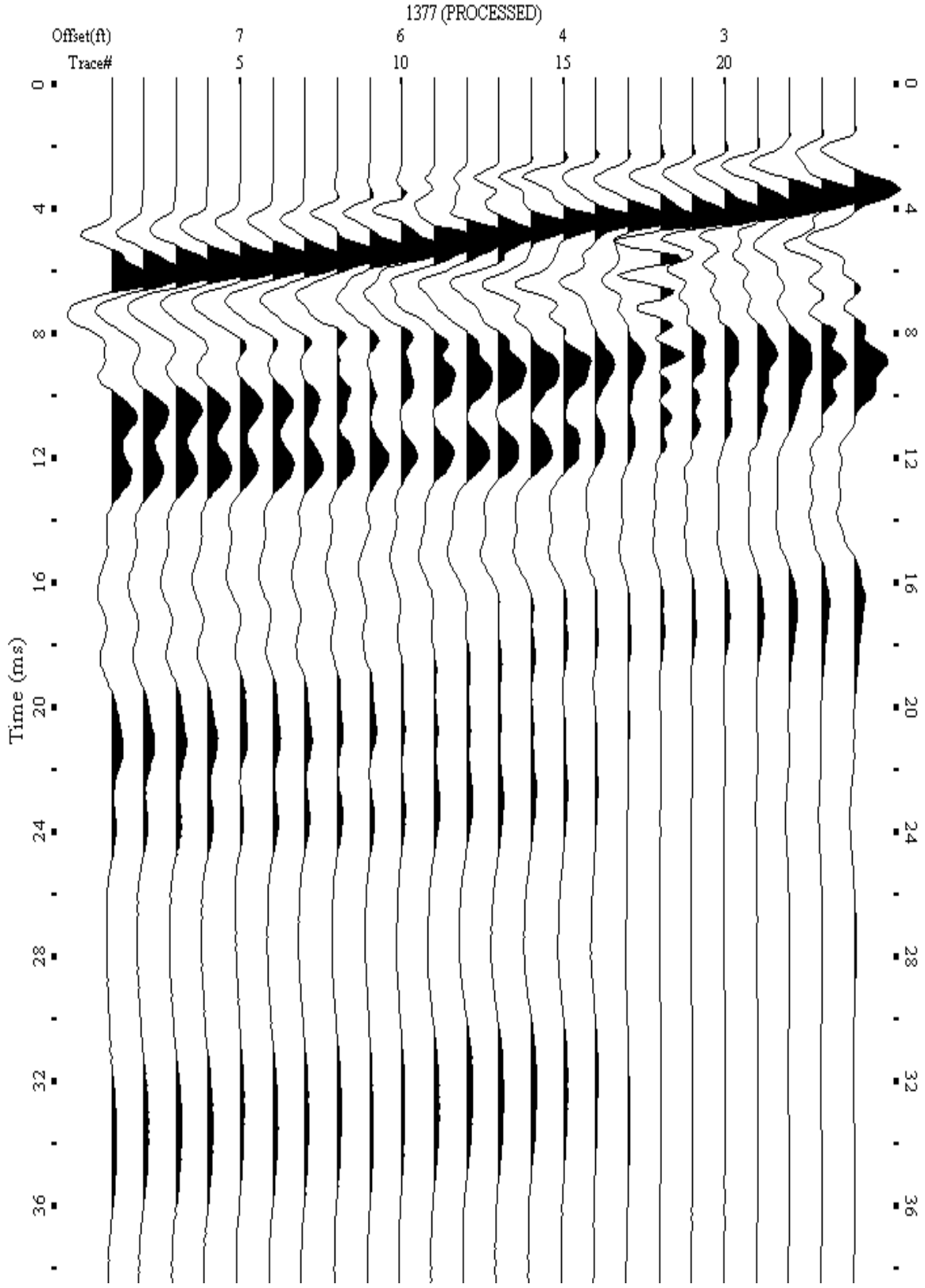

A.634: Shot Gather Line 1377 used in Pre-blast 11, Pre-blast 20, and Pre-blast 39

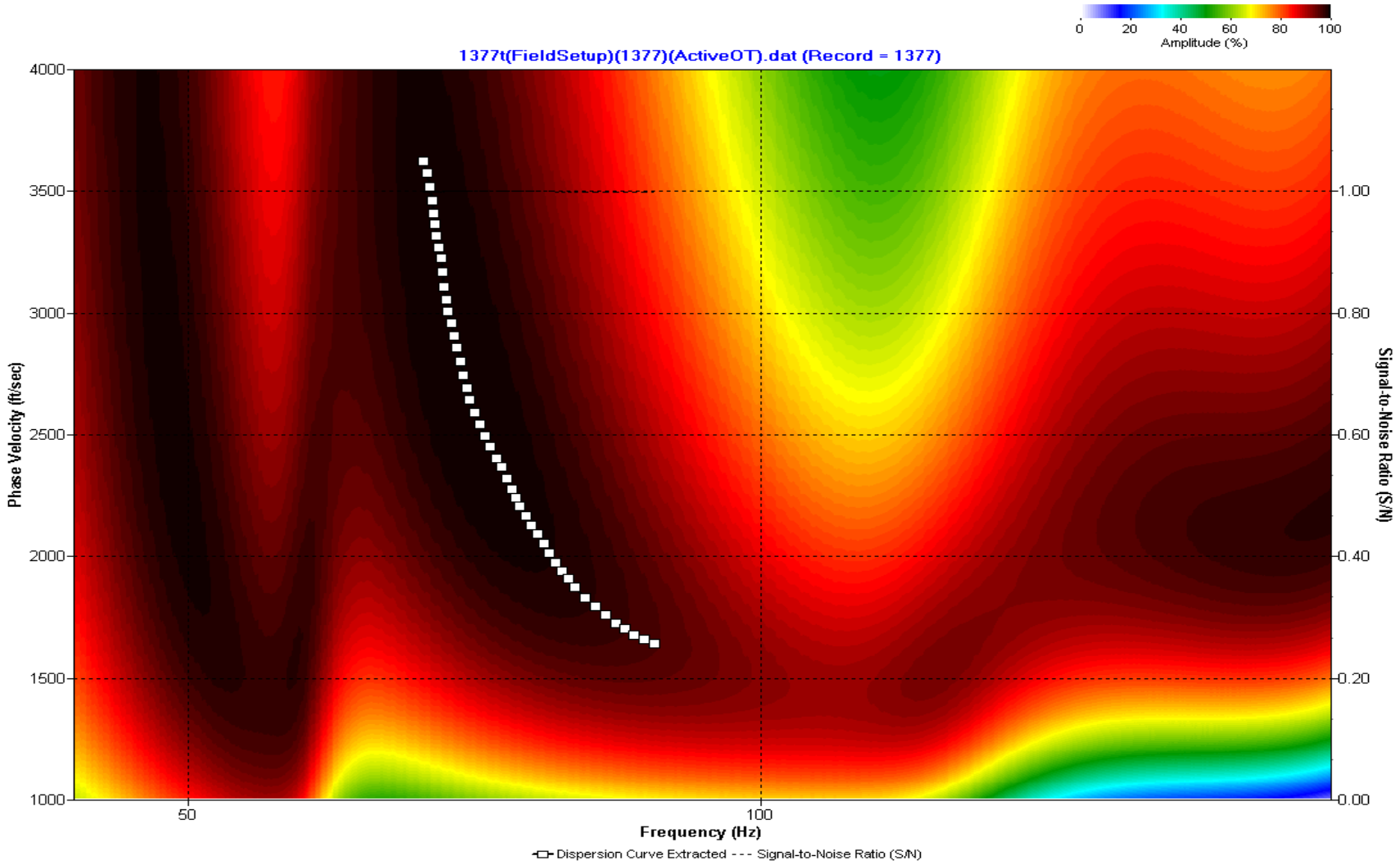

A.635: Dispersion Curve Line 1377 used in Pre-blast 11, Pre-blast 20, and Pre-blast 39

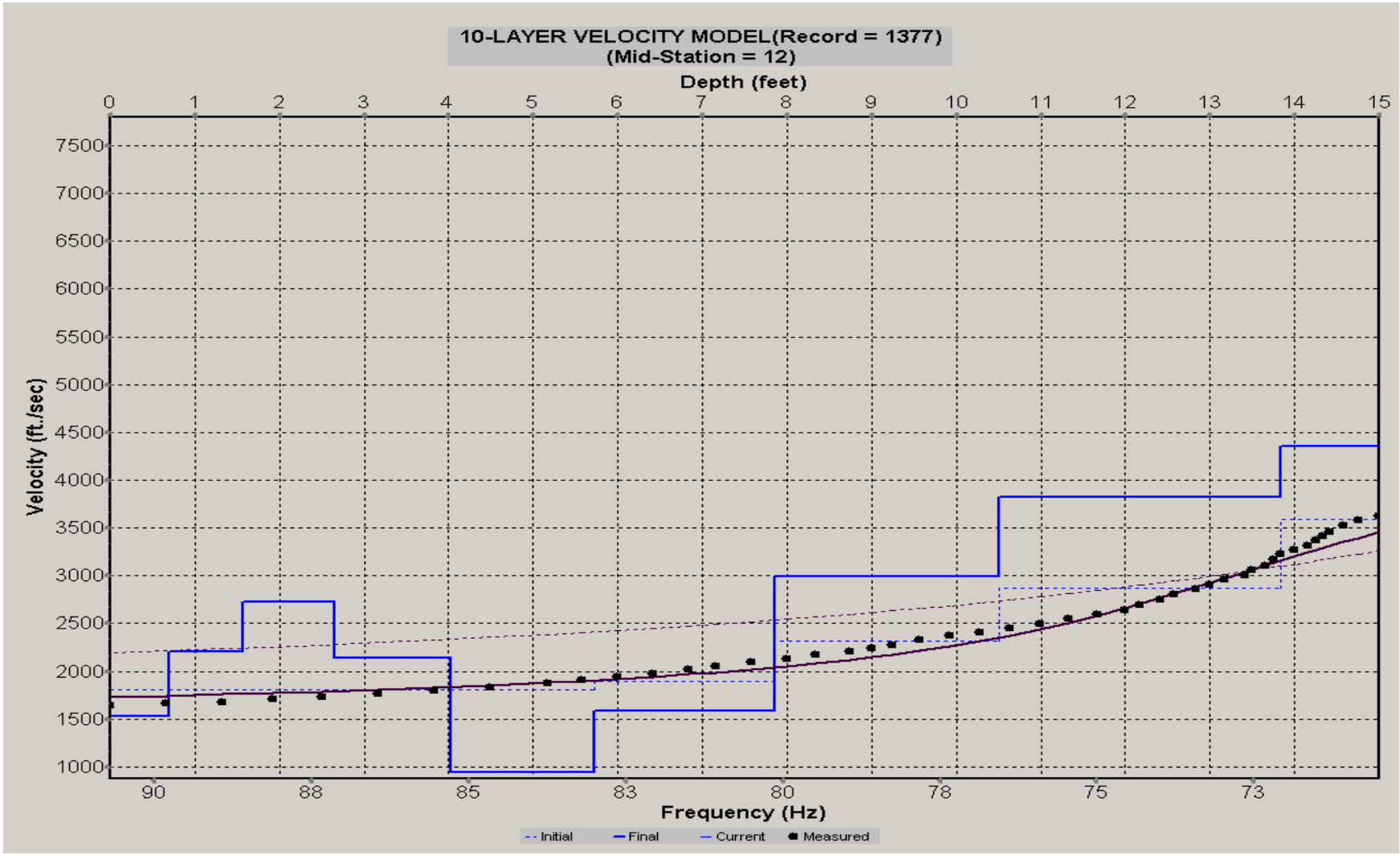

A.636: Velocity Profile Line 1377 used in Pre-blast 11, Pre-blast 20, and Pre-blast 39

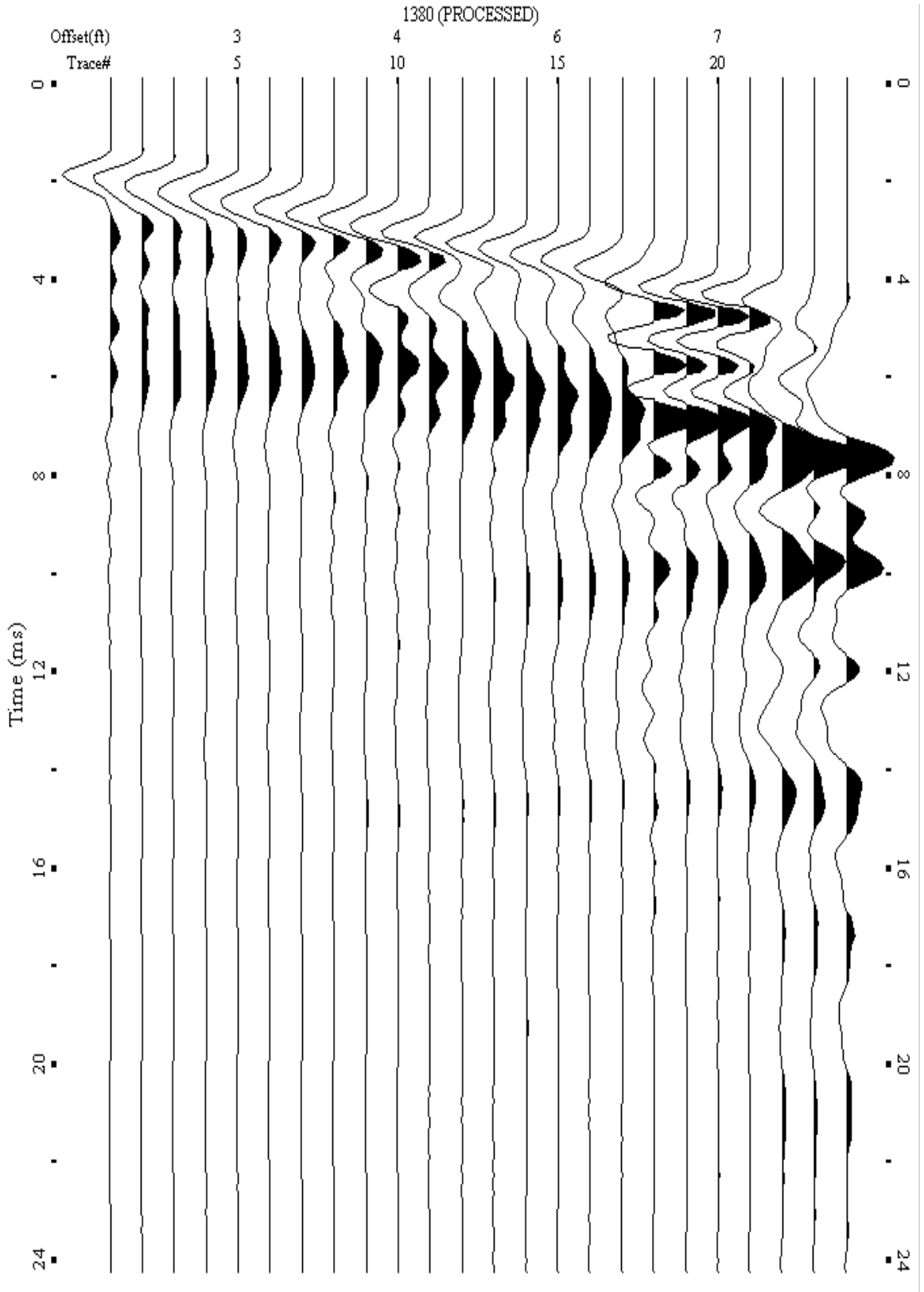

A.637: Shot Gather Line 1380 used in Pre-blast 11 and Pre-blast 39

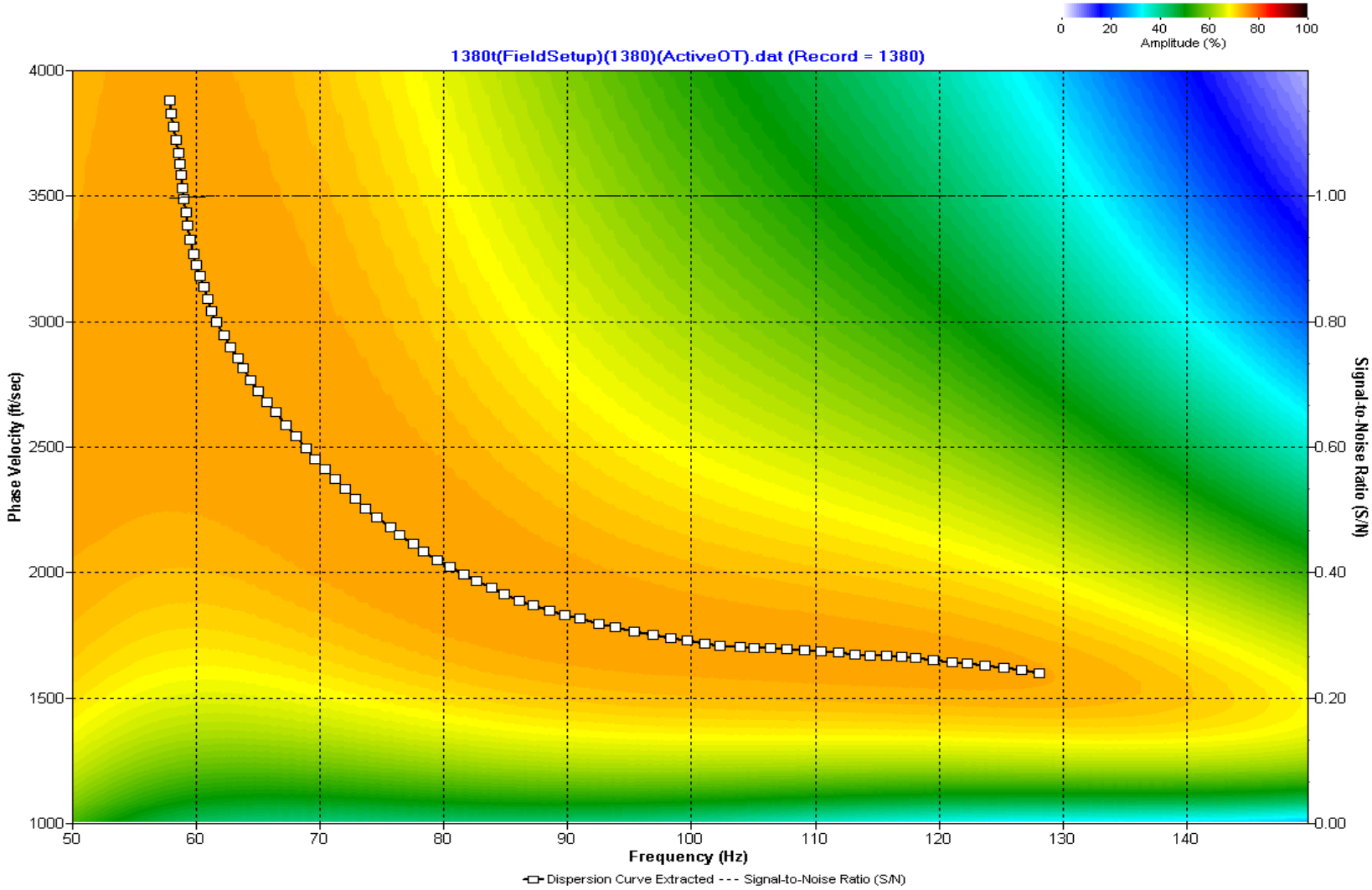

A.638: Dispersion Curve Line 1380 used in Pre-blast 11 and Pre-blast 39

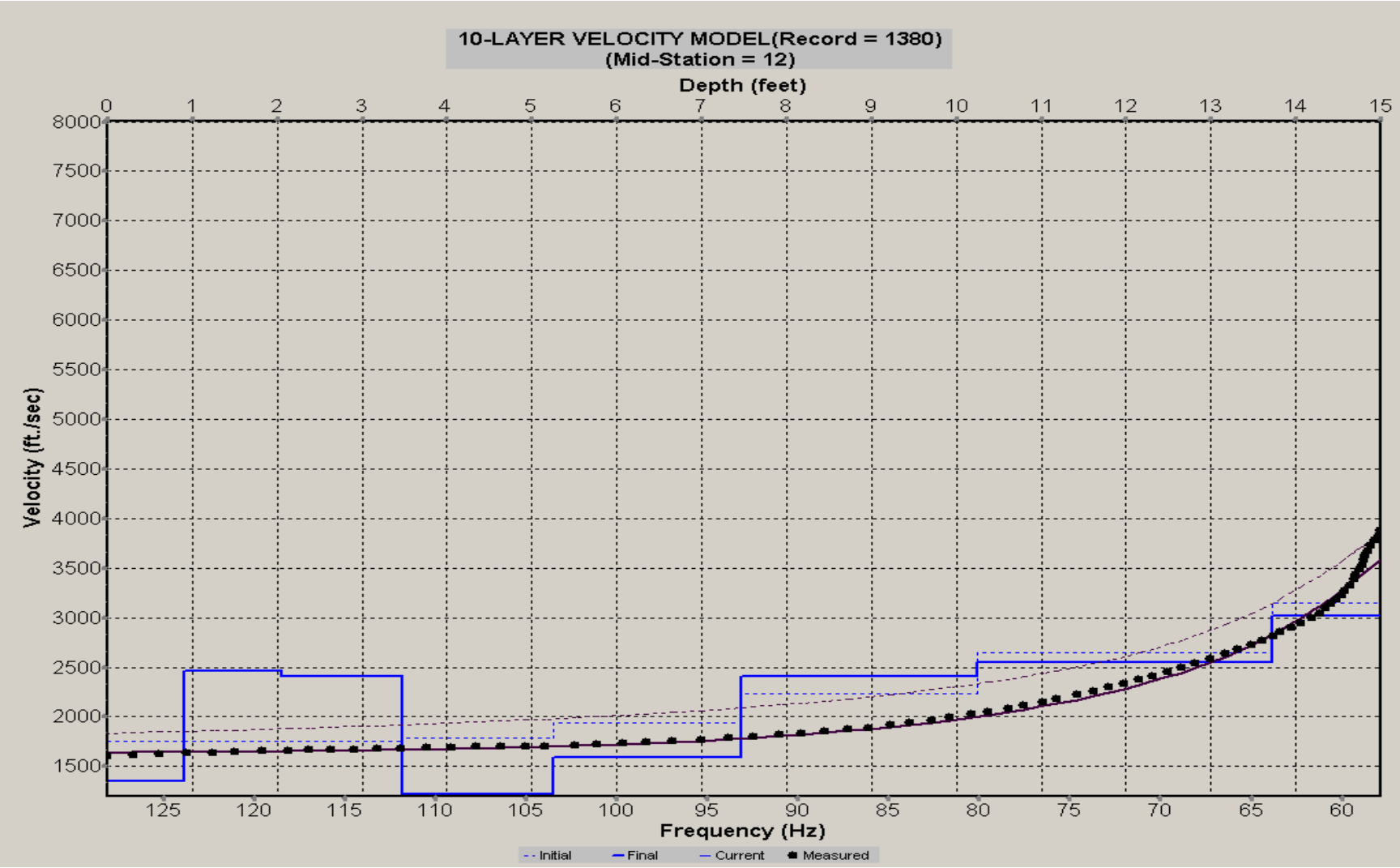

A.639: Velocity Profile Line 1380 used in Pre-blast 11 and Pre-blast 39

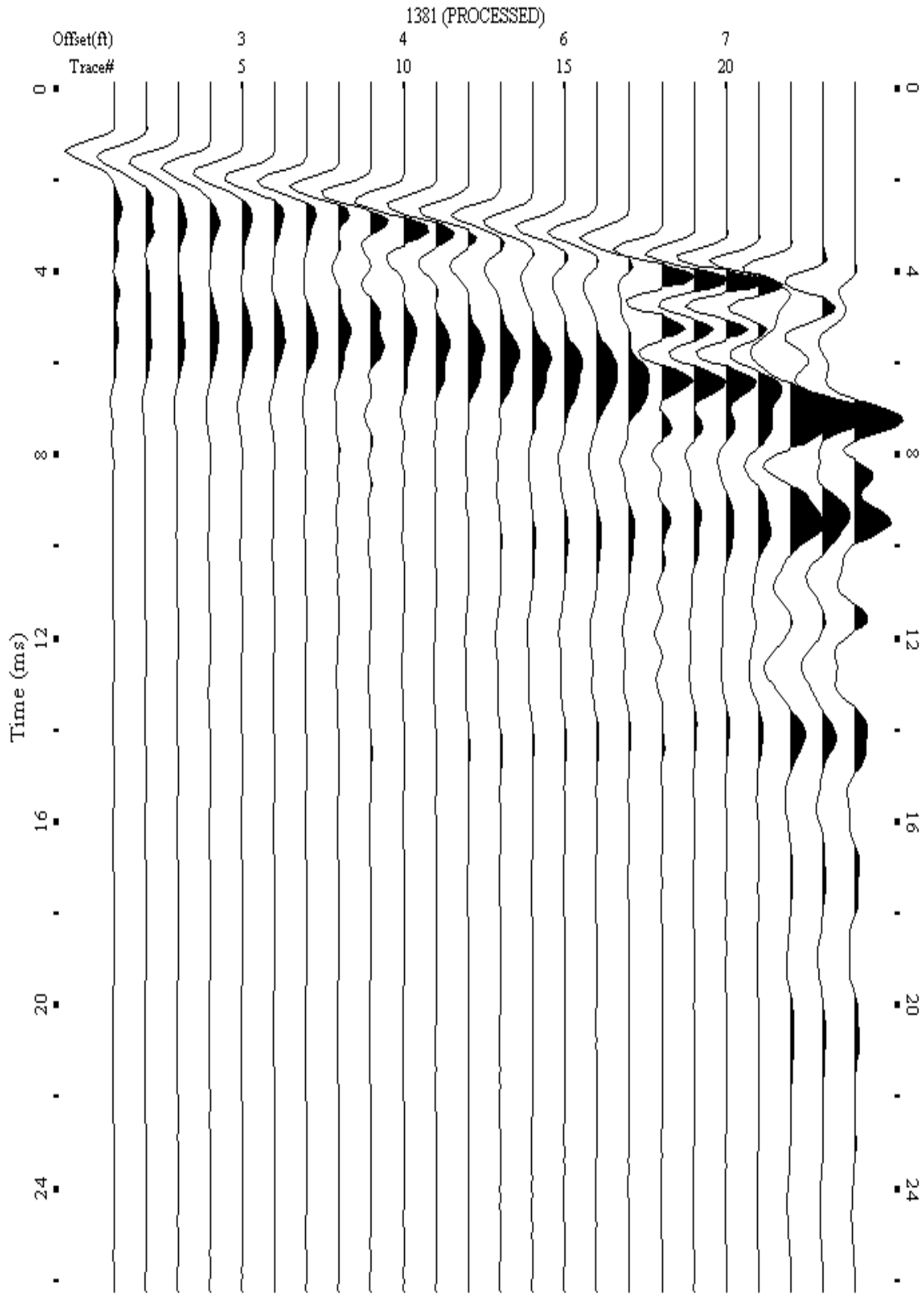

A.640: Shot Gather Line 1381 used in Pre-blast 11, Pre-blast 20, and Pre-blast 39

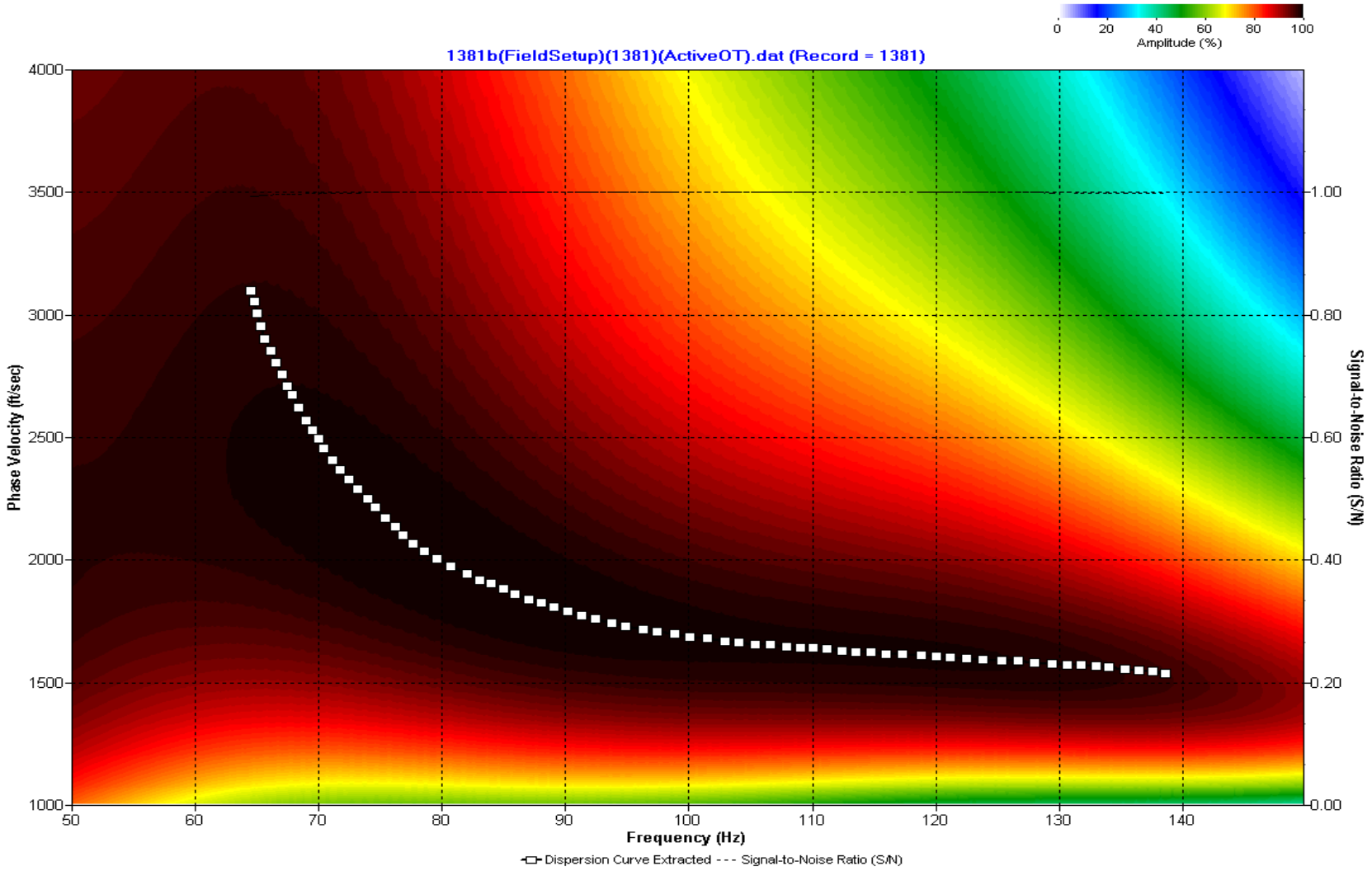

A.641: Dispersion Curve Line 1381 used in Pre-blast 11, Pre-blast 20, and Pre-blast 39

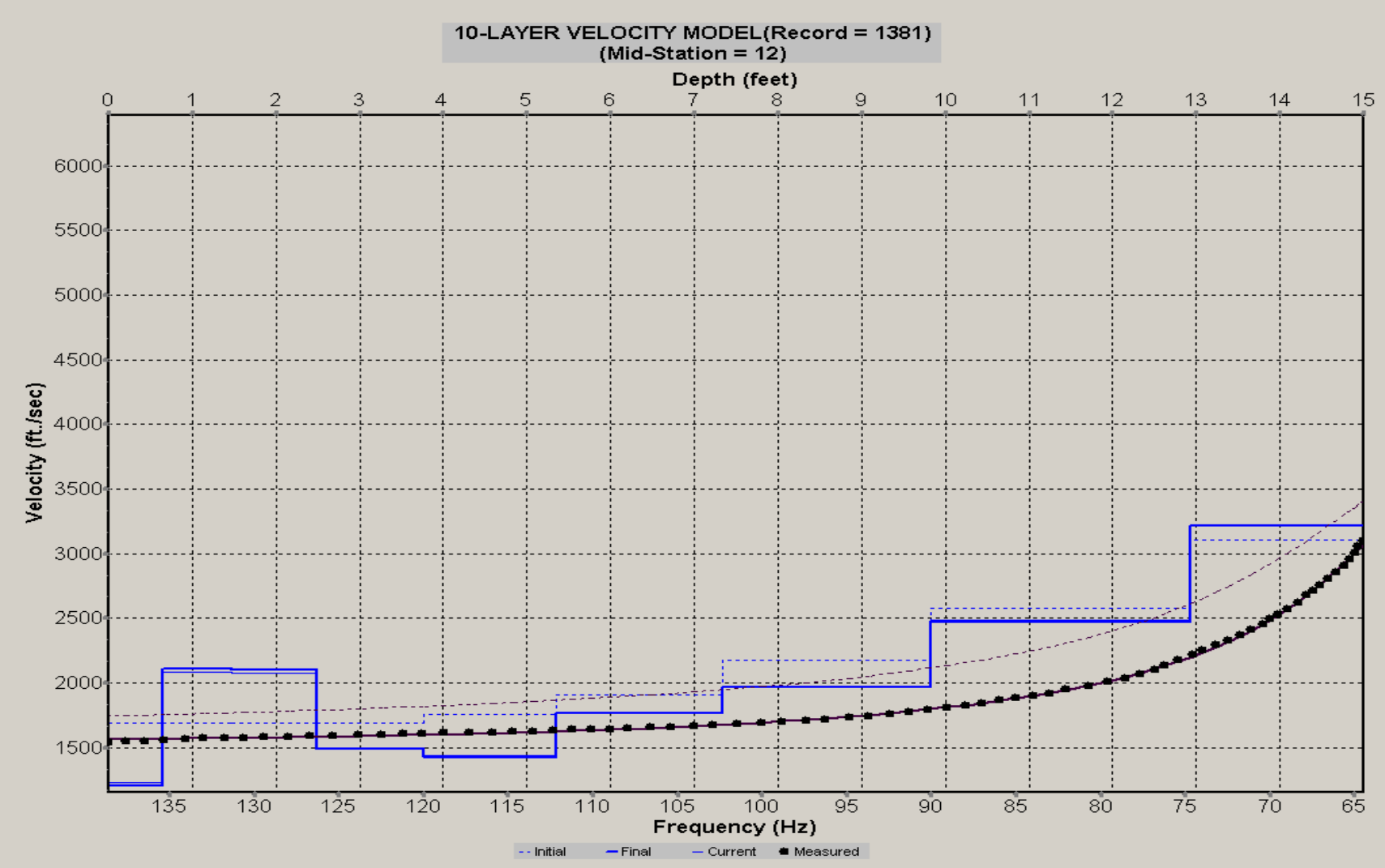

A.642: Velocity Profile Line 1381 used in Pre-blast 11, Pre-blast 20, and Pre-blast 39

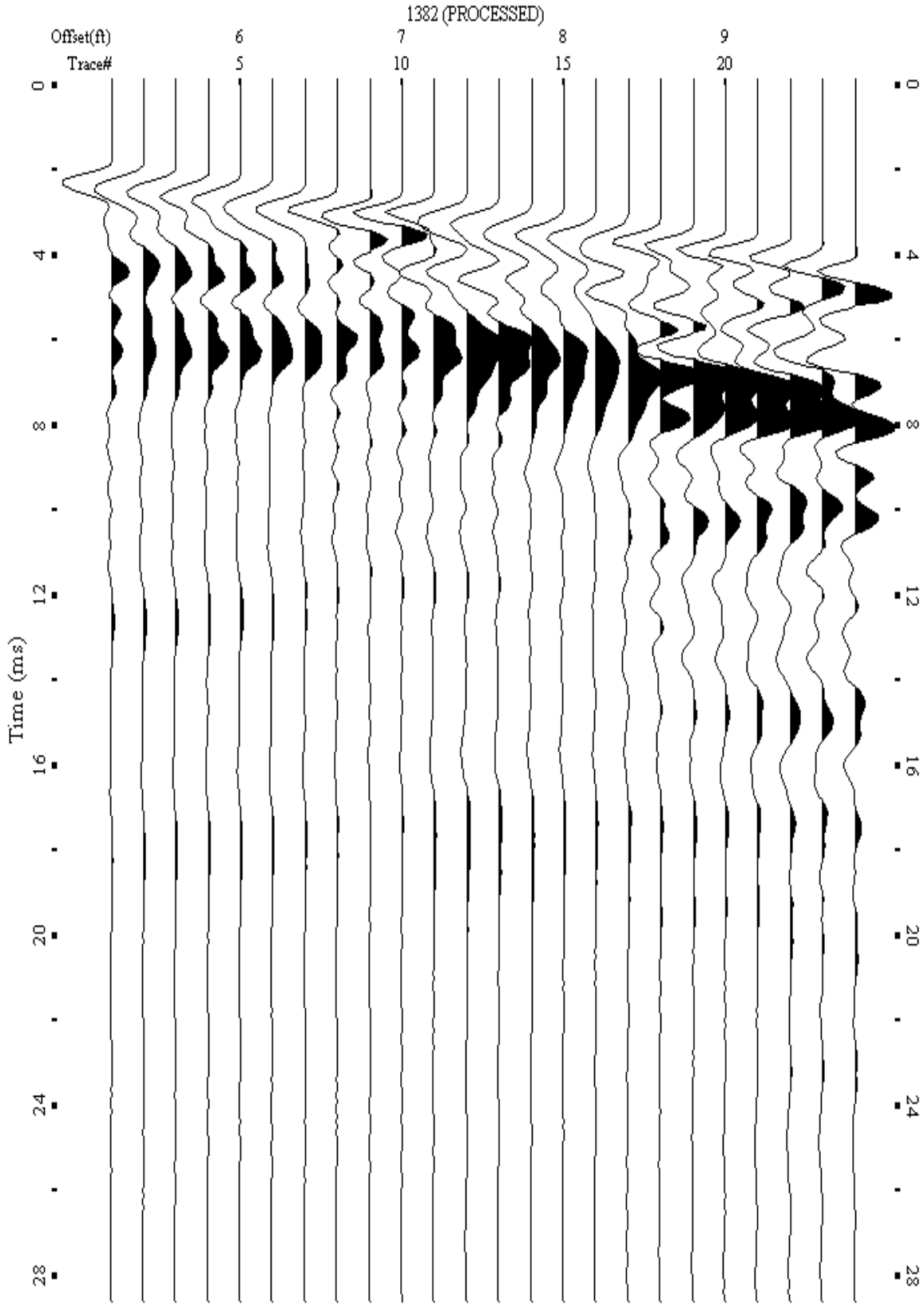

A.643: Shot Gather Line 1382 used in Pre-blast 11, Pre-blast 20, and Pre-blast 39

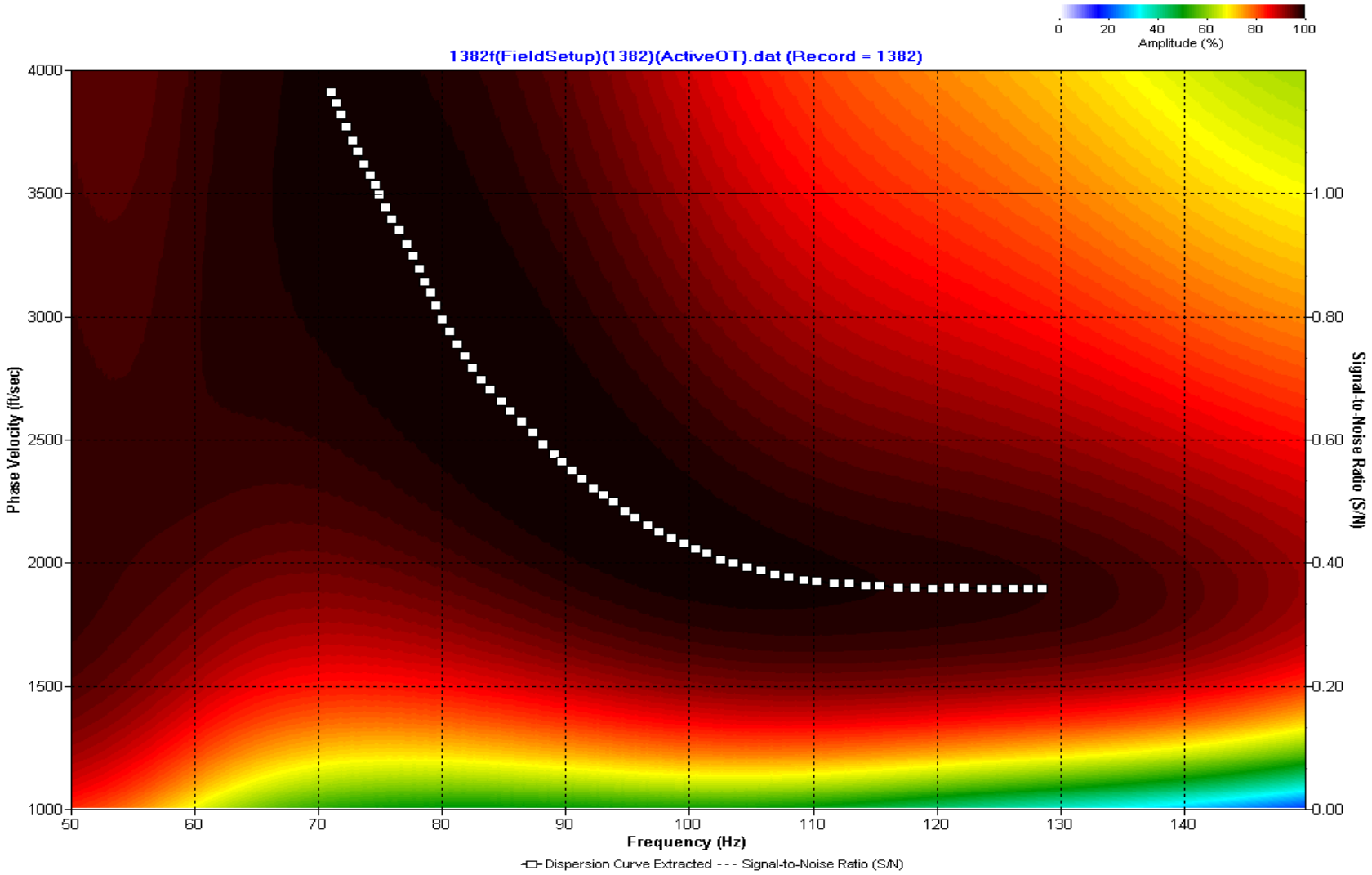

A.644: Dispersion Curve Line 1382 used in Pre-blast 11, Pre-blast 20, and Pre-blast 39

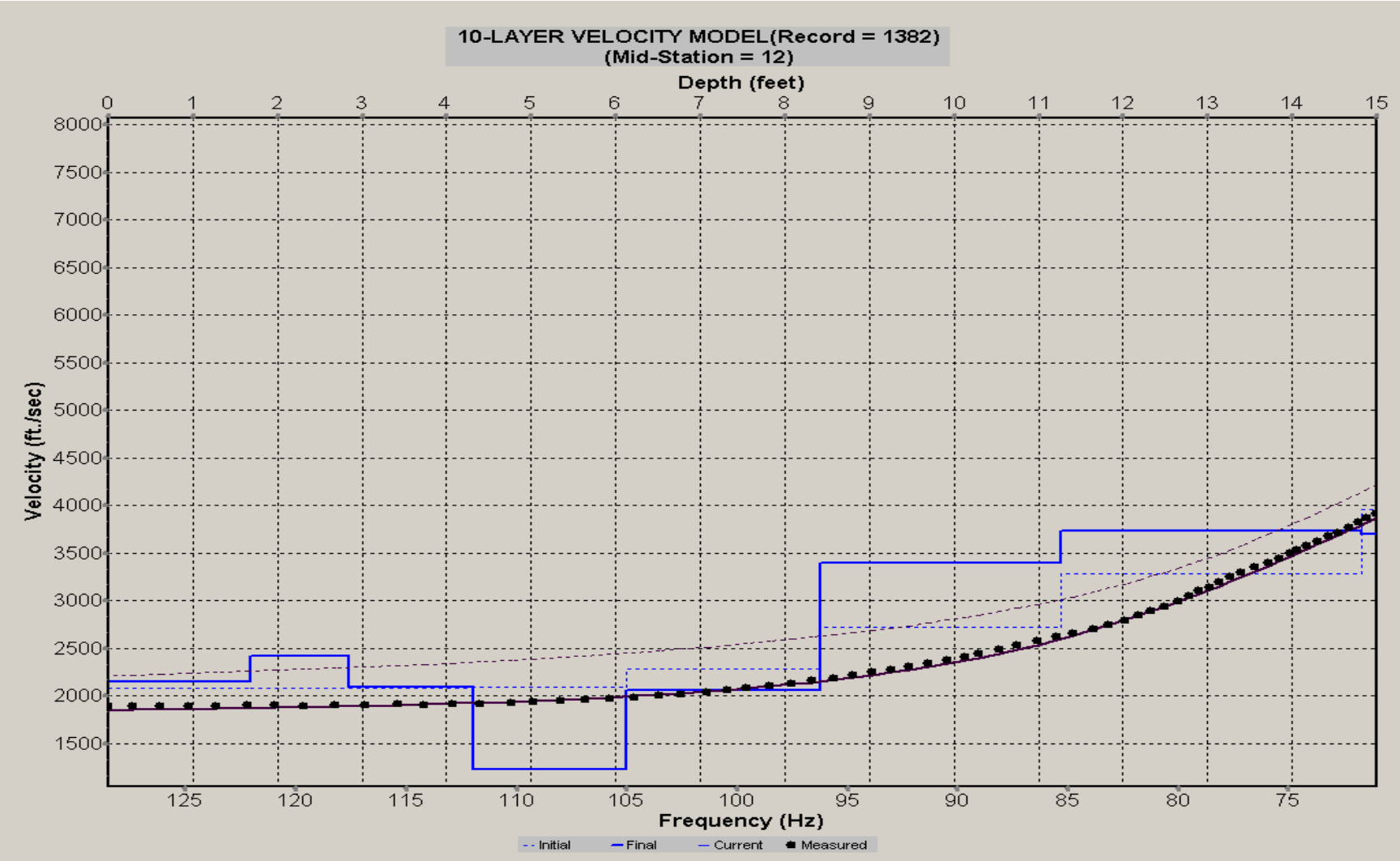

A.645: Velocity Profile Line 1382 used in Pre-blast 11, Pre-blast 20, and Pre-blast 39

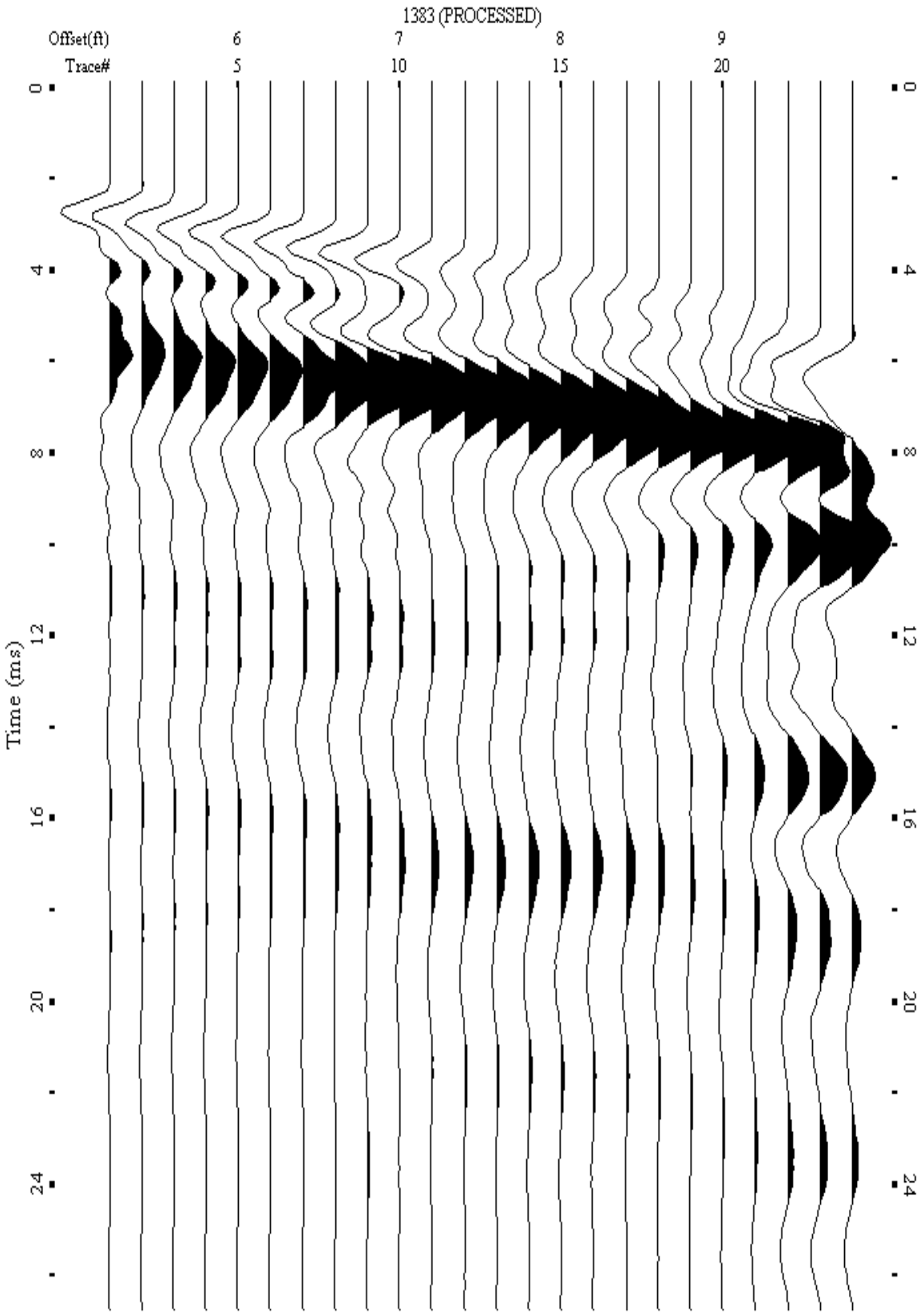

A.646: Shot Gather Line 1383 used in Pre-blast 11, Pre-blast 20, and Pre-blast 39

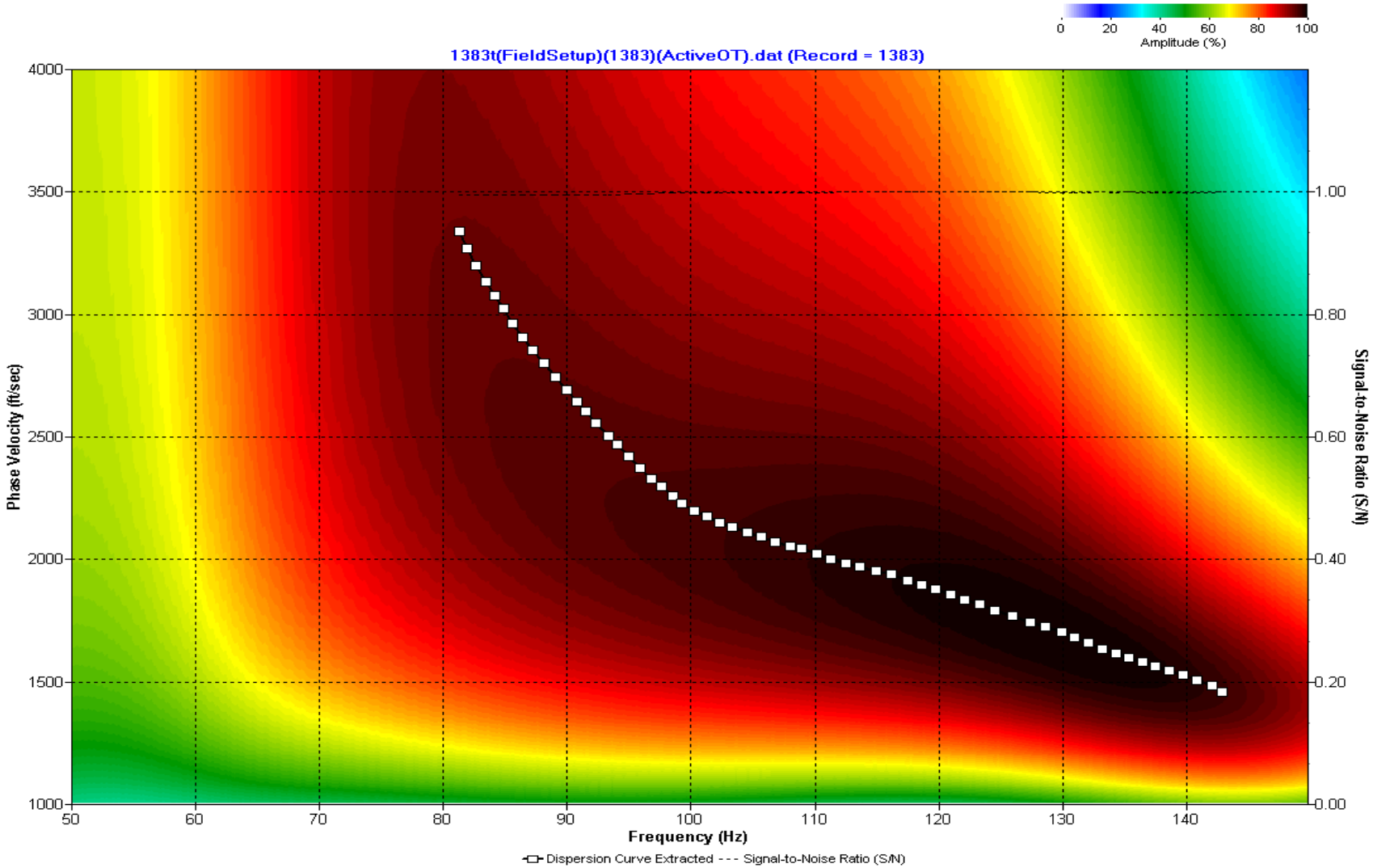

A.647: Dispersion Curve Line 1383 used in Pre-blast 11, Pre-blast 20, and Pre-blast 39

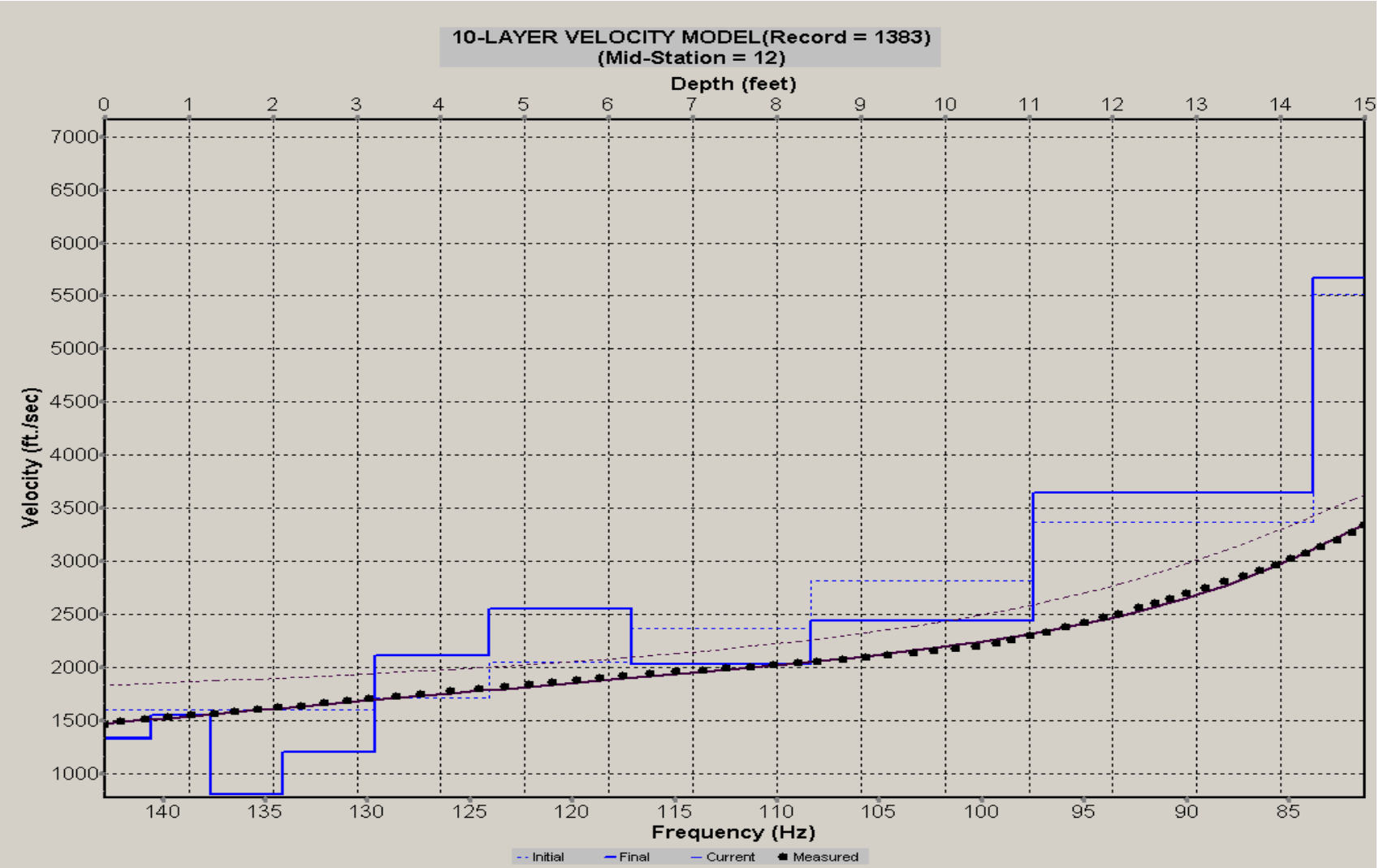

A.648: Velocity Profile Line 1383 used in Pre-blast 11, Pre-blast 20, and Pre-blast 39

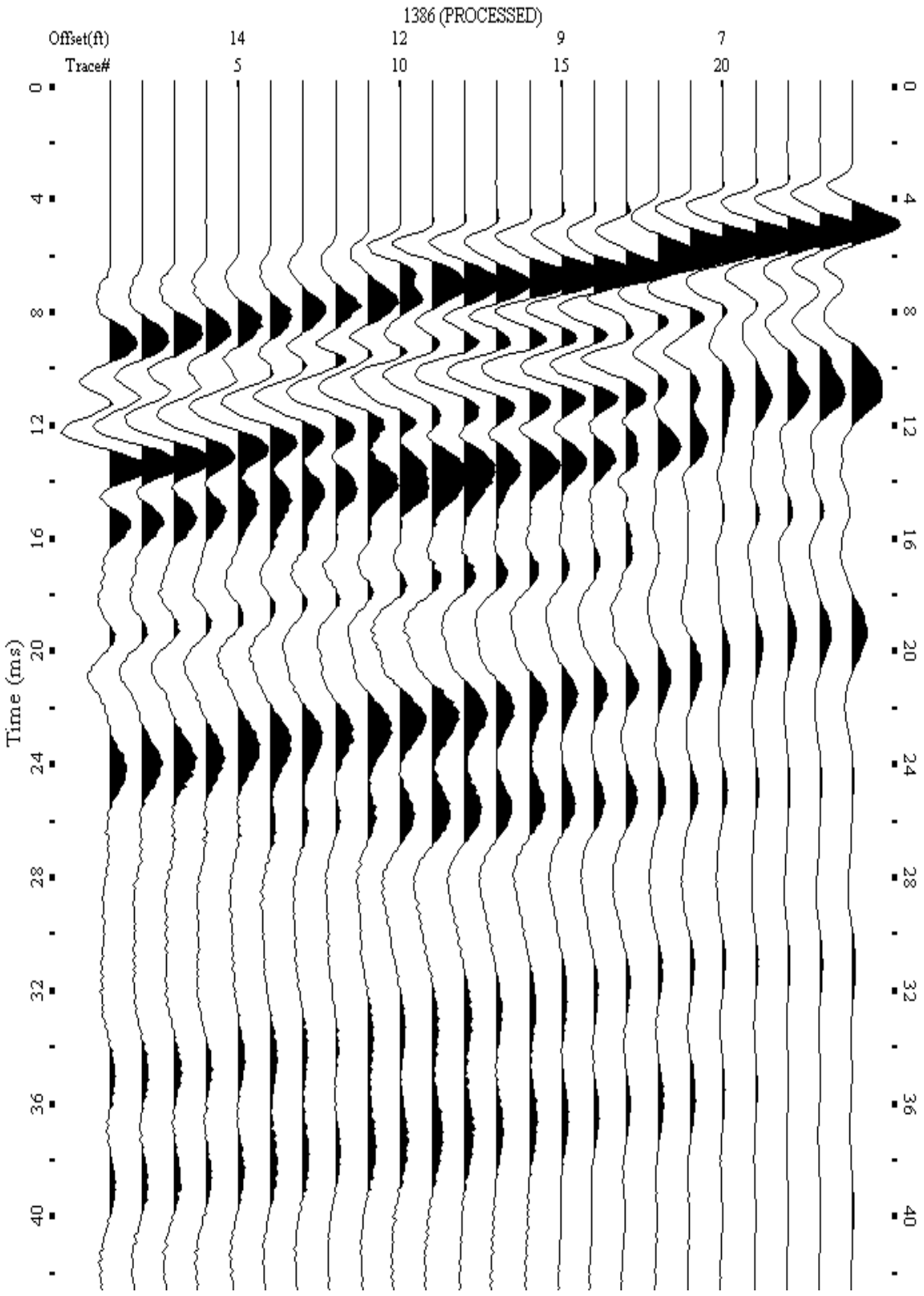

A.649: Shot Gather Line 1386 used in Pre-blast 11, Pre-blast 20, and Pre-blast 39

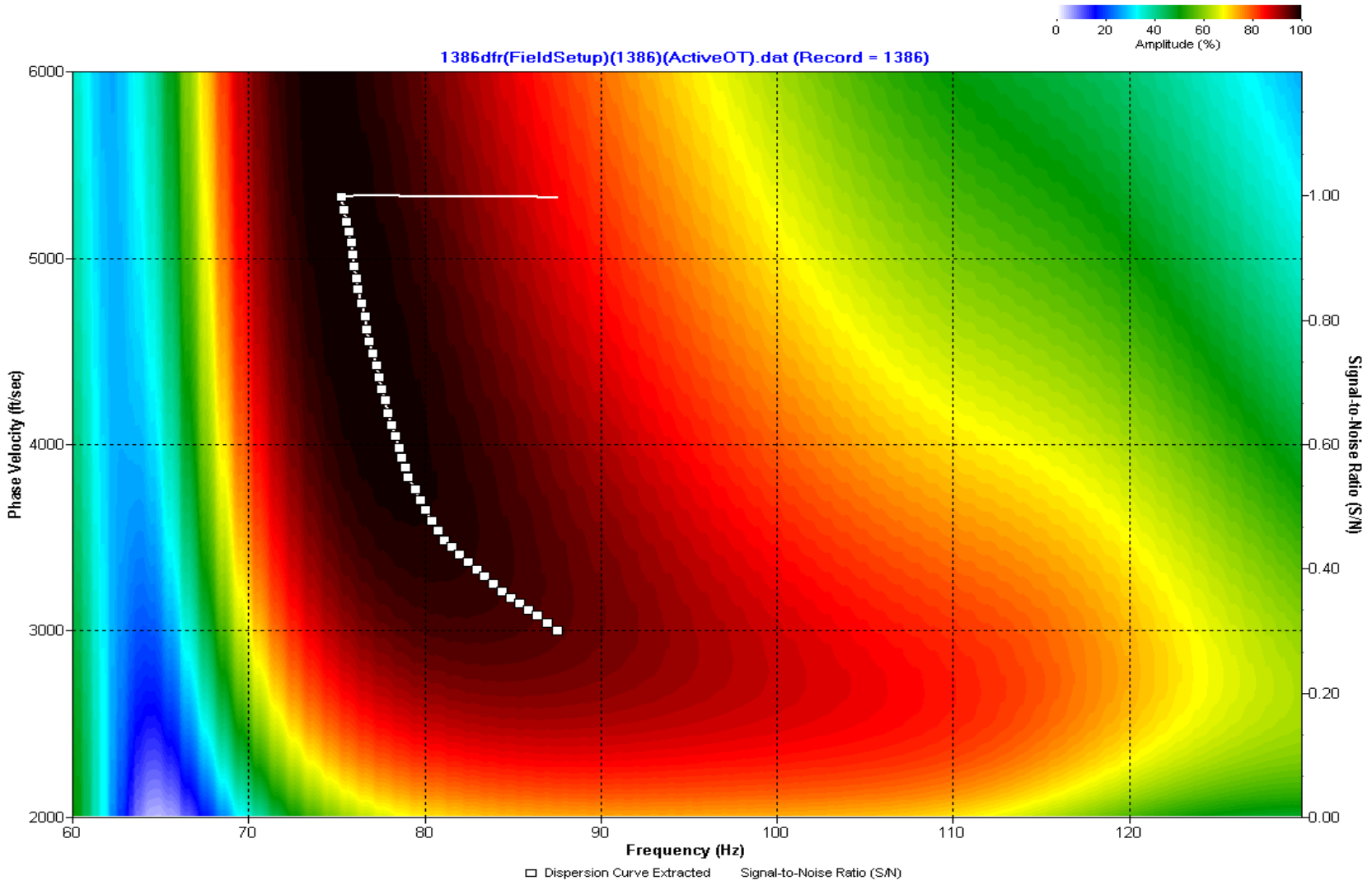

A.650: Dispersion Curve Line 1386 used in Pre-blast 11, Pre-blast 20, and Pre-blast 39

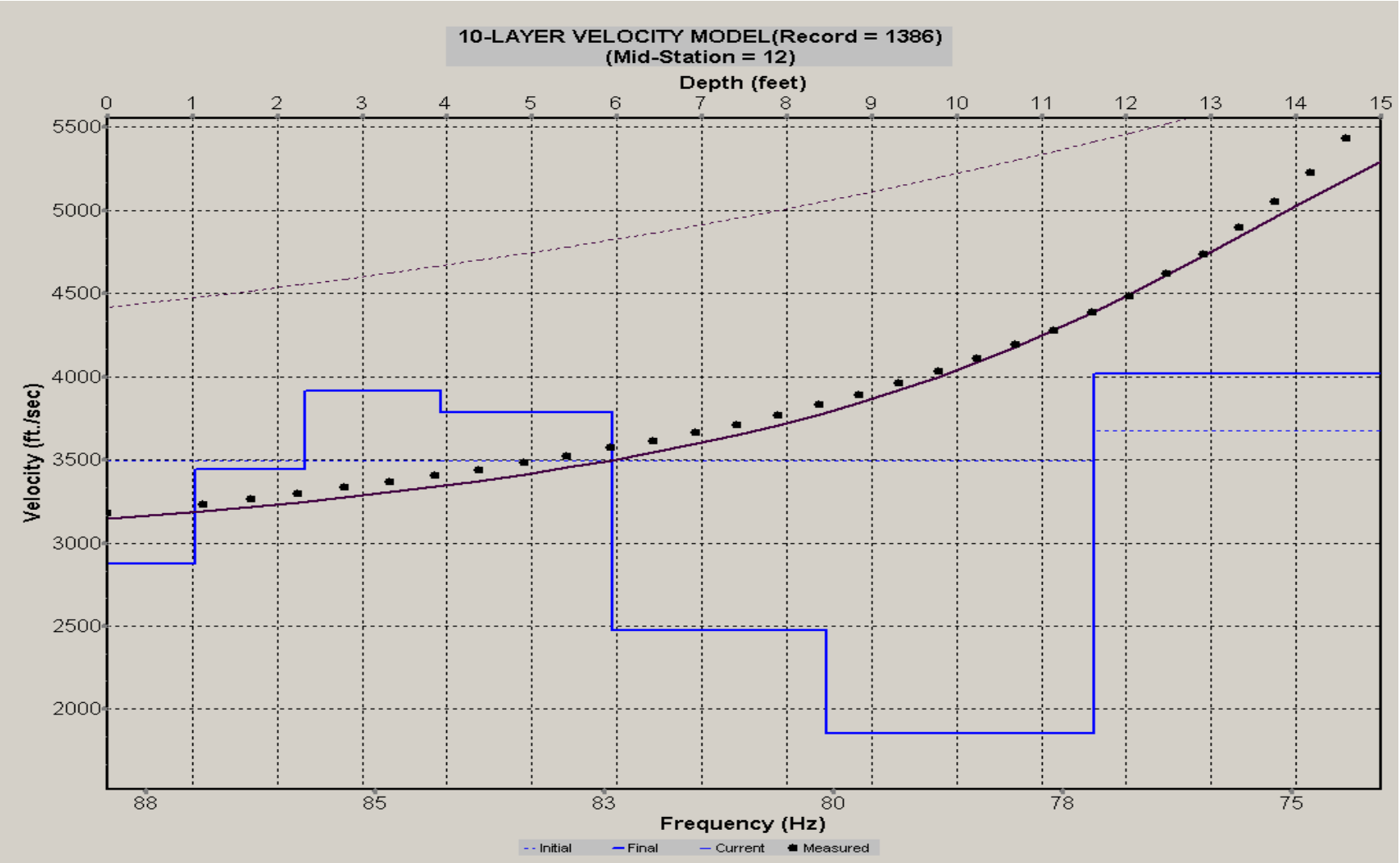

A.651: Velocity Profile Line 1386 used in Pre-blast 11, Pre-blast 20, and Pre-blast 39

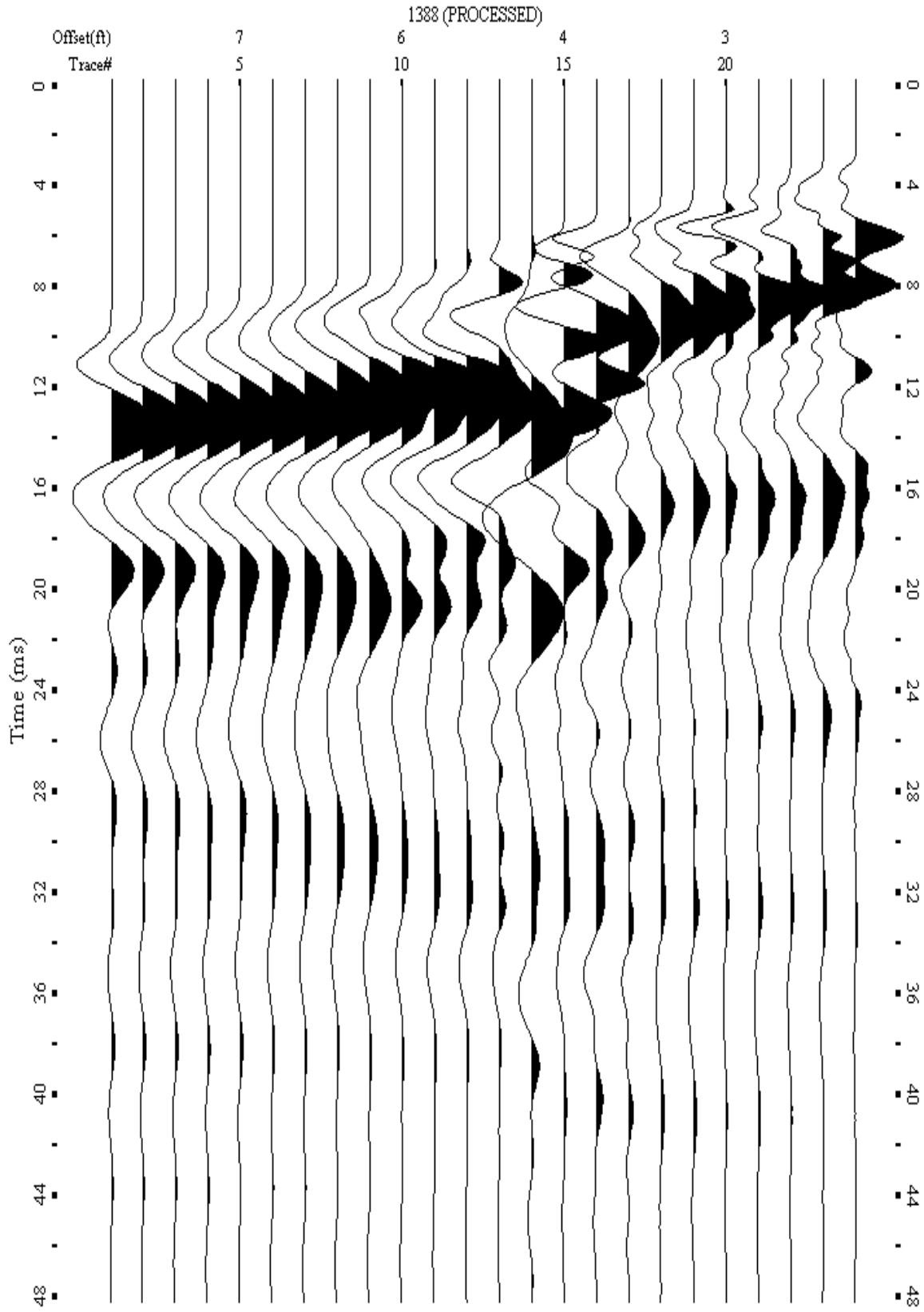

A.652: Shot Gather Line 1388 used in Pre-blast 38

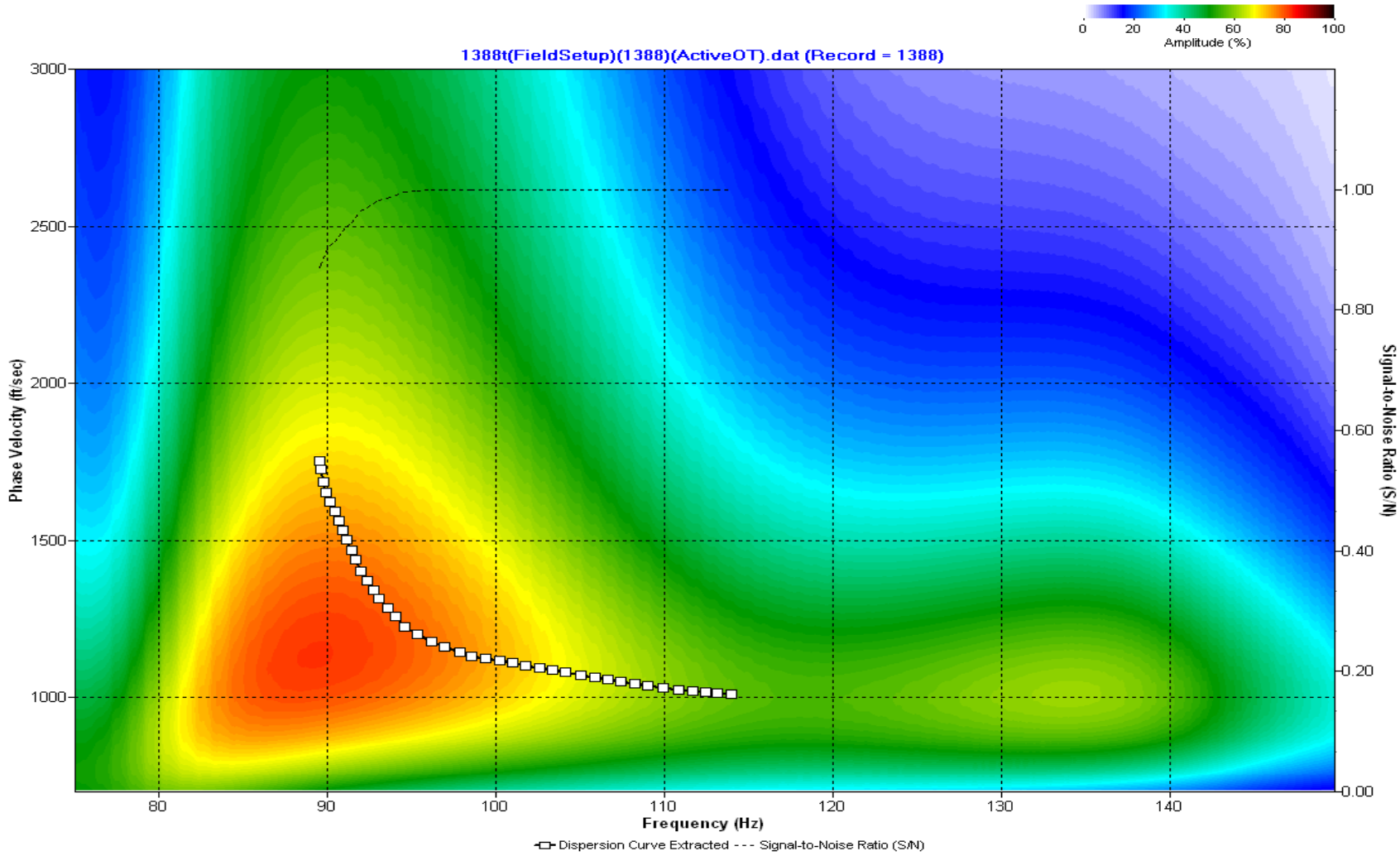

A.653: Dispersion Curve Line 1388 used in Pre-blast 38

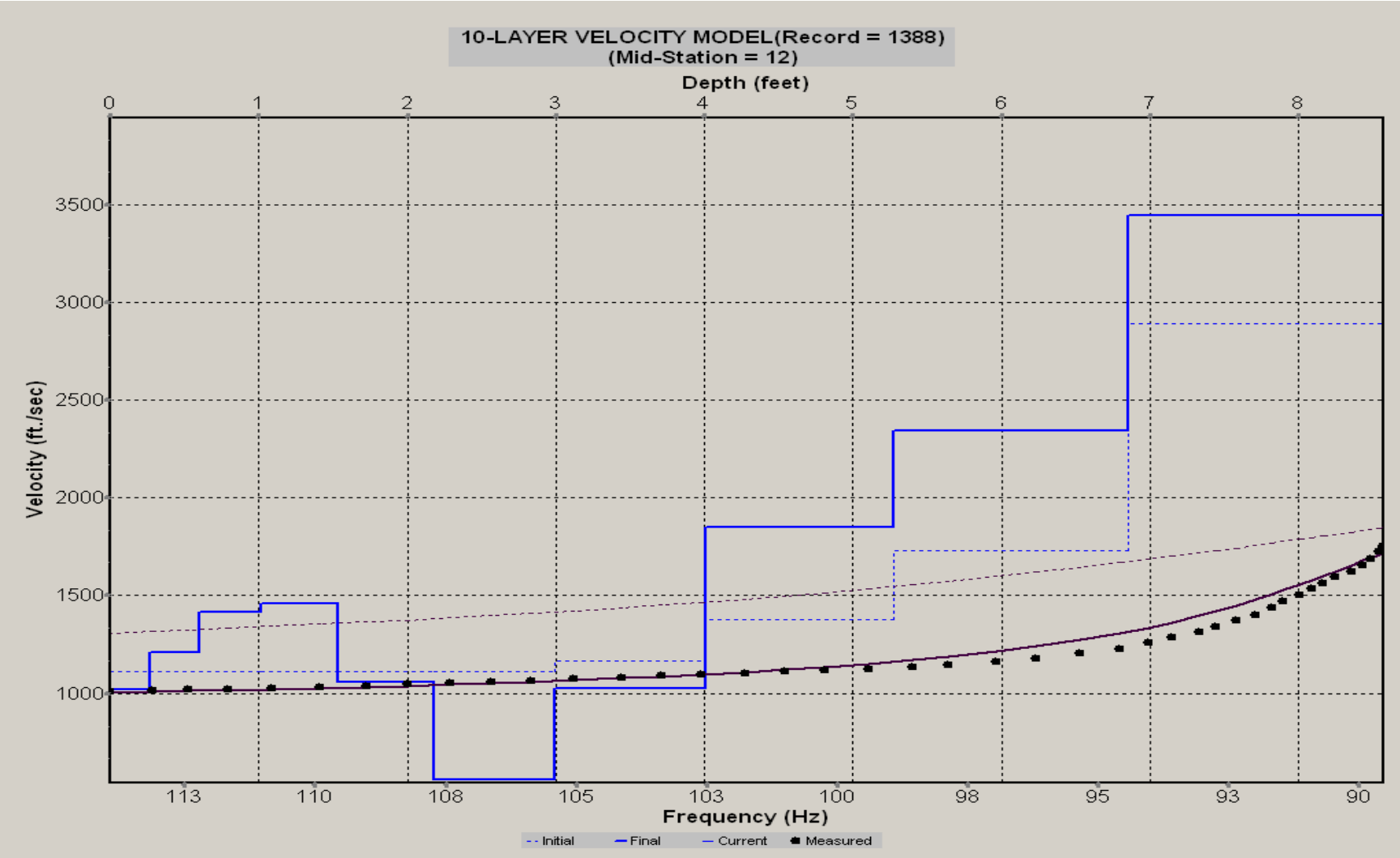

A.654: Velocity Profile Line 1388 used in Pre-blast 38

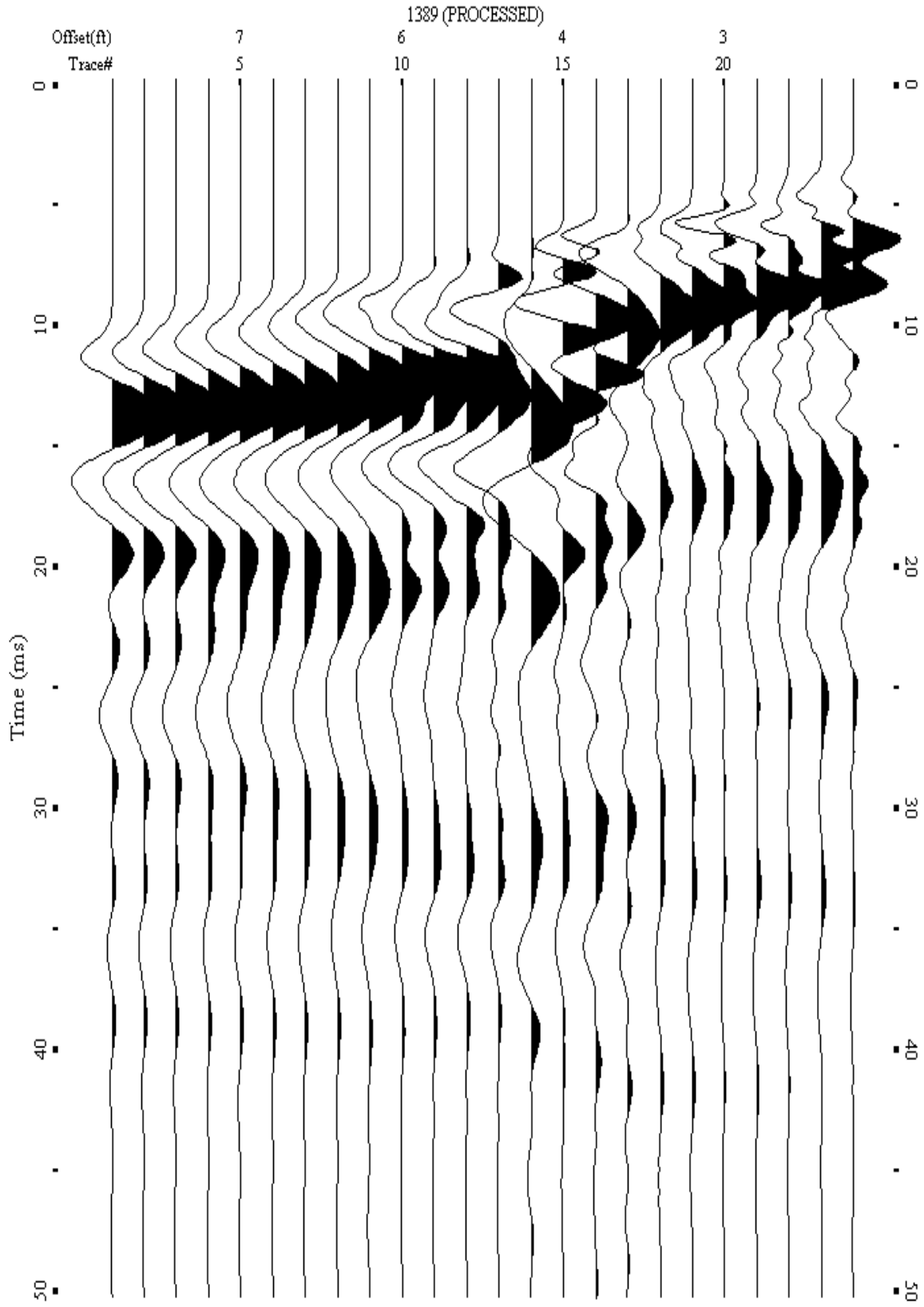

A.655: Shot Gather Line 1389 used in Pre-blast 38

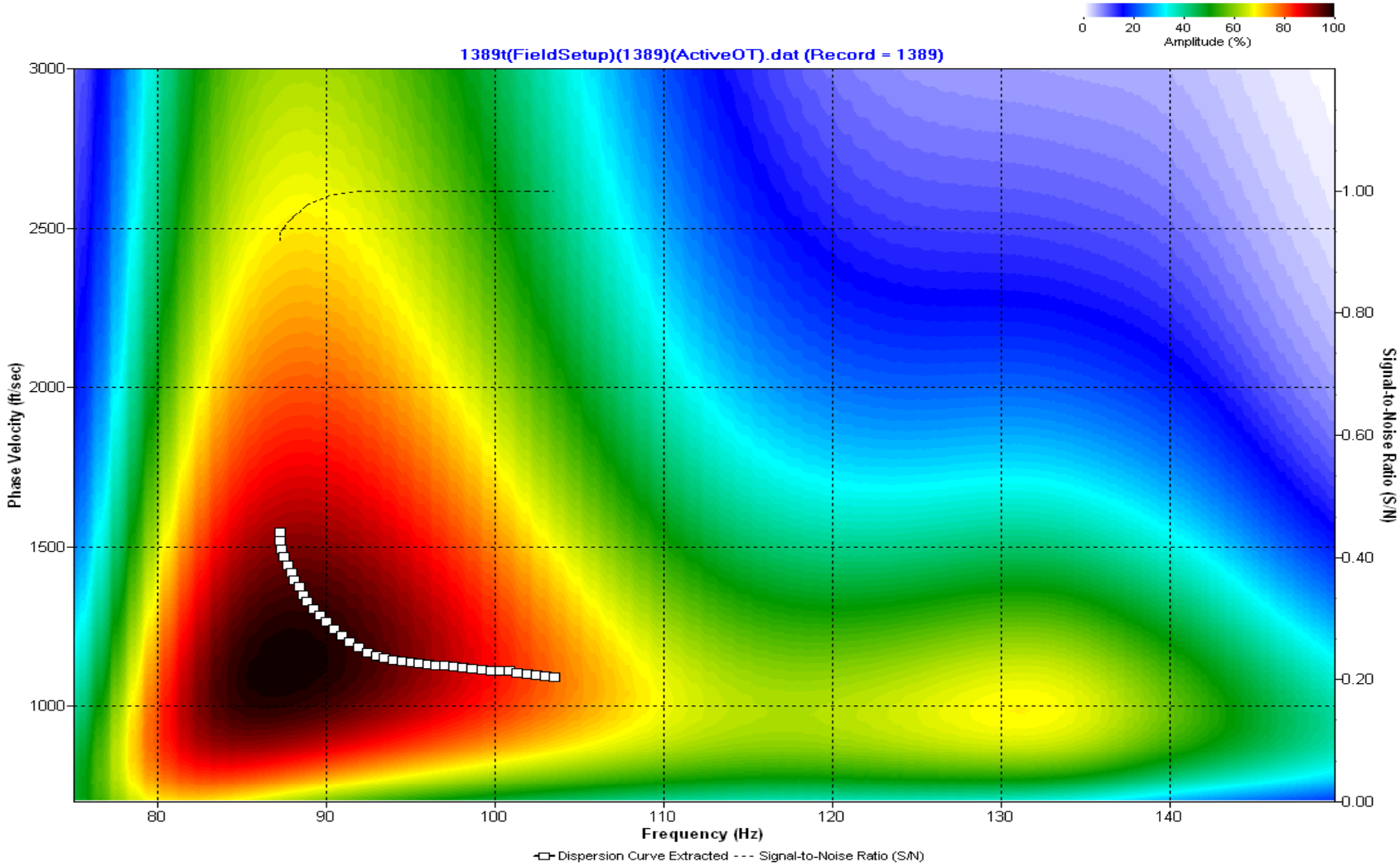

A.656: Dispersion Curve Line 1389 used in Pre-blast 38

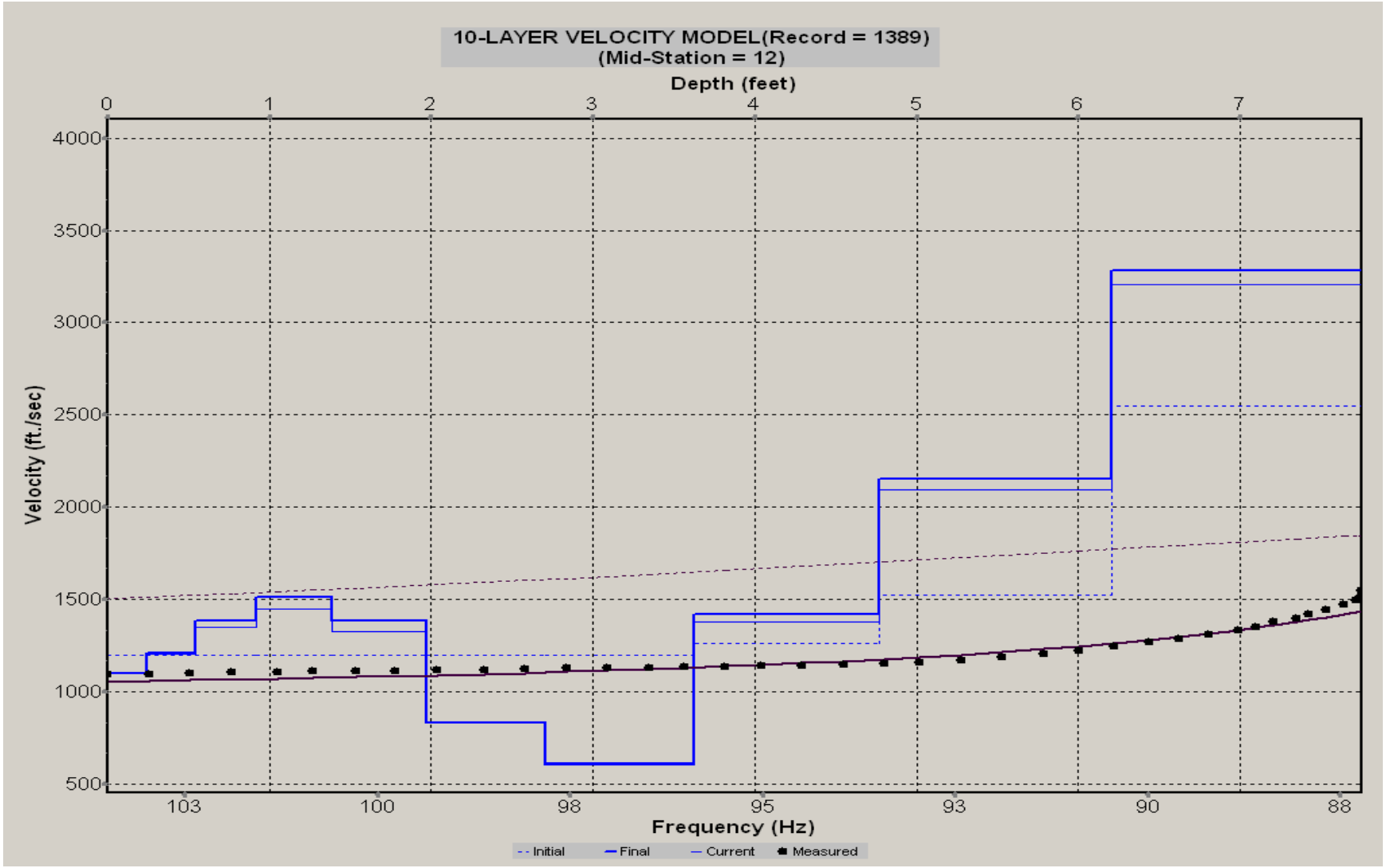

A.657: Velocity Profile Line 1389 used in Pre-blast 38

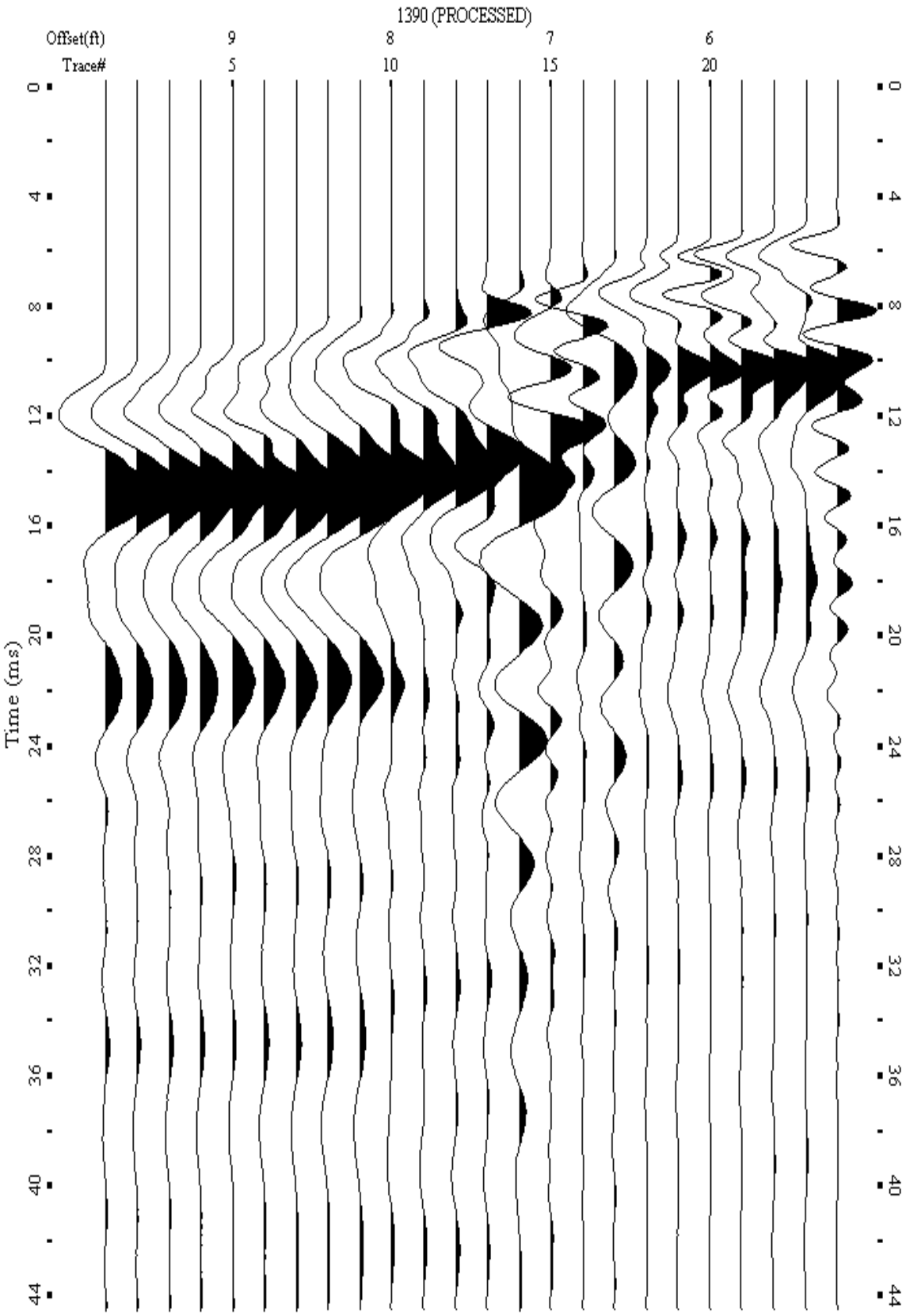

A.658: Shot Gather Line 1390 used in Pre-blast 38

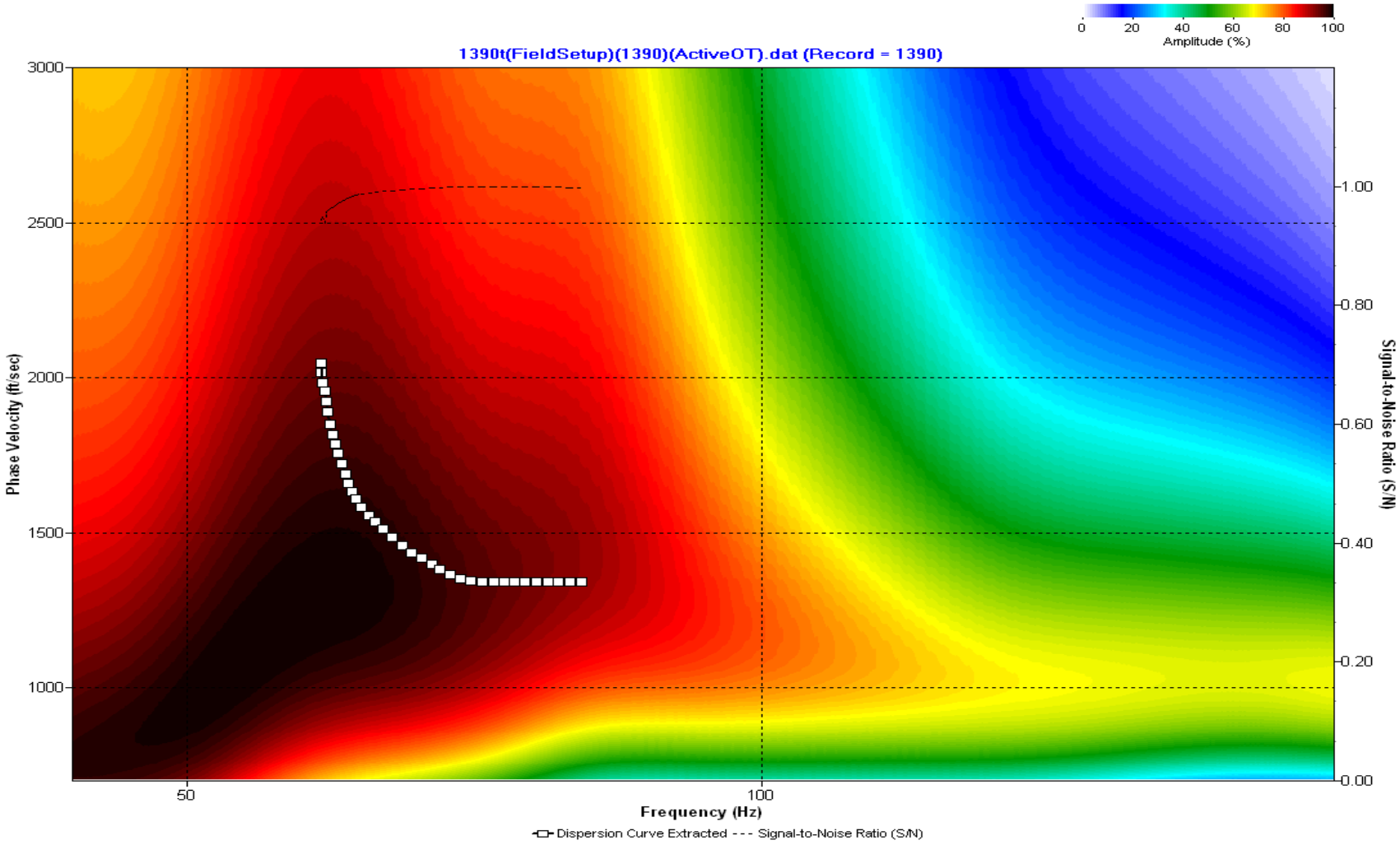

A.659: Dispersion Curve Line 1390 used in Pre-blast 38

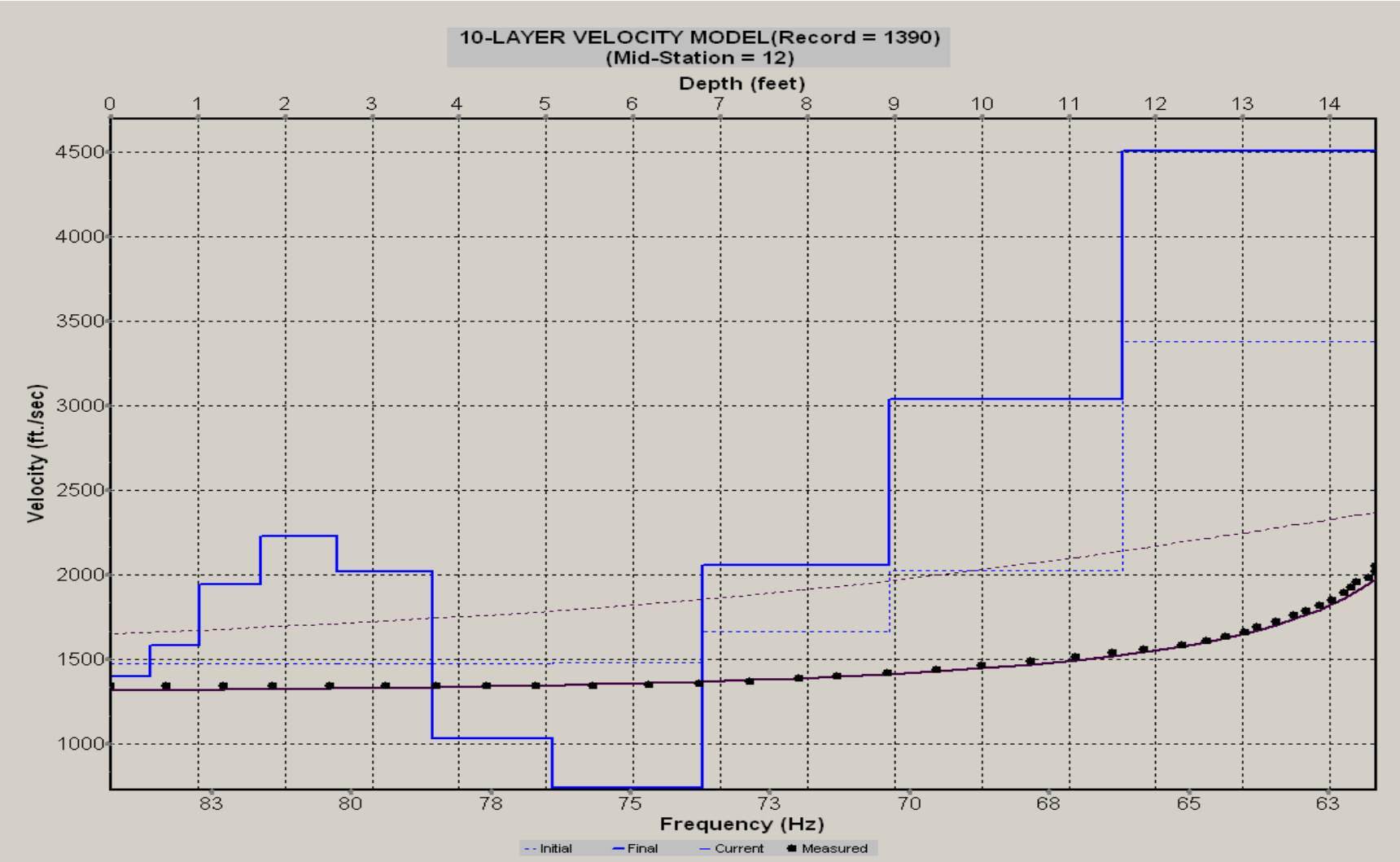

A.660: Velocity Profile Line 1390 used in Pre-blast 38

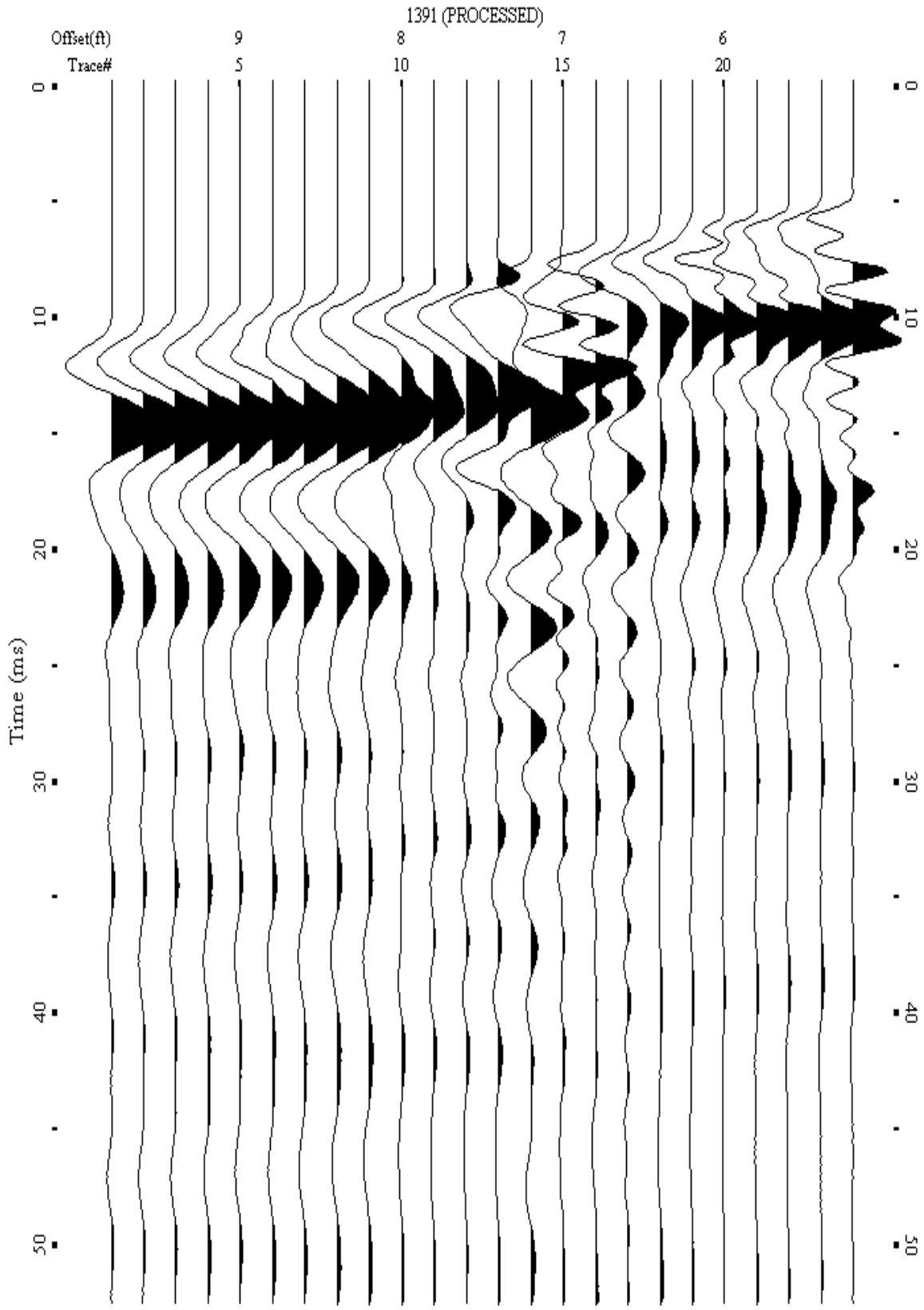

A.661: Shot Gather Line 1391 used in Pre-blast 38

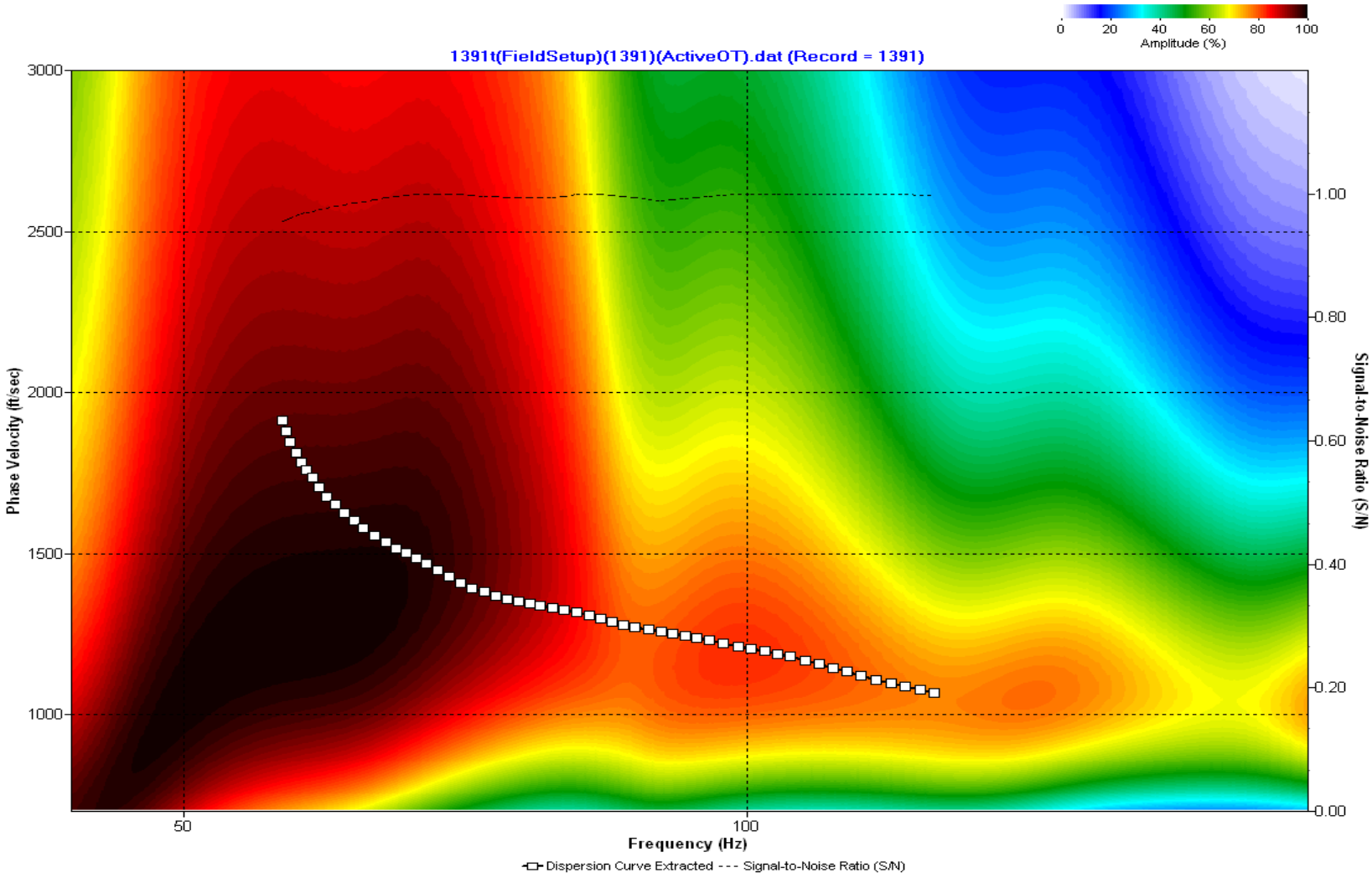

A.662: Dispersion Curve Line 1391 used in Pre-blast 38

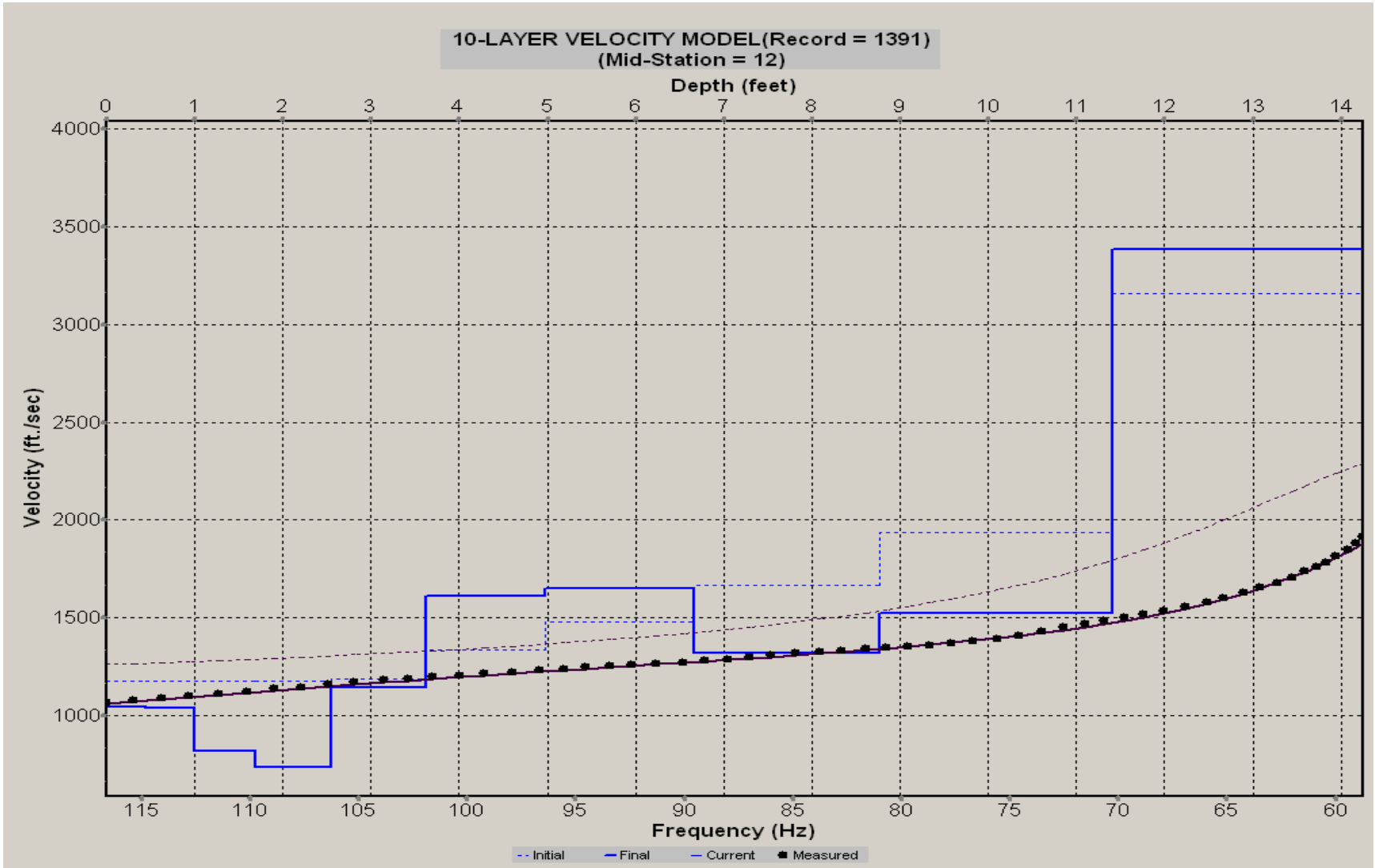

A.663: Velocity Profile Line 1391 used in Pre-blast 38

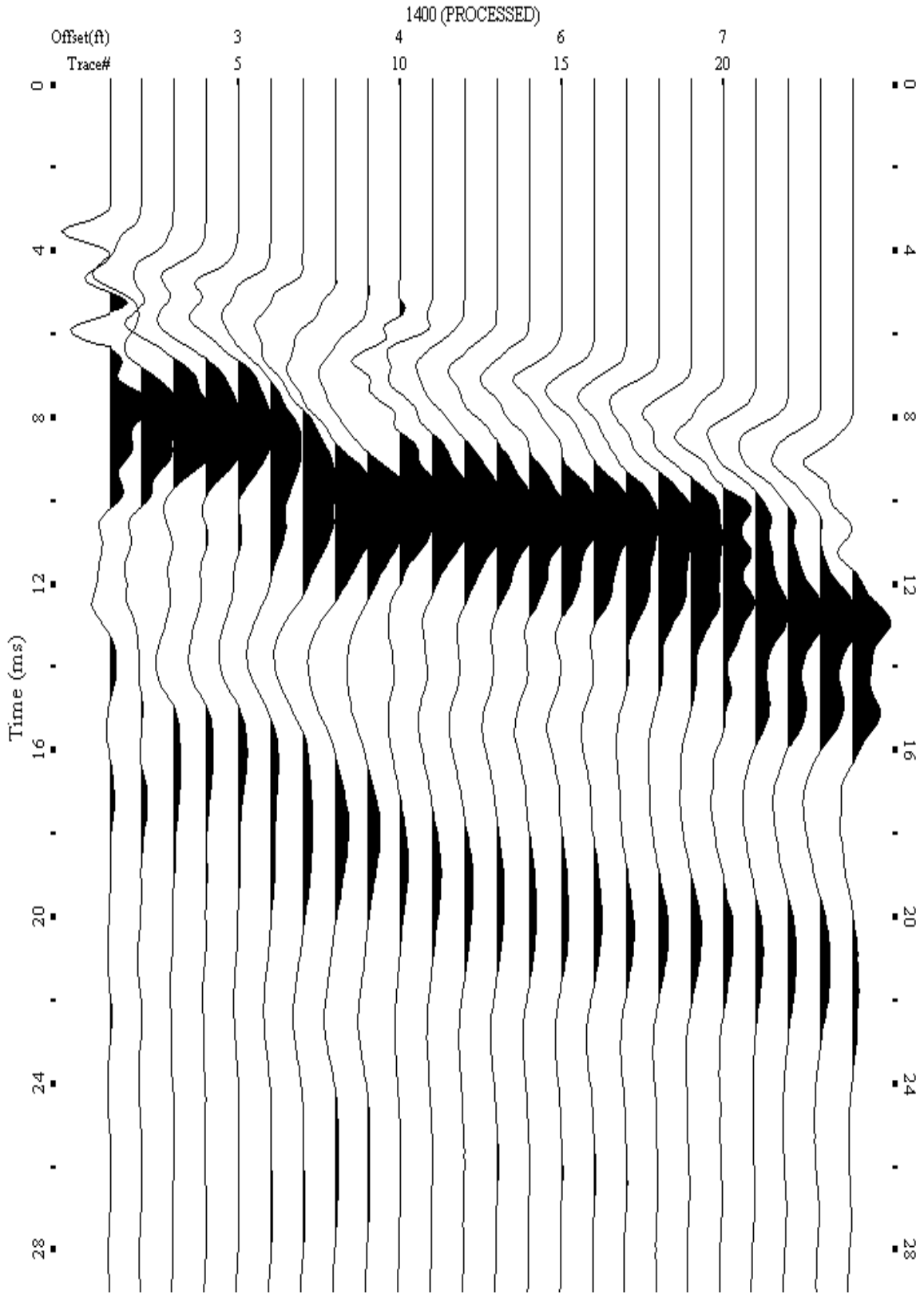

A.664: Shot Gather Line 1400 used in Pre-blast 38

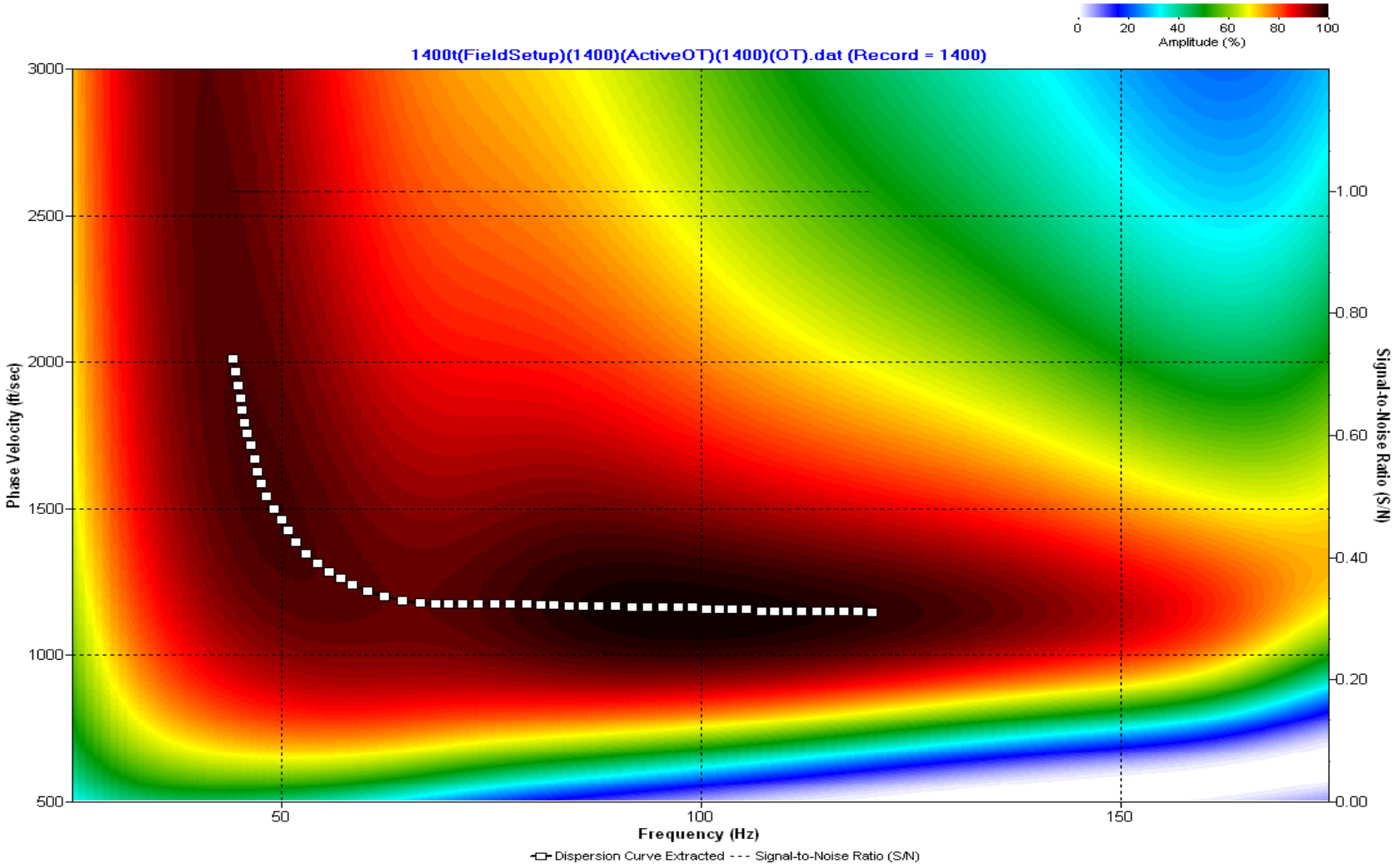

A.665: Dispersion Curve Line 1400 used in Pre-blast 38

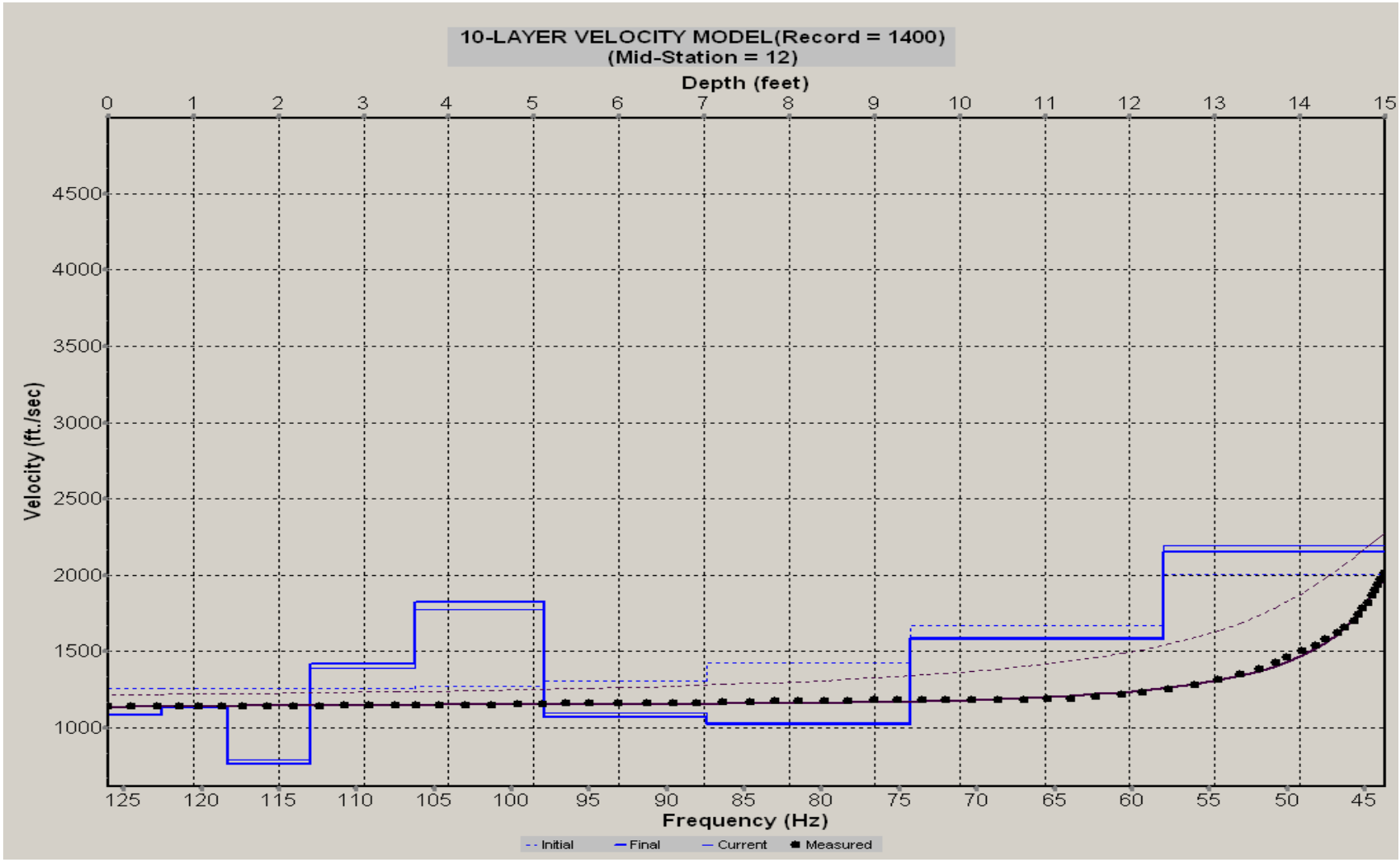

A.666: Velocity Profile Line 1400 used in Pre-blast 38

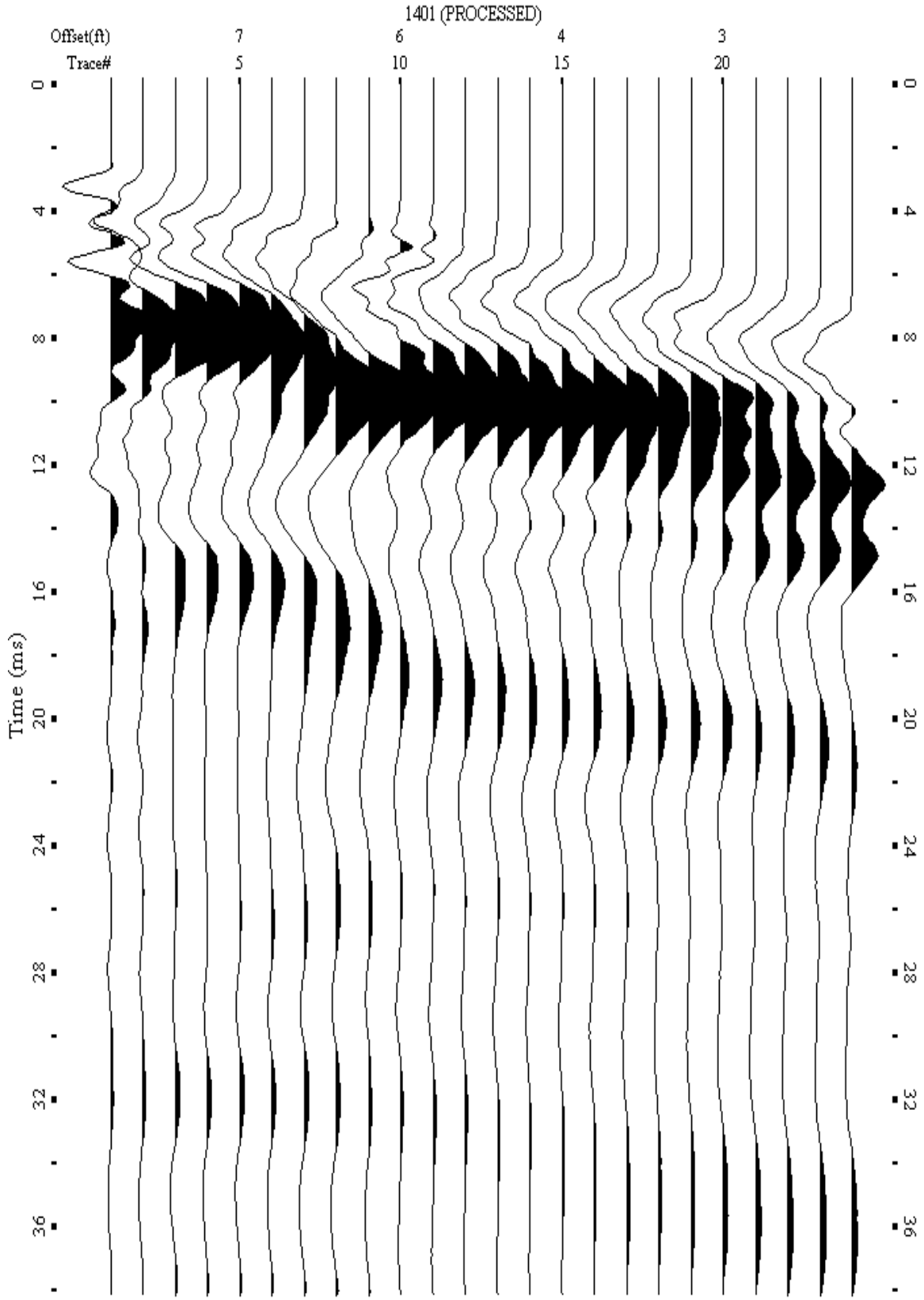

A.667: Shot Gather Line 1401 used in Pre-blast 38

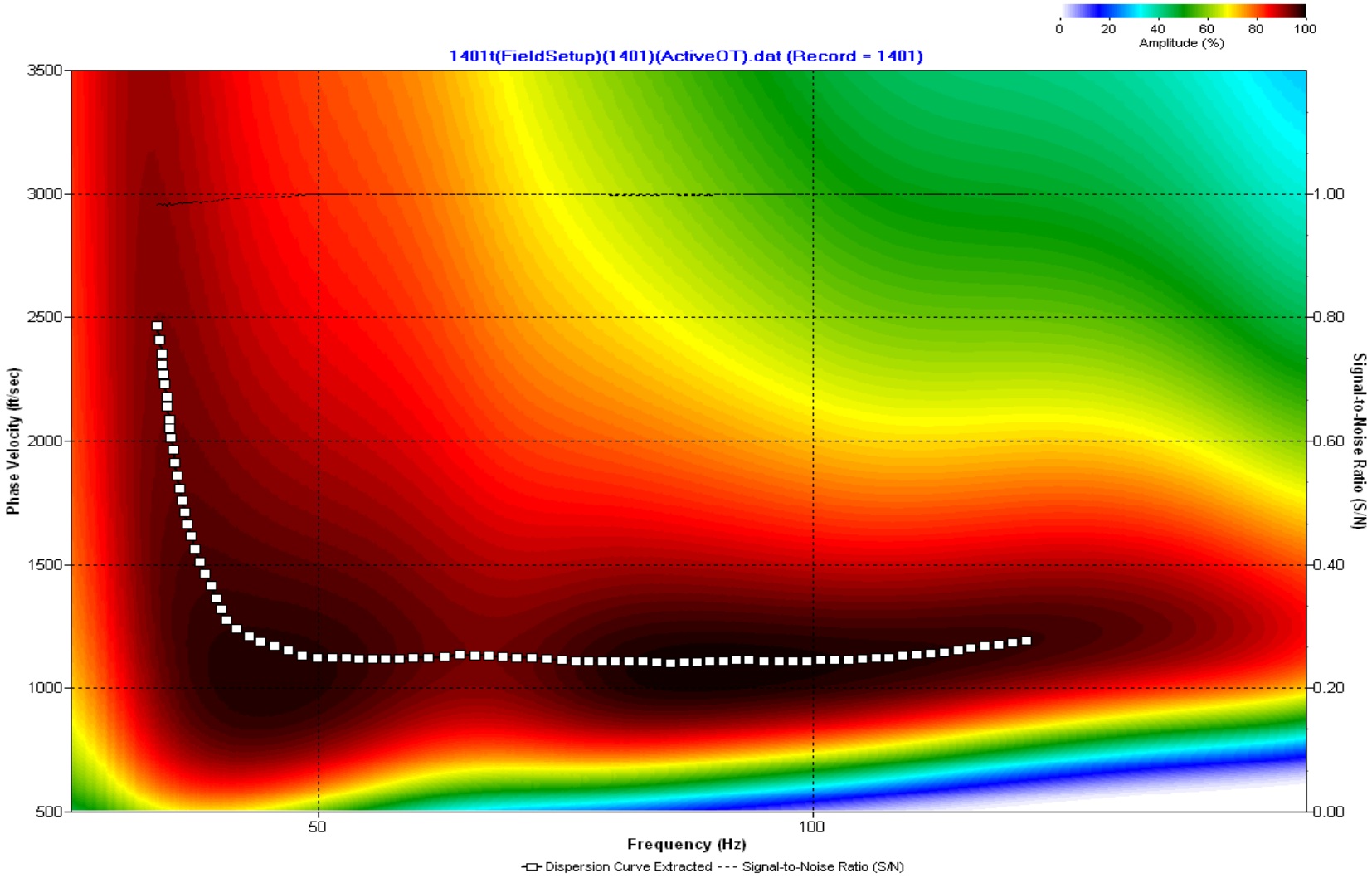

A.668: Dispersion Curve Line 1401 used in Pre-blast 38

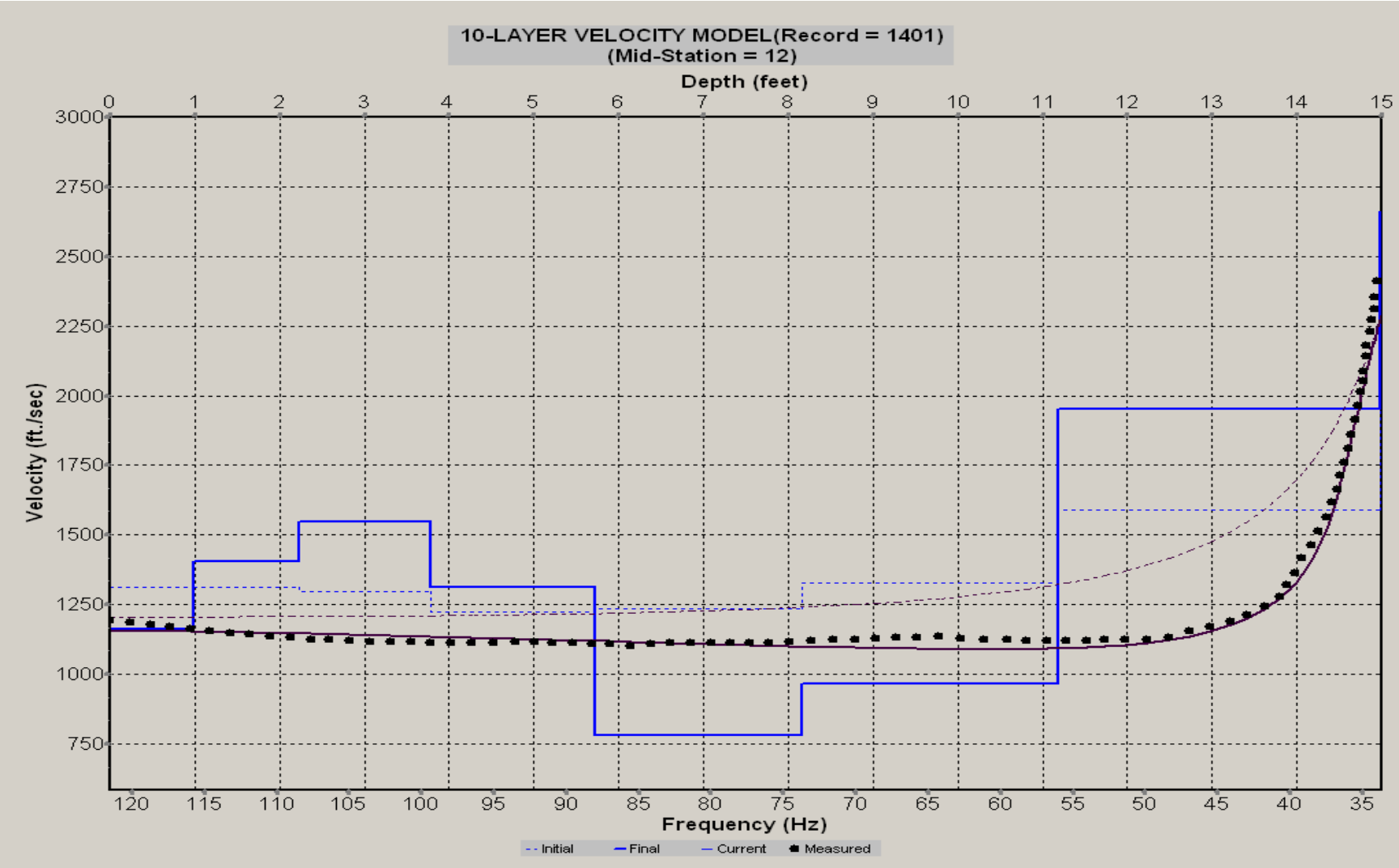

A.669: Velocity Profile Line 1401 used in Pre-blast 38

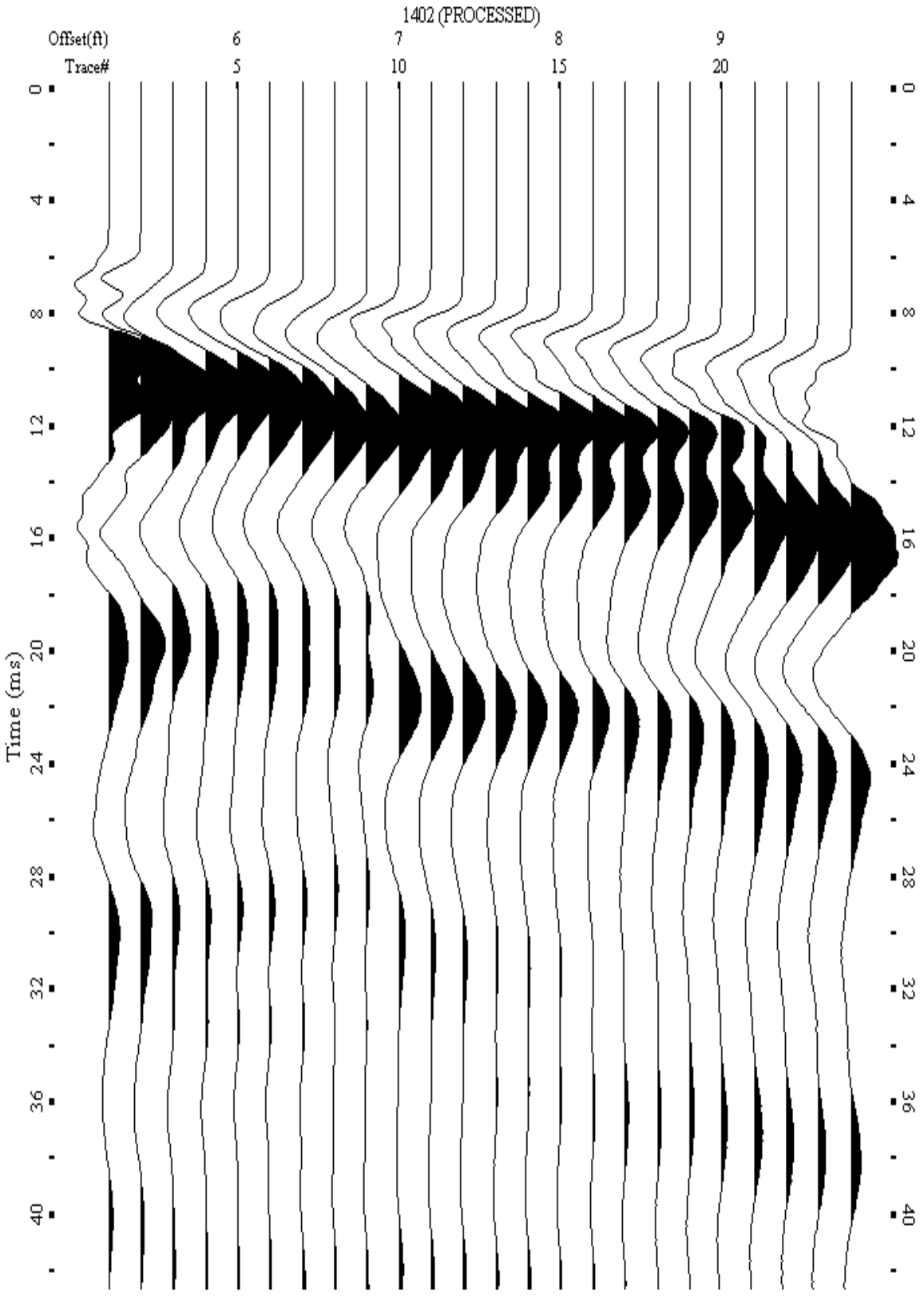

A.670: Shot Gather Line 1402 used in Pre-blast 38

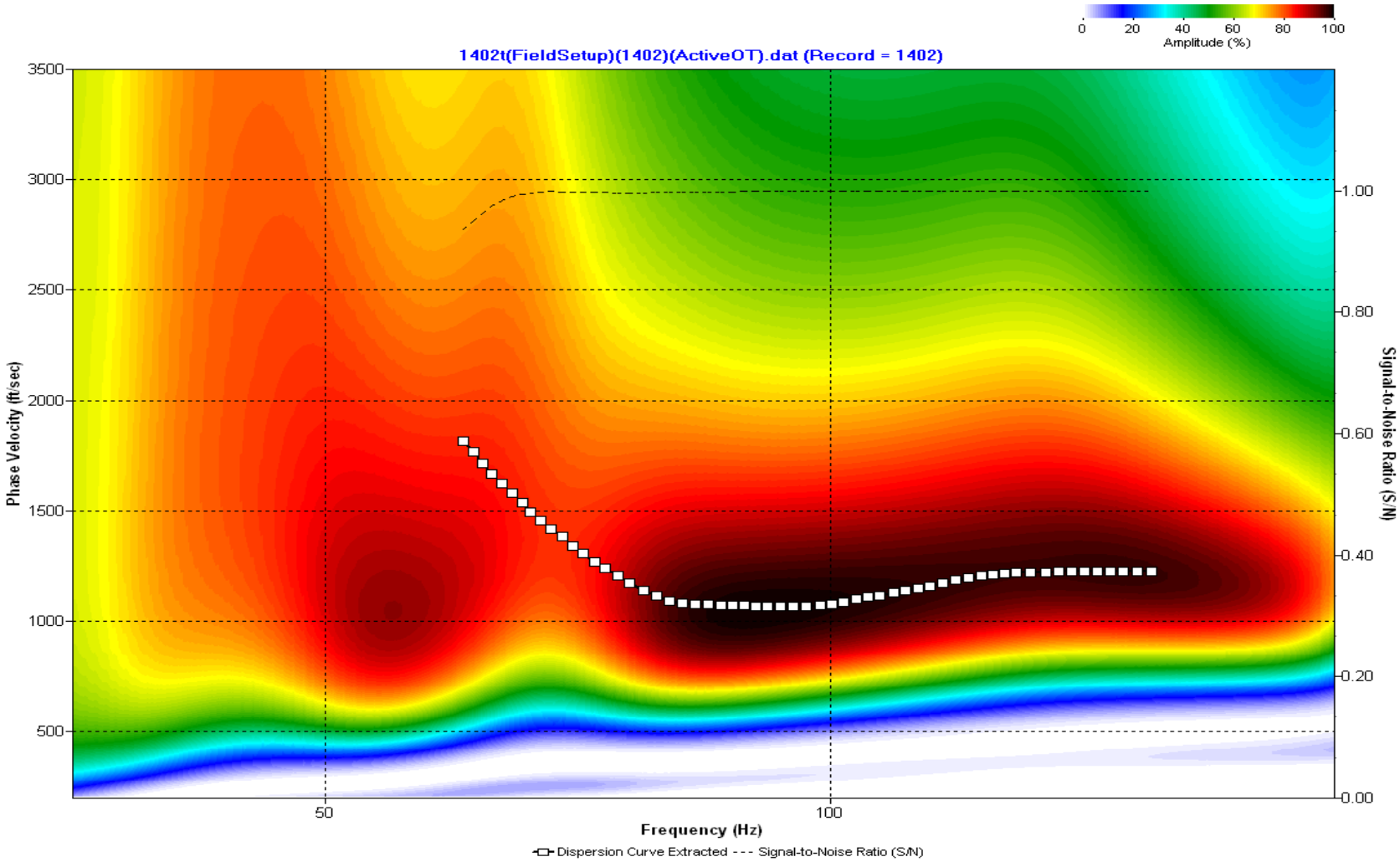

A.671: Dispersion Curve Line 1402 used in Pre-blast 38

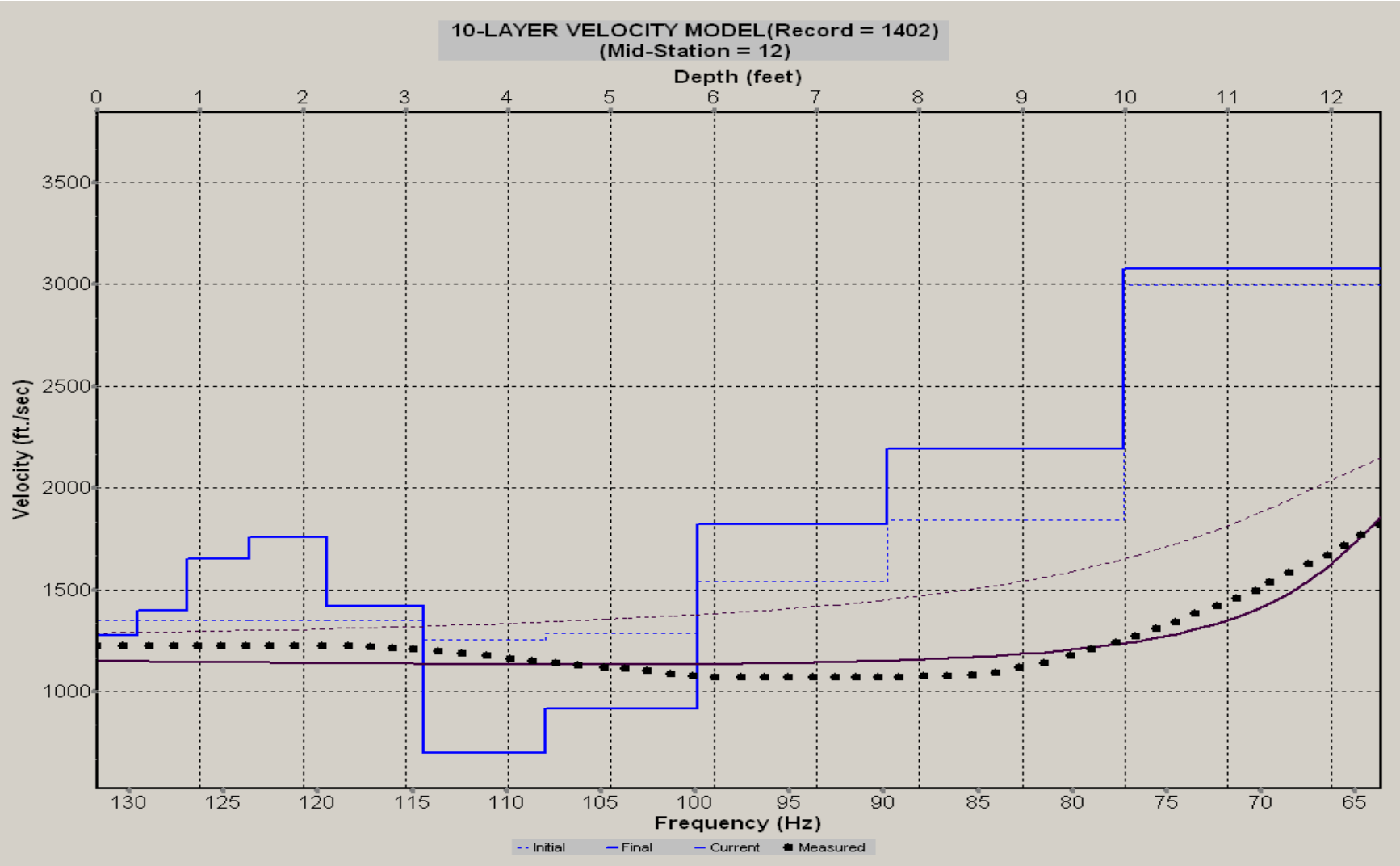

A.672: Velocity Profile Line 1402 used in Pre-blast 38

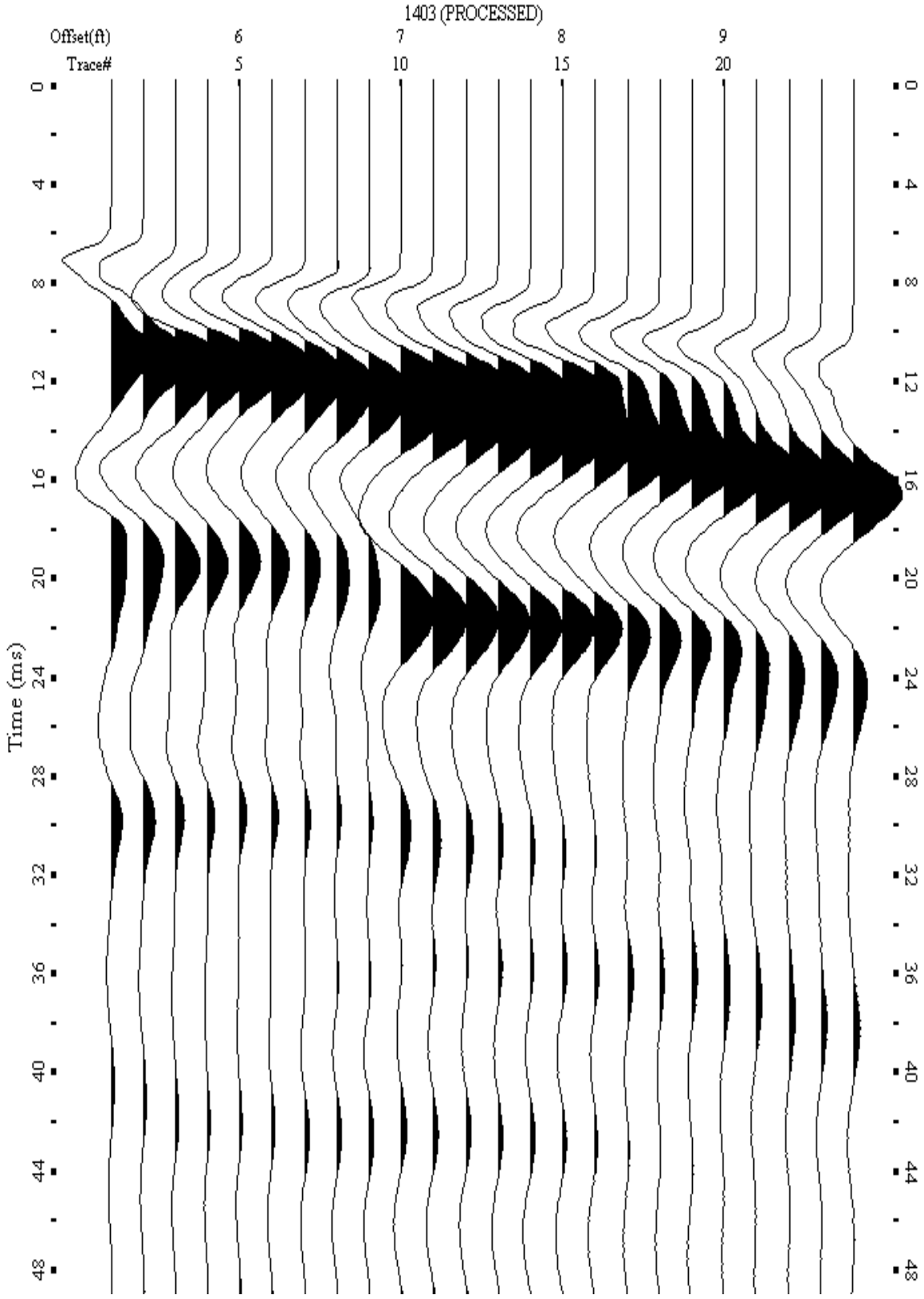

A.673: Shot Gather Line 1403 used in Pre-blast 38

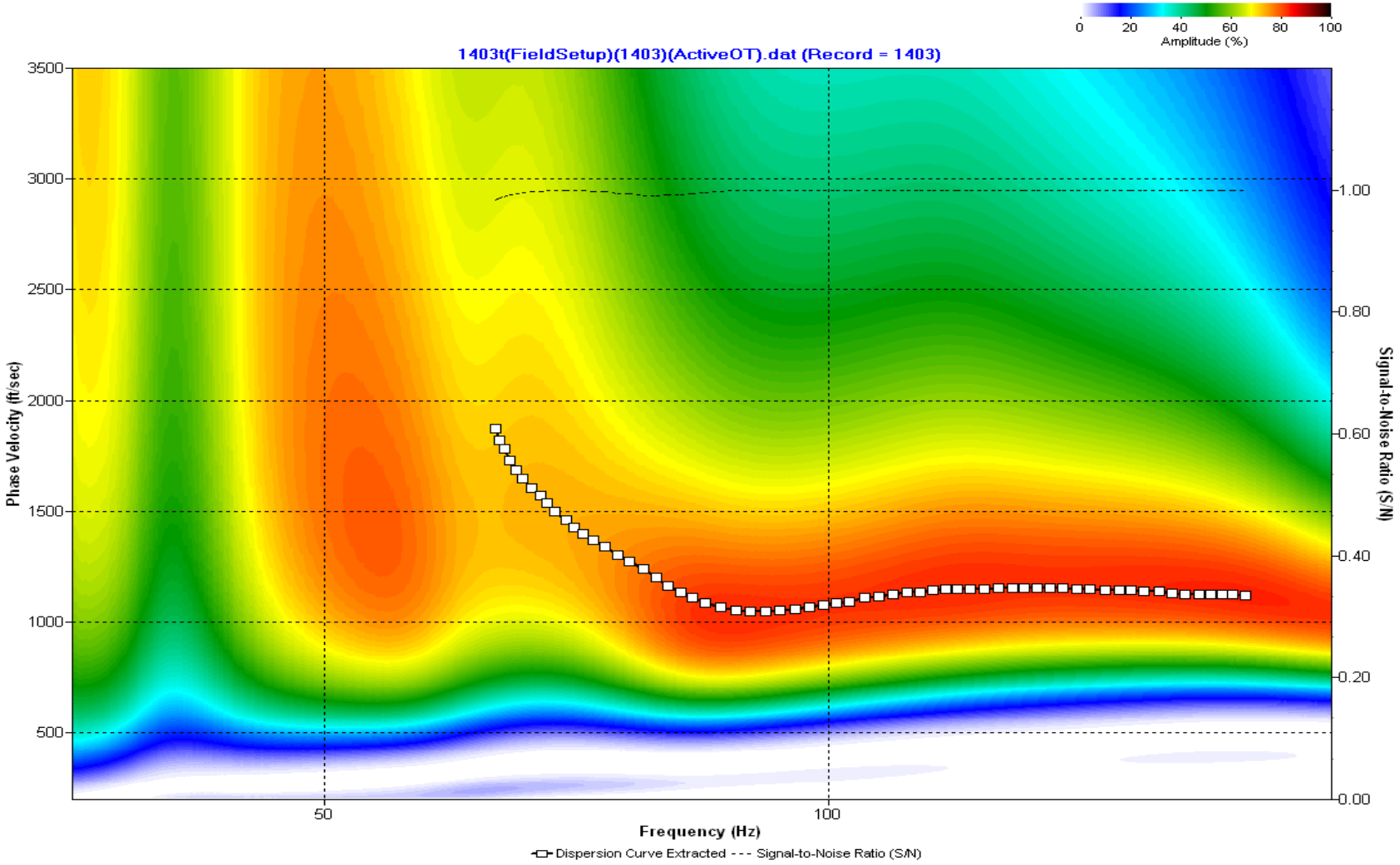

A.674: Dispersion Curve Line 1403 used in Pre-blast 38

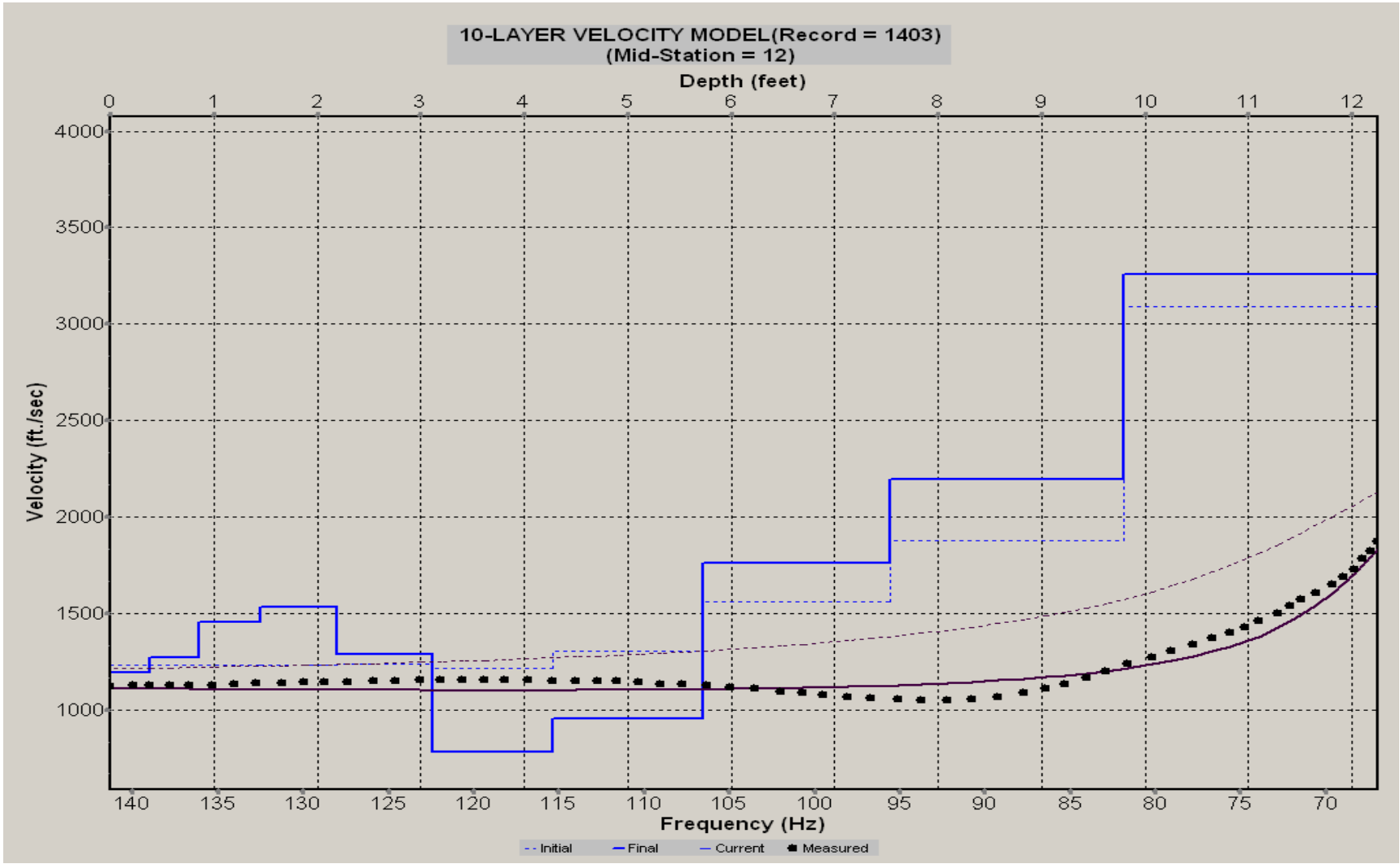

A.675: Velocity Profile Line 1403 used in Pre-blast 38

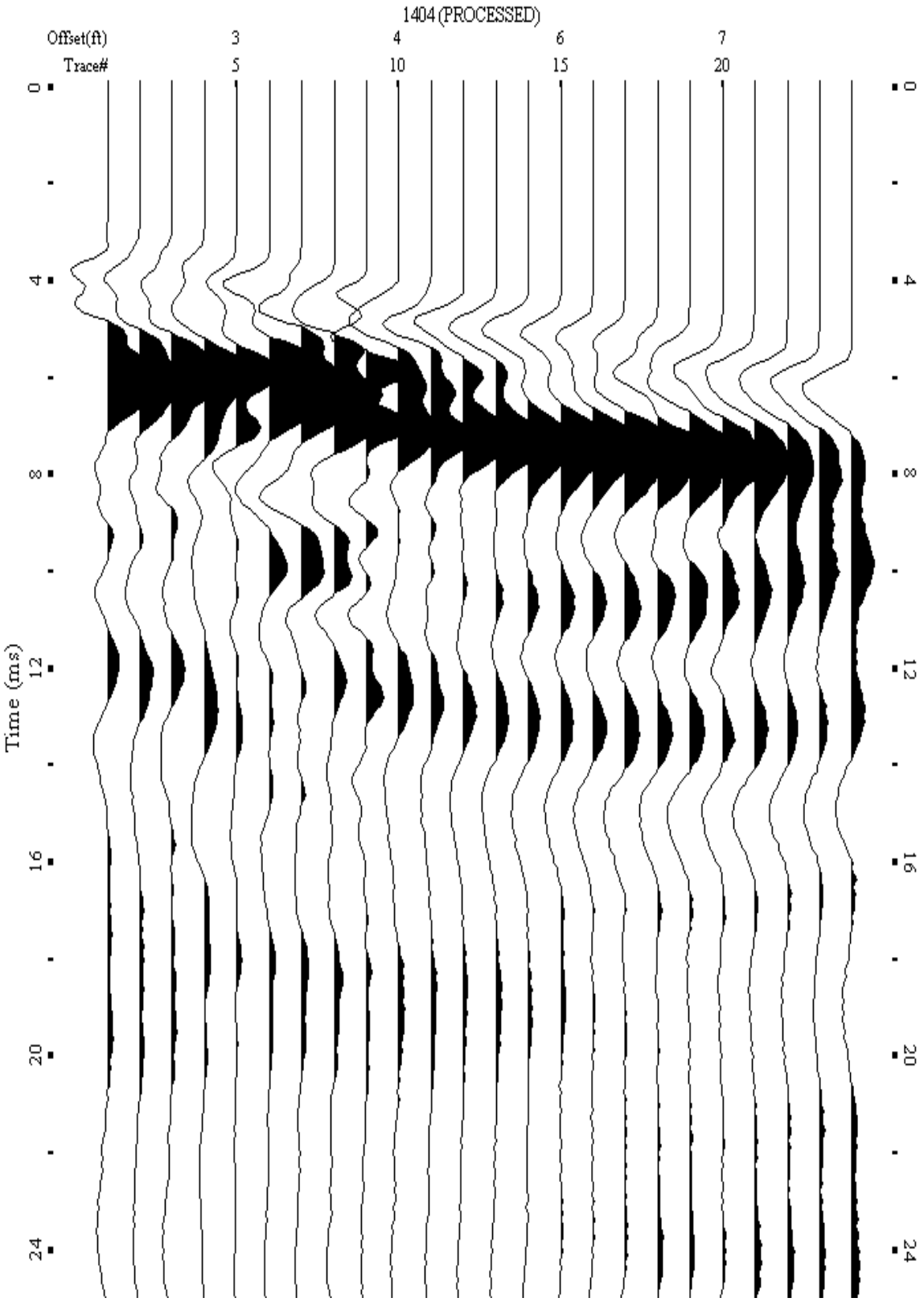

A.676: Shot Gather Line 1404 used in Pre-blast 36 and Pre-blast 37

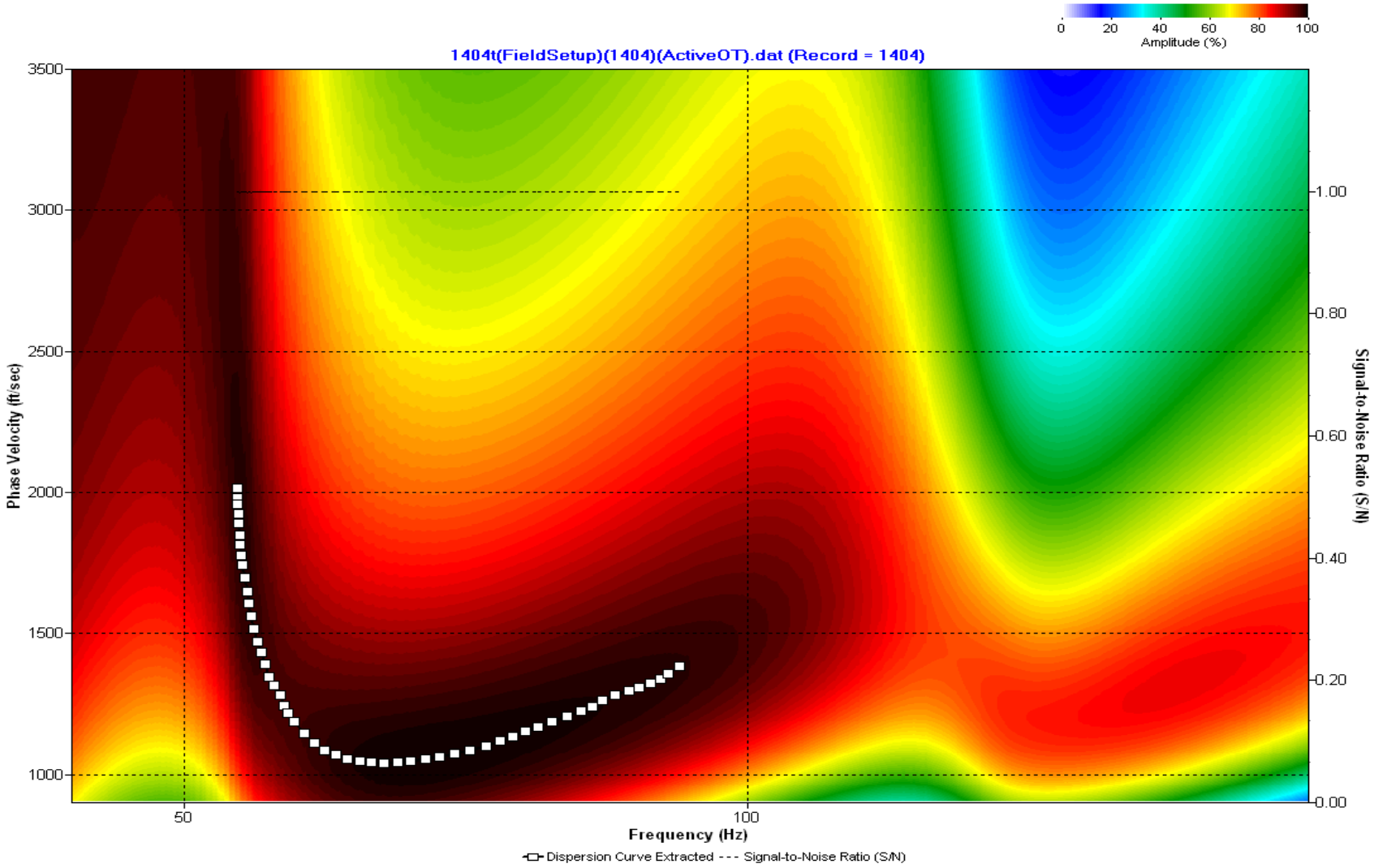

A.677: Dispersion Curve Line 1404 used in Pre-blast 36 and 37

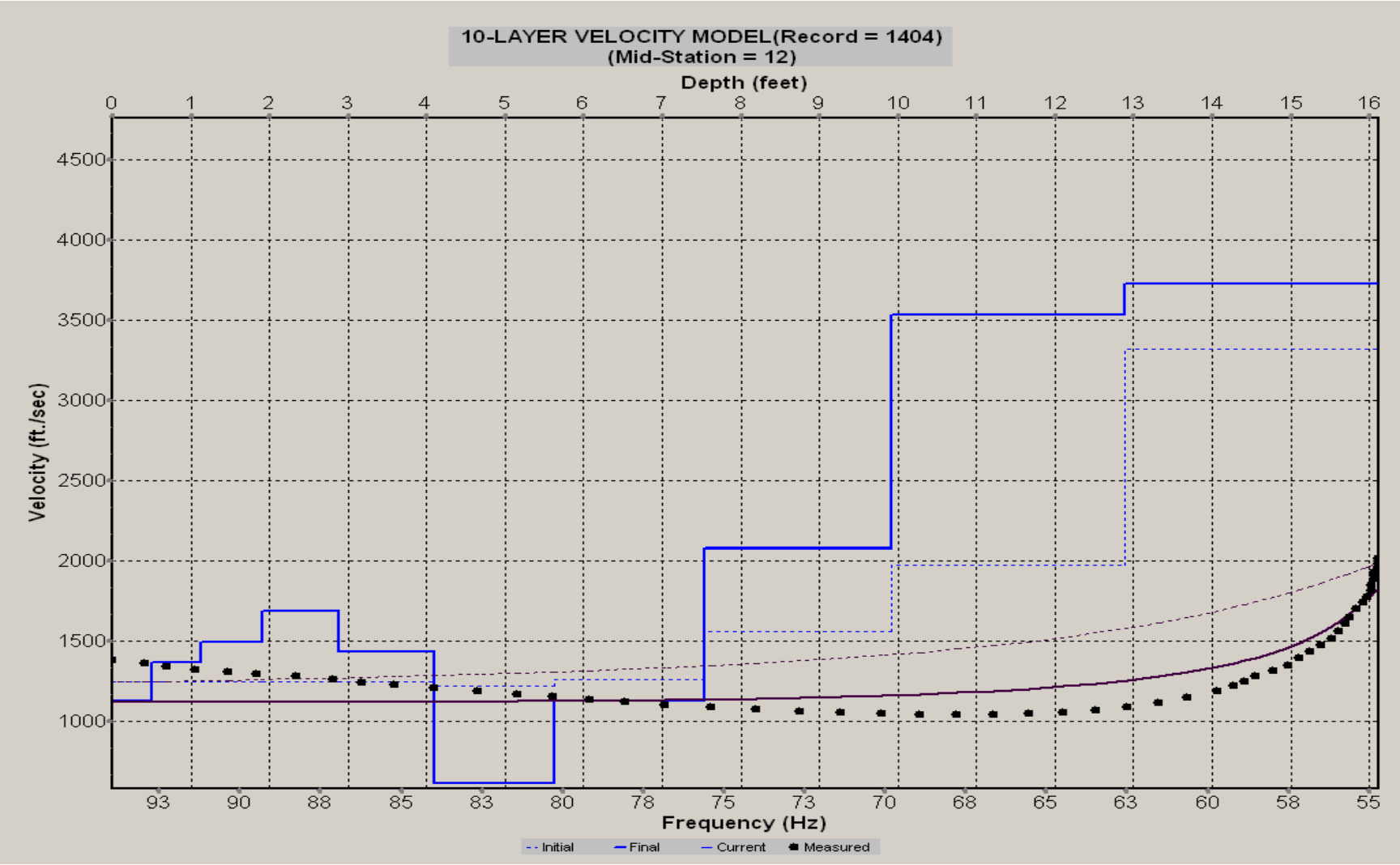

A.678: Velocity Profile Line 1404 used in Pre-blast 36 and Pre-blast 37

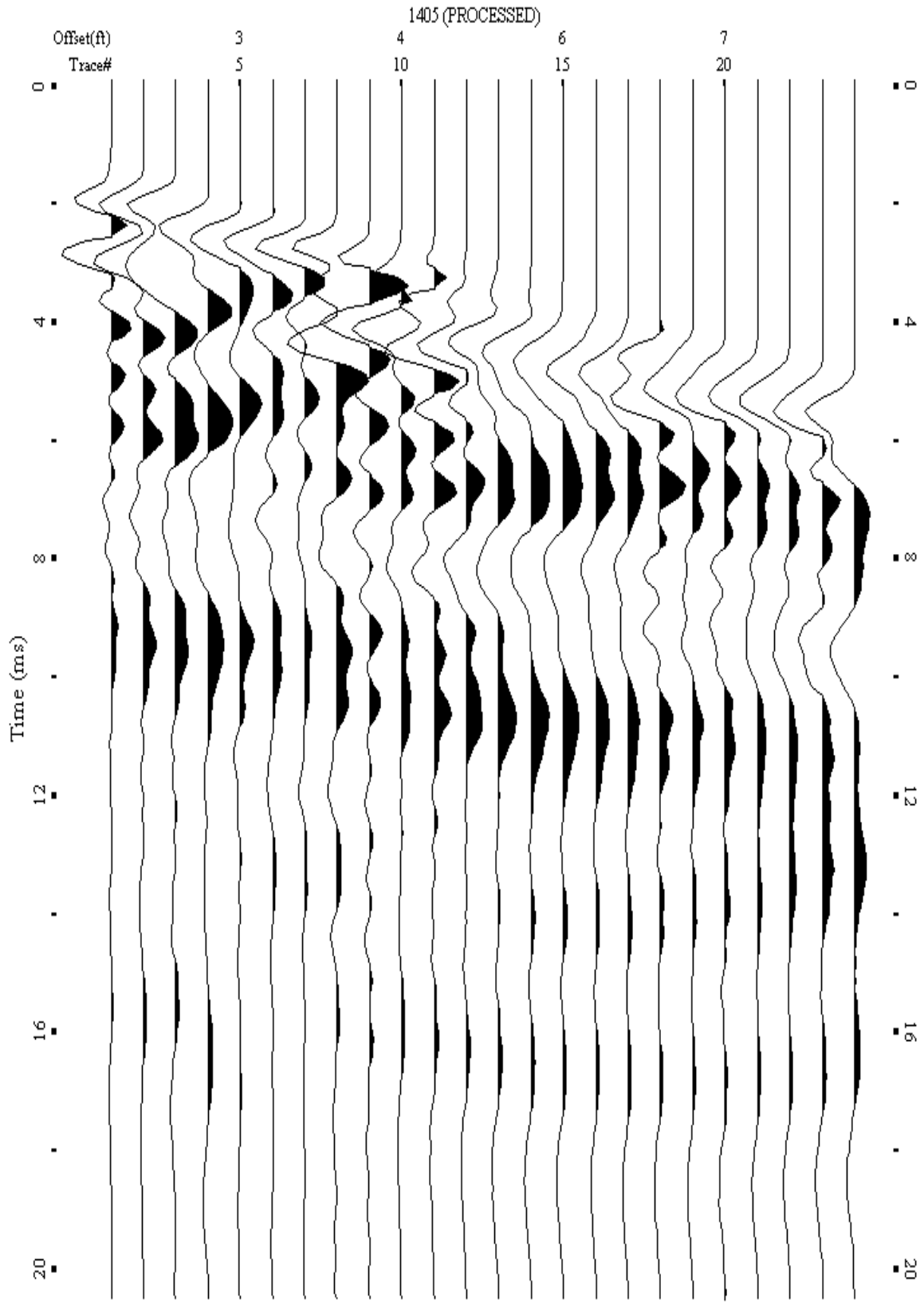

A.679: Shot Gather Line 1405 used in Pre-blast 36 and Pre-blast 37

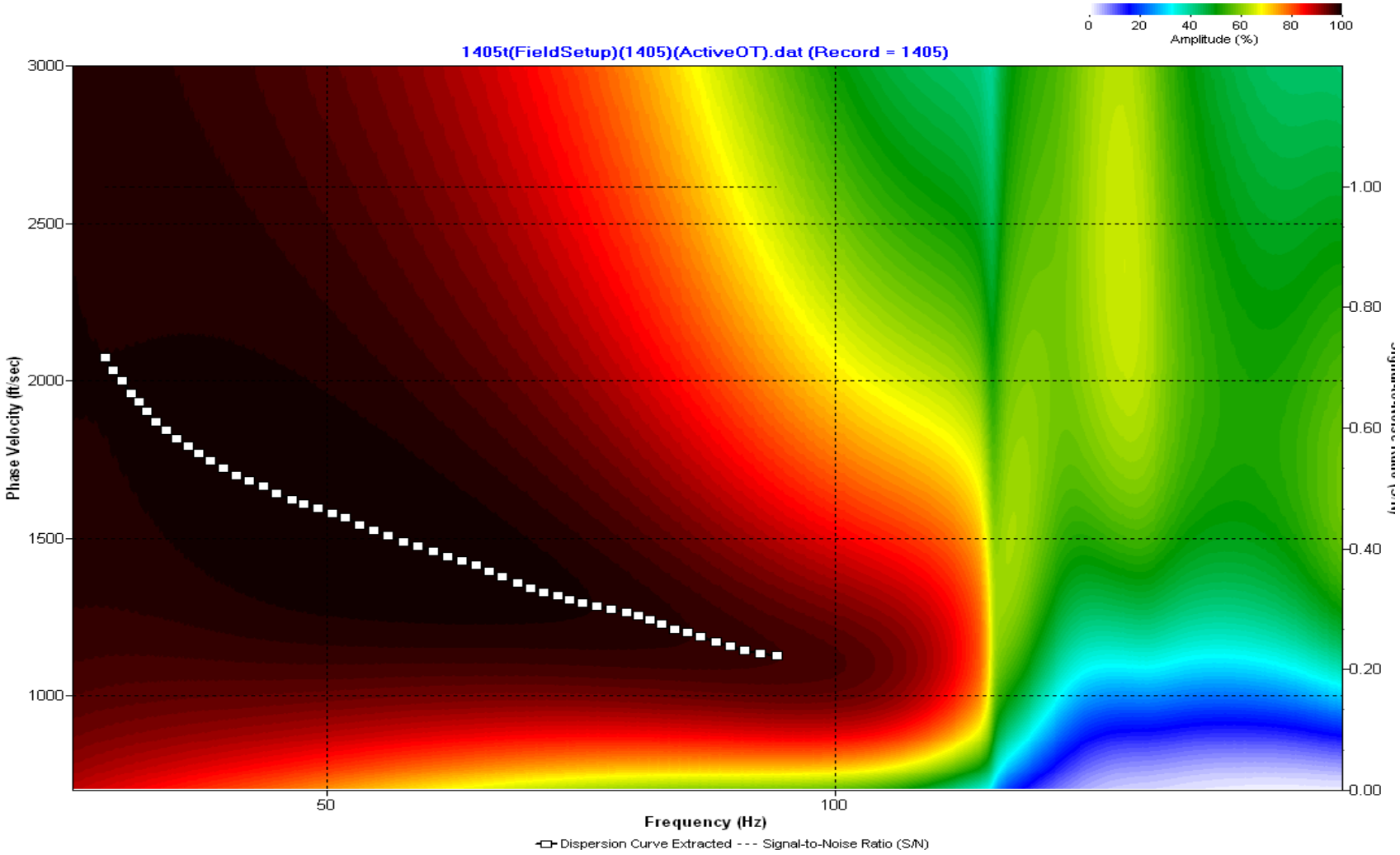

A.680: Dispersion Curve Line 1405 used in Pre-blast 36 and Pre-blast 37

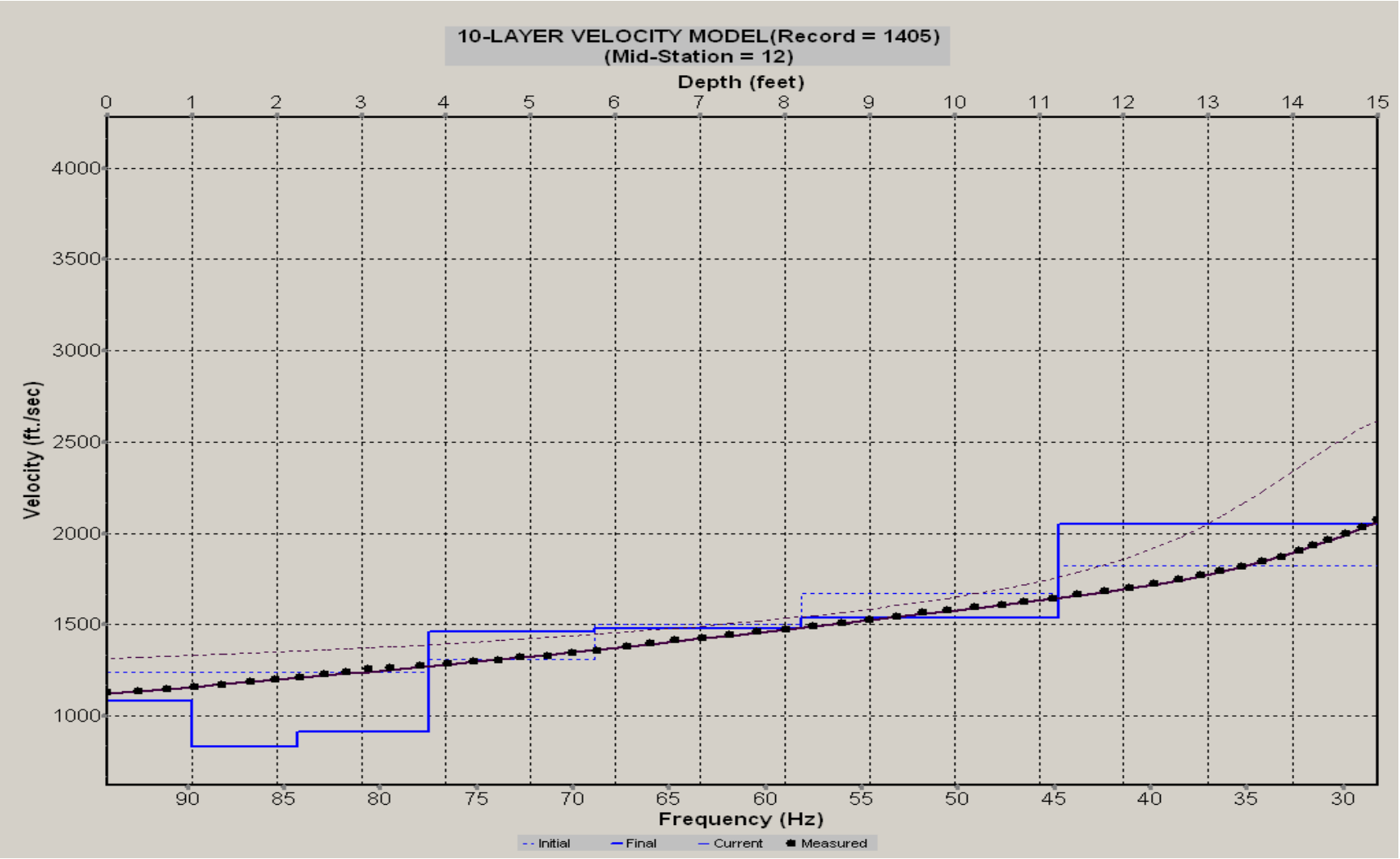

A.681: Velocity Profile Line 1405 used in Pre-blast 36 and Pre-blast 37

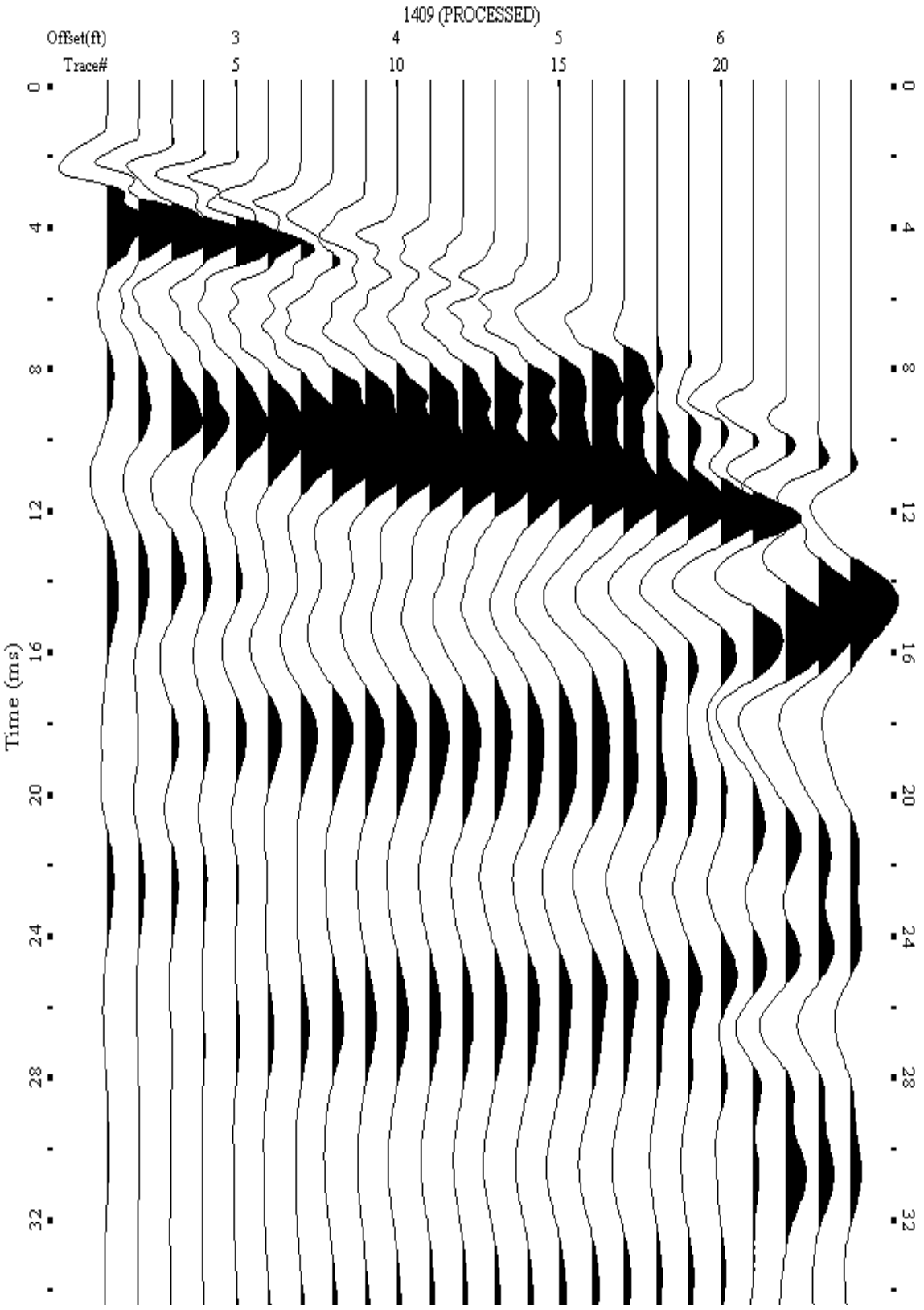

A.682: Shot Gather Line 1409 used in Post-blast 36 and Post-blast 37

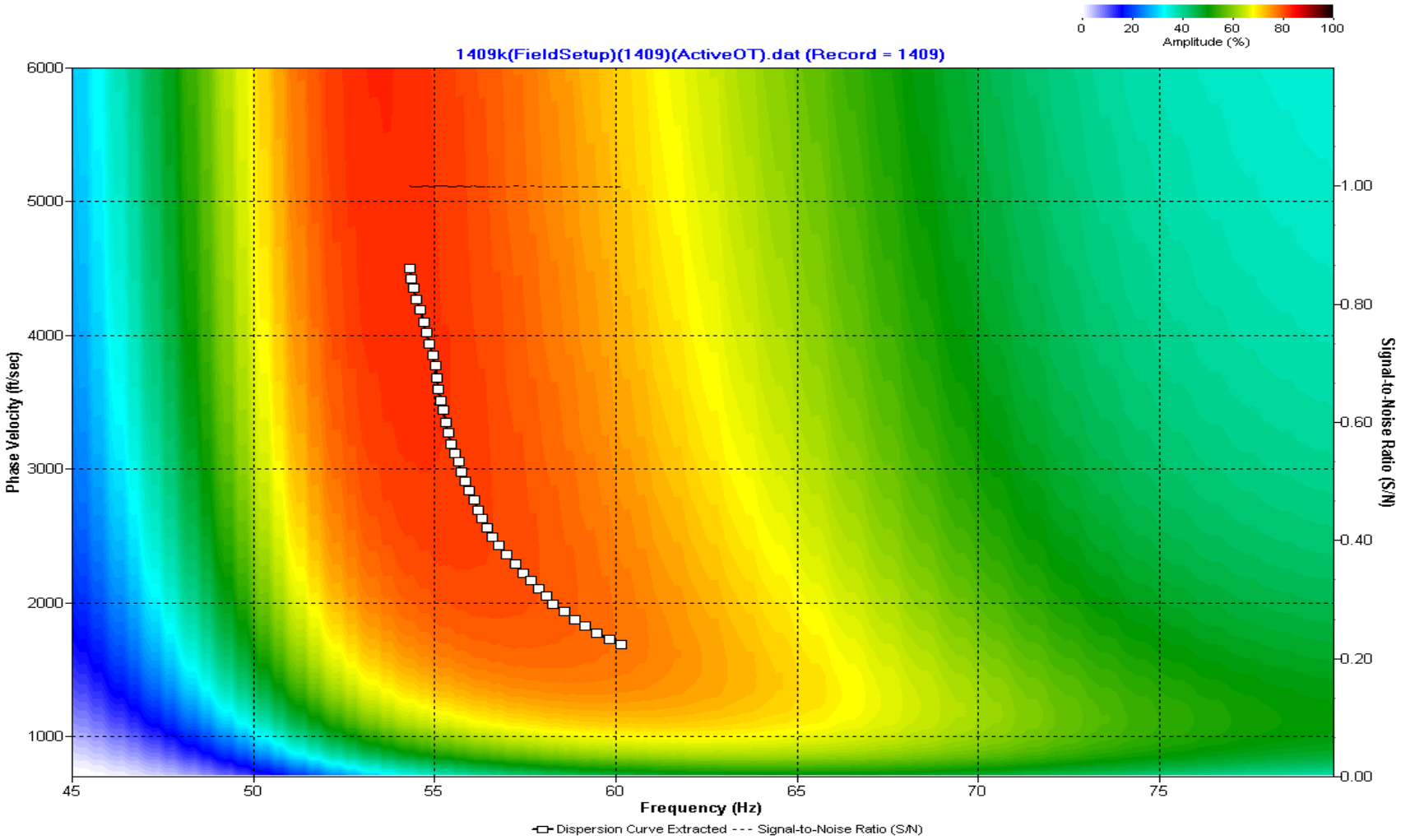

A.683: Dispersion Curve Line 1409 used in Post-blast 36 and Post-blast 37

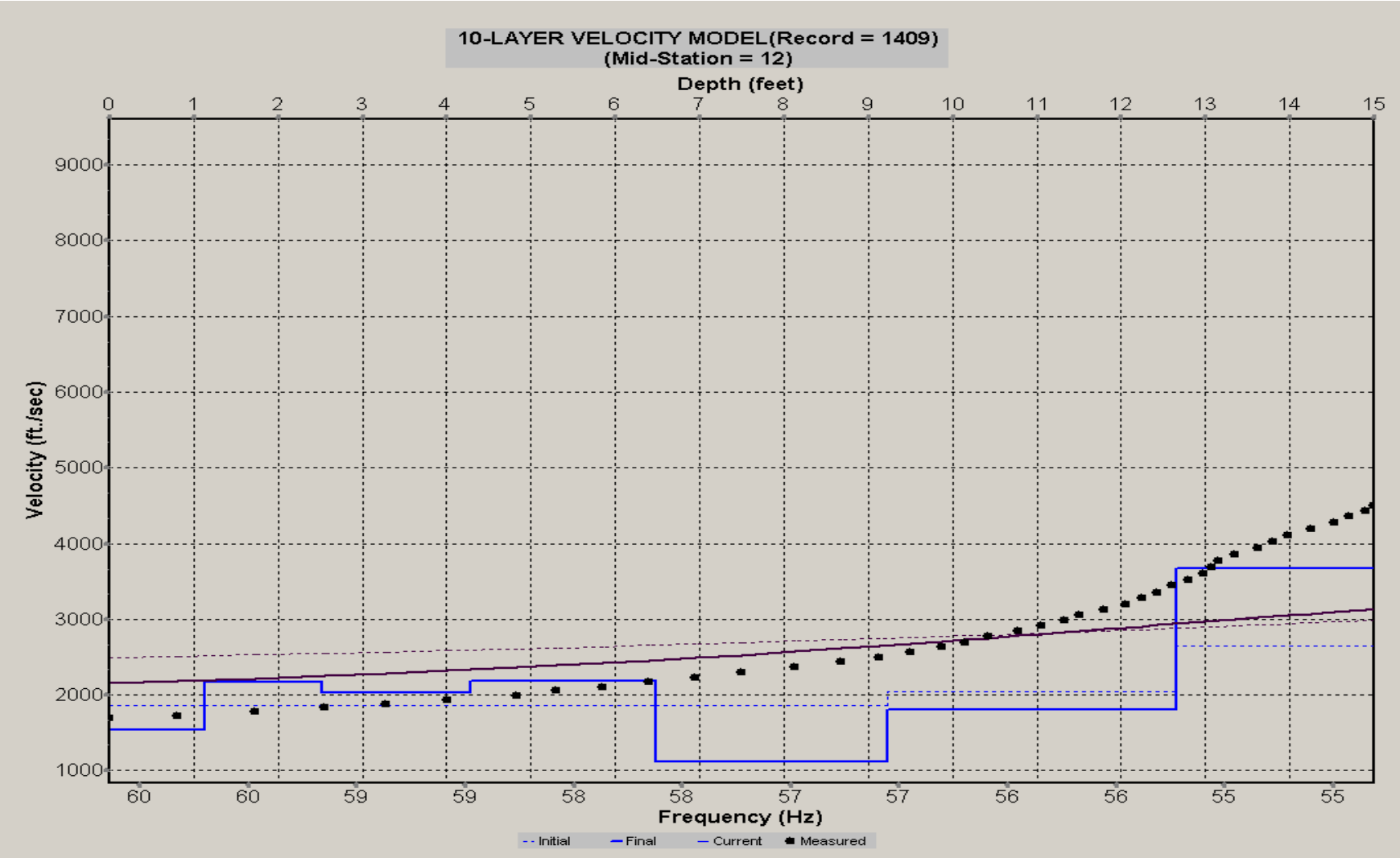

A.684: Velocity Profile Line 1409 used in Post-blast 36 and Post-blast 37

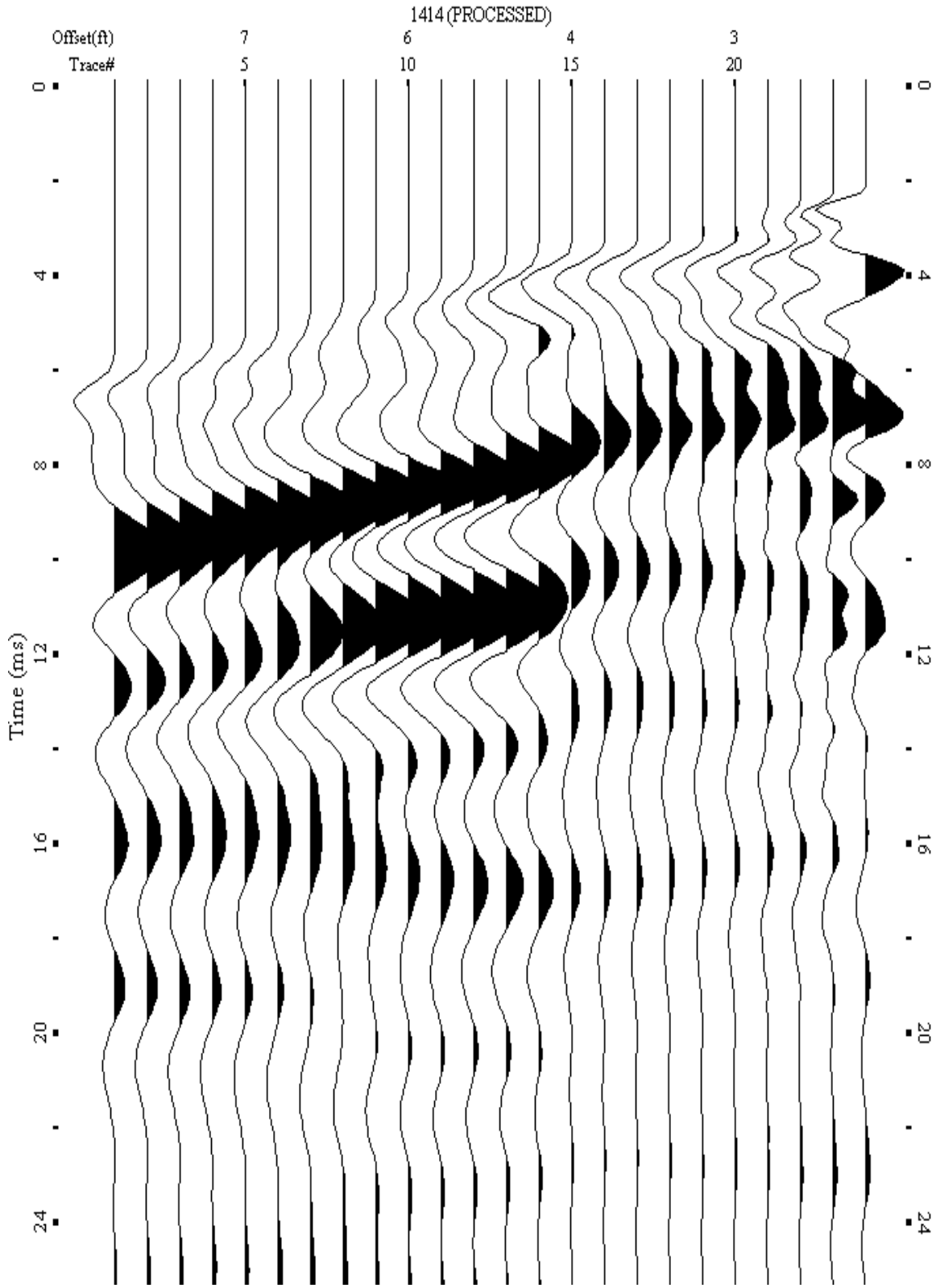

A.685: Shot Gather Line 1414 used in Pre-blast 41

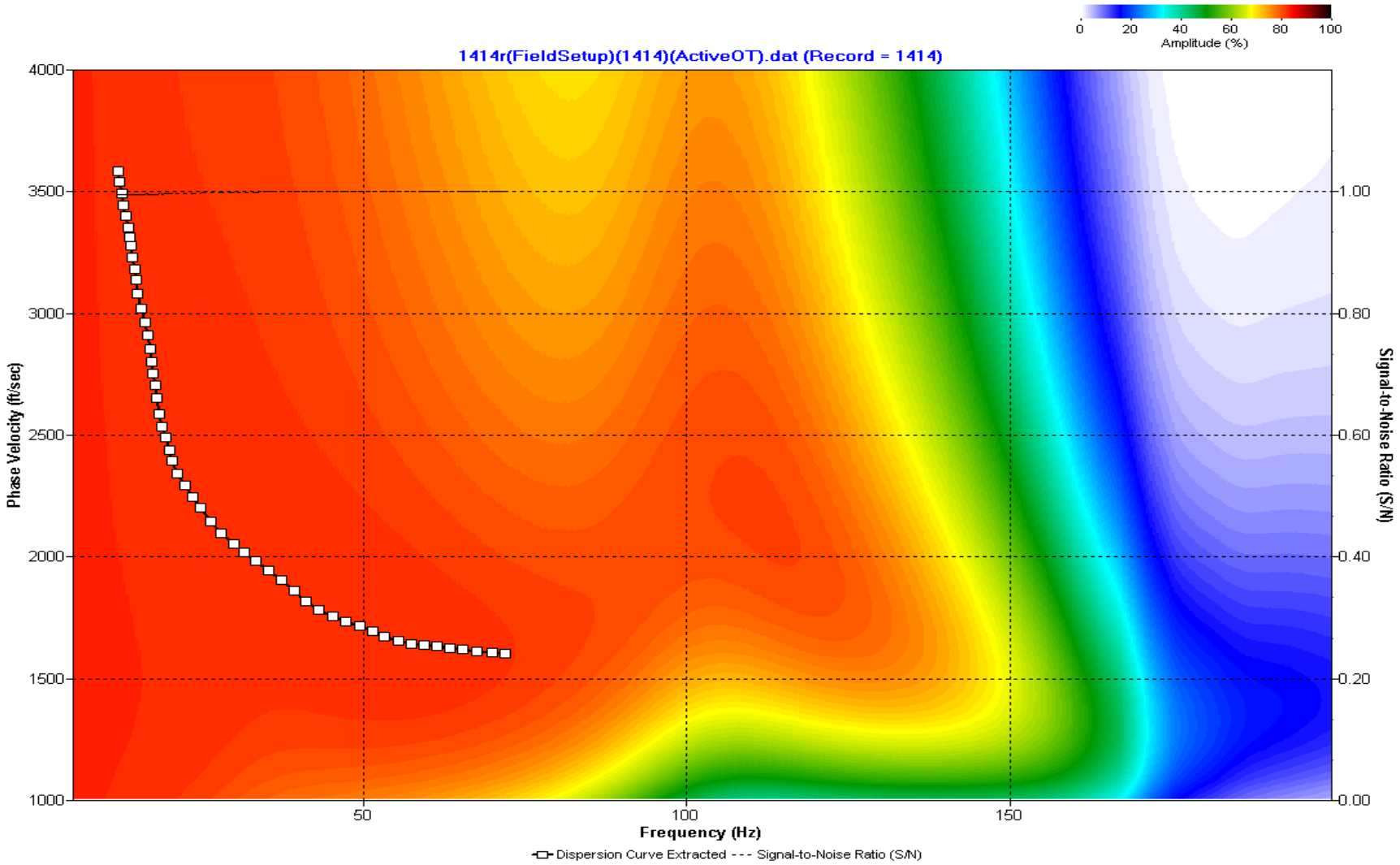

A.686: Dispersion Curve Line 1414 used in Pre-blast 41

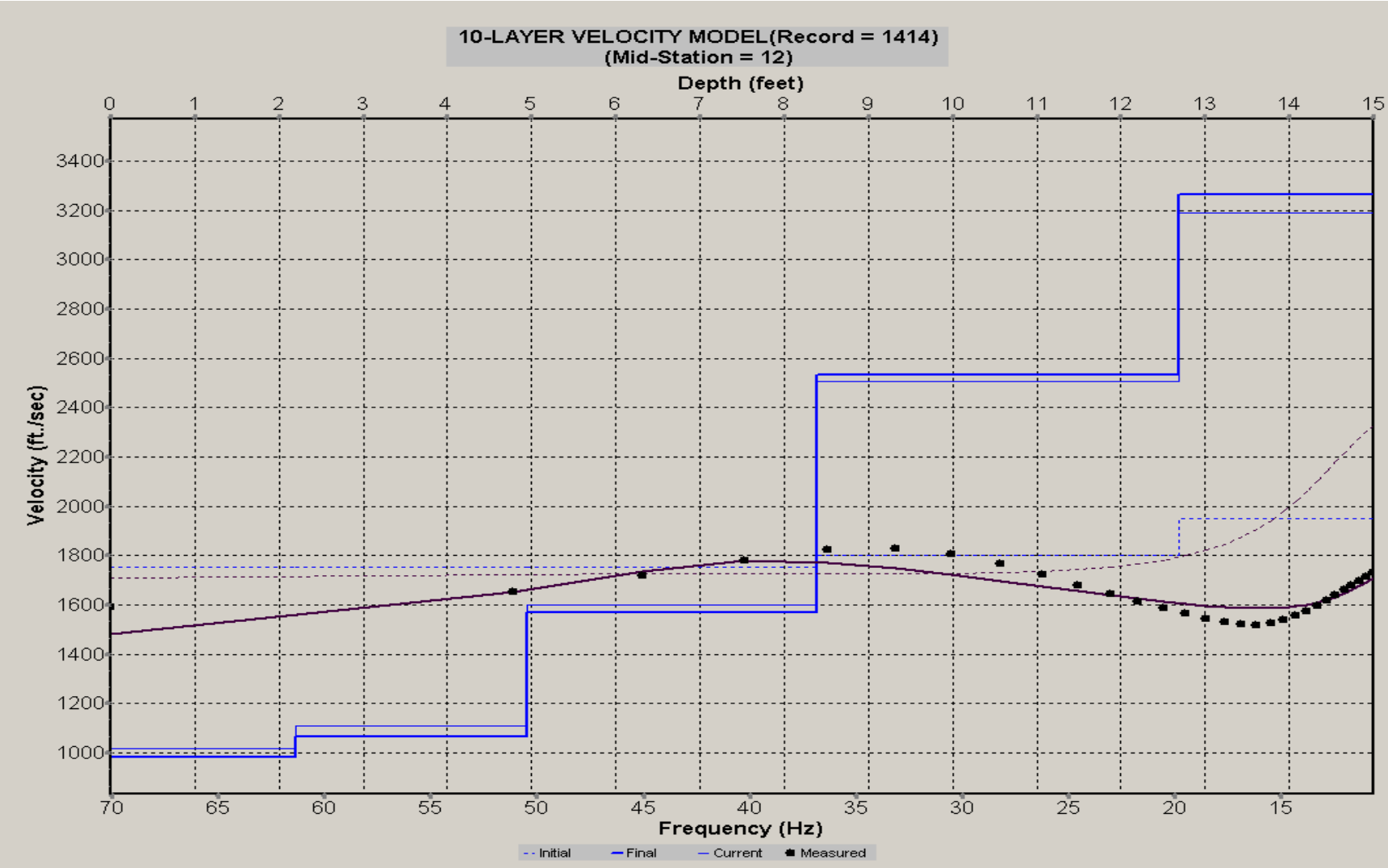

A.687: Velocity Profile Line 1414 used in Pre-blast 41

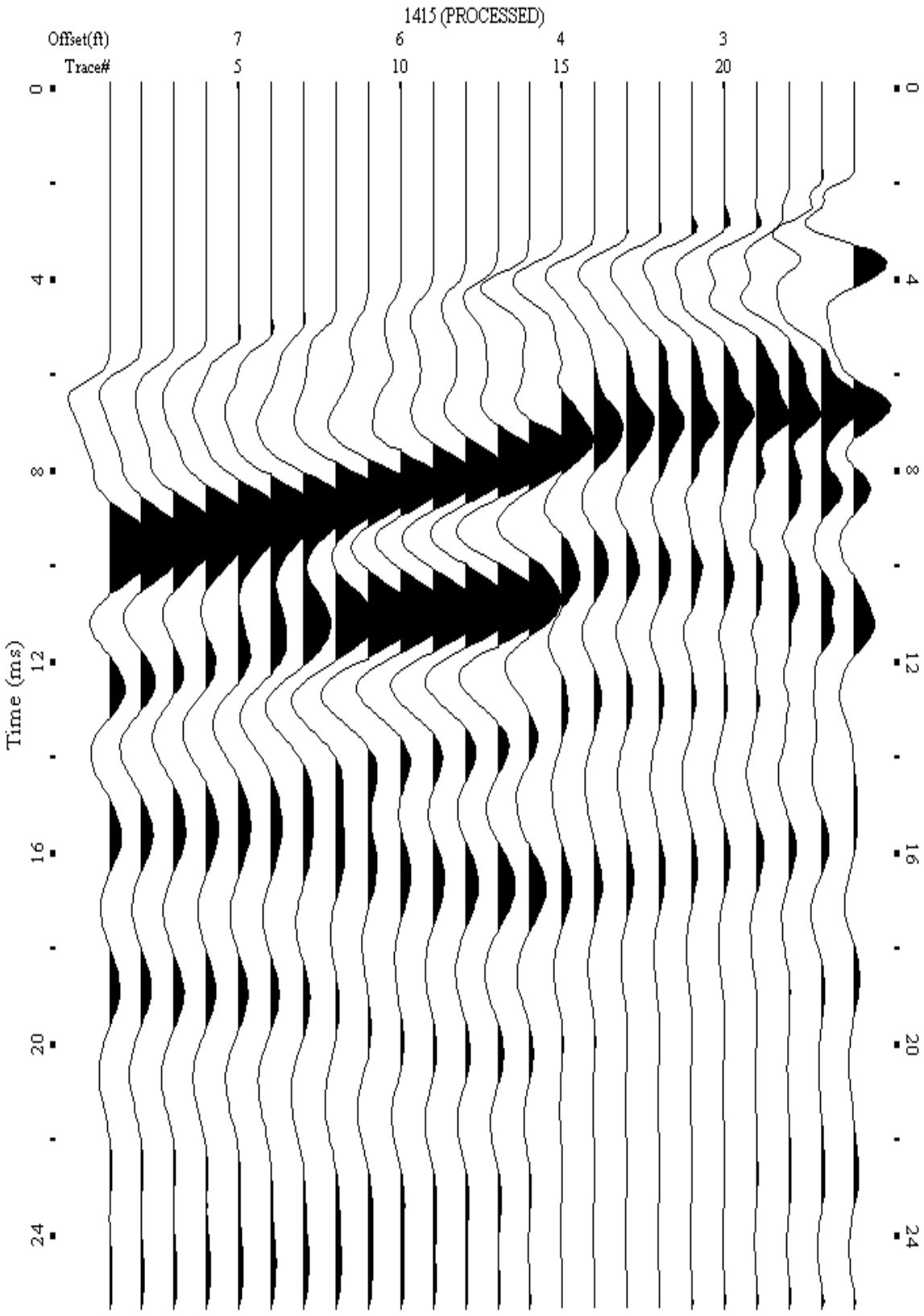

A.688: Shot Gather Line 1415 used in Post-blast 38, Pre-blast 41 and Pre-blast 42

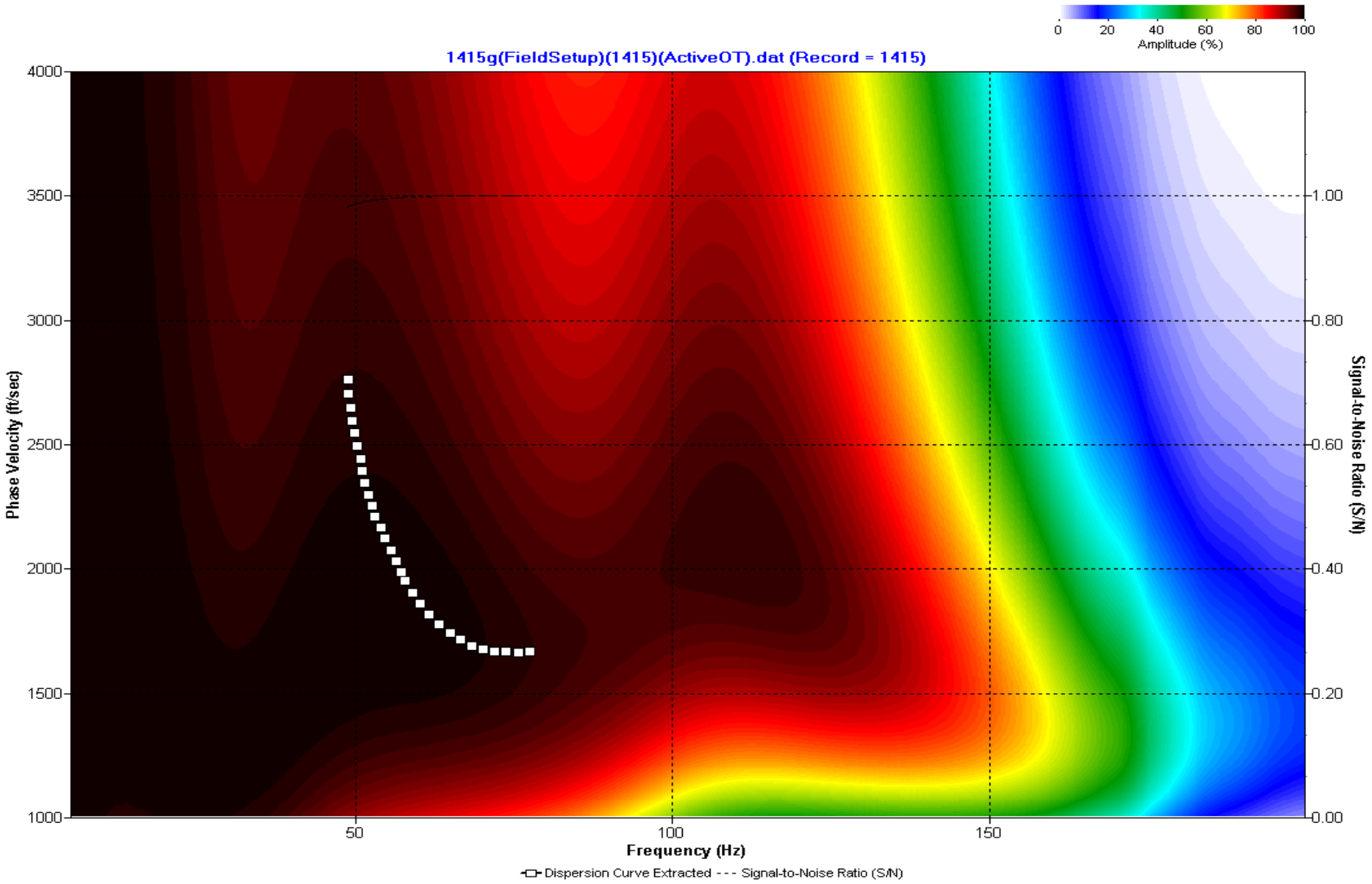

A.689: Dispersion Curve Line 1415 used in Post-blast 38, Pre-blast 41 and Pre-blast 42

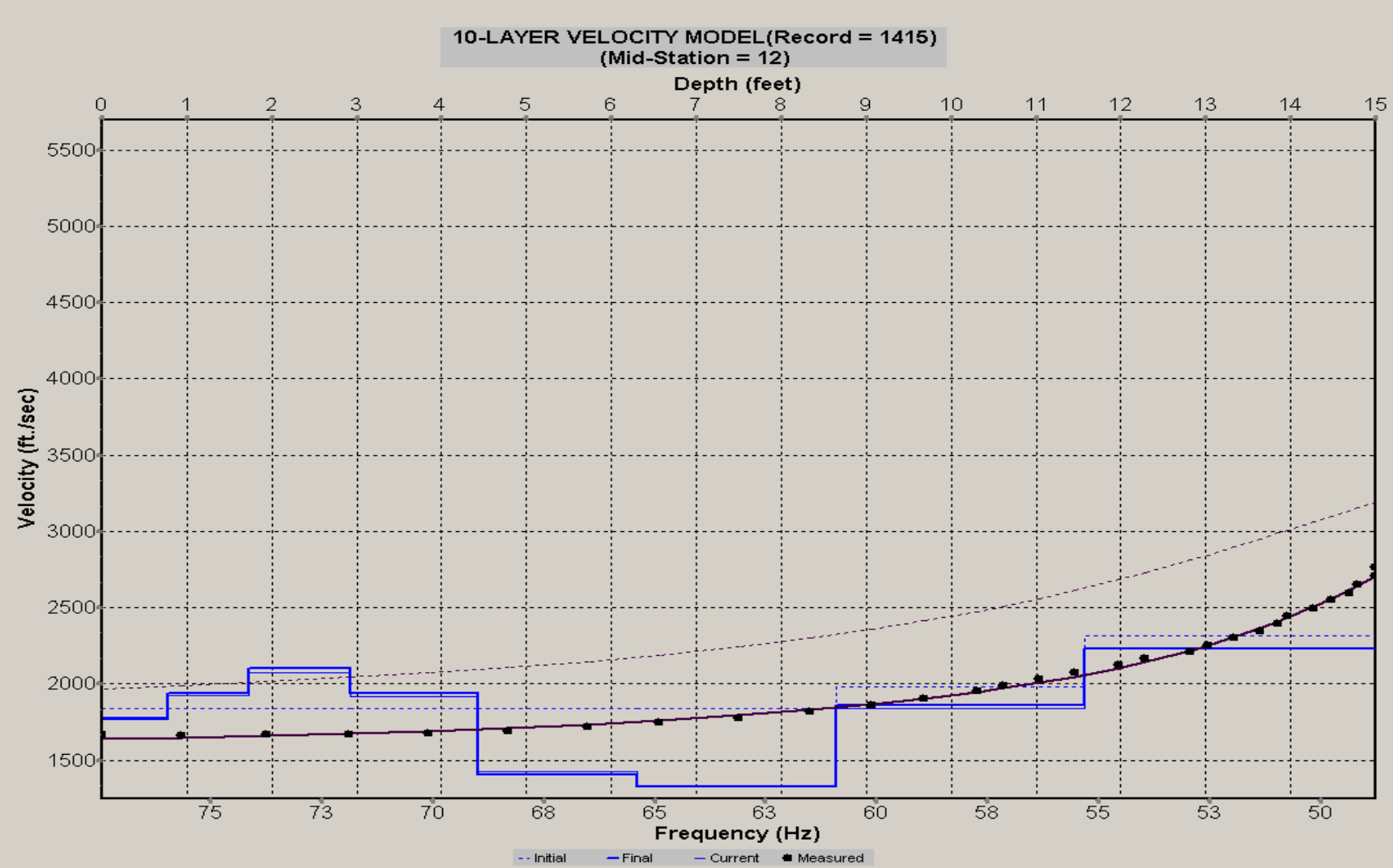

A.690: Velocity Profile Line 1415 used in Post-blast 38, Pre-blast 41 and Pre-blast 42

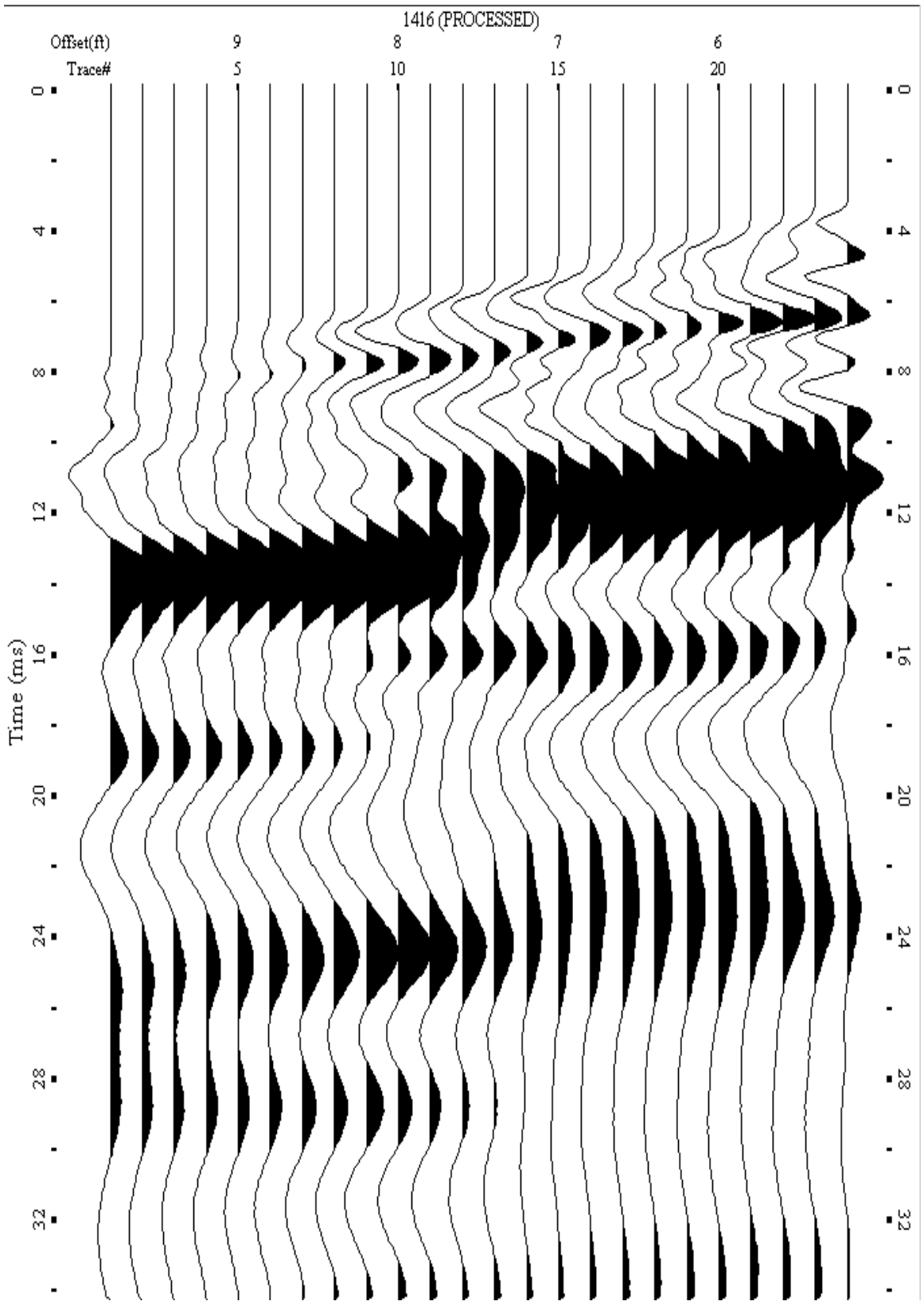

A.691: Shot Gather Line 1416 used in Post-blast 38, Pre-blast 41 and Pre-blast 42

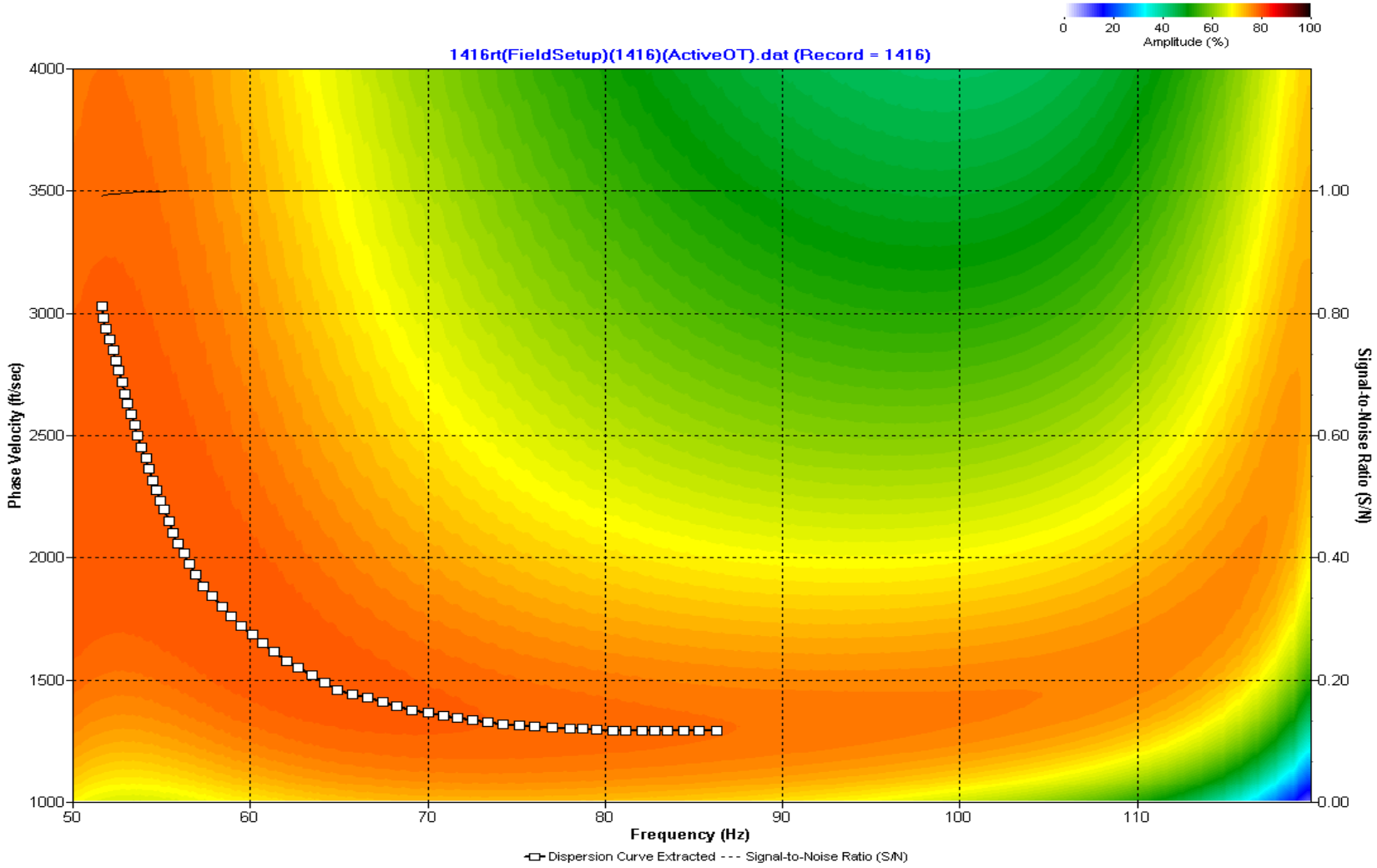

A.692: Dispersion Curve Line 1416 used in Post-blast 38, Pre-blast 41 and Pre-blast 42

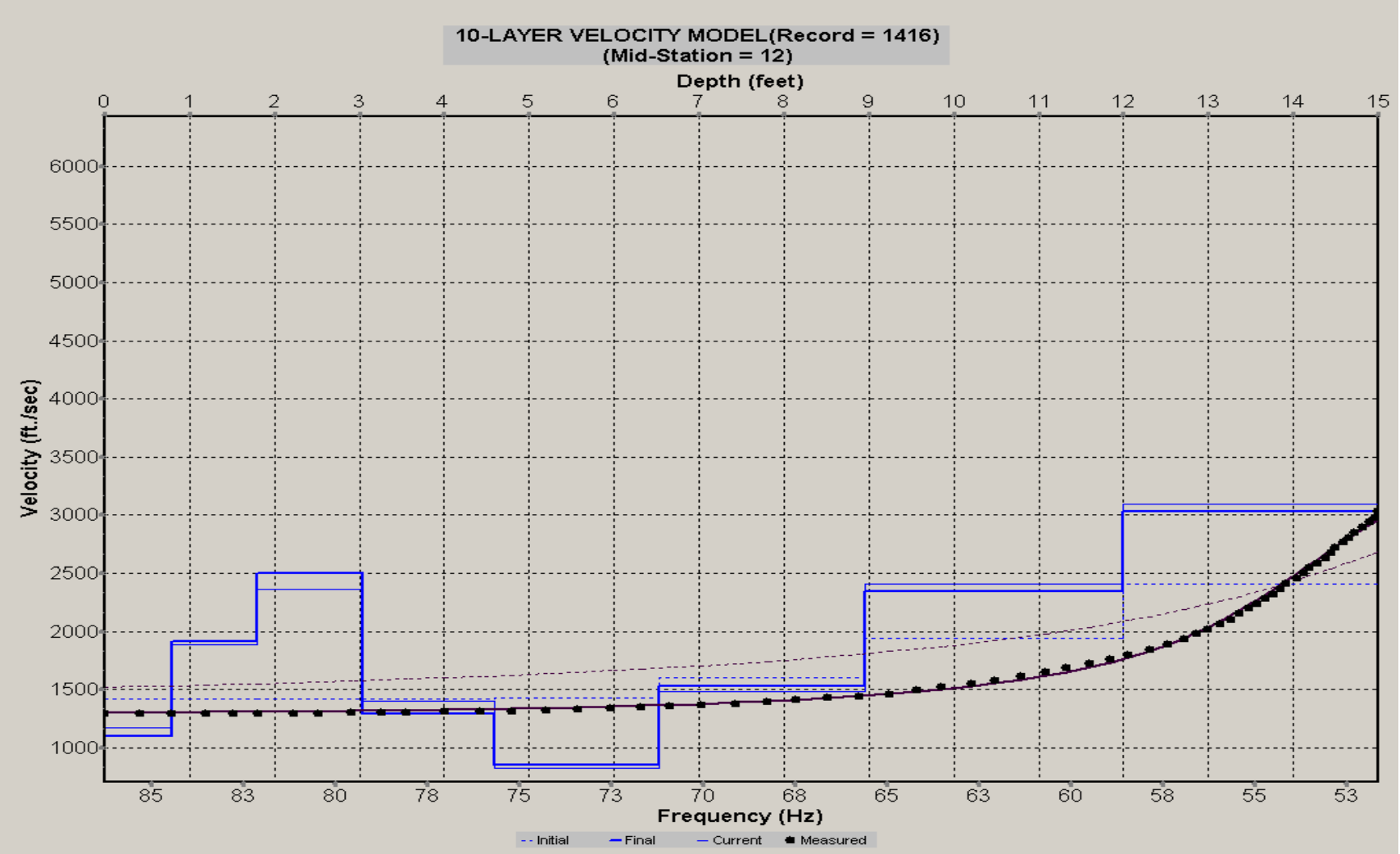

A.693: Velocity Profile Line 1416 used in Post-blast 38, Pre-blast 41 and Pre-blast 42

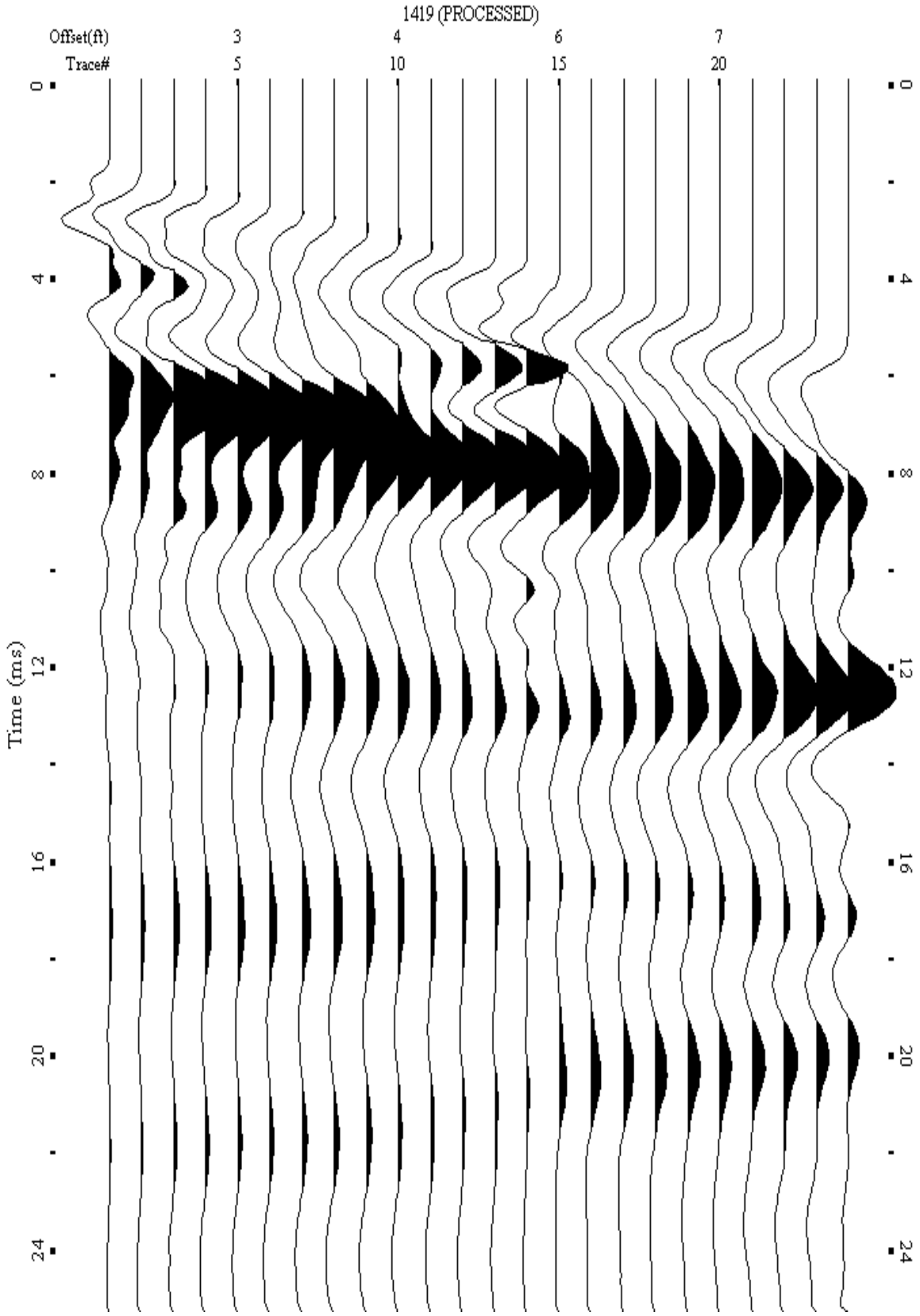

A.694: Shot Gather Line 1419 used in Post-blast 38, Pre-blast 41 and Pre-blast 42

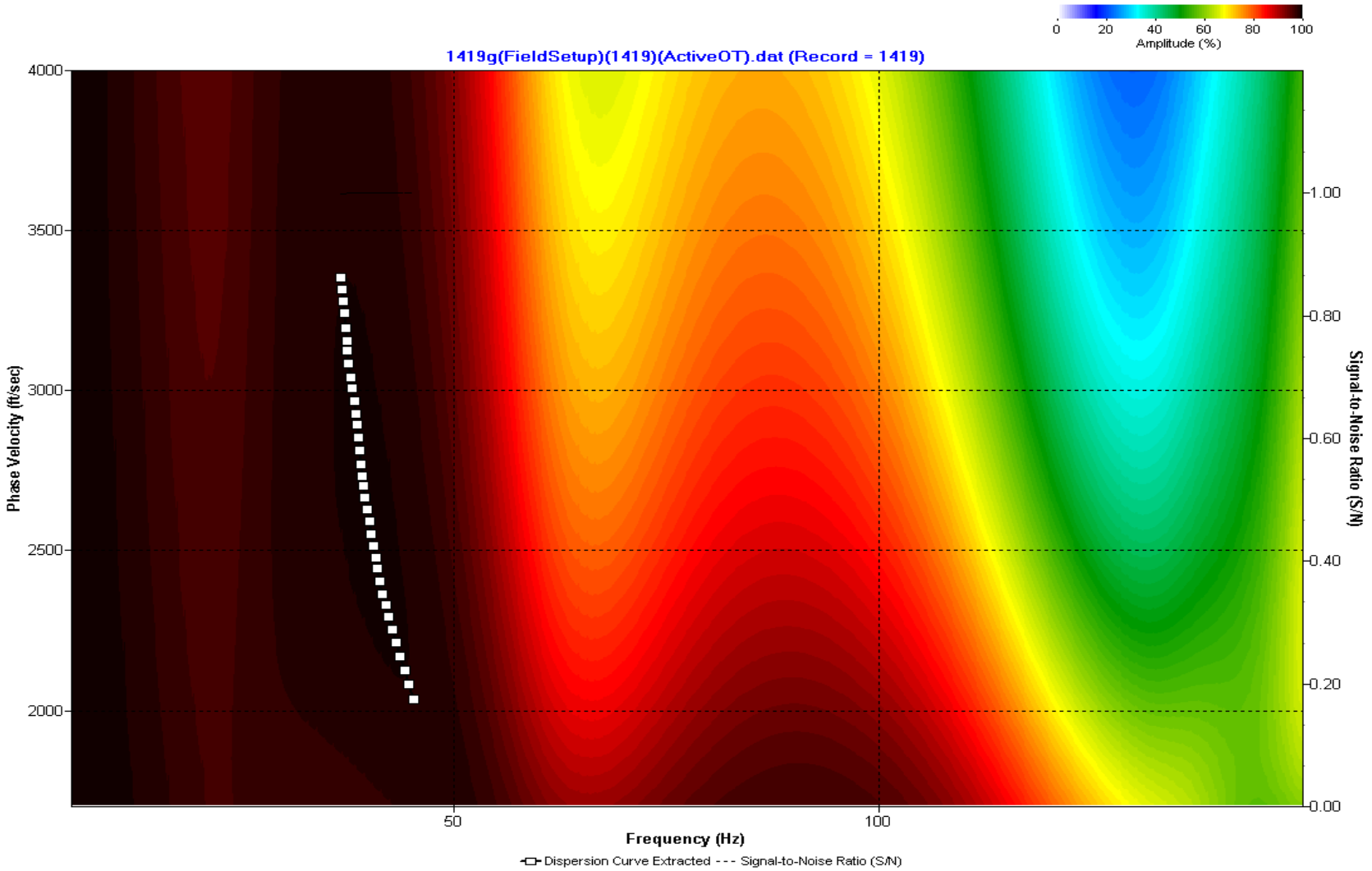

A.695: Dispersion Curve Line 1419 used in Post-blast 38, Pre-blast 41 and Pre-blast 42

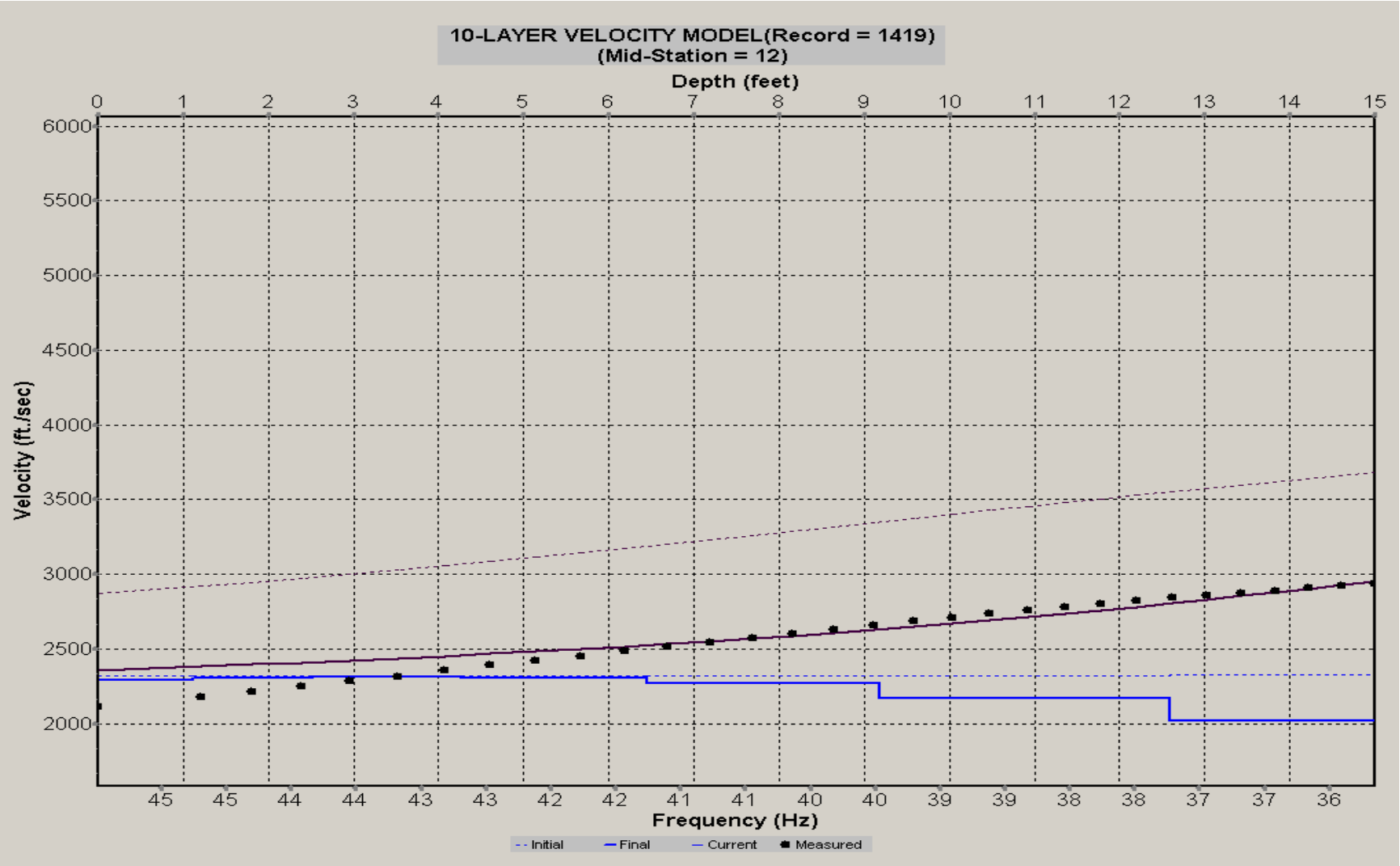

A.696: Velocity Profile Line 1419 used in Post-blast 38, Pre-blast 41 and Pre-blast 42

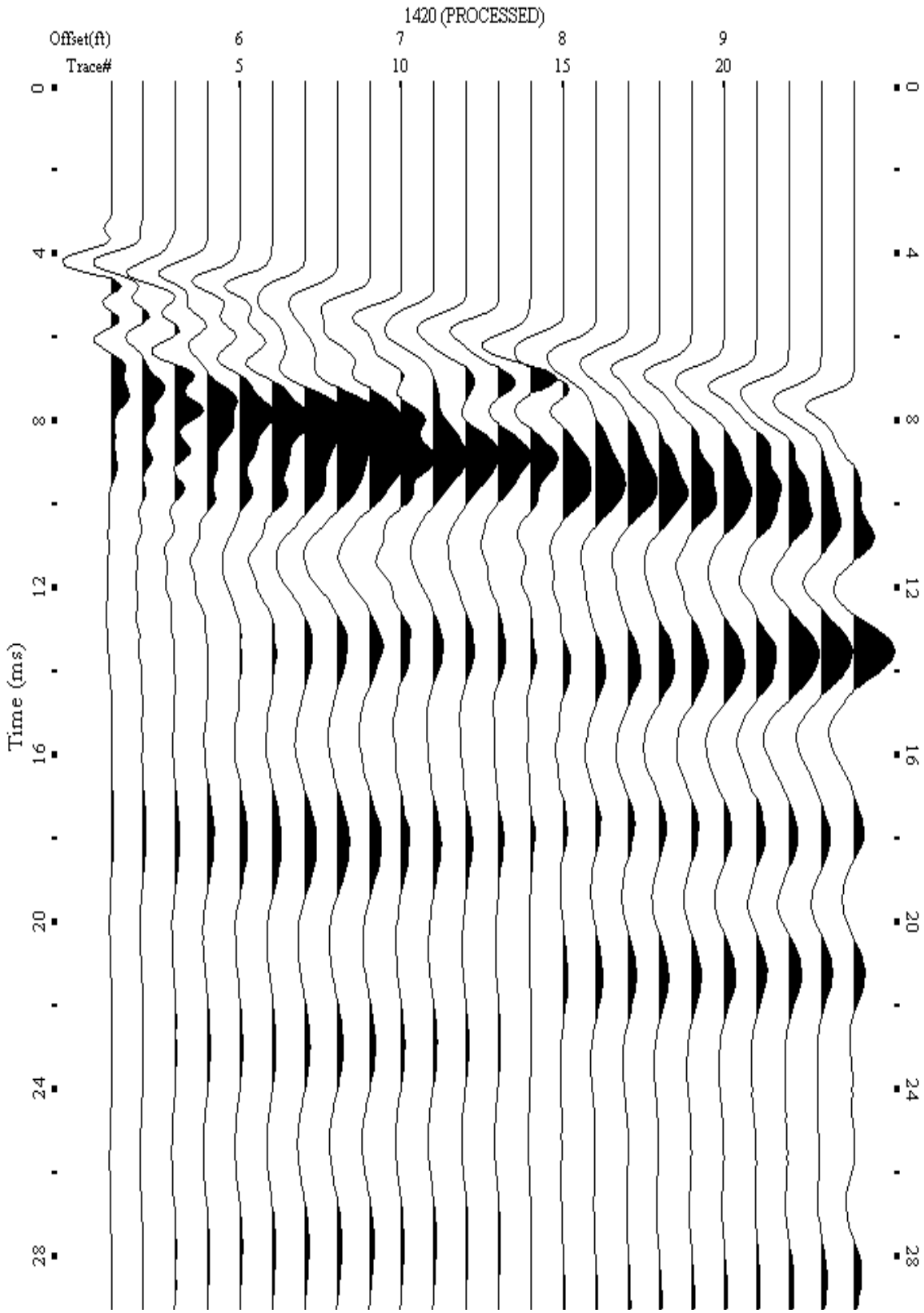

A.697: Shot Gather Line 1420 used in Pre-blast 41 and Pre-blast 42

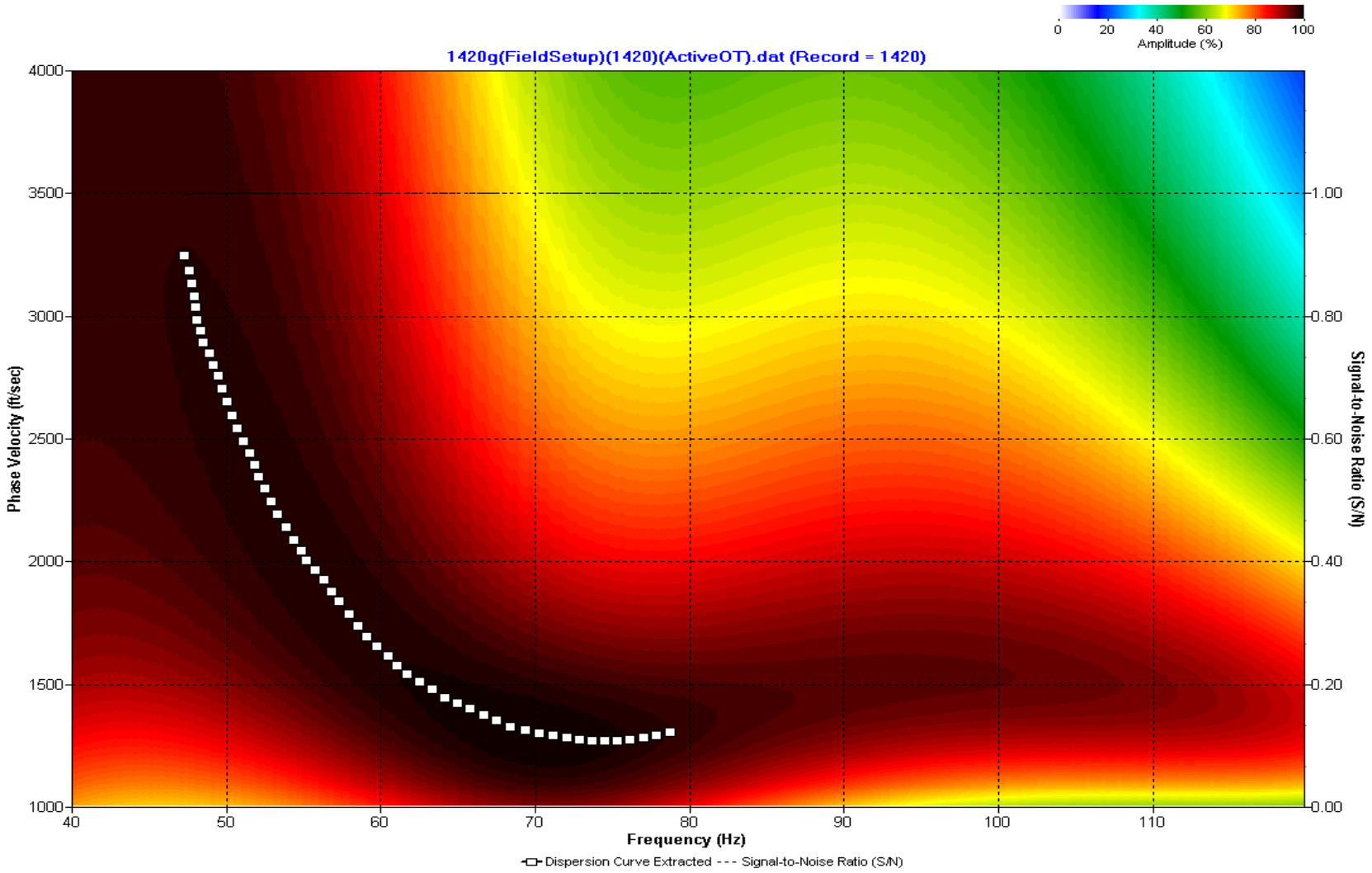

A.698: Dispersion Curve Line 1420 used in Pre-blast 41 and Pre-blast 42

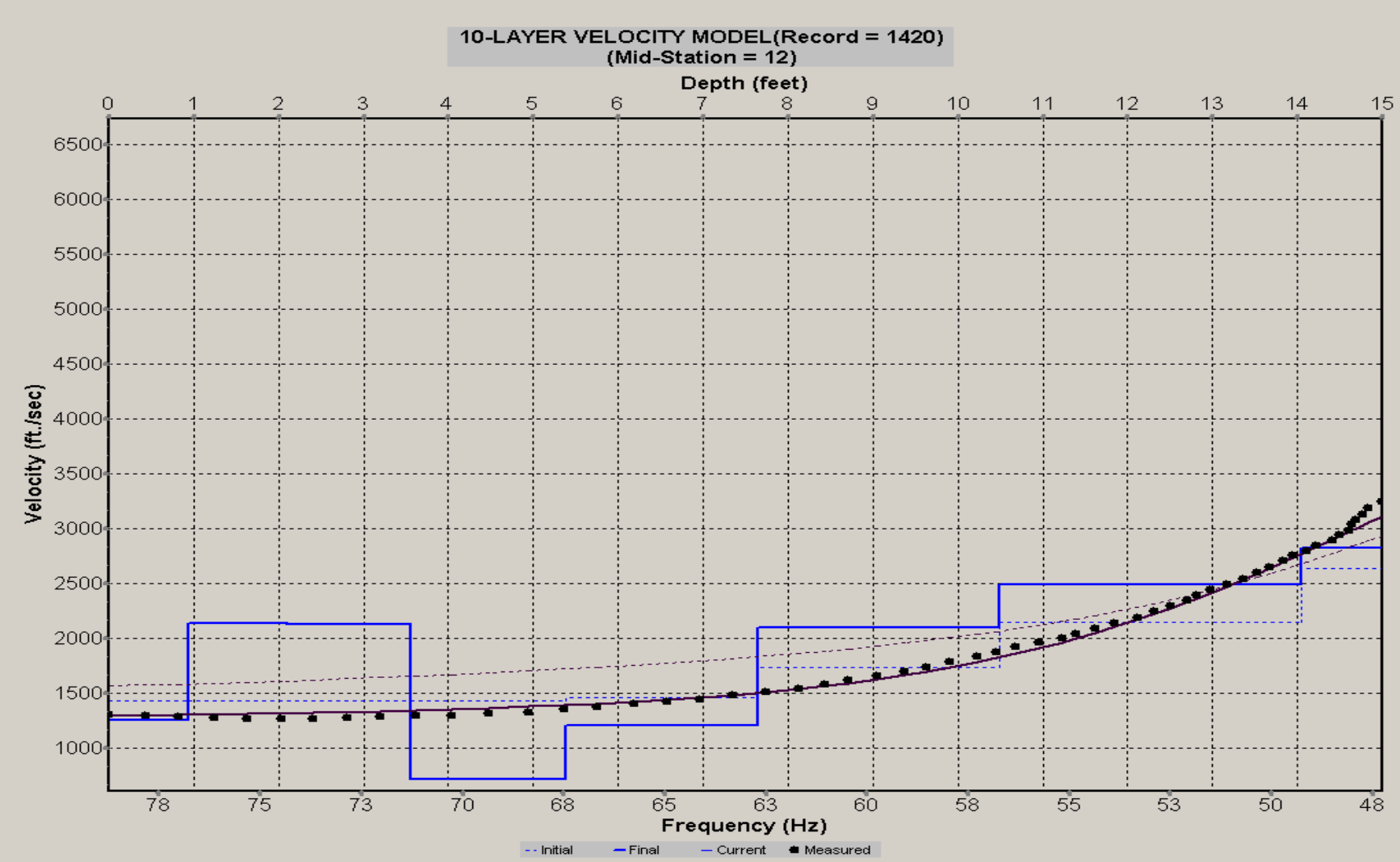

A.699: Velocity Profile Line 1420 used in Pre-blast 41 and Pre-blast 42

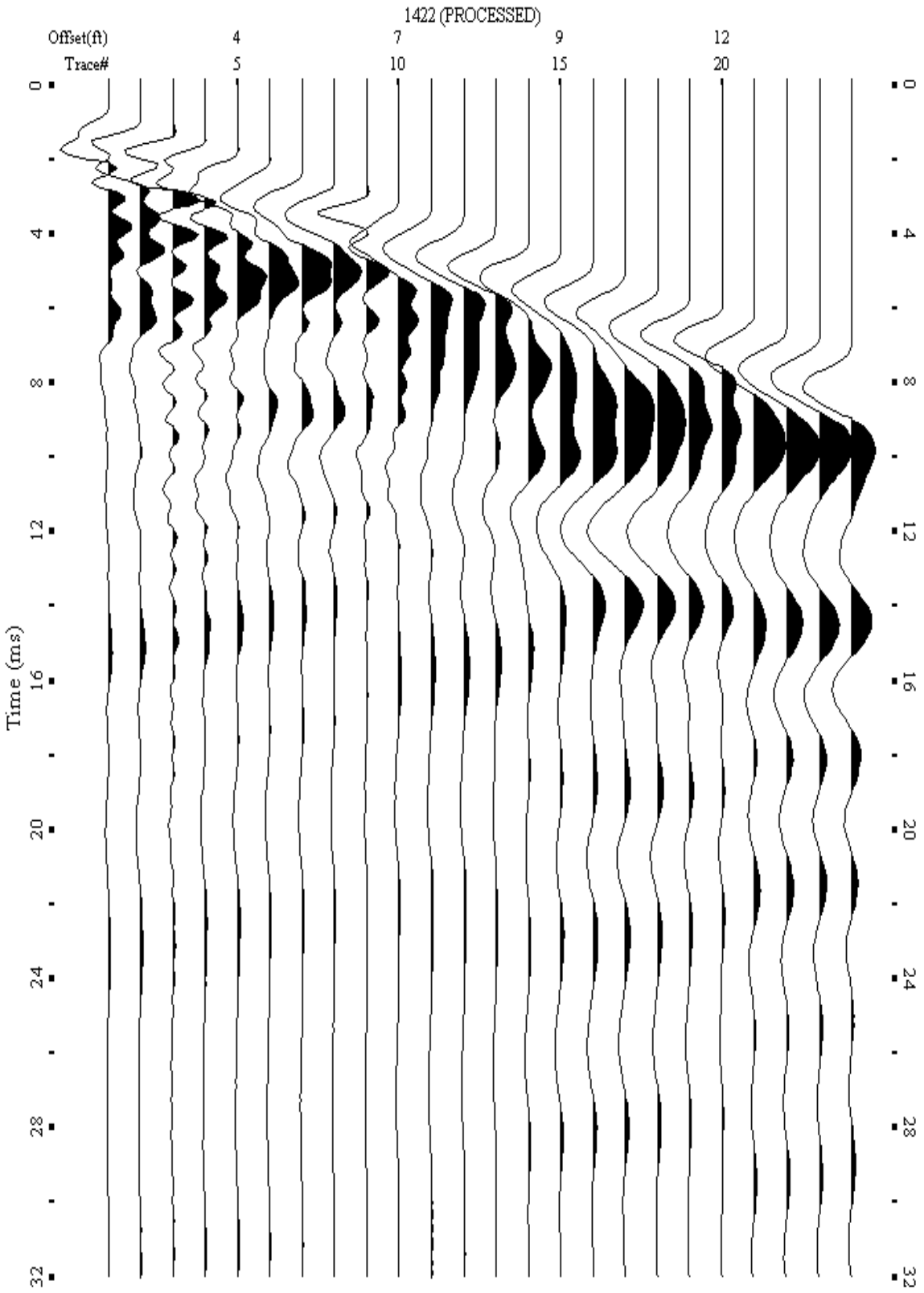

A.700: Shot Gather Line 1422 used in Post-blast 39, Pre-blast 41 and Pre-blast 42

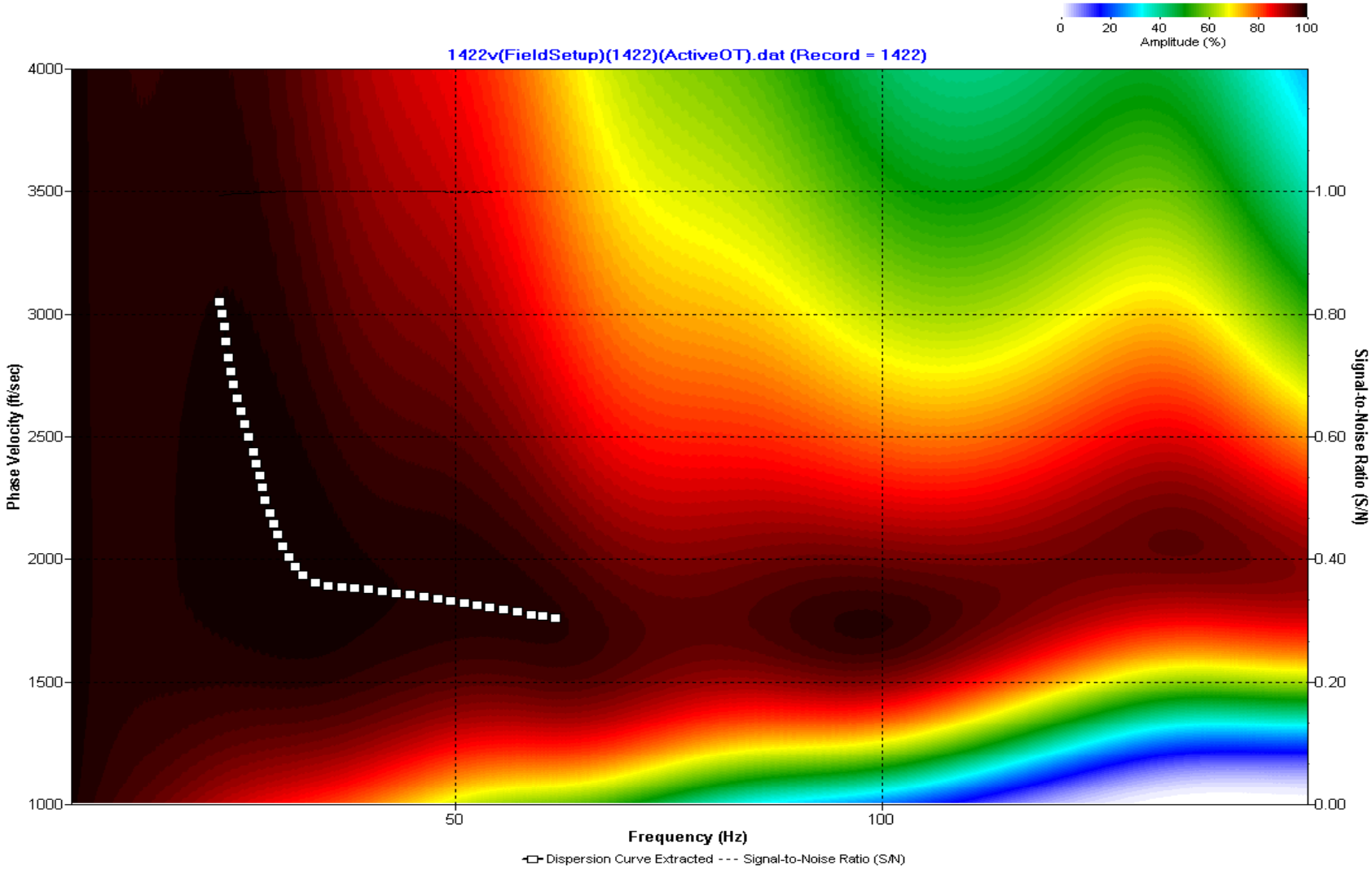

A.701: Dispersion Curve Line 1422 used in Post-blast 39, Pre-blast 41 and Pre-blast 42

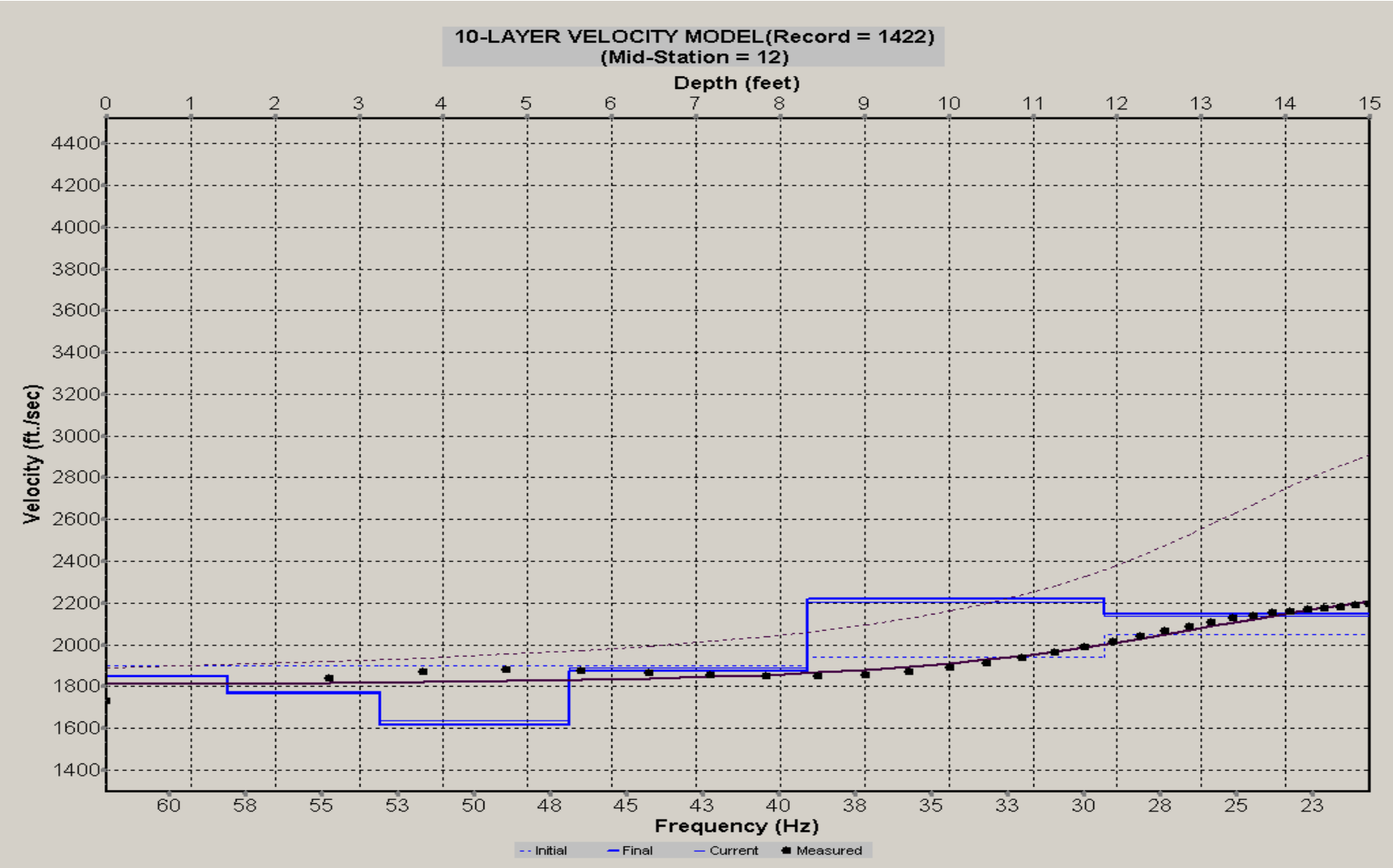

A.702: Velocity Profile Line 1422 used in Post-blast 39, Pre-blast 41 and Pre-blast 42

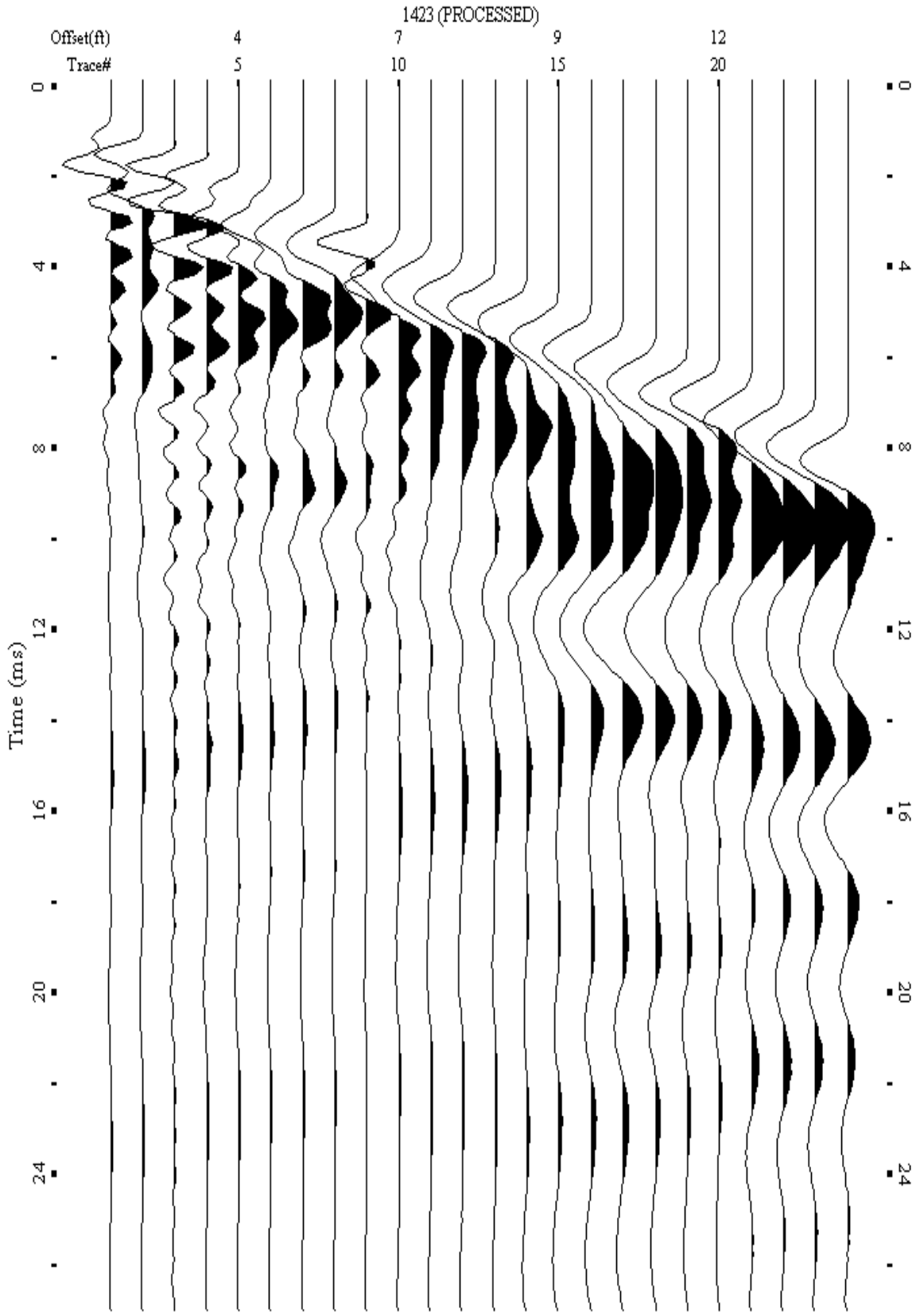

A.703: Shot Gather Line 1423 used in Pre-blast 43

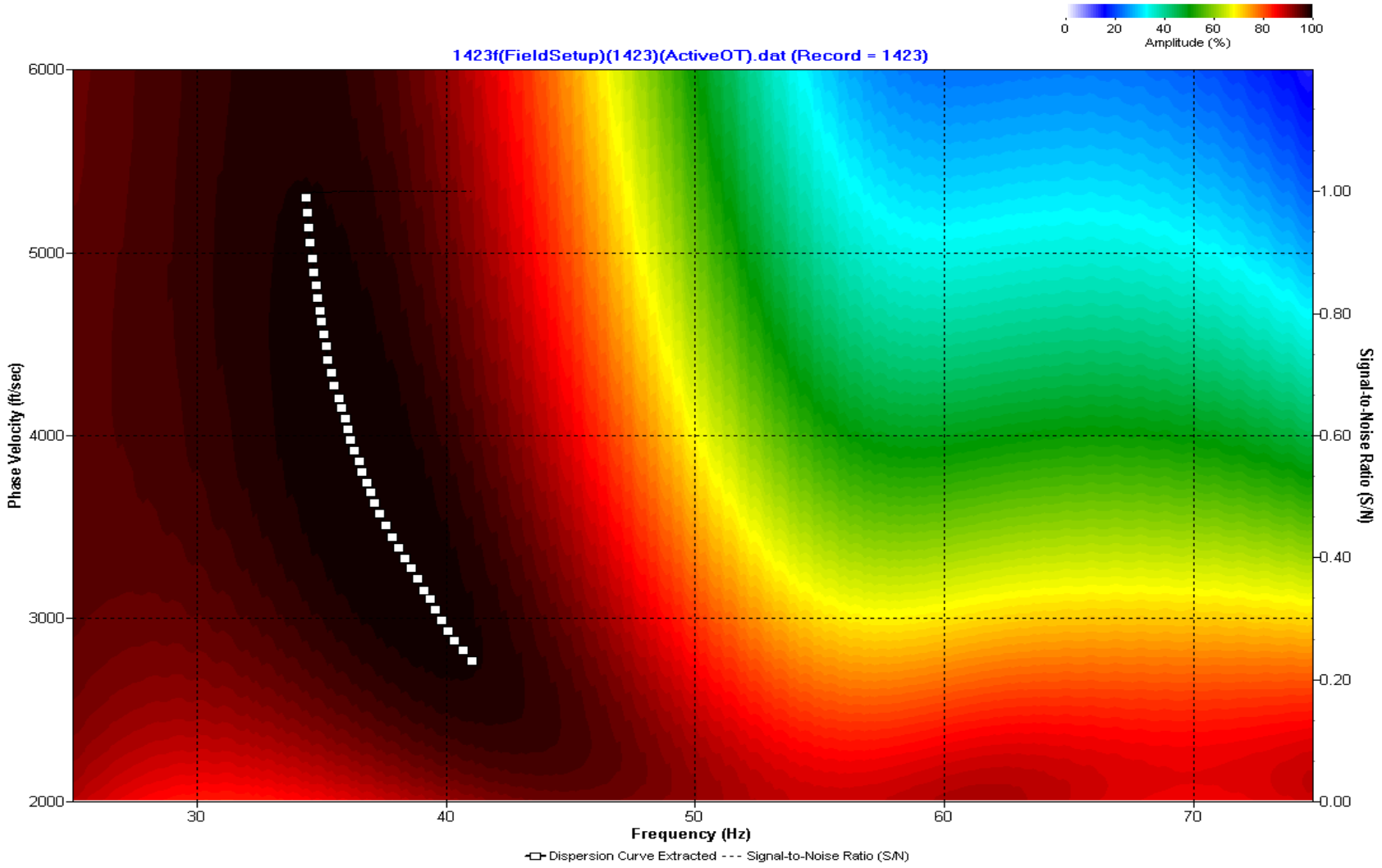

A.704: Dispersion Curve Line 1423 used in Pre-blast 43

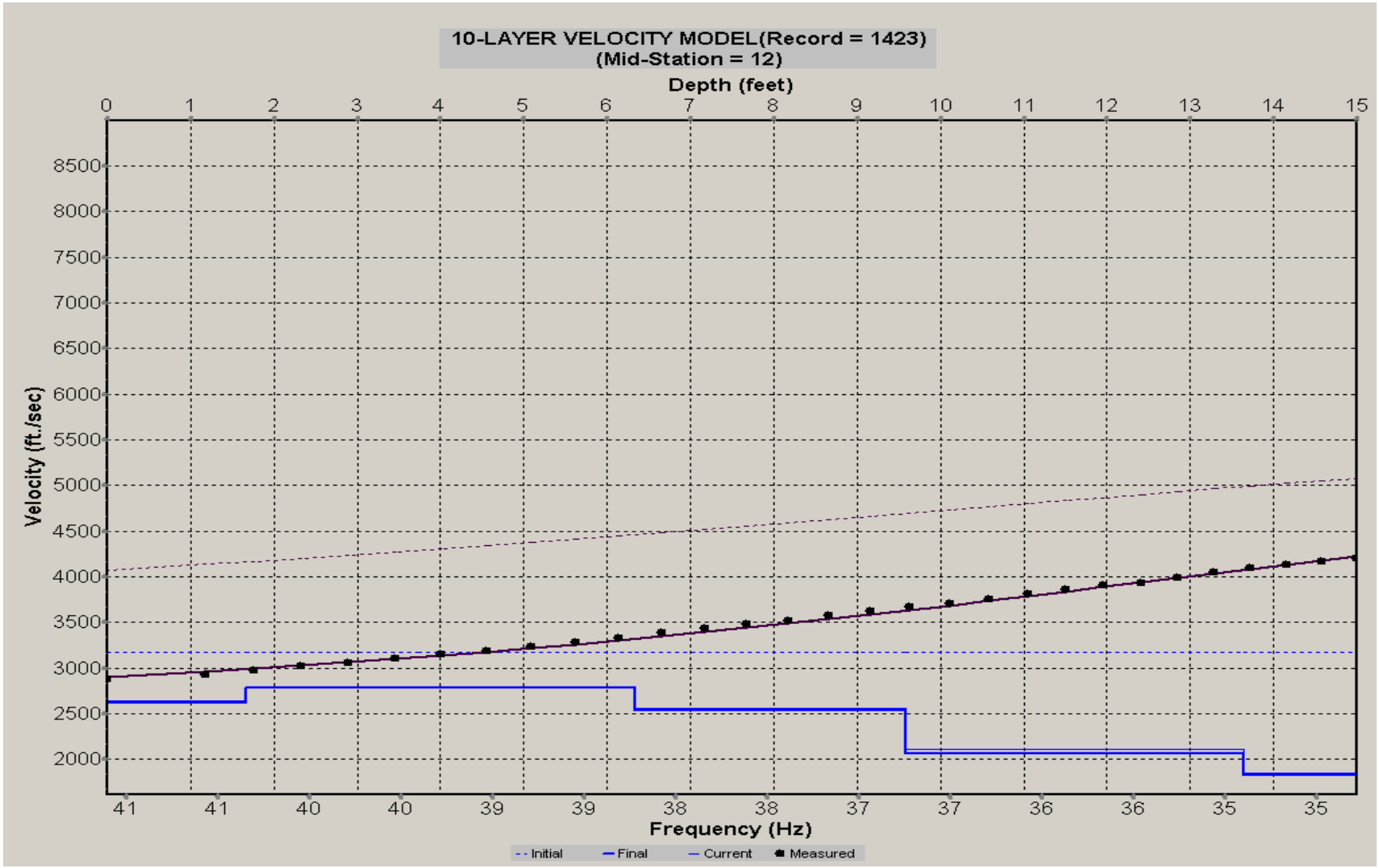

A.705: Velocity Profile Line 1423 used in Pre-blast 43

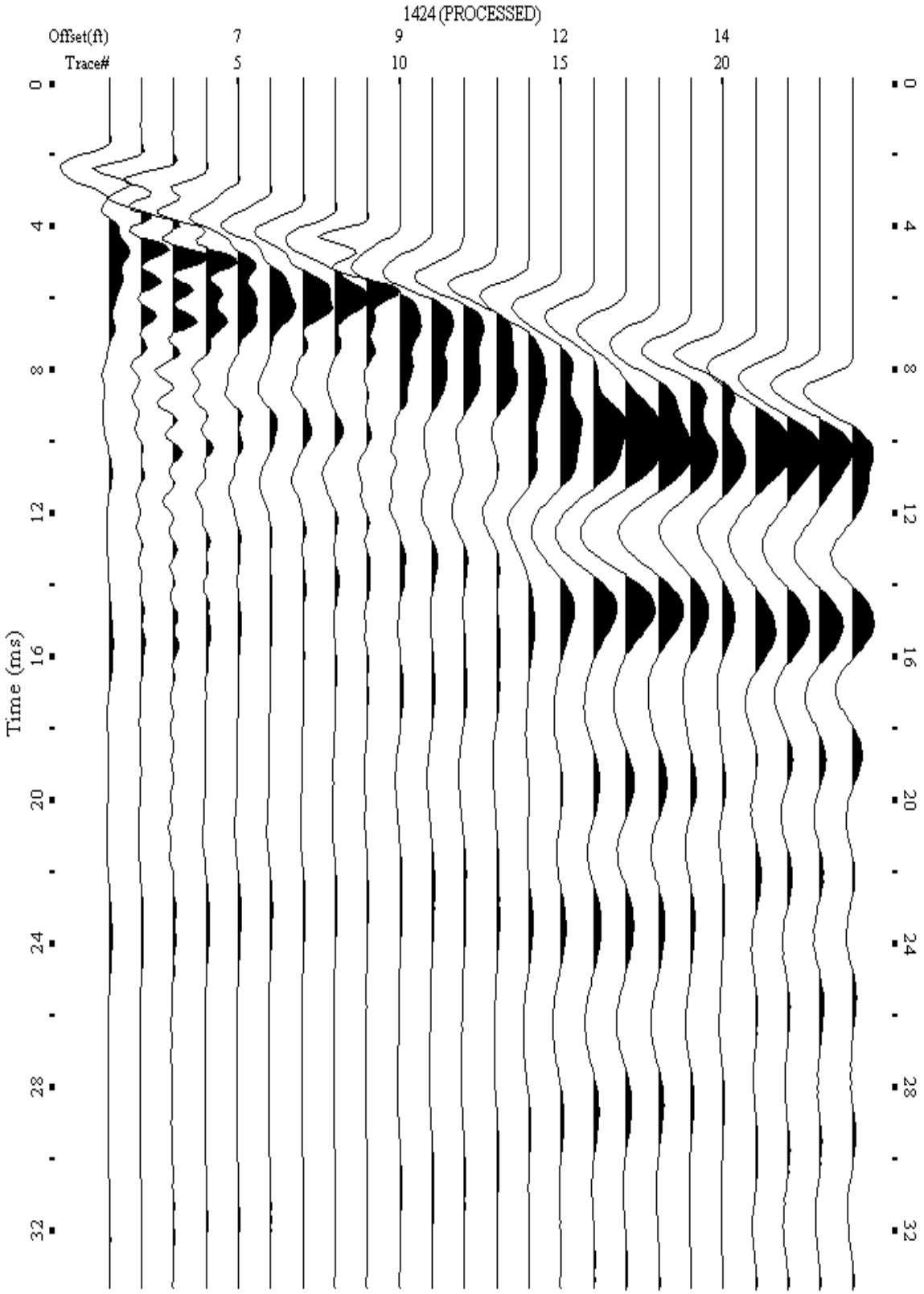

A.706: Shot Gather Line 1424 used in Post-blast 38, Post-blast 39, Pre-blast 41, Pre-blast 42 and Pre-blast 43

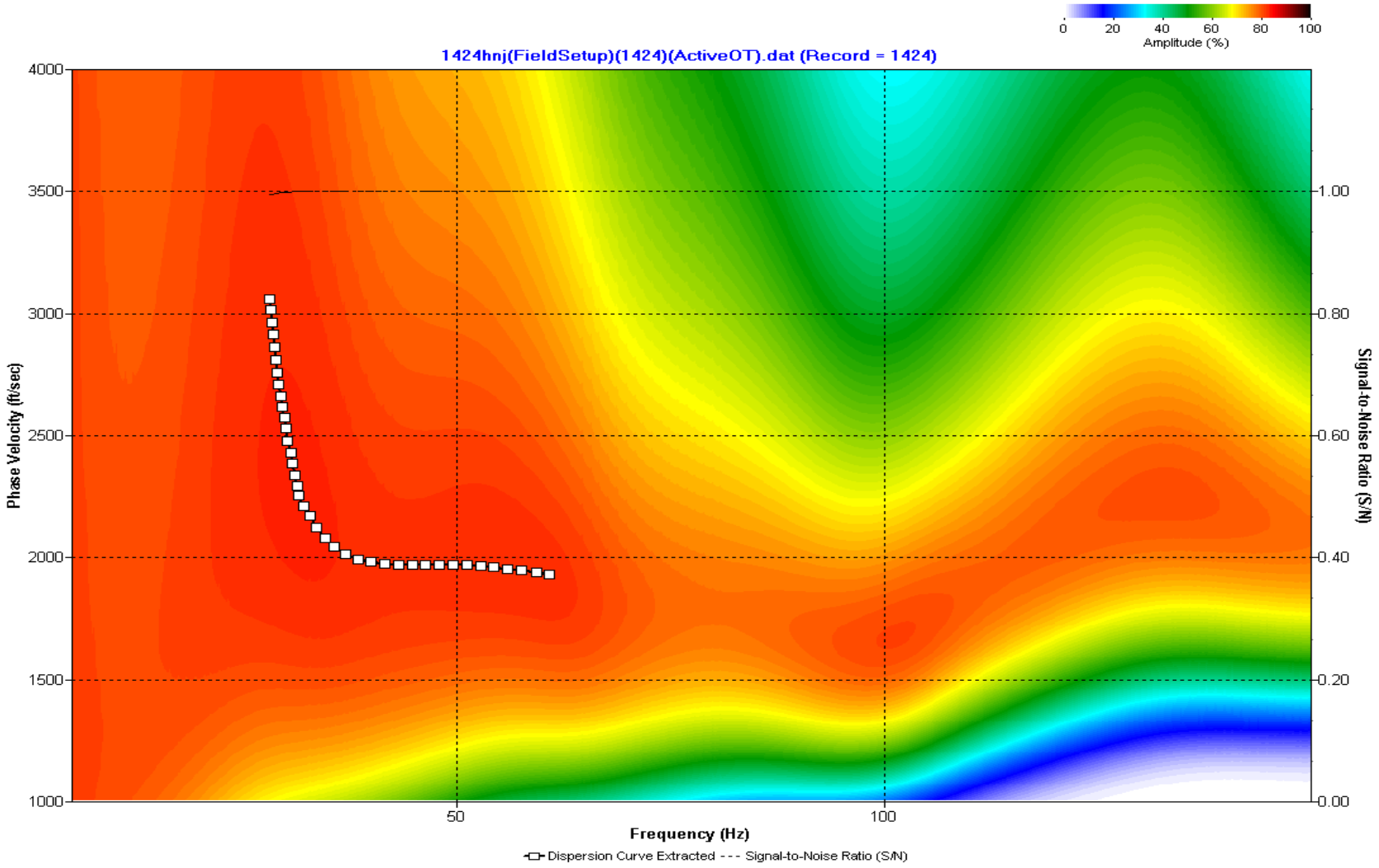

A.707: Dispersion Curve Line 1424 used in Post-blast 38, Post-blast 39, Pre-blast 41, Pre-blast 42 and Pre-blast 43

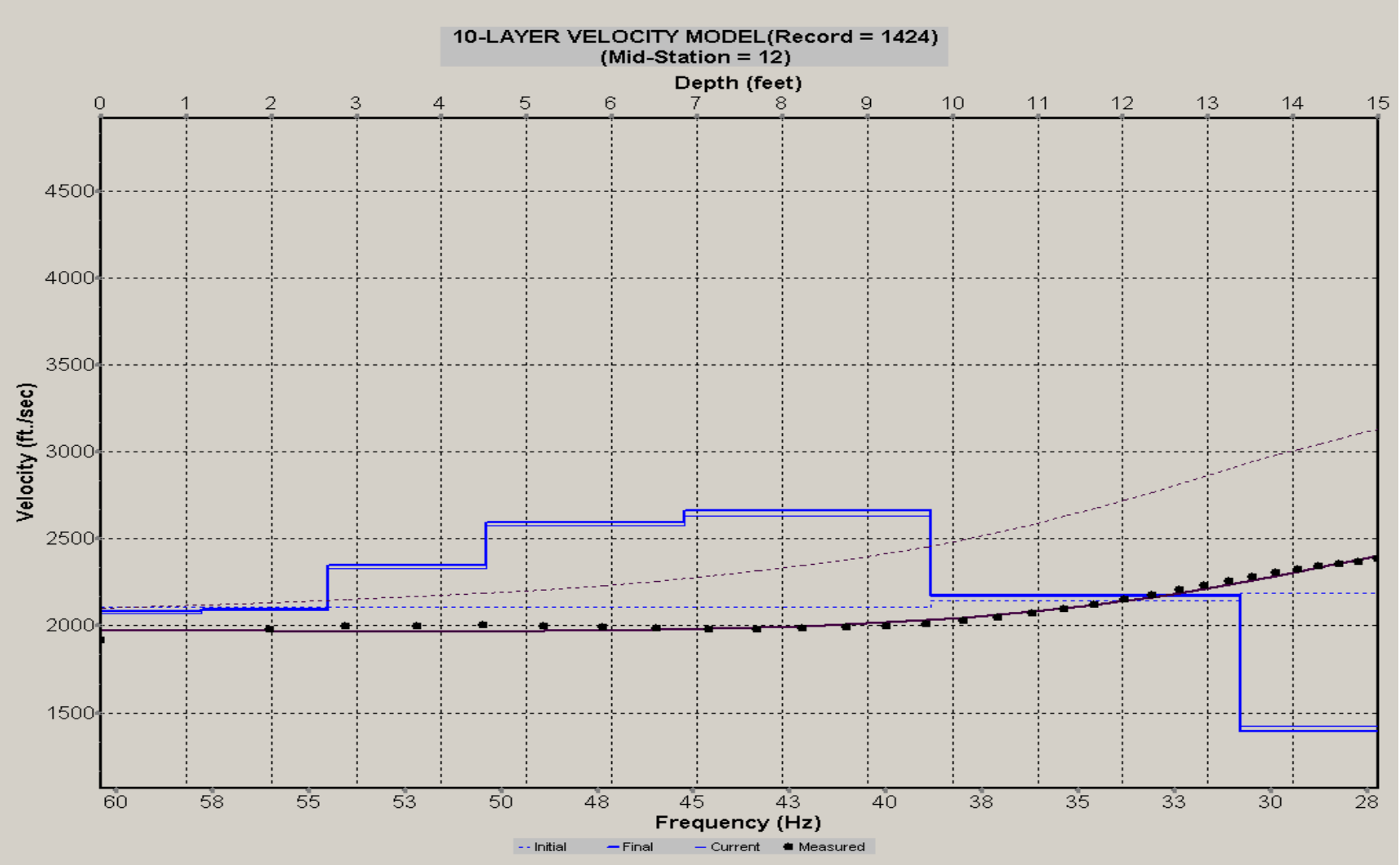

A.708: Velocity Profile Line 1424 used in Post-blast 38, Post-blast 39, Pre-blast 41, Pre-blast 42 and Pre-blast 43

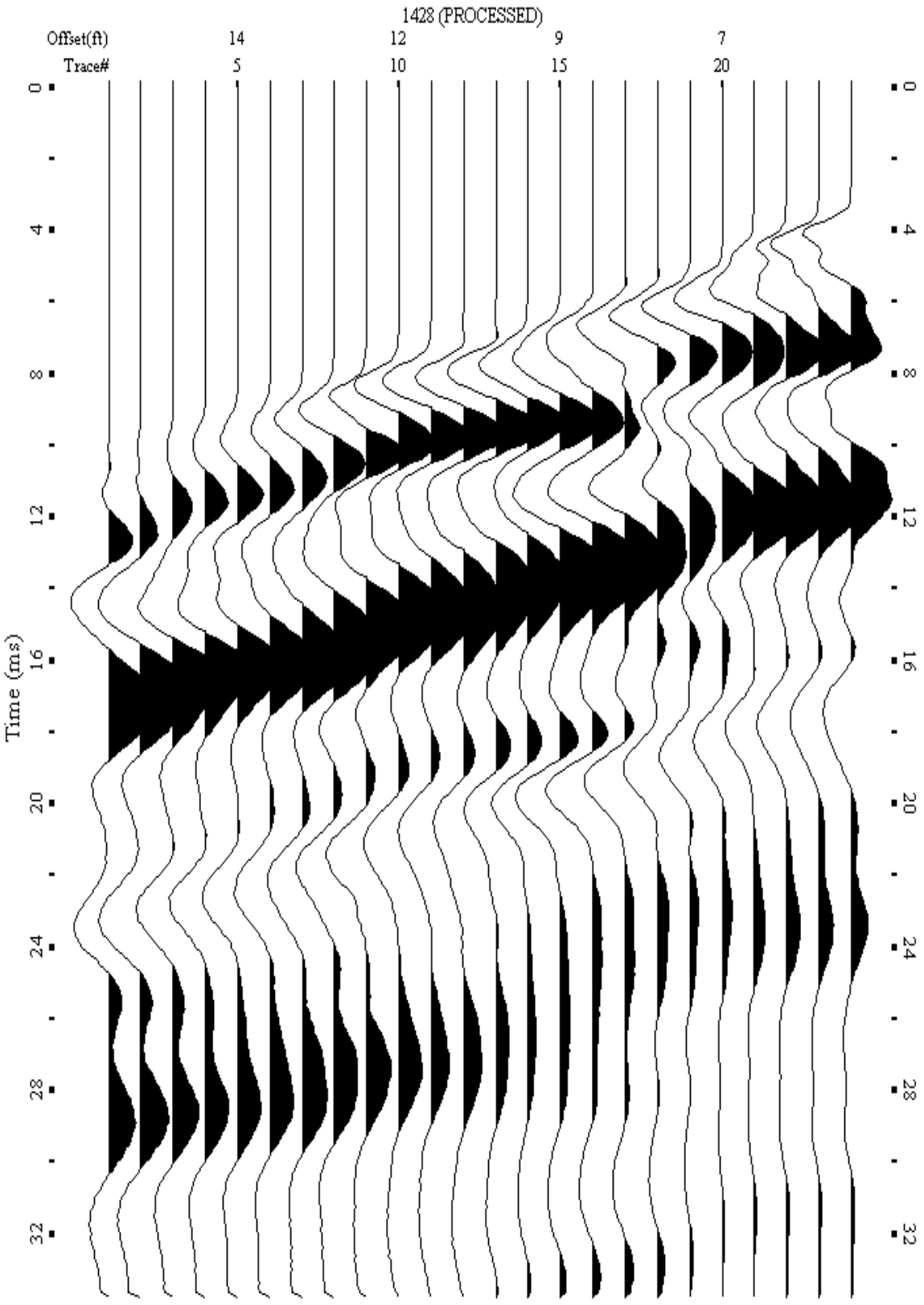

A.709: Shot Gather Line 1428 used in Post-blast 38, Post-blast 39, Pre-blast 41, Pre-blast 42 and Pre-blast 43

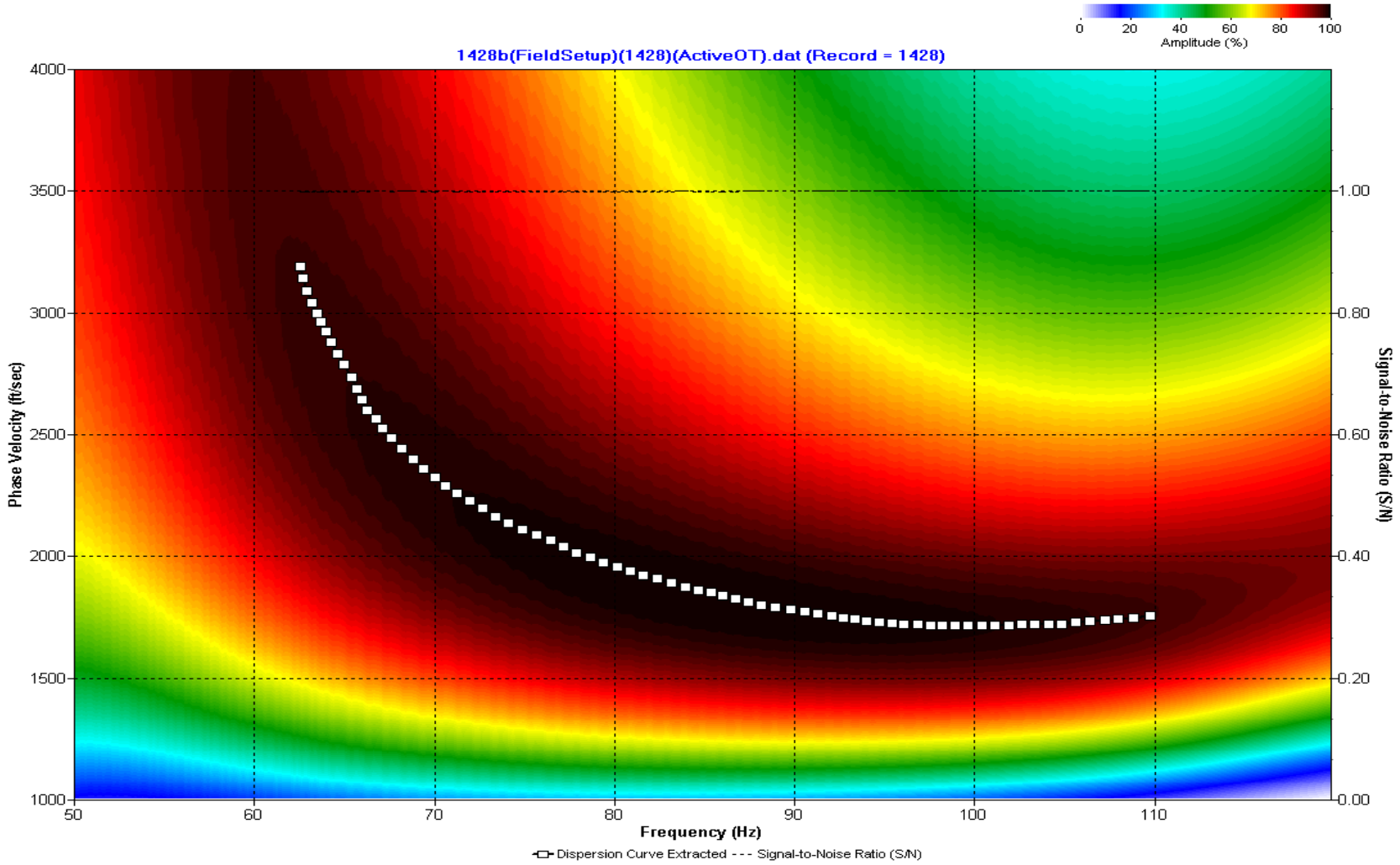

A.710: Dispersion Curve Line 1428 used in Post-blast 38, Post-blast 39, Pre-blast 41, Pre-blast 42 and Pre-blast 43

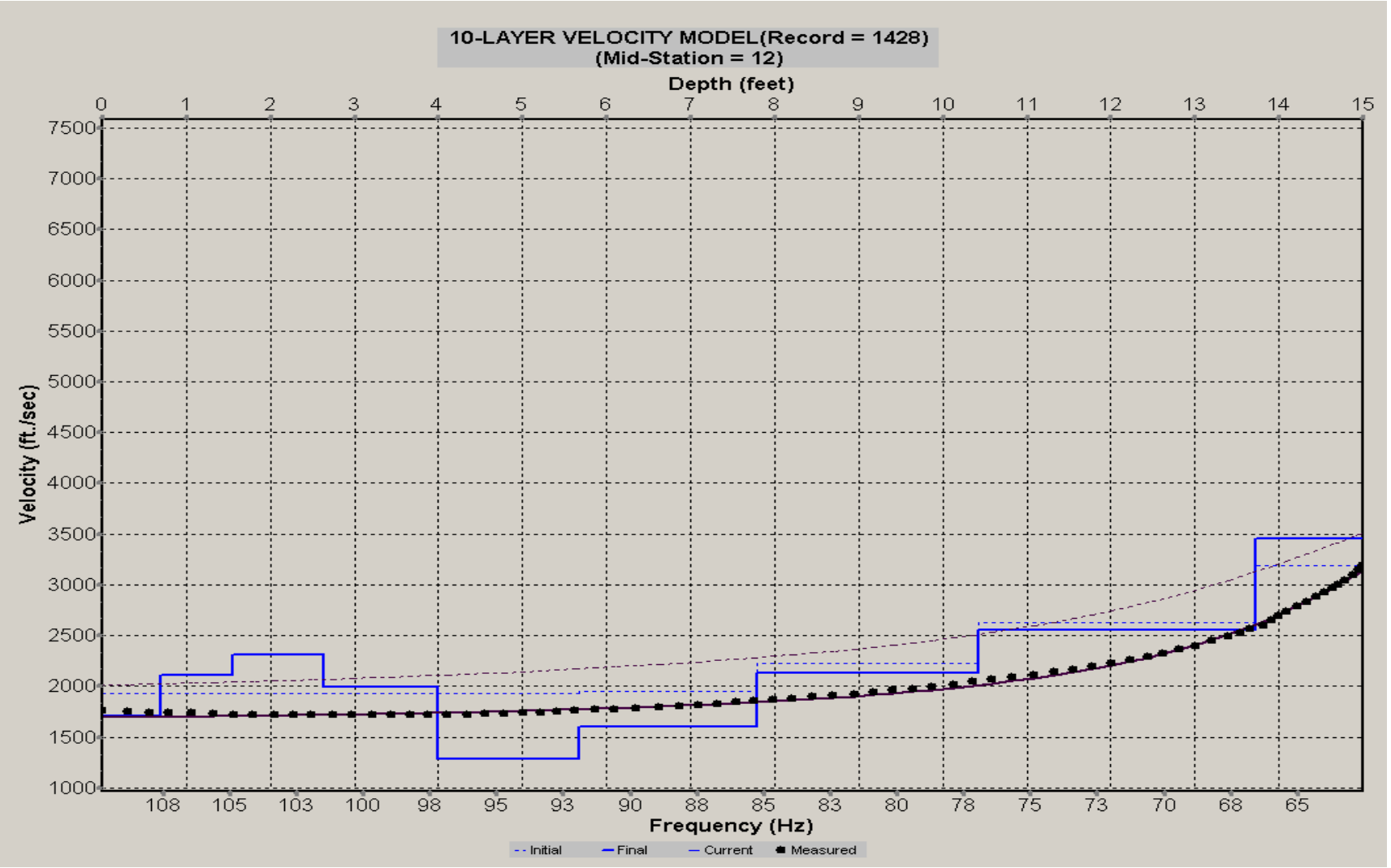

A.711: Velocity Profile Line 1428 used in Post-blast 38, Post-blast 39, Pre-blast 41, Pre-blast 42 and Pre-blast 43

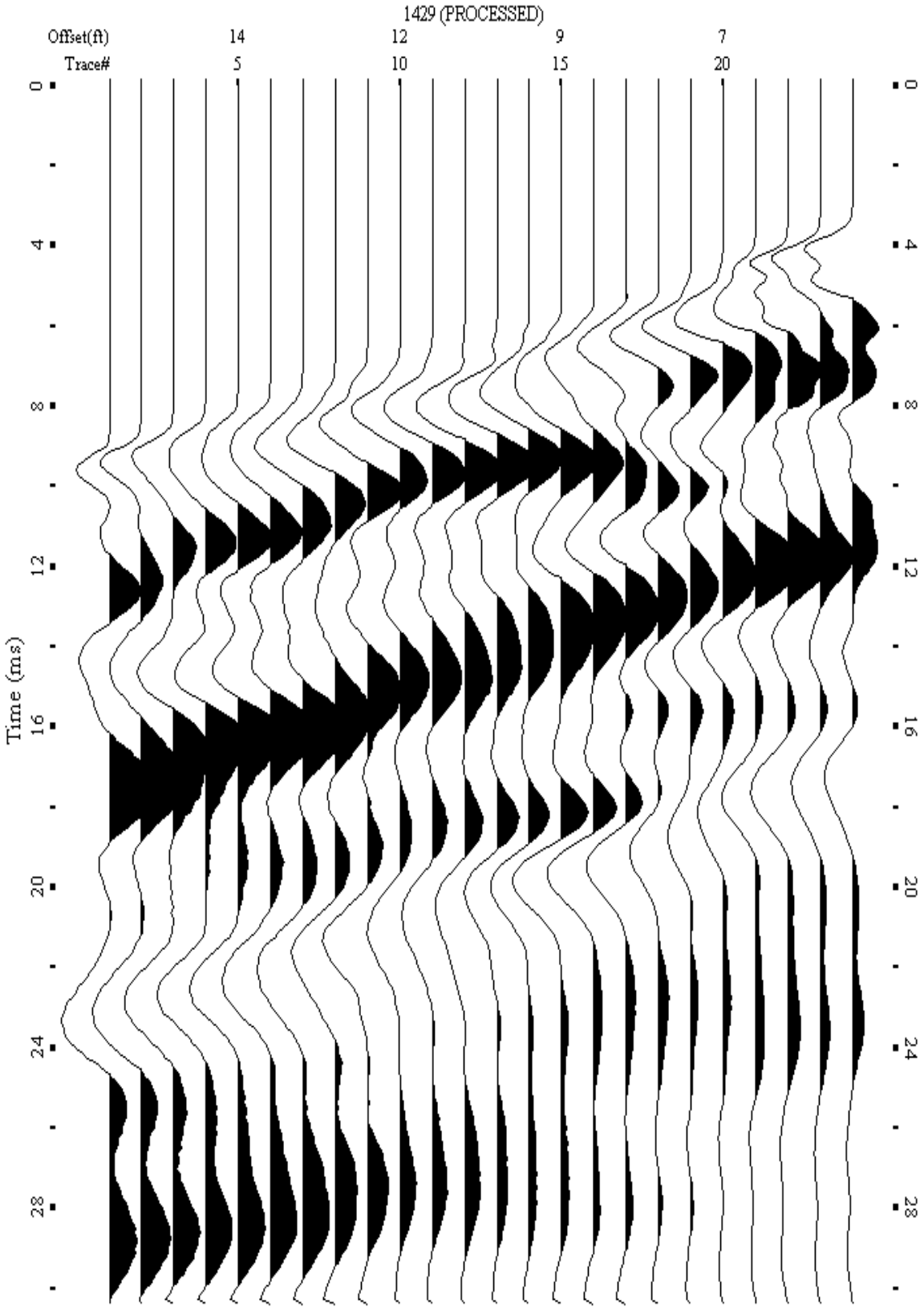

A.712: Shot Gather Line 1429 used in Pre-blast 42 and Pre-blast 43

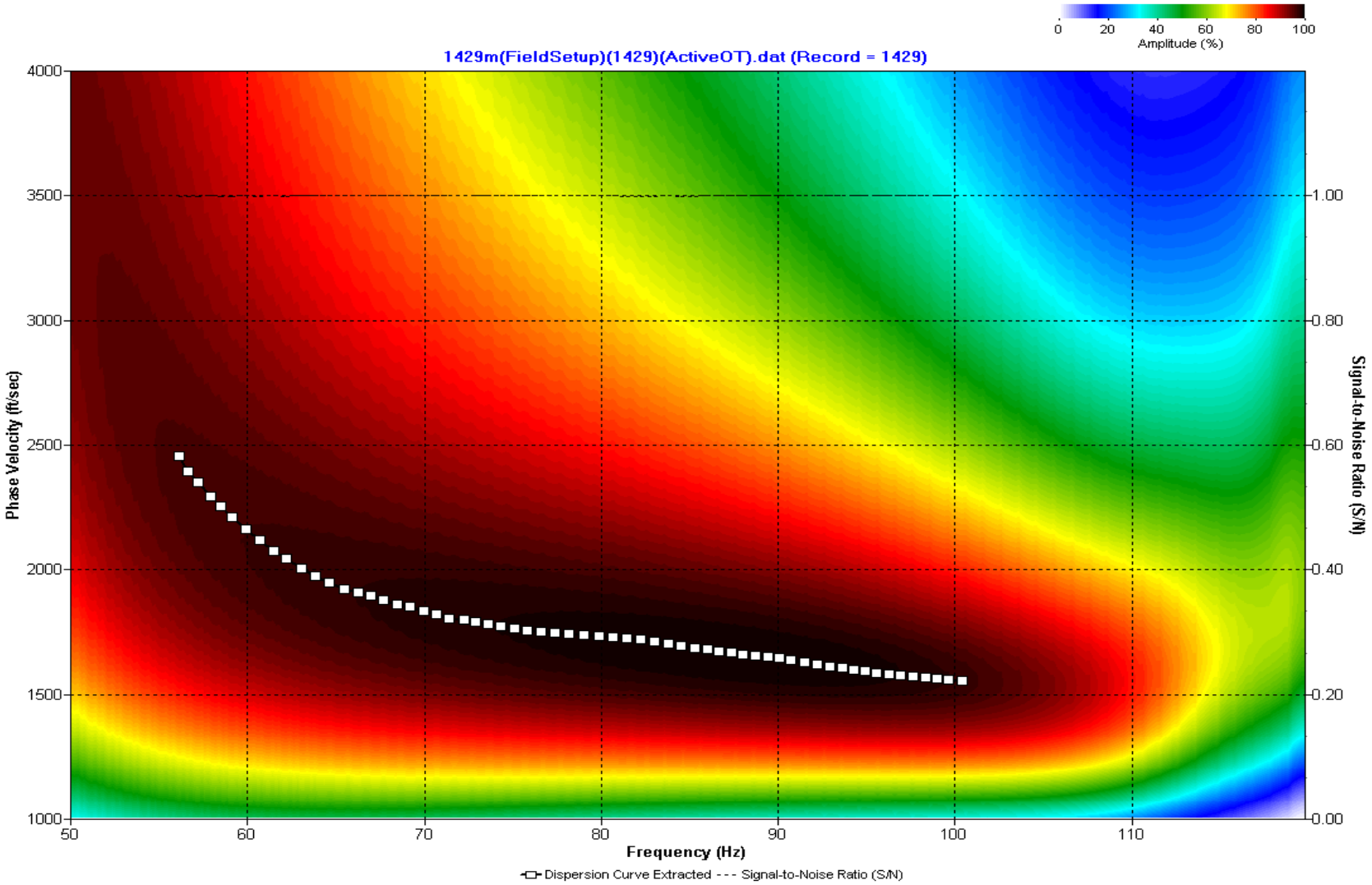

A.713: Dispersion Curve Line 1429 used in Pre-blast 42 and Pre-blast 43

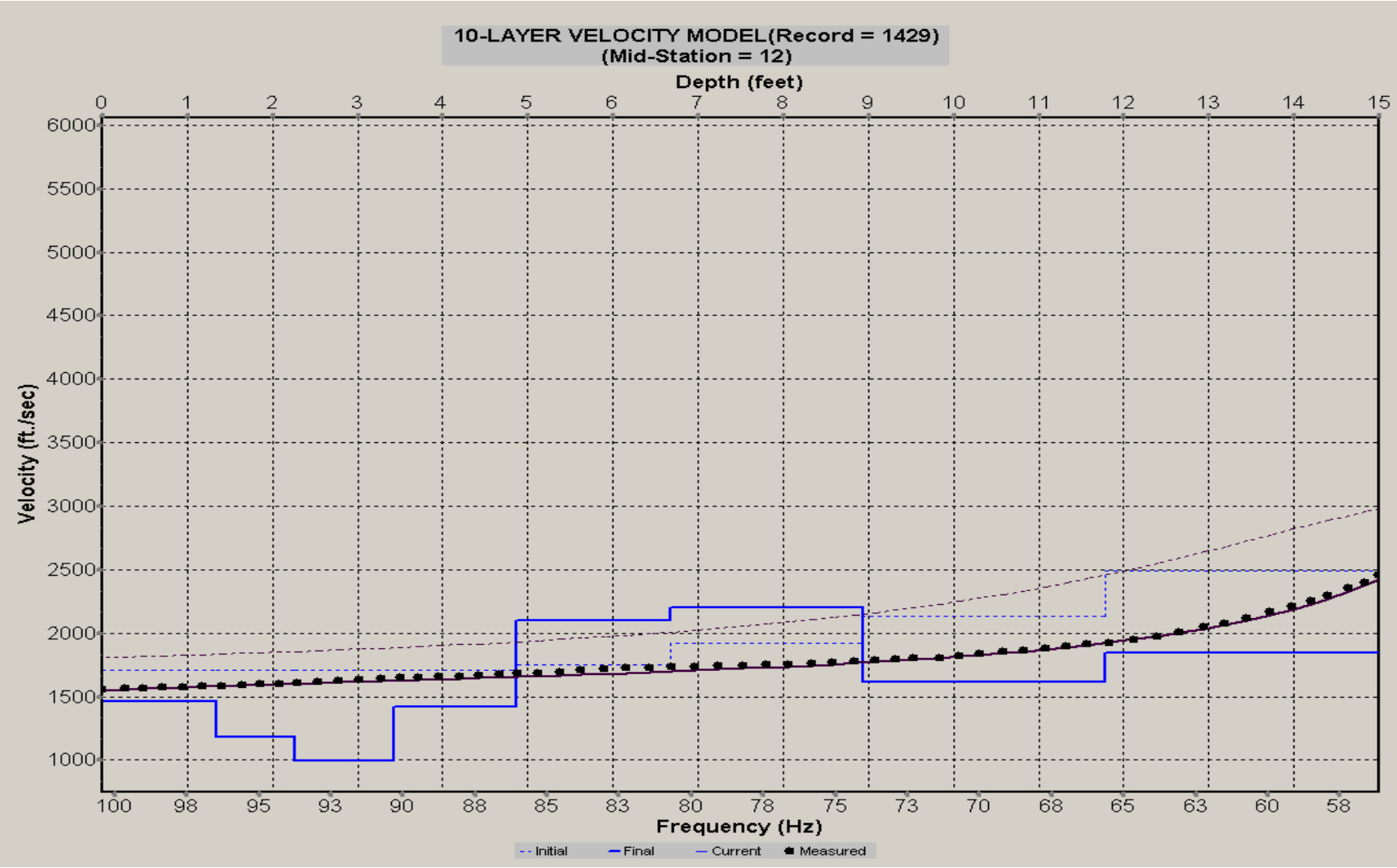

A.714: Velocity Profile Line 1429 used in Pre-blast 42 and Pre-blast 43

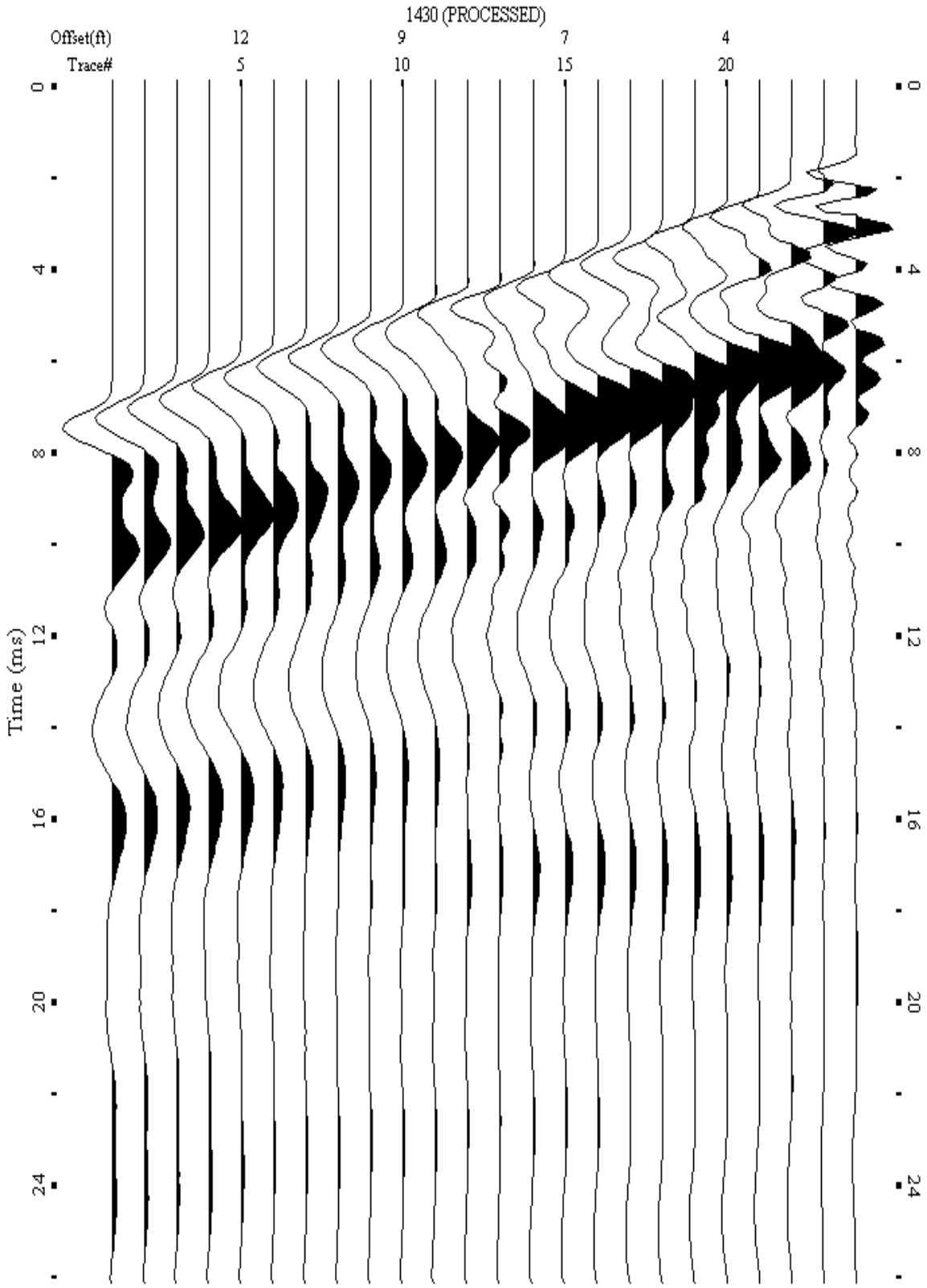

A.715: Shot Gather Line 1430 used in Post-blast 39, Post-blast 40, Pre-blast 43 and Pre-blast 44

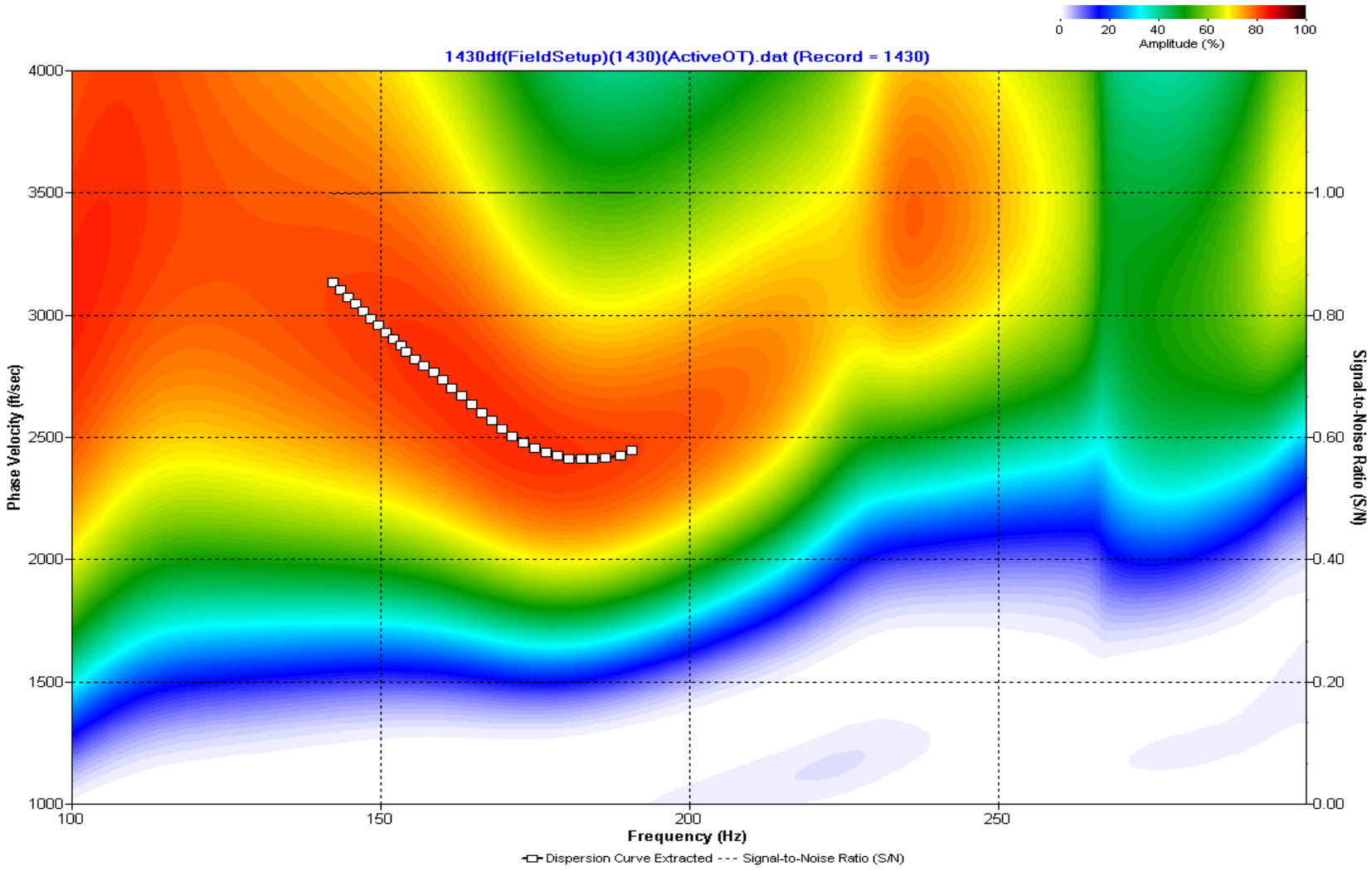

A.716: Dispersion Curve Line 1430 used in Post-blast 39, Post-blast 40, Pre-blast 43 and Pre-blast 44

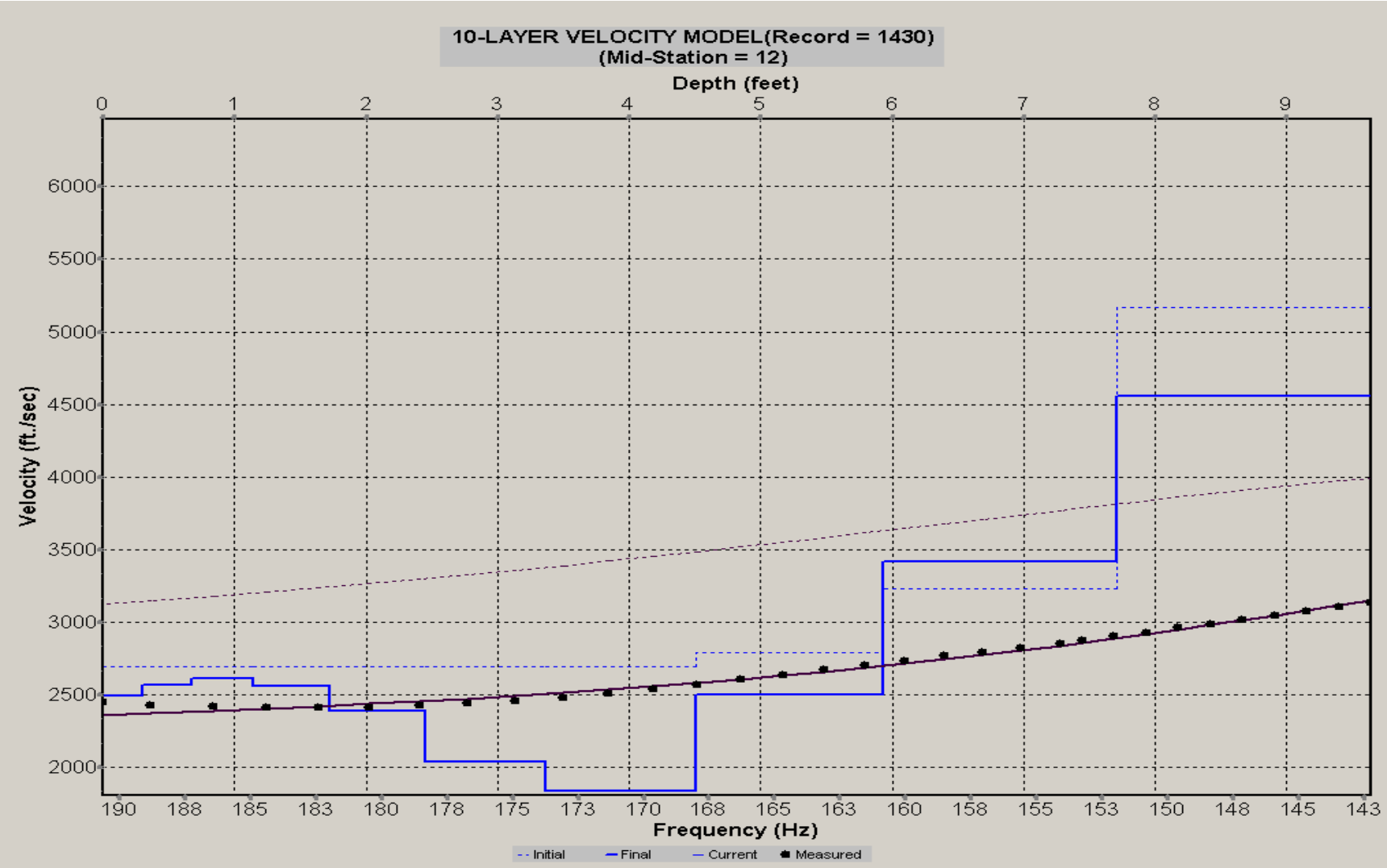

A.717: Velocity Profile Line 1430 used in Post-blast 39, Post-blast 40, Pre-blast 43 and Pre-blast 44

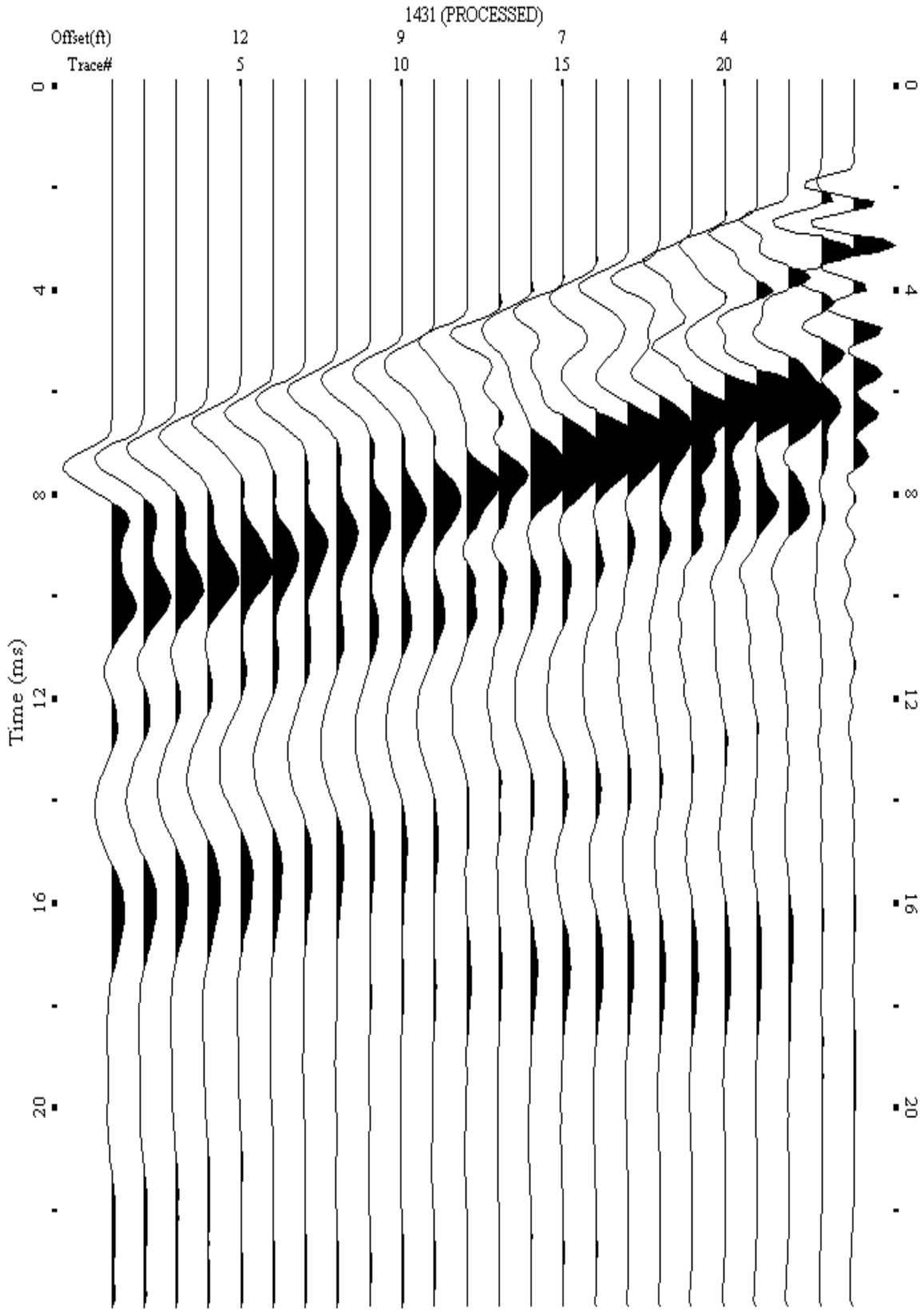

A.718: Shot Gather Line 1431 used in Post-blast 40 and Pre-blast 44

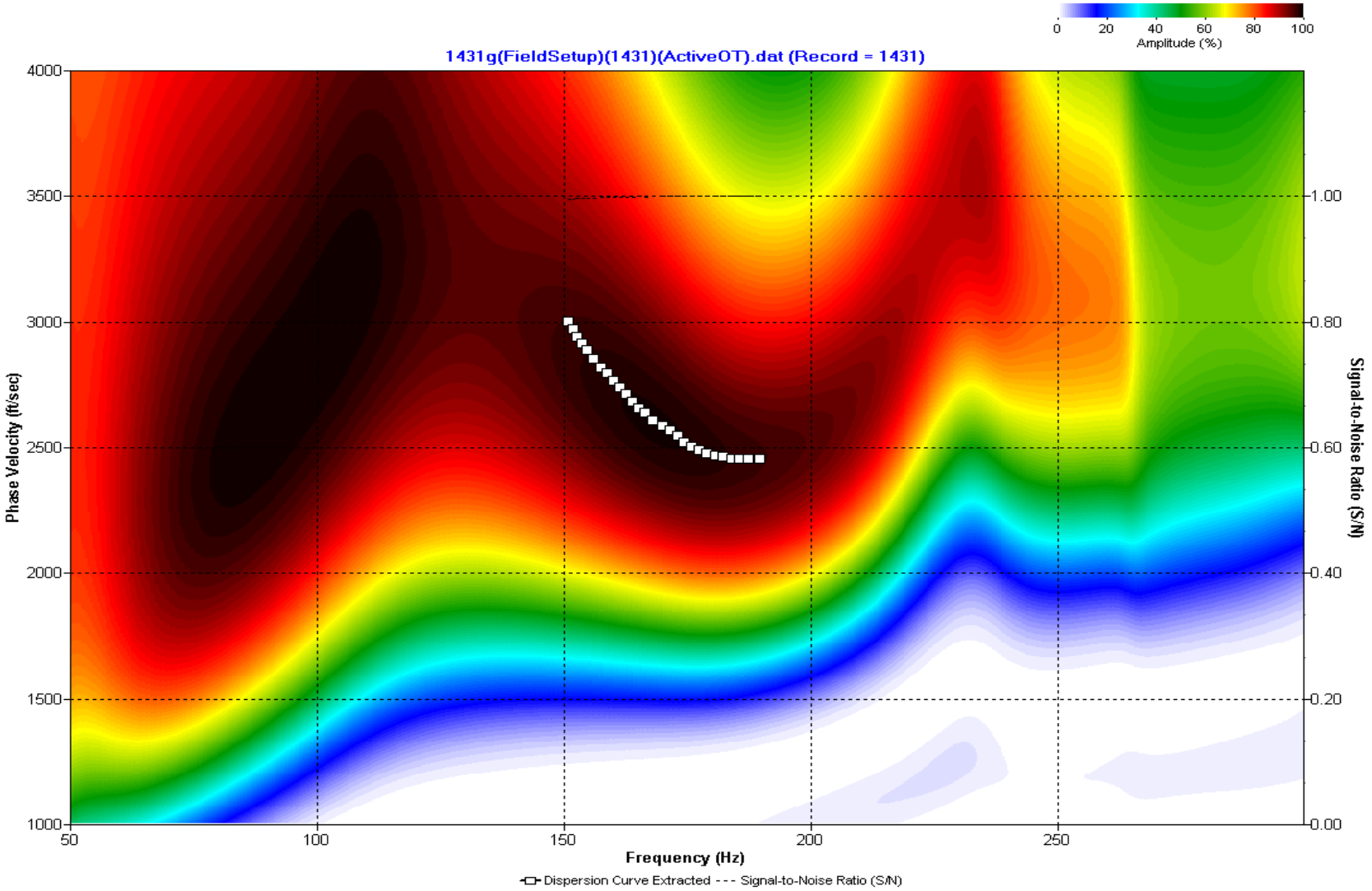

A.719: Dispersion Curve Line 1431 used in Post-blast 40 and Pre-blast 44

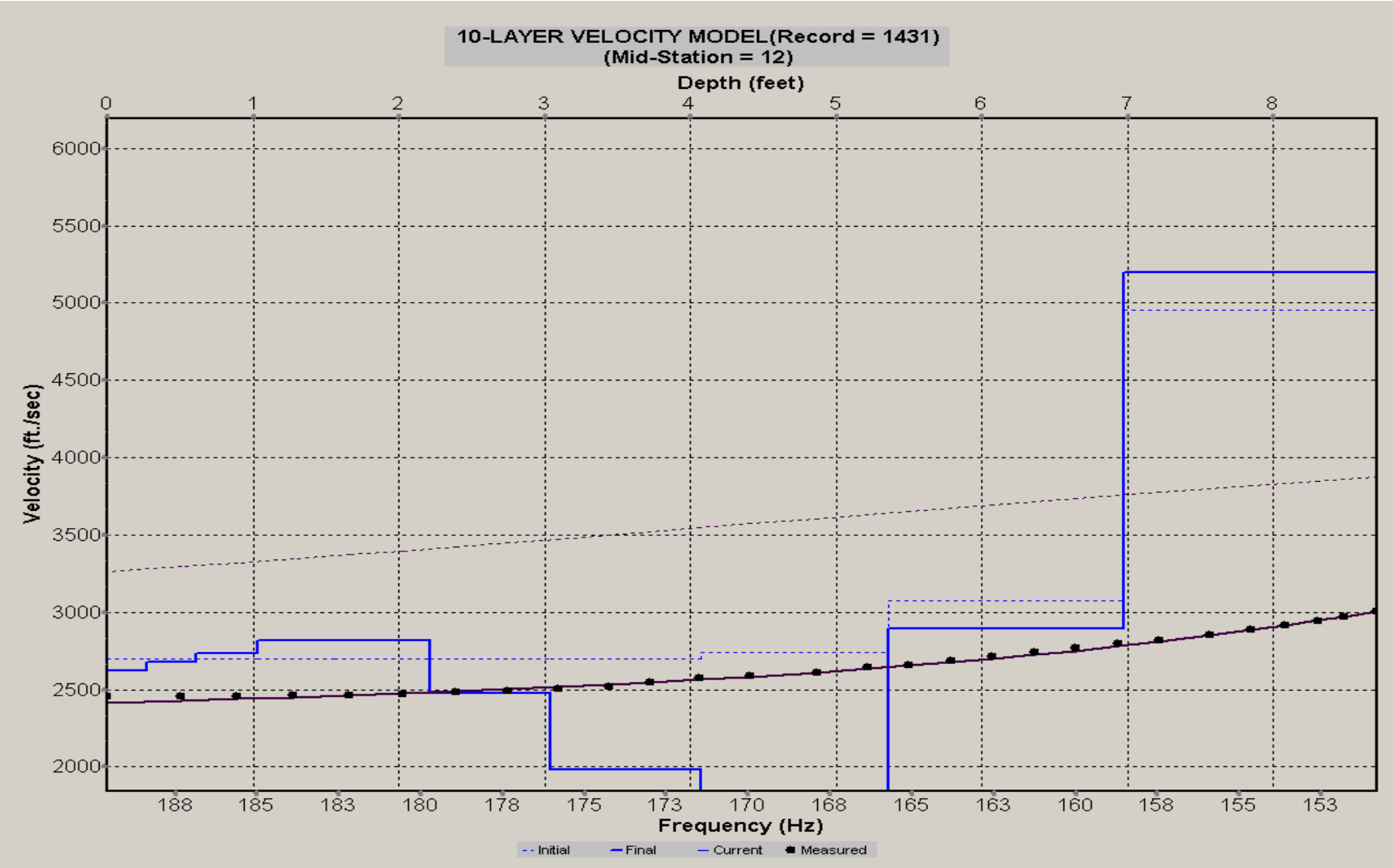

A.720: Velocity Profile Line 1431 used in Post-blast 40 and Pre-blast 44

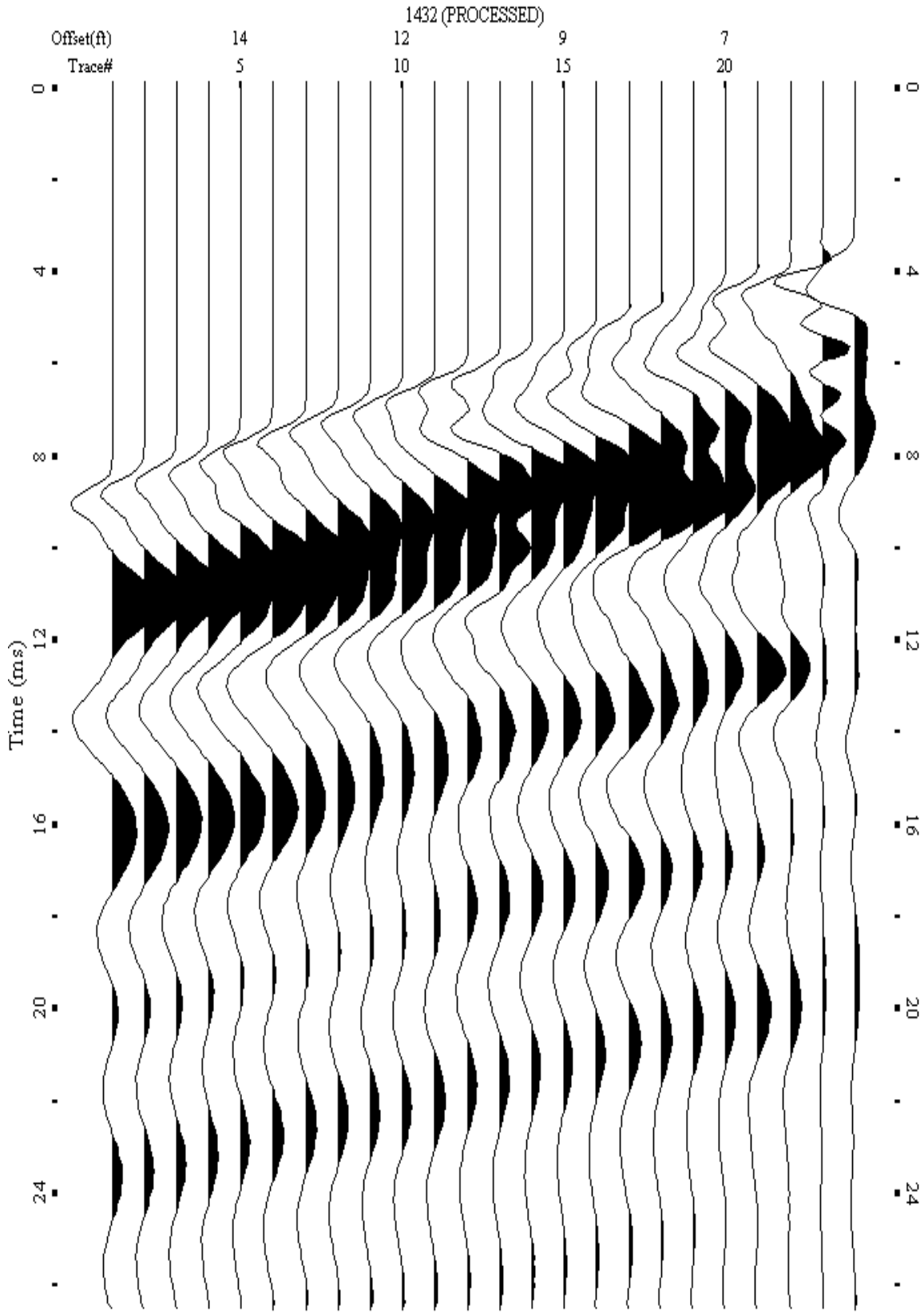

A.721: Shot Gather Line 1432 used in Post-blast 40 and Pre-blast 44

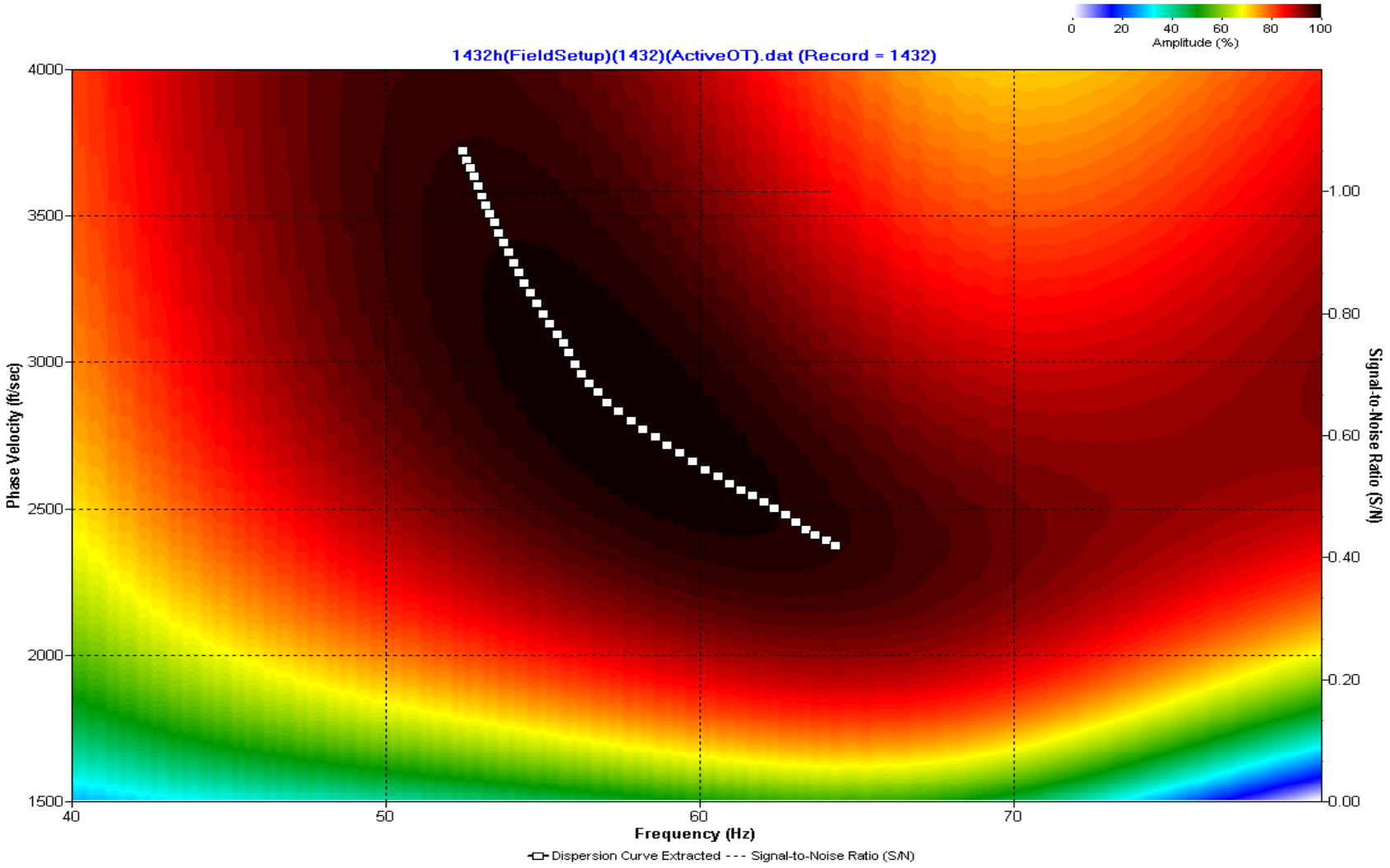

A.722: Dispersion Curve Line 1432 used in Post-blast 40 and Pre-blast 44

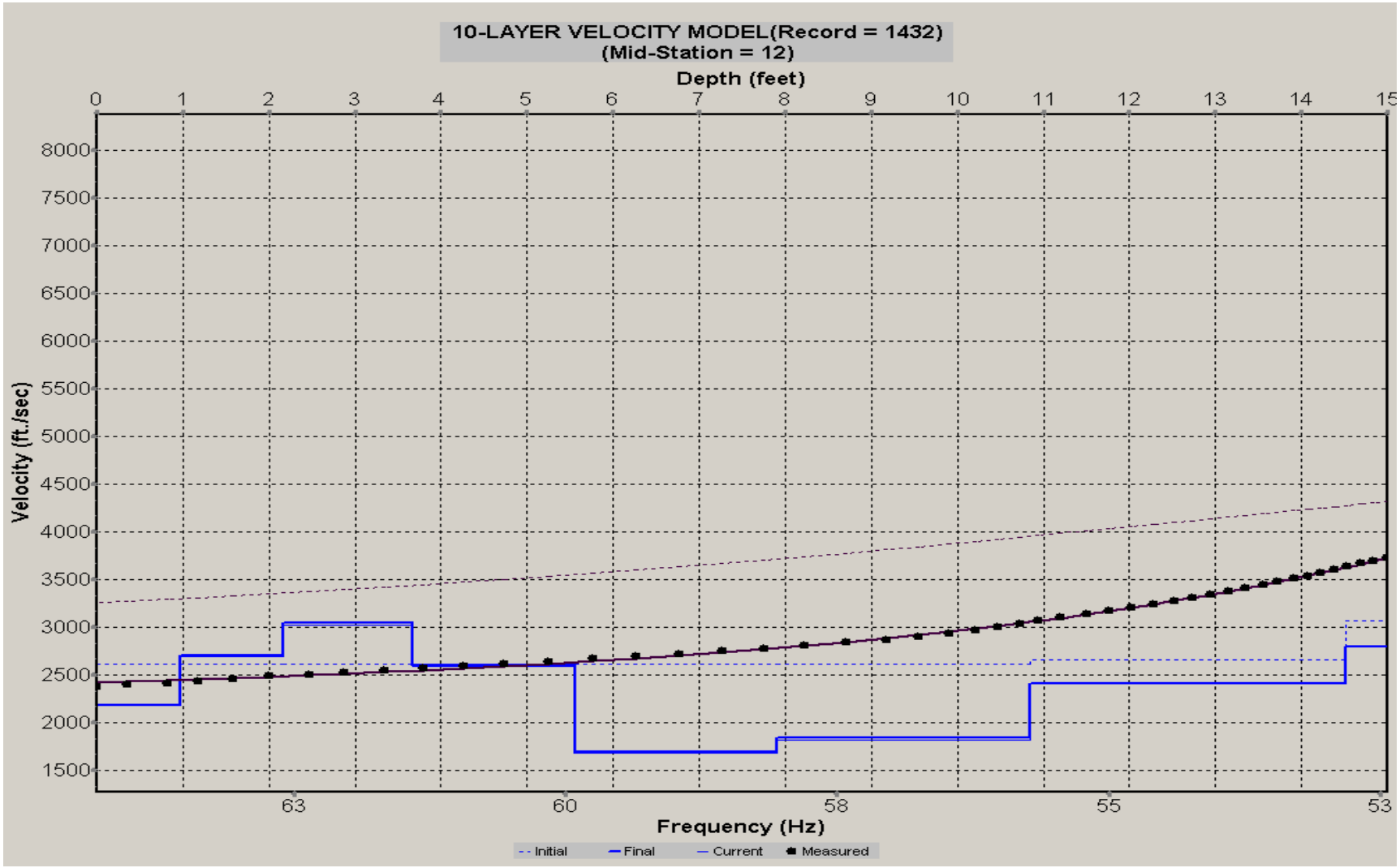

A.723: Velocity Profile Line 1432 used in Post-blast 40 and Pre-blast 44

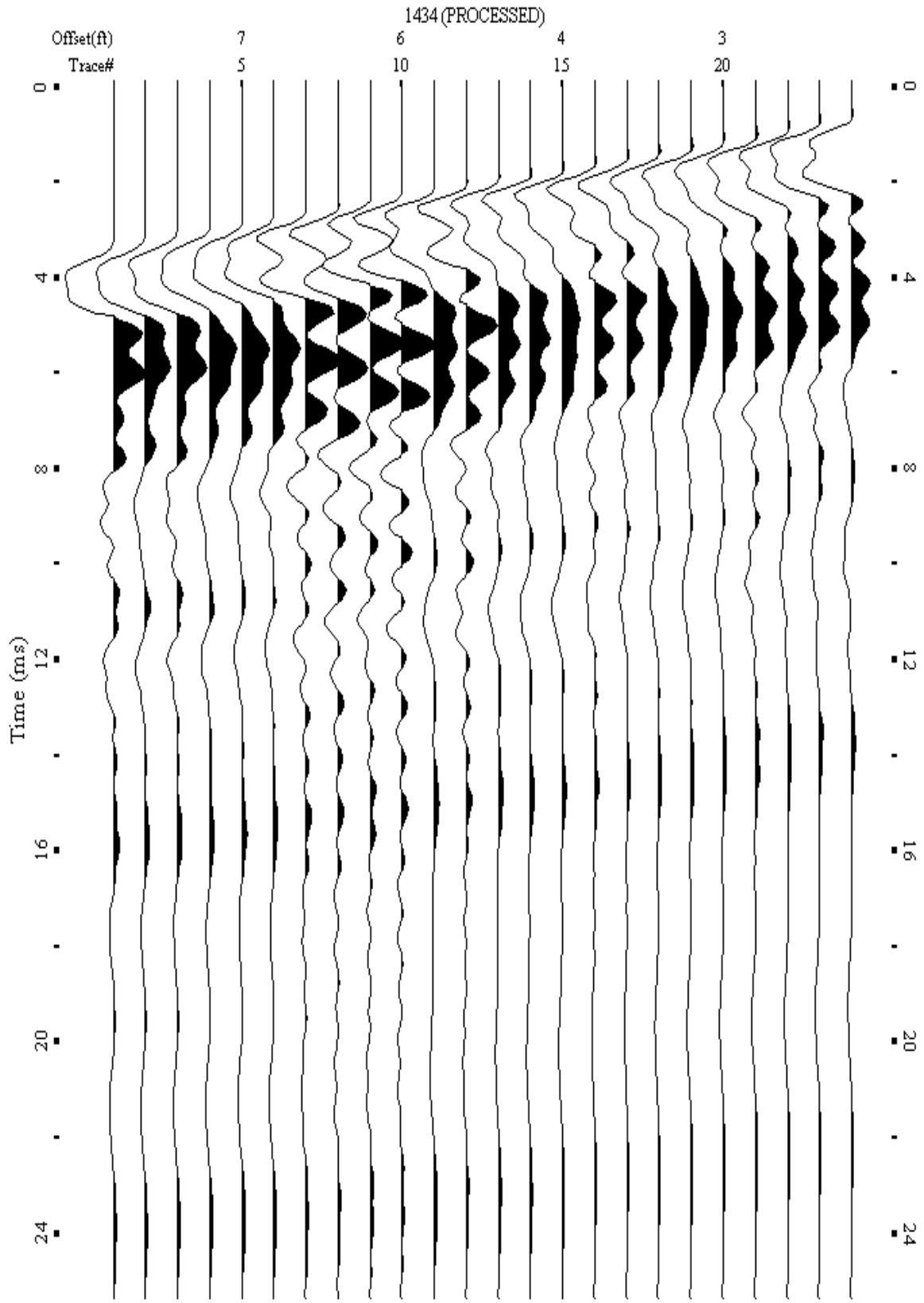

A.724: Shot Gather Line 1434 used in Post-blast 40 and Pre-blast 44

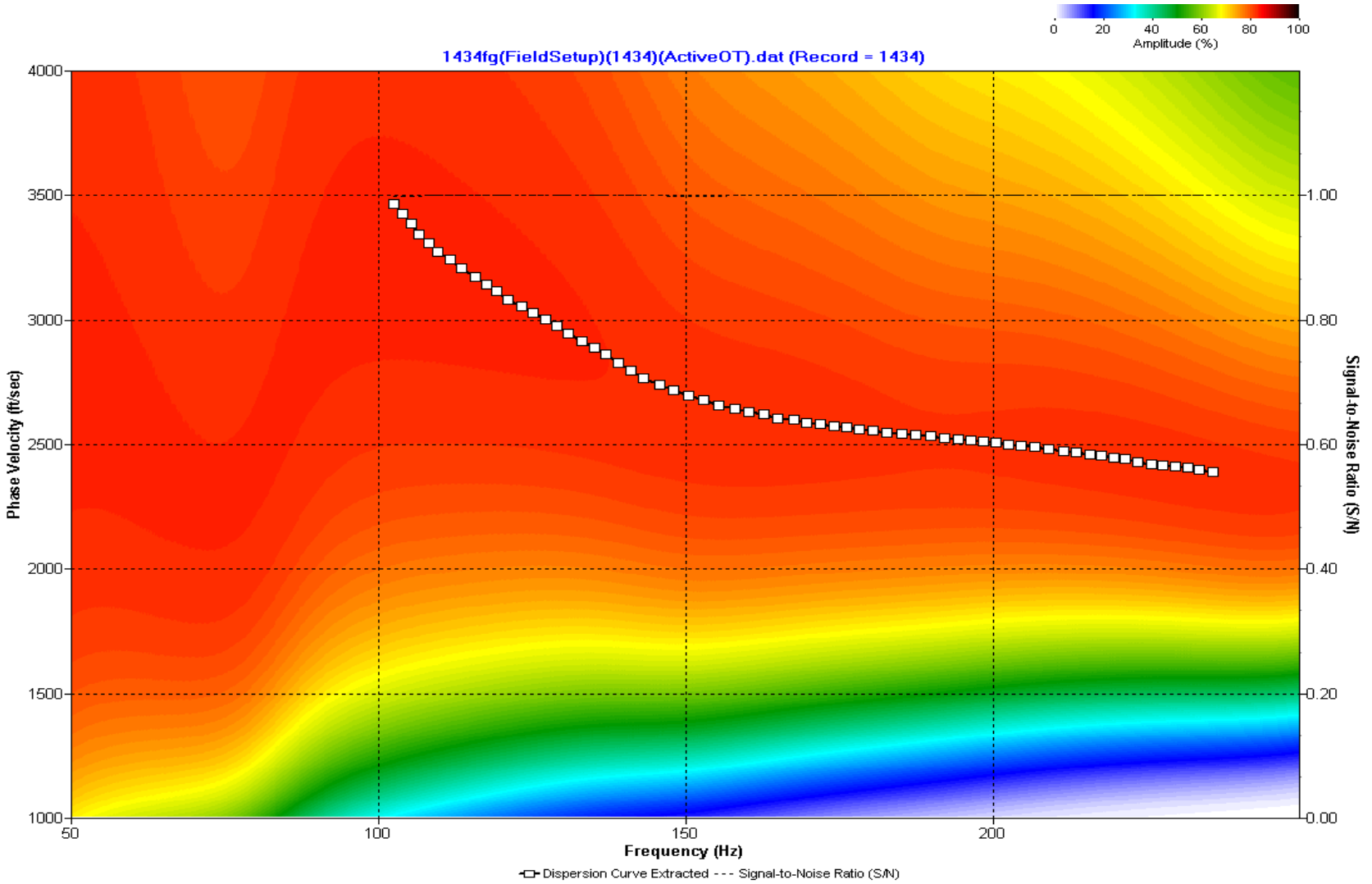

A.725: Dispersion Curve Line 1434 used in Post-blast 40 and Pre-blast 44

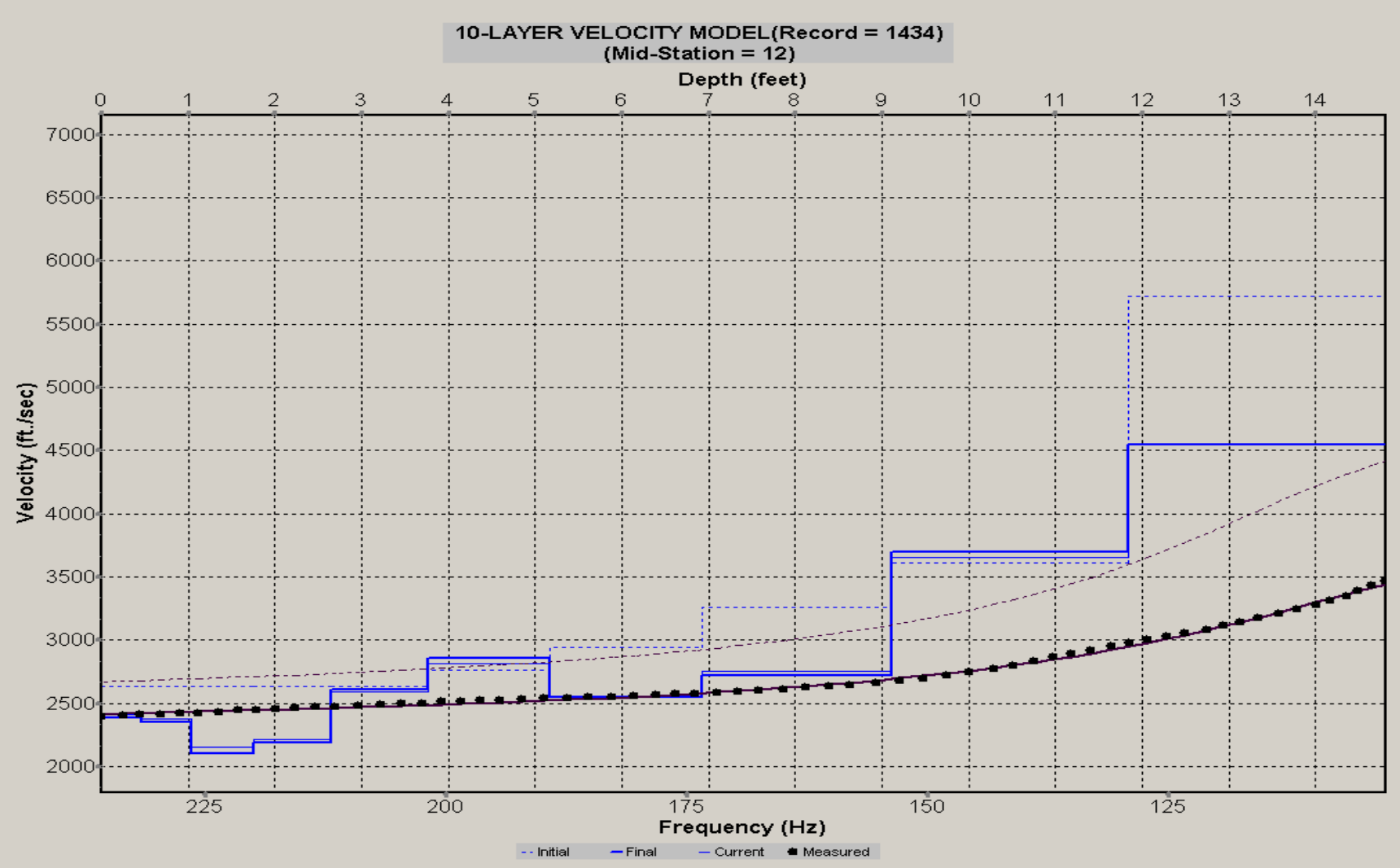

A.726: Velocity Profile Line 1434 used in Post-blast 40 and Pre-blast 44

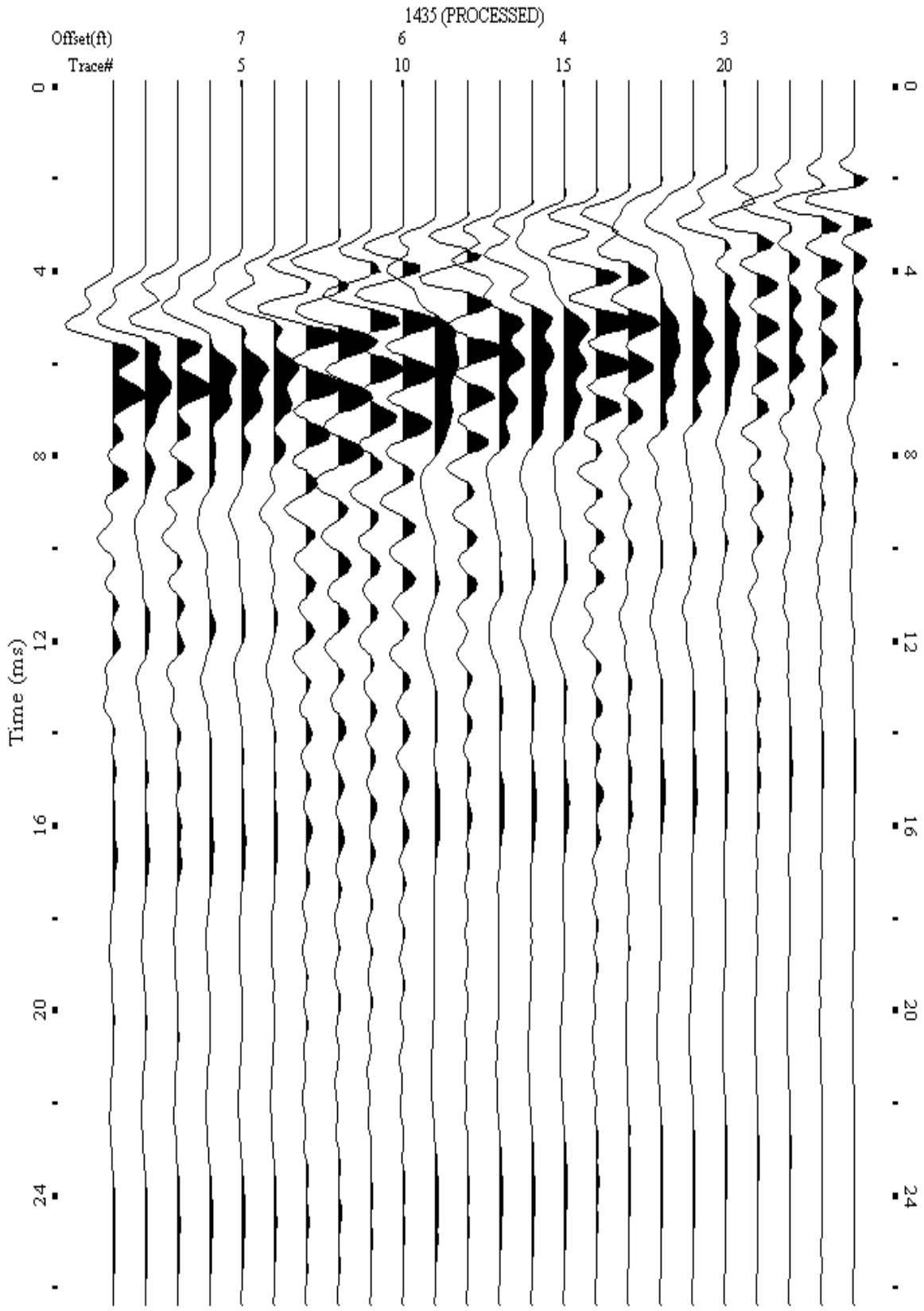

A.727: Shot Gather Line 1435 used in Post-blast 40 and Pre-blast 44

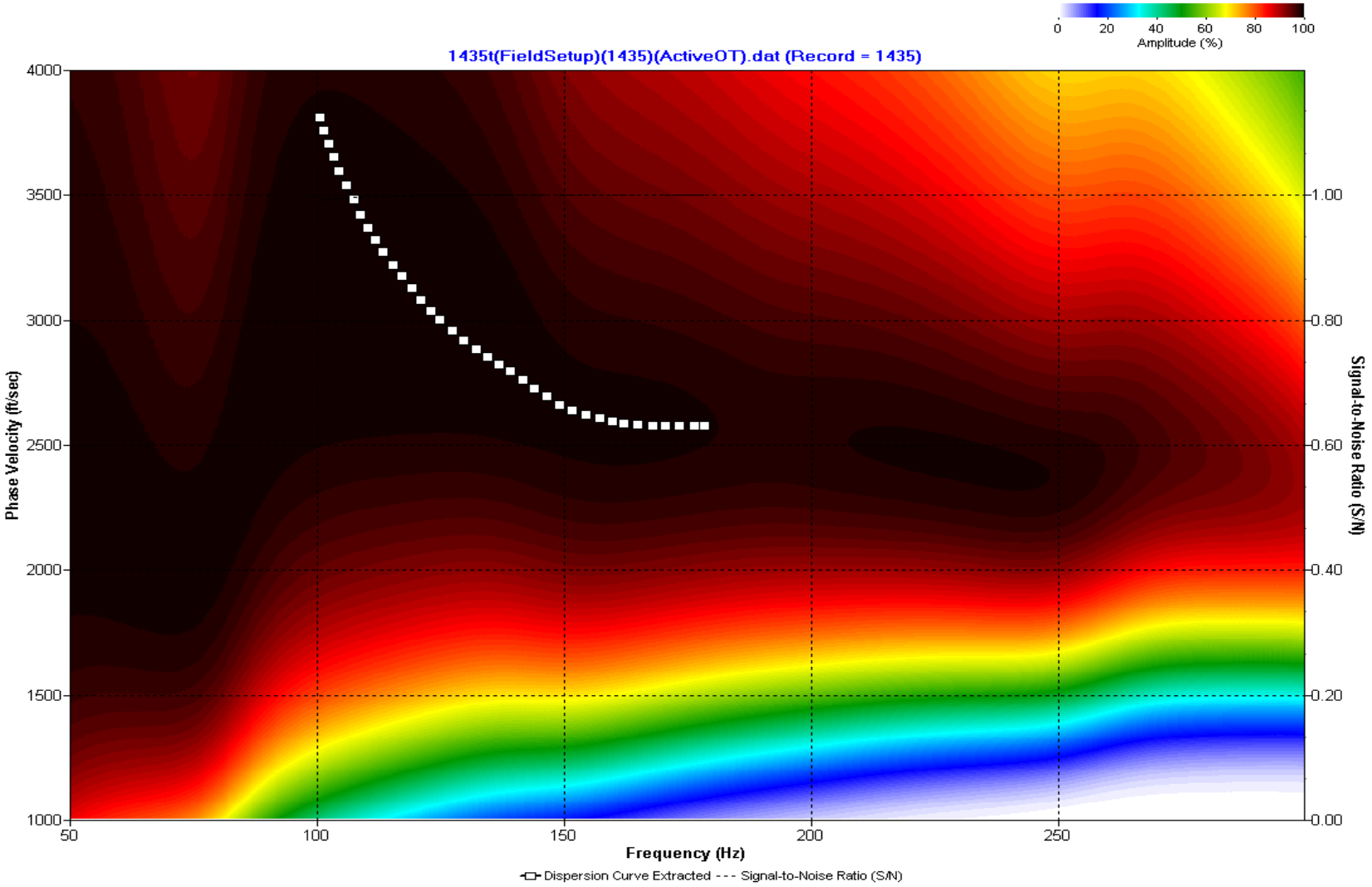

A.728: Dispersion Curve Line 1435 used in Post-blast 40 and Pre-blast 44

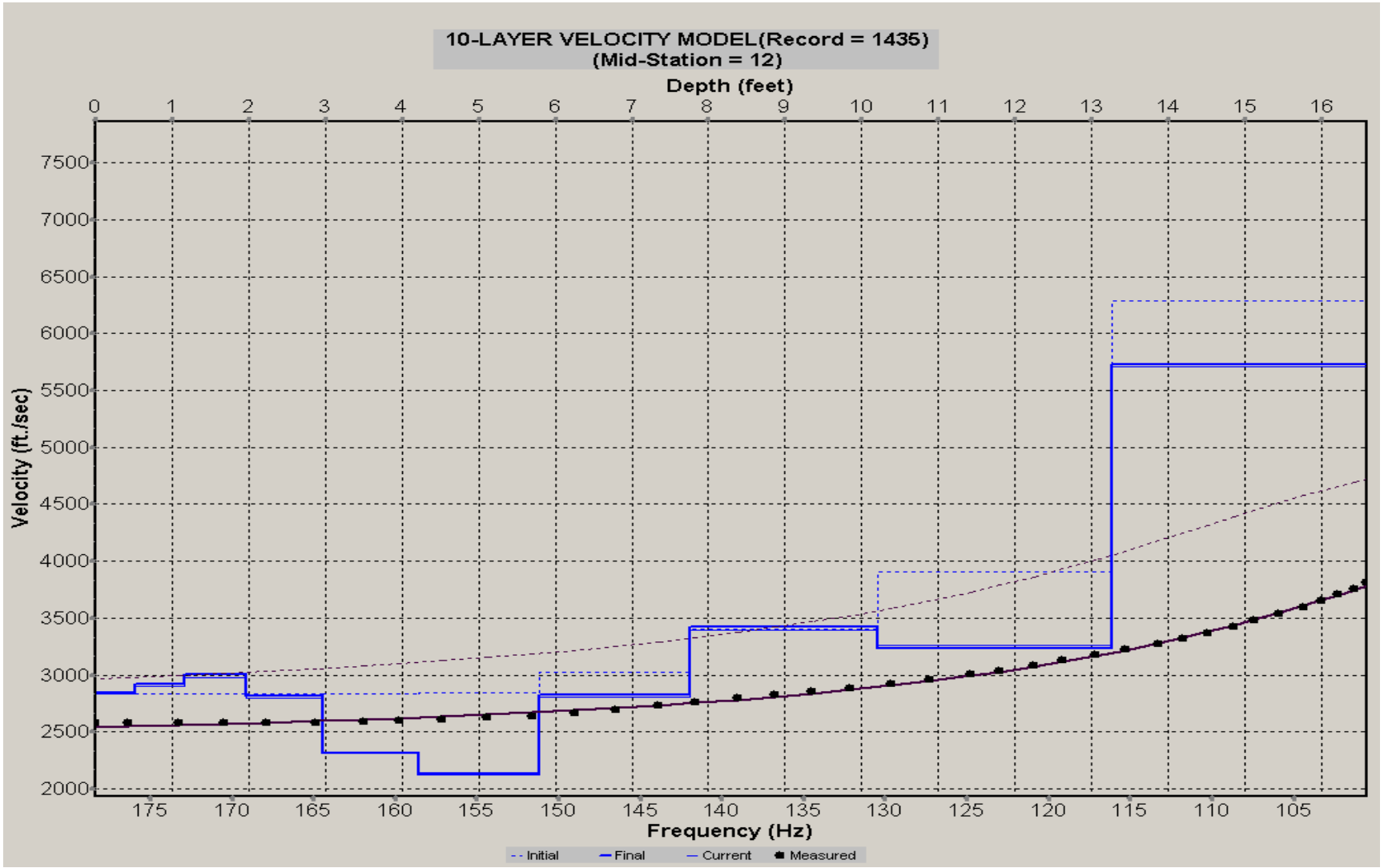

A.729: Velocity Profile Line 1435 used in Post-blast 40 and Pre-blast 44

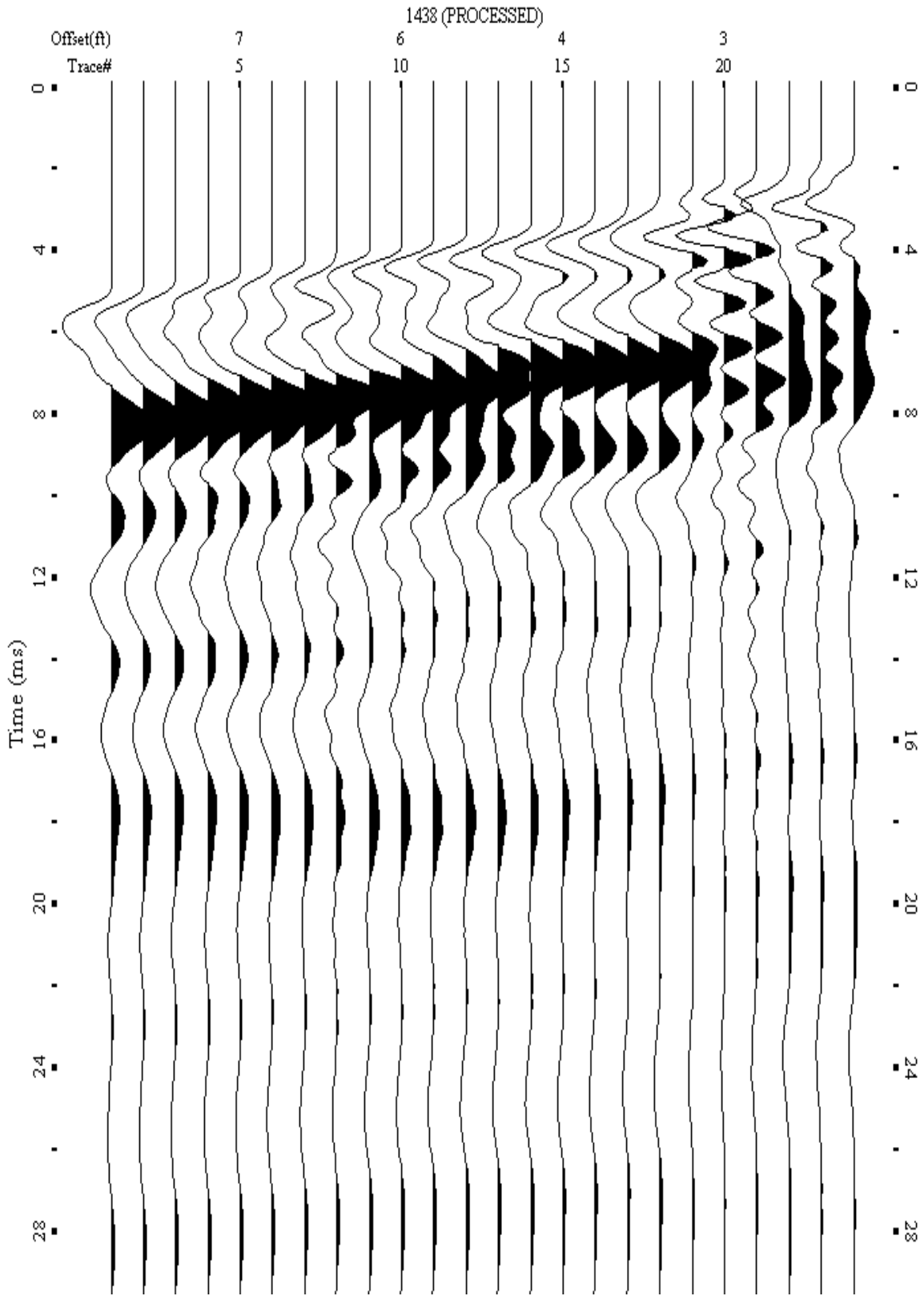

A.730: Shot Gather Line 1438 used in Post-blast 39

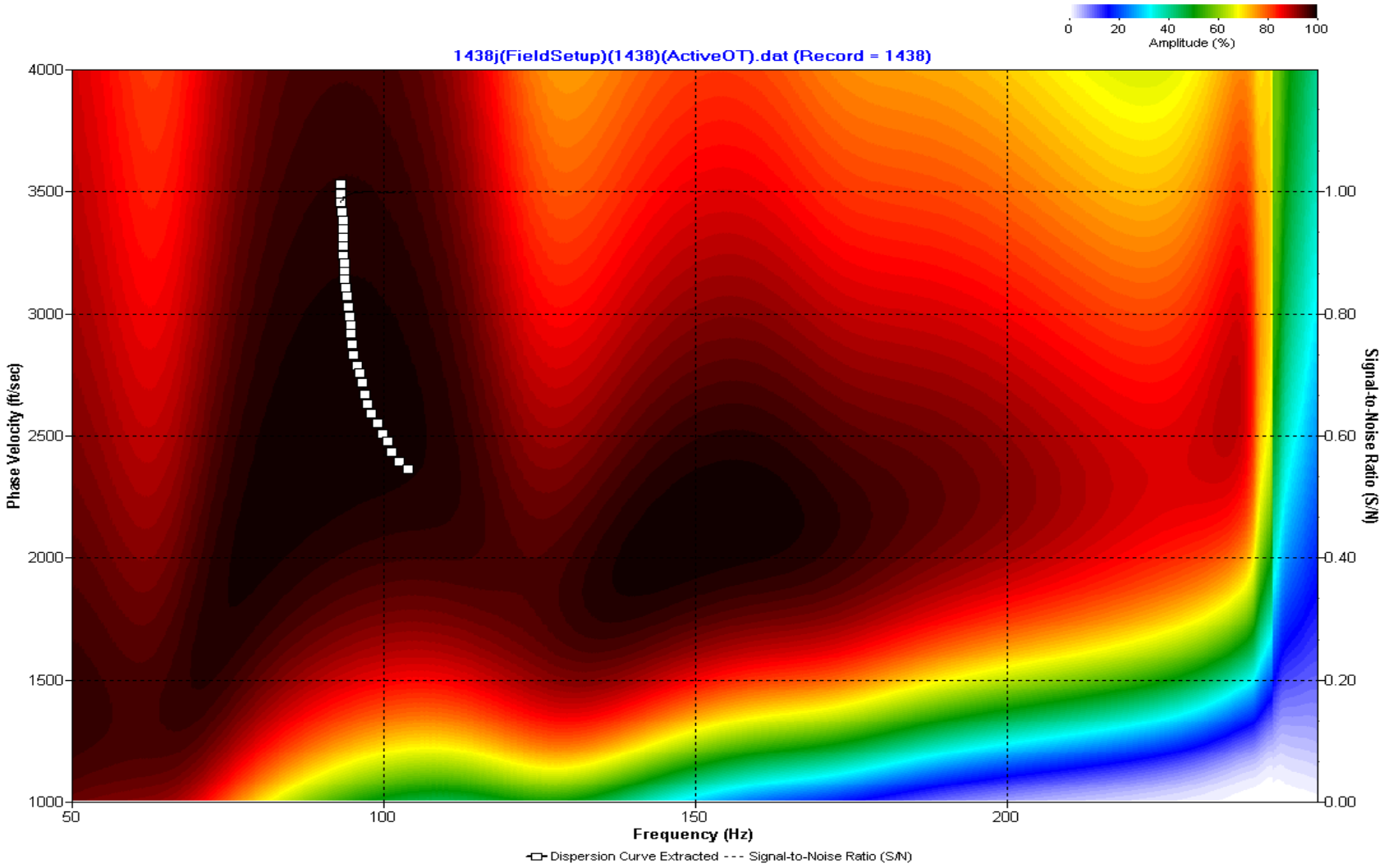

A.731: Dispersion Curve Line 1438 used in Post-blast 39

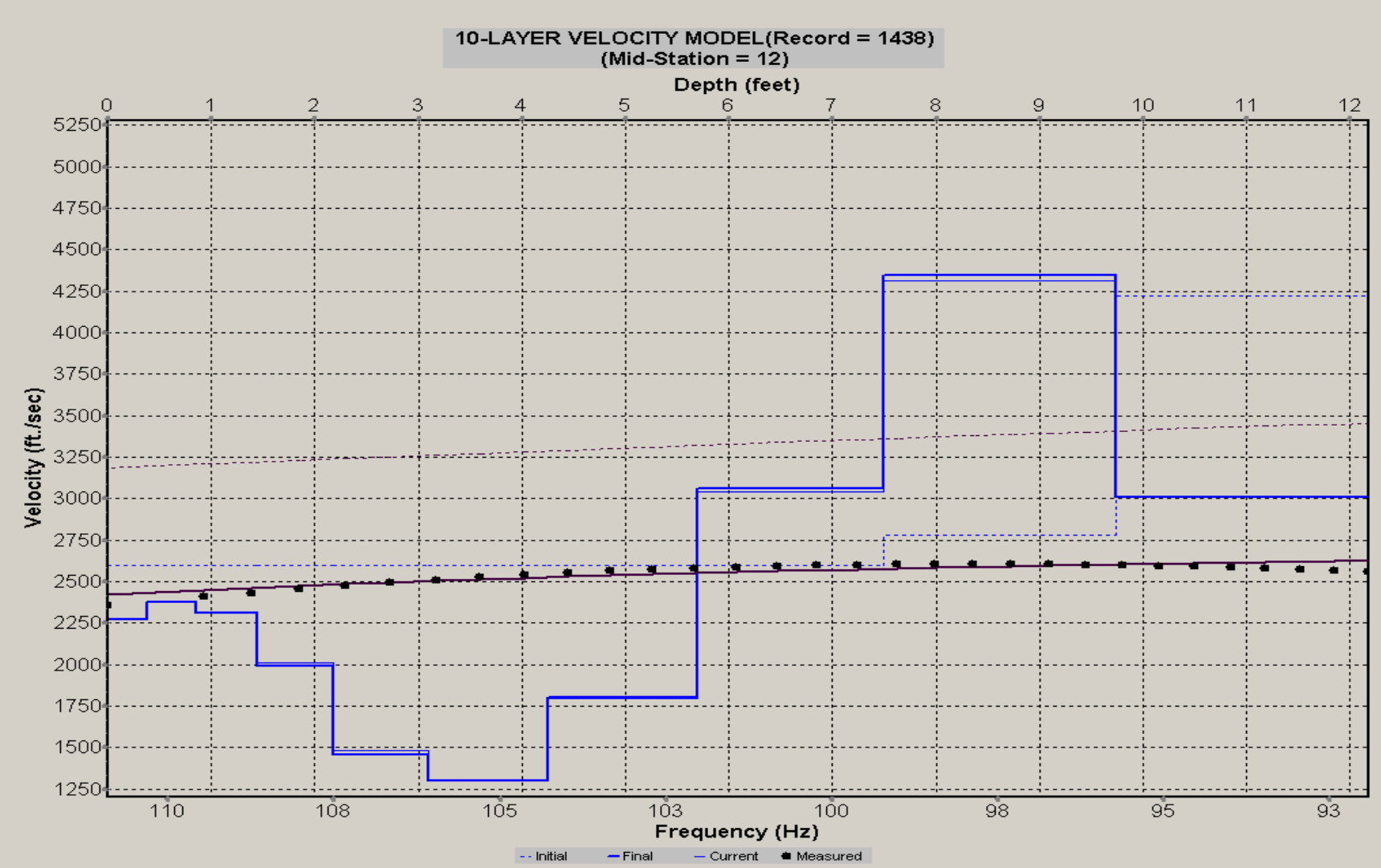

A.732: Velocity Profile Line 1438 used in Post-blast 39

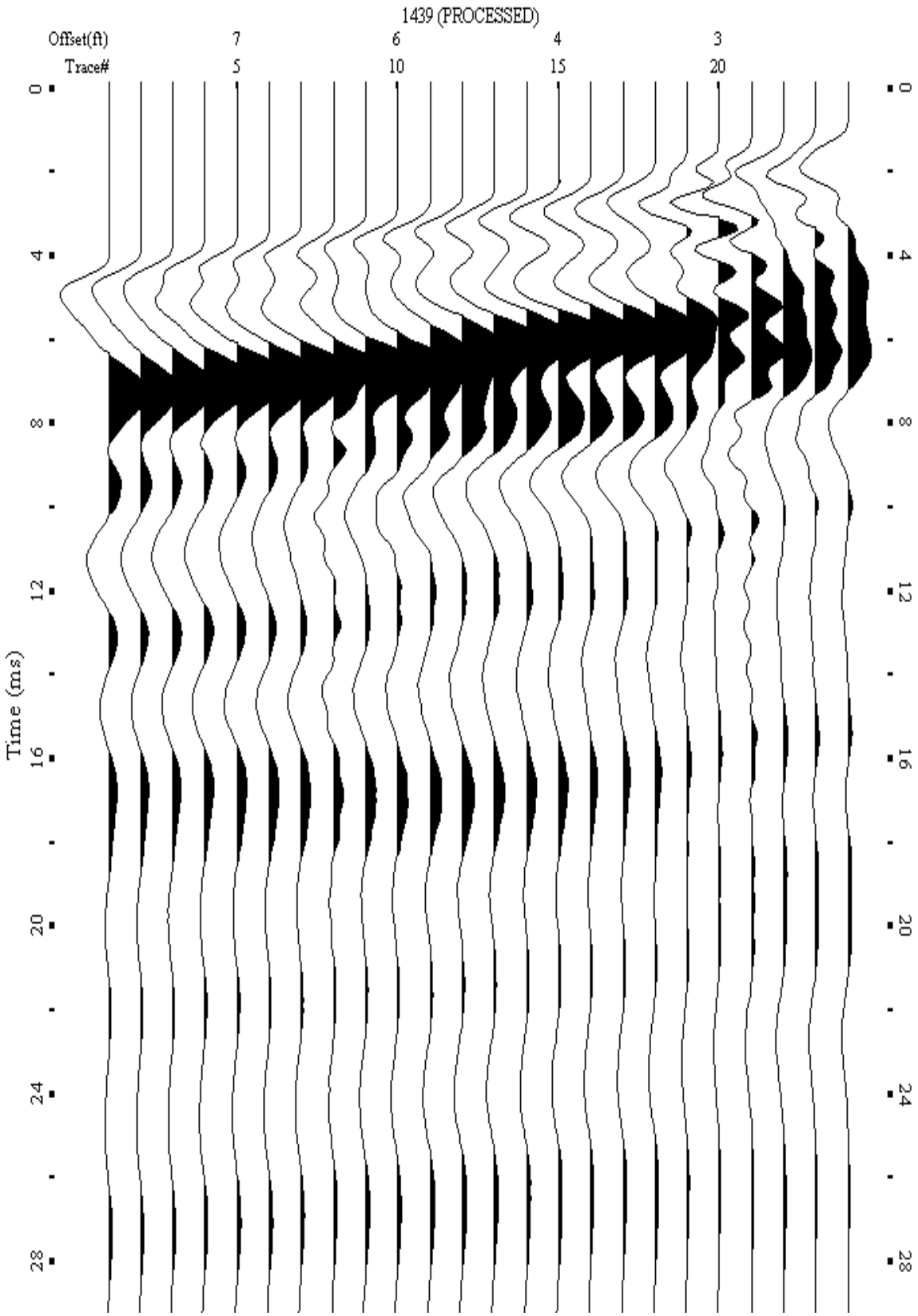

A.733: Shot Gather Line 1439 used in Pre-blast 43

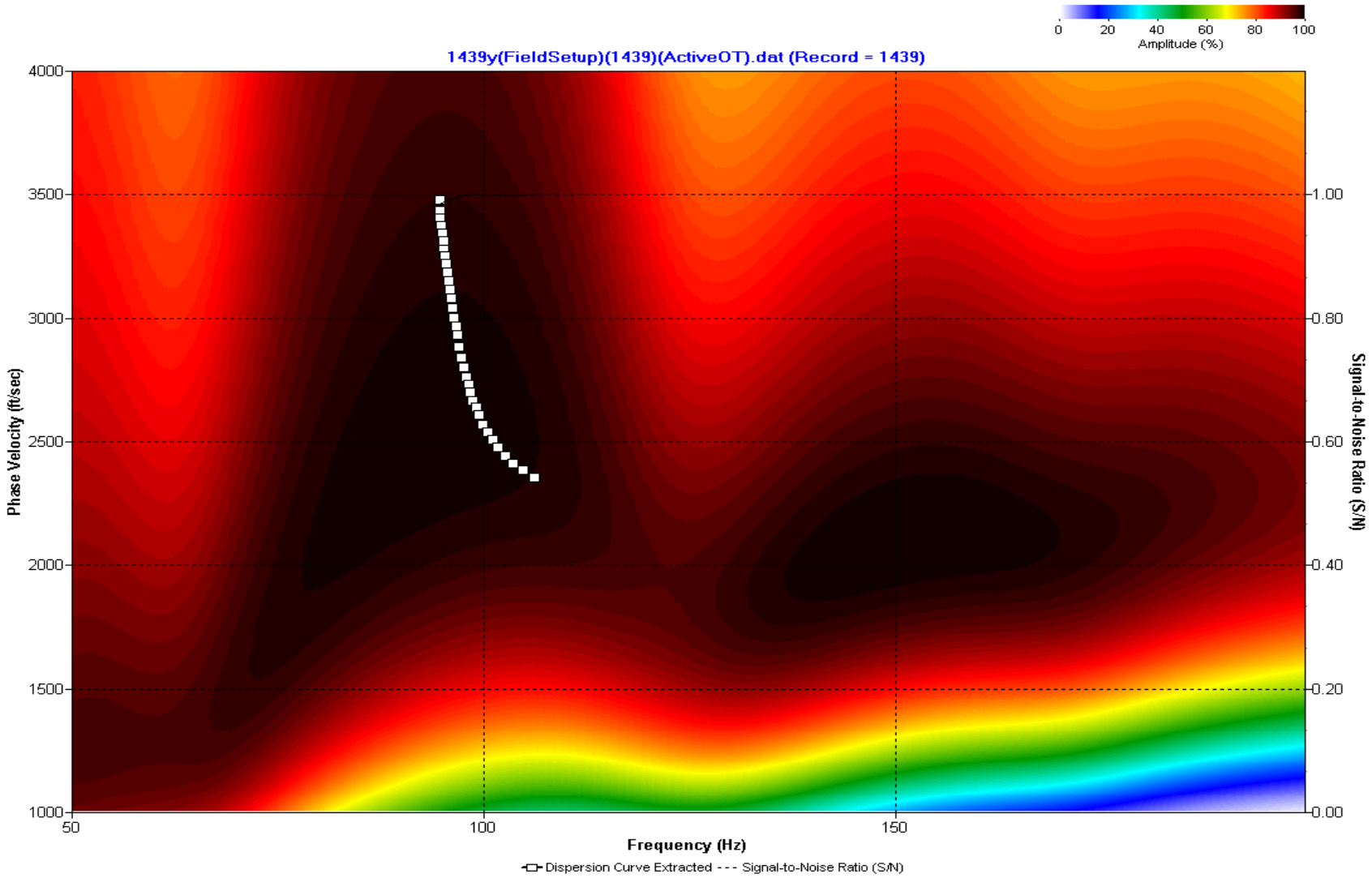

A.734: Dispersion Curve Line 1439 used in Pre-blast 43

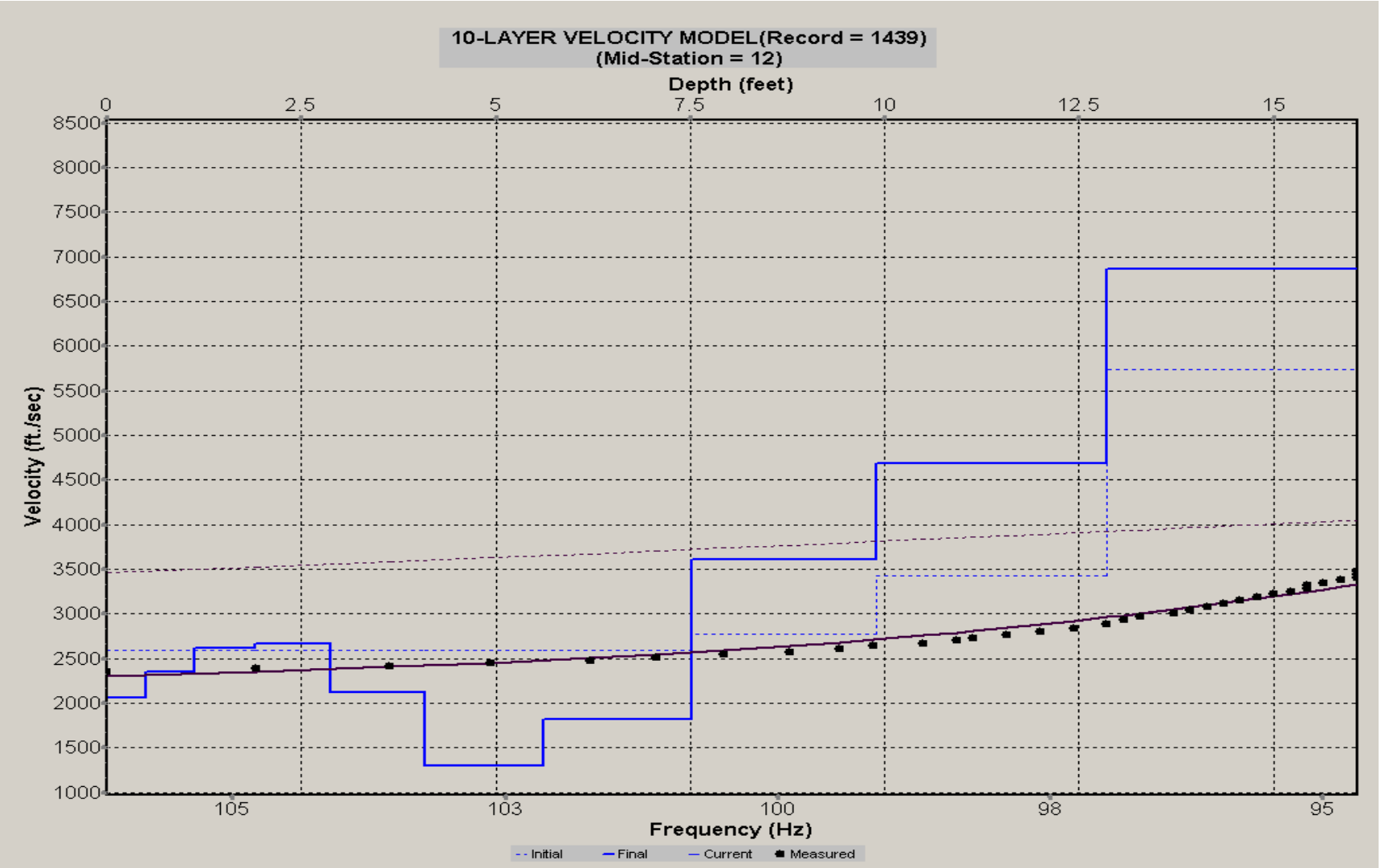

A.735: Velocity Profile Line 1439 used in Pre-blast 43

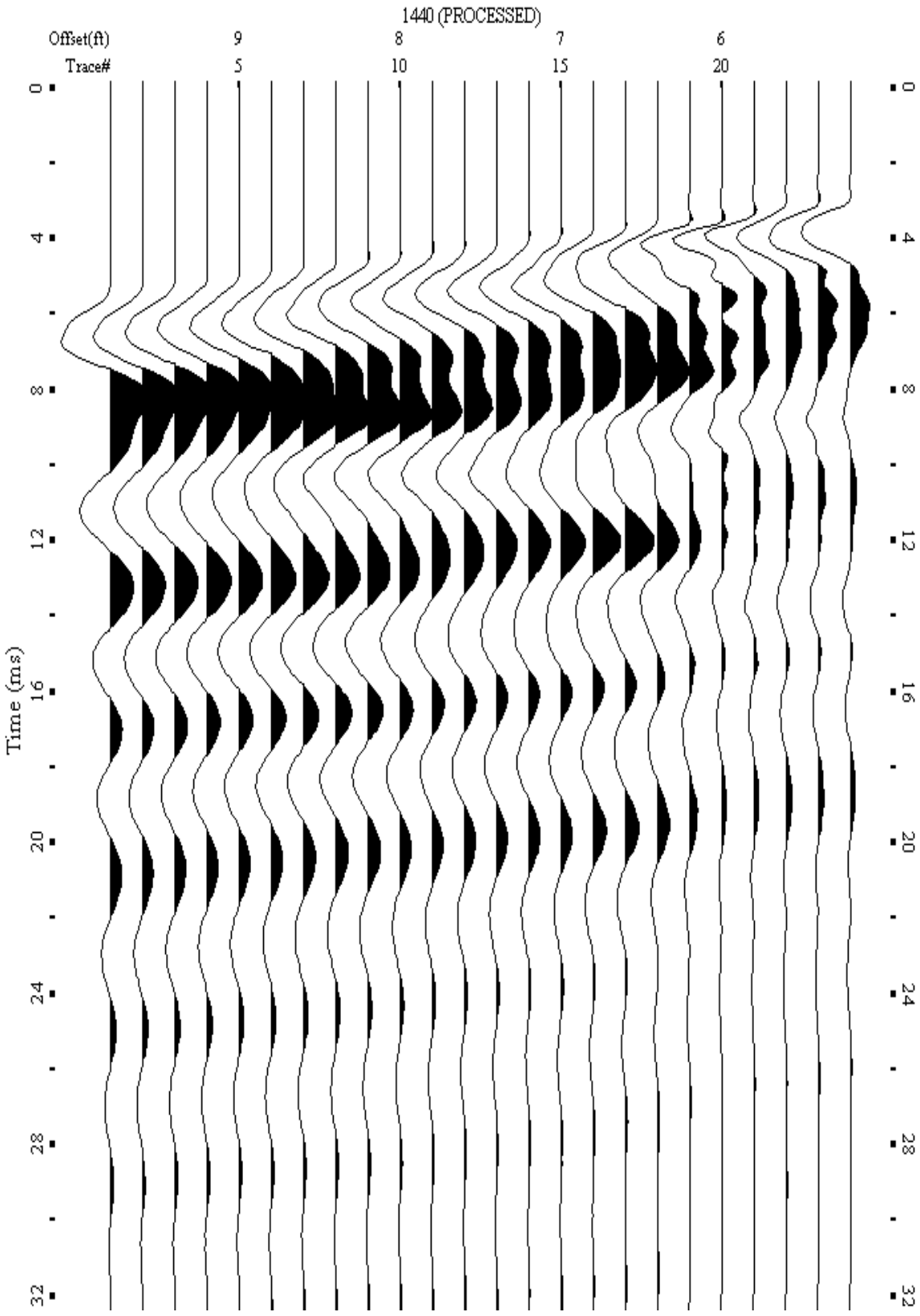

A.736: Shot Gather Line 1440 used in Post-blast 39

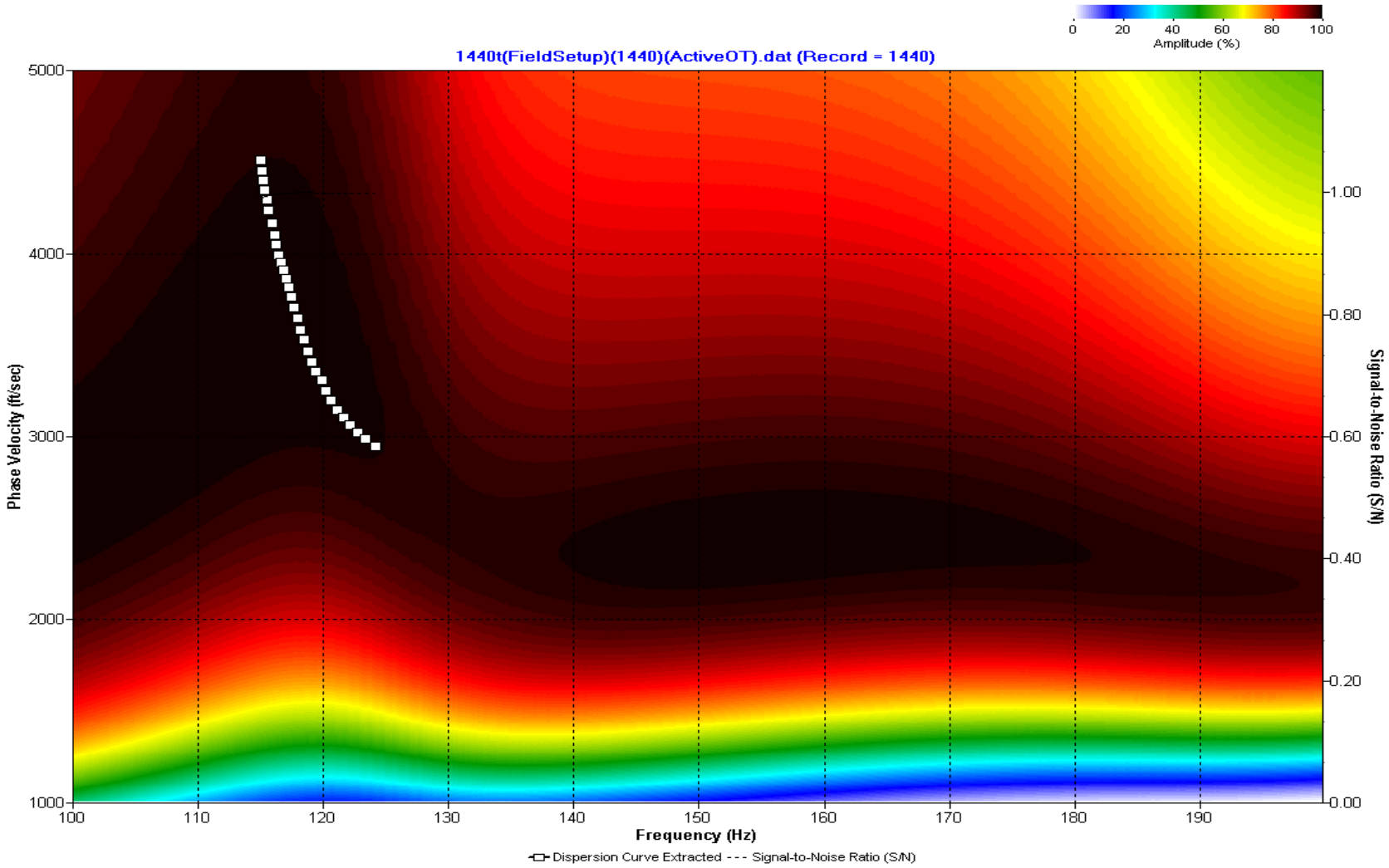

A.737: Dispersion Curve Line 1440 used in Post-blast 39

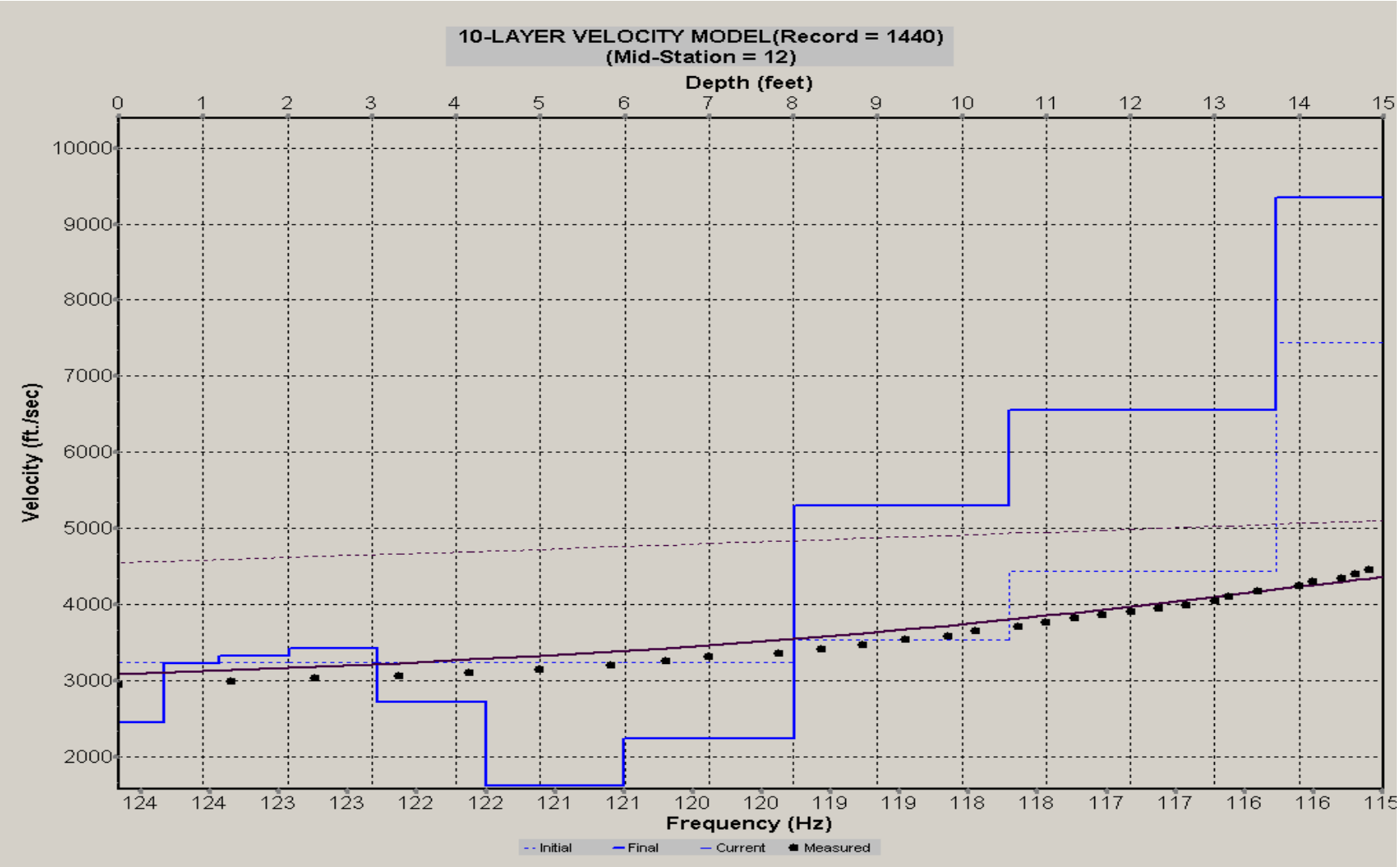

A.738: Velocity Profile Line 1440 used in Post-blast 39

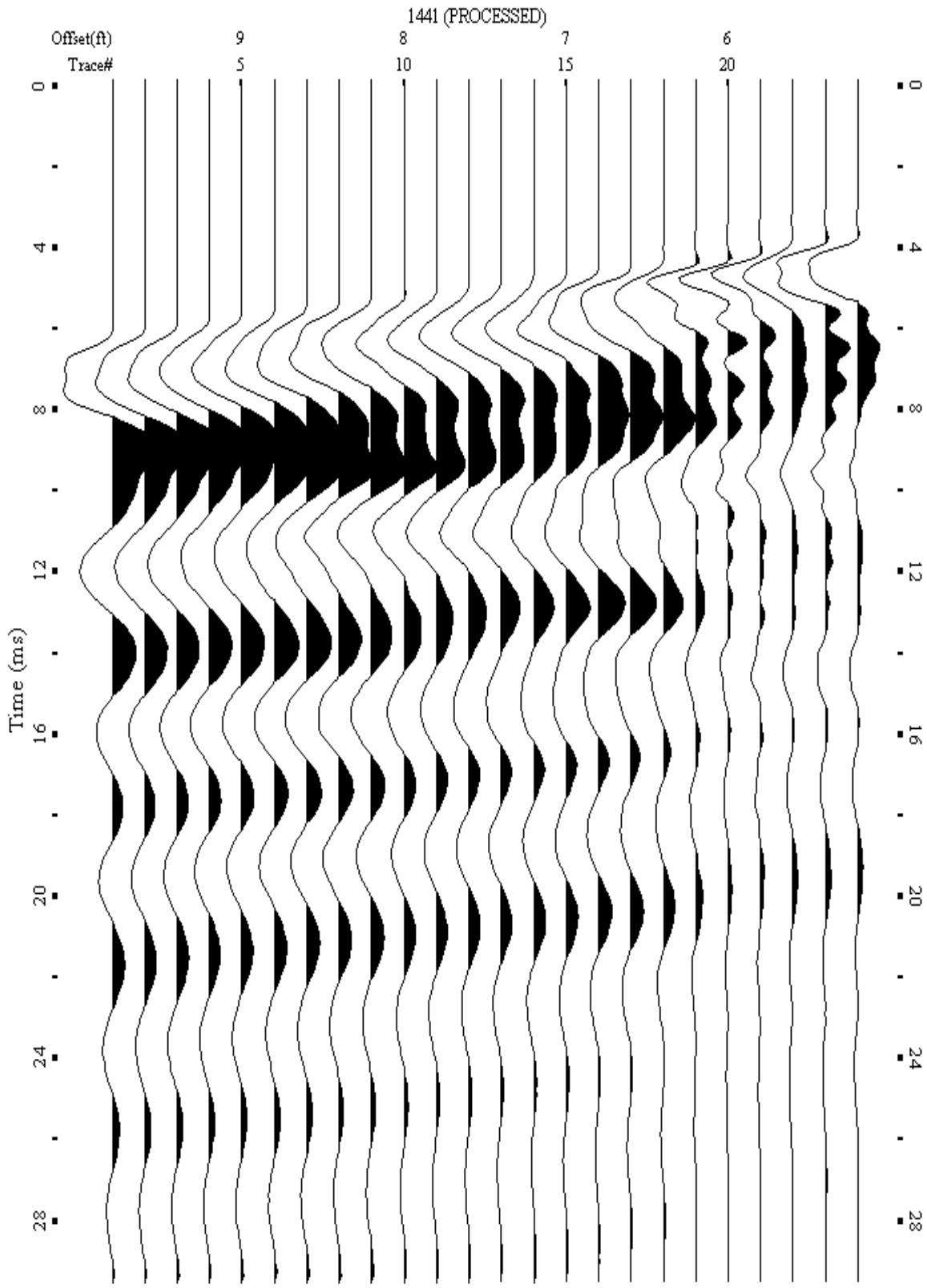

A.739: Shot Gather Line 1441 used in Post-blast 39 and Pre-blast 43

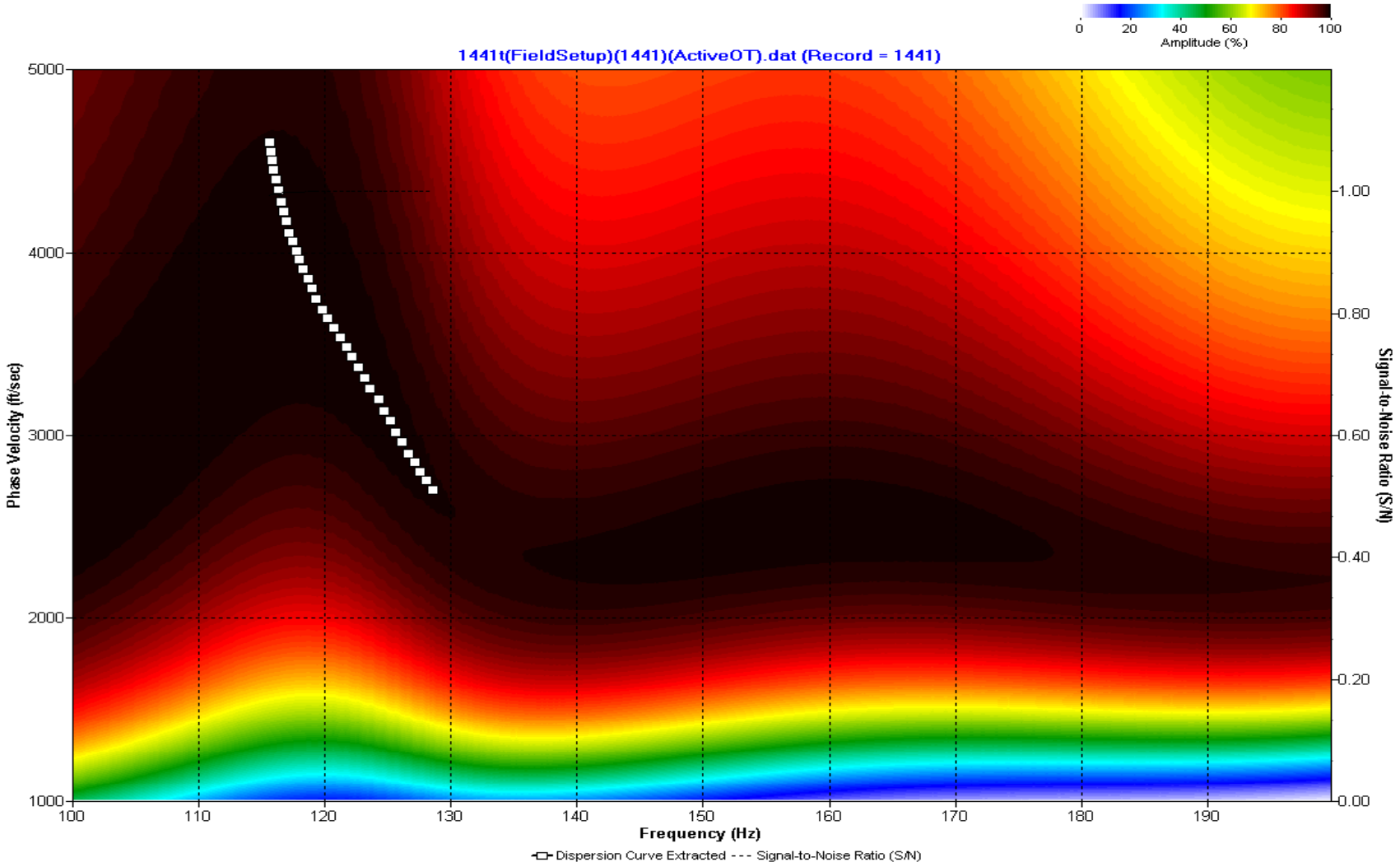

A.740: Dispersion Curve Line 1441 used in Post-blast 39 and Pre-blast 43

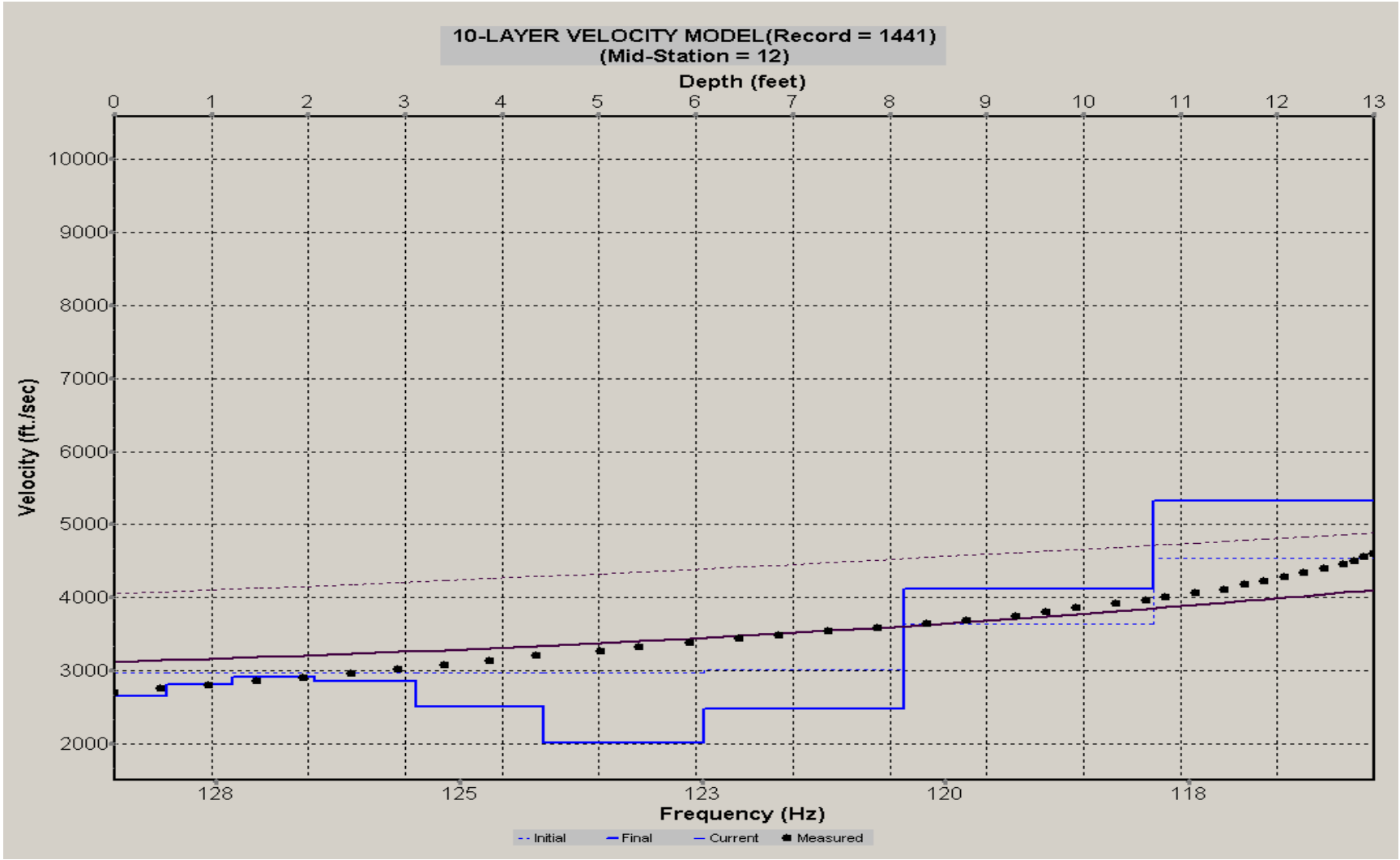

A.741: Velocity Profile Line 1441 used in Post-blast 39 and Pre-blast 43

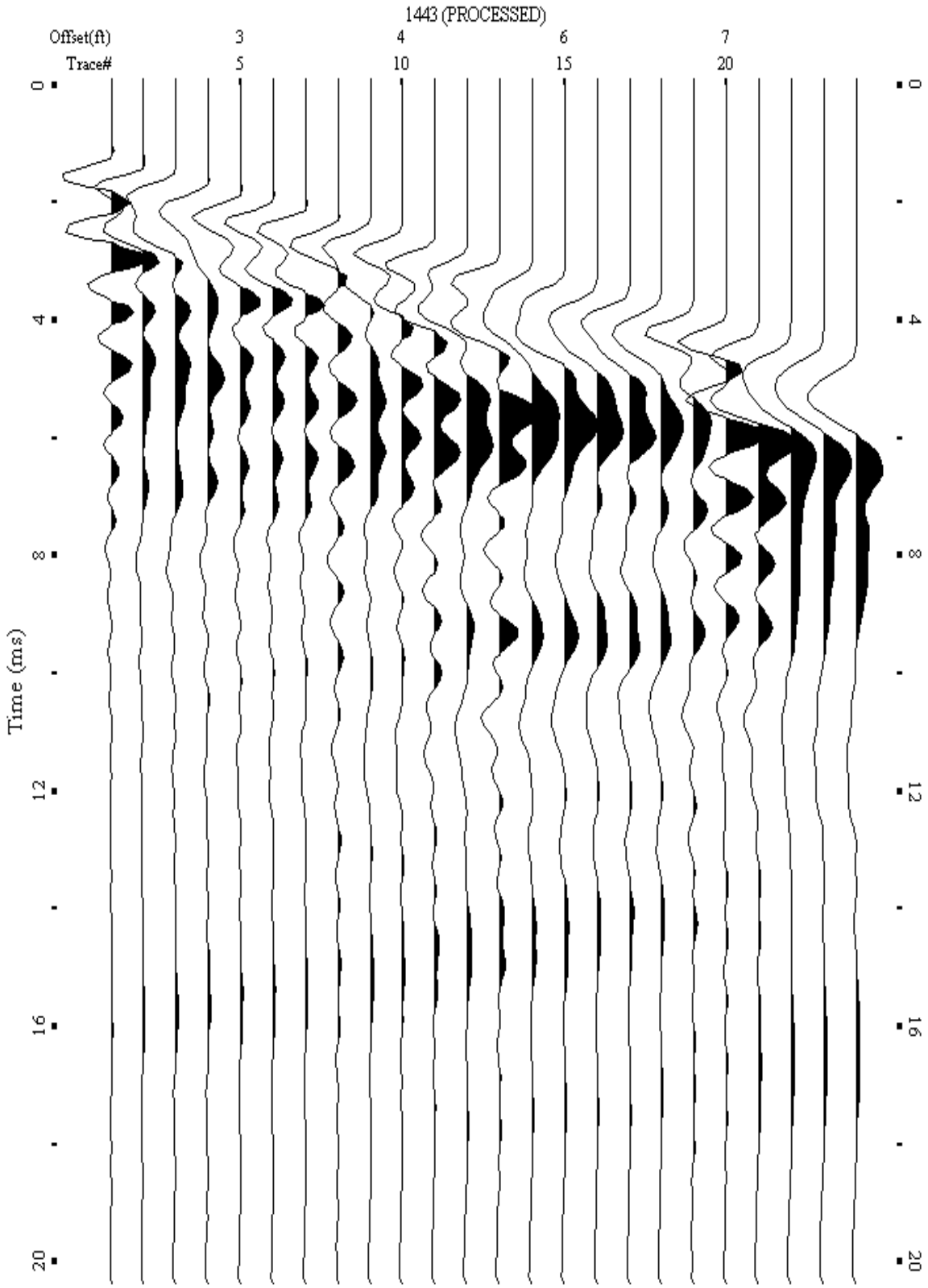

A.742: Shot Gather Line 1443 used in Post-blast 39

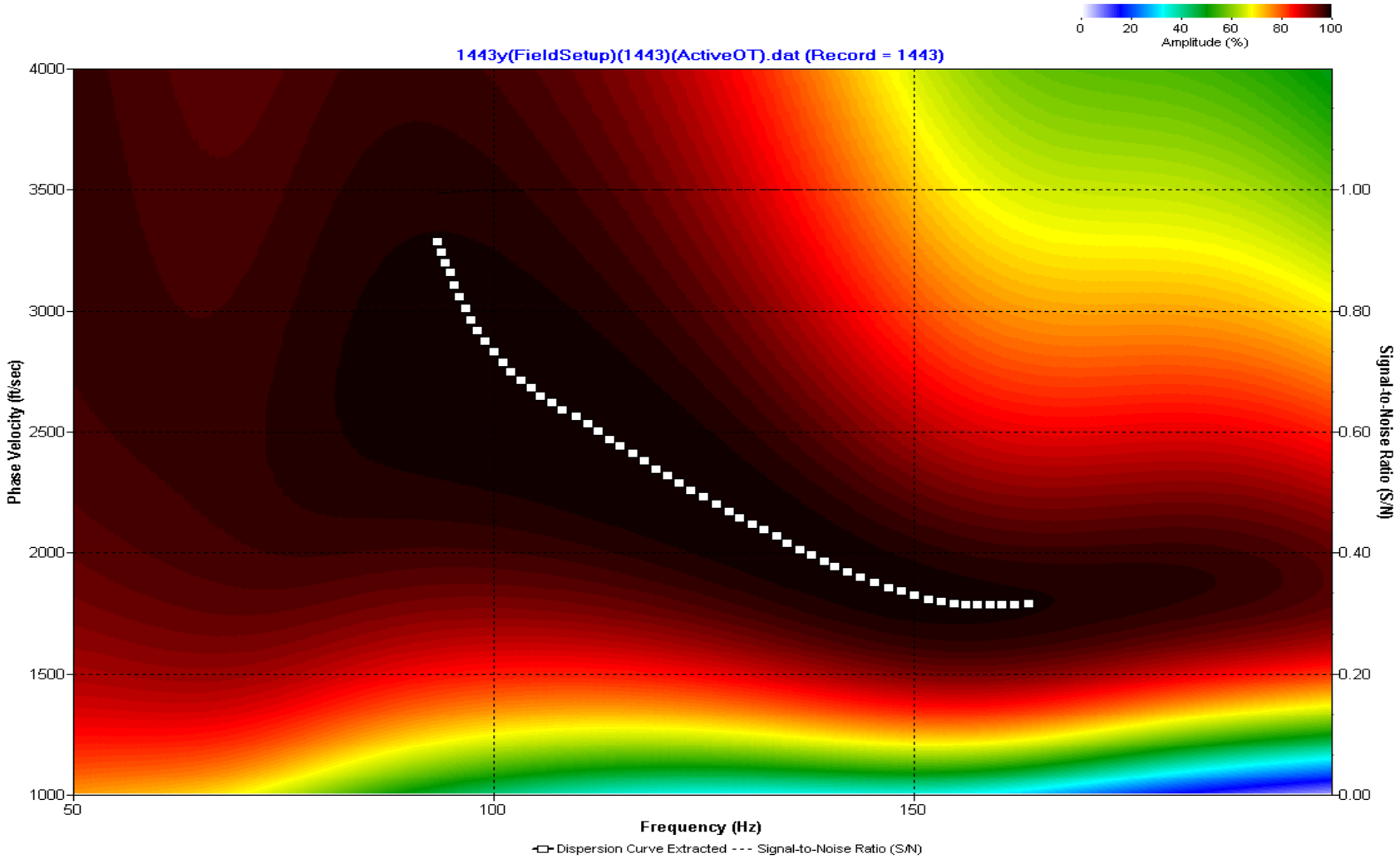

A.743: Dispersion Curve Line 1443 used in Post-blast 39

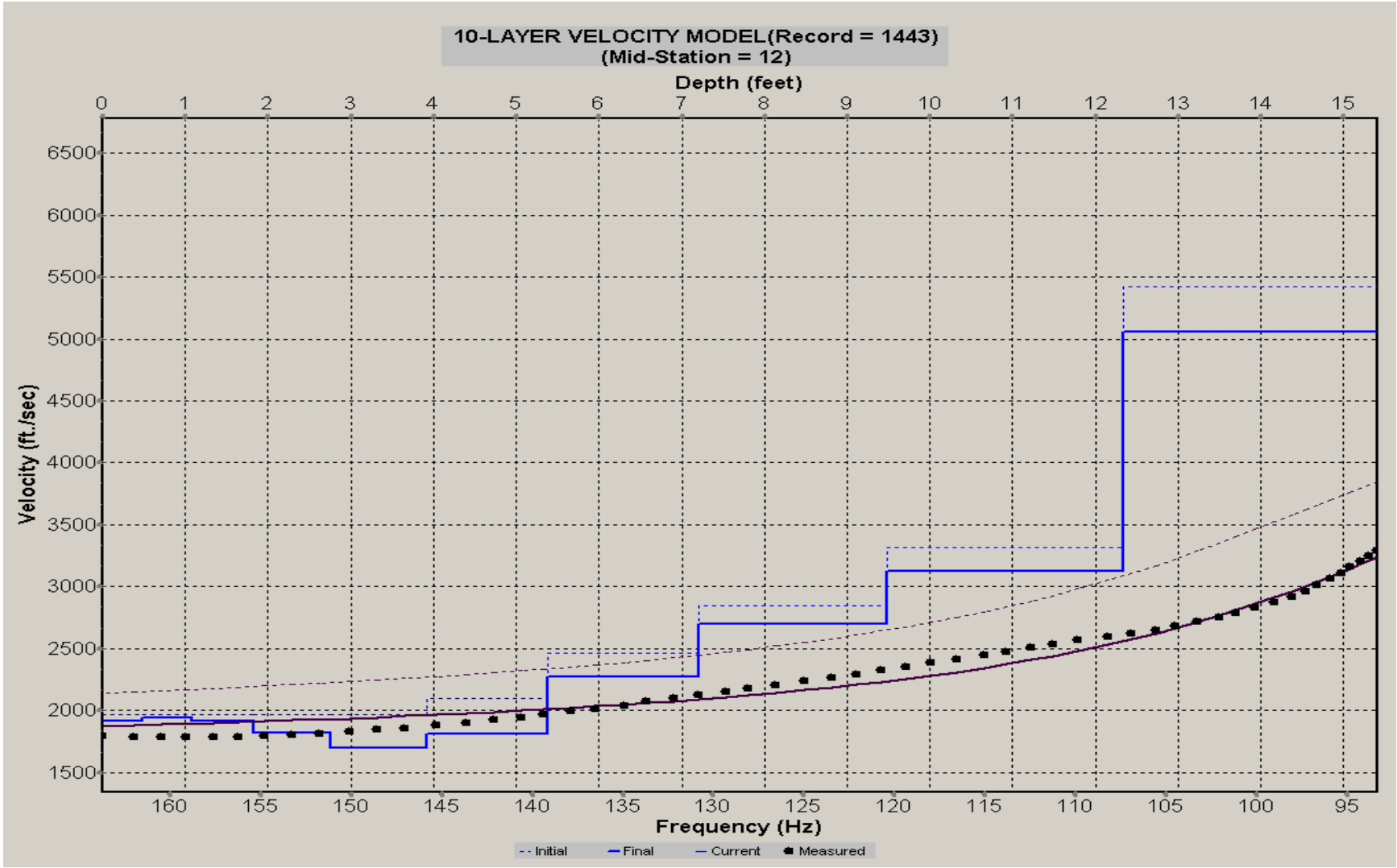

A.744: Velocity Profile Line 1443 used in Post-blast 39

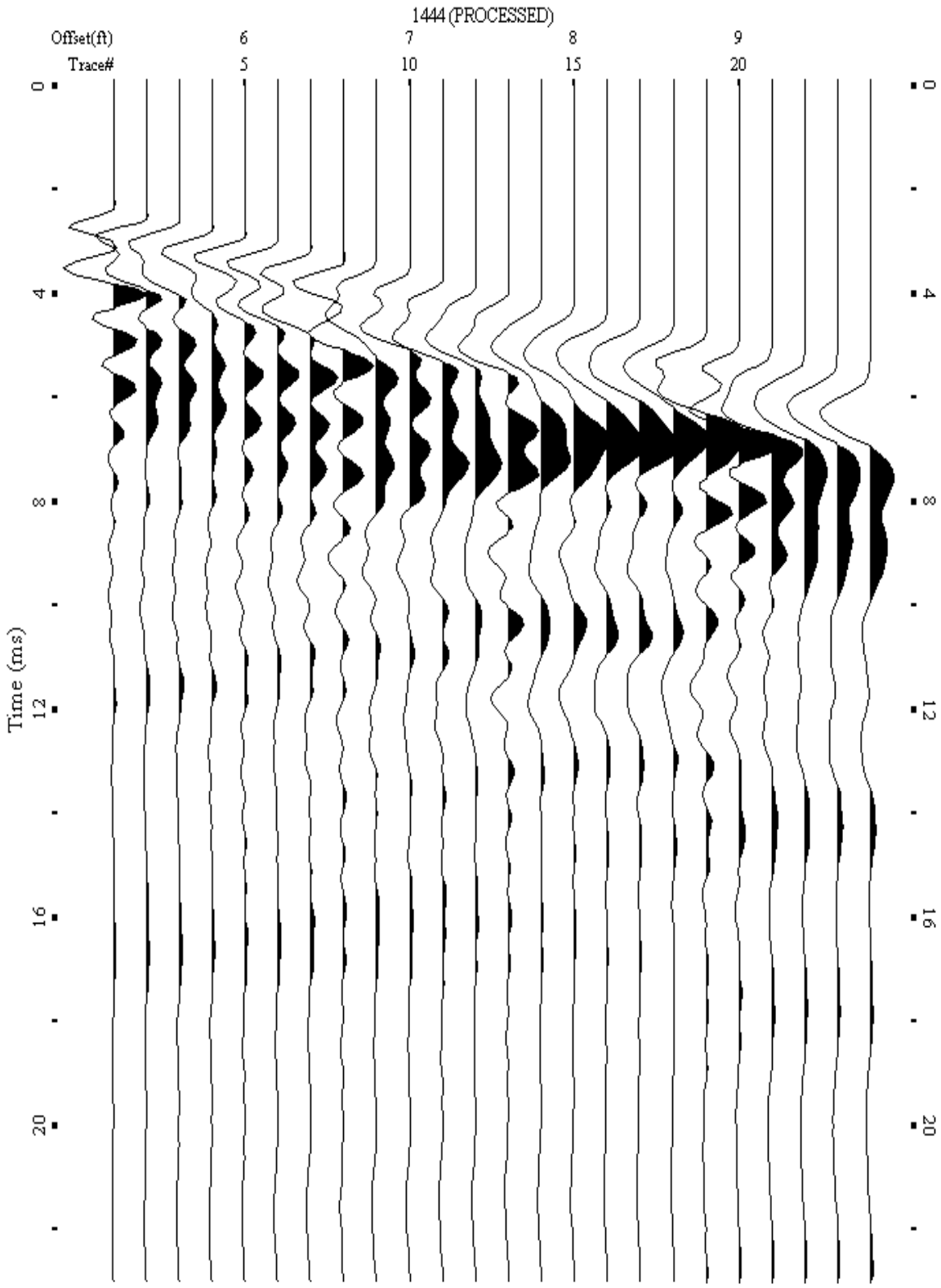

A.745: Shot Gather Line 1444 used in Post-blast 39 and Pre-blast 43

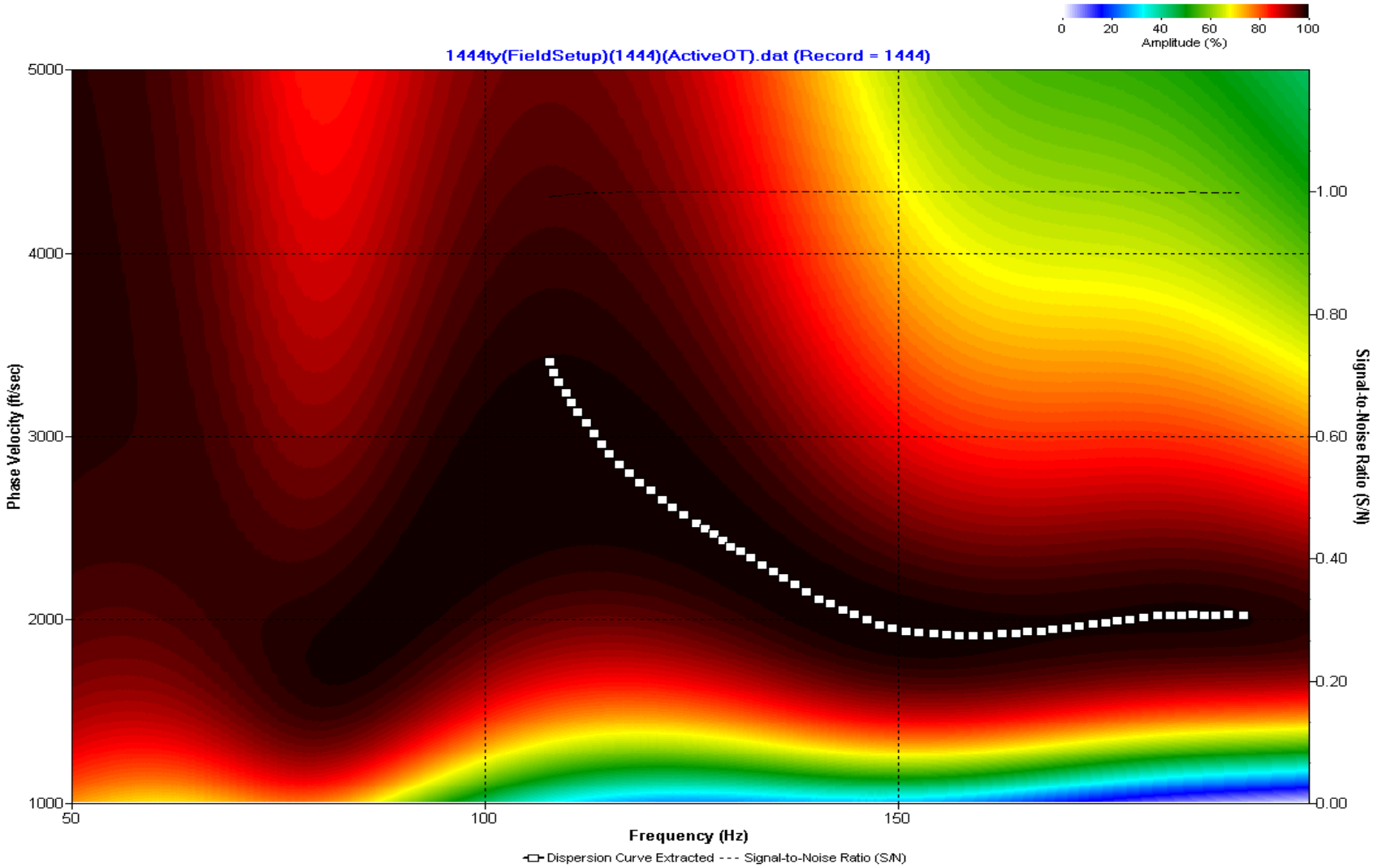

A.746: Dispersion Curve Line 1444 used in Post-blast 39 and Pre-blast 43

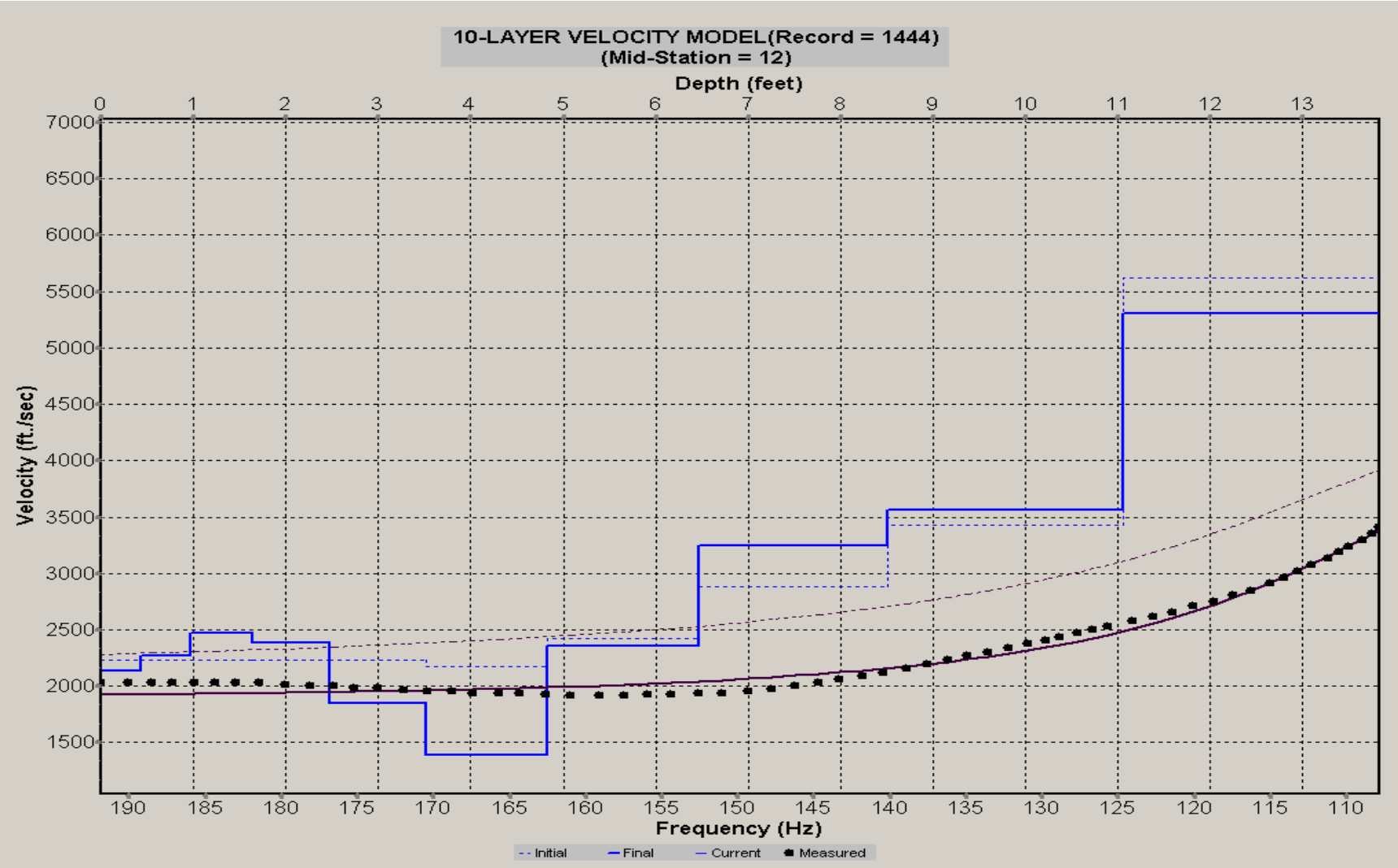

A.747: Velocity Profile Line 1444 used in Post-blast 39 and Pre-blast 43

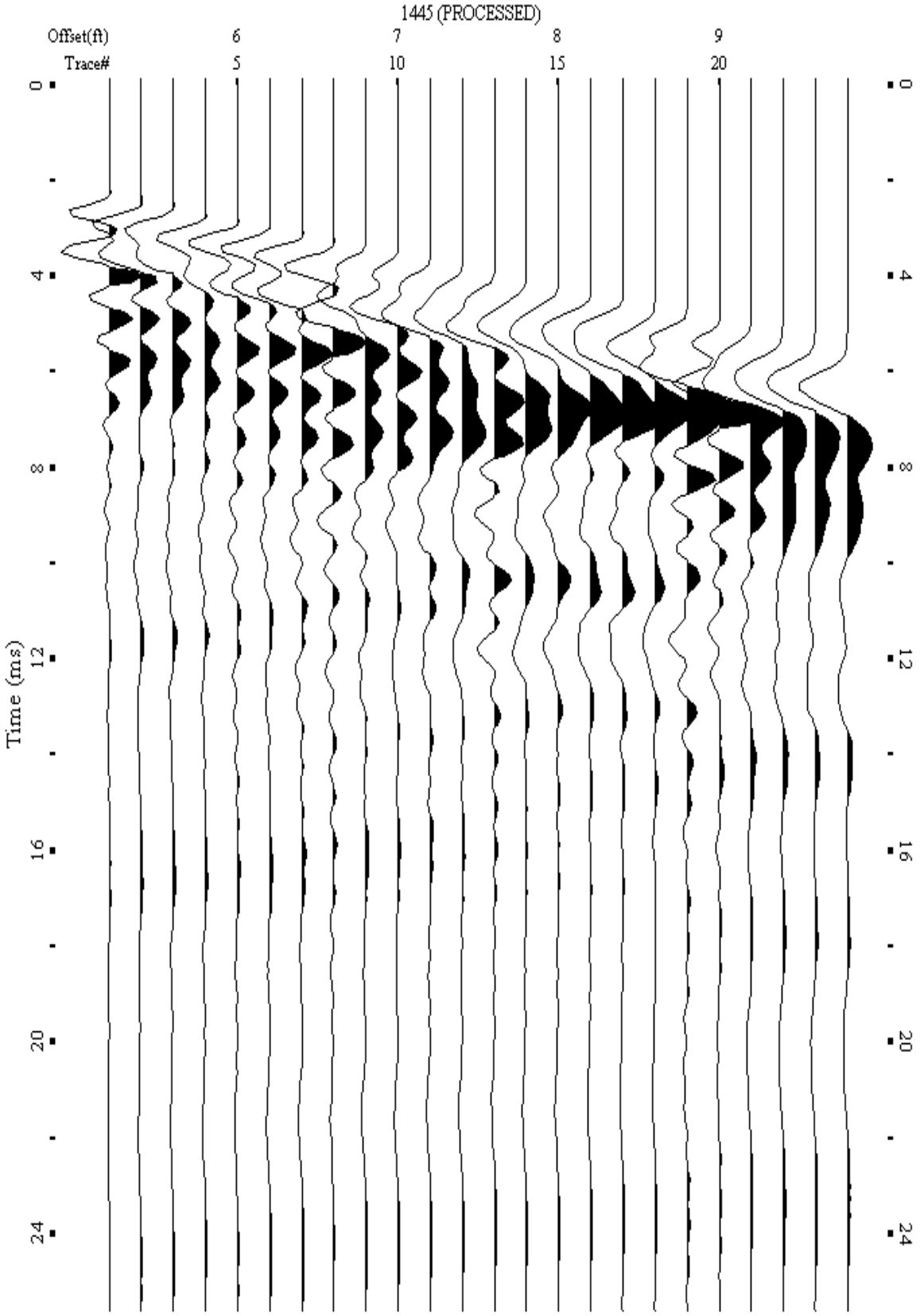

A.748: Shot Gather Line 1445 used in Post-blast 39

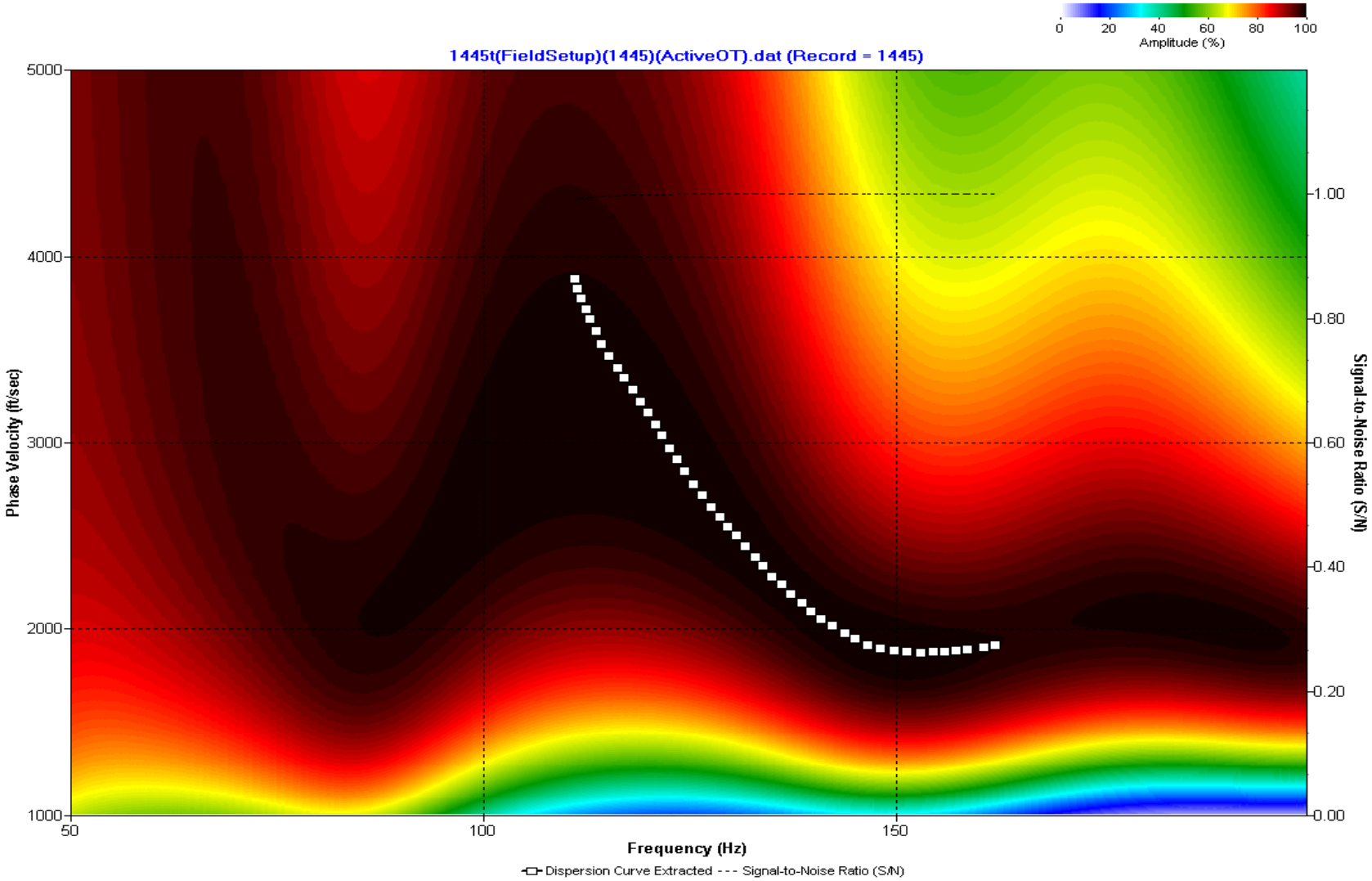

A.749: Dispersion Curve Line 1445 used in Post-blast 39

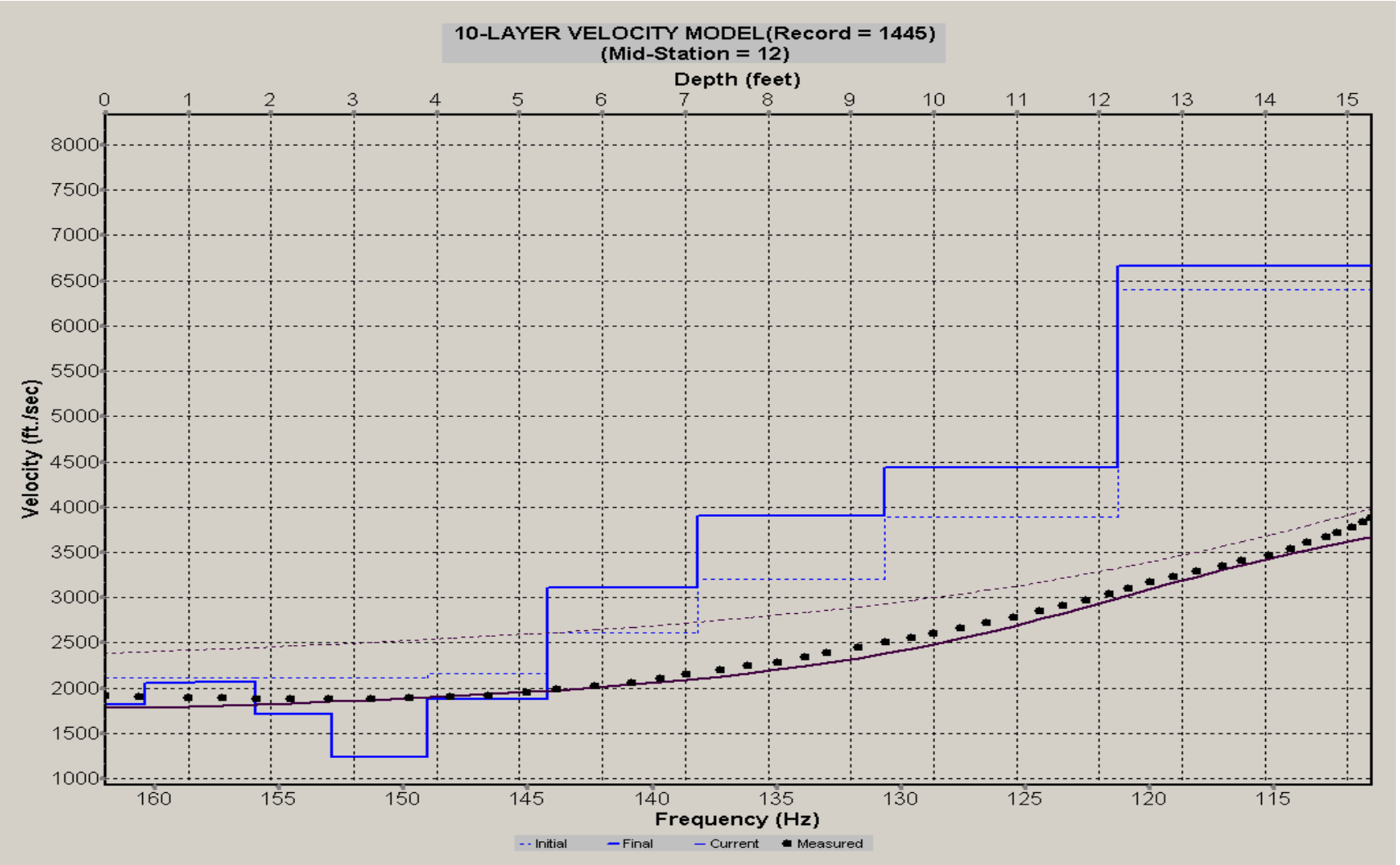

A.750: Velocity Profile Line 1445 used in Post-blast 39

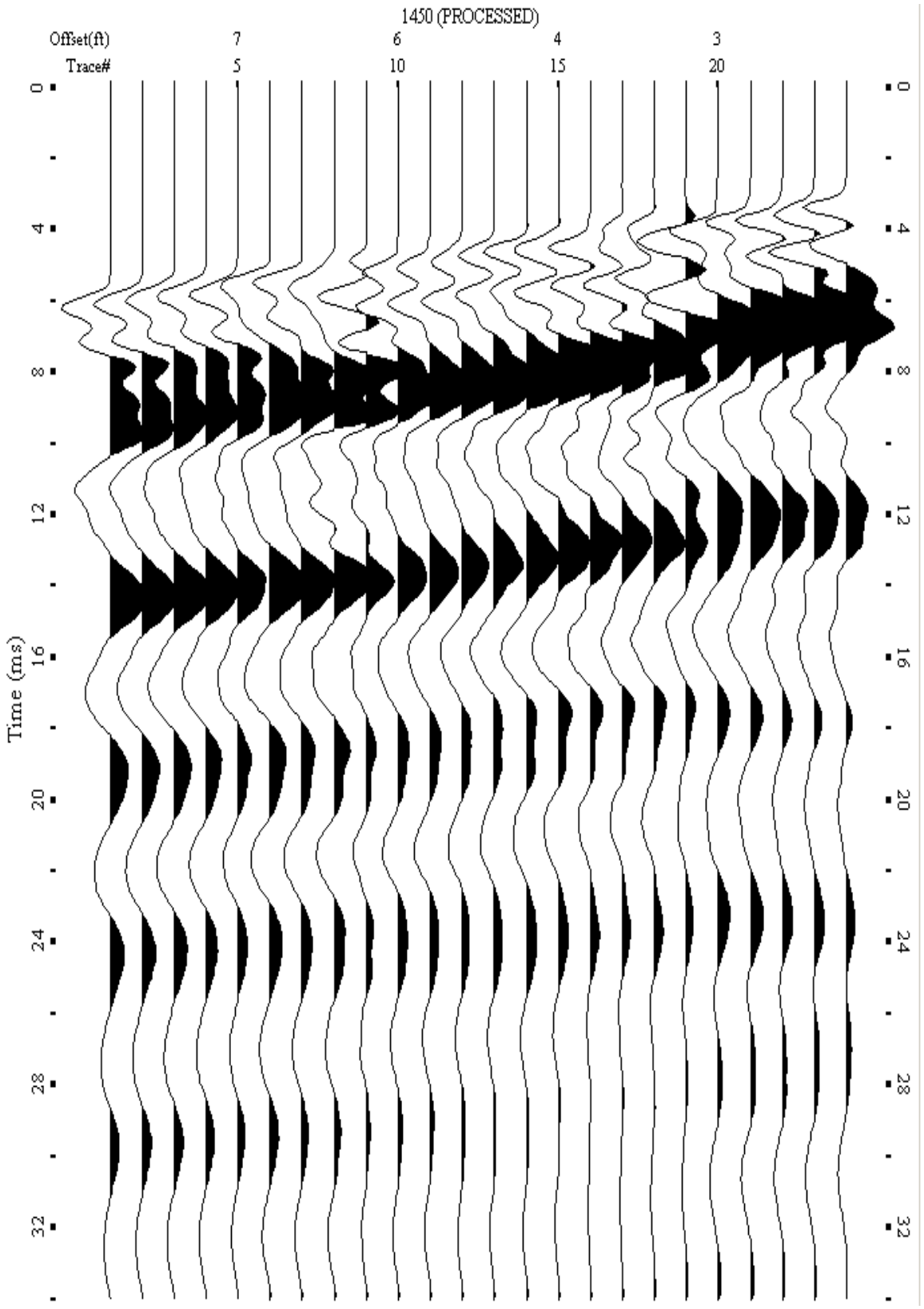

A.751: Shot Gather Line 1450 used in Post-blast 42

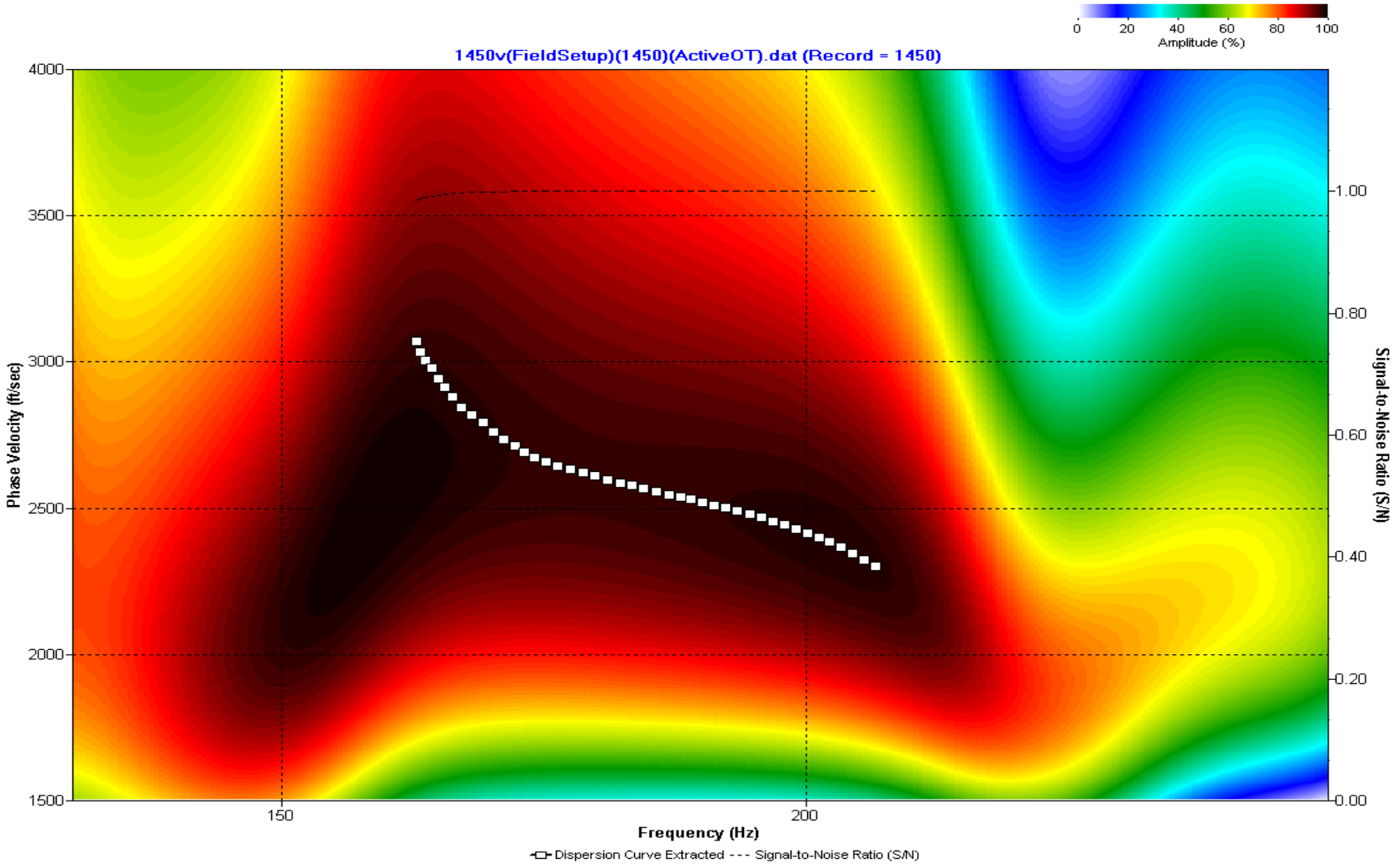

A.752: Dispersion Curve Line 1450 used in Post-blast 42

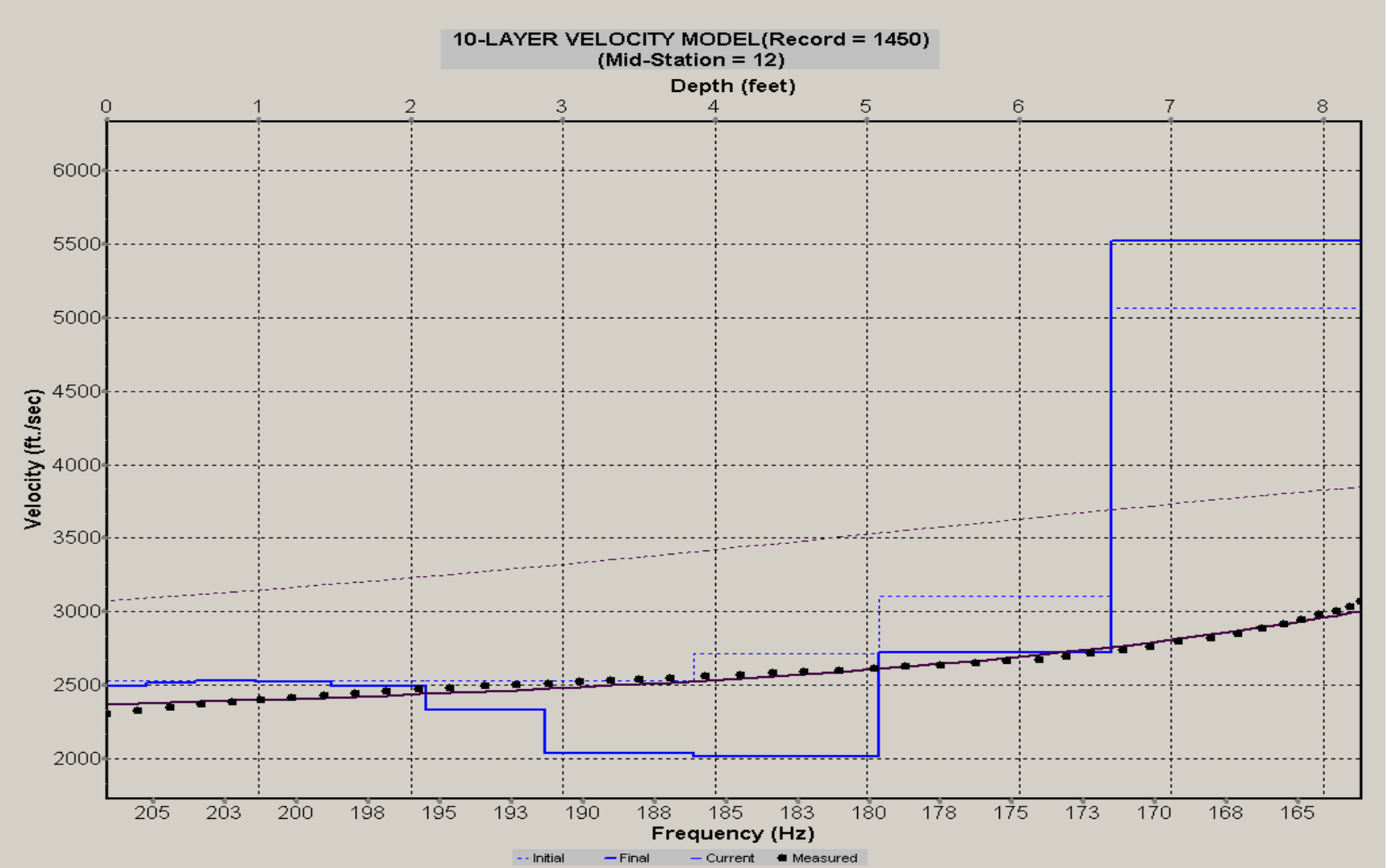

A.753: Velocity Profile Line 1450 used in Post-blast 42

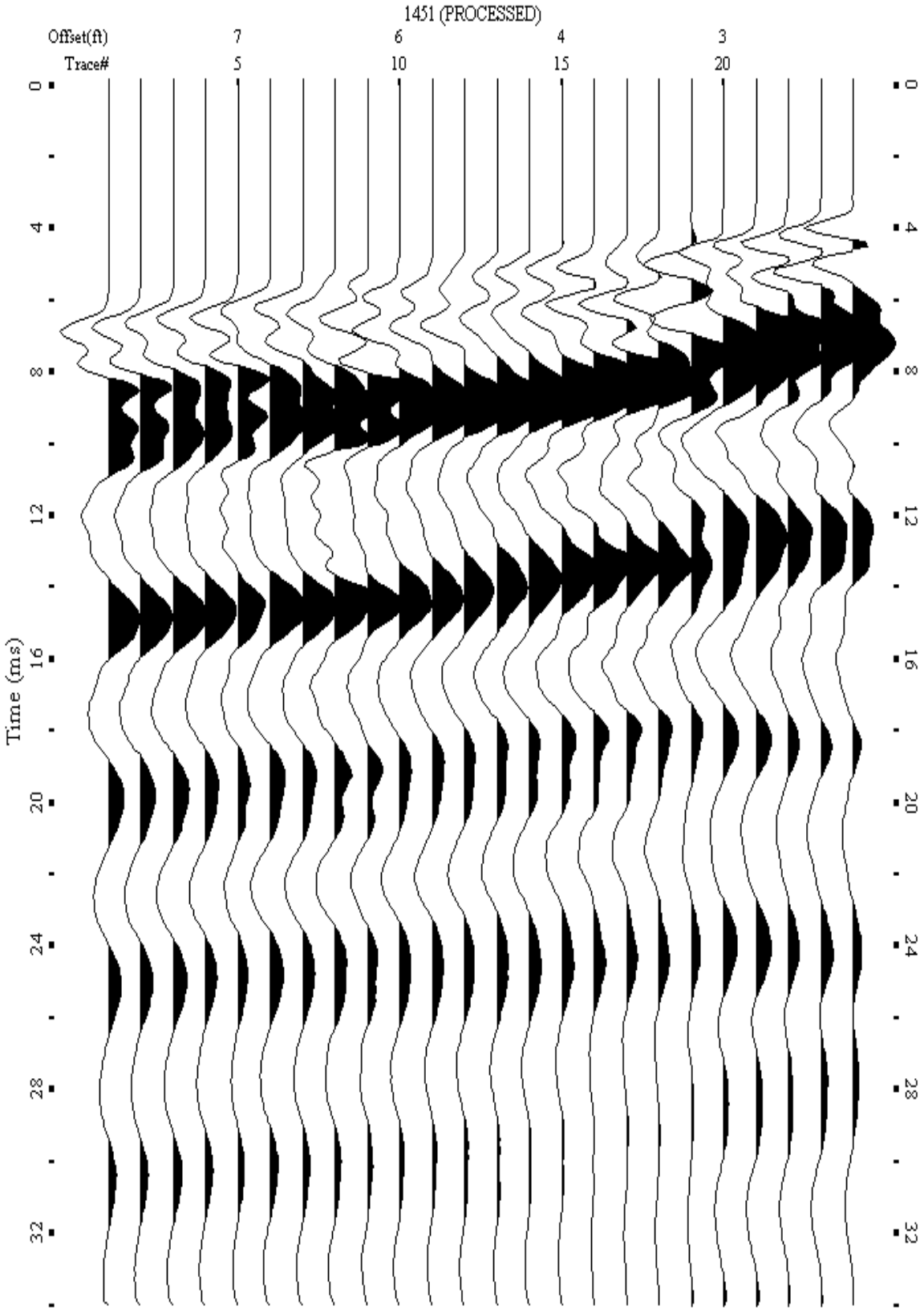

A.754: Shot Gather Line 1451 used in Post-blast 42

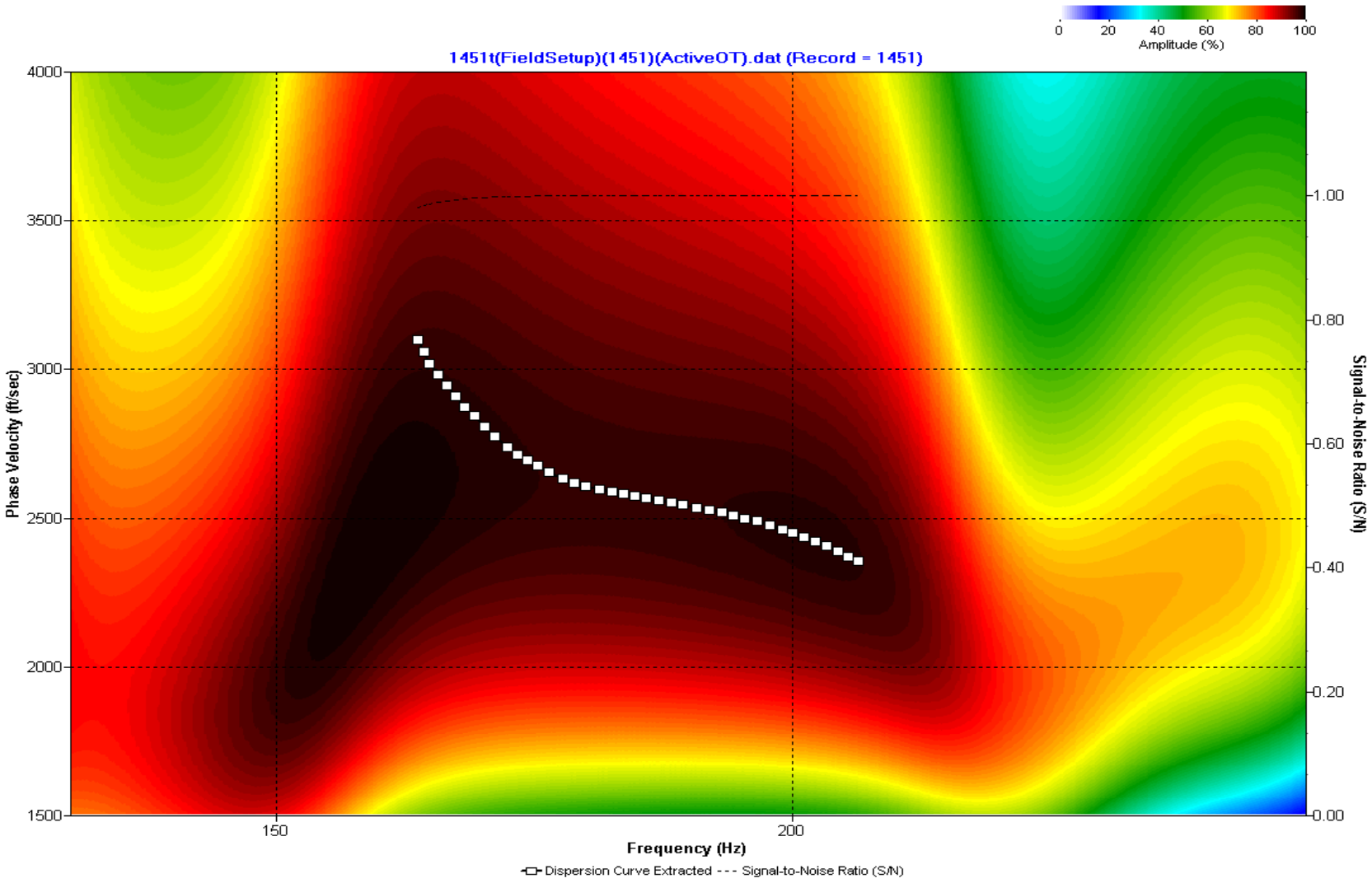

A.755: Dispersion Curve Line 1451 used in Post-blast 42

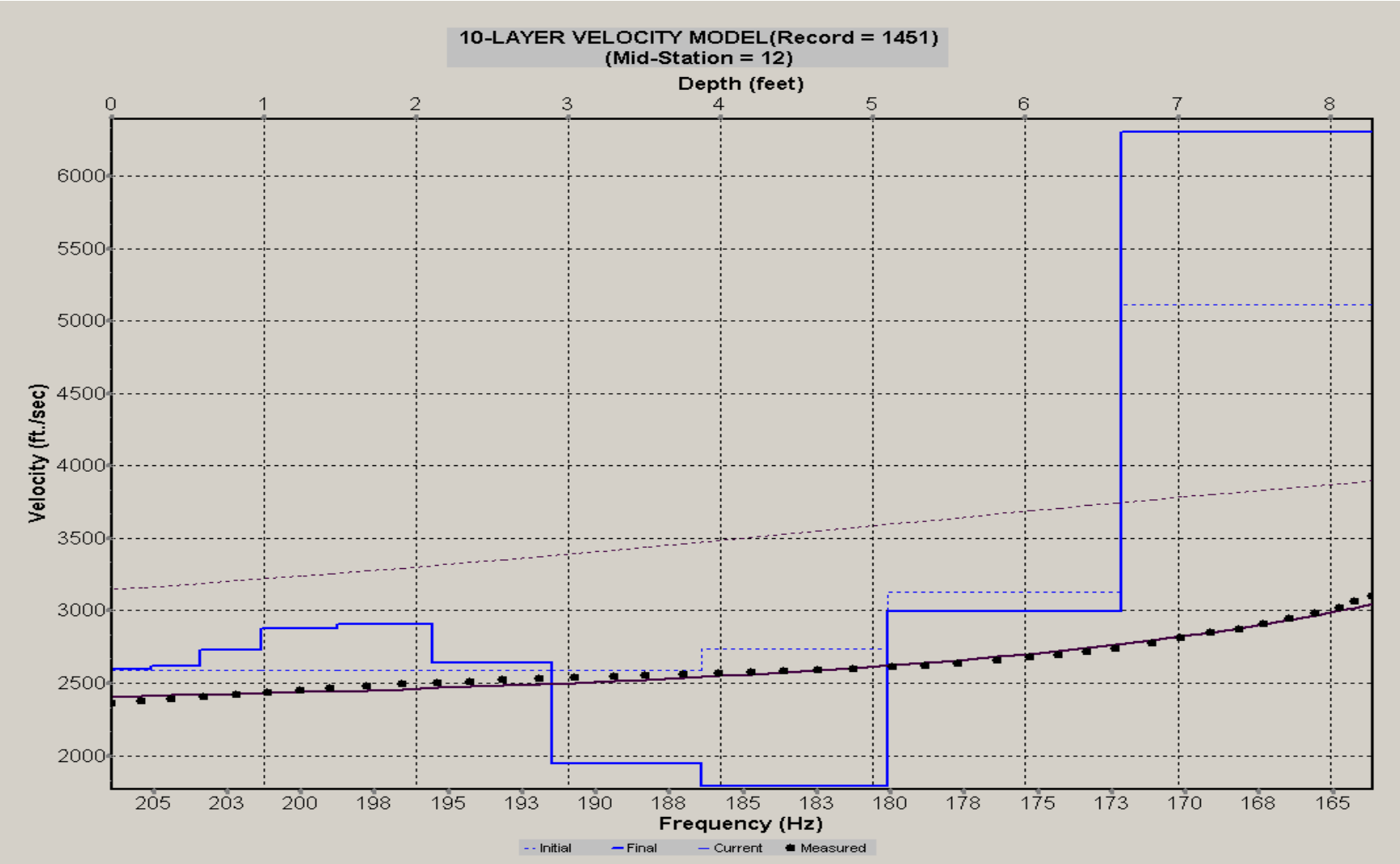

A.756: Velocity Profile Line 1451 used in Post-blast 42

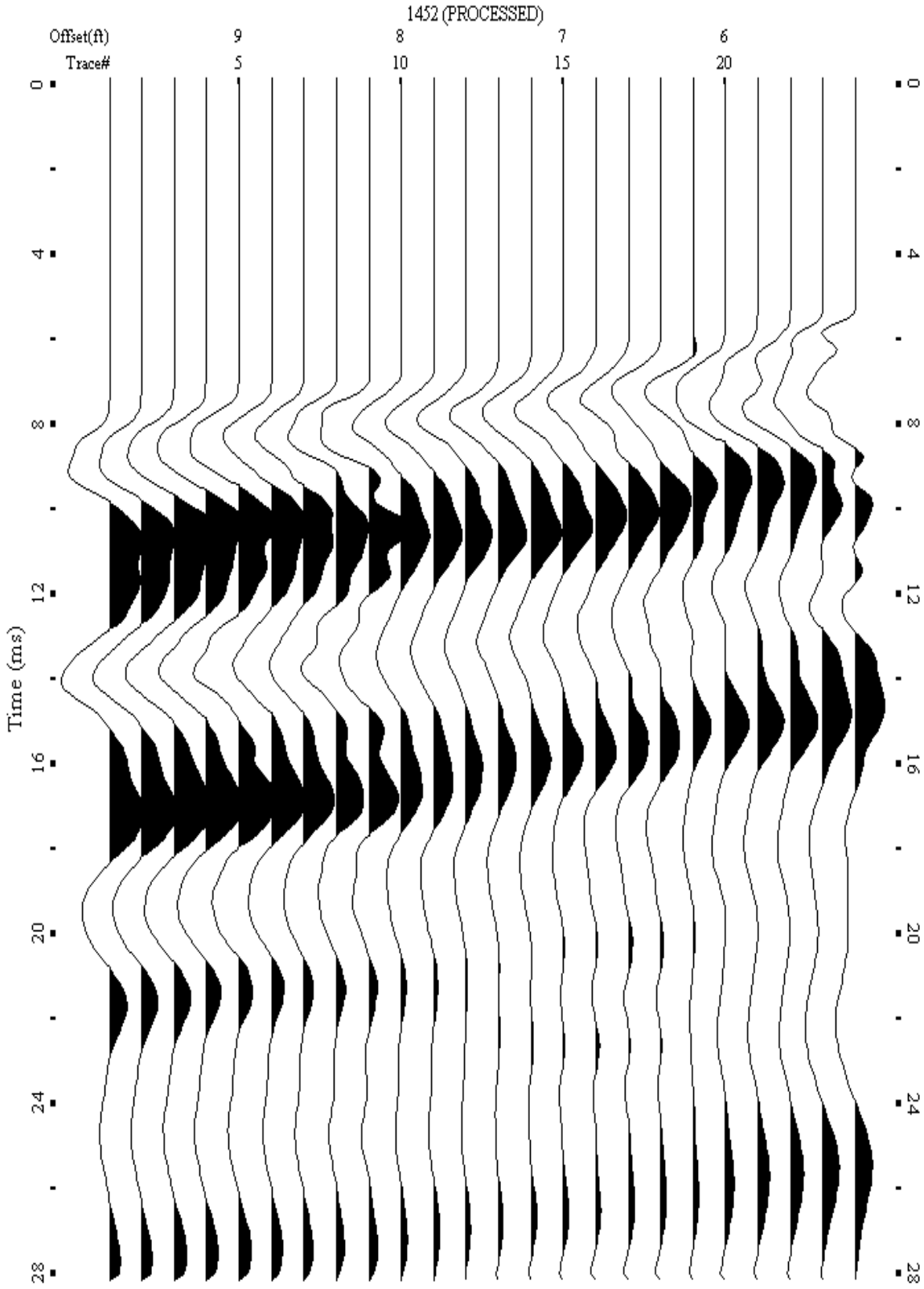

A.757: Shot Gather Line 1452 used in Post-blast 42

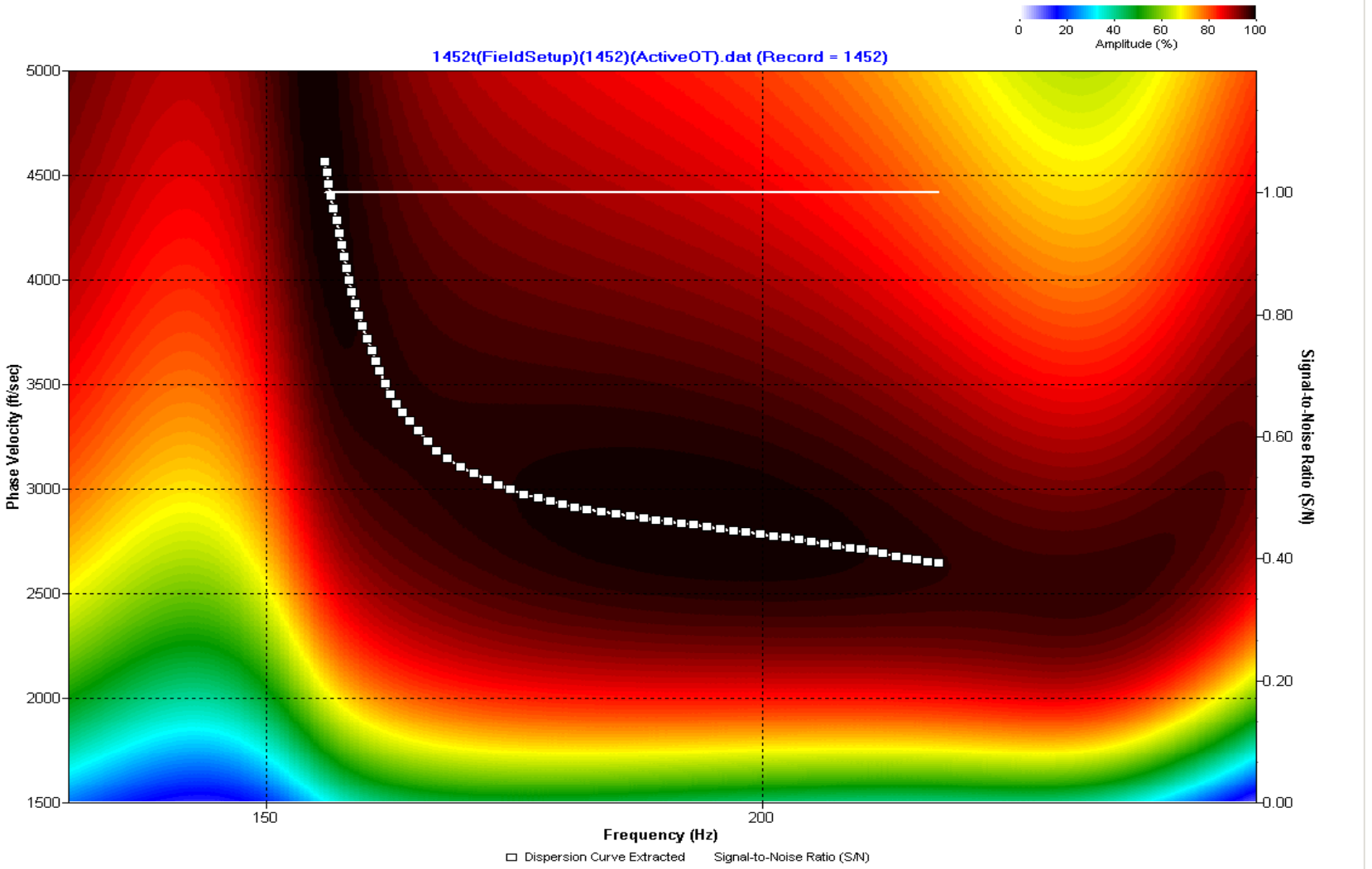

A.758: Dispersion Curve Line 1452 used in Post-blast 42

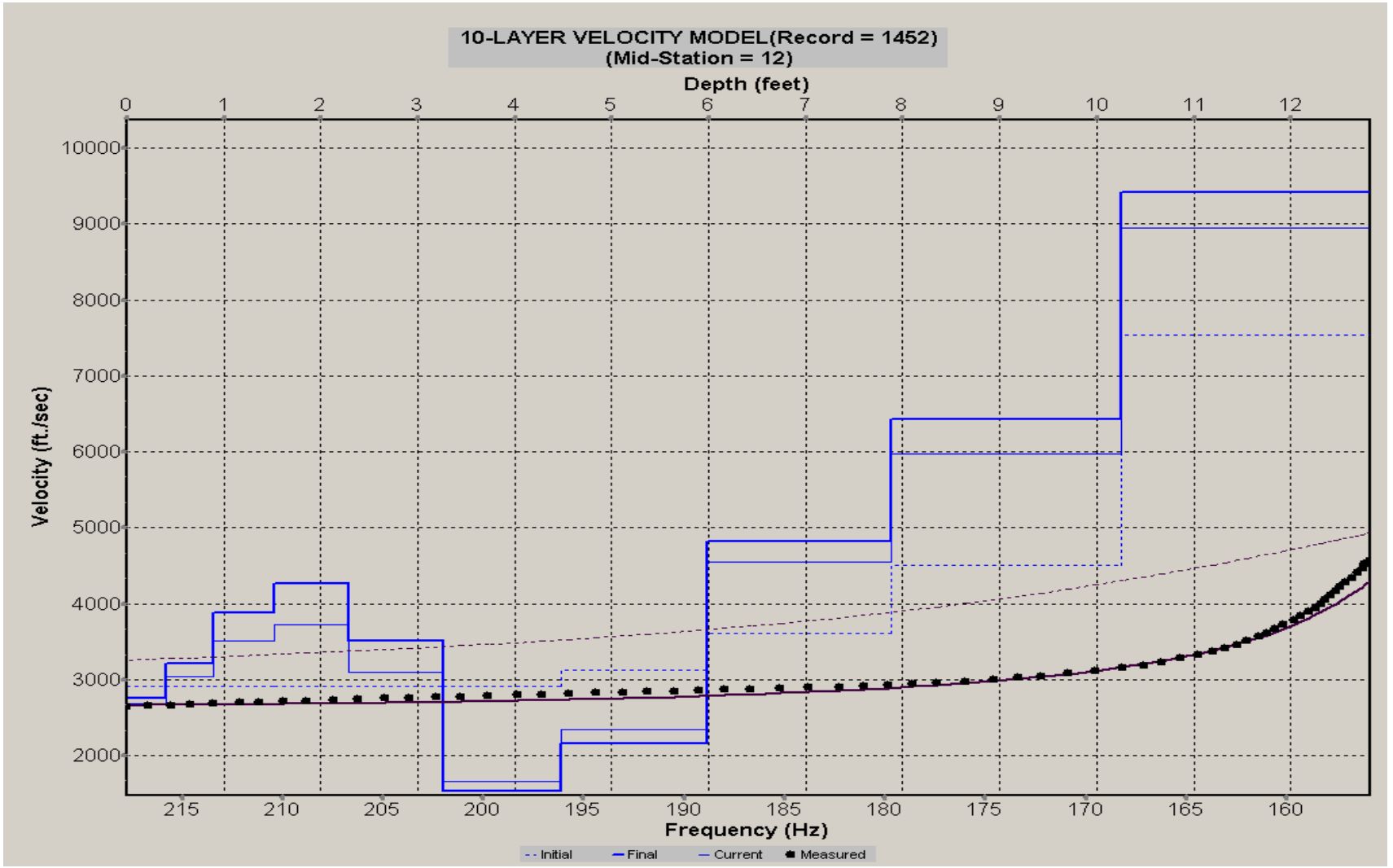

A.759: Velocity Profile Line 1452 used in Post-blast 42

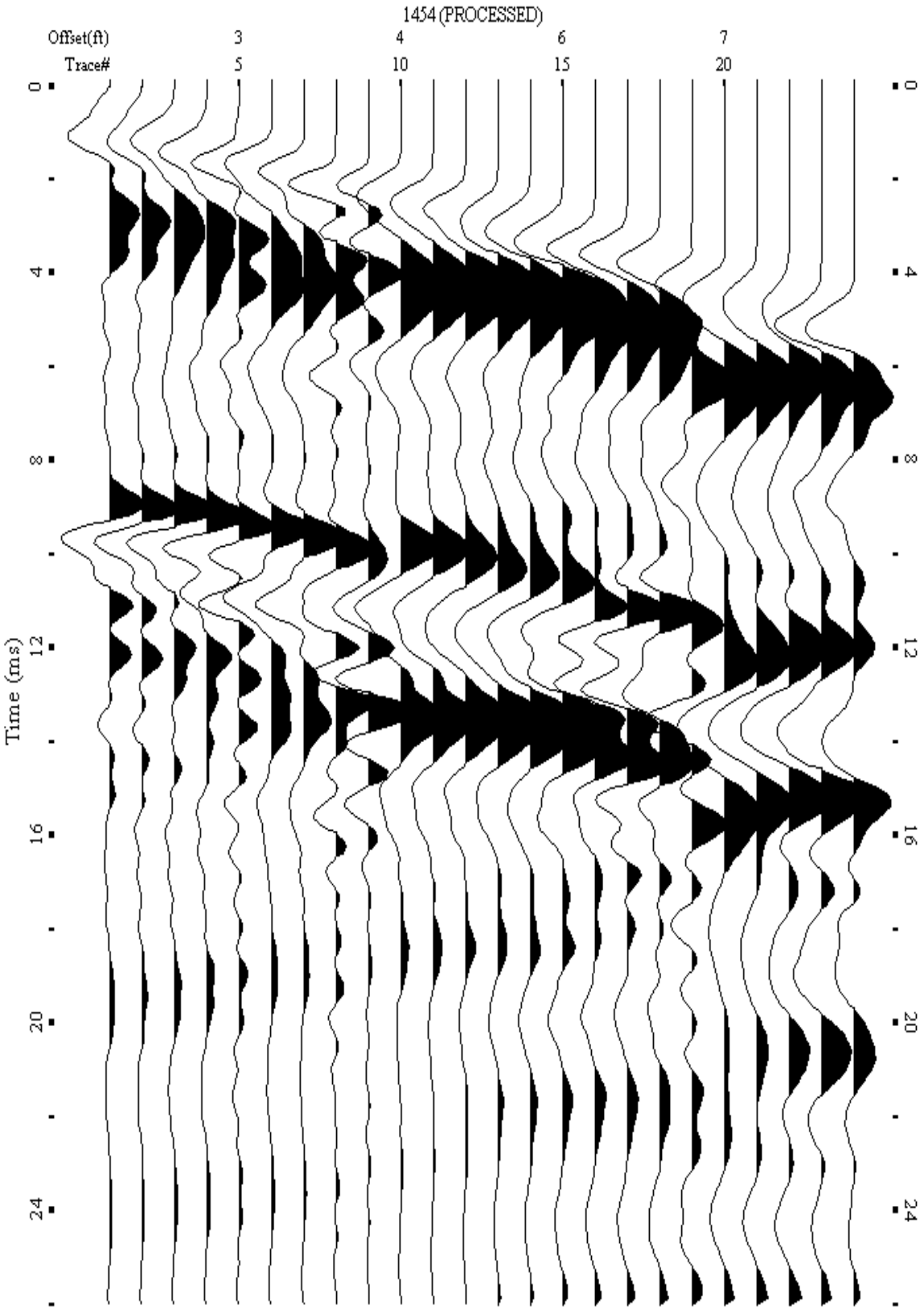

A.760: Shot Gather Line 1454 used in Post-blast 41 and Post-blast 42

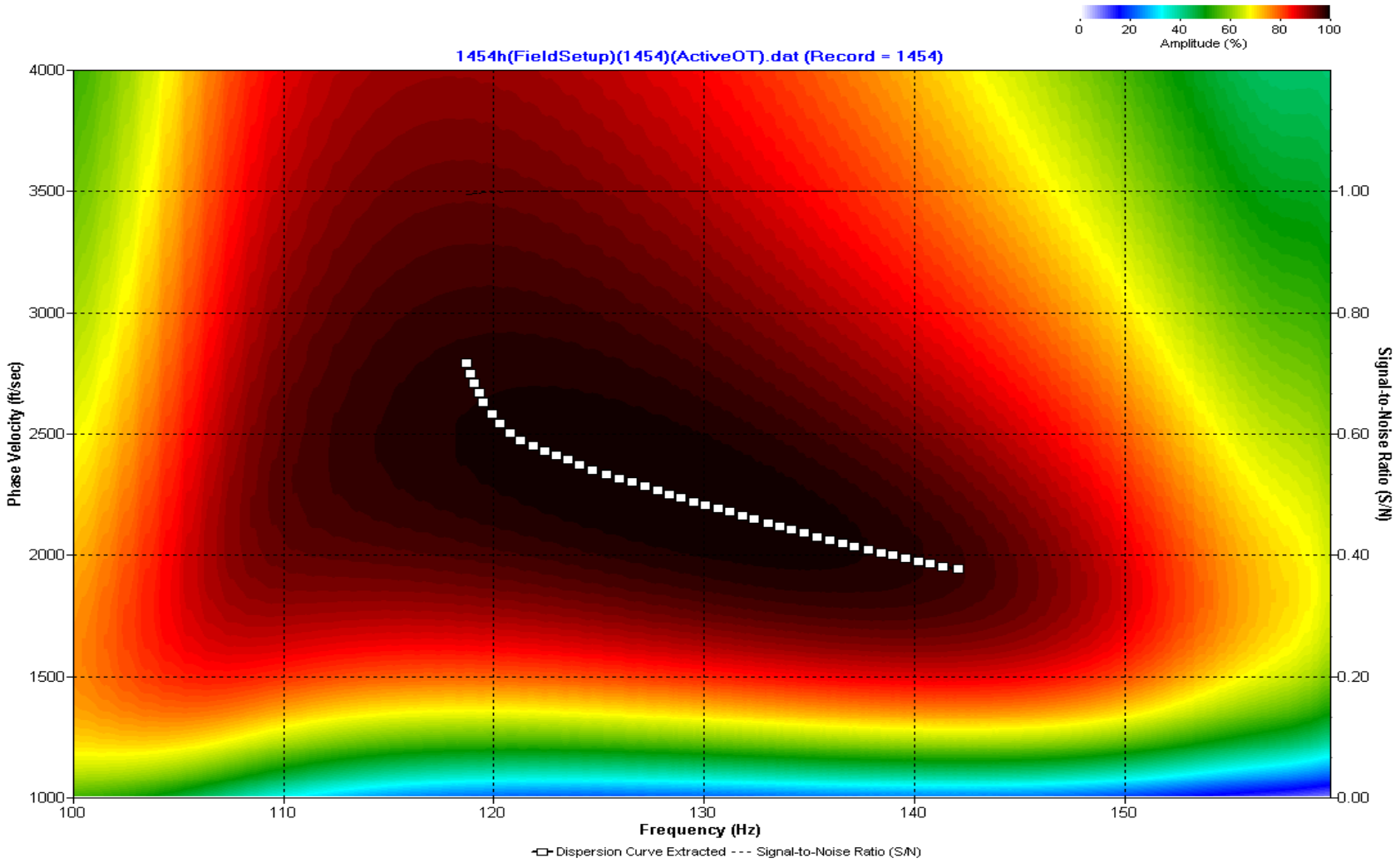

A.761: Dispersion Curve Line 1454 used in Post-blast 41 and Post-blast 42

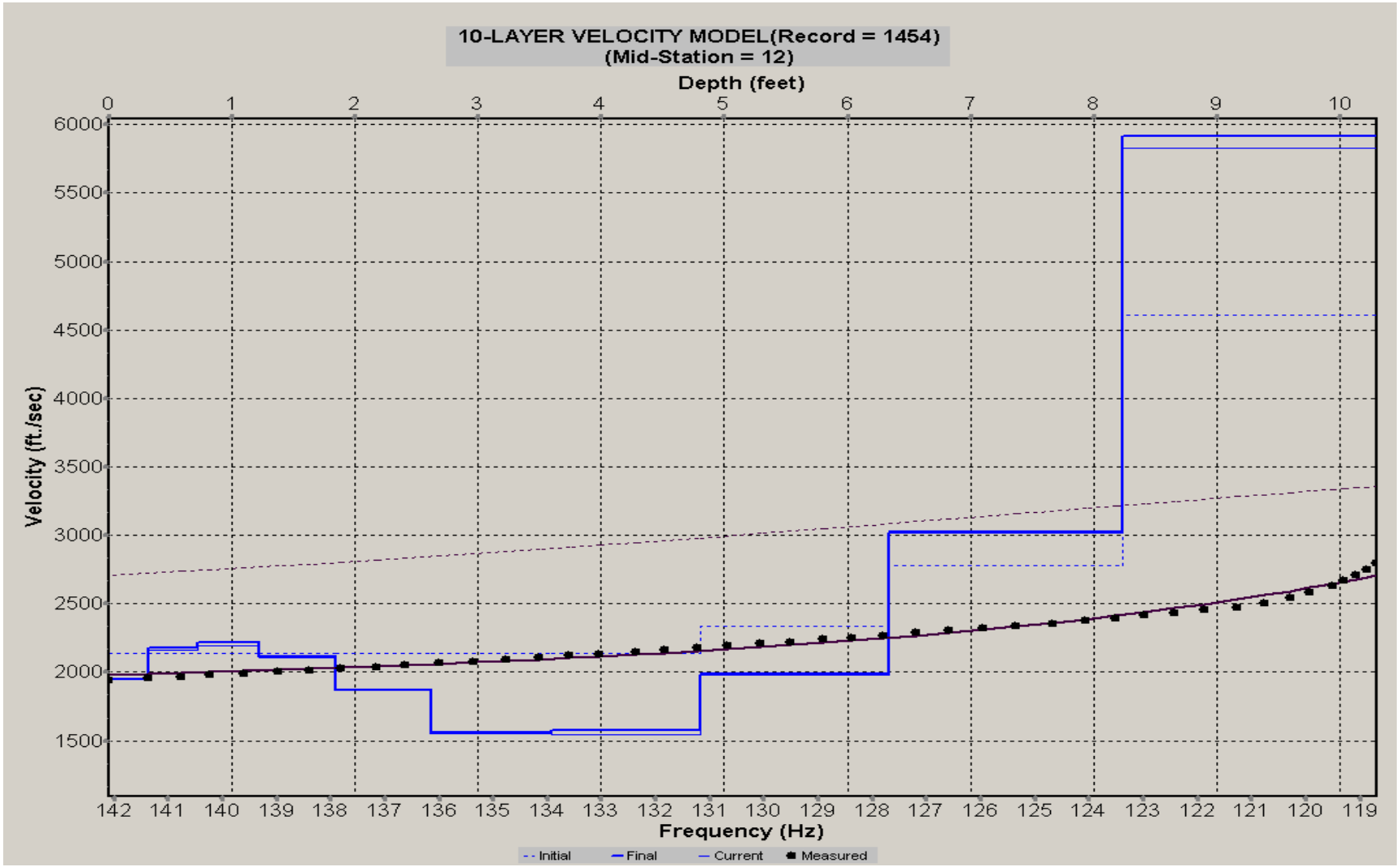

A.762: Velocity Profile Line 1454 used in Post-blast 41 and Post-blast 42

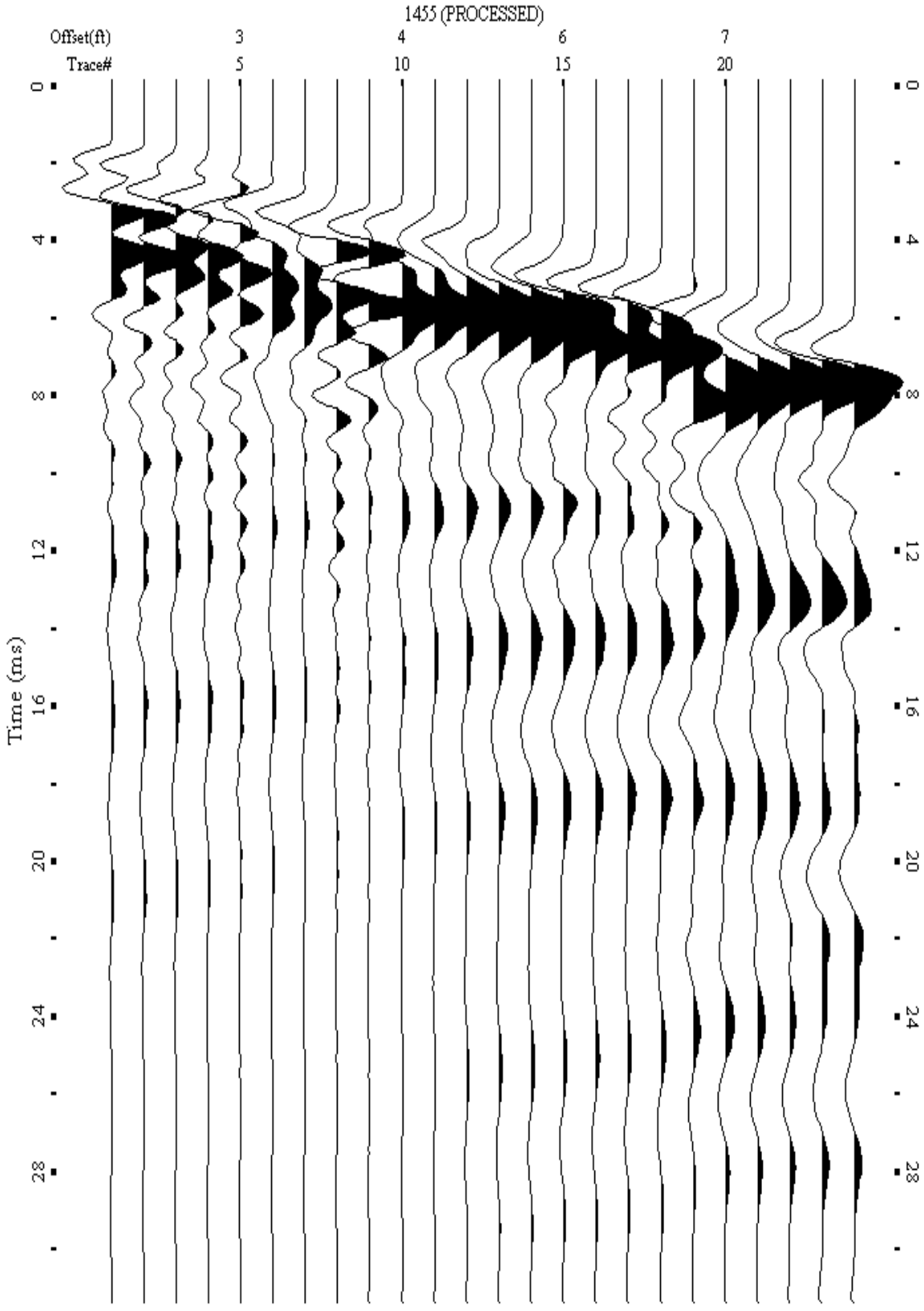

A.763: Shot Gather Line 1455 used in Post-blast 41 and Post-blast 42

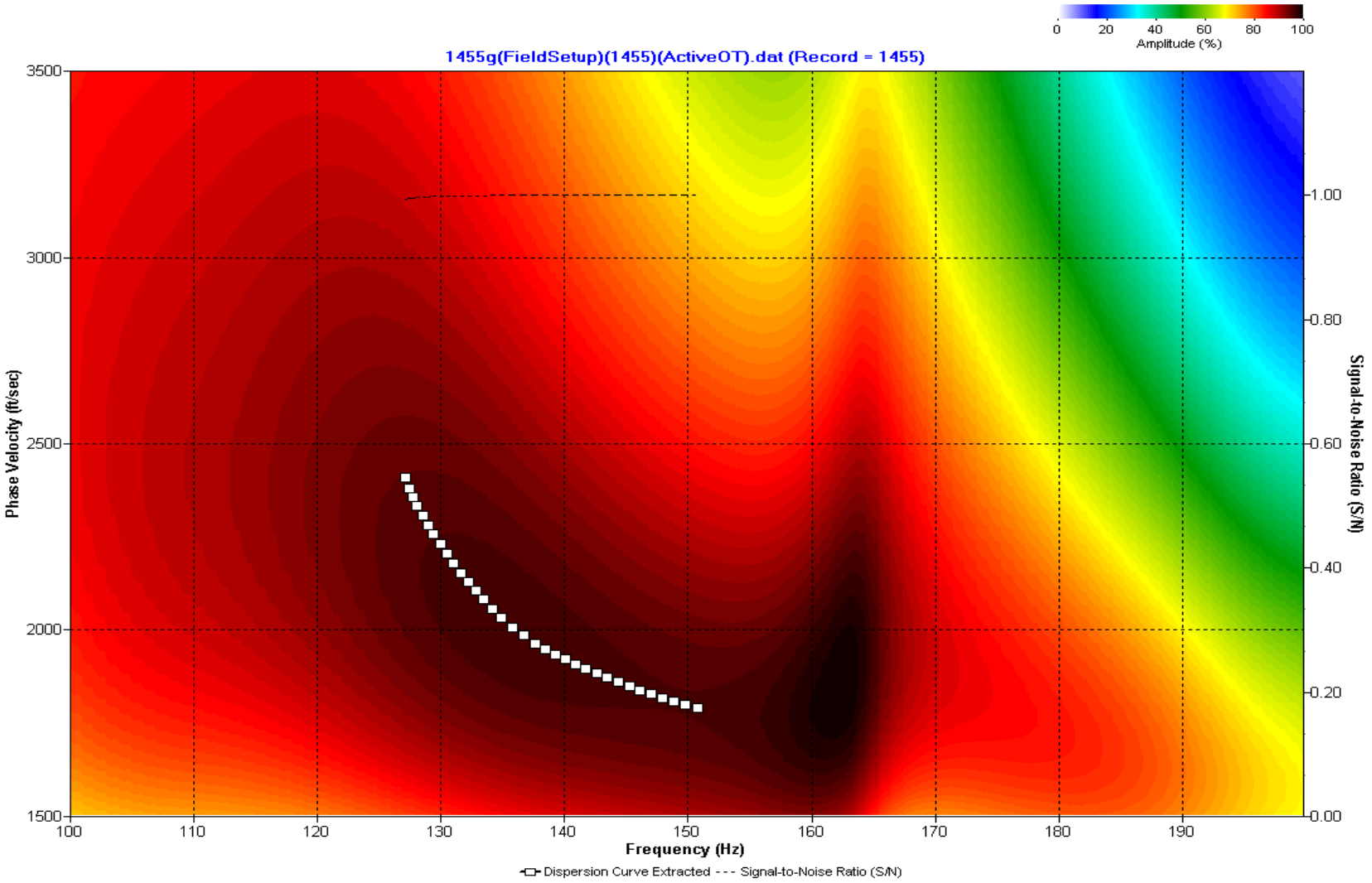

A.764: Dispersion Curve Line 1455 used in Post-blast 41 and Post-blast 42

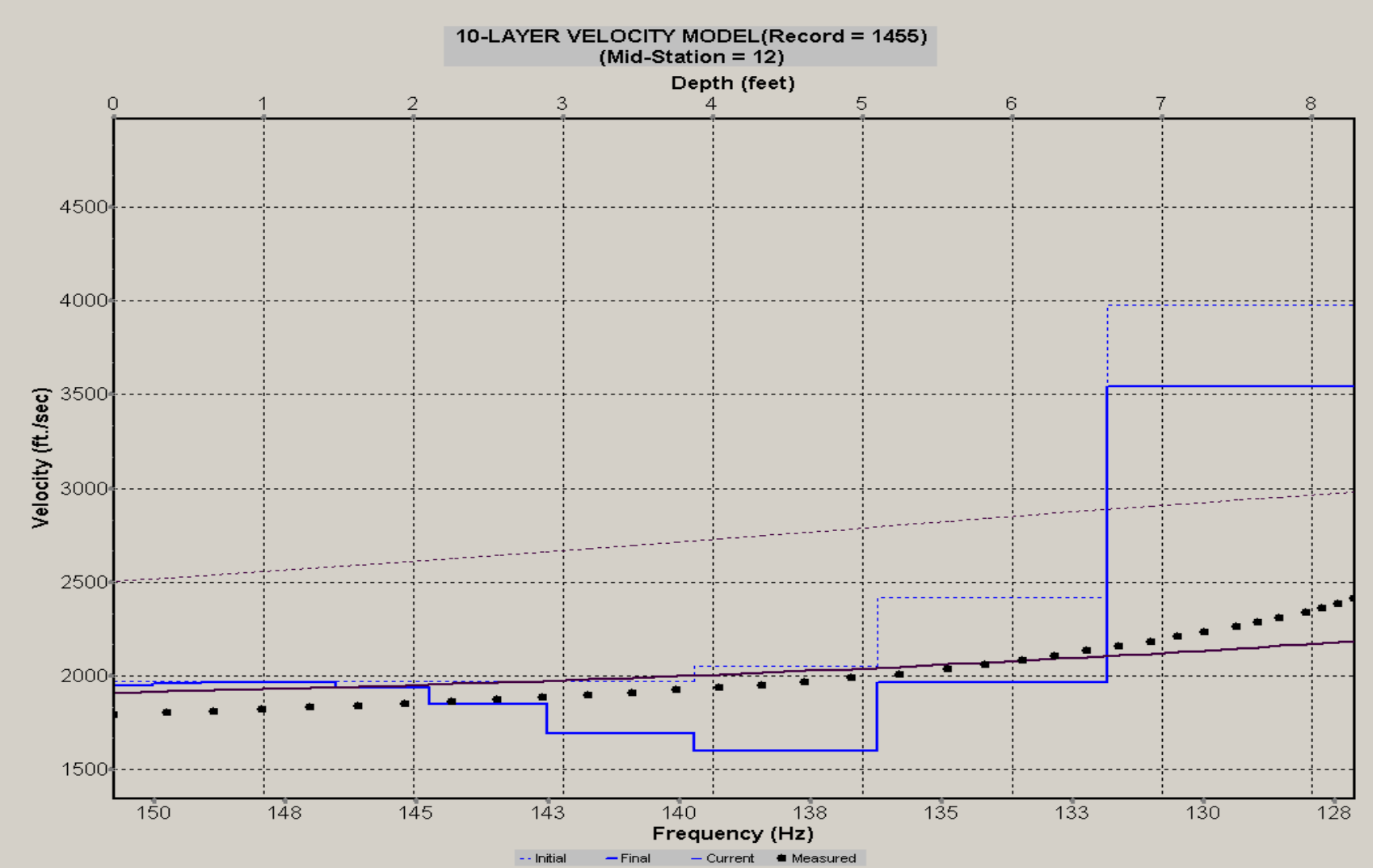

A.765: Velocity Profile Line 1455 used in Post-blast 41 and Post-blast 42

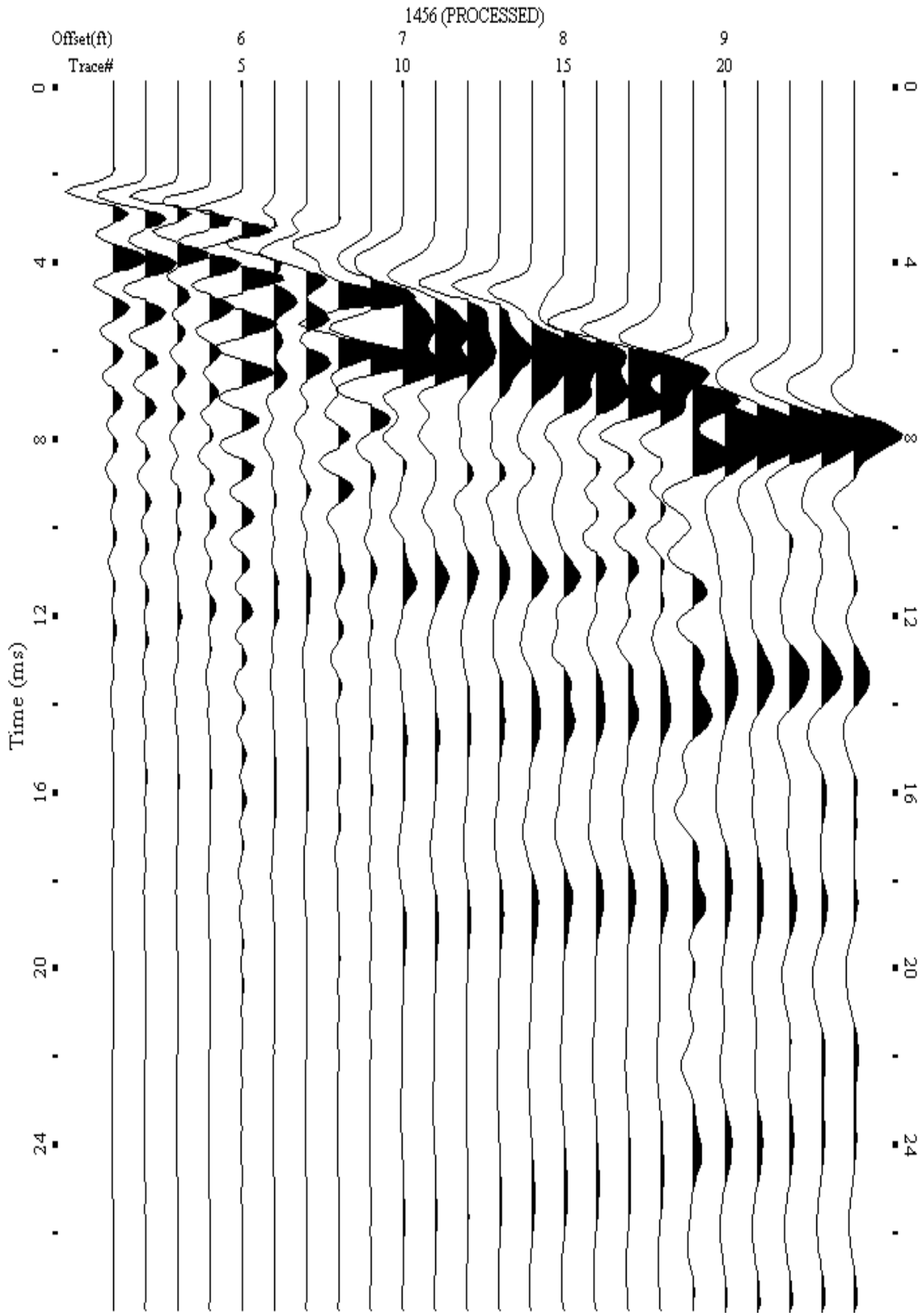

A.766: Shot Gather Line 1456 used in Post-blast 42

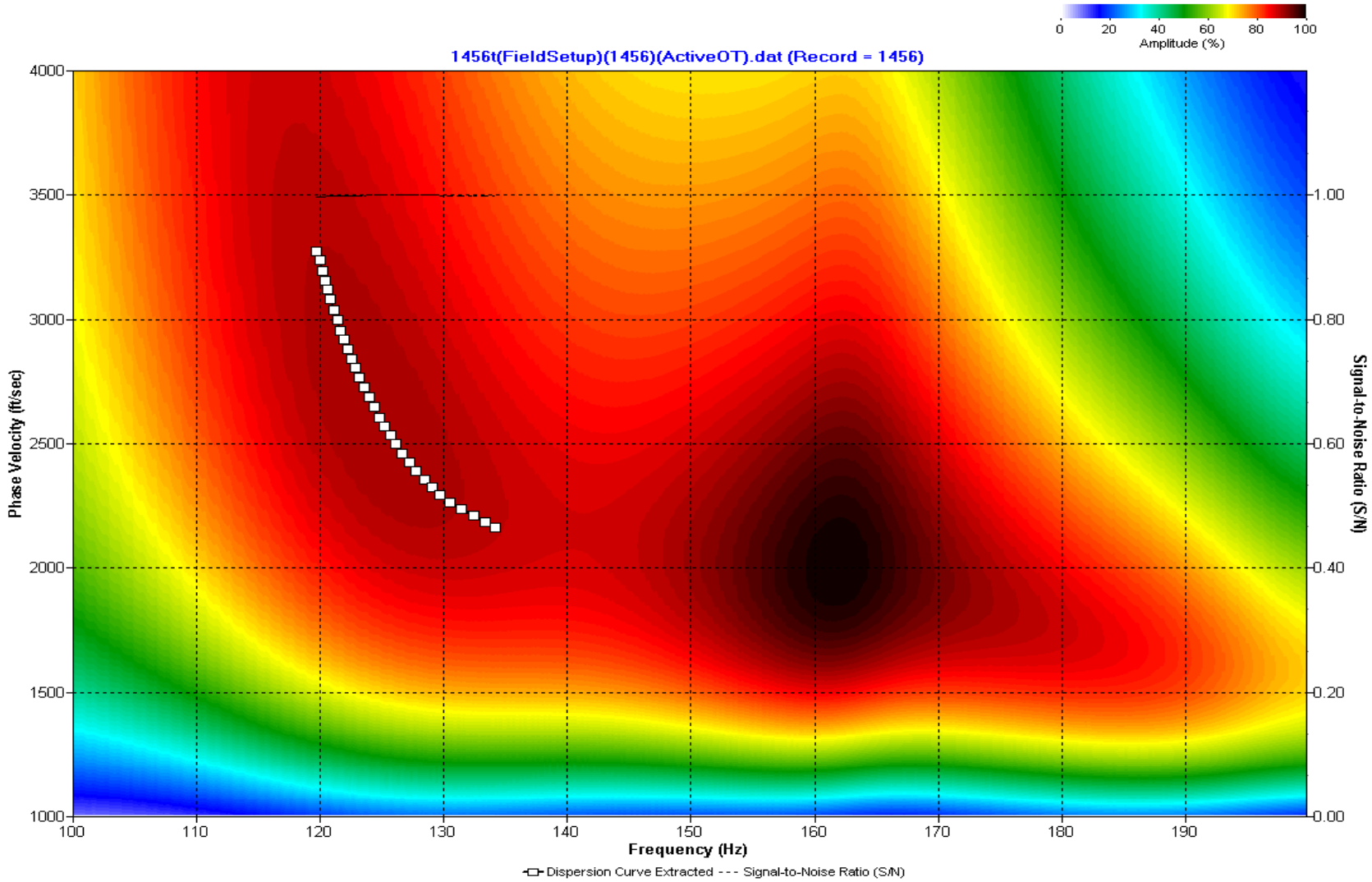

A.767: Dispersion Curve Line 1456 used in Post-blast 42

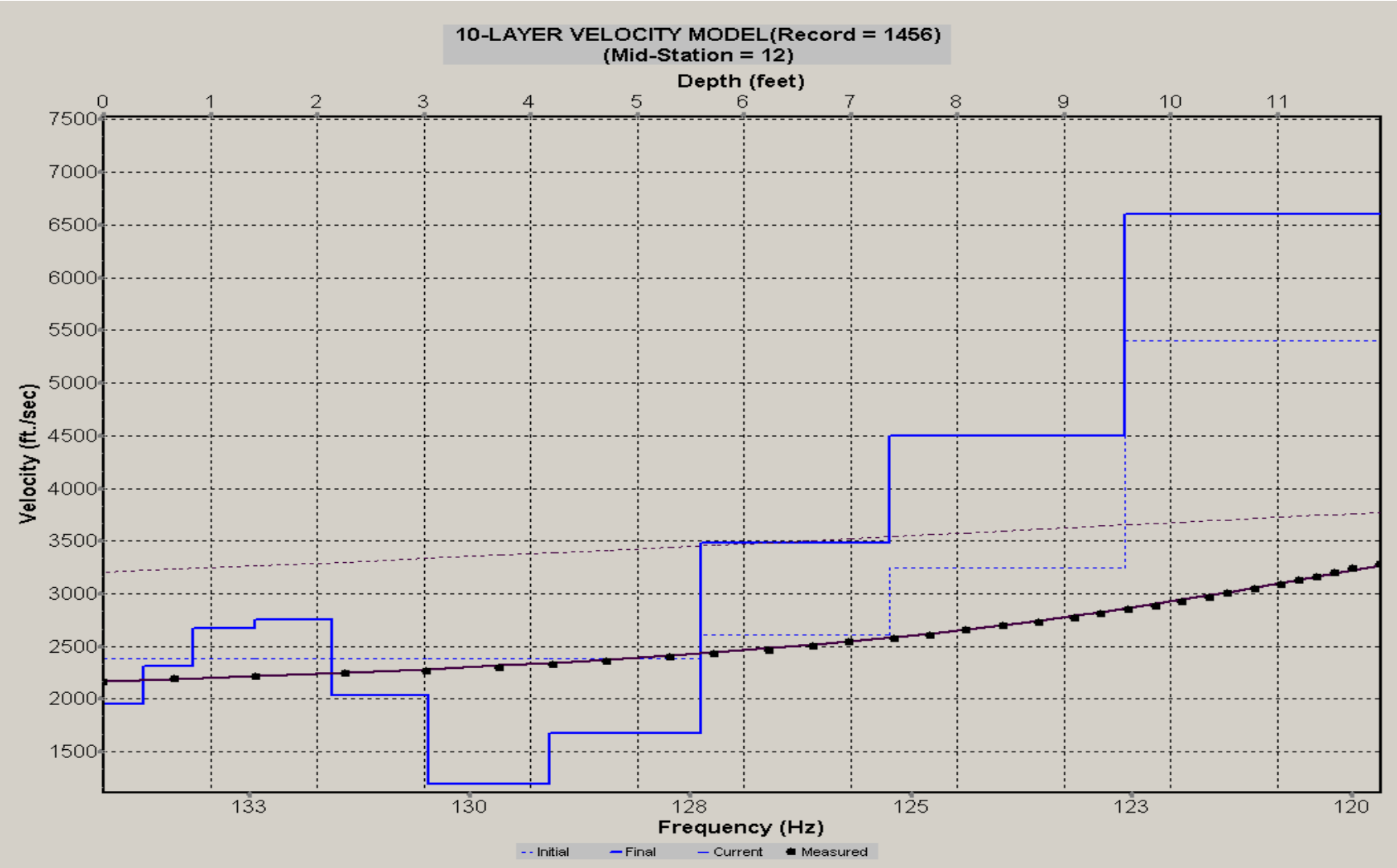

A.768: Velocity Profile Line 1456 used in Post-blast 42

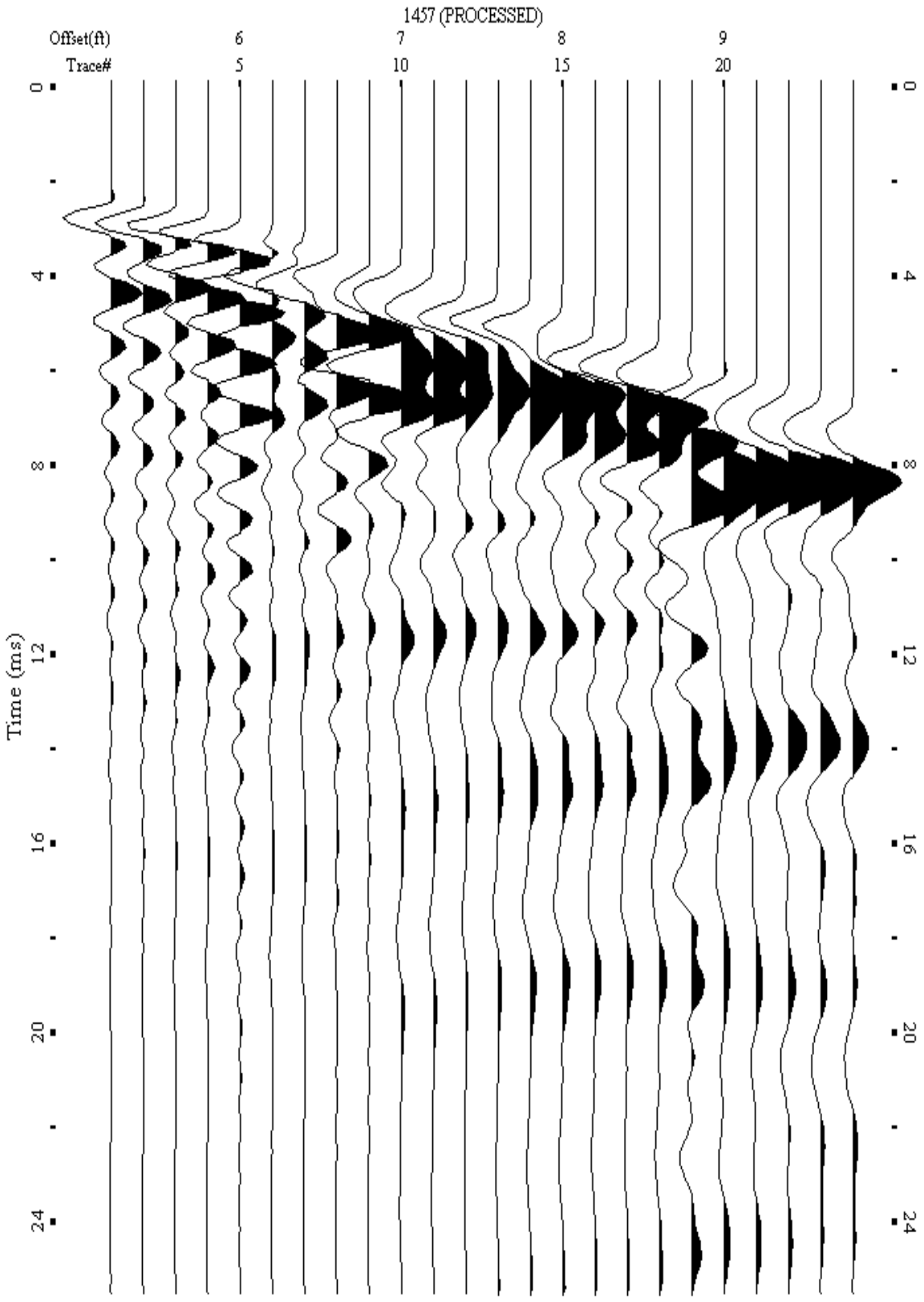

A.769: Shot Gather Line 1457 used in Post-blast 41 and Post-blast 42

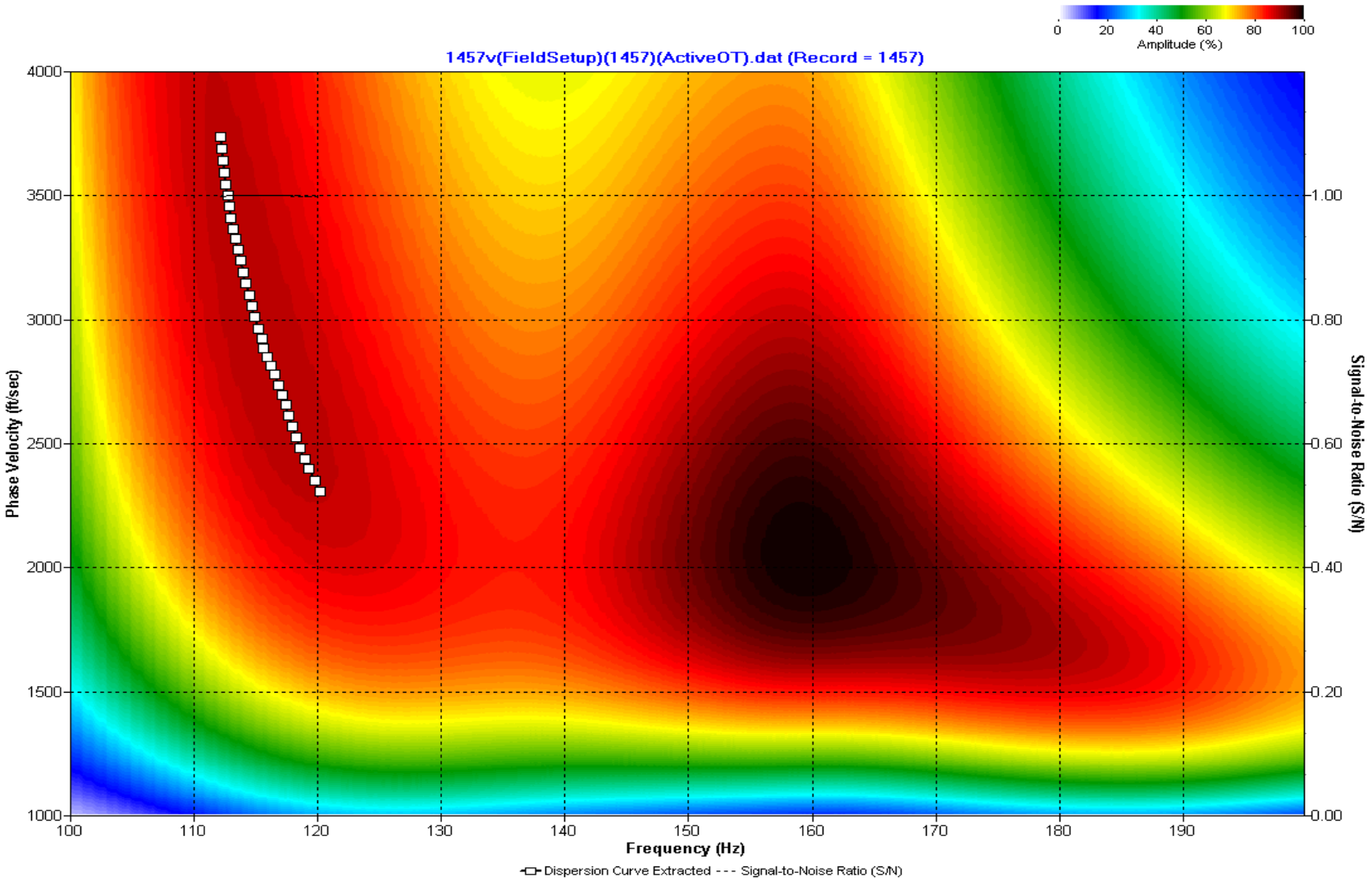

A.770: Dispersion Curve Line 1457 used in Post-blast 41 and Post-blast 42

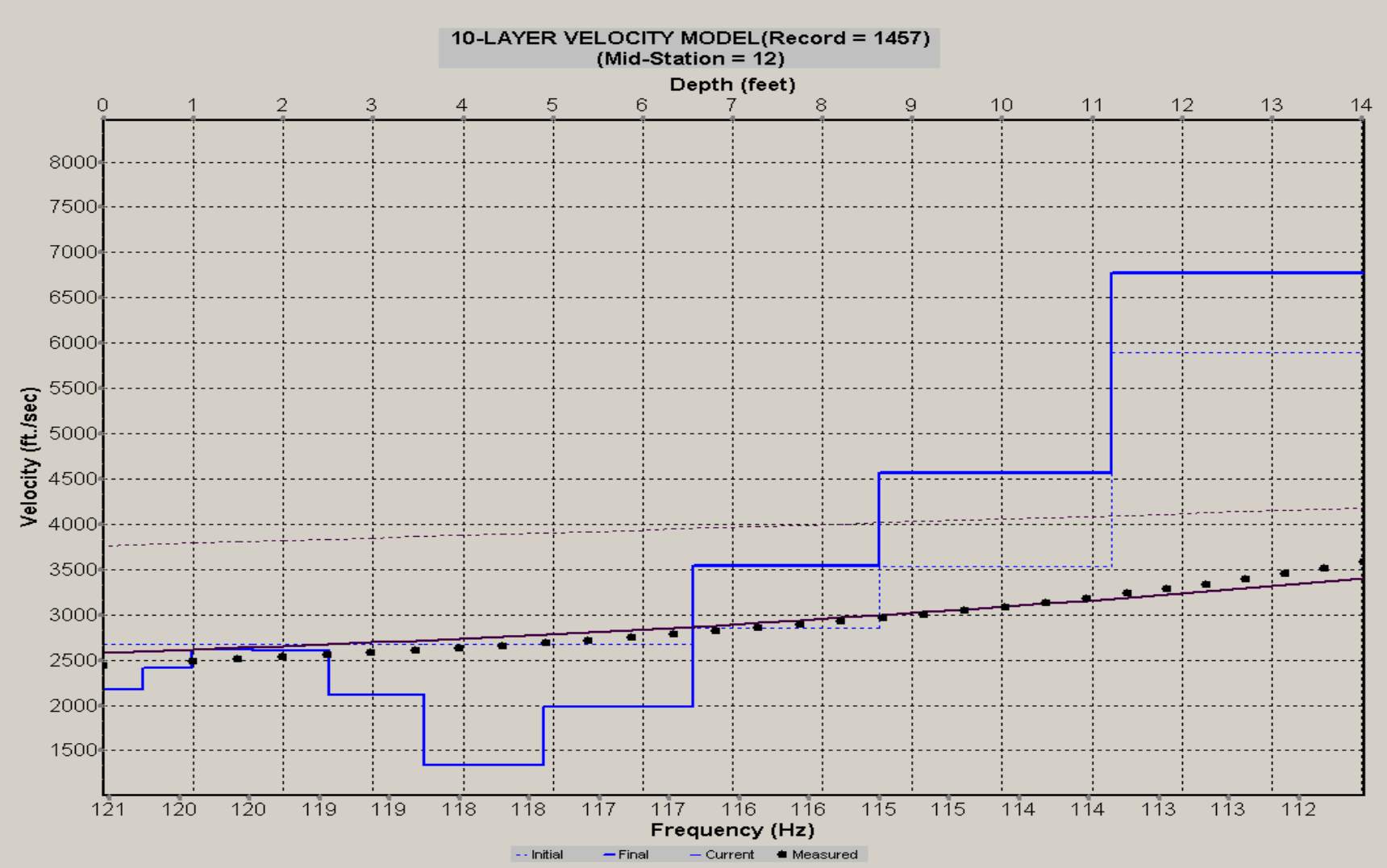

A.771: Velocity Profile Line 1457 used in Post-blast 41 and Post-blast 42

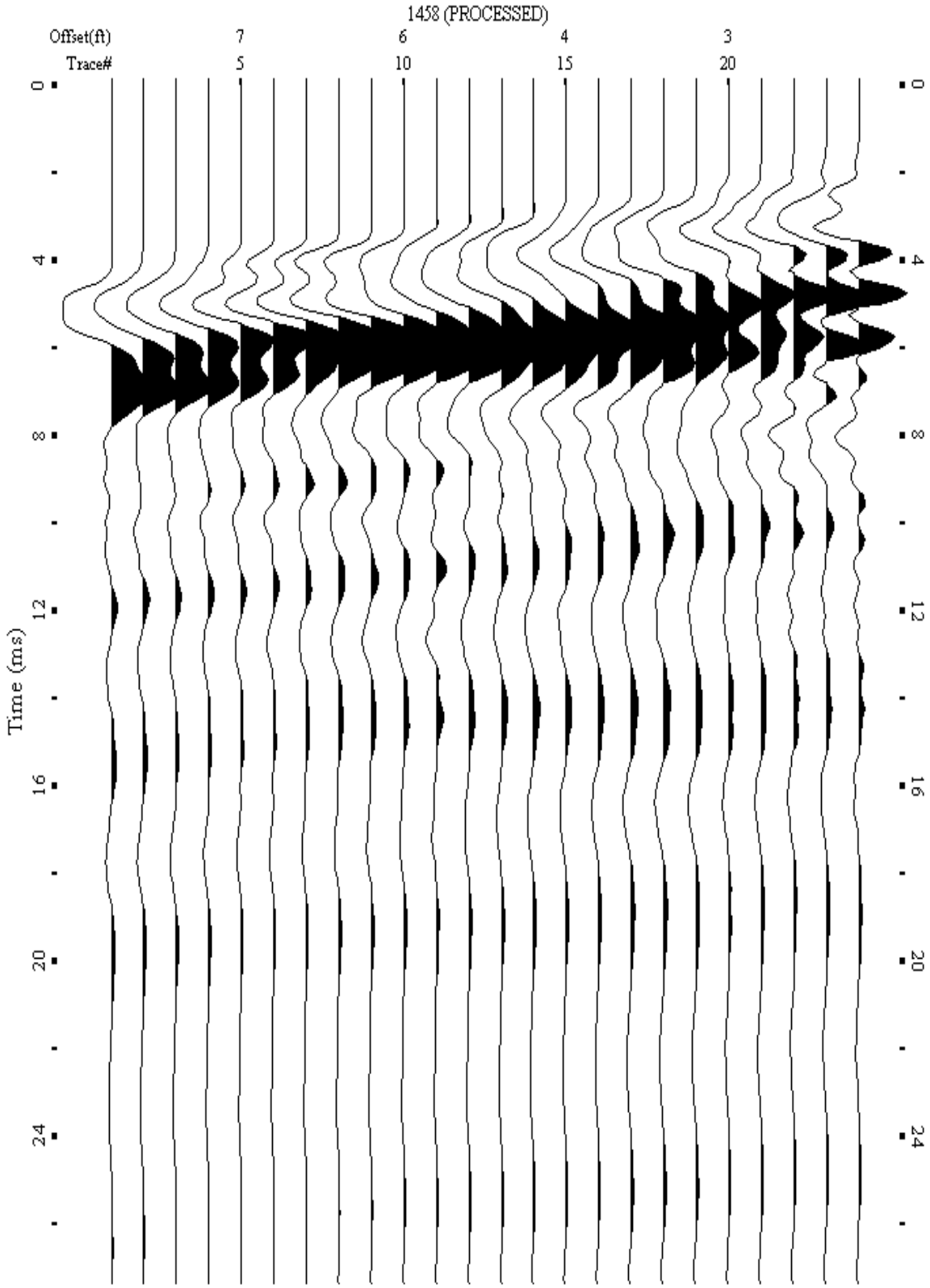

A.772: Shot Gather Line 1458 used in Post-blast 43

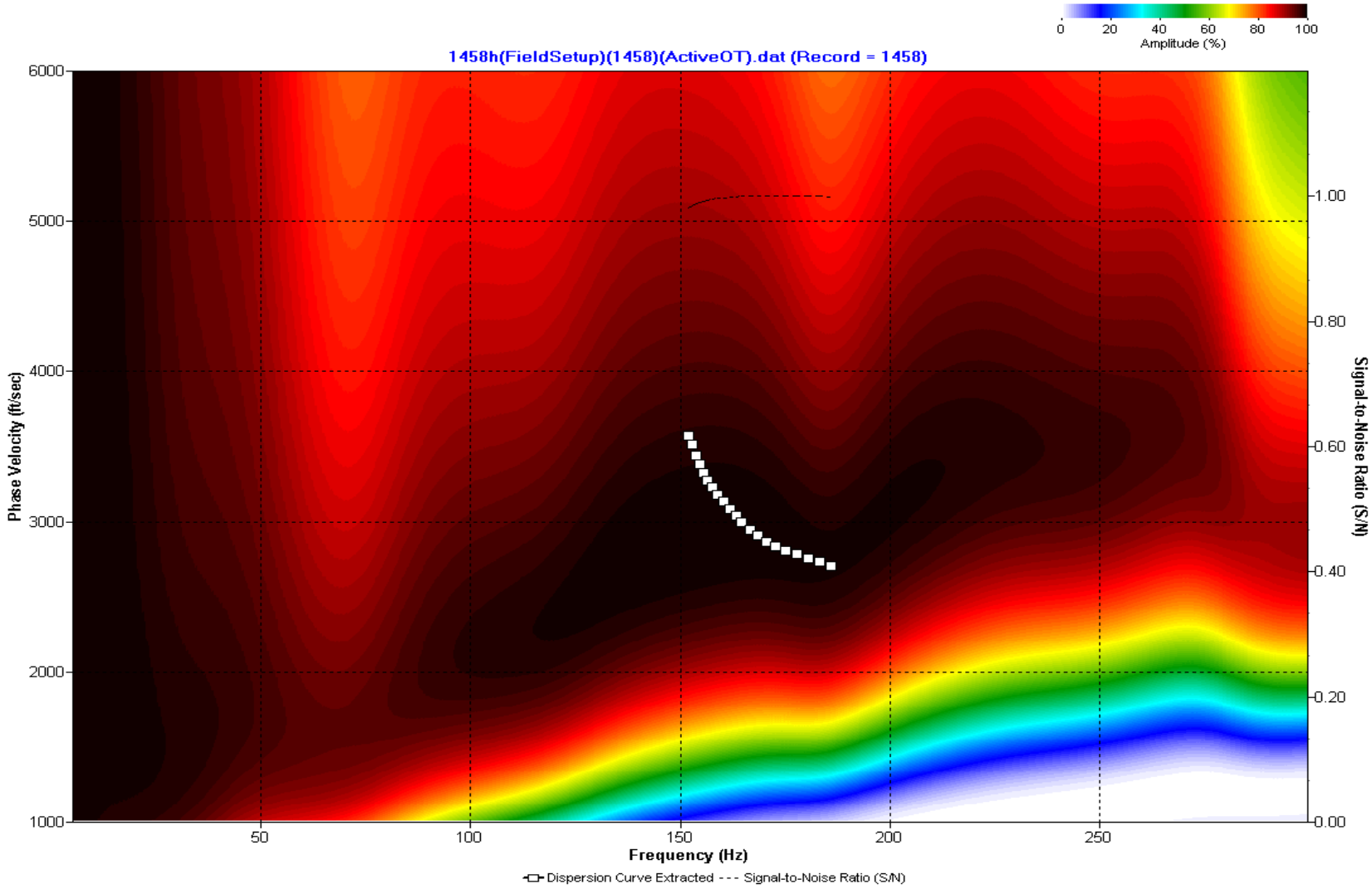

A.773: Dispersion Curve Line 1458 used in Post-blast 43

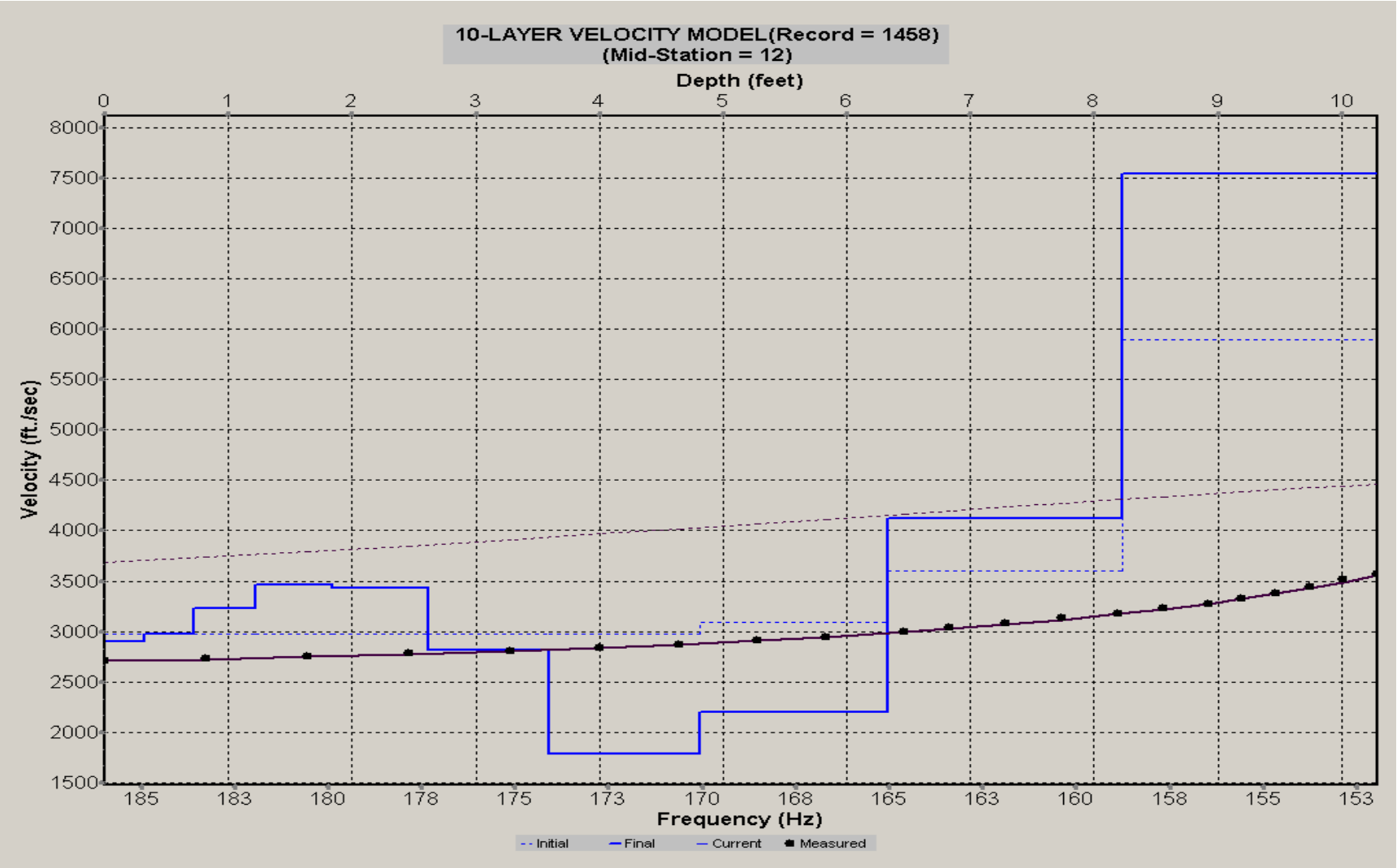

A.774: Velocity Profile Line 1458 used in Post-blast 43

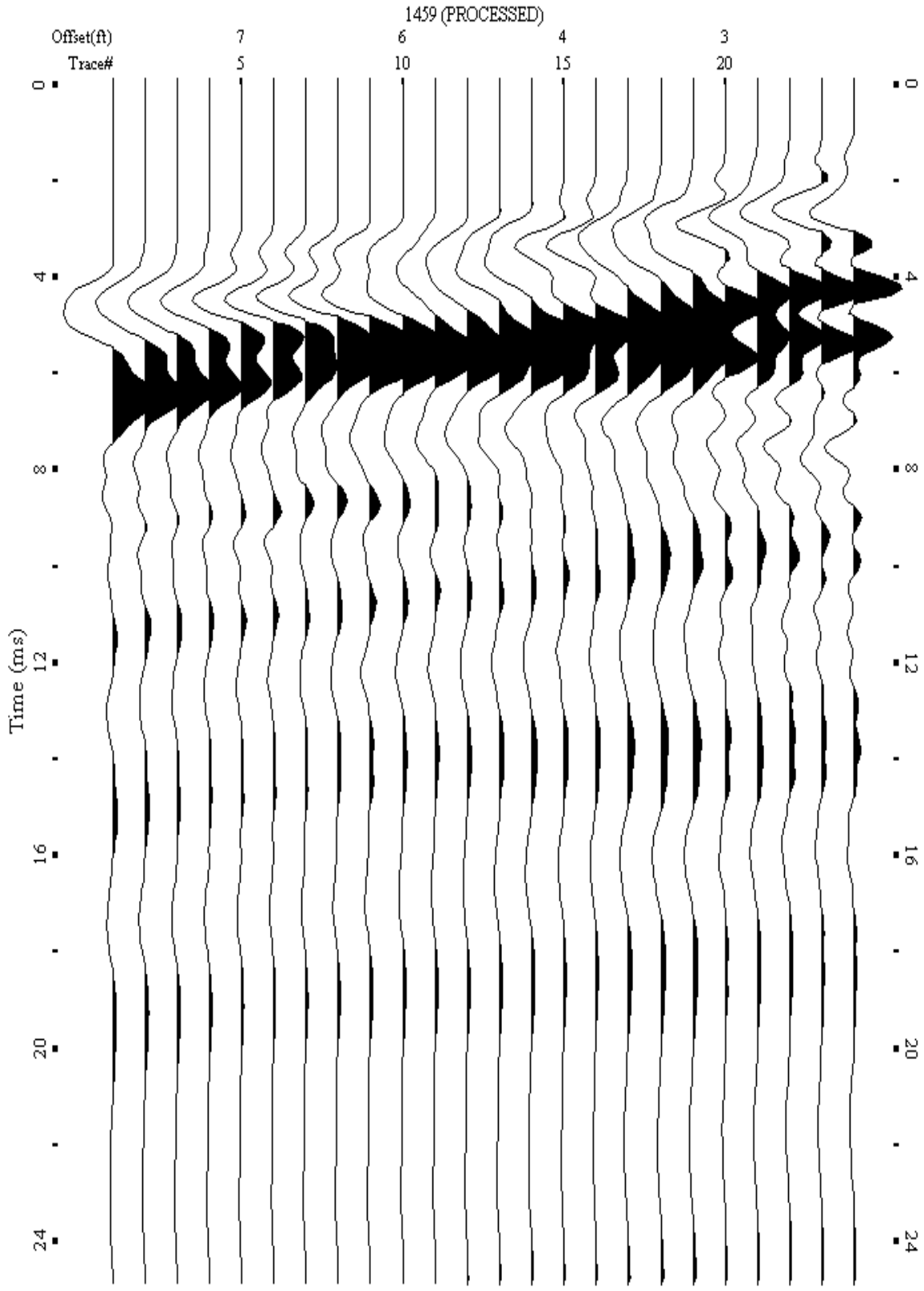

A.775: Shot Gather Line 1459 used in Post-blast 43

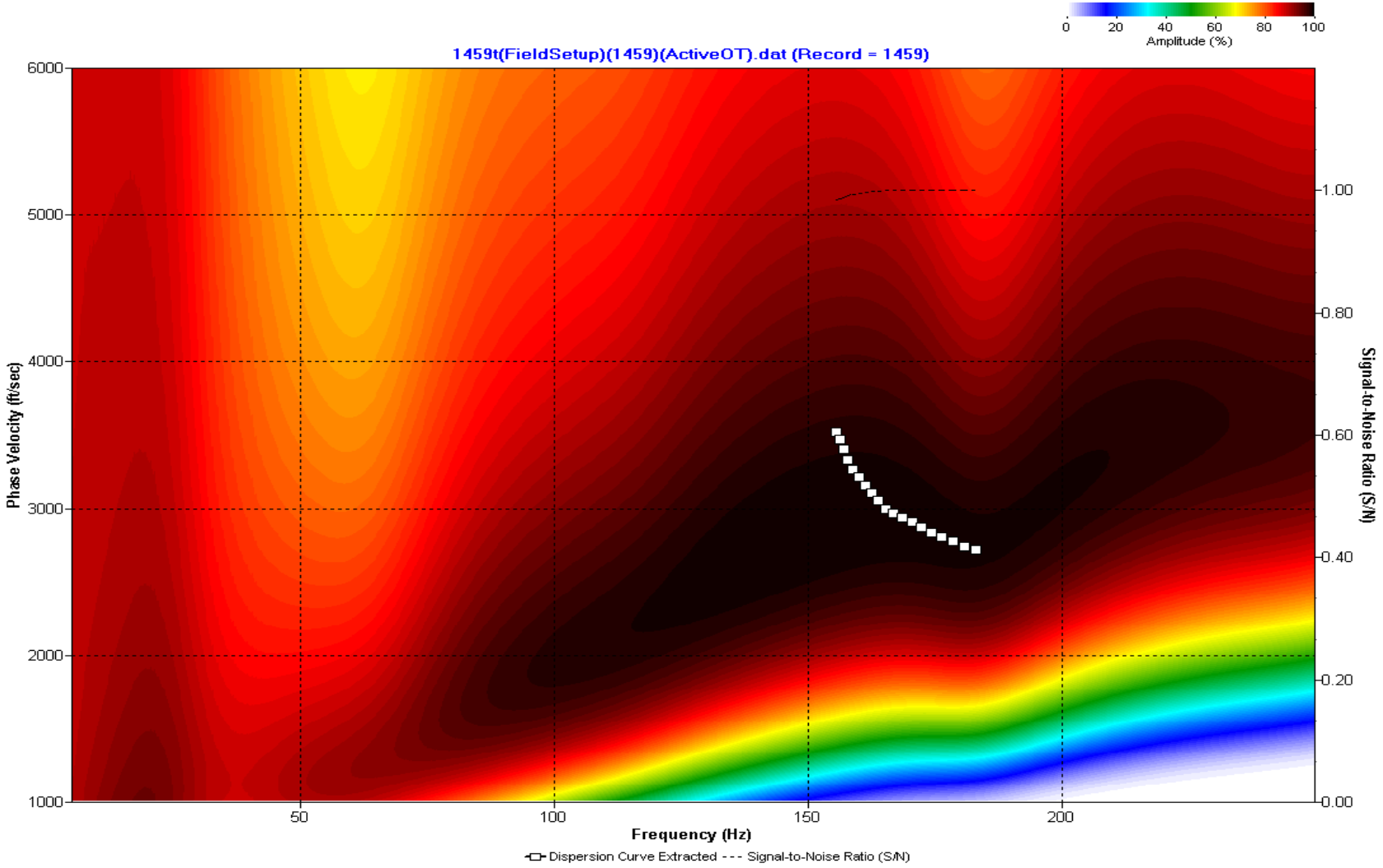

A.776: Dispersion Curve Line 1459 used in Post-blast 43

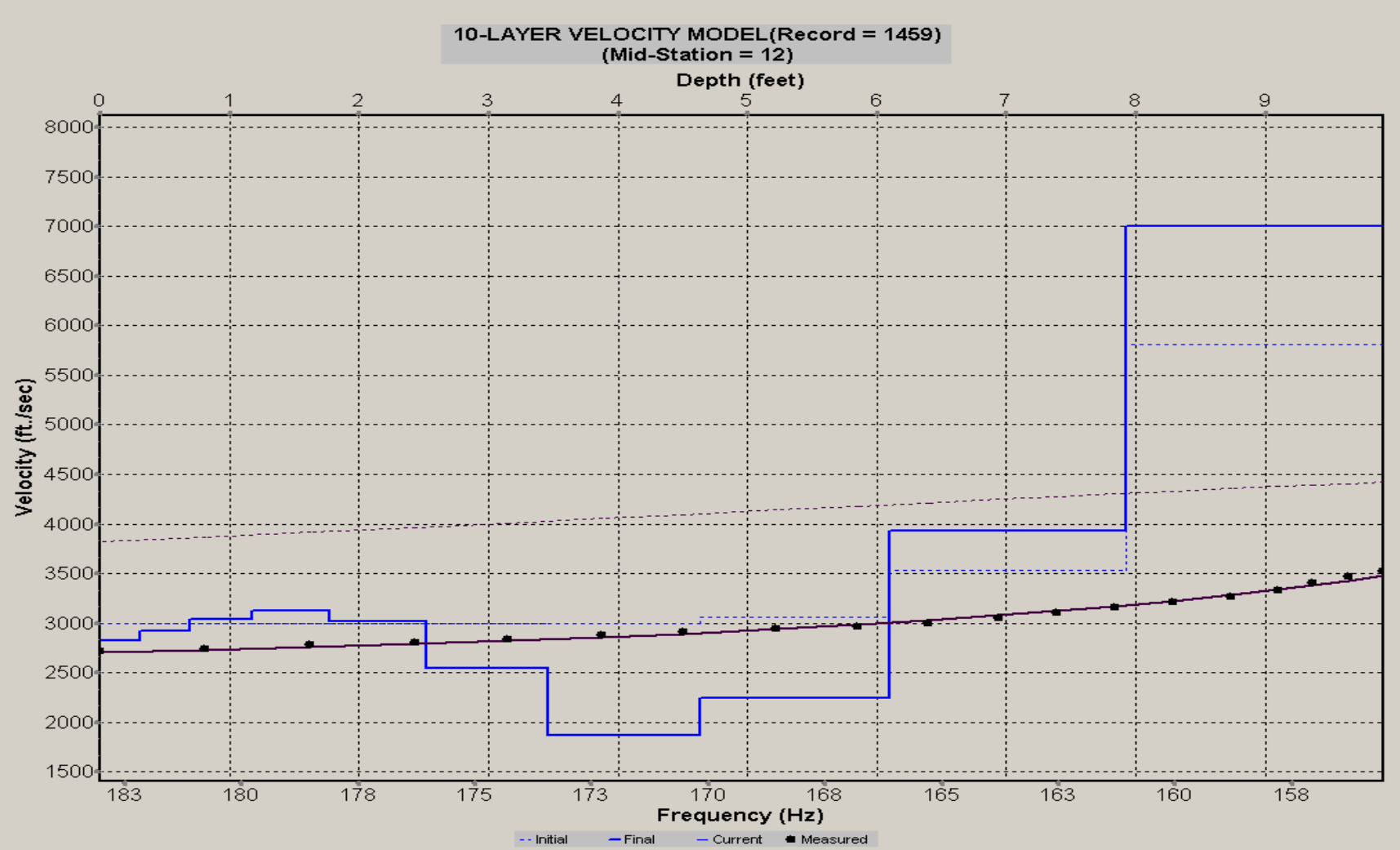

A.777: Velocity Profile Line 1459 used in Post-blast 43

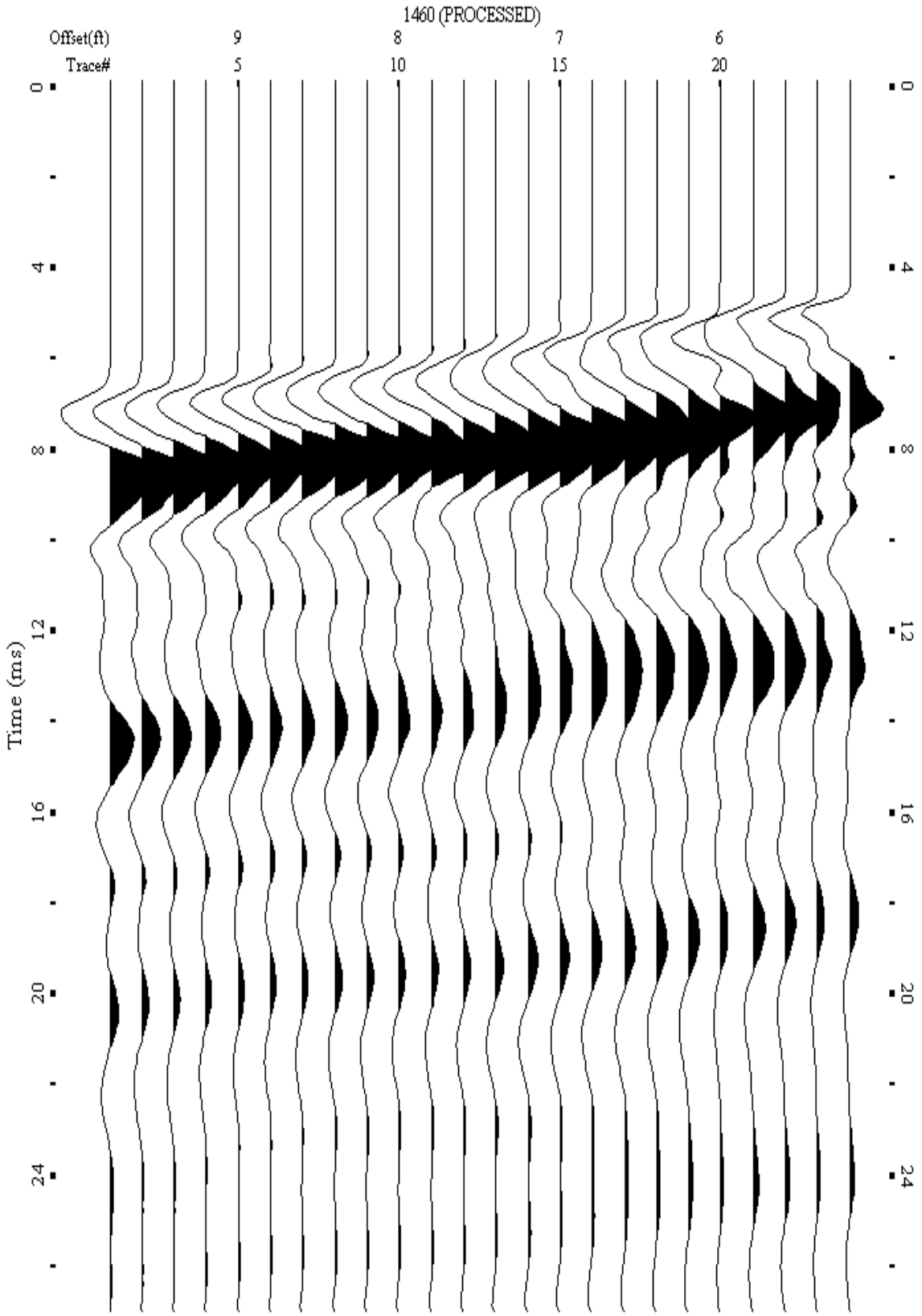

A.778: Shot Gather Line 1460 used in Post-blast 43

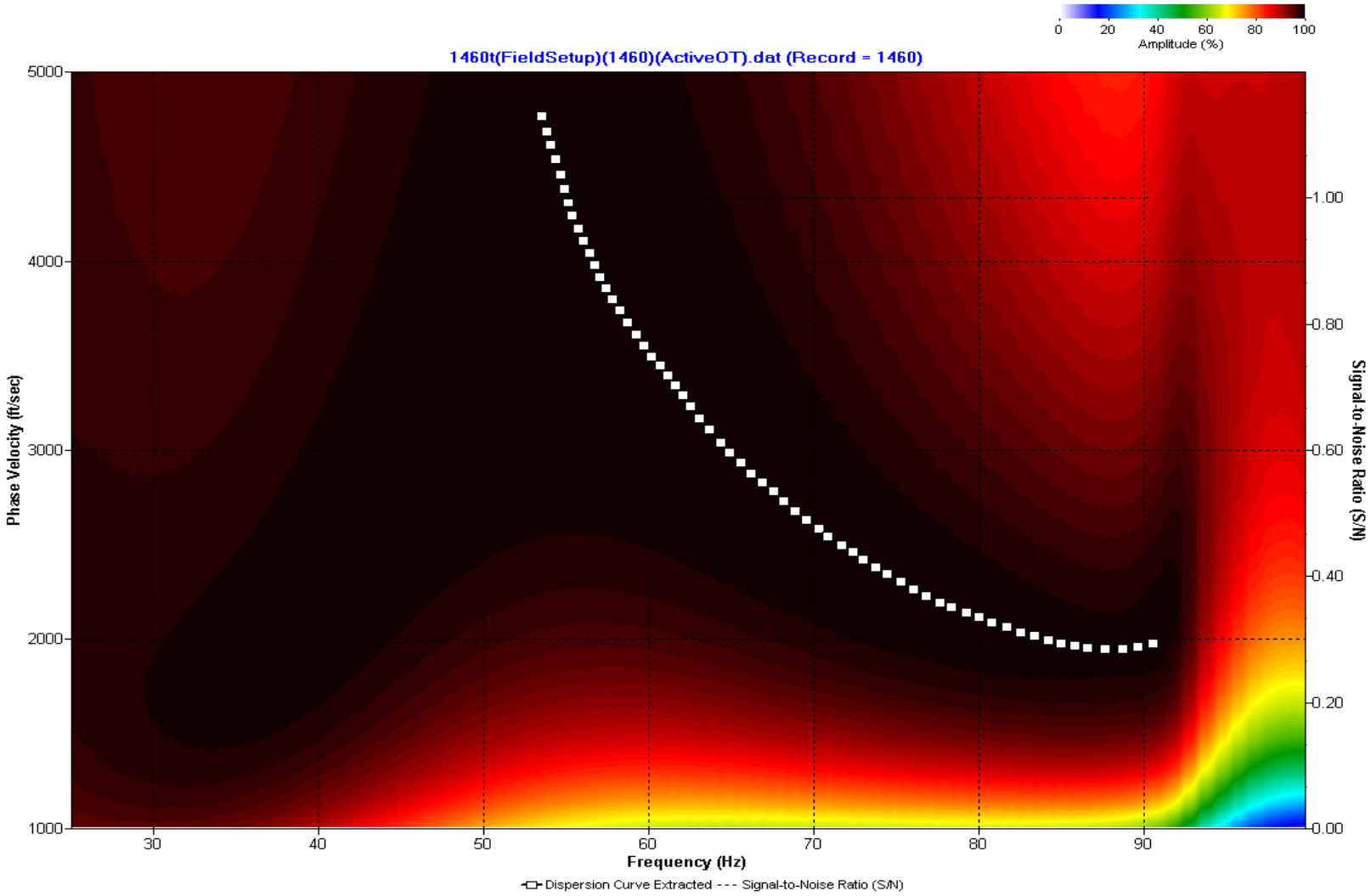

A.779: Dispersion Curve Line 1460 used in Post-blast 43

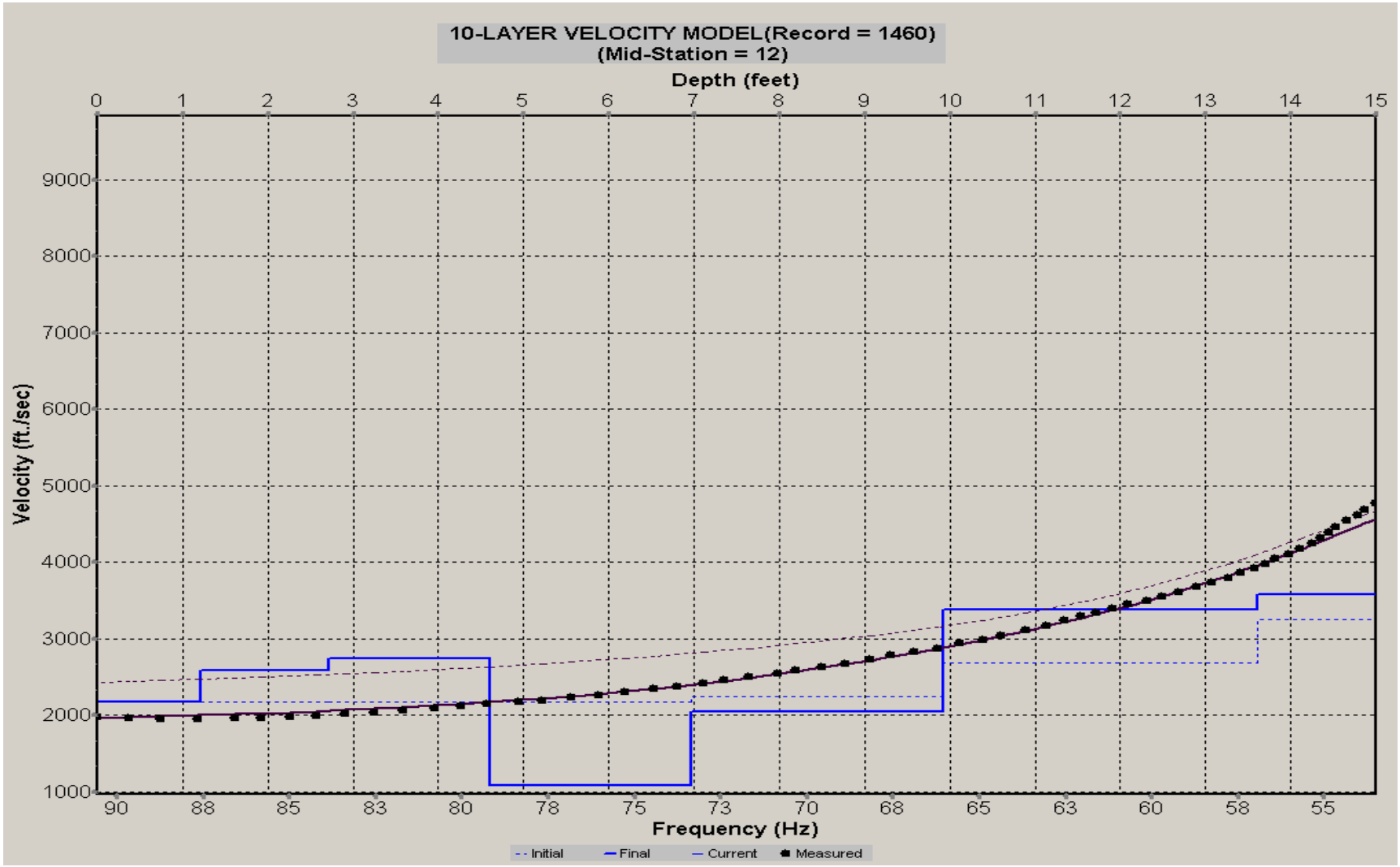

A.780: Velocity Profile Line 1460 used in Post-blast 43

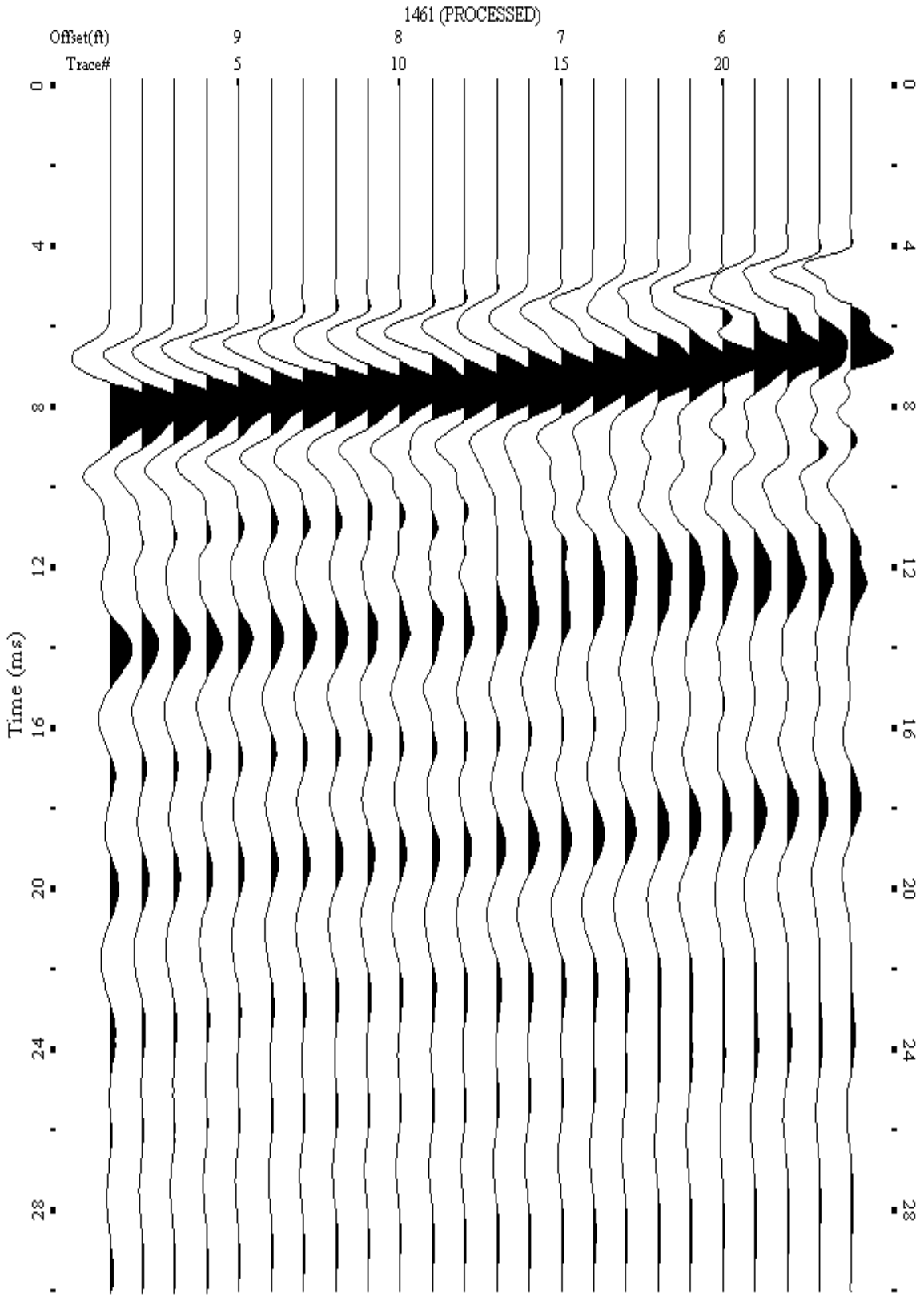

A.781: Shot Gather Line 1461 used in Post-blast 43

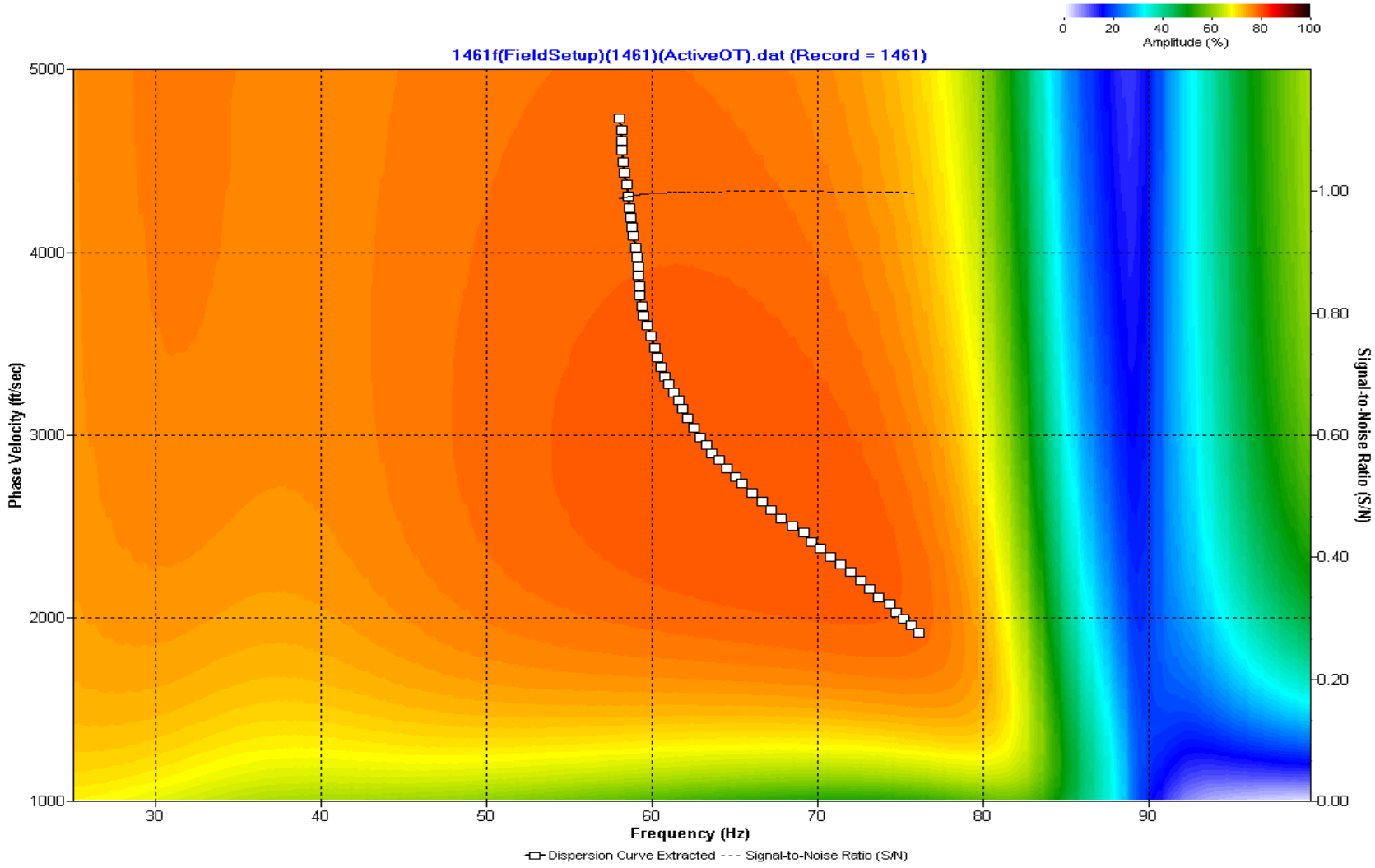

A.782: Dispersion Curve Line 1461 used in Post-blast 43

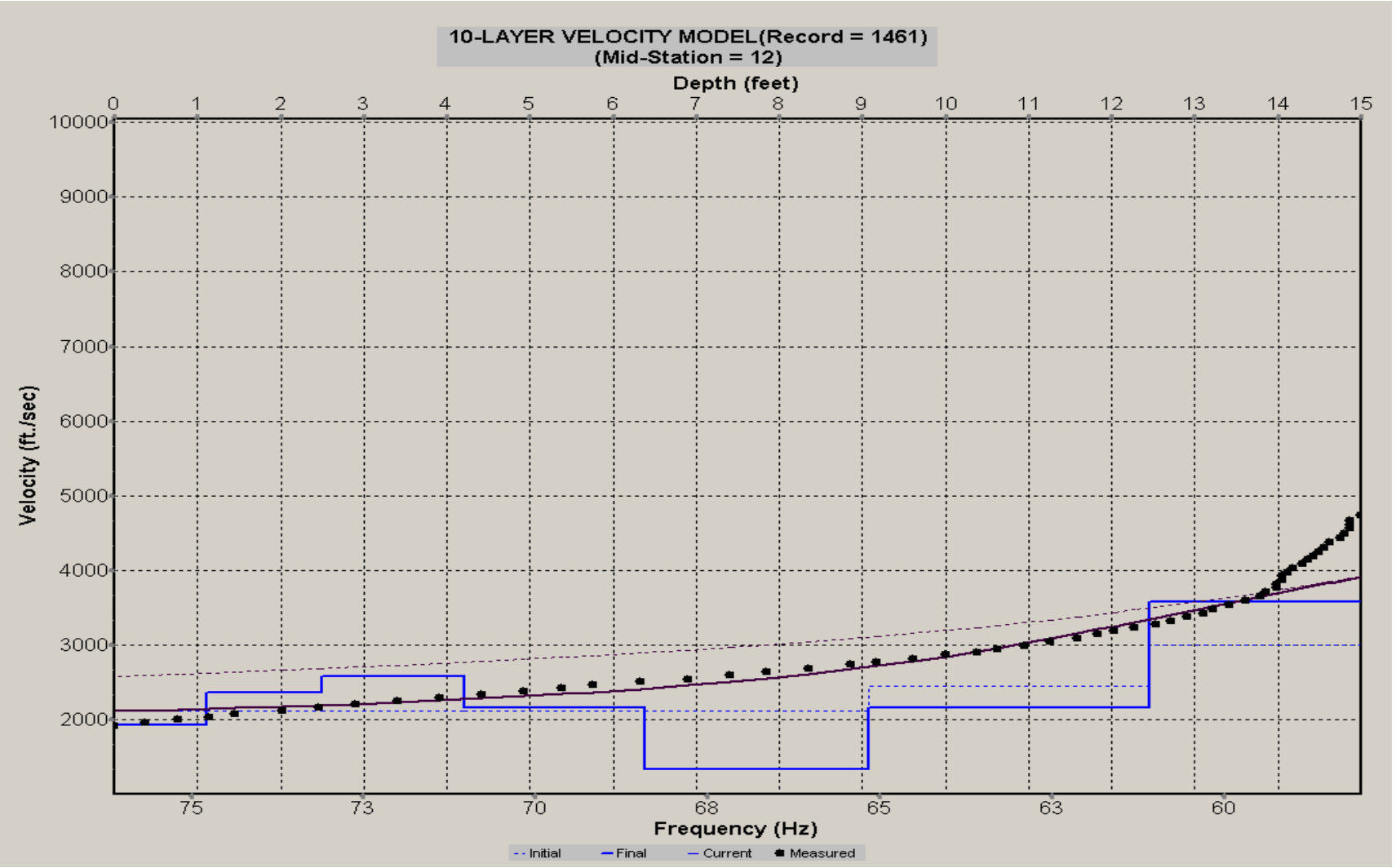

A.783: Velocity Profile Line 1461 used in Post-blast 43

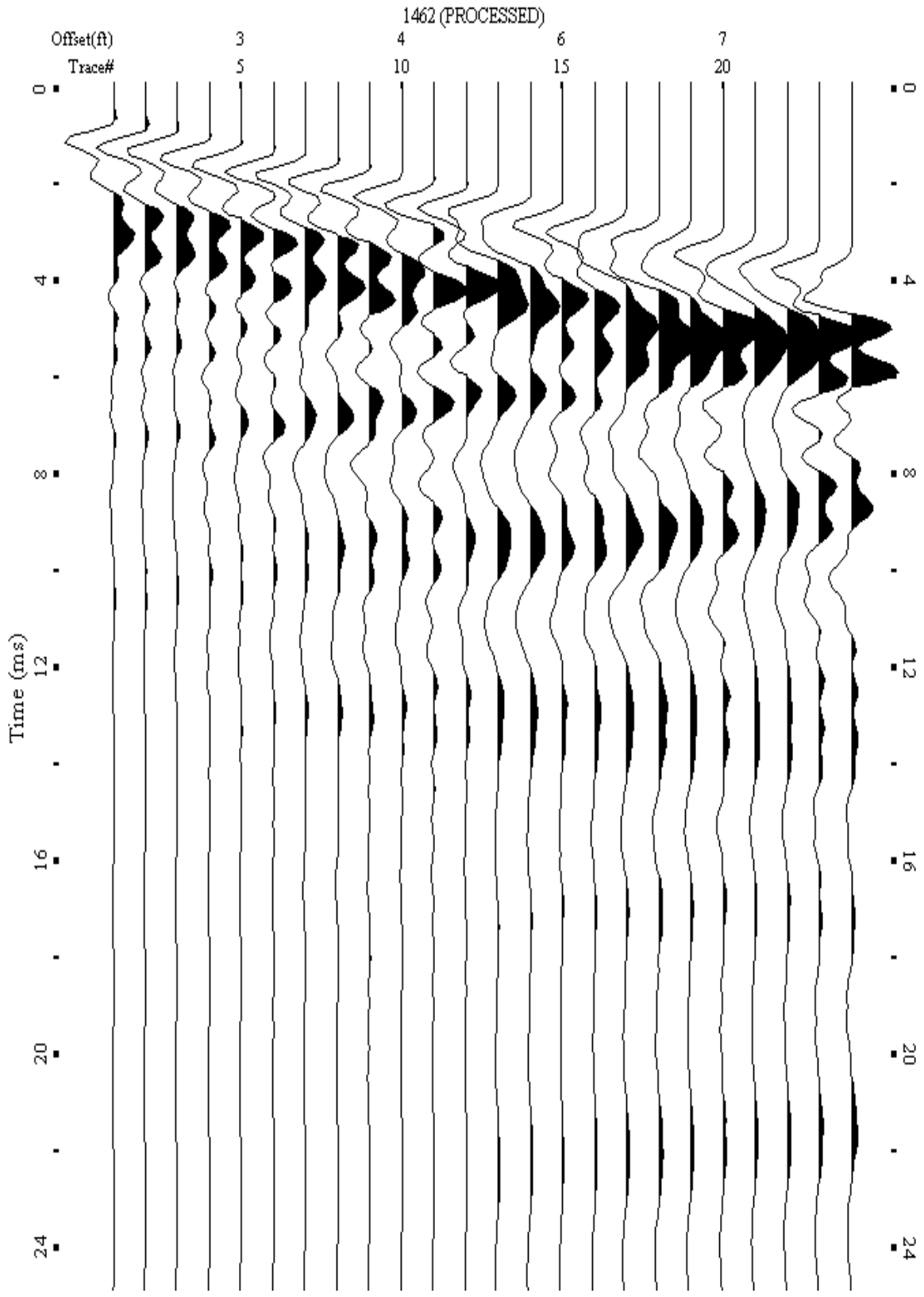

A.784: Shot Gather Line 1462 used in Post-blast 43

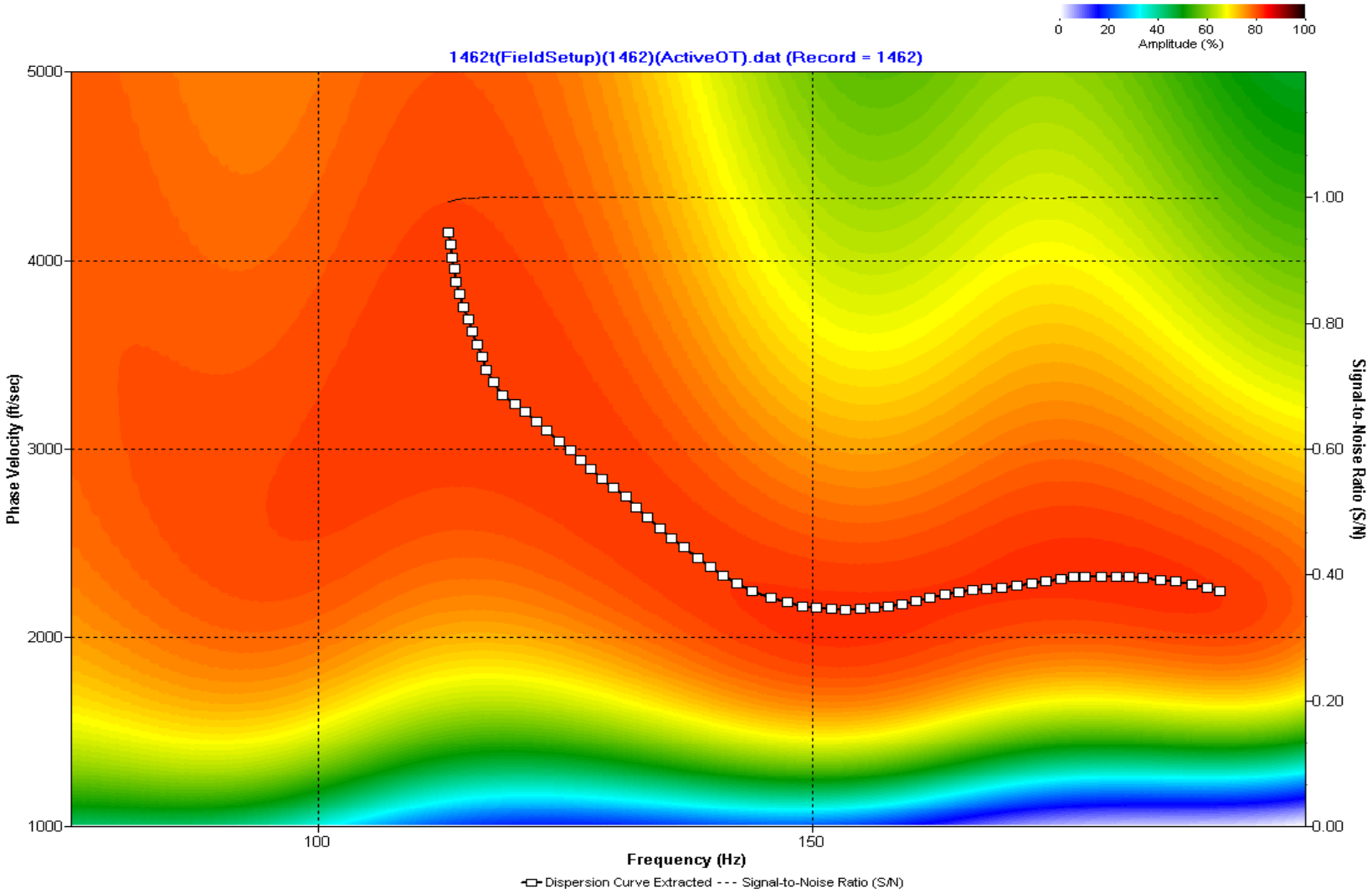

A.785: Dispersion Curve Line 1462 used in Post-blast 43

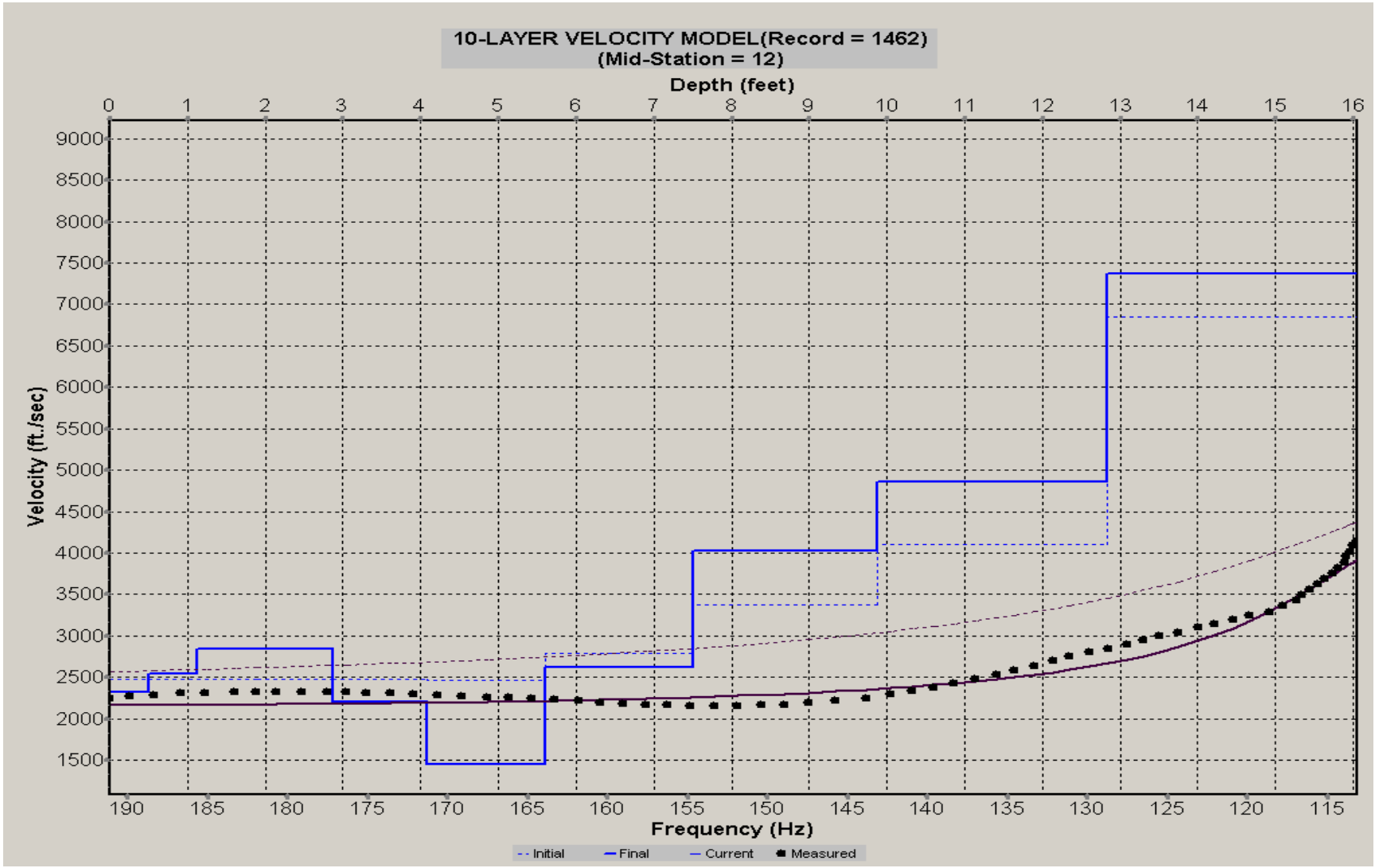

A.786: Velocity Profile Line 1462 used in Post-blast 43

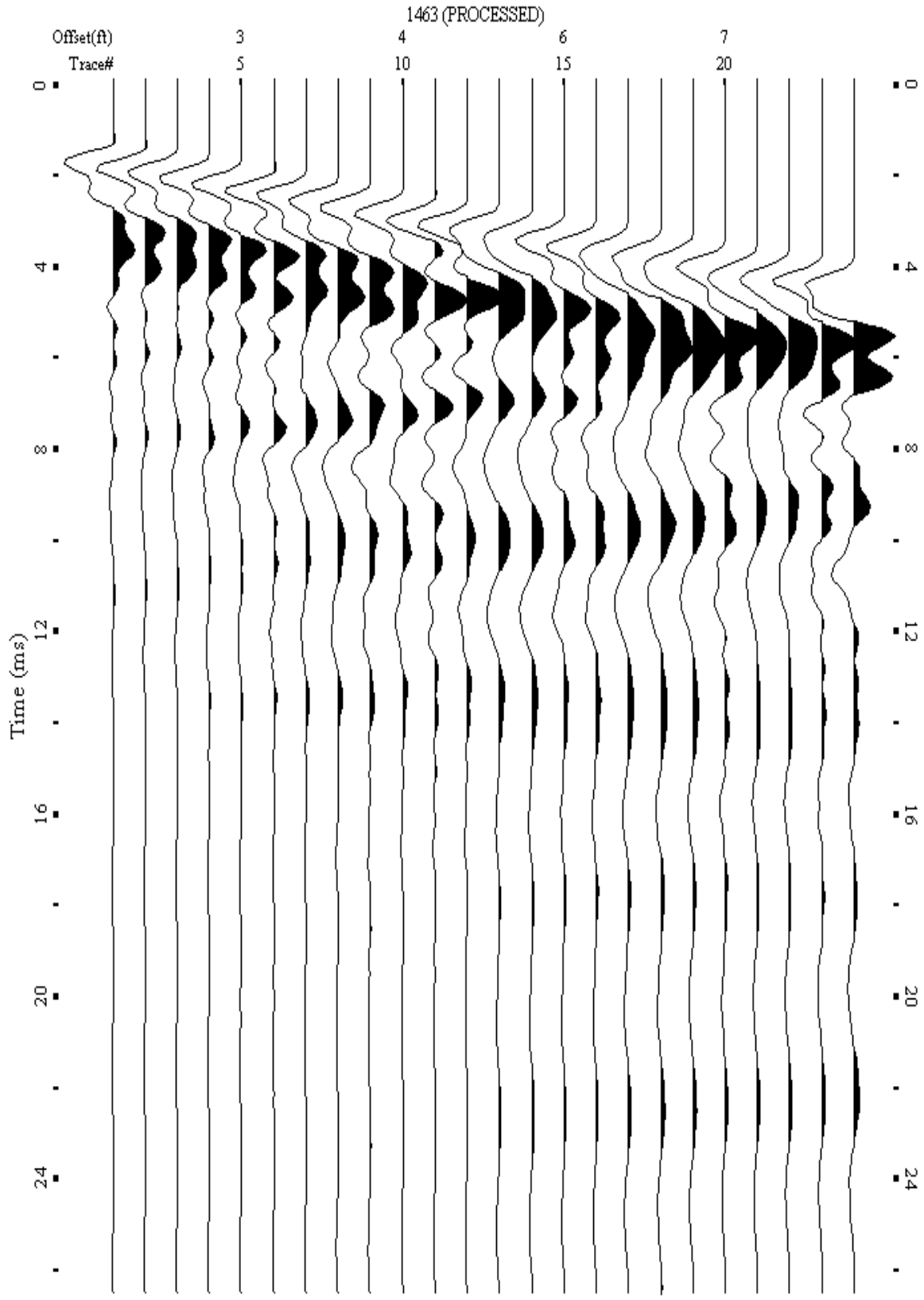

A.787: Shot Gather Line 1463 used in Post-blast 43

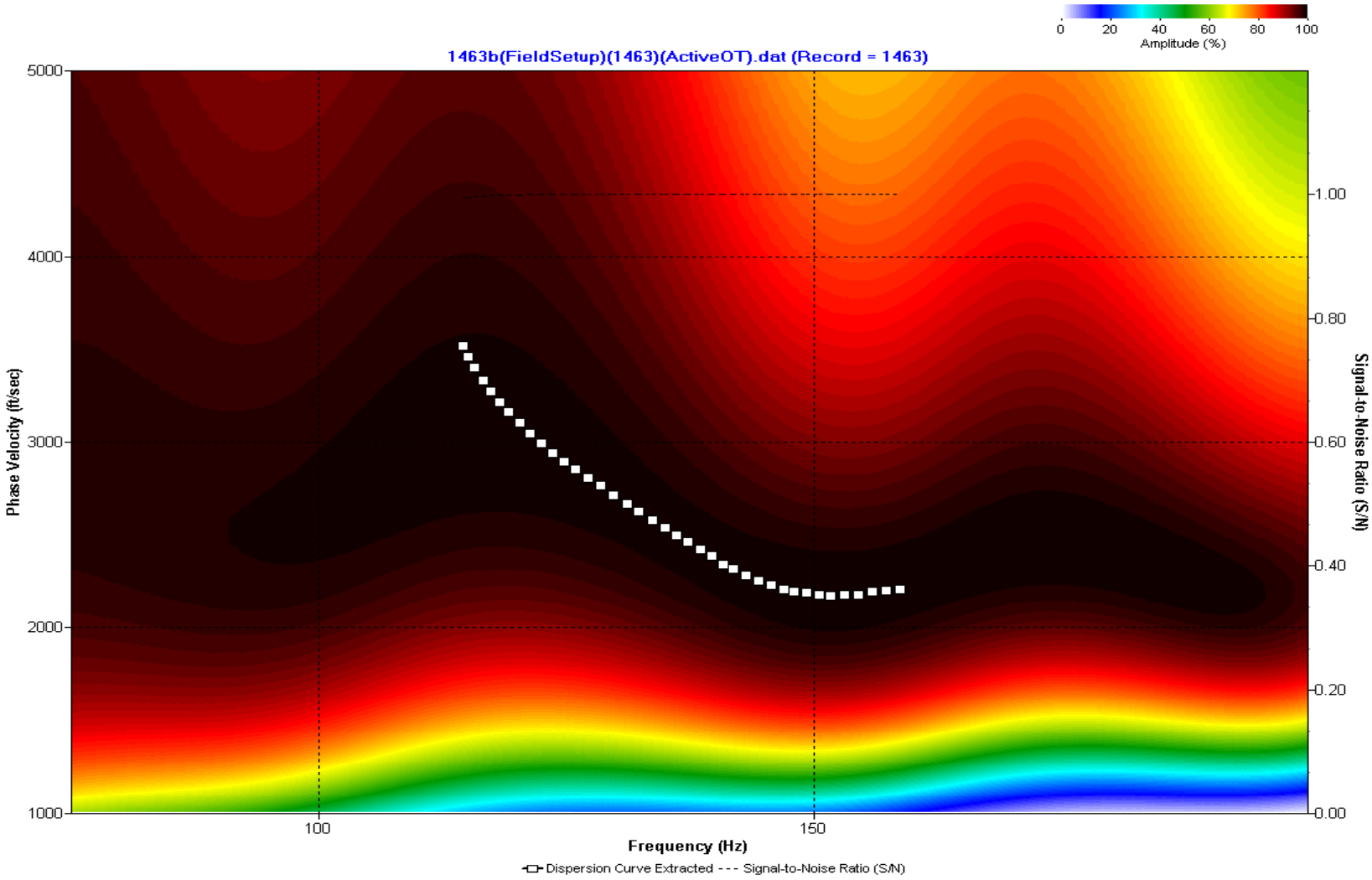

A.788: Dispersion Curve Line 1463 used in Post-blast 43

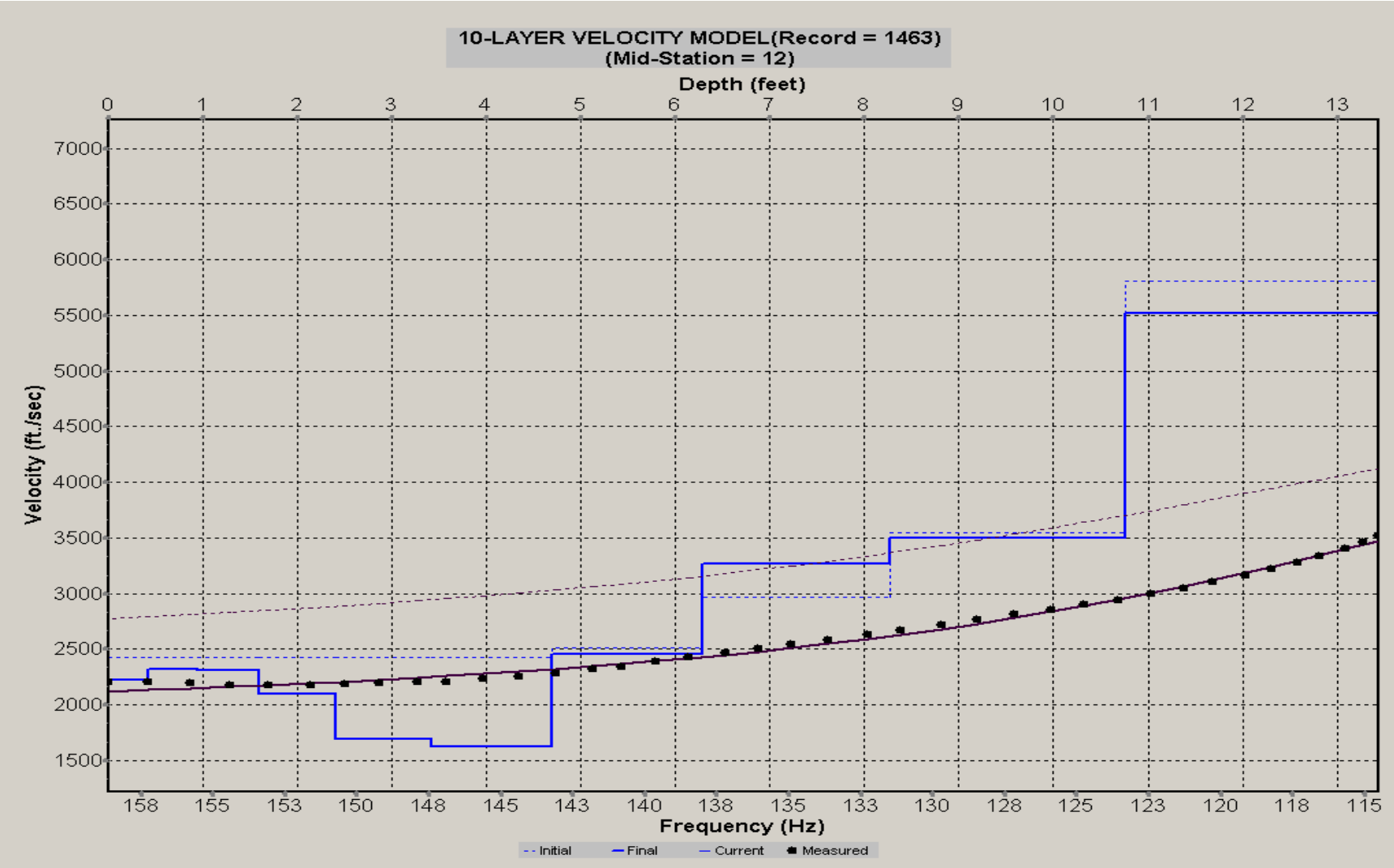

A.789: Velocity Profile Line 1463 used in Post-blast 43

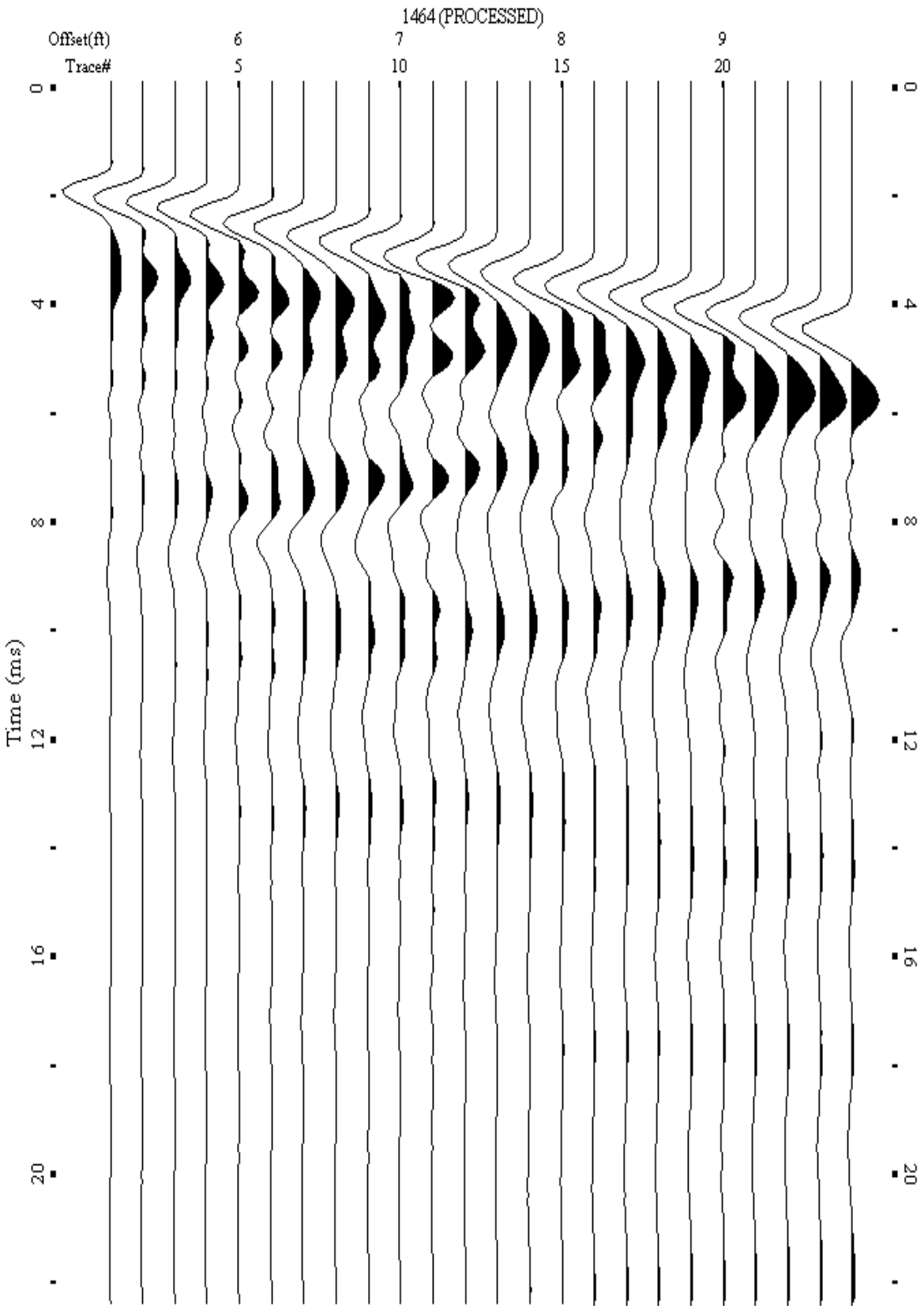

A.790: Shot Gather Line 1464 used in Post-blast 43

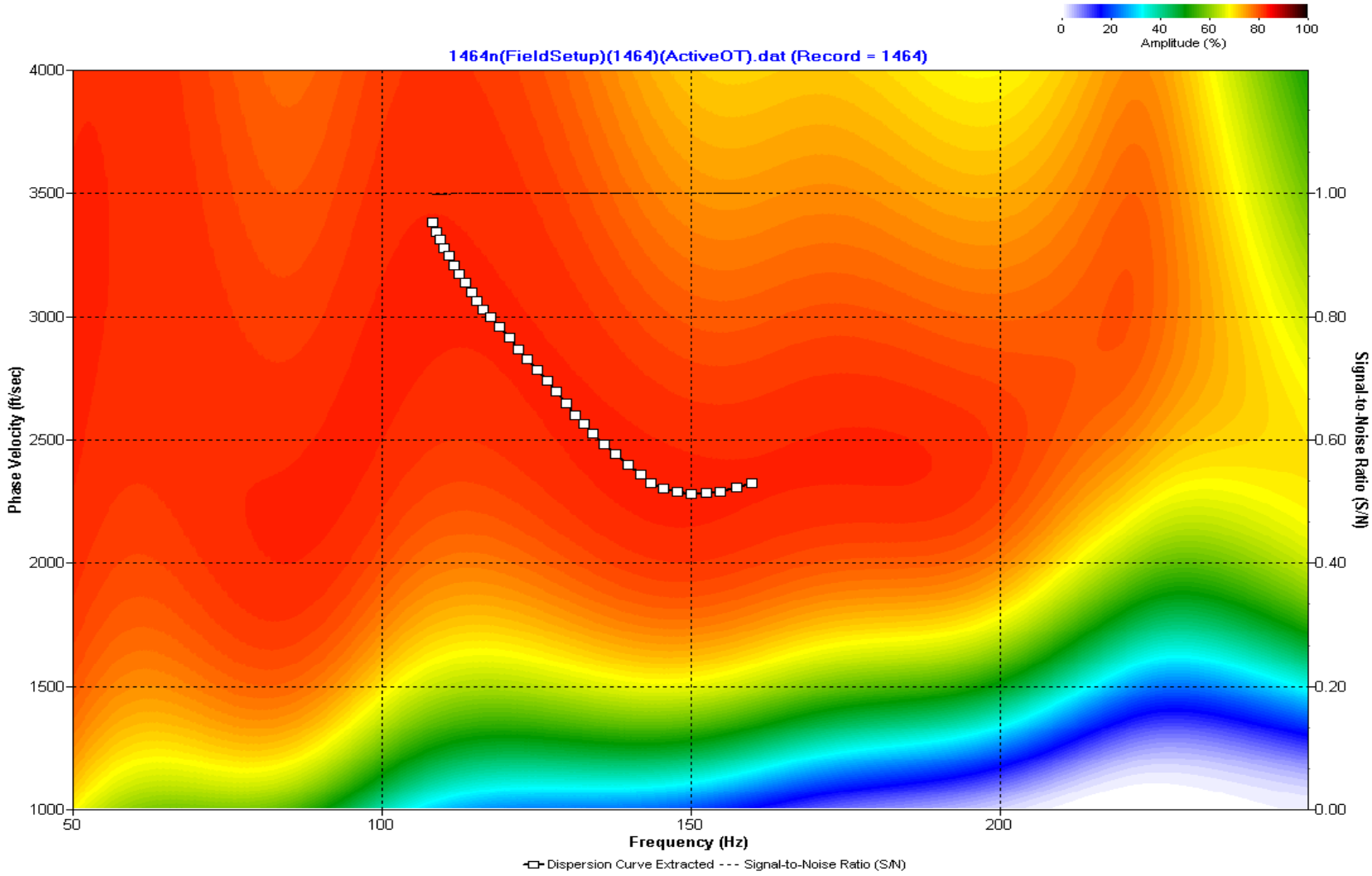

A.791: Dispersion Curve Line 1464 used in Post-blast 43

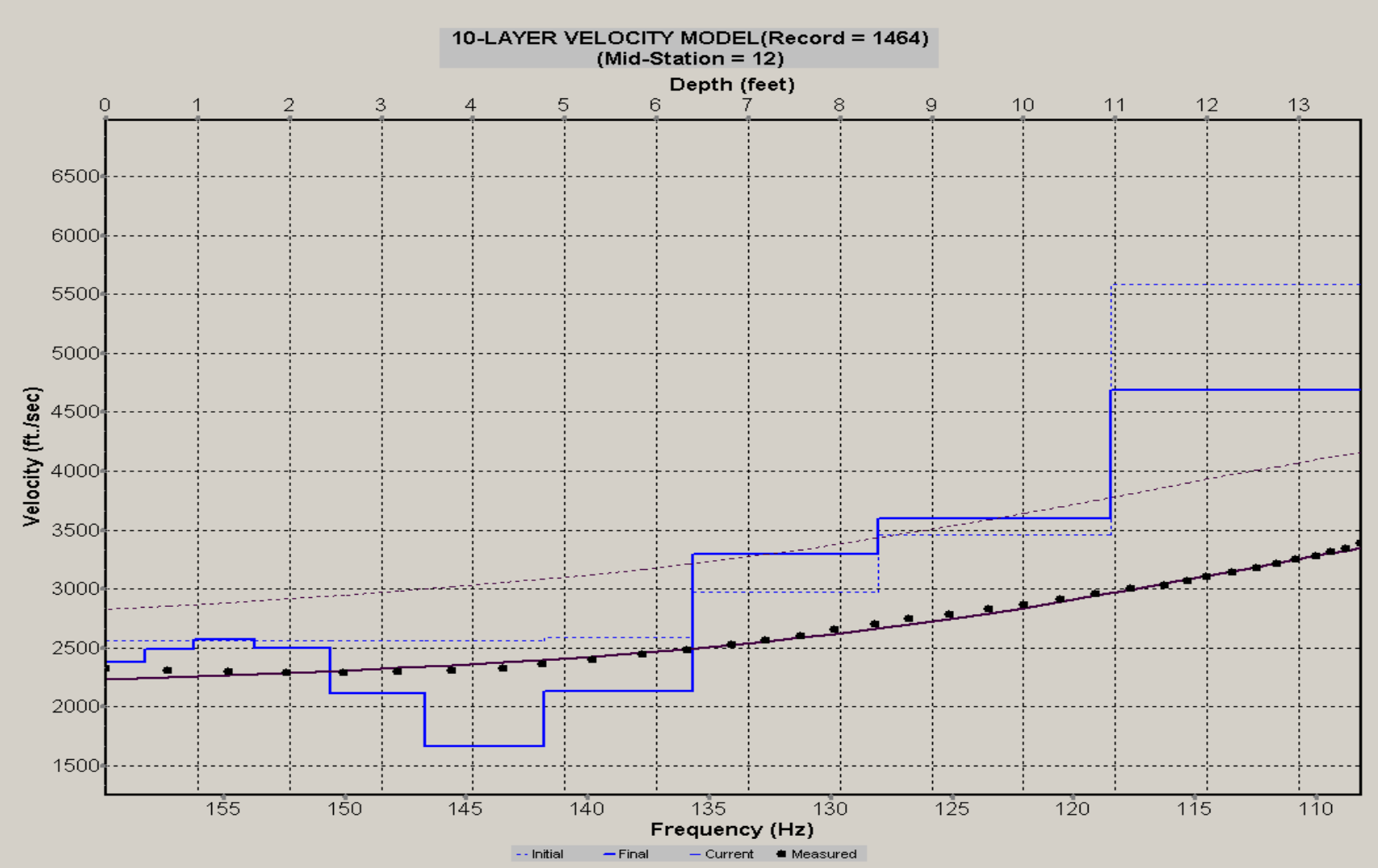

A.792: Velocity Profile Line 1464 used in Post-blast 43

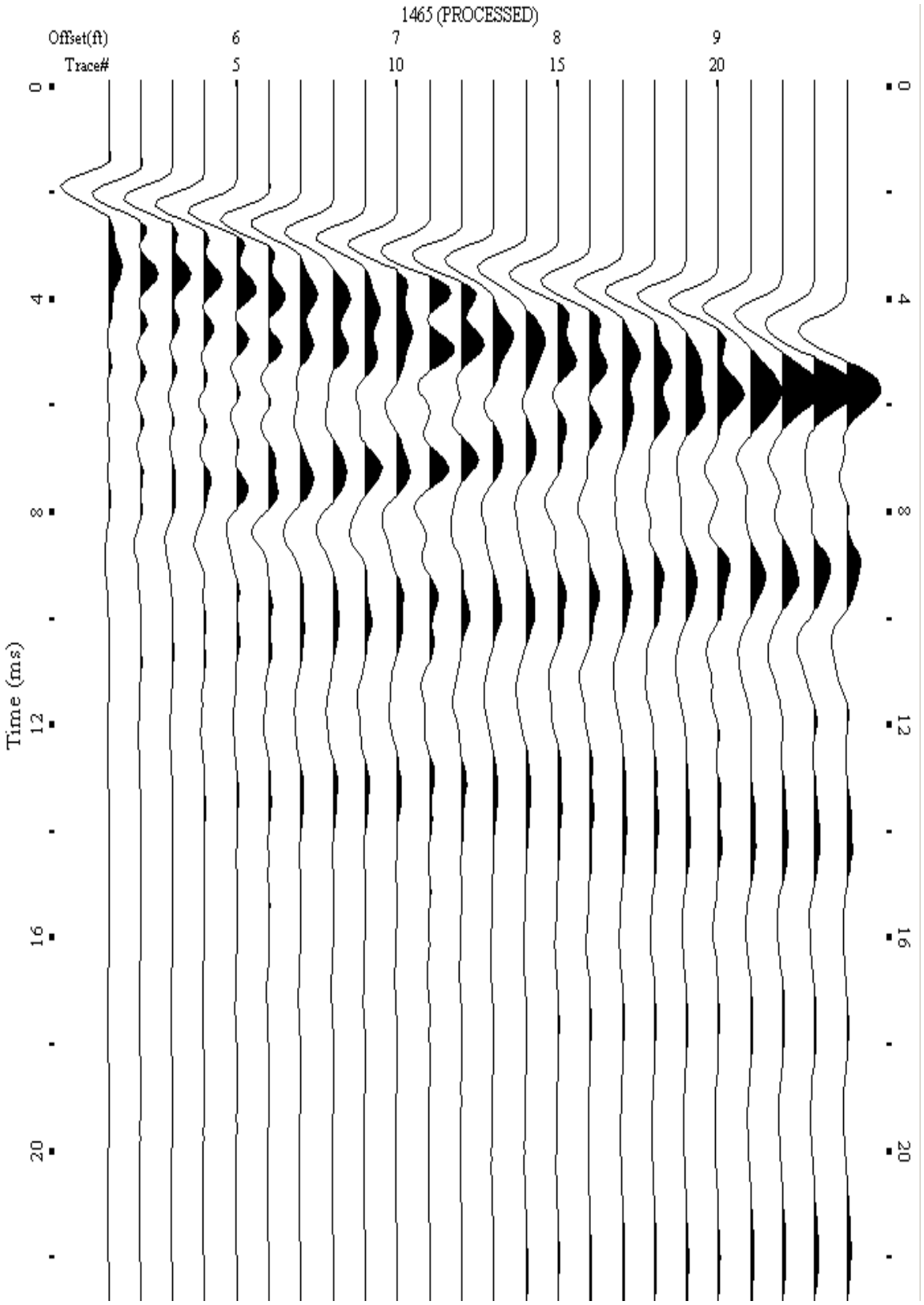

A.793: Shot Gather Line 1465 used in Post-blast 43

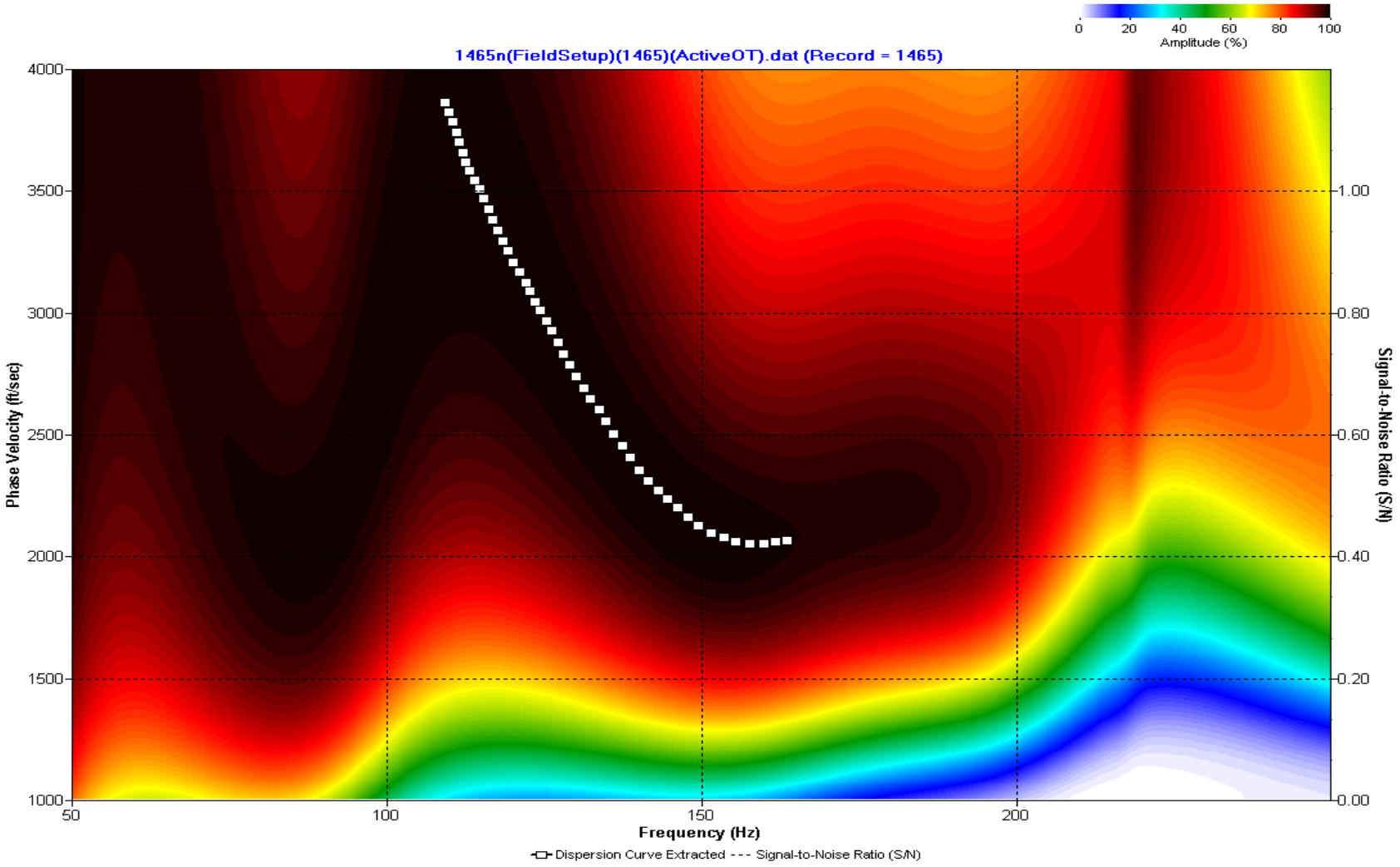

A.794: Dispersion Curve Line 1465 used in Post-blast 43

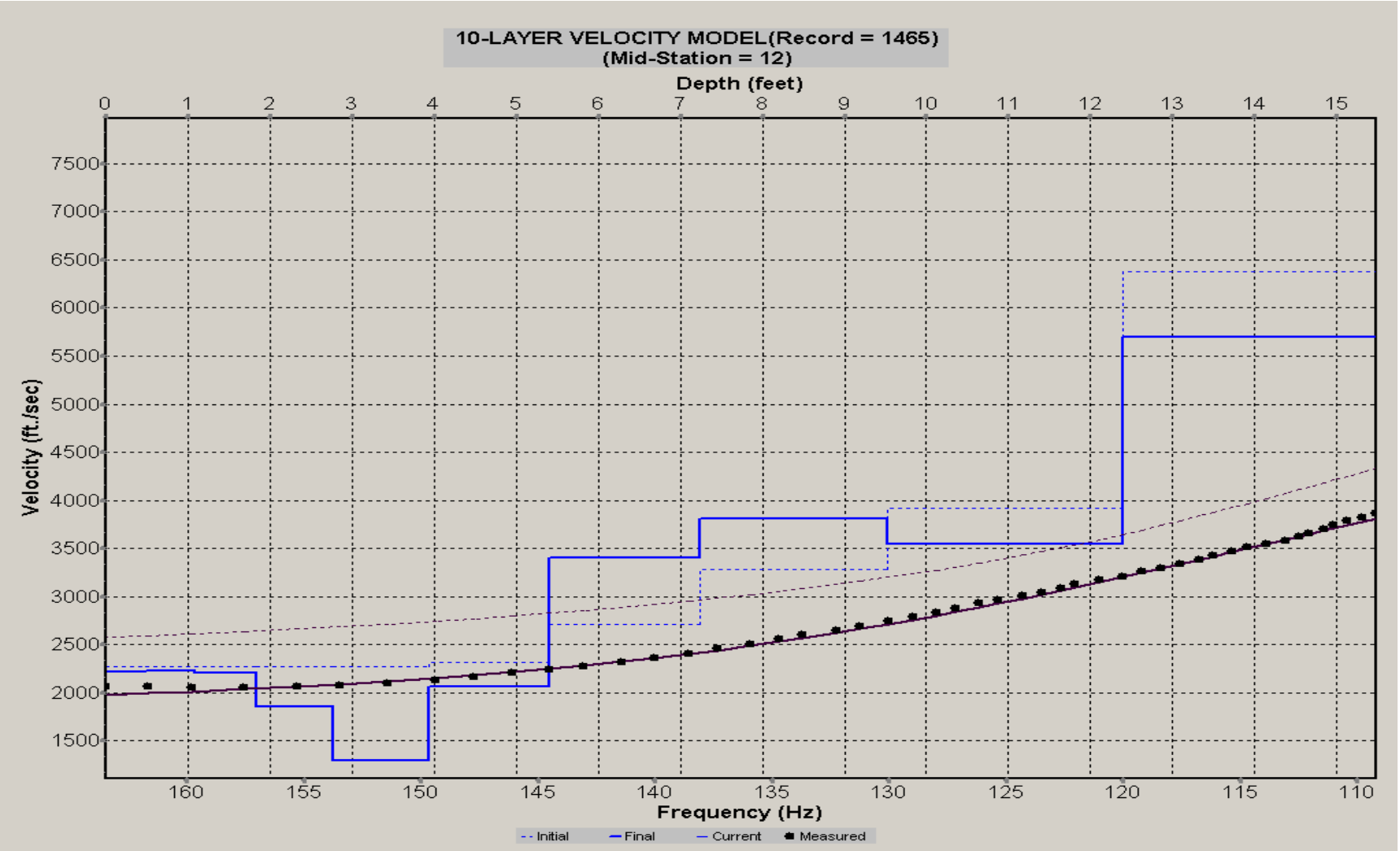

A.795: Velocity Profile Line 1465 used in Post-blast 43

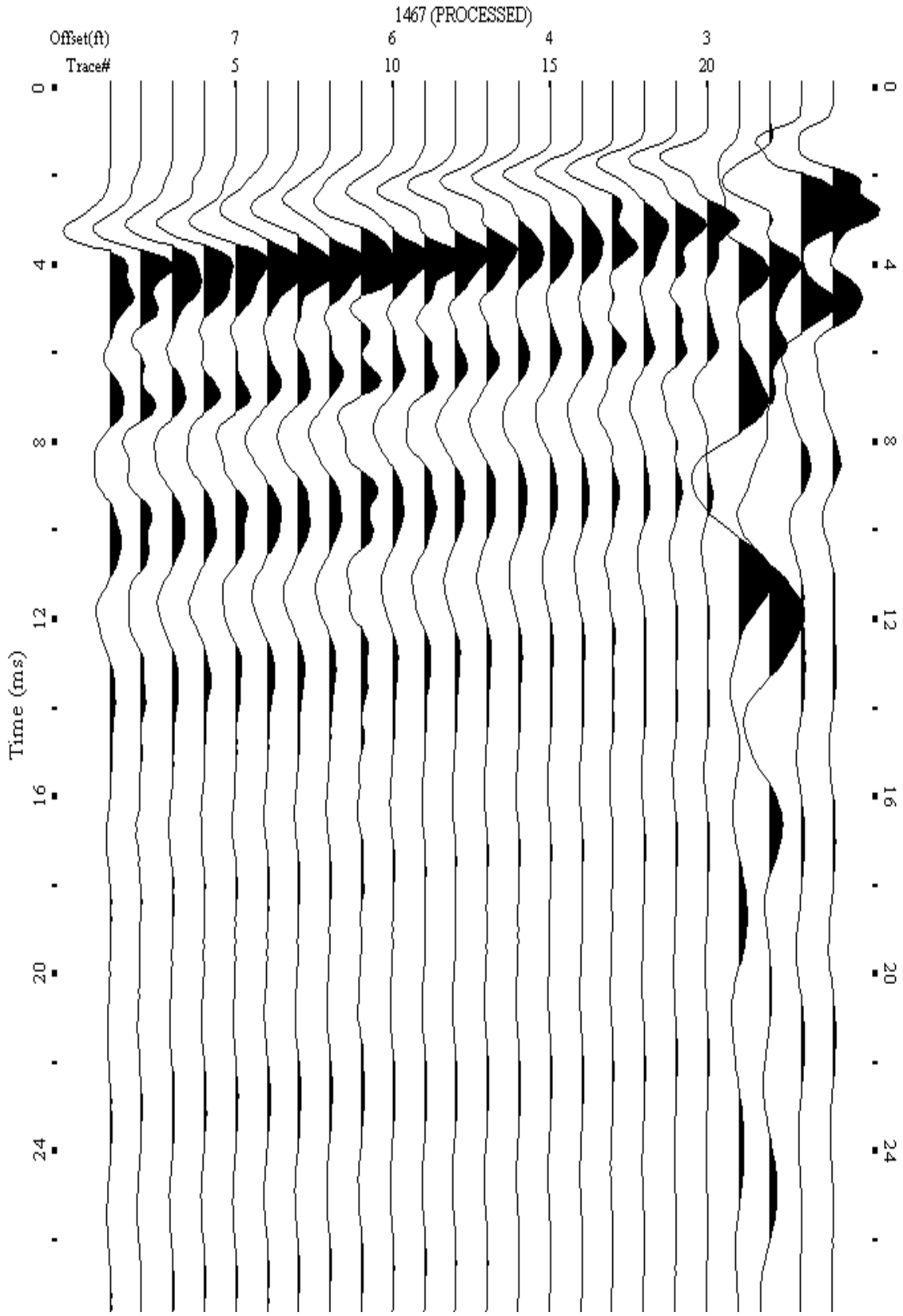

A.796: Shot Gather Line 1467 used in Post-blast 44

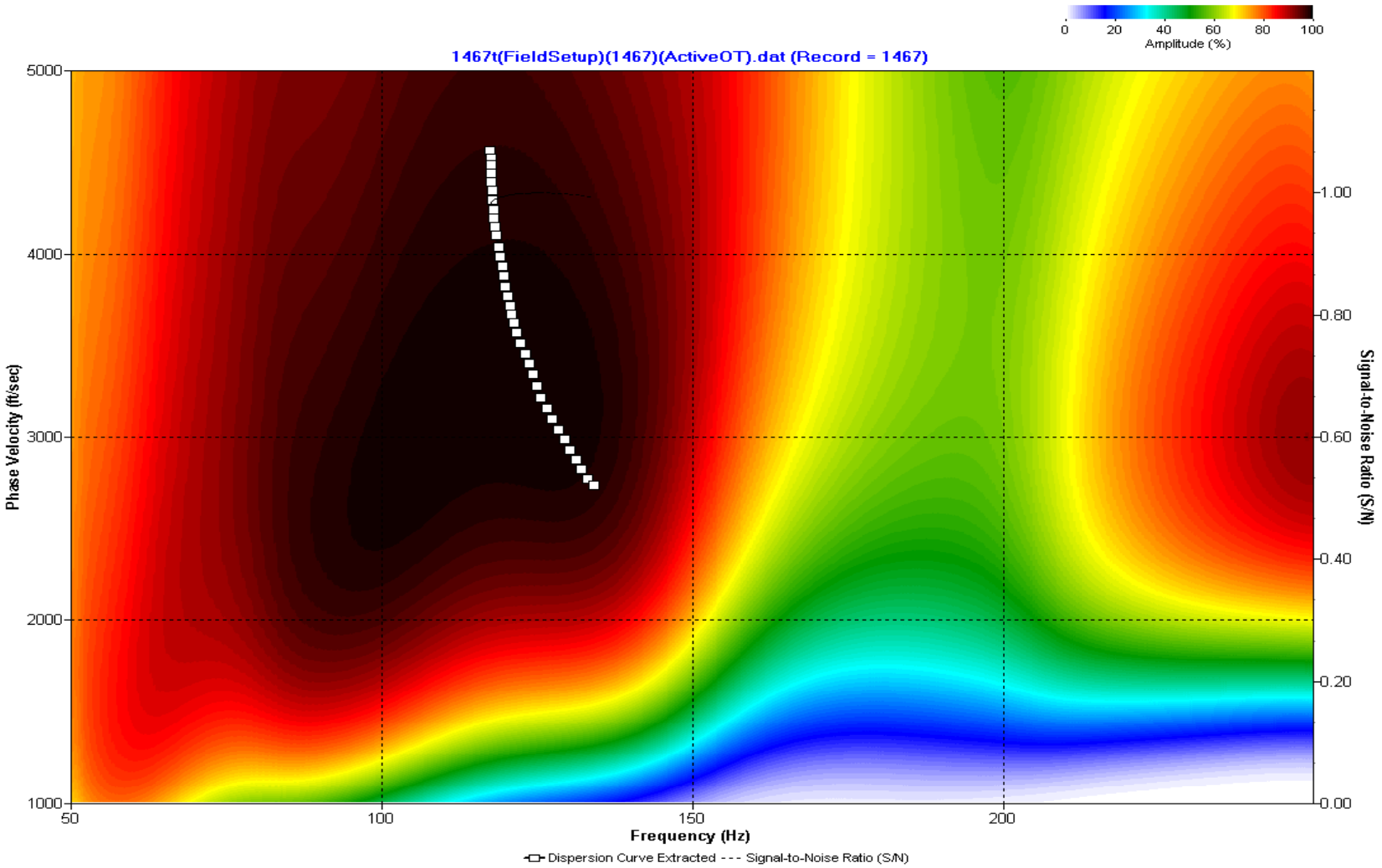

A.796: Dispersion Curve Line 1467 used in Post-blast 44

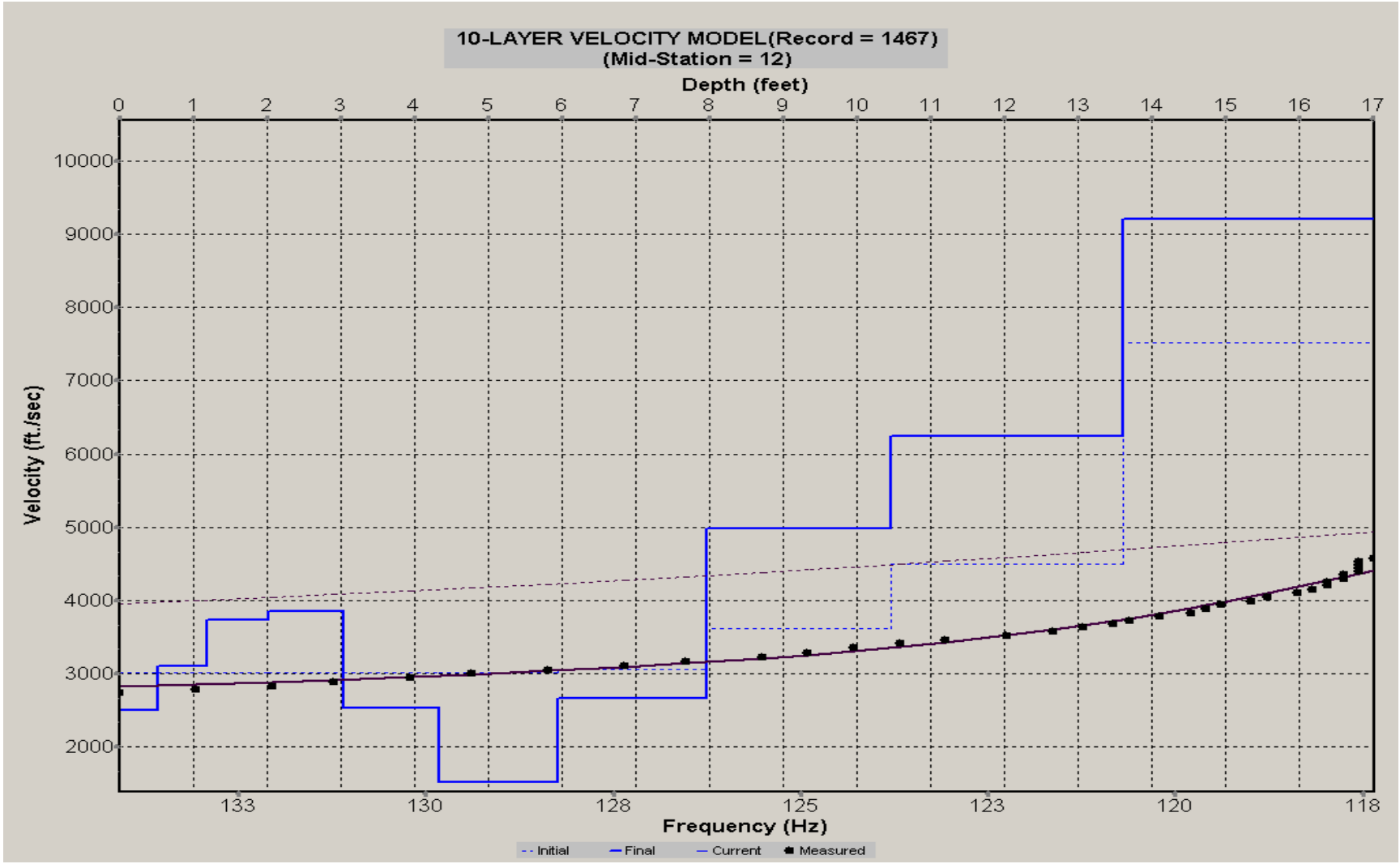

A.798: Velocity Profile Line 1467 used in Post-blast 44

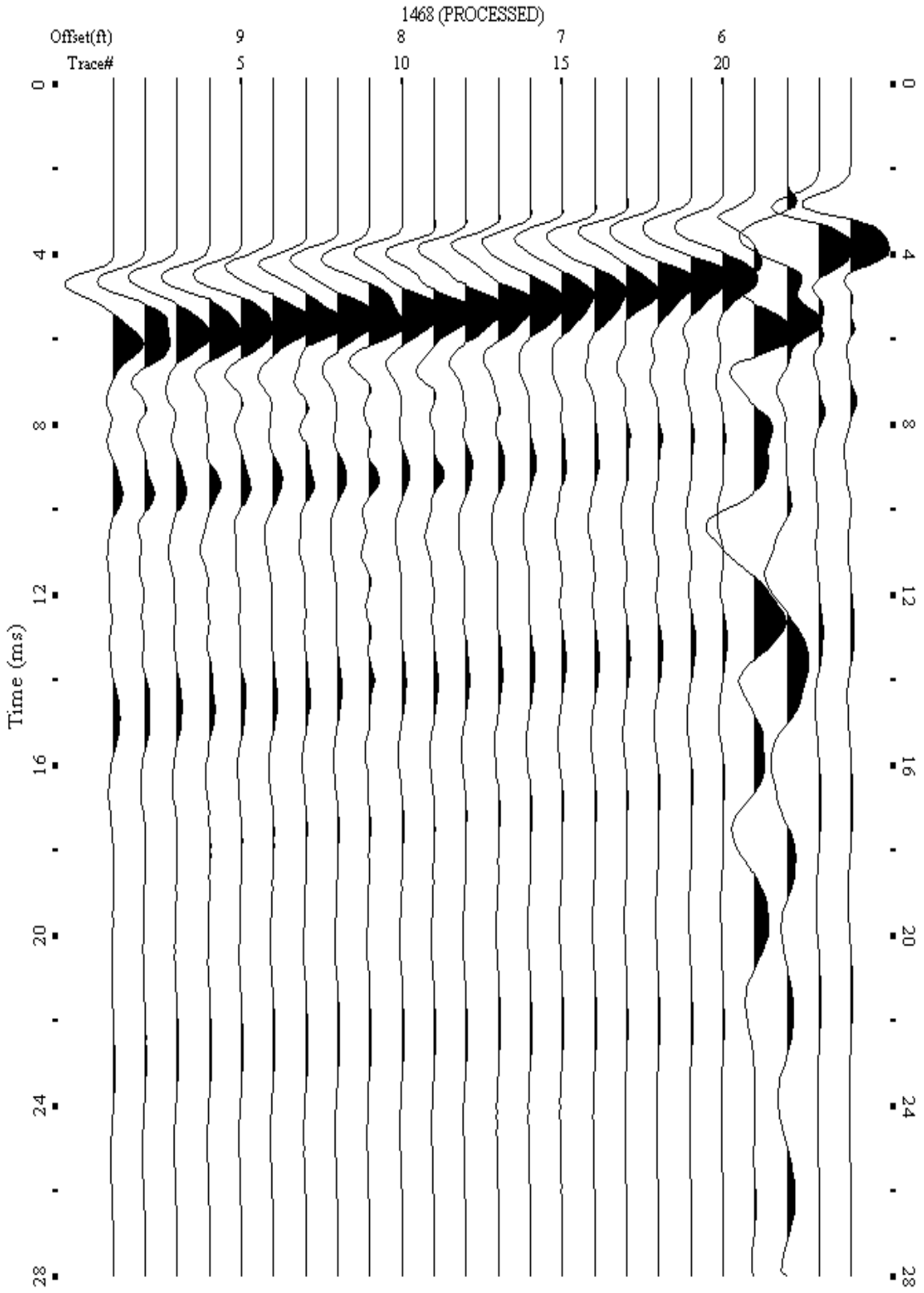

A.799: Shot Gather Line 1468 used in Post-blast 44

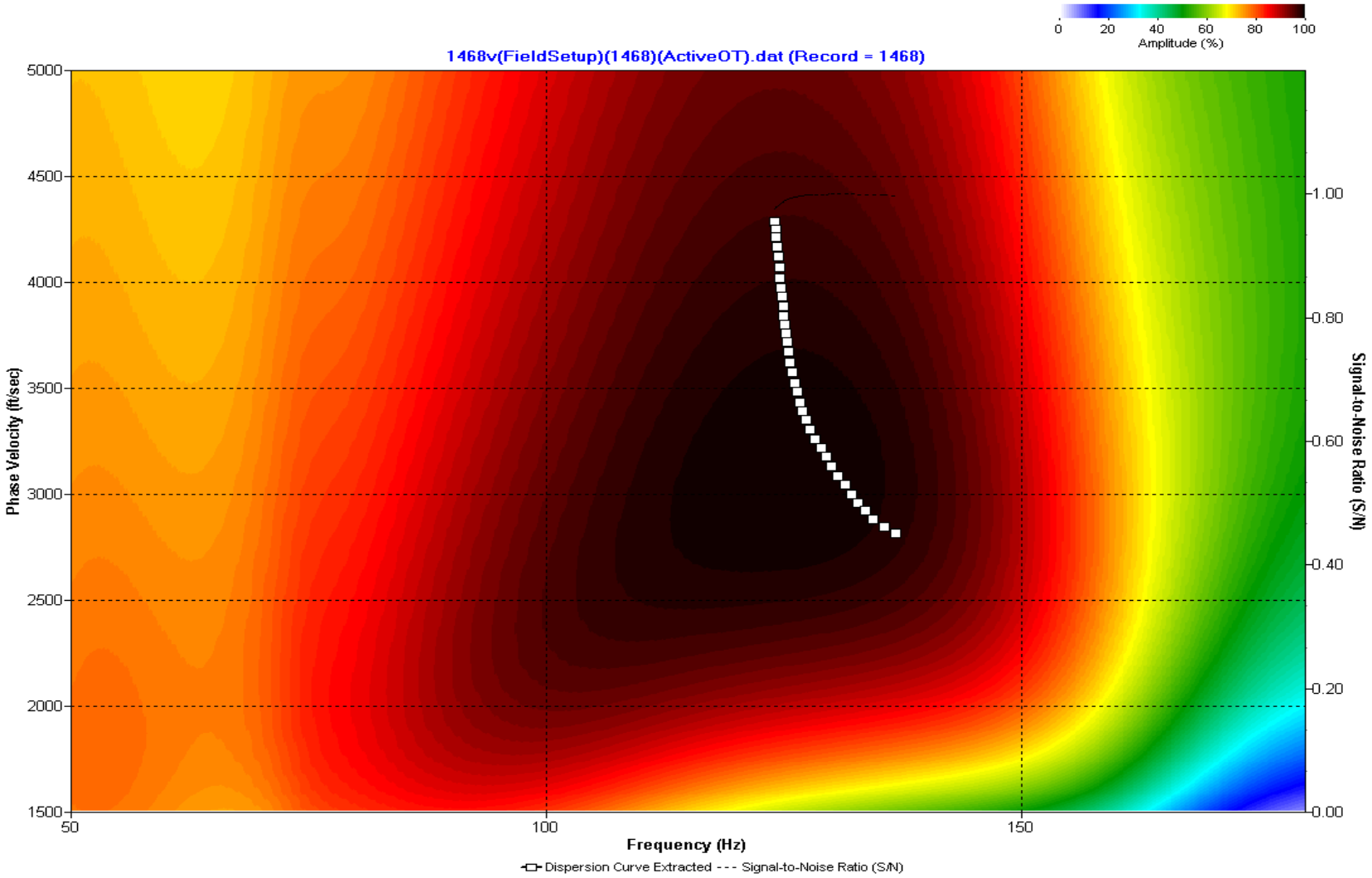

A.800: Dispersion Curve Line 1468 used in Post-blast 44

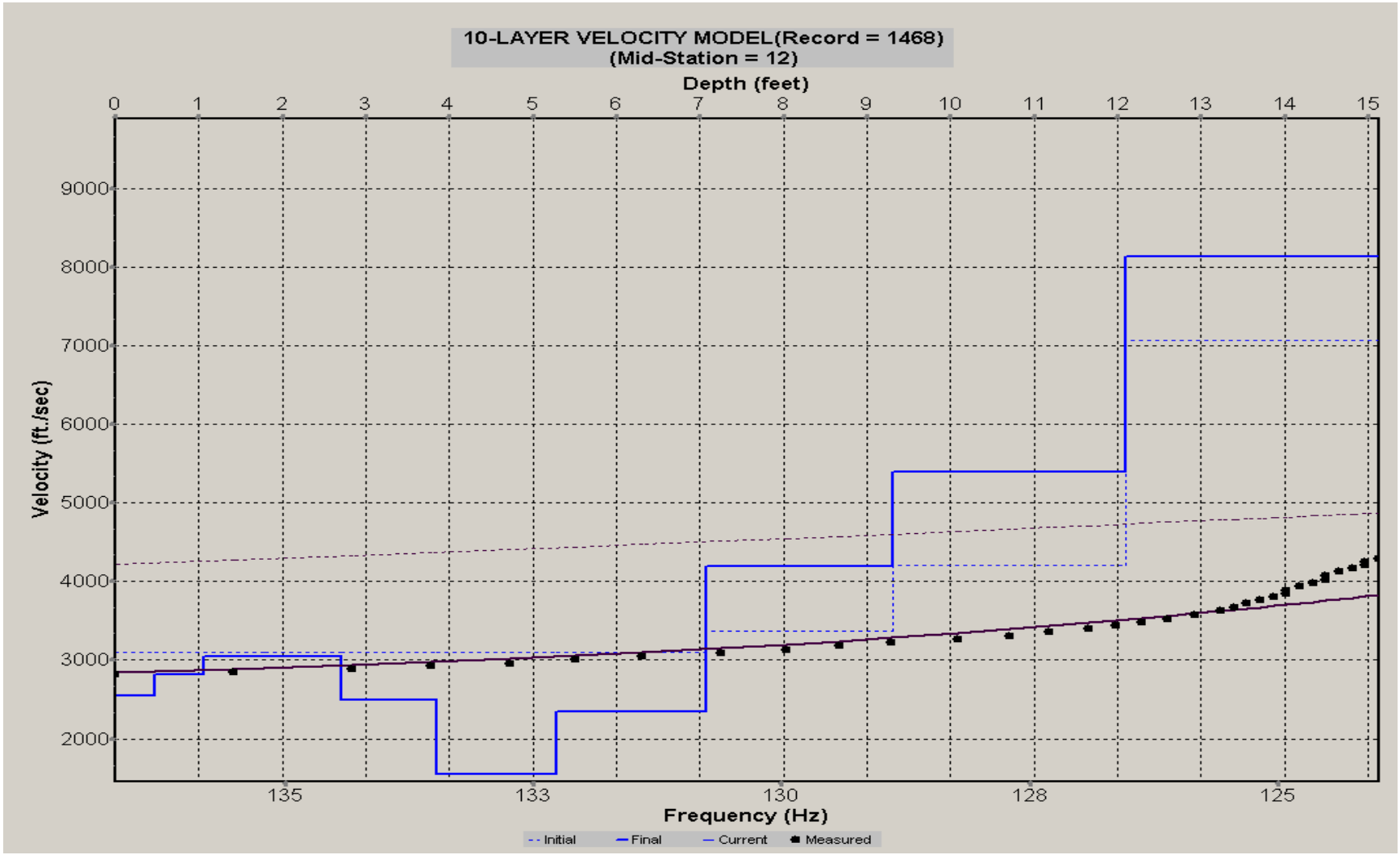

A.801: Velocity Profile Line 1468 used in Post-blast 44

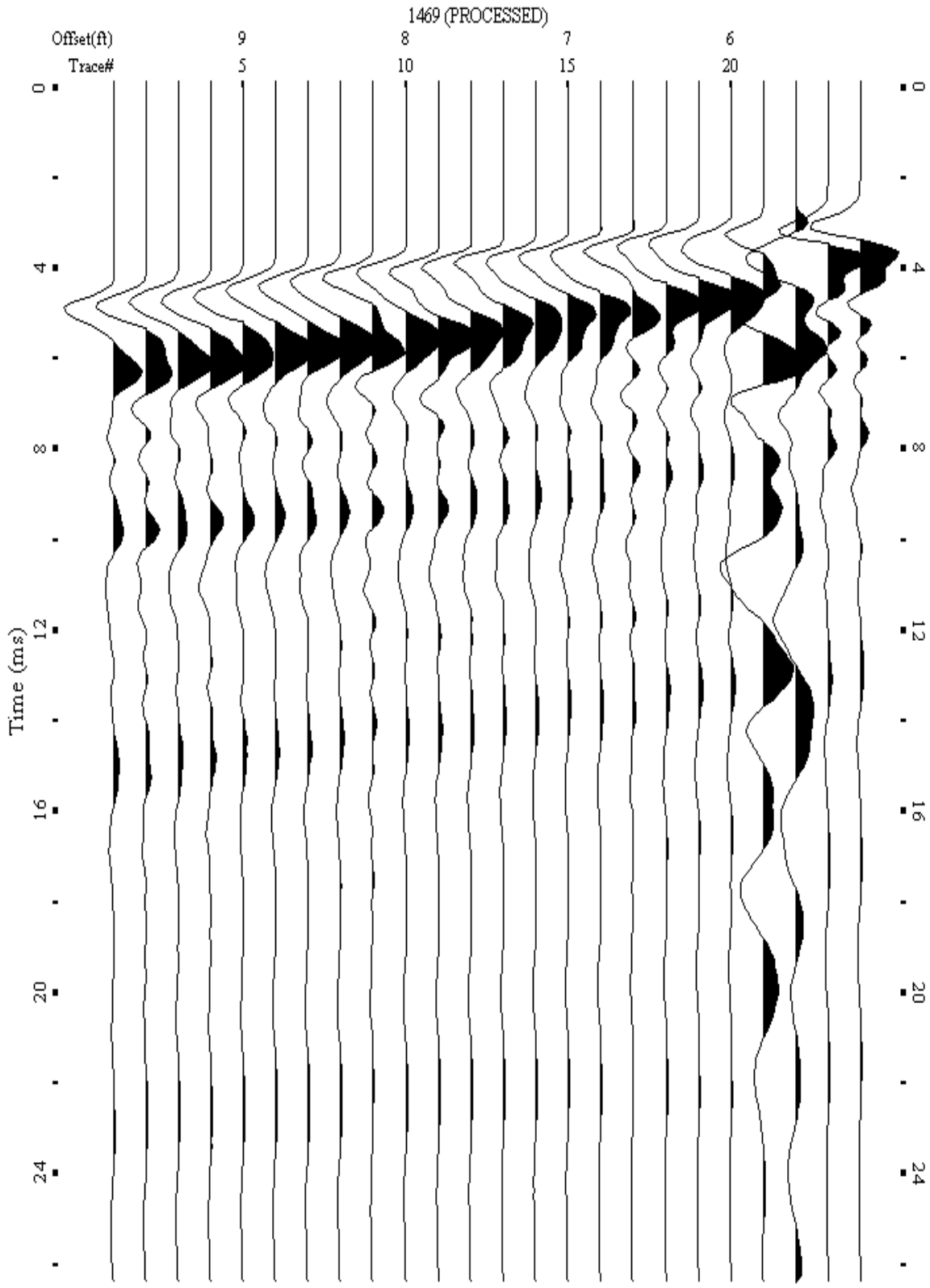

A.802: Shot Gather Line 1469 used in Post-blast 44

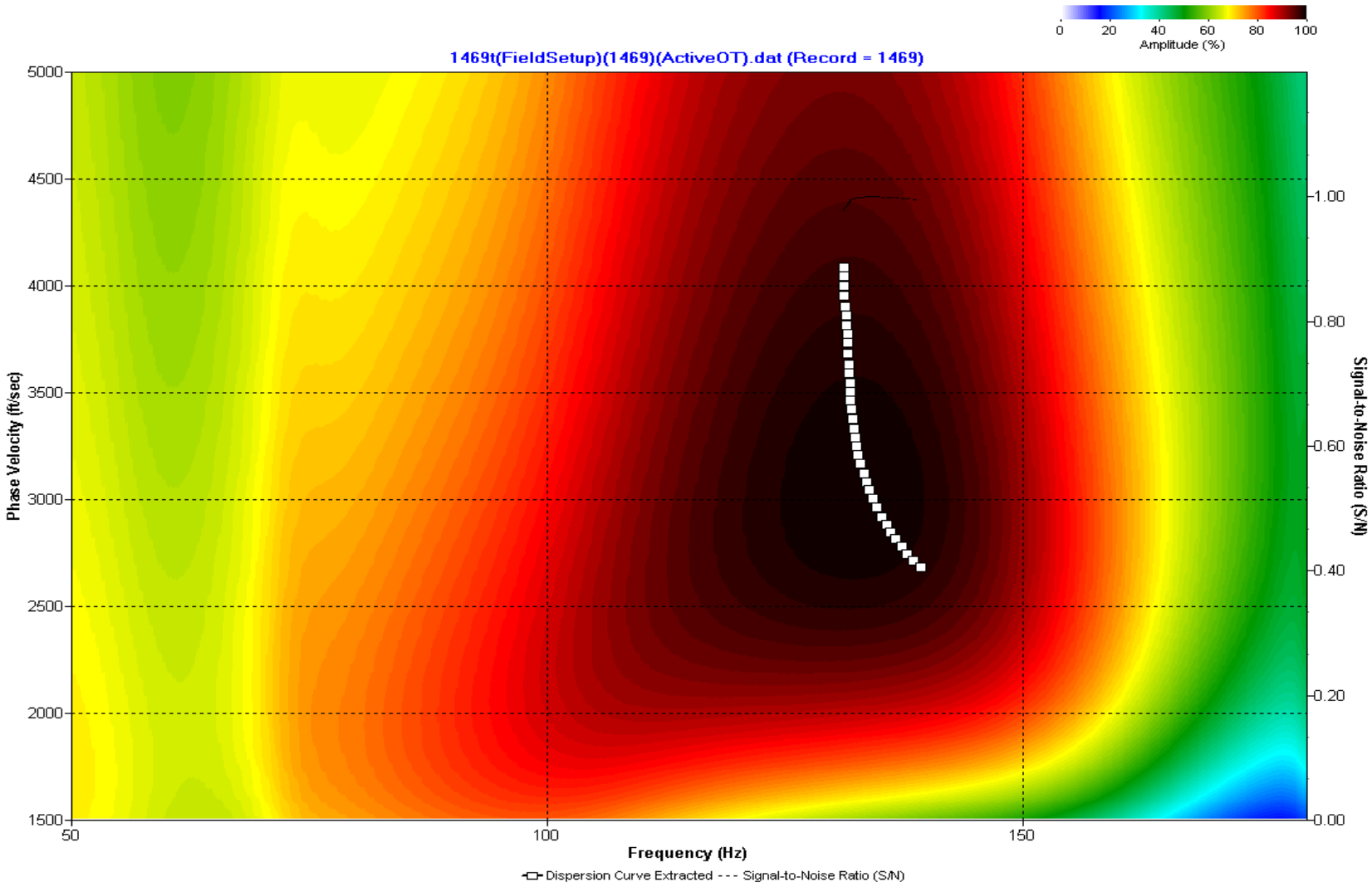

A.803: Dispersion Curve Line 1469 used in Post-blast 44

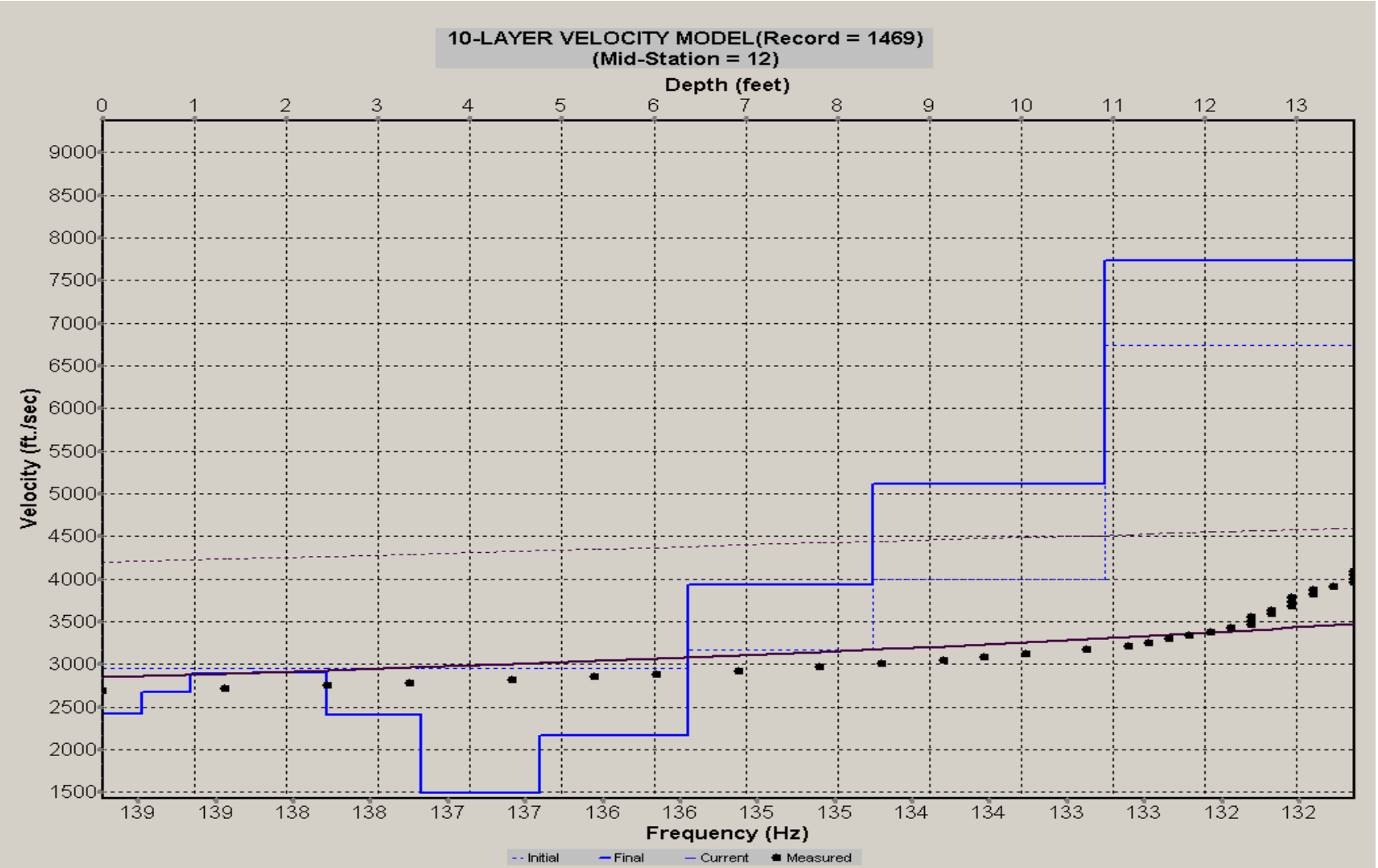

A.804: Velocity Profile Line 1469 used in Post-blast 44

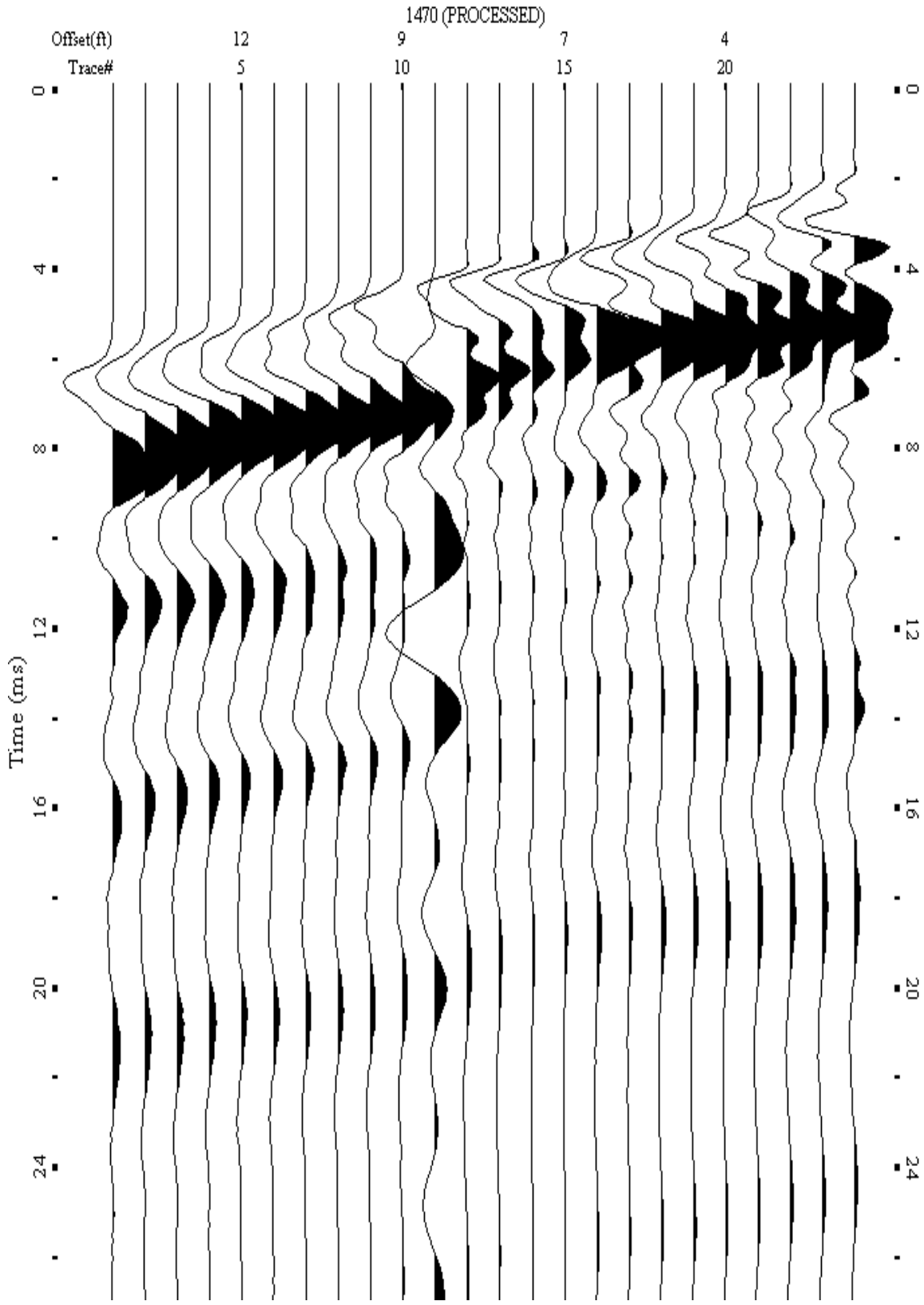

A.805: Shot Gather Line 1470 used in Post-blast 44

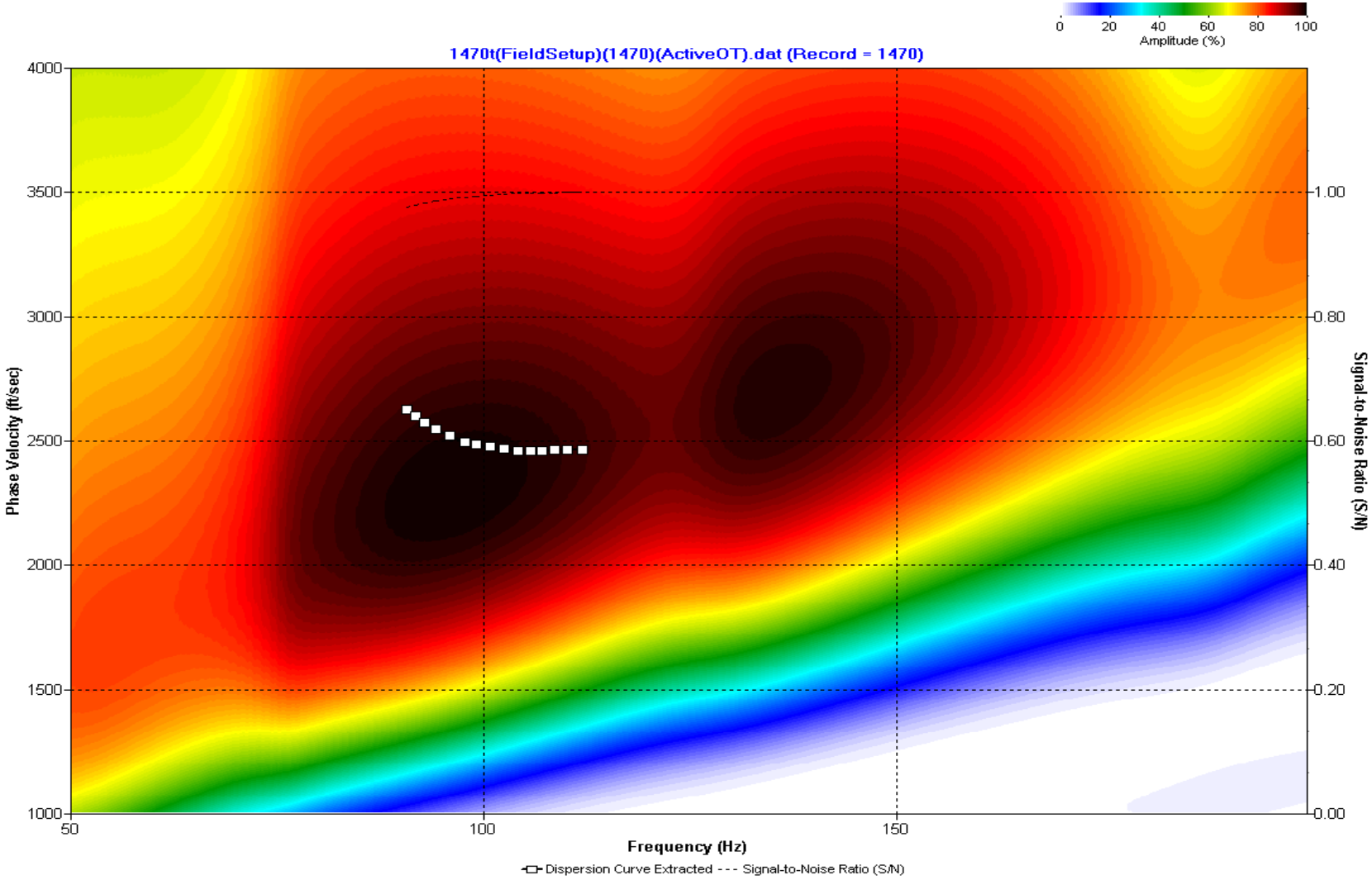

A.806: Dispersion Curve Line 1470 used in Post-blast 44

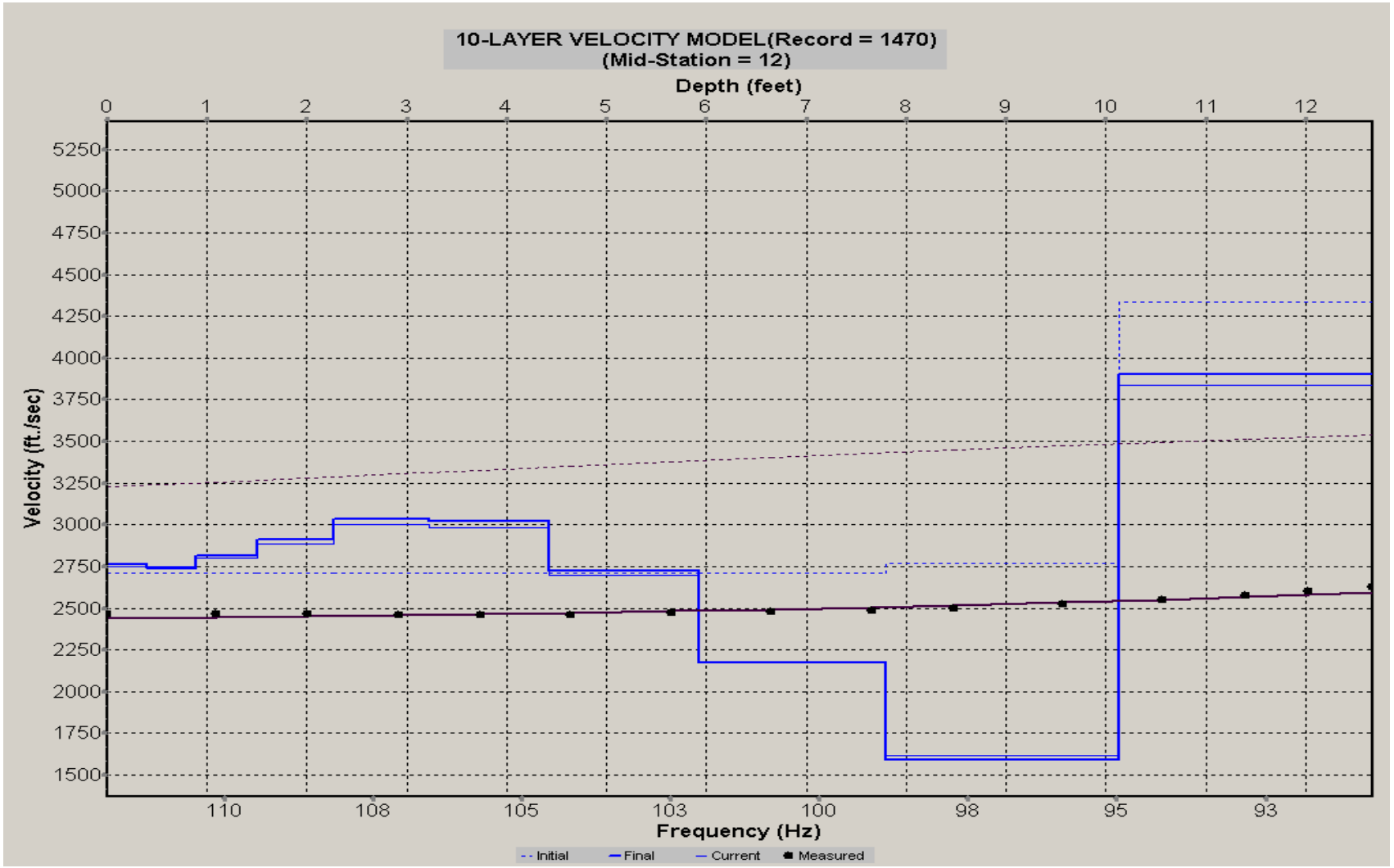

A.807: Velocity Profile Line 1470 used in Post-blast 44

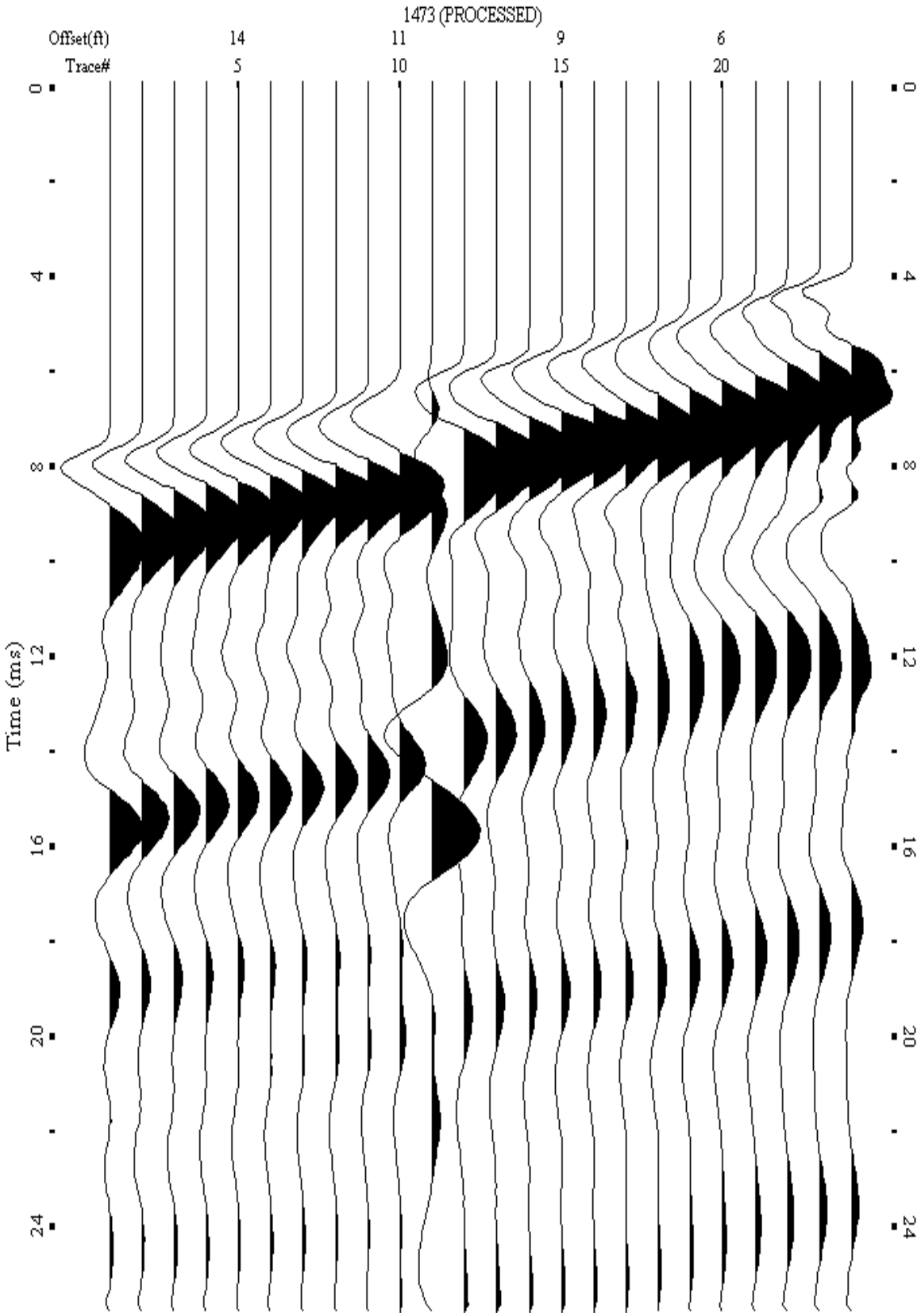

A.808: Shot Gather Line 1473 used in Post-blast 44

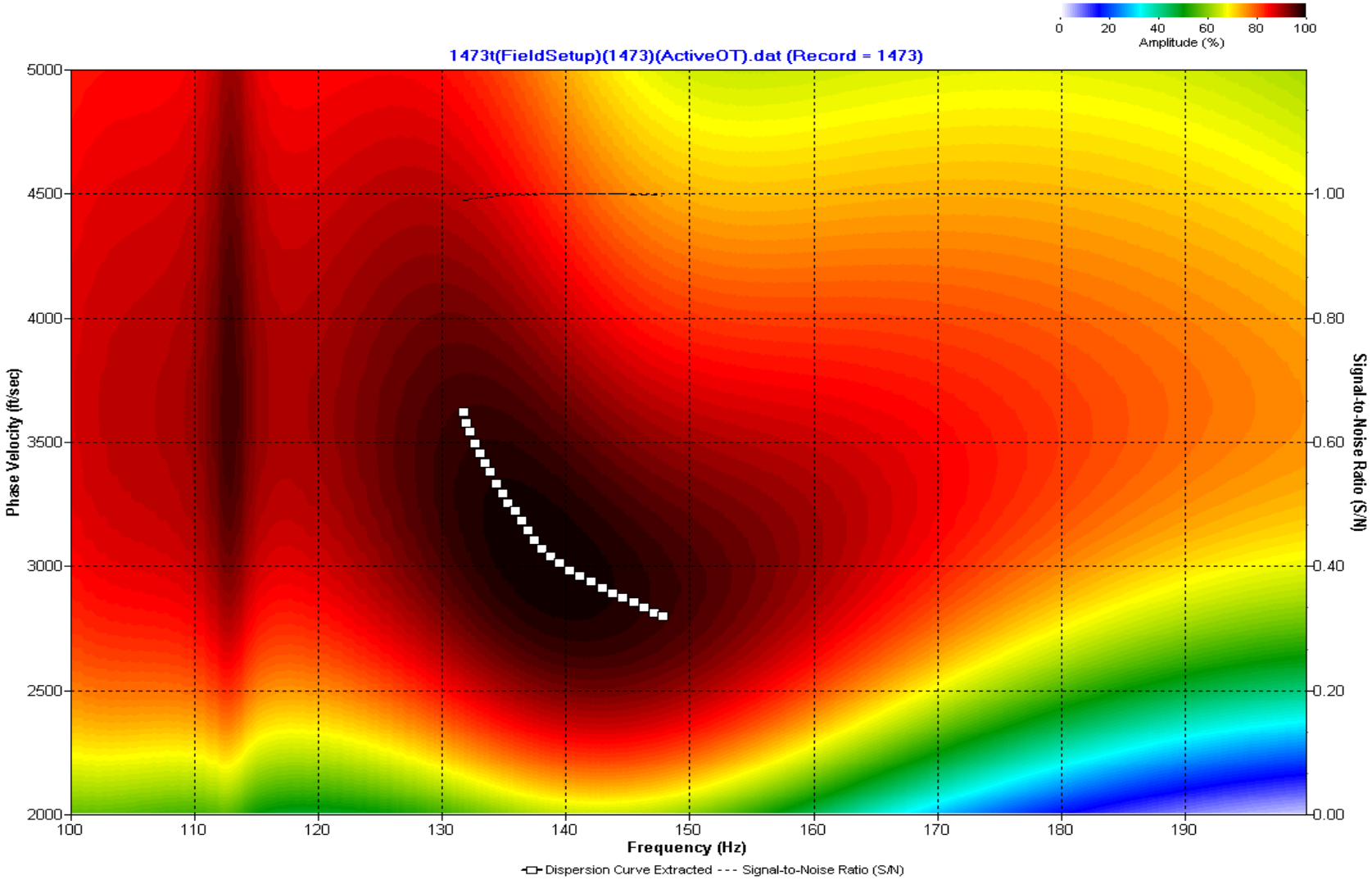

A.809: Dispersion Curve Line 1473 used in Post-blast 44

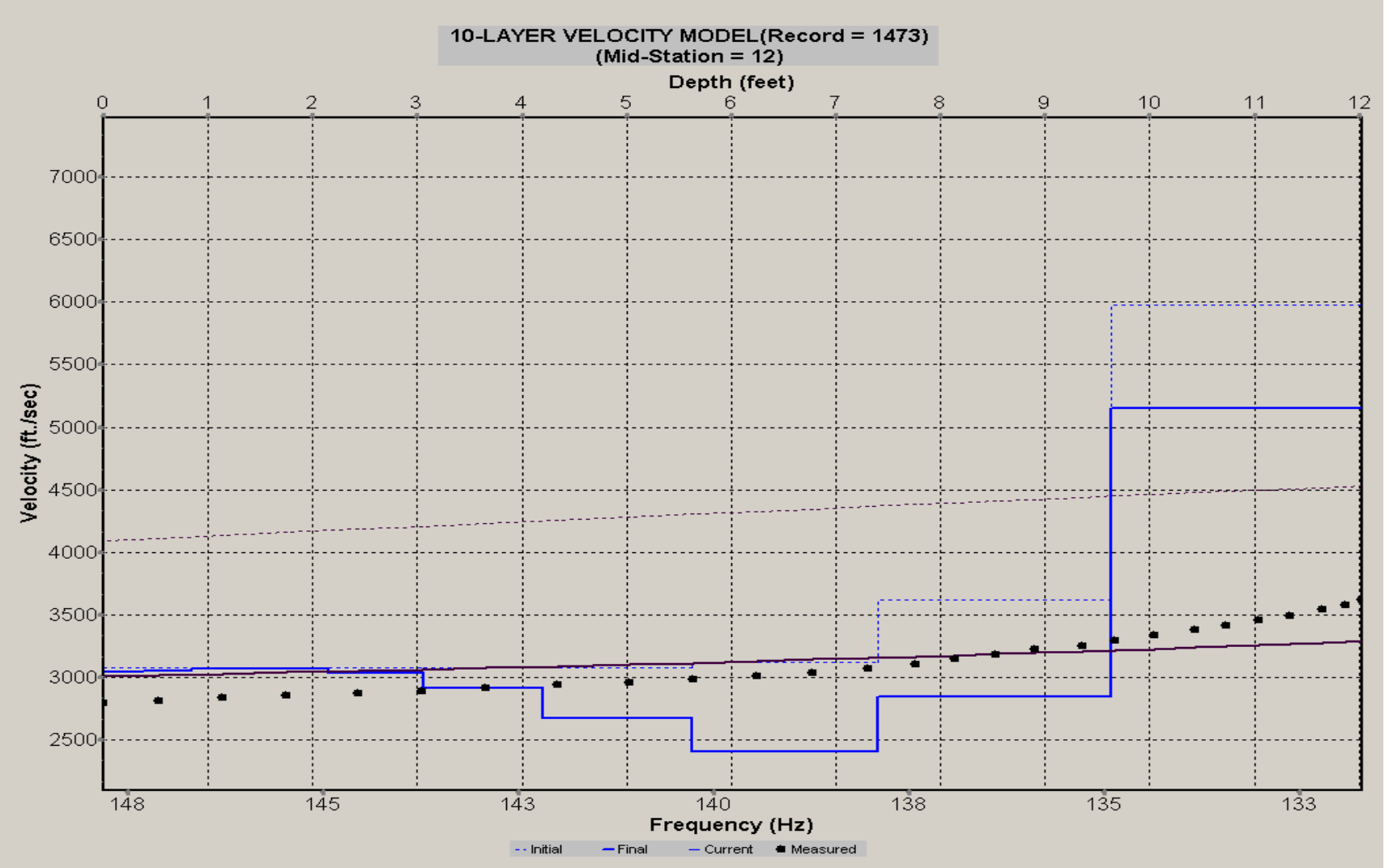

A.810: Velocity Profile Line 1473 used in Post-blast 44